



Docket No.: PF-0733 USN

Response Under 37 C.F.R. 1.116 – Expedited Procedure
Examining Group 1652

Certificate of Mailing

I hereby certify that this correspondence is being deposited with the United States Postal Service as first class mail in an envelope addressed to:
Mail Stop Appeal Brief-Patents, Commissioner for Patents, P.O. Box 1450, Alexandria, VA 22313-1450 on January 27, 2004.

By: 

Printed: Lisa McBill

IN THE UNITED STATES PATENT AND TRADEMARK OFFICE
BEFORE THE BOARD OF PATENT APPEALS AND INTERFERENCES

In re Application of: Yue et al.

Title: INTRACELLULAR SIGNALING MOLECULES

Serial No.: 10/018,170

Filing Date: December 11, 2001

Examiner: Steadman, D

Group Art Unit: 1652

Mail Stop Appeal Brief-Patents
Commissioner for Patents
P.O. Box 1450
Alexandria, VA 22313-1450

TRANSMITTAL FEE SHEET

Sir:

Transmitted herewith are the following for the above-identified application:

1. Return Receipt Postcard;
2. Petition for Extension of Time (1 pg.);
3. Brief on Appeal, including Appendix (33 pp., in triplicate);
4. Seventeen (17) References, as cited in Brief (in triplicate);
5. Copy of Declaration of L. Michael Furness Under 37 C.F.R. §1.132 (13 pp., in triplicate);
6. Copy of Declaration of Tod Bedilion Under 37 C.F.R. §1.132 (16 pp., in triplicate); and
7. Exhibit A, as cited in Brief (in triplicate).

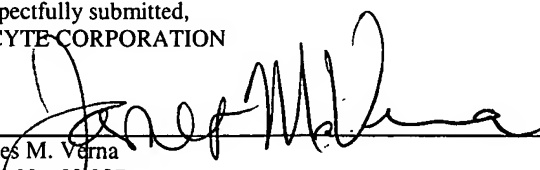
The fee has been calculated as shown below:

<input type="checkbox"/>	No additional Fee is required.	\$	
<input checked="" type="checkbox"/>	Fee for filing a Brief in support of an Appeal under 37 C.F.R. §1.17(c):	\$	330.00
<input checked="" type="checkbox"/>	Fee for Petition for Extension of Time Under 37 C.F.R. § 1.17(a):	\$	110.00
<input checked="" type="checkbox"/>	Please charge Deposit Account No. 09-0108 in the amount of:	\$	440.00

The Commissioner is hereby authorized to charge any additional fees required under 37 C.F.R. § 1.16 and § 1.17, or credit overpayment to Deposit Account No. **09-0108**. A duplicate copy of this sheet is enclosed.

Respectfully submitted,
INCYTE CORPORATION

Date: January 27, 2004


James M. Verna
Reg. No. 33,287
Direct Dial Telephone: (650) 845-5415

Customer No.: 27904
3160 Porter Drive
Palo Alto, California 94304
Phone: (650) 855-0555 or Fax: (650) 849-8886

Doc No.118841

1

10/018,170



Docket No.: PF-0733 USN

Response Under 37 C.F.R. 1.116 - Expedited Procedure
Examining Group 1652

Certificate of Mailing

I hereby certify that this correspondence is being deposited with the United States Postal Service as first class mail in an envelope addressed to:
Mail Stop Appeal Brief Patents, Commissioner for Patents, P.O. Box 1450, Alexandria, VA 22313-1450 on January 27, 2004.

By: 

Printed: Katherine Stog
Lisa McMill

IN THE UNITED STATES PATENT AND TRADEMARK OFFICE
BEFORE THE BOARD OF PATENT APPEALS AND INTERFERENCES

In re Application of: Yue et al.

Title: INTRACELLULAR SIGNALING MOLECULES

Serial No.: 10/018,170

Filing Date:

December 11, 2001

Examiner: Steadman, D

Group Art Unit:

1652

Mail Stop Appeal Brief-Patents
Commissioner for Patents
P.O. Box 1450
Alexandria, VA 22313-1450

BRIEF ON APPEAL

Sir:

Further to the Notice of Appeal filed October 22, 2003, and received by the USPTO on October 27, 2003, herewith are three copies of Appellants' Brief on Appeal. Appellants hereby request a one-month extension of time in order to file this Brief. Authorized fees include the statutory fee of \$110.00 for a one-month extension of time, as well as the \$ 330.00 fee for the filing of this Brief.

This is an appeal from the decision of the Examiner finally rejecting claims 205, 206, 208, 209, 211-215, 217, 224-226, and 228-231 of the above-identified application.

(1) REAL PARTY IN INTEREST

The above-identified application is assigned of record to **Incyte Pharmaceuticals, Inc., (now Incyte Corporation, formerly known as Incyte Genomics, Inc.)** (Reel 012671, Frame 0254) which is the real party in interest herein.

02/03/2004 AMONDAF1 00000003 090108 10018170

01 FC:1402 330.00 DA
118062

(2) RELATED APPEALS AND INTERFERENCES

Appellants, their legal representative and the assignee are not aware of any related appeals or interferences which will directly affect or be directly affected by or have a bearing on the Board's decision in the instant appeal.

(3) STATUS OF THE CLAIMS

Claims rejected: Claims 205, 206, 208, 209, 211-215, 217, 224-226, and 228-231
Claims allowed: (none)
Claims canceled: Claims 1-204, 207, 210, 216, 218, and 227
Claims withdrawn: Claims 219-223
Claims on Appeal: Claims 205, 206, 208, 209, 211-215, 217, 224-226, and 228-231
(A copy of the claims on appeal, as amended, can be found in the attached Appendix).

(4) STATUS OF AMENDMENTS AFTER FINAL

The Amendment after Final Rejection under 37 C.F.R. §1.116 filed August 27, 2003 has been entered for purposes of this appeal. See the Advisory Action, mailed December 19, 2003, indicating the Amendment would be entered upon filing of an appeal.

(5) SUMMARY OF THE INVENTION

Appellants' invention is directed to polynucleotides and polypeptides, including polynucleotides, comprising the polynucleotide sequence of SEQ ID NO:64, encoding the human annexin (INTRA-12), comprising the amino acid sequence of SEQ ID NO:12, and polypeptides comprising the amino acid sequence of SEQ ID NO:12 (Specification, e.g., at page 7, line 18 through page 8, line 2). Appellants' invention also includes complementary polynucleotides (e.g., at page 9, lines 1-6), recombinant polynucleotides encoding polypeptides comprising SEQ ID NO:12 (e.g., at page 8, lines 9-12), host cells transformed with recombinant polynucleotides, and methods of making polypeptides encoded by the claimed polynucleotides (e.g., at page 8, lines 16-21, pages 31-36 and Example X at pages 67-68). In addition, Appellants' invention comprises polypeptides, including an isolated polypeptide comprising an amino acid sequence of

SEQ ID NO:12 and compositions comprising a polypeptide comprising an amino acid sequence of SEQ ID NO:12 and a pharmaceutically acceptable excipient (Specification, e.g., at page 9, lines 31-33).

INTRA-12 has chemical and structural homology to human annexin 31 (g3688370; Specification, e.g., Table 2). The polynucleotides and polypeptides of the present invention are useful, for example, for toxicology testing, drug discovery, and diagnosis, prevention, and treatment of cancer, immune disorders, neurological disorders, and gastrointestinal disorders.

(6) ISSUES

1. Whether claims 205, 206, 208, 209, 211-215, 217, 224-226, and 228-231 directed to INTRA polypeptide sequences and the polynucleotides that encode them meet the utility requirement of 35 U.S.C. §101.

2. Whether one of ordinary skill in the art would know how to use the claimed sequences, e.g., in toxicology testing, drug development, and the diagnosis of disease, so as to satisfy the enablement requirement of 35 U.S.C. §112, first paragraph.

(7) GROUPING OF THE CLAIMS

As to Issue 1

All of the claims on appeal are grouped together.

As to Issue 2

All of the claims on appeal are grouped together.

(8) APPELLANTS' ARGUMENTS

THE FINAL REJECTION

Claims 205, 206, 208, 209, 211-215, 217, 224-226, and 228-231 stand rejected under 35 U.S.C. §§ 101 and 112, first paragraph, based on the allegation that the claimed invention lacks patentable utility. The rejection alleges in particular that:

- the claimed invention is not supported by either a specific and substantial asserted utility or a well-established utility. The specification discloses no uses for the broadly-claimed polynucleotides and polypeptides. A specific utility is one that is particular to the subject matter claimed, while a substantial utility is one that defines a “real world” use. Utilities that require or constitute carrying out further research to identify or reasonably confirm a “real world” context of use are not substantial utilities.
- there is no well-established, specific and substantial utility for the claimed polynucleotides and polypeptides because the function of the polypeptide of SEQ ID NO:12 has not been empirically determined; therefore, further experimentation would be required to determine the function of the protein.
- the specification does not disclose whether the polynucleotide of SEQ ID NO:64 is differentially expressed in different cells or tissues, and therefore the gene is not a disease marker or an appropriate target for drug discovery or toxicology testing.
- the utility of the claimed polynucleotides in toxicology testing is not specific because if any polynucleotide expressed in a human has utility in toxicology testing, then that polynucleotide has no specific utility as all polynucleotides would have such use.

Issue 1 – Whether the claims meet the utility requirement of 35 U.S.C. § 101

The rejection of claims 205, 206, 208, 209, 211-215, 217, 224-226, and 228-231 is improper, as the inventions of those claims have a patentable utility as set forth in the instant specification, and/or a utility well known to one of ordinary skill in the art.

The invention at issue is a polynucleotide sequence corresponding to a gene that is expressed in reproductive, gastrointestinal, and nervous system tissues (Specification at Table 3). The invention also comprises polypeptides encoded by the claimed polynucleotides. As such, the claimed invention has numerous practical, beneficial uses in toxicology testing, drug development, and the diagnosis of disease, none of which require knowledge of how the polypeptide actually functions.

The similarity of the claimed polypeptide to another polypeptide of known, undisputed utility by itself demonstrates utility beyond the reasonable probability required by law. INTRA-12 is, in that regard, homologous to human annexin 31 (g3688370) (Specification, e.g., at Table 2). In particular, SEQ ID NO:12 shares 98% sequence identity with annexin 31.

This is more than enough homology to demonstrate a reasonable probability that the utility of annexin 31 receptor can be imputed to the claimed invention. It is well-known that the probability that two unrelated polypeptides share more than 40% sequence homology over 70 amino acid residues is exceedingly small. Brenner *et al.*, Proc. Natl. Acad. Sci. U.S.A. 95:6073-78 (1998). Given homology in excess of 40% over many more than 70 amino acid residues, the probability that the claimed polypeptide is related to annexin 31 is, accordingly, very high.

The fact that the claimed polypeptide is a member of the annexin family alone demonstrates utility. Each of the members of this class, regardless of their particular functions, are useful. There is no evidence that any member of this class of polypeptides, let alone a substantial number of them, would not have some patentable utility. It follows that there is a more than substantial likelihood that the claimed polypeptide also has patentable utility, regardless of its actual function. The law has never required a patentee to prove more.

There is, in addition, direct proof of the utility of the claimed invention. Appellants submitted previously the Declarations of Bedilion and Furness describing some of the practical uses of the claimed invention in gene and protein expression monitoring applications as they would have been understood at the time of the patent application.

The Bedilion Declaration describes, in particular, how the claimed expressed polynucleotide can be used in gene expression monitoring applications that were well-known at the time the patent application was filed, and how those applications are useful in developing drugs and monitoring their activity. Dr. Bedilion states that the claimed invention is a useful tool when employed as a highly specific probe in a cDNA microarray:

Persons skilled in the art would appreciate that cDNA microarrays that contained the SEQ ID NO:12-encoding polynucleotides would be a more useful tool than cDNA microarrays that did not contain the polynucleotides in connection with conducting gene expression monitoring studies on proposed (or actual) drugs for treating cancer, immune disorders, neurological disorders, and gastrointestinal disorders for such purposes as evaluating their efficacy and toxicity.

The Patent Examiner does not dispute that the claimed polynucleotide can be used as a probe in cDNA microarrays and used in gene expression monitoring applications. Instead, the Patent Examiner contends that the claimed polynucleotide cannot be useful without precise knowledge of its biological function. But the law never has required knowledge of biological function to prove utility. It is the claimed invention's uses, not its functions, that are the subject of a proper analysis under the utility requirement.

In any event, as demonstrated by the Bedilion Declaration, the person of ordinary skill in the art can achieve beneficial results from the claimed polynucleotide in the absence of any knowledge as to the precise function of the protein encoded by it. The uses of the claimed polynucleotide in gene expression monitoring applications are in fact independent of its precise function.

The Furness Declaration describes, in particular, how the claimed polypeptide can be used in protein expression analysis techniques such as 2-D PAGE gels and western blots. Using the claimed invention with these techniques, persons of ordinary skill in the art can better assess, for example, the potential toxic affect of a drug candidate. (Furness Declaration at ¶ [11]).

The Patent Examiner does not dispute that the claimed polypeptide can be used in 2-D PAGE gels and western blots to perform drug toxicity testing. Instead, the Patent Examiner contends that the claimed polypeptide cannot be useful without precise knowledge of its function. But the law never has required knowledge of biological function to prove utility. It is the claimed invention's uses, not its functions, that are the subject of a proper analysis under the utility requirement.

In any event, as demonstrated by the Furness Declaration, the person of ordinary skill in the art can achieve beneficial results from the claimed polypeptide in the absence of any knowledge as to the precise function of the protein. The uses of the claimed polypeptide for gene expression monitoring applications including toxicology testing are in fact independent of its precise function.

I. The Applicable Legal Standard

To meet the utility requirement of sections 101 and 112 of the Patent Act, the patent applicant need only show that the claimed invention is "practically useful," *Anderson v. Natta*,

480 F.2d 1392, 1397, 178 USPQ 458 (CCPA 1973) and confers a “specific benefit” on the public. *Brenner v. Manson*, 383 U.S. 519, 534-35, 148 USPQ 689 (1966). As discussed in a recent Court of Appeals for the Federal Circuit case, this threshold is not high:

An invention is “useful” under section 101 if it is capable of providing some identifiable benefit. See *Brenner v. Manson*, 383 U.S. 519, 534 [148 USPQ 689] (1966); *Brooktree Corp. v. Advanced Micro Devices, Inc.*, 977 F.2d 1555, 1571 [24 USPQ2d 1401] (Fed. Cir. 1992) (“to violate Section 101 the claimed device must be totally incapable of achieving a useful result”); *Fuller v. Berger*, 120 F. 274, 275 (7th Cir. 1903) (test for utility is whether invention “is incapable of serving any beneficial end”).

Juicy Whip Inc. v. Orange Bang Inc., 51 USPQ2d 1700 (Fed. Cir. 1999).

While an asserted utility must be described with specificity, the patent applicant need not demonstrate utility to a certainty. In *Stiftung v. Renishaw PLC*, 945 F.2d 1173, 1180, 20 USPQ2d 1094 (Fed. Cir. 1991), the United States Court of Appeals for the Federal Circuit explained:

An invention need not be the best or only way to accomplish a certain result, and it need only be useful to some extent and in certain applications: “[T]he fact that an invention has only limited utility and is only operable in certain applications is not grounds for finding lack of utility.” *Envirotech Corp. v. Al George, Inc.*, 730 F.2d 753, 762, 221 USPQ 473, 480 (Fed. Cir. 1984).

The specificity requirement is not, therefore, an onerous one. If the asserted utility is described so that a person of ordinary skill in the art would understand how to use the claimed invention, it is sufficiently specific. See *Standard Oil Co. v. Montedison, S.p.a.*, 212 U.S.P.Q. 327, 343 (3d Cir. 1981). The specificity requirement is met unless the asserted utility amounts to a “nebulous expression” such as “biological activity” or “biological properties” that does not convey meaningful information about the utility of what is being claimed. *Cross v. Iizuka*, 753 F.2d 1040, 1048 (Fed. Cir. 1985).

In addition to conferring a specific benefit on the public, the benefit must also be “substantial.” *Brenner*, 383 U.S. at 534. A “substantial” utility is a practical, “real-world” utility. *Nelson v. Bowler*, 626 F.2d 853, 856, 206 USPQ 881 (CCPA 1980).

If persons of ordinary skill in the art would understand that there is a “well-established” utility for the claimed invention, the threshold is met automatically and the applicant need not make any showing to demonstrate utility. Manual of Patent Examination Procedure at

§ 706.03(a). Only if there is no “well-established” utility for the claimed invention must the applicant demonstrate the practical benefits of the invention. *Id.*

Once the patent applicant identifies a specific utility, the claimed invention is presumed to possess it. *In re Cortright*, 165 F.3d 1353, 1357, 49 USPQ2d 1464 (Fed. Cir. 1999); *In re Brana*, 51 F.3d 1560, 1566; 34 USPQ2d 1436 (Fed. Cir. 1995). In that case, the Patent Office bears the burden of demonstrating that a person of ordinary skill in the art would reasonably doubt that the asserted utility could be achieved by the claimed invention. *Id.* To do so, the Patent Office must provide evidence or sound scientific reasoning. *See In re Langer*, 503 F.2d 1380, 1391-92, 183 USPQ 288 (CCPA 1974). If and only if the Patent Office makes such a showing, the burden shifts to the applicant to provide rebuttal evidence that would convince the person of ordinary skill that there is sufficient proof of utility. *Brana*, 51 F.3d at 1566. The applicant need only prove a “substantial likelihood” of utility; certainty is not required. *Brenner*, 383 U.S. at 532.

II. Uses of the claimed polypeptides and polynucleotides for diagnosis of conditions and disorders characterized by expression of INTRA, for toxicology testing, and for drug discovery are sufficient utilities under 35 U.S.C. §§ 101 and 112, first paragraph

The claimed invention meets all of the necessary requirements for establishing a credible utility under the Patent Law: There are “well-established” uses for the claimed invention known to persons of ordinary skill in the art, and there are specific practical and beneficial uses for the invention disclosed in the patent application’s specification. These uses are explained, in detail, in the Bedilion Declaration and the Furness Declaration accompanying this brief. Objective evidence, not considered by the Patent Office, further corroborates the credibility of the asserted utilities.

A. The use of INTRA for toxicology testing, drug discovery, and disease diagnosis are practical uses that confer “specific benefits” to the public

The claimed invention has specific, substantial, real-world utility by virtue of its use in toxicology testing, drug development and disease diagnosis through gene expression profiling. These uses are explained in detail in the accompanying Bedilion Declaration and Furness Declaration, the substance of which is not rebutted by the Patent Examiner. There is no dispute that the claimed polynucleotide is in fact a useful tool in cDNA microarrays used to perform gene expression analysis and that the claimed polypeptide is a useful tool in two-dimensional polyacrylamide gel electrophoresis (“2-D PAGE”) analysis and western blots used to monitor protein expression and assess drug toxicity. These uses are sufficient to establish utilities for the claimed polynucleotide and polypeptide, respectively.

The instant application claims priority to United States Provisional Patent Application Serial No. 60/139,566 filed on June 16, 1999 (hereinafter “the Yue ‘566 application”).

1. The Bedilion Declaration

In his Declaration, Dr. Bedilion explains the many reasons why a person skilled in the art reading the Yue ‘566 application on June 16, 1999 would have understood that application to disclose the claimed polynucleotide to be useful for a number of gene expression monitoring applications, *e.g.*, as a highly specific probe for the expression of that specific polynucleotide in connection with the development of drugs and the monitoring of the activity of such drugs. (Bedilion Declaration at, *e.g.*, ¶¶ 10-15). Much, but not all, of Dr. Bedilion’s explanation concerns the use of the claimed polynucleotide in cDNA microarrays of the type first developed at Stanford University for evaluating the efficacy and toxicity of drugs, as well as for other applications. (Bedilion Declaration, ¶¶ 12 and 15).¹

In connection with his explanations, Dr. Bedilion states that the “Yue ‘566 specification would have led a person skilled in the art on June 16, 1999 who was using gene expression

¹Dr. Bedilion also explained, for example, why persons skilled in the art would also appreciate, based on the Yue ‘566 specification, that the claimed polynucleotide would be useful in connection with developing new drugs using technology, such as Northern analysis, that predated by many years the development of the cDNA technology (Bedilion Declaration, ¶ 16).

monitoring in connection with working on developing new drugs for the treatment of cancer, immune disorders, neurological disorders, and gastrointestinal disorders [a] to conclude that a cDNA microarray that contained the SEQ ID NO:12-encoding polynucleotides would be a highly useful tool, and [b] to request specifically that any cDNA microarray that was being used for such purposes contain the SEQ ID NO:12-encoding polynucleotides” (Bedilion Declaration, ¶ 15). For example, as explained by Dr. Bedilion, “[p]ersons skilled in the art would [have appreciated on June 16, 1999] that a cDNA microarray that contained the SEQ ID NO:12-encoding polynucleotides would be a more useful tool than a cDNA microarray that did not contain the polynucleotides in connection with conducting gene expression monitoring studies on proposed (or actual) drugs for treating cancer, immune disorders, neurological disorders, and gastrointestinal disorders for such purposes as evaluating their efficacy and toxicity.” *Id.*

In support of those statements, Dr. Bedilion provided detailed explanations of how cDNA technology can be used to conduct gene expression monitoring evaluations, with extensive citations to pre-June 16, 1999 publications showing the state of the art on June 16, 1999. (Bedilion Declaration, ¶¶ 10-14). While Dr. Bedilion’s explanations in paragraph 15 of his Declaration include almost three pages of text and six subparts (a)-(f), he specifically states that his explanations are not “all-inclusive.” *Id.* For example, with respect to toxicity evaluations, Dr. Bedilion had earlier explained how persons skilled in the art who were working on drug development on June 16, 1999 (and for several years prior to June 16, 1999) “without any doubt” appreciated that the toxicity (or lack of toxicity) of any proposed drug was “one of the most important criteria to be evaluated in connection with the development of the drug” and how the teachings of the Yue ‘566 application clearly include using differential gene expression analyses in toxicity studies (Bedilion Declaration, ¶ 10).

Thus, the Bedilion Declaration establishes that persons skilled in the art reading the Yue ‘566 application at the time it was filed “would have wanted their cDNA microarray to have a [SEQ ID NO:12-encoding polynucleotide probe] because a microarray that contained such a probe (as compared to one that did not) would provide more useful results in the kind of gene expression monitoring studies using cDNA microarrays that persons skilled in the art have been doing since well prior to June 16, 1999” (Bedilion Declaration, ¶ 15, item (f)). This, by itself, provides more than sufficient reason to compel the conclusion that the Yue ‘566 application

disclosed to persons skilled in the art at the time of its filing substantial, specific and credible real-world utilities for the claimed polynucleotide.

Nowhere does the Patent Examiner address the fact that, as described on pp. 33-34 of the Yue '566 application, the claimed polynucleotides can be used as highly specific probes in, for example, cDNA microarrays – probes that without question can be used to measure both the existence and amount of complementary RNA sequences known to be the expression products of the claimed polynucleotides. The claimed invention is not, in that regard, some random sequence whose value as a probe is speculative or would require further research to determine.

Given the fact that the claimed polynucleotide is known to be expressed, its utility as a measuring and analyzing instrument for expression levels is as indisputable as a scale's utility for measuring weight. This use as a measuring tool, regardless of how the expression level data ultimately would be used by a person of ordinary skill in the art, by itself demonstrates that the claimed invention provides an identifiable, real-world benefit that meets the utility requirement. *Raytheon v. Roper*, 724 F.2d 951, (Fed. Cir. 1983) (claimed invention need only meet one of its stated objectives to be useful); *In re Cortwright*, 165 F.3d 1353, 1359 (Fed. Cir. 1999) (how the invention works is irrelevant to utility); MPEP § 2107 (“Many research tools such as gas chromatographs, screening assays, and nucleotide sequencing techniques have a clear, specific, and unquestionable utility (e.g., they are useful in analyzing compounds)” (emphasis added)).

Though Applicants need not so prove to demonstrate utility, there can be no reasonable dispute that persons of ordinary skill in the art have numerous uses for information about relative gene expression including, for example, understanding the effects of a potential drug for treating cancer, immune disorders, neurological disorders, and gastrointestinal disorders. Because the patent application states explicitly that the claimed polynucleotide is known to be expressed in reproductive, gastrointestinal, and nervous system tissues and in tissues associated with cancer and inflammation (see the Yue '566 application at Table 3), and expresses a protein that is a member of the annexin family known to be associated with diseases such as cancer, immune disorders, neurological disorders, and gastrointestinal disorders, there can be no reasonable dispute that a person of ordinary skill in the art could put the claimed invention to such use. In other words, the person of ordinary skill in the art can derive more information about a potential cancer, immune disorders, neurological disorders, and gastrointestinal disorders drug candidate

or potential toxin with the claimed invention than without it (see Bedilion Declaration at, e.g., ¶ 15, subparts (e)-(f)).

The Bedilion Declaration shows that a number of pre-June 16, 1999 publications confirm and further establish the utility of cDNA microarrays in a wide range of drug development gene expression monitoring applications at the time the Yue '566 application was filed (Bedilion Declaration ¶¶ 10-14; Bedilion Exhibits A-G). Indeed, Brown and Shalon U.S. Patent No. 5,807,522 (the Brown '522 patent, Bedilion Exhibit D), which issued from a patent application filed in June 1995 and was effectively published on December 29, 1995 as a result of the publication of a PCT counterpart application, shows that the Patent Office recognizes the patentable utility of the cDNA technology developed in the early to mid-1990s. As explained by Dr. Bedilion, among other things (Bedilion Declaration, ¶ 12):

The Brown '522 patent further teaches that the “[m]icroarrays of immobilized nucleic acid sequences prepared in accordance with the invention” can be used in “numerous” genetic applications, including “monitoring of gene expression” applications (see Bedilion Tab D at col. 14, lines 36-42). The Brown '522 patent teaches (a) monitoring gene expression (i) in different tissue types, (ii) in different disease states, and (iii) in response to different drugs, and (b) that arrays disclosed therein may be used in toxicology studies (see Bedilion Tab D at col. 15, lines 13-18 and 52-58 and col. 18, lines 25-30).

Literature reviews published shortly after the filing of the Yue '566 application describing the state of the art further confirm the claimed invention's utility. Rockett et al. confirm, for example, that the claimed invention is useful for differential expression analysis regardless of how expression is regulated:

Despite the development of multiple technological advances which have recently brought the field of gene expression profiling to the forefront of molecular analysis, recognition of the importance of differential gene expression and characterization of differentially expressed genes has existed for many years.

* * *

Although differential expression technologies are applicable to a broad range of models, perhaps their most important advantage is that, in most cases, absolutely no prior knowledge of the specific genes which are up- or down-regulated is required.

* * *

Whereas it would be informative to know the identity and functionality of all genes up/down regulated by . . . toxicants, this would appear a longer term goal However, the current use of gene profiling yields a *pattern* of gene changes for a xenobiotic of unknown toxicity which may be matched to that of well characterized toxins, thus alerting the toxicologist to possible *in vivo* similarities between the unknown and the standard, thereby providing a platform for more extensive toxicological examination. (emphasis added)

Rockett et al., Differential gene expression in drug metabolism and toxicology: practicalities, problems and potential, 29 Xenobiotica No. 7, 655 (1999).

In another pre-June 16, 1999 article, Lashkari et al. state explicitly that sequences that are merely “predicted” to be expressed (predicted Open Reading Frames, or ORFs) – the claimed invention in fact is known to be expressed – have numerous uses:

Efforts have been directed toward the amplification of each predicted ORF or any other region of the genome ranging from a few base pairs to several kilobase pairs. There are many uses for these amplicons– they can be cloned into standard vectors or specialized expression vectors, or can be cloned into other specialized vectors such as those used for two-hybrid analysis. The amplicons can also be used directly by, for example, arraying onto glass for expression analysis, for DNA binding assays, or for any direct DNA assay.

Lashkari et al., Whole genome analysis: Experimental access to all genome sequenced segments through larger-scale efficient oligonucleotide synthesis and PCR, 94 Proc. Nat. Acad. Sci. 8945 (Aug. 1997) (emphasis added).

In his Declaration, Mr. Furness explains the many reasons why a person skilled in the art who read the Yue ‘566 application on June 16, 1999 would have understood that application to disclose the claimed polypeptide to be useful for a number of gene and protein expression monitoring applications, *e.g.*, in 2-D PAGE technologies, in connection with the development of drugs and the monitoring of the activity of such drugs. (Furness Declaration at, *e.g.*, ¶¶ 10-14). Much, but not all, of Mr. Furness’ explanation concerns the use of the claimed polypeptide in the creation of protein expression maps using 2-D PAGE.

2-D PAGE technologies were developed during the 1980’s. Since the early 1990’s, 2-D PAGE has been used to create maps showing the differential expression of proteins in different cell types or in similar cell types in response to drugs and potential toxic agents. Each expression pattern reveals the state of a tissue or cell type in its given environment, *e.g.*, in the presence or

absence of a drug. By comparing a map of cells treated with a potential drug candidate to a map of cells not treated with the candidate, for example, the potential toxicity of a drug can be assessed. (Furness Declaration at ¶ 10.)

The claimed invention makes 2-D PAGE analysis a more powerful tool for toxicology and drug efficacy testing. A person of ordinary skill in the art can derive more information about the state or states or tissue or cell samples from 2-D PAGE analysis with the claimed invention than without it. As Mr. Furness explains:

In view of the Yue '566 application, the Wilkins article, and other related pre-June 1999 publications, persons skilled in the art on June 16, 1999 clearly would have understood the Yue '566 application to disclose the SEQ ID NO:12 polypeptide to be useful in 2-D PAGE analyses for the development of new drugs and monitoring the activities of drugs for such purposes as evaluating their efficacy and toxicity (Furness Declaration, ¶10)

* * *

Persons skilled in the art would appreciate that a 2-D PAGE map that utilized the SEQ ID NO:12 polypeptide sequence would be a more useful tool than a 2-D PAGE map that did not utilize this protein sequence in connection with conducting protein expression monitoring studies on proposed (or actual) drugs for treating cancer, immune disorders, neurological disorders, and gastrointestinal disorders for such purposes as evaluating their efficacy and toxicity. (Furness Declaration, ¶12)

Mr. Furness' observations are confirmed in the literature published before the filing of the patent application. Wilkins, for example, describes how 2-D gels are used to define proteins present in various tissues and measure their levels of expression, the data from which is in turn used in databases:

For proteome projects, the aim of [computer-aided 2-D PAGE] analysis . . . is to catalogue all spots from the 2-D gel in a qualitative and if possible quantitative manner, so as to define the number of proteins present and their levels of expression. Reference gel images, constructed from one or more gels, for the basis of two-dimensional gel databases. (Wilkins, Tab C, p. 26).

B. The use of polynucleotides and polypeptides expressed by humans as tools for toxicology testing, drug discovery, and the diagnosis of disease is now “well-established”

The technologies made possible by expression profiling using polynucleotides and polypeptides are now well-established. The technical literature recognizes not only the prevalence of these technologies, but also their unprecedented advantages in drug development, testing and safety assessment. These technologies include toxicology testing, as described by Bedilion and Furness in their Declarations.

Toxicology testing is now standard practice in the pharmaceutical industry. See, *e.g.*, John C. Rockett et al., *supra*:

Knowledge of toxin-dependent regulation in target tissues is not solely an academic pursuit as much interest has been generated in the pharmaceutical industry to harness this technology in the early identification of toxic drug candidates, thereby shortening the developmental process and contributing substantially to the safety assessment of new drugs.

To the same effect are several other scientific publications, including Emile F. Nuwaysir et al., Microarrays and Toxicology: The Advent of Toxicogenomics, 24 Molecular Carcinogenesis 153 (1999); Sandra Steiner and N. Leigh Anderson, Expression profiling in toxicology -- potentials and limitations, 112-13 Toxicology Letters 467 (2000).

Nucleic acids useful for measuring the expression of whole classes of genes are routinely incorporated for use in toxicology testing. Nuwaysir et al. describes, for example, a Human ToxChip comprising 2089 human clones, which were selected

for their well-documented involvement in basic cellular processes as well as their responses to different types of toxic insult. Included on this list are DNA replication and repair genes, apoptosis genes, and genes responsive to PAHs and dioxin-like compounds, peroxisome proliferators, estrogenic compounds, and oxidant stress. Some of the other categories of genes include transcription factors, oncogenes, tumor suppressor genes, cyclins, kinases, phosphatases, cell adhesion and motility genes, and homeobox genes. Also included in this group are 84 housekeeping genes, whose hybridization intensity is averaged and used for signal normalization of the other genes on the chip.

See also Table 1 of Nuwaysir et al. (listing additional classes of genes deemed to be of special interest in making a human toxicology microarray).

The more genes that are available for use in toxicology testing, the more powerful the technique. "Arrays are at their most powerful when they contain the entire genome of the species they are being used to study." John C. Rockett and David J. Dix, Application of DNA Arrays to Toxicology, 107 Environ. Health Perspec. 681, No. 8 (1999). Control genes are carefully selected for their stability across a large set of array experiments in order to best study the effect of toxicological compounds. See attached email from the primary investigator on the Nuwaysir paper, Dr. Cynthia Afshari, to an Incyte employee, dated July 3, 2000, as well as the original message to which she was responding, indicating that even the expression of carefully selected control genes can be altered. Thus, there is no expressed gene which is irrelevant to screening for toxicological effects, and all expressed genes have a utility for toxicological screening.

In fact, the potential benefit to the public, in terms of lives saved and reduced health care costs, are enormous. Recent developments provide evidence that the benefits of this information are already beginning to manifest themselves. Examples include the following:

- In 1999, CV Therapeutics, an Incyte collaborator, was able to use Incyte gene expression technology, information about the structure of a known transporter gene, and chromosomal mapping location, to identify the key gene associated with Tangiers disease. This discovery took place over a matter of only a few weeks, due to the power of these new genomics technologies. The discovery received an award from the American Heart Association as one of the top 10 discoveries associated with heart disease research in 1999.
- In an April 9, 2000, article published by the Bloomberg news service, an Incyte customer stated that it had reduced the time associated with target discovery and validation from 36 months to 18 months, through use of Incyte's genomic information database. Other Incyte customers have privately reported similar experiences. The implications of this significant saving of time and expense for the number of drugs that may be developed and their cost are obvious.
- In a February 10, 2000, article in the *Wall Street Journal*, one Incyte customer stated that over 50 percent of the drug targets in its current pipeline were derived from the Incyte database. Other Incyte customers have privately reported similar experiences. By doubling the number of targets available to pharmaceutical researchers, Incyte genomic information has demonstrably accelerated the development of new drugs.

C. The similarity of the claimed polypeptide to another of undisputed utility demonstrates utility

Because there is a substantial likelihood that the claimed INTRA-12 is functionally related to annexin 31 and pemphaxin, a polypeptide of undisputed utility, there is by implication a substantial likelihood that the claimed polypeptide and the polynucleotide that encodes it are similarly useful. Appellants need not show any more to demonstrate utility. *In re Brana*, 51 F.3d at 1567.

It is undisputed that the polypeptide encoded for by the claimed polynucleotide shares more than 98% sequence identity over 345 amino acid residues with annexin 31 (g3688370) (Specification, e.g., at Table 2). The presence of multiple annexin domain signatures in SEQ ID NO:12 indicates that INTRA-12 is a member of the annexin family (see specification at Table 2). Members of the annexin family are known to function in phospholipid binding, membrane-cytoskeleton interactions, phospholipase inhibition, anticoagulation, and membrane fusion (Specification at page 4, lines 18-24) and have been implicated in cancer, neurodegenerative diseases, autoimmune diseases, and inflammatory bowel diseases (enclosed references of Bastian (1997) *Cell. Mol. Life Sci.* 53:554-556; Eberhard et al. (1994) *Am. J. Pathol.* 145:640-649; and Gerke and Moss (2002) *Physiol. Rev.* 82:331-371).

CLUSTALW analysis shows that SEQ ID NO:12 is 99.7% identical to pemphaxin (see Exhibit C of the Response to the Final Office Action of June 30, 2003). Although, the Examiner argues that SEQ ID NO:12 is "structurally distinct from pemphaxin" and therefore "cannot be pemphaxin" (Advisory Action, page 6), Applicants note that the sequence of SEQ ID NO:12 and pemphaxin share 344 out of 345 residues in common. Thus, SEQ ID NO:12 is pemphaxin. Pemphaxin acts as a cell surface cholinergic receptor involved in the regulation of keratinocyte cell adhesion and is known to be associated with the autoimmune disorder, pemphigus vulgaris (see article of Nguyen *et al.* *J. Biol. Chem.* (2000) 275:29466-29476, previously submitted as Exhibit B of the Response to the Final Office Action of June 30, 2003). Nguyen et al. identified pemphaxin in a screen for self-antigens recognized by pathogenic autoantibodies associated with the autoimmune disorder pemphigus vulgaris. Pemphaxin is believed to be one of the major proteins targeted by the autoimmune disorder. This corroborates the statement on page 7 of the

Specification that the SEQ ID NO:12 polypeptide and the polynucleotides encoding it may be useful in the diagnosis and treatment of autoimmune disorders.

Members of the annexin class of proteins have been found to be useful cell markers because of their phospholipid binding properties and their association with the plasma membrane (See the response to the Office Action of January 10, 2003 at page 22). Annexin V has been used in radionuclide imaging as a marker of apoptosis to monitor the changes in phospholipid distribution that accompany cell death (enclosed references of Blankenberg et al. (1998) Proc. Natl. Acad. Sci. U.S.A. 95:6349-6354 and Blankenberg et al. (2000) Eur. J. Nucl. Med. 27:359-367). Radionuclide imaging with radiolabeled annexins may be useful for diagnosis of stroke, neurodegenerative diseases, inflammatory diseases, myocardial ischemia, myelodysplastic disorders, organ transplantation, and cancer.

Although, the Examiner has pointed out the absence of type II calcium binding sites in annexin 31, and argues that the SEQ ID NO:12 protein "would not have the phospholipid binding ability of other annexins" (Final Office Acton, page 22), Applicants disagree. Other members of the annexin family display both calcium-dependent and calcium-independent binding to phospholipids. For example, annexin I has a calcium-independent form that associates with membranes in the absence of calcium. Phosphorylation of the calcium-independent form of annexin I by epidermal growth factor kinase converts annexin I to a calcium-dependent form that requires calcium for membrane association (See enclosed reference of Futter et al. (1993) J. Cell Biol. 120:77-83). Annexin II, annexin A11, and annexin XIII also are able to associate with membranes in the absence of calcium. (Also see the enclosed references of Jost et al. (1997) J. Cell Science 110:221-228, Lecona et al. (2003) Biochem. J. 373:437-449, and Lecat et al. (2000) J. Cell Science 113:2607-2618). Thus, the calcium binding site is not required in all annexins to confer phospholipid binding properties. The SEQ ID NO:12 polypeptide, as a member of the annexin family, more likely than not, is a phospholipid binding protein, and as such, is useful like other members of the annexin family.

The Examiner must accept the applicants' assertion that the polypeptide encoded for by the claimed invention is pemphaxin and thus has its utility unless the Examiner can demonstrate through evidence or sound scientific reasoning that a person of ordinary skill in the art would doubt that SEQ ID NO:12 is pemphaxin. See *In re Langer*, 503 F.2d 1380, 1391-92, 183 USPQ

288 (CCPA 1974). The Examiner has not provided sufficient evidence or sound scientific reasoning to the contrary.

While the Examiner has cited literature: Smith et al. (Nat. Biotech 15:1222-1223, 1997); Brenner et al. (Trends in Genetics, 15:132-133, 1999); and Seffernick et al. (J. Bacteriol. 183:2405-2410, 2001, identifying some of the difficulties that may be involved in predicting protein function, none suggests that functional homology cannot be inferred by a reasonable probability in this case. Most important, none contradicts Brenner's basic rule that sequence homology in excess of 40% over 70 or more amino acid residues yields a high probability of functional homology as well. At most, these articles individually and together stand for the proposition that it is difficult to make predictions about function with certainty. The standard applicable in this case is not, however, proof to certainty, but rather proof to reasonable probability.

The Seffernick et al. reference cited by the Examiner does not contradict the findings of Brenner et al. The Seffernick et al. reference describes two enzymes, a melamine deaminase and an atrazine chlorohydrolase, that are 98% identical, yet have different substrate specificities. These two enzymes belong to a class of bacterial amidohydrolases whose members catalyze the hydrolytic displacement of amino groups or chlorine substituents from triazine ring compounds. Notably, the substrates of the two enzymes, melamine and atrazine, have similar structures except that melamine possesses an amino group and atrazine possesses a chlorine substituent. Some other members of the amidohydrolase superfamily catalyze deamination and dechlorination reactions with both triazine ring substrates. Therefore, the 98% sequence homology between melamine deaminase and atrazine chlorohydrolase correctly predicts their functional similarity and their membership in a common enzyme family. As noted by the Examiner, Seffernick et al. recognize that "functional assignments based on >50% sequence identity are considered to be reasonably sound" (Seffernick et al., page 2409, left column, paragraph 2).

Furthermore, the Examiner has not provided evidence that any member of the annexin family, let alone a substantial number of those members, is not useful. In such circumstances, the only reasonable inference is that the polypeptide encoded by the claimed invention, like the other members of the annexin protein family, must be useful.

D. Objective evidence corroborates the utilities of the claimed invention

There is, in fact, no restriction on the kinds of evidence a Patent Examiner may consider in determining whether a “real-world” utility exists. Indeed, “real-world” evidence, such as evidence showing actual use or commercial success of the invention, can demonstrate conclusive proof of utility. *Raytheon v. Roper*, 220 USPQ2d 592 (Fed. Cir. 1983); *Nestle v. Eugene*, 55 F.2d 854, 856, 12 USPQ 335 (6th Cir. 1932). Indeed, proof that the invention is made, used or sold by any person or entity other than the patentee is conclusive proof of utility. *United States Steel Corp. v. Phillips Petroleum Co.*, 865 F.2d 1247, 1252, 9 USPQ2d 1461 (Fed. Cir. 1989).

Over the past several years, a vibrant market has developed for databases containing all expressed genes (along with the polypeptide translations of those genes), in particular genes having medical and pharmaceutical significance such as the instant sequence. (Note that while the value in these databases is enhanced by their completeness, each sequence in them is independently valuable nonetheless.) The databases sold by Appellants’ assignee, Incyte, include exactly the kinds of information made possible by the claimed invention, such as tissue and disease associations. Incyte sells its database containing the claimed sequence and millions of other sequences throughout the scientific community, including to pharmaceutical companies who use the information to develop new pharmaceuticals.

Both Incyte’s customers and the scientific community have acknowledged that Incyte’s databases have proven to be valuable in, for example, the identification and development of drug candidates. As Incyte adds information to its databases, including the information that can be generated only as a result of Incyte’s discovery of the claimed polynucleotide and its use of that polynucleotide on cDNA microarrays, the databases become even more powerful tools. Thus the claimed invention adds more than incremental benefit to the drug discovery and development process.

III. The Patent Examiner’s Rejections Are Without Merit

Rather than responding to the evidence demonstrating utility, the Examiner attempts to dismiss it altogether by arguing that the disclosed and well-established utilities for the claimed

polynucleotide and polypeptide are not "specific and substantial" utilities. (Office Action of January 10, 2003 at p. 4.) The Examiner is incorrect both as a matter of law and as a matter of fact.

A. The Precise Biological Role Or Function Of An Expressed Polynucleotide or Polypeptide Is Not Required To Demonstrate Utility

The Patent Examiner's primary rejection of the claimed invention is based on the ground that, without information as to the precise "biological role" of the claimed invention, the claimed invention's utility is not sufficiently specific. According to the Examiner, it is not enough that a person of ordinary skill in the art could use and, in fact, would want to use the claimed invention either by itself or in a microarray, 2-D gel or western blot to monitor the expression of genes for such applications as the evaluation of a drug's efficacy and toxicity. The Examiner would require, in addition, that the Appellant provide a specific and substantial interpretation of the results generated in any given expression analysis.

It may be that specific and substantial interpretations and detailed information on biological function are necessary to satisfy the requirements for publication in some technical journals, but they are not necessary to satisfy the requirements for obtaining a United States patent. The relevant question is not, as the Examiner would have it, whether it is known how or why the invention works, *In re Cortwright*, 165 F.3d 1353, 1359 (Fed. Cir. 1999), but rather whether the invention provides an "identifiable benefit" in presently available form. *Juicy Whip Inc. v. Orange Bang Inc.*, 185 F.3d 1364, 1366 (Fed. Cir. 1999). If the benefit exists, and there is a substantial likelihood the invention provides the benefit, it is useful. There can be no doubt, particularly in view of the Bedilion Declaration (at, e.g., ¶¶ 10 and 15, Bedilion) and the Furness Declaration (at, e.g., ¶¶ 10-13), that the present invention meets this test.

The threshold for determining whether an invention produces an identifiable benefit is low. *Juicy Whip*, 185 F.3d at 1366. Only those utilities that are so nebulous that a person of ordinary skill in the art would not know how to achieve an identifiable benefit and, at least according to the PTO guidelines, so-called "throwaway" utilities that are not directed to a person

of ordinary skill in the art at all, do not meet the statutory requirement of utility. Utility Examination Guidelines, 66 Fed. Reg. 1092 (Jan. 5, 2001).

Knowledge of the biological function or role of a biological molecule has never been required to show real-world benefit. In its most recent explanation of its own utility guidelines, the PTO acknowledged so much (66 F.R. at 1095):

[T]he utility of a claimed DNA does not necessarily depend on the function of the encoded gene product. A claimed DNA may have specific and substantial utility because, *e.g.*, it hybridizes near a disease-associated gene or it has gene-regulating activity.

By implicitly requiring knowledge of biological function for any claimed nucleic acid, the Examiner has, contrary to law, elevated what is at most an evidentiary factor into an absolute requirement of utility. Rather than looking to the biological role or function of the claimed invention, the Examiner should have looked first to the benefits it is alleged to provide.

B. Membership in a Class of Useful Products Can Be Proof of Utility

Despite the uncontradicted evidence that the claimed polypeptide is related to pemphaxin, a member of the annexin family, whose members indisputably are useful, the Examiner refused to impute the utility of pemphaxin to INTRA-12. In the Office Action of January 10, 2003, the Patent Examiner takes the position that unless Appellants can identify which particular annexin function is possessed by INTRA-12, utility cannot be imputed.

In order to demonstrate utility by membership in a class, the law requires only that the class not contain a substantial number of useless members. So long as the class does not contain a substantial number of useless members, there is sufficient likelihood that the claimed invention will have utility, and a rejection under 35 U.S.C. § 101 is improper. That is true regardless of how the claimed invention ultimately is used and whether or not the members of the class possess one utility or many. *See Brenner v. Manson*, 383 U.S. 519, 532 (1966); *Application of Kirk*, 376 F.2d 936, 943 (CCPA 1967).

Membership in a “general” class is insufficient to demonstrate utility only if the class contains a sufficient number of useless members such that a person of ordinary skill in the art

could not impute utility by a substantial likelihood. There would be, in that case, a substantial likelihood that the claimed invention is one of the useless members of the class. In the few cases in which class membership did not prove utility by substantial likelihood, the classes did in fact include predominately useless members. *E.g.*, *Brenner* (man-made steroids); *Kirk* (same); *Natta* (man-made polyethylene polymers).

The Examiner addresses INTRA-12 as if the general class in which it is included is not the annexin family, but rather all polynucleotides or all polypeptides, including the vast majority of useless theoretical molecules not occurring in nature, and thus not pre-selected by nature to be useful. While these “general classes” may contain a substantial number of useless members, the annexin family does not. The annexin family is sufficiently specific to rule out any reasonable possibility that INTRA-12 would not also be useful like the other members of the family.

Because the Examiner has not presented any evidence that the annexin class of proteins has any, let alone a substantial number, of useless members, the Examiner must conclude that there is a “substantial likelihood” that the INTRA-12 encoded by the claimed polynucleotides is useful. It follows that SEQ ID NO:12 and SEQ ID NO:64 also are useful.

Even if the Examiner's “common utility” criterion were correct – and it is not – the annexin family would meet it. It is undisputed that known members of the annexin family function in phospholipid binding, membrane-cytoskeleton interactions, phospholipase inhibition, anticoagulation, and membrane fusion. A person of ordinary skill in the art need not know any more about how the claimed invention functions to use it, and the Examiner presents no evidence to the contrary. Instead, the Examiner makes the conclusory observation that a person of ordinary skill in the art would need to know whether, for example, any given annexin functions in phospholipid binding, membrane-cytoskeleton interactions, or phospholipase inhibition. The Examiner then goes on to assume that the only use for INTRA-12 absent knowledge as to how INTRA-12 actually works is further study of INTRA-12 itself.

Not so. As demonstrated by Appellants, knowledge that INTRA-12 is an annexin related to annexin 31 is more than sufficient to make it useful for the diagnosis and treatment of cancer, immune disorders, neurological disorders, and gastrointestinal disorders. The Examiner must accept these facts to be true unless the Examiner can provide evidence or sound scientific reasoning to the contrary. But the Examiner has not done so.

C. Because the uses of polynucleotides encoding INTRA in toxicology testing, drug discovery, and disease diagnosis are practical uses beyond mere study of the invention itself, the claimed invention has substantial utility.

The Examiner rejected the claims at issue on the ground that the use of an invention as tool for research is not a “substantial” use. Because the Examiner’s rejection assumes a substantial overstatement of the law, and is incorrect in fact, it must be overturned.

There is no authority for the proposition that use as a tool for research is not a substantial utility. Indeed, the Patent Office has recognized that just because an invention is used in a research setting does not mean that it lacks utility (MPEP § 2107):

Many research tools such as gas chromatographs, screening assays, and nucleotide sequencing techniques have a clear, specific and unquestionable utility (e.g., they are useful in analyzing compounds). An assessment that focuses on whether an invention is useful only in a research setting thus does not address whether the specific invention is in fact “useful” in a patent sense. Instead, Office personnel must distinguish between inventions that have a specifically identified utility and inventions whose specific utility requires further research to identify or reasonably confirm.

The Patent Office’s actual practice has been, at least until the present, consistent with that approach. It has routinely issued patents for inventions whose only use is to facilitate research, such as DNA ligases. These are acknowledged by the PTO’s Training Materials themselves to be useful, as well as DNA sequences used, for example, as markers.

Only a limited subset of research uses are not “substantial” utilities: those in which the only known use for the claimed invention is to be an **object** of further study, thus merely inviting further research. This follows from *Brenner*, in which the U.S. Supreme Court held that a process for making a compound does not confer a substantial benefit where the only known use of the compound was to be the object of further research to determine its use. *Id.* at 535. Similarly, in *Kirk*, the Court held that a compound would not confer substantial benefit on the public merely because it might be used to synthesize some other, unknown compound that would confer substantial benefit. *Kirk*, 376 F.2d at 940, 945 (“What Appellants are really saying to those in the art is take these steroids, experiment, and find what use they do have as medicines.”).

Nowhere do those cases state or imply, however, that a material cannot be patentable if it has some other beneficial use in research.

Such beneficial uses beyond studying the claimed invention itself have been demonstrated, in particular those described in the Bedilion and Furness Declarations. The claimed invention is a tool, rather than an object, of research. The data generated in gene expression monitoring using the claimed invention as a tool is **not** used merely to study the claimed polynucleotide itself, but rather to study properties of tissues, cells, and potential drug candidates and toxins. Without the claimed invention, the information regarding the properties of tissues, cells, drug candidates and toxins is less complete.

Moreover, as discussed above in section II D., SEQ ID NO:12 shares homology with other members of the annexin family. Therefore, the skilled artisan would have considered INTRA to be an important and valuable tool, in particular, for use in research on cancer, immune disorders, neurological disorders, and gastrointestinal disorders. The claimed invention has numerous other uses as a research tool, each of which alone is a “substantial utility.” These include uses such as diagnostic assays (e.g., pages 51-56), chromosomal markers (e.g., pages 56-57), and ligand screening assays (e.g., page 36).

IV. By Requiring the Patent Applicant to Assert a Particular or Unique Utility, the Patent Examination Utility Guidelines and Training Materials Applied by the Patent Examiner Misstate the Law

There is an additional, independent reason to overturn the rejections: to the extent the rejections are based on Revised Interim Utility Examination Guidelines (64 FR 71427, December 21, 1999), the final Utility Examination Guidelines (66 FR 1092, January 5, 2001) and/or the Revised Interim Utility Guidelines Training Materials (USPTO Website www.uspto.gov, March 1, 2000), the Guidelines and Training Materials are themselves inconsistent with the law.

The Training Materials, which direct the Examiners regarding how to apply the Utility Guidelines, address the issue of specificity with reference to two kinds of asserted utilities:

“specific” utilities which meet the statutory requirements, and “general” utilities which do not. The Training Materials define a “specific utility” as follows:

A [specific utility] is *specific* to the subject matter claimed. This contrasts to *general* utility that would be applicable to the broad class of invention. For example, a claim to a polynucleotide whose use is disclosed simply as “gene probe” or “chromosome marker” would not be considered to be specific in the absence of a disclosure of a specific DNA target. Similarly, a general statement of diagnostic utility, such as diagnosing an unspecified disease, would ordinarily be insufficient absent a disclosure of what condition can be diagnosed.

The Training Materials distinguish between “specific” and “general” utilities by assessing whether the asserted utility is sufficiently “particular,” *i.e.*, unique (Training Materials at p.52) as compared to the “broad class of invention.” (In this regard, the Training Materials appear to parallel the view set forth in Stephen G. Kunin, Written Description Guidelines and Utility Guidelines, 82 J.P.T.O.S. 77, 97 (Feb. 2000) (“With regard to the issue of specific utility the question to ask is whether or not a utility set forth in the specification is *particular* to the claimed invention.”)).

Such “unique” or “particular” utilities never have been required by the law. To meet the utility requirement, the invention need only be “practically useful,” *Natta*, 480 F.2d 1 at 1397, and confer a “specific benefit” on the public. *Brenner*, 383 U.S. at 534. Thus, incredible “throw-away” utilities, such as trying to “patent a transgenic mouse by saying it makes great snake food,” do not meet this standard. Karen Hall, Genomic Warfare, *The American Lawyer* 68 (June 2000) (quoting John Doll, Chief of the Biotech Section of USPTO).

This does not preclude, however, a general utility, contrary to the statement in the Training Materials where “specific utility” is defined (page 5). Practical real-world uses are not limited to uses that are unique to an invention. The law requires that the practical utility be “definite,” not particular. *Montedison*, 664 F.2d at 375. Appellant is not aware of any court that has rejected an assertion of utility on the grounds that it is not “particular” or “unique” to the specific invention. Where courts have found utility to be too “general,” it has been in those cases in which the asserted utility in the patent disclosure was not a practical use that conferred a specific benefit. That is, a person of ordinary skill in the art would have been left to guess as to

how to benefit at all from the invention. In *Kirk*, for example, the CCPA held the assertion that a man-made steroid had “useful biological activity” was insufficient where there was no information in the specification as to how that biological activity could be practically used. *Kirk*, 376 F.2d at 941.

The fact that an invention can have a particular use does not provide a basis for requiring a particular use. See *Brana, supra* (disclosure describing a claimed antitumor compound as being homologous to an antitumor compound having activity against a “particular” type of cancer was determined to satisfy the specificity requirement). “Particularity” is not and never has been the *sine qua non* of utility; it is, at most, one of many factors to be considered.

As described *supra*, broad classes of inventions can satisfy the utility requirement so long as a person of ordinary skill in the art would understand how to achieve a practical benefit from knowledge of the class. Only classes that encompass a significant portion of nonuseful members would fail to meet the utility requirement. *Supra* § II.B.2 (*Montedison*, 664 F.2d at 374-75).

The Training Materials fail to distinguish between broad classes that convey information of practical utility and those that do not, lumping all of them into the latter, unpatentable category of “general” utilities. As a result, the Training Materials paint with too broad a brush. Rigorously applied, they would render unpatentable whole categories of inventions that heretofore have been considered to be patentable and that have indisputably benefitted the public, including the claimed invention. See *supra* § II.B. Thus the Training Materials cannot be applied consistently with the law.

Issue 2 – Whether claims 205, 206, 208, 209, 211-215, 217, 224-226, and 228-231 meet the enablement requirement of 35 U.S.C. § 112, first paragraph

To the extent the rejection of the claimed invention under 35 U.S.C. § 112, first paragraph, is based on the improper rejection for lack of utility under 35 U.S.C. § 101, it must be reversed.

The rejection set forth in the Office Action is based on the assertions discussed above, i.e., that the claimed invention lacks patentable utility. To the extent that the rejection under § 112, first paragraph, is based on the improper allegation of lack of patentable utility under § 101, it fails for the same reasons.

CONCLUSION

Appellants respectfully submit that rejections for lack of utility based, *inter alia*, on an allegation of “lack of specificity,” as set forth in the Office Action and as justified in the Revised Interim and final Utility Guidelines and Training Materials, are not supported in the law. Neither are they scientifically correct, nor supported by any evidence or sound scientific reasoning. These rejections are alleged to be founded on facts in court cases such as *Brenner* and *Kirk*, yet those facts are clearly distinguishable from the facts of the instant application, and indeed most if not all nucleotide and protein sequence applications. Nevertheless, the PTO is attempting to mold the facts and holdings of these prior cases, “like a nose of wax,”² to target rejections of claims to polypeptide and polynucleotide sequences, as well as to claims to methods of detecting said polynucleotide sequences, where biological activity information has not been proven by laboratory experimentation, and they have done so by ignoring perfectly acceptable utilities fully disclosed in the specifications as well as well-established utilities known to those of skill in the art. As is disclosed in the specification, and even more clearly, as one of ordinary skill in the art would understand, the claimed invention has well-established, specific, substantial and credible utilities. The rejections are, therefore, improper and should be reversed.

Moreover, to the extent the above rejections were based on the Revised Interim and final Examination Guidelines and Training Materials, those portions of the Guidelines and Training Materials that form the basis for the rejections should be determined to be inconsistent with the law.

Due to the urgency of this matter, including its economic and public health implications, an expedited review of this appeal is earnestly solicited.

If the USPTO determines that any additional fees are due, the Commissioner is hereby authorized to charge Deposit Account No. **09-0108**.

This brief is enclosed in triplicate

²“The concept of patentable subject matter under §101 is not ‘like a nose of wax which may be turned and twisted in any direction * * *.’ *White v. Dunbar*, 119 U.S. 47, 51.” (*Parker v. Flook*, 198 USPQ 193 (US SupCt 1978))

Respectfully submitted,
INCYTE CORPORATION

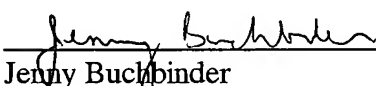
Date: January 27, 2004


James M. Verna, Ph.D.

Reg. No. 33,287

Direct Dial Telephone: (650) 845 -5415

Date: January 27, 2004


Jenny Buchbinder

Reg. No. 48,588

Direct Dial Telephone: (650) 843-7212

Customer No.: 27904

3160 Porter Drive

Palo Alto, California 94304

Phone: (650) 855-0555

Fax: (650) 849-8886

Enclosures:

1. Rockett et al., Differential gene expression in drug metabolism and toxicology: practicalities, problems and potential, 29 Xenobiotica No. 7, 655 (1999)
2. Lashkari et al., Whole genome analysis: Experimental access to all genome sequenced segments through larger-scale efficient oligonucleotide synthesis and PCR, 94 Proc. Nat. Acad. Sci. 8945 (Aug. 1997).
3. Emile F. Nuwaysir et al., Microarrays and Toxicology: The Advent of Toxicogenomics, 24 Molecular Carcinogenesis 153 (1999);
4. Sandra Steiner and N. Leigh Anderson, Expression profiling in toxicology -- potentials and limitations, 112-13 Toxicology Letters 467 (2000).
5. John C. Rockett and David J. Dix, Application of DNA Arrays to Toxicology, 107 Environ. Health Perspec. 681, No. 8 (1999).
6. Email from the primary investigator on the Nuwaysir paper, Dr. Cynthia Afshari, to an Incyte employee, dated July 3, 2000, as well as the original message to which she was responding.
7. Brenner et al., Proc. Natl. Acad. Sci. 95:6073-78 (1998).
8. Bastian Cell. Mol. Life Sci. 53:554-556 (1997).
9. Eberhard et al. Am. J. Pathol. 145:640-649 (1994).
10. Gerke and Moss Physiol. Rev. 82:331-371 (2002).
11. Nguyen et al., J. Biol. Chem. 275:29466-29476 (2000).
12. Futter et al. J. Cell Biol. 120:77-83 (1993).

13. Jost et al. J. Cell Science 110:221-228 (1997).
14. Lecona et al. Biochem. J. 373:437-449 (2003).
15. Lecat et al., J. Cell Science 113:2607-2618 (2000).
16. Blankenberg et al. Proc. Natl. Acad. Sci. U.S.A. 95:6349-6354 (1998).
17. Blankenberg et al. Eur. J. Nucl. Med. 27:359-367 (2000).
18. Declaration of Mr. Furness, under 37 C.F.R. § 1.132.
19. Declaration of Dr. Bedilion, under 37 C.F.R. § 1.132.
20. CLUSTALW alignment

APPENDIX - CLAIMS ON APPEAL

205. An isolated polypeptide comprising an amino acid sequence of SEQ ID NO:12.

206. A composition comprising a polypeptide of claim 205 and a pharmaceutically acceptable excipient.

208. A method for treating a disease or condition associated with decreased expression of functional INTRA, comprising administering to a patient in need of such treatment the composition of claim 206.

209. A method of screening for a compound that specifically binds to the polypeptide of claim 205, the method comprising:

- a) combining the polypeptide of claim 205 with at least one test compound under suitable conditions, and
- b) detecting binding of the polypeptide of claim 205 to the test compound, thereby identifying a compound that specifically binds to the polypeptide of claim 205.

211. An isolated polynucleotide encoding a polypeptide comprising an amino acid sequence of SEQ ID NO:12.

212. An isolated polynucleotide of claim 211 comprising a polynucleotide sequence of SEQ ID NO:64.

213. A recombinant polynucleotide comprising a promoter sequence operably linked to a polynucleotide of claim 211.

214. A cell transformed with a recombinant polynucleotide of claim 213.

215. A method of producing a polypeptide comprising an amino acid sequence of SEQ ID NO:12, the method comprising:

- a) culturing a cell under conditions suitable for expression of the polypeptide, wherein said cell is transformed with a recombinant polynucleotide, and said recombinant polynucleotide comprises a promoter sequence operably linked to a polynucleotide of claim 211, and
- b) recovering the polypeptide so expressed.

217. An isolated polynucleotide selected from the group consisting of:

- a) a polynucleotide comprising a polynucleotide sequence of SEQ ID NO:64,
- b) a polynucleotide completely complementary to a polynucleotide of a), and
- c) an RNA equivalent of a)-b).

224. A microarray wherein at least one element of the microarray is a polynucleotide of claim 217.

225. A method of generating an expression profile of a sample which contains polynucleotides, the method comprising:

- a) labeling the polynucleotides of the sample,
- b) contacting the microarray of claim 224 with the labeled polynucleotides of the sample under conditions suitable for the formation of a hybridization complex, and
- c) quantifying the expression of the polynucleotides in the sample.

226. An array comprising different nucleic acids affixed in distinct physical locations on a solid substrate, wherein at least one of said nucleic acids comprises a first polynucleotide sequence completely complementary to a target polynucleotide, and wherein said target polynucleotide is a polynucleotide of claim 217.

228. An array of claim 226, which is a microarray.

229. An array of claim 226, further comprising said target polynucleotide hybridized to a nucleic acid comprising said first polynucleotide sequence.

230. An array of claim 226, wherein a linker joins at least one of said nucleic acids to said solid substrate.

231. An array of claim 226, wherein each distinct physical location on the substrate contains multiple nucleic acids, and the multiple nucleic acids at any single distinct physical location have the same sequence, and each distinct physical location on the substrate contains nucleic acids having a sequence which differs from the sequence of nucleic acids at another distinct physical location on the substrate.

Differential gene expression in drug metabolism and toxicology: practicalities, problems and potential

JOHN C. ROCKETT†, DAVID J. ESDAILE‡
and G. GORDON GIBSON*

Molecular Toxicology Laboratory, School of Biological Sciences, University of Surrey,
Guildford, Surrey, GU2 5XH, UK

Received January 8, 1999

1. An important feature of the work of many molecular biologists is identifying which genes are switched on and off in a cell under different environmental conditions or subsequent to xenobiotic challenge. Such information has many uses, including the deciphering of molecular pathways and facilitating the development of new experimental and diagnostic procedures. However, the student of gene hunting should be forgiven for perhaps becoming confused by the mountain of information available as there appears to be almost as many methods of discovering differentially expressed genes as there are research groups using the technique.

2. The aim of this review was to clarify the main methods of differential gene expression analysis and the mechanistic principles underlying them. Also included is a discussion on some of the practical aspects of using this technique. Emphasis is placed on the so-called 'open' systems, which require no prior knowledge of the genes contained within the study model. Whilst these will eventually be replaced by 'closed' systems in the study of human, mouse and other commonly studied laboratory animals, they will remain a powerful tool for those examining less fashionable models.

3. The use of suppression-PCR subtractive hybridization is exemplified in the identification of up- and down-regulated genes in rat liver following exposure to phenobarbital, a well-known inducer of the drug metabolizing enzymes.

4. Differential gene display provides a coherent platform for building libraries and microchip arrays of 'gene fingerprints' characteristic of known enzyme inducers and xenobiotic toxicants, which may be interrogated subsequently for the identification and characterization of xenobiotics of unknown biological properties.

Introduction

It is now apparent that the development of almost all cancers and many non-neoplastic diseases are accompanied by altered gene expression in the affected cells compared to their normal state (Hunter 1991, Wynford-Thomas 1991, Vogelstein and Kinzler 1993, Semenza 1994, Cassidy 1995, Kleinjan and Van Hegningen 1998). Such changes also occur in response to external stimuli such as pathogenic micro-organisms (Rohn *et al.* 1996, Singh *et al.* 1997, Griffin and Krishna 1998, Lunney 1998) and xenobiotics (Sewall *et al.* 1995, Dogra *et al.* 1998, Ramana and Kohli 1998), as well as during the development of undifferentiated cells (Hecht 1998, Rudin and Thompson 1998, Schneider-Maunoury *et al.* 1998). The potential medical and therapeutic benefits of understanding the molecular changes which occur in any given cell in progressing from the normal to the 'altered' state are enormous. Such profiling essentially provides a 'fingerprint' of each step of a

* Author for correspondence; e-mail: g.gibson@surrey.ac.uk

† Current Address: US Environmental Protection Agency, National Health and Environmental Effects, Research Laboratory, Reproductive Toxicology Division, Research Triangle Park, NC 27711, USA.

‡ Rhone-Poulenc Agrochemicals, Toxicology Department, Sophia-Antipolis, Nice, France.

cell's development or response and should help in the elucidation of specific and sensitive biomarkers representing, for example, different types of cancer or previous exposure to certain classes of chemicals that are enzyme inducers.

In drug metabolism, many of the xenobiotic-metabolizing enzymes (including the well-characterized isoforms of cytochrome P450) are inducible by drugs and chemicals in man (Pelkonen *et al.* 1998), predominantly involving transcriptional activation of not only the cognate cytochrome P450 genes, but additional cellular proteins which may be crucial to the phenomenon of induction. Accordingly, the development of methodology to identify and assess the full complement of genes that are either up- or down-regulated by inducers are crucial in the development of knowledge to understand the precise molecular mechanisms of enzyme induction and how this relates to drug action. Similarly, in the field of chemical-induced toxicity, it is now becoming increasingly obvious that most adverse reactions to drugs and chemicals are the result of multiple gene regulation, some of which are causal and some of which are casually-related to the toxicological phenomenon *per se*. This observation has led to an upsurge in interest in gene-profiling technologies which differentiate between the control and toxin-treated gene pools in target tissues and is, therefore, of value in rationalizing the molecular mechanisms of xenobiotic-induced toxicity. Knowledge of toxin-dependent gene regulation in target tissues is not solely an academic pursuit as much interest has been generated in the pharmaceutical industry to harness this technology in the early identification of toxic drug candidates, thereby shortening the developmental process and contributing substantially to the safety assessment of new drugs. For example, if the gene profile in response to say a testicular toxin that has been well-characterized *in vivo* could be determined in the testis, then this profile would be representative of all new drug candidates which act via this specific molecular mechanism of toxicity, thereby providing a useful and coherent approach to the early detection of such toxicants. Whereas it would be informative to know the identity and functionality of all genes up/down regulated by such toxicants, this would appear a longer term goal, as the majority of human genes have not yet been sequenced, far less their functionality determined. However, the current use of gene profiling yields a *pattern* of gene changes for a xenobiotic of unknown toxicity which may be matched to that of well-characterized toxins, thus alerting the toxicologist to possible *in vivo* similarities between the unknown and the standard, thereby providing a platform for more extensive toxicological examination. Such approaches are beginning to gain momentum, in that several biotechnology companies are commercially producing 'gene chips' or 'gene arrays' that may be interrogated for toxicity assessment of xenobiotics. These chips consist of hundreds/thousands of genes, some of which are degenerate in the sense that not all of the genes are mechanistically-related to any one toxicological phenomenon. Whereas these chips are useful in broad-spectrum screening, they are maturing at a substantial rate, in that gene arrays are now becoming more specific, e.g. chips for the identification of changes in growth factor families that contribute to the aetiology and development of chemically-induced neoplasias.

Although documenting and explaining these genetic changes presents a formidable obstacle to understanding the different mechanisms of development and disease progression, the technology is now available to begin attempting this difficult challenge. Indeed, several 'differential expression analysis' methods have been developed which facilitate the identification of gene products that demonstrate

altered expression in cells of one population compared to another. These methods have been used to identify differential gene expression in many situations, including invading pathogenic microbes (Zhao *et al.* 1998), in cells responding to extracellular and intracellular microbial invasion (Duguid and Dinauer 1990, Ragno *et al.* 1997, Maldarelli *et al.* 1998), in chemically treated cells (Syed *et al.* 1997, Rockett *et al.* 1999), neoplastic cells (Liang *et al.* 1992, Chang and Terzaghi-Howe 1998), activated cells (Gurskaya *et al.* 1996, Wan *et al.* 1996), differentiated cells (Hara *et al.* 1991, Guimaraes *et al.* 1995a, b), and different cell types (Davis *et al.* 1984, Hedrick *et al.* 1984, Xhu *et al.* 1998). Although differential expression analysis technologies are applicable to a broad range of models, perhaps their most important advantage is that, in most cases, absolutely no prior knowledge of the specific genes which are up- or down-regulated is required.

The field of differential expression analysis is a large and complex one, with many techniques available to the potential user. These can be categorized into several methodological approaches, including:

- (1) Differential screening,
- (2) Subtractive hybridization (SH) (includes methods such as chemical cross-linking subtraction—CCLS, suppression-PCR subtractive hybridization—SSH, and representational difference analysis—RDA),
- (3) Differential display (DD),
- (4) Restriction endonuclease facilitated analysis (including serial analysis of gene expression—SAGE—and gene expression fingerprinting—GEF),
- (5) Gene expression arrays, and
- (6) Expressed sequence tag (EST) analysis.

The above approaches have been used successfully to isolate differentially expressed genes in different model systems. However, each method has its own subtle (and sometimes not so subtle) characteristics which incur various advantages and disadvantages. Accordingly, it is the purpose of this review to clarify the mechanistic principles underlying the main differential expression methods and to highlight some of the broader considerations and implications of this very powerful and increasingly popular technique. Specifically, we will concentrate on the so-called 'open' systems, namely those which do not require any knowledge of gene sequences and, therefore, are useful for isolating unknown genes. Two 'closed' systems (those utilising previously identified gene sequences), EST analysis and the use of DNA arrays, will also be considered briefly for completeness. Whilst emphasis will often be placed on suppression PCR subtractive hybridization (SSH, the approach employed in this laboratory), it is the aim of the authors to highlight, wherever possible, those areas of common interest to those who use, or intend to use, differential gene expression analysis.

Differential cDNA library screening (DS)

Despite the development of multiple technological advances which have recently brought the field of gene expression profiling to the forefront of molecular analysis, recognition of the importance of differential gene expression and characterization of differentially expressed genes has existed for many years. One of the original approaches used to identify such genes was described 20 years ago by St John and Davis (1979). These authors developed a method, termed 'differential plaque filter

hybridization', which was used to isolate galactose-inducible DNA sequences from yeast. The theory is simple: a genomic DNA library is prepared from normal, unstimulated cells of the test organism/tissue and multiple filter replicas are prepared. These replica blots are probed with radioactively (or otherwise) labelled complex cDNA probes prepared from the control and test cell mRNA populations. Those mRNAs which are differentially expressed in the treated cell population will show a positive signal only on the filter probed with cDNA from the treated cells. Furthermore, labelled cDNA from different test conditions can be used to probe multiple blots, thereby enabling the identification of mRNAs which are only up-regulated under certain conditions. For example, St John and Davis (1979) screened replica filters with acetate-, glucose- and galactose-derived probes in order to obtain genes induced specifically by galactose metabolism. Although groundbreaking in its time this method is now considered insensitive and time-consuming, as up to 2 months are required to complete the identification of genes which are differentially expressed in the test population. In addition, there is no convenient way to check that the procedure has worked until the whole process has been completed.

Subtractive Hybridization (SH)

The developing concept of differential gene expression and the success of early approaches such as that described by St John and Davis (1979) soon gave rise to a search for more convenient methods of analysis. One of the first to be developed was SH, numerous variations of which have since been reported (see below). In general, this approach involves hybridization of mRNA/cDNA from one population (tester) to excess mRNA/cDNA from another (driver), followed by separation of the unhybridized tester fraction (differentially expressed) from the hybridized common sequences. This step has been achieved physically, chemically and through the use of selective polymerase chain reaction (PCR) techniques.

Physical separation

Original subtractive hybridization technology involved the physical separation of hybridized common species from unique single stranded species. Several methods of achieving this have been described, including hydroxyapatite chromatography (Sargent and Dawid 1983), avidin-biotin technology (Duguid and Dinauer 1990) and oligodT-latex separation (Hara *et al.* 1991). In the first approach, common mRNA species are removed by cDNA (from test cells)-mRNA (from control cells) subtractive hybridization followed by hydroxyapatite chromatography, as hydroxyapatite specifically adsorbs the cDNA-mRNA hybrids. The unabsorbed cDNA is then used either for the construction of a cDNA library of differentially expressed genes (Sargent and Dawid 1983, Schneider *et al.* 1988) or directly as a probe to screen a preselected library (Zimmerman *et al.* 1980, Davis *et al.* 1984, Hedrick *et al.* 1984). A schematic diagram of the procedure is shown in figure 1.

Less rigorous physical separation procedures coupled with sensitivity enhancing PCR steps were later developed as a means to overcome some of the problems encountered with the hydroxyapatite procedure. For example, Duguid and Dinauer (1990) described a method of subtraction utilizing biotin-affinity systems as a means to remove hybridized common sequences. In this process, both the control and tester mRNA populations are first converted to cDNA and an adaptor ('oligovector',

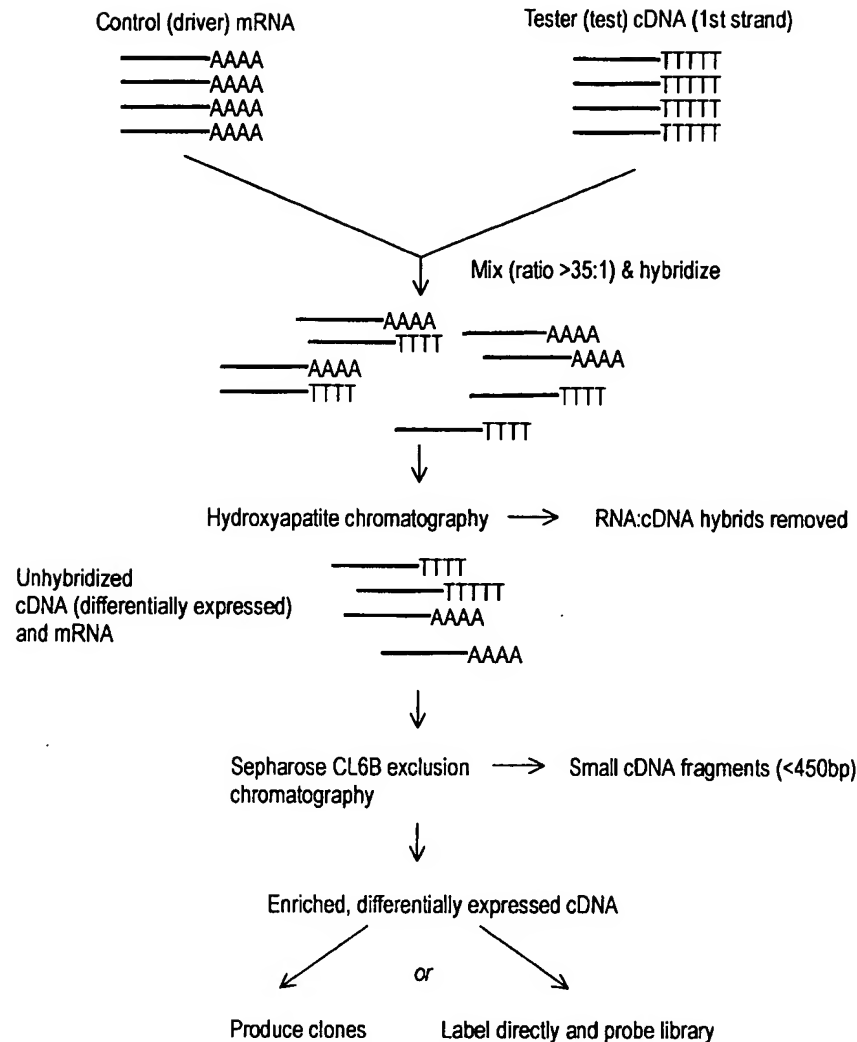


Figure 1. The hydroxyapatite method of subtractive hybridization. cDNA derived from the treated/alterd (tester) population is mixed with a large excess of mRNA from the control (driver) population. Following hybridization, mRNA-cDNA hybrids are removed by hydroxyapatite chromatography. The only cDNAs which remain are those which are differentially expressed in the treated/alterd population. In order to facilitate the recovery of full length clones, small cDNA fragments are removed by exclusion chromatography. The remaining cDNAs are then cloned into a vector for sequencing, or labelled and used directly to probe a library, as described by Sargent and Dawid (1983).

containing a restriction site) ligated to both sides. Both populations are then amplified by PCR, but the driver cDNA population is subsequently digested with the adaptor-containing restriction endonuclease. This serves to cleave the oligo-vector and reduce the amplification potential of the control population. The digested control population is then biotinylated and an excess mixed with tester cDNA. Following denaturation and hybridization, the mix is applied to a biocytin column (streptavidin may also be used) to remove the control population, including heteroduplexes formed by annealing of common sequences from the tester population. The procedure is repeated several times following the addition of fresh

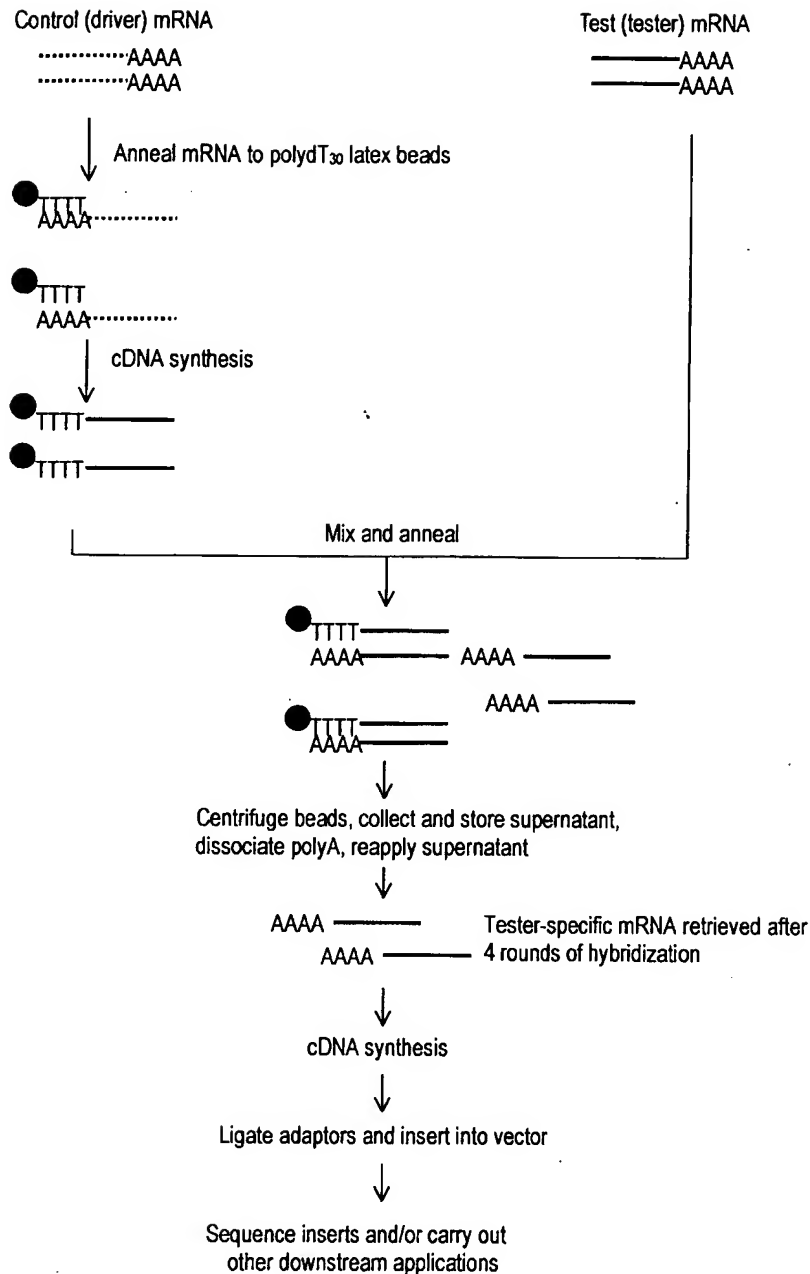


Figure 2. The use of oligodT₃₀ latex to perform subtractive hybridization. mRNA extracted from the control (driver) population is converted to anchored cDNA using polydT oligonucleotides attached to latex beads. mRNA from the treated/alterd (tester) population is repeatedly hybridized against an excess of the anchored driver cDNA. The final population of mRNA is tester specific and can be converted into cDNA for cloning and other downstream applications, as described by Hara *et al.* (1991).

control cDNA. In order to further enrich those species differentially expressed in the tester cDNA, the subtracted tester population is amplified by PCR following every second subtraction cycle. After six cycles of subtraction (three reamplification steps) the reaction mix is ligated into a vector for further analysis.

In a slightly different approach, Hara *et al.* (1991) utilized a method whereby oligo(dT₃₀) primers attached to a latex substrate are used to first capture mRNA extracted from the control population. Following 1st strand cDNA synthesis, the RNA strand of the heteroduplexes is removed by heat denaturation and centrifugation (the cDNA-oligotex-dT₃₀ forms a pellet and the supernatant is removed). A quantity of tester mRNA is then repeatedly hybridized to the immobilized control (driver) cDNA (which is present in 20-fold excess). After several rounds of hybridization the only mRNA molecules left in the tester mRNA population are those which are not found in the driver cDNA-oligotex-dT₃₀ population. These tester-specific mRNA species are then converted to cDNA and, following the addition of adaptor sequences, amplified by PCR. The PCR products are then ligated into a vector for further analysis using restriction sites incorporated into the PCR primers. A schematic illustration of this subtraction process is shown in figure 2.

However, all these methods utilising physical separation have been described as inefficient due to the requirement for large starting amounts of mRNA, significant loss of material during the separation process and a need for several rounds of hybridization. Hence, new methods of differential expression analysis have recently been designed to eliminate these problems.

Chemical Cross-Linking Subtraction (CCLS)

In this technique, originally described by Hampson *et al.* (1992), driver mRNA is mixed with tester cDNA (1st strand only) in a ratio of > 20:1. The common sequences form cDNA:mRNA hybrids, leaving the tester specific species as single stranded cDNA. Instead of physically separating these hybrids, they are inactivated chemically using 2,5 diaziridinyl-1,4-benzoquinone (DZQ). Labelled probes are then synthesized from the remaining single stranded cDNA species (unreacted mRNA species remaining from the driver are not converted into probe material due to specificity of Sequenase T7 DNA polymerase used to make the probe) and used to screen a cDNA library made from the tester cell population. A schematic diagram of the system is shown in figure 3.

It has been shown that the differentially expressed sequences can be enriched at least 300-fold with one round of subtraction (Hampson *et al.* 1992), and that the technique should allow isolation of cDNAs derived from transcripts that are present at less than 50 copies per cell. This equates to genes at the low end of intermediate abundance (see table 1). The main advantages of the CCLS approach are that it is rapid, technically simple and also produces fewer false positives than other differential expression analysis methods. However, like the physical separation protocols, a major drawback with CCLS is the large amount of starting material required (at least 10 µg RNA). Consequently, the technique has recently been refined so that a renewable source of RNA can be generated. The degenerate random oligonucleotide primed (DROP) adaptation (Hampson *et al.* 1996, Hampson and Hampson 1997) uses random hexanucleotide sequences to prime solid phase-synthesized cDNA. Since each primer includes a T7 polymerase promoter sequence

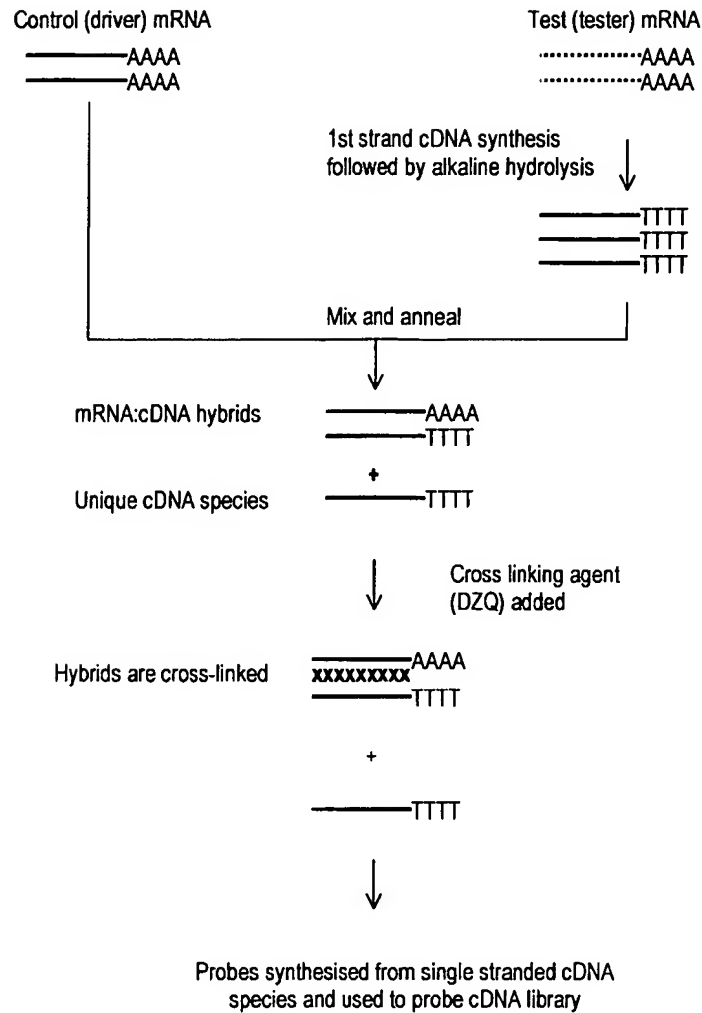


Figure 3. Chemical cross-linking subtraction. Excess driver mRNA is mixed with 1st strand tester cDNA. The common sequences form mRNA:cDNA hybrids which are cross linked with 2,5 diaziridinyl-1,4-benzoquinone (DZQ) and the remaining cDNA sequences are differentially expressed in the tester population. Probes are made from these sequences using Sequenase 2.0 DNA polymerase, which lacks reverse transcriptase activity and, therefore, does not react with the remaining mRNA molecules from the driver. The labelled probes are then used to screen a cDNA library for clones of differentially expressed sequences. Adapted from Walter *et al.* (1996), with permission.

Table 1. The abundance of mRNA species and classes in a typical mammalian cell.

mRNA class	Copies of each species/cell	No. of mRNA species in class	Mean % of each species in class	Mean mass (ng) of each species/ μ g total RNA
Abundant	12000	4	3.3	1.65
Intermediate	300	500	0.08	0.04
Rare	15	11000	0.004	0.002

Modified from Bertoli *et al.* (1995).

at the 5' end, the final pool of random cDNA fragments is a PCR-renewable cDNA population which is representative of the expressed gene pool and can be used to synthesize sense RNA for use as driver material. Furthermore, if the final pool of random cDNA fragments is reamplified using biotinylated T7 primer and random hexamer, the product can be captured with streptavidin beads and the antisense strand eluted for use as tester. Since both target and driver can be generated from the same DROP product, subtraction can be performed in both directions (i.e. for up- and down-regulated species) between two different DROP products.

Representational Difference Analysis (RDA)

RDA of cDNA (Hubank and Schatz 1994) is an extension of the technique originally applied to genomic DNA as a means of identifying differences between two complex genomes (Lisitsyn *et al.* 1993). It is a process of subtraction and amplification involving subtractive hybridization of the tester in the presence of excess driver. Sequences in the tester that have homologues in the driver are rendered unamplifiable, whereas those genes expressed only in the tester retain the ability to be amplified by PCR. The procedure is shown schematically in figure 4.

In essence, the driver and tester mRNA populations are first converted to cDNA and amplified by PCR following the ligation of an adaptor. The adaptors are then removed from both populations and a new (different) adaptor ligated to the amplified tester population only. Driver and tester populations are next melted and hybridized together in a ratio of 100:1. Following hybridization, only tester:tester homohybrids have 5' adaptors at each end of the DNA duplex and can, thus, be filled in at both 3' ends. Hence, only these molecules are amplified exponentially during the subsequent PCR step. Although tester:driver heterohybrids are present, they only amplify in a linear fashion, since the strand derived from the driver has no adaptor to which the primer can bind. Driver:driver heterohybrids have no adaptors and, therefore, are not amplified. Single stranded molecules are digested with mung bean nuclease before a further PCR-enrichment of the tester:tester homohybrids. The adaptors on the amplified tester population are then replaced and the whole process repeated a further two or three times using an increasing excess of driver (Hubank and Schatz used a tester:driver ratio of 1:400, 1:80000 and 1:800000 for the second, third and fourth hybridizations, respectively). Different adaptors are ligated to the tester between successive rounds of hybridization and amplification to prevent the accumulation of PCR products that might interfere with subsequent amplifications. The final display is a series of differentially expressed gene products easily observable on an ethidium bromide gel.

The main advantages of RDA are that it offers a reproducible and sensitive approach to the analysis of differentially expressed genes. Hubank and Schatz (1994) reported that they were able to isolate genes that were differentially expressed in substantially less than 1% of the cells from which the tester is derived. Perhaps the main drawback is that multiple rounds of ligation, hybridization, amplification and digestion are required. The procedure is, therefore, lengthier than many other differential display approaches and provides more opportunity for operator-induced error to occur. Although the generation of false positives has been noted, this has been solved to some degree by O'Neill and Sinclair (1997) through the use of HPLC-purified adaptors. These are free of the truncated adaptors which appear to be a major source of the false positive bands. A very similar technique to RDA, termed linker capture subtraction (LCS) was described by Yang and Sytowski (1996).

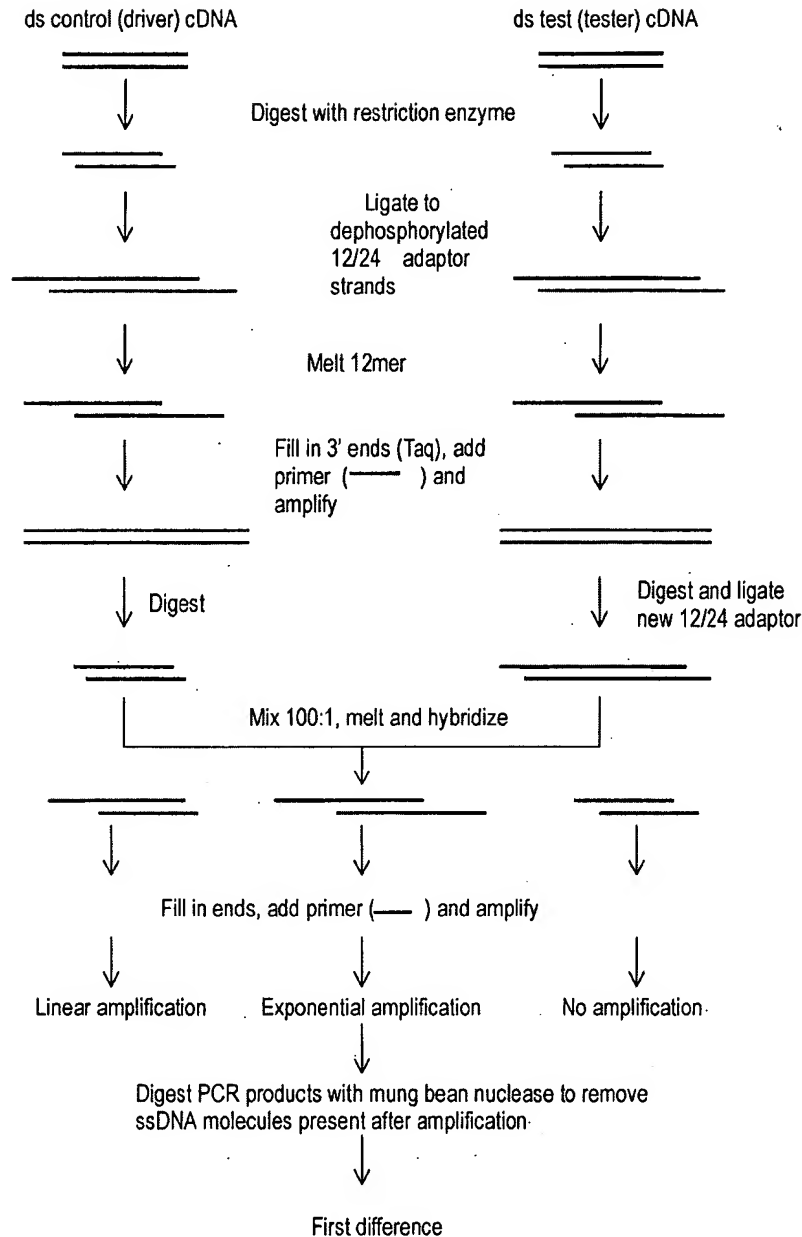


Figure 4. The representational difference analysis (RDA) technique. Driver and tester cDNA are digested with a 4-cutter restriction enzyme such as *DpnII*. The 1st set of 12/24 adaptor strands (oligonucleotides) are ligated to each other and the digested cDNA products. The 12mer is subsequently melted away and the 3' ends filled in using Taq DNA polymerase. Each cDNA population is then amplified using PCR, following which the 1st set of adaptors is removed with *DpnII*. A second set of 12/24 adaptor strands is then added to the amplified tester cDNA population, after which the tester is hybridized against a large excess of driver. The 12mer adaptors are melted and the 3' ends filled in as before. PCR is carried out with primers identical to the new 24mer adaptor. Thus, the only hybridization products which are exponentially amplified are those which are tester:tester combinations. Following PCR, ssDNA products are removed with mung bean nuclease, leaving the 'first difference product'. This is digested and a third set of 12/24 adaptors added before repeating the subtraction process from the hybridization stage. The process is repeated to the 3rd or 4th difference product, as described by Lisitsyn *et al.* (1993) and Hubank and Schatz (1994).

Suppression PCR Subtractive Hybridization (SSH)

The most recent adaptation of the SH approach to differential expression analysis was first described by Diatchenko *et al.* (1996) and Gurskaya *et al.* (1996). They reported that a 1000–5000 fold enrichment of rare cDNAs (equivalent to isolating mRNAs present at only a few copies per cell) can be obtained without the need for multiple hybridizations/subtractions. Instead of physical or chemical removal of the common sequences, a PCR-based suppression system is used (see figure 5).

In SSH, excess driver cDNA is added to two portions of the tester cDNA which have been ligated with different adaptors. A first round of hybridization serves to enrich differentially expressed genes and equalize rare and abundant messages. Equalization occurs since reannealing is more rapid for abundant molecules than for rarer molecules due to the second order kinetics of hybridization (James and Higgins 1985). The two primary hybridization mixes are then mixed together in the presence of excess driver and allowed to hybridize further. This step permits the annealing of single stranded complementary sequences which did not hybridize in the primary hybridization, and in doing so generates templates for PCR amplification. Although there are several possible combinations of the single stranded molecules present in the secondary hybridization mix, only one particular combination (differentially expressed in the tester cDNA composed of complimentary strands having different adaptors) can amplify exponentially.

Having obtained the final differential display, two options are available if cloning of cDNAs is desired. One is to transform the whole of the final PCR reaction into competent cells. Transformed colonies can then be isolated and their inserts characterized by sequencing, restriction analysis or PCR. Alternatively, the final PCR products can be resolved on a gel and the individual bands excised, reamplified and cloned. The first approach is technically simpler and less time consuming. However, ligation/transformation reactions are known to be biased towards the cloning of smaller molecules, and so the final population of clones will probably not contain a representative selection of the larger products. In addition, although equalization theoretically occurs, observations in this laboratory suggest that this is by no means perfectly accomplished. Consequently, some gene species are present in a higher number than others and this will be represented in the final population of clones. Thus, in order to obtain a substantial proportion of those gene species that actually demonstrate differential expression in the tester population, the number of clones that will have to be screened after this step may be substantial. The second approach is initially more time consuming and technically demanding. However, it would appear to offer better prospects for cloning larger and low abundance gel products. In addition, one can incorporate a screening step that differentiates different products of different sequences but of the same size (HA-staining, see later). In this way, a good idea of the final number of clones to be isolated and identified can be achieved.

An alternative (or even complementary) approach is to use the final differential display reaction to screen a cDNA library to isolate full length clones for further characterization, or a DNA array (see later) to quickly identify known genes. SSH has been used in this laboratory to begin characterization of the short-term gene expression profiles of enzyme-inducers such as phenobarbital (Rockett *et al.* 1997) and Wy-14,643 (Rockett *et al.* unpublished observations). The isolation of differentially expressed genes in this manner enables the construction of a fingerprint

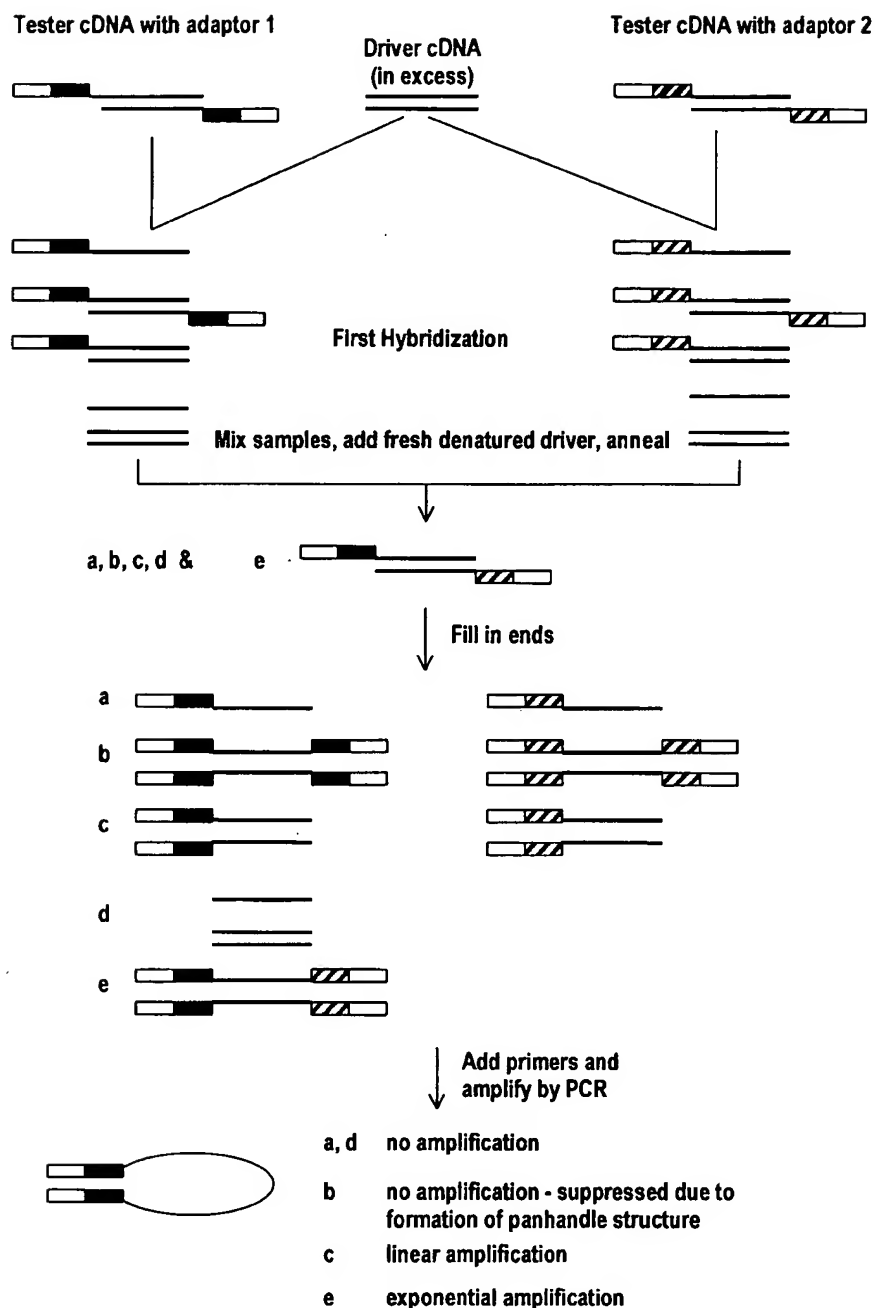


Figure 5. PCR-select cDNA subtraction. In the primary hybridization, an excess of driver cDNA is added to each tester cDNA population. The samples are heat denatured and allowed to hybridize for between 3 and 8 h. This serves two purposes: (1) to equalize rare and abundant molecules; and (2) to enrich for differentially expressed sequences—cDNAs that are not differentially expressed form type c molecules with the driver. In the secondary hybridization, the two primary hybridizations are mixed together without denaturing. Fresh denatured driver can also be added at this point to allow further enrichment of differentially expressed sequences. Type e molecules are formed in this secondary hybridization which are subsequently amplified using two rounds of PCR. The final products can be visualized on an agarose gel, labelled directly or cloned into a vector for downstream manipulation. As described by Diatchenko *et al.* (1996) and Gurskaya *et al.* (1996), with permission.

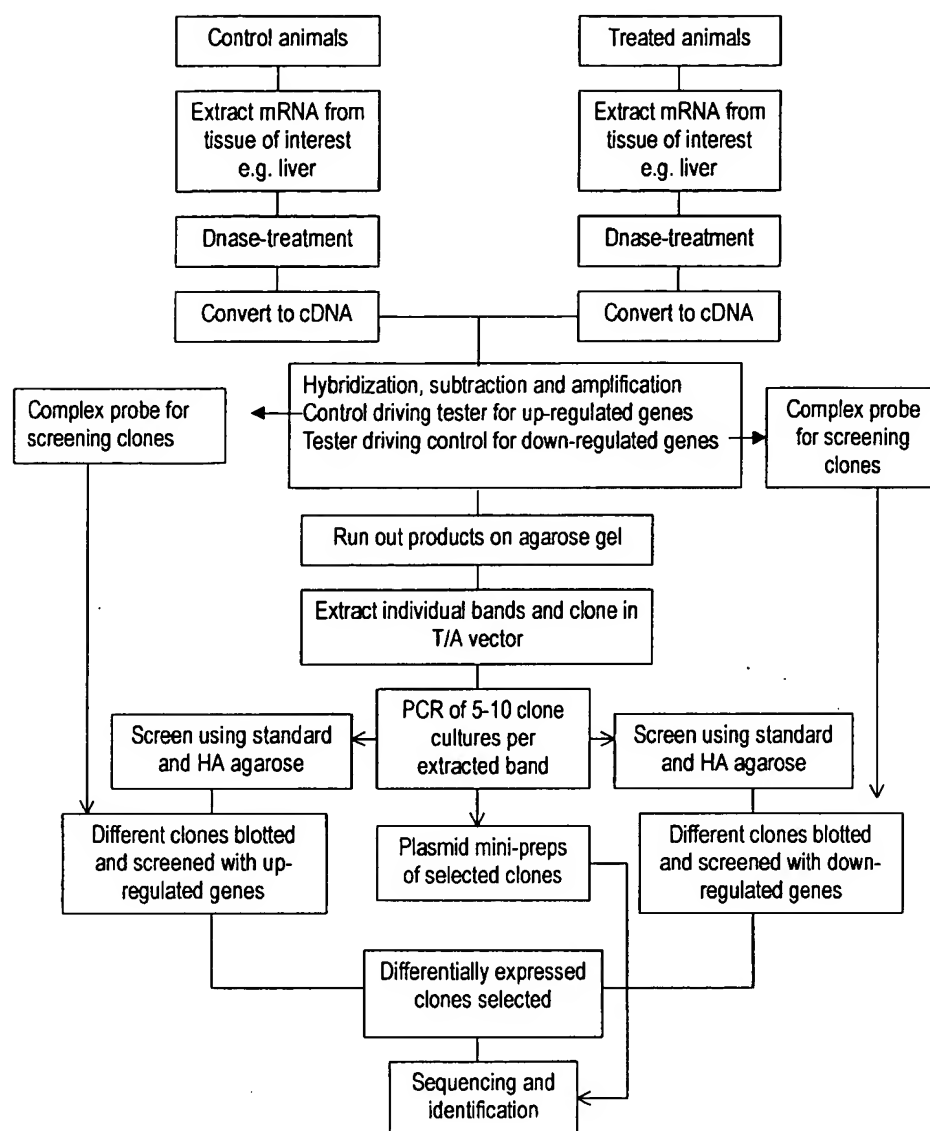


Figure 6. Flow diagram showing method used in this laboratory to isolate and identify clones of genes which are differentially expressed in rat liver following short term exposure to the enzyme inducers, phenobarbital and Wy-14,643.

of expressed genes which are unique to each compound and time/dose point. Such information could be useful in short-term characterization of the toxic potential of new compounds by comparing the gene-expression profiles they elicit with those produced by known inducers. Figure 6 shows a flow diagram of the method used to isolate, verify and clone differentially expressed genes, and figure 7 shows expression profiles obtained from a typical SSH experiment. Subsequent sub-cloning of the individual bands, sequencing and gene data base interrogation reveals many genes which are either up- or down-regulated by phenobarbital in the rat (tables 2 and 3).

One of the advantages in using the SSH approach is that no prior knowledge is required of which specific genes are up/down-regulated subsequent to xenobiotic

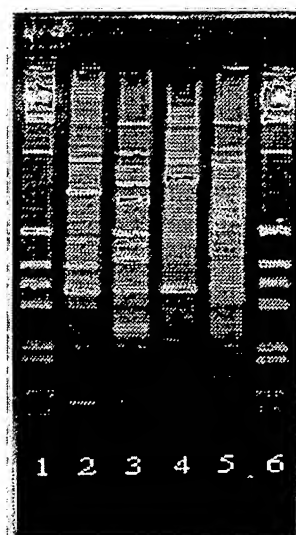


Figure 7. SSH display patterns obtained from rat liver following 3-day treatment with Wy-14,643 or phenobarbital. mRNA extracted from control and treated livers was used to generate the differential displays using the PCR-Select cDNA subtraction kit (Clontech). Lane: 1—1kb ladder; 2—genes upregulated following Wy,14-643 treatment; 3—genes downregulated following Wy,14-643 treatment; 4—genes upregulated following phenobarbital treatment; 5—genes downregulated following phenobarbital treatment; 6—1kb ladder. Reproduced from Rockett *et al.* (1997), with permission.

exposure, and an almost complete complement of genes are obtained. For example, the peroxisome proliferator and non-genotoxic hepatocarcinogen Wy,14,643, up-regulates at least 28 genes and down-regulates at least 15 in the rat (a sensitive species) and produces 48 up- and 37 down-regulated genes in the guinea pig, a resistant species (Rockett, Swales, Esda and Gibson, unpublished observations). One of these genes, CD81, was up-regulated in the rat and down-regulated in the guinea pig following Wy-14,643 treatment. CD81 (alternatively named TAPA-1) is a widely expressed cell surface protein which is involved in a large number of cellular processes including adhesion, activation, proliferation and differentiation (Levy *et al.* 1998). Since all of these functions are altered to some extent in the phenomena of hepatomegaly and non-genotoxic hepatocarcinogenesis, it is intriguing, and probably mechanistically-relevant, that CD81 expression is differentially regulated in a resistant and susceptible species. However, the down-side of this approach is that the majority of genes can be sequenced and matched to database sequences, but the latter are predominantly expressed sequence tags or genes of completely unknown function, thus partially obscuring a realistic overall assessment of the critical genes of genuine biological interest. Notwithstanding the lack of complete functional identification of altered gene expression, such gene profiling studies essentially provides a 'molecular fingerprint' in response to xenobiotic challenge, thereby serving as a mechanistically-relevant platform for further detailed investigations.

Differential Display (DD)

Originally described as 'RNA fingerprinting by arbitrarily primed PCR' (Liang and Pardee 1992) this method is now more commonly referred to as 'differential

Table 2. Genes up-regulated in rat liver following 3-day exposure to phenobarbital.

Band number (approximate size in bp)	Highest sequence similarity	FASTA-EMBL gene identification
5 (1300)	93.5%	CYP2B1
7 (1000)	95.1%	Preproalbumin Serum albumin mRNA
8 (950)	98.3%	NCI-CGAP-Pr1 <i>H. sapiens</i> (EST)
10 (850)	95.7%	CYP2B1
11 (800)	Clone 1 94.9%	CYP2B1
	Clone 2 75.3%	CYP2B2
12 (750)	93.8%	TRPM-2 mRNA Sulfated glycoprotein
15 (600)	92.9%	Preproalbumin Serum albumin mRNA
16 (55)	Clone 1 95.2%	CYP2B1
	Clone 2 93.6%	Haptoglobulin mRNA partial alpha
21 (350)	99.3%	18S, 5.8S & 28S rRNA

Bands 1–4, 6, 9, 13, 14, and 17–20 are shown to be false positives by dot blot analysis and, therefore, are not sequenced. Derived from Rockett *et al.* (1997). It should be noted that the above genes do not represent the complete spectrum of genes which are up-regulated in rat liver by phenobarbital, but simply represents the genes sequenced and identified to date.

Table 3. Genes down-regulated in rat liver following 3-day exposure to phenobarbital.

Band number (approximate size in bp)	Highest sequence similarity	FASTA-EMBL gene identification
1 (1500)	95.3%	3-oxoacyl-CoA thiolase
2 (1200)	92.3%	Hemopoxin mRNA
3 (1000)	91.7%	Alpha-2u-globulin mRNA
7 (700)	Clone 1 77.2%	<i>M. musculus</i> C1 inhibitor
	Clone 2 94.5%	Electron transfer flavoprotein
	Clone 3 91.0%	<i>M. musculus</i> Topoisomerase 1 (Topo 1)
8 (650)	Clone 1 86.9%	Soares 2NbMT <i>M. musculus</i> (EST)
	Clone 2 96.2%	Alpha-2u-globulin (s-type) mRNA
9 (600)	Clone 1 86.9%	Soares mouse NML <i>M. musculus</i> (EST)
	Clone 2 82.0%	Soares p3NMF 19.5 <i>M. musculus</i> (EST)
10 (550)	73.8%	Soares mouse NML <i>M. musculus</i> (EST)
11 (525)	95.7%	NCI-CGAP-Pr1 <i>H. sapiens</i> (EST)
12 (375)	100.0%	Ribosomal protein
13 (23)	Clone 1 97.2%	Soares mouse embryo NbME135 (EST)
	Clone 2 100.0%	Fibrinogen B-beta-chain
	Clone 3 100.0%	Apolipoprotein E gene
14 (170)	96.0%	Soares p3NMF19.5 <i>M. musculus</i> (EST)
15 (140)	97.3%	Stratagene mouse testis (EST)
Others: (300)	96.7%	<i>R. norvegicus</i> RASP 1 mRNA
(275)	93.1%	Soares mouse mammary gland (EST)

EST = Expressed sequence tag. Bands 4–6 were shown to be false positives by dot blot analysis and, therefore, were not sequenced. Derived from Rockett *et al.* (1997). It should be noted that the above genes do not represent the complete spectrum of genes which are down-regulated in rat liver by phenobarbital, but simply represents the genes sequenced and identified to date.

display' (DD). In this method, all the mRNA species in the control and treated cell populations are amplified in separate reactions using reverse transcriptase-PCR (RT-PCR). The products are then run side-by-side on sequencing gels. Those bands which are present in one display only, or which are much more intense in one

display compared to the other, are differentially expressed and may be recovered for further characterization. One advantage of this system is the speed with which it can be carried out—2 days to obtain a display and as little as a week to make and identify clones.

Two commonly used variations are based on different methods of priming the reverse transcription step (figure 8). One is to use an oligo dT with a 2-base 'anchor' at the 3'-end, e.g. 5' (dT₁₁)CA 3' (Liang and Pardee 1992). Alternatively, an arbitrary primer may be used for 1st strand cDNA synthesis (Welsh *et al.* 1992). This variant of RNA fingerprinting has also been called 'RAP' (RNA Arbitrarily Primed)-PCR. One advantage of this second approach is that PCR products may be derived from anywhere in the RNA, including open reading frames. In addition, it can be used for mRNAs that are not polyadenylated, such as many bacterial mRNAs (Wong and McClelland 1994). In both cases, following reverse transcription and denaturation, second strand cDNA synthesis is carried out with an arbitrary primer (*arbitrary* primers have a single base at each position, as compared to *random* primers, which contain a mixture of all four bases at each position). The resulting PCR, thus, produces a series of products which, depending on the system (primer length and composition, polymerase and gel system), usually includes 50–100 products per primer set (Band and Sager 1989). When a combination of different dT-anchors and arbitrary primers are used, almost all mRNA species from a cell can be amplified. When the cDNA products from two different populations are analysed side by side on a polyacrylamide gel, differences in expression can be identified and the appropriate bands recovered for cloning and further analysis.

Although DD is perhaps the most popular approach used today for identifying differentially expressed genes, it does suffer from several perceived disadvantages:

- (1) It may have a strong bias towards high copy number mRNAs (Bertioli *et al.* 1995), although this has been disputed (Wan *et al.* 1996) and the isolation of very low abundance genes may be achieved in certain circumstances (Guimeraes *et al.* 1995a).
- (2) The cDNAs obtained often only represent the extreme 3' end of the mRNA (often the 3'-untranslated region), although this may not always be the case (Guimeraes *et al.* 1995a). Since the 3' end is often not included in Genbank and shows variation between organisms, cDNAs identified by DD cannot always be matched with their genes, even if they have been identified.
- (3) The pattern of differential expression seen on the display often cannot be reproduced on Northern blots, with false positives arising in up to 70% of cases (Sun *et al.* 1994). Some adaptations have been shown to reduce false positives, including the use of two reverse transcriptases (Sung and Denman 1997), comparison of uninduced and induced cells over a time course (Burn *et al.* 1994) and comparison of DDPCR-products from two uninduced and two induced lines (Sompayrac *et al.* 1995). The latter authors also reported that the use of cytoplasmic RNA rather than total RNA reduces false positives arising from nuclear RNA that is not transported to the cytoplasm.

Further details of the background, strengths and weaknesses of the DD technique can be obtained from a review by McClelland *et al.* (1996) and from articles by Liang *et al.* (1995) and Wan *et al.* (1996).

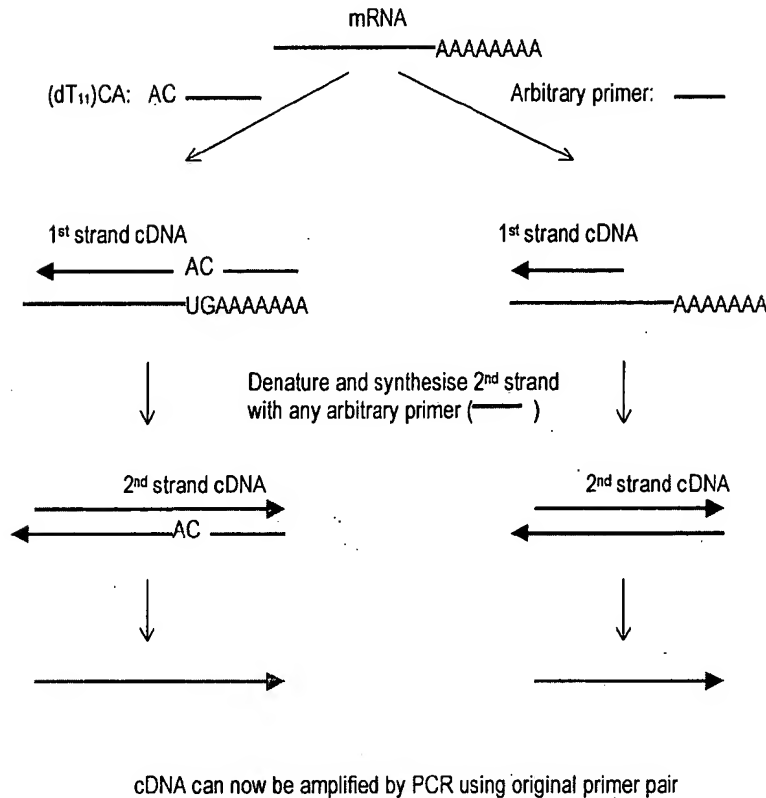


Figure 8. Two approaches to differential display (DD) analysis. 1st strand synthesis can be carried out either with a polydT₁₁NN primer (where N = G, C or A) or with an arbitrary primer. The use of different combinations of G, C and A to anchor the first strand polydT primer enables the priming of the majority of polyadenylated mRNAs. Arbitrary primers may hybridize at none, one or more places along the length of the mRNA, allowing 1st strand cDNA synthesis to occur at none, one or more points in the same gene. In both cases, 2nd strand synthesis is carried out with an arbitrary primer. Since these arbitrary primers for the 2nd strand may also hybridize to the 1st strand cDNA in a number of different places, several different 2nd strand products may be obtained from one binding point of the 1st strand primer. Following 2nd strand synthesis, the original set of primers is used to amplify the second strand products, with the result that numerous gene sequences are amplified.

Restriction endonuclease-facilitated analysis of gene expression

Serial Analysis of Gene Expression (SAGE)

A more recent development in the field of differential display is SAGE analysis (Velculescu *et al.* 1995). This method uses a different approach to those discussed so far and is based on two principles. Firstly, in more than 95% of cases, short nucleotide sequences ('tags') of only nine or 10 base pairs provide sufficient information to identify their gene of origin. Secondly, concatenation (linking together in a series) of these tags allows sequencing of multiple cDNAs within a single clone. Figure 9 shows a schematic representation of the SAGE process. In this procedure, double stranded cDNA from the test cells is synthesized with a biotinylated polydT primer. Following digestion with a commonly cutting (4bp recognition sequence) restriction enzyme ('anchoring enzyme'), the 3' ends of the cDNA population are captured with streptavidin beads. The captured population is

split into two and different adaptors ligated to the 5' ends of each group. Incorporated into the adaptors is a recognition sequence for a type IIS restriction enzyme—one which cuts DNA at a defined distance (< 20 bp) from its recognition sequence. Hence, following digestion of each captured cDNA population with the IIS enzyme, the adaptors plus a short piece of the captured cDNA are released. The two populations are then ligated and the products amplified. The amplified products are cleaved with the original anchoring enzyme, religated (concatomers are formed in the process) and cloned. The advantage of this system is that hundreds of gene tags can be identified by sequencing only a few clones. Furthermore, the number of times a given transcript is identified is a quantitative measurement of that gene's abundance in the original population, a feature which facilitates identification of differentially expressed genes in different cell populations.

Some disadvantages of SAGE analysis include the technical difficulty of the method, a large amount of accurate sequencing is required, biased towards abundant mRNAs, has not been validated in the pharmaco/toxicogenomic setting and has only been used to examine well known tissue differences to date.

Gene Expression Fingerprinting (GEF)

A different capture/restriction digest approach for isolating differentially expressed genes has been described by Ivanova and Belyavsky (1995). In this method, RNA is converted to cDNA using biotinylated oligo(dT) primers. The cDNA population is then digested with a specific endonuclease and captured with magnetic streptavidin microbeads to facilitate removal of the unwanted 5' digestion products. The use of restricted 3'-ends alone serves to reduce the complexity of the cDNA fragment pool and helps to ensure that each RNA species is represented by not more than one restriction product. An adaptor is ligated to facilitate subsequent amplification of the captured population. PCR is carried out with one adaptor-specific and one biotinylated polydT primer. The reamplified population is recaptured and the non-biotinylated strands removed by alkaline dissociation. The non-biotinylated strand is then resynthesized using a different adaptor-specific primer in the presence of a radiolabelled dNTP. The labelled immobilized 3' cDNA ends are next sequentially treated with a series of different restriction endonucleases and the products from each digestion analysed by PAGE. The result is a fingerprint composed of a number of ladders (equal to the number of sequential digests used). By comparing test versus control fingerprints, it is possible to identify differentially expressed products which can then be isolated from the gel and cloned. The advantages of this procedure are that it is very robust and reproducible, and the authors estimate that 80–93% of cDNA molecules are involved in the final fingerprint. The disadvantage is that polyacrylamide gels can rarely resolve more than 300–400 bands, which compares poorly to the 1000 or more which are estimated to be produced in an average experiment. The use of 2-D gels such as those described by Uitterlinden *et al.* (1989) and Hatada *et al.* (1991) may help to overcome this problem.

A similar method for displaying restriction endonuclease fragments was later described by Prashar and Weissman (1996). However, instead of sequential digestion of the immobilized 3'-terminal cDNA fragments, these authors simply compared the profiles of the control and treated populations without further manipulation.

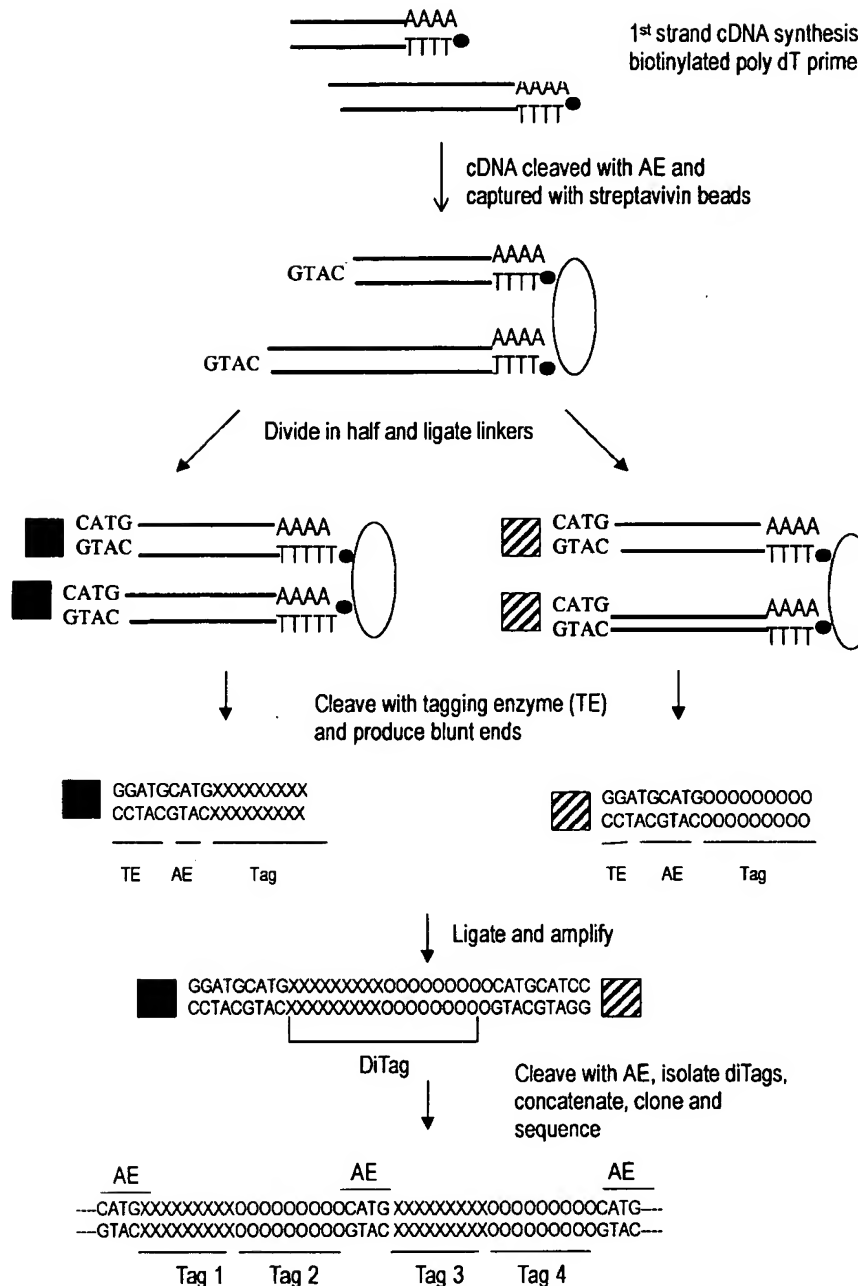


Figure 9. Serial analysis of gene expression (SAGE) analysis. cDNA is cleaved with an anchoring enzyme (AE) and the 3' ends captured using streptavidin beads. The cDNA pool is divided in half and each portion ligated to a different linker, each containing a type IIS restriction site (tagging enzyme, TE). Restriction with the type IIS enzyme releases the linker plus a short length of cDNA (XXXXXX and OOOOO indicate nucleotides of different tags). The two pools of tags are then ligated and amplified using linker-specific primers. Following PCR, the products are cleaved with the AE and the ditags isolated from the linkers using PAGE. The ditags are then ligated (during which process, concatenization occurs) and cloned into a vector of choice for sequencing. After Velculescu *et al.* (1995), with permission.

DNA arrays

'Open' differential display systems are cumbersome in that it takes a great deal of time to extract and identify candidate genes and then confirm that they are indeed up- or down-regulated in the treated compared to the control tissue. Normally, the latter process is carried out using Northern blotting or RT-PCR. Even so, each of the aforementioned steps produce a bottleneck to the ultimate goal of rapid analysis of gene expression. These problems will likely be addressed by the development of so-called DNA arrays (e.g. Gress *et al.* 1992, Zhao *et al.* 1995, Schena *et al.* 1996), the introduction of which has signalled the next era in differential gene expression analysis. DNA arrays consist of a gridded membrane or glass 'chips' containing hundreds or thousands of DNA spots, each consisting of multiple copies of part of a known gene. The genes are often selected based on previously proven involvement in oncogenesis, cell cycling, DNA repair, development and other cellular processes. They are usually chosen to be as specific as possible for each gene and animal species. Human and mouse arrays are already commercially available and a few companies will construct a personalized array to order, for example Clontech Laboratories and Research Genetics Inc. The technique is rapid in that hundreds or even thousands of genes can be spotted on a single array, and that mRNA/cDNA from the test populations can be labelled and used directly as probe. When analysed with appropriate hardware and software, arrays offer a rapid and quantitative means to assess differences in gene expression between two cell populations. Of course, there can only be identification and quantitation of those genes which are in the array (hence the term 'closed' system). Therefore, one approach to elucidating the molecular mechanisms involved in a particular disease/development system may be to combine an open and closed system—a DNA array to directly identify and quantitate the expression of known genes in mRNA populations, and an open system such as SSH to isolate unknown genes which are differentially expressed.

One of the main advantages of DNA arrays is the huge number of gene fragments which can be put on a membrane—some companies have reported gridding up to 60000 spots on a single glass 'chip' (microscope slide). These high density chip-based micro-arrays will probably become available as mass-produced off-the-shelf items in the near future. This should facilitate the more rapid determination of differential expression in time and dose-response experiments. Aside from their high cost and the technical complexities involved in producing and probing DNA arrays, the main problem which remains, especially with the newer micro-array (gene-chip) technologies, is that results are often not wholly reproducible between arrays. However, this problem is being addressed and should be resolved within the next few years.

EST databases as a means to identify differentially expressed genes

Expressed sequence tags (ESTs) are partial sequences of clones obtained from cDNA libraries. Even though most ESTs have no formal identity (putative identification is the best to be hoped for), they have proven to be a rapid and efficient means of discovering new genes and can be used to generate profiles of gene-expression in specific cells. Since they were first described by Adams *et al.* (1991), there has been a huge explosion in EST production and it is estimated that there are now well over a million such sequences in the public domain, representing over half

of all human genes (Hillier *et al.* 1996). This large number of freely available sequences (both sequence information and clones are normally available royalty-free from the originators) has enabled the development of a new approach towards differential gene expression analysis as described by Vasmatzis *et al.* (1998). The approach is simple in theory: EST databases are first searched for genes that have a number of related EST sequences from the target tissue of choice, but none or few from non-target tissue libraries. Programmes to assist in the assembly of such sets of overlapping data may be developed in-house or obtained privately or from the internet. For example, the Institute for Genomic Research (TIGR, found at <http://www.tigr.org>) provides many software tools free of charge to the scientific community. Included amongst these is the TIGR assembler (Sutton *et al.* 1995), a tool for the assembly of large sets of overlapping data such as ESTs, bacterial artificial chromosomes (BAC)s, or small genomes. Candidate EST clones representing different genes are then analysed using RNA blot methods for size and tissue specificity and, if required, used as probes to isolate and identify the full length cDNA clone for further characterization. In practice however, the method is rather more involved, requiring bioinformatic and computer analysis coupled with confirmatory molecular studies. Vasmatzis *et al.* (1998) have described several problems in this fledgling approach, such as separating highly homologous sequences derived from different genes and an overemphasis of specificity for some EST sequences. However, since these problems will largely be addressed by the development of more suitable computer algorithms and an increased completeness of the EST database, it is likely that this approach to identifying differentially expressed genes may enjoy more patronage in the future.

Problems and potential of differential expression techniques

The holistic or single cell approach?

When working with *in vivo* models of differential expression, one of the first issues to consider must be the presence of multiple cell types in any given specimen. For example, a liver sample is likely to contain not only hepatocytes, but also (potentially) Ito cells, bile ductule cells, endothelial cells, various immune cells (e.g. lymphocytes, macrophages and Kupffer cells) and fibroblasts. Other tissues will each have their own distinctive cell populations. Also, in the case of neoplastic tissue, there are almost always normal, hyperplastic and/or dysplastic cells present in a sample. One must, therefore, be aware that genes obtained from a differential display experiment performed on an animal tissue model may not necessarily arise exclusively from the intended 'target' cells, e.g. hepatocytes/neoplastic cells. If appropriate, further analyses using immunohistochemistry, *in situ* hybridization or *in situ* RT-PCR should be used to confirm which cell types are expressing the gene(s) of interest. This problem is probably most acute for those studying the differential expression of genes in the development of different cell types, where there is a need to examine homologous cell populations. The problem is now being addressed at the National Cancer Institute (Bethesda, MD, USA) where new microdissection techniques have been employed to assist in their gene analysis programme, the Cancer Genome Anatomy Project (CGAP) (For more information see web site: <http://www.ncbi.nlm.nih.gov/ncicgap/intro.html>). There are also separation techniques available that utilise cell-specific antigens as a means to isolate target cells,

e.g. fluorescence activated cell sorting (FACS) (Dunbar *et al.* 1998, Kas-Deelen *et al.* 1998) and magnetic bead technology (Richard *et al.* 1998, Rogler *et al.* 1998).

However, those taking a holistic approach may consider this issue unimportant. There is an equally appropriate view that all those genes showing altered expression within a compromised tissue should be taken into consideration. After all, since all tissues are complex mixes of different, interacting cell types which intimately regulate each other's growth and development, it is clear that each cell type could in some way contribute (positively or negatively) towards the molecular mechanisms which lie behind responses to external stimuli or neoplastic growth. It is perhaps then more informative to carry out differential display experiments using *in vivo* as opposed to *in vitro* models, where uniform populations of identical cells probably represent a partial, skewed or even inaccurate picture of the molecular changes that occur.

The incidence and possible implications of inter-individual biological variation should be considered in any approach where whole animal models are being used. It is clear that individuals (humans and animals) respond in different ways to identical stimuli. One of the best characterized examples is the debrisoquine oxidation polymorphism, which is mediated by cytochrome CYP2D6 and determines the pharmacokinetics of many commonly prescribed drugs (Lennard 1993, Meyer and Zanger 1997). The reasons for such differences are varied and complex, but allelic variations, regulatory region polymorphisms and even physical and mental health can all contribute to observed differences in individual responses. Careful thought should, therefore, be given to the specific objectives of the study and to the possible value of pooling starting material (tissue/mRNA). The effect of this can be beneficial through the ironing out of exaggerated responses and unimportant minor fluctuations of (mechanistically) irrelevant genes in individual animals, thus providing a clearer overall picture of the general molecular mechanisms of the response. However, at the same time such minor variations may be of utmost importance in deciding the ability of individual animals to succumb to or resist the effects of a given chemical/disease.

How efficient are differential expression techniques at recovering a high percentage of differentially expressed genes?

A number of groups have produced experimental data suggesting that mammalian cells produce between 8000–15000 different mRNA species at any one time (Mechler and Rabbitts 1981, Hedrick *et al.* 1984, Bravo 1990), although figures as high as 20–30000 have also been quoted (Axel *et al.* 1976). Hedrick *et al.* (1984) provided evidence suggesting that the majority of these belong to the rare abundance class. A breakdown of this abundance distribution is shown in table 1.

When the results of differential display experiments have been compared with data obtained previously using other methods, it is apparent that not all differentially expressed mRNAs are represented in the final display. In particular, rare messages (which, importantly, often include regulatory proteins) are not easily recovered using differential display systems. This is a major shortcoming, as the majority of mRNA species exist at levels of less than 0.005% of the total population (table 1). Bertioli *et al.* (1995) examined the efficiency of DD templates (heterogeneous mRNA populations) for recovering rare messages and were unable to detect mRNA

species present at less than 1.2% of the total mRNA population—equivalent to an intermediate or abundant species. Interestingly, when simple model systems (single target only) were used instead of a heterogeneous mRNA population, the same primers could detect levels of target mRNA down to 10000× smaller. These results are probably best explained by competition for substrates from the many PCR products produced in a DD reaction.

The numbers of differentially expressed mRNAs reported in the literature using various model systems provides further evidence that many differentially expressed mRNAs are not recovered. For example, DeRisi *et al.* (1997) used DNA array technology to examine gene expression in yeast following exhaustion of sugar in the medium, and found that more than 1700 genes showed a change in expression of at least 2-fold. In light of such a finding, it would not be unreasonable to suggest that of the 8000–15 000 different mRNA species produced by any given mammalian cell, up to 1000 or more may show altered expression following chemical stimulation. Whilst this may be an extreme figure, it is known that at least 100 genes are activated/upregulated in Jurkat (T-) cells following IL-2 stimulation (Ullman *et al.* 1990). In addition, Wan *et al.* (1996) estimated that interferon- γ -stimulated HeLa cells differentially express up to 433 genes (assuming 24 000 distinct mRNAs expressed by the cells). However, there have been few publications documenting anywhere near the recovery of these numbers. For example, in using DD to compare normal and regenerating mouse liver, Bauer *et al.* (1993) found only 70 of 38 000 total bands to be different. Of these, 50% (35 genes) were shown to correspond to differentially expressed bands. Chen *et al.* (1996) reported 10 genes upregulated in female rat liver following ethinyl estradiol treatment. McKenzie and Drake (1997) identified 14 different gene products whose expression was altered by phorbol myristate acetate (PMA, a tumour promoter agent) stimulation of a human myelomonocytic cell line. Kilty and Vickers (1997) identified 10 different gene products whose expression was upregulated in the peripheral blood leukocytes of allergic disease sufferers. Linskens *et al.* (1995) found 23 genes differentially expressed between young and senescent fibroblasts. Techniques other than DD have also provided an apparent paucity of differentially expressed genes. Using SH for example, Cao *et al.* (1997) found 15 genes differentially expressed in colorectal cancer compared to normal mucosal epithelium. Fitzpatrick *et al.* (1995) isolated 17 genes upregulated in rat liver following treatment with the peroxisome proliferator, clofibrate; Philips *et al.* (1990) isolated 12 cDNA clones which were upregulated in highly metastatic mammary adenocarcinoma cell lines compared to poorly metastatic ones. Prashar and Weissman (1996) used 3' restriction fragment analysis and identified approximately 40 genes showing altered expression within 4 h of activation of Jurkat T-cells. Groenink and Leegwater (1996) analysed 27 gene fragments isolated using SSH of delayed early response phase of liver regeneration and found only 12 to be upregulated.

In the laboratory, SSH was used to isolate up to 70 candidate genes which appear to show altered expression in guinea pig liver following short-term treatment with the peroxisome proliferator, WY-14,643 (Rockett, Swales, Esdaile and Gibson, unpublished observations). However, these findings have still to be confirmed by analysis of the extracted tissue mRNA for differential expression of these sequences.

Whilst the latest differential display technologies are purported to include design and experimental modifications to overcome this lack of efficiency (in both the total number of differentially expressed genes recovered and the percentage that are true

positives), it is still not clear if such adaptations are practically effective—proving efficiency by spiking with a known amount of limited numbers of artificial construct(s) is one thing, but isolating a high percentage of the rare messages already present in an mRNA population is another. Of course, some models will genuinely produce only a small number of differentially expressed genes. In addition, there are also technical problems that can reduce efficiency. For example, mRNAs may have an unusual primary structure that effectively prevents their amplification by PCR-based systems. In addition, it is known that under certain circumstances not all mRNAs have 3' polyA sites. For example, during *Xenopus* development, deadenylation is used as a means to stabilize RNAs (Voeltz and Steitz 1998), whilst preferential deadenylation may play a role in regulating Hsp70 (and perhaps, therefore, other stress protein) expression in *Drosophila* (Dellavalle *et al.* 1994). The presence of deadenylated mRNAs would clearly reduce the efficiency of systems utilizing a polydT reverse transcription step. The efficiency of any system also depends on the quality of the starting material. All differential display techniques use mRNA as their target material. However, it is difficult to isolate mRNA that is completely free of ribosomal RNA. Even if polydT primers are used to prime first strand cDNA synthesis, ribosomal RNA is often transcribed to some degree (Clontech PCR-Select cDNA Subtraction kit user manual). It has been shown, at least in the case of SSH, that a high rRNA:mRNA ratio can lead to inefficient subtractive hybridization (Clontech PCR-Select cDNA Subtraction kit user manual), and there is no reason to suppose that it will not do likewise in other SH approaches. Finally, those techniques that utilise a presubtraction amplification step (e.g. RDA) may present a skewed representation since some sequences amplify better than others.

Of course, probably the most important consideration is the temporal factor. It is clear that any given differential display experiment can only interrogate a cell at one point in time. It may well be that a high percentage of the genes showing altered expression at that time are obtained. However, given that disease processes and responses to environmental stimuli involve dynamic cascades of signalling, regulation, production and action, it is clear that all those genes which are switched on/off at different times will not be recovered and, therefore, vital information may well be missed. It is, therefore, imperative to obtain as much information about the model system beforehand as possible, from which a strategy can be derived for targeting specific time points or events that are of particular interest to the investigator. One way of getting round this problem of single time point analysis is to conduct the experiment over a suitable time course which, of course, adds substantially to the amount of work involved.

How sensitive are differential expression technologies?

There has been little published data that addresses the issue of how large the change in expression must be for it to permit isolation of the gene in question with the various differential expression technologies. Although the isolation of genes whose expression is changed as little as 1.5-fold has been reported using SSH (Groenink and Leegwater 1996), it appears that those demonstrating a change in excess of 5-fold are more likely to be picked up. Thus, there is a 'grey zone' in between where small changes could fade in and out of isolation between

experiments and animals. DD, on the other hand, is not subject to this grey zone since, unlike SH approaches, it does not amplify the difference in expression between two samples. Wan *et al.* (1996) reported that differences in expression of twofold or more are detectable using DD.

Resolution and visualization of differential expression products

It seems highly improbable with current technology that a gel system could be developed that is able to resolve all gene species showing altered expression in any given test system (be it SH- or DD-based). Polyacrylamide gel electrophoresis (PAGE) can resolve size differences down to 0.2% (Sambrook *et al.* 1989) and are used as standard in DD experiments. Even so, it is clear that a complex series of gene products such as those seen in a DD will contain unresolvable components. Thus, what appears to be one band in a gel may in fact turn out to be several. Indeed, it has been well documented (Mathieu-Daude *et al.* 1996, Smith *et al.* 1997) that a single band extracted from a DD often represents a composite of heterogeneous products, and the same has been found for SSH displays in this laboratory (Rockett *et al.* 1997). One possible solution was offered by Mathieu-Daude *et al.* (1996), who extracted and reamplified candidate bands from a DD display and used single strand conformation polymorphism (SSCP) analysis to confirm which components represented the truly differentially expressed product.

Many scientists often try to avoid the use of PAGE where possible because it is technically more demanding than agarose gel electrophoresis (AGE). Unfortunately, high resolution agarose gels such as Metaphor (FMC, Lichfield, UK) and AquaPor HR (National Diagnostics, Hesse, UK), whilst easier to prepare and manipulate than PAGE, can only separate DNA sequences which differ in size by around 1.5–2% (15–20 base pairs for a 1Kb fragment). Thus, SSH, RDA or other such products which differ in size by less than this amount are normally not resolvable. However, a simple technique does in fact exist for increasing the resolving power of AGE—the inclusion of HA-red (10-phenyl neutral red-PEG ligand) or HA-yellow (bisbenzamide-PEG ligand) (Hanse Analytik GmbH, Bremen, Germany) in a gel separates identical or closely sized products on base content. Specifically, HA-red and -yellow selectively bind to GC and AT DNA motifs, respectively (Wawer *et al.* 1995, Hanse Analytik 1997, personal communication). Since both HA-stains possess an overall positive charge, they migrate towards the cathode when an electric field is applied. This is in direct opposition to DNA, which is negatively charged and, therefore, migrates towards the anode. Thus, if two DNA clones are identical in size (as perceived on a standard high resolution agarose gel), but differ in AT/GC content, inclusion of a HA-dye in the gel will effectively retard the migration of one of the sequences compared to the other, effectively making it apparently larger and, thus, providing a means of differentiating between the two. The use of HA-red has been shown to resolve sequences with an AT variation of less than 1% (Wawer *et al.* 1995), whilst Hanse Analytik have reported that HA staining is so sensitive that in one case it was used to distinguish two 567bp sequences which differed by only a single point mutation (Hanse Analytik 1996, personal communication). Therefore, if one wishes to check whether all the clones produced from a specific band in a differential display experiment are derived from the same gene species, a small amount of reamplified or digested clone can be run on a standard high resolution gel, and a second aliquot

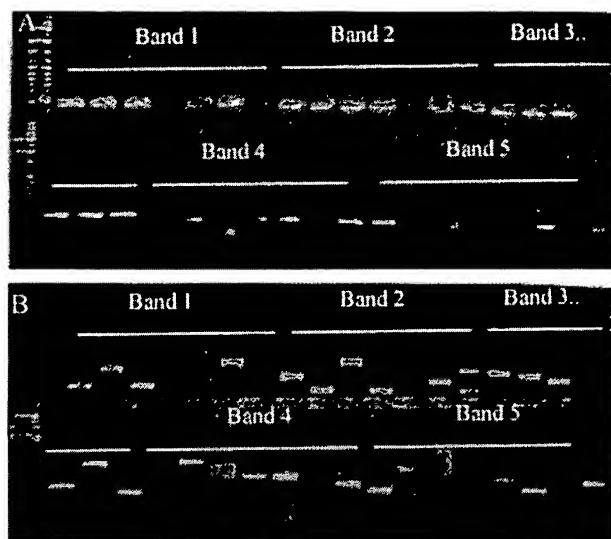


Figure 10. Discrimination of clones of identical/nearly identical size using HA-red. Bands of decreasing size (1–5) were extracted from the final display of a suppression subtractive hybridization experiment and cloned. Seven colonies were picked at random from each cloned band and their inserts amplified using PCR. The products were run on two gels, (A) a high resolution 2% agarose gel, and (B) a high resolution 2% agarose gel containing 1 U/ml HA-red. With few exceptions, all the clones from each band appear to be the same size (gel A). However, the presence of HA-red (gel B), which separates identically-sized DNA fragments based on the percentage of GC within the sequence, clearly indicates the presence of different gene species within each band. For example, even though all five re-amplified clones of band 1 appear to be the same size, at least four different gene species are represented.

in a similar gel containing one of the HA-stains. The standard gel should indicate any gross size differences, whilst the HA-stained gel should separate otherwise unresolvable species (on standard AGE) according to their base content. Geisinger *et al.* (1997) reported successful use of this approach for identifying DD-derived clones. Figure 10 shows such an experiment carried out in this laboratory on clones obtained from a band extracted from an SSH display.

An alternative approach is to carry out a 2-D analysis of the differential display products. In this approach, size-based separation is first carried out in a standard agarose gel. The gel slice containing the display is then extracted and incorporated in to a HA gel for resolution based on AT/GC content.

Of course, one should always consider the possibility of there being different gene species which are the same size and have the same GC/AT content. However, even these species are not unresolvable given some effort—again, one might use SSCP, or perhaps a denaturing gradient gel electrophoresis (DGGE) or temperature gradient field electrophoresis (TGGE) approach to resolve the contents of a band, either directly on the extracted band (Suzuki *et al.* 1991) or on the reamplified product.

The requirement of some differential display techniques to visualize large numbers of products (e.g. DD and GEF) can also present a problem in that, in terms of numbers, the resolution of PAGE rarely exceeds 300–400 bands. One approach to overcoming this might be to use 2-D gels such as those described by Uitterlinden *et al.* (1989) and Hatada *et al.* (1991).

Extraction of differentially expressed bands from a gel can be complex since, in some cases (e.g. DD, GEF), the results are visualized by autoradiographic means, such that precise overlay of the developed film on the gel must occur if the correct band is to be extracted for further analysis. Clearly, a misjudged extraction can account for many man-hours lost. This problem, and that of the use of radioisotopes, has been addressed by several groups. For example, Lohmann *et al.* (1995) demonstrated that silver staining can be used directly to visualize DD bands in horizontal PAGs. An *et al.* (1996) avoided the use of radioisotopes by transferring a small amount (20–30%) of the DNA from their DD to a nylon membrane, and visualizing the bands using chemiluminescent staining before going back to extract the remaining DNA from the gel. Chen and Peck (1996) went one step further and transferred the entire DD to a nylon membrane. The DNA bands were then visualized using a digoxigenin (DIG) system (DIG was attached to the polydT primers used in the differential display procedure). Differentially expressed bands were cut from the membrane and the DNA eluted by washing with PCR buffer prior to reamplification.

One of the advantages of using techniques such as SSH and RDA is that the final display can be run on an agarose gel and the bands visualized with simple ethidium bromide staining. Whilst this approach can provide acceptable results, overstaining with SYBR Green I or SYBR Gold nucleic acid stains (FMC) effectively enhances the intensity and sharpness of the bands. This greatly aids in their precise extraction and often reveals some faint products that may otherwise be overlooked. Whilst differential displays stained with SYBR Green I are better visualized using short wavelength UV (254 nm) rather than medium wavelength (306 nm), the shorter wavelength is much more DNA damaging. In practice, it takes only a few seconds to damage DNA extracted under 254 nm irradiation, effectively preventing reamplification and cloning. The best approach is to over stain with SYBR Green I and extract bands under a medium wavelength UV transillumination.

The possible use of 'microfingerprinting' to reduce complexity

Given the sheer number of gene products and the possible complexity of each band, an alternative approach to rapid characterization may be to use an enhanced analysis of a small section of a differential display—a 'sub-fingerprint' or 'micro-fingerprint'. In this case, one could concentrate on those bands which only appear in a particular chosen size region. Reducing the fingerprint in this way has at least two advantages. One is that it should be possible to use different gel types, concentrations and run times tailored exactly to that region. Currently, one might run products from 100–3000 + bp on the same gel, which leads to compromise in the gel system being used and consequently to suboptimal resolution, both in terms of size and numbers, and can lead to problems in the accurate excision of individual bands. Secondly, it may be possible to enhance resolution by using a 2-D analysis using a HA-stain, as described earlier. In summary, if a range of gene product sizes is carefully chosen to include certain 'relevant' genes, the 2-D system standardized, and appropriate gene analysis used, it may be possible to develop a method for the early and rapid identification of compounds which have similar or widely different cellular effects. If the prognosis for exposure to one or more other chemicals which display a similar profile is already known, then one could perhaps predict similar effects for any new compounds which show a similar micro-fingerprint.

An alternative approach to microfingerprinting is to examine altered expression in specific families of genes through careful selection of PCR primers and/or post-reaction analysis. Stress genes, growth factors and/or their receptors, cell cycling genes, cytochromes P450 and regulatory proteins might be considered as candidates for analysis in this way. Indeed, some off-the-shelf DNA arrays (e.g. Clontech's Atlas cDNA Expression Array series) already anticipated this to some degree by grouping together genes involved in different responses e.g. apoptosis, stress, DNA-damage response etc.

Screening

False positives

The generation of false positives has been discussed at length amongst the differential display community (Liang *et al.* 1993, 1995, Nishio *et al.* 1994, Sun *et al.* 1994, Sompayrac *et al.* 1995). The reason for false positives varies with the technique being used. For instance, in RDA, the use of adaptors which have not been HPLC purified can lead to the production of false positives through illegitimate ligation events (O'Neill and Sinclair 1997), whilst in DD they can arise through PCR artifacts and illegitimate transcription of rRNA. In SH, false positives appear to be derived largely from abundant gene species, although some may arise from cDNA/mRNA species which do not undergo hybridization for technical reasons.

A quick screening of putative differentially expressed clones can be carried out using a simple dot blot approach, in which labelled first strand probes synthesized from tester and driver mRNA are hybridized to an array of said clones (Hedrick *et al.* 1984, Sakaguchi *et al.* 1986). Differentially expressed clones will hybridize to tester probe, but not driver. The disadvantage of this approach is that rare species may not generate detectable hybridization signals. One option for those using SSH is to screen the clones using a labelled probe generated from the subtracted cDNA from which it was derived, and with a probe made from the reverse subtraction reaction (ClonTechniques 1997a). Since the SSH method enriches rare sequences, it should be possible to confirm the presence of clones representing low abundance genes. Despite this quick screening step, there is still the need to go back to the original mRNA and confirm the altered expression using a more quantitative approach. Although this may be achieved using Northern blots, the sensitivity is poor by today's high standards and one must rely on PCR methods for accurate and sensitive determinations (see below).

Sequence analysis

The majority of differential display procedures produce final products which are between 100 and 1000bp in size. However, this may considerably reduce the size of the sequence for analysis of the DNA databases. This in turn leads to a reduced confidence in the result—several families of genes have members whose DNA sequences are almost identical except in a few key stretches, e.g. the cytochrome P450 gene superfamily (Nelson *et al.* 1996). Thus, does the clone identified as being almost identical to gene X_0 really come from that gene, or its brother gene X_1 or its as yet undiscovered sister X_2 ? For example, using SSH, part of a gene was isolated,

which was up-regulated in the liver of rats exposed to Wy-14,643 and was identified by a FASTA search as being transferrin (data not shown). However, transferrin is known to be downregulated by hypolipidemic peroxisome proliferators such as Wy-14,643 (Hertz *et al.* 1996), and this was confirmed with subsequent RT-PCR analysis. This suggests that the gene sequence isolated may belong to a gene which is closely related to transferrin, but is regulated by a different mechanism.

A further problem associated with SH technology is redundancy. In most cases before SH is carried out, the cDNA population must first be simplified by restriction digestion. This is important for at least two reasons:

- (1) To reduce complexity—long cDNA fragments may form complex networks which prevent the formation of appropriate hybrids, especially at the high concentrations required for efficient hybridization.
- (2) Cutting the cDNAs into small fragments provides better representation of individual genes. This is because genes derived from related but distinct members of gene families often have similar coding sequences that may cross-hybridize and be eliminated during the subtraction procedure (Ko 1990). Furthermore, different fragments from the same cDNA may differ considerably in terms of hybridization and amplification and, thus, may not efficiently do one or the other (Wang and Brown 1991). Thus, some fragments from differentially expressed cDNAs may be eliminated during subtractive hybridization procedures. However, other fragments may be enriched and isolated. As a consequence of this, some genes will be cut one or more times, giving rise to two or more fragments of different sizes. If those same genes are differentially expressed, then two or more of the different size fragments may come through as separate bands on the final differential display, increasing the observed redundancy and increasing the number of redundant sequencing reactions.

Sequence comparisons also throw up another important point—at what degree of sequence similarity does one accept a result. Is 90% identity between a gene derived from your model species and another acceptably close? Is 95% between your sequence and one from the same species also acceptable? This problem is particularly relevant when the forward and reverse sequence comparisons give similar sequences with completely different gene species! An arbitrary decision seems to be to allocate genes that are definite (95% and above similarity) and then group those between 60 and 95% as being related or possible homologues.

Quantitative analysis

At some point, one must give consideration to the quantitative analysis of the candidate genes, either as a means of confirming that they are truly differentially expressed, or in order to establish just what the differences are. Northern blot analysis is a popular approach as it is relatively easy and quick to perform. However, the major drawback with Northern blots is that they are often not sensitive enough to detect rare sequences. Since the majority of messages expressed in a cell are of low abundance (see table 1), this is a major problem. Consequently, RT-PCR may be the method of choice for confirming differential expression. Although the procedure is somewhat more complex than Northern analysis, requiring synthesis of primers and optimization of reaction conditions for each gene species, it is now possible to set up high throughput PCR systems using multichannel pipettes, 96 +well plates and

appropriate thermal cycling technology. Whilst quantitative analysis is more desirable, being more accurate and without reliance on an internal standard, the money and time needed to develop a competitor molecule is often excessive, especially when one might be examining tens or even hundreds of gene species. The use of semi-quantitative analysis is simpler, although still relatively involved. One must first of all choose an internal standard that does not change in the test cells compared to the controls. Numerous reference genes have been tried in the past, for example interferon-gamma (IFN- γ , Frye *et al.* 1989), β -actin (Heuval *et al.* 1994), glyceraldehyde-3-phosphate dehydrogenase (GAPDH, Wong *et al.* 1994), dihydrofolate reductase (DHFR, Mohler and Butler 1991), β -2-microglobulin (β -2-m, Murphy *et al.* 1990), hypoxanthine phosphoribosyl transferase (HPRT, Foss *et al.* 1998) and a number of others (ClonTechniques 1997b). Ideally, an internal standard should not change its level of expression in the cell regardless of cell age, stage in the cell cycle or through the effects of external stimuli. However, it has been shown on numerous occasions that the levels of most housekeeping genes currently used by the research community do in fact change under certain conditions and in different tissues (ClonTechniques 1997b). It is imperative, therefore, that preliminary experiments be carried out on a panel of housekeeping genes to establish their suitability for use in the model system.

Interpretation of quantitative data must also be treated with caution. By comparing the lists of genes identified by differential expression one can perhaps gain insight into why two different species react in different ways to external stimuli. For example, rats and mice appear sensitive to the non-genotoxic effects of a wide range of peroxisome proliferators whilst Syrian hamsters and guinea pigs are largely resistant (Orton *et al.* 1984, Rodricks and Turnbull 1987, Lake *et al.* 1989, 1993, Makowska *et al.* 1992). A simplified approach to resolving the reason(s) why is to compare lists of up- and down-regulated genes in order to identify those which are expressed in only one species and, through background knowledge of the effects of the said gene, might suggest a mechanism of facilitated non-genotoxic carcinogenesis or protection. Of course, the situation is likely to be far more complex. Perhaps if there were one key gene protecting guinea pig from non-genotoxic effects and it was upregulated 50 times by PPs, the same gene might only be up-regulated five times in the rat. However, since both were noted to be upregulated, the importance of the gene may be overlooked. Just to complicate matters, a large change in expression does not necessarily mean a biologically important change. For example, what is the true relevance of gene Y which shows a 50-fold increase after a particular treatment, and gene Z which shows only a 5-fold increase? If one examines the literature one may find that historically, gene Y has often been shown to be up-regulated 40–60-fold by a number of unrelated stimuli—in light of this the 50-fold increase would appear less significant. However, the literature may show that gene Z has never been recorded as having more than doubled in expression—which makes your 5-fold increase all the more exciting. Perhaps even more interesting is if that same 5-fold increase has only been seen in related neoplasms or following treatment with related chemicals.

Problems in using the differential display approach

Differential display technology originally held promise of an easily obtainable 'fingerprint' of those genes which are up- or down-regulated in test animals/cells in a developmental process or following exposure to given stimuli. However, it has

become clear that the fingerprinting process, whilst still valid, is much too complex to be represented by a single technique profile. This is because all differential display techniques have common and/or unique technical problems which preclude the isolation and identification of all those genes which show changes in expression. Furthermore, there are important genetic changes related to disease development which differential expression analysis is simply not designed to address. An example of this is the presence of small deletions, insertions, or point mutations such as those seen in activated oncogenes, tumour suppressor genes and individual polymorphisms. Polymorphic variations, small though they usually are, are often regarded as being of paramount importance in explaining why some patients respond better than others to certain drug treatments (and, in logical extension, why some people are less affected by potentially dangerous xenobiotics/carcinogens than others). The identification of such point mutations and naturally occurring polymorphisms requires the subsequent application of sequencing, SSCP, DGGE or TGGE to the gene of interest. Furthermore, differential display is not designed to address issues such as alternatively spliced gene species or whether an increased abundance of mRNA is a result of increased transcription or increased mRNA stability.

Conclusions

Perhaps the main advantage of open system differential display techniques is that they are not limited by extant theories or researcher bias in revealing genes which are differentially expressed, since they are designed to amplify all genes which demonstrate altered expression. This means that they are useful for the isolation of previously unknown genes which may turn out be useful biomarkers of a particular state or condition. At least one open system (SAGE) is also quantitative, thus eliminating the need to return to the original mRNA and carry out Northern/PCR analysis to confirm the result. However, the rapid progress of genome mapping projects means that over the next 5–10 years or so, the balance of experimental use will switch from open to closed differential display systems, particularly DNA arrays. Arrays are easier and faster to prepare and use, provide quantitative data, are suitable for high throughput analysis and can be tailored to look at specific signalling pathways or families of genes. Identification of all the gene sequences in human and common laboratory animals combined with improved DNA array technology, means that it will soon no longer be necessary to try to isolate differentially expressed genes using the technically more demanding open system approach. Thus, their main advantage (that of identifying unknown genes) will be largely eradicated. It is likely, therefore, that their sphere of application will be reduced to analysis of the less common laboratory species, since it will be some time yet before the genomes of such animals as zebrafish, electric eels, gerbils, crayfish and squid, for example, will be sequenced.

Of course, in the end the question will always remain: What is the functional/biological significance of the identified, differentially expressed genes? One persistent problem is understanding whether differentially expressed genes are a cause or consequence of the altered state. Furthermore, many chemicals, such as non-genotoxic carcinogens, are also mitogens and so genes associated with replication will also be upregulated but may have little or nothing to do with the

carcinogenic effect. Whilst differential display technology cannot hope to answer these questions, it does provide a springboard from which identification, regulatory and functional studies can be launched. Understanding the molecular mechanism of cellular responses is almost impossible without knowing the regulation and function of those genes and their condition (e.g. mutated). In an abstract sense, differential display can be likened to a still photograph, showing details of a fixed moment in time. Consider the Historian who knows the outcome of a battle and the placement and condition of the troops before the battle commenced, but is asked to try and deduce how the battle progressed and why it ended as it did from a few still photographs—an impossible task. In order to understand the battle, the Historian must find out the capabilities and motivation of the soldiers and their commanding officers, what the orders were and whether they were obeyed. He must examine the terrain, the remains of the battle and consider the effects the prevailing weather conditions exerted. Likewise, if mechanistic answers are to be forthcoming, the scientist must use differential display in combination with other techniques, such as knockout technology, the analysis of cell signalling pathways, mutation analysis and time and dose response analyses. Although this review has emphasized the importance of differential gene profiling, it should not be considered in isolation and the full impact of this approach will be strengthened if used in combination with functional genomics and proteomics (2-dimensional protein gels from isoelectric focusing and subsequent SDS electrophoresis and virtual 2D-maps using capillary electrophoresis). Proteomics is attracting much recent attention as many of the changes resulting in differential gene expression do not involve changes in mRNA levels, as described extensively herein, but rather protein-protein, protein-DNA and protein phosphorylation events which would require functional genomics or proteomic technologies for investigation.

Despite the limitations of differential display technology, it is clear that many potential applications and benefits can be obtained from characterizing the genetic changes that occur in a cell during normal and disease development and in response to chemical or biological insult. In light of functional data, such profiling will provide a 'fingerprint' of each stage of development or response, and in the long term should help in the elucidation of specific and sensitive biomarkers for different types of chemical/biological exposure and disease states. The potential medical and therapeutic benefits of understanding such molecular changes are almost immeasurable. Amongst other things, such fingerprints could indicate the family or even specific type of chemical an individual has been exposed to plus the length and/or acuteness of that exposure, thus indicating the most prudent treatment. They may also help uncover differences in histologically identical cancers, provide diagnostic tests for the earliest stages of neoplasia and, again, perhaps indicate the most efficacious treatment.

The Human Genome Project will be completed early in the next century and the DNA sequence of all the human genes will be known. The continuing development and evolution of differential gene expression technology will ensure that this knowledge contributes fully to the understanding of human disease processes.

Acknowledgements

We acknowledge Drs Nick Plant (University of Surrey), Sally Darney and Chris Luft (US EPA at RTP) for their critical analysis of the manuscript prior to submission. This manuscript has been reviewed in accordance with the policy of the

US Environmental Protection Agency and approved for publication. Approval does not signify that the contents reflect the views and policies of the Agency, nor does mention of trade names constitute endorsement or recommendation for use.

References

- ADAMS, M. D., KELLEY, J. M., GOCAYNE, J. D., DUBNICK, M., POLYMERPOULOS, M. H., XIAO, H., MERRIL, C. R., WU, A., OLDE, B., MORENO, R. F., KERLAVAGE, A. R., McCOMBIE, W. R. and VENTOR, J. C., 1991, Complementary DNA sequencing: expressed sequence tags and human genome project. *Science*, **252**, 1651–1656.
- AN, G., LUO, G., VELTRI, R. W. and O'HARA, S. M., 1996, Sensitive non-radioactive differential display method using chemiluminescent detection. *Biotechniques*, **20**, 342–346.
- AXEL, R., FEIGELSON, P. and SCHULTZ, G., 1976, Analysis of the complexity and diversity of mRNA from chicken liver and oviduct. *Cell*, **7**, 247–254.
- BAND, V. and SAGER, R., 1989, Distinctive traits of normal and tumor-derived human mammary epithelial cells expressed in a medium that supports long-term growth of both cell types. *Proceedings of the National Academy of Sciences, USA*, **86**, 1249–1253.
- BAUER, D., MULLER, H., REICH, J., RIEDEL, H., AHRENKIEL, V., WARTHOF, P. and STRAUSS, M., 1993, Identification of differentially expressed mRNA species by an improved display technique (DDRT-PCR). *Nucleic Acids Research*, **21**, 4272–4280.
- BERTIOLI, D. J., SCHLICHTER, U. H. A., ADAMS, M. J., BURROWS, P. R., STEINBISS, H.-H. and ANTONIW, J. F., 1995, An analysis of differential display shows a strong bias towards high copy number mRNAs. *Nucleic Acids Research*, **23**, 4520–4523.
- BRAVO, R., 1990, Genes induced during the G0/G1 transition in mouse fibroblasts. *Seminars in Cancer Biology*, **1**, 37–46.
- BURN, T. C., PETROVICK, M. S., HOHAUS, S., ROLLINS, B. J. and TENEN, D. G., 1994, Monocyte chemoattractant protein-1 gene is expressed in activated neutrophils and retinoic acid-induced human myeloid cell lines. *Blood*, **84**, 2776–2783.
- CAO, J., CAI, X., ZHENG, L., GENG, L., SHI, Z., PAO, C. C. and ZHENG, S., 1997, Characterisation of colorectal cancer-related cDNA clones obtained by subtractive hybridisation screening. *Journal of Cancer Research and Clinical Oncology*, **123**, 447–451.
- CASSIDY, S. B., 1995, Uniparental disomy and genomic imprinting as causes of human genetic disease. *Environmental and Molecular Mutagenesis*, **25** (Suppl 26), 13–20.
- CHANG, G. W. and TERZAGHI-HOWE, M., 1998, Multiple changes in gene expression are associated with normal cell-induced modulation of the neoplastic phenotype. *Cancer Research*, **58**, 4445–4452.
- CHEN, J., SCHWARTZ, D. A., YOUNG, T. A., NORRIS, J. S. and YAGER, J. D., 1996, Identification of genes whose expression is altered during mitosis suppression in livers of ethinyl estradiol-treated female rats. *Carcinogenesis*, **17**, 2783–2786.
- CHEN, J. J. W. and PECK, K., 1996, Non-radioactive differential display method to directly visualise and amplify differential bands on nylon membrane. *Nucleic Acid Research*, **24**, 793–794.
- CLON TECHNIQUES, 1997a, PCR-Select Differential Screening Kit—the next step after Clontech PCR-Select cDNA subtraction. *ClonTechniques*, **XII**, 18–19.
- CLON TECHNIQUES, 1997b, Housekeeping RT-PCR amplimers and cDNA probes. *ClonTechniques*, **XII**, 15–16.
- DAVIS, M. M., COHEN, D. I., NIELSEN, E. A., STEINMETZ, M., PAUL, W. E. and HOOD, L., 1984, Cell-type-specific cDNA probes and the murine I region: the localization and orientation of Ad alpha. *Proceedings of the National Academy of Sciences (USA)*, **81**, 2194–2198.
- DELLAVALLE, R. P., PETERSON, R. and LINDQUIST, S., 1994, Preferential deadenylation of HSP70 mRNA plays a key role in regulating Hsp70 expression in *Drosophila melanogaster*. *Molecular and Cell Biology*, **14**, 3646–3659.
- DERISI, J. L., VASHWANATH, R. L. and BROWN, P., 1997, Exploring the metabolic and genetic control of gene expression on a genomic scale. *Science*, **278**, 680–686.
- DIATCHENKO, L., LAU, Y.-F. C., CAMPBELL, A. P., CHENCHIK, A., MOQADAM, F., HUANG, B., LUKYANOV, K., GURSKAYA, N., SVERDLOV, E. D. and SIEBERT, P. D., 1996, Suppression subtractive hybridisation: A method for generating differentially regulated or tissue-specific cDNA probes and libraries. *Proceedings of the National Academy of Sciences (USA)*, **93**, 6025–6030.
- DOGRA, S. C., WHITELAW, M. L. and MAY, B. K., 1998, Transcriptional activation of cytochrome P450 genes by different classes of chemical inducers. *Clinical and Experimental Pharmacology and Physiology*, **25**, 1–9.
- DUGUID, J. R. and DINAUER, M. C., 1990, Library subtraction of *in vitro* cDNA libraries to identify differentially expressed genes in scrapie infection. *Nucleic Acids Research*, **18**, 2789–2792.
- DUNBAR, P. R., OGG, G. S., CHEN, J., RUST, N., VAN DER BRUGGEN, P. and CERUNDOLO, V., 1998, Direct isolation, phenotyping and cloning of low-frequency antigen-specific cytotoxic T lymphocytes from peripheral blood. *Current Biology*, **26**, 413–416.

- FITZPATRICK, D. R., GERMAIN -LEE, E. and VALLE, D., 1995, Isolation and characterisation of rat and human cDNAs encoding a novel putative peroxisomal enoyl-CoA hydratase. *Genomics*, **27**, 457-466.
- FOSS, D. L., BAARSCH, M. J. and MURTAUGH, M. P., 1998, Regulation of hypoxanthine phosphoribosyltransferase, glyceraldehyde-3-phosphate dehydrogenase and beta-actin mRNA expression in porcine immune cells and tissues. *Animal Biotechnology*, **9**, 67-78.
- FRYE, R. A., BENZ, C. C. and LIU, E., 1989, Detection of amplified oncogenes by differential polymerase chain reaction. *Oncogene*, **4**, 1153-1157.
- GEISINGER, A., RODRIGUEZ, R., ROMERO, V. and WETTSTEIN, R., 1997, A simple method for screening cDNAs arising from the cloning of RNA differential display bands. *Elsevier Trends Journals Technical Tips Online*, <http://tto.trends.com>, document T01110.
- GRESS, T. M., HOEISEL, J. D., LENNON, G. G., ZEHETNER, G. and LEHRACH, H., 1992, Hybridisation fingerprinting of high density cDNA filter arrays with cDNA pools derived from whole tissues. *Mammalian Genome*, **3**, 609-619.
- GRIFFIN, G. and KRISHNA, S., 1998, Cytokines in infectious diseases. *Journal of the Royal College of Physicians, London*, **32**, 195-198.
- GROENINK, M. and LEEGWATER, A. C. J., 1996, Isolation of delayed early genes associated with liver regeneration using Clontech PCR-select subtraction technique. *Clontechniques*, **XI**, 23-24.
- GUIMARAES, M. J., BAZAN, J. F., ZLOTNIK, A., WILES, M. V., GRIMALDI, J. C., LEE, F. and MCCLANAHAN, T., 1995b, A new approach to the study of haematopoietic development in the yolk sac and embryoid bodies. *Development*, **121**, 3335-3346.
- GUIMARAES, M. J., LEE, F., ZLOTNIK, A. and MCCLANAHAN, T., 1995a, Differential display by PCR: novel findings and applications. *Nucleic Acids Research*, **23**, 1832-1833.
- GURSKAYA, N. G., DIATCHENKO, L., CHENCHIK, P. D., SIEBERT, P. D., KHASPEKOV, G. L., LUKYANOV, K. A., VAGNER, L. L., ERMOLAEVA, O. D., LUKYANOV, S. A. and SVERDLOV, E. D., 1996, Equalising cDNA subtraction based on selective suppression of polymerase chain reaction: Cloning of Jurkat cell transcripts induced by phytohemagglutinin and phorbol 12-Myristate 13-Acetate. *Analytical Biochemistry*, **240**, 90-97.
- HAMPSON, I. N. and HAMPSON, L., 1997, CCLS and DROP—subtractive cloning made easy. *Life Science News* (A publication of Amersham Life Science), **23**, 22-24.
- HAMPSON, I. N., HAMPSON, L. and DEXTER, T. M., 1996, Directional random oligonucleotide primed (DROP) global amplification of cDNA: its application to subtractive cDNA cloning. *Nucleic Acids Research*, **24**, 4832-4835.
- HAMPSON, I. N., POPE, L., COWLING, G. J. and DEXTER, T. M., 1992, Chemical cross linking subtraction (CCLS): a new method for the generation of subtractive hybridisation probes. *Nucleic Acids Research*, **20**, 2899.
- HARA, E., KATO, T., NAKADA, S., SEKIYA, S. and ODA, K., 1991, Subtractive cDNA cloning using oligo(dT)30-latex and PCR: isolation of cDNA clones specific to undifferentiated human embryonal carcinoma cells. *Nucleic Acids Research*, **19**, 7097-7104.
- HATADA, I., HAYASHIZAKE, Y., HIROTSUNE, S., KOMATSUBARA, H. and MUKAI, T., 1991, A genomic scanning method for higher organisms using restriction sites as landmarks. *Proceedings of the National Academy of Sciences (USA)*, **88**, 9523-9527.
- HECHT, N., 1998, Molecular mechanisms of male sperm cell differentiation. *Bioessays*, **20**, 555-561.
- HEDRICK, S., COHEN, D. I., NIELSEN, E. A. and DAVIS, M. E., 1984, Isolation of T cell-specific membrane-associated proteins. *Nature*, **308**, 149-153.
- HERTZ, R., SECKBACH, M., ZAKIN, M. M. and BAR-TANA, J., 1996, Transcriptional suppression of the transferrin gene by hypolipidemic peroxisome proliferators. *Journal of Biological Chemistry*, **271**, 218-224.
- HEUVAL, J. P. V., CLARK, G. C., KOHN, M. C., TRITSCHER, A. M., GREENLEE, W. F., LUCIER, G. W. and BELL, D. A., 1994, Dioxin-responsive genes: Examination of dose-response relationships using quantitative reverse transcriptase-polymerase chain reaction. *Cancer Research*, **54**, 62-68.
- HILLIER, L. D., LENNON, G., BECKER, M., BONALDO, M. F., CHIAPELLI, B., CHISSOE, S., DIETRICH, N., DUBUQUE, T., FAVELLO, A., GISH, W., HAWKINS, M., HULTMAN, M., KUCABA, T., LACY, M., LE, M., LE, N., MARDIS, E., MOORE, B., MORRIS, M., PARSONS, J., PRANGE, C., RIFKIN, L., ROHLFING, T., SCHELLENBERG, K., SOARES, M. B., TAN, F., THIERRY-MEG, J., TREVASKIS, E., UNDERWOOD, K., WOHLDMAN, P., WATERSTON, R., WILSON, R. and MARRA, M., 1996, Generation and analysis of 280,000 human expressed sequence tags. *Genome Research*, **6**, 807-828.
- HUBANK, M. and SCHATZ, D. G., 1994, Identifying differences in mRNA expression by representational difference analysis. *Nucleic Acids Research*, **22**, 5640-5648.
- HUNTER, T., 1991, Cooperation between oncogenes. *Cell*, **64**, 249-270.
- IVANOVA, N. B. and BELYAVSKY, A. V., 1995, Identification of differentially expressed genes by restriction endonuclease-based gene expression fingerprinting. *Nucleic Acids Research*, **23**, 2954-2958.
- JAMES, B. D. and HIGGINS, S. J., 1985, *Nucleic Acid Hybridisation* (Oxford: IRL Press Ltd).
- KAS-DEELEN, A. M., HARMSSEN, M. C., DE MAAR, E. F. and VAN SON, W. J., 1998, A sensitive method for

- quantifying cytomegalic endothelial cells in peripheral blood from cytomegalovirus-infected patients. *Clinical Diagnostic and Laboratory Immunology*, 5, 622-626.
- KILTY, I. and VICKERS, P., 1997, Fractionating DNA fragments generated by differential display PCR. *Strategies Newsletter* (Stratagene), 10, 50-51.
- KLEINJAN, D.-J. and VAN HEYNINGEN, V., 1998, Position effect in human genetic disease. *Human and Molecular Genetics*, 7, 1611-1618.
- KO, M. S., 1990, An 'equalized cDNA library' by the reassociation of short double-stranded cDNAs. *Nucleic Acids Research*, 18, 5705-5711.
- LAKE, B. G., EVANS, J. G., CUNNINGHAME, M. E. and PRICE, R. J., 1993, Comparison of the hepatic effects of Wy-14,643 on peroxisome proliferation and cell replication in the rat and Syrian hamster. *Environmental Health Perspectives*, 101, 241-248.
- LAKE, B. G., EVANS, J. G., GRAY, T. J. B., KOROSI, S. A. and NORTH, C. J., 1989, Comparative studies of nafenopin-induced hepatic peroxisome proliferation in the rat, Syrian hamster, guinea pig and marmoset. *Toxicology and Applied Pharmacology*, 99, 148-160.
- LENNARD, M. S., 1993, Genetically determined adverse drug reactions involving metabolism. *Drug Safety*, 9, 60-77.
- LEVY, S., TODD, S. C. and MAECKER, H. T., 1998, CD81(TAPA-1): a molecule involved in signal transduction and cell adhesion in the immune system. *Annual Review of Immunology*, 16, 89-109.
- LIANG, P. and PARDEE, A. B., 1992, Differential display of eukaryotic messenger RNA by means of the polymerase chain reaction. *Science*, 257, 967-971.
- LIANG, P., AVERBOUKH, L., KEYOMARSI, K., SAGER, R. and PARDEE, A., 1992, Differential display and cloning of messenger RNAs from human breast cancer versus mammary epithelial cells. *Cancer Research*, 52, 6966-6968.
- LIANG, P., AVERBOUKH, L. and PARDEE, A. B., 1993, Distribution & cloning of eukaryotic mRNAs by means of differential display refinements and optimisation. *Nucleic Acids Research*, 21, 3269-3275.
- LIANG, P., BAUER, D., AVERBOUKH, L., WARTHOF, P., ROHRWILD, M., MULLER, H., STRAUSS, M. and PARDEE, A. B., 1995, Analysis of altered gene expression by differential display. *Methods in Enzymology*, 254, 304-321.
- LINSKENS, M. H., FENG, J., ANDREWS, W. H., ENLOW, B. E., SAATI, S. M., TONKIN, L. A., FUNK, W. D. and VILLEPONTEAU, B., 1995, Cataloging altered gene expression in young and senescent cells using enhanced differential display. *Nucleic Acids Research*, 23, 3244-3251.
- LISITSYN, N., LISITSYN, N. and WIGLER, M., 1993, Cloning the differences between two complex genomes. *Science*, 259, 946-951.
- LOHMANN, J., SCHICKLE, H. and BOSCH, T. C. G., 1995, REN Display, a rapid and efficient method for non-radioactive differential display and mRNA isolation. *Biotechniques*, 18, 200-202.
- LUNNEY, J. K., 1998, Cytokines orchestrating the immune response. *Reviews in Science and Technology*, 17, 84-94.
- MAKOWSKA, J. M., GIBSON, G. G. and BONNER, F. W., 1992, Species differences in ciprofibrate induction of hepatic cytochrome P4504A1 and peroxisome proliferation. *Journal of Biochemical Toxicology*, 7, 183-191.
- MALDARELLI, F., XIANG, C., CHAMOUN, G. and ZEICHNER, S. L., 1998, The expression of the essential nuclear splicing factor SC35 is altered by human immunodeficiency virus infection. *Virus Research*, 53, 39-51.
- MATHIEU-DAUDE, F., CHENG, R., WELSH, J. and MCCLELLAND, M., 1996, Screening of differentially amplified cDNA products from RNA arbitrarily primed PCR fingerprints using single strand conformation polymorphism (SSCP) gels. *Nucleic Acids Research*, 24, 1504-1507.
- MCKENZIE, D. and DRAKE, D., 1997, Identification of differentially expressed gene products with the castaway system. *Strategies Newsletter* (Stratagene), 10, 19-20.
- MCCLELLAND, M., MATHIEU-DAUDE, F. and WELSH, J., 1996, RNA fingerprinting and differential display using arbitrarily primed PCR. *Trends in Genetics*, 11, 242-246.
- MECHLER, B. and RABBITTS, T. H., 1981, Membrane-bound ribosomes of myeloma cells. IV. mRNA complexity of free and membrane-bound polysomes. *Journal of Cell Biology*, 88, 29-36.
- MEYER, U. A. and ZANGER, U. M., 1997, Molecular mechanisms of genetic polymorphisms of drug metabolism. *Annual Review of Pharmacology and Toxicology*, 37, 269-296.
- MOHLER, K. M. and BUTLER, L. D., 1991, Quantitation of cytokine mRNA levels utilizing the reverse transcriptase-polymerase chain reaction following primary antigen-specific sensitization in vivo—I. Verification of linearity, reproducibility and specificity. *Molecular Immunology*, 28, 437-447.
- MURPHY, L. D., HERZOG, C. E., RUDICK, J. B., TITO FOJO, A. and BATES, S. E., 1990, Use of the polymerase chain reaction in the quantitation of the *mdr-1* gene expression. *Biochemistry*, 29, 10351-10356.
- NELSON, D. R., KOYMANS, L., KAMATAKI, T., STEGEMAN, J. J., FEYEREISEN, R., WAXMAN, D. J., WATERMAN, M. R., GOTOH, O., COON, M. J., ESTABROOK, R. W., GUNSALUS, I. C. and NEBERT, D. W., 1996, Update on new sequences, gene mapping, accession numbers and nomenclature. *Pharmacogenetics*, 6, 1-42.

- NISHIO, Y., AIELLO, L. P. and KING, G. L., 1994, Glucose induced genes in bovine aortic smooth muscle cells identified by mRNA differential display. *FASEB Journal*, **8**, 103–106.
- O'NEILL, M. J. and SINCLAIR, A. H., 1997, Isolation of rare transcripts by representational difference analysis. *Nucleic Acids Research*, **25**, 2681–2682.
- ORTON, T. C., ADAM, H. K., BENTLEY, M., HOLLOWAY, B. and TUCKER, M. J., 1984, Clobazart: species differences in the morphological and biochemical response of the liver following chronic administration. *Toxicology and Applied Pharmacology*, **73**, 138–151.
- PELKONEN, O., MAENPAA, J., TAAVITSAINEN, P., RAUTIO, A. and RAUNIO, H., 1998, Inhibition and Induction of human cytochrome P450 (CYP) enzymes. *Xenobiotica*, **28**, 1203–1253.
- PHILIPS, S. M., BENDALL, A. J. and RAMSHAW, I. A., 1990, Isolation of genes associated with high metastatic potential in rat mammary adenocarcinomas. *Journal of the National Cancer Institute*, **82**, 199–203.
- PRASHAR, Y. and WEISSMAN, S. M., 1996, Analysis of differential gene expression by display of 3' end restriction fragments of cDNAs. *Proceedings of the National Academy of Sciences (USA)*, **93**, 659–663.
- RAGNO, S., ESTRADA, I., BUTLER, R. and COLSTON, M. J., 1997, Regulation of macrophage gene expression following invasion by *Mycobacterium tuberculosis*. *Immunology Letters*, **57**, 143–146.
- RAMANA, K. V. and KOHLI, K. K., 1998, Gene regulation of cytochrome P450—an overview. *Indian Journal of Experimental Biology*, **36**, 437–446.
- RICHARD, L., VELASCO, P. and DETMAR, M., 1998, A simple immunomagnetic protocol for the selective isolation and long-term culture of human dermal microvascular endothelial cells. *Experimental Cell Research*, **240**, 1–6.
- ROCKETT, J. C., ESDAILE, D. J. and GIBSON, G. G., 1997, Molecular profiling of non-genotoxic hepatocarcinogenesis using differential display reverse transcription-polymerase chain reaction (ddRT-PCR). *European Journal of Drug Metabolism and Pharmacokinetics*, **22**, 329–333.
- RODRICKS, J. V. and TURNBULL, D., 1987, Inter-species differences in peroxisomes and peroxisome proliferation. *Toxicology and Industrial Health*, **3**, 197–212.
- ROGLER, G., HAUSMANN, M., VOGL, D., ASCHENBRENNER, E., ANDUS, T., FALK, W., ANDRESEN, R., SCHOLMERICH, J. and GROSS, V., 1998, Isolation and phenotypic characterization of colonic macrophages. *Clinical and Experimental Immunology*, **112**, 205–215.
- ROHN, W. M., LEE, Y. J. and BENVENISTE, E. N., 1996, Regulation of class II MHC expression. *Critical Reviews in Immunology*, **16**, 311–330.
- RUDIN, C. M. and THOMPSON, C. B., 1998, B-cell development and maturation. *Seminars in Oncology*, **25**, 435–446.
- SAKAGUCHI, N., BERGER, C. N. and MELCHERS, F., 1986, Isolation of a cDNA copy of an RNA species expressed in murine pre-B cells. *EMBO Journal*, **5**, 2139–2147.
- SAMBROOK, J., FRITSCH, E. F. and MANIATIS, T., 1989, Gel electrophoresis of DNA. In N. Ford, M. Nolan and M. Fergusen (eds), *Molecular Cloning—A laboratory manual*, 2nd edition (New York: Cold Spring Harbour Laboratory Press), Volume 1, pp. 6–37.
- SARGENT, T. D. and DAWID, I. B., 1983, Differential gene expression in the gastrula of *Xenopus laevis*. *Science*, **222**, 135–139.
- SCHENA, M., SHALON, D., HELLER, R., CHAI, A., BROWN, P. O. and DAVIS, R. W., 1996, Parallel human genome analysis: Microarray-based expression monitoring of 1000 genes. *Proceedings of the National Academy of Sciences (USA)*, **93**, 10614–10619.
- SCHNEIDER, C., KING, R. M. and PHILIPSON, L., 1988, Genes specifically expressed at growth arrest of mammalian cells. *Cell*, **54**, 787–793.
- SCHNEIDER-MAUNOURY, S., GILARDI-HEBENSTREIT, P. and CHARNAY, P., 1998, How to build a vertebrate hindbrain. Lessons from genetics. *C R Academy of Science III*, **321**, 819–834.
- SEMENZA, G. L., 1994, Transcriptional regulation of gene expression: mechanisms and pathophysiology. *Human Mutations*, **3**, 180–199.
- SEWALL, C. H., BELL, D. A., CLARK, G. C., TRITSCHER, A. M., TULLY, D. B., VANDEN HEUVEL, J. and LUCIER, G. W., 1995, Induced gene transcription: implications for biomarkers. *Clinical Chemistry*, **41**, 1829–1834.
- SINGH, N., AGRAWAL, S. and RASTOGI, A. K., 1997, Infectious diseases and immunity: special reference to major histocompatibility complex. *Emerging Infectious Diseases*, **3**, 41–49.
- SMITH, N. R., LI, A., ALDERSLEY, M., HIGH, A. S., MARKHAM, A. F. and ROBINSON, P. A., 1997, Rapid determination of the complexity of cDNA bands extracted from DDRT-PCR polyacrylamide gels. *Nucleic Acids Research*, **25**, 3552–3554.
- SOMPAYRAC, L., JANE, S., BURN, T. C., TENEN, D. G. and DANNA, K. J., 1995, Overcoming limitations of the mRNA differential display technique. *Nucleic Acids Research*, **23**, 4738–4739.
- ST JOHN, T. P. and DAVIS, R. W., 1979, Isolation of galactose-inducible DNA sequences from *Saccharomyces cerevisiae* by differential plaque filter hybridisation. *Cell*, **16**, 443–452.
- SUN, Y., HEGAMER, G. and COLBURN, N. H., 1994, Molecular cloning of five messenger RNAs differentially expressed in preneoplastic or neoplastic JB6 mouse epidermal cells: one is homologous to human tissue inhibitor of metalloproteinases-3. *Cancer Research*, **54**, 1139–1144.

- SUNG, Y. J. and DENMAN, R. B., 1997, Use of two reverse transcriptases eliminates false-positive results in differential display. *Biotechniques*, **23**, 462-464.
- SUTTON, G., WHITE, O., ADAMS, M. and KERLAVAGE, A., 1995, TIGR Assembler; A new tool for assembling large shotgun sequencing projects. *Genome Science and Technology*, **1**, 9-19.
- SUZUKI, Y., SEKIYA, T. and HAYASHI, K., 1991, Allele-specific polymerase chain reaction: a method for amplification and sequence determination of a single component among a mixture of sequence variants. *Analytical Biochemistry*, **192**, 82-84.
- SYED, V., GU, W. and HECHT, N. B., 1997, Sertoli cells in culture and mRNA differential display provide a sensitive early warning assay system to detect changes induced by xenobiotics. *Journal of Andrology*, **18**, 264-273.
- UITERLINDEN, A. G., SLAGBOOM, P., KNOOK, D. L. and VUJL, J., 1989, Two-dimensional DNA fingerprinting of human individuals. *Proceedings of the National Academy of Sciences (USA)*, **86**, 2742-2746.
- ULLMAN, K. S., NORTHROP, J. P., VERWEIJ, C. L. and CRABTREE, G. R., 1990, Transmission of signals from the T lymphocyte antigen receptor to the genes responsible for cell proliferation and immune function: the missing link. *Annual Review of Immunology*, **8**, 421-452.
- VASMATZIS, G., ESSAND, M., BRINKMANN, U., LEE, B. and PASTON, I., 1998, Discovery of three genes specifically expressed in human prostate by expressed sequence tag database analysis. *Proceedings of the National Academy of Sciences (USA)*, **95**, 300-304.
- VELCULESCU, V. E., ZHANG, L., VOGELSTEIN, B. and KINZLER, K. W., 1995, Serial analysis of gene expression. *Science*, **270**, 484-487.
- VOELTZ, G. K. and STEITZ, J. A., 1998, AuuuA sequences direct mRNA deadenylation uncoupled from decay during *Xenopus* early development. *Molecular and Cell Biology*, **18**, 7537-7545.
- VOGELSTEIN, B. and KINZLER, K. W., 1993, The multistep nature of cancer. *Trends in Genetics*, **9**, 138-141.
- WALTER, J., BELFIELD, M., HAMPSON, I. and READ, C., 1997, A novel approach for generating subtractive probes for differential screening by CCLS. *Life Science News*, **21**, 13-14.
- WAN, J. S., SHARP, S. J., POIRIER, G. M.-C., WAGAMAN, P. C., CHAMBERS, J., PYATI, J., HOM, Y.-L., GALINDO, J. E., HUVAR, A., PETERSON, P. A., JACKSON, M. R. and ERLANDER, M. G., 1996, Cloning differentially expressed mRNAs. *Nature Biotechnology*, **14**, 1685-1691.
- WALTER, J., BELFIELD, M., HAMPSON, I. and READ, C., 1997, A novel approach for generating subtractive probes for differential screening by CCLS. *Life Science News*, **21**, 13-14.
- WANG, Z. and BROWN, D. D., 1991, A gene expression screen. *Proceedings of the National Academy of Sciences (USA)*, **88**, 11505-11509.
- WAWER, C., RUGGEBERG, H., MEYER, G. and MUYZER, G., 1995, A simple and rapid electrophoresis method to detect sequence variation in PCR-amplified DNA fragments. *Nucleic Acids Research*, **23**, 4928-4929.
- WELSH, J., CHADA, K., DALAL, S. S., CHENG, R., RALPH, D. and MCCLELLAND, M., 1992, Arbitrarily primed PCR fingerprinting of RNA. *Nucleic Acids Research*, **20**, 4965-4970.
- WONG, H., ANDERSON, W. D., CHENG, T. and RIABOWOL, K. T., 1994, Monitoring mRNA expression by polymerase chain reaction: the 'primer-dropping' method. *Analytical Biochemistry*, **223**, 251-258.
- WONG, K. K. and MCCLELLAND, M., 1994, Stress-inducible gene of *Salmonella typhimurium* identified by arbitrarily primed PCR of RNA. *Proceedings of the National Academy of Sciences (USA)*, **91**, 639-643.
- WYNFORD-THOMAS, D., 1991, Oncogenes and anti-oncogenes; the molecular basis of tumour behaviour. *Journal of Pathology*, **165**, 187-201.
- XHU, D., CHAN, W. L., LEUNG, B. P., HUANG, F. P., WHEELER, R., PIEDRAFITA, D., ROBINSON, J. H. and LIEW, F. Y., 1998, Selective expression of a stable cell surface molecule on type 2 but not type 1 helper T cells. *Journal of Experimental Medicine*, **187**, 787-794.
- YANG, M. and SYTOWSKI, A. J., 1996, Cloning differentially expressed genes by linker capture subtraction. *Analytical Biochemistry*, **237**, 109-114.
- ZHAO, N., HASHIDA, H., TAKAHASHI, N., MISUMI, Y. and SAKAKI, Y., 1995, High-density cDNA filter analysis: a novel approach for large scale quantitative analysis of gene expression. *Gene*, **156**, 207-213.
- ZHAO, X. J., NEWSOME, J. T. and CIHLAR, R. L., 1998, Up-regulation of two *Candida albicans* genes in the rat model of oral candidiasis detected by differential display. *Microbial Pathogenesis*, **25**, 121-129.
- ZIMMERMANN, C. R., ORR, W. C., LECLERC, R. F., BARNARD, C. and TIMBERLAKE, W. E., 1980, Molecular cloning and selection of genes regulated in *Aspergillus* development. *Cell*, **21**, 709-715.

Whole genome analysis: Experimental access to all genome sequenced segments through larger-scale efficient oligonucleotide synthesis and PCR

DEVAL A. LASHKARI*†, JOHN H. MCCUSKER‡, AND RONALD W. DAVIS*§

*Departments of Genetics and Biochemistry, Beckman Center, Stanford University, Stanford, CA 94305; and ‡Department of Microbiology, 3020 Duke University Medical Center, Durham, NC 27710

Contributed by Ronald W. Davis, May 20, 1997

ABSTRACT The recent ability to sequence whole genomes allows ready access to all genetic material. The approaches outlined here allow automated analysis of sequence for the synthesis of optimal primers in an automated multiplex oligonucleotide synthesizer (AMOS). The efficiency is such that all ORFs for an organism can be amplified by PCR. The resulting amplicons can be used directly in the construction of DNA arrays or can be cloned for a large variety of functional analyses. These tools allow a replacement of single-gene analysis with a highly efficient whole-genome analysis.

The genome sequencing projects have generated and will continue to generate enormous amounts of sequence data. The genomes of *Saccharomyces cerevisiae*, *Escherichia coli*, *Haemophilus influenzae* (1), *Mycoplasma genitalium* (2), and *Methanococcus jannaschii* (3) have been completely sequenced. Other model organisms have had substantial portions of their genomes sequenced as well, including the nematode *Caenorhabditis elegans* (4) and the small flowering plant *Arabidopsis thaliana* (5). This massive and increasing amount of sequence information allows the development of novel experimental approaches to identify gene function.

One standard use of genome sequence data is to attempt to identify the functions of predicted open reading frames (ORFs) within the genome by comparison to genes of known function. Such a comparative analysis of all ORFs to existing sequence data is fast, simple, and requires no experimentation and is therefore a reasonable first step. While finding sequence homologies/motifs is not a substitute for experimentation, noting the presence of sequence homology and/or sequence motifs can be a useful first step in finding interesting genes, in designing experiments and, in some cases, predicting function. However, this type of analysis is frequently uninformative. For example, over one-half of new ORFs in *S. cerevisiae* have no known function (6). If this is the case in a well studied organism such as yeast, the problem will be even worse in organisms that are less well studied or less manipulable. A large, experimentally determined gene function database would make homology/motif searches much more useful.

Experimental analysis must be performed to thoroughly understand the biological function of a gene product. Scaling up from classical "cottage industry" one-gene-oriented approaches to whole-genome analysis would be very expensive and laborious. It is clear that novel strategies are necessary to efficiently pursue the next phase of the genome projects—whole-genome experimental analysis to explore gene expression, gene product function, and other genome functions. Model organisms, such as *S. cerevisiae*, will be extremely

important in the development of novel whole-genome analysis techniques and, subsequently, in improving our understanding of other more complex and less manipulable organisms.

The genome sequence can be systematically used as a tool to understand ORFs, gene product function, and other genome regions. Toward this end, a directed strategy has been developed for exploiting sequence information as a means of providing information about biological function (Fig. 1). Efforts have been directed toward the amplification of each predicted ORF or any other region of the genome ranging from a few base pairs to several kilobase pairs. There are many uses for these amplicons—they can be cloned into standard vectors or specialized expression vectors, or can be cloned into other specialized vectors such as those used for two-hybrid analysis. The amplicons can also be used directly by, for example, arraying onto glass for expression analysis, for DNA binding assays, or for any direct DNA assay (7). As a pilot study, synthetic primers were made on the 96-well automated multiplex oligonucleotide synthesizer (AMOS) instrument (8) (Fig. 2). These oligonucleotides were used to amplify each ORF on yeast chromosome V. The current version of this instrument can synthesize three plates of 96 oligonucleotides each (25 bases) in an 8-hr day. The amplification of the entire set of PCR products was then analyzed by gel electrophoresis (Fig. 3). Successful amplification of the proper length product on the first attempt was 95%. This project demonstrates that one can go directly from sequence information to biological analysis in a truly automated, totally directed manner.

These amplicons can be incorporated directly in arrays or the amplicons can be cloned. If the amplicons are to be cloned, novel sequences can be incorporated at the 5' end of the oligonucleotide to facilitate cloning. One potential problem with cloning PCR products is that the cloned amplicons may contain sequence alterations that diminish their utility. One option would be to resequence each individual amplicon. However, this is expensive, inefficient, and time consuming. A faster, more cost-effective, and more accurate approach is to apply comparative sequencing by denaturing HPLC (9). This method is capable of detecting a single base change in a 2-kb heteroduplex. Longer amplicons can be analyzed by use of appropriate restriction fragments. If any change is detected in a clone, an alternate clone of the same region can be analyzed. Modifying the system to allow high throughput analysis by denaturing HPLC is also relatively simple and straightforward.

If amplicons are used directly on arrays without cloning, it is important to note that, even if single PCR product bands are observed on gels, the PCR products will be contaminated with various amounts of other sequences. This contamination has the potential to affect the results in, for example, expression

The publication costs of this article were defrayed in part by page charge payment. This article must therefore be hereby marked "advertisement" in accordance with 18 U.S.C. §1734 solely to indicate this fact.

© 1997 by The National Academy of Sciences 0027-8424/97/948945-3\$2.00/0
PNAS is available online at <http://www.pnas.org>.

†Present address: Synteni, Inc., 6519 Dumbarton Circle, Fremont, CA 94555.

§To whom reprint requests should be addressed at: Department of Biochemistry, Beckman Center, B400, Stanford University, Stanford, CA 94305-5307. e-mail: gilbert@cmgm.stanford.edu.

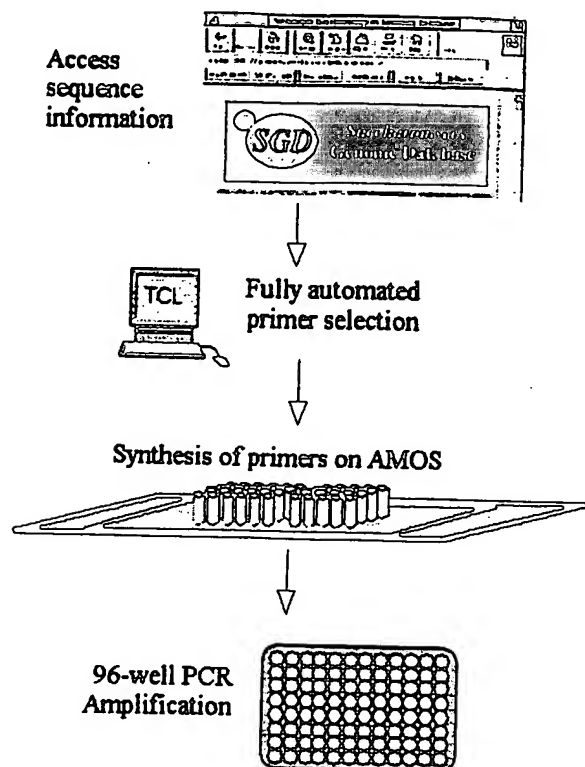


FIG. 1. Overview of systematic method for isolating individual genes. Sequence information is obtained automatically from sequence databases. The data are input into primer selection software specifically designed to target ORFs as designated by database annotations. The output file containing the primer information is directly read by a high-throughput oligonucleotide synthesizer, which makes the oligonucleotides in 96-well plates (AMOS, automated multiplex oligonucleotide synthesizer). The forward and reverse primers are synthesized in the same location on separate plates to facilitate the downstream handling of primers. The amplicons are generated by PCR in 96-well plates as well.

analysis. On the other hand, direct use of the amplicons is much less labor intensive and greatly decreases the occurrence of mistakes in clone identification, a ubiquitous problem associated with large clone set archiving and retrieving.

Any large-scale effort to capture each ORF within a genome must rely on automation if cost is to be minimized while efficiency is maximized. Toward that end, primers targeting ORFs were designed automatically using simple new scripts and existing primer selection software. These script-selected primer sequences were directly read by the high-throughput synthesizer and the forward and reverse primers were synthesized in separate plates in corresponding wells to facilitate automated pipetting and PCR amplifications. Each of the resulting PCR products, generated with minimum labor, contains a known, unique ORF.

Large-scale genome analysis projects are dependent on newly emerging technologies to make the studies practical and economically feasible. For example, the cost of the primers, a significant issue in the past, has been reduced dramatically to make feasible this and other projects that require tens of thousands of oligonucleotides. Other methods of high-throughput analysis are also vital to the success of functional analysis projects, such as microarraying and oligonucleotide chip methods (10–14).

Changes in attitude are also required. One of the major costs of commercial oligonucleotides is extensive quality control such that virtually 100% of the supplied oligonucleotides are successfully synthesized and work for their intended purpose.

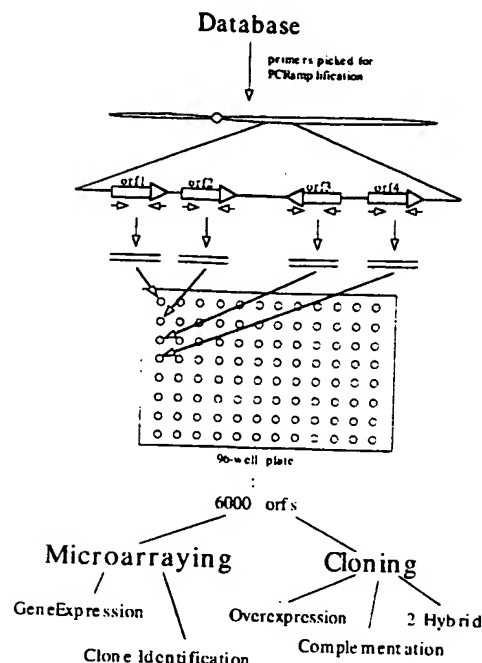


FIG. 2. Overall approach for using database of a genome to direct biological analysis. The synthesis of the 6,000 ORFs (orfs) for each gene of *S. cerevisiae* can be used in many applications utilizing both cloning and microarraying technology.

Considerable cost reduction can be obtained by simply decreasing the expected successful synthesis rate to 95–97%. One can then achieve faster and cheaper whole genome coverage by simply adding a single quality control at the end of the experiment and batching the failures for resynthesis.

The directed nature of the amplicon approach is of clear advantage. The sequence of each ORF is analyzed automatically, and unique specific primers are made to target each ORF. Thus, there is relatively little time or labor involved—for example, no random cloning and subsequent screening is required because each product is known. In the test system, primers for 240 ORFs from chromosome V were systematically synthesized, beginning from the left arm and continuing through to the right arm. At no point was there any manual analysis of sequence information to generate the collection. In many ways, now that the sequence is known, there is no need for the researcher to examine it.

These amplicons can be arrayed and expression analysis can be done on all arrayed ORFs with a single hybridization (10). Those ORFs that display significant differential expression patterns under a given selection are easily identified without the laborious task of searching for and then sequencing a clone. Once scaled up, the procedure provides even greater returns on effort, because a single hybridization will ultimately provide a "snapshot" of the expression of all genes in the yeast genome. Thus, the limiting factor in whole genome analysis will not be the analysis process itself, but will instead be the ability of researchers to design and carry out experimental selections.

Current expression and genetic analysis technologies are geared toward the analysis of single genes and are ill suited to analyze numerous genes under many conditions. Additional difficulties with current technologies include: the effort and expense required to analyze expression and make mutants, the potential duplication of effort if done by different laboratories, and the possibility of conflicting results obtained from different laboratories. In contrast, whole genome analysis not only is more efficient, it also provides data of much higher quality; all genes are assayed and compared in parallel under exactly

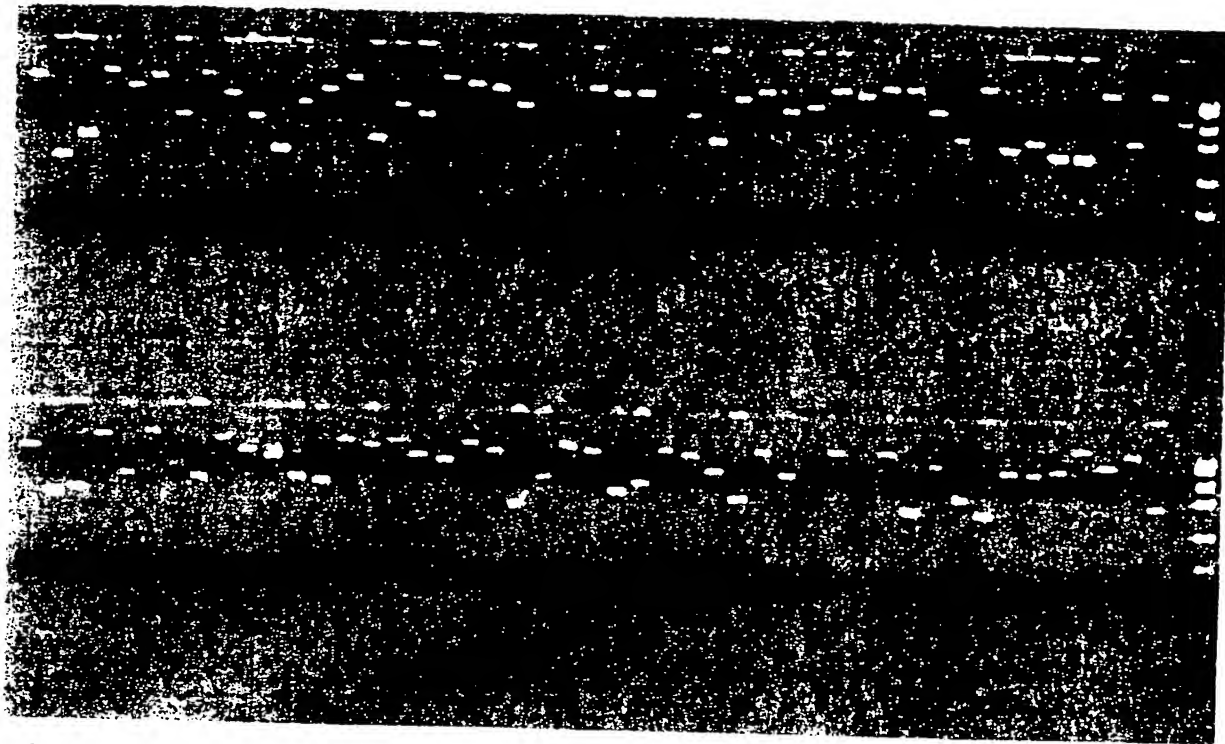


FIG. 3. Gel image of amplifications. Using the method described in Fig. 1, amplicons were generated for ORFs of *S. cerevisiae* chromosome V. One plate of 96 amplification reactions is shown.

the same conditions. In addition, amplicons have many applications beyond gene expression. For example, one recent approach is to incorporate a unique DNA sequence tag, synthesized as part of each gene specific primer, during amplification. The tags or molecular bar codes, when reintroduced into the organism as a gene deletion or as a gene clone, can be used much more efficiently than individual mutations or clones because pools of tagged mutants or transformants can be analyzed in parallel. This parallel analysis is possible because the tags are readily and quantitatively amplified even in complex mixtures of tags (13).

These ORF genome arrays and oligonucleotide tagged libraries can be used for many applications. Any conventional selection applied to a library that gives discrete or multiple products can use these technologies for a simple direct read-out. These include screens and selections for mutant complementation, overexpression suppression (15, 16), second-site suppressors, synthetic lethality, drug target overexpression (17), two-hybrid screens (18), genome mismatch scanning (19), or recombination mapping.

The genome projects have provided researchers with a vast amount of information. These data must be used efficiently and systematically to gain a truly comprehensive understanding of gene function and, more broadly, of the entire genome which can then be applied to other organisms. Such global approaches are essential if we are to gain an understanding of the living cell. This understanding should come from the viewpoint of the integration of complex regulatory networks, the individual roles and interactions of thousands of functional gene products, and the effect of environmental changes on both gene regulatory networks and the roles of all gene products. The time has come to switch from the analysis of a single gene to the analysis of the whole genome.

Support was provided by National Institutes of Health Grants R37H60198 and P01H600205.

1. Fleischmann, R. D., Adams, M. D., White, O., Clayton, R. A., Kirkness, E. F., *et al.* (1995) *Science* **269**, 496–512.
2. Fraser, C. M., Gocayne, J. D., White, O., Adams, M. D., Clayton, R. A., *et al.* (1995) *Science* **270**, 397–403.
3. Bult, C. J., White, O., Olsen, G. J., Zhou, L., Fleischmann, R. D., *et al.* (1996) *Science* **273**, 1058–1073.
4. Sulston, J., Du, Z., Thomas, K., Wilson, R., Hillier, L., Staden, R., Halloran, N., Green, P., Thierry-Mieg, J., Qiu, L., Dear, S., Coulson, A., Craxton, M., Durbin, R., Berks, M., Metzstein, M., Hawkins, T., Ainscough, R., & Waterston, R. (1992) *Nature (London)* **356**, 37–41.
5. Newman, T., de Bruijn, F. J., Green, P., Keegstra, K., Kende, H., *et al.* (1994) *Plant Physiol.* **106**, 1241–1255.
6. Oliver, S. (1996) *Nature (London)* **379**, 597–600.
7. Lashkari, D. A. (1996) Ph.D. dissertation (Stanford Univ., Stanford, CA).
8. Lashkari, D. A., Hunicke-Smith, S. P., Norgren, R. M., Davis, R. W., & Brennan, T. (1995) *Proc. Natl. Acad. Sci. USA* **92**, 7912–7915.
9. Oefner, P. J. & Underhill, P. A. (1995) *Am. J. Hum. Genet.* **57**, A266.
10. Schena, M., Shalon, D., Davis, R. W., & Brown, P. O. (1995) *Science* **270**, 467–470.
11. Fodor, S. P., Read, J. L., Pirrung, M. C., Stryer, L., Lu, A. T., & Solas, D. (1991) *Science* **251**, 767–773.
12. Chee, M., Yang, R., Hubbell, E., Berno, A., Huang, X. C., Stern, D., Winkler, J., Lockhart, D. J., Morris, M. S., & Fodor, S. P. (1996) *Science* **274**, 610–614.
13. Shoemaker, D. D., Lashkari, D. A., Morris, D., Mittmann, M., & Davis, R. W. (1996) *Nat. Genet.* **14**, 450–456.
14. Smith, V., Chou, K., Lashkari, D., Botstein, D., & Brown, P. O. (1996) *Science* **274**, 2069–2074.
15. Magdolen, V., Drubin, D. G., Mages, G., & Bandlow, W. (1993) *FEBS Lett.* **316**, 41–47.
16. Ramer, S. W., Elledge, S. J., & Davis, R. W. (1992) *Proc. Natl. Acad. Sci. USA* **89**, 11589–11593.
17. Rine, J., Hansen, W., Hardeman, E., & Davis, R. W. (1983) *Proc. Natl. Acad. Sci. USA* **80**, 6750–6754.
18. Fields, S., & Song, O. (1989) *Nature (London)* **340**, 245–246.
19. Nelson, S. F., McCusker, J. H., Sander, M. A., Kee, Y., Modrich, P., & Brown, P. O. (1994) *Nat. Genet.* **4**, 11–18.

IN PERSPECTIVE

Claudio J. Conti, Editor

Microarrays and Toxicology: The Advent of Toxicogenomics

Emile F. Nuwaysir,¹ Michael Bittner,² Jeffrey Trent,² J. Carl Barrett,¹ and Cynthia A. Afshari¹

¹Laboratory of Molecular Carcinogenesis, National Institute of Environmental Health Sciences, Research Triangle Park, North Carolina

²Laboratory of Cancer Genetics, National Human Genome Research Institute, Bethesda, Maryland

The availability of genome-scale DNA sequence information and reagents has radically altered life-science research. This revolution has led to the development of a new scientific subdiscipline derived from a combination of the fields of toxicology and genomics. This subdiscipline, termed toxicogenomics, is concerned with the identification of potential human and environmental toxicants, and their putative mechanisms of action, through the use of genomics resources. One such resource is DNA microarrays or "chips," which allow the monitoring of the expression levels of thousands of genes simultaneously. Here we propose a general method by which gene expression, as measured by cDNA microarrays, can be used as a highly sensitive and informative marker for toxicity. Our purpose is to acquaint the reader with the development and current state of microarray technology and to present our view of the usefulness of microarrays to the field of toxicology. *Mol. Carcinog.* 24:153-159, 1999. © 1999 Wiley-Liss, Inc.

Key words: toxicology; gene expression; animal bioassay

INTRODUCTION

Technological advancements combined with intensive DNA sequencing efforts have generated an enormous database of sequence information over the past decade. To date, more than 3 million sequences, totaling over 2.2 billion bases [1], are contained within the GenBank database, which includes the complete sequences of 19 different organisms [2]. The first complete sequence of a free-living organism, *Haemophilus influenzae*, was reported in 1995 [3] and was followed shortly thereafter by the first complete sequence of a eukaryote, *Saccharomyces cerevisiae* [4]. The development of dramatically improved sequencing methodologies promises that complete elucidation of the *Homo sapiens* DNA sequence is not far behind [5].

To exploit more fully the wealth of new sequence information, it was necessary to develop novel methods for the high-throughput or parallel monitoring of gene expression. Established methods such as northern blotting, RNase protection assays, S1 nuclease analysis, plaque hybridization, and slot blots do not provide sufficient throughput to effectively utilize the new genomics resources. Newer methods such as differential display [6], high-density filter hybridization [7,8], serial analysis of gene expression [9], and cDNA- and oligonucleotide-based microarray "chip" hybridization [10-12] are possible solutions to this bottleneck. It is our belief that the microarray approach, which allows the monitoring of expression levels of thousands of genes simultaneously, is a tool of unprecedented power for use in toxicology studies.

Almost without exception, gene expression is altered during toxicity, as either a direct or indirect result of toxicant exposure. The challenge facing toxicologists is to define, under a given set of experimental conditions, the characteristic and specific pattern of gene expression elicited by a given toxicant. Microarray technology offers an ideal platform for this type of analysis and could be the foundation for a fundamentally new approach to toxicology testing.

MICROARRAY DEVELOPMENT AND APPLICATIONS

cDNA Microarrays

In the past several years, numerous systems were developed for the construction of large-scale DNA arrays. All of these platforms are based on cDNAs or oligonucleotides immobilized to a solid support. In the cDNA approach, cDNA (or genomic) clones of interest are arrayed in a multi-well format and amplified by polymerase chain reaction. The products of this amplification, which are usually 500- to 2000-bp clones from the 3' regions of the genes of interest, are then spotted onto solid support by using high-speed robotics. By using this method, microarrays of up to 10 000 clones can be generated by spotting onto a glass substrate

*Correspondence to: Laboratory of Molecular Carcinogenesis, National Institute of Environmental Health Sciences, 111 Alexander Drive, Research Triangle Park, NC 27709.

Received 8 December 1998; Accepted 5 January 1999

Abbreviations: PAH, polycyclic aromatic hydrocarbon; NIEHS, National Institute of Environmental Health Sciences.

[13,14]. Sample detection for microarrays on glass involves the use of probes labeled with fluorescent or radioactive nucleotides.

Fluorescent cDNA probes are generated from control and test RNA samples in single-round reverse-transcription reactions in the presence of fluorescently tagged dUTP (e.g., Cy3-dUTP and Cy5-dUTP), which produces control and test products labeled with different fluors. The cDNAs generated from these two populations, collectively termed the "probe," are then mixed and hybridized to the array under a glass coverslip [10,11,15]. The fluorescent signal is detected by using a custom-designed scanning confocal microscope equipped with a motorized stage and lasers for fluor excitation [10,11,15]. The data are analyzed with custom digital image analysis software that determines for each DNA feature the ratio of fluor 1 to fluor 2, corrected for local background [16,17]. The strength of this approach lies in the ability to label RNAs from control and treated samples with different fluorescent nucleotides, allowing for the simultaneous hybridization and detection of both populations on one microarray. This method eliminates the need to control for hybridization between arrays. The research groups of Drs. Patrick Brown and Ron Davis at Stanford University spearheaded the effort to develop this approach, which has been successfully applied to studies of *Arabidopsis thaliana* RNA [10], yeast genomic DNA [15], tumorigenic versus non-tumorigenic human tumor cell lines [11], human T-cells [18], yeast RNA [19], and human inflammatory disease-related genes [20]. The most dramatic result of this effort was the first published account of gene expression of an entire genome, that of the yeast *Saccharomyces cerevisiae* [21].

In an alternative approach, large numbers of cDNA clones can be spotted onto a membrane support, albeit at a lower density [7,22]. This method is useful for expression profiling and large-scale screening and mapping of genomic or cDNA clones [7,22–24]. In expression profiling on filter membranes, two different membranes are used simultaneously for control and test RNA hybridizations, or a single membrane is stripped and reprobed. The signal is detected by using radioactive nucleotides and visualized by phosphorimager analysis or autoradiography. Numerous companies now sell such cDNA membranes and software to analyze the image data [25–27].

Oligonucleotide Microarrays

Oligonucleotide microarrays are constructed either by spotting prefabricated oligos on a glass support [13] or by the more elegant method of direct in situ oligo synthesis on the glass surface by photolithography [28–30]. The strength of this approach lies in its ability to discriminate DNA molecules based on single base-pair difference. This allows the application of this method to the fields of medical diagnos-

tics, pharmacogenetics, and sequencing by hybridization as well as gene-expression analysis.

Fabrication of oligonucleotide chips by photolithography is theoretically simple but technically complex [29,30]. The light from a high-intensity mercury lamp is directed through a photolithographic mask onto the silica surface, resulting in deprotection of the terminal nucleotides in the illuminated regions. The entire chip is then reacted with the desired free nucleotide, resulting in selected chain elongation. This process requires only $4n$ cycles (where n = oligonucleotide length in bases) to synthesize a vast number of unique oligos, the total number of which is limited only by the complexity of the photolithographic mask and the chip size [29,31,32].

Sample preparation involves the generation of double-stranded cDNA from cellular poly(A)⁺ RNA followed by antisense RNA synthesis in an in vitro transcription reaction with biotinylated or fluor-tagged nucleotides. The RNA probe is then fragmented to facilitate hybridization. If the indirect visualization method is used, the chips are incubated with fluor-linked streptavidin (e.g., phycoerythrin) after hybridization [12,33]. The signal is detected with a custom confocal scanner [34]. This method has been applied successfully to the mapping of genomic library clones [35], to de novo sequencing by hybridization [28,36], and to evolutionary sequence comparison of the *BRCA1* gene [37]. In addition, mutations in the cystic fibrosis [38] and *BRCA1* [39] gene products and polymorphisms in the human immunodeficiency virus-1 clade B protease gene [40] have been detected by this method. Oligonucleotide chips are also useful for expression monitoring [33] as has been demonstrated by the simultaneous evaluation of gene-expression patterns in nearly all open reading frames of the yeast strain *S. cerevisiae* [12]. More recently, oligonucleotide chips have been used to help identify single nucleotide polymorphisms in the human [41] and yeast [42] genomes.

THE USE OF MICROARRAYS IN TOXICOLOGY

Screening for Mechanism of Action

The field of toxicology uses numerous in vivo model systems, including the rat, mouse, and rabbit, to assess potential toxicity and these bioassays are the mainstay of toxicology testing. However, in the past several decades, a plethora of in vitro techniques have been developed to measure toxicity, many of which measure toxicant-induced DNA damage. Examples of these assays include the Ames test, the Syrian hamster embryo cell transformation assay, micronucleus assays, measurements of sister chromatid exchange and unscheduled DNA synthesis, and many others. Fundamental to all of these methods is the fact that toxicity is often preceded by, and results in, alterations in gene expression. In many cases, these changes in gene expression are a

far more sensitive, characteristic, and measurable endpoint than the toxicity itself. We therefore propose that a method based on measurements of the genome-wide gene expression pattern of an organism after toxicant exposure is fundamentally informative and complements the established methods described above.

We are developing a method by which toxicants can be identified and their putative mechanisms of action determined by using toxicant-induced gene expression profiles. In this method, in one or more defined model systems, dose and time-course parameters are established for a series of toxicants within a given prototypic class (e.g., polycyclic aromatic hydrocarbons (PAHs)). Cells are then treated with these agents at a fixed toxicity level (as measured by cell survival), RNA is harvested, and toxicant-induced gene expression changes are assessed by hybridization to a cDNA microarray chip (Figure 1). We have developed a custom DNA chip, called ToxChip v1.0, specifically for this purpose and will discuss it in more detail below. The changes in gene expression induced by the test agents in the model systems are analyzed, and the common set of changes unique to that class of toxicants, termed a toxicant signature, is determined.

This signature is derived by ranking across all experiments the gene-expression data based on rela-

tive fold induction or suppression of genes in treated samples versus untreated controls and selecting the most consistently different signals across the sample set. A different signature may be established for each prototypic toxicant class. Once the signatures are determined, gene-expression profiles induced by unknown agents in these same model systems can then be compared with the established signatures. A match assigns a putative mechanism of action to the test compound. Figure 2 illustrates this signature method for different types of oxidant stressors, PAHs, and peroxisome proliferators. In this example, the unknown compound in question had a gene-expression profile similar to that of the oxidant stressors in the database. We anticipate that this general method will also reveal cross talk between different pathways induced by a single agent (e.g., reveal that a compound has both PAH-like and oxidant-like properties). In the future, it may be necessary to distinguish very subtle differences between compounds within a very large sample set (e.g., thousands of highly similar structural isomers in a combinatorial chemistry library or peptide library). To generate these highly refined signatures, standard statistical clustering techniques or principal-component analysis can be used.

For the studies outlined in Figure 2, we developed the custom cDNA microarray chip ToxChip v1.0.

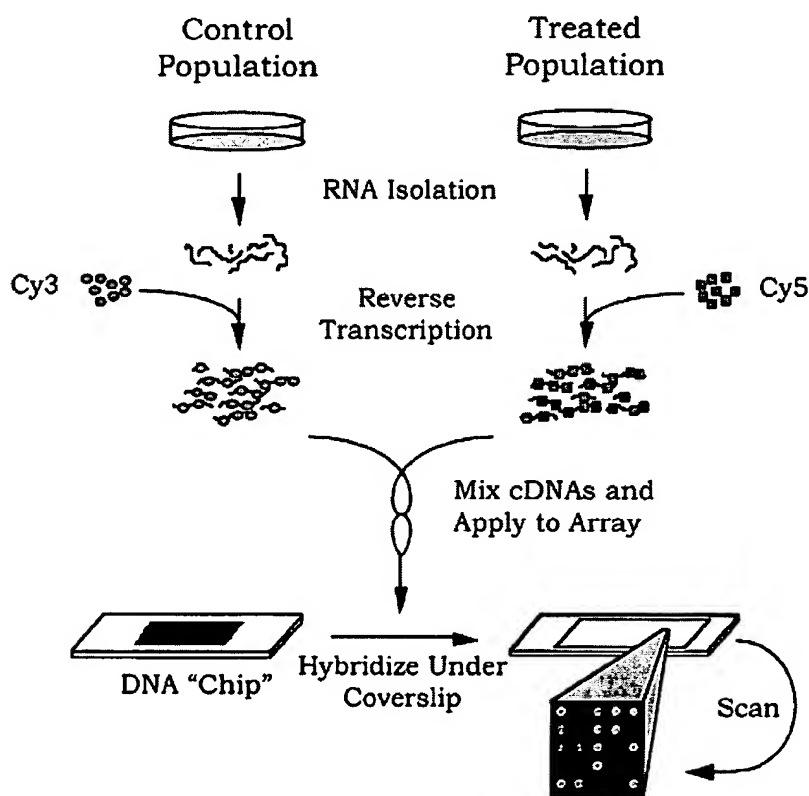


Figure 1. Simplified overview of the method for sample preparation and hybridization to cDNA microarrays. For illus-

trative purposes, samples derived from cell culture are depicted, although other sample types are amenable to this analysis.

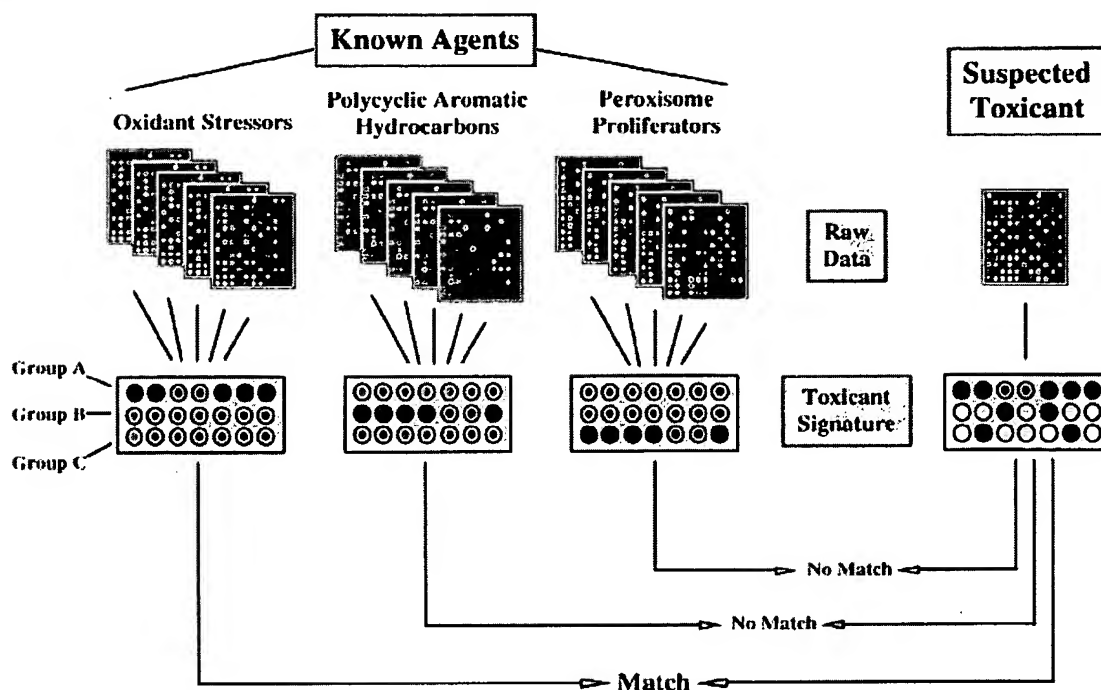


Figure 2. Schematic representation of the method for identification of a toxicant's mechanism of action. In this method, gene-expression data derived from exposure of model systems to known toxicants are analyzed, and a set of changes characteristic to that type of toxicant (termed the toxicant signature) is identified. As depicted, oxidant stressors produce

consistent changes in group A genes (indicated by red and green circles), but not group B or C genes (indicated by gray circles). The set of gene-expression changes elicited by the suspected toxicant is then compared with these characteristic patterns, and a putative mechanism of action is assigned to the unknown agent.

The 2090 human genes that comprise this subarray were selected for their well-documented involvement in basic cellular processes as well as their responses to different types of toxic insult. Included on this list are DNA replication and repair genes, apoptosis genes, and genes responsive to PAHs and dioxin-like compounds, peroxisome proliferators, estrogenic compounds, and oxidant stress. Some of the other categories of genes include transcription factors, oncogenes, tumor suppressor genes, cyclins, kinases, phosphatases, cell adhesion and motility genes, and homeobox genes. Also included in this group are 84 housekeeping genes, whose hybridization intensity is averaged and used for signal normalization of the other genes on the chip. To date, very few toxicants have been shown to have appreciable effects on the expression of these housekeeping genes. However, this housekeeping list will be revised if new data warrant the addition or deletion of a particular gene. Table 1 contains a general description of some of the different classes of genes that comprise ToxChip v1.0.

When a toxicant signature is determined, the genes within this signature are flagged within the database. When uncharacterized toxicants are then screened, the data can be quickly reformatted so that blocks of genes representing the different signatures

are displayed [11]. This facilitates rapid, visual interpretation of data. We are also developing ToxChip v2.0 and chips for other model systems, including rat, mouse, *Xenopus*, and yeast, for use in toxicology studies.

Animal Models in Toxicology Testing

The toxicology community relies heavily on the use of animals as model systems for toxicology testing. Unfortunately, these assays are inherently expensive, require large numbers of animals and take a long time to complete and analyze. Therefore, the National Institute of Environmental Health Sciences (NIEHS), the National Toxicology Program, and the toxicology community at large are committed to reducing the number of animals used, by developing more efficient and alternative testing methodologies. Although substantial progress has been made in the development of alternative methods, bioassays are still used for testing endpoints such as neurotoxicity, immunotoxicity, reproductive and developmental toxicology, and genetic toxicology. The rodent cancer bioassay is a particularly expensive and time-consuming assay, as it requires almost 4 yr, 1200 animals, and millions of dollars to execute and analyze [43]. In vitro experiments of the type outlined in Figure 2 might provide evidence that an unknown

Table 1. ToxChip v1.0: A Human cDNA Microarray Chip Designed to Detect Responses to Toxic Insult

Gene category	No. of genes on chip
Apoptosis	72
DNA replication and repair	99
Oxidative stress/redox homeostasis	90
Peroxisome proliferator responsive	22
Dioxin/PAH responsive	12
Estrogen responsive	63
Housekeeping	84
Oncogenes and tumor suppressor genes	76
Cell-cycle control	51
Transcription factors	131
Kinases	276
Phosphatases	88
Heat-shock proteins	23
Receptors	349
Cytochrome P450s	30

*This list is intended as a general guide. The gene categories are not unique, and some genes are listed in multiple categories.

agent is (or is not) responsible for eliciting a given biological response. This information would help to select a bioassay more specifically suited to the agent in question or perhaps suggest that a bioassay is not necessary, which would dramatically reduce cost, animal use, and time.

The addition of microarray techniques to standard bioassays may dramatically enhance the sensitivity and interpretability of the bioassay and possibly reduce its cost. Gene-expression signatures could be determined for various types of tissue-specific toxicants, and new compounds could be screened for these characteristic signatures, providing a rapid and sensitive *in vivo* test. Also, because gene expression is often exquisitely sensitive to low doses of a toxicant, the combination of gene-expression screening and the bioassay might allow the use of lower toxicant doses, which are more relevant to human exposure levels, and the use of fewer animals. In addition, gene-expression changes are normally measured in hours or days, not in the months to years required for tumor development. Furthermore, microarrays might be particularly useful for investigating the relationship between acute and chronic toxicity and identifying secondary effects of a given toxicant by studying the relationship between the duration of exposure to a toxicant and the gene-expression profile produced. Thus, a bioassay that incorporates gene-expression signatures with traditional endpoints might be substantially shorter, use more realistic dose regimens, and cost substantially less than the current assays do.

These considerations are also relevant for branches of toxicology not related to human health and not using rodents as model systems, such as aquatic toxicology and plant pathology. Bioassays based on the flathead minnow, *Daphnia*, and *Arabidopsis* could

also be improved by the addition of microarray analysis. The combination of microarrays with traditional bioassays might also be useful for investigating some of the more intractable problems in toxicology research, such as the effects of complex mixtures and the difficulties in cross-species extrapolation.

Exposure Assessment, Environmental Monitoring, and Drug Safety

The currently used methods for assessment of exposure to chemical toxicants are based on measurement of tissue toxin levels or on surrogate markers of toxicity, termed biomarkers (e.g., peripheral blood levels of hepatic enzymes or DNA adducts). Because gene expression is a sensitive endpoint, gene expression as measured with microarray technology may be useful as a new biomarker to more precisely identify hazards and to assess exposure. Similarly, microarrays could be used in an environmental-monitoring capacity to measure the effect of potential contaminants on the gene-expression profiles of resident organisms. In an analogous fashion, microarrays could be used to measure gene-expression endpoints in subjects in clinical trials. The combination of these gene-expression data and more established toxic endpoints in these trials could be used to define highly precise surrogates of safety.

Gene-expression profiles in samples from exposed individuals could be compared to the profiles of the same individuals before exposure. From this information, the nature of the toxic exposure can be determined or a relative clinical safety factor estimated. In the future it may also be possible to estimate not only the nature but the dose of the toxicant for a given exposure, based on relative gene-expression levels. This general approach may be particularly appropriate for occupational-health applications, in which unexposed and exposed samples from the same individuals may be obtainable. For example, a pilot study of gene expression in peripheral-blood lymphocytes of Polish coke-oven workers exposed to PAHs (and many other compounds) is under consideration at the NIEHS. An important consideration for these types of studies is that gene expression can be affected by numerous factors, including diet, health, and personal habits. To reduce the effects of these confounding factors, it may be necessary to compare pools of control samples with pools of treated samples. In the future it may be possible to compare exposed sample sets to a national database of human-expression data, thus eliminating the need to provide an unexposed sample from the same individual. Efforts to develop such a national gene-expression database are currently under way [44,45]. However, this national database approach will require a better understanding of genome-wide gene expression across the highly diverse human population and of the effects of environmental factors on this expression.

Alleles, Oligo Arrays, and Toxicogenetics

Gene sequences vary between individuals, and this variability can be a causative factor in human diseases of environmental origin [46,47]. A new area of toxicology, termed toxicogenetics, was recently developed to study the relationship between genetic variability and toxicant susceptibility. This field is not the subject of this discussion, but it is worthwhile to note that the ability of oligonucleotide arrays to discriminate DNA molecules based on single base-pair differences makes these arrays uniquely useful for this type of analysis. Recent reports demonstrated the feasibility of this approach [41,42]. The NIEHS has initiated the Environmental Genome Project to identify common sequence polymorphisms in 200 genes thought to be involved in environmental diseases [48]. In a pilot study on the feasibility of this application to the Environmental Genome Project, oligonucleotide arrays will be used to resequence 20 candidate genes. This toxicogenetic approach promises to dramatically improve our understanding of interindividual variability in disease susceptibility.

FUTURE PRIORITIES

There are many issues that must be addressed before the full potential of microarrays in toxicology research can be realized. Among these are model system selection, dose selection, and the temporal nature of gene expression. In other words, in which species, at what dose, and at what time do we look for toxicant-induced gene expression? If human samples are analyzed, how variable is global gene expression between individuals, before and after toxicant exposure? What are the effects of age, diet, and other factors on this expression? Experience, in the form of large data sets of toxicant exposures, will answer these questions.

One of the most pressing issues for array scientists is the construction of a national public database (linked to the existing public databases) to serve as a repository for gene-expression data. This relational database must be made available for public use, and researchers must be encouraged to submit their expression data so that others may view and query the information. Researchers at the National Institutes of Health have made laudable progress in developing the first generation of such a database [44,45]. In addition, improved statistical methods for gene clustering and pattern recognition are needed to analyze the data in such a public database.

The proliferation of different platforms and methods for microarray hybridizations will improve sample handling and data collection and analysis and reduce costs. However, the variety of microarray methods available will create problems of data compatibility between platforms. In addition, the near-infinite variety of experimental conditions under

which data will be collected by different laboratories will make large-scale data analysis extremely difficult. To help circumvent these future problems, a set of standards to be included on all platforms should be established. These standards would facilitate data entry into the national database and serve as reference points for cross-platform and inter-laboratory data analysis.

Many issues remain to be resolved, but it is clear that new molecular techniques such as microarray hybridization will have a dramatic impact on toxicology research. In the future, the information gathered from microarray-based hybridization experiments will form the basis for an improved method to assess the impact of chemicals on human and environmental health.

ACKNOWLEDGMENTS

The authors would like to thank Drs. Robert Maronpot, George Lucier, Scott Masten, Nigel Walker, Raymond Tennant, and Ms. Theodora Deverenux for critical review of this manuscript. EFN was supported in part by NIEHS Training Grant #ES07017-24.

REFERENCES

1. <http://www.ncbi.nlm.nih.gov/Web/Genbank/index.html>
2. <http://www.ncbi.nlm.nih.gov/Entrez/Genome/org.html>
3. Fleischmann RD, Adams MD, White O, et al. Whole-genome random sequencing and assembly of *Haemophilus influenzae* Rd. *Science* 1995;269:496-512.
4. Goffeau A, Barrell BG, Bussey H, et al. Life with 6000 genes. *Science* 1996;274:546, 563-567.
5. <http://www.perkin-elmer.com/press/prc5448.html>
6. Liang P, Pardee AB. Differential display of eukaryotic messenger RNA by means of the polymerase chain reaction. *Science* 1992;257:967-971.
7. Pietu G, Alibert O, Guichard V, et al. Novel gene transcripts preferentially expressed in human muscles revealed by quantitative hybridization of a high density cDNA array. *Genome Res* 1996;6:492-503.
8. Zhao ND, Hashida H, Takahashi N, Misumi Y, Sakaki Y. High-density cDNA filter analysis—A novel approach for large-scale, quantitative analysis of gene expression. *Gene* 1995;156:207-213.
9. Velculescu VE, Zhang L, Vogelstein B, Kinzler KW. Serial analysis of gene expression. *Science* 1995;270:484-487.
10. Schena M, Shalon D, Davis RW, Brown PO. Quantitative monitoring of gene-expression patterns with a complementary DNA microarray. *Science* 1995;270:467-470.
11. DeRisi J, Penland L, Brown PO, et al. use of a cDNA microarray to analyse gene expression patterns in human cancer. *Nat Genet* 1996;14:457-460.
12. Wodicka L, Dong HL, Mittmann M, Ho MH, Lockhart DJ. Genome-wide expression monitoring in *Saccharomyces cerevisiae*. *Nat Biotechnol* 1997;15:1359-1367.
13. Marshall A, Hodgson J. DNA chips: An array of possibilities. *Nat Biotechnol* 1998;16:27-31.
14. <http://www.synteni.com>
15. Shalon D, Smith SJ, Brown PO. A DNA microarray system for analyzing complex DNA samples using two-color fluorescent probe hybridization. *Genome Res* 1996;6:639-645.
16. Chen Y, Dougherty ER, Bittner ML. Ratio-based decisions and the quantitative analysis of cDNA microarray images. *Biomedical Optics* 1997;2:364-374.
17. Khan J, Simon R, Bittner M, et al. Gene expression profiling of alveolar rhabdomyosarcoma with cDNA microarrays. *Cancer Res* 1998;58:5009-5013.
18. Schena M, Shalon D, Heller R, Chai A, Brown PO, Davis RW. Parallel human genome analysis: Microarray-based expression monitoring of 1000 genes. *Proc Natl Acad Sci USA* 1996;93:10614-10619.

19. Lashkari DA, DeRisi JL, McCusker JH, et al. Yeast microarrays for genome wide parallel genetic and gene expression analysis. *Proc Natl Acad Sci USA* 1997;94:13057-13062.
20. Heller RA, Schena M, Chai A, et al. Discovery and analysis of inflammatory disease-related genes using cDNA microarrays. *Proc Natl Acad Sci USA* 1997;94:2150-2155.
21. DeRisi JL, Iyer VR, Brown PO. Exploring the metabolic and genetic control of gene expression on a genomic scale. *Science* 1997;278:680-686.
22. Drmanac S, Stavropoulos NA, Labat I, et al. Gene-representing cDNA clusters defined by hybridization of 57,419 clones from infant brain libraries with short oligonucleotide probes. *Genomics* 1996;37:29-40.
23. Milosavljevic A, Savkovic S, Crkvenjakov R, et al. DNA sequence recognition by hybridization to short oligomers: Experimental verification of the method on the *E. coli* genome. *Genomics* 1996;37:77-86.
24. Drmanac S, Drmanac R. Processing of cDNA and genomic kilobase-size clones for massive screening, mapping and sequencing by hybridization. *Biotechniques* 1994;17:328-329, 332-336.
25. <http://www.resgen.com/>
26. <http://www.genomesystems.com/>
27. <http://www.clontech.com/>
28. Pease AC, Solas DA, Fodor SPA. Parallel synthesis of spatially addressable oligonucleotide probe matrices. Abstract. Abstracts of Papers of the American Chemical Society 1992;203:34.
29. Pease AC, Solas D, Sullivan EJ, Cronin MT, Holmes CP, Fodor SPA. Light-generated oligonucleotide arrays for rapid DNA sequence analysis. *Proc Natl Acad Sci USA* 1994;91:5022-5026.
30. Fodor SPA, Read JL, Pirrung MC, Stryer L, Lu AT, Solas D. Light-directed, spatially addressable parallel chemical synthesis. *Science* 1991;251:767-773.
31. McGall G, Labadie J, Brock P, Wallraff G, Nguyen T, Hinsberg W. Light-directed synthesis of high-density oligonucleotide arrays using semiconductor photoresists. *Proc Natl Acad Sci USA* 1996;93:13555-13560.
32. Lipshutz RJ, Morris D, Chee M, et al. Using oligonucleotide probe arrays to access genetic diversity. *Biotechniques* 1995;19:442-447.
33. Lockhart DJ, Dong HL, Byrne MC, et al. Expression monitoring by hybridization to high-density oligonucleotide arrays. *Nat Biotechnol* 1996;14:1675-1680.
34. <http://www.mdyn.com/>
35. Sapolsky RJ, Lipshutz RJ. Mapping genomic library clones using oligonucleotide arrays. *Genomics* 1996;33:445-456.
36. Chee M, Yang R, Hubbell E, et al. Accessing genetic information with high-density DNA arrays. *Science* 1996;274:610-614.
37. Hacia JG, Makalowski W, Edgemon K, et al. Evolutionary sequence comparisons using high-density oligonucleotide arrays. *Nat Genet* 1998;18:155-158.
38. Cronin MT, Fucini RV, Kim SM, Masino RS, Wespi RM, Miyada CG. Cystic fibrosis mutation detection by hybridization to light-generated DNA probe arrays. *Hum Mutat* 1996;7:244-255.
39. Hacia JG, Brody LC, Chee MS, Fodor SPA, Collins FS. Detection of heterozygous mutations in BRCA1 using high density oligonucleotide arrays and two-colour fluorescence analysis. *Nat Genet* 1996;14:441-447.
40. Kozal MJ, Shah N, Shen NP, et al. Extensive polymorphisms observed in HIV-1 clade B protease gene using high-density oligonucleotide arrays. *Nat Med* 1996;2:753-759.
41. Wang DG, Fan JB, Siao CJ, et al. Large-scale identification, mapping, and genotyping of single-nucleotide polymorphisms in the human genome. *Science* 1998;280:1077-1082.
42. Winzeler EA, Richards DR, Conway AR, et al. Direct allelic variation scanning of the yeast genome. *Science* 1998;281:1194-1197.
43. Chhabra RS, Huff JE, Schwetz BS, Selkirk J. An overview of prechronic and chronic toxicity carcinogenicity experimental-study designs and criteria used by the National Toxicology Program. *Environ Health Perspect* 1990;86:313-321.
44. Ermolaeva O, Rastogi M, Pruitt KD, et al. Data management and analysis for gene expression arrays. *Nat Genet* 1998;20:19-23.
45. <http://www.nhgri.nih.gov/DIR/LCG/15K/HTML/dbase.html>
46. Samson M, Libert F, Doranz BJ, et al. Resistance to HIV-1 infection in Caucasian individuals bearing mutant alleles of the CCR-5 chemokine receptor gene. *Nature* 1996;382:722-725.
47. Bell DA, Taylor JA, Paulson DF, Robertson CN, Mohler JL, Lucier GW. Genetic risk and carcinogen exposure—A common inherited defect of the carcinogen-metabolism gene glutathione-S-transferase M1 (Gstm1) that increases susceptibility to bladder cancer. *J Natl Cancer Inst* 1993;85:1159-1164.
48. <http://www.niehs.nih.gov/envgenom/home.html>



Toxicology Letters 112–113 (2000) 467–471

Toxicology
Letters

www.elsevier.com/locate/toxlet

Expression profiling in toxicology — potentials and limitations

Sandra Steiner *, N. Leigh Anderson

Large Scale Biology Corporation, 9620 Medical Center Drive, Rockville, MD 20850-3338, USA

Abstract

Recent progress in genomics and proteomics technologies has created a unique opportunity to significantly impact the pharmaceutical drug development processes. The perception that cells and whole organisms express specific inducible responses to stimuli such as drug treatment implies that unique expression patterns, molecular fingerprints, indicative of a drug's efficacy and potential toxicity are accessible. The integration into state-of-the-art toxicology of assays allowing one to profile treatment-related changes in gene expression patterns promises new insights into mechanisms of drug action and toxicity. The benefits will be improved lead selection, and optimized monitoring of drug efficacy and safety in pre-clinical and clinical studies based on biologically relevant tissue and surrogate markers. © 2000 Elsevier Science Ireland Ltd. All rights reserved.

Keywords: Proteomics; Genomics; Toxicology

1. Introduction

The majority of drugs act by binding to protein targets, most to known proteins representing enzymes, receptors and channels, resulting in effects such as enzyme inhibition and impairment of signal transduction. The treatment-induced perturbations provoke feedback reactions aiming to compensate for the stimulus, which almost always are associated with signals to the nucleus, resulting in altered gene expression. Such gene expression regulations account for both the

pharmacological action and the toxicity of a drug and can be visualized by either global mRNA or global protein expression profiling. Hence, for each individual drug, a characteristic gene regulation pattern, its molecular fingerprint, exists which bears valuable information on its mode of action and its mechanism of toxicity.

Gene expression is a multistep process that results in an active protein (Fig. 1). There exist numerous regulation systems that exert control at and after the transcription and the translation step. Genomics, by definition, encompasses the quantitative analysis of transcripts at the mRNA level, while the aim of proteomics is to quantify gene expression further down-stream, creating a snapshot of gene regulation closer to ultimate cell function control.

* Corresponding author. Tel.: +1-301-4245989; fax: +1-301-7624892.

E-mail address: steiner@lsbc.com (S. Steiner)

2. Global mRNA profiling

Expression data at the mRNA level can be produced using a set of different technologies such as DNA microarrays, reverse transcript imaging, amplified fragment length polymorphism (AFLP), serial analysis of gene expression (SAGE) and others. Currently, DNA microarrays are very popular and promise a great potential. On a typical array, each gene of interest is represented either by a long DNA fragment (200–2400 bp) typically generated by polymerase chain reaction (PCR) and spotted on a suitable substrate using robotics (Schena et al., 1995; Shalon et al., 1996) or by several short oligonucleotides (20–30 bp) synthesized directly onto a solid support using photolabile nucleotide chemistry (Fodor et al., 1991; Chee et al., 1996). From control and treated tissues, total RNA or mRNA is isolated and reverse transcribed in the presence of radioactive or fluorescent labeled nucleotides, and the labeled probes are then hybridized to the arrays. The intensity of the array signal is measured for each gene transcript by either autoradiography or laser scanning confocal microscopy. The ratio between the signals of control and treated samples reflect the relative drug-induced change in transcript abundance.

3. Global protein profiling

Global quantitative expression analysis at the protein level is currently restricted to the use of two-dimensional gel electrophoresis. This technique combines separation of tissue proteins by isoelectric focusing in the first dimension and by sodium dodecyl sulfate slab gel electrophoresis-based molecular weight separation on the second, orthogonal dimension (Anderson et al., 1991). The product is a rectangular pattern of protein spots that are typically revealed by Coomassie Blue, silver or fluorescent staining (Fig. 2). Protein spots are identified by mass spectrometry following generation of peptide mass fingerprints (Mann et al., 1993) and sequence tags (Wilkins et al., 1996). Similar to the mRNA approach, the ratio between the optical density of spots from control and treated samples are compared to search for treatment-related changes.

4. Expression data analysis

Bioinformatics forms a key element required to organize, analyze and store expression data from either source, the mRNA or the protein level. The overall objective, once a mass of high-quality

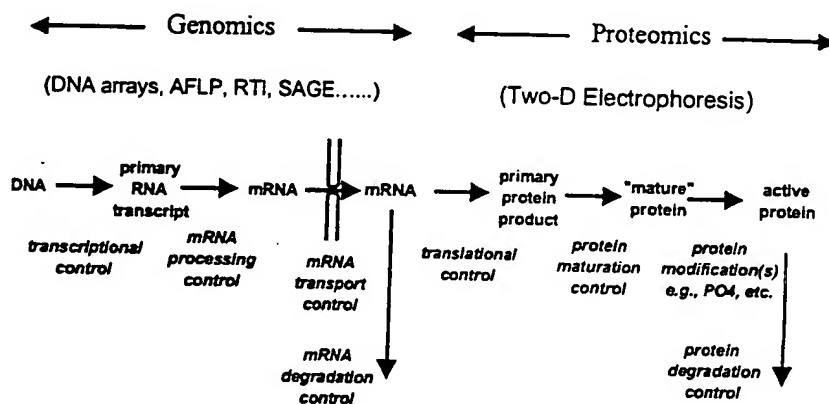
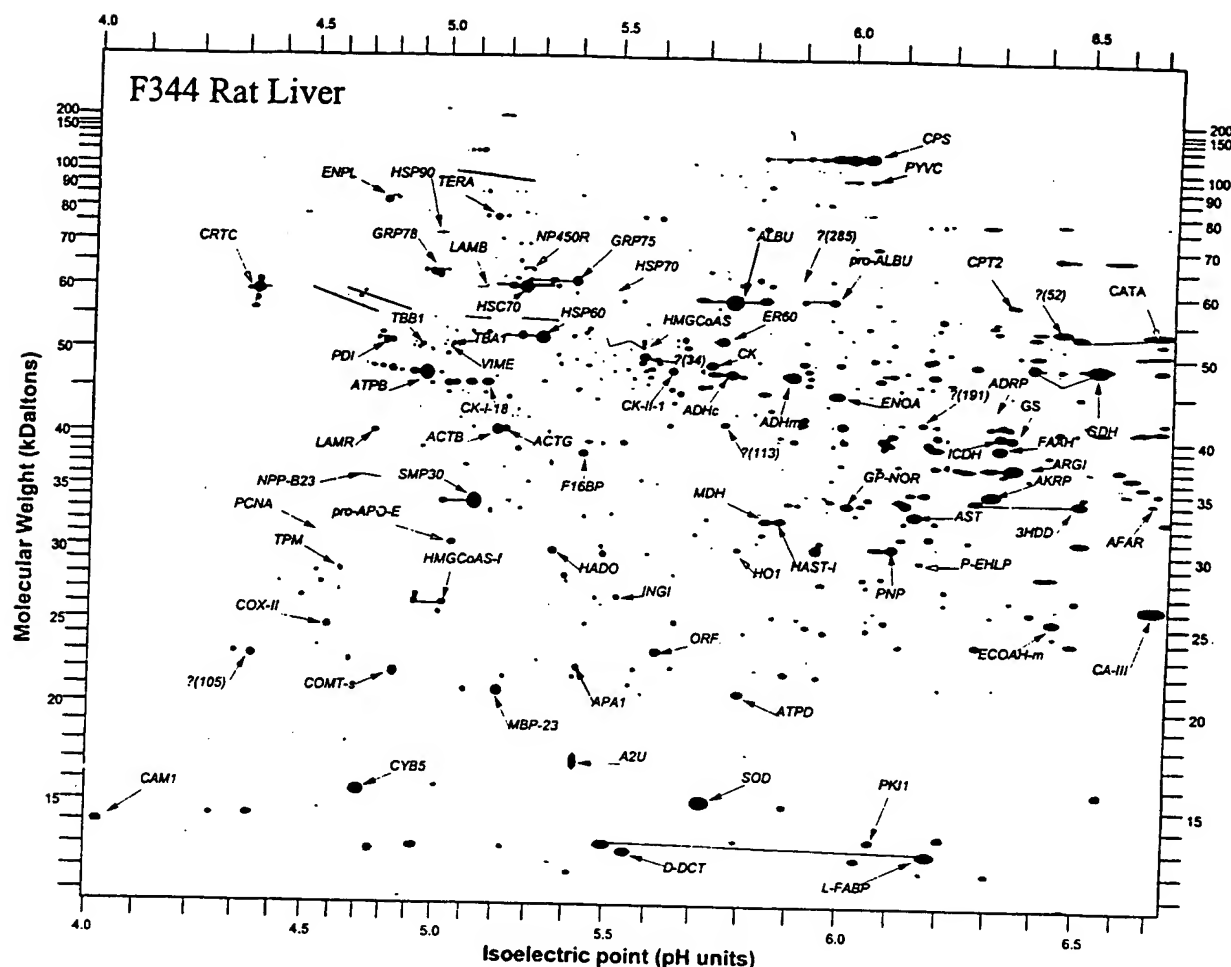


Fig. 1. Production of an active protein is a multistep process in which numerous regulation systems exert control at various stages of expression. Molecular fingerprints of drugs can be visualized through expression profiling at the mRNA level (genomics) using a variety of technologies and at the protein level (proteomics) using two-dimensional gel electrophoresis.



5. Comparison of global mRNA and protein expression profiling

There are several synergies and overlaps of data obtained by mRNA and protein expression analysis. Low abundant transcripts may not be easily quantified at the protein level using standard two-dimensional gel electrophoresis analysis and their detection may require prefractionation of samples. The expression of such genes may be preferably quantified at the mRNA level using techniques allowing PCR-mediated target amplifi-

cation. Tissue biopsy samples typically yield good quality of both mRNA and proteins; however, the quality of mRNA isolated from body fluids is often poor due to the faster degradation of mRNA when compared with proteins. RNA samples from body fluids such as serum or urine are often not very 'meaningful', and secreted proteins are likely more reliable surrogate markers for treatment efficacy and safety. Detection of post-translational modifications, events often related to function or nonfunction of a protein, is restricted to protein expression analysis and rarely can be predicted by mRNA profiling. Information on subcellular localization and translocation of proteins has to be acquired at the level of the protein in combination with sample prefractionation procedures. The growing evidence of a poor correlation between mRNA and protein abundance (Anderson and Seilhamer, 1997) further suggests that the two approaches, mRNA and protein profiling, are complementary and should be applied in parallel.

6. Expression profiling and drug development

Understanding the mechanisms of action and toxicity, and being able to monitor treatment efficacy and safety during trials is crucial for the successful development of a drug. Mechanistic insights are essential for the interpretation of drug effects and enhance the chances of recognizing potential species specificities contributing to an improved risk profile in humans (Richardson et al., 1993; Steiner et al., 1996b; Aicher et al., 1998). The value of expression profiling further increases when links between treatment-induced expression profiles and specific pharmacological and toxic endpoints are established (Anderson et al., 1991, 1995, 1996; Steiner et al. 1996a). Changes in gene expression are known to precede the manifestation of morphological alterations, giving expression profiling a great potential for early compound screening, enabling one to select drug candidates with wide therapeutic windows reflected by molecular fingerprints indicative of high pharmacological potency and low toxicity (Arce et al., 1998). In later phases of drug devel-

opment, surrogate markers of treatment efficacy and toxicity can be applied to optimize the monitoring of pre-clinical and clinical studies (Doherty et al., 1998).

7. Perspectives

The basic methodology of safety evaluation has changed little during the past decades. Toxicity in laboratory animals has been evaluated primarily by using hematological, clinical chemistry and histological parameters as indicators of organ damage. The rapid progress in genomics and proteomics technologies creates a unique opportunity to dramatically improve the predictive power of safety assessment and to accelerate the drug development process. Application of gene and protein expression profiling promises to improve lead selection, resulting in the development of drug candidates with higher efficacy and lower toxicity. The identification of biologically relevant surrogate markers correlated with treatment efficacy and safety bears a great potential to optimize the monitoring of pre-clinical and clinical trials.

References

- Aicher, L., Wahl, D., Arce, A., Grenet, O., Steiner, S., 1998. New insights into cyclosporine A nephrotoxicity by proteome analysis. *Electrophoresis* 19, 1998–2003.
- Anderson, N.L., Seilhamer, J., 1997. A comparison of selected mRNA and protein abundances in human liver. *Electrophoresis* 18, 533–537.
- Anderson, N.L., Esquer-Blasco, R., Hofmann, J.P., Anderson, N.G., 1991. A two-dimensional gel database of rat liver proteins useful in gene regulation and drug effects studies. *Electrophoresis* 12, 907–930.
- Anderson, L., Steele, V.K., Kelloff, G.J., Sharma, S., 1995. Effects of oltipraz and related chemoprevention compounds on gene expression in rat liver. *J. Cell. Biochem. Suppl.* 22, 108–116.
- Anderson, N.L., Esquer-Blasco, R., Richardson, F., Foxworthy, P., Eacho, P., 1996. The effects of peroxisome proliferators on protein abundances in mouse liver. *Toxicol. Appl. Pharmacol.* 137, 75–89.
- Arce, A., Aicher, L., Wahl, D., Esquer-Blasco, R., Anderson, N.L., Cordier, A., Steiner, S., 1998. Changes in the liver proteome of female Wistar rats treated with the hypoglycemic agent SDZ PGU 693. *Life Sci.* 63, 2243–2250.

- Chee, M., Yang, R., Hubbell, E., Berno, A., Huang, X.C., Stern, D., Winkler, J., Lockhart, D.J., Morris, M.S., Fodor, S.P., 1996. Accessing genetic information with high-density DNA arrays. *Science* 274, 610-614.
- Doherty, N.S., Littman, B.H., Reilly, K., Swindell, A.C., Buss, J., Anderson, N.L., 1998. Analysis of changes in acute-phase plasma proteins in an acute inflammatory response and in rheumatoid arthritis using two-dimensional gel electrophoresis. *Electrophoresis* 19, 355-363.
- Fodor, S.P., Read, J.L., Pirrung, M.C., Stryer, L., Lu, A.T., Solas, D., 1991. Light-directed, spatially addressable parallel chemical synthesis. *Science* 251, 767-773.
- Mann, M., Hojrup, P., Roepstorff, P., 1993. Use of mass spectrometric molecular weight information to identify proteins in sequence databases. *Biol. Mass Spectrom.* 22, 338-345.
- Richardson, F.C., Strom, S.C., Copple, D.M., Bendele, R.A., Probst, G.S., Anderson, N.L., 1993. Comparisons of protein changes in human and rodent hepatocytes induced by the rat-specific carcinogen, methapyrilene. *Electrophoresis* 14, 157-161.
- Schena, M., Shalon, D., Davis, R.W., Brown, P.O., 1995. Quantitative monitoring of gene expression patterns with a complementary DNA microarray. *Science* 251, 467-470.
- Shalon, D., Smith, S.J., Brown, P.O., 1996. A DNA microarray system for analyzing complex DNA samples using two-color fluorescent probe hybridization. *Genome Res.* 6, 639-645.
- Steiner, S., Wahl, D., Mangold, B.L.K., Robison, R., Raynackers, J., Meheus, L., Anderson, N.L., Cordier, A., 1996a. Induction of the adipose differentiation-related protein in liver of etomoxir treated rats. *Biochem. Biophys. Res. Commun.* 218, 777-782.
- Steiner, S., Aicher, L., Raynackers, J., Meheus, L., Esquer-Blasco, R., Anderson, L., Cordier, A., 1996b. Cyclosporine A mediated decrease in the rat renal calcium binding protein calbindin-D 28 kDa. *Biochem. Pharmacol.* 51, 253-258.
- Wilkins, M.R., Gasteiger, E., Sanchez, J.C., Appel, R.D., Hochstrasser, D.F., 1996. Protein identification with sequence tags. *Curr. Biol.* 6, 1543-1544.

Application of DNA Arrays to Toxicology

John C. Rockett and David J. Dix

Reproductive Toxicology Division, National Health and Environmental Effects Research Laboratory, U.S. Environmental Protection Agency, Research Triangle Park, North Carolina, USA

Docket No.: PF-0733 USN
USSN: 10/018,170
Ref. No. 5 of 17

DNA array technology makes it possible to rapidly genotype individuals or quantify the expression of thousands of genes on a single filter or glass slide, and holds enormous potential in toxicologic applications. This potential led to a U.S. Environmental Protection Agency-sponsored workshop titled "Application of Microarrays to Toxicology" on 7-8 January 1999 in Research Triangle Park, North Carolina. In addition to providing state-of-the-art information on the application of DNA or gene microarrays, the workshop catalyzed the formation of several collaborations, committees, and user's groups throughout the Research Triangle Park area and beyond. Potential application of microarrays to toxicologic research and risk assessment include genome-wide expression analyses to identify gene-expression networks and toxicant-specific signatures that can be used to define mode of action, for exposure assessment, and for environmental monitoring. Arrays may also prove useful for monitoring genetic variability and its relationship to toxicant susceptibility in human populations. **Key words:** DNA arrays, gene arrays, microarrays, toxicology. *Environ Health Perspect* 107:681-685 (1999). [Online 6 July 1999]
<http://ehpnet1.niehs.nih.gov/docs/1999/107p681-685rockett/abstract.html>

Decoding the genetic blueprint is a dream that offers manifold returns in terms of understanding how organisms develop and function in an often hostile environment. With the rapid advances in molecular biology over the last 30 years, the dream has come a step closer to reality. Molecular biologists now have the ability to elucidate the composition of any genome. Indeed, almost 20 genomes have already been sequenced and more than 60 are currently under way. Foremost among these is the Human Genome Mapping Project. However, the genomes of a number of commonly used laboratory species are also under intensive investigation, including yeast, *Arabidopsis*, maize, rice, zebra fish, mouse, rat, and dog. It is widely expected that the completion of such programs will facilitate the development of many powerful new techniques and approaches to diagnosing and treating genetically and environmentally induced diseases which afflict mankind. However, the vast amount of data being generated by genome mapping will require new high-throughput technologies to investigate the function of the millions of new genes that are being reported. Among the most widely heralded of the new functional genomics technologies are DNA arrays, which represent perhaps the most anticipated new molecular biology technique since polymerase chain reaction (PCR).

Arrays enable the study of literally thousands of genes in a single experiment. The potential importance of arrays is enormous and has been highlighted by the recent publication of an entire *Nature Genetics* supplement dedicated to the technology (1). Despite this huge surge of interest, DNA arrays are still little used and largely unproven, as demonstrated by the high ratio of review and press articles to actual data papers. Even so, the potential they offer

has driven venture capitalists into a frenzy of investment and many new companies are springing up to claim a share of this rapidly developing market.

The U.S. Environmental Protection Agency (EPA) is interested in applying DNA array technology to ongoing toxicologic studies. To learn more about the current state of the technology, the Reproductive Toxicology Division (RTD) of the National Health and Environmental Effects Research Laboratory (NHEERL; Research Triangle Park, NC) hosted a workshop on "Application of Microarrays to Toxicology" on 7-8 January 1999 in Research Triangle Park, North Carolina. The workshop was organized by David Dix, Robert Kavlock, and John Rockett of the RTD/NHEERL. Twenty-two intramural and extramural scientists from government, academia, and industry shared information, data, and opinions on the current and future applications for this exciting new technology. The workshop had more than 150 attendees, including researchers, students, and administrators from the EPA, the National Institute of Environmental Health Sciences (NIEHS), and a number of other establishments from Research Triangle Park and beyond. Presentations ranged from the technology behind array production through the sharing of actual experimental data and projections on the future importance and applications of arrays. The information contained in the workshop presentations should provide aid and insight into arrays in general and their application to toxicology in particular.

Array Elements

In the context of molecular biology, the word "array" is normally used to refer to a series of DNA or protein elements firmly attached in

a regular pattern to some kind of supportive medium. DNA array is often used interchangeably with gene array or microarray. Although not formally defined, microarray is generally used to describe the higher density arrays typically printed on glass chips. The DNA elements that make up DNA arrays can be oligonucleotides, partial gene sequences, or full-length cDNAs. Companies offering pre-made arrays that contain less than full-length clones normally use regions of the genes which are specific to that gene to prevent false positives arising through cross-hybridization. Sequence verification of cDNA clone identity is necessary because of errors in identifying specific clones from cDNA libraries and databases. Premade DNA arrays printed on membranes are currently or imminently available for human, mouse, and rat. In most cases they contain DNA sequences representing several thousand different sequence clusters or genes as delineated through the National Center for Biotechnology Information UniGene Project (2). Many of these different UniGene clusters (putative genes) are represented only by expressed sequence tags (ESTs).

Array Printing

Arrays are typically printed on one of two types of support matrix. Nylon membranes are used by most off-the-shelf array providers such as Clontech Laboratories, Inc. (Palo Alto, CA), Genome Systems, Inc. (St. Louis, MO), and Research Genetics, Inc. (Huntsville, AL). Microarrays such as those produced by Affymetrix, Inc. (Santa Clara, CA), Incyte Pharmaceuticals, Inc. (Palo Alto, CA), and many do-it-yourself (DIY) arraying groups use glass wafers or slides. Although standard microscope slides may be used, they must be preprepared to facilitate sticking of the DNA to the glass. Several different

Address correspondence to J. Rockett, Reproductive Toxicology Division (MD-72), National Health and Environmental Effects Research Laboratory, U.S. EPA, Research Triangle Park, NC 27711 USA. Telephone: (919) 541-2678. Fax: (919) 541-4017. E-mail: rockett.john@epa.gov

The authors thank R. Kavlock for envisioning the application of array technology to toxicology at the U.S. Environmental Protection Agency. We also thank T. Wall and B. Deitz for administrative assistance.

This document has been reviewed in accordance with EPA policy and approved for publication. Mention of companies, trade names, or products does not signify endorsement of such by the EPA.

Received 23 March 1999; accepted 22 April 1999.

coatings have been successfully used, including silane and lysine. The coating of slides can easily be carried out in the laboratory, but many prefer the convenience of precoated slides available from suppliers.

Once the support matrix has been prepared, the DNA elements can be applied by several methods. Affymetrix, Inc., has developed a unique photolithographic technology for attaching oligonucleotides to glass wafers. More commonly, DNA is applied by either noncontact or contact printing. Noncontact printers can use thermal, solenoid, or piezoelectric technology to spray aliquots of solution onto the support matrix and may be used to produce slide or membrane-based arrays. Cartesian Technologies, Inc. (Irvine, CA) has developed nQUAD technology for use in its PixSys printers. The system couples a syringe pump with the microsolenoid valve, a combination that provides rapid quantitative dispensing of nanoliter volumes (down to 4.2 nL) over a variable volume range. A different approach to noncontact printing uses a solid pin and ring combination (Genetic MicroSystems, Inc., Woburn, MA). This system (Figure 1) allows a broader range of sample, including cell suspensions and particulates, because the printing head cannot be blocked up in the same way as a spray nozzle. Fluid transfer is controlled in this system primarily by the pin dimensions and the force of deposition, although the nature of the support matrix and the sample will also affect transfer to some degree.

In contact printing, the pin head is dipped in the sample and then touched to the support matrix to deposit a small aliquot. Split pins were one of the first contact-printing devices to be reported and are the suggested format for DIY arrayers, as described by Brown (3). Split pins are small metal pins with a precise groove cut vertically in the middle of the pin tip. In this system, 1–48 split pins are positioned in the pin-head. The split pins work by simple capillary action, not unlike a fountain pen—when the pin heads are dipped in the sample, liquid is drawn into the pin groove. A small (fixed) volume is then deposited each time the split pins are gently touched to the support matrix. Sample (100–500 pL depending on a variety of parameters) can be deposited on multiple slides before refilling is required, and array densities of > 2,500 spots/cm² may be produced. The deposit volume depends on the split size, sample fluidity, and the speed of printing. Split pins are relatively simple to produce and can be made in-house if a suitable machine shop is available. Alternatively, they can be obtained directly from companies such as TeleChem International, Inc. (Sunnyvale, CA).

Irrespective of their source, printers should be run through a preprint sequence prior to producing the actual experimental

arrays: the first 100 or so spots of a new run tend to be somewhat variable. Factors affecting spot reproducibility include slide treatment homogeneity, sample differences, and instrument errors. Other factors that come into play include clean ejection of the drop and clogging (nQUAD printing) and mechanical variations and long-term alteration in print-head surface of solid and split pins. However, with careful preparation it is possible to get a coefficient of variance for spot reproducibility below 10%.

One potential printing problem is sample carryover. Repeated washing, blotting, and drying (vacuum) of print pins between samples is normally effective at reducing sample carryover to negligible amounts. Printing should also be carried out in a controlled environment. Humidified chambers are available in which to place printers. These help prevent dust contamination and produce a uniform drying rate, which is important in determining spot size, quality, and reproducibility.

In summary, although several printing technologies are available, none are particularly outstanding and the bottom line is that they are still in a relatively early stage of evolution.

Array Hybridization

The hybridization protocol is, practically speaking, relatively straightforward and those with previous experience in blotting should have little difficulty. Array hybridizations are, in essence, reverse Southern/Northern blots—instead of applying a labeled probe to the target population of DNA/RNA, the labeled population is applied to the probe(s). With membrane-based arrays, the control and treated mRNA populations are normally converted to cDNA and labeled with isotope (e.g., ³²P) in the process. These labeled populations are then hybridized independently to parallel or serial arrays and the hybridization signal is detected with a phosphorimager. A less commonly used alternative to radioactive probes is enzymatic detection. The probe may be biotinylated, haptenylated, or have alkaline phosphatase/horseradish peroxidase attached. Hybridization is detected by enzymatic reaction yielding a color reaction (4). Differences in hybridization signals can be detected by eye or, more accurately, with the help of digital imaging and commercially available software. The labeling of the test populations for slide-based microarrays uses a slightly different approach. The probe typically consists of two samples of poly(A)⁺ RNA (usually from a treated and a control population) that are converted to cDNA; in the process each is labeled with a different fluor. The independently labeled probes are then mixed together and hybridized to a single microarray slide and the resulting combined fluorescent signal is scanned. After

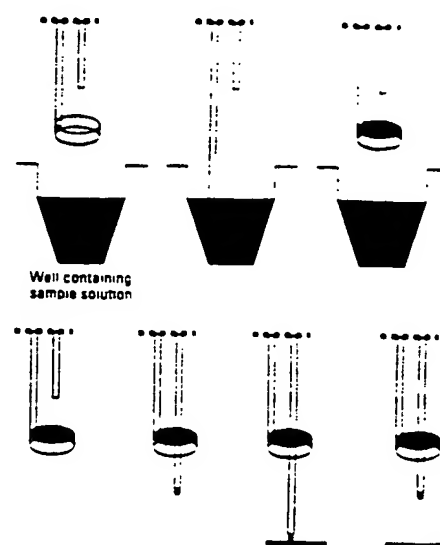


Figure 1. Genetic Microsystems (Woburn, MA) pin ring system for printing arrays. The pin ring combination consists of a circular open ring oriented parallel to the sample solution, with a vertical pin centered over the ring. When the ring is dipped into a solution and lifted, it withdraws an aliquot of sample held by surface tension. To spot the sample, the pin is driven down through the ring and a portion of the solution is transferred to the bottom of the pin. The pin continues to move downward until the pendant drop of solution makes contact with the underlying surface. The pin is then lifted, and gravity and surface tension cause deposition of the spot onto the array. Figure from Flowers et al. (14), with permission from Genetic Microsystems.

normalization, it is possible to determine the ratio of fluorescent signals from a single hybridization of a slide-based microarray.

cDNA derived from control and treated populations of RNA is most commonly hybridized to arrays, although subtractive hybridization or differential display reactions may also be used. Fluorophore- or radiolabeled nucleotides are directly incorporated into the cDNA in the process of converting RNA to cDNA. Alternatively, 5' end-labeled primers may be used for cDNA synthesis. These are labeled with a fluorophore for direct visualization of the hybridized array. Alternatively, biotin or a hapten may be attached to the primer, in which case fluorescent streptavidin or antibody must be applied before a signal can be generated. The most commonly used fluorophores at present are cyanine (Cy)3 and Cy5 (Amersham Pharmacia Biotech AB, Uppsala, Sweden). However, the relative expense of these fluorescent conjugates has driven a search for cheaper alternatives. Fluorescein, rhodamine, and Texas red have all been used, and companies such as Molecular Probes, Inc. (Eugene, OR) are developing a series of labeled nucleotides with a wide range of excitation and emission spectra which may prove to function as well as the Cy dyes.

Analysis of DNA Microarrays

Membrane-based arrays are normally analyzed on film or with a phosphorimager, whereas chip-based arrays require more specialized scanning devices. These can be divided into three main groups: the charge-coupled device camera systems, the nonconfocal laser scanners, and the confocal laser scanners. The advantages and disadvantages of each system are listed in Table 1.

Because a typical spot on a microarray can contain $> 10^8$ molecules, it is clear that a large variation in signal strength may occur. Current scanners cannot work across this many orders of magnitude (4 or 5 is more typical). However, the scanning parameters can normally be adjusted to collect more or less signal, such that two or three scans of the same array should permit the detection of rare and abundant genes.

When a microarray is scanned, the fluorescent images are captured by software normally included with the scanner. Several commercial suppliers provide additional software for quantifying array images, but the software tools are constantly evolving to meet the developing needs of researchers, and it is prudent to define one's own needs and clarify the exact capabilities of the software before its purchase. Issues that should be considered include the following:

- Can the software locate offset spots?
- Can it quantitate across irregular hybridization signals?
- Can the arrayed genes be programmed in for easy identification and location?
- Can the software connect via the Internet to databases containing further information on the gene(s) of interest?

One of the key issues raised at the workshop was the sensitivity of microarray technology. Experiments by General Scanning, Inc. (Watertown, MA), have shown that by using the Cy dyes and their scanner, signal can be detected down to levels of < 1 fluor molecule per square micrometer, which translates to detecting a rare message at approximately one copy per cell or less.

Array Applications

Although arrays are an emerging technology certain to undergo improvement and alteration, they have already been applied successfully to a number of model systems. Arrays are at their most powerful when they contain the entire genome of the species they are being used to study. For this reason, they have strong support among researchers utilizing yeast and *Caenorhabditis elegans* (5). The genomes of both of these species have been sequenced and, in the case of yeast, deposited onto arrays for examination of gene expression (6,7). With both of these species, it is relatively easy to perturb individual gene expression. Indeed, *C.*

Table 1. Advantages and disadvantages of different microarray scanning systems.

	CCD camera system	Nonconfocal laser scanner	Confocal laser scanner
Advantages	Few moving parts	Relatively simple optics	Small depth of focus reduces artifacts
	Fast scanning of bright samples	—	May have high light collection efficiency
Disadvantages	Less appropriate for dim samples	Low light collection efficiency	Small depth of focus requires scanning precision
	Optical scatter can limit performance	Background artifacts not rejected	
		Resolution typically low	

CCD, charge-coupled device.
From Kawasaki (13).

elegans knockouts can be made simply by soaking the worms in an antisense solution of the gene to be knocked out.

By a process of systematic gene disruption, it is now possible to examine the cause and effect relationships between different genes in these simple organisms. This kind of approach should help elucidate biochemical pathways and genetic control processes, deconvolute polygenic interactions, and define the architecture of the cellular network. A simple case study of how this can be achieved was presented by Butow [University of Texas Southwestern Medical Center, Dallas, TX (Figure 2)]. Although it is the phenotypic result of a single gene knockout that is being examined, the effect of such perturbation will almost always be polygenic. Polygenic interactions will become increasingly important as researchers begin to move away from single gene systems when examining the nature of toxicologic responses to external stimuli. This is especially important in toxicology because the phenotype produced by a given environmental insult is never the result of the action of a single gene; rather, it is a complex interaction of one or multiple cellular pathways. Phenomena such as quantitative trait (the continuous variation of phenotype), epistasis (the effect of alleles of one or more genes on the expression of other genes), and penetrance (proportion of individuals of a given genotype that display a particular phenotype) will become increasingly evident and important as toxicologists push toward the ultimate goal of matching the responses of individuals to different environmental stimuli.

Analysis of the transcriptome (the expression level of all the genes in a given cell population) was a use of arrays addressed by several speakers. Unfortunately, current gene nomenclature is often confusing in that single genes are allocated multiple names (usually as a result of independent discovery by different laboratories), and there was a call for standardization of gene nomenclature. Nevertheless, once a transcriptome has been assembled it can then be transferred onto arrays and used to screen any chosen system. The EPA MicroArray Consortium (EPAMAC) is assembling testes

transcriptomes for human, rat, and mouse. In a slightly different approach, Nuwaysir et al. (8) describes how the NIEHS assembled what is effectively a "toxicological transcriptome"—a library of human and mouse genes that have previously been proven or implicated in responses to toxicologic insults. Clontech Laboratories, Inc. (Palo Alto, CA), has begun a similar process by developing stress/toxicology filter arrays of rat, mouse, and human genes. Thus, rather than being tissue or cell specific, these stress/toxicology arrays can be used across a variety of model systems to look for alterations in the expression of toxicologically important genes and define the new field of toxicogenomics. The potential to identify toxicant families based on tissue- or cell-specific gene expression could revolutionize drug testing. These molecular signatures or fingerprints could not only point to the possible toxicity/carcinogenicity of newly discovered compounds (Figure 3), but also aid in elucidating their mechanism of action through identification of gene expression networks. By extension, such signatures could provide easily identifiable biomarkers to assess the degree, time, and nature of exposure.

DNA arrays are primarily a tool for examining differential gene expression in a given model. In this context they are referred to as closed systems because they lack the ability of other differential expression technologies, e.g., differential display and subtractive hybridization, to detect previously unknown genes not present on the array. This would appear to limit the power of DNA arrays to the imaginations and preconceptions of the researcher in selecting genes previously characterized and thought to be involved in the model system. However, the various genome sequencing projects have created a new category of sequence—the EST—that has partially mollified this deficiency. ESTs are cDNAs expressed in a given tissue that, although they may share some degree of sequence similarity to previously characterized genes, have not been assigned specific genetic identity. By incorporating EST clones into an array, it is possible to monitor the expression of these unknown genes. This can enable the identification of previously uncharacterized genes that may have biologic

significance in the model system. Filter arrays from Research Genetics and slide arrays from Incyte Pharmaceuticals both incorporate large numbers of ESTs from a variety of species.

A further use of microarrays is the identification of single nucleotide polymorphisms (SNPs). These genomic variations are abundant—they occur approximately every 1 kb or so—and are the basis of restriction fragment length polymorphism analysis used in forensic analysis. Affymetrix, Inc., designed chips that contain multiple repeats of the same gene sequence. Each position is present with all four possible bases. After the hybridization of the sample, the degree of hybridization to the different sequences can be measured and the exact sequence of the target gene deduced. SNPs are thought to be of vital importance in drug metabolism and toxicology. For example, single base differences in the regulatory region or active site of some genes can account for huge differences in the activity of that gene. Such SNPs are thought to explain why some people are able to metabolize certain xenobiotics better than others. Thus, arrays provide a further tool for the toxicologist investigating the nature of susceptible subpopulations and toxicologic response.

There are still many wrinkles to be ironed out before arrays become a standard tool for toxicologists. The main issues raised at the workshop by those with hands-on experience were the following:

- Expense: the cost of purchasing/contracting this technology is still too great for many individual laboratories.

- Clones: the logistics of identifying, obtaining, and maintaining a set of nonredundant, non-contaminated, sequence-verified, species/cell/tissue/field-specific clones.
- Use of inbred strains: where whole-organism models are being used, the use of inbred strains is important to reduce the potentially confusing effects of the individual variation typically seen in outbred populations.
- Probe: the need for relatively large amounts of RNA, which limits the type of sample (e.g., biopsy) that can be used. Also, different RNA extraction methods can give different results.
- Specificity: the ability to discriminate accurately between closely related genes (e.g., the cytochrome p450 family) and splice variants.
- Quantitation: the quantitation of gene expression using gene arrays is still open to debate. One reason for this is the different incorporation of the labeling dyes. However, the main difficulty lies in knowing what to normalize against. One option is to include a large number of so-called housekeeping genes in the array. However, the expression of these genes often change depending on the tissue and the toxicant, so it is necessary to characterize the expression of these genes in the model system before utilizing them. This is clearly not a viable option when screening multiple new compounds. A second option is to include on the array genes from a nonrelated species (e.g., a plant gene on an animal array) and to spike the probe with synthetic RNA(s) complementary to the gene(s).
- Reproducibility: this is sometimes questionable, and a figure of approximately two or three repeats was used as the minimum number required to confirm initial findings.

Again, however, most people advocated the use of Northern blots or reverse transcriptase PCR to confirm findings.

- Sensitivity: concerns were voiced about the number of target molecules that must be present in a sample for them to be detected on the array.
- Efficiency: reproducible identification of 1.5- to 2-fold differences in expression was reported, although the number of genes that undergo this level of change and remain undetected is open to debate. It is important that this level of detection be ultimately achieved because it is commonly perceived that some important transcription factors and their regulators respond at such low levels. In most cases, 3- to 5-fold was the minimum change that most were happy to accept.
- Bioinformatics: perhaps the greatest concern was how to accurately interpret the data with the greatest accuracy and efficiency. The biggest headache is trying to identify networks of gene expression that are common to different treatments or doses. The amount of data from a single experiment is huge. It may be that, in the future, several groups individually equipped with specialized software algorithms for studying their favorite genes or gene systems will be able to share the same hybridized chips. Thus, arrays could usher in a new perspective on collaboration and the sharing of data.

EPAMAC

Perhaps the main reason most scientists are unable to use array technology is the high cost involved, whether buying off-the-shelf membranes, using contract printing services, or

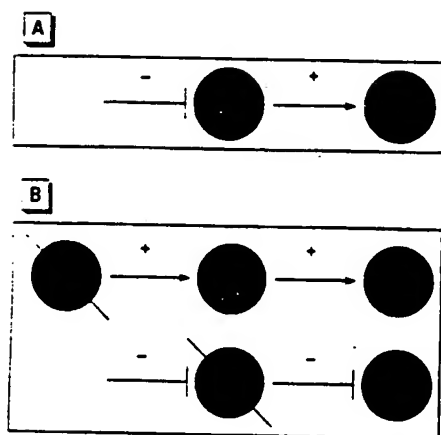


Figure 2. Potential effects of gene knockout within positively and negatively regulated gene expression networks. i_1 is limiting in wild type for expression of i_2 . (A) A simple, two-component, linear regulatory network operating on gene i_2 , where i_1 is a positive effector of i_2 and j_n is either a positive or negative effector of i_1 . This network could be deduced by examining the consequence of (B) deleting j_n on the expression of i_1 and i_2 , where the expression of i_2 would be decreased or increased depending on whether j_n was a positive or negative regulator. These and other connected components of even greater complexity could be revealed by genome-wide expression analysis. From Butow (15).

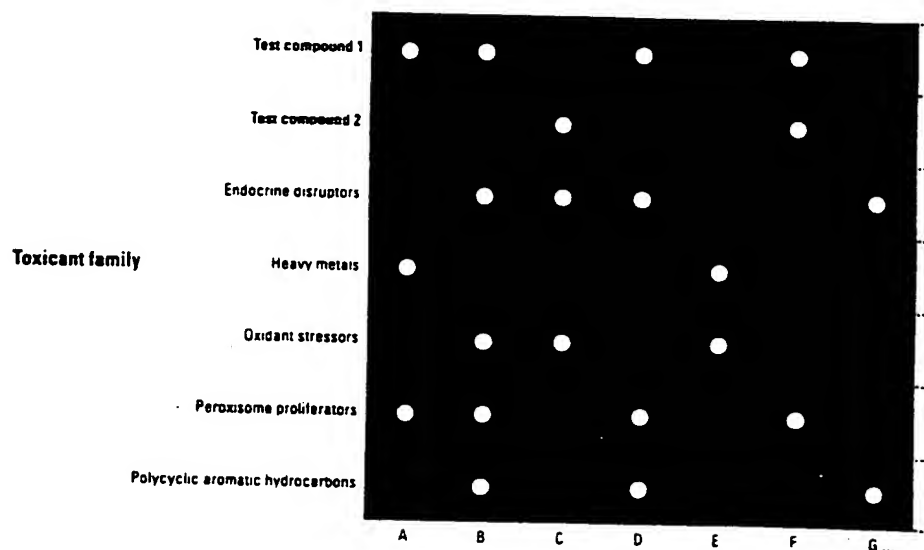


Figure 3. Gene expression profiles—also called fingerprints or signatures—of known toxicants or toxicant families may, in the future, be used to identify the potential toxicity of new drugs, etc. In this example, the genetic signature of test compound 1 is identical to that of known peroxisome proliferators, whereas that of test compound 2 does not match any known toxicant family. Based on these results, test compound 2 would be retained for further testing and test compound 1 would be eliminated.

producing chips in-house. In view of this, researchers at the RTD/NHEERL initiated the EPAMAC. This consortium brings together scientists from the EPA and a number of extramural labs with the aim of developing microarray capability through the sharing of resources and data. EPAMAC researchers are primarily interested in the developmental and toxicologic changes seen in testicular and breast tissue, and a portion of the workshop was set aside for EPAMAC members to share their ideas on how the experimental application of microarrays could facilitate their research. One of the central areas of interest to EPAMAC members is the effect of xenobiotics on male fertility and reproductive health. Of greatest concern is the effect of exposure during critical periods of development and germ cell differentiation (9), and how this may compromise sperm counts and quality following sexual maturation (10). As well as spermatogenic tissue, there is also interest in how residual mRNA found in mature sperm (11) could be used as an indicator of previous xenobiotic effects (it is easier to obtain a semen sample than a testicular biopsy). Arrays will be used to examine and compare the effect of exposure to heat and chemicals in testicular and epididymal gene expression profiles, with the aim of establishing relationships/associations between changes in developmental landmarks and the effects on sperm count and quality. Cluster, pattern, and other analysis of such data should help identify hidden relationships between genes that may reveal potential mechanisms of action and uncover roles for genes with unknown functions.

Summary

The full impact of DNA arrays may not be seen for several years, but the interest shown at this regional workshop indicates the high level of interest that they foster. Apart from educating and advertising the various technologies in this field, this workshop brought together a number of researchers from the Research Triangle Park area who are already using DNA arrays. The interest in sharing ideas and experiences led to the initiation of a Triangle array user's group.

Array technology is still in its infancy. This means that the hardware is still improving and there is no current consensus for standard procedures, quantitation, and interpretation. Consistency in spotting and scanning arrays is not yet optimized, and this is one of the most critical requirements of any experiment. In addition, one of the dark regions of array technology—strife in the courts over who owns what portions of it—has further muddled the future and is a potential barrier toward the development of consensus procedures.

Perhaps the greatest hurdle for the application of arrays is the actual interpretation of data. No specialists in bioinformatics attended the workshop, largely because they are rare and because as yet no one seems clear on the best method of approaching data analysis and interpretation. Cross-referencing results from multiple experiments (time, dose, repeats, different animals, different species) to identify commonly expressed genes is a great challenge. In most cases, we are still a long way from understanding how the expression of gene *X* is related to the expression of gene *Y*, and ordering gene expression to delineate causal relationships.

To the ordinary scientist in the typical laboratory, however, the most immediate problem is a lack of affordable instrumentation. One can purchase premade membranes at relatively affordable prices. Although these may be useful in identifying individual genes to pursue in more detail using other methods, the numbers that would be required for even a small routine toxicology experiment prohibit this as a truly viable approach. For the toxicologist, there is a need to carry out multiple experiments—dose responses, time curves, multiple animals, and repeats. Glass-based DNA arrays are most attractive in this context because they can be prepared in large batches from the same DNA source and accommodate control and treated samples on the same chip. Another problem with current off-the-shelf arrays is that they often do not contain one or more of the particular genes a group is interested in. One alternative is to obtain and/or produce a set of custom clones and have contract printing of membranes or slides carried out by a company such as Genomic Solutions, Inc. (Ann Arbor, MI). This approach

is less expensive than laying out capital for one's own entire system, although at some point it might make economic sense to print one's own arrays.

Finally, DNA arrays are currently a team effort. They are a technology that uses a wide range of skills including engineering, statistics, molecular biology, chemistry, and bioinformatics. Because most individuals are skilled in only one or perhaps two of these areas, it appears that success with arrays may be best expected by teams or collaborators consisting of individuals having each of these skills.

Those considering array applications may be amused or goaded on by the following quote from *Fortune* magazine (12):

Microprocessors have reshaped our economy, spawned vast fortunes and changed the way we live. Gene chips could be even bigger.

Although this comment may have been designed to excite the imagination rather than accurately reflect the truth, it is fair to say that the age of functional genomics is upon us. DNA arrays look set to be an important tool in this new age of biotechnology and will likely contribute answers to some of toxicology's most fundamental questions.

REFERENCES AND NOTES

1. The chipping forecast. *Nat Genet* 21(Suppl 1):3-60 (1999).
2. National Center for Biotechnology Information. The Unigene System. Available: www.ncbi.nlm.nih.gov/Schuler/UniGene [cited 22 March 1999].
3. Brown PO. The Brown Lab. Available: <http://cmgm.Stanford.edu/pbrown> [cited 22 March 1999].
4. Chen JJ, Wu R, Yang PC, Huang JY, Sher YP, Han MH, Kao WC, Lee PJ, Chiu TF, Chang F, et al. Profiling expression patterns and isolating differentially expressed genes by cDNA microarray system with colorimetry detection. *Genomics* 51:313-324 (1998).
5. Ward S. DNA Microarray Technology to Identify Genes Controlling Spermatogenesis. Available: www.mcbaizona.edu/wardlab/microarray.html [cited 22 March 1999].
6. Marton MJ, DeRisi JL, Bennett HA, Iyer VR, Meyer MR, Roberts CJ, Stoughton R, Burchard J, Slade D, Dai H, et al. Drug target validation and identification of secondary drug target effects using DNA microarrays. *Nat Med* 4:1293-1301 (1998).
7. Brown PO. The Full Yeast Genome on a Chip. Available: <http://cmgm.stanford.edu/pbrown/yeastchip.html> [cited 22 March 1999].
8. Nuwaysir EF, Bitner M, Trent J, Barrett JC, Afshari CA. Microarrays and toxicology: the advent of toxicogenomics. *Mol Carcinog* 24(3):153-159 (1999).
9. Hecht NB. Molecular mechanisms of male germ cell differentiation. *Bioessays* 20:555-561 (1998).
10. Zacharewski TR, Timothy R, Zacharewski. Available: <http://bch.msu.edu/faculty/zachar.htm> [cited 22 March 1999].
11. Kramer JA, Krawetz SA. RNA in spermatozoa: implications for the alternative haploid genome. *Mol Hum Reprod* 3:473-478 (1997).
12. Stipp D. Gene chip breakthrough. *Fortune*, March 31:56-73 (1997).
13. Kawasaki E (General Scanning Instruments, Inc., Watertown, MA). Unpublished data.
14. Flowers P, Overback J, Mace ML Jr, Pagliughi FM, Eggers WJE, Yonkers M, Honkanen P, Montagu J, Rose SD. Development and Performance of a Novel Microarraying System Based on Surface Tension Forces. Available: <http://www.geneticmicro.com/resources/html/coldspring.html> [cited 22 March 1999].
15. Butow R (University of Texas Medical Center, Dallas, TX). Unpublished data.

SPEAKERS

Cindy Afshari NIEHS	Abdel Elkhouloun Research Genetics, Inc.
Linda Birnbaum U.S. EPA	Sue Fenton U.S. EPA
Ron Butow University of Texas Southwestern Medical Center	Norman Hecht University of Pennsylvania
Alex Chenchik Clontech Laboratories, Inc.	Pat Murban Paradigm Genetics, Inc.
David Dix U.S. EPA	Bob Kavlock U.S. EPA
	Ernie Kawasaki General Scanning, Inc.

Steve Krawetz Wayne State University	Jim Samet U.S. EPA
Nick Mace Genetic Microsystems, Inc.	Sam Ward University of Arizona
Scott Mordecai Affymetrix, Inc.	Jaff Weich U.S. EPA
Kevin Morgan Glaxo Wellcome, Inc.	Reen Wu University of California at Davis
Elaine Poplin Research Genetics, Inc.	Tom Zacharewski Michigan State University
Don Rose Cartesian Technologies, Inc.	

Subject: RE: [Fwd: Toxicology Chip]

Date: Mon. 3 Jul 2000 08:09:45 -0400

From: "Afshari.Cynthia" <afshari@niehs.nih.gov>

To: "Diana Hamlet-Cox" <dianahc@incyte.com>

You can see the list of clones that we have on our 12K chip at:
<http://manuel.niehs.nih.gov/maps/guest/clonesrch.cfm>

We selected a subset of genes (2000K) that we believed critical to toxic response and basic cellular processes and added a set of clones and ESTs to this. We have included a set of control genes (80-) that were selected by the NHGRI because they did not change across a large set of array experiments. However, we have found that some of these genes change significantly after toxic treatments and are in the process of looking at the variation of each of these 80- genes across our experiments.

Our chips are constantly changing and being updated and we hope that our data will lead us to what the toxchip should really be.

I hope this answers your question.

Cindy Afshari

> -----

> From: Diana Hamlet-Cox
 > Sent: Monday, June 26, 2000 8:52 PM
 > To: afshari@niehs.nih.gov
 > Subject: [Fwd: Toxicology Chip]

> Dear Dr. Afshari,

> Since I have not yet had a response from Bill Grigg, perhaps he was not the right person to contact.

> Can you help me in this matter? I don't need to know the sequences, necessarily, but I would like very much to know what types of sequences are being used, e.g., GPCRs (more specific?), ion channels, etc.

> Diana Hamlet-Cox

> ----- Original Message -----

> Subject: Toxicology Chip
 > Date: Mon. 19 Jun 2000 18:31:48 -0700
 > From: Diana Hamlet-Cox <dianahc@incyte.com>
 > Organization: Incyte Pharmaceuticals
 > To: grigg@niehs.nih.gov

> Dear Colleague:

> I am doing literature research on the use of expressed genes as pharmacotoxicology markers, and found the Press Release dated February 29, 2000 regarding the work of the NIEHS in this area. I would like to know if there is a resource I can access (or you could provide?) that would give me a list of the 12,000 genes that are on your Human ToxChip Microarray. In particular, I am interested in the criteria used to select sequences for the ToxChip, including any control sequences included in the microarray.

> Thank you for your assistance in this request.

> Diana Hamlet-Cox, Ph.D.
 > Incyte Genomics, Inc.

> --

> =====

> This email message is for the sole use of the intended recipient(s) and
> may contain confidential and privileged information subject to
> attorney-client privilege. Any unauthorized review, use, disclosure or
> distribution is prohibited. If you are not the intended recipient,
> please contact the sender by reply email and destroy all copies of the
> original message.

> *****

>
>
>

Assessing sequence comparison methods with reliable structurally identified distant evolutionary relationships

STEVEN E. BRENNER^{*†‡}, CYRUS CHOTHIA^{*}, AND TIM J. P. HUBBARD[§]

^{*}MRC Laboratory of Molecular Biology, Hills Road, Cambridge CB2 2QH, United Kingdom; and [§]Sanger Centre, Wellcome Trust Genome Campus, Hinxton, Cambs CB10 1SA, United Kingdom

Communicated by David R. Davies, National Institute of Diabetes, Bethesda, MD, March 16, 1998 (received for review November 12, 1997)

ABSTRACT Pairwise sequence comparison methods have been assessed using proteins whose relationships are known reliably from their structures and functions, as described in the SCOP database [Murzin, A. G., Brenner, S. E., Hubbard, T. & Chothia C. (1995) *J. Mol. Biol.* 247, 536–540]. The evaluation tested the programs BLAST [Altschul, S. F., Gish, W., Miller, W., Myers, E. W. & Lipman, D. J. (1990) *J. Mol. Biol.* 215, 403–410], WU-BLAST2 [Altschul, S. F. & Gish, W. (1996) *Methods Enzymol.* 266, 460–480], FASTA [Pearson, W. R. & Lipman, D. J. (1988) *Proc. Natl. Acad. Sci. USA* 85, 2444–2448], and SSEARCH [Smith, T. F. & Waterman, M. S. (1981) *J. Mol. Biol.* 147, 195–197] and their scoring schemes. The error rate of all algorithms is greatly reduced by using statistical scores to evaluate matches rather than percentage identity or raw scores. The E-value statistical scores of SSEARCH and FASTA are reliable: the number of false positives found in our tests agrees well with the scores reported. However, the P-values reported by BLAST and WU-BLAST2 exaggerate significance by orders of magnitude. SSEARCH, FASTA $ktup = 1$, and WU-BLAST2 perform best, and they are capable of detecting almost all relationships between proteins whose sequence identities are $>30\%$. For more distantly related proteins, they do much less well; only one-half of the relationships between proteins with 20–30% identity are found. Because many homologs have low sequence similarity, most distant relationships cannot be detected by any pairwise comparison method; however, those which are identified may be used with confidence.

Sequence database searching plays a role in virtually every branch of molecular biology and is crucial for interpreting the sequences issuing forth from genome projects. Given the method's central role, it is surprising that overall and relative capabilities of different procedures are largely unknown. It is difficult to verify algorithms on sample data because this requires large data sets of proteins whose evolutionary relationships are known unambiguously and independently of the methods being evaluated. However, nearly all known homologs have been identified by sequence analysis (the method to be tested). Also, it is generally very difficult to know, in the absence of structural data, whether two proteins that lack clear sequence similarity are unrelated. This has meant that although previous evaluations have helped improve sequence comparison, they have suffered from insufficient, imperfectly characterized, or artificial test data. Assessment also has been problematic because high quality database sequence searching attempts to have both sensitivity (detection of homologs) and specificity (rejection of unrelated proteins); however, these complementary goals are linked such that increasing one causes the other to be reduced.

Sequence comparison methodologies have evolved rapidly, so no previously published tests have evaluated modern versions of programs commonly used. For example, parameters in BLAST (1) have changed, and WU-BLAST2 (2)—which produces gapped alignments—has become available. The latest version of FASTA (3) previously tested was 1.6, but the current release (version 3.0) provides fundamentally different results in the form of statistical scoring.

The previous reports also have left gaps in our knowledge. For example, there has been no published assessment of thresholds for scoring schemes more sophisticated than percentage identity. Thus, the widely discussed statistical scoring measures have never actually been evaluated on large databases of real proteins. Moreover, the different scoring schemes commonly in use have not been compared.

Beyond these issues, there is a more fundamental question: in an absolute sense, how well does pairwise sequence comparison work? That is, what fraction of homologous proteins can be detected using modern database searching methods?

In this work, we attempt to answer these questions and to overcome both of the fundamental difficulties that have hindered assessment of sequence comparison methodologies. First, we use the set of distant evolutionary relationships in the SCOP: Structural Classification of Proteins database (4), which is derived from structural and functional characteristics (5). The SCOP database provides a uniquely reliable set of homologs, which are known independently of sequence comparison. Second, we use an assessment method that jointly measures both sensitivity and specificity. This method allows straightforward comparison of different sequence searching procedures. Further, it can be used to aid interpretation of real database searches and thus provide optimal and reliable results.

Previous Assessments of Sequence Comparison. Several previous studies have examined the relative performance of different sequence comparison methods. The most encompassing analyses have been by Pearson (6, 7), who compared the three most commonly used programs. Of these, the Smith-Waterman algorithm (8) implemented in SSEARCH (3) is the oldest and slowest but the most rigorous. Modern heuristics have provided BLAST (1) the speed and convenience to make it the most popular program. Intermediate between these two is FASTA (3), which may be run in two modes offering either greater speed ($ktup = 2$) or greater effectiveness ($ktup = 1$). Pearson also considered different parameters for each of these programs.

To test the methods, Pearson selected two representative proteins from each of 67 protein superfamilies defined by the PIR database (9). Each was used as a query to search the database, and the matched proteins were marked as being homologous or unrelated according to their membership of PIR.

Abbreviation: EPO, errors per query.

[†]Present address: Department of Structural Biology, Stanford University, Fairchild Building D-109, Stanford, CA 94305-5126

[‡]To whom reprint requests should be addressed. e-mail: brenner@hyper.stanford.edu.

The publication costs of this article were defrayed in part by page charge payment. This article must therefore be hereby marked "advertisement" in accordance with 18 U.S.C. §1734 solely to indicate this fact.

© 1998 by The National Academy of Sciences 0027-8424/98/956073-06\$05.00/0
PNAS is available online at <http://www.pnas.org>.

superfamilies. Pearson found that modern matrices and "ln-scaling" of raw scores improve results considerably. He also reported that the rigorous Smith-Waterman algorithm worked slightly better than FASTA, which was in turn more effective than BLAST.

Very large scale analyses of matrices have been performed (10), and Henikoff and Henikoff (11) also evaluated the effectiveness of BLAST and FASTA. Their test with BLAST considered the ability to detect homologs above a predetermined score but had no penalty for methods which also reported large numbers of spurious matches. The Henikoffs searched the SWISS-PROT database (12) and used PROSITE (13) to define homologous families. Their results showed that the BLOSUM62 matrix (14) performed markedly better than the extrapolated PAM-series matrices (15), which previously had been popular.

A crucial aspect of any assessment is the data that are used to test the ability of the program to find homologs. But in Pearson's and the Henikoffs' evaluations of sequence comparison, the correct results were effectively unknown. This is because the superfamilies in PIR and PROSITE are principally created by using the same sequence comparison methods which are being evaluated. Interdependency of data and methods creates a "chicken and egg" problem, and means for example, that new methods would be penalized for correctly identifying homologs missed by older programs. For instance, immunoglobulin variable and constant domains are clearly homologous, but PIR places them in different superfamilies. The problem is widespread: each superfamily in PIR 48.00 with a structural homolog is itself homologous to an average of 1.6 other PIR superfamilies (16).

To surmount these sorts of difficulties, Sander and Schneider (17) used protein structures to evaluate sequence comparison. Rather than comparing different sequence comparison algorithms, their work focused on determining a length-dependent threshold of percentage identity, above which all proteins would be of similar structure. A result of this analysis was the HSP equation; it states that proteins with 25% identity over 80 residues will have similar structures, whereas shorter alignments require higher identity. (Other studies also have used structures (18–20), but these focused on a small number of model proteins and were principally oriented toward evaluating alignment accuracy rather than homology detection.)

A general solution to the problem of scoring comes from statistical measures (i.e., E-values and P-values) based on the extreme value distribution (21). Extreme value scoring was implemented analytically in the BLAST program using the Karlin and Altschul statistics (22, 23) and empirical approaches have been recently added to FASTA and SSEARCH. In addition to being heralded as a reliable means of recognizing significantly similar proteins (24, 25), the mathematical tractability of statistical scores "is a crucial feature of the BLAST algorithm" (1). The validity of this scoring procedure has been tested analytically and empirically (see ref. 2 and references in ref. 24). However, all large empirical tests used random sequences that may lack the subtle structure found within biological sequences (26, 27) and obviously do not contain any real homologs. Thus, although many researchers have suggested that statistical scores be used to rank matches (24, 25, 28), there have been no large rigorous experiments on biological data to determine the degree to which such rankings are superior.

A Database for Testing Homology Detection. Since the discovery that the structures of hemoglobin and myoglobin are very similar though their sequences are not (29), it has been apparent that comparing structures is a more powerful (if less convenient) way to recognize distant evolutionary relationships than comparing sequences. If two proteins show a high degree of similarity in their structural details and function, it

is very probable that they have an evolutionary relationship though their sequence similarity may be low.

The recent growth of protein structure information combined with the comprehensive evolutionary classification in the SCOP database (4, 5) have allowed us to overcome previous limitations. With these data, we can evaluate the performance of sequence comparison methods on real protein sequences whose relationships are known confidently. The SCOP database uses structural information to recognize distant homologs, the large majority of which can be determined unambiguously. These superfamilies, such as the globins or the immunoglobulins, would be recognized as related by the vast majority of the biological community despite the lack of high sequence similarity.

From SCOP, we extracted the sequences of domains of proteins in the Protein Data Bank (PDB) (30) and created two databases. One (PDB90D-B) has domains which were all <90% identical to any other, whereas (PDB40D-B) had those <40% identical. The databases were created by first sorting all protein domains in SCOP by their quality and making a list. The highest quality domain was selected for inclusion in the database and removed from the list. Also removed from the list (and discarded) were all other domains above the threshold level of identity to the selected domain. This process was repeated until the list was empty. The PDB40D-B database contains 1,323 domains, which have 9,044 ordered pairs of distant relationships, or ~0.5% of the total 1,749,006 ordered pairs. In PDB90D-B, the 2,079 domains have 53,988 relationships, representing 1.2% of all pairs. Low complexity regions of sequence can achieve spurious high scores, so these were masked in both databases by processing with the SEG program (27) using recommended parameters: 12 1.8 2.0. The databases used in this paper are available from <http://sss.stanford.edu/sss/>, and databases derived from the current version of SCOP may be found at <http://scop.mrc-lmb.cam.ac.uk/scop/>.

Analyses from both databases were generally consistent, but PDB40D-B focuses on distantly related proteins and reduces the heavy overrepresentation in the PDB of a small number of families (31, 32), whereas PDB90D-B (with more sequences) improves evaluations of statistics. Except where noted otherwise, the distant homolog results here are from PDB40D-B. Although the precise numbers reported here are specific to the structural domain databases used, we expect the trends to be general.

Assessment Data and Procedure. Our assessment of sequence comparison may be divided into four different major categories of tests. First, using just a single sequence comparison algorithm at a time, we evaluated the effectiveness of different scoring schemes. Second, we assessed the reliability of scoring procedures, including an evaluation of the validity of statistical scoring. Third, we compared sequence comparison algorithms (using the optimal scoring scheme) to determine their relative performance. Fourth, we examined the distribution of homologs and considered the power of pairwise sequence comparison to recognize them. All of the analyses used the databases of structurally identified homologs and a new assessment criterion.

The analyses tested BLAST (1), version 1.4.9MP; and WU-BLAST2 (2), version 2.0a13MP. Also assessed was the FASTA package, version 3.0i76 (3), which provided FASTA and the SSEARCH implementation of Smith-Waterman (8). For SSEARCH and FASTA, we used BLOSUM45 with gap penalties -12/-1 (7, 16). The default parameters and matrix (BLOSUM62) were used for BLAST and WU-BLAST2.

The "Coverage Vs. Error" Plot. To test a particular protocol (comprising a program and scoring scheme), each sequence from the database was used as a query to search the database. This yielded ordered pairs of query and target sequences with associated scores, which were sorted, on the basis of their scores, from best to worst. The ideal method would have

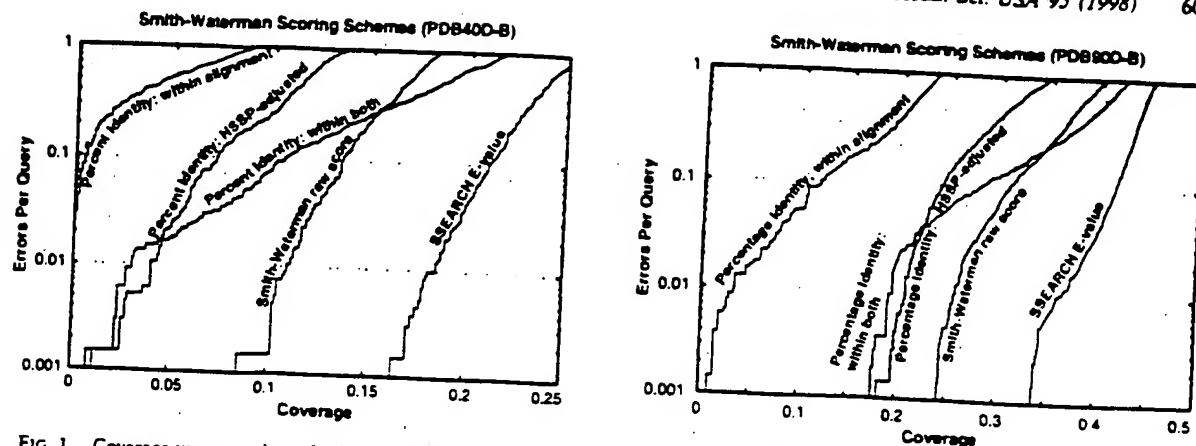


FIG. 1. Coverage vs. error plots of different scoring schemes for SSEARCH Smith-Waterman. (A) Analysis of PDB400-B database. (B) Analysis of PDB900-B database. All of the proteins in the database were compared with each other using the SSEARCH program. The results of this single set of comparisons were considered using five different scoring schemes and assessed. The graphs show the coverage and errors per query (EPQ) for statistical scores, raw scores, and three measures using percentage identity. In the coverage vs. error plot, the x axis indicates the fraction of all homologs in the database (known from structure) which have been detected. Precisely, it is the number of detected pairs of proteins with the same fold divided by the total number of pairs from a common superfamily. PDB400-B contains a total of 9,044 homologs, so a score of 10% indicates identification of 904 relationships. The y axis reports the number of EPQ. Because there are 1,323 queries made in the PDB400-B all-vs.-all comparison, 13 errors corresponds to 0.01, or 1% EPQ. The y axis is presented on a log scale to show results over the widely varying degrees of accuracy which may be desired. The scores that correspond to the levels of EPQ and coverage are shown in Fig. 4 and Table 1. The graph demonstrates the trade-off between sensitivity and selectivity. As more homologs are found (moving to the right), more errors are made (moving up). The ideal method would be in the lower right corner of the graph, which corresponds to identifying many evolutionary relationships without selecting unrelated proteins. Three measures of percentage identity are plotted. Percentage identity within alignment is the degree of identity within the aligned region of the proteins, without consideration of the alignment length. Percentage identity within both is the number of identical residues in the aligned region as a percentage of the average length of the query and target proteins. The HSP equation (17) is $H = 290.15I^{-0.542}$ where I is length for $10 < I < 80$; $H > 100$ for $I < 10$; $H = 24.7$ for $I > 80$. The percentage identity HSP-adjusted score is the percent identity within the alignment minus H . Smith-Waterman raw scores and E-values were taken directly from the sequence comparison program.

perfect separation, with all of the homologs at the top of the list and unrelated proteins below. In practice, perfect separation is impossible to achieve so instead one is interested in drawing a threshold above which there are the largest number of related pairs of sequences consistent with an acceptable error rate.

Our procedure involved measuring the coverage and error for every threshold. Coverage was defined as the fraction of structurally determined homologs that have scores above the selected threshold; this reflects the sensitivity of a method. Errors per query (EPQ), an indicator of selectivity, is the number of nonhomologous pairs above the threshold divided by the number of queries. Graphs of these data, called coverage vs. error plots, were devised to understand how

protocols compare at different levels of accuracy. These graphs share effectively all of the beneficial features of Receiver Operating Characteristic (ROC) plots (33, 34) but better represent the high degrees of accuracy required in sequence comparison and the huge background of nonhomologs.

This assessment procedure is directly relevant to practical sequence database searching, for it provides precisely the information necessary to perform a reliable sequence database search. The EPQ measure places a premium on score consistency; that is, it requires scores to be comparable for different queries. Consistency is an aspect which has been largely

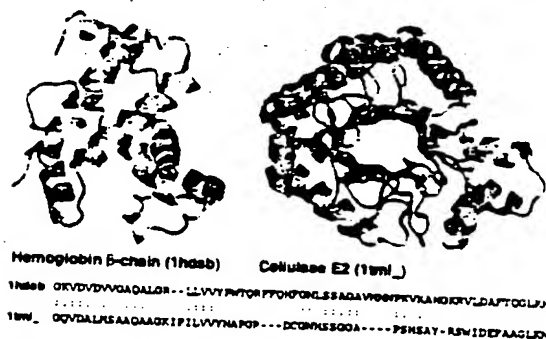


FIG. 2. Unrelated proteins with high percentage identity. Hemoglobin beta-chain (PDB code 1hds chain b, ref. 38, *Left*) and cellulase E2 (PDB code 1tml, ref. 39, *Right*) have 39% identity over 64 residues, a level which is often believed to be indicative of homology. Despite this high degree of identity, their structures strongly suggest that these proteins are not related. Appropriately, neither the raw alignment score of 85 nor the E-value of 1.3 is significant. Proteins rendered by RASMO (40).

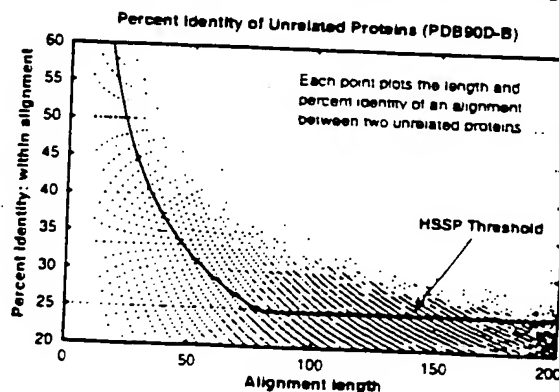


FIG. 3. Length and percentage identity of alignments of unrelated proteins in PDB400-B: Each pair of nonhomologous proteins found with SSEARCH is plotted as a point whose position indicates the length and the percentage identity within the alignment. Because alignment length and percentage identity are quantized, many pairs of proteins may have exactly the same alignment length and percentage identity. The line shows the HSP threshold (though it is intended to be applied with a different matrix and parameters).

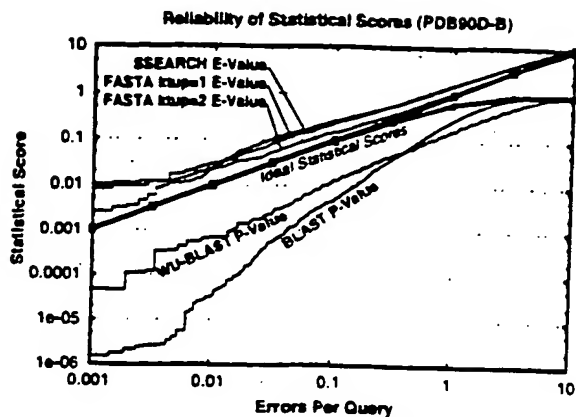


FIG. 4. Reliability of statistical scores in PDB90D-B: Each line shows the relationship between reported statistical score and actual error rate for a different program. E-values are reported for SSEARCH and FASTA, whereas P-values are shown for BLAST and WU-BLAST. If the scoring were perfect, then the number of errors per query and the E-values would be the same, as indicated by the upper bold line. (P-values should be the same as EPO for small numbers, and diverges at higher values, as indicated by the lower bold line.) E-values from SSEARCH and FASTA are shown to have good agreement with EPO but underestimate the significance slightly. BLAST and WU-BLAST are overconfident, with the degree of exaggeration dependent upon the score. The results for PDB40D-B were similar to those for PDB90D-B despite the difference in number of homologs detected. This graph could be used to roughly calibrate the reliability of a given statistical score.

ignored in previous tests but is essential for the straightforward or automatic interpretation of sequence comparison results. Further, it provides a clear indication of the confidence that should be ascribed to each match. Indeed, the EPQ measure should approximate the expectation value reported by database searching programs, if the programs' estimates are accurate.

The Performance of Scoring Schemes. All of the programs tested could provide three fundamental types of scores. The first score is the percentage identity, which may be computed in several ways based on either the length of the alignment or the lengths of the sequences. The second is a "raw" or "Smith-Waterman" score, which is the measure optimized by the Smith-Waterman algorithm and is computed by summing the substitution matrix scores for each position in the alignment and subtracting gap penalties. In BLAST, a measure

related to this score is scaled into bits. Third is a statistical score based on the extreme value distribution. These results are summarized in Fig. 1.

Sequence Identity. Though it has been long established that percentage identity is a poor measure (35), there is a common rule-of-thumb stating that 30% identity signifies homology. Moreover, publications have indicated that 25% identity can be used as a threshold (17, 36). We find that these thresholds, originally derived years ago, are not supported by present results. As databases have grown, so have the possibilities for chance alignments with high identity; thus, the reported cutoffs lead to frequent errors. Fig. 2 shows one of the many pairs of proteins with very different structures that nonetheless have high levels of identity over considerable aligned regions. Despite the high identity, the raw and the statistical scores for such incorrect matches are typically not significant. The principal reasons percentage identity does so poorly seem to be that it ignores information about gaps and about the conservative or radical nature of residue substitutions.

From the PDB90D-B analysis in Fig. 3, we learn that 30% identity is a reliable threshold for this database only for sequence alignments of at least 150 residues. Because one unrelated pair of proteins has 43.5% identity over 62 residues, it is probably necessary for alignments to be at least 70 residues in length before 40% is a reasonable threshold, for a database of this particular size and composition.

At a given reliability, scores based on percentage identity detect just a fraction of the distant homologs found by statistical scoring. If one measures the percentage identity in the aligned regions without consideration of alignment length, then a negligible number of distant homologs are detected. Use of the HSP equation improves the value of percentage identity, but even this measure can find only 4% of all known homologs at 1% EPQ. In short, percentage identity discards most of the information measured in a sequence comparison.

Raw Scores. Smith-Waterman raw scores perform better than percentage identity (Fig. 1), but ln-scaling (7) provided no notable benefit in our analysis. It is necessary to be very precise when using either raw or bit scores because a 20% change in cutoff score could yield a tenfold difference in EPQ. However, it is difficult to choose appropriate thresholds because the reliability of a bit score depends on the lengths of the proteins matched and the size of the database. Raw score thresholds also are affected by matrix and gap parameters.

Statistical Scores. Statistical scores were introduced partly to overcome the problems that arise from raw scores. This scoring scheme provides the best discrimination between homologous proteins and those which are unrelated. Most

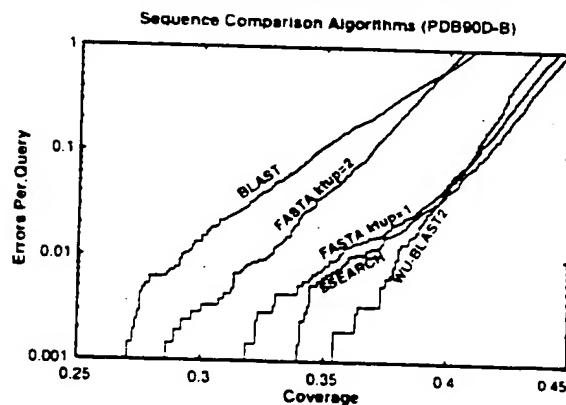
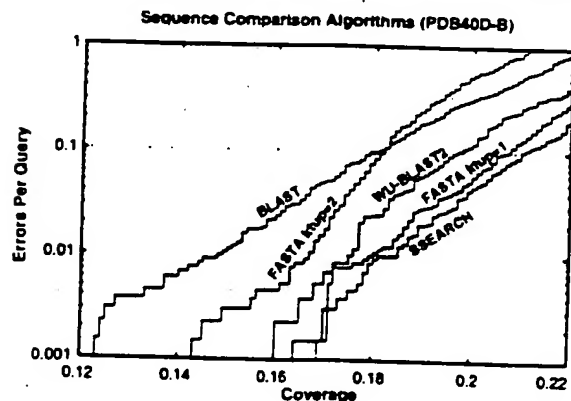


FIG. 5. Coverage vs. error plots of different sequence comparison methods: Five different sequence comparison methods are evaluated, each using statistical scores (E- or P-values). (A) PDB40D-B database. In this analysis, the best method is the slow SSEARCH, which finds 18% of relationships at 1% EPQ. FASTA ktup = 1 and WU-BLAST are almost as good. (B) PDB90D-B database. The quick WU-BLAST program provides the best coverage at 1% EPQ on this database, although at higher levels of error it becomes slightly worse than FASTA ktup = 1 and SSEARCH.

likely, its power can be attributed to its incorporation of more information than any other measure: it takes account of the full substitution and gap data (like raw scores) but also has details about the sequence lengths and composition and is scaled appropriately.

We find that statistical scores are not only powerful, but also easy to interpret. SSEARCH and FASTA show close agreement between statistical scores and actual number of errors per query (Fig. 4). The expectation value score gives a good, slightly conservative estimate of the chances of the two sequences being found at random in a given query. Thus, an E-value of 0.01 indicates that roughly one pair of nonhomologs of this similarity should be found in every 100 different queries. Neither raw scores nor percentage identity can be interpreted in this way, and these results validate the suitability of the extreme value distribution for describing the scores from a database search.

The P-values from BLAST also should be directly interpretable but were found to overstate significance by more than two orders of magnitude for 1% EPO for this database. Nonetheless, these results strongly suggest that the analytic theory is fundamentally appropriate. WU-BLAST2 scores were more reliable than those from BLAST, but also exaggerate expected confidence by more than an order of magnitude at 1% EPO.

Overall Detection of Homologs and Comparison of Algorithms. The results in Fig. 5A and Table 1 show that pairwise sequence comparison is capable of identifying only a small fraction of the homologous pairs of sequences in PDB40D-B. Even SSEARCH with E-values, the best protocol tested, could find only 18% of all relationships at a 1% EPO. BLAST, which identifies 15%, was the worst performer, whereas FASTA $k_{\text{tup}} = 1$ is nearly as effective as SSEARCH. FASTA $k_{\text{tup}} = 2$ and WU-BLAST2 are intermediate in their ability to detect homologs. Comparison of different algorithms indicates that those capable of identifying more homologs are generally slower. SSEARCH is 25 times slower than BLAST and 6.5 times slower than FASTA $k_{\text{tup}} = 1$. WU-BLAST2 is slightly faster than FASTA $k_{\text{tup}} = 2$, but the latter has more interpretable scores.

In PDB90D-B, where there are many close relationships, the best method can identify only 38% of structurally known homologs (Fig. 5B). The method which finds that many relationships is WU-BLAST2. Consequently, we infer that the differences between FASTA $k_{\text{tup}} = 1$, SSEARCH, and WU-BLAST2 programs are unlikely to be significant when compared with variation in database composition and scoring reliability.

Fig. 6 helps to explain why most distant homologs cannot be found by sequence comparison: a great many such relationships have no more sequence identity than would be expected by chance. SSEARCH with E-values can recognize >90% of the homologous pairs with 30–40% identity. In this region, there are 30 pairs of homologous proteins that do not have significant E-values, but 26 of these involve sequences with <50 residues. Of sequences having 25–30% identity, 75% are identified by SSEARCH E-values. However, although the number of homologs grows at lower levels of identity, the detection falls off sharply: only 40% of homologs with 20–25% identity

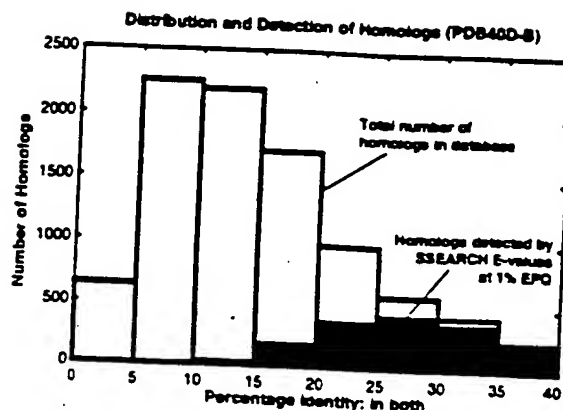


FIG. 6. Distribution and detection of homologs in PDB40D-B. Bars show the distribution of homologous pairs PDB40D-B according to their identity (using the measure of identity in both). Filled regions indicate the number of these pairs found by the best database searching method (SSEARCH with E-values) at 1% EPO. The PDB40D-B database contains proteins with <40% identity, and as shown on this graph, most structurally identified homologs in the database have diverged extremely far in sequence and have <20% identity. Note that the alignments may be inaccurate, especially at low levels of identity. Filled regions show that SSEARCH can identify most relationships that have 25% or more identity, but its detection wanes sharply below 25%. Consequently, the great sequence divergence of most structurally identified evolutionary relationships effectively defeats the ability of pairwise sequence comparison to detect them.

are detected and only 10% of those with 15–20% can be found. These results show that statistical scores can find related proteins whose identity is remarkably low; however, the power of the method is restricted by the great divergence of many protein sequences.

After completion of this work, a new version of pairwise BLAST was released: BLASTGP (37). It supports gapped alignments, like WU-BLAST2, and dispenses with sum statistics. Our initial tests on BLASTGP using default parameters show that its E-values are reliable and that its overall detection of homologs was substantially better than that of ungapped BLAST, but not quite equal to that of WU-BLAST2.

CONCLUSION

The general consensus amongst experts (see refs. 7, 24, 25, 27 and references therein) suggests that the most effective sequence searches are made by (i) using a large current database in which the protein sequences have been complexity masked and (ii) using statistical scores to interpret the results. Our experiments fully support this view.

Our results also suggest two further points. First, the E-values reported by FASTA and SSEARCH give fairly accurate estimates of the significance of each match, but the P-values provided by BLAST and WU-BLAST2 underestimate the true

Table 1. Summary of sequence comparison methods with PDB40D-B

Method	Relative Time*	1% EPO Cutoff	Coverage at 1% EPO
SSEARCH % identity: within alignment	25.5	>70%	<0.1
SSEARCH % identity: within both	25.5	34%	3.0
SSEARCH % identity: HSP-scaled	25.5	35% (HSSP = 9.8)	4.0
SSEARCH Smith-Waterman raw scores	25.5	142	10.5
SSEARCH E-values	25.5	0.03	16.4
FASTA $k_{\text{tup}} = 1$ E-values	3.9	0.03	17.9
FASTA $k_{\text{tup}} = 2$ E-values	1.4	0.03	16.7
WU-BLAST2 P-values	1.1	0.003	17.5
BLAST P-values	1.0	0.00016	14.8

*Times are from large database searches with genome proteins.

extent of errors. Second, SSEARCH, WU-BLAST2, and FASTA ktup = 1 perform best, though BLAST and FASTA ktup = 2 detect most of the relationships found by the best procedures and are appropriate for rapid initial searches.

The homologous proteins that are found by sequence comparison can be distinguished with high reliability from the huge number of unrelated pairs. However, even the best database searching procedures tested fail to find the large majority of distant evolutionary relationships at an acceptable error rate. Thus, if the procedures assessed here fail to find a reliable match, it does not imply that the sequence is unique; rather, it indicates that any relatives it might have are distant ones.**

**Additional and updated information about this work, including supplementary figures, may be found at <http://sss.stanford.edu/sss/>.

The authors are grateful to Drs. A. G. Murzin, M. Levitt, S. R. Eddy, and G. Mitchison for valuable discussion. S.E.B. was principally supported by a St. John's College (Cambridge, UK) Benefactors' Scholarship and by the American Friends of Cambridge University. S.E.B. dedicates his contribution to the memory of Rabbi Albert T. and Clara S. Bilgray.

1. Altschul, S. F., Gish, W., Miller, W., Myers, E. W. & Lipman, D. J. (1990) *J. Mol. Biol.* 215, 403-410.
2. Altschul, S. F. & Gish, W. (1996) *Methods Enzymol.* 266, 460-480.
3. Pearson, W. R. & Lipman, D. J. (1988) *Proc. Natl. Acad. Sci. USA* 85, 2444-2448.
4. Murzin, A. G., Brenner, S. E., Hubbard, T. & Chothia, C. (1995) *J. Mol. Biol.* 247, 536-540.
5. Brenner, S. E., Chothia, C., Hubbard, T. J. P. & Murzin, A. G. (1996) *Methods Enzymol.* 266, 635-643.
6. Pearson, W. R. (1991) *Genomics* 11, 635-650.
7. Pearson, W. R. (1995) *Protein Sci.* 4, 1145-1160.
8. Smith, T. F. & Waterman, M. S. (1981) *J. Mol. Biol.* 147, 195-197.
9. George, D. G., Hunt, L. T. & Barker, W. C. (1996) *Methods Enzymol.* 266, 41-59.
10. Vogt, G., Etzold, T. & Argos, P. (1995) *J. Mol. Biol.* 249, 816-831.
11. Henikoff, S. & Henikoff, J. G. (1993) *Proteins* 17, 49-61.
12. Bairoch, A. & Apweiler, R. (1996) *Nucleic Acids Res.* 24, 21-25.
13. Bairoch, A., Bucher, P. & Hofmann, K. (1996) *Nucleic Acids Res.* 24, 189-196.
14. Henikoff, S. & Henikoff, J. G. (1992) *Proc. Natl. Acad. Sci. USA* 89, 10915-10919.
15. Dayhoff, M., Schwartz, R. M. & Orcutt, B. C. (1978) in *Atlas of Protein Sequence and Structure*, ed. Dayhoff, M. (National Bio-
medical Research Foundation, Silver Spring, MD), Vol. 5, Suppl. 3, pp. 345-352.
16. Brenner, S. E. (1996) Ph.D. thesis. (University of Cambridge, UK).
17. Sander, C. & Schneider, R. (1991) *Proteins* 9, 56-68.
18. Johnson, M. S. & Overington, J. P. (1993) *J. Mol. Biol.* 233, 716-738.
19. Barton, G. J. & Sternberg, M. J. E. (1987) *Protein Eng.* 1, 89-94.
20. Lesk, A. M., Levitt, M. & Chothia, C. (1986) *Protein Eng.* 1, 77-78.
21. Arratia, R., Gordon, L. & M. W. (1986) *Ann. Stat.* 14, 971-993.
22. Karlin, S. & Altschul, S. F. (1990) *Proc. Natl. Acad. Sci. USA* 87, 2264-2268.
23. Karlin, S. & Altschul, S. F. (1993) *Proc. Natl. Acad. Sci. USA* 90, 5873-5877.
24. Altschul, S. F., Boguski, M. S., Gish, W. & Wootton, J. C. (1994) *Nat. Genet.* 6, 119-129.
25. Pearson, W. R. (1996) *Methods Enzymol.* 266, 227-258.
26. Lipman, D. J., Wilbur, W. J., Smith, T. F. & Waterman, M. S. (1984) *Nucleic Acids Res.* 12, 215-226.
27. Wootton, J. C. & Federhen, S. (1996) *Methods Enzymol.* 266, 554-571.
28. Waterman, M. S. & Vingron, M. (1994) *Stat. Science* 9, 367-381.
29. Perutz, M. F., Kendrew, J. C. & Watson, H. C. (1965) *J. Mol. Biol.* 13, 669-678.
30. Abola, E. E., Bernstein, F. C., Bryant, S. H., Koetzle, T. F. & Weng, J. (1987) in *Crystallographic Databases: Information Content, Software Systems, Scientific Applications*, eds. Allen, F. H., Bergerhoff, G. & Sievers, R. (Data Comm. Intl. Union Crystallogr., Cambridge, UK), pp. 107-132.
31. Brenner, S. E., Chothia, C. & Hubbard, T. J. P. (1997) *Curr. Opin. Struct. Biol.* 7, 369-376.
32. Orengo, C., Michie, A., Jones, S., Jones, D. T., Swindells, M. B. & Thornton, J. (1997) *Structure (London)* 5, 1093-1108.
33. Zweig, M. H. & Campbell, G. (1993) *Clin. Chem.* 39, 561-577.
34. Gribskov, M. & Robinson, N. L. (1996) *Comput. Chem.* 20, 25-33.
35. Fitch, W. M. (1966) *J. Mol. Biol.* 16, 9-16.
36. Chung, S. Y. & Subbiah, S. (1996) *Structure (London)* 4, 1123-1127.
37. Altschul, S. F., Madden, T. L., Schaffer, A. A., Zhang, J., Zhang, Z., Miller, W. & Lipman, D. J. (1997) *Nucleic Acids Res.* 25, 3389-3402.
38. Girling, R., Schmidt, W., Jr., Houston, T., Amma, E. & Huisman, T. (1979) *J. Mol. Biol.* 131, 417-433.
39. Spezio, M., Wilson, D. & Karplus, P. (1993) *Biochemistry* 32, 9906-9916.
40. Sayle, R. A. & Milner-White, E. J. (1995) *Trends Biochem. Sci.* 20, 374-376.

Annexins in cancer and autoimmune diseases

B. C. Bastian

Klinik und Poliklinik für Hautkrankheiten, Julius-Maximilians Universität Würzburg, Josef-Schneider-Str. 2, D-97080 Würzburg (Germany)

Abstract. Several annexins have been implicated in the pathogenesis of benign and malignant neoplasms of different origins. In some tumours a suppressive action of annexins has been shown, whereas studies of other tumours indicate an involvement of annexins in tumour progression. In the light of the expression of annexins at distinct episodes of fetal development these observations point towards a functional role of annexins in cellular development and differentiation. This view is supported by data that link certain annexins to distinct pathways of signal transduction. Auto-antibodies against several annexins have been detected in patients with autoimmune diseases such as systemic lupus erythematosus, rheumatoid arthritis and inflammatory bowel disease. Until now it is unclear whether their presence reflects a relevant pathogenetic mechanism or merely represents an unspecific expression of a raised autoimmunity in these patients.

Key words. Annexins; neoplasms; pathology; autoimmune diseases; auto-antibodies; differentiation.

Expression of annexins in tumours

The finding that several annexins are subject to growth-dependent regulation of expression, together with their participation in signalling pathways and cell-cell adhesion, has awoken interest in their role in the pathogenesis of cancer. Considering the related structural properties of the annexins it is of interest that tumour suppressing and promoting attributes have also been demonstrated for different annexins.

In 1983 Hattori et al. reported that AX-1 can induce differentiation in the human histiocytic lymphoma cell line U937 [1]. In their experiments a similar effect could be obtained by treatment of the cells for 6 days with dexamethasone. This dexamethasone-inducible differentiation could be blocked by a monoclonal anti-AX-1 antibody, suggesting that the dexamethasone effect was mediated by AX-1. However, other investigators failed to confirm AX-1 mRNA and protein induction by dexamethasone in U937 cells [2] as well as in primary human macrophages [3]. That these discrepancies might be a reflection of different culture conditions has been shown by Schlaepfer et al. [4]. The cellular level of AX-1 varies with the growth state of cells, with proliferating cells having significantly higher cellular levels and synthesis rates than quiescent cells. Differentiation induction by AX-1 was also reported for the human lung cell adenocarcinoma cell line A549 [5, 6] and the human squamous cell carcinoma cell line SqCC/Y1 [7]. Immunohistochemical analyses have revealed increased

expression of AX-1 in a variety of central and peripheral nervous system tumours [8] and squamous cell carcinoma of the skin [9].

AX-2 has also been shown to underlie a growth-dependent regulation and to be inducible by mitogenic substances [10, 11]. In contrast to the described tumour suppressive effects assigned to AX-1 the association of AX-2 phosphorylation with retroviral transformation has raised the suspicion that AX-2 could be involved in the pathogenesis of cancer [12–14]. AX-2 has been shown to be highly abundant in human hepatocellular carcinoma but not in normal liver, human fetal tissue or regenerating rat liver after injury [15]. Overexpression of AX-2 mRNA and protein have further been demonstrated in human pancreatic cancer and pancreatic cancer derived cell lines [16, 17], multi-drug resistant small cell lung cancer [18], and high but not low grade gliomas [19, 20]. In the Eker rat hereditary renal carcinoma model, a dominant disorder with a defect in the rat analogue of the human tuberous sclerosis (*TSC2*) gene, a differential analysis showed the AX-2 heavy chain to be one of four genes with increased expression compared to normal animals [21]. Low baseline AX-2 expressions and strong increases after induction of differentiation are found in the PC12 rat adrenal pheochromocytoma and the F9 murine teratocarcinoma cell lines [22, 23]. Tressler et al. have demonstrated that AX-2 and AX-6 expressed on murine RAW117 lymphoma cells serve as adhesion molecules for tumour cell–endothelial cell binding [24, 25]. They showed that AX-2 and AX-6 are present on the external plasma membrane and that the binding of tumour cells could be significantly reduced by antibodies against AX-2 or AX-6. These findings indicate a pivotal role of certain AXs in cell-cell interaction.

Current address: Cancer Genetics Program, University of California San Francisco, Cancer Center, Box 0808, San Francisco (California 94143-0808, USA), Fax +1 415 476 8218, e-mail: bastian@cc.ucsf.edu

AXs-1, 2, 4, 5 and 6 were also shown to be expressed by cultured osteoblasts and the human osteosarcoma cell line MG-63 [26]. In this study the amount of AX-5 found in MG-63 cells was three times higher than in the primary osteoblast cultures. The authors also noted an influence on AX-5 levels on the state of growth of the culture. Karube et al. found a decrease of AX-5 mRNA and protein in carcinomas of the uterine cervix and endometrium when compared to normal tissues [27]. As AX-5 has been shown to exert an inhibitory action on protein kinase C [28, 29] the decreased levels of AX-5 might lead to a dysregulated activation of protein kinase C.

In contrast to AX-1 and -2 which are regulated during normal cell growth, the expression of AX-6 appears to be constitutive in most cell lines [30]. Tumour suppressive effects have been assigned to AX-6 in certain model systems. AX-6 is not expressed in the human squamous cell carcinoma line A431 which is characterized by a lack of contact inhibition and reduced growth factor requirement. After transfection with the AX-6 gene A431 cells stopped proliferating after reaching confluence [31] and grew smaller tumours than the non-transfected cells in mice [32]. Recently, AX-6 has been demonstrated to be differentially expressed in a murine melanoma cell line when compared to a syngeneic Melan-a-immortalized melanocyte cell line [33].

Acute promyelocytic leukemia (APL) is a disorder characterized by a balanced t(15;17) translocation in which the breakpoint involves the retinoic acid receptor- α and the *PML* gene [34]. AX-8 was shown to be overexpressed in APL cells in the majority of cases [35, 36]. As the AX-8 gene is located on chromosome 10 its overexpression cannot be directly related to the translocation. Interestingly, all-trans-retinoic acid, a strikingly effective drug to induce remissions in APL patients, is able to reduce the AX-8 expression in the APL-derived cell line NB4 [35]. This has been shown to be due to transcriptional regulation of the AX-8 gene [36]. The negative response of AX-8 expression to all-trans-retinoic acid supports the notion that AX-8 might act as a signal transducer involved in regulation of cell growth and differentiation.

Annexins as potential auto-antigens in autoimmune diseases

Auto-antibodies against AX-1 in patients with rheumatic diseases such as systemic lupus erythematosus (SLE) and rheumatoid arthritis (RA) were first described by Hirata et al. in 1981 [37]. These investigators found that patients' sera were able to abrogate the inhibitory action of a partly purified rabbit lipocortin on phospholipase A₂. This effect was decreased after absorption of the IgM fraction but not the IgG fraction of the sera, which suggests that circulating IgM antibodies

against AX-1 were present in those patients. Later, AX-1 of the IgM and to a lesser extent of the IgG-type were found in patients with RA and SLE using a recombinant human AX-1 and a correlation with disease activity was claimed [38]. Initially, it was suggested that corticosteroids might, by the induction of AX-1, induce the formation of AX-1 auto-antibodies, and that their presence might impair the inhibitory action of corticosteroids on phospholipase A₂ [38]. However, a causal role of corticosteroids in the induction of AX-1 auto-antibodies seems unlikely, because asthma patients treated with corticosteroids do not show AX-1 auto-antibodies [39]. Furthermore, no association of AX-1 auto-antibodies with either serum phospholipase A₂ levels or activity could be shown [40]. Patients with SLE were also reported to have auto-antibodies against AX-5 [41]. In this study the auto-antibodies were more common in patients who additionally had positive anti-cardiolipin antibodies or lupus anticoagulant. AX-1 auto-antibodies have also been demonstrated in patients with inflammatory bowel diseases, such as Crohn's disease or ulcerative colitis, who lack any association with corticosteroid treatment [42]. Interestingly, in this study patients with active confirmed bacterial diarrhoea had the highest titres of AX-1 auto-antibodies, suggesting that their presence might not be confined to autoimmune diseases but might reflect a nonspecific reaction to inflammation. This view is supported by studies demonstrating auto-antibodies against AX-1, AX-2, AX-3, AX-4, AX-5, and AX-6 in a plethora of inflammatory and neoplastic skin diseases without a clear correlation to any disease group including autoimmune diseases [43, 44]. For obvious reasons, a final judgement on the relevance of AX auto-antibodies requires the elucidation of the functions of AXs.

- 1 Hattori T., Hoffman T. and Hirata F. (1983) Differentiation of a histiocytic lymphoma cell line by lipomodulin a phospholipase inhibitory protein. *Biochem. Biophys. Res. Commun.* 111: 551-559
- 2 Isacke C. M., Lindberg R. A. and Hunter T. (1989) Synthesis of p36 and p35 is increased when U-937 cells differentiate in culture but expression is not inducible by glucocorticoids. *Molec. Cell Biol.* 9: 232-240
- 3 Bronnegard M. O., Andersson O., Edwall J., Lund G., Norstedt G. and Carlstedt-Duke J. (1988) Human calpactin II (lipocortin I) messenger ribonucleic acid is not induced by glucocorticoids. *Molec. Endocrinol.* 2: 732-739
- 4 Schlaepfer D. D. and Haigler H. T. (1990) Expression of annexins as a function of cellular growth state. *J. Cell Biol.* 111: 19685-21061
- 5 Croxtall J. D., Waheed S., Choudhury Q., Anand R. and Flower R. J. (1993) N-terminal peptide fragments of lipocortin-1 inhibit A549 cell growth and block EGF-induced stimulation of proliferation. *Int. J. Cancer* 54: 153-158
- 6 Croxtall J. D. and Flower R. J. (1992) Lipocortin 1 mediates dexamethasone-induced growth arrest of the A549 lung adenocarcinoma cell line. *Proc. Natl Acad. Sci. USA* 89: 3571-3575
- 7 Violette S. M., King I., Browning J. L., Pepinsky R. B., Wallner B. P. and Sartorelli A. C. (1990) Role of lipocortin I in the glucocorticoid induction of the terminal differentiation of a human squamous carcinoma. *J. Cell Physiol.* 142: 70-77

- 8 Johnson M. D., Kamsio-Pratt J., Pepinsky R. B. and Whetsell W. O. J. (1989) Lipocortin-1 immunoreactivity in central and peripheral nervous system glial tumours. *Hum. Pathol.* 20: 772-776
- 9 Bastian B. C., van der Piepen U., Römisch J., Pâques E. P. and Bröcker E. B. (1993) Localization of annexins in normal and diseased human skin. *J. Dermatol. Sci.* 6: 225-234
- 10 Chiang Y., Schneiderman M. H. and Vishwanatha J. K. (1993) Annexin II expression is regulated during mammalian cell cycle. *Cancer Res.* 53: 6017-6021
- 11 Kreutzer J. C. and Hirschhorn R. R. (1990) The growth-regulated gene *IB6* is identified as the heavy chain of calpactin I. *Exp. Cell Res.* 188: 153-159
- 12 Radke K., Gilmore T. and Martin G. S. (1980) Transformation by Rous sarcoma virus: a cellular substrate for transformation-specific protein phosphorylation contains phosphotyrosine. *Cell* 21: 821-828
- 13 Erikson E. and Erikson R. L. (1980) Identification of a cellular protein substrate phosphorylated by the avian sarcoma virus-transforming gene product. *Cell* 21: 829-836
- 14 Ozaki T. and Sakiyama S. (1993) Molecular cloning of rat calpactin I heavy-chain cDNA whose expression is induced in v-src-transformed rat culture cell lines. *Oncogene* 8: 1707-1710
- 15 Frohlich M., Motte P., Galvin K., Takahashi H., Wands J. and Ozturk M. (1990) Enhanced expression of the protein kinase substrate p36 in human hepatocellular carcinoma. *Molec. Cell Biol.* 10: 3216-3223
- 16 Vishwanatha J. K., Chiang Y., Kumble K. D., Hollingsworth M. A. and Pour P. M. (1993) Enhanced expression of annexin II in human pancreatic carcinoma cells and primary pancreatic cancers. *Carcinogenesis* 14: 2575-2579
- 17 Kumble K. D., Hirota M., Pour P. M. and Vishwanatha J. K. (1992) Enhanced levels of annexins in pancreatic carcinoma cells of Syrian hamsters and their intrapancreatic allografts. *Cancer Res.* 52: 163-167
- 18 Cole S. P., Pinkoski M. J., Bhardwaj G. and Deeley R. G. (1992) Elevated expression of annexin II (lipocortin II, p36) in a multidrug resistant small cell lung cancer cell line. *Br. J. Cancer* 65: 498-502
- 19 Reeves S. A., Chavez-Kappel C., Davis R., Rosenblum M. and Israel M. A. (1992) Developmental regulation of annexin II (Lipocortin 2) in human brain and expression in high grade glioma. *Cancer Res.* 52: 6871-6876
- 20 Roseman B. J., Bollen A., Hsu J., Lamborn K. and Israel M. A. (1994) Annexin II marks astrocytic brain tumours of high histologic grade. *Oncol. Res.* 6: 561-567
- 21 Hino O., Kobayashi E., Nishizawa M., Kubo Y., Kobayashi T., Hirayama Y. et al. (1995) Renal carcinogenesis in the Eker rat. *J. Cancer Res. Clin. Oncol.* 121: 602-605
- 22 Fox M. T., Prentice D. A. and Hughes J. P. (1991) Increases in p11 and annexin II proteins correlate with differentiation in the PC12 pheochromocytoma. *Biochem. Biophys. Res. Commun.* 177: 1188-93
- 23 Harder T., Thiel C. and Gerke V. (1993) Formation of the annexin IIp112 complex upon differentiation of F9 teratocarcinoma cells. *J. Cell Sci.* 104: 1109-1117
- 24 Tressler R. J., Yeatman T. and Nicolson G. L. (1994) Extracellular annexin VI expression is associated with divalent cation-dependent endothelial cell adhesion of metastatic RAW117 large-cell lymphoma cells. *Exp. Cell Res.* 215: 395-400
- 25 Tressler R. J., Updyke T. V., Yeatman T. and Nicolson G. L. (1993) Extracellular annexin II is associated with divalent cation-dependent tumour cell-endothelial cell adhesion of metastatic RAW117 large-cell lymphoma cells. *J. Cell Biochem.* 53: 265-276
- 26 Mohiti J., Walker J. H. and Caswell A. M. (1995) Studies on annexins in primary cultures of human osteoblasts and in the human osteosarcoma cell line MG-63. *Biochem. Soc. Trans.* 23: 36S
- 27 Karube A., Shidara Y., Hayasaka K., Maki M. and Tanaka T. (1995) Suppression of calphobindin I (CPB I) production in carcinoma of uterine cervix and endometrium. *Gynecol. Oncol.* 58: 295-300
- 28 Shibata S., Sato H. and Maki M. (1992) Calphobindins (placental annexins) inhibit protein kinase C. *J. Biochem.* 112: 552-556
- 29 Schlaepfer D. D., Jones J. J. and Haigler H. T. (1992) Inhibition of protein kinase C by annexin V. *Biochemistry* 31: 1886-1891
- 30 Moss S. E., Jacob S. M., Davies A. A. and Crumpton M. J. (1992) A growth-dependent post-translational modification of annexin VI. *Biochim. Biophys. Acta* 1160: 120-126
- 31 Theobald J., Smith P. D., Jacob S. M. and Moss S. E. (1994) Expression of annexin VI in A431 carcinoma cells suppresses proliferation: a possible role for annexin VI in cell growth regulation. *Biochim. Biophys. Acta* 1223: 383-390
- 32 Theobald J., Hanby A., Patel K. and Moss S. E. (1995) Annexin VI has tumour-suppressor activity in human A431 squamous epithelial carcinoma cells. *Br. J. Cancer* 71: 786-788
- 33 Francia G., Mitchell S. D., Moss S. E., Hanby A. M., Marshall J. F. and Hart I. R. (1996) Identification by differential display of annexin-VI, a gene differentially expressed during melanoma progression. *Cancer Res.* 56: 3855-3858
- 34 Warrell R. P., de Thé, H., Wang Z. Y. and Degos L. (1993) Acute promyelocytic leukemia. *New Engl. J. Med.* 329: 177-189
- 35 Chang K. S., Wang G., Freireich E. J., Daly M., Naylor S. L., Trujillo J. M. et al. (1992) Specific expression of the annexin VIII gene in acute promyelocytic leukemia. *Blood* 79: 1802-1810
- 36 Sarkar A., Yang P., Fan Y. H., Mu Z. M., Hauptmann R., Adolf G. R. et al. (1994) Regulation of the expression of annexin VIII in acute promyelocytic leukemia. *Blood* 84: 279-286
- 37 Hirata F., del Carmine R., Nelson C. A., Axelrod, J., Schiffmann E., Warabi A. et al. (1981) Presence of autoantibody for phospholipase inhibitory protein, lipomodulin, in patients with rheumatic diseases. *Proc. Natl Acad. Sci. USA* 78: 3190-3194
- 38 Goulding N. J., Podgorski M. R., Hall N. D., Flower R. J., Browning J. L., Pepinsky R. B. et al. (1989) Autoantibodies to recombinant lipocortin-1 in rheumatoid arthritis and systemic lupus erythematosus. *Ann. Rheum. Dis.* 48: 843-850
- 39 Wilkinson J. R., Podgorski M. R., Godolphin J. L., Goulding N. J. and Lee T. H. (1990) Bronchial asthma is not associated with autoantibodies to lipocortin-1. *Clin. Exp. Allergy* 20: 189-192
- 40 Pruzanski W., Goulding N. J., Flower R. J., Gladman D. D., Urowitz M. B., Goodman P. J. et al. (1994) Circulating group II phospholipase A2 activity and antilipocortin antibodies in systemic lupus erythematosus. Correlative study with disease activity. *J. Rheumatol.* 21: 252-257
- 41 Matsuda J., Saitoh N., Gohchi K., Gotoh M. and Tsukamoto M. (1994) Anti-annexin V antibody in systemic lupus erythematosus patients with lupus anticoagulant and/or anticardiolipin antibody. *Am. J. Hematol.* 47: 56-58
- 42 Stevens T. R., Smith S. F. and Rampton D. S. (1993) Antibodies to human recombinant lipocortin-I in inflammatory bowel disease. *Clin. Sci.* 84: 381-386
- 43 Kraus M., Römisch J., Bastian B. C., Pâques E. P. and Hartmann A. A. (1992) Detection of human anti-annexin autoantibodies by enzyme immunoassays. *J. Immunoassay* 13: 411-439
- 44 Bastian B. C., Nuss B., Römisch J., Kraus M. and Bröcker E. B. (1994) Autoantibodies to annexins: a diagnostic marker for cutaneous disorders? *J. Dermatol. Sci.* 8: 194-202

Alterations of Annexin Expression in Pathological Neuronal and Glial Reactions

Immunohistochemical Localization of Annexins I, II (p36 and p11 Subunits), IV, and VI in the Human Hippocampus

David A. Eberhard, Morry D. Brown, and
Scott R. VandenBerg

From the Department of Pathology (Neuropathology),
University of Virginia Health Sciences Center,
Charlottesville, Virginia

Annexins are Ca^{2+} -dependent membrane-binding proteins that are potentially important in Ca^{2+} -induced neurotoxicity or neuroprotection. To address the possible involvement of annexins in cellular reactions to brain injury and neurodegenerative disease, we studied the immunohistochemical localization of annexins I, II (p36 and p11), IV, and VI in the adult human hippocampus. Formalin-fixed, paraffin-embedded tissue from autopsy cases representing hypoxic-ischemic injury, seizure disorders, Alzheimer's disease, and age-related controls were examined. Neurons showed cytoplasmic immunoreactivity for annexin I, whereas annexin VI was distributed in patterns suggesting plasma membrane and perisynaptic locations. The cytoarchitectural distribution of annexin VI within neurons was altered in pathological states and annexin VI was strongly associated with neuronal granulovacuolar bodies in Alzheimer's disease. Reactive astrocytes expressed annexins I, II (p36 and p11), and IV, whereas quiescent astrocytes were minimally immunoreactive. Significant annexin immunoreactivity was also detected in oligodendrocytes (annexin IV), ependymocytes (I, II, and IV), choroid plexus (I, IV, and VI), meningeal epithelium (I, II, IV, and VI), and vascular endothelium (II and IV) and smooth muscle (I, IV, and VI). This is the first comparative study of immunoreactivities for multiple annexins in human brain. Neurons and

glia display selective and different profiles of annexin protein expression and show immunohistochemical changes in pathological conditions, which suggest involvement of annexins in neuronal and glial reactions to injury. (Am J Pathol 1994, 145:640-649)

The annexins are a family of proteins that are defined by a conserved COOH-terminal domain that confers Ca^{2+} -dependent binding to membranes containing acidic phospholipids. The NH₂-terminal sequence of each annexin is unique and presumably confers functional specificity to the protein. A variety of roles for annexins in cellular physiology have been proposed, such as mediation of membrane trafficking events and membrane-cytoskeleton interactions, regulation of phospholipase activity and eicosanoid release, receptor signal transduction, modulation, or formation of Ca^{2+} channels, and control of cellular proliferation and differentiation.^{1,2} However, at present there is little understanding of the specific functions of particular annexins *in vivo*.

Annexins are widely distributed among species and tissues. In the mammalian nervous system, different annexins are expressed in various cell types.³⁻⁶ The patterns of annexin expression in the brain may change during development^{3,7} and in pathological states.^{8,9} To better define the relationship of annexins to cellular reactions to injury and de-

DAE was supported by grant T32 NS 7236 from NINCDS and MDB was supported by a GEM fellowship of the National Consortium for Graduate Degrees for Minorities in Engineering and Science, Inc.

Accepted for publication June 12, 1994

Address reprint requests to Dr. Scott R. VandenBerg, Department of Pathology (Neuropathology), Box 214, University of Virginia Health Sciences Center, Charlottesville, VA 22908

generation in the have compared t and p36 subunits a variety of cond and neuronal dar damage, chronic mer's disease w ations in both the tectural patterns changes occurrence of annexin V ins I, II, and IV ir gest that the an and glial respor

Materials and

Case Materiz

Hippocampal si cases (13 male tients (ages 35 acute or chror garded as cont zure disorders: sclerosis and fe trogliosis witho tients with histic logical findings Four patients events that occ three showed n gliosis and one patients were and showed a Postmortem int hours (median were used as mortem fixation istry. These co cerebral neoc sented a varie processes, inf mer's disease.

Tissue Proc Immunohisti

In most cases in 10 to 20% temperature fc embedding in freshly dissec

generation in the human central nervous system, we have compared the distributions of annexins I, II (p11 and p36 subunits), IV, and VI in the hippocampus after a variety of conditions associated with glial reactions and neuronal damage. In this study, hypoxic ischemic damage, chronic seizure-related injury, and Alzheimer's disease were accompanied by specific alterations in both the cellular distributions and cytoarchitectural patterns of the annexins. The most prominent changes occurred with the cytoarchitectural distribution of annexin VI in neurons and increases of annexins I, II, and IV in reactive astroglia. These data suggest that the annexins may be involved in neuronal and glial responses to acute and chronic injury.

Materials and Methods

Case Material

Hippocampal sections from a total of 20 postmortem cases (13 male, 7 female) were examined. Four patients (ages 35 to 66 years) with no history of either acute or chronic neurological disorders were regarded as controls. Six patients had histories of seizure disorders: two had asymmetric hippocampal sclerosis and four showed mild to moderate hilar astrogliosis without significant neuronal loss. Four patients with histories of chronic dementia had pathological findings diagnostic of Alzheimer's disease.¹⁰ Four patients had significant hypoxic/ischemic events that occurred 4 days to 2 weeks before death: three showed neuronal loss in hippocampal CA1 with gliosis and one had a subacute infarct in CA1. Two patients were terminally unresponsive after shock and showed acute neuronal injury without gliosis. Postmortem intervals for all cases ranged from 2 to 24 hours (median, 12 hours). Neurosurgical specimens were used as controls to assess the effects of postmortem fixation delay on annexin immunohistochemistry. These consisted of gray and white matter from cerebral neocortex and hippocampus and represented a variety of diseases, including inflammatory processes, infarcts, seizure disorders, and Alzheimer's disease.

Tissue Processing and Immunohistochemistry

In most cases the entire brain was fixed by immersion in 10 to 20% phosphate-buffered formalin at room temperature for 2 weeks before dissection and routine embedding in paraffin. In three cases, the brains were freshly dissected and hippocampal slices were fixed

for 3 to 4 days at 4 C in phosphate-buffered 10% formalin before paraffin embedding. The control neurosurgical specimens were fixed and processed under a variety of conditions, ranging from rapid immersion and fixation of fresh tissue in 10% buffered zinc formalin for 48 hours at 4 C to routine fixation for 8 to 24 hours at room temperature. Fixed tissue was embedded in either regular temperature or low melting point paraffin (42 C). Variations in tissue processing did not affect the cellular and cytoarchitectural localizations of specific annexin immunoreactivities related to either normal or disease states. The overall intensity of immunostaining was somewhat less robust in deeper regions of the postmortem brains fixed by whole immersion compared with fresh tissue sections that were more rapidly fixed.

Immunohistochemistry was performed for annexins I, II (p11 and p36), IV, and VI and for glial fibrillary acidic protein (GFAP) in all cases; for S100 β and β A4-amyloid in Alzheimer's disease cases; and for synaptophysin, HAM 56, and factor VIII in selected other cases. Primary antibodies were obtained from the following sources and used at the indicated concentrations in phosphate-buffered saline (PBS): 1) monoclonal mouse IgG antibodies directed to annexin I, annexin II (p36 monomer), annexin II (p11 subunit), annexin IV, and annexin VI (each at 1:500; Zymed Laboratories, Inc., South San Francisco, CA); 2) rabbit polyclonal antibodies directed to GFAP (1:1400; Dako Corp., Carpinteria, CA); 3) monoclonal mouse IgG directed to synaptophysin (SY38, 1:10; Boehringer Mannheim Corp., Indianapolis, IN); 4) rabbit polyclonal antibodies directed to β 4-amyloid (1:10; Boehringer Mannheim Corp.); 5) rabbit polyclonal antibodies directed to S100 β (1:2000; Chemicon International, Inc., Temecula, CA); 6) monoclonal mouse IgG antibodies directed to human macrophage antigen (HAM 56, 1:100; Dako Corp.); and 7) monoclonal mouse IgG antibodies directed to factor VIII (1:10; Dako Corp.). The specificities of the antiannexin antibodies were confirmed by Western blotting of normal and neoplastic human brain tissues and of cultured U251 human glioma cells.

Paraffin sections, 5 μ thick, were prepared for immunohistochemistry by deparaffinization in xylene, preincubation for 30 minutes at 22 C with methanolic H₂O₂ (1.75%), and hydration in graded alcohols. For annexin II (p11 subunit or p36) immunohistochemistry sections were then treated either with pepsin (Sigma Chemical Co., St. Louis, MO) 4 mg/ml in 0.01 N HCl for 15 to 30 minutes at 37 C or by microwaving at 750 W in 10 mmol/L sodium citrate buffer (pH 6) for three to four consecutive 5-minute intervals, replacing evaporated buffer volume with H₂O after each inter-

val. The patterns of p11 immunoreactivity produced after each of these treatments were identical. For p36, microwave pretreatment allowed detection of immunoreactivity but pepsin pretreatment did not. For detection of β A4 epitopes, sections were incubated with 88% formic acid for 5 minutes at 22 C. All sections were then rinsed in PBS, blocked with 1.5% nonimmune serum in PBS (horse serum for monoclonal antibodies or goat serum for polyclonal antibodies), and incubated with the primary antibodies for 18 to 24 hours at 4 C. Primary antibody was labeled by the avidin-biotin complex method¹¹ using the Vectastain Elite kit (Vector Laboratories Inc., Burlingame, CA) and visualized with peroxidase-coupled anti-mouse or anti-rabbit antibodies using diaminobenzidine (DAB) as the chromogen. The sections were counterstained with hematoxylin.

Dual-label immunohistochemistry for p11 and GFAP was performed by first visualizing p11 with microwave pretreatment as described above using aminoethylcarbazole (AEC) as chromogen. The sections were then incubated with pepsin (4 mg/ml in 0.01 N HCl, 15 minutes at 37 C), rinsed in PBS, and blocked with nonimmune goat serum. GFAP was then visualized as described above, using DAB-Ni complex as chromogen. Dual labeling for β A4 and p11 was performed by first visualizing β A4 with formic acid pretreatment as described above using AEC as chromogen; p11 was then visualized with pepsin or microwave pretreatment as described above using DAB-Ni complex as chromogen.

Annexin Nomenclature

Studies cited herein have used a variety of designations for the annexin proteins. The system used here is that of Crumpton and Dedman:¹² p37, annexin I; p36, annexin II monomer; p32, annexin IV; p67/68, annexin VI.

Results

Normal Hippocampus

The cellular localizations of annexins I, II (p36 and p11), IV, and VI are summarized in Table 1.

Annexin I

Moderate to strong immunoreactivity for annexin I was present in neurons, subependymal and subpial astrocytes, choroid plexus epithelium, ependyma, and vascular smooth muscle (Figure 1A). In neurons,

Table 1. Cellular Localization of Annexins in Human Hippocampus and Associated Structures

	Annexin			
	I	II	IV	VI
Neurons	++	-	-	+++
Subependymal/subpial astrocytes	++	+++	++	-
Parenchymal astrocytes	-	-	+	-
Oligodendrocytes	-	-	++	-
Ependyma	+++	+++	+++	+
Choroid plexus	+++	+	+++	+++
Meningothelium	+++	+++	+++	+++
Endothelium	+	+++	+++	-
Smooth muscle	++	-	++	++

annexin I was primarily confined to the soma in a diffuse to granular cytoplasmic pattern (Figure 3F), sometimes with a perinuclear distribution. The intensity of the annexin I immunoreactivity of the hippocampal neurons ranged from most intense in bipolar neurons of the stratum oriens, to moderate in the pyramidal neurons of the cornu ammonis, and to only mild in the granular cells of the dentate gyrus. Immunoreactivity in other cell types generally showed a diffuse cytoplasmic pattern. Subependymal and subpial astrocytes exhibited moderate immunoreactivity in cell bodies and larger processes. In contrast, annexin I was not detected in nonreactive parenchymal astrocytes and oligodendroglia. The neuropil showed a faint to mild diffuse staining, somewhat less in white matter compared with gray matter. Immunoreactivity in vascular endothelium was mild and variable.

Annexin II (p36 and p11)

Immunoreactivities for annexin II (p36 and p11) showed similar cellular and cytoarchitectural distributions (Figure 1B). In ependymocytes and subependymal and subpial astrocytes, immunoreactivity was usually most intense at the cell periphery but was sometimes cytoplasmic. Immunostaining in deep white matter was variable and when present was associated with perivascular astroglia. Annexin II p36 and p11 were absent in neurons, nonreactive parenchymal astrocytes, oligodendrocytes, and neuropil. In other cell types, p11 and p36 immunoreactivities were strong in arachnoid meningotheilium and vascular endothelium, whereas staining of the choroid plexus epithelium and vascular smooth muscle was variable and mild.

Annexin IV

Moderate to strong cytoplasmic immunoreactivity for annexin IV was present in subependymal and subpial

Figure
 (C).
 bodie
 more
 p11
 assoc
 prim
 temp

astro
 eper
 smo
 sube
 fuse
 large
 nexi
 cyto
 tion,
 cell
 app
 periv
 perir
 mem
 tect
 Ar
 eper
 end
 was
 type

Anr.

Mod
 pre

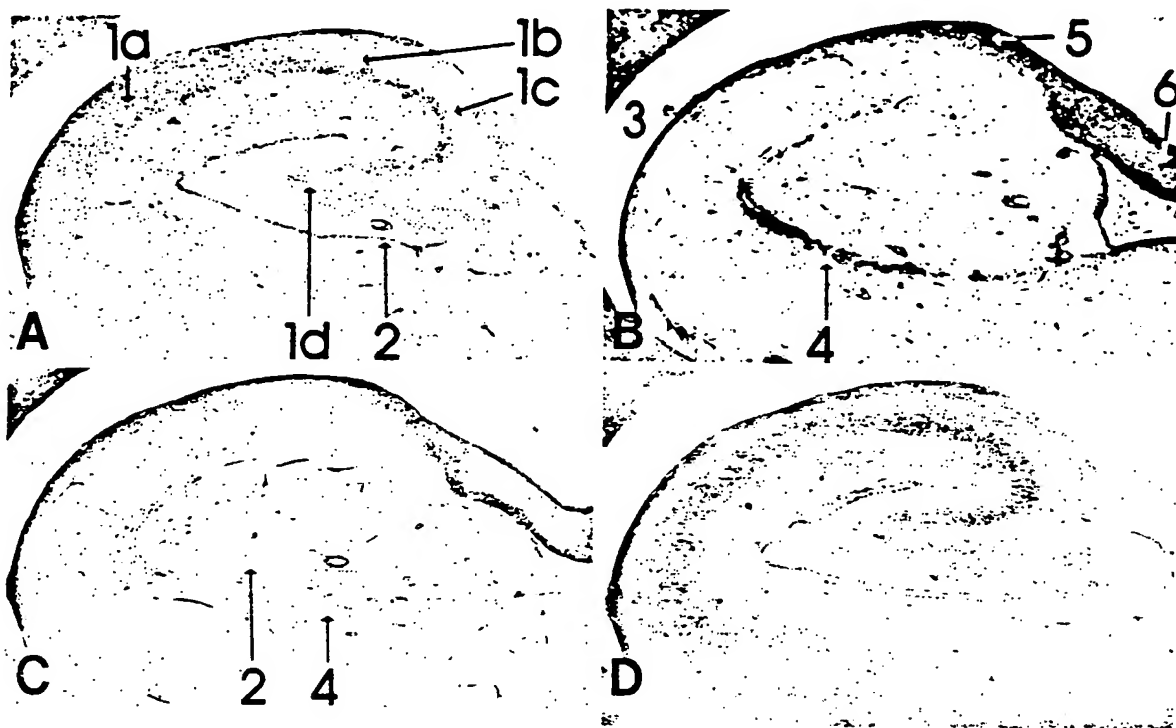


Figure 1. Annexin immunohistochemistry of normal hippocampus. Adjacent tissue sections were processed for annexin I (A), p11 (B), annexin IV (C), and annexin VI (D) using biotin-avidin immunohistochemistry with hematoxylin counterstain. A: Annexin I was present in neuronal cell bodies in the dentate gyrus and Ammon's horn, glia in hippocampal fissure, fimbria, and alveus, and ependyma and vessels. B: Dense p11 immunoreactivity was associated with glia in fimbria, alveus, and hippocampal fissure, and with vessels and ependyma. C: The distribution of annexin IV immunoreactivity resembled that of p11 but the staining was less dense and more diffuse. Immunoreactivity in dentate granule cell layer was associated with glia. D: Annexin VI was prominent in pyramidal and granule cell layers and dentritic fields. Staining in fimbria and alveus was primarily axonal. Original magnification, $\times 17.5$. 1, Ammon's horn (a, CA1; b, CA2; c, CA3; d, CA4); 2, granule cell layer of dentate gyrus; 3, temporal horn of lateral ventricle; 4, hippocampal fissure; 5, alveus; 6, fimbria.

astrocytes, oligodendroglia, choroid plexus, ependyma, arachnoid meningotheilium, vascular smooth muscle, and endothelium (Figure 1C). The subependymal and subpial astrocytes contained diffuse or granular staining patterns in cytoplasm and larger processes. In choroid plexus epithelium, annexin IV was distributed in a relatively coarse granular cytoplasmic pattern, often with subapical accumulation, and in ependymocytes was usually localized to cell borders. Annexin IV in oligodendroglia was most apparent in populations exhibiting perineuronal and perivascular satellitosis where it was present as a thin perinuclear cytoplasmic rim or outlining the plasma membrane (Figure 3H). Annexin IV was never detected in neurons.

Annexin IV was also detected in the nuclei of some ependymocytes, astrocytes, oligodendrocytes, and endothelial cells. The presence of nuclear staining was not correlated with cytoplasmic staining or the type of lesion, clinical history, or patient age.

Annexin VI

Moderate to strong annexin VI immunoreactivity was present in neurons, choroid plexus epithelium, arach-

noid meningotheilium, and vascular smooth muscle (Figure 1D). In pyramidal neurons, annexin VI was primarily localized to the plasma membranes of dendritic processes and perikarya and in neuropil in a granular or punctate pattern similar to that of synaptophysin (Figure 3, A and B). Bipolar neurons in the stratum oriens displayed dense cytoplasmic staining of soma and proximal processes, whereas the immunoreactivity in granule cells was less prominent. The only immunoreactivity in the white matter was confined to axonal fibers. Annexin VI in the choroid plexus epithelium was concentrated in the apical and basal regions, whereas ependyma displayed negligible immunoreactivity. Annexin VI was not detected in non-reactive astrocytes, oligodendroglia, and endothelial cells.

Pathological States

All the types of acute central nervous system damage and chronic degeneration were associated with alterations of the cytoarchitectural distribution of annexin VI in affected neurons and increased expression of annexins I, II, and IV in reactive astrocytes.

However, the intraneuronal distribution of annexin VI and the relative degree of expression for the annexins showed some differences in the various pathological processes.

Neuronal Annexins

In subacute hypoxic ischemic injury, seizure damage, and Alzheimer's disease, the surviving CA2 pyramidal neurons displayed increased annexin VI immunoreactivity within the somal cytoplasm (Figure 3E). The differences in staining intensities of the CA2 neurons compared with those in other areas was often quite marked. Similar but more variable changes were present in the CA3 and CA4 neurons. In Alzheimer's disease, the granulovacuolar bodies within degenerating pyramidal neurons were strongly immunoreactive for annexin VI. The vacuolar membranes of these bodies were consistently labeled, whereas the granular bodies were more variably stained (Figure 3E). In contrast, annexin VI was never detected in neurofibrillary tangles or neuritic plaques.

Each case of acute hypoxic ischemic injury displayed a unique pattern of annexin VI immunoreactivity within neurons. The first was a concentration of immunoreactivity within proximal dendritic segments in CA2-4 (Figure 3C) or within the somal cytoplasm in CA1-2 (Figure 3D). The other was a markedly heterogeneous distribution of immunoreactivity within pyramidal neurons, including focal staining of plasma membrane and vesicular structures within the cytoplasm.

In contrast to annexin VI, annexin I immunoreactivity in neurons showed no consistent pattern of alteration in the various disease states. In Alzheimer's disease, staining within neurons was excluded from intracellular neurofibrillary tangles and granulovacuolar bodies in degenerating neurons.

Glial Annexins

Reactive astrocytes were identified by prominent cytoplasm and processes with strong GFAP immunoreactivity. Astrocytes in the endfolium region adjacent to the granular cell layer appeared to be the most sensitive to developing reactive changes in response to hypoxic ischemic injury and seizures. In more severe cases reactive astrocytes were more widely distributed, particularly in areas of neuronal loss or infarction. In Alzheimer's disease, reactive astrocytes were diffusely distributed, often in association with senile plaques and degenerating neurons.

Reactive astrocyte populations displayed variable expression of annexins I, II, and IV. In general, annexin immunoreactivity was most prominent within cells and the surrounding neuropil in regions of more severe gliosis, eg, adjacent to an infarct (Figure 2A). The intracellular pattern of annexin I immunoreactivity was always diffuse (Figure 3F). Annexin IV was diffusely distributed within gemistocytic astrocytes (Figure 3, H) or in punctate, granular, or vesicular patterns within fibrillary astrocytes. In contrast, annexin II p11 and p36 were usually most strongly localized at the cell periphery. In Alzheimer's disease, astrocytic p11/p36 was also localized to discrete plaque-like areas (Figure 2B). Dual-label immunohistochemistry showed that p11 immunoreactive astrocytes, when present, were only in close proximity to diffuse and mature β -amyloid plaques and were not associated with either dystrophic neurites or extracellular neurofibrillary tangles. However, many β -amyloid plaques were not associated with p11/p36 immunoreactivity. In contrast to the focal pattern of p11/p36 expression, GFAP and S100 β immunoreactive astrocytes were more widely distributed (Figure 3G). Annexin I or IV immunoreactive astrocytes did not show a plaque-like pattern and were distributed without any specific relationship to neuritic plaques, neurofibrillary tangles, or degenerating neurons.

Only annexin IV could be consistently identified in activated microglia with ramified, rod, and amoeboid morphologies. These cell populations were also immunoreactive for the HAM-56 macrophage antigen but not GFAP or factor VIII. Annexin IV immunoreactivity was distributed in granular or vesicular patterns within the cytoplasm and processes.

Discussion

Previous studies have described the isolation and biochemical characterization of the major species of annexins in mammalian brain, which include annexins I, II, IV, and VI.^{4,13} Little is known, however, about the specific cellular distribution or physiological roles of this family of proteins in the human nervous system. This study examined the comparative cellular localization of the major annexins in the human hippocampus, which contains physiologically distinct neuronal cell types and undergoes well-characterized pathological changes in response to injury and degenerative processes. Annexin VI was selectively distributed in neurons and annexins II and IV in glia, whereas annexin I was present in both neurons and astroglia. These data concur with previous findings in non-

Fig
 nen
 x 15
 orig

hur
 plic
 spc
 cor
 sut
 has
 dog
 of a
 am
 ast
 res
 Lik
 rea
 The
 cor
 of t
 prc
 lan
 twr

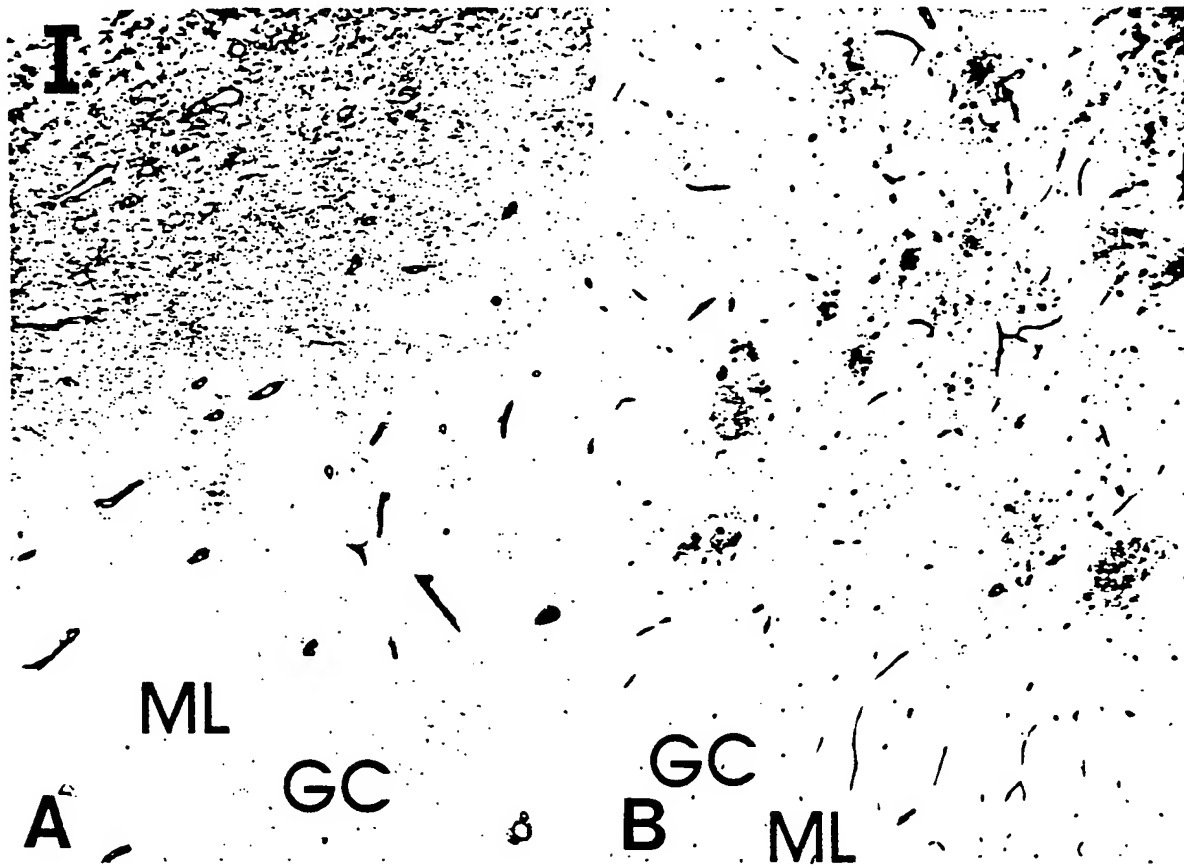


Figure 2. Pathological patterns of p11 immunoreactivity. **A:** Subacute infarct in CA1. The region adjacent to the infarct was densely stained. Annexins I, II (p36), and IV showed similar patterns. (Biotin-avidin immunoperoxidase with hematoxylin counterstain, original magnification $\times 150$.) **B:** Alzheimer's disease. Staining was associated with plaques in CA4. (Biotin-avidin immunoperoxidase with hematoxylin counterstain, original magnification $\times 60$.) I, infarct; GC, granule cell layer of dentate gyrus; ML, molecular layer of dentate gyrus.

human mammalian brain.^{3-5,13} Our findings also implicate the annexins in neuronal and astroglial responses to acute and chronic neurodegenerative conditions.

Annexin I has been shown to be a major cellular substrate for the EGF receptor tyrosine kinase¹⁴ and has also received much attention as a putative endogenous anti-inflammatory agent.¹⁵ The localization of annexin I immunoreactivity in neurons of the cornu ammonis and dentate gyrus and in subependymal astrocytes, ependymocytes, and choroid plexus corresponds to the localization of the EGF receptor.¹⁶ Like annexin I, the EGF receptor is also expressed in reactive astrocytes but not in quiescent astrocytes.¹⁷ The parallel distributions of these proteins are thus consistent with a role for annexin I in mediating effects of EGF on neurons and glia. Annexin I has also been proposed to play a role in regulating glial prostaglandin production, based on the relationships between annexin I expression, phospholipase A₂ activ-

ity, and eicosanoid release in cultured astrocytes.¹⁸ Annexin I in rat hippocampus has a neuronal and glial distribution like that described here⁵ and is present in synaptic plasma membrane fractions as a covalent dimer,¹⁹ presumably due to cross-linking by transglutaminase.²⁰ In human brain, Johnson et al⁶ detected annexin I immunoreactivity in ependyma, subependymal astrocytes, choroid plexus, and reactive astrocytes associated with brain injury, but unlike this study, not in neurons. The most obvious explanation for this variance would be differences in the epitopes recognized by the antibodies used in these studies; it is possible that posttranslational modifications of annexin I in neurons, such as cross-linking, could mask immunoreactive epitopes.

Annexin VI immunoreactivity was associated with neuronal cell membranes and processes in a pattern suggestive of terminal and perisynaptic locations and was the only annexin that was not detected in

114-115



reactive o
 secretory
 ing conce
 One poter
 and chorc
 membran
 involved
 granules
 totic recy
 VI is requ
 diocytotic
 chain do
 binding
 and IV...
 suggesti
 teins.⁴ A
 the activ
 sarcopla
 been id
 that ann
 naling n

Expre
 cells wa
 lations e
 tectural
 were qu
 p36 we
 branes
 wherea
 active i
 godenc
 sometim
 These
 likely r
 as pro
 toplasm
 IV in r
 blasts.
 gester
 ponem
 protein
 with c

Two
 teristic
 nexin
 pyran
 p36⁺

Figure
 memb
 bodies
 per left
 reacti
 plasm
 oligod.
 x 52

reactive or quiescent macroglia. The choroid plexus secretory epithelium showed strong annexin VI staining concentrated in the subplasmalemmal region. One potential role for annexin VI in synaptic terminals and choroid plexus is regulation of clathrin-mediated membrane trafficking. Clathrin-coated vesicles are involved in the biogenesis of dense-core secretory granules and synaptic vesicles, and in the endocytotic recycling of vesicles after exocytosis.²¹ Annexin VI is required for the budding of clathrin-coated endocytotic pits *in vitro*.²² Although the clathrin heavy chain does not exhibit Ca^{2+} -dependent membrane binding properties, it co-purifies with annexins VI and IV prepared from brain using this technique, suggesting an association with the annexin proteins.⁴ Annexin VI has also been shown to modulate the activity of a ryanodine-sensitive Ca^{2+} channel in sarcoplasmic reticulum.²³ Ryanodine receptors have been identified in neurons,²⁴ raising the possibility that annexin VI might modulate neuronal Ca^{2+} signaling mechanisms.

Expression of annexins II (p11/p36) and IV in neural cells was limited to glia. However, the glial cell populations expressing these annexins and the cytoarchitectural distribution of immunoreactivity within cells were quite different. Immunoreactivities for p11 and p36 were associated primarily with plasma membranes and processes of reactive astrocytes, whereas annexin IV staining was cytoplasmic in reactive astrocytes and was also present in some oligodendrocyte populations, activated microglia, and sometimes in the nuclei of glial (and endothelial) cells. These different patterns of annexin localization most likely reflect roles in different cellular activities, such as proliferation,²⁵ migration,²⁶ and extension of cytoplasmic processes.^{25,27} The localization of annexin IV in nuclei has been previously reported in fibroblasts.²⁸ Intracellular functions of annexins are suggested by the discoveries that annexin II is a component of the DNA polymerase α -primer recognition protein complex,²⁹ and of a novel annexin associated with calyculin.³⁰

Two patterns of annexin localization were characteristic of Alzheimer's disease: the association of annexin VI with granulovacuolar bodies in degenerating pyramidal neurons and expression of annexin II (p11/p36) by astrocytes closely associated with some

β -amyloid plaques. Granulovacuolar bodies contain immunoreactivities for cytoskeletal epitopes similar to those found in neurofibrillary tangles and neuritic plaques, and thus seem to be related to neurofibrillary degeneration.³¹ The presence of strong annexin VI immunoreactivity associated with the membranes of granulovacuolar bodies (but not with neurofibrillary tangles or neuritic plaques) suggests that annexin VI could be important in their formation, perhaps involving an aberrant vesicular trafficking pathway. The occasional association of p11/p36 immunoreactive astrocytes with extracellular β -amyloid deposits in Alzheimer's hippocampus suggests that some amyloid plaques may contain a component that stimulates annexin II expression. Plaques are heterogeneous in composition, containing variable amounts of amyloid precursor derivatives, neuritic components, microglia, and secondary substances such as immunoglobulins and complement factors.³² It seems likely that plaque components other than amyloid and neurites are related to annexin II expression in plaque-associated astrocytes, because p11/p36 immunoreactivity was inconstantly present in mature or immature plaques and was not seen in reactive astrocytes associated with extracellular neurofibrillary tangles, which, like neuritic plaques, contain paired helical filaments.

The increased expression of annexins in pathological states may represent a neural tissue response that serves to limit damage. Membrane degradation by phospholipases represents one mechanism underlying neuronal injury after hypoxia ischemia, excitotoxin exposure, seizures, and in chronic neurodegenerative diseases.³³ Annexins, which inhibit phospholipase activity *in vitro*, could thus act as endogenous neuroprotective agents. In subacute and chronic states (posthypoxic, seizures, and Alzheimer's disease) annexin VI immunoreactivity was consistently increased within the cytoplasm of pyramidal neuronal soma in CA2. Neurons in this region are more resistant to injury than those in other regions of the hippocampus, raising the possibility that an increase in annexin VI expression could represent a response promoting neuronal survival or recovery from injury. An alternative explanation is that annexin VI may accumulate in neuronal soma because of disruption of normal axonal-dendritic transport mechanisms, because an-

Figure 3. Cellular localization of annexins. **A-E:** Annexin VI. Immunoreactivity in normal CA2 (**A**) and CA1 (**B**) was associated with neuronal membranes and neuropil. In acute hypoxic ischemic injury, annexin VI was concentrated within dendritic segments in CA2 (**C**) and neuronal cell bodies in CA1 (**D**). In Alzheimer's disease (**E**), annexin VI was selectively increased within CA2 neurons (lower right) but not in CA1 neurons (upper left) and was also associated with granulovacuolar bodies (inset). **F:** Annexin I immunoreactivity was present in both pyramidal neurons and reactive astrocytes (inset). **G:** Dual-labeling for p11 (AEC, red) and GFAP (DAB-Ni, black) demonstrated p11 immunoreactivity in an Alzheimer's plaque-associated astrocyte (arrowhead) and capillaries, whereas other astrocytes stained only for GFAP (arrows). **H:** Annexin IV was present in oligodendrocytes and reactive astrocytes (inset). Biotin-avidin immunoperoxidase with hematoxylin counterstain, magnifications: **A-D**, $\times 338$; **E**, $\times 52$; inset, $\times 676$; **F**, $\times 180$; inset, $\times 541$; **G**, $\times 226$; **H**, $\times 541$; inset, $\times 609$.

nexin VI has been identified in the slow component of axonal transport in rat peripheral nerve.³⁴

The presence of annexin I immunoreactivity in neurons is also compatible with the hypothesis that neuronal annexins could confer resistance to Ca^{2+} -induced neuronal injury. Although annexin I did not show patterns of expression in neuronal populations which clearly corresponded with their relative degrees of resistance or susceptibility to injury, recent studies have directly demonstrated neuroprotective properties of endogenous annexin I. Surprisingly, the active protein appears to reside in the extracellular space, because intraventricular administration of annexin I in live rats decreased the sizes of cerebral lesions induced by ischemia⁹ or glutamate receptor agonist,³⁵ whereas injection of neutralizing antibody had the opposite effect. Potential sources of endogenous extracellular annexin I could include local release by neurons and reactive astrocytes or secretion into the cerebrospinal fluid by choroid plexus, because annexin I has been shown to be selectively secreted by other cell types.^{36,37} Annexin I could also be released from damaged tissue or inflammatory cells. Although this study confirms previous observations that annexin I is increased in injured brain tissue,^{9,9} we found that annexins II and IV were also increased. The role(s) of these annexins in neuroprotection has yet to be studied.

Annexins in the cerebral vascular endothelium are probably not related to special physiological functions, such as the blood-brain barrier, because relatively high levels of annexins I, II, IV, and VI are present in cultured human umbilical vein endothelial cells.³⁸ It is quite possible that we did not detect significant annexin VI immunoreactivity in the endothelium because of the relatively strong reaction in adjacent vascular smooth muscle and neuropil. Our data regarding annexin expression in cerebrovascular smooth muscle agree with a previous report that smooth muscle cells express annexin VI but not annexin II.³⁹

Annexins are widely distributed throughout the body and therefore could be involved in pathophysiological processes in nonneural tissues and brain. Annexin I expression is increased in rat renal tubules during recovery from ischemia,⁴⁰ supporting a hypothesis that annexins may participate in general cellular and tissue mechanisms for limiting injury and promoting repair. Further studies of multiple annexins, as described here in the human hippocampus, may define patterns of expression that are unique or common to various types of cells and pathological states, suggesting links between specific annexins and cellular functions.

Acknowledgments

We thank Dr. C. Creutz for helpful discussions.

References

1. Klee CB: Ca^{2+} -dependent phospholipid- (and membrane-) binding proteins. *Biochemistry* 1988; 27:6645-6653
2. Burgoyne RD, Geisow MJ: The annexin family of calcium-binding proteins. *Cell Calcium* 1989; 10:1-10
3. Burgoyne RD, Cambray-Deakin MA, Norman K-M: Developmental regulation of tyrosine kinase substrate p36 (calpactin heavy chain) in rat cerebellum. *J Mol Neurosci* 1989; 1:47-54
4. Woolgar JA, Boustead CM, Walker JH: Characterization of annexins in mammalian brain. *J Neurochem* 1990; 54:62-71
5. Stribos PJLM, Tilders FJH, Carey F, Forder R, Rothwell NJ: Localization of immunoreactive lipocortin-1 in the brain and pituitary gland of the rat: effects of adrenalectomy, dexamethasone, and colchicine treatment. *Brain Res* 1991; 553:249-260
6. Spreca A, Rambotti MG, Giambanco I, Pula G, Bianchi R, Ceccarelli P, Donato R: Immunocytochemical localization of annexin V (CaBP33), a Ca^{2+} -dependent phospholipid- and membrane-binding protein, in the rat nervous system and skeletal muscles and in the porcine heart. *J Cell Physiol* 1992; 152:567-598
7. Reeves SA, Chavez-Kappel C, Davis R, Rosenblum M, Israel MA: Developmental regulation of annexin II (lipocortin-2) in human brain and expression in high grade glioma. *Cancer Res* 1992; 52:6871-6876
8. Johnson MD, Kamso-Pratt JM, Whetsell WO, Pepinsky RB: Lipocortin-1 immunoreactivity in the normal human central nervous system and lesions with astrogliosis. *Am J Clin Pathol* 1989; 92:424-429
9. Relton JK, Stribos PJ, O'Shaughnessy CT, Carey F, Forder RA, Tilders FJ, Rothwell NJ: Lipocortin-1 is an endogenous inhibitor of ischemic damage in the rat brain. *J Exp Med* 1991; 174:305-310
10. Knatchaturian ZS: Diagnosis of Alzheimer's disease. *Arch Neurol* 1995; 42:1097-1104
11. Hsu S, Raine L, Fanger H: Use of avidin-biotin-peroxidase complex (ABC) in immunoperoxidase techniques: a comparison between ABC and unlabeled antibody (PAP) procedures. *J Histochem Cytochem* 1981; 29:577-580
12. Crumpton MJ, Dedman JR: Protein terminology tangle. *Nature* 1990; 345:212
13. Regnoul F, Rendon A, Pradel RA: Biochemical characterization of annexins I and II isolated from pig nervous tissue. *J Neurochem* 1991; 56:1985-1996
14. Fava RA, Cohen S: Isolation of a calcium-dependent 35-kilodalton substrate for the epidermal growth factor receptor/kinase from A431 cells. *J Biol Chem* 1984; 259:2636-2645

15. Fic
the
16. We
ca
rec
toc
17. Bir
LB
in
ea.
18. Ge
P,
inc
cy:
19. Pra
mc
19
20. An
inc
su-
me
11
21. Ja
rin
65
22. Lir
qu
19
23. Di
De
tiv.
kD
24. So
ma
14
25. Sc
a
11
26. Br.
ca-
ma
Ce
27. Fo
an
the
Cc
28. We
tor
ex:
teir

15. Flow RJJ: Lipocortin and the mechanisms of action of the glucocorticoids. *Br J Pharmacol* 1988, 94:987-1015
16. Werner MH, Nanney LB, Stoscheck CM, King LE: Localization of immunoreactive epidermal growth factor receptors in human nervous system. *J Histochem Cytochem* 1988, 36:81-86
17. Birecree E, Whetsell WO, Stoscheck C, King LE, Nanney LB: Immunoreactive epidermal growth factor receptors in neuritic plaques from patients with Alzheimer's disease. *J Neuropathol Exp Neurol* 1988, 47:549-560
18. Gebicke-Haerter PJ, Schobert A, Dieter P, Honegger P, Hertting G: Regulation and glucocorticoid-independent induction of lipocortin I in cultured astrocytes. *J Neurochem* 1991, 57:175-183
19. Pradel LA, Rendon A: Annexin I is present in different molecular forms in rat cerebral cortex. *FEBS Lett* 1993, 327:41-44
20. Ando Y, Imamura S, Owada MK, Kannagi R: Calcium-induced intracellular cross-linking of lipocortin I by tissue transglutaminase in A431 cells: augmentation by membrane phospholipids. *J Biol Chem* 1991, 266:1101-1108
21. Jackson AP: Endocytosis in the brain: the role of clathrin light-chains. *Biochem Soc Transact* 1992, 20:653-655
22. Lin HC, Sudhof TC, Anderson RGW: Annexin I is required for the budding of clathrin-coated pits. *Cell* 1992, 70:283-291
23. Diaz-Munoz M, Hamilton S, Kaetzel MA, Hazarika P, Dedman JR: Modulation of Ca^{2+} release channel activity from sarcoplasmic reticulum by annexin VI (67-kDa calcimedlin). *J Biol Chem* 1990, 265:15894-15899
24. Sorrentino V, Volpe P: Ryanodine receptors: how many, where, and why? *Trends Pharmacol Sci* 1993, 14:98-103
25. Schlaepfer DD, Haigler HT: Expression of annexins as a function of cellular growth state. *J Cell Biol* 1990, 111:229-238
26. Braslau DL, Ringo DL, Rocha V: Synthesis of novel calcium-dependent proteins associated with mammary epithelial cell migration and differentiation. *Exp Cell Res* 1984, 155:213-21
27. Fox MT, Prentice DA, Hughes JP: Increases in p11 and annexin II proteins correlate with differentiation in the PC12 pheochromocytoma. *Biochem Biophys Res Commun* 1991, 177:1188-1193
28. Walker JH, Boustead CM, Brown R, Koster JJ, Middleton CA: Tissue and subcellular distribution of endonexin, a calcium-dependent phospholipid-binding protein. *Biochem Soc Trans* 1990, 18:1235-1236
29. Jindal HK, Chaney WG, Anderson CW, Davis RG, Vishwanatha JK: The protein-tyrosine kinase substrate, calpactin I heavy chain (p36), is part of the primer recognition protein complex that interacts with DNA polymerase α . *J Biol Chem* 1991, 266:5169-5176
30. Mizutani A, Usuda N, Tokumitsu H, Minami H, Yasui K, Kobayashi R, Hidaka H: CAP-50, a newly identified annexin, localizes in the nuclei of cultured fibroblast 3Y1 cells. *J Biol Chem* 1992, 267:13498-13504
31. Bondareff W, Wischik CM, Novak M, Roth M: Sequestration of tau by granulovacuolar degeneration in Alzheimer's disease. *Am J Pathol* 1991, 139:641-648
32. Alafuzoff I, Adolfsson R, Grundke-Iqbal I, Winblad B: Blood-brain barrier in Alzheimer dementia and in nondemented elderly: an immunocytochemical study. *Acta Neuropathol* 1987, 73:160-166
33. Choi DW: Glutamate neurotoxicity and diseases of the nervous system. *Neuron* 1988, 1:623-634
34. Sekimoto S, Tashiro T, Komiya Y: Two 68-kDa proteins in slow axonal transport belong to the 70-kDa heat shock protein family and the annexin family. *J Neurochem* 1991, 56:1774-1782
35. Black MD, Carey F, Crossman AR, Relton JK, Rothwell NJ: Lipocortin-1 inhibits NMDA receptor-mediated neuronal damage in the striatum of the rat. *Brain Res* 1992, 585:135-140
36. Solito E, Rauge G, Melli M, Parenti L: Dexamethasone induces the expression of the mRNA of lipocortin 1 and 2 and the release of lipocortin 1 and 5 in differentiated, but not undifferentiated U-937 Cells. *FEBS Lett* 1991, 291:236-244
37. Christmas P, Callaway J, Fallon J, Jones J, Haigler HT: Selective secretion of annexin I, a protein without a signal sequence, by the human prostate gland. *J Biol Chem* 1991, 266:2499-507
38. Romisch J, Schuler E, Bastian B, Burger T, Dunkel FG, Schwinn A, Hartmann AA, Paques EP: Annexins I to VI: quantitative determination in different human cell types and in plasma after myocardial infarction. *Blood Coagul Fibrinol* 1992, 3:11-17
39. Iida H, Hatae T, Shibata Y: Immunocytochemical localization of 67 kD Ca^{2+} binding protein (p67) in ventricular, skeletal, and smooth muscle cells. *J Histochem Cytochem* 1992, 40:1899-1907
40. McKanna JA, Chuncharunee A, Munger KA, Breyer JA, Cohen S, Harris RC: Localization of p35 (annexin I, lipocortin 1) in normal adult rat kidney and during recovery from ischemia. *J Cell Physiol* 1992, 153:467-476

Annexins: From Structure to Function

VOLKER GERKE AND STEPHEN E. MOSS

Institute for Medical Biochemistry, Center for Molecular Biology of Inflammation, University of Münster, Münster, Germany; and Department of Cell Biology, Institute of Ophthalmology, University College London, London, United Kingdom

I. Introduction: Overview of the Annexin Family	331
II. Biochemical Properties of Annexins and Their Three-Dimensional Structure	332
A. Molecular structures	332
B. Annexins as membrane binding proteins: canonical and atypical properties	336
C. Nonlipid annexin ligands	338
D. Modulation of annexin properties by posttranslational modifications	342
III. Molecular Evolution of the Annexin Family and Regulation of Annexin Gene Expression	343
A. Molecular phylogeny of annexins	343
B. Gene structures	344
C. Regulation of gene expression	345
IV. Functional Diversity Within the Annexin Family	347
A. Annexins in membrane traffic and organization	347
B. Annexins and ion channels	353
C. Extracellular annexin activities	356
D. Annexin transgenesis and targeted gene disruption	358
V. Annexins and Human Disease	359
A. Disorders of the heart and circulation	359
B. Annexins and physiological stress	361
C. Annexins and cancer	361
VI. Conclusion	362

Gerke, Volker, and Stephen E. Moss. Annexins: From Structure to Function. *Physiol Rev* 82: 331–371, 2002; 10.1152/physrev.00030.2001.—Annexins are Ca^{2+} and phospholipid binding proteins forming an evolutionary conserved multigene family with members of the family being expressed throughout animal and plant kingdoms. Structurally, annexins are characterized by a highly α -helical and tightly packed protein core domain considered to represent a Ca^{2+} -regulated membrane binding module. Many of the annexin cores have been crystallized, and their molecular structures reveal interesting features that include the architecture of the annexin-type Ca^{2+} binding sites and a central hydrophilic pore proposed to function as a Ca^{2+} channel. In addition to the conserved core, all annexins contain a second principal domain. This domain, which NH_2 -terminally precedes the core, is unique for a given member of the family and most likely specifies individual annexin properties in vivo. Cellular and animal knock-out models as well as dominant-negative mutants have recently been established for a number of annexins, and the effects of such manipulations are strikingly different for different members of the family. At least for some annexins, it appears that they participate in the regulation of membrane organization and membrane traffic and the regulation of ion (Ca^{2+}) currents across membranes or Ca^{2+} concentrations within cells. Although annexins lack signal sequences for secretion, some members of the family have also been identified extracellularly where they can act as receptors for serum proteases on the endothelium as well as inhibitors of neutrophil migration and blood coagulation. Finally, deregulations in annexin expression and activity have been correlated with human diseases, e.g., in acute promyelocytic leukemia and the antiphospholipid antibody syndrome, and the term *annexinopathies* has been coined.

I. INTRODUCTION: OVERVIEW OF THE ANNEXIN FAMILY

Nature has achieved the means to tightly control intracellular Ca^{2+} concentrations, thereby enabling the

ion to serve second messenger functions in a variety of processes which couple extracellular signals to cellular responses. Systems regulating intracellular Ca^{2+} levels thus are considered part of the intricate Ca^{2+} signaling network. They include gated Ca^{2+} channels and energy-

dependent pumps, which are located in organelle membranes and the plasma membrane, as well as intracellular Ca^{2+} binding proteins serving as regulated Ca^{2+} buffers. Other classes of Ca^{2+} binding proteins participate more directly in Ca^{2+} signaling as they display altered properties in response to Ca^{2+} binding. Annexins can be considered a subgroup of the latter, although their precise position within Ca^{2+} signaling chains remains elusive. Moreover, a growing body of evidence suggests that annexins can also function in their Ca^{2+} -free conformation in a hitherto unknown fashion, thereby increasing the functional diversity among these proteins.

The name annexin is derived from the Greek *annex* meaning "bring/hold together" and was chosen to describe the principal property of all or at least nearly all annexins, i.e., the binding to and possibly holding together of certain biological structures, in particular membranes. The name also has a somewhat historical flavor as it takes into account the point that a number of the groups who independently of one another discovered annexins were in search for such scaffolding or bridging proteins. However, initially, i.e., at the date of their discoveries in the late 1970s and early 1980s, annexins received diverse and unrelated names referring to their biochemical properties. These included synexin (for granule aggregating protein, Ref. 52), chromobindins (proteins binding to chromaffin granules, Ref. 54), calmedins (proteins mediating Ca^{2+} signals, Ref. 199), lipocortins (steroid-inducible lipase inhibitors, Ref. 85), and calpactins (proteins binding Ca^{2+} , phospholipid, and actin, Ref. 101). Intensive biochemical work, protein and cDNA sequencing, as well as gene cloning led to the realization that all such proteins identified shared key biochemical properties as well as gene structure and sequence features. Hence, the concept of a novel multigene family arisen by gene duplication was developed and the common name annexin was introduced to solve the terminology tangle (55).

By definition, an annexin protein has to fulfill two major criteria. First, it must be capable of binding in a Ca^{2+} -dependent manner to negatively charged phospholipids. Second, it has to contain as a conserved structural element the so-called annexin repeat, a segment of some 70 amino acid residues. Molecular structures obtained for a number of annexins over the past decade helped to extend the similarities to the three-dimensional level. Moreover, they defined a hitherto unknown structural fold, the conserved annexin domain, which is built of four annexin repeats packed into a highly α -helical disk, and which now is considered to be a general membrane binding module. Once clearly defined and advanced by genome sequencing work, the annexin family has grown steadily in the 1990s, and with the turn of the century, now amounts to more than 160 unique annexin proteins present in more than 65 different species ranging from fungi and protists to plants and higher vertebrates (Fig. 1)

(202, 204). In this review we summarize the biochemical and structural properties of annexins, putting a particular emphasis on novel aspects of annexin interactions with lipids and other biological ligands. For a detailed discussion of the canonical annexin properties, their structural organization, and intracellular as well as tissue distribution, the interested reader is referred to previous reviews (51, 97, 244).

Having accumulated a wealth of biochemical and structural knowledge, we are still in need of assigning a physiological function to the annexin family as a whole, or better, because they are likely to differ, to individual annexins. Recent knock-out models, both at the cellular and the animal level, as well as the development and use of dominant-negative mutant proteins have introduced the first direct approaches for analyzing annexin function. They underscore the concept of functional diversity within the family. Moreover, it has recently become clear that certain dysregulations in annexin expression and activity can be correlated with human diseases and that this has led to the introduction of the term *annexinopathies*. Although we still have to await final proof of a direct correlation, we decided to concentrate our review on such recent developments leading to the proposal of some models concerning annexin function.

II. BIOCHEMICAL PROPERTIES OF ANNEXINS AND THEIR THREE-DIMENSIONAL STRUCTURE

A. Molecular Structures

1. Structures of annexin protein cores: the conserved membrane binding modules

Each annexin is composed of two principal domains: the divergent NH_2 -terminal "head" and the conserved COOH -terminal protein core. The latter harbors the Ca^{2+} and membrane binding sites and is responsible for mediating the canonical membrane binding properties. An annexin core comprises four (in annexin A6 eight) segments of internal and interannexin homology that are easily identified in a linear sequence alignment (for review, see Ref. 244). It forms a highly α -helical and tightly packed disk with a slight curvature and two principle sides. The more convex side contains novel types of Ca^{2+} binding sites, the so-called type II and type III sites (335), and faces the membrane when an annexin is associated peripherally with phospholipids. The more concave side points away from the membrane and thus appears accessible for interactions with the NH_2 -terminal domain and/or possibly cytoplasmic binding partners (Fig. 2). The first structure known for an annexin core was that solved by Huber et al. (134) for annexin A5 in 1990. In the

Name	Synonyms/Former name(s)	Human gene symbol	Non-human gene symbol
annexin A1	lipocortin 1, annexin I	ANXA1	Anxa1
annexin A2	calpactin 1, annexin II	ANXA2	Anxa2
annexin A3	annexin III	ANXA3	Anxa3
annexin A4	annexin IV	ANXA4	Anxa4
annexin A5	annexin V	ANXA5	Anxa5
annexin A6	annexin VI	ANXA6	Anxa6
annexin A7	synexin, annexin VII	ANXA7	Anxa7
annexin A8	annexin VIII	ANXA8	Anxa8
annexin A9	annexin XXXI	ANXA9	Anxa9
annexin A10		ANXA10	Anxa10
annexin A11	annexin XI	ANXA11	Anxa11
annexin A12	unassigned		
annexin A13	annexin XIII	ANXA13	Anxa13

Name	Organism/Former name	Gene symbol
annexin B9	3 species of insect, annexin IX	Anxb9
annexin B10	4 species of insect, annexin X	Anxb10
annexin B11	1 species of insect, annexin	Anxb11
annexin B12	Cnidaria, annexin XII	Anxb12
	3 species of flatworms, 5 annexins 10 species of roundworms, 5 annexins (including <i>C. elegans</i> annexins XV-XVII,XXX)	

Name	Organism/Former name	Gene symbol
annexin C1	<i>Dictyostelium</i> and <i>Neurospora</i> annexin XIV	Anxc1
annexin C2-C5	4 species of fungi/molds/alveolates	Anxc2-c5

Name	Organism/Former name	Gene symbol
annexin D1-D25	35 species including annexin XVIII and annexins XXII-XXIX	Anxd1-d25

Name	Organism/Former name	Gene symbol
annexin E1	<i>Giardia</i> annexin XXI	Anxe1
annexin E2	<i>Giardia</i> annexin XIX	Anxe2
annexin E3	<i>Giardia</i> annexin XX	Anxe3

FIG. 1. The new annexin nomenclature. The five major annexin groups (A–E) are shown, with details of the most extensively studied family members. The nomenclature is that proposed by Reg Morgan and Pilar Fernandez and endorsed by participants at the 50th Harden Conference on Annexins held at Wye College, UK, September 1–5, 1999. A more extensive list of annexin subfamilies and species is posted at the European annexin web site (<http://www24.brinkster.com/annexins/>). There are several important points to note. The vertebrate annexins (A1–A13) are unlikely to be widely represented in invertebrate species. The oldest of this group, namely, annexins A7, A11, and A13, are possible exceptions, and an annexin A11 ortholog has been described in the mollusk *Aplysia*. Within the B group, the *Caenorhabditis elegans* annexins have yet to be assigned numbers. In the C group, the *Dictyostelium* annexin, originally described incorrectly as annexin VII (synexin), is now established as being orthologous to the *Neurospora* annexin.

meantime, more than 10 crystal structures for annexin cores have been described showing a remarkable conservation of the overall three-dimensional fold. Aspects of molecular annexin structures have been reviewed in detail previously (see, for example, Refs. 133, 178, 305), and

the purpose of this review is to discuss only recent and novel developments in this area.

Recent findings include the elucidation of the first structures of annexins from lower eukaryotes and plants. Liemann et al. (177) crystallized the core of annexin C1

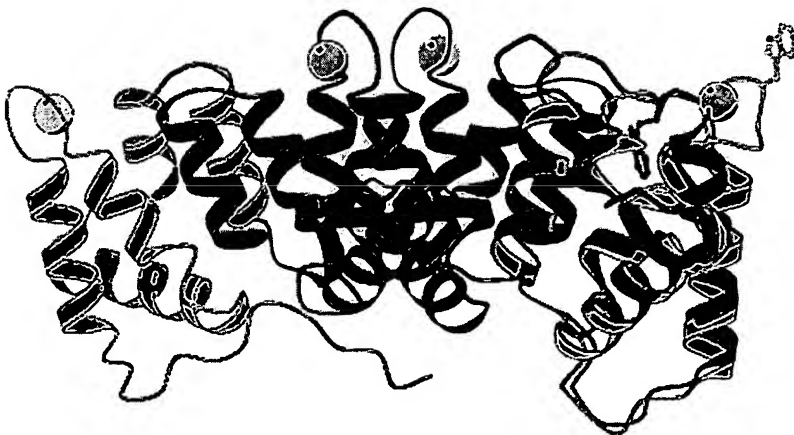


FIG. 2. Crystal structure of human annexin A5. The ribbon drawing illustrates the highly α -helical folding of the protein core that forms a slightly curved disk. Different colors were chosen to highlight the four annexin repeats that are given in green (repeat I), blue (repeat II), red (repeat III), and violet/cyan (repeat IV). The NH_2 -terminal domain appears unstructured and extends along the concave side of the molecule (green). The high and low Ca^{2+} forms are shown in a superposition revealing the conformational change in repeat III, which leads to an exposure of Trp-187 (violet for the low and cyan for the high Ca^{2+} form). Bound Ca^{2+} are depicted as yellow spheres. [Image kindly provided by R. Huber, S. Liemann, and A. Lewit-Bentley, as modified from Ref. 178.]

from *Dictyostelium discoideum*, whereas Hofmann et al. (127) elucidated the structure of a plant annexin, annexin D11 from *Capsicum annuum*, which revealed not only the typical annexin fold but also differences to nonplant annexins in annexin repeats I and III and in the membrane binding loops. Another recent advance is the introduction of benzodiazepine and benzothiazepine derivatives as annexin ligands and their cocrystallization with annexins. The benzothiazepine K201 was first described to bind to annexin A5 and inhibit its Ca^{2+} channel activity, most likely by restraining a hinge movement of the two annexin A5 modules formed by annexin repeats I/IV and II/III, respectively (149, 150). Other structurally related benzodiazepine compounds have subsequently been identified as ligands for various annexins with the interaction being based on similar structural principles (126). However, a possible pharmacological role of these interactions remains to be shown. Crystal structure determination and biochemical characterization in combination with site-directed mutagenesis have also proven powerful in recent years in characterizing the contribution of certain residues to the overall fold of annexin cores and/or their biochemical properties. Conserved arginine residues present in the so-called endonexin fold of each homology segment, for example, were shown to be crucial for stabilizing the tertiary structure of annexin A5. On the other hand, substitution by alanine of different serine and threonine residues and the unique tryptophan in the same annexin results in altered membrane binding underscoring the importance of these residues in mediating intermolecular, i.e., annexin-phospholipid, contacts (31, 32). Moreover, mutational analysis revealed that the aspartate residue at position 226 of annexin A5 participates as a molecular switch in a Ca^{2+} - and pH-dependent conformational change (294). Like many other annexins, annexin A4 is a substrate of protein kinase C (PKC), at least in vitro reactions, and Kaetzel et al. (147) have attempted to monitor structural changes resulting from this phosphorylation. They show that replacement by glutamate of the PKC acceptor site, threonine-6, causes a release of the NH_2 -terminal domain from the protein core indicative of a regulatory role in the membrane aggregation displayed by this annexin. Annexin B12 has also been subjected to detailed scrutiny by mutagenesis involving cysteine substitutions for spin labeling purposes (see below) and the glutamate at position 105. This residue has been found to participate in the formation of intermolecular Ca^{2+} binding sites in a hexameric form of the molecule (185), and replacement of Glu-105 by lysine stabilizes this hexamer by favoring extensive hydrogen bonding (35).

Recently, techniques other than crystallization of the soluble proteins have been introduced to study in detail structural properties of annexins, in particular when

bound to membrane or phospholipid surfaces. They include cryoelectron microscopy, which led to the identification of highly structured junctions formed by different annexins between opposing membranes (167), and atomic force microscopy (AFM), which enabled the high-resolution analysis of two-dimensional crystals of annexin A5 formed on planar lipid bilayers (248, 249). Two-dimensional crystals of annexin A6 formed on artificial lipid monolayers were also obtained and characterized recently, revealing an intrinsic flexibility of this eight-annexin repeat-containing molecule. Here the two lobes of annexin A6, i.e., repeats I-IV and V-VIII, respectively, were found to bind to the phospholipid in both parallel or antiparallel orientation, with the latter providing a structural basis for membrane cross-linking (6). Evidence for conformational changes occurring in annexins upon membrane binding was obtained by analyzing membrane-bound annexin A5 with transmission and internal reflection infrared spectroscopy. Interestingly, it was inferred from these studies that a new β -structure with interstrand hydrogen bonds oriented parallel to the membrane surface is formed upon interaction with a lipid monolayer. On the other hand, analyses of two-dimensional crystals of the same annexin on membrane surfaces by high-resolution electron microscopy and AFM, and crystal structure analysis of a cross-linked form of annexin A2 capable of binding membranes, do not provide evidence for substantial conformational alterations accompanying the canonical Ca^{2+} -dependent membrane binding (26, 29, 229, 248). Relatively subtle changes, however, might occur. These include the exposure of the unique tryptophan in repeat 3 of annexin A5 observed in high Ca^{2+} (47, 174). Thus, despite the wealth of structural information on soluble as well as membrane-bound annexins, it is not clear whether the peripheral and Ca^{2+} -dependent membrane binding of annexins as a whole, or individual annexins, requires or is accompanied by conformational changes. Moreover, the structural basis of (possible) membrane insertions of annexins triggered by certain environmental changes like hydrogen ion concentration (see below) need to be described in more detail, possibly also by integrating into such analyses the characterization of folding properties of individual annexin repeats such as the first repeat of annexin A1 (49, 94).

2. Structures of the unique NH_2 -terminal annexin domains and their complexes with protein ligands

Molecular details of the three-dimensional folds of annexin molecules are mostly restricted to the protein core domains (see above) and unique NH_2 -terminal regions of the smaller annexins containing NH_2 -terminal sequences of 16 or fewer residues. In these structures, the NH_2 -terminal sequences extend along the concave side of

the molecule partially engaged in hydrophobic interactions with the protein core. In annexin A3, a direct effect of the NH₂-terminal domain on properties displayed by the core has been shown by replacing Trp-5 (in the unique NH₂-terminal sequence) by alanine. The W5A mutant protein shows a much stronger phospholipid binding, and although having a similar overall structure has a more disordered NH₂-terminal domain. Interestingly, through urea-induced denaturation analysis, it became apparent that the NH₂-terminal domain, even though comprising only 16 residues, unfolds separately from the protein core (128). Thus it appears that the short NH₂-terminal domains of the smaller annexins, located on the concave side of the folded molecule, affect the Ca²⁺-dependent phospholipid binding executed by the convex, or opposite, side possibly through stabilizing or destabilizing slightly different conformations of the molecule. This underscores the regulatory importance of even the small NH₂-terminal domains, a notion that had previously been postulated due to the presence of sites for posttranslational modifications in these regions (see below). Moreover, the finding that subtle differences in the NH₂-terminal sequence, which do not affect the overall structure, result in significantly altered properties could at least in part explain functional diversity among otherwise highly conserved annexins.

Recently, the first complete structure of a longer annexin, annexin A1, has been determined at high resolution (255). Annexin A1 has an NH₂-terminal domain of 40 residues, the first 10–14 of which represent the binding site for a protein ligand of the S100 family, S100A11 (188, 273). Interestingly, in the Ca²⁺-free crystals of annexin A1, this NH₂-terminal sequence forms an amphipathic α -helix and replaces a helix in the tightly packed core domain (helix D of repeat III), which in turn is unwound and partially extrudes from the protein surface (255). Such a structure could have interesting mechanistic and regulatory consequences. Given the tight internal packing of the NH₂-terminal helix, one would assume that this sequence is not available for S100A11 binding in Ca²⁺-free annexin A1. However, upon Ca²⁺-dependent membrane binding, the D helix of repeat III could be forced back into the position described for the Ca²⁺-loaded annexin A1 core (335), thereby freeing the NH₂-terminal helix and enabling this sequence to interact with S100A11. Moreover, such movement could be the prerequisite for the membrane aggregation activity described for annexin A1, e.g., by making accessible a second membrane binding site or a site for homophilic annexin 1 interaction (for a hypothetical model see Fig. 3). Thus, in the case of annexin A1, Ca²⁺ could have a dual regulatory function. First, it could trigger membrane attachment through the convex side of the molecule, and second, by inducing the switch of helix D, it would enable the membrane-bound

protein to interact with cellular protein ligands (S100A11) and/or a second membrane surface. In this respect, it is interesting to note that thermodynamic analyses revealed cooperativity in the binding of Ca²⁺ to annexin A1 (257). Finally, the conformational switch postulated by Rosengarth et al. (255) could also modulate the accessibility of phosphorylatable residues in the NH₂-terminal domain of annexin A1 for their respective kinases (see below), thereby guaranteeing a spatially restricted, probably membrane-dependent, regulation of annexin A1 activities.

The structure of the very same NH₂-terminal domain of annexin A1 comprising residues 1–14 has also been solved in complex with its S100A11 ligand. Cocystals of S100A11, a homodimeric protein containing two EF hand-type Ca²⁺ binding sites, with the NH₂-terminal annexin A1 peptide revealed a 1:1 stoichiometry, with the two peptides occupying hydrophobic pockets on two opposite sides of the S100A11 dimer (246). The structure of the complex proved to be very similar to that of the NH₂-terminal sequence of annexin A2 bound to a related S100 protein, S100A10 (247). In both annexins (A1 and A2), the first 14 residues form amphipathic α -helices providing the binding sites for two ligands of the S100 protein family (15, 142, 188, 273). At least in the case of annexin A2, it has been shown that the formation of a heterotetrameric complex containing the S100A10 dimer and two annexin A2 chains significantly alters the properties of this annexin in vitro and also within cells (for reviews, see Refs. 97, 330). Importantly, the annexin A2-S100A10 complex can aggregate membrane vesicles at micromolar Ca²⁺ levels, a property not shared with monomeric annexin A2 or, as a matter of fact, any other annexin. The structure of the NH₂-terminal annexin A2 peptide in complex with S100A10, in combination with high-resolution images of junctions formed between adjacent membranes by the annexin A2-S100A10 complex, now provides the first detailed structural explanation of this aggregation activity. It appears that due to the highly symmetric nature of the structures, the complex links annexin A2-bound membrane surfaces through the dimerization of S100A10, i.e., the two annexin A2 subunits of the membrane-linking complex are bound to two separate bilayers with the S100A10 dimer connecting them through binding to the NH₂-terminal domains (167, 175, 247). A similar scenario could hold true for the annexin A1-S100A11 complex, which in contrast to annexin A2-S100A10 requires Ca²⁺ binding to the S100 protein and probably Ca²⁺/membrane-bound annexin (see above) for complex formation. Nevertheless, we are still in need of high-resolution structures of complete annexin A2-S100A10 and annexin A1-S100A11 complexes to prove or disprove this attractive model, as well as some evidence that the annexin A1-S100A11 exists in vivo.

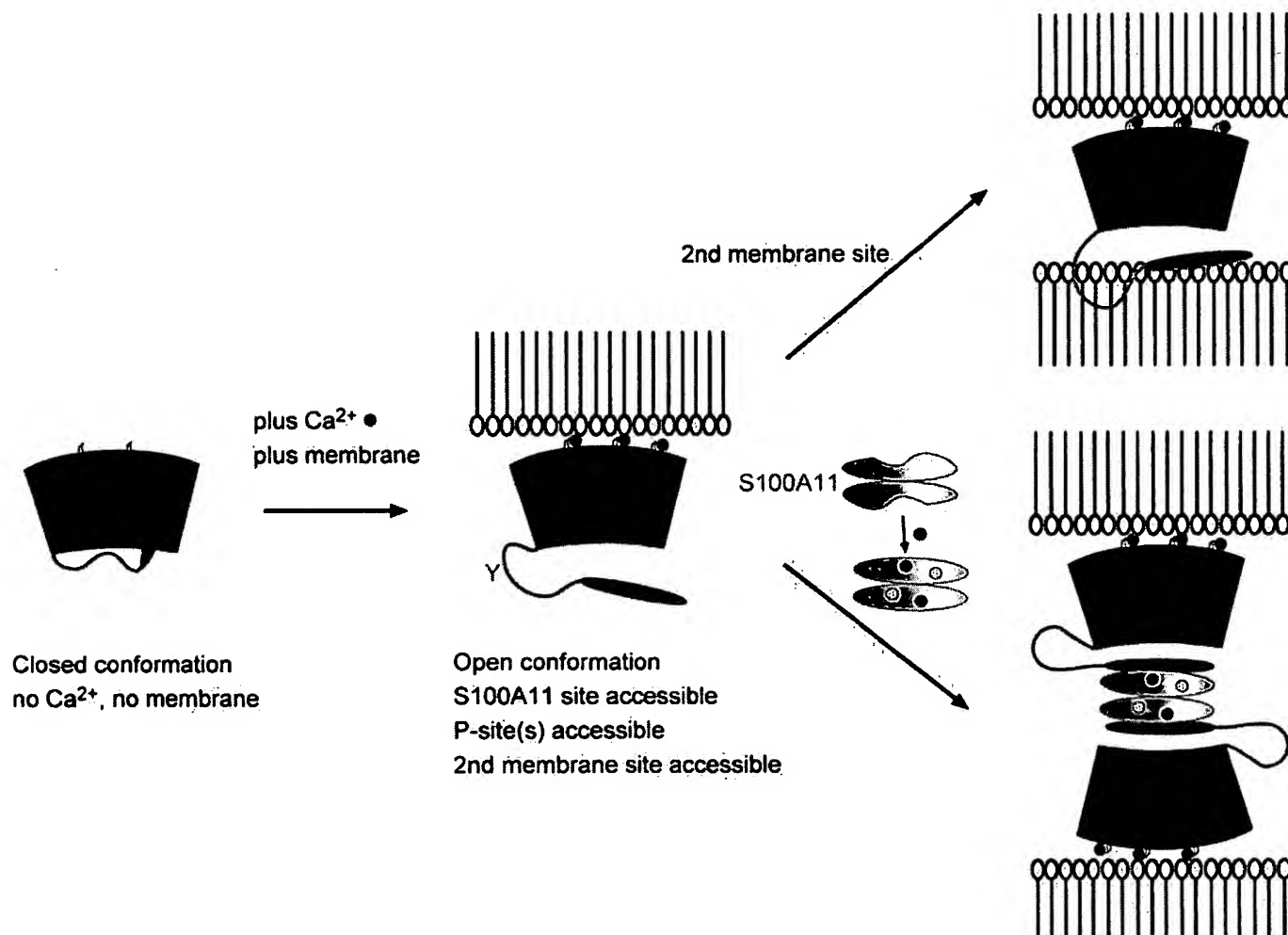


FIG. 3. Model describing the switch of helix D in the annexin A1 structure and its implications for membrane aggregation. In the crystal structure of Ca^{2+} -free annexin A1 (red), the NH_2 -terminal α -helix, which contains the S100A11 binding site (brown), is replacing helix D of the third repeat (255). Ca^{2+} -dependent membrane binding could be accompanied by a conformational change establishing the Ca^{2+} -bound crystal structure of the annexin A1 core (335) and, most likely, a more accessible NH_2 -terminal domain. As a result, the NH_2 -terminal domain can interact with a second membrane surface or the S100A11 dimer, which itself requires Ca^{2+} binding to establish an interaction-competent conformation. An as yet hypothetical annexin A1/S100A11 heterotetramer would represent an entity capable of linking membrane surfaces (see text and Ref. 255 for details).

B. Annexins as Membrane Binding Proteins: Canonical and Atypical Properties

1. Ca^{2+} -dependent phospholipid binding and vesicle aggregation

Biochemically, annexins are defined as soluble, hydrophilic proteins that bind to negatively charged phospholipids in a Ca^{2+} -dependent manner (they are Ca^{2+} /phospholipid binding proteins). This binding is reversible, and removal of Ca^{2+} by Ca^{2+} chelating agents will lead to a liberation of annexins from the phospholipid matrix. The interaction of annexins with negatively charged phospholipids observed *in vitro* is thought to reflect in a more physiological scenario the binding to cellular membranes, in particular, the cytosolic leaflets of the plasma mem-

brane and various organelle membranes. This canonical annexin property is retained within the annexin cores, the conserved annexin modules most likely representing building blocks designed for peripheral membrane association. However, although Ca^{2+} -dependent phospholipid binding is shared by all annexins, individual members differ significantly in their Ca^{2+} sensitivity and phospholipid headgroup specificity. A large number of reports analyzing the Ca^{2+} -regulated phospholipid binding of annexins *in vitro* have been published, and a comprehensive overview has been given by Raynal and Pollard (244).

Although differences in the binding to phospholipids with different headgroups (e.g., phosphatidic acid, phosphatidylserine, phosphatidylinositol) have long been recognized in *in vitro* studies, it has only recently become

clear that annexin cores also show specificity with respect to their membrane binding in living cells. Through expression of chimeric proteins containing different annexin cores fused to the green fluorescent protein (GFP), it was possible to visualize the distribution of such annexin cores in living cells. Strikingly different distributions were observed within a given cell type showing, e.g., an endosomal localization for the annexin A1 core, an association with certain plasma membrane structures for the annexin A4 core, and a nonmembranous, cytosolic distribution for the annexin A2 core (245). Such live cell experiments have to be extended to reveal annexin dynamics and to circumvent the potential problem that in fixed cells annexin distributions could be subjected to artifacts due to the presence or absence of Ca^{2+} in the fixation/permeabilization buffers. Although the annexin cores carry specificity with respect to membrane binding, an additional layer of such specificity is most likely added by the unique NH_2 -terminal domains of the annexins as in live cells full-length proteins show distributions often differing from the respective cores (73, 196, 245). Moreover, it remains to be seen how interactions with other protein ligands and posttranslational modifications (see below) affect the specific localizations of annexins to certain cellular sites.

Although well described in vitro, the physiological importance of Ca^{2+} -dependent phospholipid (and membrane) binding is not understood. However, interesting models have been put forward to assign functions to a peripherally associated and abundant membrane binding protein like, e.g., annexin A5. In situ, annexin A5 can form two-dimensional crystals on planar lipid bilayers containing negatively charged phospholipids (26, 229, 248, 249). Such crystalline or semi-crystalline arrangement will most likely affect membrane properties including rigidity, fluidity, and lipid segregation and can therefore participate in the regulation and/or stabilization of membrane domains. Indeed, electron paramagnetic resonance (EPR) spectroscopy reveals that Ca^{2+} -dependent binding of annexin A5 to phospholipid vesicles parallels a rigidification of the membrane (193). Moreover, it was shown that binding of this annexin to the surface of T cells (by an as yet unknown mechanism) delays programmed cell death most likely by generating a certain (in this case extracellular) membrane constraint which in turn interferes with the release of CD4^+ membrane particles (99). On the other hand, membrane binding also affects the annexin protein, as annexin A5, thermodynamically a marginally stable protein (like annexin A1; Refs. 256, 328) is protected to a significant degree from thermal denaturation by Ca^{2+} /phospholipid binding (338).

Annexins are not only capable of binding phospholipid-containing membranes but at least in some cases, e.g., annexins A1, A2, A4, A6 and A7, also mediate membrane vesicle aggregation. Again, phospholipid composi-

tion and Ca^{2+} sensitivity for this aggregation activity differ for individual members (for review, see Ref. 244). As molecular structures of annexins reveal one Ca^{2+} /lipid-binding surface (see above), several models have been put forward to explain an aggregation activity based on the linking of membrane surfaces (see also Ref. 97). One proposal, based on the self-association properties of several annexins, is a protein-protein interaction of annexin molecules bound to two separate membranes (for reviews, see Refs. 51, 244; recent example in Ref. 180). A second explanation is based on the identification of a second membrane binding site in annexin A1 (for review, see Ref. 97 and also discussion in Ref. 23). A sequence in the unique NH_2 -terminal domain of annexin A1, residues 24–35, constitutes a crucial part of this second binding domain and when fused to the core of annexin A5 can confer membrane aggregation activity to this otherwise inactive annexin (40). In contrast to the Ca^{2+} -dependent primary membrane binding via the annexin A1 core, the secondary binding is mainly hydrophobic in nature, and it appears that lateral aggregation of annexin A1 molecules bound to one membrane surface precedes the aggregation mediated through the secondary binding site (24). Interestingly, recent crystal structure determination of full-length annexin A1 suggests that the NH_2 -terminal domain of this annexin only becomes fully accessible when the protein core is linked to a membrane surface via its Ca^{2+} /phospholipid binding sites (255). This could indicate that the second (NH_2 -terminal) membrane binding site in annexin A1 is dormant in the cytosolic protein and only becomes activated when the protein associates with membranes. A third alternative of aggregation activity is probably realized in annexin A6, the only member of the family identified so far with eight instead of four annexin repeats. Here a duplication of the core domain has generated a second Ca^{2+} -dependent phospholipid-binding module, thus allowing for two spatially separated membrane interactions (6). Yet another route is taken by annexin A2 and possibly also other annexins capable of interacting with dimeric protein ligands of the S100 family (see below). The NH_2 -terminal domain of annexin A2 harbors a highly specific binding site for the small dimeric S100 protein S100A10, with protein-protein interaction leading to the formation of a heterotetrameric complex. In this complex, two annexin A2 molecules are noncovalently linked via a S100A10 dimer bound to their NH_2 -terminal domains, thereby generating an entity capable of binding simultaneously to two membrane surfaces through the two annexin A2 cores (175). Thus it appears that although several annexins mediate membrane-membrane contacts, the way this is achieved differs from member to member. This could explain the different Ca^{2+} concentrations required by different annexins for half-maximal vesicle aggregation (for review, see Ref. 244) and also the differing dimensions of annexin-dependent junc-

tions observed in high-resolution cryoelectron microscopy of lipid vesicles aggregated by different annexins in the presence of Ca^{2+} (167).

2. Ca^{2+} -independent lipid binding

Although Ca^{2+} -dependent phospholipid binding remains the criterion of choice for defining an annexin protein biochemically, additional "atypical" lipid binding properties have begun to emerge in recent years. These properties again vary between the different annexins analyzed so far, but it appears that the single most important parameter regulating Ca^{2+} -independent membrane binding is the pH value chosen to analyze the interaction. Annexin A5, for example, binds to and apparently penetrates the bilayer of phosphatidylserine (PS) vesicles at pH 4 (158), and at pH 5 was shown to induce a leakage of PS vesicles (124). Both activities are observed in the absence of Ca^{2+} , whereas at neutral pH Ca^{2+} binding to the protein appears to be a prerequisite for the lipid interaction (158). Most likely, this switch in properties is accompanied by a conformational change in the annexin A5 molecule, which has been shown to occur between pH 4.6 and 4 when the acid-induced unfolding of the protein was analyzed (16). This change is characterized by solvent exposure of a unique tryptophan residue in annexin A5 (Trp-187), and thus is reminiscent of a Ca^{2+} -induced exposure of the same tryptophan at neutral pH (192, 293–296). Conformational changes leading to Ca^{2+} -independent phospholipid binding *in vitro* have also been proposed to occur when Ca^{2+} sites in annexin 2 were inactivated by mutagenesis (79), although such mutations interfere with the intracellular membrane localization of this and other annexins (145, 245).

Considerable progress in analyzing Ca^{2+} -independent annexin-membrane interactions occurring at lower pH has come recently through the introduction of site-directed spin labeling. By engineering protein mutants with unique cysteines and specifically derivatizing these cysteines with a paramagnetic nitroxide side chain, the groups of Haigler, Langen, and Hubbell (168, 169) were able to probe the structure of annexin B12 bound to membranes at lower pH. Combined with the use of reagents that selectively and photoactivatably label amino acid side chains exposed to the hydrophobic domain of the bilayer, they could show that annexin B12 inserts into the bilayer of PS/phosphatidylcholine (PC)-containing vesicles. This insertion is likely to be accompanied by the formation of a continuous transmembrane α -helix. In the solution structure of the molecule, this part forms a helix-loop-helix motif, and it is tempting to speculate that the switch from the helix-loop-helix motif to the transmembrane helix drives a reversible membrane insertion (138, 168, 169). Based on these observations, Langen et al. (168) propose concerted conformational changes in all four

annexin repeats of annexin B12, which are triggered by low pH and involve the formation of several elongated transmembrane helices from helix-loop(turn)-helix structures found in solution (Fig. 4). As a consequence, the entire molecule can assume a transmembrane topology as defined by accessibility to proteases present on either side of the membrane (289). The pH-dependent switch in conformation could be induced by the protonation of certain carboxylate residues found in or close to the loop of the helix-loop-helix motif, which upon deprotonation could drive the protein back to the solution conformation (168). Such a model could also hold true for other annexins, as all have similar solution structures, and its reversibility could perhaps explain why and how certain annexins under certain circumstances can span a lipid bilayer. The latter could be of particular importance in the case of annexins A1 and A2, which also appear to have extracellular activities and for which cell surface receptors have been described (see below). At least in the case of annexins A1 and A6, pH-driven membrane insertion has been identified (103, 258), although it is not clear whether this could lead to membrane translocation.

In addition to the points discussed above, Ca^{2+} -independent membrane associations have also been observed for several annexins at neutral pH. Examples for these types of Ca^{2+} -independent interactions are the association of annexins A2 and A6 with endosomal membranes (120, 145, 160, 275), the binding of annexin A2 to A549 cell membranes (182), and the interaction of annexin A5 with the plasma membrane of platelets (for review, see Ref. 322). At least in part it appears that such interactions are mediated through a binding of the respective annexin to a protein ligand that is itself associated with or embedded in the cellular membrane.

C. Nonlipid Annexin Ligands

1. Annexin complexes with EF hand-type Ca^{2+} binding proteins

The EF hand denotes a helix-loop-helix Ca^{2+} binding motif that is present in a large number of proteins comprising the EF hand superfamily with its distinct subfamilies (for review, see Ref. 154). Several EF hand proteins, in particular those of the S100 subfamily, form complexes with members of the annexin family. S100 proteins are small (~10 kDa) proteins characterized by two consecutive EF hands connected by a flexible linker region and flanked by unique NH_2 - and COOH -terminal extensions. Similar to calmodulin, they are thought to interact with and thereby regulate cellular target proteins in a Ca^{2+} -dependent manner (for reviews, see Refs. 68, 267). Three S100 proteins, S100A6, S100A10, and S100A11, were shown to bind specifically to three different annexins, annexins A11, A2, and A1, respectively. The best charac-

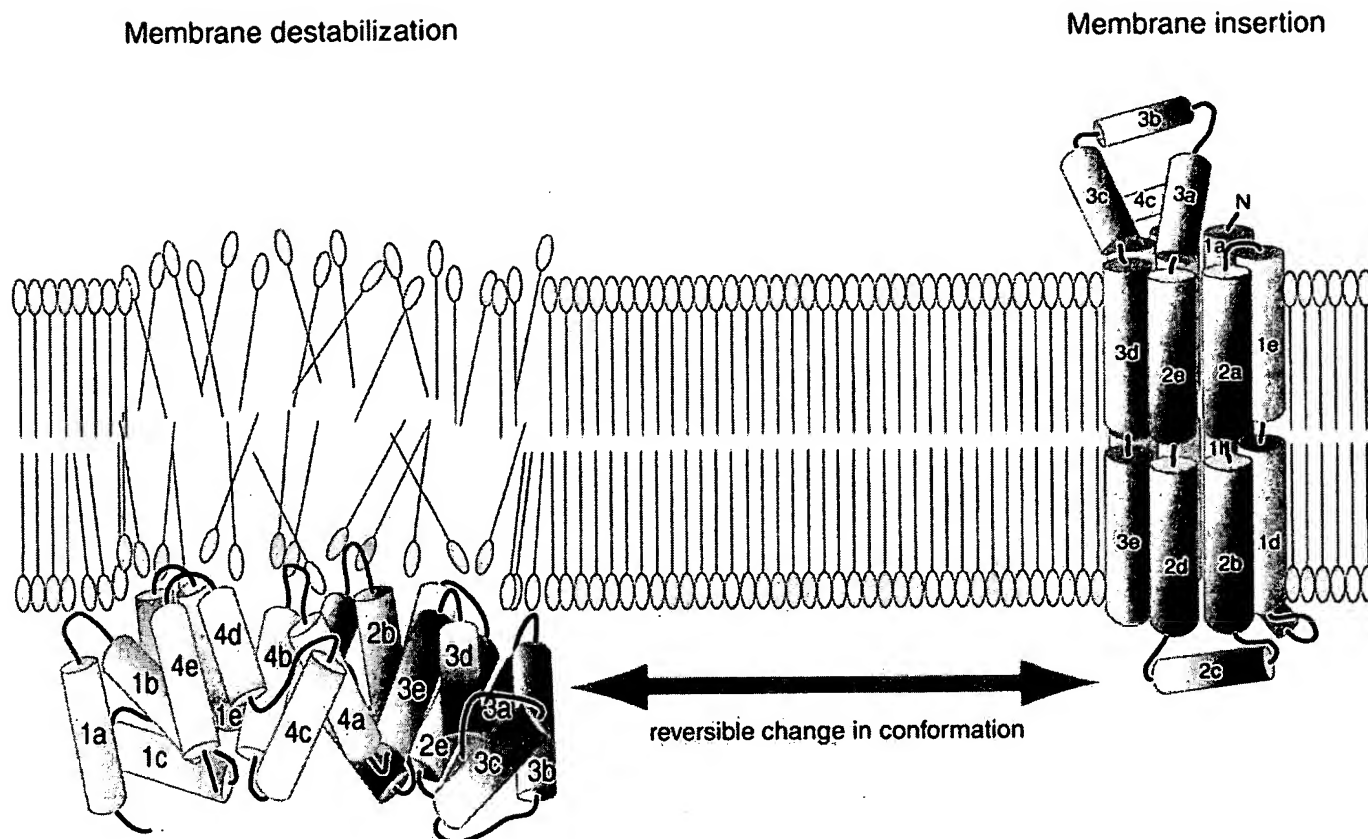


FIG. 4. Peripheral membrane binding and insertion by an annexin. Two potential interaction states for a monomeric annexin molecule with the cytoplasmic leaflet of a hypothetical membrane are shown. The peripherally bound annexin on the *left* assumes the tertiary structure depicted in Figure 2 and has been postulated to increase membrane permeability by apposition of its convex upper surface with the lipid bilayer, which in turn has been suggested to lead to ion flow. The fully membrane integrated structure on the *right* is based on that proposed by Langen and co-workers (168, 169), after protonation at acidic pH, destabilization of the native α -helical structure, and refolding into the seven-transmembrane spanning configuration. Although the proposed structure is obliged to have NH_2 and COOH termini on opposing sides of the bilayer, the orientation shown in the figure is arbitrary.

terized of these annexin-S100 complexes is the annexin A2-S100A10 (p11) heterotetramer. Here it was clearly established that complex formation is highly specific, occurs *in vivo*, can be regulated by posttranslational modifications in the annexin, and modulates properties displayed by the isolated subunits (for review, see Ref. 97). S100A10 is the only member of the S100 family that has suffered deletions and mutations in its two EF hand loops, rendering the Ca^{2+} sites nonfunctional. However, it appears that the resulting conformation of the protein represents a permanently active state with respect to its capacity to bind the annexin A2 target (143, 246, 247). The S100A10 binding site on annexin A2 is restricted to the NH_2 -terminal 14 residues and peptides corresponding to this sequence bind to S100A10 with high specificity and affinity. Moreover, such peptides disrupt by competition preformed annexin A2-S100A10 complexes and therefore

can be used as tools for studying complex function (161). At least in studies with synthetic peptides, an important feature of this binding site is the NH_2 -terminal acetylation of the NH_2 -terminal serine residue of annexin A2, a post-translational modification occurring with high efficiency in eukaryotic cells (15). On the other hand, annexin A2, expressed recombinantly in bacteria and lacking the *N*-acetyl group, is also capable of binding p11, although the affinity of this interaction has not been compared with that of the acetylated protein (151). The apparent discrepancy in these results remains to be resolved, in particular since only an acetylated NH_2 -terminal annexin peptide is capable of disrupting the annexin A2-S100A10 heterotetramer (161).

Complex formation between annexin A1 and S100A11 is based on very similar principles, although in this case Ca^{2+} binding to the S100 protein is required to

establish the interaction-competent form of S100A11 (188, 246, 273). Moreover, it remains to be established if and when this interaction occurs *in vivo*. In contrast to the heterotetrameric annexin A2-S100A10 complexes, standard isolation protocols do not yield annexin A1-S100A11 complexes but only the separated subunits. Likewise, a strong colocalization has not been reported so far, although ectopic expression studies using mutant proteins indicate that annexin A1 can target S100A11 to endosomal membranes in baby hamster kidney (BHK) cells (274). It appears likely that the strict Ca^{2+} dependence of the annexin A1-S100A11 interaction interferes with the visualization or isolation of complexes once Ca^{2+} drops below a certain threshold within the cells or during isolation. On the basis of the high structural similarity of the annexin A2-S100A10 and annexin A1-S100A11 complexes, it is likely that both are heterotetrameric entities with the capacity of linking membrane surfaces in a symmetric manner (see Fig. 3 for annexin A1). While the former complex is known to exist in resting cells irrespective of cellular Ca^{2+} transients (but perhaps regulated by PKC phosphorylation in the NH_2 -terminal sequence of annexin A2; Ref. 144), the latter is probably dependent on (perhaps locally restricted) Ca^{2+} rises and could be of importance during Ca^{2+} -regulated membrane transport events.

The third annexin-S100 protein interaction described to date is that between annexin A11 and S100A6 (312). Although the S100 binding site in annexin A11 is also located in the NH_2 -terminal domain (303, 311), the mode of complex formation is likely to be different. Annexin A11 contains a long NH_2 -terminal domain of almost 200 residues rich in glycine, tyrosine, and proline residues, which resembles that of annexin A7 and possibly lacks a well-ordered three-dimensional fold (177), or contains segments with pro- β -helices (190). However, sequences within the NH_2 -terminal domain of annexin A11 do not resemble the amphipathic helices found in annexins A1 and A2 and thus are unlikely to fit in a homologous manner in a binding pocket formed by the S100 dimer. The physiological consequences of the annexin A11-S100A6 interaction remain to be established, although it is interesting to note that only one NH_2 -terminal splice form of annexin A11 can interact with S100A6 at least *in vitro* (302). Other annexin-S100 interactions have been described, e.g., that of annexin A6 with S100A1 and S100B (96), but the structural basis and physiological significance of such complexes is less well defined. The reader is referred to the S100 literature for further detail (e.g., Ref. 68).

In contrast to S100 proteins, sorcin is a member of the EF hand superfamily containing four and not two of the helix-loop-helix motifs. It binds in a Ca^{2+} -dependent manner to the GYP-rich NH_2 -terminal domain of annexin A7 (28) with the NH_2 -terminal domain of sorcin being required for the interaction (327). Complex formation can

recruit sorcin to the membrane of chromaffin granules, which are a prime site of annexin A7 localization. Moreover, binding of sorcin inhibits the chromaffin granule aggregation mediated by annexin A7 (28), thus underscoring the regulatory importance of complex formation. The common picture emerging from the interaction analyses is that it is most likely to be the annexins that are affected in their properties by EF hand protein binding, rather than the other way round. Although the structural basis of the interaction probably differs between the different complexes, a common feature is the importance of the NH_2 -terminal annexin domain for binding. Protein binding to this unique domain in the respective annexin can have a number of consequences ranging from the establishment of a different physical entity capable of interconnecting membranes (see, for example, Fig. 3) to a protein complex with altered biochemical properties.

2. Annexin interactions with cytoskeletal proteins

A number of annexins have been described as cytoskeleton, in particular F-actin, binding proteins, and it has been suggested that at least some members of the family could participate in regulating membrane-cytoskeleton dynamics. Here we do not survey the entire literature in this area but only focus on recent developments. For an overview of the earlier literature, the reader is referred to previous reviews (97, 244).

Annexin A1 binds to F-actin and also interacts with profilin, a G-actin binding protein and regulator of actin polymerization. Complex formation between annexin A1 and profilin modifies the profilin effect on actin polymerization. Because of the partially overlapping intracellular localization of the two proteins, it is tempting to speculate that the annexin A1-profilin interaction participates in regulating the membrane-associated cytoskeleton (2). In addition to this interaction with a protein involved in actin cytoskeleton dynamics, some colocalization of annexin A1 with tubulin and cytokeratin-8 has also been reported. In A549 human lung adenocarcinoma cells, striking patches of annexin A1 immunolabeling are found at the plasma membrane, which are also positive for these two cytoskeletal proteins (313). It is not clear, however, whether this colocalization reflects a functional interaction.

Annexin A2 is another F-actin binding annexin that also has a Ca^{2+} -dependent filament bundling activity. This bundling activity is particularly pronounced in the case of the heterotetrameric annexin A2-S100A10 complex (for review, see Refs. 97, 330). Recently, the F-actin binding site has been mapped to the COOH terminus of annexin A2, underscoring the specificity of the interaction (80). Annexin A2 is not associated with stress fibers or cytoplasmic actin filaments but appears to play a role in the organization of membrane-associated actin at sites of cho-

lesterol-rich membrane domains. Evidence for this view is severalfold. In the presence of Ca^{2+} , annexin A2 binds to and possibly promotes the lateral association of glycosphingolipid- and cholesterol-rich lipid microdomains (rafts) (8, 119). It has been proposed that in smooth muscle cells this association promotes the binding of annexin A6, which itself mediates the formation of a reversible membrane contact with the actin cytoskeleton (8, 9). On the other hand, annexin A2 could also carry out this task by itself or in conjunction with other actin binding proteins, since cholesterol-sequestering agents specifically release annexin A2 together with the cortical cytoskeletal proteins α -actinin, ezrin, and actin from membranes of BHK and endothelial cells (120; J. König and V. Gerke, unpublished observations). Moreover, expression in epithelial cells of a mutant annexin A2 protein causing the submembrane aggregation of annexin A2 and its ligand S100A10 results in the simultaneous aggregation of a transmembrane raft protein (CD44) and a redirection of actin bundles toward these clusters (216). Thus, due to its Ca^{2+} -dependent membrane and F-actin binding and its intracellular location at sites of membrane rafts, annexin A2 could serve as an organizer of these membrane microdomains and their connection to the actin cytoskeleton.

Annexin A5 has been observed to relocate to the cortical membrane cytoskeleton after activation of platelets. This relocation appears to involve both binding to the plasma membrane and to a specific actin isoform, γ -actin, and is paralleled by an association with the platelet membrane of cytosolic phospholipase A_2 , suggesting an interaction between this phospholipase and annexin A5 (319–321). Annexin A6, another actin-binding annexin, has been implicated in mediating in a Ca^{2+} -dependent manner membrane-cytoskeleton contacts in smooth muscle cells (9). Spectrin is another binding partner of annexin A6 in the cortical cytoskeleton. Because annexin A6 promotes a cysteine protease-dependent type of budding of clathrin-coated vesicles at the plasma membrane, it has been proposed that the protein participates in disconnecting the clathrin lattice from the spectrin membrane cytoskeleton during the final stages of coated pit budding (148). With the exception of annexin A2 (98), it is not known whether other annexins share this spectrin binding property. In addition to the family members mentioned above, F-actin binding annexins have recently also been identified in the killifish medaka (297) and in plants (131), although their functional roles in these organisms have not been addressed so far.

3. Other ligands

In addition to Ca^{2+} , phospholipid, EF hand type proteins, and cytoskeleton-associated proteins, a number of other annexin ligands ranging from proteins to RNA and

smaller molecules have been described. An account of such binding partners is given in previous reviews (97, 244), and only the most recent findings are summarized here. Moreover, this section primarily focuses on intracellular binding partners, whereas extracellular protein ligands are discussed when we review extracellular activities of annexins (see sect. IV C).

Annexin protein ligands other than the ones summarized above include the cytosolic phospholipase A_2 , which interacts with annexin A1 (156) and the p120 Ras GTPase activating protein (GAP), which through its C2 domain binds to annexin A6 (60). Within annexin A6, the binding site has been mapped to the unique linker region connecting the two four-repeat lobes of the protein (44). This region is not found in other annexins, thus emphasizing the specificity of the interaction. Recently, two protein kinases, Fyn (a src kinase family member) and Pyk2 (a member of the focal adhesion kinase family), have also been found in the annexin A6-p120GAP complex, indicating that annexins could also participate in certain signaling events (43). A link between annexin A6 and signaling has also been inferred from its association with activated PKC- α , which was described in skeletal muscle (272). Another binding partner for annexin A6 was identified in clathrin-coated vesicles isolated from adrenocortical tissue. In a subpopulation of these vesicles, which also contain the transferrin receptor, annexin A6 tightly associates with the GTPase dynamin known to participate in the pinching off of clathrin-coated endocytic vesicles (318). In the vesicle preparations, annexin A2 was shown to bind to a yet unidentified 200-kDa protein, suggesting that these two annexins could participate in defining specific protein-lipid interaction domains during endocytosis (see also below). A similar function has been suggested for annexin A13, which interacts with the C2 domain of the Nedd4 ubiquitin protein ligase, thereby participating in the apical membrane targeting of Nedd4 in polarized epithelial cells (231). Annexin A13 exists in two NH_2 -terminal splice variants, a and b, with 13b being specifically targeted to the apical transport vesicles also containing raft components (see below). The binding of annexin A13 to Nedd4 was initially identified in a yeast two-hybrid screen and a number of annexin-protein interactions, e.g., that of annexin A5 with the intracellular domain of the vascular endothelial growth factor (VEGF) receptor Flk-1 (334), have been reported using similar approaches. Interestingly, in all cases reported it has been the protein ligand and never the annexin that was used as the bait in the initial screen.

Some annexins have also been shown to bind to other cellular macromolecules. Annexins A2, A4, A5, A6, and the *Caenorhabditis elegans* protein annexin B7 interact with carbohydrates, in particular glycosaminoglycans, and in some cases the binding sites have been mapped to certain regions within the respective annexin molecule

(83, 139, 152, 159, 265). These interactions are likely to come into play when annexins are present extracellularly, but their functional significance remains to be proven. Nucleic acids comprise yet another class of macromolecules reported to bind to annexins in a Ca^{2+} -dependent manner. Whereas annexin A1 interacts with purine-rich RNA and pyrimidine-rich DNA, annexin A2 has been found associated with mRNA of a distinct polysomal subpopulation (123, 326). It is not known whether and how annexin binding affects stability or functional state of the mRNAs, e.g., in terms of translation efficiency. However, because of the sequence specific binding (A. Vedeler, personal communication) and the fact that annexins A1 and A2 are also actin binding proteins, it has been speculated that the annexin proteins participate in the intracellular positioning of certain mRNAs via an interaction with both the mRNA and the actin cytoskeleton. Single nucleotides binding to certain annexin proteins have also been described in recent reports. While ATP binds to annexins A1 (118) and A6 (for review, see Ref. 11), annexin A7 not only interacts with but also catalyzes the hydrolysis of GTP (34). This latter observation led to the suggestion that annexin A7 acts as an atypical G protein involved in mediating the Ca^{2+} /GTP signal during exocytotic membrane fusion (34). However, although GTP and GDP were present in immunoprecipitates of annexin A7 from permeabilized chromaffin cells, the ratio of GTP to GDP was apparently not influenced by Ca^{2+} , raising questions as to how the GTPase activity might be regulated in vivo. Clearly, further work is required to improve our understanding of how annexins interact with nucleotides, especially as annexins lack a consensus nucleotide binding site. In this context, the three-dimensional structures of annexins complexed to nucleotides will be particularly informative, together with the identification of proteins that might modulate any catalytic activity ascribed to annexins, such as the activator proteins, dissociation inhibitors, and exchange factors that collectively regulate other GTPases.

D. Modulation of Annexin Properties by Posttranslational Modifications

Annexins are long known to be targets for posttranslational modifications. In fact, annexin A2 was initially isolated as a major *v-src* protein kinase substrate, and the tyrosine kinase activity of the epidermal growth factor (EGF) receptor has long been known to phosphorylate annexin A1 (see previous reviews, Refs. 51, 97, 111 and also Ref. 259 for an overview). More recently, additional phosphorylations by signal transducing kinases of these and other annexins have been reported with at least some of them affecting annexin properties. Other tyrosine kinases recognizing annexins A1 and A2 as substrates are

those associated with the platelet-derived growth factor (PDGF) receptor, the hepatocyte growth factor/scatter factor, and the insulin receptor (for review, see Ref. 259). In the latter case, annexin A2 only undergoes insulin-triggered tyrosine phosphorylation when receptor internalization is occurring (22). To some extent, this mimics the tyrosine phosphorylation of annexin A1 upon activation and internalization of the EGF receptor and indicates that both annexins and their phosphorylation are mechanistically linked to the internalization/endocytic sorting of certain ligand bound receptors (see also below). Although these phosphorylations are known to occur in vivo, their physiological consequences have not been established. In vitro or in situ studies, however, have revealed alterations in the Ca^{2+} /membrane binding of annexins A1 and A2 phosphorylated at Tyr-20 (by the EGF receptor kinase, Ref. 61) and Tyr-23 (by the src kinase, Ref. 102), respectively. Tyrosine phosphorylated annexin A1 is more susceptible to NH_2 -terminal proteolysis, thus showing altered phospholipid vesicle binding and aggregation activities (for review, see Ref. 111). Moreover, in contrast to the nonphosphorylated form, it requires Ca^{2+} for the association with the membrane of multivesicular endosomes (92). In the case of annexin A2, tyrosine phosphorylation decreases its affinity for phospholipids and interferes with capability of the annexin A2-S100A10 complex to aggregate chromaffin granules at micromolar Ca^{2+} concentrations (132, 236). A mutual influence of Tyr-23 phosphorylation and phospholipid binding is also corroborated by the finding that phosphorylation of annexin A2 by pp60^{src} is significantly enhanced when the protein is bound to PS containing vesicle (17). Recently, annexins A7 and A11 were also described to be phosphorylated on tyrosine residues, in this case in rat vascular smooth muscle cells in response to PDGF. In vitro both annexins are also phosphorylated by the Ca^{2+} -dependent tyrosine kinase Pyk-2, the src tyrosine kinase, and the EGF receptor kinase, but the physiological consequences of these phosphorylations have not yet been described (91).

A number of serine/threonine kinases that phosphorylate annexins have also been described. Phosphorylation sites again reside in the unique NH_2 -terminal domains of the annexins, and the modifications in some cases have been shown to affect biochemical properties of the annexins, in particular their affinity for Ca^{2+} /phospholipid (already reviewed in Refs. 97, 244). PKC, for example, has long been known to phosphorylate a number of annexins, with annexin A5 being a remarkable exception as it can serve as a PKC inhibitor (261). The strongest evidence for PKC phosphorylation regulating annexin activities in cells has accumulated in the case of annexin A2 and its involvement in Ca^{2+} -regulated exocytosis in adrenal chromaffin cells. Here, nicotine stimulation leads to annexin A2 phosphorylation by PKC with activation of PKC being a prerequisite for regulated exocytosis (63, 263). A link be-

tween secretion and PKC phosphorylation has also been obtained recently in the case of annexin A7, with PKC phosphorylation activating the Ca^{2+} -dependent membrane fusion displayed by this annexin (33). Other kinases acting on annexins are casein kinase I, which phosphorylates annexin A2, and a yet to be defined histidine-specific kinase which phosphorylates annexin A1 (95, 208). Recent evidence for a participation in intracellular signaling has been obtained for annexin A1, whose expression levels have been coupled to regulation of the extracellular signal-regulated kinase (ERK) pathway in RAW macrophages (1).

As pointed out above, annexin phosphorylation often results in an altered susceptibility toward proteolysis. Although this could be considered a mere indication of a conformational change, it could also reflect an important intracellular consequence of the posttranslational modification directly linked to altered properties displayed by the modified annexin. Cleavage generally occurs in the unique NH_2 -terminal annexin domain with the resulting NH_2 -terminally truncated molecule showing, as revealed in particular for annexins A1 and A2, an altered sensitivity toward Ca^{2+} /phospholipid (for review see Refs. 111, 244) and a different intracellular location (245, 275). In addition, it appears at least in the case of annexin A1 that NH_2 -terminal cleavage by an intracellular protease can occur without prior phosphorylation and can thus itself be considered the regulatory event. This has been shown in human neutrophils where removal by a membrane localized metalloprotease of the NH_2 -terminal eight residues of annexin A1 results in a protein species with a decreased Ca^{2+} requirement for binding to secretory vesicles and the plasma membrane, an event possibly linked to the exocytosis of different vesicle populations (206, 207). In annexin A2, another recently observed modification is a *S*-glutathiolation of Cys-8 in the NH_2 -terminal domain, which is observed after oxidative stress, e.g., in tumor necrosis factor (TNF)- α -treated cells (304). Modification of this cysteine, which is located in the S100A10 binding sequence, does not affect the interaction with S100A10 (143). On the other hand, a general cysteine modification of the annexin A2-S100A10 complex by *N*-ethylmaleimide (NEM), which most likely also affects Cys-8, strongly inhibits the ability of the complex to aggregate lipid vesicles (282). It is not clear whether cysteine residues participate directly in the aggregation activity or whether their derivatization interferes with certain conformational changes in the molecule required for the activity. However, as annexin A2 has been implicated in membrane trafficking events possibly requiring its aggregation activity (see below), NEM, which is frequently used as an inhibitor of membrane fusion, could also affect annexin A2.

Hence, a variety of posttranslational modifications on annexins which also include the *N*-myristoylation of an-

nexin A13a and -b (77, 336) have been described, with most of them affecting the Ca^{2+} and/or membrane binding properties of the molecules and thus their most probable intracellular activity. Future analyses have to reveal how these modifications are mechanistically linked to the different annexin functions.

III. MOLECULAR EVOLUTION OF THE ANNEXIN FAMILY AND REGULATION OF ANNEXIN GENE EXPRESSION

Ever since annexins were first reported in the literature they have been categorized as a structurally conserved family of Ca^{2+} binding proteins. The structural conservation remains a defining characteristic, but the discovery of human annexins A9 and A10 (201, 204) provides what appear to be exceptions to the unifying ability of annexins to bind Ca^{2+} . Nevertheless, the conservation of annexin primary structures extends throughout multicellular eukaryotic species, and the abundance of annexin sequences provides unique insights not only into the evolution of the annexin gene family, but also genetic molecular evolution in a broader sense. For readers seeking detailed accounts of annexin evolution, there are several excellent recent articles (203, 200, 204); here we focus on the major features of annexin phylogeny and ask whether or not functional insight can be gained by examination of molecular relationships between annexins.

A. Molecular Phylogeny of Annexins

Annexins have been described in most eukaryotic organisms, with the exception of those yeasts for which genomic sequences are available. The absence of recognizable annexin-like sequences in *Saccharomyces cerevisiae* had been anticipated by a number of investigators in the field who had used both biochemical and molecular genetic screens in what ultimately proved to be unfruitful searches for yeast annexins. Nevertheless, given the genetic diversity of yeasts, it remains possible that an ancestral eukaryotic annexin will be discovered in certain yeast species.

The simplest organisms known to express annexins are the protist *Giardia lamblia* and the fungus *Neurospora crassa*. The existence of at least three annexins in the protist is surprising given the simplicity of the organism and that more sophisticated multicellular eukaryotes such as *Hydra vulgaris* and *Dictyostelium discoideum* have at most one or two annexins. A long-running question in annexin evolution is whether any of the annexins discovered in these primitive organisms represents the ancestor of the modern vertebrate annexins. Early studies describing the *D. discoideum* annexin as a direct ortholog of vertebrate annexin A7 (106) now appear to be incor-

rect. However, the *D. discoideum* annexin does occupy an interesting niche in annexin evolution. The *D. discoideum* and *N. crassa* annexins share ~40% amino acid sequence identity, which given their evolutionary distance suggests they may be orthologs. Indeed, this annexin has now been discovered in the oyster mushroom and potato fungus (R. Morgan and M. Fernandez, personal communication), suggesting the evolutionary segregation of this annexin to this group of organisms.

A second major group of annexins distinct from the vertebrate cohort have been described in plants (64). Plant annexins are characterized by their lack of variable NH₂-terminal domains and, at least in modern flowering plants, by the absence of type II Ca²⁺ binding sites in repeats 2 and 3. Thus, from an evolutionary viewpoint, plant annexins have evolved in quite distinct ways to those in the animal phyla. The position of the fungal and mold annexins relative to either the animal or plant kingdoms is unclear, but sequence identity of ~40% between *D. discoideum* annexin C1 and human annexin A11 raises the possibility that the former is a direct ancestor of the latter. Analysis of the structure of the annexin A11 gene (10) revealed it to be the common ancestor of up to nine descendant annexins (A1, A2, A3, A4, A5, A6, A8, A9, and A10), indicating that at the time of the early chordate radiation 500–600 million years ago the first vertebrate genomes probably contained the genes for only three annexins, namely, annexins A13, A7, and A11. Exon splicing patterns within the core tetrads of annexins A13, A7, and A11 support the idea that A11 is a descendant of A7 and that this in turn evolved from A13. However, orthologs of annexins A7, A11, and A13 have not been formally identified in any nonvertebrate species, and any direct lineage between annexins in organisms such as *D. discoideum* and vertebrates remains conjectural.

A final point of interest to emerge from studies on the molecular evolution of the annexins concerns the origins of annexin A6. This annexin is unique within the family in that it comprises two of the tetrad repeats found in all other annexins. The two tetrads are joined by a short linking sequence, and it was previously hypothesized that annexin A6 was formed by tandem duplication and fusion of a single tetrad (285, 286). Because the 5'-tetrad of annexin A6 is most closely related to annexin A5, it was proposed that the progenitor of this duplication event was the 5'-tetrad. However, the recent discovery and analysis of the annexin A10 gene provides an alternative and much more persuasive explanation for the origins of annexin A6 (204). First, annexin A10 has greater similarity to the 3'-tetrad of annexin A6 than the two halves of annexin A6 have to one another, and significantly, an unusual single codon deletion near the start of repeat three is present in both annexin A10 and the 3'-tetrad of annexin A6. These and other phylogenetic data suggest that the two four-repeat annexins A5 and A10, which are located on human

chromosome 4q26 and 4q33, respectively, may have duplicated and fused to form the 5'- and 3'-lobes of annexin A6 early in chordate evolution.

Collectively, these phylogenetic studies enable us to put the annexins into a meaningful evolutionary context, but they tell us little about annexin function. Because the invertebrate and plant annexins do not have mammalian orthologs, analysis of annexin function in these simpler organisms may yield little information about the functions of the vertebrate family. Despite the difficulty in extracting functional insight from phylogenetic analysis, the fact that the family of 12 mammalian annexins have been tightly conserved over several 100 million years suggests that these proteins do indeed have important physiological roles.

B. Gene Structures

1. Conservation of genomic structure in the annexins

The structural organization of annexin genes is highly conserved, at least with regard to the positions of intron-exon boundaries (286). Most four-repeat annexins comprise 12–15 exons, the variation depending in large part on the length of the NH₂-terminal domains. Thus annexins A7 and A11 have long NH₂ termini encoded by up to six exons, whereas annexin A5 has a short NH₂ terminus encoded by two exons. For several annexins, particularly those with long NH₂ termini, alternative splicing adds to the diversity of annexin isoforms, which may in turn amplify functional variability within the family as a whole. Annexin A6, which has a duplicated tetrad core and therefore 8 conserved repeats, comprises 26 exons and is the largest annexin gene extending over ~60 kb (285). Within the conserved repeats, the tendency is for intron sizes to be considerably smaller than for those introns that lie between the first two or three exons. In many mammalian annexin genes, the first two or three introns are frequently 10 kb or more, whereas introns within the tetrad core are often <1 kb. Almost all alternative splicing of annexin RNA transcripts occurs within exons that encode the variable NH₂ termini. Given that annexin NH₂ termini contain binding motifs for protein partners and sites for posttranslational modifications, alternative splicing in these domains may contribute to the regulation of annexin function. Perhaps the best-characterized exception to this general rule is the alternative splicing of exon 21 in the seventh repeat of ANXA6. Exclusion of this 18-nucleotide exon gives rise to the characteristic appearance of annexin A6 on gel electrophoresis or Western blotting as a closely spaced polypeptide doublet (205).

Cladistic analysis of the mammalian annexin gene family reveals that annexins fall into three major groups. One group comprises the earliest vertebrate annexins,

these being A7, A11, and A13. A second group includes annexins A4, A5, and A8, and the third group comprises annexins A1, A2, and A3, with annexins A9 and A10 as somewhat distant members. Annexin A6 is more difficult to categorize, because the 5'-tetrad is most closely related to the A4,A5,A8 group and the 3'-tetrad to the A1,A2,A3 group. Nevertheless, the cladistic demarcation of these groups raises the question of whether or not they correspond to functional groupings. Despite the lack of clear functional data for most annexins, it is certainly possible to identify some cohesion within these groups. For example, annexins A1 and A2 both bind proteins of the S100 family, both are physiological substrates for protein serine/threonine and tyrosine kinases, and both are suggested to function in the endocytic pathway. In contrast, annexins A4 and A5 are more closely linked with regulation of ion flow (see sect. *ivB*), and annexin A6, which arguably belongs in both groups, has been proposed to have roles that impinge on both the endocytic pathway and regulation of Ca^{2+} signaling. Although such notions are purely speculative, the possibility that annexin clades may represent functional groupings might be relevant to the issue of functional redundancy and therefore the design of gene knock-out experiments.

2. Structural and regulatory features

The completion of the human genome sequencing project, together with increasingly sophisticated algorithms for detecting and analyzing DNA sequences, has led to the identification of unusual and interesting elements within certain annexin genes. The most detailed analyses have been conducted for the annexin A5 and A11 genes (10, 137, 251). The rat and mouse annexin A5 genes are unusual in having two promoters. In both species, the promoter proximal to the gene has a high GC content and lacks a TATA box; this is also true for the human and chick annexin A5 genes (48, 76, 227), and all have an abundance of binding sites for the ubiquitous SP1 transcription factor. In contrast, the distal promoter in the rat and mouse annexin A5 genes has a TATA box and conserved binding sites for transcription factors such as AP1, the glucocorticoid receptor, and MyoD. The significance of these observations is not clear, but the possibility exists that under certain conditions, perhaps during cell differentiation, proliferation, or transformation, transcription from the distal promoter results in an annexin A5 transcript that omits exon 2 in which the start methionine is located. Such a transcript would initiate translation within the first conserved repeat, and the protein thus generated would be predicted to lack the NH_2 terminus and have a molecular mass ~ 3 kDa smaller than the full-length protein. Although there are no reports of the natural occurrence of such an annexin A5 splice variant, *in vitro* studies of recombinant annexin A5 showed that a

mutant lacking the NH_2 terminus was unable to mediate a Ca^{2+} influx into phospholipid vesicles (20). Further investigation of these annexin A5 splice forms supported by a clearer understanding of annexin A5 function could reveal the significance of the two promoters for this gene.

The mouse annexin A5 gene also contains an endogenous retrovirus (251) located in intron 4. The MuERV-L sequence is believed to exist in only 100–200 copies in the mouse genome, although there is no evidence that its presence has any impact on the regulation of annexin A5 expression. The same gene also contains a region of Z-DNA (alternating purine-pyrimidine tract) in intron 6, and other Z-DNA sequences have been identified in the annexin A6 (287) and A11 genes (10). Given the abundance of repetitive elements in mammalian genomes, it is not surprising that *Alu* sequences, long interspersed nuclear elements (LINEs), mammalian-wide interspersed repeats (MIRs), and other less common elements have all been described in various annexin genes. For the most part, these appear to be no more than genomic landmarks, but in the case of annexin A6, a LINE-2 element named ALF (for annexin A6 LINE-2 fragment) was shown to function as a potent and highly specific T-cell silencer that may play a role in the downregulation of annexin A6 in T cells exposed to phorbol ester and calcium ionophore (69). This sequence was also shown to be present in other genes including interleukin-4 and PKC- β , both of which are similarly downregulated by this combination of agonists in T cells.

C. Regulation of Gene Expression

Annexins are frequently described as being ubiquitous. This is true in the sense that any single cell type appears to express a range of annexins, or an "annexin fingerprint," but no single annexin is expressed in all cells, implying that regulation of annexin gene expression is tightly controlled. Insight into the mechanisms of annexin gene regulation can be gained by direct investigation of the relevant gene promoters or by indirect analysis of annexin expression.

1. Annexin gene promoters

Relatively few vertebrate annexins have been subjected to detailed promoter analysis. Two annexin A1 genes have been investigated in pigeons, one of which is strongly inducible by prolactin, and both of which bind Y-box factors (237, 323). The promoters for these genes have been partially characterized, but the most detailed analyses have been performed on the human annexin A1 (70, 290), A6 (70), and A7 (301) gene promoters. The annexin A1 gene promoter contains CAAT and TATA boxes that were shown in deletion studies to be essential for minimal promoter activity. Analysis of the annexin A1

promoter also permitted investigation of the sensitivity to dexamethasone, a glucocorticoid analog. Although one study found the promoter to be unresponsive to treatment with dexamethasone (70), the other reported some level of induction (290). The different results may correspond to the use of different cell lines in each report or may reflect the exposure times used which in the former case extended to 8 h, and in the latter to 24 h. Despite these differences, both studies support the notion that annexin A1 is not a glucocorticoid primary response gene. Interestingly, studies on the cytokine responsiveness of the annexin A1 promoter showed the gene to be induced by interleukin-6 (290). This result is consistent with a role for annexin A1 in the acute phase response to inflammation.

The human annexin A6 gene promoter also contains CAAT and TATA boxes, although these are somewhat distal to the transcription start site and in this case the minimal promoter lies downstream of and does not include these elements (70). The most unusual feature of the annexin A6 promoter is a potent T cell-specific silencer located ~600 bases 5' to the transcription start site (69). This element was discussed in section III B2. The human annexin A7 gene promoter has also been serially dissected, and it lacks CAAT and TATA boxes but is GC rich and contains many SP1 binding sites (301). The phylogenetically related annexin A11 gene promoter also lacks CAAT and TATA boxes, and it too is GC rich (10). The presence of SP1 binding sites in most, if not all, annexin promoters so far examined, is consistent with their broad patterns of expression, but the existence of other regulatory elements, or in the case of annexin A5 an alternative promoter, suggests that under certain circumstances tight transcriptional control may be exerted.

2. Annexin expression in development and differentiation

The annexin literature contains many reports in which the expression of individual annexins is correlated with cell proliferation, differentiation, or transformation. For the most part, these studies do not reveal any great insight into annexin function, so in this review we focus on instances where annexin expression is developmentally regulated and in which the annexin exhibits a particularly striking and suggestive association with a certain cell type or cellular localization. Many of the clearest examples of potential functional correlates are to be found in the simple eukaryotes. In these cases, the presence of only a few annexins together with fewer cell types allows a more straightforward interpretation of the observations.

Hydra vulgaris expresses at least two annexins, of which annexin B12 (formerly annexin XII) is the best characterized. Annexin B12 was discovered first (270) and is clearly the major annexin in *Hydra*, being expressed at

an estimated 100-fold excess of a second as yet uncharacterized annexin. Immunofluorescence analysis of whole *Hydra* revealed the staining pattern of the two annexins to be segregated, with annexin B12 being largely confined to epithelial battery cells throughout the tentacles, with the second *Hydra* annexin being maximally located in the cytoplasm of nematocytes (269). The epithelial battery cells differentiate from gastric ectodermal epithelial stem cells, whereas nematocytes differentiate from interstitial cells. The battery epithelial cells and nematocytes are closely aligned in *Hydra* tentacles; both are motile and both are actively turned over. The presence of annexins in these cells therefore fits with current models of annexin function in cell matrix adhesion and cell membrane plasticity and remodeling. The nematode worm *C. elegans* is somewhat more complex in that it expresses four annexins (annexins B5 to B8), of which annexin B7 is the best characterized. Annexin B7 (originally nex-1) was discovered using classical protein biochemical techniques as a major 32-kDa polypeptide exhibiting reversible Ca^{2+} -dependent binding to phospholipids (53). Immunocytochemical and electron microscopic investigation of this protein revealed it to be associated with a well-defined subset of cell types and structures including the membrane systems of the secretory glands in the pharynx and the uterine wall and vulva. However, the most striking and most intense localization was to the convoluted membranes of the spermathecal valve. These membranes undergo major conformational changes as eggs pass through the valve, suggesting a possible role for annexin B7 in the regulation of membrane fluidity or membrane-membrane and membrane-cytoskeleton interactions. So far, only annexin B7 has been isolated and biochemically characterized, although annexins B6 and B8 (nex-2 and nex-3, respectively) have been shown by RT-PCR to be actively transcribed (57). Of these, annexin B6 has an unusually long NH_2 terminus similar to those that characterize annexins A7 and A11, indicating possible evolutionary linkage with the modern annexins. Although genetic studies have not yet been reported for these annexins, the emergence of RNA interference as a particularly effective technique for preventing gene expression in *C. elegans* (81) opens the way for a detailed and potentially highly informative analysis of annexin function in this organism.

Despite the prevalence of annexins in most eukaryotic species, relatively little is known about developmental regulation of annexin gene expression. A few studies have focused on mammalian annexin gene expression in the developing mouse brain (115, 116), the results of which revealed distinct patterns of temporal and spatial regulation of individual annexins. Other investigators reported developmental regulation of expression of at least four annexins in the loach *Misgurnus fossilis* (140) and the medaka fish *Oryzias latipes* (219). The latter study extended to whole mount RNA in situ hybridization to

examine the localization of four annexins during embryogenesis. As with the investigation of nematode annexins, this work identified tightly controlled annexin expression associated with specific organs or cell types. The annexin expressed earliest in medaka embryogenesis is a likely ortholog of annexin A11, which appears transiently in the prechordal mesendoderm and hindbrain. The three other medaka annexins, which may be orthologs of annexins A1, A4, and A5, all appear later in embryogenesis but in a range of tissues including liver, floor plate, and skin.

These studies represent only a small part of a large and fragmentary literature relating to the developmental, cell growth, and differentiation-dependent regulation of annexin expression. The picture that emerges from these studies is that for many annexins expression patterns are broad, which might imply fundamental roles in cell physiology for most members of the family. For the majority of annexins, functions suggested on the basis of observations made in a single cell type may therefore be incorrect. However, other annexins are undoubtedly restricted in their patterns of expression, sometimes with regard to cell and tissue development and sometimes in terminally differentiated cells. In these cases, exemplified by annexin A13, which is clearly involved in apical vesicle transport in certain polarized epithelial cells, it is more reasonable to predict a specialized cell type-specific function. In simpler eukaryotes with fewer annexins, of which several examples have been described here, there is now the prospect of combining genetics with developmental analysis to provide new information about function. Even if the absence of orthologous annexins in vertebrates presents a bar to direct extrapolation of function, the knowledge will impinge on the experimental design of genetic approaches to annexin function in species such as the mouse.

IV. FUNCTIONAL DIVERSITY WITHIN THE ANNEXIN FAMILY

A. Annexins in Membrane Traffic and Organization

A priori, annexins are intracellular proteins, and their denominating property, i.e., binding in a Ca^{2+} -regulated manner to negatively charged phospholipid surfaces, strongly argues for their functioning in conjunction with such phospholipids that are enriched in the cytoplasmic leaflets of cellular membranes. Exceptions are, however, disturbed cells undergoing apoptosis which display negatively charged phospholipids on their surface. In fact, it is the canonical annexin property of Ca^{2+} -dependent binding to acidic phospholipids which led to the introduction of annexin A5 as a diagnostic tool for labeling the surface of apoptotic cells. It has to be emphasized here that this diagnostic binding, albeit very useful, does not necessarily

have any implications for the *in vivo* function of annexin A5.

A large number of reports have provided circumstantial and also more direct evidence for annexins functioning in intracellular membrane organization. These include the detailed analyses of annexin distributions within different types of mostly cultured cells. A survey of these localization studies has been presented before (97). As a whole it appears that different annexins show strikingly different subcellular distributions and often reside in both a cytosolic and a membrane-associated pool, with a switch between the two typically being regulated by Ca^{2+} . The respective target membranes identified for different annexins are in most cases the plasma membrane and membranes of the biosynthetic or the endocytic pathway, and it has therefore been concluded that annexins function in these membrane trafficking steps.

More recently, studies on the intracellular location of annexins have been extended to live cells in approaches using GFP fusions. Such analyses revealed that annexin A1 associates with membranes of the endosomal, transferrin-accessible system of HeLa cells in a manner dependent on active Ca^{2+} binding sites being present in the protein. Moreover, it was shown that removal of the unique NH_2 -terminal domain of the protein results in a change in intracellular localization with the annexin A1-core being targeted to late endosomal membranes. Interestingly, this also appears to be specific since protein cores of other annexins (annexins A2 and A4) show different distributions in live HeLa cells (245). In light of the finding that proteolytic cleavage within the NH_2 -terminal domain of annexin A1 is likely to occur within cells (possibly triggered by phosphorylation, see above), the distinct localizations of full-length and NH_2 -terminally truncated annexin A1 could reflect distinct functions of the two species. Full-length annexin A2 localizes to the plasma membrane in living HeLa and HepG2 cells and also to membranes of the endosomal system in living BHK and rat basophilic leukemia cells (196, 245, 342). In the latter case, inspection by evanescent field microscopy of pinocytic vesicles formed under mildly hyperosmotic conditions revealed the presence of annexin A2-GFP in actin tails propelling these pinosomes. Moreover, formation of such pinocytic rockets is inhibited by overexpression of a mutant protein dominantly interfering with the annexin A2 localization, thus suggesting an important role of this annexin in organizing interfaces between certain membranes or membrane domains and the actin cytoskeleton (196). An annexin A7-GFP chimera was also localized recently to discrete intracellular structures, in this case in differentiated myoblasts (45). Upon subcellular fractionation, the annexin A7-containing membranes copurify with caveolin-3, but a role of annexin A7 in, e.g., the establishment or stabilization of tubules during myogen-

esis, remains to be shown and is not as yet evident in annexin A7-deficient mice (see sect. IV D).

1. Annexins in the biosynthetic pathway

A number of annexin proteins, including annexins A1, A2, A3, A6, A7, A11, A13, and B7, have been linked to exocytotic processes, more specifically post-*trans*-Golgi network events in the biosynthetic pathway (for reviews, see Refs. 30, 51, 97, 244). The most compelling evidence for such an involvement which go beyond the mere localization of the protein to secretory organelle membranes and/or the plasma membrane has been reported for annexins A2 and A13. Annexin A2 has been identified as a cytosolic protein that can retard the rundown of secretory responsiveness to Ca^{2+} stimulation of permeabilized chromaffin cells when added exogenously as a purified protein. In this assay, the annexin A2-S100A10 complex, which is localized in several cell types to the sites of plasma membrane/secretory granule membrane contact and/or intergranule contact (212, 276, 277) and which is capable of aggregating vesicles (see above), is more efficient than the monomeric annexin protein. Moreover, PKC phosphorylation of annexin A2 is required for the activity (263) (recall that PKC is activated upon nicotinic stimulation of chromaffin cells), and a peptide corresponding to an NH_2 -terminal annexin A2 sequence containing the PKC site inhibits catecholamine secretion in nicotine-stimulated chromaffin cells. Interestingly, it appears that the function of the annexin A2-S100A10 complex in chromaffin granule exocytosis is restricted to adrenergic cells as the S100A10 subunit is not expressed in the noradrenergic cell type (38) (for review, see Ref. 5). By correlation, it was also inferred that the annexin A2-S100A10 complex participates in lung surfactant secretion from alveolar type II cells as phenothiazines inhibited this secretion in a manner similar to their inhibition of annexin A2-S100A10-mediated vesicle aggregation (181). Yet another Ca^{2+} -triggered exocytosis event is the regulated secretion of different granule contents from endothelial cells, the most prominent being the von Willebrand factor stored in Weibel-Palade bodies. With the use of a whole cell patch-clamp approach combined with membrane capacitance recordings, it was shown that disruption of the annexin A2-S100A10 complex by a competitor peptide corresponding to the S100A10 binding site on annexin A2 markedly inhibits the Ca^{2+} -dependent exocytotic membrane fusion (161). Annexin A2 and S100A10 in endothelial cells are located at the plasma membrane and not found on Weibel-Palade bodies. Hence, it has been proposed that the complex indirectly functions in endothelial granule exocytosis by organizing the plasma membrane in a manner supporting the granule-plasma membrane fusion event (161, 213). In line with this proposal, annexin A2 is found concentrated at certain subdomains

of the plasma membrane and seems to provide a link between such subdomains and the actin cytoskeleton (see below).

Annexin A13, a myristoylated member of the family occurring in two NH_2 -terminal splice variants (a and b), is only expressed in a limited subset of polarized epithelial cells. Here, the 13b variant is localized specifically to the TGN, post-TGN carrier vesicles, and the apical plasma membrane. Antibodies directed against the unique exon encoded sequence in the annexin A13b splice form interfere with carrier vesicle transport to the apical but not the basolateral membrane domain of permeabilized Madin-Darby canine kidney (MDCK) cells, suggesting a very specific role of the protein in this transport step (77). Annexin A13b binds to sphingolipid- and cholesterol-rich domains (rafts) that bud off the TGN and that are destined for the apical plasma membrane in a transport step requiring a microtubule minus end-directed motor (214). The TGN budding is inhibited by annexin A13b antibodies and stimulated by myristoylated but not unmyristoylated annexin A13b (165). The other splice variant, annexin A13a, also stimulates apical biosynthetic transport but, in contrast to annexin A13b, also appears to be involved in the basolateral delivery in polarized cells (172). Due to their specific and in some cases regulated association with raft domains, the involvement of annexin A13 isoforms in post-TGN transport to the plasma membrane could be based on a membrane-organizing effect and thus could mirror the situation discussed for annexin A2 in Ca^{2+} -regulated exocytosis in endothelial cells. Thus the membrane-organizing capacity of annexins, which differs in extent, regulation, and target membrane between different members of the family, could represent the mechanistic basis of annexin effects in membrane transport events.

Other biosynthetic membrane transport steps affected by annexins include Ca^{2+} -dependent secretion in neutrophils, which in a streptolysin-O (SLO)-permeabilized cell system is stimulated by annexins A1 and A3 (254), and Ca^{2+} -induced insulin secretion in pancreatic β -cells, which in SLO-permeabilized cells is inhibited by annexin A11 antibodies (135). However, in all cases, live cell experiments, e.g., the injection of antibodies or interfering peptides/proteins or the generation of cells deficient in specific annexins combined with a subsequent characterization of transport steps in the modified cells, are required to corroborate and more specifically define the role of annexins in exocytosis.

2. Annexins in the endocytic pathway

Membranes of the endosomal system have also been identified as target structures for several annexins, and the mode of membrane binding has been studied extensively, both in terms of the specific target membrane

selected by the individual annexins and in terms of the structural requirements for membrane binding within the annexin molecule. Some of the literature describing annexin-endosome interactions has been reviewed before (97, 108). More recently, the specificity and thus most likely functional importance of such interactions has received support by a number of observations regarding annexins A1, A2, and A6. Live cell experiments analyzing the intracellular distribution of annexin-GFP chimeras have underscored the importance of the unique NH₂-terminal domain in positioning the individual annexin at certain target membranes (see above). Annexin A1, for example, is found on early, transferrin-accessible endosomes in BHK and HeLa cells, although some protein is also present on multivesicular endosomes, at least in mouse fibroblasts (92, 245, 275). Upon removal of the NH₂-terminal domain, the resulting annexin 1 core domain redistributes to late endosomes with the interaction still being Ca²⁺ dependent and specific, i.e., not observed with other highly homologous annexin cores (245, 275). This switch could also occur under certain cellular con-

ditions, e.g., when upon internalization of the EGF receptor annexin A1 becomes phosphorylated on Tyr-20 and thus more susceptible to NH₂-terminal proteolysis (see above). The proteolysis removes at least part of the NH₂-terminal domain and thus not only the sequence required for localizing the protein to early endosomes but also the binding site for the annexin A1 ligand S100A11. As a result, a putative heterotetrameric annexin A1-S100A11 complex capable of linking membrane surfaces would be disrupted. Together with the finding that the association of annexin 1 with multivesicular endosomes is regulated through phosphorylation by internalized EGF receptors, the proposed role of the protein in mediating the inward vesiculation in multivesicular endosomes (92) could be envisaged as depicted in Figure 5. Annexin A1 in its Ca²⁺-regulated complex with S100A11 (which is targeted to early endosomes by annexin A1, Ref. 274) could organize the limiting membrane of multivesicular endosomes *in statu nascendi*, i.e., early endosomes or budding endosomal carrier vesicles in the process of becoming multivesicular, in a way that supports the inward vesiculation.

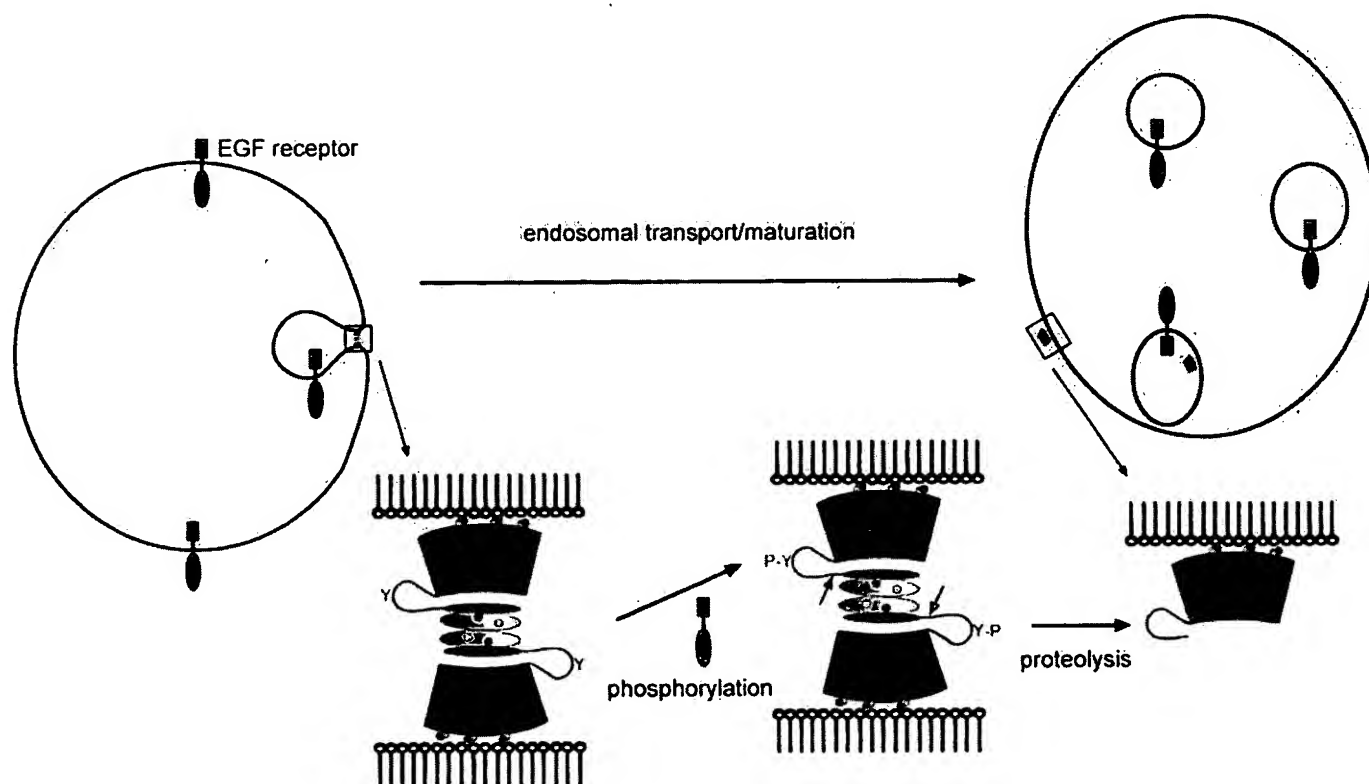


FIG. 5. Model describing a potential participation of annexin A1-S100A11 in the inward vesiculation process generating multivesicular endosomes. Owing to its potential membrane linking properties, the as of yet hypothetical heterotetramer of annexin A1 (red) and S100A11 (orange) could stabilize membrane interactions required for inward budding. Phosphorylation of Tyr-20 of annexin A1 by the internalized epidermal growth factor (EGF) receptor (92) renders the protein more susceptible for proteolysis occurring in the NH₂-terminal domain. Proteolytic cleavage would release the S100A11 dimer (together with the NH₂-terminal annexin A1 sequence) in a process that could accompany the actual membrane fission and internal vesicle release. As a result, an NH₂-terminal foreshortened annexin A1 would be present on multivesicular/late endosomal membranes, a localization in line with that of ectopically expressed annexin A1 core-green fluorescent protein (245).

Once the inward budding is about to be completed with the final fusion process, annexin A1 becomes phosphorylated by internalized receptors destined for degradation. This leads to limited proteolysis and thus disruption of the complex between annexin 1 and S100A11 in a process which might be coupled to the actual fusion. This activity might not be essential for endosome maturation/transport to occur but might facilitate the kinetics by providing a supporting membrane scaffold. Whether and how this model relates to observed stimulatory effects of annexin A1 on cell proliferation, EGF receptor synthesis, and phosphorylation remains to be established (62).

Annexin A2 was also identified on early endosomes (in addition to its localization at the plasma membrane and on certain secretory granules). Interestingly, its interaction with endosomal membranes occurs in the absence of Ca^{2+} and is primarily mediated by the NH_2 -terminal domain, which upon fusion to an annexin A1 core can transfer this unique property to the otherwise Ca^{2+} -sensitive annexin A1 (120, 145, 160). It is not clear whether the NH_2 -terminal annexin A2 sequence in question interacts with a protein receptor, e.g., a 200-kDa protein identified in ligand blotting experiments in certain clathrin-coated vesicle preparations (318), or specifically associates with a unique lipid structure, e.g., cholesterol-rich membrane domains that are required for this atypical annexin-membrane interaction (120, 160). Annexin A2 is not distributed evenly over the early endosomal compartment. Immunoaffinity approaches reveal that it is enriched on Rab11- (and also transferrin receptor-) but not Rab5-positive endosomes of Chinese hamster ovary (CHO) cells, whereas it is not found in transferrin receptor-positive recycling endosomes of polarized MDCK cells (93, 315). In BHK cells, on the other hand, endosomes isolated on immobilized annexin A2 antibodies are positive for the transferrin receptor but not the early endosomal antigen EEA1. This correlates with the ultrastructural colocalization of annexin A2 and the transferrin receptor on endosomes of BHK cells (341). Thus it appears that the fine tuning of annexin A2 localization within the early endosomal compartment is handled differently in different cells, possibly in conjunction with its proposed function as a scaffolding protein organizing and/or stabilizing rafts (see below).

A similar scenario could hold true for annexin A6, which has been localized to different endosomal membranes in different cells. In rat liver hepatocytes, it is found on an apical endocytic compartment, whereas it is present on late endosomes/prelysosomes of NRK fibroblasts (218, 235). Furthermore, some annexin A6 is also associated with the plasma membrane and clathrin-coated vesicles (179, 318), where it could function in facilitating coated pit budding. Earlier experiments employing immobilized plasma membranes and taking the loss of clathrin from such membranes as a measure for

coated pit budding reported an inhibitory effect when the cytosol required in this Ca^{2+} - and ATP-dependent reaction was depleted of annexin A6 (179). More recently, with the use of the same assay, it was shown that annexin A6 is only required for a certain type of coated pit budding, one sensitive to the cysteine protease inhibitor ALLN. The involvement of annexin A6 depended on its association with spectrin indicative of a function of the protein in remodeling the spectrin lattice as a prerequisite for efficient budding (148). Moreover, the same study revealed that microinjection of a truncated annexin A6 mutant inhibited low-density lipoprotein (LDL) uptake, thus paralleling the inhibitory effect of the mutant on coated pit budding in the *in vitro* assay. Other coated pit budding events (those not affected by ALLN) do not require annexin A6, thus providing a possible explanation for the finding that receptor-mediated endocytosis in annexin A6-negative A 431 cells is not stimulated by ectopic overexpression of the protein (288). On the other hand, ectopic overexpression of annexin A6 in CHO cells has a stimulatory effect on LDL receptor endocytosis, however, only when the receptor itself is overexpressed as well. In these experiments, annexin A6 remained associated with LDL-containing vesicles also at later stages of the endocytic pathway, possibly suggesting additional functions of the protein in late endocytic events (107). Such functions are likely to include trafficking events leading to LDL degradation, since microinjection of a mutated annexin A6 into NRK cells causes a retention of LDL in the prelysosomal compartment (234).

3. Annexins and phagocytosis

A translocation of different annexins to the membrane of maturing phagosomes has been observed in a number of phagocytic cells and has been taken as an indication for the involvement of the proteins in phagocytosis (previously reviewed in Ref. 97). Such observations have been extended in the recent past showing, for example, that annexins A1–A5 are present on isolated phagosomes from J774 macrophages, with the levels of annexin A4 (but not those of the other annexins) increasing with age of the maturing phagosomes (66). In another study using macrophage-like cells and analyzing Fc receptor-mediated phagocytosis, annexins A7 and A11 in addition to the members mentioned above were found to translocate to the phagosomes upon particle ingestion (230). In differentiated human monocytes, phagocytic uptake of *Brucella* bacteria (opsonized or nonopsonized) is accompanied by a recruitment of annexin A1-positive structures to the site of entry (164), whereas neutrophils phagocytosing yeast cells show a translocation of annexin A11 to the periphagosomal region (284). When the same cells take up an attenuated strain of *Mycobacterium tuberculosis*, the intracellular distribution of annexins A1

and A5 remains unchanged while annexins A3, A4, and A6 are translocated from the cytoplasm to the proximity of the bacteria containing phagosomes. In the case of annexin A4, this even occurs in Ca^{2+} -depleted neutrophils (189). Similar observations have also been made in human dendritic cells phagocytosing *M. tuberculosis* (170). Although these reports point to a role of the respective annexins in phagosome maturation, e.g., by facilitating certain transport or phagosome-endosome fusion steps, they so far only represent circumstantial evidence. We are still in need of functional approaches, e.g., analysis of phagocytosis in cells with an altered annexin expression or in the presence of dominantly interfering compounds, to make a conclusive connection between annexins and phagocytosis.

4. Annexins and the establishment/stabilization of membrane domains

Recent years have seen a formulation of the concept of membrane microdomains (rafts) being involved in aspects of membrane transport and also representing platforms for signaling events (for review, see Refs. 27, 281). Rafts are lateral assemblies of membrane patches rich in sphingolipids and cholesterol, which due to their high content of saturated hydrocarbon chains form a liquid-ordered phase in the more disordered background of glycerolipids containing unsaturated fatty acid chains. Biochemically, rafts (or detergent-resistant membrane complexes, DRMs) are defined by their resistance toward treatment with nonionic detergent in the cold and their ability to float to low density in sucrose density gradients. A number of membrane proteins have been described as raft associated. Typically, these proteins contain a certain fatty acid, isoprene or lipid moiety (e.g., glycosylphosphatidylinositol or GPI) which helps anchor them in the membrane raft. Most of the typical lipid and also protein components of rafts described to date are those found in the exoplasmic leaflet of the bilayer. The inner leaflet of these microdomains is less well characterized, although it appears to contain glycerophospholipids with a higher degree of saturation than the total plasma membrane (88) and also is likely to be enriched in cholesterol (281). Moreover, information on proteins associating specifically with the cytoplasmic side of rafts and thereby possibly regulating their assembly and dynamics is rather scarce. It is here where annexins could come into play as several members of the family have been identified in raft preparations and seem to associate with rafts in a manner which is in some cases but not strictly regulated by Ca^{2+} . Recent evidence in support of this view is summarized below for different annexins.

Rafts and membrane microdomains are not restricted to the plasma membrane but are also found in membranes of the biosynthetic (Golgi) and the endoso-

mal system (209, 279, 280). Annexin A1, a substrate of the EGF receptor kinase implicated in endosomal sorting of the receptor (see above), is also a substrate of PKC and localizes with the active enzyme to the endosomal compartment. After PKC activation initiated by exposure of cells to phorbol esters, downregulation of the enzyme appears to occur via translocation from the plasma membrane to endosomes, a process which is inhibited by caveolin binding drugs. Because PKC translocation and thus its colocalization with annexin A1 does not depend on the endosomal GTPase Rab5, it has been proposed that the transport is mediated through caveolae, cell surface invaginations containing a subset of lipid rafts which are formed by polymerization of the cholesterol-binding caveolin proteins (238; for review on caveolae, see Refs. 3, 136). Thus it appears that annexin A1 could also be involved in the downregulation of membrane-bound PKC through caveolae-mediated traffic to endosomes. Although evidence in support of this hypothesis is vague and circumstantial, several lines of research have strongly and more directly implicated annexin A2 in the organization and dynamics of membrane rafts. In several types of cells, annexin A2 associates with membrane rafts (biochemically defined as described above) in both a Ca^{2+} -dependent and a Ca^{2+} -independent manner. These include adrenal chromaffin cells where, after nicotine stimulation and in the presence of $1 \mu\text{M}$ Ca^{2+} , the protein translocates to Triton X-100 (TX-100)-insoluble membrane subdomains (262) as well as MDCK, polarized mammary epithelial, and smooth muscle cells where raft association is also Ca^{2+} dependent (8, 119, 216). On the other hand, BHK as well as bovine endothelial cells contain annexin A2, whose association with rafts is not sensitive to Ca^{2+} chelation but correlates with the amount of membrane cholesterol (50, 120). Interestingly, annexin A2 associated Ca^{2+} independently with BHK or endothelial cell membranes can be specifically released together with a subset of cortical cytoskeletal elements (actin, α -actinin, ezrin, and moesin) by sequestration of membrane cholesterol, suggesting a link between raft-associated annexin A2 and the membrane underlying actin cytoskeleton (120; König and Gerke, unpublished observations).

A role of annexin A2 as an organizer of membrane domains has gained further support in the case of the Ca^{2+} -dependently raft-associated protein. In the sarcolemma of smooth muscle cells, the dynamics of rafts, their lateral assembly, and association with the actin cytoskeleton appear to be regulated by changes in intracellular Ca^{2+} concentrations occurring during smooth muscle contraction. These changes correlate with the Ca^{2+} -dependent association of annexin A2 with membrane rafts and the translocation of annexin A6 to a membrane-cytoskeleton complex. Hence, it was proposed that an initial Ca^{2+} rise in smooth muscle cells triggers the binding of annexin A2 to lipid rafts and a clustering of these rafts

which is promoted by lateral annexin assembly. As a consequence, the spatial organization of, e.g., membrane receptors, is altered leading to a second Ca^{2+} transient further elevating intracellular Ca^{2+} . This is proposed to trigger a translocation of annexin A6 to the sarcolemma where it could be involved in the formation of bonds between the plasma membrane and the actin cytoskeleton (8). Annexin A2 is a F-actin binding protein itself (98) and thus could also participate more directly in the formation of membrane-cytoskeleton links. In a recent study it was shown to colocalize in basolateral lipid rafts of mammary epithelial cells with the hyaluronic acid receptor CD44. Antibody-induced clustering of CD44 leads to a similar clustering of annexin A2. Even more interestingly, clustering of annexin A2 at the cytoplasmic side of the membrane, which was achieved through ectopic expression of a *trans*-dominant annexin A2 mutant protein, led to the enrichment of CD44 in the annexin A2-positive patches. Moreover, a reorientation of F-actin toward the annexin A2 clusters was observed (216). A rearrangement of cortical actin can also be induced by certain pathogens, e.g., enteropathogenic *Escherichia coli* (EPEC), which induce the formation of actin-rich pedestals underneath their site of host cell attachment. Interestingly, bacterial attachment triggers a clustering of membrane raft components and a recruitment of annexin A2 to the attachment sites, suggesting that annexin A2 could participate in this process by stabilizing raft patches and their linkage to the actin cytoskeleton beneath adhering EPEC (343).

Collectively, these findings indicate that annexin A2 could represent a cytoplasmic protein peripherally associating with the cytoplasmic leaflet of membrane rafts, thereby stabilizing these domains and providing a link with the cortical actin cytoskeleton. Such a function would depend crucially on the membrane association of annexin A2 and therefore could be regulated in two ways, by membrane cholesterol content and local Ca^{2+} concentration, as indeed shown recently for annexin A2 associated with endosomal membranes (279, 341) or artificial liposomes containing cholesterol (7). This dual regulation mode reflects itself in the structure of the molecule as the NH_2 -terminal domain mediates a Ca^{2+} -independent interaction with cholesterol-rich membrane domains (160) and the COOH-terminal protein core harbors the Ca^{2+} -regulated binding site. As depicted in Figure 6, this could mean that some annexin A2 binds to cholesterol-containing membrane domains or specific receptors therein, already in the absence of Ca^{2+} . Once Ca^{2+} rises, e.g., during regulated exocytosis, at the sarcolemma upon smooth muscle cell activation or during certain types of endosomal fusion (129), additional annexin A2 molecules are recruited to the same sites providing a sort of membrane scaffold and, given they reside in complex with the S100A10 dimer, contact sites to other membranes or the cytoskeleton. In this view the annexin serves a more

structural role in the membrane periphery affecting indirectly a number of membrane transport events, thus functioning in a manner similar to that discussed for membrane skeleton proteins, e.g., spectrin or spectrin-associated proteins present on intracellular membranes (14, 197, 340).

As already mentioned, annexin A6 has also been implicated in the organization of membrane domains, in particular their association with the cytoskeleton in smooth muscle cells (8, 9). It could serve a similar function in mammary epithelial cells as a fraction of annexin A6 is recovered from the TX-100-insoluble fraction from these cells in a manner which appears to be regulated during polarization of the cells (171). Moreover, annexin A6 associates with raft fractions from synaptic plasma membranes in a Ca^{2+} -dependent manner (217). Whether and how this relates to the spectrin binding of annexin A6 and its proposed function in clathrin-coated pit budding remains to be shown. The sole annexin whose association with lipid rafts was shown to be functionally important for membrane trafficking events is annexin A13b (see also above). Together with its NH_2 -terminal splice variant, annexin A13a, it is the only member of the family that can be NH_2 -terminally myristoylated (77, 336). Annexin A13b is located in the apical compartment of polarized MDCK cells and found on the *trans*-Golgi network, at the apical cell surface and on exocytic apical carrier vesicles whose formation is inhibited by anti-annexin A13b antibody (165). As judged by several criteria including flotation in Optiprep gradients of TX-100-insoluble fractions obtained from apical carrier vesicles, annexin A13b clearly is a raft-associated protein, and it was proposed to function by binding to apical rafts that bud off the *trans*-Golgi network (165). Recently, it was also shown that annexin A13b participates in mediating the apical membrane targeting of the ubiquitin ligase Nedd4. The enzyme contains a C2 domain and associates with lipid rafts in a Ca^{2+} -dependent manner, most likely through an interaction of this Ca^{2+} -sensitive C2 domain with the raft-associating annexin A13b (231). Annexin A13a differs from the 13b variant by a deletion of 41 amino acid residues from the unique NH_2 -terminal domain and a somewhat broader intracellular distribution as it is also found at the basolateral membrane. Interestingly, its association with lipid rafts differs between the apical and the basolateral compartment of polarized epithelial cells with only the latter requiring Ca^{2+} . Moreover, and in contrast to annexin A13b, the 13a variant appears to be involved in the basolateral transport route (172). Thus different annexins seem to participate to differing extents in the organization of membrane domains (e.g., lipid rafts) with their association with these domains and thus their role in the process being regulated by changes in cytosol conditions (Ca^{2+} , pH?) and membrane lipid content (cholesterol, acidic phospholipids).

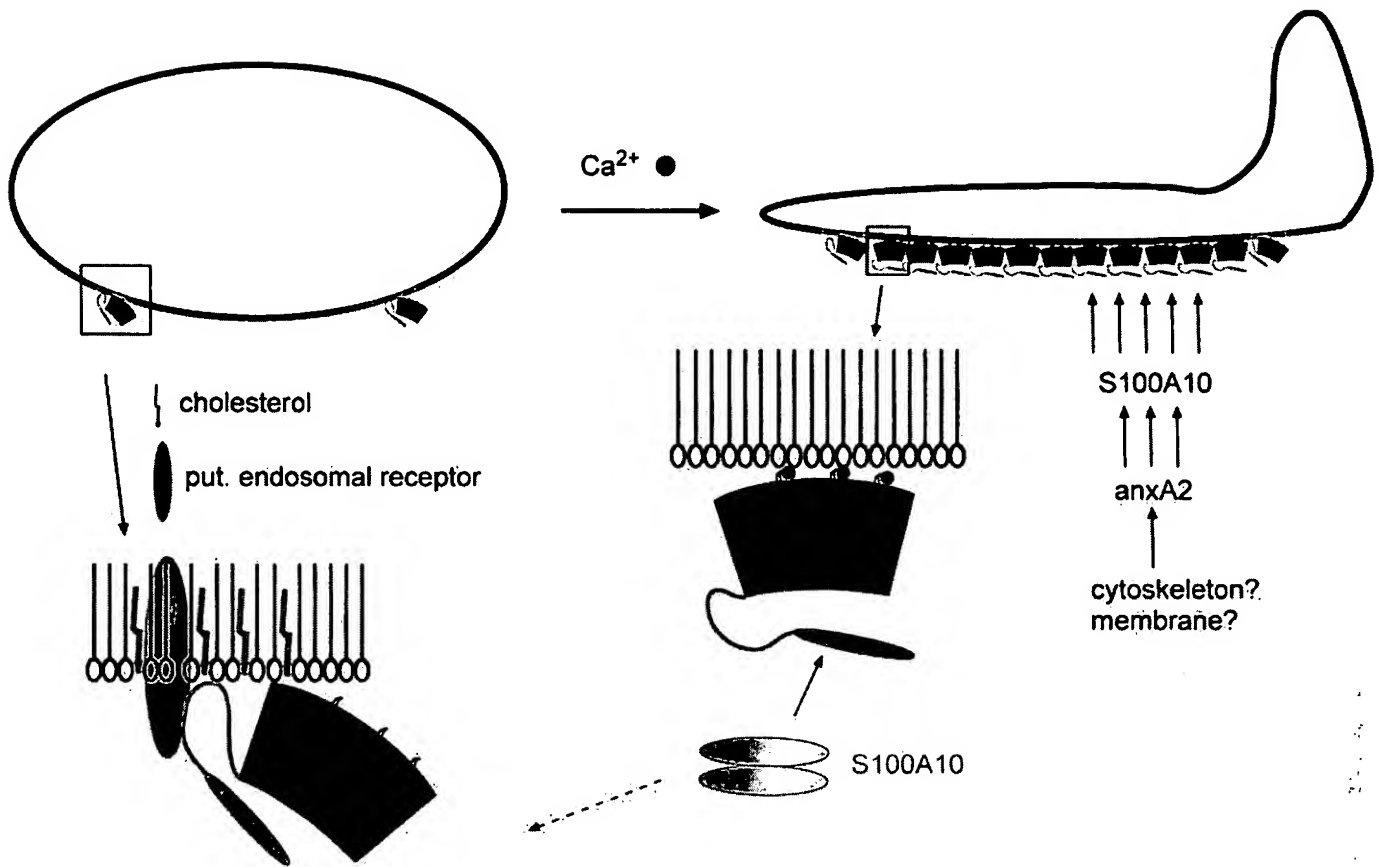


FIG. 6. Ca^{2+} -independent and Ca^{2+} -dependent interactions of annexin A2 with endosomal membranes. In the absence of Ca^{2+} , annexin A2 (blue) binds to endosomes in a manner requiring membrane cholesterol and a unique sequence in the NH_2 -terminal domain of the protein. The amount of endosome-associated annexin A2 increases significantly in the presence of Ca^{2+} , with the membrane binding now being driven by the canonical and Ca^{2+} -dependent membrane interaction. A high-density packing of annexin A2 molecules could be envisaged, which is in line with cryoelectron microscopy studies of annexin A2 bound to artificial bilayers (167). Such annexin A2 assemblies could stabilize certain membrane domains/organizations, and after S100A10-dependent formation of the annexin A2-S100A10 heterotetramer, these domains could be linked to a second membrane or cytoskeleton surface.

B. Annexins and Ion Channels

In section 11B we discussed the Ca^{2+} -dependent and Ca^{2+} -independent interactions between annexins and phospholipid membranes. In the former case, such interactions depend largely on the conserved annexin core and the Ca^{2+} -binding sites therein, and in both cases a degree of reversibility is a characteristic of membrane binding for most members of the annexin family. A major challenge in the annexin field has been to understand what annexins do once membrane bound. For some annexins there is increasingly persuasive evidence for roles in vesicle trafficking and/or membrane organization, but for most annexins, the functional significance of reversible membrane binding remains elusive. However, one intriguing possibility to have emerged in the last decade is that membrane-associated annexins might function either as ion channels and/or ion channel regulators. If correct, such activities would point to annexins as both effectors

and regulators of ion fluxes and place these proteins as key mediators in the control of cellular Ca^{2+} homeostasis.

1. Regulation of ion channel activity by annexins

The first study to implicate any annexin in the regulation of ion flow demonstrated that purified annexin A6 increased the mean open time and opening frequency of the sarcoplasmic reticulum ryanodine-sensitive Ca^{2+} channel (67). This modulatory activity appeared to be specific because there was no effect of annexin A6 on sarcoplasmic K^+ or Cl^- currents. These findings suggested that annexin A6 might have a role in the regulation of intracellular Ca^{2+} signaling in cardiomyocytes and skeletal muscle cells, cell types in which annexin A6 is known to be expressed at high levels. However, annexin A6 only exhibited this property when added to the luminal side of the membrane, and annexin A6 is generally considered to be a cytosolic protein. The problem of under-

standing the effect of annexin A6 in this system was further compounded by the subsequent observation that purified annexin A6 exhibits Ca^{2+} channel activity in artificial phospholipid membranes (19). This raises the possibility that changes in the Ca^{2+} permeability observed in sarcoplasmic reticulum membranes attributed to the ryanodine receptor may have been partly or wholly due to annexin A6 itself. Another study, this time demonstrating a cytosolic effect of annexin A6, showed that the introduction of a neutralizing antibody to annexin A6 led to an increase in K^+ currents in dorsal root ganglia (DRG) and spinal cord neurons, and to an increase in Ca^{2+} currents in DRG (211). A model in which displacement of annexin A6 from intracellular membranes leads to amplification of the Ca^{2+} signal is consistent with work showing that elevation of cytosolic Ca^{2+} induced by hydrogen peroxide is associated with translocation of annexin A6 from the cytoplasmic face of the plasma membrane (130). Another study, again supporting a role for annexin A6 in the regulation of Ca^{2+} influx, showed that ectopic expression of annexin A6 in epithelial A431 cells leads to attenuation of Ca^{2+} influx stimulated by EGF (84). A431 cells normally lack annexin A6 and exhibit a sustained elevation of intracellular Ca^{2+} after exposure to EGF. This work showed that whereas Ca^{2+} release from intracellular stores was unaffected by annexin A6, membrane hyperpolarization and consequent Ca^{2+} influx was inhibited. Interestingly, this inhibitory activity was only observed for the larger of the two splice forms of annexin A6, an effect that also directly correlated with splice variant-specific growth suppression in these cells.

Annexins A2 and A4 have also been demonstrated to modulate the activity of ion channels, although in both cases the effects were observed on Cl^- rather than Ca^{2+} channels. Annexin A4 is located at the apical cell plasma membrane in polarized colonic T84 cells, and in electrophysiological experiments it was found that introduction of purified recombinant annexin A4 into T84 cells through the patch electrode led to inhibition of the Ca^{2+} -induced Cl^- current (146). Consistent with this, an antibody to annexin A4 and also an antisense oligonucleotide to annexin A4 mRNA, both reduced the threshold for Cl^- current activation. Activation of the Ca^{2+} -dependent Cl^- conductance occurs in response to mobilization of Ca^{2+} from intracellular stores or, in patched cell experiments, by introduction of calmodulin-dependent protein kinase II (CaMKII). Inhibition of CaMKII using a specific peptide blocked the activation of the Ca^{2+} -dependent Cl^- channel observed with the antibody to annexin A4 (37). Annexin A4 is not believed to activate or inhibit CaMKII, nor to act as a substrate for the kinase, suggesting that it may inhibit the Cl^- channel through a direct protein-protein interaction. Regulation of the Cl^- channel by annexin A4 might also involve inositol 3,4,5,6-tetrakisphosphate [$\text{Ins}(3,4,5,6)\text{P}_4$]. In electrophysiological experiments in

T84 cells, the potency of $\text{Ins}(3,4,5,6)\text{P}_4$ as an inhibitor of the Ca^{2+} -dependent Cl^- channel was doubled in the presence of annexin A4, when annexin A4 was added at a concentration at which it has no inhibitory effect when used alone (339). These observations suggest a function for annexin A4 as part of a complex signaling pathway involving both protein kinases and intracellular Ca^{2+} . The involvement of annexin A2 in Cl^- channel regulation is less well characterized but no less intriguing. A single study reported that introduction of a synthetic peptide corresponding to the NH_2 -terminal domain of annexin A2 into endothelial cells via a patch electrode led to rundown of the osmotic-regulated Cl^- channel (213). In a control experiment, a similar peptide with a single amino acid substitution that eliminated S100A10 binding was shown to be without effect. These results imply that correct assembly of the annexin A2/S100A10 heterotetramer is required for the integrity of this current. The reason for this is unclear, but in many cells the annexin A2/S100A10 complex is stably associated with the submembraneous actin cytoskeleton, which in turn may have a functional interface with volume-sensitive Cl^- channels (VSCC). Indeed, specialized membrane-cytoskeleton compartments rich in cholesterol, caveolin, and ERM (ezrin, radixin, moesin) proteins are implicated in VSCC function and also contain annexin A2 (316). Furthermore, chicken DT40 cells containing a targeted disruption of the annexin A2 gene exhibit a more hyperpolarized resting membrane potential, consistent with dysregulation of chloride homeostasis (163). Collectively, these studies suggest that whereas annexin A4 may be involved in a direct molecular interplay with the Ca^{2+} -dependent Cl^- channel, the effect of annexin A2 on VSCCs might be an indirect consequence of a possible role in the regulation of membrane cytoskeleton interactions.

2. Annexin-dependent ion fluxes

The problem of defining specific functions for individual annexins is a recurring theme in annexin research. When annexin A1 (lipocortin) was first described as an inhibitor of phospholipase A_2 (PLA_2), this was widely accepted as an explanation for the apparent anti-inflammatory activity of annexin A1. However, as the family expanded, it rapidly became clear that all annexins can inhibit PLA_2 by Ca^{2+} -dependent sequestration of the phospholipid substrate (59). Although the inhibition of PLA_2 is therefore now believed to be nonspecific and probably nonphysiological, the anti-inflammatory activity of annexin A1 is nevertheless specific to this protein, and recently a more convincing mechanism has emerged to explain its activity (see sect. *ivCI*). A similar history surrounds the idea that annexins might function as ion channels. The first annexin to be shown to have Ca^{2+} channel activity was annexin A7 (233, 252), but this was soon

extended to annexin A5 (253), and in conjunction with X-ray crystallographic studies, most annexins have now been demonstrated to have Ca^{2+} channel activity (19, 29, 134, 232). Just as PLA_2 inhibition by annexins was shown to be the consequence of a shared biochemical property, so it appears that the Ca^{2+} channel activity of annexins may be due to a common structural feature, namely, the central hydrophilic pore in the annexin core (see sect. II A1). However, in contrast to the anti-inflammatory activity of annexin A1, no annexin has ever been shown to exhibit Ca^{2+} channel activity in a living cell. Moreover, the general view of annexins as peripheral membrane binding proteins presents a conceptual obstacle to the idea that these proteins could function as ion channels. Despite this, the selectivity of the annexin ion channel for Ca^{2+} , together with pharmacological and electrophysiological properties that correspond to those of as yet uncharacterized Ca^{2+} channels in nonexcitable cells, ensures continuing interest in this subject.

To understand how annexins might function as Ca^{2+} channels, it is necessary to examine the way in which annexins interact with phospholipid membranes. In experiments using artificial lipid bilayers, the interaction between annexins and membranes depends on four key variables; these are the phospholipid composition of the bilayer, the concentration of the annexin, the concentration of Ca^{2+} , and the transmembrane voltage (125). For ion channel activity to occur, the annexin must first bind to the membrane, and then some poorly understood gating process must follow that leads to Ca^{2+} flux. Because the first step depends on the availability of free Ca^{2+} , the observation that as Ca^{2+} concentration increases the Ca^{2+} channel activity decreases may appear counterintuitive. However, a Ca^{2+} binding site in the proposed channel makes the current-voltage curve for annexin A5 nonlinear (253), and it is established that annexin A5 becomes more tightly membrane bound at elevated Ca^{2+} levels and that this has the effect of stabilizing the membrane (104, 210). For Ca^{2+} channel activity to occur, membrane destabilization is required. In addition, several annexins display anticooperativity of binding, such that as the protein concentration increases, so membrane binding decreases (125). Annexins also bind to membranes with higher affinity at increasingly negative resting membrane potentials, although in the absence of Ca^{2+} the membrane potential negativity required for annexin binding extends well out of the accepted physiological range. However, the requirement for a negative potential difference is reduced as the free Ca^{2+} concentration increases. In applying a reductionist approach to the analysis of annexin ion channel activity and membrane binding, one should keep in mind that some of these variables may have little influence *in vivo*, whereas other factors (such as other divalent cations, posttranslational modifications, and co-factors) could well come into play. Also, when one con-

siders the issue of annexin-specific channel activity, it is important to note that with regard to these four variables annexins behave quite differently. For example, whereas high free Ca^{2+} concentration leads to tight binding of annexin A5 to membranes, this is not the case for either annexins A6 or A7. Thus, under conditions of high free Ca^{2+} , annexins A6 and A7 display more Ca^{2+} channel activity than annexin A5 (125).

Recent studies have added a fifth key variable, namely, pH, to the parameters that govern the interactions between annexins and phospholipid membranes (see sect. II B). Several investigators have reported that mildly acidic pH favors the Ca^{2+} -independent binding of annexins to phospholipid membranes (158, 168), and spin labeling experiments using derivatized recombinant *Hydra* annexin B12 showed that protonation led to gross changes in the structure of the protein, proposed to correspond to the assembly of transmembrane α -helices which form a new membrane-spanning molecule with a central hydrophilic pore (168) (Fig. 4). Subsequent experiments showed that at pH 5.0 and below, annexins A5 and B12 both label with a photoactivatable agent that partitions into the hydrophobic domain of a lipid bilayer and that both proteins form ion channels at low pH but not at neutral pH (138). Further studies supporting the idea that annexin B12 forms a transmembrane structure showed that when added to the opposite side of the bilayer to the purified annexin, pronase caused an increase to preannexin values in the conductance of the probe nonactin (289). The conclusion of these carefully controlled studies is that the pronase effect can only be explained if annexin B12 forms a structure that spans the lipid bilayer. The key points to emerge from these studies is that the pH-dependent insertion of annexins into lipid bilayers is reversible and that it is inhibited by free Ca^{2+} . The reversibility is significant because it suggests that a dynamic equilibrium may exist between the soluble cytosolic annexin, the peripherally membrane-bound form, and the membrane-inserted form. At neutral pH it can be argued that the equilibrium is heavily biased away from the membrane-inserted form, which is consistent with reports that channel activity for annexins, despite being widely reported at neutral pH, is actually exceedingly rare (125, 138). Despite the topographical appeal of this model, there is resistance to the idea that the tightly folded α -helical annexin core could unfold and insert into membranes. Nevertheless, molecular rearrangements of this sort are not unprecedented because members of the Bcl family of pro- and antiapoptotic proteins undergo similar pH-dependent insertion into acidic phospholipid bilayers (198, 268, 271). A second problem concerns the requirement for a pH < 6.0 to induce annexin membrane insertion, given that in healthy living cells the intracellular pH probably never falls below 6.5.

In considering these problems there is a need to

interpret the findings of *in vitro* studies in terms of how annexins might function as ion channels in living cells. Thus, if annexin A5 does function as a Ca^{2+} channel, the expectation might be that such an activity would be favored under conditions of intracellular acidification and membrane hyperpolarization. In B lymphocytes, exposure to physiological concentrations of peroxide leads to a Ca^{2+} influx accompanied by membrane hyperpolarization and intracellular acidification from pH 7.3 to pH 7.0. Other Ca^{2+} mobilizing agonists such as thapsigargin or antibody to the B cell receptor do not change membrane polarity or cytosolic pH. Targeted disruption of the annexin A5 gene in B cells leads to loss of the Ca^{2+} influx component of the peroxide response, but Ca^{2+} responses to other agonists are unaffected in such cells (163). Significantly, this study also showed that in experiments using a photoactivatable agent to label annexin A5 in synthetic lipid bilayers, exposure of the protein to peroxide led to membrane insertion independently of any requirement for acidification. These results support a role for annexin A5 either as a Ca^{2+} channel or as an essential signaling intermediate in a Ca^{2+} influx pathway. Further cellular evidence for a Ca^{2+} channel role for annexin A5 comes from studies on mineralizing chondrocytes (157). The deposition of new bone by chondrocytes is mediated by matrix vesicles, PS-rich structures with a proteinaceous core that binds Ca^{2+} upon entry, to form calcium phosphate crystals. The Ca^{2+} influx channels in matrix vesicles share many properties with annexin A5 Ca^{2+} channels *in vitro*. Thus both are blocked by Zn^{2+} , activated by ATP, and inhibited by GTP, and maximal Ca^{2+} influx is observed when annexin A5 is associated Ca^{2+} -independently with the vesicles (4). These studies, together with those in B cells, provide evidence that annexin A5 may indeed function as a Ca^{2+} channel under certain conditions. However, definitive proof may be difficult to obtain, and even if this is eventually established, the question of whether or not annexin A5 functions as a peripherally bound or integral membrane protein may take longer to answer.

C. Extracellular Annexin Activities

Although annexins *per se* are intracellular proteins, i.e., they localize to the cytoplasm and/or intracellular organelles and lack signal sequences guiding them to the canonical secretory pathway, a number of properties have been attributed to extracellular annexins. Although it is still a mystery whether and to what extent regulated secretion of annexins can occur, the recent description of cell or extracellular matrix receptors for different annexins supports the physiological (or pathophysiological) meaning of such extracellular properties. The more recent findings along these lines will be summarized below. For a detailed and more complete account of extracellular

annexin activities described in the past, the reader is referred to the review by Raynal and Pollard (244).

1. Annexin A1 and the control of inflammatory responses

Annexin A1 (lipocortin I) has long been suggested to function as a cellular mediator of anti-inflammatory glucocorticoids since its expression and secretion in several cell types is induced by glucocorticoids (see, for example, Refs. 46, 228, 308) and since exogenously administered protein exhibits anti-inflammatory activities in several animal models of inflammation (for reviews, see Refs. 85, 86, 260). Although this effect has initially been attributed to the capability of annexin A1 to inhibit PLA_2 and thus the production of eicosanoids, it has become clear more recently that the anti-inflammatory activity of the protein is most likely due to interference with granulocyte recruitment, migration, and/or activation at sites of inflammation (for reviews, see Refs. 105, 221, 222).

Inflammatory processes are characterized by a localized emigration of neutrophils and other leukocytes from the blood into the inflamed tissue. This process crucially depends on strictly regulated interactions between the leukocytes and the endothelial lining of the vessels ranging from leukocyte rolling on the endothelium to firm adhesion of the blood cells and finally their transendothelial migration (for reviews, see Refs. 176, 298). The transition from rolling to firm adhesion of neutrophils requires their activation by soluble or surface-bound mediators like chemokines and other chemoattractants that also provide a gradient along which neutrophils navigate toward the site of inflammation. Glucocorticoids delay this extravasation of leukocytes, and several lines of evidence have implicated annexin A1 as a central mediator of this glucocorticoid effect. In neutrophils adhering to activated endothelium, annexin A1 is mobilized and externalized through an as yet unknown mechanism resulting in a downregulation of neutrophil transmigration (224). Most likely this is due to an inhibitory effect on transmigration of the released annexin A1, which has been described *in vitro* and *in vivo* with exogenously applied protein as well as peptides derived from the unique NH_2 -terminal domain of annexin A1 (for reviews, see Refs. 105, 221, 222). Such NH_2 -terminal peptides typically covering residues 1–25 of the annexin A1 sequence in their NH_2 -terminally acetylated form (Ac1–25), as well as the entire molecule, are also capable of restricting leukocyte migration and thus tissue damage in animal models of splanchnic artery occlusion/reperfusion and myocardial ischemia/reperfusion injury (56, 58). Thus *in vitro* systems as well as a number of animal models have proven the antimigratory effect of annexin A1 (and the unique NH_2 -terminal peptides) on leukocyte extravasation, and the protective influence of the protein/peptides in several pathophysiological situa-

tions has sparked interest in their pharmacological potential.

Given these well-established effects of annexin A1 on neutrophil extravasation, two questions arise. First, what is the mechanistic basis of the effect, and second, can endogenous annexin A1 function as a modulator of leukocyte extravasation, e.g., by downregulating inflammatory responses to prevent chronic inflammation? To explain the antimigratory effects, a direct action of extracellular annexin A1 on leukocytes had long been postulated and indeed been proven in a number of studies. Among other things, the NH₂-terminal annexin A1 peptide Ac1-25 was shown to affect directly a number of neutrophil functions, and preincubation of neutrophils with the annexin A1 peptide resulted in decreased migration of these cells through untreated endothelial monolayers (226, 331). Proteinaceous binding sites for annexin A1 have been shown to exist on human monocytes and neutrophils as well as on monocytic U937 cells, with bound annexin A1 in the latter case being colocalized and coimmunoprecipitated with $\alpha_4\beta_1$ -integrins (75, 291). Compelling evidence has been obtained recently for a specific binding of annexin A1 (and its NH₂-terminal peptides) to the formyl peptide receptor (FPR) on neutrophils. FPR is a heptahelical, G protein-coupled receptor recognized by bacterial peptides of the prototype formyl-Met-Leu-Phe (fMLP) which are thought to provide the chemoattractant gradient for guiding neutrophils toward the site of bacterial infection. When employed in an *in vitro* transmigration model, antagonistic fMLP peptides were shown to reverse the inhibitory effect of annexin A1 (and its NH₂-terminal peptide) on neutrophil transmigration, and ectopically expressed FPR was specifically triggered by the annexin A1 peptides (331). As the annexin A1 peptides can also desensitize the FPR on neutrophils toward fMLP challenge, it appears that their inhibitory action on neutrophil extravasation is based on their binding to and activation/desensitization of the FPR. Such a role of the FPR in mediating the anti-inflammatory effect of annexin A1 has been corroborated by *in vivo* experiments employing FPR knockout mice (225). FPR activation by annexin A1 peptides can occur also in nonmyeloid cells leading, e.g., in human lung A549 cells, to the induction of acute phase protein expression, thus arguing for a more widespread role of the annexin A1-FPR interaction (U. Rescher, A. Danielczyk, A. Markoff, and V. Gerke, unpublished observations).

Although this provides a mechanistic explanation for the pharmacological action of exogenously applied annexin A1 (or NH₂-terminal annexin A1 peptides), it is not clear whether such scenarios could also hold true for endogenously released annexin A1. Regulated externalization of annexin A1 has been described for endothelium-adherent leukocytes (224, 291), but it is not clear whether the amounts released are sufficient to trigger the

FPR. Moreover, with the mechanism of secretion unknown, it remains possible that the extracellular annexin A1 stems at least in part from lysed cells. Thus we are in need of identifying in molecular terms a system promoting regulated annexin A1 release. The protein does not follow the classical secretory pathway because its release is not inhibited by brefeldin A, monensin, or nocodazole (228). However, in neutrophils, some annexin A1 colocalizes with gelatinase in gelatinase storage granules, and this appears to be released to the cell surface upon adhesion of the neutrophils to endothelial monolayers (223). Nonetheless, it is not clear how the protein reaches the lumen of the granules and whether this relates to the Ca²⁺-dependent secretion of annexin A1 in activated human neutrophils, which was described recently in a proteomic approach (25). Whatever model is favored, for active secretion to occur the transport of annexin A1 across the bilayer (that of the plasma membrane or of internal membranes of secretory organelles) is required, and it is not yet clear how that can happen. In this context, the pH-induced conformational change allowing annexin A1 to insert into the bilayer (see above) might be hypothesized, but it remains to be shown whether such insertion (possibly followed by a release at the other side of the bilayer) can occur under physiological conditions met in cells.

2. Extracellular activities of other annexins

This section focuses on recent developments relating to extracellular activities of annexins A2 and A5. Extracellular annexin A2 has been described as a surface-bound receptor for a number of different molecules, indicating that it might act as a more general surface anchor and not as a specific receptor of a given ligand. Best studied is probably the interaction of elements of the plasmin/plasminogen activator system with annexin A2 present on the surface of endothelial cells. Annexin A2 binds both plasminogen and the tissue plasminogen activator (tPA), with the former interaction being inhibited by the atherogenic lipoprotein A and the latter being blocked by homocysteine (for review, see Ref. 114). The tPA binding site on annexin A2 has been mapped to the NH₂-terminal domain and encompasses residues 7-12. This sequence contains an accessible cysteine residue at position 8 (142), and it is this cysteine that is derivatized by homocysteine leading to the reduction in tPA binding (112). Thus annexin A2 present on the surface of endothelial cells could play a role in fibrinolytic surveillance by anchoring key components of the fibrinolytic cascade. Increased homocysteine levels would interfere with this annexin A2 action, thus providing a possible explanation for a link between increased homocysteine levels and the risk of atherogenesis (113). The antithrombogenic action of annexin A2 could also be directly associated with the

hemorrhagic disorder in patients suffering from acute promyelocytic leukemia, as will be discussed below. However, we have to take into account that annexin A2 is probably not the only cell surface receptor for tPA on the endothelium (90). Moreover, in addition to binding to tPA and stimulating the conversion of plasminogen to plasmin, annexin A2 (in complex with its S100A10 ligand) can also inhibit the plasmin-mediated lysis of fibrin polymers and can inhibit plasmin activity by stimulating its autolytic digestion (41, 42, 82). Thus the relation between extracellular annexin A2 and the regulation of thrombogenesis is likely to be complex.

Annexin A2 present on the surface of endothelial cells has also been described to represent the binding site for β_2 -glycoprotein I, a phospholipid-binding protein from plasma known as an autoantigen in the antiphospholipid antibody syndrome. This interaction indicates that the association of β_2 -glycoprotein I with endothelial cells is not mediated directly by phospholipids but depends on annexin A2 (186). Other ligands for cell-surface bound annexin A2 are procathepsin B (on human breast carcinoma and glioma cells) (187) and a vitamin D analog that appears to use annexin A2 as a receptor on rat osteoblast-like cells with the interaction being inhibited by Ca^{2+} (12, 13). It is not clear whether and how this relates to the finding that gene expression of annexin A2 itself is up-regulated by 1,25-dihydroxyvitamin D_3 and that extracellular annexin A2 stimulates the proliferation of osteoclast precursors by activating T cells to secrete granulocyte-macrophage colony stimulating factor (194). However, as already discussed above for annexin A1, it remains to be shown whether, how, and to what extent annexin A2 is actively exported from, for example, endothelial cells and whether such export can be regulated under physiological conditions. Moreover, for annexin A2 acting as a cell surface receptor, it requires anchoring on or in the cell membrane, the mechanism for which has so far not been elucidated.

Several functions have also been proposed for extracellular annexin A5. It was originally described as an anticoagulant protein, and this activity most likely depends on its Ca^{2+} -regulated binding to anionic phospholipids, possibly those exposed on the surface of activated platelets or endothelial cells. This binding could interfere with the accessibility of such sites for coagulation factors, thereby preventing their local accumulation/activation (for review, see Ref. 244). More recently, antibody-mediated inhibition of an anticoagulant property of annexin A5 has been proposed to occur in recurrent pregnancy losses observed in patients with antiphospholipid syndrome (for review, see Ref. 240). As discussed in detail in section v, annexin A5 binds to the apical surface of placental syncytiotrophoblasts and by shielding these coagulation-promoting surfaces could be important for the maintenance of blood flow through the placenta. Anti-annexin A5 anti-

bodies that are found in patients with antiphospholipid syndrome (and also in the sera of patients suffering from systemic lupus erythematosus, Ref. 266) decrease the ability of annexin A5 to form a shield on the trophoblast surface and could thus cause placental thrombosis (240, 241, 243, 333). In vitro annexin A5 was also shown to interact with the NH_2 -terminal (extracellular) domain of polycystin 1, the major protein affected in autosomal dominant polycystic kidney disease, although the in vivo relevance of this interaction remains to be established (A. Markoff, N. Bogdanova, U. Rescher, F. Qian, B. Dworniczak, G. Germino, Y. Horst, and V. Gerke, unpublished observations). Moreover, the protein is capable of binding to components of the extracellular matrix, in particular types II and X collagens. Such binding could relate to the finding that annexin A5 (as a Ca^{2+} channel, see above) affects the Ca^{2+} uptake in chondrocyte-derived matrix vesicles in a manner depending on the binding to collagens types II and X (for review, see Ref. 329). The annexin A5 knock-out models underway should answer the question whether annexin A5 has a crucial role to play in such processes.

D. Annexin Transgenesis and Targeted Gene Disruption

Modulation of gene expression by either transgenic expression or targeted gene disruption has been used in many species to gain insight into protein function. Given the historical difficulty of assigning functions to annexins, it is perhaps surprising that such studies appeared relatively recently in the annexin literature. This might have been partly due to the expectation that annexins would be discovered in yeast, in which genetic manipulation is facile, or could reflect an unwillingness by funding agencies to support what are seen to be risky projects. Despite the absence of annexins in yeast, the presence of annexins in roundworms and insects leads one to hope that eventually mutants will be established in these organisms that might give clues to function. Indeed, the first genetic experiment involving annexins reported that disruption of annexin C1 in *Dictyostelium* did not lead to any adverse effects when cells were cultured under normal conditions (71). However, the cells were significantly disadvantaged when cultured in low external Ca^{2+} , exhibiting defects in growth, motility, and chemotaxis, observations that support a role for annexin C1 either as a Ca^{2+} mediator or as a regulator of Ca^{2+} homeostasis (72). The only transgenic studies reported to date describe the effects of overexpression of annexin A6 targeted to cardiomyocytes. These animals display left ventricular dilation and cardiomyopathy and die of heart failure at a relatively young age. Studies on isolated cardiomyocytes from young animals revealed that overexpression of annexin A6 was associ-

ated with a lower resting level of cytosolic Ca^{2+} and smaller Ca^{2+} spikes associated with attenuation of contractility when the cardiomyocytes were electronically paced (109). These results correlate inversely with studies on annexin A6 expression in failing human hearts (described in sect. vA2). Perhaps unexpectedly in view of these results, annexin A6 null mutant mice are healthy and fertile and fail to exhibit any cardiovascular defects with regard to heart rate, blood pressure, and circulatory collapse in response to endotoxic shock (121). However, in certain respects, the mouse is not an ideal model for human cardiovascular function, partly because the mouse heart beats almost maximally so that any "enhancement" in cardiomyocyte contractility would be difficult to detect. Indeed, in isolated cardiomyocytes from annexin A6 knock-out mice in which contraction rate can be regulated, significantly increased mechanical properties linked to altered Ca^{2+} handling are observed, when compared with cells from wild-type littermates (G. Song, S. E. Moss, and M. Duchon, unpublished observations).

The lack of an overt phenotype in annexin A6 knock-out mice contrasts with studies on annexin A7. Targeted disruption of annexin A7 in mice led to embryonic lethality at *day 10* due to cerebral hemorrhage. Mice heterozygous for the mutation are viable and fertile but have defects in insulin secretion, although the insulin content of islet cells is considerably higher than in wild-type mice (299). Investigation of this phenotype revealed that expression of the inositol 1,4,5-trisphosphate (InsP_3) receptor was also reduced, leading to the failure of InsP_3 to release intracellular calcium. Although this observation explains the phenotype and establishes a potential link between annexin A7 and Ca^{2+} signaling, it is not clear why a partial reduction in annexin A7 expression levels should be accompanied by a parallel loss of InsP_3 receptor expression. In a separate annexin A7 gene knock-out project, the null mutant mice were found to be healthy and viable and no different from control mice with regard to glucose-stimulated insulin secretion, although cardiomyocytes isolated from these mice showed alterations in their frequency-induced shortening (122). However, as observed with annexin A6 knock-out mice, cardiomyocytes lacking annexin A7 manifested disturbances in power-contraction frequency. Although there are other examples of gene disruption studies in which different groups reported distinct phenotypes, and in the case of annexin A7 there were differences in design of targeting constructs and disruption sites, reconciliation of the embryonic lethality and minimal phenotype reported by these two groups represents a considerable challenge. In other ongoing studies, mice containing a targeted disruption of the annexin A1 gene are reported to be viable and healthy (R. Flower, personal communication), and matings between mice heterozygous for a disrupting mutation of the annexin A5 gene yield viable pups (K. von der Mark and E.

Pöschl, personal communication). Although systematic analysis of annexin null mutant mice is therefore still at an early stage, these preliminary observations exemplify not only the potential value of gene knockout in exploring annexin function, but also the need to keep an open mind with regard to the interpretation of phenotype.

V. ANNEXINS AND HUMAN DISEASE

A. Disorders of the Heart and Circulation

1. Annexins and cardiovascular biology

As yet, no human diseases have been described in which a mutation in an annexin gene is a primary cause. However, there is evidence that through changes in expression, properties, or localization, annexins may contribute to the pathophysiology of disease phenotypes. The most striking examples of these secondary effects have been termed "annexinopathies" (239) and are characterized by dysregulation of what may be the normal antithrombotic properties of extracellular annexins. As discussed earlier, annexin A2 on the surface of vascular endothelial cells can act as a receptor for tPA, so its presence would favor a thrombolytic environment and might therefore make a positive contribution to the overall health of the vasculature. Conversely, changes in endothelial cell behavior leading to reduced cell surface expression of annexin A2 or metabolic changes that chemically modify annexin A2 could be hypothesized to lead to predisposition to cardiovascular disease. Of numerous risk factors implicated in atherothrombotic vascular disease, elevated plasma homocysteine is of particular relevance. Homocysteine is a metabolic derivative of dietary methionine and was shown to incorporate into the NH_2 terminus of annexin A2 replacing Cys-8, a key residue in mediating the tPA processive activity of annexin A2 (113). In this study, substitution of Cys-8 with homocysteine led to a ~65% loss in tPA binding capacity, consistent with the development of reduced thromboresistance in homocysteinemic individuals. A second risk factor with a well-established link to cardiovascular disease is oxidative stress. In a recent study, annexin A2 was identified as a major cellular target for glutathiolation in response to oxidative stress induced by hydrogen peroxide or $\text{TNF-}\alpha$. Interestingly, the reactive cysteine identified as the target for glutathione in this study was again Cys-8 in the annexin A2 NH_2 terminus (304). A third risk factor shown in epidemiological studies to be linked to cardiovascular disease is alcohol consumption, although the effect of moderate intake is protective rather than deleterious. One recent study reported that vascular endothelial cells cultured in the presence of low concentrations of ethanol exhibited a doubling of cell surface fibrinolytic activity

that correlated with a sustained increase in annexin A2 mRNA and protein (306). Although these studies do not prove that annexin A2 is directly involved in the development of or susceptibility to cardiovascular disease, they support the idea that metabolic changes known to influence risk could be mediated at least in part by chemical modifications in and transcriptional regulation of annexin A2.

2. Heart disease

Because of the importance of Ca^{2+} homeostasis in the heart, and the abundance of annexins A2, A5, and A6 in cardiomyocytes and the supporting cellular infrastructure, there is considerable interest in elucidating the roles of cardiac annexins. Immunocytochemical studies identified annexins A5 and A6 in both myocytes and nonmyocytes in a variety of species, and most of these reported a concentration of annexin A5 with the sarcolemma and Z line in cardiomyocytes (141, 183, 191, 317, 332) and a preferential localization of annexin A6 with the sarcolemma and intercalated disks (184, 191, 317). In addition, annexin A5 has been reported to be localized to the nucleus and nuclear membrane in neonatal differentiating myocytes and becomes associated with the sarcolemma only in terminally differentiated adult cells (183). In a parallel study, annexin A6 was found colocalized with uncharacterized subcellular structures in neonatal myocytes and was only associated with the sarcolemma in adult cells (184). Although the function of cardiac annexin A5 is not known, the benzothiazepine derivative K201, which blocks the Ca^{2+} channel activity of annexin A5 in vitro (150), has been shown to protect the myocardium against the cytotoxic effects of Ca^{2+} associated with ischemia/reperfusion injury (110).

Several other lines of evidence suggest that annexins have important functions in the heart. The most striking of these is the demonstration that cardiomyocyte-specific overexpression of annexin A6 in transgenic mice leads to hypertrophy and heart failure (109) (see also sect. IV D). This study prompted several investigations into annexin expression in heart disease, both in a variety of animal models and also in humans with end-stage heart failure. The picture that emerges from these studies is that the expression levels of annexins A2, A5, and A6 are largely unaffected during ventricular hypertrophy (141), but that during end-stage heart failure the levels of annexin A6 fall in cardiomyocytes whereas those of annexins A2 and A5 rise (292). Other investigators reported similar rises in annexins A2 and A5 during heart failure, but restricted to nonmuscle cells (18), and also elevation of annexin A6 in interstitial tissue (317). The significance of these changes is not clear, but given that overexpression of annexin A6 reduces the contractility of cardiomyocytes (109) and that the opposite effect is observed in annexin A6 null mutant

mice (Song et al., unpublished observations), it is possible that downregulation of annexin A6 during heart failure is a form of molecular compensation that favors improved cardiomyocyte function.

3. Annexins as anticoagulants

As discussed in section VA1, there is growing evidence that annexin A2 has an antithrombotic role at the endothelial cell surface. More direct evidence for the involvement of annexin A2 in disease pathology emerged from studies on leukemic cells from patients with acute promyelocytic leukemia (APL). Patients with APL exhibit an increased tendency to hemorrhagic diathesis and respond well to treatment with all-*trans*-retinoic acid. APL leukocytes were found to strongly overexpress annexin A2 at the cell surface and also to stimulate the generation of plasmin from tPA twice as efficiently as other leukemic cells (195). Plasmin generation was blocked by anti-annexin A2 antibodies and could be induced in non-APL cells by ectopic expression of annexin A2. Moreover, exposure of APL cells to all-*trans*-retinoic acid led to a marked reduction in annexin A2 mRNA and protein which correlated with diminished tPA binding. This study provides the clearest evidence so far for any member of the annexin family having a direct role in the pathophysiology of a human disease.

Like annexin A2, annexin A5 has also been suggested to have an antithrombotic role that becomes compromised in disease. However, whereas annexin A2 appears to function as an intermediary in the fibrinolytic cascade, annexin A5 has been proposed to have a more direct role, by forming a molecular shield that insulates the apical surfaces of placental villi from the activities of circulating coagulant proteins. Anticoagulant activity is a feature of all Ca^{2+} binding annexins and can be explained by simple Ca^{2+} -dependent sequestration of the phospholipid matrix with which procoagulant factors interact. In this respect, annexins behave in exactly the same way as when first described as inhibitors of PLA_2 , since the enzyme also requires both Ca^{2+} and phospholipid as cofactor and substrate, respectively. Although this type of anticoagulant activity and PLA_2 inhibition have long been viewed as purely in vitro properties of annexins, there is now evidence that the anticoagulant activity of annexin A5 might be of biological importance in the recurrent pregnancy losses associated with antiphospholipid syndrome (240). A diagnostic observation in patients with antiphospholipid syndrome is the presence in the serum of antibodies against a range of proteins or phospholipids, including annexin A5, prothrombin, cardiolipin, β_2 -glycoprotein-I, and phosphatidylethanolamine (78, 314), and a number of studies suggest that displacement of the annexin A5 shield by anti-annexin A5 antibodies is causative in the generation of a thrombogenic environment and consequent fetal loss. For example, displacement of annexin A5

from the syncytiotrophoblast surface with either specific antisera or Ca^{2+} chelator (242) leads to accelerated coagulation of plasma, and in a mouse model, infusion of anti-annexin A5 antibodies led to placental infarction and pregnancy wastage (333). However, not all investigators take the same view. Several clinical studies failed to detect either anti-annexin A5 antibodies (278) or any changes in expression or localization of annexin A5 (166) in women with pregnancy loss associated with antiphospholipid syndrome. Another study found no evidence that displacement of annexin A5 using antiphospholipid antibodies increased the thrombogenicity of the cell surface (21). If annexin A5 really does have a protective function in the placenta as an anticoagulant, the mechanism of its activity is likely to be considerably more complex than proposed in current models, suggesting that the protein forms an antithrombotic shield in two-dimensional crystalline arrays on the exposed phospholipid surface.

B. Annexins and Physiological Stress

Physiological stress occurs at the cellular level in many disease states and is typically associated with the activation of certain signaling pathways, changes in cell morphology and activity, and modulation of gene expression. Many of these changes can be induced in normal cells by using osmotic, temperature, and oxidative shock, and new research suggests that members of the annexin family may be involved in the cellular response to stress. Annexin A1 was reported to have chaperone activity in vitro experiments in which the purified protein was demonstrated to protect the enzymes citrate synthase and glutamate dehydrogenase from heat inactivation (155). Furthermore, heat shock, hydrogen peroxide, and sodium arsenite were all demonstrated to induce expression of annexin A1 and also translocation of the protein from the cytosol to the nucleus in A549 and HeLa cells (250). The same set of agonists also activated the annexin A1 gene promoter in experiments using a reporter gene. Other annexins have also been shown to be regulated by cytotoxic stress. For example, annexin A4 was shown to be induced in human non-small-cell lung carcinoma cells by the antimitotic drug paclitaxel and to concentrate in the nuclei of stressed cells (117). The correlation between annexin translocation to the nucleus and cellular stress extends to annexin A5, which exhibits the same behavior in primary cultures of vascular endothelial cells grown under conditions of mild hyperoxidative stress (S. M. Sacre and S. E. Moss, unpublished observations). Annexin A5 has also been identified in a screen for proteins induced by hypoxic stress in cultured human cervical epithelial cells (65). Annexin A2 was also found to be induced by hypoxia in this study and by hyperoxidative stress in a model of renal cell carcinoma (307). Thus, at

least in certain cell types, annexins A2 and A5 appear to be upregulated by changes in cellular redox state, irrespective of whether these tend toward a more reducing or a more oxidative environment. The idea that members of the annexin family might have stress-related functions is also supported by studies in plants (100, 162, 310). One of these studies reported that an annexin from *Arabidopsis thaliana* possesses catalase activity and that expression of this annexin restored the ability of a delta oxyR mutant strain of *E. coli* to grow in the presence of peroxide (100). Although such enzyme activity has never been convincingly demonstrated for any animal annexin, there is growing evidence that annexin function may be directly influenced by oxidative and perhaps other stresses. Annexin A2 is glutathiolated in HeLa cells exposed to peroxide (304), annexin A6 has been reported to contribute to the Ca^{2+} signal in macrophages exposed to peroxide by dissociation from the plasma membrane (130), and targeted disruption of the annexin A5 gene in B cells leads to loss of the Ca^{2+} influx response to peroxide (163). Mechanical stress has also been shown to influence annexin behavior. Relaxation of human foreskin fibroblasts grown on collagen matrices led to the enrichment of annexins A2 and A6 with shed membrane vesicles (173), and mild hyperosmolar shock leads to the association of GFP-tagged annexin A2 with mobile endocytic vesicles in rat basophilic leukemia cells (196). Collectively, these studies suggest that physiological stress may be important in the regulation not only of annexin gene expression but also the activities and intracellular localization of at least some annexins.

C. Annexins and Cancer

Annexins A1 and A2 were first discovered as major cellular substrates for phosphorylation on tyrosine by the EGF receptor and the transforming gene product of the Rous sarcoma virus, respectively, implicating these proteins in signaling pathways known to be subverted or involved in cancer. Nevertheless, evidence in support of causative roles for any annexin in the development of cancer or in cell transformation is still mainly circumstantial. Recent studies have reported a correlation between the level of annexin A1 expression in RAW 264.7 macrophages and the cellular responsiveness to lipopolysaccharide (LPS) of components of the mitogen-activated protein (MAP) kinase pathway (1). Cells expressing reduced levels of annexin A1 exhibited potentiation of LPS-induced MAP kinase activation, with elevated annexin A1 expression having the inverse correlation. A similar investigation reported a correlation between annexin A1 expression and mobilization of intracellular Ca^{2+} in MCF-7 breast carcinoma cells (89). In this case, overexpression of annexin A1 led to abrogation of Ca^{2+} release after activation of purinergic or bradykinin receptors, whereas

downregulation of annexin A1 using antisense had the converse effect. Another recent study provided evidence that annexin A1 overexpression in rat 2 fibroblasts leads to direct inhibition of cytosolic PLA₂, which in turn depresses the serum response element of *c-fos* (215). These authors also used deletion mutants to map the functional site in annexin A1 to a domain comprising the first conserved annexin repeat. Collectively, these studies all imply a growth-suppressive role for annexin A1 despite the apparent mechanistic diversity underlying each case. The difficulty comes in reconciling the reported effects of annexin A1 on MAP kinase signaling, *c-fos* induction, and Ca²⁺ mobilization to a single function. Does annexin A1 really regulate signal transduction pathways via interactions with multiple cellular targets, or can these observations be explained by a more general effect of annexin A1 on Ca²⁺ signaling or endocytosis? And, the conclusions of these studies are not supported by work showing that annexin A1 is strongly upregulated in a prostate cancer cell line (324), esophageal cancer (74), a stomach cancer cell line (283), mammary adenocarcinoma (220), and hepatocarcinoma (62). Interestingly, the latter study also showed that annexin A1 is upregulated during normal hepatocyte proliferation after partial hepatectomy and that the proliferative rate of both normal and malignant hepatocytes was attenuated by antisense to annexin A1. These results suggest a link between annexin A1 and cell proliferation, rather than malignant transformation per se, and they suggest that cell growth is associated with elevated rather than reduced levels of annexin A1. It must be hoped that clarification of these apparently contradictory lines of evidence will come from analysis of annexin A1 null mutant mice.

Other annexins have also been linked with cell growth and transformation, frequently in studies using similar experimental designs to those described above for annexin A1. For example, overexpression of annexin A5 in MCF-7 cells leads to inhibition of phorbol ester-mediated activation of the MAP kinase pathway (264), and heterologous expression of annexin A6 at physiological levels in human A431 carcinoma cells leads to inhibition of growth factor-mediated Ca²⁺ influx (84) and slower tumor growth in mice (309). Interestingly, the correlation between expression of annexin A6 and growth suppression extends to melanoma, where a genetic screen identified annexin A6 as a protein downregulated in the transition from a nonmetastatic to a metastatic phenotype (87). A similar result was recently obtained for annexin 2, which appears to be downregulated in prostate cancer (39), and annexin A7, which is expressed at low levels in the most metastatic malignant melanomas (153). Interestingly, a recent study examining loss of heterozygosity (LOH) at the annexin A7 locus in prostate cancer specimens identified this LOH in 35% of the primary prostate tumors. Analysis of annexin A7 expression in prostate

tumor microarrays revealed low levels of expression in metastatic and local recurrences of hormone refractory prostate cancer compared with primary tumors. Moreover, the same study showed that ectopic expression of annexin A7 in two prostate tumor cell lines reduced cell proliferation and that heterozygous annexin A7 knock-out mice (+/−) have a more cancer-prone phenotype (300). A potential role of an annexin as tumor suppressor gene is not without precedent, since Theobald et al. (309) had reported that annexin A6 has tumor suppressor activity in human A 431 cells.

The advent of global gene expression analysis using proteomics and DNA chip technology has also revealed changes in annexin gene expression in numerous cancers and other diseased or stressed cell states (36, 74, 283, 325, 337). There are several searchable web sites reporting these findings, and for one of the most informative, interested readers are referred to <http://genome-www.stanford.edu/> for the results of the NC160 Cancer Microarray Project. Some of the most striking findings here include upregulation of annexin A5 in melanomas and annexin A9 in prostate and colon cancers and downregulation of annexin A5 in leukemias and annexin A1 in prostate cancers. Correlations of this type are intriguing and suggest that changes in the levels of expression of certain annexins may influence patterns of cellular behavior, such as motility, invasiveness, and proliferative rate, without actually initiating the transformation process. As such, annexins may yet prove to have therapeutic potential in the treatment of malignant disease.

VI. CONCLUSION

Annexins comprise a multigene family of Ca²⁺-regulated membrane binding proteins that has evolved into different branches with members expressed widely throughout the animal and plant kingdoms. The conserved Ca²⁺/membrane binding unit present in all annexins (the core domain) can be viewed as a tool invented by nature to peripherally dock proteins to membranes. Such docking can occur at high density, possibly enabling the annexins to organize membranes, e.g., by assembling interacting phospholipids into certain domains, or at low density, under which circumstances annexins may increase membrane permeability. Membrane insertion shown for some annexins to occur in vitro at lower pH might follow such peripheral association, but conditions possibly inducing this in vivo and potential physiological consequences still need to be established. The second principal annexin domain located at the NH₂-terminal end is unique for a given member and specifies or fine-tunes its intracellular (in some cases also extracellular) interactions with certain target membranes or protein ligands. Such interactions may either affect annexin properties or

may be affected by annexin binding. The basis of annexin function as a whole most likely resides in their unique mode of membrane interaction, which in turn can influence a number of membrane-related events, e.g., membrane traffic and the organization of compartment membranes and the plasma membrane. Through their apparent ability to organize, perturb, or integrate into membranes with which they interact, annexins may therefore have roles as effectors, regulators, and mediators of Ca^{2+} signals. Such biological activities have now been shown for some annexins, and further knockout as well as mutant models are under development to decipher the roles of other members of the family. However, we still have a long way to go to understand the precise functions of individual annexins. Redundancy in the family coupled to the problem of dealing with scaffolding or structural functions for many annexins will demand imaginative experimental approaches and rigorous objectivity in the interpretation of the results.

We owe a major debt of thanks to the many annexin workers who provided prepublication information, including Rod Flower, Klaus von der Mark, Ernst Pöschl, Angelika Noegel, Annie Vedeler, and Thorsten Kirsch. We also thank Reg Morgan, Pilar Fernandez, and Harry Haigler as well as members of our laboratories for proofreading the manuscript or parts thereof.

Work in the Moss laboratory is funded by the Wellcome Trust, Medical Research Council, Leukemia Research Fund, Arthritis Research Campaign, British Heart Foundation, Fight for Sight, and Guide Dogs for the Blind. Work in the Gerke laboratory is funded by the Deutsche Forschungsgemeinschaft, the European Union, and the Interdisciplinary Center for Clinical Research of the University of Münster.

Address for reprint requests and other correspondence: V. Gerke, Institute for Medical Biochemistry, ZMBE, Univ. of Münster, von-Esmarch-Str. 56, D-48149 Münster, Germany.

REFERENCES

- ALLDRIDGE LC, HARRIS HJ, PLEVIN R, HANNON R, AND BRYANT, CE. The annexin protein lipocortin 1 regulates the MAPK/ERK pathway. *J Biol Chem* 274: 37620–37628, 1999.
- ALVAREZ-MARTINEZ MT, PORTE F, LIAUTARD JP, AND SRI-WIDADA J. Effects of profilin-annexin I association on some properties of both profilin and annexin I. *Biochim Biophys Acta* 1399: 331–340, 1997.
- ANDERSON RG. The caveolae membrane system. *Annu Rev Biochem* 67: 199–225, 1998.
- ARISPE N, ROJAS E, GENGGE BR, WU LNY, AND WUTHIER RE. Similarity in calcium channel activity of annexin V and matrix vesicles in planar lipid bilayers. *Biophys J* 71: 1764–1775, 1996.
- AUNIS D AND LANGLEY K. Physiological aspects of exocytosis in chromaffin cells of the adrenal medulla. *Acta Physiol Scand* 167: 89–97, 1999.
- AVILA-SAKAR AJ, KRETSINGER RH, AND CREUTZ CE. Membrane-bound 3D structures reveal the intrinsic flexibility of annexin VI. *J Struct Biol* 130: 54–62, 2000.
- AYALA-SANMARTIN J, HENRY J, AND PRADEL L. Cholesterol regulates membrane binding and aggregation by annexin 2 at submicromolar Ca^{2+} concentrations. *Biochim Biophys Acta* 1510: 18–28, 2001.
- BABIYCHUK EB AND DRAEGER A. Annexins in cell membrane dynamics: Ca^{2+} -regulated association of lipid microdomains. *J Cell Biol* 150: 1113–1124, 2000.
- BABIYCHUK EB, PALSTRA RJ, SCHALLER J, KAMPFER U, AND DRAEGER A. Annexin VI participates in the formation of a reversible, membrane cytoskeleton complex in smooth muscle cells. *J Biol Chem* 274: 35191–35195, 1999.
- BANCES P, FERNANDEZ M-R, RODRIGUEZ-GARCIA M-I, MORGAN RO, AND FERNANDEZ M-P. Annexin A11 (ANXA11) gene structure as the progenitor of paralogous annexins and source of orthologous cDNA isoforms. *Genomics* 69: 95–103, 2000.
- BANDOROWICZ-PIKULA S, DANIELUK M, WRZOSEK A, BUS R, BUCHET R, AND PIKULA S. Annexin VI: an intracellular target for ATP. *Acta Biochim Pol* 46: 810–812, 1999.
- BARAN DT, QUAIL JM, RAY R, AND HONEYMAN T. Binding of $1\alpha,25$ -dihydroxyvitamin D(3) to annexin II: effect of vitamin D metabolites and calcium. *J Cell Biochem* 80: 259–265, 2001.
- BARAN DT, QUAIL JM, RAY R, LESZYK L, AND HONEYMAN T. Annexin II is the membrane receptor that mediates the rapid actions of $1\alpha,25$ -dihydroxyvitamin D(3). *J Cell Biochem* 78: 34–46, 2000.
- BECK KA, BUCHANAN JA, MALHOTRA V, AND NELSON WJ. Golgi spectrin: identification of an erythroid alpha spectrin homolog associated with the Golgi complex. *J Cell Biol* 127: 707–723, 1994.
- BECKER T, WEBER K, AND JOHNSON N. Protein-protein recognition via short amphiphilic helices: a mutational analysis of the binding site of annexin II for p11. *EMBO J* 9: 4207–4213, 1990.
- BEERMANN B, HINZ H-J, HOFMANN A, AND HUBER R. Acid induced unfolding of annexin V wild type shows two intermediate states. *FEBS Lett* 423: 265–269, 1998.
- BELLAGAMBA C, HUBAISHY I, BJORGE JD, FITZPATRICK SL, FUJITA DJ, AND WAISMAN DM. Tyrosine phosphorylation of annexin II tetramer is stimulated by membrane binding. *J Biol Chem* 272: 3195–3199, 1997.
- BENEVOLENSKY D, BELIKOVA Y, MOHAMMADZADEH R, TROUVE P, MAROTTE F, RUSSO-MARIE F, SAMUEL JL, AND CHARLEMAGNE D. Expression and localization of the annexins II, V, and VI in myocardium from patients with end-stage heart failure. *Lab Invest* 80: 123–133, 2000.
- BENZ J, BERGNER A, HOFMANN A, DEMANGE P, GÖTTIG P, LIEMANN S, HUBER R, AND VOGES D. The structure of recombinant human annexin VI in crystals and membrane-bound. *J Mol Biol* 260: 638–643, 1996.
- BERENDES R, BURGER A, VOGES D, DEMANGE P, AND HUBER R. Calcium influx through annexin V ion channels into large unilamellar vesicles measured with fura-2. *FEBS Lett* 317: 131–134, 1993.
- BEVERS EM, JANSSEN MP, WILLEMS GM, AND ZWAAL FA. No evidence for enhanced thrombin formation through displacement of annexin V by antiphospholipid antibodies. *Thromb Haemostasis* 83: 792–794, 2000.
- BIENER Y, FEINSTEIN R, MAYAK M, KABURAGI Y, KADOWAKI T, AND ZICK Y. Annexin II is a novel player in insulin signal transduction. *J Biol Chem* 271: 29489–29496, 1996.
- BITTO E AND CHO W. Roles of individual domains of annexin I in its vesicle binding and vesicle aggregation: a comprehensive mutagenesis study. *Biochemistry* 37: 10231–10237, 1998.
- BITTO E, LI M, TIKHONOV AM, SCHLOSSMANN ML, AND CHO W. Mechanism of annexin I-mediated membrane aggregation. *Biochemistry* 39: 13469–13477, 2000.
- BOUSSAC M AND GARIN J. Calcium-dependent secretion in human neutrophils: a proteomic approach. *Electrophoresis* 21: 665–672, 2000.
- BRISSON A, MOSSER G, AND HUBER R. Structure of soluble and membrane-bound annexin V. *J Mol Biol* 220: 199–203, 1991.
- BROWN DA AND LONDON E. Functions of lipid rafts in biological membranes. *Annu Rev Cell Dev Biol* 14: 111–136, 1998.
- BROWNAWELL A AND CREUTZ C. Calcium-dependent binding of sorcin to the N-terminal domain of synexin (annexin VII). *J Biol Chem* 272: 22182–22190, 1997.
- BURGER A, BERENDES R, LIEMANN S, BENZ J, HOFMANN A, GÖTTIG P, HUBER R, GERKE V, THIEL C, RÖMISCH J, AND WEBER K. The crystal structure and ion channel activity of human annexin II, a peripheral membrane protein. *J Mol Biol* 257: 839–847, 1996.
- BURGOYNE RD. Calpactin in exocytosis. *Nature* 331: 20, 1988.
- CAMPOS B, MO YD, MEALY TR, LI CW, SWAIRIO MA, BALCH C, HEAD JF, RETZINGER G, DEDMAN JR, AND SEATON BA. Mutational and crystallographic analyses of interfacial residues suggest direct interac-

- tions with phospholipid membrane components. *Biochemistry* 37: 8004–8010, 1998.
32. CAMPOS B, WANG S, RETZINGER GS, KAETZEL MA, SEATON BA, KARIN NJ, JOHNSON JD, AND DEDMAN JR. Mutation of highly conserved arginine residues disrupts the structure and function of annexin V. *Arch Med Res* 30: 360–367, 1999.
 33. CAO HUY H AND POLLARD HB. Activation of annexin 7 by protein kinase C in vitro and in vivo. *J Biol Chem* 276: 12813–12821, 2001.
 34. CAO HUY H, SRIVASTAVA M, AND POLLARD HB. Membrane fusion protein synexin (annexin VII) as a Ca^{2+} /GTP sensor in exocytotic secretion. *Proc Natl Acad Sci USA* 93: 10797–10802, 1996.
 35. CARTAILLER J, HAIGLER HT, AND LUECKE H. Annexin XII E105K crystal structure: identification of a pH-dependent switch for mutant hexamerization. *Biochemistry* 39: 2475–2483, 2000.
 36. CELIS A, RASMUSSEN HH, CELIS P, BASSE B, LAURIDSEN JB, RATZ G, HEIN B, OSTERGAARD M, WOLF H, ORNSTOFT T, AND CELIS JE. Short-term culturing of low-grade superficial bladder transitional cell carcinomas leads to changes in the expression levels of several proteins involved in key cellular activities. *Electrophoresis* 20: 355–361, 1999.
 37. CHAN HC, KAETZEL MA, GOTTER AL, DEDMAN JR, AND NELSON DJ. Annexin IV inhibits calmodulin-dependent protein kinase II-activated chloride conductance. A novel mechanism for ion channel regulation. *J Biol Chem* 269: 32464–32468, 1994.
 38. CHASSEROT-GOLAZ S, VITALE N, SAGOT I, DELOUCHE B, DIRRIG S, PRADEL LA, HENRY JP, AUNIS D, AND BADER M-F. Annexin II in exocytosis: catecholamine secretion requires the translocation of p36 to the subplasmalemmal region in chromaffin cells. *J Cell Biol* 133: 1217–1236, 1996.
 39. CHETCUTI A, MARGAN SH, RUSSELL P, MANN S, MILLAR DS, CLARK SJ, ROGERS J, HANDELSMANN DJ, AND DONG Q. Loss of annexin II heavy and light chains in prostate cancer and its precursors. *Cancer Res* 61: 6331–6334, 2001.
 40. CHO W AND BITTO E. Structural determination of the vesicle aggregation activity of annexin I. *Biochemistry* 38: 14094–14100, 1999.
 41. CHOI K-S, FITZPATRICK SL, FILIPENKO NR, FOGG DK, KASSAM G, MAGGIOCCO AM, AND WAISMAN DM. Regulation of plasmin-dependent fibrin clot lysis by annexin II heterotetramer. *J Biol Chem* 276: 25212–25221, 2001.
 42. CHOI K-S, GHUMAN J, KASSAM G, KANG H-M, FITZPATRICK SL, AND WAISMAN DM. Annexin II tetramer inhibits plasmin-dependent fibrinolysis. *Biochemistry* 37: 648–655, 1998.
 43. CHOW A, DAVIS AJ, AND GAWLER DJ. Identification of a novel protein complex containing annexin VI, Fyn, Pyk2, and the P120(GAP) C2 domain. *FEBS Lett* 469: 88–92, 2000.
 44. CHOW A AND GAWLER DJ. Mapping the site of interaction between annexin VI and the p120GAP C2 domain. *FEBS Lett* 460: 166–172, 1999.
 45. CLEMEN CS, HOFMANN A, ZAMPARELLI C, AND NOEGEL AA. Expression and localization of annexin VII (synexin) isoforms in differentiating myoblasts. *J Muscle Res Cell Motil* 20: 669–679, 1999.
 46. COMERA C AND RUSSO-MARIE F. Glucocorticoid induced annexin 1 secretion by monocytes and peritoneal leukocytes. *Br J Pharmacol* 115: 1043–1047, 1995.
 47. CONCHA NO, HEAD JF, KAETZEL MA, DEDMAN JR, AND SEATON BA. Rat annexin V crystal structure: Ca^{2+} -induced conformational changes. *Science* 261: 1321–1324, 1993.
 48. COOKSON BT, ENGELHARDT S, SMITH C, BAMFORD HA, PROCHAZKA M, AND TAIT JF. Organization of the human annexin V (ANX5) gene. *Genomics* 20: 463–467, 1994.
 49. CORDIER-OSCHENBEIN F, GUEROIS R, BALEUX F, HUYNH-DINH T, CHAFOTTE A, NEUMANN J-M, AND SANSON A. Folding properties of an annexin I domain: a (1)H-(15)N NMR and CD study. *Biochemistry* 35: 10347–10357, 1996.
 50. CORVERA S, DIBONAVENTURE C, AND SHPETNER HS. Cell confluence-dependent remodeling of endothelial membranes mediated by cholesterol. *J Biol Chem* 275: 31414–31421, 2000.
 51. CREUTZ CE. The annexins and exocytosis. *Science* 258: 924–931, 1992.
 52. CREUTZ CE, PAZOLES CJ, AND POLLARD HB. Identification and purification of an adrenal medullary protein (synexin) that causes calcium-dependent aggregation of chromaffin granules. *J Biol Chem* 253: 2858–2866, 1978.
 53. CREUTZ CE, SNYDER SL, DAIGLE SN, AND REDICK J. Identification, localization, and functional implications of an abundant nematode annexin. *J Cell Biol* 132: 1079–1092, 1996.
 54. CREUTZ CE, ZAKS WJ, HAMMAN HC, CRANE S, MARTIN WH, GOULD KL, ODDIE KM, AND PARSONS SJ. Identification of chromaffin granule-binding proteins. *J Biol Chem* 262: 1860–1868, 1987.
 55. CRUMPTON MJ AND DEDMAN JR. Protein terminology tangle. *Nature* 345: 212, 1990.
 56. CUZZOCREA S, TAILOR A, ZINGARELLI B, SALZMAN AL, FLOWER RJ, SZABO C, AND PERRETTI M. Lipocortin 1 protects against splanchnic artery occlusion and reperfusion injury by affecting neutrophil migration. *J Immunol* 159: 5089–5097, 1997.
 57. DAIGLE SN AND CREUTZ CE. Transcription, biochemistry and localization of nematode annexins. *J Cell Sci* 112: 1901–1913, 1999.
 58. D'AMICO M, DI FILIPPO C, LA M, SOLITO E, MCLEAN PG, FLOWER RJ, OLIANI SM, AND PERRETTI M. Lipocortin 1 reduces myocardial ischemia-reperfusion injury by affecting local leukocyte recruitment. *FASEB J* 14: 1867–1869, 2000.
 59. DAVIDSON FF, DENNIS EA, POWELL M, AND GLENNEY JR. Inhibition of phospholipase A_2 by "lipocortins" and calpactins. *J Biol Chem* 262: 1698–1705, 1987.
 60. DAVIS AJ, BUTT JT, WALKER JH, MOSS SE, AND GAWLER DJ. The CaLB domain of p120(GAP) mediates protein-protein interactions with Ca^{2+} -dependent membrane binding proteins: evidence for a direct interaction between annexin VI and p120(GAP). *J Biol Chem* 271: 24333–24336, 1996.
 61. DE BK, MISONO KS, LUKAS TJ, MROCZKOWSKI B, AND COHEN S. A calcium-dependent 35-kilodalton substrate for epidermal growth factor receptor/kinase isolated from normal tissue. *J Biol Chem* 261: 13784–13792, 1986.
 62. DE COUPADE C, GILLET R, BENNOUN M, BRIAND P, RUSSO-MARIE F, AND SOLITO E. Annexin I expression and phosphorylation are upregulated during liver regeneration and transformation in antithrombin III SV40 large T antigen transgenic mice. *Hepatology* 31: 371–380, 2000.
 63. DELOUCHE B, PRADEL LA, AND HENRY JP. Phosphorylation by protein kinase C of annexin 2 in chromaffin cells stimulated by nicotine. *J Neurochem* 68: 1720–1727, 1997.
 64. DELMER DP AND POTIKHA TS. Structures and functions of annexins in plants. *Cell Mol Life Sci* 53: 546–553, 1997.
 65. DENKO N, SCHINDLER C, KOONG A, LADEROUTE K, GREEN C, AND GIACCIA A. Epigenetic regulation of gene expression in cervical cancer cells by the tumor microenvironment. *Clin Cancer Res* 6: 480–487, 2000.
 66. DIAKONOVA M, GERKE V, ERNST J, LAUTARD J-P, VAN DER VUSSE G, AND GRIFFITHS G. Localization of five annexins in J774 macrophages and on isolated phagosomes. *J Cell Sci* 110: 1199–1213, 1997.
 67. DIAZ-MUNOZ M, HAMILTON SL, KAETZEL MA, HAZARIKA P, AND DEDMAN JR. Modulation of calcium release channel activity from sarcoplasmic reticulum by annexin VI (67 kDa-calmodulin). *J Biol Chem* 265: 15894–15899, 1990.
 68. DONATO R. Functional roles of S100 proteins, calcium-binding proteins of the EF-hand type. *Biochim Biophys Acta* 1450: 191–231, 1999.
 69. DONNELLY SR, HAWKINS TE, AND MOSS SE. A conserved nuclear element with a role in mammalian gene regulation. *Hum Mol Genet* 8: 1723–1728, 1999.
 70. DONNELLY SR AND MOSS SE. Functional analysis of the human annexin I and VI gene promoters. *Biochem J* 332: 681–687, 1998.
 71. DÖRING V, SCHLEICHER M, AND NOEGEL AA. *Dictyostelium* annexin VII (synexin). cDNA sequence and isolation of a gene disruption mutant. *J Biol Chem* 266: 17509–17515, 1991.
 72. DÖRING V, VERETOUT F, ALBRECHT R, MÜHLBAUER B, SCHLATTERER C, SCHLEICHER M, AND NOEGEL AA. The in vivo role of annexin VII (synexin): characterization of an annexin VII-deficient *Dictyostelium* mutant indicates an involvement in Ca^{2+} -regulated processes. *J Cell Sci* 108: 2065–2076, 1995.
 73. EBERHARD D, KARNS LR, VANDENBERG SR, AND CREUTZ CE. Control of the nucleocytoplasmic partitioning of annexin II by a nuclear export signal and by p11 binding. *J Cell Sci* 114: 3155–3166, 2001.
 74. EMMERT-BUCK MR, GILLESPIE JW, PAWELETZ CP, ORNSTEIN DK, BASRUR V, APPELLA E, WANG QH, HUANG J, HU N, TAYLOR P, AND PETRICONE EF. An approach to proteomic analysis of human tumors. *Mol Carcinog* 27: 158–165, 2000.

75. EUZGER HS, FLOWER RJ, GOULDING NJ, AND PERRETTI M. Differential modulation of annexin I binding sites on monocytes and neutrophils. *Mediators Inflamm* 8: 53–62, 1999.
76. FERNÁNDEZ M-P, MORGAN RO, FERNÁNDEZ M-R, AND CARCEDO M-T. The gene encoding human annexin V has a TATA-less promoter with a high G+C content. *Gene* 149: 253–260, 1994.
77. FIEDLER K, LAFONT F, PARTON RG, AND SIMONS K. Annexin XIIIb: a novel epithelial specific annexin is implicated in vesicular traffic to the apical plasma membrane. *J Cell Biol* 128: 1043–1053, 1995.
78. FIELD SL, BRIGHTON TA, MCNEIL HP, AND CHESTERMAN CN. Recent insights into antiphospholipid antibody-mediated thrombosis. *Baillieres Best Pract Res Clin Haematol* 12: 407–422, 1999.
79. FLIPENKO NR AND WAISMAN DM. Characterization of Ca^{2+} -binding sites of annexin II tetramer. *J Biol Chem* 275: 38877–38884, 2000.
80. FLIPENKO NR AND WAISMAN DM. The C-terminus of annexin II mediates binding to F-actin. *J Biol Chem* 276: 5310–5315, 2001.
81. FIRE A, XU S, MONTGOMERY MK, KOSTAS SA, DRIVER SE, AND MELLO CC. Potent and specific genetic interference by double-stranded RNA in *Caenorhabditis elegans*. *Nature* 391: 806–811, 1998.
82. FITZPATRICK SL, KASSAM G, CHOI KS, KANG HM, FOGG DK, AND WAISMAN DM. Regulation of plasmin activity by annexin II tetramer. *Biochemistry* 39: 1021–1028, 2000.
83. FITZPATRICK SL, KASSAM G, MANRO A, BRAAT CE, LOUIE P, AND WAISMAN DM. Fucoidan-dependent conformational changes in annexin II tetramer. *Biochemistry* 39: 2140–2148, 2000.
84. FLEET A, ASHWORTH R, KUBISTA H, EDWARDS H, BOLSOVER S, MOBBS P, AND MOSS SE. Inhibition of EGF-dependent calcium influx by annexin VI is splice form-specific. *Biochem Biophys Res Commun* 260: 540–546, 1999.
85. FLOWER RJ. Background and discovery of lipocortins. *Agents Actions* 17: 255–262, 1986.
86. FLOWER RJ AND ROTHWELL NJ. Lipocortin-1: cellular mechanisms and clinical relevance. *Trends Pharmacol Sci* 15: 71–76, 1994.
87. FRANCA G, MITCHELL SD, MOSS SE, HANBY AM, MARSHALL JF, AND HART IR. Identification by differential display of annexin-VI, a gene differentially expressed during melanoma progression. *Cancer Res* 56: 3855–3858, 1996.
88. FREDRIKSSON EK, SHIPKOVA PA, SHEETS ED, HOLOWKA D, BAIRD B, AND MCLAFFERTY FW. Quantitative analysis of phospholipids in functionally important membrane domains from RBL-2H3 mast cells using tandem high-resolution mass spectrometry. *Biochemistry* 38: 8056–8063, 1999.
89. FREY BM, REBER BF, VISHWANATH BS, ESCHER G, AND FREY FJ. Annexin I modulates cell functions by controlling intracellular calcium release. *FASEB J* 13: 2235–2245, 1999.
90. FUKAO H, UESHIMA S, TAKAISHI T, OKADO K, AND MATSUO O. Enhancement of tissue type plasminogen activator (tPA) activity by purified tPA receptor expressed in human endothelial cells. *Biochim Biophys Acta* 1356: 111–120, 1997.
91. FURGE LL, CHEN K, AND COHEN S. Annexin VII and annexin XI are tyrosine phosphorylated in peroxyvanadate-treated dogs and in platelet derived growth factor-treated rat vascular smooth muscle cells. *J Biol Chem* 274: 33504–33509, 1999.
92. FUTTER CE, FELDER S, SCHLESSINGER J, ULLRICH A, AND HOPKINS CR. Annexin I is phosphorylated in the multivesicular body during the processing of the epidermal growth factor receptor. *J Cell Biol* 120: 77–83, 1993.
93. GAGESCU R, DEMAUREX N, PARTON RG, HUNZIKER W, HUBER L, AND GRUENBERG J. The recycling endosome of Madin-Darby canine kidney cells is a mildly acidic compartment rich in raft components. *Mol Biol Cell* 11: 2775–2791, 2000.
94. GAO J, LI Y, AND YAN H. NMR solution structure of domain 1 of human annexin I shows an autonomous folding unit. *J Biol Chem* 274: 2971–2977, 1999.
95. GAO ZH, METHERRALL J, AND VIRSHUP DM. Identification of casein kinase I substrates by in vitro expression cloning screening. *Biochem Biophys Res Commun* 268: 562–566, 2000.
96. GARBUGLIA M, VERZINI M, AND DONATO R. Annexin VI binds S100A1 and S100B and blocks the ability of S100A1 and S100B to inhibit desmin and GFAP assemblies into intermediate filaments. *Cell Calcium* 24: 177–191, 1998.
97. GERKE V AND MOSS SE. Annexins and membrane dynamics. *Biochim Biophys Acta* 1357: 129–154, 1997.
98. GERKE V AND WEBER K. Identity of p36K phosphorylated upon Rous sarcoma virus transformation with a protein from brush borders: calcium-dependent binding to nonerythroid spectrin and F-actin. *EMBO J* 3: 227–233, 1984.
99. GIDON-JEANGIRARD C, HUGEL B, HOLL V, TOTI F, LAPLANCHE JL, MEYER D, AND FREYSSINET JM. Annexin V delays apoptosis while exerting an external constraint preventing the release of CD4+ and PrPc+ membrane particles in a human T lymphocyte model. *J Immunol* 162: 5712–5718, 1999.
100. GIDROL X, SABELLI PA, FERN YS, AND KUSH AK. Annexin-like protein from *Arabidopsis thaliana* rescues DeltaoxyR mutant of *Escherichia coli* from H_2O_2 stress. *Proc Natl Acad Sci USA* 93: 11268–11273, 1996.
101. GLENNEY JR, TACK B, AND POWELL MA. Calpactins: two distinct Ca^{2+} -regulated phospholipid and actin-binding proteins isolated from bovine lung and placenta. *J Biol Chem* 104: 503–511, 1987.
102. GLENNEY JR AND TACK BF. Amino-terminal sequence of p36 and associated p11: identification of the site of tyrosine phosphorylation and homology with S-100. *Proc Natl Acad Sci USA* 82: 7884–7888, 1985.
103. GOLCZAK M, KICINSKA A, BANDOROWICZ J, BUCHET R, SZEWCZYK A, AND PIKULA S. Acidic pH-induced folding of annexin VI is a prerequisite for its insertion into lipid bilayers and formation of ion channels by the protein molecule. *FASEB J* 15: 1083–1085, 2001.
104. GOOSSENS ELJ, REUTELINGSPERGER CPM, JONGSMA FHM, KRAAYENHOF R, AND HERMENS WT. Annexin V perturbs or stabilises phospholipid membranes in a calcium-dependent manner. *FEBS Lett* 359: 155–158, 1995.
105. GOULDING NJ, EUZGER HS, BUTT SK, AND PERRETTI M. Novel pathways for glucocorticoid effects on neutrophils in chronic inflammation. *Inflamm Res* 47: S158–S165, 1998.
106. GREENWOOD M AND TSANG A. Sequence and expression of annexin VII of *Dictyostelium discoideum*. *Biochim Biophys Acta* 1088: 429–432, 1991.
107. GREWAL T, HEEREN J, MEWAWALA D, SCHNITGERHANS T, WENDT D, SALOMON G, ENRICH C, BEISIEGEL U, AND JÄCKLE S. Annexin VI stimulates endocytosis and is involved in the trafficking of LDL to the prelysosomal compartment. *J Biol Chem* 275: 33806–33813, 2000.
108. GRUENBERG J AND EMANS N. Annexins in membrane traffic. *Trends Cell Biol* 3: 224–227, 1993.
109. GUNTESKI-HAMBLIN AM, SONG GJ, WALSH RA, FRENZKE M, BOIVIN GP, DORN GW II, KAETZEL MA, HORSEMAN ND, AND DEDMAN JR. Annexin VI overexpression targeted to heart alters cardiomyocyte function in transgenic mice. *Am J Physiol Heart Circ Physiol* 270: H1091–H1100, 1996.
110. HACHIDA M, LU H, KANEKO N, HORIKAWA Y, OHKADO A, GU H, ZHANG XL, HOSHI H, NONOYAMA M, NAKANISHI T, AND KOYANAGI H. Protective effect of JTV519 (K201), a new 1,4-benzothiazepine derivative, on prolonged myocardial preservation. *Transplant Proc* 31: 996–1000, 1999.
111. HAIGLER HT AND SCHLAEPFER DD. Annexin I phosphorylation and secretion. In: *The Annexins*, edited by Moss SE. London: Portland, 1992, p. 11–34.
112. HAJJAR K, MAURI L, JACOVINA AT, ZHONG F, MIRZA UA, PADOVAN JC, AND CHAIT BT. Tissue plasminogen activator binding to the annexin II tail domain. Direct modulation by homocysteine. *J Biol Chem* 273: 9987–9993, 1998.
113. HAJJAR KA AND JACOVINA AT. Modulation of annexin II by homocysteine: implications for atherothrombosis. *J Invest Med* 46: 364–369, 1998.
114. HAJJAR KA AND KRISHNAN S. Annexin II: a mediator of the plasmin/plasminogen activator system. *Trends Cardiovasc Med* 9: 128–138, 1999.
115. HAMRE KM, CHEPENIK KP, AND GOLDOWITZ D. The annexins: specific markers of midline structures and sensory neurons in the developing murine central nervous system. *J Comp Neurol* 352: 421–435, 1995.
116. HAMRE KM, KELLER-PECK CR, CAMPBELL RM, PETERSON AC, MULLEN RJ, AND GOLDOWITZ D. Annexin IV is a marker of roof and floor plate development in the murine CNS. *J Comp Neurol* 368: 527–537, 1996.
117. HAN EK, TAHIR SK, CHERIAN SP, COLLINS N, AND NG SC. Modulation of paclitaxel resistance by annexin IV in human cancer cell lines. *Br J Cancer* 83: 83–88, 2000.

118. HAN H-Y, LEE Y-H, OH J-Y, NA D-S, AND LEE B-J. NMR analysis of the interaction of human annexin I with ATP, Ca(2+), and Mg(2+). *FEBS Lett* 425: 523-527, 1998.
119. HARDER T AND GERKE V. The annexin II(2)p11(2) complex is the major component of the Triton X-100 insoluble low-density fraction prepared from MDCK cells in the presence of Ca(2+). *Biochim Biophys Acta* 1223: 375-382, 1994.
120. HARDER T, KELLNER R, PARTON RG, AND GRUENBERG J. Specific release of membrane-bound annexin II and cortical cytoskeletal elements by sequestration of membrane cholesterol. *Mol Biol Cell* 8: 533-545, 1997.
121. HAWKINS TE, ROES J, REES D, MONKHOUSE J, AND MOSS SE. Immunological development and cardiovascular function are normal in annexin VI null mutant mice. *Mol Cell Biol* 19: 8028-8032, 1999.
122. HERR C, SMYTH N, ULLRICH S, YUN F, SASSE P, HESCHELER J, FLEISCHMANN B, LASEK K, BRIXTIS K, SCHWINGER RH, FÄSSLER R, SCHRODER R, AND NOEGEL AA. Loss of annexin A7 leads to alterations in frequency-induced shortening of isolated murine cardiomyocytes. *Mol Cell Biol* 21: 4119-4128, 2001.
123. HIRATA A AND HIRATA F. Lipocortin (annexin) I heterotetramer binds to purine RNA and pyrimidine DNA. *Biochem Biophys Res Commun* 265: 200-204, 1999.
124. HOEKSTRA D, BUIST AR, KLAPPE K, AND REUTELINGSPIERGER CP. Interaction of annexins with membranes: the N-terminus as a governing parameter as revealed with a chimeric annexin. *Biochemistry* 32: 14194-14202, 1993.
125. HOFMANN A, BENZ J, LIEMANN S, AND HUBER R. Voltage dependent binding of annexin V, annexin VI and annexin VII core to acidic phospholipid membranes. *Biochim Biophys Acta* 1330: 254-264, 1997.
126. HOFMANN A, ESCHERICH A, LEWIT-BENTLEY A, BENZ J, RAGUENES-NICOL C, RUSSO-MARIE F, GERKE V, MARODER L, AND HUBER R. Interactions of benzodiazepine derivatives with annexins. *J Biol Chem* 273: 2885-2894, 1998.
127. HOFMANN A, PROUST J, DOROWSKI A, SCHANTZ R, AND HUBER R. Annexin 24 from *Capsicum annuum*: X-ray structure and biochemical characterization. *J Biol Chem* 275: 8072-8082, 2000.
128. HOFMANN A, RAGUENES-NICOL C, FAVIER-PERRON B, MESONERO J, HUBER R, RUSSO-MARIE F, AND LEWIT-BENTLEY A. The annexin A3-membrane interaction is modulated by an N-terminal tryptophan. *Biochemistry* 39: 7712-7721, 2000.
129. HOLROYD C, KISTNER U, ANNAERT W, AND JAHN R. Fusion of endosomes involved in synaptic vesicle recycling. *Mol Biol Cell* 10: 3035-3044, 1999.
130. HOYAL CR, THOMAS AP, AND FORMAN HJ. Hydroperoxide-induced increases in intracellular calcium due to annexin VI translocation and inactivation of plasma membrane Ca²⁺-ATPase. *J Biol Chem* 271: 29205-29210, 1996.
131. HU S, BRADY SR, KOVAR DR, STAIGER CJ, CLARK GB, ROUX SJ, AND MUDAY GK. Technical advance: identification of plant actin-binding proteins by F-actin affinity chromatography. *Plant J* 24: 127-137, 2000.
132. HUBAISHY I, JONES PG, BJORGE J, BELLAGAMBA C, FITZPATRICK S, FUJITA DJ, AND WAISMAN DM. Modulation of annexin II tetramer by tyrosine phosphorylation. *Biochemistry* 34: 14527-14534, 1995.
133. HUBER R, BERENDES R, BURGER A, LUECKE H, AND KARSHIKOV A. Annexin V: crystal structure and its implication on function. In: *The Annexins*, edited by Moss SE. London: Portland, 1992, p. 105-124.
134. HUBER R, RÖMISCH J, AND PAQUES EP. The crystal and molecular structure of human annexin V, an anticoagulant calcium, membrane binding protein. *EMBO J* 9: 3867-3874, 1990.
135. IINO S, SUDO T, NIWA T, FUKOSAWA T, HIDAKA H, AND NIKI I. Annexin XI may be involved in Ca(2+) or GTP-gammaS-induced insulin secretion in the pancreatic beta-cell. *FEBS Lett* 479: 46-50, 2000.
136. IKONEN E AND PARTON RG. Caveolins and cellular cholesterol balance. *Traffic* 1: 212-217, 2000.
137. IMAI Y AND KOHSAKA S. Structure of rat annexin V gene and molecular diversity of its transcripts. *Eur J Biochem* 232: 327-334, 1995.
138. ISAS JM, CARTAILLER JP, SOKOLOV Y, PATEL DR, LANGEN R, LUECKE H, HALL JE, AND HAIGLER HT. Annexins V and XII insert into bilayers at mildly acidic pH and form ion channels. *Biochemistry* 39: 3015-3022, 2000.
139. ISHITSUKA R, KOJIMA K, UTSUMI H, OGAWA H, AND MATSUMOTO I. Glycosaminoglycan binding properties of annexin IV, V, and VI. *J Biol Chem* 273: 9935-9941, 1998.
140. IVANENKOV VV, WEBER K, AND GERKE V. The expression of different annexins in the fish embryo is developmentally regulated. *FEBS Lett* 352: 227-230, 1994.
141. JANS SW, DE JONG YF, REUTELINGSPIERGER CP, VAN DER VUSSE GJ, AND VAN BILSEN M. Differential expression and localization of annexin V in cardiac myocytes during growth and hypertrophy. *Mol Cell Biochem* 178: 229-236, 1998.
142. JOHNSON N, MARRIOTT G, AND WEBER K. p36, the major cytoplasmic substrate of src tyrosine protein kinase, binds to its p11 subunit via a short amino-terminal amphipathic helix. *EMBO J* 7: 2435-2442, 1988.
143. JOHNSON N AND WEBER K. Alkylation of cysteine 82 of p11 abolishes the complex formation with the tyrosine protein kinase substrate p36 (annexin 2, calpactin 2, lipocortin 2). *J Biol Chem* 265: 14464-14468, 1990.
144. JOST M AND GERKE V. Mapping of a regulatory important site for protein kinase C phosphorylation in the N-terminal domain of annexin II. *Biochim Biophys Acta* 1313: 283-289, 1996.
145. JOST M, ZEUSCHNER D, SEEMANN J, WEBER K, AND GERKE V. Identification and characterization of a novel type of annexin-membrane interaction: Ca²⁺ is not required for the association of annexin II with endosomal membranes. *J Cell Sci* 110: 221-228, 1997.
146. KAETZEL MA, CHANG CHAN H, DUBINSKY WP, DEDMAN JR, AND NELSON DJ. A role for annexin IV in epithelial cell function. Inhibition of calcium-activated chloride conductance. *J Biol Chem* 269: 5297-5302, 1994.
147. KAETZEL MA, MO YD, MEALY TR, CAMPOS B, BERGSMASCHUTTER W, BRISSON A, DEDMAN JR, AND SEATON BA. Phosphorylation mutants elucidate the mechanism of annexin IV-mediated membrane aggregation. *Biochemistry* 40: 4192-4199, 2001.
148. KAMAL A, YING Y, AND ANDERSON RG. Annexin VI-mediated loss of spectrin during coated pit budding is coupled to delivery of LDL to lysosomes. *J Cell Biol* 142: 937-947, 1998.
149. KANEKO N, AGO H, MATSUDA R, INAGAKI E, AND MIYANO M. Crystal structure of annexin V with its ligand K-201 as a calcium channel activity inhibitor. *J Mol Biol* 274: 16-20, 1997.
150. KANEKO N, MATSUDA R, TODA M, AND SHIMAMOTO K. Inhibition of annexin V-dependent Ca(2+) movement in large unilamellar vesicles by K201, a new 1,4-benzothiazepine derivative. *Biochim Biophys Acta* 1330: 1-7, 1997.
151. KANG H-M, KASSAM G, JARVIS SE, FITZPATRICK SL, AND WAISMAN DM. Characterization of human recombinant annexin II tetramer purified from bacteria: role of N-terminal acetylation. *Biochemistry* 36: 2041-2050, 1997.
152. KASSAM G, MANRO A, BRAAT CE, LOUIE P, FITZPATRICK SL, AND WAISMAN DM. Characterization of the heparin binding properties of annexin II tetramer. *J Biol Chem* 272: 15093-15100, 1997.
153. KATAOKA TR, ITO A, ASADA H, WATABE K, NISHIYAMA K, NAKAMOTO K, ITAMI S, YOSHIKAWA K, ITO M, NOJIMA H, AND KITAMURA Y. Annexin VII as a novel marker for invasive phenotype of malignant melanoma. *Jpn J Cancer Res* 91: 75-83, 2000.
154. KAWASAKI H AND KRETSINGER RH. Calcium-binding proteins 1: EF-hands. *Protein Profile* 2: 297-490, 1995.
155. KIM GY, LEE HB, LEE SO, RHEE HJ, AND NA DS. Chaperone-like function of lipocortin 1. *Biochem Mol Biol Int* 43: 521-528, 1997.
156. KIM SW, RHEE HJ, KO J, KIM YJ, KIM HG, YANG JM, CHOI EC, AND NA DS. Inhibition of cytosolic phospholipase A₂ by annexin I. Specific interaction model and mapping of interaction site. *J Biol Chem* 276: 15712-15719, 2001.
157. KIRSCH T, NAH HD, DEMUTH DR, HARRISON G, GOLUB EE, ADAMS SL, AND PACIFICI M. Annexin V-mediated calcium flux across membranes is dependent on the lipid composition: implications for cartilage mineralization. *Biochemistry* 36: 3359-3367, 1997.
158. KÖHLER G, HERING U, ZSCHÖRNIG O, AND ARNOLD K. Annexin V interaction with phosphatidylserine-containing vesicles at low and neutral pH. *Biochemistry* 36: 8189-8194, 1997.
159. KOJIMA K, YAMAMOTO K, IRIMURA T, OGAWA H, AND MATSUMOTO I. Characterization of carbohydrate binding protein p33/41: relation with annexin IV, molecular basis of the doublet forms (p33 and p41), and modulation for the carbohydrate binding activity phospholipids. *J Biol Chem* 271: 7679-7685, 1996.

160. KÖNIG J AND GERKE V. Modes of annexin-membrane interactions analyzed by employing chimeric annexin proteins. *Biochim Biophys Acta*. In press.
161. KÖNIG J, PRENEN J, NILIUS B, AND GERKE V. The annexin II-p11 complex is involved in regulated exocytosis in bovine pulmonary artery endothelial cells. *J Biol Chem* 273: 19679–19684, 1998.
162. KOVACS I, AYAYDIN F, OBERSCHALL A, IPACS I, BOTTKA S, PONGOR S, DUDITS D, AND TOTTH EC. Immunolocalization of a novel annexin-like protein encoded by a stress and abscisic acid responsive gene in alfalfa. *Plant J* 15: 185–197, 1998.
163. KUBISTA H, HAWKINS TE, PATEL DR, HAIGLER HT, AND MOSS SE. Annexin 5 mediates a peroxide-induced Ca^{2+} influx in B cells. *Curr Biol* 9: 1403–1406, 1999.
164. KUSUMAWATI A, CAZAVIEILLE C, PORTE F, BETTACHE S, LIAUTARD J-P, AND SRI WIDADA J. Early events and implication of F-actin and annexin I associated structures in the phagocytic uptake of *Brucella suis* by the J774A.1 murine cell line and human monocytes. *Microb Pathog* 28: 343–352, 2000.
165. LAFONT F, LECAT S, VERKADE P, AND SIMONS K. Annexin XIIIb associates with lipid microdomains to function in apical delivery. *J Cell Biol* 142: 1413–1427, 1998.
166. LAKASING L, CAMPA JS, POSTON R, KHAMASHTA MA, AND POSTON L. Normal expression of tissue factor, thrombomodulin, and annexin V in placentas from women with antiphospholipid syndrome. *Am J Obstet Gynecol* 181: 180–189, 1999.
167. LAMBERT O, GERKE V, BADER MF, PORTE F, AND BRISSON A. Structural analysis of junctions formed between lipid membranes and several annexins by cryoelectron microscopy. *J Mol Biol* 272: 42–55, 1997.
168. LANGEN R, ISAS JM, HUBBEL WL, AND HAIGLER HT. A transmembrane form of annexin XII detected by site-directed spin labeling. *Proc Natl Acad Sci USA* 95: 14060–14065, 1998.
169. LANGEN R, ISAS JM, LUECKE H, HAIGLER HT, AND HUBBEL WL. Membrane-mediated assembly of annexins studied by site-directed spin labeling. *J Biol Chem* 273: 22453–22458, 1998.
170. LARSSON M, MAJEED M, ERNST JD, MAGNUSSON KE, STENDAHL O, AND FORSUN U. Role of annexins in endocytosis of antigens in immature human dendritic cells. *Immunology* 92: 501–511, 1997.
171. LAVAILLE F, RAINTEAU D, MASSEY-HARROUCHE D, AND METZ F. Establishment of plasma membrane polarity in mammary epithelial cells correlates with changes in prolactin trafficking and in annexin VI recruitment to membranes. *Biochim Biophys Acta* 1464: 83–94, 2000.
172. LECAT S, VERKADE P, THIELE C, FIEDLER K, SIMONS K, AND LAFONT F. Different properties of two isoforms of annexin XIII in MDCK cells. *J Cell Sci* 113: 2607–2618, 2000.
173. LEE T-L, LIN Y-C, MOCHITATE K, AND GRINNELL F. Stress-relaxation of fibroblasts in collagen matrices triggers ectocytosis of plasma membrane vesicles containing actin, annexins II and VI, and β_1 integrin receptors. *J Cell Sci* 105: 167–177, 1993.
174. LEWITT-BENTLEY A, MORERA S, HUBER R, AND BODO G. The effect of metal binding on the structure of annexin V and implications for membrane binding. *Eur J Biochem* 210: 73–77, 1992.
175. LEWITT-BENTLEY A, RETY S, SOPKOVA-DE OLIVEIRA SANTOS J, AND GERKE V. S100-annexin complexes: some insights from structural studies. *Cell Biol Int* 24: 799–802, 2000.
176. LEY K. Molecular mechanisms of leukocyte recruitment in the inflammatory process. *Cardiovasc Res* 32: 733–742, 1996.
177. LIEMANN S, BRINGEMEIER I, BENZ J, GÖTTIG P, HOFMANN A, HUBER R, NOEGEL AA, AND JACOB U. Crystal structure of the C-terminal tetrad repeat from synexin (annexin VII) of *Dictyostelium discoideum*. *J Mol Biol* 270: 79–88, 1997.
178. LIEMANN S AND LEWITT-BENTLEY A. Annexins: a novel family of calcium- and membrane-binding proteins in search of a function. *Structure* 3: 233–237, 1995.
179. LIN HC, SUDHOF TC, AND ANDERSON RG. Annexin VI is required for budding of clathrin-coated pits. *Cell* 70: 283–291, 1992.
180. LIU L. Calcium-dependent self-association of annexin II: a possible implication in exocytosis. *Cell Signal* 11: 317–324, 1999.
181. LIU L, TAO JQ, LI HL, AND ZIMMERMAN UJ. Inhibition of lung surfactant secretion from alveolar type II cells and annexin II tetramer-mediated membrane fusion by phenothiazines. *Arch Biochem Biophys* 342: 322–328, 1997.
182. LIU L, TAO J-Q, AND ZIMMERMAN U-JP. Annexin II binds to the membrane of A549 cells in a calcium-dependent and calcium-independent manner. *Cell Signal* 9: 299–304, 1997.
183. LUCKCUCK T, TROTTER PJ, AND WALKER JH. Localization of annexin V in the adult and neonatal heart. *Biochem Biophys Res Commun* 238: 622–628, 1997.
184. LUCKCUCK T, TROTTER PJ, AND WALKER JH. Localization of annexin VI in the adult and neonatal heart. *Cell Biol Int* 22: 199–205, 1998.
185. LUECKE H, CHANG BT, MAILLIARD WS, SCHLAEPFER DD, AND HAIGLER HT. Crystal structure of the annexin XII hexamer and implications for bilayer insertion. *Nature* 378: 512–515, 1995.
186. MA K, SIMANTOV R, ZHANG JC, SILVERSTEIN R, HAJJAR KA, AND MCCRAE KR. High affinity binding of beta 2-glycoprotein I to human endothelial cells is mediated by annexin 2. *J Biol Chem* 275: 15541–15548, 2000.
187. MAI J, FINLEY RL, WAISMAN DM, AND SLOANE BF. Human procathepsin B interacts with the annexin II tetramer on the surface of tumor cells. *J Biol Chem* 275: 12806–12812, 2000.
188. MAILLIARD WS, HAIGLER HT, AND SCHLAEPFER DD. Calcium dependent binding of S100C to the N-terminal domain of annexin I. *J Biol Chem* 271: 719–725, 1996.
189. MAJEED M, PERSKVIST N, ERNST JD, ORSELJUS K, AND STENDAHL O. Roles of calcium and annexins in phagocytosis and elimination of an attenuated strain of *Mycobacterium tuberculosis* in human neutrophils. *Microb Pathog* 24: 309–320, 1998.
190. MATSUSHIMA N, CREUTZ CE, AND KRETSINGER RH. Polyproline, beta-turn helices. Novel secondary structures proposed for the tandem repeats within rhodopsin, synaptophysin, synexin, gliadin, RNA polymerase II, hordein, and gluten. *Proteins* 7: 125–155, 1990.
191. MATTEO RG AND MORAVEC CS. Immunolocalization of annexins IV, V and VI in the failing and non-failing human heart. *Cardiovasc Res* 45: 961–970, 2000.
192. MEERS P AND MEALY T. Relationship between annexin V tryptophan exposure, calcium, and phospholipid binding. *Biochemistry* 32: 5411–5418, 1993.
193. MEGLI FM, SELVAGGI M, LIEMANN S, QUAGLIARIELLO E, AND HUBER R. The calcium-dependent binding of annexin V to phospholipid vesicles influences the bilayer inner fluidity. *Biochemistry* 37: 10540–10546, 1998.
194. MENAA C, DEVLIN RD, REDDY SV, GAZITT Y, CHOI SJ, AND ROODMAN GD. Annexin II increases osteoclast formation by stimulating the proliferation of osteoclast precursors in human marrow cultures. *J Clin Invest* 103: 1605–1613, 1999.
195. MENELL JS, CESARMAN GM, JACOVINA TA, MCLAUGHLIN MA, LEV AE, AND HAJJAR KA. Annexin II and bleeding in acute promyelocytic leukemia. *N Engl J Med* 340: 994–1004, 1999.
196. MERRIFIELD CJ, RESCHER U, ALMERS W, PROUST J, GERKE V, SECHI AS, AND MOSS SE. Annexin 2 has an essential role in actin-based macropinocytic rocketing. *Curr Biol* 11: 1136–1141, 2001.
197. MICHAELY P, KAMAL A, ANDERSON RG, AND BENNETT V. A requirement for ankyrin to clathrin coated pit budding. *J Biol Chem* 274: 35908–35913, 1999.
198. MINN AJ, VELEZ P, SCHENDEL SL, LIANG H, MUCHMORE SW, FESIK SW, FILL M, AND THOMPSON CB. Bcl-x(L) forms an ion channel in synthetic lipid membranes. *Nature* 385: 353–357, 1997.
199. MOORE PB, KRAUS FRIEDMANN N, AND DEDMAN JR. Unique calcium-dependent hydrophobic binding proteins: possible independent mediators of intracellular calcium distinct from calmodulin. *J Cell Sci* 72: 121–133, 1984.
200. MORGAN RO, BELL DW, TESTA JR, AND FERNANDEZ MP. Genomic locations of *ANX11* and *ANX13* and the evolutionary genetics of human annexins. *Genomics* 48: 100–110, 1998.
201. MORGAN RO, BELL DW, TESTA JR, AND FERNANDEZ M-P. Human annexin 31 genetic mapping and origin. *Gene* 227: 33–38, 1999.
202. MORGAN RO AND FERNANDEZ MP. Distinct annexin subfamilies in plants and protists diverged prior to animal annexins and from a common ancestor. *J Mol Evol* 44: 178–188, 1997.
203. MORGAN RO AND FERNANDEZ MP. Annexin gene structures and molecular evolutionary genetics. *Cell Mol Life Sci* 53: 508–515, 1997.
204. MORGAN RO, JENKINS NA, GILBERT DJ, COPELAND NG, BALSARA BR, TESTA JR, AND FERNANDEZ MP. Novel human and mouse annexin A10 are linked to the genome duplications during early chordate evolution. *Genomics* 60: 40–49, 1999.
205. MOSS SE AND CRUMPTON MJ. Alternative splicing gives rise to two

- forms of the p68 calcium-binding protein. *FEBS Lett* 261: 299–302, 1990.
206. MOVITZ C AND DAHLGREN C. Endogenous cleavage of annexin I generates a truncated protein with a reduced calcium requirement for binding to neutrophil secretory vesicles and plasma membrane. *Biochim Biophys Acta* 1468: 231–238, 2000.
 207. MOVITZ C, SJOLIN C, AND DAHLGREN C. Cleavage of annexin I in human neutrophils by a membrane-localized metalloprotease. *Biochim Biophys Acta* 1416: 101–108, 1999.
 208. MUIMO R, HORNICKOVA Z, RIEMEN C, GERKE V, MATTHEWS H, AND MEHTA A. Histidine phosphorylation of annexin I in airway epithelia. *J Biol Chem* 275: 36632–36636, 2000.
 209. MUKHERJEE S AND MAXFIELD FR. Role of membrane organization and membrane domains in endocytic lipid trafficking. *Traffic* 1: 203–211, 2000.
 210. MUKHOPADHYAY S AND CHO WH. Interactions of annexin V with phospholipid monolayers. *Biochim Biophys Acta* 1279: 58–62, 1996.
 211. NACIFF JM, BEHBEHANI MM, KAETZEL MA, AND DEDMAN JR. Annexin VI modulates Ca^{2+} and K^{+} conductances of spinal cord and dorsal root ganglion neurons. *Am J Physiol Cell Physiol* 271: C2004–C2015, 1996.
 212. NAKATA T, SOBUE K, AND HIROKAWA N. Conformational change and localization of calpactin I complex involved in exocytosis as revealed by quick-freeze deep-etch electron microscopy and immunocytochemistry. *J Cell Biol* 110: 13–25, 1990.
 213. NILIUS B, GERKE V, PRENEN J, SZÜCS G, HEINKE S, WEBER K, AND DROOGMANS G. Annexin II modulates volume-activated chloride currents in vascular endothelial cells. *J Biol Chem* 271: 30631–30636, 1996.
 214. NODA Y, OKADA Y, SAITO N, SETOU M, XU Y, ZHANG Z, AND HIROKAWA N. Kifc3, a microtubule minus end-directed motor for the apical transport of annexin XIIIb-associated Triton-insoluble membranes. *J Cell Biol* 155: 77–88, 2001.
 215. OH J, RHEE HJ, KIM S, KIM SB, YOU H, KIM JH, AND NA DS. Annexin-I inhibits PMA-induced *c-fos* SRE activation by suppressing cytosolic phospholipase A_2 signal. *FEBS Lett* 477: 244–248, 2000.
 216. OLIFERENKO S, PAIHA K, HARDER T, GERKE V, SCHWARZLER C, SCHWARZ H, BEUG H, GÜNTHER U, AND HUBER L. Analysis of CD44-containing lipid rafts: recruitment of annexin II and stabilization by the actin cytoskeleton. *J Cell Biol* 146: 843–854, 1999.
 217. ORITO A, KUMANOGOH H, YASAKA K, SOKAWA J, HIDAKA H, SOKAWA Y, AND MAEKAWA S. Calcium-dependent association of annexin VI, protein kinase C α , and neurocalcin α on the raft fraction derived from the synaptic plasma membrane. *J Neurosci Res* 64: 235–241, 2001.
 218. ORTEGA D, POL A, BIERMER M, JÄCKLE S, AND ENRICH C. Annexin VI defines an apical endocytic compartment in rat liver hepatocytes. *J Cell Sci* 111: 261–269, 1998.
 219. OSTERLOH D, WITTBRODT J, AND GERKE V. Characterization and developmentally regulated expression of four annexins in the killifish medaka. *DNA Cell Biol* 17: 835–847, 1998.
 220. PENCIL SD AND TOTH M. Elevated levels of annexin I protein in vitro and in vivo in rat and human mammary adenocarcinoma. *Clin Exp Metastasis* 16: 113–121, 1998.
 221. PERRETTI M. Endogenous mediators that inhibit the leukocyte-endothelium interaction. *Trends Pharmacol Sci* 18: 418–425, 1997.
 222. PERRETTI M. Lipocortin 1 and chemokine modulation of granulocyte and monocyte accumulation in experimental inflammation. *Gen Pharmacol* 31: 545–552, 1998.
 223. PERRETTI M, CHRISTIAN H, WHELLER SK, AJELLO I, MUGRIDGE KG, MORRIS JF, FLOWER RJ, AND GOULDING NJ. Annexin I is stored within gelatinase granules of human neutrophil and mobilized on the cell surface upon adhesion but not phagocytosis. *Cell Biol Int* 24: 163–174, 2000.
 224. PERRETTI M, CROXTALL JD, WHELLER SK, GOULDING NJ, HANNON R, AND FLOWER RJ. Mobilizing lipocortin 1 in adherent human leukocytes downregulates their transmigration. *Nature Med* 2: 1259–1262, 1996.
 225. PERRETTI M, GETTING SJ, SOLITO E, MURPHY PM, AND GAO JL. Involvement of the receptor for formylated peptides in the in vivo antimigratory actions of annexin I and its mimetics. *Am J Pathol* 158: 1969–1973, 2001.
 226. PERRETTI M, WHELLER SK, CHOUDHURY Q, CROXTALL JD, AND FLOWER RJ. Selective inhibition of neutrophil function by a peptide derived from lipocortin 1 N-terminus. *Biochem Pharmacol* 50: 1037–1042, 1995.
 227. PFANNMÜLLER E, TURNAY J, BERTLING W, AND VON DER MARK K. Organisation of the chicken annexin V gene and its correlation with the tertiary structure of the protein. *FEBS Lett* 336: 467–471, 1993.
 228. PHILIP JG, FLOWER RJ, AND BUCKINGHAM JC. Blockade of the classical pathway of protein secretion does not affect the cellular exportation of lipocortin I. *Regul Peptides* 73: 133–139, 1998.
 229. PIGAULT C, FOLLENIUS WA, SCHMUTZ M, FREYSSINET JM, AND BRISSON A. Formation of two-dimensional arrays of annexin V on phosphatidylserine-containing liposomes. *J Mol Biol* 236: 199–208, 1994.
 230. PITTIS MG AND GARCIA RC. Annexin VII and XI are present in a human macrophage-like cells line. Differential translocation on FcR-mediated phagocytosis. *J Leukoc Biol* 66: 845–850, 1999.
 231. PLANT PJ, LAFONT F, LECAT S, VERKADE P, SIMONS K, AND ROTIN D. Apical membrane targeting of Nedd 4 is mediated by an association of its C2 domain with annexin XIIIb. *J Cell Biol* 149: 1473–1483, 2000.
 232. POLLARD HB, GUY HR, ARISPE N, DE LA FUENTE M, LEE G, ROJAS EM, POLLARD JR, SRIVASTAVA M, ZHANG-KECK Z-Y, MEREZHINSKAYA N, CAO-HUY H, BURNS AL, AND ROJAS E. Calcium channel and membrane fusion activity of synexin and other members of the annexin gene family. *Biophys J* 62: 15–18, 1992.
 233. POLLARD HB AND ROJAS E. Ca^{2+} -activated synexin forms highly selective, voltage-gated Ca^{2+} channels in phosphatidylserine bilayer membranes. *Proc Natl Acad Sci USA* 85: 2974–2978, 1988.
 234. PONS M, GREWAL T, RIUS E, SCHNITGERHANS T, JACKLE S, AND ENRICH C. Evidence for the involvement of annexin 6 in the trafficking between the endocytic compartment and lysosomes. *Exp Cell Res* 269: 13–22, 2001.
 235. PONS M, IHRKE G, KOCH S, BIERMER M, POL A, JÄCKLE S, AND ENRICH C. Late endocytic compartments are major sites of annexin VI localization in NRK fibroblasts and polarized WIF-B hepatoma cells. *Exp Cell Res* 257: 33–47, 2000.
 236. POWELL MA AND GLENNEY JR JR. Regulation of calpactin I phospholipid binding by calpactin I light-chain binding and phosphorylation by $p60^{src}$. *Biochem J* 247: 321–328, 1987.
 237. PRATT SL AND HORSEMAN ND. Identification of two Y-Box binding proteins that interact with the promoters of columbid annexin I genes. *Gene* 214: 147–156, 1998.
 238. PREVOSTEL C, ALICE V, JOUBERT D, AND PARKER PJ. Protein kinase C actively downregulates through caveolae-dependent traffic to an endosomal compartment. *J Cell Sci* 113: 2575–2584, 2000.
 239. RAND JH. “Annexinopathies”—a new class of diseases. *N Engl J Med* 340: 1035–1036, 1999.
 240. RAND JH. Antiphospholipid antibody-mediated disruption of the annexin V antithrombotic shield: a thrombogenic mechanism for the antiphospholipid syndrome. *J Autoimmun* 15: 107–111, 2000.
 241. RAND JH AND WU XX. Antibody-mediated disruption of the annexin V antithrombotic shield: a new mechanism for thrombosis in the antiphospholipid syndrome. *Thromb Haemostasis* 82: 649–655, 1999.
 242. RAND JH, WU XX, ANDREE HA, LOCKWOOD CJ, GULLER S, SCHER J, AND HARPEL PC. Pregnancy loss in the antiphospholipid-antibody syndrome—a possible thrombogenic mechanism. *N Engl J Med* 337: 154–160, 1997.
 243. RAND JH, WU XX, GULLER S, GIL J, GUHA A, SCHER J, AND LOCKWOOD CJ. Reduction of annexin-V (placental anticoagulant protein-I) on placental villi of women with antiphospholipid antibodies and recurrent spontaneous abortion. *Am J Obstet Gynecol* 171: 1566–1572, 1994.
 244. RAYNAL P AND POLLARD HB. Annexins: the problem of assessing the biological role for a gene family of multifunctional calcium- and phospholipid-binding proteins. *Biochim Biophys Acta* 1197: 63–93, 1994.
 245. RESCHER U, ZOBIAK N, AND GERKE V. Intact Ca^{2+} binding sites are required for targeting annexin I to endosomal membranes in living HeLa cells. *J Cell Sci* 113: 3931–3938, 2000.
 246. RETY S, OSTERLOH D, ARIE J-P, TABARIES S, SEEMANN J, RUSSO-MARIE F, GERKE V, AND LEWIT-BENTLEY A. Structural basis of the $Ca(2+)$ -

- dependent association between S100C (S100A11) and its target, the N-terminal part of annexin I. *Structure* 8: 175–184, 2000.
247. RETY S, SOPKOVA J, RENOARD M, OSTERLOH D, TABARIES S, RUSSO-MARIE F, AND LEWIT-BENTLEY A. The crystal structure of a complex of p11 with the annexin II N-terminal peptide. *Nature Struct Biol* 6: 89–95, 1999.
 248. REVIKINE I, BERGSMAS-SCHUTTER W, AND BRISSON A. Growth of protein 2-D crystals on supported planar lipid bilayers imaged in situ by AFM. *J Struct Biol* 121: 356–361, 1998.
 249. REVIKINE I, BERGSMAS-SCHUTTER W, MAZERES-DUBUT C, GOVORUKHINA N, AND BRISSON A. Surface topography of the p3 and p6 annexin V crystal forms determined by atomic force microscopy. *J Struct Biol* 131: 234–239, 2000.
 250. RHEE HJ, KIM GY, HUH JW, KIM SW, AND NA DS. Annexin I is a stress protein induced by heat, oxidative stress and a sulfhydryl-reactive agent. *Eur J Biochem* 267: 3220–3225, 2000.
 251. RODRIGUEZ-GARCIA M-I, MORGAN RO, FERNANDEZ M-R, BANCES P, AND FERNANDEZ M-P. Mouse annexin V genomic organization includes an endogenous retrovirus. *Biochem J* 337: 125–131, 1999.
 252. ROJAS E AND POLLARD HB. Membrane capacity measurements suggest a calcium-dependent insertion of synexin into phosphatidylserine bilayers. *FEBS Lett* 217: 25–31, 1987.
 253. ROJAS E, POLLARD HB, HAIGLER HT, PARRA C, AND BURNS AL. Calcium-activated endonexin II forms calcium channels across acidic phospholipid bilayer membranes. *J Biol Chem* 265: 21207–21215, 1990.
 254. ROSALES JL AND ERNST JD. Calcium-dependent neutrophil secretion: characterization and regulation by annexins. *J Immunol* 159: 6195–6202, 1997.
 255. ROSENGARTH A, GERKE V, AND LUECKE H. X-ray structure of full-length annexin I and implications for membrane aggregation. *J Mol Biol* 306: 489–498, 2001.
 256. ROSENGARTH A, RÖSGEN J, HINZ H-J, AND GERKE V. A comparison of the energetics of annexin I and annexin V. *J Mol Biol* 288: 1013–1025, 1999.
 257. ROSENGARTH A, RÖSGEN J, HINZ H-J, AND GERKE V. Folding energetics of ligand binding proteins. II. Cooperative binding of Ca^{2+} ions to annexin I. *J Mol Biol* 306: 825–835, 2001.
 258. ROSENGARTH A, WINTERGALEN A, GALLA H-J, HINZ H-J, AND GERKE V. Ca^{2+} independent interaction of annexin I with phospholipid membranes. *FEBS Lett* 438: 279–284, 1998.
 259. ROTHUT B. Participation of annexins in protein phosphorylation. *Cell Mol Life Sci* 53: 522–526, 1997.
 260. RUSSO-MARIE F. Lipocortins as antiphospholipase A_2 and anti-inflammatory proteins. In: *Biochemistry, Molecular Biology and Physiology of Phospholipase A_2 and Its Regulatory Factors*, edited by Mukherjee AB. New York: Plenum, 1990, p. 197–210.
 261. RUSSO-MARIE F. Annexin V and phospholipid metabolism. *Clin Chem Lab Med* 37: 287–291, 1999.
 262. SAGOT I, REGNOUF F, HENRY JP, AND PRADEL LA. Translocation of cytosolic annexin 2 to a Triton-insoluble membrane subdomain upon nicotine stimulation of chromaffin cultured cells. *FEBS Lett* 410: 229–234, 1997.
 263. SARAFIAN T, PRADEL L-A, HENRY J-P, AUNIS D, AND BADER M-F. The participation of annexin II (Calpactin I) in calcium-evoked exocytosis requires protein kinase C. *J Cell Biol* 114: 1135–1147, 1991.
 264. SATO H, OGATA H, AND DE LUCA LM. Annexin V inhibits the 12-O-tetradecanoylphorbol-13-acetate-induced activation of Ras/extracellular signal-regulated kinase (ERK) signaling pathway upstream of Shc in MCF-7 cells. *Oncogene* 19: 2904–2912, 2000.
 265. SATOH A, HAZUKI H, KOJIMA K, HIRABAYASHI J, AND MATSUMOTO I. Ligand-binding properties of annexin from *Caenorhabditis elegans* (annexin 16, Nex-1). *J Biochem (Tokyo)* 128: 377–381, 2000.
 266. SATOH A, SUZUKI K, TAKAYAMA E, KOJIMA K, HIDAKA T, KAWAKAMI M, MATSUMOTO I, AND OHSUZU F. Detection of anti-annexin IV and V antibodies in patients with antiphospholipid syndrome and systemic lupus erythematosus. *J Rheumatol* 26: 1715–1720, 1999.
 267. SCHAFER BW AND HEIZMANN CW. The S100 family of EF-hand calcium-binding proteins: functions and pathology. *Trends Biochem Sci* 21: 134–140, 1996.
 268. SCHENDEL SL, XIE Z, MONTAL MO, MATSUYAMA S, MONTAL M, AND REED JC. Channel formation by antiapoptotic protein Bcl-2. *Proc Natl Acad Sci USA* 94: 5113–5118, 1997.
 269. SCHLAEPFER DD, BODE HR, AND HAIGLER HT. Distinct cellular expression pattern of annexins in *Hydra vulgaris*. *J Cell Biol* 118: 911–928, 1992.
 270. SCHLAEPFER DD, FISHER DA, BRANDT ME, BODE HR, JONES JM, AND HAIGLER HT. Identification of a novel annexin in *Hydra vulgaris*. *J Biol Chem* 267: 9529–9539, 1992.
 271. SCHLESINGER PH, GROSS A, YIN XM, YAMAMOTO K, SAITO M, WAKSMAN G, AND KORSMEYER SJ. Comparison of the ion channel characteristics of proapoptotic BAX and antiapoptotic BCL-2. *Proc Natl Acad Sci USA* 94: 11357–11362, 1997.
 272. SCHMITZ-PFEIFFER C, BROWNE CL, WALKER J, AND BIDEN TJ. Activated protein kinase C α associates with annexin VI from skeletal muscle. *Biochem J* 330: 675–681, 1998.
 273. SEEMANN J, WEBER K, AND GERKE V. Structural requirements for annexin I-S100C complex formation. *Biochem J* 319: 123–129, 1996.
 274. SEEMANN J, WEBER K, AND GERKE V. Annexin I targets S100C to early endosomes. *FEBS Lett* 413: 185–190, 1997.
 275. SEEMANN J, WEBER K, OSBORN M, PARTON RG, AND GERKE V. The association of annexin I with early endosomes is regulated by Ca^{2+} and requires an intact N-terminal domain. *Mol Biol Cell* 7: 1359–1374, 1996.
 276. SENDA T, OKABE T, MATSUDA M, AND FUJITA H. Quick-freeze, deep-etch visualization of exocytosis in anterior pituitary secretory cells: localization and possible roles of actin and annexin II. *Cell Tissue Res* 277: 51–60, 1994.
 277. SENDA T, YAMASHITA K, OKABE T, SUGIMOTO N, AND MATSUDA M. Intergranule bridges in the anterior pituitary cell and their possible involvement in Ca^{2+} -induced granule-granule fusion. *Cell Tissue Res* 292: 513–519, 1998.
 278. SIATAK C, LAMBERT M, CARON C, AMIRAL J, HACHULLA E, HATRON PY, AND GOUDEMAND J. Low prevalence of anti-annexin V antibodies in antiphospholipid syndrome with fetal loss. *Rev Med Intern* 20: 762–765, 1999.
 279. SIMONS K AND GRUENBERG J. Jamming the endosomal system: lipid rafts and lysosomal storage diseases. *Trends Cell Biol* 10: 459–462, 2000.
 280. SIMONS K AND IKONEN E. Functional rafts in cell membranes. *Nature* 387: 569–572, 1997.
 281. SIMONS K AND TOOMRE D. Lipid rafts and signal transduction. *Nature Rev* 1: 31–39, 2000.
 282. SINGH TK AND LIU L. Modification of cysteine residues by N-ethylmaleimide inhibits annexin II tetramer mediated liposome aggregation. *Arch Biochem Biophys* 381: 135–140, 2000.
 283. SINHA P, HUTTER G, KOTTGEN E, DIETEL M, SCHADENDORF D, AND LAGE H. Increased expression of annexin I and thioredoxin detected by two-dimensional gel electrophoresis of drug resistant human stomach cancer cells. *J Biochem Biophys Methods* 37: 105–116, 1998.
 284. SJOLIN C, MOVITZ C, LUNDQVIST H, AND DAHLGREN C. Translocation of annexin XI to neutrophil subcellular organelles. *Biochim Biophys Acta* 1326: 149–156, 1997.
 285. SMITH PD, DAVIES A, CRUMPTON MJ, AND MOSS SE. Structure of the human annexin VI gene. *Proc Natl Acad Sci USA* 91: 2713–2717, 1994.
 286. SMITH PD AND MOSS SE. Structural evolution of the annexin supergene family. *Trends Genet* 10: 241–246, 1994.
 287. SMITH PD AND MOSS SE. Z-DNA-forming sequences at a putative duplication site in the human annexin VI-encoding gene. *Gene* 138: 239–242, 1994.
 288. SMYTHE E, SMITH PD, JACOB SM, THEOBALD J, AND MOSS SE. Endocytosis occurs independently of annexin VI in human A431 cells. *J Cell Biol* 124: 301–306, 1994.
 289. SOKOLOV Y, MAILLIARD WS, TRANNGO N, ISAS M, LUECKE H, HAIGLER HT, AND HALL JE. Annexins V and XII alter the properties of planar lipid bilayers seen by conductance probes. *J Gen Physiol* 115: 571–582, 2000.
 290. SOLITO E, DE COUPADE C, PARENTE L, FLOWER RJ, AND RUSSO-MARIE F. IL-6 stimulates annexin 1 expression and translocation and suggests a new biological role as class II acute phase protein. *Cytokine* 10: 514–521, 1998.
 291. SOLITO E, ROMERO IA, MARULLO S, RUSSO-MARIE F, AND WEKSLER BB. Annexin 1 binds to U937 monocytic cells and inhibits their adhesion to microvascular endothelium. *J Immunol* 165: 1573–1581, 2000.
 292. SONG GJ, CAMPOS B, WAGONER LE, DEDMAN JR, AND WALSH RA.

- Altered cardiac annexin mRNA and protein levels in the left ventricle of patients with end-stage heart failure. *J Mol Cell Cardiol* 30: 443–451, 1998.
293. SOPKOVA J, RENOUDARD M, AND LEWIT BA. The crystal structure of a new high-calcium form of annexin V. *J Mol Biol* 234: 816–825, 1993.
 294. SOPKOVA-DE OLIVEIRA SANTOS J, VINCENT M, TABARIES S, CHEVALIER A, KERBOEUF D, RUSSO-MARIE F, LEWIT-BENTLEY A, AND GALLAY J. Annexin A5 D226K structure and dynamics: identification of a molecular switch for the large scale conformational change of domain III. *FEBS Lett* 493: 122–128, 2001.
 295. SOPKOVA J, VINCENT M, TAKAHASHI M, LEWIT-BENTLEY A, AND GALLAY J. Conformational flexibility of domain III of annexin V studied by fluorescence of tryptophan 187 and circular dichroism: the effect of pH. *Biochemistry* 37: 11962–11970, 1998.
 296. SOPKOVA J, VINCENT M, TAKAHASHI M, LEWIT-BENTLEY A, AND GALLAY J. Conformational flexibility of domain II of annexin V at membrane/water interfaces. *Biochemistry* 38: 5447–5458, 1999.
 297. SPENNEBERG R, OSTERLOH D, AND GERKE V. Phospholipid vesicle binding and aggregation by four novel fish annexins are differently regulated by Ca^{2+} . *Biochim Biophys Acta* 1448: 311–319, 1998.
 298. SPRINGER TA. Traffic signals for lymphocyte recirculation and leukocyte emigration: the multistep paradigm. *Cell* 76: 301–314, 1994.
 299. SRIVASTAVA M, ATWATER I, GLASMAN M, LEIGHTON X, GOPING G, CAO HUY H, MILLER G, PICHEL J, WESTPHAL H, MEARS D, ROJAS E, AND POLLARD HB. Defects in inositol 1,4,5-trisphosphate receptor expression, Ca^{2+} signaling, and insulin secretion in the *anx7(+/-)* knockout mouse. *Proc Natl Acad Sci USA* 96: 13783–13788, 1999.
 300. SRIVASTAVA M, BUBENDORF L, SRIKANTAN V, FOSSOM L, NOLAN L, GLASMAN M, LEIGHTON X, FEHRLE W, PITTALUGA S, RAFFELD M, KOIVISTO P, WILLI N, GASSER TC, KONONEN J, SAUTER G, KALLIONIEMI OP, SRIVASTAVA S, AND POLLARD HP. Anx7, a candidate tumor suppressor gene for prostate cancer. *Proc Natl Acad Sci USA* 98: 4575–4580, 2001.
 301. SRIVASTAVA M AND POLLARD HB. Low in vivo levels of human anx7 (annexin vii) gene expression are due to endogenous inhibitory promoter sequences. *Cell Biol Int* 24: 475–481, 2000.
 302. SUDO T AND HIDAKA H. Regulation of calyculin (S100A6) binding by alternative splicing in the N-terminal regulatory domain of annexin XI isoforms. *J Biol Chem* 273: 6351–6357, 1998.
 303. SUDO T AND HIDAKA H. Characterization of the calyculin (S100A6) binding site of annexin XI-A by site-directed mutagenesis. *FEBS Lett* 444: 11–14, 1999.
 304. SULLIVAN DM, WEHR NB, FERGUSSON MM, LEVINE RL, AND FINKEL T. Identification of oxidant-sensitive proteins: TNF- α induces protein glutathiolation. *Biochemistry* 39: 11121–11128, 2000.
 305. SWAIRJO MA AND SEATON BA. Annexin structure and membrane interactions: a molecular perspective. *Annu Rev Biophys Biomol Struct* 23: 193–213, 1994.
 306. TABENGWA EM, ABOU-AGAG LH, BENZA RL, TORRES JA, AIKENS ML, AND BOOYSE FM. Ethanol-induced up-regulation of candidate plasminogen receptor annexin II in cultured human endothelial cells. *Alcohol Clin Exp Res* 24: 754–761, 2000.
 307. TANAKA T, KONDO S, IWASA Y, HIAI H, AND TOYOKUNI S. Expression of stress-response and cell proliferation genes in renal cell carcinoma induced by oxidative stress. *Am J Pathol* 156: 2149–2157, 2000.
 308. TAYLOR AD, PHILIP JG, JOHN CD, COVER PO, MORRIS JF, FLOWER RJ, AND BUCKINGHAM JC. Annexin I (lipocortin 1) mediates the glucocorticoid inhibition of cyclic adenosine 3',5'-monophosphate-stimulated prolactin secretion. *Endocrinology* 141: 2209–2219, 2000.
 309. THEOBALD J, HANBY A, PATEL K, AND MOSS SE. Annexin VI has tumour-suppressor activity in human A431 squamous epithelial carcinoma cells. *Br J Cancer* 71: 786–788, 1995.
 310. THONAT C, MATHIEU C, CREVECOEUR M, PENEL C, GASPAR T, AND BOYER N. Effects of a mechanical stimulation on localization of annexin-like proteins in *Bryonia dioica* internodes. *Plant Physiol* 114: 981–988, 1997.
 311. TOKUMITSU H, MIZUTANI A, AND HIDAKA H. Calyculin-binding site located on the NH₂-terminal domain of rabbit CAP-50 (annexin XI): functional expression of CAP-50 in *Escherichia coli*. *Arch Biochem Biophys* 303: 302–306, 1993.
 312. TOKUMITSU H, MIZUTANI A, MINAMI H, KOBAYASHI R, AND HIDAKA H. A calyculin-associated protein is a newly identified member of the Ca^{2+} /phospholipid-binding proteins, annexin family. *J Biol Chem* 267: 8919–8924, 1992.
 313. TRAVERSO V, MORRIS JF, FLOWER RJ, AND BUCKINGHAM J. Lipocortin 1 (annexin I) in patches associated with the membrane of a lung adenocarcinoma cell line and in the cytoplasm. *J Cell Sci* 111: 1405–1418, 1998.
 314. TRIPLETT DA AND ASHERSON RA. Pathophysiology of the catastrophic antiphospholipid syndrome (CAPS). *Am J Hematol* 65: 154–159, 2000.
 315. TRISCHLER M, STOOORVOGEL W, AND ULLRICH O. Biochemical analysis of distinct Rab5- and Rab11-positive endosomes along the transferrin pathway. *J Cell Sci* 112: 4773–4783, 1999.
 316. TROUET D, NILIUS B, JACOBS A, REMACLE C, DROOGMANS G, AND EGERMONT J. Caveolin-1 modulates the activity of the volume-regulated chloride channel. *J Physiol (Lond)* 520: 113–119, 1999.
 317. TROUPE P, LEGOT S, BELIKOVA I, MAROTTE F, BENEVOLENSKY D, RUSSO-MARIE F, SAMUEL JL, AND CHARLEMAGNE D. Localization and quantitation of cardiac annexins II, V, and VI in hypertensive guinea pigs. *Am J Physiol Heart Circ Physiol* 276: H1159–H1166, 1999.
 318. TURPIN E, RUSSO-MARIE F, DUBOIS T, DE PAILLERETS C, ALFSEN A, AND BOMSEL M. In adrenocortical tissue, annexins II and VI are attached to clathrin coated vesicles in a calcium-independent manner. *Biochim Biophys Acta* 1402: 115–130, 1998.
 319. TZIMA E, TROTTER PJ, HASTINGS AD, ORCHARD MA, AND WALKER JH. Investigation of the relocation of cytosolic phospholipase A₂ and annexin V in activated platelets. *Thromb Res* 97: 421–429, 2000.
 320. TZIMA E, TROTTER PJ, ORCHARD MA, AND WALKER JH. Annexin V binds to the actin-based cytoskeleton at the plasma membrane of activated platelets. *Exp Cell Res* 251: 185–193, 1999.
 321. TZIMA E, TROTTER PJ, ORCHARD MA, AND WALKER JH. Annexin V relocates to the platelet cytoskeleton upon activation and binds to a specific isoform of actin. *Eur J Biochem* 267: 4720–4730, 2000.
 322. TZIMA E AND WALKER JH. Platelet annexin V: the ins and outs. *Platelets* 11: 245–251, 2000.
 323. UHRIN P AND HORSEMAN ND. Regulation of the annexin Icp35 gene in transfected mammary gland cell lines. *Biochem Mol Biol Int* 30: 305–310, 1993.
 324. VAARALA MH, PORVARI K, KYLLONEN A, AND VIHKO P. Differentially expressed genes in two LNCaP prostate cancer cell lines reflecting changes during prostate cancer progression. *Lab Invest* 80: 1259–1268, 2000.
 325. VAN GINKEL PR, GEE RL, WALKER TM, HU DN, HEIZMANN CW, AND POLANS AS. The identification and differential expression of calcium-binding proteins associated with ocular melanoma. *Biochim Biophys Acta* 1448: 290–297, 1998.
 326. VEDELER A AND HOLLAS H. Annexin II is associated with mRNA which may constitute a distinct subpopulation. *Biochem J* 348: 565–572, 2000.
 327. VERZILI D, ZAMPARELLI C, MATTEI B, NOEGEL AA, AND CHIANCONE E. The sorcin-annexin VII calcium-dependent interaction requires the sorcin N-terminal domain. *FEBS Lett* 471: 197–200, 2000.
 328. VOGL T, JATZKE C, HINZ H-J, BENZ J, AND HUBER R. Thermodynamic stability of annexin V E17G: equilibrium parameters from an irreversible unfolding reaction. *Biochemistry* 36: 1657–1668, 1997.
 329. VON DER MARK K AND MOLLENHAUER J. Annexin V interactions with collagen. *Cell Mol Life Sci* 53: 539–545, 1997.
 330. WAISMAN DM. Annexin II tetramer: structure and function. *Mol Cell Biochem* 149/150: 301–322, 1995.
 331. WALTHER A, RIEHEMANN K, AND GERKE V. A novel ligand of the formyl peptide receptor: annexin I regulates neutrophil extravasation by interacting with the FPR. *Mol Cell* 5: 831–840, 2000.
 332. WANG LM, RAHMAN MM, IIDA H, INAI T, KAWABATA S, IWANAGA S, AND SHIBATA Y. Annexin V is localized in association with Z-line of rat cardiac myocytes. *Cardiovasc Res* 30: 363–371, 1995.
 333. WANG X, CAMPOS B, KAETZEL MA, AND DEDMAN JR. Annexin V is critical in the maintenance of murine placental integrity. *Am J Obstet Gynecol* 180: 1008–1016, 1999.
 334. WEN Y, EDELMAN JL, KANG T, AND SACHS G. Lipocortin V may function as a signaling protein for vascular endothelial growth factor receptor-2/Ftk-1. *Biochem Biophys Res Commun* 258: 713–721, 1999.
 335. WENG X, LUECKE H, SONG IS, KANG DS, KM SH, AND HUBER R. Crystal

- structure of human annexin I at 2.5 Å resolution. *Protein Sci* 2: 448–458, 1993.
336. WICE BM AND GORDON JI. A strategy for isolation of cDNAs encoding proteins affecting human intestinal epithelial cell growth and differentiation: characterization of a novel gut-specific N-myristoylated annexin. *J Cell Biol* 116: 405–422, 1992.
337. WILLIAMS K, CHUBB C, HUBERMAN E, AND GIOMETTI CS. Analysis of differential protein expression in normal and neoplastic human breast epithelial cell lines. *Electrophoresis* 19: 333–343, 1998.
338. WU F, FLACH CR, SEATON BA, MEALY TR, AND MENDELSON R. Stability of annexin V in ternary complex with Ca^{2+} and anionic phospholipids: IR studies of monolayers and bulk phases. *Biochemistry* 38: 792–799, 1999.
339. XIE W, KAETZEL MA, BRUZIK KS, DEDMAN JR, SHEARS SB, AND NELSON DJ. Inositol 3,4,5,6-tetrakisphosphate inhibits the calmodulin-dependent protein kinase II-activated chloride conductance in T84 colonic epithelial cells. *J Biol Chem* 271: 14092–14097, 1996.
340. XU J, ZIEMNICKA D, MERZ GS, AND KOTULA L. Human spectrin src homology 3 domain binding protein 1 regulates macropinocytosis in NIH 3T3 cells. *J Cell Sci* 113: 3805–3814, 2000.
341. ZEUSCHNER D, STOORVOGEL W, AND GERKE V. Association of annexin 2 with recycling endosomes requires either calcium or cholesterol-stabilized membrane domains. *Eur J Cell Biol* 80: 499–507, 2001.
342. ZOBIACK N, GERKE V, AND RESCHER U. Complex formation and sub-membranous localization of annexin 2 and S100A10 in live HepG2 cells. *FEBS Lett* 500: 137–140, 2001.
343. ZOBIACK N, RESCHER U, LAARMANN S, MICHGEHL S, SCHMIDT MA, AND GERKE V. Cell surface attachment of pedestal-forming enteropathogenic *E. coli* induces a clustering of raft components and a recruitment of annexin 2. *J Cell Sci*. In press.

Pemphigus Vulgaris Antibody Identifies Pemphaxin

A NOVEL KERATINOCYTE ANNEXIN-LIKE MOLECULE BINDING ACETYLCHOLINE*

Received for publication, April 13, 2000, and in revised form, July 3, 2000
Published, JBC Papers in Press, July 17, 2000, DOI 10.1074/jbc.M003174200

Vu Thuong Nguyen, Assane Ndoeye, and Sergei A. Grando†

From the Department of Dermatology, University of California at Davis, Sacramento, California 95817

Because pemphigus vulgaris (PV) IgGs adsorbed on the rDsg3-Ig-His baculoprotein induced blisters in neonatal mice, it was proposed that anti-desmoglein 3 (Dsg 3) autoantibody causes PV. However, we found that rDsg3-Ig-His absorbs autoantibodies to different antigens, including a non-Dsg 3 keratinocyte protein of 130 kDa. This prompted our search for novel targets of PV autoimmunity. The PV IgG eluted from a 75-kDa keratinocyte protein band both stained epidermis in a pemphigus-like pattern and induced acantholysis in keratinocyte monolayers. Screening of a keratinocyte λ gt11 cDNA library with this antibody identified clones carrying cDNA inserts encoding a novel molecule exhibiting ~40% similarity with annexin-2, named pemphaxin (PX). Recombinant PX (rPX-His) was produced in *Escherichia coli* M15 cells, and, because annexins can act as cholinergic receptors, its conformation was tested in a cholinergic radioligand binding assay. rPX-His specifically bound [3 H]acetylcholine, suggesting that PX is one of the keratinocyte cholinergic receptors known to be targeted by disease-causing PV antibodies. Preabsorption of PV sera with rPX-His eliminated acantholytic activity, and eluted antibody immunoprecipitated native PX. This antibody alone did not cause skin blisters *in vivo*, but its addition to the preabsorbed PV IgG fraction restored acantholytic activity, indicating that acantholysis in PV results from synergistic action of antibodies to different keratinocyte self-antigens, including both acetylcholine receptors and desmosomal cadherins.

skin adhesion in which keratinocytes (KC), the stratified epithelial cells comprising the epidermis, lose their ability to adhere to one another (acantholysis) (1). Acantholysis leads to an intra-epidermal split and separation of the suprabasal epidermal layer, which is clinically manifested by blistering that denudes skin and oral mucosa. Introduction of glucocorticosteroids into the treatment of PV patients decreased mortality from 90 to 10% (reviewed in Ref. 2). Long-term corticosteroid therapy of PV patients is life-saving but causes severe side effects, including death (3, 4). This urges development of non-hormonal therapy of pemphigus acantholysis. The pathophysiology of PV includes an array of IgG autoantibodies reacting with keratinocyte self-antigens with the apparent molecular mass ranging from 12 to 190 kDa (reviewed in Ref. 5), including a 130-kDa keratinocyte polypeptide (6, 7). The notion that autoantibodies are the main cause of PV stems from the fact that passive transfer of pemphigus, but not normal, IgGs to neonatal mice can induce skin lesions characteristic of PV (8). Using pemphigus antibodies eluted from the 130-kDa band as a probe, Amagai *et al.* (9) screened the human keratinocyte λ gt11 cDNA library and found that two of the clones recognized by these PV antibodies represented a novel desmosomal cadherin termed desmoglein (Dsg) 3. The hypothesis that PV, a disease of skin adhesion, is caused by an antibody to Dsg 3, an adhesion molecule, prompted experiments toward elucidation of the biological effects of anti-Dsg 3 antibody. However, acantholysis could not be documented in keratinocyte monolayers treated with anti-Dsg 3 antibody. Several recombinant Dsg 3 (rDsg3) proteins were produced and used to test if adsorbed antibodies can elicit skin blistering in neonatal mice upon passive transfer (10, 11). Although rDsg3 could absorb PV antibodies to Dsg 3, it failed to absorb all disease-causing antibody, and PV IgGs depleted of antibodies to Dsg 3 kept binding to KC in murine epidermis and inducing gross skin blisters (10, 12). Only creation of a chimeric baculoprotein that included both the extracellular epitope of Dsg 3 and an Fc portion of human IgG₁ could fulfill both goals: elimination of all disease-causing antibodies from pemphigus serum and induction of gross skin blisters in neonatal mice injected with concentrated eluants (13, 14). Explanations of this phenomenon include: 1) a possibility that the IgG portion rendered the rDsg3 with appropriate conformational epitope, which could be tested by crystallography; and 2) a possibility that the tertiary structure of the chimera mimicked non-Dsg 3 targets of pemphigus autoimmunity, which could be tested by characterizing the antigenic profile of the eluted IgG. Neither possibility was tested. Recently, it has become evident that anti-Dsg 3 antibody alone is not sufficient to cause skin blisters (15). A role for an autoantibody to another desmosomal cadherin, Dsg1, was

Pemphigus vulgaris (PV¹) is a potentially lethal disease of

* This work was supported by the International Pemphigus Research Fund. Preliminary reports of these findings were presented at the Third Tricontinental Meeting of the Society for Investigative Dermatology, the European Society for Dermatological Research, and the Japanese Society for Investigative Dermatology, Cologne, Germany, May 9, 1998, and at the 60th Annual Meeting of the Society for Investigative Dermatology, Chicago, Illinois, May 7, 1999, and May 12, 2000, and published in abstract form in the *Journal of Investigative Dermatology* 110:486, 1998, and *Journal of Investigative Dermatology* 112:250, 1999, respectively. The costs of publication of this article were defrayed in part by the payment of page charges. This article must therefore be hereby marked "advertisement" in accordance with 18 U.S.C. Section 1734 solely to indicate this fact.

The nucleotide sequence(s) reported in this paper has been submitted to the GenBank™/EBI Data Bank with accession number(s) AF230929.

† To whom correspondence should be addressed: Dept. of Dermatology, University of California, Davis, UC Davis Medical Center, 4860 Y St., Suite 3400, Sacramento, CA 95817. Tel.: 916-734-6057; Fax: 916-734-6793; E-mail: sagrando@ucdavis.edu.

¹ The abbreviations used are: PV, pemphigus vulgaris; PX, pemphaxin; ACh, acetylcholine; DIF, direct immunofluorescence; Dsg, desmoglein; FITC, fluorescein isothiocyanate; IIF, indirect immunofluorescence; IPTG, isopropyl-D-thiogalactoside; KC, keratinocytes; KGM, serum-free keratinocyte growth medium; PBS, phosphate-buffered saline; PCR, polymerase chain reaction; PrBCM, propylbenzylcholine

mustard; rDsg, recombinant Dsg; rPX-His, recombinant PX; PAGE, polyacrylamide gel electrophoresis; TBS, Tris-buffered saline; bp, base pair(s); kb, kilobase(s); kbp, kilobase pair(s).

proposed to explain skin blisters in PV patients (16). However, well-documented cases of generalized disease in PV patients lacking Dsg1 antibody (17) argued in favor of the existence of a yet unidentified disease-causing non-Dsg1/Dsg 3 antibody that could have been nonspecifically preabsorbed with rDsg3-Ig constructs. Furthermore, intraperitoneal injection of the PV IgG, which did not have anti-Dsg1 activity, into neonatal *Dsg3* knockout mice (*i.e.* *Dsg3^{null}* mice) resulted in gross skin blisters (5). It should be mentioned that neonatal *Dsg3^{null}* mice lack the true PV phenotype, in that they do not develop spontaneous skin blisters (5, 18), which has already justified their use in passive transfer experiments by different research groups studying the nature of disease-causing PV antibodies (5, 15).

Recently, we have compared antibodies eluted from rDsg3 (rDsg3-His) and rDsg3-Ig (rDsg3-Ig-His), which were used in the original preabsorption experiments (10, 13, 14), and demonstrated that the two Dsg 3 constructs adsorb antibodies with different antigenic specificities (19). The PV IgGs eluted from rDsg3-His reacted predominantly with the 130-kDa protein band present in normal human KC in addition to a few weakly stained bands that varied among test PV sera. In marked contrast, the antibodies eluted from rDsg3-Ig-His recognized several different protein bands, including a non-Dsg 3 130-kDa band in the immunoblot of Dsg 3-/- keratinocyte proteins. Thus, crossreactivity of *Dsg3-Ig-His* with non-Dsg 3 antibodies explains how this chimeric baculoprotein could absorb all disease-causing PV IgG.

The vast majority of pemphigus patients develop antibodies that immunoprecipitate keratinocyte membrane proteins binding the covalent cholinergic radioligand [³H]propylbenzilylcholine mustard ([³H]PrBCM) (5) and compete with a cholinergic radioligand, [³H]atropine, for binding to the cell membrane of intact human KC in culture (20). The nature of the acetylcholine (ACh) receptor(s) targeted by PV autoimmunity remains to be determined. Addition to either muscarinic or nicotinic antagonists to keratinocyte monolayers in both cases results in acantholysis (reviewed in Refs. 21, 22), whereas cholinergic agonists stimulate cell-to-cell adhesion of KC, and can reverse, attenuate, or prevent acantholysis in keratinocyte monolayers when added to culture after, simultaneously with, or prior to PV IgG, respectively (20). The anti-acantholytic activity of cholinergic agonists suggests a novel avenue for development of non-hormonal treatment of pemphigus.

In this study, we demonstrate the nature of a novel target for non-Dsg 3 disease-causing PV IgG. Screening of the keratinocyte cDNA expression library with PV IgG immunoaffinity-purified on a 75-kDa area of the immunoblotting membrane revealed a novel human annexin-like molecule, which we named pemphaxin (PX). We produced recombinant PX (rPX-His) and demonstrated that this protein acts as a cholinergic receptor in the radioligand binding assay with [³H]ACh. PV IgG specifically recognized rPX-His, and preabsorption of PV sera with rPX-His eliminated the acantholytic activity that could be restored by adding back the anti-PX antibody eluted from the affinity column. Thus, disease-causing PV antibody identified PX, a novel human annexin that acts as a keratinocyte cell surface receptor for ACh, and, therefore, may mediate known biological effects of this cytotransmitter on adhesion and motility of KC.

EXPERIMENTAL PROCEDURES

Sources of Sera and Tissue—The sera and IgG fractions were from well-established PV patients, and from healthy volunteers. This study had been approved by the University of California Davis Human Subjects Review Committee. The diagnosis of PV was made based on the results of both comprehensive clinical and histological examinations together with immunological studies, which included direct immunofluorescence (DIF), indirect immunofluorescence (IIF) on various epi-

thelial substrates, immunoblotting, and immunoprecipitation, following standard protocols (23). The serum samples were stored frozen at -80 °C until use in experiments. The serum IgG fractions were isolated using 40% ammonium sulfate followed by dialysis with Ca²⁺- and Mg²⁺-free phosphate-buffered saline (PBS; Life Technologies, Inc., Gaithersburg, MD), lyophilized, and reconstituted in PBS as detailed elsewhere (5). The protein concentration was determined using the Micro BCA kit (Pierce). The samples of normal human neonatal foreskins that were used to start keratinocyte cell cultures were transported to the laboratory in culture medium, and the samples of normal human abdominoplasty skin that served as a source of keratinocyte membrane protein for immunoblotting were frozen immediately after harvesting.

Immunoaffinity Purification of Acantholytic Anti-keratinocyte PV Antibody—The enriched fraction of human keratinocyte membrane protein (5) was used as a substrate in immunoblotting experiments aimed at characterizing novel PV antigens. The epidermis was separated from the dermis by incubation in RPMI 1640 medium (Sigma), supplemented to contain 200 mM EDTA for 90 min at 37 °C and 5% CO₂ (24), and harvested into a 50-ml polyethylene centrifuge tube filled with ice-cold Tris-buffered saline (TBS), pH 7.4, that contained the following protease inhibitors: 2 mM phenylmethylsulfonyl fluoride, 0.1 mg/ml bacitracin, 10 µg/ml leupeptin, 10 µg/ml soybean trypsin inhibitor, 10 µg/ml pepstatin A, and 10 µg/ml chymostatin (all from Sigma). The epidermis was then washed three times by centrifugation, put on ice, and homogenized with a PowerGen tissue-and-cell disrupter (Fisher Scientific, Santa Clara, CA) in the same buffer containing 20 mM Ca²⁺. Large organelles and epidermal debris were removed by centrifugation at 2000 × *g* for 45 min at 4 °C, and the cell membrane fraction was pelleted from the supernatant by centrifugation at 80,000 × *g* for 1 h at 4 °C. The pellet was solubilized in sodium dodecyl sulfate-polyacrylamide gel electrophoresis (SDS-PAGE) buffer containing 2% SDS and 5% β-mercaptoethanol, boiled for 5 min, and cleared by centrifugation at 40,000 × *g* for 1 h at 4 °C. Western blotting of SDS-PAGE-resolved proteins was performed as reported previously (5) with minor modifications. Briefly, the proteins were separated on a 7.5% SDS-PAGE gel and transferred to an Immobilon-P membrane (Millipore Corp., Bedford, MA), which was blocked, first with 5% milk in TBS for 1 h at 37 °C and then with TBS containing 1% normal goat serum, 3% dried milk, and 0.05% Tween 20 (Sigma) overnight at 4 °C, and cut into 4-mm wide vertical strips. Each strip was exposed to a primary antibody, *i.e.* PV or normal human serum, for 1 h at room temperature and then washed thoroughly. The protein bands recognized by PV and normal human IgGs were visualized by biotinylated goat anti-human IgG antibody (Pierce) and developed using a biotin/avidin system (Vectastain ABC system; Vector Laboratories, Burlingame, CA). The specificity of binding was determined in negative control experiments, in which the primary antibodies were omitted. The PV IgG fractions were isolated from the immunoblotting membrane areas that were recognized uniquely by PV IgG, but not normal human IgG, following a procedure described previously (25). Briefly, approximately 3-mm wide horizontal strips carrying a keratinocyte membrane protein with a particular molecular mass of ±3 kDa were cut out from the immunoblotting membrane and incubated overnight with PV serum diluted 1:5 in TBS containing 20 mM CaCl₂, 0.05% Tween 20 (Sigma), and 1% non-fat skim milk to allow antibody binding. The strips were then washed thoroughly, and the antibodies were eluted by a 3-min incubation at 37 °C in a solution containing 500 µl of 20 mM sodium citrate, 1% milk, and 0.05% Tween 20 (pH 3.2) and immediately neutralized by adjusting the pH to 7.4 with the 2 M Tris base.

Immunofluorescence Screening Experiments—The IIF experiments testing the ability of PV IgG eluted from the strips of immunoblotting membranes to specifically stain KC in the tissue samples were performed as described previously (5) with minor modifications. Briefly, 4- to 8-mm cryostat sections of freshly frozen normal human skin, monkey esophagus, or murine skin were incubated overnight at 4 °C with the immunoaffinity-purified PV IgG fractions, after which the tissue sections were washed and binding of primary antibody was visualized by incubating the tissue section with fluorescein isothiocyanate (FITC)-labeled goat anti-human IgG antibody (Pierce) for 1 h at room temperature. The specificity of antibody binding was demonstrated by omitting the primary antibody, which abolished the staining. The immunofluorescence images were obtained using a fluorescence microscope (Axiovert 135, Carl Zeiss Inc., Thornwood, NY) with a charge-coupled device video camera (Photon Technology International, Monmouth Junction, NJ) attached.

Cell Culture Screening Experiments—Acantholytic activity of the eluted PV IgGs, which stained the stratified epithelial substrate in a

pemphigus-like, "intercellular" pattern, were tested in the monolayers of normal human foreskin KC isolated from the epidermis and grown at 37 °C in serum-free keratinocyte growth medium (KGM; Life Technologies, Inc.) containing 0.09 mM Ca^{2+} in a humid 5% CO_2 incubator, as detailed elsewhere (26). To observe changes in cell morphology, second passage KC were seeded into 6-well tissue culture plates at a cell density of 1×10^5 /well and grown to confluence (i.e. for 5–7 days) in 2 ml of KGM per well. The monolayers were then fed with equal amounts of test PV (experiment) or normal human serum (control) IgG fractions, 10 $\mu\text{g}/\text{ml}$ KGM, and returned to a 5% CO_2 incubator for a 12-h incubation at 37 °C. After incubation, the cells were fixed with 3% glutaraldehyde and stained with the trypan blue dye solution (Sigma), and the images of the experimental and control keratinocyte monolayers were captured using a camera-adapted light microscope (Olympus Corp., Lake Success, NY).

Screening of cDNA Library—Following standard procedures (27), the human keratinocyte $\lambda\text{gt}11$ cDNA library (CLONTECH, Palo Alto, CA) was screened with PV antibody that was immunoaffinity-purified from a 75-kDa keratinocyte membrane protein band. Briefly, the host bacteria Y1090r- were grown overnight, infected with phages from the library for 30 min, plated on Mg^{2+} -containing agar plates, and grown overnight at 37 °C. Over 3 million plaques formed on the bacterial lawns were screened by lifting isopropyl-D-thiogalactoside (IPTG; Sigma) containing nitrocellulose filters (Millipore Corp.). After blocking with 3% dry milk (Sigma) in TBS, the filters were incubated for 2 h at room temperature with the immunoaffinity-purified antibody. The plaques specifically recognized by the antibody were visualized using horseradish peroxidase-conjugated goat anti-human IgG (Bio-Rad, Hercules, CA). The positive plaques were isolated and rescreened until a single clone was isolated. The insert from isolated clones were amplified using a pair of cloning primers specific for the $\lambda\text{gt}11$ vector: 5'-ggggggggtaccggatccccgtgacgggtttccatag-3' (forward) and 5'-cccggatccataggtaccaagctattttgacacagacca-3' (reverse). The polymerase chain reaction (PCR) products were purified from the gel using the silica membrane spin-column technology (QIAquick Spin, Qiagen, Santa Clarita, CA) and sequenced in both directions with a pair of specific sequence primers: 5'-gactctggagccg-3' (forward) and 5'-ggtagcgaccggcg-3' (reverse) using an automated DNA sequencing system (ABI Prism 377, Perkin-Elmer). Homology searches were run against the GenBank® nucleotide and protein sequence data bases using the BLAST search program from the National Center of Biological Information web site. The amino acid multiple sequence alignment was performed using Gene Jockey III software (Biosoft, Cambridge, UK). The cDNA insert was removed from the purified $\lambda\text{gt}11$ phagemid and subcloned into pBluescript vector (Stratagene, La Jolla, CA) for further characterization.

PCR Experiments—PCR was performed as described by us elsewhere (5). Briefly, each reaction had a final volume of 50 μl containing the DNA templates, 1 \times PCR buffer (Promega, Madison, WI); 0.2 mM each of dATP, dCTP, dGTP, dTTP; 2 units of *Taq* DNA polymerase (Promega); and 1 μM each of the sense and antisense primers. The reaction mixture was first heated at 95 °C for 5 min and hot-started with 2 units of DNA *Taq*-polymerase (Life Technologies, Inc.) followed by 35 cycles (or 15 cycles for cloning experiments) of denaturing at 95 °C for 60 s, annealing at an appropriate temperature (optimized for primers used in each PCR) for 60 s, and extension at 72 °C for 120 s. In the final cycle, the extension was increased to 8 min. The PCR products were electrophoresed on 2% agarose gels containing 1 $\mu\text{g}/\text{ml}$ ethidium bromide and photographed under fluorescent UV illumination (AlphaImager 2000, Alpha Innotech Corp., San Leandro, CA). The size of the PCR product was estimated by using a 100- or a 250-bp DNA ladder standard (Life Technologies, Inc.).

Expression of rPX-His in Escherichia coli—The expression vector pQE-30 (Qiagen), which is designed to express proteins containing a 6xHis-tag at the N-terminal, was used to express rPX-His. The vector was linearized by digestion with the *Sph*I and *Kpn*I restriction enzymes for 1 h at 37 °C, then purified from an agarose gel, and incubated at 37 °C with 5 units of alkaline phosphatase (Promega) to enhance the efficiency of ligation. cDNA from the PX $\lambda\text{gt}11$ clone was amplified by PCR with the following primers: 5'-ccgcatgcgatgacgatgacaaaatgtctgtgactggcggaagatggc-3' (forward) and 5'-cccggatccataggtaccaagctattttgacacagacca-3' (reverse). The forward primer was designed to have an additional *Sph*I restriction site, which allows the insert to be ligated in-frame with the 6xHis gene of the pQE-30 vector. The PCR product was double digested with *Sph*I and *Kpn*I restriction enzymes and purified. Digested product was directionally cloned into unique *Sph*I and *Kpn*I sites in the multiple cloning site of the pQE-30 vector. The ligated vector was used to transform *E. coli* expression

strain M15 (Qiagen). Transformed cells were plated on a NYZ agar plate containing 25 $\mu\text{g}/\text{ml}$ kanamycin and 100 $\mu\text{g}/\text{ml}$ ampicillin and grown overnight. To verify the clone that produced the rPX-His protein, transformed bacterial colonies were blotted to a marked nitrocellulose filter and inversely placed on an IPTG-containing NYZ agar plate and grown for 4 h. The filter was then treated with denaturing buffer, neutralized, blocked with 3% non-fat milk in TBS and screened for colonies that produced rPX-His using anti-RGS-His monoclonal antibody (Qiagen). Positive clones were selected from the original plate, and their plasmids were sequenced with a specific primer to confirm that the correct PX cDNA had proper frame and orientation. A representative clone was inoculated into NYZ medium containing 25 $\mu\text{g}/\text{ml}$ kanamycin and 100 $\mu\text{g}/\text{ml}$ ampicillin. The culture was incubated, with shaking, at 37 °C until an A_{600} of 0.6 was reached, and IPTG was added to a final concentration of 2 mM. Culture samples (2 ml each) were collected every hour during 4 h and centrifuged, and the bacterial pellets were dissolved in sample buffer and analyzed by SDS-PAGE with Coomassie Blue staining.

Production and Purification of rPX-His—Large scale rPX-His production was performed in 1 liter of medium, as described above. The cell pellet was lysed at room temperature by stirring the pellet in a buffered solution containing 8 M urea, pH 8.0 (lysis solution). Once the solution became translucent, the cellular debris was removed by centrifugation at $40,000 \times g$ for 1 h at 4 °C. The clarified supernatant was incubated with nickel-nitrilotriacetic acid-agarose resin (Ni-NTA, Qiagen) to capture the His-tagged protein. The resin was washed with several volumes of buffered 8 M urea, pH 6.3, until a A_{280} of about 0.001 was achieved, and loaded into a column. The rPX-His protein was eluted from the column using either denaturing or non-denaturing condition. The denatured rPX-His was eluted with a buffer containing 8 M urea, pH 5.9 and 4.5, resolved by SDS-PAGE, and analyzed by immunoblotting with PV IgG. Or, the immobilized rPX-His was first renatured over a period of 1.5 h in a linear 6 to 1 M urea gradient in 500 mM NaCl, 20% glycerol, 20 mM Tris-Cl, pH 7.4, containing protease inhibitors, and then eluted with a non-denaturing buffer containing 50 mM NaH_2PO_4 , 300 mM NaCl, and 250 mM imidazole, pH 8.0. The purified renatured rPX-His was used in the radioligand binding assays as well as for immunoaffinity purification of anti-PX PV antibody.

Radioligand Binding Assays with rPX-His—Nitrocellulose filters (13-mm diameter, catalog no. HAWPO1300, Millipore Corp.) with a total protein capacity of 160 $\mu\text{g}/\text{cm}^2$ were placed into the bottom of each well of a bovine serum albumin-pretreated 24-well standard cell-and-tissue culture plate (Nalco Nunc International, Denmark). One μg of the affinity-purified rPX-His was diluted in 300 μl of PBS and loaded into each filter for overnight incubation at 4 °C to allow complete absorption of rPX-His by the filter (determined in a series of preliminary experiments by measuring the optical density at 280 nm of free rPX-His remaining in the solution). The membranes carrying rPX-His were blocked with 2% bovine serum albumin for 1 h at room temperature, after which the plates were put on ice, washed three times with ice-cold PBS, and exposed in triplicate for 1 h to increasing, from 0 to 1000 nM, concentrations of [^3H]ACh iodide (82.0 mCi/mmol, NEN Life Science Products, Boston, MA). Nonspecific binding was measured in parallel wells, in which the filters were exposed to the same increasing doses [^3H]ACh in the presence of 100-fold concentrations of non-labeled ACh iodide (Sigma). The filters were then washed thoroughly with ice-cold PBS, placed in 6-ml vials containing 5 ml of liquid scintillation mixture (Ecolite, ICN, Costa Mesa, CA), and their radioactivity was counted in the liquid scintillation counter (model 1409, Wallac Inc., Gaithersburg, MD). The specific binding was computed by subtracting the nonspecific binding from total binding, and the binding capacity (B_{max}) and dissociation constant (K_d) were calculated using the ligand binding analysis software Prism (GraphPad, San Diego, CA). In a separate set of radioligand binding experiments, we investigated the ability of the cholinergic radioligand [^3H]PrBCM (5 mCi/mmol of the customized [^3H]PrBCM; NEN Life Products) to label rPX-His and the ability of the nicotinic agonist nicotine and the muscarinic agonist muscarine (both from Sigma) to abolish rPX-His labeling with [^3H]PrBCM. Prior to the assay, [^3H]PrBCM was cyclized in 10 mM PBS at 30 °C for 20 min to activate the aziridinum ions (28).

Immunoaffinity Purification and Characterization of Anti-PX PV IgG—PV sera were diluted 1:5 in Immunopure Gentle binding buffer (Pierce) and incubated overnight at 4 °C with rPX-His immobilized on Ni-NTA resin. The pass-through serum fraction was collected, and the IgGs were isolated using 40% ammonium sulfate precipitation followed by dialysis against Ca^{2+} - and Mg^{2+} -free PBS. The rPX-His column with bound PV antibody was washed 10 times with TBS containing 300 mM NaCl, and the immunoaffinity-purified anti-PX IgG fraction was eluted

from the column by Immunopure Gentle elution buffer and desalted on a D-Salt Exellulose plastic desalting column (both from Pierce). The pattern of specific binding of the eluted antibody was examined by IIF on human skin and monkey esophagus. The antigenic profile of the eluted PV IgG was identified by immunoprecipitation of metabolically labeled human keratinocyte proteins (see below), which is considered the most sensitive and specific approach to characterize the antigenic specificity pemphigus antibodies (7).

Metabolic Labeling of Cultured KC and Immunoprecipitation Assay—Second passage human foreskin KC were grown to approximately 90% confluence, washed thoroughly with prewarmed (37 °C) PBS, incubated for 15 min at 37 °C in methionine-free Dulbecco's modified Eagle's medium (Life Technologies, Inc.) containing 15% newborn calf serum, and then exposed to 100 μ Ci/ml [³⁵S]methionine (1000 Ci/mmol, Amersham Pharmacia Biotech, Arlington Heights, IL) in 1.8 mM Ca²⁺ labeling medium for 16 h in a humid, 5% CO₂ incubator at 37 °C. The keratinocyte monolayers were then washed thoroughly, and the cells were scraped with a rubber policeman; pelleted by centrifugation at 300 \times g for 5 min at 4 °C; resuspended in ice-cold 10 mM TBS containing 0.025% NaN₃, 20 mM Ca²⁺, 1% Nonidet P-40 (Amersham Pharmacia Biotech) and the protease inhibitors 1 mM iodoacetamide, 2 mM phenylmethylsulfonyl fluoride, 5 μ g/ml leupeptin, 5 μ g/ml pepstatin A, and 5 μ g/ml chymostatin; put on ice; and homogenized. Solubilized [³⁵S]methionine-labeled proteins were separated by centrifugation at 40,000 \times g for 60 min at 4 °C and used as a source of naturally folded keratinocyte proteins. The radiolabeled keratinocyte protein solution was incubated with immunoaffinity-purified anti-PX PV IgG overnight at 4 °C with gentle shaking. The immune complexes were precipitated with slurry protein A-Sepharose suspension, washed, and resolved by 7.5% SDS-PAGE. The gels were fixed and enhanced with 1 M sodium salicylate, and the radioactivity was analyzed using the storage phosphor autoradiography feature of the Storm system (Molecular Dynamics, Mountain View, CA).

Antibody Transfer to Neonatal Mice—The PV phenotype was induced in neonatal mice by passive transfer of PV patients' serum IgG fractions to normal Balb/c mice (8). The IgGs were injected intraperitoneally through a 30-gauge needle at a dose of 20 mg/g of body weight per day into 10- to 12-h-old pups. The neonates always received the same amounts of PV IgG (experiment) and normal human IgG (control). The latter was isolated from normal human serum purchased from Sigma Chemical Co. The mice were sacrificed when fully developed skin lesions could be seen or, if no gross lesions could be observed, approximately 24 h after the last injection. The lesional and perilesional skin samples were collected and examined by staining with hematoxylin and eosin and by DIF with FITC-conjugated goat anti-human IgG antibody (Pierce).

Statistics—The results of quantitative experiments were expressed as mean \pm S.D. Significance was determined using the Student's *t* test.

RESULTS

Selection of an Immunoaffinity-purified Acantholytic Anti-keratinocyte PV IgG as a Candidate for cDNA Library Screening—In an attempt to identify the pathogenic PV antibody, we investigated the ability of different fractions of immunoaffinity-purified anti-keratinocyte PV IgGs to: 1) stain the stratified epithelial substrates in a fishnet-like, "intercellular" pattern, which is diagnostic of PV (1); and 2) induce acantholysis in keratinocyte monolayers, which has become a standard approach to test disease-causing ability of PV antibodies (29, 30). Among tested PV IgG fractions, the antibody eluted from the horizontal strip excised from the 75-kDa area of the immunoblotting membrane produced intercellular epithelial staining of both normal human skin and monkey esophagus in IIF experiments (Fig. 1, A and B). Treatment of confluent monolayers of normal human KC with this immunoaffinity-purified PV IgG fraction, but not with normal human IgG, produced changes of the cell morphology characteristic of pemphigus acantholysis (Fig. 1, C and D). No acantholysis could be seen in cultures treated with equal amounts of PV IgG eluted from the 130-kDa area of immunoblots of normal human keratinocyte proteins (data not shown). Therefore, PV IgG immunoaffinity-purified on a 75-kDa band was selected to probe the λ gt11 human keratinocyte cDNA expression library.

Isolation of cDNA Clones Encoding PX and Sequence Anal-

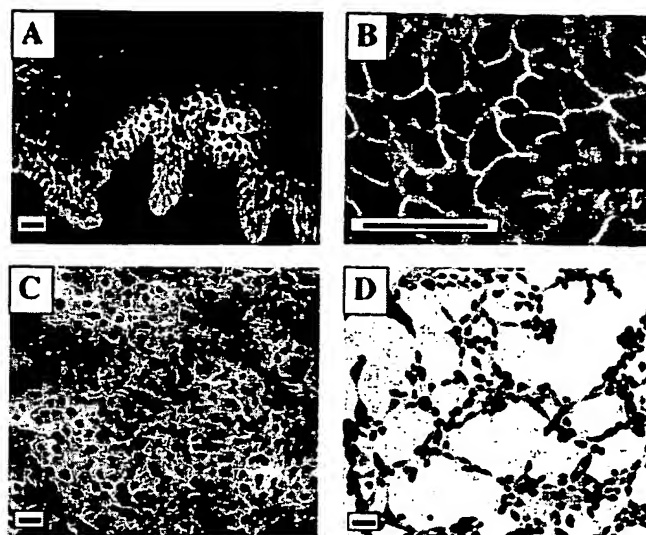
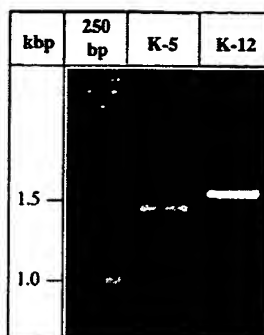


FIG. 1. Selection of the acantholytic anti-keratinocyte PV IgG fraction for screening human keratinocyte λ gt11 cDNA library. A and B, the PV IgG immunoaffinity-purified on the horizontal strip excised from the 75-kDa area of the immunoblotting membrane produced intercellular epithelial staining of both normal human skin (A) and monkey esophagus (B) in IIF experiments. FITC-labeled rabbit anti-human IgG was used as a secondary antibody. No staining was seen when the PV IgG was omitted or replaced with an irrelevant antibody (not shown). Scale bars, 50 μ m. C and D, A confluent monolayer of second passage normal human foreskin KC was incubated with either normal human IgG (C; negative control) or equal amount of the PV IgG that was immunoaffinity-purified on a 75-kDa band (D) for 12 h, and then fixed and stained with the trypan blue dye. The cell morphology is characteristic of pemphigus acantholysis was induced by anti-75 kDa PV antibody (D). No such changes could be observed in a parallel control experiment in which a confluent keratinocyte monolayer was treated with PV IgG immunoaffinity-purified on the 130-kDa horizontal strip (not shown). Scale bars, 50 μ m.

ysis—Approximately 3×10^6 plaques of λ gt11 human keratinocyte cDNA expression library were screened with the affinity-purified antibody from three PV sera (codes: PRC-45, PRC-46, and PRC-47), which contained the anti-75-kDa band acantholytic PV IgG that stained the stratified epithelium in a pemphigus-like pattern. In the first round of screening, four plaques were found to be positive for antibody binding. However, only two clones, designated as K5 and K12, remained immunoreactive after subsequent rescreeing. Because PV IgG eluted from the filter blotted with both K5 and K12 clones stained monkey esophagus in a pemphigus-like pattern (data not shown), both clones were selected for further characterization. PCR amplification of the cDNA insert using a pair of λ gt11 cloning primer revealed that K5 and K12 clones carried the 1.3- and 1.4-kb cDNA inserts, respectively (Fig. 2A). Unexpectedly, sequence analysis of the cDNA inserts from both clones predicted the same open reading frame of 1035 bp, encoding a full-length protein comprised of 345 amino acids (Fig. 2B) with a calculated molecular mass of 38.3 kDa. Examination of the nucleotide sequence revealed an in-frame stop codon situated upstream of the first ATG codon, which indicated that a complete coding region was identified. There were two tandem ATG potential translation initiation codons after the upstream in-frame stop codon. The first one most likely represented the initiation codon, because it was preceded with the Kozak consensus sequence (31). No poly(A) tail was detected. A BLAST search of the GenBank® data base at the NCBI web site showed that the nucleotide sequence encoded a previously unknown molecule. The deduced amino acid sequence revealed a high degree of homology to the members of the Ca²⁺-dependent annexin protein gene family. The strong-

A



B

-226 ATCGGCGGAATTCGCCCCACTTTCCTCTACCAGGCCACACCGGAGGCAGTG -175
 -174 CTCACACAGGCAAGCTACCAGGCCACAACGACACCCACCTCCTGGCACCTCTGAGCATCCACGTACTTGCAAGAACTCTT -88
 -87 GCTCACATCAGCTAAGAGATTGCACCTGCTGACCTAGAGATTCCGGCCTGTGCTCCTGTGCTGCTGAGCAGGGCAACCAAGTAGCACC -1

1 ATG TCT GTG ACT GGC GGG AAG ATG GCA CCG TCC CTC ACC CAG GAG ATC CTC AGC CAC CTG GGC CTG 66
 1 Met Ser Val Thr Gly Gly Lys Met Ala Pro Ser Leu Thr Gln Glu Ile Leu Ser His Leu Gly Leu 22

67 GCC AGC AAG ACT GCA GCG TGG GGG ACC CTG GGC ACC CTC AGG ACC TTC TTG AAC TTC AGC GTG GAC 132
 23 Ala Ser Lys Thr ala Ala Trp Gly Thr Leu Gly Thr Leu Arg Thr Phe Leu Asn Phe Ser Val Asp 44

133 AAG GAT GCG CAG AGG CTA CTG AGG GCC ATT ACT GGC CAA GGC GTG GAC CGC AGT GCC ATT GTG GAC 198
 45 Lys Asp Ala Gln Arg Leu Leu Arg Ala Ile Thr Gly Gln Gly Val Asp Arg Ser Ala Ile Val Asp 66

199 GTG CTG ACC AAC CGG AGC AGA GAG CAA AGG CAG CTC ATC TCA CGA AAC TTC CAG GAG CGC ACC CAA 264
 67 Val Leu Thr Asn Arg Ser Arg Glu Gln Arg Gln Leu Ile Ser Arg Asn Phe Gln Glu Arg Thr Gln 88

265 CAG GAC CTG ATG AAG TCT CTA CAG GCA GCA CTT TCC GGC AAC CTG GAG AGG ATT GTG ATG GCT CTG 330
 89 Gln Asp Leu Met Lys Ser Leu Gln Ala Ala Leu Ser Gly Asn Leu Glu Arg Ile Val Met Ala Leu 110

331 CTG CAG CCC ACA GCC CAG TTT GAC GCC CAG GAA TTG AGG ACA GCT CTG AAG GCC TCA GAT TCT GCT 396
 111 Leu Gln Pro Thr Ala Gln Phe Asp Ala Gln Glu Leu Arg Thr Ala Leu Lys Ala Ser Asp Ser Ala 132

397 GTG GAC GTG GCC ATT GAA ATT CTT GCC ACT CGA ACC CCA CCC CAG CTG CAG GAG TGC TTG GCA GTC 462
 133 Val Asp Val Ala Ile Glu Ile Leu Ala Thr Arg Thr Pro Pro Gln Leu Gln Glu Cys Leu Ala Val 154

463 TAC AAA CAC AAT TTC CAG GTG GAG GCT GTG GAT GGC ATC ACA TCT GAG ACC AGT GGC ATC TTG CAG 528
 155 Tyr Lys His Asn Phe Gln Val Glu Ala Val Asp Gly Ile Thr Ser Glu Thr Ser Gly Ile Leu Gln 176

529 GAC CTG CTG TTG GCC CTG GCC AAG GGG GGC CGT GAC AGC TAC TCT GGA ATC ATT GAC TAT AAT CTG 594
 177 Asp Leu Leu Leu Ala Leu Ala Lys Gly Gly Arg Asp Ser Tyr Ser Gly Ile Ile Asp Tyr Asn Leu 198

595 GCA GAA CAA GAT GTC CAG GCA CTG CAG CGG GCA GAA GGA CCT AGC AGA GAG GAA ACA TGG GTC CCA 660
 199 Ala Glu Gln Asp Val Gln Ala Leu Gln Arg Ala Glu Gly Pro Ser Arg Glu Glu Thr Trp Val Pro 220

661 GTC TTC ACC CAG CGA AAT CCT GAA CAC CTC ATC CGA GTG TTT GAT CAG TAC CAG CGG AGC ACT GGG 726
 221 Val Phe Thr Gln Arg Asn Pro Glu His Leu Ile Arg Val Phe Asp Gln Tyr Gln Arg Ser Thr Gly 242

727 CAA GAG CTG GAG GAG GCT GTC CAG AAC CGT TTC CAT GGA GAT GCT CAG GTG GCT CTG CTC GGC CTA 792
 243 Leu Glu Gln Glu Glu Ala Val Gln Asn Arg Phe His Gly Asp Ala Gln Val Ala Leu Leu Gly Leu 264

793 GCT TCG GTG ATC AAG AAC ACA CCG CTG TAC TTT GCT GAC AAA CTT CAT CAA GCC CTC CAG GAA ACT 858
 265 Ala Ser Val Ile Lys Asn Thr Pro Leu Tyr Phe Ala Asp Lys Leu His Gln Ala Leu Gln Glu Thr 286

859 GAG CCC AAT TAC CAA GTC CTG ATT CGC ATC CTT ATC TCT CGA TGT GAG ACT GAC CTT CTG AGT ATC 924
 287 Glu Pro Asn Tyr Gln Val Leu Ile Arg Ile Leu Ile Ser Arg Cys Glu Thr Asp Leu Leu Ser Ile 308

925 AGA GCT GAG TTC AGG AAG AAA TTT GGG AAG TCC CTC TAC TCT TCT CTC CAG GAT GCA GTG AAA GGG 990
 309 Arg Ala Glu Phe Arg Lys Lys Phe Gly Lys Ser Leu Tyr Ser Ser Leu Gln Asp Ala Val Lys Gly 330

991 GAT TGC CAG TCA GCC CTC CTG GCC TTG TGC AGG GCT GAA GAC ATG TGAGACTTCCTGCCCCACCCACATG 1062
 331 Asp Cys Gln Ser Ala Leu Leu Ala Leu Cys Arg Ala Glu Asp Met 345

1063 ACATCCGAGGATCTGAGATTTCCTGTGTTGGCTGAACCTGGGAGACCAGCTGGGCCTCCAAGTAGGATAACCCCTCACTGAGCACCC 1156
 1150 GGATTCC

FIG. 2. Identification of pemphaxin (PX)—a novel human annexin-like molecule—using the anti-75-kDa band immunoaffinity-purified PV IgG as a probe. A, PCR amplification of cDNA inserts from λ gt11 phages isolated from the clones K5 and K12 using specific λ gt11 forward and reverse cloning primers. The 1.5- and 1.6-kbp PCR products carried copies of 1.3- and 1.4-kbp cDNA inserts, respectively, from the two clones that were specifically recognized by affinity-purified PV IgG as a result of screening of 3 million plaques of a λ gt11 human keratinocyte cDNA expression library. Sequence analysis of both cDNA inserts revealed that both encoded for the same novel molecule, PX. B, the nucleotide sequence and the predicted amino acid sequence of PX. The in-frame upstream and downstream stop codons are underlined. The Kozak sequence that precedes the potential initiation ATG codon is double underlined. C, multiple amino acid sequence alignment of PX with the annexin-2 sequences reported for different species showing that PX shares the same amino acids in most of the conserved regions. Shaded regions indicate the identical amino acid residues among all compared sequences. The arrow denotes potential glycosylation site. The asterisks denote the potential type II Ca^{2+} binding sites. The potential actin bundling site is underlined. Anx-2, annexin-2.

Pemphaxin
Human Anx-2
Bovine Anx-2
Rat Anx-2
Chick Anx-2

HETVGGKMAPSLTQHTTSHGGLASK-TAAMGTLTGLRTFLAYSVDKDAQRLLRAITGQGVRSATVDVYKRSRERQOLY
HETV-----HETLCKSLGSDHSTPPSAYGSKVAYTNDADERDALNIETALKTGQVDEVTIWNILATKRNENACROOL
HETV-----HETLCKSLGSDHSTPPSAYGSKVAYTNDADERDALNIETALKTGQVDEVTIWNILATKRNENACROOL
HETV-----HETLCKSLGSDHSTPPSAYGSKVAYTNDADERDALNIETALKTGQVDEVTIWNILATKRNENACROOL
HETV-----HETLCKSLGSDHSLPPSAYATVKAYSNTDADRDAALAAKTKTGQVDEVTIWNILATKRSNBEROOL

Pemphaxin
Human Anx-2
Bovine Anx-2
Rat Anx-2
Chick Anx-2

SRNFOETFOODTKSLQAALSGNLRIVMAKLOPTAGPDAOBLRTALKASDSAVDVATLRLATETPPPOLORCLAVYKHNPF
AFAYDRKTKKRLSAALKSALSCHLEAVILGLKTPAQYDASHTKASMKGLGTDEDSLHETLCSTNOBLQKINRVYKRM
AFAYDRKTKKRLSAALKSALSCHLEAVILGLKTPAQYDASHTKASMKGLGTDEDSLHETLCSTNOBLQKINRVYKRM
AFAYDRKTKKRLSAALKSALSCHLEAVILGLKTPAQYDASHTKASMKGLGTDEDSLHETLCSTNOBLQKINRVYKRM
AFAYDRKTKKRLSAALKSALSCHLEAVILGLKTPAQYDASHTKASMKGLGTDEDSLHETLCSTNOBLQKINRVYKRM

Pemphaxin
Human Anx-2
Bovine Anx-2
Rat Anx-2
Chick Anx-2

QVEAVDGYTSTSGILQDMLLALAKGGRDSYSGIIPYNLAEDVQALORAEKRSREE---TWVPVPTORNPEHLIRVTDQ
KTDLKEDLISDTSGDFRKHVALAKGRAEDGSDVLYELIDODARELYDAGVKRKGTDVPMISINTERSVPELOKVYDR
KTDLKEDLISDTSGDFRKHVALAKGRAEDGSDVLYELIDODARELYDAGVKRKGTDVPMISINTERSVPELOKVYDR
KTDLKEDLISDTSGDFRKHVALAKGRAEDGSDVLYELIDODARELYDAGVKRKGTDVPMISINTERSVPELOKVYDR
KTDLKEDLISDTSGDFRKHVALAKGRAEDGSDVLYELIDODARELYDAGVKRKGTDVPMISINTERSVPELOKVYDR

Pemphaxin
Human Anx-2
Bovine Anx-2
Rat Anx-2
Chick Anx-2

YQRSTGQBLEAVQNRPHGDAQVALIGLASVKEHTPTLYEADKRLHQALQESTEPNYO
YKSYSPYDMLHSIRKEVKGLENAPLNLVQCIQNKQLYFADRLYDSMKGKGTADK
YKSYSPYDMLHSIRKEVKGLENAPLNLVQCIQNKQLYFADRLYDSMKGKGTADK
YKSYSPYDMLHSIRKEVKGLENAPLNLVQCIQNKQLYFADRLYDSMKGKGTADK
YKSYSPYDMLHSIRKEVKGLENAPLNLVQCIQNKQLYFADRLYDSMKGKGTADK

Pemphaxin
Human Anx-2
Bovine Anx-2
Rat Anx-2
Chick Anx-2

GKSLYYSLLQDQAVKGCQSALLALCRAEPM
GKSLYYSLLQDQTKGDTYKQKALLYLGGDD
GKSLYYSLLQDQTKGDTYKQKALLYLGGDD
GKSLYYSLLQDQTKGDTYKQKALLYLGGDD
GKSLYYSLLQDQTKGDTYKQKALLYLGGDD

FIG. 2—continued

est similarity, approximately 40%, was observed with annexin-2 present in chicken (GenBank[®] accession number P17785), cow (P04272), rat (Q07936) and humans (NP004030). The amino acid sequence alignment (Fig. 2C) revealed several conserved regions, including the type II Ca²⁺ binding sites (32, 33) and the actin bundling site that plays a role in Ca²⁺-dependent bundling of actin microfilaments by annexins (34). Because of its homology to the members of the annexin protein gene family, we tentatively named this newly discovered PV antigen pemphaxin (*i.e.* pemphigus + annexin = pemphaxin).

Expression of the rPX-His Fusion Protein in *E. coli* and Its Affinity Purification—To allow experiments with immunoaffinity-purified anti-PX PV antibody, we produced a full-length recombinant PX. Because both K5 and K12 clones carried full-length cDNAs encoding the complete open reading frame of PX, we chose to directionally clone the K5 cDNA to the pQE-30 expression vector, which was designed to express PX protein carrying a poly-His tag at its N terminus. The cloned pQE-30-PX was transformed into *E. coli* M15 cells, and the colonies expressing rPX-His were selected by screening with anti-RGS-His monoclonal antibody. Antibody staining revealed six strongly positive colonies that contained correct PX inserts, as confirmed by subsequent sequencing. Clone 1 was selected for a time course characterization of PX expression. As seen in Fig. 3A, the transfected bacteria began to produce rPX-His after induction with 2 mM IPTG, and the amount of this fusion protein, estimated by the time course study with the time points of 1, 2, 3, and 4 h, gradually increased and reached saturation at 4 h after induction. As expected from the deduced molecular mass of PX, the newly produced rPX-His migrated with a 40-kDa protein band on the 12% SDS-PAGE gel. No proteins were induced by IPTG in control, non-transfected *E. coli* M15 cells (data not shown). The rPX-His was isolated from the mixture of *E. coli* proteins on the Ni-NTA column via its His residues. The rPX-His fusion protein was eluted from the column, and its purity was confirmed by finding a single band in 12% SDS-PAGE-resolved eluant (Fig. 3A, lane PX). The ability of rPX-His to exhibit PX conformational epitope(s) recognized by PV antibody was confirmed by immunoblotting of affinity-

purified rPX-His with the three PV sera that were used in the cDNA library screening experiments (Fig. 3B).

Cholinergic Radioligand Binding by rPX-His—Cholinergic ligand binding properties of annexins-1, -2, and -3 (35) suggested that PX also acts as a cholinergic receptor binding ACh on the cell surface of KC. To test this hypothesis, rPX-His was used in a standard radioligand binding assay. The saturable specific binding was achieved with the reversible cholinergic radioligand [^3H]ACh (Fig. 4A). The analysis of binding kinetics revealed the K_d value of 909 nM and a B_{max} of 176 pmol/mg of protein, indicating that, on the cell membrane of KC, PX may act as a low affinity receptor for endogenously produced and secreted ACh.

Because we demonstrated in a previous study (5) that 85% of pemphigus patients develop autoantibodies, which immunoprecipitate a keratinocyte membrane protein covalently labeled with the cholinergic radioligand [^3H]PrBCM, we further asked whether [^3H]PrBCM can specifically label rPX-His. The specificity of [^3H]PrBCM binding to rPX-His was demonstrated in the binding inhibition experiment using non-labeled cholinergic ligands ACh, nicotine, and muscarine as competitors (Fig. 4B). As expected, ACh as well as its nicotinic and muscarinic congeners decreased significantly ($p < 0.05$) the amount of [^3H]PrBCM bound to rPX-His, indicating that PX exhibits dual, muscarinic and nicotinic pharmacology. The dose-dependent radioligand binding inhibition assay with [^3H]PrBCM could not be performed because of the irreversible nature of its binding to a receptor molecule, via an alkylation reaction (36).

Characterization of Immunoaffinity-purified Anti-PX PV Antibody—The anti-PX PV IgG was immunoaffinity-purified on rPX-His immobilized on the Ni-NTA column via its His tags, and the PV IgG fraction eluted from the resin was characterized by: 1) IIF assay using human skin and monkey esophagus as substrates; and 2) immunoprecipitation assay with metabolically radiolabeled keratinocyte proteins. In the IIF assays, the immunoaffinity-purified anti-PX PV IgG stained, in a distinct fishnet-like, pemphigus pattern, the stratified squamous epithelium in human skin and monkey esophagus (Fig. 5, A and

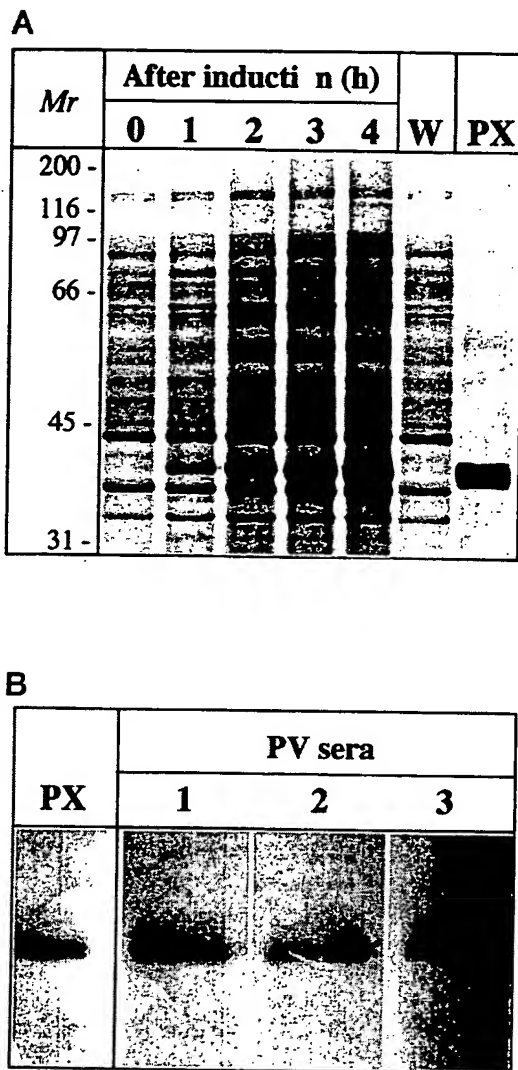


FIG. 3. Expression of the rPX-His fusion protein in *E. coli* and its affinity purification. A, the time-course study of the expression of rPX-His. The selected *E. coli* M15 cells transformed with pQE30-PX were grown in NYZ medium to an optical density of 0.6, at 600 nm and induced with 2 mM IPTG. 1-ml samples of bacterial culture were collected before induction and at 1, 2, 3, and 4 h post induction. The protein extracts of these samples were analyzed on 12% SDS-PAGE gel stained with Coomassie Blue. A sample of rPX-His purified on a Ni-NTA column is designated as PX, and the wash-through fraction is designated as W. No additional proteins were produced in the control experiments in which non-transfected *E. coli* M15 cells were induced with IPTG (not shown). B, the conformational epitope of rPX-His allows its immunorecognition by PV IgG. Western blots of affinity-purified rPX-His were stained with sera from the three PV patients whose IgG fraction was used to screen λ gt11 human keratinocyte cDNA expression libraries. Binding of anti-PX PV IgG was visualized using horseradish peroxidase-conjugated goat anti-human IgG antibody. No staining could be seen in the negative control experiment in which the primary antibody was omitted (not shown). In the reference lane, denoted PX, the rPX-His fusion protein is visualized by staining with Coomassie Blue.

B). The epithelia of other types, such as those lining human bronchi, lung alveoli, small and large intestine, and renal glomeruli, did not exhibit specific staining (data not shown), indicating that the stratified epithelium is a major site of the epithelial expression of PX in human beings. We did not test non-epithelial tissues in this study.

Although addition of a 6xHis-tag to PX should not alter its conformational epitope, we sought to rule out even a remote possibility that, in addition to anti-PX, the rPX-His fusion protein absorbs antibodies of other specificities. The purity of

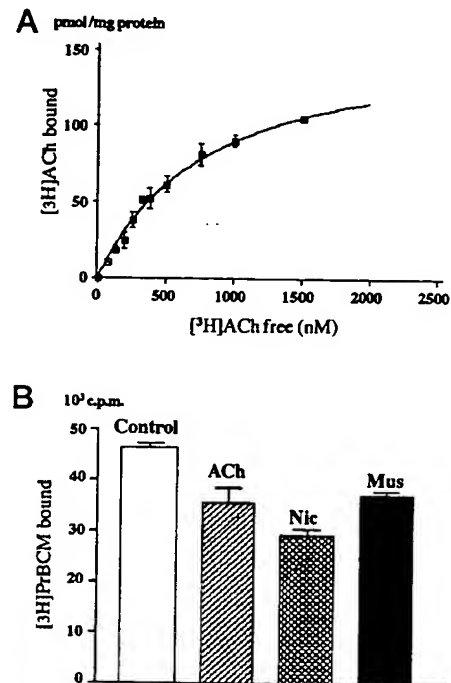


FIG. 4. Cholinergic radioligand-binding to rPX-His. A, saturable binding of the reversible cholinergic radioligand [3 H]ACh to rPX-His in a standard radioligand binding assay detailed under "Experimental Procedures." The analysis of the specific binding revealed a B_{max} of 176 pmol/mg of protein with a K_d of 909 nM. B, blocking of rPX-His labeling by [3 H]PrBCM in the presence of ACh, the nicotinic ligand nicotine (Nic) or the muscarinic ligand muscarine (Mus). The data are mean \pm S.D. of triplicate measurements of [3 H]PrBCM radioactivity (in cpm) associated with rPX-His after its 30-min incubation with 5 nM [3 H]PrBCM at room temperature in the presence or absence of 10 μ M of non-labeled cholinergic drugs ACh, Nic, or Mus.

PV IgG eluted from rPX-His was tested in an immunoprecipitation assay, which allows an antibody to recognize its antigen in the native form, to increase the sensitivity and specificity of antibody characterization. The immunoprecipitation assay showed that the affinity-purified anti-PX PV IgG precipitated keratinocyte proteins with apparent molecular masses of 40 and 80 kDa (Fig. 5C). Because the deduced molecular mass of PX is 38.3 kDa, these results suggested that PX exists as a monomer and a homodimer in KC. This hypothesis was further supported by demonstration of the predicted reciprocal changes in the relative amounts of the 40- and 80-kDa products depending on the presence or absence of the reducing agent β -mercaptoethanol in the SDS-PAGE buffer (Fig. 5C). Indeed, the covalent linkage of two annexins in a dimer is common for certain annexins (reviewed in Ref. 37).

Absorption of Disease-causing PV Antibodies with rPX-His.—To determine the pathophysiological significance of anti-PX antibody in pemphigus, we next asked if depletion of the PV IgG fraction of anti-PX antibody could affect the ability of PV IgG to cause gross skin blisters in neonatal mice. Equal amounts of the intact whole PV IgG fraction (positive control) and the PV IgGs that either passed through the Ni-NTA column containing immobilized rPX-His or were eluted from the column were injected intraperitoneally into 10- to 12-h-old Balb/c mice at a concentration of 20 mg of IgG/g of body weight per day. Only the mice that received non-absorbed PV IgGs reproducibly developed pemphigus-like gross skin lesions between the 16th and 24th h after a single injection. The mice injected repeatedly with either the pass-through (Fig. 5D) or the immunoaffinity-purified anti-PX IgGs (not shown) did not develop any macro- or microscopic skin changes, despite deposition of injected IgGs in mouse epidermis in both cases (Fig.

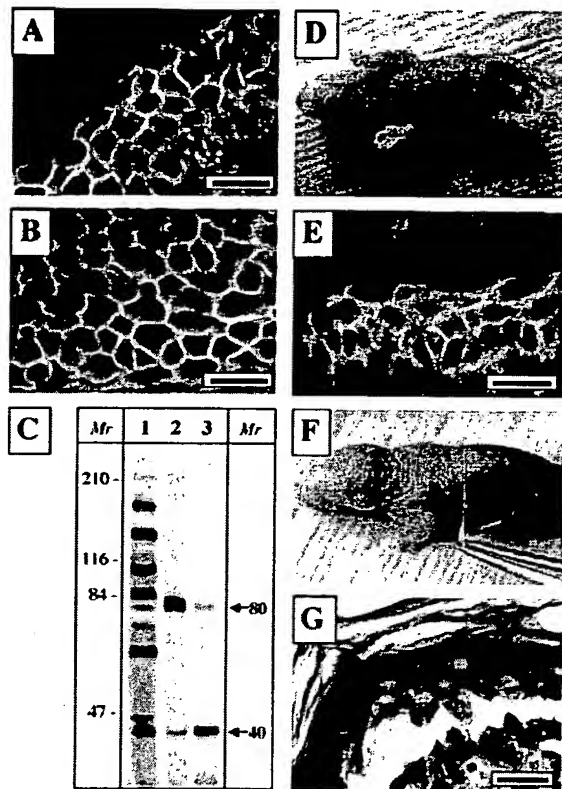


FIG. 5. Characterization of immunoaffinity-purified anti-PX PV antibody. A and B, characterization of immunoaffinity-purified anti-PX PV IgG by IIF. Typical pemphegus-like, "intercellular" staining pattern produced due to binding of the PV IgG fraction eluted from rPX-His to normal human epidermis (A) and monkey esophagus (B). No staining could be seen in negative control experiments stained by a secondary antibody without anti-PX PV IgG (not shown). Scale bars, 50 μ m. C, characterization of immunoaffinity-purified anti-PX PV IgG by immunoprecipitation. The whole PV serum (lane 1) or PV IgG eluted from rPX-His (lanes 2 and 3) were used to immunoprecipitate 35 S-metabolically labeled human keratinocyte protein extract, as detailed under "Experimental Procedures." The immunoprecipitate in lanes 1 and 3 was diluted in SDS-PAGE buffer containing both 2% SDS and 5% β -mercaptoethanol, which allowed predominant visualization of rPX-His in the form of a 40-kDa monomer. The immunoprecipitate resolved in lane 2 was treated without the reducing agent β -mercaptoethanol, which produced a reciprocal staining picture, because omission of β -mercaptoethanol allowed predominant visualization of rPX-His in a form of a naturally assembled homodimer with an apparent molecular mass of 80 kDa. D and E, results of passive transfer of PV IgG preabsorbed with rPX-His to a neonatal Balb/c mouse. Lack of any visible alteration of skin integrity in a pup injected intraperitoneally during 2 days with the pass-through PV IgG fraction in a total dose of 40 mg/g body weight. Demonstration of the deposits of injected pass-through PV IgGs in the epidermis of this mouse by DIF (E). Scale bar, 50 μ m. F and G, results of the passive transfer experiment using the pass-through PV IgG fraction that was supplemented with the immunoaffinity-purified anti-rPX-His IgG. An extensive blister with a loosely attached peripheral skin (positive Nikolsky sign) in a neonate approximately 16 h after a single intraperitoneal injection of 20 mg/g PV IgG (F). The skin blister in this pup resulted from a typical PV-like suprabasilar acantholysis observed by hematoxylin and eosin examination of the perilesional skin (G). The fishnet-like deposits of injected IgG in the epidermis of this mouse were confirmed by DIF (not shown). Scale bar, 50 μ m.

5E). These results indicated that, although absorption with rPX-His eliminates the acantholytic activity of PV serum, the anti-PX antibody alone is not sufficient to induce acantholysis and gross skin blisters in neonatal mice. Therefore, we hypothesized that, although anti-PX antibody is essential for acantholysis development, it is not the only one in the pool of disease-causing PV antibodies that are required to break the integrity of live epidermis.

To test this hypothesis, we sought to determine if acantho-

lytic activity of preabsorbed PV IgGs could be restored by adding back the adsorbed anti-PX antibody. As seen in Fig. 5 (F and G), the pups injected with the pass-through PV IgGs supplemented with anti-PX IgG eluted from the affinity column produced the PV phenotype that was indistinguishable from the epidermal acantholysis and gross skin blisters produced by non-adsorbed PV IgG (not shown). These results clearly indicated that, in addition to anti-PX antibody, the pool of disease-causing PV IgG contains autoantibodies to other keratinocyte self-antigens and suggested that a cumulative effect of anti-keratinocyte antibodies of different specificities is required to break up the integrity of live epidermis and induce skin blistering.

DISCUSSION

In this study we selected the PV IgG fraction that can both stain the epithelial substrates in the pemphigus-like pattern and induce acantholysis in keratinocyte monolayers to probe λ gt11 keratinocyte cDNA library for novel targets of disease-causing PV antibodies. The PV antibody immunoaffinity-purified on a 75-kDa keratinocyte protein band identified a novel human annexin-like molecule, which we termed PX. Recombinant PX was produced and shown to bind specifically ACh and its nicotinic and muscarinic congeners. The obtained results indicate that PX may serve as a cell surface cholinergic receptor mediating a novel ACh signaling pathway involved in the physiological control of cell-to-cell adhesion and that autoimmunity to PX may lead to acantholysis.

Pemphigus is an autoimmune disease with a complex pathophysiology. Both humoral (38) and cellular (39) effectors of autoimmune aggression against KC are involved in the pathogenesis of this disease, and it has been demonstrated that local activation of trypsin-like serine proteases, such as plasminogen activator (40), complement (41), eicosanoids (42), and proinflammatory cytokines (29, 43), all can contribute to acantholysis. The precise mechanism leading to acantholysis in PV, however, is yet to be determined. It is currently held that an autoantibody to the 130-kDa adhesion molecule Dsg 3 causes pemphigus by disrupting directly the keratinocyte cell-to-cell bridges or desmosomes (44, 45). The intuitive notion that the disease of skin adhesion is caused by an antibody to the adhesion molecule, however, awaits its direct experimental confirmation. Meanwhile, Kitajima *et al.* (46) demonstrated that desmosome formation induced by switching the incubation medium from a low to a high Ca^{2+} content is not inhibited by the binding of PV IgG to the cell membrane of cultured KC. In agreement with this report, we could not detect any morphological changes in the keratinocyte monolayers treated with the anti-130-kDa PV IgG for 16 h, whereas the acantholysis in cell monolayers usually develops within 12 h after addition of the whole PV IgG fraction (20, 29, 30). Fan *et al.* (47) attempted to create an animal model of PV by immunizing four different strains of mice, Balb/c, DBA/1, SJL/J, and HRS/J, with full-length Dsg 3 protein, recombinant extracellular portion of Dsg 3, and the synthetic peptides spanning the entire Dsg 3. However, they found no signs of pemphigus, oral or cutaneous, in any of the animals, despite relatively high, up to 1/2560, titer of circulating anti-Dsg 3 antibodies produced by immunized animals. Furthermore, even after the immune sera were concentrated 10-fold and inoculated into neonatal mice, the mice of only one strain, Balb/c, developed the lesion. These results demonstrated that, at the serum titers that are equivalent or exceeding those found in PV patients, the anti-Dsg 3 antibody is not sufficient to cause pemphigus symptoms. The suprapharmacological doses of this antibody, however, can physically interfere with cell-to-cell adhesion, as illustrated by the occurrence of microscopic changes in the oral mucosa of immuno-

deficient Rag-2 knockout mice grafted with a spleen producing anti-Dsg 3 antibodies (48). Unfortunately, the interpretation of findings in mice with adoptively transferred anti-Dsg 3 antibodies in the study of Amagai *et al.* (48) is complicated by its rather controversial nature, which includes direct conflict with the existing data. For instance, according to Amagai *et al.* (48), lack of skin changes in Balb/c mice immunized with Dsg 3 is attributed to inability of this strain of mice to produce anti-Dsg 3 antibody, whereas Fan *et al.* (47) achieved high anti-Dsg 3 antibody titers in these animals, albeit without any mucocutaneous signs of PV. Furthermore, Amagai *et al.* (48) opine that, by analogy with the interpretation of the *Dsg3^{null}* phenotype (18), a transient hair loss accompanied by transient microscopic alterations of keratinocyte adhesion in the oral cavity, which is all that can be observed in the recipient Rag-2^{-/-} mice, should be interpreted as the PV phenotype. However, the following facts argue against this interpretation: 1) hair loss is not a sign of PV (1); 2) true PV is a disease severe enough to kill approximately 90% of patients, if left untreated (reviewed in Ref. 2); and 3) neither recipient Rag-2^{-/-} mice nor *Dsg3^{null}* mice develop spontaneous skin blisters (5, 15, 18). Nevertheless, the notion about the pathophysiological significance of Dsg 3 antibody in PV has been supported by the results of *in vivo* experiments in which pemphigus antibodies affinity-purified on the rDsg3-Ig chimera induced gross skin blisters in neonatal mice (13, 14). Unfortunately, the profile of PV IgGs adsorbed by the rDsg3-Ig-His baculoprotein has never been shown, leaving unresolved the purity and specificity of the antibodies used in the passive transfer experiments. Therefore, we had to characterize the antigenic reactivity of PV IgG adsorbed with rDsg3-Ig-His in our laboratory (19). We established that the antibodies adsorbed on rDsg3-Ig-His are directed toward several keratinocyte proteins, including an unknown 130-kDa self-antigen recognized in the Western blot of keratinocyte proteins of *Dsg3^{null}* mice.

To select the PV IgG fraction that most likely contains disease-causing antibody, we screened PV IgG fractions eluted from different areas of the immunoblotting membrane for their ability to both: 1) stain epidermis in a fishnet-like, pemphigus pattern; and 2) produce acantholysis in keratinocyte monolayers. The anti-75-kDa band PV IgG met both criteria. Failure of the antibody eluted from the 130-kDa area of the immunoblotting membrane to fulfill both criteria was not surprising, because in the past this antibody was selected for the cDNA screening experiments that identified Dsg 3 based on the first criteria only (9). In our study, anti-75-kDa band PV antibody caused acantholysis, which could be observed at 0.09 mM Ca²⁺ in KGM. Although expression of Dsg 3 in KC requires preincubation of the cells at high, from 1.8 to 2.55 mM, extracellular Ca²⁺ (9, 49, 50), we and other workers have previously demonstrated that binding of disease-causing PV IgGs to KC and acantholysis in cell monolayers both occur at as low as 0.1 mM Ca²⁺ (20, 29). This fact suggests that, in addition to blocking the "adhesive sites" of desmosomal cadherins with anti-Dsg PV IgG, binding of pemphigus antibodies to KC initiates an intracellular signaling cascade that can lead to disassembly of other types of intercellular junctions comprised of classical cadherins, such as tight junctions, adherence junctions, and gap junctions, all of which can mediate keratinocyte cell-to-cell adhesion at low Ca²⁺ (51–53).

Screening of the λ gt11 keratinocyte cDNA expression library with the acantholytic anti-75-kDa band PV antibody identified PX, a novel human annexin-like molecule. It appeared that two of 3×10^6 plaques labeled with PV IgGs carried cDNA encoding for the same previously unknown annexin-like molecule with the predicted molecular mass of the translated product of 38.3

kDa. Sequence alignment with known annexins showed that PX shares the same amino acids in most of the conserved regions and is ~40% similar to annexin-2. Annexin-2 may exist as a monomer, dimer, heterodimer, or heterotetramer in which two annexin-2 molecules combine with two smaller subunits, p11, that resemble the S-100 protein of the calmodulin family (54). Because the PV IgG immunoaffinity-purified on rPX-His labeled keratinocyte proteins with apparent molecular masses of 40 and 80 kDa, it can be postulated that PX forms homodimers.

Annexins comprise a unique family of Ca²⁺- and phospholipid-binding proteins encoded by some 20 different genes, which are ubiquitous among eukaryotic organisms, single-celled organisms, and plants and animals (reviewed in Refs. 55, 56). Individual annexins have been described under the names anchorin, calcimedlin, calelectrin, calpactin, calphobindin, chromobindin, endonexin, lipocortin, and synexin. Different annexins have been shown to: 1) participate in ligand-mediated cell signaling both directly, by forming Ca²⁺-sensitive, voltage-gated Ca²⁺ channels, and indirectly, by generating membrane-derived second messengers; 2) mediate anti-inflammatory action of glucocorticosteroids via inhibition of phospholipase A₂; 3) regulate and directly mediate cell-to-cell adhesion; 4) mediate endo- and exocytosis; 5) inhibit blood coagulation; 6) regulate Ca²⁺-dependent Cl⁻ conductance; and 7) participate in the processes of cell proliferation, apoptosis, and virus infection (reviewed in Refs. 37, 57–60).

PX turned out to be a sixth protein of the annexin protein gene family identified in normal human skin to date. Annexins-1, -2, -5, -6, and -7 have been demonstrated previously (61, 62). Expression of annexins in epidermis is differentiation-dependent (63). Annexin-1 immunoreactivity is found almost entirely around the perimeter of KC, especially tonofilament/desmosome-rich prickle KC (61). It has been noted that raising intracellular Ca²⁺ results in peripheral relocations of annexins-2, -4, -5, and -6 from the perinuclear areas (64). Annexin-2 has been shown to be directly involved in regulation of cell adhesion and migration (65). The presence in PX of the conserved sites providing for Ca²⁺ binding and for bundling of actin filaments suggests that PX, just like annexin-2, regulates assembly and maintenance of the cytoskeletal units. This actin polymerization is now believed to play a crucial role in epithelial cell-to-cell adhesion, because disruption of this process in an animal model causes skin lesions indistinguishable from PV lesions (66).

Although annexins lack a leader sequence (and do not pass the Golgi apparatus), they are found on the keratinocyte cell surface, where they can function as receptors. Extracellular annexins have been demonstrated to bind collagen, tenascin, and plasminogen activator (65, 67–70). Binding of tenascin-C to annexin-2 provokes three cellular responses: loss of adhesion, lateral migration, and enhanced cell division (71). Tenascin expression is induced in pemphigus skin as well as in the skin of other blistering dermatoses (72).

To characterize PX, we produced full-length recombinant protein using pQE-30 vector, which contained IPTG-inducible promoter transformed into the *E. coli* M-15 competent cells. Plasmid purified from this clone was analyzed by restriction enzyme analysis and sequencing. Both confirmed that the PX DNA insert was 100% correct. The rPX-His was affinity-purified and used in standard receptor-ligand binding assays with the cholinergic radioligand [³H]ACh. The analysis of the saturable binding of [³H]ACh showed that PX can function as a low affinity cholinergic receptor on the cell membrane of KC. These results were expected, because choline, which itself serves as a pharmacological agonist of cholinergic receptors (73, 74), has

been shown to specifically bind to annexin-1, -2, and -3 (35). Likewise, rPX-His could be specifically tagged with a covalent cholinergic radioligand [^3H]PrBCM, which was previously used by us to label keratinocyte membrane proteins immunoprecipitated by 85% of pemphigus patients (5).

The results of pharmacological experiments demonstrated that rPX-His exhibited conformational structure, thus allowing specific binding of cholinergic ligands. Post-translational modification is not required for ligand binding to single-unit ACh receptors, such as the muscarinic receptor (75, 76). However, the affinity of ACh binding by the wild-type PX, which can form dimers, may be different from that shown by rPX-His *in vitro*, because the bacterial system in which it was expressed was not capable of post-translational modification, such as glycosylation, which is known to play an important role in ligand binding by multi-subunit ACh receptors such as the nicotinic receptor (77). Thus, PX can act as a novel keratinocyte cell surface receptor for the cytotoxin ACh, synthesized and secreted by human KC in autocrine and paracrine fashions, and mediate known effects of ACh and cholinergic drugs on keratinocyte adhesion (reviewed in Refs. 21, 22). PX can also represent, at least in part, the putative keratinocyte cholinergic receptors targeted by PV IgG (5, 20).

The drugs that act at keratinocyte cholinergic receptors have been shown to alter cell motility and adhesion. Exposure of suspended KC to ACh results in attachment and spreading of the cells on the dish surface and development of intercellular contacts within 20–30 min, whereas non-stimulated cells accomplish this process within 90–120 min. On the other hand, exposure of a confluent keratinocyte monolayer to pharmacological antagonists of ACh leads to a characteristic acantholytic response. The cells retract their cytoplasmic projections, lose cell-to-cell attachments, detach from each other, and become round in shape and non-motile—characteristics that remarkably resemble pemphigus acantholysis *in vitro* (20). We have previously reported that ACh and its muscarinic and nicotinic congeners can prevent and reverse acantholysis produced in keratinocyte cultures by PV IgG (20). A receptor/ligand type of interaction of disease-causing PV IgG, with its target being a keratinocyte cell membrane protein, was first proposed by Patel *et al.* (78) based on the results of time-course study of the fate of the PV antibody/antigen complex. A direct evidence of activation of second messenger systems in response to PV IgG binding to KC have been obtained in the studies showing changes with phospholipase C, inositol 1,4,5-trisphosphate, transmembrane flux and intracellular levels of Ca^{2+} , intracellular cAMP/cGMP ratios, and activity and intracellular location of protein kinase C (reviewed in Refs. 5, 79). Therefore, binding of anti-PX antibody to KC may lead to acantholysis by competing with the natural agonist ACh, thus interrupting physiological regulation of keratinocyte adhesion. In keeping with the notion that autoantibody-mediated ligation of PX on the cell membrane of KC can alter the cell adhesive function are the results showing that an antibody to annexin-2 inhibits cell-to-cell attachment (80).

To determine the role of anti-PX antibody in pemphigus pathophysiology, we preabsorbed PV sera with rPX-His and tested acantholytic activities of both the PV IgGs depleted of anti-PX antibody and the PV IgG eluted from rPX-His. Neither IgG fraction could induce micro- or macroscopic mucocutaneous lesions in neonatal Balb/c mice. Addition of the adsorbed anti-PX PV IgG to the preabsorbed IgG fraction restored its acantholytic activity. These findings suggested that anti-PX antibody is one of the major contributors to skin blistering in PV patients. The fact that anti-PX PV antibody alone was sufficient to cause acantholysis *in vitro* (Fig. 1) but could not do

so *in vivo* was not surprising. Obviously, the cell-to-cell adhesion of KC cultured at low Ca^{2+} is less sophisticated than that taking place in live epidermis, with regard to a variety of adhesion molecules and control mechanisms, which include local anti-acantholytic factors such as interleukin-10 (30). Needless to say, the integrity of the epidermal barrier in higher species relies on more than a single molecule. For example, inactivation of an adhesion molecule such as Dsg 3 does not lead to skin blisters and is well compatible with the normal life span of *Dsg3^{null}* mice (5, 18), whereas a loss of immunological tolerance to keratinocyte self-antigens in PV is potentially lethal in 90% of patients (reviewed in Ref. 2). Therefore, to explain clinical and immunological correlations in PV, we propose a “multi-hit” hypothesis, which postulates that acantholysis in PV results from simultaneous and cumulative effects of autoantibodies directed toward different keratinocyte self-antigens, including the “structural” antigens, such as desmosomal cadherins, and “functional” antigens, such as cell surface receptors regulating function of the adhesion and cytoskeletal units.

The rationale behind our emphasis on the importance of “functional” targets of PV autoimmunity stems from recent discoveries of the genetic defects that underlie certain skin diseases. For instance, patients with genetic defects of the adhesion molecules Dsg1 and desmoplakin develop neither macroscopic nor light- or electron-microscopic alterations of keratinocyte cell-to-cell adhesion but produce instead a palmoplantar keratoderma, represented by linear and focal hyperkeratosis on palms and soles (81–83). In marked contrast, intra-epidermal split and PV-like skin lesions in patients with keratosis follicularis, or Darier-White disease, and patients with benign familial pemphigus, or Hailey-Hailey disease, result from a mutation in the genes coding for Ca^{2+} pumps, the ATP2A2 and ATP2C1, respectively (84, 85). Calcium metabolism in the epidermis of PV patients may also be altered. We have recently found that PV patients develop autoantibodies to the novel human $\alpha 9$ ACh receptor subunit that comprises ACh-gated Ca^{2+} channels on the cell membrane of human KC (19).

In summary, in this study we identified PX, a novel annexin-like molecule, which can function as a keratinocyte cholinergic receptor mediating biological effects of ACh on KC, including regulation of cell-to-cell adhesion. PX is targeted by PV autoimmunity and may represent one of the major targets for acantholytic autoantibodies. Further studies should be directed to elucidate the biochemical mechanisms by which the anti-PX antibody alters keratinocyte adhesion *in vitro* and the biological effect(s) caused by cholinergic ligand binding to PX. Furthermore, because annexins are well known mediators of anti-inflammatory effects of glucocorticosteroids in the skin (86), and because glucocorticosteroids can directly protect KC from the acantholytic effect of PV IgG *in vitro* (87), it will be important to elucidate possible relationships between the effects of glucocorticosteroids on PX and keratinocyte adhesion. Such an association may lead toward development of non-hormonal treatment of PV, because cholinergic drugs that, just like glucocorticosteroids, exhibit direct anti-acantholytic activity (20) may do so by competing with PV IgG for binding to PX on the cell membrane of KC.

Acknowledgments—We thank Dr. Henry Tesluk, Department of Pathology, and Drs. Thomas R. Stevenson and Thomas P. Whetzel, Department of Surgery, University of California Davis Medical Center for facilitating obtainments of large quantities of keratinocyte membrane protein for immunoblotting.

REFERENCES

1. Cohen, L. M., Skopicki, D. K., Harriest, T. J., and Clark, W. H., Jr. (1997) in *Lever's Histopathology of the Skin* (Elder, D., Elenitas, R., Jaworsky, C., and

- Johnson, B. J., eds 8th Ed., pp. 209–252, Lippincott-Raven, Philadelphia
2. Robinson, J. C., Lozada-Nur, F., and Frieden, I. (1997) *Oral Surg. Oral Med. Oral Pathol. Oral Radiol. Endod.* 84, 349–355
3. Rosenberg, F. R., Sanders, S., and Nelson, C. T. (1976) *Arch. Dermatol.* 112, 962–970
4. Ahmed, A. R., and Moy, R. (1982) *J. Am. Acad. Dermatol.* 7, 221–228
5. Nguyen, V. T., Lee, T. X., Ndoye, A., Shultz, L. D., Pittelkow, M. R., Dahl, M. V., Lynch, P. J., and Grando, S. A. (1998) *Arch. Dermatol.* 134, 971–980
6. Stanley, J. R., Yaar, M., Hawley-Nelson, P., and Katz, S. I. (1982) *J. Clin. Invest.* 70, 281–288
7. Stanley, J. R., Koulou, L., and Thivolet, C. (1984) *J. Clin. Invest.* 74, 313–320
8. Anhalt, G. J., Labib, R. S., Voorhees, J. J., Beals, T. F., and Diaz, L. A. (1982) *N. Engl. J. Med.* 306, 1189–1196
9. Amagai, M., Klaus-Kovtun, V., and Stanley, J. R. (1991) *Cell* 67, 869–877
10. Amagai, M., Karpati, S., Prussick, R., Klaus-Kovtun, V., and Stanley, J. R. (1992) *J. Clin. Invest.* 90, 919–926
11. Memar, O. M., Rajaraman, S., Thotakura, R., Tying, S. K., Fan, J. L., Seetharamaiah, G. S., Lopez, A., Jordan, R. E., and Prabhakar, B. S. (1996) *J. Invest. Dermatol.* 106, 261–268
12. Memar, O. M. (1995) *Characterization of the Pemphigus Vulgaris Antibigen (Desmoglein 3) Expressed in Insect Cells: Induction of Blister-Causing Antibodies*, University of Texas Medical Branch Editorial Offices, Galveston, TX
13. Amagai, M., Hashimoto, T., Shimizu, N., and Nishikawa, T. (1994) *J. Clin. Invest.* 94, 59–67
14. Amagai, M., Nishikawa, T., Nousari, H. C., Anhalt, G. J., and Hashimoto, T. (1998) *J. Clin. Invest.* 102, 775–782
15. Mahoney, M. G., Wang, Z., Rothenberger, K., Koch, P. J., Amagai, M., and Stanley, J. R. (1999) *J. Clin. Invest.* 103, 461–468
16. Udey, M. C., and Stanley, J. R. (1999) *J. Am. Med. Assoc.* 282, 572–576
17. Ding, X., Diaz, L. A., Fairley, J. A., Guidice, G. J., and Liu, Z. (1999) *J. Invest. Dermatol.* 112, 739–743
18. Koch, P. J., Mahoney, M. G., Ishikawa, H., Pulkkinen, L., Uitto, J., Shultz, L., Murphy, G. F., Whitaker-Menezes, D., and Stanley, J. R. (1997) *J. Cell Biol.* 137, 1091–1102
19. Nguyen, V. T., Ndoye, A., and Grando, S. A. (2000) *Am. J. Pathol.*, in press
20. Grando, S. A., and Dahl, M. V. (1993) *J. Eur. Acad. Dermatol. Venereol.* 2, 72–86
21. Grando, S. A., and Horton, R. M. (1997) *Curr. Opin. Dermatol.* 4, 262–268
22. Grando, S. A. (1997) *J. Invest. Dermatol. Symp. Proc.* 2, 41–48
23. Beutner, E. H., Chorzelski, T. P., and Jablonska, S. (1985) *Int. J. Dermatol.* 24, 405–421
24. Ohata, Y., Hashimoto, T., and Nishikawa, T. (1995) *Clin. Exp. Dermatol.* 20, 454–458
25. Nguyen, V., Kadunce, D. P., Hendrix, J. D., Gammon, W. R., and Zone, J. J. (1993) *J. Invest. Dermatol.* 100, 349–355
26. Grando, S. A., Cabrera, R., Hostager, B. S., Bigliardi, P. L., Blake, J. S., Herron, M. J., Dahl, M. V., and Nelson, R. D. (1993) *Skin Pharmacol.* 6, 135–147
27. Huynh, T. V., Young, R. A., and Davis, R. W. (1985) in *DNA Cloning: A Practical Approach* (Glover, D. M., ed) Vol. 1, pp. 49–78, IRL Press, Oxford
28. Taylor, I. K., Cuthbert, A. W., and Young, M. (1975) *Eur. J. Pharmacol.* 31, 319–326
29. Feliciani, C., Toto, P., Amerio, P., Mohammad, S., Coscione, P. S., Amerio, P., Shivji, G., Wang, B., and Sauder, S. N. (2000) *J. Invest. Dermatol.* 114, 71–77
30. Toto, P., Feliciani, C., Amerio, P., Suzuki, H., Wang, B., Shivji, G. M., Woodley, D., and Sauder, D. N. (2000) *J. Immunol.* 164, 522–529
31. Kozak, M. (1987) *Nucleic Acids Res.* 15, 8125–8148
32. Jost, M., Weber, K., and Gerke, V. (1994) *Biochem. J.* 298, 553–559
33. Jost, M., Thiel, C., Weber, K., and Gerke, V. (1992) *Eur. J. Biochem.* 207, 923–930
34. Jones, P. G., Moore, G. J., and Waisman, D. M. (1992) *J. Biol. Chem.* 267, 13993–13997
35. Zimmerman, U. J., Hennigan, B. B., Liu, L., Campbell, C. H., and Fisher, A. B. (1995) *Biochem. Mol. Biol. Int.* 35, 307–315
36. Curtis, C. A., Wheatley, M., Bansal, S., Birdsall, N. J., Eveleigh, P., Pedder, E. K., Poyner, D., and Hulme, E. C. (1989) *J. Biol. Chem.* 264, 489–495
37. Siever, D. A., and Erickson, H. P. (1997) *Int. J. Biochem. Cell Biol.* 29, 1219–1223
38. Lin, M. S., Mascaro, J. M., Jr., Liu, Z., Espana, A., and Diaz, L. A. (1997) *Clin. Exp. Immunol.* 107, Suppl. 1, 9–15
39. Grando, S. A., Glukhenky, B. T., Drannik, G. N., Kostromin, A. P., Boiko, Y., and Senyuk, O. F. (1989) *Autoimmunity* 3, 247–260
40. Hashimoto, K., Wun, T. C., Baird, J., Lazarus, G. S., and Jensen, P. J. (1989) *J. Invest. Dermatol.* 92, 310–314
41. Kawana, S., Geoghegan, W. D., Jordan, R. E., and Nishiyama, S. (1989) *J. Invest. Dermatol.* 92, 588–592
42. Grando, S. A., Glukhenky, B. T., Drannik, G. N., Epshtein, E. V., Kostromin, A. P., and Korostash, T. A. (1989) *Arch. Dermatol.* 125, 925–930
43. Grando, S. A., Glukhenky, B. T., Drannik, G. N., Kostromin, A. P., Chernyavsky, A. I., and Barabash, T. M. (1990) *J. Clin. Lab. Immunol.* 32, 137–141
44. Amagai, M. (1999) *J. Dermatol. Sci.* 20, 92–102
45. Stanley, J. R. (1995) *Ciba Found. Symp.* 189, 107–120
46. Kitajima, Y., Inoue, S., and Yae, H. (1987) *J. Invest. Dermatol.* 89, 167–171
47. Fan, J. L., Memar, O., McCormick, D. J., and Prabhakar, B. S. (1999) *J. Immunol.* 163, 6228–6235
48. Amagai, M., Tsunoda, K., Suzuki, H., Nishifuji, K., Koyasu, S., and Nishikawa, T. (2000) *J. Clin. Invest.* 105, 625–631
49. Iwatsuki, K., Harada, H., Yokote, R., and Kaneko, F. (1995) *Br. J. Dermatol.* 133, 209–216
50. Karpati, S., Amagai, M., Prussick, R., Cehrs, K., and Stanley, J. R. (1993) *J. Cell Biol.* 122, 409–415
51. Rajasekaran, A. K., Hojo, M., Huima, T., and Rodriguez-Boulant, E. (1996) *J. Cell Biol.* 132, 451–463
52. Witcher, L. L., Collins, R., Puttagunta, S., Mechanic, S. E., Munson, M., Gumbiner, B., and Cowin, P. (1996) *J. Biol. Chem.* 271, 10904–10909
53. Fujimoto, K., Nagafuchi, A., Tsukita, S., Kuraoka, A., Ohokuma, A., and Shibata, Y. (1997) *J. Cell Sci.* 110, 311–322
54. Creutz, C. E. (1992) *Science* 258, 924–931
55. Smith, P. D., and Moss, S. E. (1994) *Trends Genet.* 10, 241–245
56. Morgan, R. O., and Fernandez, M. P. (1997) *Cell. Mol. Life Sci.* 53, 508–515
57. Demange, P., Voges, D., Benz, J., Liemann, S., Goettig, P., Berendes, R., Burger, A., and Huber, R. (1994) *Trends Biochem. Sci.* 19, 272–276
58. Moss, S. E. (1997) *Trends Cell Biol.* 7, 87–89
59. Donnelly, S. R., and Moss, S. E. (1997) *Cell. Mol. Life Sci.* 53, 533–538
60. Reutelsperger, C. P. M., and Van Heerde, W. L. (1997) *Cell. Mol. Life Sci.* 53, 527–532
61. Fava, R. A., Nanney, L. B., Wilson, D., and King, L. E., Jr. (1993) *J. Invest. Dermatol.* 101, 732–737
62. Culard, J. F., Basset-Seguin, N., Calas, B., Guilhou, J. J., and Martin, F. (1992) *J. Invest. Dermatol.* 98, 436–441
63. Ma, A. S., and Ozers, L. J. (1996) *Arch. Dermatol. Res.* 288, 596–603
64. Barwise, J. L., and Walker, J. H. (1996) *J. Cell Sci.* 109, 247–255
65. Chung, C. Y., and Erickson, H. P. (1994) *J. Cell Biol.* 126, 539–548
66. Vasioukhin, V., Bauer, C., Yin, M., and Fuchs, E. (2000) *Cell* 100, 209–219
67. Nakao, H., Watanabe, M., and Maki, M. (1994) *Eur. J. Biochem.* 223, 901–908
68. Falcone, D. J., Borth, W., Mathew, J., Guevara, C., and Hajjar, K. A. (1995) *FASEB J.* 9, 412 (abstr.)
69. Hajjar, K. A., and Menell, J. S. (1997) *Ann. N. Y. Acad. Sci.* 811, 337–349
70. Von Der Mark, K., and Mollenhauer, J. (1997) *Cell. Mol. Life Sci.* 53, 539–545
71. Chung, C. Y., Murphy-Ullrich, J. E., and Erickson, H. P. (1996) *Mol. Biol. Cell* 7, 883–892
72. Schenk, S., Bruckner-Tuderman, L., and Chiquet-Ehrismann, R. (1995) *Br. J. Dermatol.* 133, 13–22
73. Ulus, I. H., Millington, W. R., Buyukusyal, R. L., and Kiran, B. K. (1988) *Biochem. Pharmacol.* 37, 2747–2755
74. Sterz, R., Peper, K., Simon, J., Ebert, J. P., Edge, M., Pagala, M., and Bradley, R. J. (1986) *Brain Res.* 385, 99–114
75. van Koppen, C. J., and Nathanson, N. M. (1990) *J. Biol. Chem.* 265, 20887–20892
76. Matus-Leibovitch, N., Mengod, G., and Oron, Y. (1992) *Biochem. J.* 285, 753–758
77. Shtrom, S. S., and Hall, Z. W. (1996) *J. Biol. Chem.* 271, 25506–25514
78. Patel, H. P., Diaz, L. A., Anhalt, G. J., Labib, R. S., and Takahashi, Y. (1984) *J. Invest. Dermatol.* 83, 409–415
79. Kitajima, Y., Aoyama, Y., and Seishima, M. (1999) *J. Invest. Dermatol. Symp. Proc.* 4, 137–144
80. Tressler, R. J., Updyke, T. V., Yeatman, T., and Nicolson, G. L. (1993) *J. Cell. Biochem.* 53, 265–276
81. Rickman, L., Simrak, D., Stevens, H. P., Hunt, D. M., King, I. A., Bryant, S. P., Eady, R. A., Leigh, I. M., Arneemann, J., Magee, A. I., Kelsell, D. P., and Buxton, R. S. (1999) *Hum. Mol. Genet.* 8, 971–976
82. Whitlock, N. V., Ashton, G. H., Dopping-Hepenstal, P. J., Gratian, M. J., Keane, F. M., Eady, R. A., and McGrath, J. A. (1999) *J. Invest. Dermatol.* 113, 940–946
83. Armstrong, D. K., McKenna, K. E., Purkis, P. E., Green, K. J., Eady, R. A., Leigh, I. M., and Hughes, A. E. (1999) *Hum. Mol. Genet.* 8, 143–148
84. Hu, Z., Bonifas, J. M., Beech, J., Bench, G., Shigihara, T., Ogawa, H., Ikeda, S., Mauro, T., and Epstein, E. H., Jr. (2000) *Nat. Genet.* 24, 61–65
85. Sakuntabhai, A., Ruiz-Perez, V., Carter, S., Jacobsen, N., Burge, S., Monk, S., Smith, M., Munro, C. S., O'Donovan, M., Craddock, N., Kucherlapati, R., Rees, J. L., Owen, M., Lathrop, G. M., Monaco, A. P., Strachan, T., and Hovnanian, A. (1999) *Nat. Genet.* 21, 271–277
86. Bastian, B. C., Sellert, C., Seekamp, A., Roemisch, J., Paques, E. P., and Broecker, E. B. (1993) *J. Invest. Dermatol.* 101, 359–363
87. Swanson, D. L., and Dahl, M. V. (1983) *J. Invest. Dermatol.* 81, 258–260

Annexin I Is Phosphorylated in the Multivesicular Body During the Processing of the Epidermal Growth Factor Receptor

Clare E. Futter, Stephen Felder,* Joseph Schlessinger,* Axel Ullrich,† and Colin R. Hopkins

MRC Laboratory for Molecular Cell Biology, University College, London; and *Department of Pharmacology, New York University Medical Center, New York; †Max Planck Institute, D-8033 Martinsried, Germany

Abstract. We have previously shown that an active epidermal growth factor receptor (EGF-R) kinase is necessary for efficient sorting of the EGF-R to the lysosome, and we have shown that this occurs in the multivesicular body (MVB), where EGF-R are sorted away from recycling receptors by being removed to the internal vesicles of the MVB. The aim of the present study was to identify substrates of the EGF-R kinase associated with MVBs which might play a role in this sorting process. We used a density shift technique to isolate MVBs and show that the major substrates phosphorylated in vitro within MVBs which contain an active EGF-R kinase are the EGF-R itself and annexin I. Annexin I is associated with both plasma membrane

and MVBs in a calcium-independent manner but can be phosphorylated in vitro only in MVBs. Phosphorylation of calcium-independent annexin I in isolated MVBs converts it to a form that requires calcium for membrane association. In cells with an active EGF-R kinase the amount of calcium-independent annexin I in MVBs is reduced, suggesting that a phosphorylation-induced conversion of the calcium independent to the calcium-dependent form also occurs in vivo. Our observations, together with the known properties of annexin I in mediating membrane fusion, suggest that inward vesiculation in MVBs is induced by the EGF-R and is mediated by phosphorylated annexin I.

WHEN EGF binds to its receptor the intrinsic tyrosine kinase of the receptor is activated, resulting in phosphorylation of the receptor itself and various other proteins (Ushiro and Cohen, 1980). During this time the EGF-EGF-receptor (EGF-R)¹ complex is rapidly internalized and processed within the endocytic pathway where it becomes degraded (Carpenter and Cohen, 1976). A mutant EGF-R lacking an active kinase is internalized in response to EGF at the same rate as the wild type EGF-R but the kinase-negative EGF-R is not efficiently degraded and a significant proportion of the mutant EGF-R recycle to the cell surface (Honegger et al., 1987; Felder et al., 1990). By EM we have shown that saturating concentrations of EGF stimulate internalization of both wild type and kinase negative EGF-R to multivesicular bodies but within this compartment they have distinctly different distributions (Felder et al., 1990). Since only wild type EGF-R are efficiently transferred to the internal vesicles of the multivesicular body (MVB) we have proposed that removal of EGF-R from the perimeter membrane of the endocytic pathway allows them to be degraded.

While it is possible that the activated EGF-R kinase initiates a series of events in the plasma membrane which results in sorting at the level of the MVB it is also possible that the

EGF-R kinase is active in the endosome where it triggers the events that lead to its degradation. The aim of the present study was to determine whether there are substrates of the EGF-R kinase specifically associated with MVBs. We have adapted a previously described density shift protocol (Futter and Hopkins, 1989) to isolate highly purified MVBs containing EGF-R and show that the major substrates of the EGF-R kinase in MVBs are the EGF-R itself and annexin I. Since annexin I is a protein which interacts with membranes and actin-containing cytoskeletal elements (Glenney et al., 1987) and can promote phospholipid vesicle fusion in vitro (Ernst et al., 1990), it could regulate the production of internal vesicles within MVBs.

Materials and Methods

Cell Lines

NIH 3T3 cells, strain 2.2, transfected with plasmid bearing either the full-length cDNA for the human EGF-R (HER14 cells), or the cDNA encoding the human EGF-R with lysine 721 replaced with alanine (K721A cells), and each expressing roughly 400,000 receptors per cell, were used (Honegger et al., 1987). Cells were maintained in DME supplemented with 10% FCS at 37°C in a 5% CO₂ atmosphere.

Colloidal Gold Complexes

Gold particles (10 nm) were prepared using the tannic acid method of Slot and Geuze, (1985), and were stabilized with the mAb 108, according to

1. Abbreviations used in this paper: EGF-R, epidermal growth factor receptor; MVB, multivesicular body.

standard procedures (DeMey, 1986). The complexes were stored in 0.02% azide at 4°C, and were washed by centrifugation in an airfuge (Beckman Instruments, Palo Alto, CA) at 150,000 g for 5 min immediately before use.

Iodination

EGF (mouse EGF; Sigma Chemical Co., Poole, UK) was iodinated according to the method of Hunter and Greenwood (1962) and protein A was iodinated using iodobeads (Pierce, Chester, UK).

Incubation Procedures

All incubations were performed in DME containing 20 mM Hepes, pH 7.4, 2 mg/ml BSA. EGF was used at a concentration of 20 nM. 108-gold was used at a concentration that gave OD₅₈₀ of 0.3–0.4. Incubations were performed at 37°C unless otherwise indicated and for the times indicated in Results. Where the proportion of cell-associated ¹²⁵I-EGF that was plasma membrane bound was to be determined, cells were incubated in acetic acid-saline, pH 2.5, for 5 min at 4°C to remove plasma membrane-bound EGF, before digestion of the cells in 5 M NaOH.

Subcellular Fractionation Procedure

Cells were washed three times at 4°C with lysis buffer (10 mM triethanolamine, pH 7.4, 0.25 M sucrose, 1 mM EDTA, 200 μM orthovanadate, 1 mM PMSF). Cells were scraped off the dish in the minimum volume of lysis buffer and lysed by eight strokes through a 21 g needle. Unbroken cells and nuclei were removed by centrifugation at 800 g for 5 min at 4°C. The resulting postnuclear supernatant was layered onto a 12 ml 26–52% sucrose gradient, containing triethanolamine, EDTA, orthovanadate, and PMSF at the same concentrations and pH as the lysis buffer. Gradients were then centrifuged in a Beckman SW40 rotor at 200,000 g for 15 h at 4°C in a Beckman L70 ultracentrifuge. Gradients were fractionated from the bottom into 15 × 0.9-ml fractions.

EM

Cells and fractions were fixed in dilute Karnovsky fixative, postfixed in osmium tetroxide, and embedded and sectioned so that the full thickness of the pellet could be examined. Sections were stained in aqueous uranyl acetate and lead citrate and examined in a CM12 Philips electron microscope.

SDS-PAGE and Western Blotting

SDS-PAGE was performed under reducing conditions. Proteins on SDS-polyacrylamide gels were electrophoretically transferred to nitrocellulose for 16 h in a transfer apparatus (Bio-Rad Laboratories, Cambridge, MA) at a constant current of 100 mA. After incubation with either rabbit anti-EGF-R antiserum, RK2 (Kris et al., 1985), rabbit anti-phosphotyrosine antiserum, or rabbit anti-annexin I antiserum (a gift from S. Moss, University College, London), blots were washed and incubated in ¹²⁵I-protein A. Blots were analyzed by autoradiography and, where quantitation was performed, radioactive bands were excised, and counted.

In Vitro Phosphorylation Studies

Cell fractions were resuspended in 20 mM Hepes, pH 7.4, 150 mM NaCl. Fractions were incubated for 15 min at 4°C in the presence of 5 mM MgCl₂, 20 μM orthovanadate, and [γ -³²P]ATP (5 μM). Reactions were stopped by the addition of 10% TCA, and TCA precipitates were examined by SDS-PAGE.

To examine the effects of phosphorylation on calcium dependence of membrane association of MVB proteins, phosphorylation reactions were performed as above. MVBs were then washed twice with 20 mM Hepes, pH 7.4, 150 mM NaCl, 200 μM orthovanadate, containing either 1.5 mM EDTA or 1.5 mM CaCl₂, by centrifugation in a Beckman TL100.4 rotor at 200,000 g for 1 h at 4°C in a Beckman TLX ultracentrifuge, and the pellets were examined by SDS-PAGE.

Annexin I Immunoprecipitation

To identify annexin I, *in vitro* phosphorylation assays were carried out as above, but were stopped by the addition of NDET (10 mM Tris, pH 7.4, 1% NP-40, 0.4% deoxycholate, 66 mM EDTA), containing 1 mM PMSF, 200 μM orthovanadate and 0.2% SDS. Samples were clarified by centrifugation (14,000 g for 5 min), and were then incubated with a rabbit polyclonal

antibody against annexin I. Antibody-bound proteins were immunoprecipitated using *Staphylococcus aureus*, and the washed immunoprecipitate was analyzed by SDS-PAGE.

Results

Isolation of Highly Purified Endosomes by Density-shift Using EGF-R Antibody-Gold Complexes

We have previously shown in H.Ep.2 cells that antibody to the transferrin receptor complexed to colloidal gold can be used to modify the density of endocytic compartments involved in the processing of the EGF-receptor complex, so that they can be purified by sucrose density centrifugation (Futter and Hopkins, 1989). In the present study we extended this technique to NIH-3T3 cells transfected with either the wild type human EGF receptor or a human EGF receptor with a point mutation in the putative ATP binding site, rendering the receptor kinase negative (Honegger et al., 1987). To isolate endocytic compartments containing EGF-R by density shift we employed a mAb (108) to EGF-R complexed to colloidal gold. The 108 antibody binds to the external domain of the EGF-R and has been shown, when saturating EGF concentrations are used, not to stimulate internalization or kinase activity of the EGF-R, or to interfere with EGF binding (Bellot et al., 1990). To induce a sufficient increase in density of endocytic compartments containing 108-gold, it was necessary to stimulate cells with saturating concentrations of EGF. Under these conditions both the kinase positive and negative EGF-R are internalized at similar rates (Felder et al., 1990). Our previous studies using gold complexes to density shift endocytic compartments showed that gold-loaded endosomes will pellet through 52% sucrose whereas gold-loaded plasma membranes will not (Futter and Hopkins, 1989). To begin we established the rate of EGF-R internalization by following ¹²⁵I-EGF uptake, and showed that >70% was internalized within 20 min of EGF stimulation (Fig. 1 a).

Fig. 1 b shows the recovery of EGF and EGF-R in the pellet after sucrose density gradient fractionation of cells after similar stimulation with EGF. Recovery of EGF-R was assessed by Western blotting with anti-EGF-R antibody. The increase in recovery of EGF and EGF-R in the pellet with increasing lengths of incubation after EGF stimulation showed similar kinetics to that of EGF-stimulated internalization, showing that endocytic compartments rather than plasma membrane pellet under the fractionation conditions used.

Examination of the endosome pellet isolated by fractionation of 108-gold-loaded cells expressing the wild type EGF-R 20 min after EGF stimulation showed that all membranous elements labeled with gold were endosomal, many of which were clearly identifiable as MVBs (Fig. 2 a). Quantitation of the number of vesicles which contained gold by counting random sections showed that 34% of vesicle profiles found in the pellet contained gold. Vesicle profiles which lacked gold presumably contained gold particles in another section plane. Electron microscopic examination of the pellet from cells expressing the kinase negative EGF-R showed that 14% of the vesicle profiles contained gold. This lower figure compared to the wild type fraction is consistent

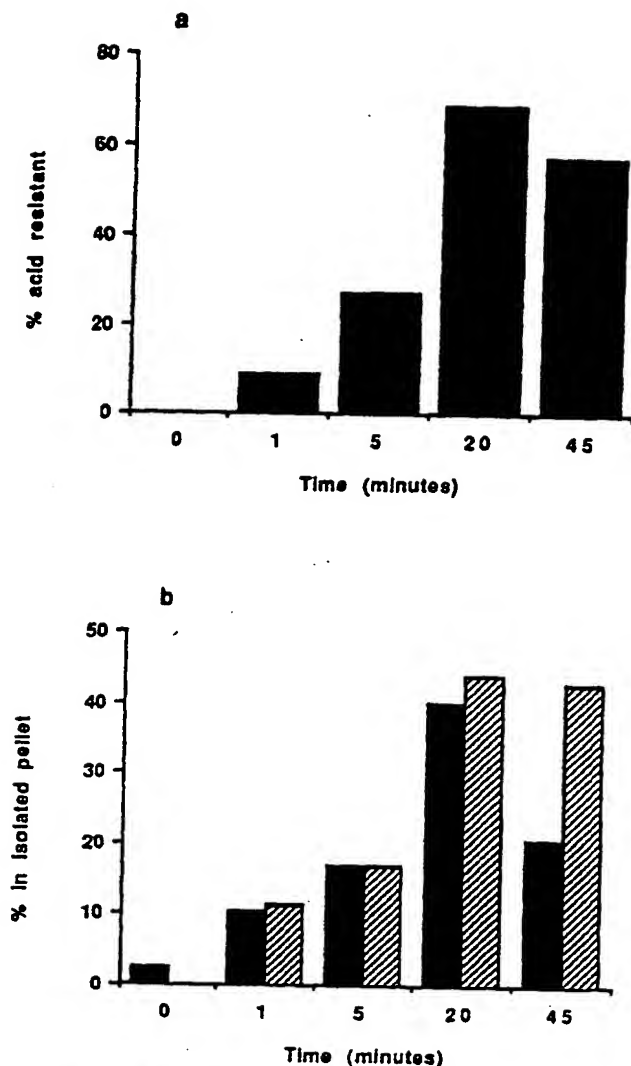


Figure 1. (a) Cells expressing wild type EGF-R were stimulated with 125 I-EGF for the indicated times. The percent of total cell-associated EGF that had been internalized was determined by acid stripping. (b) Cells expressing wild type EGF-R were incubated with 108-gold for 30 min and were then stimulated with 125 I-EGF for the indicated times. Cells were lysed and fractionated. The percent of postnuclear supernatant 125 I-EGF (▨) and EGF-R (■) that was recovered in the pellet after sucrose density gradient fractionation was determined. Quantitation of the EGF-R was performed by blotting gradient fractions with anti-EGF-R antibody. Iodinated protein A and autoradiography were used to visualize bands, which were excised and counted.

with observations on intact cells (Felder et al., 1990) which have shown that there is significantly less EGF-R in the MVB compartment of kinase negative cells. It should be noted nevertheless that the majority of gold-loaded elements in the pellets from the kinase negative cells are MVBs (Fig. 2 b). Presumably the other gold-containing elements of the endocytic pathway were too buoyant to pellet. Previous studies have shown, through measurement of marker enzyme activities and by EM, that in a number of different cell lines nonendosomal organelles do not pellet under the fractionation conditions used (Beardmore et al., 1988; Futter et al., 1989; Beaumelle and Hopkins, 1990). However amorphous mate-

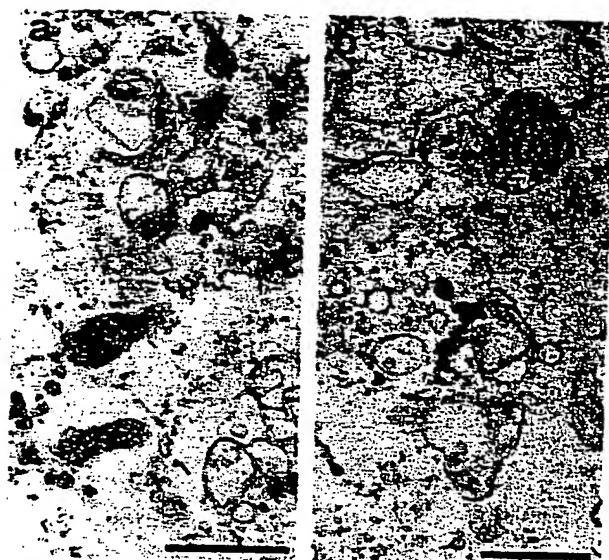


Figure 2. Cells expressing either wild type (a) or kinase negative (b) EGF-R were incubated with 108-gold for 30 min, and were then stimulated with EGF for 20 min. Cells were then lysed and fractionated, and the pellet after sucrose gradient fractionation was processed for microscopy. All membranous elements that contain gold are endosomal, many of which are MVBs. Amorphous material, presumably of cytoskeletal nature, consistently pellets with endosome fractions. Bar, 0.5 μ m.

rial, presumably a component of the cytoskeleton, consistently pellets with endosome fractions.

The Fate of the Plasma Membrane during Density Shift Separation of Gold-loaded Endosomes

When cells were stimulated with EGF for 1 min after preincubation with 108-gold (when the majority of EGF-R are plasma membrane associated), the density of the plasma membrane fraction was increased. Thus, in the absence of 108-gold binding, plasma membrane was found in a peak in fractions 8–12 (Fig. 3 a) while binding of 108-gold to the plasma membrane caused a shift to fraction 6 (Fig. 3 b). After stimulation of cells with EGF for one minute EGF-R was still found in fraction 6 (Fig. 3 c). EM of this fraction showed that it was composed of large vesicle profiles bearing EGF-R-gold particles on their outer surfaces (results not shown), in contrast to MVBs where the gold particles were found only on the inner surfaces of the perimeter membrane.

Substrates Phosphorylated in Endosomes and Plasma Membrane Isolated from Cells Expressing Wild type EGF-R Kinase

To determine whether proteins are phosphorylated in MVBs as a result of activation of the EGF-R kinase, phosphorylation was examined in endosomes isolated from NIH 3T3 cells expressing either the wild type or the kinase negative EGF-R. Endosomes were isolated 20 min after EGF stimulation when the majority of both kinase negative and wild type EGF-R are in MVBs (Felder et al., 1990) and the density shifted fractions are composed primarily of MVBs (Fig. 2). When MVBs isolated from NIH 3T3 cells expressing the wild type EGF-R were incubated with [γ - 32 P]ATP in vitro

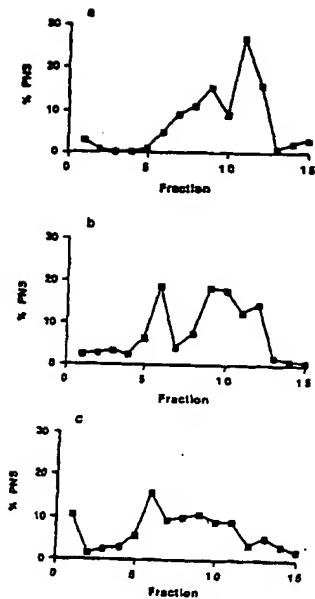


Figure 3 Cells expressing wild type EGF-R were incubated with no gold (a), 108-gold for 30 min (b), or 108-gold for 30 min, followed by stimulation with EGF for 1 min (c). Cells were lysed and fractionated and gradient fractions were analyzed by Western blotting with anti-EGF-R antibody. Iodinated protein A and autoradiography were used to visualize bands, which were excised and counted.

two major phosphorylated substrates were detected, the EGF-R itself and a protein of approximately 35 kD (Fig. 4 a). The 35-kD protein could be immunoprecipitated with anti-annexin I antibody (Fig. 4 b).

To determine whether annexin I is phosphorylated in plasma membrane fractions in addition to MVBs, plasma membrane fractions were isolated from cells stimulated with EGF for one minute. When these fractions were incubated with [γ - 32 P]ATP in vitro several substrates were phosphorylated including the EGF-R (Fig. 4 a), but immunoprecipitation with annexin I antibody showed they did not include annexin I (Fig. 4 b).

MVB and plasma membrane fractions from cells expressing the kinase negative EGF-R, used as a control, showed that neither the EGF-R nor the 35-kD protein were phosphorylated (Fig. 4, a and b).

To confirm that the phosphorylation of annexin I in the MVB was due to the presence of an active EGF-R kinase we carried out a parallel study using H.Ep.2 cells in which we have shown previously that EGF-R containing MVBs can be isolated by density shift when loaded with anti-transferrin receptor-gold complexes and stimulated with EGF (Futter and Hopkins, 1989). Western blotting the isolated MVBs showed that EGF stimulation of transferrin receptor-gold-loaded cells resulted in a fivefold increase in the amount of EGF-R that co-localized with transferrin receptor in MVBs (results not shown). In vitro phosphorylation assays showed that a number of proteins became phosphorylated in MVBs isolated from H.Ep.2 cells, but only in MVBs that contained an active EGF-R kinase did the EGF-R and a 35-kD protein become phosphorylated (Fig. 5 a). Immunoprecipitation confirmed this protein was annexin I (Fig. 5 b).

We conclude that annexin I is present in isolated MVBs and that it can be phosphorylated in vitro in the presence of an active EGF-R kinase.

Phosphorylation and the Calcium Dependence of Annexin I Binding to MVBs and Plasma Membrane

Annexin I has been isolated as an EDTA eluate of mem-

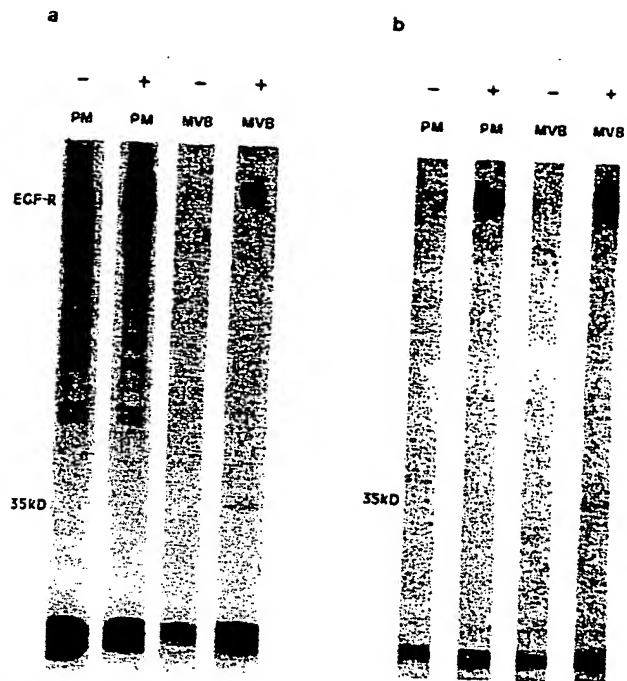


Figure 4. NIH 3T3 cells expressing either the wild type (+) or the kinase negative (−) EGF-R were incubated with 108-gold for 30 min. Cells were then stimulated with EGF for 1 min to isolate a plasma membrane fraction (PM) or for 20 min to isolate an MVB fraction (MVB). Cells were then lysed and fractionated. The PM fraction was taken from fraction 6 and the MVB fraction was taken from the pellet after sucrose gradient fractionation. In vitro phosphorylation reactions were performed on the isolated fractions as described in Materials and Methods. Either the whole fraction (a) or an anti-annexin I immunoprecipitation of the fraction (b) were analyzed by SDS-PAGE on a 10% gel. The EGF-R is present in anti-annexin I immunoprecipitations because the fractions contain anti-EGF-R gold, but in control immunoprecipitations that do not include anti-annexin I antibody, annexin I is not immunoprecipitated. Gel loadings with respect to the EGF-R are 1:2:1:1.4 for −PM: +PM: −MVB: +MVB.

branes and shown to associate with phospholipids in a calcium dependent manner (Glenney et al., 1987). Haigler et al., (1987) have shown that in addition to the calcium-dependent form there is a form of annexin I in human placenta which associates with membranes independently of calcium and can be phosphorylated by the EGF-R kinase. Phosphorylation of this form of annexin I converts the protein into a form that associates with membranes only in the presence of calcium. The MVBs used in the present study are isolated in the presence of EDTA and so the annexin I that is phosphorylated in vitro must remain associated with membranes in the absence of calcium. In order to determine the effect of phosphorylation on the calcium dependence of annexin I in MVBs, isolated fractions were incubated with [γ - 32 P]ATP and then washed two times in lysis buffer containing either 1.5 mM EDTA or 1.5 mM Ca^{2+} . The membrane pellet was examined by SDS-PAGE. After washing in EDTA phosphorylated annexin I was no longer associated with the MVB pellet. However in the presence of calcium the protein remained associated with MVBs (Fig. 6).



Figure 5. H.Ep.2 cells were incubated with B3/25 (anti-transferrin receptor)-gold for 60 min and were then incubated in the presence (+) or absence (-) of EGF for 20 min (in the continued presence of B3/25-gold). Cells were then lysed and fractionated. In vitro phosphorylation reactions were performed on the MVB fractions as described in Materials and Methods. Either the whole fraction (a) or an anti-annexin I immunoprecipitation of the fraction (b) were analyzed by SDS-PAGE on a 10% gel.

The Influence of EGF-R Kinase on the Amount of Annexin I Associated with Plasma Membrane and MVBs

To determine whether an active EGF-R kinase is necessary for association of annexin I with MVBs isolated MVBs were Western blotted with anti-annexin I antibody and the amount of annexin I relative to EGF-R was quantitated. Annexin I was present in MVB fractions from cells expressing the wild type EGF-R and also those expressing the kinase negative EGF-R. However MVBs from NIH 3T3 cells containing wild type EGF-R had three- to fourfold less annexin I (relative to EGF-R) than kinase negative MVBs (Fig. 7). Similarly annexin I was present in MVBs from H.Ep.2 cells iso-

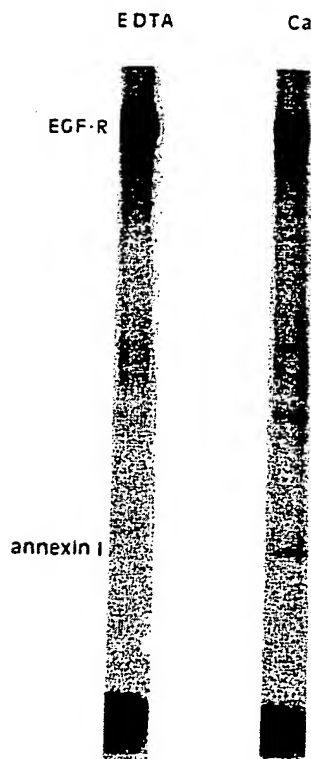


Figure 6. NIH 3T3 cells expressing wild type EGF-R were incubated with 108-gold for 30 min and were then stimulated with EGF for 20 min. Cells were then lysed and fractionated. In vitro phosphorylation reactions were performed on the MVB fractions as described in Materials and Methods. MVBs were then washed in the presence of EDTA (EDTA) or calcium (Ca). Washed pellets were analyzed by SDS-PAGE on a 10% gel.

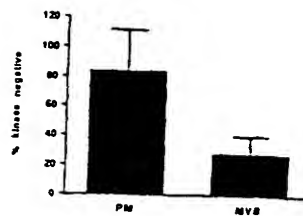


Figure 7. (a) NIH 3T3 cells expressing wild type (+) or kinase negative (-) EGF-R were incubated with 108 gold for 30 min. Cells were then stimulated with EGF for 1 min and a plasma membrane fraction isolated (PM) or for 20 min and an MVB fraction iso-

lated (MVB). Fractions were Western blotted with anti-EGF-R antibody and anti-annexin-I antibody. Iodinated protein A and autoradiography were used to visualize bands, which were excised and counted. The amount of annexin I (relative to the EGF-R) in fractions from wild type cells is expressed as a % of that in the corresponding fractions from kinase negative cells. Results are mean \pm SEM of four observations.

lated using transferrin receptor gold with or without prior EGF stimulation, but MVBs containing an active EGF-R kinase contained approximately twofold less annexin I (relative to transferrin receptor) than MVBs lacking an active EGF-R kinase (results not shown). We conclude therefore that an active EGF-R kinase is not necessary for association of annexin I with MVBs. In addition, the reduction in the amount of calcium-independent annexin I in MVBs containing an active EGF-R kinase is consistent with the phosphorylation of annexin I in vivo, as we have shown phosphorylation of annexin I in vitro to cause its release from MVBs in the presence of calcium chelator. To confirm, as our in vitro results would suggest, that the loss of calcium-independent annexin I through phosphorylation occurs in MVBs rather than on the plasma membrane, the amount of annexin I associated with plasma membrane fractions containing wild type and those containing kinase negative EGF-R was compared. Plasma membrane fractions containing wild type EGF-R and those containing kinase negative EGF-R contained similar levels of annexin I relative to EGF-R (Fig. 7), suggesting that the release of calcium independent annexin I through phosphorylation does not occur on the plasma membrane.

Discussion

We have shown in previous studies that an active EGF-R kinase is necessary for lysosomal sorting (Honegger et al., 1987; Felder et al., 1990). Other investigators have also shown a reduction in EGF-stimulated degradation of EGF in cells expressing a kinase negative EGF-R but they have concluded that this is due to a reduced internalization rate, rather than to defective lysosomal sorting (Glenney et al., 1988; Chen et al., 1989; Wiley et al., 1991). Most recently Felder et al. (1992) obtained data to suggest that the role of the EGF-R kinase in internalization concerns primarily high affinity EGF-R. At the saturating concentrations of EGF used in the present study our previous biochemical and morphological studies (Felder et al., 1990) clearly show that there is a similar rate of internalization of both the wild type and the kinase negative EGF-R and it is in the MVB that the pathways of the wild type and kinase negative EGF-R diverge. A recent study of another growth factor receptor kinase, the receptor for colony stimulating factor 1, has shown that an active kinase is not necessary for internalization but is a requirement for lysosomal sorting (Carlberg et al., 1991).

The requirement for an active EGF-R kinase for efficient degradation indicates that either the EGF-R must be autophosphorylated to be efficiently targeted to lysosomes, or the kinase phosphorylates a substrate necessary for lysosomal targeting. When kinase positive and kinase negative EGF-R are expressed in the same cell, heterodimers form in response to EGF and the kinase negative EGF-R becomes tyrosine phosphorylated (Honegger et al., 1990). However, in this system kinase negative EGF-R are still predominantly recycled. It is therefore likely that phosphorylation of a substrate accessible only in the MVB is necessary for degradation. This would require the EGF-R kinase to be active in the MVB. There is considerable evidence that the EGF-R kinase is active in the endosome. Autophosphorylation activity of the EGF-R kinase has been demonstrated *in vitro* in endosome fractions from A431 cells (Cohen and Fava, 1985) and rat liver (Kay et al., 1986; Lai et al., 1989). We and others (Carpentier et al., 1987; Nesterov et al., 1990) have shown that EGF stimulation results in prolonged autophosphorylation of the EGF-R, suggesting that the EGF-R kinase is still active after internalization *in vivo*. Wada et al. (1992) have shown that the EGF-R kinase is more highly phosphorylated in the endosome than on the plasma membrane. Moreover the internalized EGF-R kinase can phosphorylate a synthetic substrate introduced into permeabilized cells (Nesterov et al., 1990).

In this study we searched for substrates of the EGF-R kinase associated with MVBs. Western blotting isolated MVBs with anti-phosphotyrosine antibody failed to reveal any major substrates of the EGF-R kinase apart from the EGF-R itself. However, when highly purified MVBs containing the wild type EGF-R are incubated with [γ - 32 P]ATP the major proteins phosphorylated are the EGF-R itself and annexin I. Neither proteins are phosphorylated in MVBs containing the kinase negative EGF-R. Similarly when MVBs from H.Ep.2 cells are isolated using transferrin receptor gold in the presence or absence of EGF, only in endosomes isolated from cells that have been stimulated with EGF does annexin I become phosphorylated. In contrast, annexin I is not phosphorylated in plasma membrane fractions whether or not an active EGF-R kinase is present. We have demonstrated therefore that in the presence of an active EGF-R kinase annexin I can be phosphorylated in MVBs, but not plasma membrane, *in vitro*. It is likely that annexin I is phosphorylated directly by the EGF-R kinase, rather than through activation of an intermediate kinase, as annexin I is efficiently phosphorylated by purified EGF-R kinase (De et al., 1986; Huang et al., 1986) and there is no evidence of an intermediate substrate in the MVB preparations.

Our *in vitro* results are consistent with the kinetics of phosphorylation of annexin I *in vivo*. Sawyer and Cohen (1985) showed that annexin I is not phosphorylated until the majority of EGF-R have been internalized and suggested that annexin I is phosphorylated by the endosomal EGF-R kinase. Cohen and Fava (1985) showed that purified annexin I added to a partially purified intracellular vesicle fraction could be phosphorylated by the EGF-R kinase, and that this reaction was dependent upon the presence of calcium. In the present study we show an association of endogenous annexin I with endosomes that is independent of calcium but this form of annexin I can be phosphorylated by the EGF-R kinase and upon phosphorylation requires calcium for membrane as-

sociation. This is in agreement with the studies of Haigler et al. (1987) who showed that phosphorylation of the calcium-independent form of annexin I in human placental membranes converts it into a form that requires calcium for membrane association. The nature of the calcium-independent interaction of annexin I with membranes is unknown but we have shown here that the association is independent of the density of EGF-R within the membrane. The interaction therefore presumably does not involve a direct interaction with the EGF-R such as has been described for the EGF-R kinase substrates, Phospholipase C γ (Miesenhelder et al., 1989), GAP (Bouton et al., 1991), Raf-1 (App et al., 1991), and Vav (Bustelo et al., 1992; Margolis et al., 1992) which interact with EGF-R via SH2 domains. Quantitation of the total amount of annexin I in plasma membrane and MVB fractions has shown that the presence or absence of an active EGF-R kinase has little effect on the amount of annexin I in plasma membrane fractions but the presence of an active EGF-R kinase causes a reduction in the amount of annexin I in MVB fractions. These results are consistent with annexin I being phosphorylated in MVBs and thus converted to a form that is eluted during fractionation in the presence of calcium chelator.

Wada et al. (1992) in a study of phosphoproteins associated with endosomes of rat liver did not report annexin I associated with endosomes. Wada et al. (1992) did however detect a 55-kD phosphoprotein associated with endosomes. We were not able to detect this substrate in either NIH 3T3 or H.Ep.2 cells, either after *in vitro* phosphorylation or by Western blotting isolated fractions with anti-phosphotyrosine antibody (results not shown). These differences may arise because different stages of processing of the EGF-R were examined. Wada et al. (1992) studied endosomes isolated a maximum of 15 min after EGF stimulation. At this time point the authors were unable to demonstrate sequestration of EGF-R within intra-luminal vesicles in the liver. That sequestration of EGF-R in intra-luminal vesicles does occur in the liver has been shown by Renfrew and Hubbard (1992). In agreement with our proposal the latter authors suggest that movement of EGF-R from the limiting membrane of endosomes to the lumen of lysosomes permits degradation of the EGF-R. Wada et al. (1992) may thus have been examining early events in the processing of the EGF-R, before removal of EGF-R from the limiting membrane.

Thus we have shown that annexin I is associated with plasma membrane and MVBs in a calcium-independent manner and can be phosphorylated *in vitro* in the presence of an active EGF-R kinase in MVBs, but not in plasma membrane. Phosphorylation of the calcium-independent form of annexin I converts it into a form that requires calcium for membrane association. MVBs, but not plasma membrane, containing an active EGF-R kinase contain less calcium-independent annexin I than those that do not contain an active EGF-R kinase. We believe therefore that calcium-independent annexin I is phosphorylated *in vivo* in MVBs whereupon it is released during fractionation in the presence of calcium chelator.

The requirement for the EGF-R kinase to be active for transfer to the inner vesicles of MVBs (Felder et al., 1990), together with the demonstration here that annexin I is a major phosphorylated substrate in MVBs, suggest that annexin I may play a role in mediating inward vesiculation. Mem-

brane invagination to form free vesicles is a well-established process at other membrane boundaries but it is important to note that in these situations the evaginating face of the membrane is cytoplasmic. In contrast, during inward vesiculation in MVBs the evaginating face of the membrane is luminal. Annexin I has been shown to mediate vesicle aggregation and a model has been proposed whereby annexin molecules bind to phospholipid vesicles and fusion between neighboring membranes is mediated by interaction of annexin molecules (Blackwood and Ernst, 1990; Ernst et al., 1991). In the MVB interaction of neighbouring molecules of annexin I on the perimeter membrane may have a role in driving inward vesiculation. Release of annexin I through phosphorylation may then be required for the inward release of vesicles from the perimeter membrane. Subfractionation of the MVB to analyse the protein composition of the perimeter membrane and inner vesicles and the development of in vitro systems to study inward vesiculation may allow the molecular dissection of the events leading to the formation of internal vesicles in the MVB.

The authors would like to thank Adele Gibson and Mark Shipman for expert technical assistance.

C. R. Hopkins was supported by an MRC programme grant.

Received for publication 17 July 1992 and in revised form 14 September 1992.

References

- Ando, Y., S. Imamura, Y.-M. Hong, M. K. Owada, T. Kakunaga, and R. Kanag. 1989. Enhancement of calcium sensitivity of lipocortin I in phospholipid binding induced by limited proteolysis and phosphorylation at the amino terminus as analysed by phospholipid affinity column chromatography. *J. Biol. Chem.* 264:6948-6955.
- App, H., R. Hazan, A. Zilberstein, A. Ullrich, J. Schlessinger, and U. Rapp. 1991. Epidermal growth factor stimulates association and kinase activity of Raf-1 with the epidermal growth factor receptor. *Mol. Cell Biol.* 11:913-919.
- Beardmore, J., K. E. Howell, K. Miller, and C. R. Hopkins. 1987. Isolation of an endocytic compartment from A431 cells using a density modification procedure employing a receptor-specific monoclonal antibody complexed with colloidal gold. *J. Cell Sci.* 87:495-506.
- Beaumelle, B. D., A. Gibson, and C. R. Hopkins. 1990. Isolation and preliminary characterization of the major membrane boundaries of the endocytic pathway in lymphocytes. *J. Cell Biol.* 111:1811-1823.
- Bellot, F. B., W. Moolenaar, R. Kris, B. Mirakhor, A. Ullrich, J. Schlessinger, and S. Felder. 1990. High-affinity epidermal growth factor binding is specifically reduced by a monoclonal antibody and appears necessary for early responses. *J. Cell Biol.* 110:491-502.
- Blackwood, R. A., and J. D. Ernst. 1990. Characterisation of Ca^{2+} -dependent phospholipid binding, vesicle aggregation and membrane fusion by annexins. *Biochem. J.* 226:195-200.
- Bouton, A. H., S. B. Klausner, R. R. Vines, H.-C. R. Wang, J. B. Gibbs, and J. T. Parsons. 1991. Transformation by pp60^{src} or stimulation of cells with epidermal growth factor induces the stable association of tyrosine phosphorylated cellular proteins with GTPase-activating protein. *Mol. Cell Biol.* 11:945-953.
- Bustelo, X. R., J. A. Ledbetter, and M. Barbacid. 1992. Product of the vav proto-oncogene defines a new class of protein tyrosine kinase substrates. *Nature (Lond.)* 356:68-70.
- Carlberg, K., P. Tapkey, C. Haystead, and L. Rohrschneider. 1991. The role of kinase activity and the kinase insert region in ligand-induced internalisation and degradation of the c-fms protein. *EMBO (Eur. Mol. Biol. Organ.) J.* 10:877-883.
- Carpenter, G., and S. Cohen. 1976. ¹²⁵I-labeled human epidermal growth factor binding, internalization and degradation in human fibroblasts. *J. Cell Biol.* 71:159-171.
- Carpentier, J. L., M. F. White, L. Orci, and C. R. Kahn. 1987. Direct visualization of the epidermal growth factor receptor during its internalization in A431 cells. *J. Cell Biol.* 105:2751-2762.
- Chen, W. S., C. S. Lazar, K. A. Lund, J. B. Welsh, C. P. Chang, G. M. Walton, C. J. Der, T. S. Wiley, G. N. Gill, and M. G. Rosenfeld. 1989. Functional independence of the epidermal growth factor receptor from a domain required for ligand-induced internalization and calcium regulation. *Cell* 59:33-43.
- Cohen, S., and R. A. Fava. 1985. Internalization of functional epidermal growth factor: receptor/kinase complexes in A-431 cells. *J. Biol. Chem.* 260:12351-12358.
- De, B. K., K. S. Misono, T. J. Lukas, B. Mroczkowski, and S. Cohen. 1986. A calcium-dependent 35-kd substrate for epidermal growth factor receptor/kinase isolated from normal tissue. *J. Biol. Chem.* 261:13784-13792.
- DeMey, J. 1986. The preparation and use of gold probes. In *Practical Applications in Pathology and Biology*. Polak, J. M., and Van Noorden, S., editors. 115-145. Wright, Bristol.
- Ernst, J. D., E. Hoyer, R. A. Blackwood, and T. L. Mok. 1991. Identification of a domain that mediates vesicle aggregation reveals functional diversity of annexin repeats. *J. Biol. Chem.* 266:6670-6673.
- Felder, S., K. Miller, G. Moehren, A. Ullrich, J. Schlessinger, and C. R. Hopkins. 1990. Kinase activity controls the sorting of the epidermal growth factor receptor within the multivesicular body. *Cell* 61:623-624.
- Felder, S., J. LaVin, A. Ullrich, and J. Schlessinger. 1992. Kinetics of binding, endocytosis, and recycling of EGF receptor mutants. *J. Cell Biol.* 117:203-212.
- Futter, C. E., and C. R. Hopkins. 1989. Subfractionation of the endocytic pathway: isolation of compartments involved in the processing of internalised epidermal growth factor receptor complexes. *J. Cell Sci.* 94:685-694.
- Glemney, J. R., B. Tack, and M. A. Powell. 1987. Calpactins: Two distinct Ca^{2+} -regulated phospholipid- and actin-binding proteins isolated from lung and placenta. *J. Cell Biol.* 104:503-511.
- Glemney, J. R., W. S. Chen, C. S. Lazar, G. M. Walton, L. M. Zokas, M. G. Rosenfeld, and G. N. Gill. 1988. Ligand-induced endocytosis of the epidermal growth factor receptor is blocked by mutational inactivation and by micro-injection of anti-phosphotyrosine antibodies. *Cell* 52:685-695.
- Haigler, H. T., D. D. Schlaepfer, and W. H. Burgess. 1987. Characterisation of lipocortin I and an immunologically unrelated 33-kDa protein as epidermal growth factor receptor/kinase substrates and phospholipase A₂ inhibitors. *J. Biol. Chem.* 262:6921-6930.
- Honegger, A. M., T. J. Dull, F. Bellot, E. Van Obberghen, D. Szapary, A. Schmidt, A. Ullrich, and J. Schlessinger. 1987. Point mutation at the ATP binding site of EGF-receptor abolishes protein tyrosine kinase activity and alters cellular routing. *Cell* 51:199-209.
- Honegger, A. M., A. Schmidt, A. Ullrich, and J. Schlessinger. 1990. Separate endocytic pathways of kinase-defective and -active epidermal growth factor receptor mutants expressed in the same cells. *J. Cell Biol.* 110:1541-1554.
- Huang, K. S., B. P. Wallner, R. J. Mattaliano, R. Tizard, C. Burne, A. Frey, C. Hession, P. McGray, L. K. Sinclair, E. Pingchang Chow, J. L. Brown, K. L. Ramachandran, J. Tang, J. E. Smart, and R. B. Pepinsky. 1986. Two human 35 kd inhibitors of phospholipase A₂ are related to substrates of pp60^{src} and of the epidermal growth factor receptor/kinase. *Cell* 46:191-199.
- Hunter, W. M., and F. C. Greenwood. 1962. Preparation of iodine-131 labeled human growth hormone of high specific activity. *Nature (Lond.)* 194:490-495.
- Kay, D. J., W. H. Lai, M. Uchihashi, M. M. Khan, B. I. Posner, and J. J. M. Bergeron. 1986. Epidermal growth factor receptor kinase translocation and activation in vivo. *J. Biol. Chem.* 261:8473-8480.
- Kris, R. M., I. Lax, W. Gullick, M. D. Waterfield, A. Ullrich, M. Fridkin, and J. Schlessinger. 1985. Antibodies against a synthetic peptide as a probe for the kinase activity of the avian EGF receptor and v-erbB protein. *Cell* 40:619-625.
- Lai, W. H., P. H. Cameron, J. J. Doherty, B. I. Posner, and J. J. M. Bergeron. 1989. Ligand-mediated autophosphorylation activity of the epidermal growth factor receptor during internalization. *J. Cell Biol.* 109:2751-2760.
- Margolis, B., P. Hu, S. Katzav, W. Li, J. M. Oliver, A. Ullrich, A. Weiss, and J. Schlessinger. 1992. Tyrosine phosphorylation of vav proto-oncogene product containing SH2 domain and transcription factor motifs. *Nature (Lond.)* 356:71-73.
- Nesterov, A., G. Reshetnikova, N. Vinogradova, and N. Nikolsky. 1990. Functional state of the epidermal growth factor-receptor complexes during their internalisation in A431 cells. *Mol. Cell Biol.* 10:5011-5014.
- Renfrew, C. A., and A. L. Hubbard. 1991. Degradation of epidermal growth factor receptor in rat liver. *J. Biol. Chem.* 266:21265-21273.
- Sawyer, S. T., and S. Cohen. 1985. Epidermal growth factor stimulates the phosphorylation of the calcium-dependent 35000-Dalton substrate in intact A-431 cells. *J. Biol. Chem.* 260:8233-8236.
- Slot, J. W., and H. I. Geuze. 1985. A new method of preparing gold probes for multiple labeling cytochemistry. *Eur. J. Cell Biol.* 38:87-93.
- Ushiro, H., and S. Cohen. 1980. Identification of phosphotyrosine as a product of epidermal growth factor-activated protein kinase in A-431 cell membranes. *J. Biol. Chem.* 255:8363-8365.
- Wada, I., W. H. Lai, B. I. Posner, and J. J. Bergeron. 1992. Association of the tyrosine phosphorylated epidermal growth factor receptor with a 55-kD tyrosine phosphorylated protein at the cell surface and in endosomes. *J. Cell Biol.* 116:321-330.
- Wiley, H. S., J. J. Herbst, B. J. Walsh, D. A. Lauffenburger, M. G. Rosenfeld, and G. N. Gill. 1991. The role of tyrosine kinase activity in endocytosis, compartmentation, and down-regulation of the epidermal growth factor receptor. *J. Biol. Chem.* 266:11083-11094.

Identification and characterization of a novel type of annexin-membrane interaction: Ca^{2+} is not required for the association of annexin II with early endosomes

Matthias Jost^{1,*}, Dagmar Zeuschner¹, Joachim Seemann², Klaus Weber² and Volker Gerke^{1,†}

¹Institute for Medical Biochemistry, ZMBE, University of Münster, von-Esmarch-Str. 56, D-48149 Münster, Germany

²Department of Biochemistry, Max Planck Institute for Biophysical Chemistry, Am Fassberg 11, D-37077 Göttingen, Germany

*Present address: Department of Cell Biology, The Scripps Research Institute, La Jolla, CA 92037, USA

†Author for correspondence

SUMMARY

Annexin II, a member of a family of Ca^{2+} and membrane binding proteins, has been implicated in regulating membrane organization and membrane transport during endocytosis and Ca^{2+} regulated secretion. To characterize the mechanistic aspects of the annexin II action we studied parameters which determine the endosomal association of annexin II. Immunoblot analysis of subcellular membrane fractions prepared from BHK cells in the presence of a Ca^{2+} chelating agent reveals that annexin II remains associated with endosomal membranes under such conditions. This annexin II behaviour is atypical for the Ca^{2+} regulated annexins and is corroborated by the finding that ectopically expressed annexin II mutants with inactivated Ca^{2+} binding sites continue to co-fractionate with endosomal membranes. The Ca^{2+} -independent membrane association

of annexin II is also not affected by introducing mutations interfering with the complex formation of annexin II with its intracellular protein ligand p11. However, a deletion of the unique N-terminal domain of annexin II, in particular the sequence spanning residues 15 to 24, abolishes the Ca^{2+} -independent association of the protein with endosomes. These results describe a novel, Ca^{2+} -independent type of annexin-membrane interaction and provide a first explanation for the observed preference of different annexins for different cellular membranes. In the case of annexin II this specificity could be mediated through specific membrane receptors interacting with a unique sequence in the annexin II molecule.

Key words: Ca^{2+} /phospholipid binding protein, Endocytosis, Membrane-cytoskeleton interaction

INTRODUCTION

The Ca^{2+} -dependent regulation of membrane-cytoskeleton and membrane-membrane interactions plays an important role in a number of biological processes ranging from the control of cell and organelle shape to that of certain membrane traffic events. Among the components thought to be involved in such Ca^{2+} -mediated processes are the annexins, members of a multigene family of Ca^{2+} /phospholipid-binding proteins widely distributed among species. Typically, all annexins share as a characteristic biochemical property the ability to bind to negatively charged phospholipids and cellular membranes in a Ca^{2+} -dependent manner, and some members of the family also interact Ca^{2+} -dependently with certain cytoskeletal elements (for reviews see Creutz, 1992; Raynal and Pollard, 1994). These annexin properties are displayed by a well conserved protein core domain which is resistant to limited proteolysis and comprises a four- or eightfold repetition of a segment of 70-80 amino acid residues, the annexin repeat. Each annexin repeat harbours one or two novel types of Ca^{2+} binding sites. These differ in architecture from the EF hand motif (Moews and Kretsinger, 1975) and involve in addition to other elements

a highly conserved acidic amino acid whose carboxyl oxygens are crucially important for Ca^{2+} coordination (Huber et al., 1990; Weng et al., 1993; Jost et al., 1992, 1994). Unique within the individual members of the annexin family is the N-terminal domain which precedes the protein core and varies in length and sequence. It is thought to be of regulatory importance as it harbours in several annexins phosphorylation sites for different signal transducing kinases (for review see Raynal and Pollard, 1994).

Annexin II is implicated in several membrane transport steps. These include the Ca^{2+} -regulated secretion since annexin II, which is a prominent component in chromaffin granule preparations, is able to aggregate these vesicles at Ca^{2+} levels which are close to those observed in stimulated chromaffin cells, and partially restores the secretory responsiveness in permeabilized chromaffin cells (Ali et al., 1989; Sarafian et al., 1991; for review see Creutz, 1992). Such Ca^{2+} -regulated function of annexin II in the exocytotic pathway seems to depend on a complex formation of the protein with its intracellular ligand, the S100 protein p11. Complex formation, which leads to an annexin II₂p11₂ heterotetramer, is mediated through the N-terminal domain of annexin II (for review see

Weber, 1992) and is a prerequisite for anchoring annexin II in the cortical region of cultured cells (Thiel et al., 1992; Jost et al., 1994). Based on these findings it had been suggested that the annexin II-p11 complex may participate in Ca^{2+} -regulated exocytosis by linking exocytotic vesicles to the cortical cytoskeleton and/or the plasma membrane and thereby positioning the vesicle at the correct place in the cell (for reviews see Creutz, 1992; Gerke, 1996).

Several lines of evidence indicate that annexin II is also involved in endocytotic processes. The protein is found on isolated early endosomal membranes and is one of the few proteins transferred from a donor to an acceptor endosomal membrane in an *in vitro* fusion assay (Emans et al., 1993). Moreover, ectopic expression of a *trans*-dominant mutant for the annexin II-p11 complex, which leads to the intracellular aggregation of annexin II and p11, specifically affects early endosomes which are translocated to the site of the aggregates (Harder and Gerke, 1993). Finally, in a cell-free system purified annexin II reconstitutes in conjunction with arachidonic acid a Ca^{2+} -dependent fusion among endosomes which previously had been washed with the Ca^{2+} chelating EDTA (Mayorga et al., 1994).

The mechanism by which annexin II affects fusion properties and/or the organization and intracellular location of endosomal membranes is not known. To shed light on this mechanism and to elucidate the structural requirements for an annexin II-endosome interaction we analyzed the subcellular fractionation of ectopically expressed mutant derivatives of annexin II. We show that the co-fractionation of annexin II with endosomal membranes is not regulated by Ca^{2+} - and p11-binding. This Ca^{2+} -independent membrane association does, however, depend on the presence of amino acids 15 to 24 of the unique N-terminal domain of annexin II.

MATERIALS AND METHODS

Expression constructs

The cDNA encoding human annexin II (Huang et al., 1986) served as a template for oligonucleotide-directed mutagenesis (Kunkel, 1985) which was employed to generate mutant cDNAs encoding defective Ca^{2+} (CM) and/or p11 (PM) binding sites (Jost et al., 1994). The mutants containing a deletion of the region encoding the N-terminal 14 or 24 amino acid residues were constructed by PCR using the wild-type (WT) cDNA as a template and the oligonucleotides $\Delta 1$ (5' CTGTGCAAGCTCGAATTCGAGATGTCTCACTCTACACC 3') or $\Delta 2$ (5' CTACACCCCGAATTCATATATGTCTGTCAAAGCC 3') as sense and the oligonucleotide $\Delta 3$ (5' GACCTGTTATCTAGAAGCATGGTG 3') as antisense primers, respectively. All annexin II cDNAs also contained a single nucleotide exchange resulting in a glutamic acid for alanine replacement at amino acid position 65. This substitution installed the epitope for the monoclonal antibody H28 and thus enabled us to use this antibody to specifically detect the recombinantly expressed annexin II derivatives (Thiel et al., 1991). For expression in BHK cells the individual annexin II cDNAs were cloned into the pCMV5 vector to yield the constructs pCMV-WT, pCMV-PM, pCMV-CM, pCMV-PMCM, pCMV- $\Delta 1$ -14, and pCMV- $\Delta 1$ -24. The presence of the individual mutations was verified by dideoxy sequencing (Sanger et al., 1977).

Cell culture and transfection

Hamster BHK cells were grown in Dulbecco's modified Eagle's medium (Gibco-BRL) supplemented with 10% fetal calf serum (Boehringer,

Mannheim). Transient transfection employed a modified calcium phosphate precipitation method (Chen and Okayama, 1987) using 20 μg of the respective plasmid DNA per 100 mm dish of cells grown to 50% confluency. After addition of the DNA, cells were incubated for 12 to 16 hours at 35°C in 3% CO_2 , then washed with PBS and cultivated in fresh medium using normal culture conditions. Between 30 and 40% of the total cell population was expressing the exogenous protein 40 hours following transfection, as revealed by routine immunofluorescence analysis with the monoclonal antibody H28.

Fractionation of endosomal membranes

Labeling and fractionation of endosomes was carried out essentially as described by Gorvel et al. (1991) and Aniento et al. (1996). Briefly, four 100 mm dishes of untreated BHK cells or six dishes of transfected cells were incubated at 37°C with 2 mg/ml horseradish peroxidase (HRP) in IM (internalization medium: Dulbecco's modified Eagle's medium supplement with 10 mM Hepes, pH 7.4). To label early endosomes the HRP incubation was carried out for five minutes. Late endosomal labeling was achieved by treating the cells for five minutes with HRP in IM followed by a 45 minute chase in IM supplement with 2 mg/ml bovine serum albumin. Subsequently, the cells were lysed in HB buffer (0.25 M sucrose, 3 mM imidazole-HCl, pH 7.4) followed by a low speed centrifugation to yield a post-nuclear supernatant (PNS). The PNS was brought to 40.6% sucrose, 3 mM imidazole-HCl, pH 7.4, and placed at the bottom of a SW 60 centrifugation tube (Beckman). This load was overlaid with 1.5 ml of 35% sucrose, 3 mM imidazole-HCl, pH 7.4, then with 1 ml 25% sucrose, 3 mM imidazole-HCl, pH 7.4, and finally with 0.5 ml HB buffer. In some experiments, the sucrose solutions were supplemented with 1 mM EDTA to reduce the free Ca^{2+} concentration. The step gradient was centrifuged at 35,000 rpm for 60 minutes at 4°C. Fractions containing late and multivesicular endosomes were collected at the 25% sucrose-HB interface and early endosomes were enriched at the 25%-35% sucrose interface. Fractions containing heavy membranes (HM) were collected at the 35%-40.6% sucrose interface. The activity of endocytosed HRP present in the different fractions was analyzed as described (Gorvel et al., 1991) and latency was measured according to Bomsel et al. (1990). Proteins present in the different fractions were concentrated by chloroform/methanol precipitation (Wessel and Flügge, 1984) and 10 μg of each fraction (as determined according to Bradford, 1976) were separated by SDS-polyacrylamide gel electrophoresis (PAGE) (Laemmli, 1970) and analyzed by immunoblotting (Towbin et al., 1987).

Immunofluorescence analysis of annexin II and transferrin receptor distribution

BHK cells grown on glass coverslips were co-transfected with an expression construct encoding the human transferrin receptor (hTfR) cDNA (pCMV-hTfR; Harder and Gerke, 1993) and with one of the expression constructs encoding wild-type (WT) or mutant annexin II derivatives (pCMV-WT, pCMV-PMCM, pCMV- $\Delta 1$ -24). At 40 hours post transfection the cells were incubated for 1 hour in serum-free medium and then for 30 minutes in serum-free medium containing 20 $\mu\text{g}/\text{ml}$ human transferrin (Boehringer) to obtain an efficient hTfR internalization into early and recycling endosomes. Subsequently, the coverslips were washed briefly in cold PBS and placed, cells facing down, for 10 minutes at 4°C onto a 50 μl drop of a solution containing activated streptolysin O (SLO; obtained from Dr S. Bhakdi, University of Mainz, FRG; Bhakdi et al., 1993). SLO was employed at 5 $\mu\text{g}/\text{ml}$ in intracellular transport buffer (ICT; 78 mM KCl, 4 mM MgCl_2 , 8.37 mM CaCl_2 , 10 mM EGTA and 1 mM DTT; Burke and Gerace, 1986). EGTA in the ICT buffer was omitted in experiments analyzing the Ca^{2+} -dependent association of $\Delta 1$ -24 annexin II with endosomes. Following incubation at 4°C the excess SLO that did not bind to the plasma membrane was removed by two washes with cold ICT. For permeabilization the coverslips were placed on pre-warmed drops of ICT for 10 minutes at 37°C. The effectiveness of permeabilization could be

measured by LDH release. The cells were then washed for an additional 10 minutes with cold ICT to obtain an efficient depletion of the cytosol. For double immunofluorescence staining of the transfected hTfR and annexin II, the cells were fixed for 2 minutes in -20°C cold methanol, washed with PBS and incubated with the first antibodies in a humid chamber for 45 minutes at room temperature. Mouse anti-human CD71 (IgG2A; Pharmingen) was employed to label the hTfR and the mouse monoclonal H28 (IgG1; Osborn et al., 1988) was used to specifically detect the ectopically expressed annexin II derivatives. The coverslips were then washed 3×10 minutes with PBS and incubated for 45 minutes with the corresponding fluorescently labeled secondary antibodies (isotype-specific antibodies directed against mouse IgG1 and IgG2A, respectively). After three final PBS washes the coverslips were mounted in Moviol 4-88 (Hoechst). Cells were examined with a Zeiss axiophot photomicroscope and photography employed Kodak P3200 film.

Antibodies

The polyclonal rabbit antibodies directed against annexins II and IV as well as the mouse monoclonal anti-annexin II antibody H28 have been described (Gerke and Weber, 1984; Osborn et al., 1988). Antibodies against the early endosome-associated protein EEA1 (Mu et al., 1995) were kindly provided by Dr Ban-Hock Toh (Monash Medical School, Melbourne, Australia). Peroxidase coupled antibodies (Dako) were used as secondary antibodies and immunoreactive bands were visualised using the ECL chemoluminescence system (Amersham-Buchler). For double immunofluorescence analysis of transfected cells ectopically expressing hTfR and annexin II, FITC-coupled goat anti-mouse IgG2A and Texas red-coupled goat anti-mouse IgG1 (Southern Biotechnology Associated Inc.) were employed as secondary antibodies.

RESULTS

The association of annexin II with endosomal membranes in the presence and absence of Ca²⁺

To analyze whether and how Ca²⁺ ions affect the association of annexin II with endosomal membranes we probed subcellular fractions of BHK cells prepared in the absence or presence of the Ca²⁺ chelating EDTA with an annexin II antibody. In these experiments an enrichment of annexin II in a given subcellular fraction was assessed by comparing the respective immunoblot signal to that obtained when an equal amount of total protein from the starting material for gradient fractionation, the post nuclear supernatant (PNS), was analyzed. Fig. 1 reveals that annexin II is enriched in fractions containing early endosomal membranes and to a lesser extent in those containing late endosomes when cell lysis and subsequent gradient fractionation are carried out in the absence of EDTA (as already shown by Emans et al., 1993). Unexpectedly the cofractionation with early endosomes is not affected by including EDTA in all buffers used in the subcellular fractionation indicating that the annexin II binding to early endosomes still occurs at submicromolar Ca²⁺ concentrations (Fig. 1). A Ca²⁺-independent association of annexin II with endosomes is also corroborated by ultrastructural analyses of mechanically perforated MDCK cells. When these cells are incubated in a physiological buffer in the absence of Ca²⁺ prior to fixation they retain the majority of their endosome associated annexin II although the soluble protein and a substantial fraction of the plasma membrane associated annexin II is lost (Harder et al., 1997).

Further immunoblot analysis reveals that annexin IV is another annexin present in BHK cell fractions containing endosomal membranes (Fig. 1). However, in contrast to

annexin II, annexin IV is enriched to an equal extent in fractions containing early and in those containing late endosomes and its co-fractionation with the respective membrane fractions is sensitive to Ca²⁺ chelation (Fig. 1). Thus, annexin IV exhibits a behaviour typical for an annexin, i.e. a Ca²⁺-regulated interaction with membranes, whereas annexin II appears to associate with the endosomal membranes in a manner atypical for an annexin. To verify the enrichment of early endosomes in the different experiments, the gradient fractions obtained were also subjected to immunoblot analysis with an antibody against EEA1, a protein of 180 kDa specifically associated with early endosomes (Mu et al., 1995; a representative example revealing the specific enrichment of EEA1 in fractions containing early endosomes is shown in Fig. 1). Moreover, in all endosome fractionation experiments the enrichment and integrity of the different endosomal membranes was routinely monitored by following the fate of HRP internalized from the fluid phase (see Materials and Methods for details).

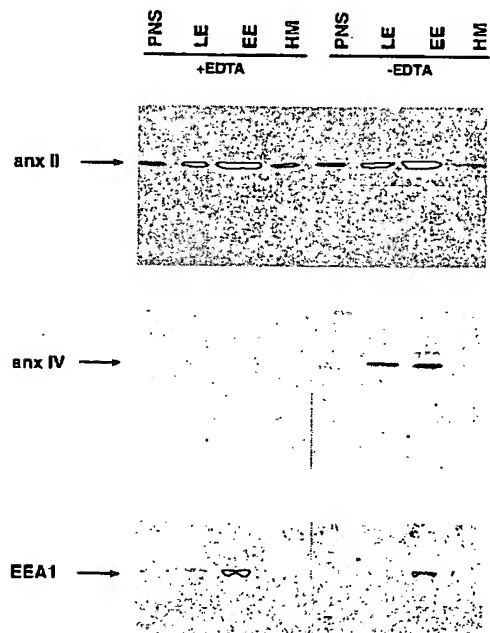
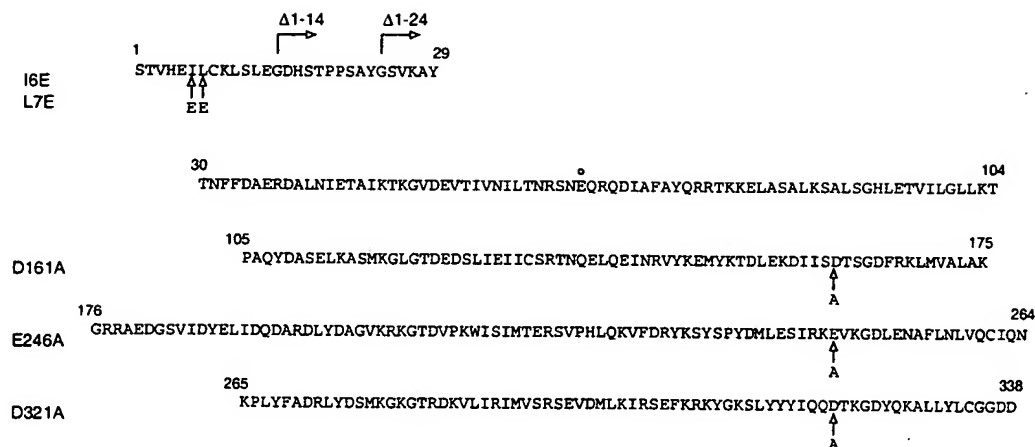


Fig. 1. Association of annexin II and annexin IV with different membrane fractions from BHK cells. A post-nuclear supernatant (PNS) was prepared from BHK cells and subjected to flotation gradient fractionation in the presence (+) or absence (-) of 1 mM EDTA. Fractions enriched in late (LE) and early endosomes (EE) as well as those containing heavy membranes (HM) were collected. Equal amounts of protein from these fractions (as determined according to Bradford, 1976) were subjected to SDS-PAGE and subsequent immunoblotting using polyclonal antibodies directed against annexins II (upper panel) and IV (middle panel). A control immunoblot using antibodies against the early endosome-associated protein EEA1 is shown in the bottom panel. Note that annexin II is enriched in fractions containing endosomal, in particular early endosomal, membranes and that this enrichment is not affected by the inclusion of the Ca²⁺ chelating EDTA. In contrast, annexin IV is equally enriched in fractions containing early and late endosomal membranes and this association is sensitive to Ca²⁺ chelation.

Fig. 2. Amino acid sequence of human annexin II and of annexin II mutants used in this study. The sequence (Huang et al., 1986) is given in the one letter code. The dot indicates a Glu for Ala replacement which is shared by all annexin II derivatives described here and which reconstitutes the epitope for the monoclonal antibody H28 (Osborn et al., 1988; Thiel et al., 1991). Vertical arrows mark the amino acid

substitutions introduced to inactivate the type II Ca^{2+} binding sites (D161A, E246A, D321A, generating CM annexin II) and the p11 binding site (I6E, L7E, generating PM annexin II). The positions of the novel N-termini of the truncation mutants, $\Delta 1-14$ and $\Delta 1-24$ annexin II, are indicated by horizontal arrows.



Intact Ca^{2+} and p11 binding sites are not required for an endosomal association of annexin II

As the subcellular fractionation data suggested a novel type of annexin-membrane interaction for the annexin II-endosome association (one not sensitive to Ca^{2+}) we analyzed the structural requirements for this association in more detail. Therefore we employed a transfection approach to express ectopically in BHK cells certain annexin II mutant proteins. The subcellular distribution of these derivatives was determined by flotation gradient fractionation of a PNS prepared from the transfected cells and subsequent immunoblot analysis of the different fractions using a monoclonal antibody specifically recognizing the ectopically expressed but not the endogenous annexin II (Thiel et al., 1991).

In a first approach we analyzed the behaviour of an annexin II mutant with inactivated type II Ca^{2+} binding sites. These sites are located in repeats 2, 3 and 4 of annexin II and they were rendered inactive by introducing alanine in place of the crucial acidic amino acids serving as so-called cap residues in this type of Ca^{2+} binding site (D161A, E246A, D321A; CM annexin II; Fig. 2). The impairment of the Ca^{2+} -sites had been verified previously by our biochemical analyses (Thiel et al., 1992; Jost et al., 1992). An expression construct encoding wild-type (WT) annexin II was used in control experiments. Fractionation of BHK cells transiently expressing the WT annexin II reveals that this ectopically expressed protein shows the co-fractionation with endosomal membranes already observed for the endogenous annexin II (Fig. 3). Moreover, this co-fractionation is observed both in the absence and in the presence of a Ca^{2+} chelating agent (not shown).

A very similar result is obtained when the subcellular distribution of the mutant protein with inactivated Ca^{2+} -sites is revealed by gradient fractionation, i.e. CM annexin II also co-fractionates with early endosomal membranes (not shown). To exclude the possibility that CM annexin II associates with endosomes through a p11-mediated binding to endogenous (intact) annexin II, we decided to analyze the subcellular distribution of a CM derivative with an inactivated p11 binding site.

p11 binding is mediated through the N-terminal 14 amino acids of annexin II with the hydrophobic side chains at positions 6 and 7 (Ile and Leu, respectively) representing major contact sites (Johnsson et al., 1988; Becker et al., 1990). Therefore, we introduced glutamic acid residues in place of Ile-6 and Leu-7 (I6E, L7E; Fig. 2) to inactivate the p11 binding site. This PM (p11-minus) mutation was combined with the CM replacements generating PMCM annexin II. As revealed by ligand blotting and Ca^{2+} -dependent liposome pelleting this mutant protein was impaired in both p11 and Ca^{2+} binding (not shown). Gradient analysis of BHK cells expressing PMCM annexin II shows that this mutant continues to co-fractionate with early endosomal membranes (Fig. 3). Since PMCM annexin II remains monomeric these results show unambiguously that Ca^{2+} binding to annexin II is not required for its cofractionation with early endosomal membranes. Interestingly, the somewhat lesser but reproducibly observed enrichment of endogenous (Fig. 1) and transfected WT annexin II (Fig. 3) in fractions containing late endosomes is not seen in the case of the PMCM derivative (Fig. 3). Likewise, the CM annexin II mutant shows an enrichment only in early endosomal but not in late endosomal fractions (not shown). This indicates that the cofractionation of annexin II with late endosomal membranes requires intact Ca^{2+} binding sites in the protein and thus differs mechanistically from the Ca^{2+} -independent association of annexin II with early endosomes.

The signal for localizing annexin II Ca^{2+} -independently to endosomal membranes resides in the N-terminal domain

To identify the region in the annexin II molecule mediating the Ca^{2+} -independent association with endosomes we generated two N-terminally truncated derivatives which were again expressed in BHK cells and subjected to the fractionation protocol described above. We chose the N-terminal domain for a more detailed analysis since this region is highly variable within the individual annexins and thus likely to be involved in mediating specific properties. In a first truncation mutant we deleted the entire p11 binding site, i.e. amino acids 1-14 (Johnsson et al.,

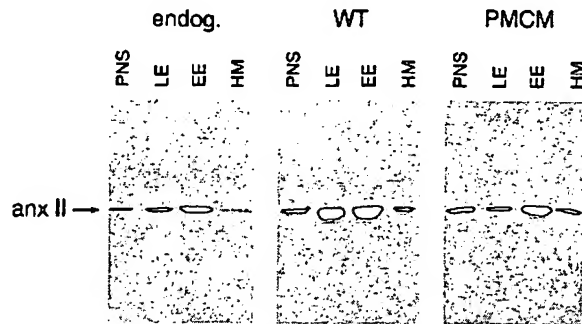


Fig. 3. Flotation gradient analysis of membranes from BHK cells ectopically expressing annexin II derivatives. BHK cells were transfected with expression constructs encoding wild-type (WT) annexin II or a mutant derivative containing inactivated Ca²⁺ binding sites as well as an inactivated p11 binding site (PMCM). Membranes present in a PNS from such cells were subjected to sucrose gradient fractionation and fractions enriched in late endosomes (LE), early endosomes (EE), and heavy membranes (HM) were analyzed by immunoblotting using a monoclonal antibody (H28) specifically recognizing the ectopically expressed annexin II. The distribution of endogenous annexin II (endog.) among the membrane fractions from non-transfected BHK cells was determined by immunoblotting with a polyclonal annexin II antibody and is given for comparison. Preparation of the PNS and gradient fractionation were carried out in the absence of EDTA to specifically analyze the consequences of the Ca²⁺-site mutations. Note that PMCM annexin II which is incapable of forming the heterotetrameric annexin II-p11 complex and which does not bind Ca²⁺ continues to co-fractionate with endosomal membranes.

1988), and introduced a novel start by replacing the amino acids at positions 14 and 15 (Gly and Asp) by methionine and serine (Fig. 2). As expected from the properties displayed by PMCM annexin II, i.e. a protein mutant incapable of binding p11, the Δ 1-14 annexin II derivative continues to co-fractionate with endosomal membranes in the presence of 1 mM EDTA (Fig. 4A). This shows again that p11 binding is not required and further reveals that the entire p11 binding site is dispensable for a Ca²⁺-independent association with endosomes.

An additional 10 amino acid residues were deleted in the second truncation mutant, Δ 1-24 annexin II, in which Gly-24 was replaced by the novel start-methionine (Fig. 2). The rationale for choosing this mutation was twofold. First, we wanted to delete or render inactive two phosphorylation sites of potential regulatory importance (Tyr-23 phosphorylated by pp60^{src} and Ser-25 phosphorylated by protein kinase C; for review see Gerke, 1992). Second, since Lys-27 is part of the discontinuous epitope of the monoclonal annexin II antibody H28 we decided to leave this residue unaffected (Thiel et al., 1991). This enabled us to detect the Δ 1-24 derivative by immunoblotting with the H28 antibody. Subcellular fractionation of BHK cells ectopically expressing Δ 1-24 annexin II reveals that this derivative fails to co-fractionate with endosomal membranes in the presence of a Ca²⁺ chelating agent (Fig. 4B). An enrichment of Δ 1-24 annexin II in membrane fractions containing endosomes is, however, observed when the preparation of the PNS and the subsequent gradient analysis are carried out in the absence of EDTA (Fig. 4B). Thus, the annexin II core starting at residue 25 displays the Ca²⁺-sensitive interaction with BHK membranes typical for an annexin, showing a preference for early and to a lesser extent late endosomes.

However, the Ca²⁺-independent association with these structures requires the sequence spanning residues 15 to 24. Fig. 4 also shows an immunoblot analysis employing EEA1 antibodies on gradient fractions prepared from BHK cells expressing the Δ 1-24 annexin II mutant. This control reveals that the fractionation properties of early endosomes are not affected by the ectopic expression of the annexin II mutant. Thus, the loss of Ca²⁺-independent membrane binding in the case of the Δ 1-24 mutant protein is solely due to the deletion of an important sequence in the protein and not caused by any putative secondary effects on the endosomal membranes in the transfected cells.

To corroborate the results obtained by subcellular fractionation we also collected morphological data on the subcellular localization of different annexin II mutants. Therefore, BHK cells were co-transfected with expression plasmids encoding the annexin II derivatives and the human transferrin receptor (hTfR) which was included as a marker for early endosomes in the transfected cells. At 40 hours following transfection the cells were permeabilized with streptolysin O (SLO) and then incubated in an intracellular transport buffer (ICT) to release

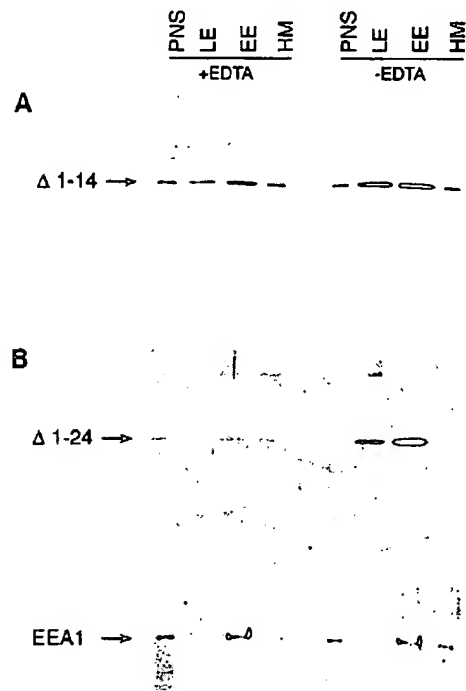
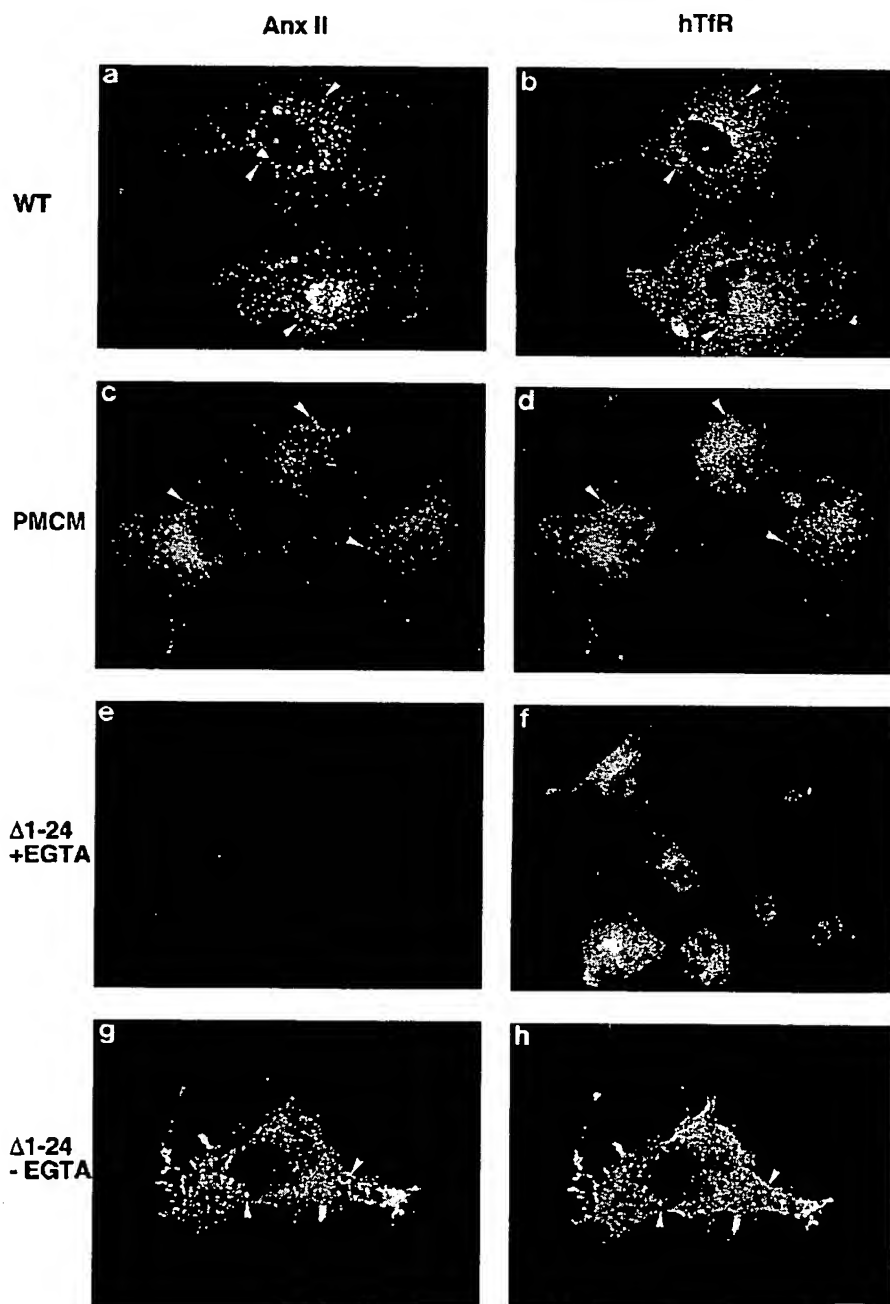


Fig. 4. Effect of N-terminal deletions on the Ca²⁺-independent co-fractionation of annexin II with endosomal membranes. Cellular membranes (LE, EE, HM) obtained by gradient fractionation of a PNS prepared from BHK cells ectopically expressing Δ 1-14 (A) or Δ 1-24 (B) annexin II were subjected to immunoblotting using the H28 monoclonal antibody specifically recognizing the mutant proteins. Subcellular fractionation was carried out in the presence (+) or absence (-) of 1 mM EDTA. Note that the deletion of amino acids 1-24 but not that of residues 1-14 renders the molecule incapable of co-fractionating with endosomal membranes in the presence of EDTA. A control immunoblot with the EEA1 antibody of the fractions obtained from Δ 1-24 annexin II-transfected cells is shown in the bottom part of B and reveals that the gradient fractionation of early endosomes is not affected in these cells.

the cytosolic fraction of annexin II (see Materials and Methods) before subjecting them to double immunofluorescence using antibodies specifically recognizing the ectopically expressed hTfR and annexin II derivatives, respectively. Fig. 5 reveals that WT annexin II and the PMCM mutant protein co-localize to a large extent with hTfR positive structures thus showing the early endosomal localization already established for endogenous annexin II at the light and electron microscope level (Emans et al., 1993; Harder and Gerke, 1993). In line with our biochemical analyses this annexin II distribution is observed after incubating the permeabilized cells prior to fixation in ICT

buffer containing the Ca^{2+} chelating EGTA (Fig. 5). In contrast, the $\Delta 1$ -24 mutant protein fails to show any endosomal or other intracellular membrane association under such conditions (Fig. 5). However, when Ca^{2+} is not chelated during the incubation of the permeabilized cells in ICT buffer the $\Delta 1$ -24 derivative remains associated with intracellular structures which to a large extent are hTfR positive (Fig. 5). These data are in line with the subcellular fractionation (Fig. 4) and thus support the conclusion that the unique N-terminal domain of annexin II is required for its Ca^{2+} -independent association with endosomal membranes. When this domain is truncated the resulting $\Delta 1$ -

Fig. 5. Localization of ectopically expressed annexin II derivatives and human transferrin receptor in SLO-permeabilized BHK cells. BHK cells were co-transfected with expression constructs encoding the human transferrin receptor (hTfR) and one of the annexin II derivatives (WT, PMCM, or $\Delta 1$ -24 annexin II, respectively). At 40 hours following transfection efficient hTfR uptake was induced by exogenously supplemented transferrin. Subsequently the cells were permeabilized with SLO and depleted of cytosol by incubation in an intracellular transport buffer (ICT) containing EGTA (see Materials and Methods). This treatment releases the cytosolic annexin II pool which to some extent masks the membrane-bound fraction in immunofluorescence analyses of directly fixed cells (Osborn et al., 1988; Harder and Gerke, 1993). In the case of cells expressing the $\Delta 1$ -24 annexin II the cytosol was released either in the presence (e,f) or absence (g,h) of 10 mM EGTA to analyze the effect of Ca^{2+} on the intracellular distribution of this mutant. The cells were then fixed and processed for double immunofluorescence using antibodies directed against annexin II (a,c,e,g) and hTfR (b,d,f,h), which only recognized the ectopically expressed and not the endogenous proteins. Note that WT and PMCM annexin II co-localize to a large extent with hTfR positive endosomal structures in a manner not affected by the EGTA which is included in the ICT buffer (arrowheads in a,b and c,d, respectively). In contrast, $\Delta 1$ -24 annexin II fails to show any membrane association under such conditions (e and f). A co-localization of $\Delta 1$ -24 annexin II with hTfR positive endosomes is, however, observed when EGTA is omitted during cytosol depletion, i.e. in the presence of Ca^{2+} (g and h).



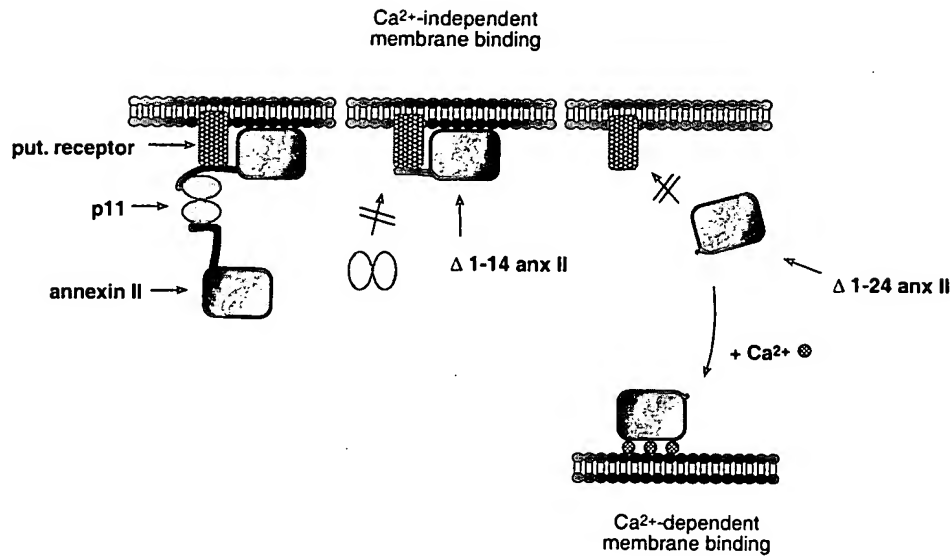


Fig. 6. Model depicting different modes of an annexin II-membrane interaction. The Ca²⁺-independent association with a target membrane described here is mediated through the sequence spanning residues 15 to 24 which could bind to a receptor specific for this membrane. This interaction would leave the very N-terminal 14 residues of annexin II accessible for p11 binding. Removal of the entire N-terminal region encompassing residues 1 to 24 generates a mutant derivative ($\Delta 1-24$ annexin II) whose membrane association strictly depends on the presence of Ca²⁺.

24 mutant protein requires Ca²⁺ for an interaction with endosomal membranes. Interestingly and as also seen in the gradient analysis the Ca²⁺-dependent membrane association of the $\Delta 1-24$ mutant protein remains to be specific for early and to a lesser extent late endosomal membranes, most likely because the phospholipid composition of these membranes is best suited for interacting with the annexin II core.

DISCUSSION

Members of the annexin family of Ca²⁺-regulated membrane binding proteins are present on most and possibly all intracellular membranes including the plasma membrane (Gruenberg and Emans, 1993). Specificity with respect to the target membrane of the individual annexins is thought to be conferred through the N-terminal domains which vary between the different members of the family. The Ca²⁺ sensitivity for a reversible and peripheral membrane binding, on the other hand, is most likely carried through the protein core comprising four or eight annexin repeats. These repeats harbour the type II and type III Ca²⁺ binding sites (for reviews see Huber et al., 1992; Swairjo and Seaton, 1994) and isolated core domains bind Ca²⁺-dependently to phospholipid vesicles and chromaffin granules (Glenney, 1986; Johnsson et al., 1986; Drust and Creutz, 1988). Most likely, the EDTA-sensitive, i.e. Ca²⁺ regulated, co-fraction of $\Delta 1-24$ annexin II with endosomes (Figs 4, 5) is the consequence of such a Ca²⁺-dependent interaction of the annexin II core domain with endosomal membranes. In this case specificity is probably carried through a certain phospholipid composition of the endosomal membranes which is better suited for binding the annexin II core than that of other cellular membranes.

A different mechanism must be responsible for mediating the Ca²⁺-independent association of annexin II with early endosomes described here. The association depends on the presence of the unique N-terminal domain of the annexin II molecule with the sequence encompassing amino acids 15-24 being of critical importance. In contrast, p11 binding and the resulting annexin II-

p11 complex formation are not required. This type of Ca²⁺-independent binding to certain cellular membranes has not been observed for an annexin before. It could be mediated through a specific receptor for annexin II on early endosomal membranes. This putative receptor would bind to the N-terminal annexin II domain, most likely to the sequence spanning residues 15 to 24, in a manner not regulated by Ca²⁺ (Fig. 6). Such an interaction could be accompanied in the presence of Ca²⁺ by a binding of the annexin II core to endosomal membrane phospholipids. Moreover, it would leave the very N-terminal region (residues 1 to 14) accessible for p11 binding thus enabling the annexin II-p11 complex formation to occur on endosomal membranes. Alternatively, the second part of the N-terminal domain, i.e. amino acids 15-24, could be involved in establishing or stabilizing a conformation of the core domain which allows for a Ca²⁺-independent interaction of this core domain with endosomal membranes. Future experiments, e.g. the identification of the putative annexin II receptor (protein or a certain lipid structure) on endosomes, have to resolve this question.

Within cells annexin II is not restricted to endosomes but is also found on the plasma membrane and/or in the cortical cytoskeleton colocalizing with molecules of the spectrin family (for review see Gerke, 1992). Interestingly, Ca²⁺ as well as p11 binding are required for establishing the tight association with the cortical cytoskeleton (Thiel et al., 1992; Jost et al., 1994) indicating that different structural requirements underlie the association of annexin II with endosomes and the cortical cytoskeleton, respectively. This could reflect the existence of functionally distinct annexin II pools and/or different modes of regulation. Cortical annexin II could be involved in stabilizing a peripheral localization of endosomes, possibly by providing a physical link between the endosomal membrane and the cortical cytoskeleton (Harder and Gerke, 1993). It may also serve an alternative or additional role in structuring or organizing endosomal membranes (or domains of the plasma membrane).

At least in certain cell types, e.g. adrenal chromaffin cells, annexin II has also been implicated in exocytotic processes, in particular in Ca²⁺ regulated secretion (Ali et al., 1989; Sarafian

et al., 1991). While the exact mechanism by which annexin II acts in exocytotic membrane transport is not known it has been suggested that a heterotetrameric annexin II-p11 complex could provide physical linkage between different chromaffin granule membranes and/or between the granule and the plasma membrane (Nakata et al., 1990; for review see Creutz, 1992). Conceptually, annexin II could therefore be involved in different membrane transport steps by serving a structural role in organizing membranes and/or membrane-cytoskeleton interactions. Specificity could then be guaranteed by certain phospholipid compositions allowing for a Ca^{2+} -dependent binding through the annexin II core domain or specific receptors (e.g. on endosomes) interacting Ca^{2+} -independently with a region in the N-terminal domain.

We thank Thomas Harder, Rob Parton and Jean Gruenberg for fruitful discussions and for communicating results prior to publication. Thanks also to Ban-Hock Toh for kindly providing antibodies against the EEA1 protein. This work was supported in part by grants from the Deutsche Forschungsgemeinschaft (Ge 514/2-2 and Ge 514/2-3) and the Human Frontier Science Program Organization (HFSP) to V.G.

REFERENCES

- Ali, S. M., Geisow, M. J. and Burgoyne, R. D. (1989). A role for calpactin in calcium dependent exocytosis in adrenal chromaffin cells. *Nature* **340**, 313-315.
- Aniento, F., Gu, F., Parton, R. G. and Gruenberg, J. (1996). An endosomal β COP is involved in the pH-dependent formation of transport vesicles destined for late endosomes. *J. Cell Biol.* **133**, 29-41.
- Bhakdi, S., Weller, U., Walev, I., Martin, E., Jonas, D. and Palmer, M. (1993). A guide to the use of pore-forming toxins for controlled permeabilization of cell membranes. *Med. Microbiol. Immunol.* **182**, 167-175.
- Becker, T., Weber, K. and Johnsson, N. (1990). Protein-protein recognition via short amphiphilic helices; a mutational analysis of the binding site of annexin II for p11. *EMBO J.* **9**, 4207-4213.
- Bomse, M., Parton, R., Kurznetsov, S. A., Schroer, T. A. and Gruenberg, J. (1990). Microtubule- and motor-dependent fusion in vitro between apical and basolateral endocytic vesicles from MDCK cells. *Cell* **62**, 719-731.
- Bradford, M. M. (1976). A rapid and sensitive method for quantitation of microgram quantities of protein utilizing the principle of protein dye-binding. *Anal. Biochem.* **72**, 248-254.
- Burke, B. and Gerace, L. (1986). A cell free system to study reassembly of the nuclear envelope at the end of mitosis. *Cell* **44**, 639-652.
- Chen, C. and Okayama, H. (1987). High-efficiency transformation of mammalian cells by plasmid DNA. *Mol. Cell. Biol.* **7**, 2745-2752.
- Creutz, C. E. (1992). The annexins and exocytosis. *Science* **258**, 924-931.
- Drust, D. S. and Creutz, C. E. (1988). Aggregation of chromaffin granules by calpactin at micromolar levels of calcium. *Nature* **331**, 88-91.
- Emans, N., Gorvel, J. P., Walter, C., Gerke, V., Kellner, R., Griffiths, G. and Gruenberg, J. (1993). Annexin II is a major component of fusogenic endosomal vesicles. *J. Cell Biol.* **120**, 1357-1369.
- Gerke, V. and Weber, K. (1984). Identity of p36K phosphorylated upon Rous sarcoma virus transformation with a protein from brush borders; calcium-dependent binding to nonerythroid spectrin and F-actin. *EMBO J.* **3**, 227-233.
- Gerke, V. (1992). Evolutionary conservation and three-dimensional folding of the tyrosine kinase substrate annexin II. In *The Annexins* (ed. S. E. Moss), pp. 47-59. Portland Press, London.
- Gerke, V. (1996). Annexins and membrane traffic. In *Annexins: Molecular Structure to Cell Function* (ed. B. A. Seaton). Landes Science Publishers, Georgetown, TX (in press).
- Glenney, J. R. Jr (1986). Phospholipid-dependent Ca^{2+} -binding by the 36-kDa tyrosine kinase substrate (calpactin) and its 33-kDa core. *J. Biol. Chem.* **261**, 7247-7252.
- Gorvel, J. P., Chavrier, P., Zerial, M. and Gruenberg, J. (1991). rab5 controls early endosome fusion in vitro. *Cell* **64**, 915-925.
- Gruenberg, J. and Emans, N. (1993). Annexins in membrane transport. *Trends Cell Biol.* **3**, 224-227.
- Harder, T. and Gerke, V. (1993). The subcellular distribution of early endosomes is affected by the annexin IIp11₂ complex. *J. Cell Biol.* **123**, 1119-1132.
- Harder, T., Kellner, R., Parton, R. G. and Gruenberg, J. (1997). Specific release of membrane bound annexin II and cortical cytoskeletal elements by sequestration of membrane cholesterol. *Mol. Biol. Cell* (in press).
- Huang, K. S., Wallner, B. P., Mattaliano, R. J., Tizard, R., Burne, C., Frey, A., Hession, C., McGray, P., Sinclair, L. K., Chow, E. P., Browning, J. L., Ramachandran, K. L. J. T., Smart, J. E. and Pepinsky, R. B. (1986). Two human 35 kd inhibitors of phospholipase A₂ are related to substrates of p60^{v-src} and the epidermal growth factor receptor/kinase. *Cell* **46**, 191-199.
- Huber, R., Römisch, J. and Paques, E. P. (1990). The crystal and molecular structure of human annexin V, an anticoagulant calcium, membrane binding protein. *EMBO J.* **9**, 3867-3874.
- Huber, R., Berendes, R., Burger, A., Luecke, H. and Karshikov, A. (1992). Annexin V: crystal structure and its implications on function. In *The Annexins* (ed. S. E. Moss), pp. 105-124. Portland Press, London.
- Johnsson, N., Vanderkerckhove, J., van Damme, J. and Weber, K. (1986). Binding sites for calcium, lipid and p11 on p36, the substrate of retroviral tyrosine-specific protein kinases. *FEBS Lett.* **198**, 361-364.
- Johnsson, N., Marriotti, G. and Weber, K. (1988). p36, the major cytoplasmic substrate of src tyrosine protein kinase, binds to its p11 subunit via a short amino-terminal amphiphatic helix. *EMBO J.* **7**, 2435-2442.
- Jost, M., Thiel, C., Weber, K. and Gerke, V. (1992). Mapping of three unique Ca^{2+} -binding sites in human annexin II. *Eur. J. Biochem.* **207**, 923-930.
- Jost, M., Weber, K. and Gerke, V. (1994). Annexin II contains two types of Ca^{2+} -binding sites. *Biochem. J.* **3**, 553-559.
- Kunkel, T. A. (1985). Rapid and efficient site-specific mutagenesis without phenotypic selection. *Proc. Nat. Acad. Sci. USA* **82**, 488-492.
- Laemmli, U. K. (1970). Cleavage of structural proteins during the assembly of the head of bacteriophage T4. *Nature* **227**, 680-685.
- Mayorga, L. S., Beron, W., Sarrouf, M. N., Colombo, M. I., Creutz, C. and Stahl, P. D. (1994). Calcium-dependent fusion among endosomes. *J. Biol. Chem.* **269**, 30927-30934.
- Moews, P. C. and Kretsinger, R. H. (1975). Refinement of the structure of carp muscle calcium-binding parvalbumin by model building and difference Fourier analysis. *J. Mol. Biol.* **91**, 6645-6653.
- Mu, F.-T., Callaghan, J. M., Steele-Mortimer, O., Stenmark, H., Parton, R. G., Campbell, P. L., McCluskey, J., Yeo, J.-P., Tock, E. P. C. and Toh, B.-H. (1995). EEA1, an early endosome-associated protein. *J. Biol. Chem.* **270**, 13503-13511.
- Nakata, T., Sobue, K. and Hirokawa, N. (1990). Conformational change and localization of calpactin I complex involved in exocytosis as revealed by quick-freeze, deep-etch electron microscopy and immunocytochemistry. *J. Cell Biol.* **110**, 13-25.
- Osborn, M., Johnsson, N., Wehland, J. and Weber, K. (1988). The submembrane location of p11 and its interaction with the p36 substrate of pp60 src kinase in situ. *Exp. Cell Res.* **175**, 81-96.
- Raynal, P. and Pollard, H. B. (1994). Annexins: the problem of assessing the biological role for a gene family of multifunctional calcium- and phospholipid-binding proteins. *Biochim. Biophys. Acta* **1197**, 63-93.
- Sanger, F., Nicklen, S. and Coulson, A. R. (1977). DNA-sequencing with chain-terminating inhibitors. *Proc. Nat. Acad. Sci. USA* **74**, 5463-5467.
- Sarafian, T., Pradel, L. A., Henry, J. P., Aunis, D. and Bader, M. F. (1991). The participation of annexin II (calpactin I) in calcium-evoked exocytosis requires protein kinase C. *J. Cell Biol.* **114**, 1135-1147.
- Swairjo, M. A. and Seaton, B. A. (1994). Annexin structure and membrane interactions: a molecular perspective. *Annu. Rev. Biophys. Biomol. Struct.* **23**, 193-213.
- Thiel, C., Weber, K. and Gerke, V. (1991). Characterization of a discontinuous epitope on annexin II by site-directed mutagenesis. *FEBS Lett.* **285**, 59-62.
- Thiel, C., Osborn, M. and Gerke, V. (1992). The tight association of the tyrosine kinase substrate annexin II with the submembrane cytoskeleton depends on intact p11- and Ca^{2+} -binding sites. *J. Cell Sci.* **103**, 733-742.
- Towbin, H., Staehelin, T. and Gordon, J. (1979). Electrophoretic transfer of proteins from polyacrylamide gels to nitrocellulose sheets: procedure and some applications. *Proc. Nat. Acad. Sci. USA* **76**, 4350-4354.
- Weber, K. (1992). Annexin II: interaction with p11. In *The Annexins* (ed. S. E. Moss), pp. 61-68. Portland Press, London.
- Weng, X., Luecke, H., Song, I. S., Kang, D. S., Kim, S. H. and Huber, R. (1993). Crystal structure of human annexin I at 2.5 Å resolution. *Protein Sci.* **2**, 448-458.
- Wessel, D. and Flügge, U. J. (1984). A method for the quantitative recovery of proteins in dilute solution in the presence of detergents and lipids. *Anal. Biochem.* **138**, 141-143.

Structural and functional characterization of recombinant mouse annexin A11: influence of calcium binding

Emilio LECONA*, Javier TURNAY*, Nieves OLMO*, Ana GUZMÁN-ARÁNGUEZ*, Reginald O. MORGAN†, Maria-Pilar FERNÁNDEZ† and M^a Antonia LIZARBE*¹

*Departamento de Bioquímica y Biología Molecular, Facultad de Ciencias Químicas, Universidad Complutense, 28040 Madrid, Spain, and †Departamento de Bioquímica y Biología Molecular, Facultad de Medicina, Universidad de Oviedo, 33006 Oviedo, Spain

Annexin A11 is one of the 12 vertebrate subfamilies in the annexin superfamily of calcium/phospholipid-binding proteins, distinguishable by long, non-homologous N-termini rich in proline, glycine and tyrosine residues. As there is negligible structural information concerning this annexin subfamily apart from primary sequence data, we have cloned, expressed and purified recombinant mouse annexin A11 to investigate its structural and functional properties. CD spectroscopy reveals two main secondary-structure contributions, α -helix and random coil (approx. 30 % each), corresponding mainly to the annexin C-terminal tetrad and the N-terminus respectively. On calcium binding, an increase in α -helix and a decrease in random coil are detected. Fluorescence spectroscopy reveals that its only tryptophan residue, located at the N-terminus, is completely exposed to the solvent; calcium binding promotes a change in tertiary structure, which does not affect this tryptophan residue but involves the movement of approximately four tyrosine residues to a more hydrophobic environment. These calcium-

induced structural changes produce a significant thermal stabilization, with an increase of approx. 14 °C in the melting temperature. Annexin A11 binds to acidic phospholipids and to phosphatidylethanolamine in the presence of calcium; weaker calcium-independent binding to phosphatidylserine, phosphatidic acid and phosphatidylethanolamine was also observed. The calcium-dependent binding to phosphatidylserine is accompanied by an increase in α -helix and a decrease in random-coil contents, with translocation of the tryptophan residue towards a more hydrophobic environment. This protein induces vesicle aggregation but requires non-physiological calcium concentrations *in vitro*. A three-dimensional model, consistent with these data, was generated to conceptualize annexin A11 structure–function relationships.

Key words: calcium binding, CD spectroscopy, fluorescence spectroscopy, phospholipid binding, thermal stability.

INTRODUCTION

The annexin gene family comprises calcium-binding proteins with a unique ancestry, a tetrad structure of homologous internal repeats, and the common property of reversible binding to acidic phospholipid-rich membranes in the presence of this cation (see [1–3] for reviews), although some protein members lack the requisite consensus for high-affinity type II calcium-binding sites [4]. The annexin core structure is composed of four (eight in annexin A6) homologous domains of approx. 68 amino acids, universally conserved throughout annexin evolution [5,6]. In contrast, the N-terminal region shows greater variability in length and amino acid sequence [1,3]. Since the solution of the annexin A5 crystal structure [7], several other annexins have been crystallized; all of them display a protein core resembling a slightly curved disc in which the four repeated domains arrange around a central hydrophilic pore. Each domain comprises a folded leaf α -helix bundle (helices A, B, D and E) organized as anti-parallel cylinders capped by a fifth α -helix (helix C). The interaction with membranes takes place on the convex side of the molecule where the principal calcium-binding sites are located. Calcium binding is established with carbonyl oxygen atoms in the loop connecting helices A and B, and with a bidentate carbonyl group from glutamic or aspartic residues located in the loop connecting helices D and E, approx. 38 residues downstream

in each repeat. The N-terminal region connects domains I and IV in annexins with a short N-terminus, such as annexin A5, and is located in the concave region of the molecule, opposite to the calcium-binding sites [7]. Rosengarth et al. [8] have solved the X-ray structure of full-length annexin A1 in the absence of calcium, showing that the N-terminus interacts with domain III through an amphipathic α -helix present in the N-terminal domain replacing helix 3D.

The structural characteristics of annexins, especially A1, A2 and A5, have been extensively analysed [7–12]. However, knowledge is more limited for other members of this family, and is unavailable for annexin A11 which has an unusual N-terminus. The core domain of annexin A11 shows the highest similarity to all other human annexins [13,14] and its evolutionary origin lies near the root of this family tree [6,15], beginning with the sequential duplication of annexin A13 to annexins A7 and A11 around the emergence of chordates [16,17]. All these observations support the view of annexin A11 as a structural prototype, founding member and key functional model of chordate annexins.

Several functions have been described for annexins *in vitro*, including anti-coagulatory and anti-inflammatory activities and involvement in signal transduction, membrane fusion, endo- and exocytosis as well as calcium-channel regulation. However, little is known about their physiological role *in vivo* [1,3]. Despite their gross structural similarity, annexins have diverged

Abbreviations used: CCA, convex constraint algorithm; DTT, dithiothreitol; IPTG, isopropyl β -D-thiogalactoside; Ni-NTA, Ni²⁺-nitrilotriacetate; PA, phosphatidic acid; PC, phosphatidylcholine; PE, phosphatidylethanolamine; PG, phosphatidylglycerol; PS, phosphatidylserine; rTEV, recombinant tobacco etch virus.

¹ To whom correspondence should be addressed (e-mail lizarbe@bbm1.ucm.es).

significantly in terms of their gene regulation, tissue-specific expression patterns, subcellular localization of different isoforms and features peculiar to individual subfamilies [16,18–20]. Moreover, self-association, heterologous annexin interactions and the interaction with other proteins have been described to act as regulatory mechanisms for the function of some of these proteins [1–3].

The main structural differences among metazoan annexins appear in the non-homologous N-terminal extension, so the structural analysis of annexin A11 could reveal some features relevant to its functional specificity. This annexin possesses an extensive N-terminal region, rich in proline, glycine and tyrosine residues [21,22]. Although several studies have pointed out various functional properties of annexin A11, including its possible role in insulin secretion [23], structural data are limited to the primary structure. The N-terminal region of annexin A11 has been proposed to be responsible for its autoantigenicity [24], nuclear localization [25] and tyrosine phosphorylation [26]. Moreover, the interaction with calyculin (S100A6) is established through amino acids 45–62 [27], analogous to that described for annexins A1 and A2 with other S100 proteins, namely S100A11 and S100A10, or for p53 with S100B [28–30]. Annexin A11 also binds, through the N-terminus, to the penta-EF-hand family proteins ALG-2 (apoptosis-linked gene-2) [31] and sorcin [32].

According to all these observations, annexin A11 is probably involved in several biological processes and its N-terminal region participates prominently in most of them. The aim of the present study is to perform a structural characterization of recombinant annexin A11 to allow a better understanding of the biological role of this protein. We have analysed some of the changes that take place on calcium binding as this is a key aspect of its functionality. We also studied the binding of annexin A11 to different phospholipid vesicles, as well as the consequent structural changes, to gain insight into the interaction of this protein with biological membranes, as this process may differ from other annexins due to its distinctive N-terminus.

EXPERIMENTAL

Construction of expression vectors

The mouse annexin cDNA was cloned previously (U65986) [14]. The 2.4 kb clone containing the full-length cDNA sequence was used as a template to isolate the coding portion of mouse annexin A11 by PCR. Oligonucleotide primers, 23 bp long, were synthesized according to the published sequence for both ends of the coding cDNA. The oligonucleotide sequences created *NcoI* and *EcoRI* restriction sites to facilitate the insertion of coding cDNA into either expression plasmid pPROEX-HTb (Life Technologies, Prat de Llobregat, Spain) or pTrc99A (AP Biotech, Cerdanyola, Spain). The identities of the final constructs pHisA11M and pTrcA11M were verified by restriction digestion and DNA sequencing.

Protein expression and purification

JA221 *Escherichia coli* cells were transformed with the annexin A11 expression constructs pTrcA11M or pHisA11M. Cells were grown at 37 °C in Luria–Bertani medium containing 100 µg/ml ampicillin until the cultures reached A_{600} 0.5. Recombinant protein expression was induced by the addition of 1 mM isopropyl β -D-thiogalactoside (IPTG) for different incubation times (1–16 h) and at temperatures over the range 25–37 °C. The protein expression of total cell homogenates was analysed by SDS/PAGE and then by

Coomassie Blue staining or Western blotting. Optimal conditions for the induction of the expression of recombinant annexin A11 in both cases were 4 h in the presence of 1 mM IPTG at 25 °C.

Spectroscopic characterization was performed using recombinant annexin A11 produced in bacteria transformed with the construction pHisA11M under the optimal expression conditions described above. Cells were collected after induction with IPTG by centrifugation at 6000 *g* for 15 min and resuspended in 50 mM Tris (pH 8.0), containing 0.1 M NaCl, 2.5 mM EGTA, 2 mM PMSF and 1 mM dithiothreitol (DTT), and ruptured by sonication cycles at 4 °C. After stirring for 90 min at 4 °C, the homogenate was centrifuged at 27000 *g* for 90 min at 4 °C. The supernatant was loaded on to an Ni²⁺-nitrilotriacetate (Ni-NTA)-agarose column, washed with buffer A [50 mM Tris (pH 8.0)/0.1 M NaCl/1.5 mM 2-mercaptoethanol] containing 20 mM imidazole. The recombinant protein was eluted with a linear gradient of buffer A containing 20–250 mM imidazole, and dialysed against 50 mM Tris (pH 8.0), containing 0.1 M NaCl and 1 mM EGTA. After the addition of 1 mM DTT, the protein was digested with 10 units/ml recombinant tobacco etch virus (rTEV) protease (Life Technologies) at 4 °C for 20–22 h and dialysed against buffer B [50 mM Tris (pH 8.0)/0.1 M NaCl]. Digested annexin was separated from the undigested form and from the rTEV protease by an additional Ni-NTA-agarose affinity chromatography, taking advantage of the presence of a poly(His) tag in the latter molecules. Finally, annexin A11 was dialysed against buffer B containing 1 mM EGTA, to remove traces of Ni²⁺ that induce alterations in the UV-visible spectra, and then against buffer B without EGTA.

The identity of both digested and non-digested proteins was confirmed by amino acid analysis (Beckman 6300 amino acid analyser) as described previously [33], which also allowed the determination of protein concentration. The molar absorption coefficient at 280 nm was obtained from the UV-visible spectra, after subtraction of apparent absorption due to light scattering and determination of the protein concentration by amino acid analyses from aliquots taken directly from the cuvette.

CD measurements

CD spectra were recorded at 20 °C in a Jasco J-715 spectropolarimeter equipped with a Neslab RTE-111 thermostat. The far-UV CD spectra were monitored between 200 and 250 nm using thermostatically controlled cuvettes of 0.1 cm pathlength. Melting curves were determined by monitoring the ellipticity changes at 208 or 220 nm between 20 and 80 °C at 60 °C/h. All the samples were first dialysed against 20 mM Hepes (pH 8.0) and 0.1 M NaCl, to minimize pH changes during heating. To analyse the influence of calcium concentration on the far-UV spectrum and on the melting temperature (T_m), different protein samples from the same stock were prepared with increasing CaCl₂ concentrations up to 75 mM. Samples with equivalent maximal ionic strength, obtained by the addition of NaCl instead of CaCl₂, were used as the control. Far-UV spectra and melting temperatures were also registered for annexin A11 in the presence of 50 nm phosphatidylserine (PS) small unilamellar vesicles (molar ratio of PS/annexin A11 is 800:1), in the absence (1 mM EGTA) or presence of 200 µM CaCl₂.

All spectra were averaged over six scans (ten for annexin A11 in the presence of vesicles) and were corrected by subtracting buffer contribution (with or without PS vesicles) from parallel spectra in the absence of protein; units are always expressed as molar ellipticity/residue ($[\theta]_{MRW}$). Prediction of the secondary structure from the far-UV spectra was performed using the convex constraint algorithm (CCA) as described by Perczel et al. [34].

Fluorescence spectroscopy

Fluorescence emission spectra were recorded at 20 °C on an SLM Aminco 8000C spectrofluorimeter with excitation wavelengths of 275 nm (global emission) and 295 nm (tryptophan emission), and 4 nm excitation and emission bandwidths. The spectra were monitored between 295 and 400 nm for global emission or 305 and 400 nm for tryptophan emission, using a 0.4 cm excitation pathlength and 1.0 cm emission pathlength cuvette. Scattering was minimized by crossed Glan–Thompson polarizers. Titration of calcium influence at both excitation wavelengths was performed by sequential addition of CaCl_2 in the absence or presence of 50 nm PS vesicles (molar ratio of PS/annexin A11 is 800:1) and correcting the spectra for dilution. Acrylamide quenching of tryptophan fluorescence was measured using emission spectra exciting at 295 nm at increasing acrylamide concentration, taking into account the effects of dilution as described previously [9]. Care was taken to avoid the inner filter effect and the solutions presented always UV absorption at the excitation wavelength below 0.04. The Stern–Volmer quenching constant (K_{SV}) was calculated from the plot of F_0/F at 340 nm against acrylamide concentration, according to the equation $F_0/F = 1 + K_{SV}[Q]$, where F_0 is the fluorescence intensity at zero quencher concentration and F the intensity at a given quencher concentration ($[Q]$).

Tyrosine titration

Titration was performed by the addition of aliquots of 1 M NaOH to the protein sample in the absence or presence of 50 mM CaCl_2 , using a 1 cm pathlength cuvette. After each addition, the pH was measured in the cuvette with a microelectrode and the UV–visible absorption spectrum was recorded. Absorption at 295 nm due to tyrosinate was determined after subtraction of the apparent absorption due to light scattering and taking into account the dilution of the sample. The number of tyrosine residues titrated at each pH was calculated from the molar ratio [tyrosinate]/[annexin A11], and the plot of this value against pH renders the titration curve.

Binding to phospholipids and vesicle aggregation assays

Unilamellar vesicles of PS (Avanti Polar Lipids), phosphatidylcholine (PC), phosphatidylglycerol (PG), phosphatidic acid (PA) and phosphatidylethanolamine (PE) (all purchased from Sigma) were obtained by hydration of a thin film of dried phospholipids in 50 mM Tris (pH 8.0) containing 0.1 M NaCl, followed by sonication and extrusion through polycarbonate filters of either 100 or 400 nm (Lipex Biomembranes). PE vesicles were stabilized by the addition of PC (PE/PC in the ratio 4:1) to avoid artifacts due to the formation of hexagonal-phase structures in pure PE liposomes. Small unilamellar vesicles (50 nm) were prepared from freshly obtained 400 nm vesicles by further extrusion through 50 nm polycarbonate filters.

Purified annexin A11 and 400 nm vesicles were mixed in a lipid/protein constant molar ratio of 800:1 with variable calcium concentrations in 50 mM Tris (pH 8.0) and 0.1 M NaCl and kept at room temperature (20 °C) for 15 min. The final mixture (300 μl) was ultracentrifuged at 134000 g at 4 °C for 1 h (Airfuge Beckman); the pellet and the supernatant were separated and analysed by SDS/PAGE followed by silver nitrate staining or Western blotting. Under these experimental conditions, almost no sedimentation of free protein was detected in a phospholipid-free

control. Gels or films were scanned and densitometric analysis was performed, obtaining volumograms on a photodocumentation system obtained from UVItec (Cambridge, U.K.) and using the UVIBand V.97 software.

Vesicle aggregation was studied using 100 nm vesicles (obtained by extrusion through 100 nm polycarbonate filters; 0.1 mg/ml PS) in the presence of increasing annexin A11 concentrations at 25 °C and triggering the reaction by adding the corresponding volume from a concentrated CaCl_2 stock solution. Absorption at 360 nm was measured immediately after the addition of calcium in a thermostatically controlled cuvette for at least 10 min.

Other procedures

The isolation of chicken annexin A5 was performed as described previously [9,35]. SDS/PAGE was performed by the method of Laemmli [36]. Western blotting was performed as described previously [37] using either polyclonal anti-bovine annexin A11 antibodies (dilution 1:8000; kindly provided by Dr Hiroyoshi Hidaka, D. Western Therapeutics Institute, Nagoya, Japan) and a secondary antibody conjugated with horseradish peroxidase (Bio-Rad, Madrid, Spain), or using directly a monoclonal peroxidase-conjugated anti-poly(His) (Sigma). Polyclonal antibodies against recombinant mouse annexin A11 were raised in rabbit following standard methods. Annexin A11 concentration in pure preparations was determined from the UV–visible spectra, except for CD spectroscopy, where quantitative amino acid analysis was used. Regression fitting of the experimental data to different equations was performed using SigmaPlot software v.8.02 obtained from SPSS (Chicago, IL, U.S.A.).

RESULTS

Purification of recombinant mouse annexin A11

The expression of recombinant annexin A11 cloned in the vector pTrec99A is low in all the experimental conditions assayed; the protein is extensively degraded even at 25 °C and short induction times, and is mainly expressed in an insoluble form. On the other hand, the cloning of the protein in the vector pPROEX-HTb, which introduces a His tag in the N-terminus, allows a significantly greater expression and minimizes degradation. According to the Western blots, using antibodies against the wild-type protein or against the poly(His) tag (Figure 1A), the degradation of the protein takes place from the N-terminus. Moreover, the His tag enables easy purification of annexin A11 expressed in *E. coli* at 25 °C for 4 h.

Figures 1(B) and 1(C) show the electrophoretic and Western-blot analyses of samples from the main steps of the purification process. Bacteria were collected by centrifugation and homogenized in the presence of 2.5 mM EGTA to obviate interactions of the recombinant annexin with bacterial membrane phospholipids and 1 mM DTT to prevent incorrect disulphide bond formation. Centrifugation of the cell homogenate allows the separation of the soluble and insoluble fractions (Figures 1B and 1C, lanes j–l). Approx. 50% of the recombinant annexin A11 remains insoluble either in inclusion bodies or associated with the membrane fraction. After removing EGTA by dialysis, the soluble fraction was purified by affinity chromatography in Ni-NTA–agarose. Whereas bacterial proteins do not bind to Ni-NTA–agarose (Figures 1B and 1C, lane m), annexin A11 with the His tag elutes only in the presence of imidazole (Figures 1B and 1C, lane n). Removal of imidazole by dialysis in the absence

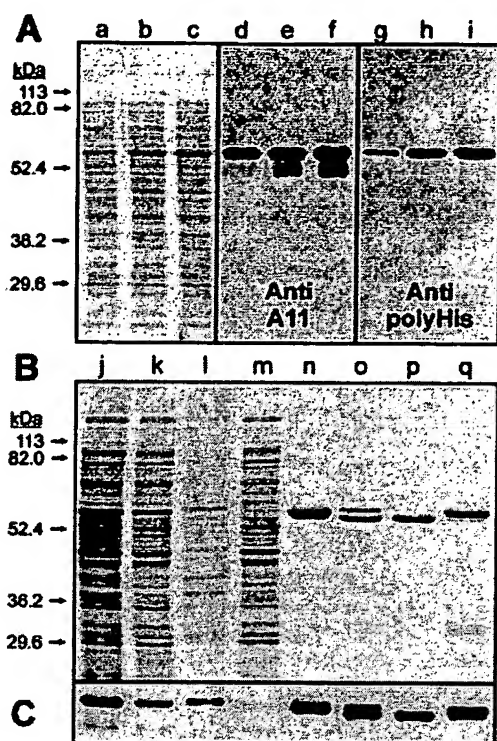


Figure 1 SDS/PAGE analysis of recombinant annexin A11 expression and purification

(A) Expression of annexin A11 was induced in exponentially growing JA221 cells by the addition of 1 mM IPTG and incubation at 25 °C for 4 h (lanes a, d and g), 6 h (lanes b, e and h) and 8 h (lanes c, f and i), and the expression was analysed by SDS/PAGE followed by Coomassie Blue staining (lanes a–c) and Western blotting using antibodies raised against either bovine annexin A11 (lanes d–f) or the poly(His) tag (lanes g–i). Purification of recombinant annexin A11 from bacterial cultures induced for 4 h with 1 mM IPTG at 25 °C was performed, followed by SDS/PAGE analysis and Coomassie Blue staining (B) and Western-blot analysis with anti-(annexin A11) antibodies (C). (B, C) Lane j, bacterial homogenate after protein expression induction; lanes k and l, supernatant and sediment respectively after centrifugation of the homogenized material in the presence of 2.5 mM EGTA; lane m, flow-through of the Ni-NTA chromatography; lane n, pool of fractions containing annexin A11; lane o, digestion of poly(His) tag containing annexin A11 with rTEV protease; lane p, purified digested annexin A11 without the poly(His) tag; lane q, material retained in the Ni-NTA-agarose chromatography after digestion with rTEV protease.

of bivalent-cation chelating agents induces the autoaggregation and precipitation of the protein containing the His tag; a similar process takes place if calcium is added to solutions of this protein. As this tag is likely to be involved in the autoaggregation of the protein, this extension was removed to perform the spectroscopic characterization of the protein. Digestion of the protein for 20 h at 4 °C in the presence of 10 units/ml rTEV protease yielded over 70% of digested protein (Figures 1B and 1C, lane o). Separation of the digested annexin A11 from the undigested protein and from the enzyme was achieved by a further chromatographic step in Ni-NTA-agarose; the protease and the undigested annexin A11 are bound to the resin, whereas the digested protein elutes in the flow-through (Figures 1B and 1C, lanes p and q).

Identity of the purified proteins was confirmed through amino acid analyses and antibodies against the recombinant protein recognized wild-type annexin A11 from cell extracts in the Western blot. The molar absorption coefficient ($51761 \text{ M}^{-1} \cdot \text{cm}^{-1}$) was determined from the absorption spectrum in the UV–visible region after correction for apparent absorption and determination of protein concentration by amino acid analysis.

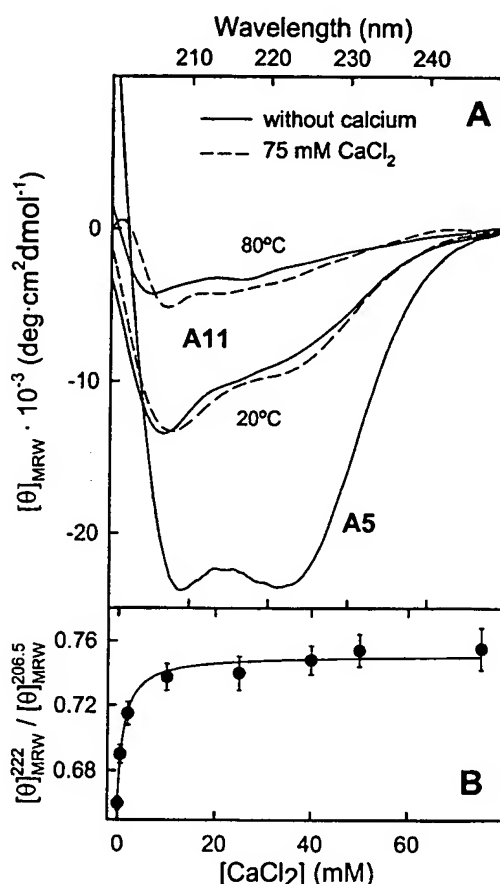


Figure 2 Far-UV CD spectra of annexin A11

(A) Representative far-UV CD spectra of annexin A11 without calcium (—) and in the presence of 75 mM CaCl_2 (---) at 20 and 80 °C are shown in comparison with that of chicken annexin A5 at 20 °C in the absence of calcium, and were registered in 50 mM Hepes (pH 8.0) and 0.1 M NaCl. (B) Variation in the ratio between molar ellipticities/residue at 222 and 206.5 nm with calcium concentration. Results are expressed as means \pm S.D. for at least three different spectra (each of them averaged over six scans).

CD analysis

The CD spectrum of annexin A11 in the far-UV region is shown in Figure 2(A) in comparison with the spectrum of chicken annexin A5 as reference. Annexin A11 in the absence of calcium presents a minimum at 206.5 nm with a molar ellipticity/residue of $-13440 \text{ degrees} \cdot \text{cm}^2 \cdot \text{dmol}^{-1}$. This spectrum differs significantly from that of annexin A5, which has a relatively short N-terminal extension of approx. 15 residues and whose spectrum in the absence of calcium presents two minima at 208 and 222 nm showing much higher negative molar ellipticities. The contribution of the different secondary-structure elements, calculated according to the CCA method, reveals that whereas annexin A5 possesses over 70% of α -helix, the main contributions to annexin A11 structure are α -helix (29%), random coil (31%) and β -turns (26%).

Calcium concentrations required for reproducing the annexin conformational rearrangements induced in the absence of phospholipids are almost three orders of magnitude higher than those required in their presence [1,2,10]. Hence, calcium concentrations in the millimolar range were used throughout these experiments. Addition of calcium to annexin A11 induces small but significant changes in the far-UV CD spectrum. Figure 2(A) also shows the spectrum of annexin A11 saturated

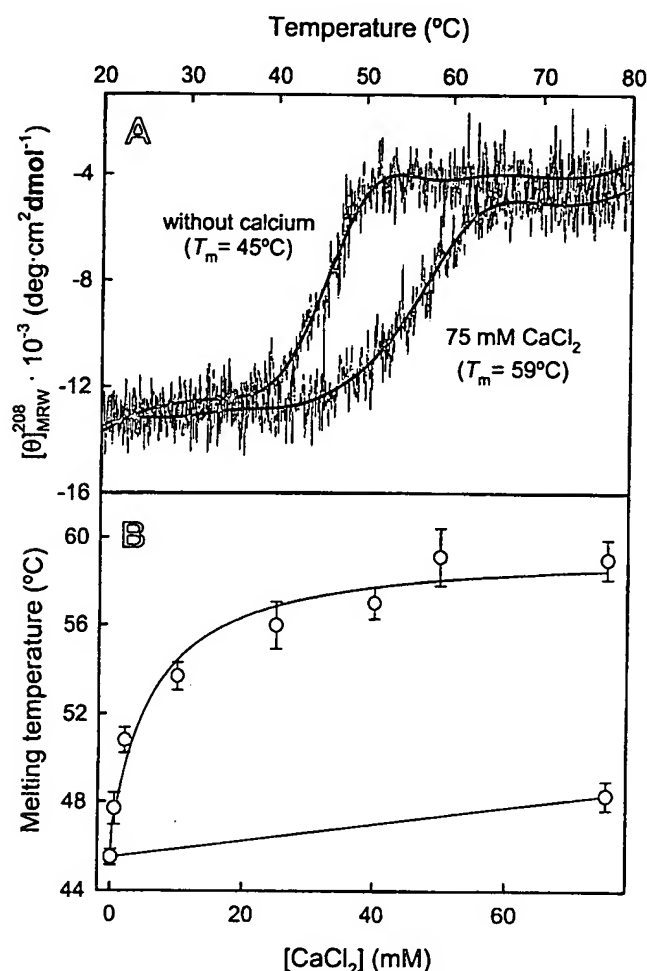


Figure 3 Influence of calcium binding on the thermal stability of annexin A11

(A) Melting curves of annexin A11 in the absence or in the presence of 75 mM CaCl_2 in 20 mM Hepes (pH 8.0) and 0.1 M NaCl. The original unsmoothed data are presented as thin lines together with the results from noise reduction using the Standard Analysis software obtained from Jasco. (B) Dependence of the melting temperature on CaCl_2 concentration (O) was analysed by determining T_m values at different calcium concentrations. Results represent the means \pm S.D. for at least two independent determinations at each CaCl_2 concentration. O, effect of an increase in ionic strength using an NaCl concentration equal to the highest CaCl_2 concentration.

with calcium (75 mM CaCl_2 ; molar ratio of calcium/protein is approx. 80000:1). These changes are not induced by the increase in the ionic strength of the solvent, since no changes in the spectrum are observed when NaCl concentration is increased up to 325 mM, equivalent to the presence of 75 mM CaCl_2 in a buffer containing 100 mM NaCl. Comparison of the spectra in the absence and presence of 75 mM CaCl_2 shows a shift in the minimum from 206.5 to 208 nm; this shift is already observed at 2 mM CaCl_2 and is maintained at higher calcium concentrations. Moreover, a gradual increase in the ratio between molar ellipticities at 222 and 206.5 nm is observed, showing a hyperbolic dependence with the calcium concentration (Figure 2B). These changes suggest a slight increase in α -helix content induced by calcium binding. In fact, CCA analysis of the spectrum at 75 mM calcium yields a 5% increase in the secondary structure (approx. 34%), with a parallel decrease in random coil (approx. 24%).

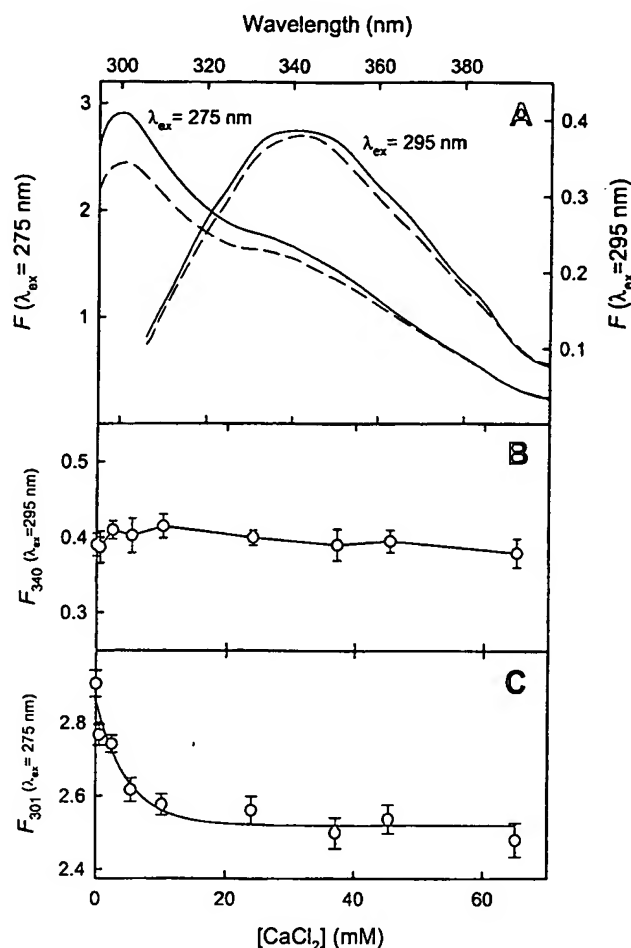


Figure 4 Fluorescence emission spectra of annexin A11 after calcium binding

(A) Emission spectra at excitation wavelengths of 275 and 295 nm in the absence of calcium (—) or presence of 75 mM CaCl_2 (---) were registered at 25 $^{\circ}\text{C}$ at 295–410 nm ($\lambda_{ex} = 275 \text{ nm}$) or 305–410 nm ($\lambda_{ex} = 295 \text{ nm}$). Fluorescence is expressed in arbitrary units; the scale for fluorescence emission at an excitation wavelength of 295 nm has been expanded (right axis). Variations in the fluorescence intensity in the emission maxima of tryptophan (340 nm, $\lambda_{ex} = 295 \text{ nm}$) and tyrosine (301 nm, $\lambda_{ex} = 275 \text{ nm}$) with calcium concentration have been plotted in (B) and (C) respectively.

Thermal stability

The stability of annexin A11 was analysed by monitoring the molar ellipticity at 208 nm as a function of temperature. In the absence of calcium, the melting curve shows a co-operative unfolding of the protein with a T_m of approx. 45 $^{\circ}\text{C}$ (Figure 3A). The binding of calcium by annexin A11 induces a highly significant increase in the thermal stability of the protein; in the presence of 75 mM CaCl_2 , there is an increase of approx. 14 $^{\circ}\text{C}$ in the T_m , with a slight loss of co-operativity (Figure 3A). The variation in the T_m with calcium concentration can be adjusted to a rectangular hyperbola, showing a midpoint effect at 6.3 mM (Figure 3B). Thermal stabilization induced by calcium is specific and is not due to alterations in the polarity of the solvent, as an increase in ionic strength with NaCl up to 325 mM induces only a slight increase in the T_m of approx. 2.8 $^{\circ}\text{C}$.

Fluorescence emission analysis

Figure 4(A) shows the fluorescence emission spectra of annexin A11 at excitation wavelengths of 275 and 295 nm in the absence

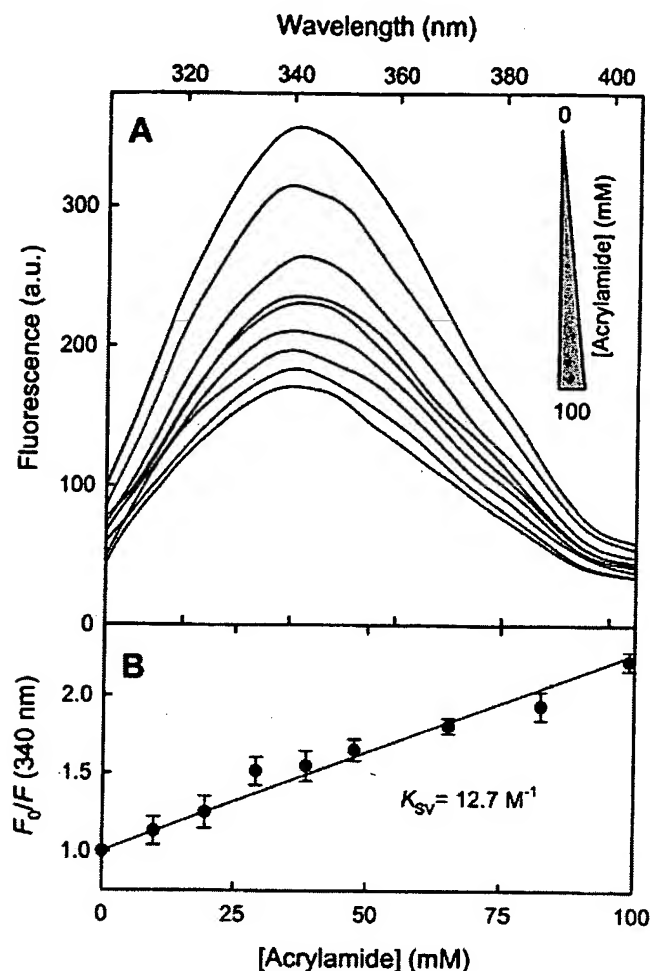


Figure 5 Acrylamide quenching of tryptophan emission

Fluorescence emission ($\lambda_{ex} = 295 \text{ nm}$) at 20°C of the unique tryptophan residue in annexin A11 was quenched by sequential addition of a concentrated acrylamide stock solution up to 100 mM. A representative experiment is shown in (A). Fluorescence intensities at 340 nm were plotted against acrylamide concentration and fitted to the Stern–Volmer equation (B). Results are expressed as means \pm S.D. for three independent experiments.

of calcium or in the presence of 75 mM CaCl_2 . The maximum in the fluorescence emission spectrum of the unique tryptophan residue of annexin A11 (Trp^{23}) appears at 340 nm and its position was not altered when calcium was added to the solvent, and no significant changes were observed in the quantum yield of this residue up to 75 mM CaCl_2 (Figure 4B). A maximum in the fluorescence emission spectrum at 301 nm is obtained using an excitation wavelength of 275 nm. This maximum is almost exclusively due to tyrosine residues and its position is not altered in the presence of calcium. However, as shown in Figure 4(C), a hyperbolic decrease of approx. 15% in the quantum yield of these residues is observed in a calcium concentration-dependent manner, showing a midpoint at 3.4 mM CaCl_2 , and this effect is almost saturated at concentrations higher than 20 mM.

Acrylamide quenching of tryptophan emission

To analyse the degree of exposure to the solvent of Trp^{23} , we have studied the effect of acrylamide on the fluorescence emission spectrum obtained at an excitation wavelength of 295 nm. Figure 5(A) shows the emission spectra of the tryptophan residue at increasing acrylamide concentrations up to 100 mM, which

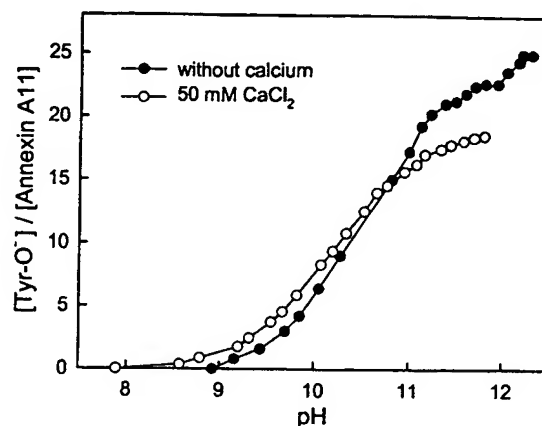


Figure 6 Tyrosine titration of annexin A11

Annexin A11 tyrosine titration was performed by sequential addition of aliquots of 1 M NaOH to a protein sample in 50 mM Tris (pH 8.0) and 0.1 M NaCl and by registration of UV–visible absorption spectra. The number of titrated tyrosine residues was calculated from the variation in absorbance at 295 nm [due to tyrosinate (Tyr-O^-)] relative to protein concentration, either in the absence of calcium (●) or with 50 mM CaCl_2 (○).

does not induce artifacts due to the internal filter effect. A gradual decrease in the emission intensity is induced by the quencher without modification in the position of the maximum. Consequently, the tryptophan residue is accessible to acrylamide and must be at least partially exposed. The Stern–Volmer analysis of the variation in the emission intensity at 340 nm as a function of acrylamide concentration is shown in Figure 5(B); the quenching constant calculated from this plot is 12.7 M^{-1} .

Tyrosine titration

Tyrosine titration was achieved by registration of the UV–visible spectra of the recombinant annexin A11, in the absence or presence of 50 mM CaCl_2 , at increasing pH by the addition of NaOH. At this calcium concentration, binding in the absence of phospholipids should be saturated. Appearance of tyrosinate (Tyr-O^-) residues was followed at 295 nm.

Titration in the absence of calcium distinguishes two main populations of tyrosine residues: buried tyrosine residues with a pK_a of approx. 12 and tyrosine residues, which are at least partially exposed, with a pK_a of approx. 10.5; an additional subpopulation of partially exposed tyrosine residues can also be suggested with a pK_a of 11.6 (Figure 6). Under these conditions, 23 of the 25 tyrosine residues are at least partially exposed. After the addition of 50 mM CaCl_2 , only 19 of the total 25 tyrosine residues of the protein remain exposed. It was not possible to titrate the buried tyrosine residues because protein aggregates at pH higher than 11.9 in the presence of calcium.

Phospholipid binding and vesicle aggregation

We have analysed the interaction of recombinant annexin A11 with phospholipid vesicles (400 nm) by ultracentrifugation and electrophoretic analysis of the supernatants and pellets either in the absence (1 mM EGTA) or presence of 500 μM CaCl_2 . Figure 7 shows the result of the analysis using liposomes composed of acidic (PA, PS or PG) and neutral (PC or PE/PC in the ratio 4:1) phospholipids. Our results suggest that recombinant annexin A11 is not capable of interacting with PC vesicles in the presence or absence of calcium. However, it is capable of

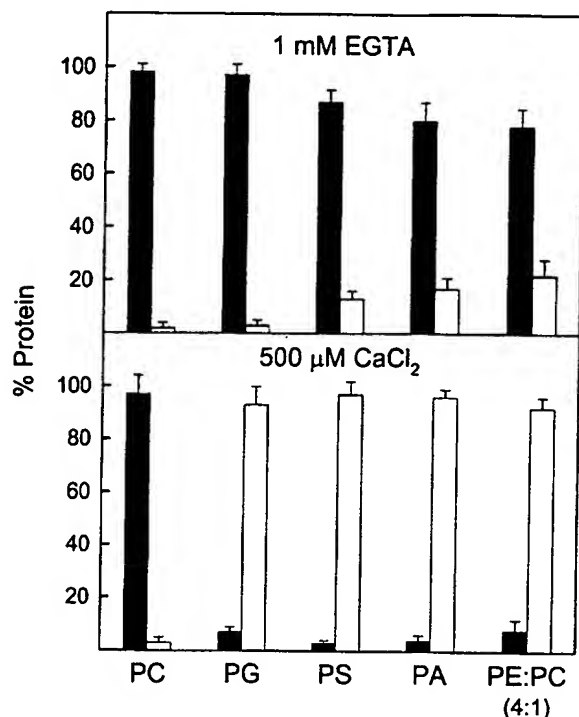


Figure 7 Binding of annexin A11 to phospholipid vesicles

The binding of annexin A11 to 400 nm vesicles with different phospholipid compositions [PC, PG, PS, PA or PE/PC in the ratio 4 : 1] was performed by ultracentrifugation in the absence of calcium (1 mM EGTA) or in the presence of 500 μ M CaCl_2 and using a lipid/protein molar ratio of 800 : 1. The percentage of annexin A11 in the pellets (white bars) and in the supernatants (black bars) was analysed by SDS/PAGE followed by Western-blot analysis using anti-(annexin A11) antibodies and densitometry of the films.

interacting with the neutral phospholipid PE, and with PA, PS and PG, in the presence of 500 μ M CaCl_2 . Furthermore, we have found that annexin A11 interacts in a calcium-independent manner, although to a lower extent, with PE (approx. 22 %) and that there is a certain degree of calcium-independent interaction with PA (approx. 17 %) and PS (approx. 15 %).

A more detailed analysis of the calcium dependence in the interaction of annexin A11 with PS vesicles is shown in Figure 8(A). Approx. 15 % of annexin A11 binds to the vesicles in the absence of calcium, and the bound protein percentage follows a hyperbolic dependence on calcium concentration. At 28 μ M CaCl_2 , 50 % of the total binding to PS vesicles was achieved. Additionally, annexin A11 induces aggregation of PA vesicles at 500 μ M CaCl_2 , but does not induce PS vesicle aggregation at calcium concentrations lower than 1 mM, even at high protein concentrations. Figure 8(B) shows that no aggregation is found at 500 μ M CaCl_2 using a relatively high annexin A11 concentration (110 nM). At 1 mM CaCl_2 , slow vesicle aggregation is observed in the absence of annexin, but addition of the protein speeds up this process in a concentration-dependent manner, from 5.5 to 110 nM (Figure 8B).

Spectroscopic analysis of annexin A11 in the presence of phospholipid vesicles

We have analysed the possible conformational changes in annexin A11 after its binding to PS vesicles using CD spectroscopy in the far-UV region (Figure 9A). The addition of PS vesicles (50 nm) in the presence of 1 mM EGTA induces a slight modification of

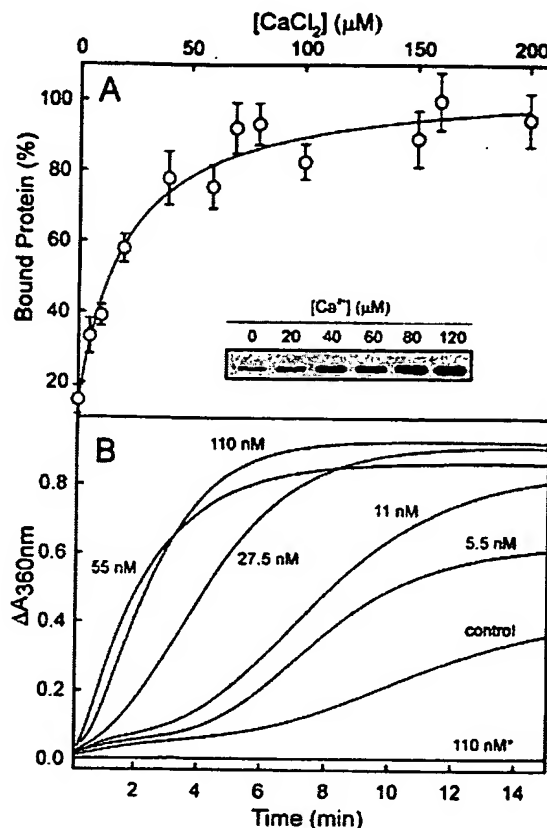


Figure 8 Calcium-dependent aggregation and binding of annexin A11 to PS vesicles

(A) Annexin A11 was mixed with PS vesicles (400 nm) at a lipid/protein molar ratio of 800 : 1 in the presence of increasing calcium concentrations. Quantification of the percentage of bound protein was done by ultracentrifugation and SDS/PAGE analysis of the pellets and supernatants, followed either by silver nitrate staining or by immunodetection of annexin A11. The inset shows a representative experiment analysed by Western blot. (B) Annexin A11-induced aggregation of PS vesicles (100 nm; 0.1 mg/ml) was followed by monitoring the changes in absorbance at 360 nm at 25 °C after the addition of 1 mM CaCl_2 . The different protein concentrations are indicated (5.5–110 nM). The self-aggregation of PS vesicles in the presence of 1 mM CaCl_2 (control) is also shown. No vesicle aggregation was observed in the presence of 500 μ M CaCl_2 even at 110 nM protein concentration indicated by an asterisk.

the spectrum, which mainly affects the region between 200 and 210 nm probably due to light-scattering effects. When 200 μ M CaCl_2 is added to the mixture, a concentration high enough to induce an almost total binding of annexin A11 to PS vesicles, a more significant change is observed in the spectrum with a less negative minimum at 208 nm and an increase in the negative ellipticity at 222 nm. These changes are consistent with an increase in the α -helical content (approx. 9 % according to CCA analysis) and a parallel decrease in the random-coil structure. The CD spectrum of annexin A11 with PC vesicles does not change after the addition of calcium and is almost identical with that obtained with PS in the absence of calcium (results not shown).

The influence of phospholipid vesicles, in the absence or presence of calcium, on the thermal stability of annexin A11 has been analysed by monitoring the changes in molar ellipticity at 220 nm to avoid light-scattering artifacts (Figure 9B). In the absence of vesicles, the T_m of annexin A11 is 45 °C as described above at 208 nm (Figures 3A and 9B). The addition of PS in the absence of calcium does not change this value but involves a loss of co-operativity and a modification in the final state at 80 °C. On the other hand, addition of calcium to a final concentration

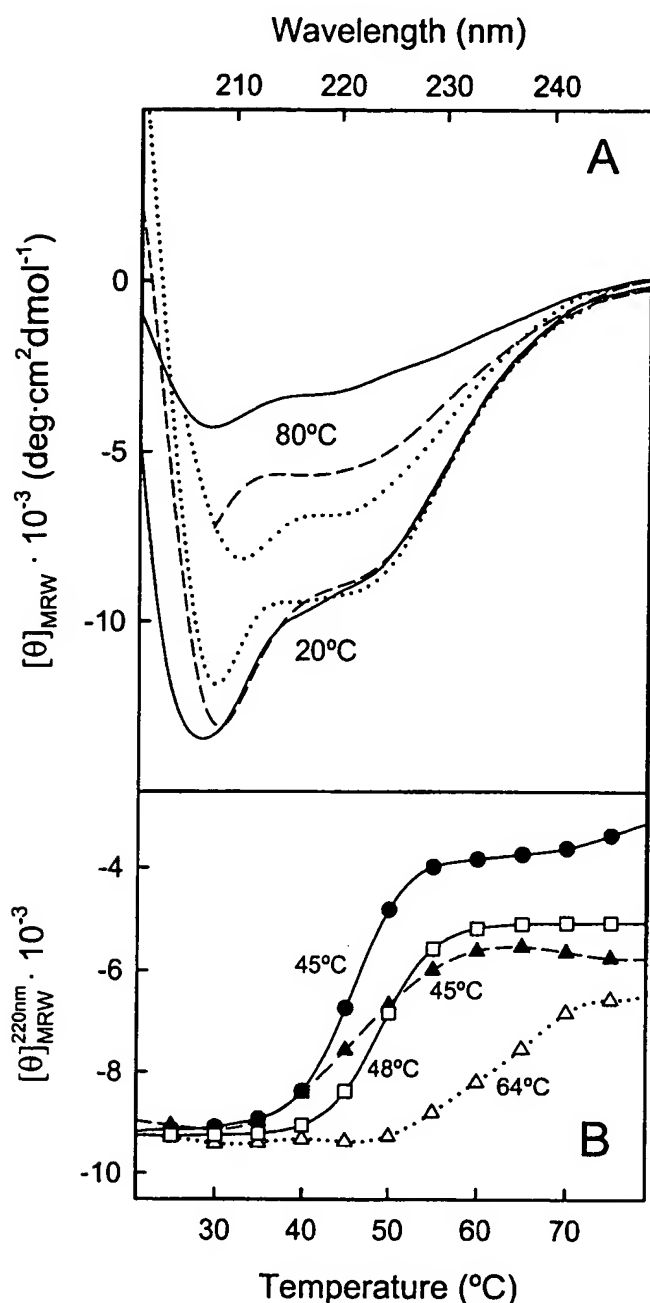


Figure 9 CD analysis of the interaction of PS vesicles with annexin A11

(A) Representative far-UV CD spectra of annexin A11 (0.12 mg/ml) in the absence (—) or presence of PS vesicles (molar ratio of lipid/protein is 800:1) either without (1 mM EGTA; ---) or with 200 μM CaCl_2 (.....) at 20 and 80 $^{\circ}\text{C}$. Spectra of annexin A11 with PC vesicles either in the absence or presence of calcium are not shown, as they are almost identical with those with PS vesicles in the presence of 1 mM EGTA. (B) Annexin A11 melting curves in the absence (1 mM EGTA; ●) or presence of PS vesicles without (\blacktriangle) or with 200 μM CaCl_2 (\square) as well as in the presence of PC vesicles and 200 μM CaCl_2 (\triangle). Molar ellipticity/residue was registered at 220 nm; noise reduction was performed using the Standard Analysis software. Melting temperatures determined from the maximum of the first derivative of each curve are also shown.

of 200 μM increases the T_m up to 64 $^{\circ}\text{C}$; this process is less cooperative and the final denatured state is different. When this analysis is performed under the same experimental conditions but using PC vesicles in the presence of 200 μM CaCl_2 , only a slight increase in the T_m (approx. 3 $^{\circ}\text{C}$) is observed.

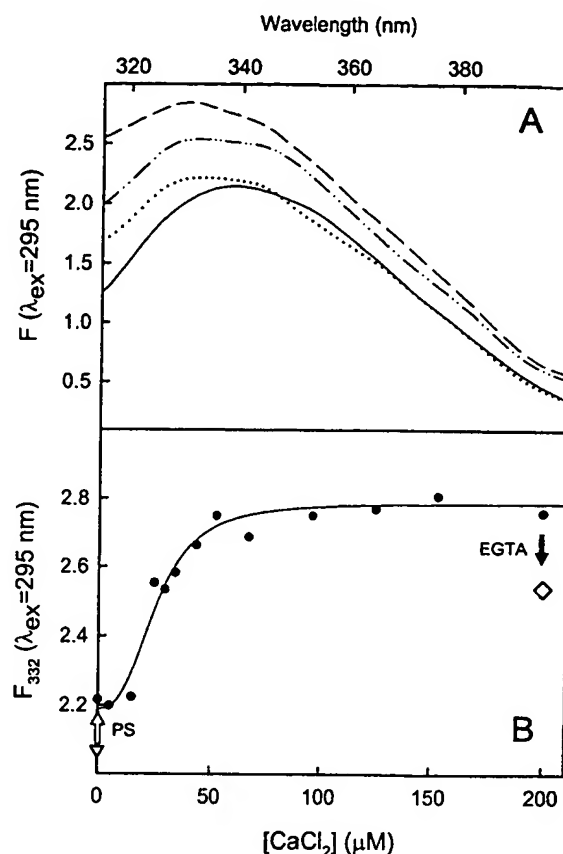


Figure 10 Analysis of the tryptophan fluorescence emission spectra after the binding of annexin A11 to PS vesicles

(A) Emission spectra at the excitation wavelength of 295 nm in the absence (—) or presence of PS vesicles without (1 mM EGTA) (.....) and with 200 μM CaCl_2 (---); --- shows the spectra after the addition of EGTA (1 mM final concentration) to the sample with 200 μM CaCl_2 . All spectra were recorded at 20 $^{\circ}\text{C}$ from 305 to 400 nm. (B) Effect of increasing calcium concentration on annexin A11 tryptophan fluorescence intensity at 332 nm in the presence of PS vesicles (●). The fluorescence intensities at 332 nm in the absence of PS vesicles and calcium (▼) and after the addition of PS vesicles (white arrow) and 200 μM CaCl_2 , followed by addition of EGTA at 1 mM final concentration (black arrow, ◇) are shown.

When annexin A11 is thermally denatured in the absence of phospholipid vesicles, macroscopic aggregation of the protein is observed. However, this process is prevented in the presence of vesicles with or without calcium. Thus the spectra of the denatured protein significantly differ and some secondary structure remains mainly in the presence of calcium and PS, as shown in Figure 9(A).

Fluorescence emission spectra of annexin A11 at an excitation wavelength of 295 nm are shown in Figure 10(A) in the absence or presence of PS vesicles and without (1 mM EGTA) or with 200 μM CaCl_2 . Addition of vesicles to annexin A11 induces a shift in the position of the emission maximum from approx. 340 to 332 nm. Addition of calcium does not modify this wavelength but increases the tryptophan quantum yield. The variation in fluorescence intensity at 332 nm with calcium concentration shows a midpoint effect at 25 μM CaCl_2 (Figure 10B). In Figure 10(B), the inverted triangle indicates the emission intensity in the absence of phospholipids (lower due to the maximum position shift), and the diamond indicates the decrease in intensity achieved by the addition of EGTA (1 mM final concentration) to the sample with PS vesicles and 200 μM CaCl_2 . The changes

in the fluorescence emission spectrum are not fully reversible after removal of calcium, as the tryptophan maximum remains at 332 nm and only a slight decrease in the quantum yield is observed.

Structural model

The sequence and deduced secondary structure of annexin A11 were expanded into a multiple-sequence alignment to facilitate comparative and evolutionary studies, and a virtual three-dimensional model was created by sequence-threading through the crystallography coordinates of known annexin structures. Annexin A11 homologues, identified in 20 vertebrate species, are represented by the mammal, bird, amphibian and fish proteins aligned in Figure 11(A). The greater sequence variability, alignment gaps and unique amino acid composition of the N-termini are evident, with an increased percentage of proline (28%), glycine (20%) and tyrosine (9%) and a tryptophan residue (Trp²³), which contrast with conserved type II calcium-binding sites and congruent structures of the tetrad core, in spite of the evolutionary distances between these species. Secondary-structure predictions (<http://www.expasy.org>) determined that the N-terminus would be expected to adopt a random-coil conformation except for one short α -helical segment ('h' strings in Figure 11A), whereas each tetrad core repeat contains the five α -helices common to other annexins. The observation that the 12 paralogous human annexins exhibit only 45–55% amino acid identity suggested that subfamily differences might be accounted for by variable sites non-critical for function as well as by synaptomorphic sites under functional constraint acting as determinants of subfamily specificity. Although annexin A11 was an ancestral progenitor of other paralogous annexins and thus shares many features in common [16], we sought to identify sites uniquely conserved among annexin A11 members. The DIVERGE v1.04 program from Gu [38] (available at <http://www.phyba.iastate.edu/>) computed 'evolutionary impact' values for each residue in a global sequence alignment and identified Cys²²⁴ and Cys⁴⁰⁹ as structurally relevant differences from other annexins with high divergence impact that implied functional specificity for annexin A11. Together with four other cysteine residues common to other annexins, these may contribute additional structural stability and redox susceptibility to annexin A11 members.

A three-dimensional model of annexin A11 was generated using the DeepView/Swiss-PdbViewer v3.7 computer program [39] and the Swiss-Model server (<http://www.expasy.org/>). These utilized public X-ray crystallography data [40] for full-length pig annexin A1 and human and rat annexin A5 (Protein Data Bank entries 1MCX, 1ANX and 1A8A) in the 'high-calcium' form to thread the mouse annexin A11 amino acid sequence into a three-dimensional model for the homologous tetrad core region (Figure 11B). This representation serves to illustrate the spatial proximity between residues and domains that might otherwise appear distant in sequence alignment format. Thus the residues involved in the type II calcium binding to phospholipids (mkGxGT-38aa-D/E) appear co-ordinated on the external convex surface of the molecule near Cys⁴⁰⁹, whereas the N-terminus (where Trp²³ is located) is orientated towards the opposite, concave (cytosolic) side of the molecule. DeepView program identified four tyrosine residues classified as not exposed to the solvent and within potentially buried α -helical coils: Tyr³¹² and Tyr⁴⁷¹ (<1% exposure); Tyr⁴⁹¹ (<2%); and Tyr³⁹⁶ (<4%) (Figure 11A). Thus it is highly probable that these residues are among those showing a higher pK_a value in the tyrosine titration in the presence of calcium. The other five core tyrosine residues were

predicted to be exposed (24–28% exposure). When the three-dimensional model of annexin A11 was obtained by comparison with the only known annexin X-ray structure in the absence of calcium (full-length pig annexin A1; PDB entry 1HM6), only Tyr³¹² and Tyr⁴⁷¹ were predicted to be completely buried (<1% exposure); Tyr⁴⁹¹ and Tyr³⁹⁶ present approx. 10 and 15% exposure respectively. The interchangeability of Tyr and Phe at certain positions between fish and higher vertebrates suggests the functional importance of bulky and/or hydrophobic residues at these positions relative to the interloop calcium-binding ligands. This model is consistent with our experimental findings and testifies to the structural relevance of uncharged cysteine and tyrosine residues to annexin function.

DISCUSSION

The eukaryotic annexin superfamily has been widely studied since the identification of its first members 25 years ago. The resolution of the crystal structure of some of these proteins with a short or truncated N-terminal extension [7,41–43] has provided a detailed structural knowledge of the core domain and the effects of calcium binding on this structure. However, the structural diversity of N-termini and the disparate functions assigned to these proteins emphasize the significant contribution of this distinctive extension to the functional divergence of animal annexins. The N-terminus is therefore considered to be a specific regulatory domain of annexins [1–3], although its structure and relationship with the core domain still remain poorly understood. Whereas the 314-amino-acid tetrad core region of annexin A11 is highly conserved, its extensive N-terminal region varies in length among vertebrate members (171–221 residues) and presents a high content of proline, glycine and tyrosine residues [21,22]. These unusual features aroused our interest in performing a structural study of annexin A11.

Annexin A11 has been isolated previously from bovine and rabbit lung [22,44] or as a fusion protein with glutathione S-transferase or with the mannose-binding protein [27,31]. However, to perform a spectroscopic characterization, the protein should be similar to the wild-type form and relatively large amounts of purified protein were required. We achieved a high yield in the expression of soluble annexin A11 in *E. coli* by the addition of a His tag, even though approx. 50% of the protein remains insoluble in the cell homogenate. This insertion also minimizes the extent of degradation and simplifies the purification process via affinity chromatography, which further removes N-terminally degraded forms. The requirement for chelating agents to prevent precipitation when imidazole is removed after the chromatography points out that the His tag is capable of inducing autoaggregation of annexin A11, acting as a bridge between different molecules in the presence of cations such as Ni²⁺ or Ca²⁺. Although the addition of calcium induces aggregation of the protein containing the His tag, this does not occur when the tag is removed. The use of reducing agents throughout the purification procedure prevents the oxidation of the redox-sensitive free cysteine residues that seem to be important for annexin A11 function, as mentioned above. Recombinant annexin A11 was obtained with only small modifications from the wild-type, a change in position 2 from Ser to Gly and the addition of Gly-Ala at the N-terminus, which are not likely to have any effect on the structure or functional properties of annexin A11.

The main secondary-structure element present in the highly conserved annexin core is the α -helix [7–10]. Accordingly, the CCA analysis of the CD spectrum of annexin A5, which possesses a very short N-terminus of 15 amino acid residues and whose



α -helix (29 %), random coil (31 %) and β -turns (26 %). The remaining 14 % is assigned to extended β -strands; however, this percentage must arise from artifacts derived from the application of the CCA, since secondary-structure predictions based on the

amino acid sequence indicate a very low theoretical percentage of these structures. There are no structural studies concerning this annexin, but the structural features of the core domain and the relatively high degree of similarity to other annexins of known three-dimensional structure suggest that the α -helical contribution probably arises from the protein core. From the studies performed with the N-terminus, the existence of an α -helix involved in S100A6 binding has been suggested [27,45], in a way similar to those described for p53 with S100B, and annexins A1 and A2 with S100A11 and S100A10 respectively [28–30].

According to the secondary-structure predictions based on the amino acid sequence of the N-terminal extension, this region would be mainly in random coil except for the theoretical amphipathic α -helix. However, the particular amino acid sequence of the N-terminus (rich in glycine, proline, tyrosine and glutamine) suggests the formation of poly(Pro) β -turn helices that would be responsible for the high β -turn percentage detected. These atypical secondary structures have been detected in the N-terminus of annexin A7 [46], whose sequence, although shorter, is quite similar to that of annexin A11. Accordingly, the N-terminus would account for both random-coil and β -turn contributions predicted from the CD spectra.

In general, the annexin core domain is known to be quite stable, with a higher T_m for those annexins with a short N-terminus [10]. The presence of a long N-terminal extension could induce a destabilization of the core domain. In fact, the T_m for annexin A11 is approx. 6 °C lower than that of human annexin A5, which has one of the lowest T_m among mammalian annexins. The change in the negative molar ellipticity at 208 nm with increase in temperature is mainly a reflection of α -helices unfolding to unordered structure. As the melting curve shows only one co-operative transition, the unfolding of the protein core and any hypothetical α -helix from the N-terminus must take place simultaneously.

Calcium binding does not greatly affect the CD spectrum of annexin A11. For other members of the family, the secondary-structure changes described after calcium binding are also small, implying mainly three-dimensional modifications of the calcium-phospholipid-binding sites with an increase in the percentage of α -helix and a rearrangement of the protein core [9,10,47]. The analysis of the CD spectra of annexin A11 reveals a hyperbolic increase in the ratio between molar ellipticities at 222 and 206.5 nm with calcium concentration. On calcium binding, this ratio increases towards that of pure α -helix, pointing to a higher contribution of this structure with a concomitant decrease in random coil. This hypothesis is also supported by the CCA analyses of the spectra, which suggest a 5–6% increase in α -helix with an equivalent decrease in random coil. Even though it has been described that saturation with calcium of annexins with short N-termini induces a similar increase in the percentage of α -helix [9,10], the total number of residues involved should be considered. Thus, whereas only 16–19 residues change in annexin A5 core, 25–30 residues may become α -helical in annexin A11. Owing to the structural similarity among the protein cores in different annexins, the increase in the α -helical content in annexin A11 cannot be completely explained by the conformational rearrangements of the protein core, and probably involves changes in its N-terminus as well.

In contrast with the relatively small conformational changes observed, calcium induces a great thermal stabilization, increasing the T_m by approx. 14 °C. This increase is larger than that observed for other mammalian annexins such as human annexin A5 (approx. 10 °C) [10]. Moreover, the calcium-bound states of annexin A5 and annexin A11 have a similar thermal stability,

whereas calcium-free annexin A11 shows a lower stability. Taking into account the degree of homology of the annexin core, differences, quite probably in the N-terminal region, are responsible for the changes in protein stability. Therefore we propose that the long N-terminus in annexin A11 has a destabilizing effect in the calcium-free state; structural changes after calcium binding contribute to stabilization of the protein and the T_m of annexin A11 approaches that of annexin A5. It remains to be explained how this interaction could take place, but it is tempting to speculate with a mechanism resembling that described for annexin A1 [8]. This annexin binds to S100A11 through an amphipathic α -helix, which, in a calcium-free state, inserts into domain III, displacing helix 3D. The full-length crystal structure of annexin A1 has been obtained recently, showing that calcium binding induces the refolding of helix 3D pushing the N-terminus outside the annexin core [48], thus enabling the interaction with S100A11. In addition to the stabilizing effects, this mechanism also involves an increase in α -helix due to the refolding of helix 3D.

Tertiary structure analysis through fluorescence studies reveals that Trp²³ is completely exposed to the polar solvent either in the presence or absence of calcium, as the maximum of emission remains at 340 nm under both conditions and there is no decrease in intensity due to calcium binding. Acrylamide quenching also supports this observation, as the obtained Stern–Volmer constant is 12.7 M⁻¹, characteristic of an almost totally exposed tryptophan residue. Whereas free tryptophan residues or *N*-acetyl-tryptophan-amide show a K_{SV} of approx. 16 · M⁻¹, exposed tryptophan residues in proteins present values between 10 and 14 M⁻¹ [49]. On the other hand, tyrosine emission decreases with increase in calcium concentration. This decrease is probably due to a change in the microenvironment of some tyrosine residues to a more hydrophobic one, where interactions that stabilize the polar group of this residue result in the quenching of emission. To confirm this observation, tyrosine titration was performed in the calcium-free and calcium-bound state. According to the titration, in the absence of calcium two tyrosine residues are buried, whereas the calcium-bound state presents six buried tyrosine residues. Therefore the addition of calcium induces a conformational change in annexin A11 that implies the translocation of some tyrosine residues from a polar to a hydrophobic environment, whereas Trp²³ remains unaltered. Taking into account the similarity between the putative amphipathic α -helix in the N-terminus of annexin A11 and that described in the N-terminus of annexin A1, one could speculate that the N-terminus would be even more exposed to the solvent in the presence of calcium. Thus at least some of the tyrosine residues internalized in the presence of calcium are probably located in the protein core. This hypothesis is strongly supported by the surface analysis of the proposed structural model, where the highly conserved residues 312, 396, 471 and 491 are predicted to be buried in the protein core. Among these residues, Tyr³¹² and Tyr³⁹⁶ could be the ones buried in the calcium-free state, as they are the only ones predicted as buried in the calcium-free model. It is not possible to locate the remaining two tyrosine residues titrated as internal in the presence of calcium, as the three-dimensional models cannot predict the structure and position of the N-terminus.

Functionally, annexin A11 interacts with acidic phospholipid and PE vesicles in a calcium-dependent fashion, whereas no binding is observed with PC, as shown previously with wild-type annexin A11 [22]. Partial binding in the absence of calcium was observed to PE, PA and PS vesicles as described for other annexins [50–52]. Phospholipid specificity is generally conserved in calcium-independent binding, and

this is likely to be the case for annexin A11. There must be two contributions to the interaction with phospholipids under these conditions: a specific polar recognition and a hydrophobic interaction. The N-terminus of annexin A11 may be able to insert into the bilayer and establish hydrophobic contacts with the phospholipids, but this would imply a reorientation of the N-terminus from the concave/cytosolic side towards the cell membrane.

Binding of annexin A11 to PS vesicles shows a hyperbolic dependence on calcium concentration. The interaction requires calcium concentrations in the micromolar range, with 50% binding achieved at 28 μ M. Consequently, there is a great increase in calcium affinity in the presence of phospholipids as has been observed for other annexins [1,2,47]. Calcium requirement for PS binding of annexin A11 is higher than that of annexin A2 and lower than that for annexin A5 [1]. These differences could account for the development of divergent functions throughout vertebrate evolution. Annexin A11 induces PS vesicle aggregation only at non-physiological calcium concentrations (> 1 mM) at which this cation itself acts as a bridge for vesicle aggregation. However, annexin A11 is able to accelerate the aggregation process in a protein concentration-dependent manner. These results formulate a role for annexin A11 in aggregation processes *in vivo*, where the presence of other proteins such as S100A6 could modify calcium requirements, as described for other annexins. For example, calcium requirement of annexin A2 for the induction of vesicle aggregation is significantly reduced in the presence of S100A10 [53].

Spectroscopic analyses of the interaction of annexin A11 with PS vesicles give further support to the above observations. Addition of PS vesicles in the absence of calcium induces only a small change in the CD spectrum, which does not affect the thermal stability of the protein, although a loss of co-operativity in the melting curve is observed. Taking into account that annexin A11 is capable of interacting weakly with PS in a calcium-independent manner, this interaction could be responsible for the observed conformational change. However, CD spectroscopy shows that annexin A11 suffers a conformational rearrangement after vesicle binding in the presence of calcium. Calcium-dependent binding to PS vesicles induces an increase in α -helical content similar to the addition of calcium in the absence of phospholipids, but to a higher extent (approx. 9% versus 5–6%). The observed change is again too large to be exclusively due to changes in the protein core; therefore the N-terminus is likely to be involved in this process.

Calcium-dependent binding to PS vesicles is also accompanied by a large increase (approx. 20 °C) in thermal stability, higher than that described for calcium binding alone, and the loss of co-operativity is also remarkable. All these changes must be the consequence of a strong specific interaction, as they are not observed when using PC vesicles. In this case, the small increase in T_m could be due only to binding of calcium to the protein without interaction with the vesicles, and thus no loss of co-operativity is displayed.

In addition to these results, fluorescence studies support a role of the N-terminus in both calcium-independent and calcium-dependent interactions with PS vesicles. The environment of the N-terminal Trp²³ was modified when vesicles were added to the protein preparation in the absence of calcium, with a significant blue-shift in the emission maximum corresponding to a change from an almost total exposure to the solvent to a more hydrophobic environment. However, taking into account that the quantum yield was not modified significantly, this residue probably remained partially in contact with the solvent. Once again, this observation supports the notion of a weak calcium-

independent interaction, probably through the N-terminus of annexin A11 establishing hydrophobic contacts with the bilayer.

Addition of calcium to the annexin/vesicle mixture is characterized by an increase in the tryptophan quantum yield, which presents a midpoint effect almost coincident to that observed in the ultracentrifugation studies. This increase is probably due to the insertion of Trp²³ into the lipid bilayer, which would protect this residue from solvent quenching. Furthermore, the addition of excess EGTA is not able to reverse the interaction, so there must be a hydrophobic component in the binding that accounts for this effect.

This original structural characterization of annexin A11 reveals that the N-terminus, the longest of all known mammalian annexins and containing unusual composition and repeat patterns, contributes significantly to the overall annexin structure. The analysis of the structural conservation of annexin A11 using a combination of primary- and secondary-structure analyses, three-dimensional models and the evolutionary divergence offers a novel insight into its key functional determinants. This annexin has one of the lowest melting temperatures *in vitro* (45 °C) and calcium binding promotes subtle rearrangements in the secondary and tertiary structures of the protein to induce significant thermal stabilization. The recombinant protein binds to acidic phospholipids in a calcium-dependent manner as described for other annexins; it also shows calcium-independent binding, but to a lower extent. These results suggest that the binding of annexin A11 to PS vesicles presents both hydrophobic and polar contributions due to the N-terminus and the annexin core respectively. According to the spectroscopic data, a two-step mechanism can be proposed. First, a weak interaction is established through surface hydrophobic contacts with some degree of polar specificity; secondly, after the addition of calcium, a tight binding to the lipid bilayer takes place, enabling in this way the partial insertion of the N-terminus, which reinforces the interaction. It remains however to be determined whether calyculin, sorcin or ALG-2 interaction with annexin A11 will influence its binding to lipid bilayers.

We are grateful to Dr Hiroyoshi Hidaka for kindly providing a polyclonal antibody raised against bovine annexin A11. This work was supported by grant nos. PM98-0083, PB98-1529 and BMC2002-01407 from the Dirección General de Investigación (Spain).

REFERENCES

- 1 Raynal, P. and Pollard, H. B. (1994) Annexins: the problem of assessing the biological role for a gene family of multifunctional calcium- and phospholipid-binding proteins. *Biochim. Biophys. Acta* **1197**, 63–93.
- 2 Swairjo, M. A. and Seaton, B. A. (1994) Annexin structure and membrane interactions: a molecular perspective. *Annu. Rev. Biophys. Struct.* **23**, 193–213.
- 3 Gerke, V. and Moss, S. E. (2002) Annexins: from structure to function. *Physiol. Rev.* **82**, 331–371.
- 4 Morgan, R. O. and Fernandez, M. P. (1998) Expression profile and structural divergence of novel human annexin 31. *FEBS Lett.* **434**, 300–304.
- 5 Liemann, S. and Huber, R. (1997) Three-dimensional structure of annexins. *Cell. Mol. Life Sci.* **53**, 516–521.
- 6 Morgan, R. O., Jenkins, N. A., Gilbert, D. J., Copeland, N. G., Balsara, B. R., Testa, J. R. and Fernandez, M. P. (1999) Novel human and mouse annexin A10 are linked to the genome duplications during early chordate evolution. *Genomics* **60**, 40–49.
- 7 Huber, R., Römisch, J. and Pâques, E. P. (1990) The crystal and molecular structure of human annexin V, an anticoagulant protein that binds to calcium and membranes. *EMBO J.* **9**, 3867–3873.
- 8 Rosengarth, A., Gerke, V. and Luecke, H. (2001) X-ray structure of full-length annexin 1 and implications for membrane aggregation. *J. Mol. Biol.* **306**, 489–498.
- 9 Arboledas, D., Olmo, N., Lizarbe, M. A. and Turnay, J. (1997) Role of the N-terminus in the structure and stability of chicken annexin V. *FEBS Lett.* **416**, 217–220.
- 10 Turnay, J., Olmo, N., Gasset, M., Iloro, I., Arrondo, J. L. R. and Lizarbe, M. A. (2002) Calcium-dependent conformational rearrangements and protein stability in chicken annexin A5. *Biophys. J.* **83**, 2280–2291.

- 11 Burger, A., Berendes, R., Liemann, S., Benz, J., Hofman, A., Göttig, P., Huber, R., Gerke, V., Carsten, T., Römisch, J. et al. (1996) The crystal structure and ion channel activity of human annexin II, a peripheral membrane protein. *J. Mol. Biol.* **257**, 839–847
- 12 Rosengarth, A., Rösger, J., Hinz, H. J. and Gerke, V. (1999) A comparison of the energetics of annexin I and annexin V. *J. Mol. Biol.* **288**, 1013–1025
- 13 Morgan, R. O. and Fernandez, M. P. (1995) Molecular phylogeny of annexins and identification of a primitive homologue in *Giardia lamblia*. *Mol. Biol. Evol.* **12**, 967–979
- 14 Fernandez, M. P., Jenkins, N. A., Gilbert, D. J., Copeland, N. G. and Morgan, R. O. (1996) Sequence and chromosomal localization of mouse annexin XI. *Genomics* **37**, 366–374
- 15 Morgan, R. O., Bell, D. W., Testa, J. R. and Fernandez, M. P. (1998) Genomic locations of ANX11 and ANX13 and the evolutionary genetics of human annexins. *Genomics* **48**, 100–110
- 16 Bances, P., Fernández, M. R., Rodríguez-García, M. I., Morgan, R. O. and Fernandez, M. P. (2000) Annexin A11 (ANXA11) gene structure as the progenitor of paralogous annexins and source of orthologous cDNA isoforms. *Genomics* **69**, 95–103
- 17 Iglesias, J. M., Morgan, R. O., Jenkins, N. A., Copeland, N. G., Gilbert, D. J. and Fernandez, M. P. (2002) Comparative genetics and evolution of annexin A13 as the founder gene of vertebrate annexins. *Mol. Biol. Evol.* **19**, 608–618
- 18 Towle, C., Weissbach, L. and Treadwell, B. V. (1992) Alternatively spliced annexin XI transcripts encode proteins that differ near the amino-terminus. *Biochim. Biophys. Acta* **1131**, 223–226
- 19 Fiedler, K., Lafont, F., Parton, R. G. and Simons, K. (1995) Annexin XIIIb: a novel epithelial specific annexin is implicated in vesicular traffic to the apical plasma membrane. *J. Cell Biol.* **128**, 1043–1053
- 20 Sable, C. L. and Riches, D. W. H. (1999) Cloning and functional activity of a novel truncated form of annexin IV in mouse macrophages. *Biochem. Biophys. Res. Commun.* **258**, 162–167
- 21 Towle, C. A. and Treadwell, B. V. (1992) Identification of a novel mammalian annexin. cDNA cloning, sequence analysis, and ubiquitous expression of the annexin XI gene. *J. Biol. Chem.* **267**, 5416–5423
- 22 Tokumitsu, H., Mizutani, A., Minami, H., Kobayashi, R. and Hidaka, H. (1992) A calyculin-associated protein is a newly identified member of the Ca^{2+} /phospholipid-binding proteins, annexin family. *J. Biol. Chem.* **267**, 8919–8924
- 23 Iino, S., Sudo, T., Niwa, T., Fukasawa, T., Hidaka, H. and Niki, I. (2000) Annexin XI may be involved in Ca^{2+} - or GTP- γ S-induced insulin secretion in the pancreatic β -cell. *FEBS Lett.* **479**, 46–50
- 24 Misaki, Y., Pruijn, G. J. M., van der Kemp, A. W. C. M. and van Venrooij, W. J. (1994) The 56K autoantigen is identical to human annexin XI. *J. Biol. Chem.* **269**, 4240–4246
- 25 Mizutani, A., Watanabe, N., Kitao, T., Tokumitsu, H. and Hidaka, H. (1995) The long amino-terminal tail domain of annexin XI is necessary for its nuclear localization. *Arch. Biochem. Biophys.* **318**, 157–165
- 26 Furge, L. L., Chen, K. and Cohen, S. (1999) Annexin VII and annexin XI are tyrosine phosphorylated in peroxovanadate-treated dogs and in platelet-derived growth factor-treated rat vascular smooth muscle cells. *J. Biol. Chem.* **274**, 33504–33509
- 27 Sudo, T. and Hidaka, H. (1999) Characterization of the calyculin (S100A6) binding site of annexin XI-A by site-directed mutagenesis. *FEBS Lett.* **444**, 11–14
- 28 Mäler, L., Sastry, M. and Chazin, W. J. (2002) A structural basis for S100 protein specificity derived from comparative analysis of apo and Ca^{2+} -calyculin. *J. Mol. Biol.* **317**, 279–290
- 29 Réty, S., Sopkova, J., Renouard, M., Osterloh, D., Gerke, V., Tabaries, S., Russo-Marie, F. and Lewit-Bentley, A. (1999) The crystal structure of a complex of p11 with the annexin II N-terminal peptide. *Nat. Struct. Biol.* **6**, 89–95
- 30 Réty, S., Osterloh, D., Arié, J. P., Tabaries, S., Seemann, J., Russo-Marie, F., Gerke, V. and Lewit-Bentley, A. (2000) Structural basis of the Ca^{2+} -dependent association between S100C (S100A11) and its target, the N-terminal part of annexin I. *Structure Fold. Res.* **8**, 175–184
- 31 Satoh, H., Shibata, H., Nakano, Y., Kitauro, Y. and Maki, M. (2002) ALG-2 interacts with the amino-terminal domain of annexin XI in a Ca^{2+} -dependent manner. *Biochem. Biophys. Res. Commun.* **291**, 1166–1172
- 32 Brownawell, A. M. and Creutz, C. E. (1997) Calcium-dependent binding of sorcin to the N-terminal domain of synexin (annexin VII). *J. Biol. Chem.* **272**, 22182–22190
- 33 Gómez-Guillén, M. C., Turnay, J., Fernández-Díaz, M. D., Olmo, N., Lizarbe, M. A. and Montero, P. (2002) Structural and physical properties of gelatine extracted from different marine species: a comparative study. *Food Hydrocolloids* **16**, 25–34
- 34 Perczel, A., Park, K. and Fasman, G. D. (1992) Analysis of the circular dichroism spectrum of proteins using the convex constraint algorithm: a practical guide. *Anal. Biochem.* **203**, 83–93
- 35 Turnay, J., Plannmüller, E., Lizarbe, M. A., Bertling, W. and von der Mark, K. (1995) Collagen binding activity of recombinant and N-terminally modified annexin V (anchoring II). *J. Cell. Biochem.* **58**, 208–220
- 36 Laemmli, U. K. (1970) Cleavage of structural proteins during the assembly of the head of bacteriophage T4. *Nature (London)* **227**, 680–685
- 37 Turnay, J., Olmo, N., Lizarbe, M. A. and von der Mark, K. (2002) Changes in the expression of annexin A5 gene during *in vitro* chondrocyte differentiation: influence of cell attachment. *J. Cell. Biochem.* **84**, 132–142
- 38 Gu, X. (1999) Statistical methods for testing functional divergence after gene duplication. *Mol. Biol. Evol.* **16**, 1664–1674
- 39 Guex, N., Diemand, A. and Peitsch, M. C. (1999) Protein modelling for all. *Trends Biol. Sci.* **24**, 364–367
- 40 Berman, H. M., Westbrook, J., Feng, Z., Gilliland, G., Bhat, T. N., Weissig, H., Shindyalov, I. N. and Bourne, P. E. (2000) The protein data bank. *Nucleic Acids Res.* **28**, 235–242
- 41 Weng, X., Luecke, H., Song, I. S., Kang, D. S., Kim, S. H. and Huber, R. (1993) Crystal structure of human annexin I at 2.5 Å resolution. *Protein Sci.* **2**, 448–458
- 42 Bewley, M. C., Boustead, C. M., Walker, J. H. and Huber, R. (1993) Structure of chicken annexin V at 2.25-Å resolution. *Biochemistry* **32**, 3923–3928
- 43 Luecke, H., Chang, B. T., Mailliard, W. S., Schlaepfer, D. D. and Haigler, H. T. (1995) Crystal structure of the annexin XII hexamer and implications for bilayer insertion. *Nature (London)* **378**, 512–515
- 44 Mizutani, A., Usuda, N., Tokumitsu, H., Minami, H., Yasui, K., Kobayashi, R. and Hidaka, H. (1992) CAP-50, a newly identified annexin, localizes in nuclei of cultured fibroblast 3Y1 cells. *J. Biol. Chem.* **267**, 13498–13504
- 45 Tokumitsu, H., Mizutani, A. and Hidaka, H. (1993) Calyculin-binding site located on the NH_2 -terminal domain of rabbit CAP-50 (annexin XI): functional expression of CAP-50 in *Escherichia coli*. *Arch. Biochem. Biophys.* **303**, 302–306
- 46 Matsushima, N., Creutz, C. E. and Kretzinger, R. H. (1990) Polyproline, β -turn helices. Novel secondary structures proposed for the tandem repeats within rhodopsin, synaptophysin, synexin, gliadin, RNA polymerase II, hordein, and gluten. *Proteins* **7**, 125–155
- 47 Sopkova, J., Vincent, M., Takahashi, M., Lewit-Bentley, A. and Gallay, J. (1999) Conformational flexibility of domain III of annexin V at membrane/water interfaces. *Biochemistry* **38**, 5447–5458
- 48 Rosengarth, A. and Luecke, H. (2003) A calcium-driven conformational switch of the N-terminal and core domains of annexin A1. *J. Mol. Biol.* **326**, 1317–1325
- 49 Lakowicz, J. R. (1999) Quenching of fluorescence. In *Principles of Fluorescence Spectroscopy*, 2nd edn (Lakowicz, J. R., ed.), pp. 237–265. Kluwer Academic/Plenum, New York
- 50 Jost, M., Zeuschner, D., Seemann, J., Weber, K. and Gerke, V. (1997) Identification and characterization of a novel type of annexin-membrane interaction: Ca^{2+} is not required for the association of annexin II with endosomal membranes. *Biochim. Biophys. Acta* **110**, 221–228
- 51 König, J. and Gerke, V. (2000) Modes of annexin-membrane interactions analyzed by employing chimeric annexin proteins. *Biochim. Biophys. Acta* **1498**, 174–180
- 52 Tzima, E. and Walker, J. H. (2000) Platelet annexin V: the ins and outs. *Platelets* **11**, 245–251
- 53 Lambert, O., Gerke, V., Bader, M. F., Porte, F. and Brisson, A. (1997) Structural analysis of junctions formed between lipid membranes and several annexins by cryo-electron microscopy. *J. Mol. Biol.* **272**, 42–55
- 54 Koradi, R., Billeter, M. and Wüthrich, K. (1996) MOLMOL: a program for display and analysis of macromolecular structures. *J. Mol. Graph.* **14**, 51–55

Received 4 November 2002/10 March 2003; accepted 11 April 2003

Published as BJ Immediate Publication 11 April 2003, DOI 10.1042/BJ20021721

Different properties of two isoforms of annexin XIII in MDCK cells

Sandra Lecat^{1,2,*}, Paul Verkade^{1,2}, Christoph Thiele³, Klaus Fiedler⁴, Kai Simons^{1,2} and Frank Lafont^{1,2,‡}

¹Cell Biology and Biophysics Programme, European Molecular Biology Laboratory, Meyerhofstrasse 1, D-69117 Heidelberg, Germany

²Max Planck Institute for Molecular Biology and Genetics, Pfotenhauerstrasse 110, D-01307 Dresden, Germany

³Department of Neurobiology, University of Heidelberg, Im Neuenheimer Feld 364, D-69120, Heidelberg, Germany

⁴Cell Biology Department Biozentrum, University of Basel, Klingelbergstrasse, 70, CH 4056 Basel, Switzerland

*Present address: Département des Récepteurs et Protéines Membranaires, Ecole Supérieure de Biotechnologie de Strasbourg, Strasbourg, France

‡Author for correspondence at present address: Département de Biochimie, Sciences II, 30 quai Ernest-Ansermet, CH-1211 Genève 4, Switzerland
(e-mail: Frank.Lafont@biochem.unige.ch)

The online version of this article contains additional data and is available at <http://www.unige.ch/sciences/biochimie/Lafont/JCSLecatY2K.html>

Accepted 9 May; published on WWW 22 June 2000

SUMMARY

Annexins form a family of proteins that are widely expressed and known to bind membranes in the presence of calcium. Two isoforms of the annexin XIII subfamily are expressed in epithelia. We previously reported that annexin XIIIb is apically localized in MDCK cells and that it is involved in raft-mediated delivery of apical proteins. We have now analyzed the properties of annexin XIIIa, which differs from annexin XIIIb by a deletion of 41 amino acids in the amino-terminal domain, and is distributed both apically and basolaterally. Annexin XIIIa binding to membranes is independent of calcium but requires its myristoyl amino-terminal modification, as observed with annexin XIIIb. Our biochemical and functional data show

that annexin XIIIa behaves differently in the apical and in the basolateral compartments. Whereas annexin XIIIa apically can associate with rafts independently of calcium, the basolateral pool requires calcium for this. Annexin XIIIa, like annexin XIIIb, stimulates apical transport of influenza virus hemagglutinin but, in contrast, only annexin XIIIa inhibits basolateral transport of vesicular stomatitis virus G protein. Our results suggest that annexin XIIIa and XIIIb have specific roles in epithelial cells, and because of their structural similarities, these isoforms offer interesting tools for unravelling the functions of annexins.

Key words: Membrane traffic, MDCK cell, Protein sorting, Annexin

INTRODUCTION

13 annexins have so far been identified in mammals, but members of the family are spread out all over the eukaryotic kingdom (Morgan and Fernandez, 1997). Each annexin has a distinct N terminus and annexins are homologous in the C-terminal core, a domain of 30 kDa that harbors calcium binding sites (Liemann and Huber, 1997). In vitro binding experiments between purified annexins and liposomes have suggested that calcium ions bridge the protein to the negatively charged head group of phospholipids. Annexins are described as calcium-dependent phospholipid-binding proteins that translocate from the cytosol to the membrane in response to an elevation of the intracellular calcium concentration. This property of the core domain was demonstrated in artificial systems but seems to operate in living cells as well (Campos et al., 1990; Ernst, 1991; Trotter et al., 1994, 1995; Selbert et al., 1995, 1996; Barwise and Walker, 1996; Chasserot et al., 1996).

How annexins perform their functions after membrane binding remains unclear (Liemann and Lewit-Bentley, 1995; Lecat and Lafont, 1999). Based on the finding that annexins can aggregate or even fuse membranes in a calcium-dependent manner in vitro, annexins have been proposed to regulate membrane fusion events (Ernst et al., 1991; Creutz, 1992;

Emans et al., 1993; Bitto and Cho, 1998). Studies in the cellular context confirmed that several annexins play a role in membrane trafficking but there is little support for their proposed function in membrane fusion (Harder and Gerke, 1993; Burgoyne and Clague, 1994; Donnelly and Moss, 1997; Carroll et al., 1998; Kamal et al., 1998; König et al., 1998). Annexins were also shown to have calcium-channel activities upon association with liposomes (Chen et al., 1993; Demange et al., 1994; Arispe et al., 1996; Liemann et al., 1996; Hofmann et al., 1997). In vitro studies have suggested that annexins I and XII can be inserted into the bilayer (Luecke et al., 1995; Langen et al., 1998; Rosengarth et al., 1998); however, studies in cells have not substantiated a role for annexins to form calcium channels. Instead, annexins have been shown to regulate the activity of several ion channels (Kaetzel et al., 1994; Nilius et al., 1996).

We previously cloned the cDNA encoding canine annexins XIIIa and XIIIb from an epithelial Madin-Darby Canine Kidney II cell (MDCKII) cDNA library (Fiedler et al., 1995). Annexin XIIIb has an insertion of 41 amino acids after the first four amino acids of the sequence that are common to both isoforms. We demonstrated that annexin XIIIb is involved in apical exocytosis of polarized MDCKII and is associated with specific lipid microdomains (Fiedler et al., 1995; Lafont et al., 1998b).

Apical exocytosis, contrary to basolateral exocytosis, is dependent on the integrity of these microdomains, called 'rafts' (Keller and Simons, 1998). Rafts consist of assemblies of sphingolipids and cholesterol (Simons and Ikonen, 1997), which form liquid-ordered phases segregated in a dynamic fashion from the other lipids (Ahmed et al., 1997; Brown and London, 1997; Brown, 1998; Rietveld and Simons, 1998). They function by forming platforms for proteins that specifically partition into these lipid assemblies (Simons and Ikonen, 1997; Brown and London, 1998). Annexin XIIIa was identified by northern blot analysis as an intestinal-specific annexin and shown by immunofluorescence studies on tissues to localize mainly at the apical plasma membrane of enterocytes with a faint staining on their basolateral plasma membrane (Wice and Gordon, 1992). The localization of annexin XIIIa could not be inferred from these studies, however, because the antibody used recognized two proteins: a 36 kDa protein corresponding to annexin XIIIa and a 40 kDa protein that we later identified as annexin XIIIb. In this paper, we have compared the subcellular distribution and functional properties of annexin XIIIa with those of annexin XIIIb in MDCKII cells.

MATERIALS AND METHODS

R agents

Detergents were the following: SDS (BioRad Laboratories, Hercules, CA, USA), Triton X-100 (Serva, Heidelberg, Germany), NP-40 (FlukaAG, Buchs, Switzerland). IPTG, methyl- β -cyclodextrin, sodium butyrate (NaBu) and proteinase inhibitors were from Sigma Chemical Co. (Deisenhofen, Germany). Restriction endonucleases were from New England Biolabs (Schwabach/Taunus, Germany) and cloned pfu polymerase from Stratagene (La Jolla, CA, USA). pOPRSVI-CAT vector was from Stratagene.

Cell culture

Media and reagents for cell culture were purchased from Gibco BRL (Eggenstein, Germany). Madin-Darby Canine Kidney (MDCK) type II cells were cultured as described (Pimplikar et al., 1994) on TranswellTM polycarbonate filters (0.4 μ m pore size) from Costar (Cambridge, MA, USA) or on plastic dishes. MDCKII Lac switchable cells were given by Dr E. E. Schneeberger and cultivated the same way as wild-type MDCKII except when transfected (McCarthy et al., 1996). After transfection, the selection was maintained with 0.6 mg/ml G418 geneticin (Gibco BRL). 293 cells were grown in MEM medium supplemented with 10% fetal calf serum (FCS) and 1% non-essential amino acids in addition to the general components such as penicillin/streptomycin and glutamine.

Preparation of antibodies and immunoblotting

The affinity-purified anti-annexin XIII-II antibody preparation was according to Fiedler et al. (1995). 12% SDS-PAGE gels were run using the BioRad mini-gel system unless otherwise mentioned. Polyclonal rabbit anti-VIP21/cav1 amino-terminal N20 was purchased from Santa Cruz Biotechnology, Inc. (Santa Cruz, CA, USA). Monoclonal mouse anti-GP114 was from our laboratory (Balcarova-Ständer et al., 1984). Goat anti-rabbit and goat anti-mouse horseradish peroxidase-conjugated antibodies were from BioRad (Munich, Germany). The immunoblots were revealed with ECL (Amersham International).

Construction of recombinant adenoviruses expressing annexin XIIIa and annexin XIIIb

Recombinant adenoviruses expressing annexin XIIIa, annexin XIIIb and non-myristoylated annexin XIIIa were produced as described

previously (He et al., 1998). Briefly, the annexin XIII sequences were amplified by PCR to obtain a *KpnI-XbaI* fragment using TCG GGT ACC AAA AAC GAA ATG GGC as 5' primer for the myristoylated annexins and, in order to create a non-myristoylated mutant, the codon for the amino-terminal glycine GGC was replaced by one for alanine GCC in the 5' primer. The 3' primer was ATA TCT AGA TCA GTG CAA GAG GGC C in all the constructs. The fragments were cloned in the pShuttle-CMV vector and recombinant adenoviral plasmids were generated by homologous recombination with the pAdEasy-1 vector (He et al., 1998). Transfection of 293 cells was performed by lipofection. Amplified adenoviruses were purified by CsCl gradient centrifugation and stored at -20°C in storage buffer (5 mM Tris-HCl, pH 8.0, 50 mM NaCl, 0.1% BSA, 25% glycerol).

Cloning of annexin XIII sequences for stable expression in MDCKII Lac switchable cells

The annexin XIII sequences were amplified by PCR to obtain a *XbaI-KpnI* fragment containing a suitable Kozack sequence before the ATG and a c-myc tag at the carboxy terminus. For the amplification of the annexin XIIIb sequence, the 5' primer was TCG TCT AGA GCC ACC ATG GGC AAT CGT CAT AGC C, these last four nucleotides being replaced by GCC A for amplifying the annexin XIIIa sequence. As 5' primer for the non-myristoylated mutants, the codon for the amino-terminal glycine GGC was replaced by one for alanine GCC. For all constructs, the 3' primer was ATA GGT ACC TCA GTT CAA GTC TTC TTC GCT TAT GAG TTT TTG CTC GTG CAA GAG GGC CAC, where the bold characters correspond to the c-myc tag, EQKLISEEDLN. The fragments were inserted in pOPRSVI-1 vector, a derivative of the pOPRSVI-CAT vector containing a polylinker instead of the CAT gene (Daniele Zacchetti, EMBL; Cheong et al., 1999).

Infection and transfection of MDCKII cells

For transient overexpression of annexin XIII by adenovirus infection, MDCKII cells grown on 1.2 cm filters for 3 days were infected on the apical side at 37°C for 1 hour in 500 μ l of culture medium with 1 μ l of virus stock. The expression was carried on for 16 hours before further analysis. For stable overexpression of annexin XIII, the MDCKII Lac switchable cells were transfected by electroporation and the clones were selected for their resistance to G418. 24 clones of each transfection were screened by immunofluorescence with anti-annexin XIII-II antibody for the expression of the exogenous proteins, after having induced their synthesis with 5 mM IPTG and 1 mM NaBu for 16 hours at 37°C.

Immunoelectron microscopy and immunofluorescence analysis

The locations of the transiently overexpressed annexin XIIIa, annexin XIIIb or non-myristoylated annexin XIIIa in polarized cells were determined at the electron-microscope level using anti-annexin XIII-II antibody at 1/200 dilution, according to Lafont et al. (1998b). For immunofluorescence studies, cells grown on filters were washed twice in PBS⁺ buffer (PBS containing 0.9 mM CaCl₂ and 0.5 mM MgCl₂), fixed with methanol at -20°C for 6 minutes and then processed for immunolabeling. The myc-tag was not accessible either to the polyclonal or the monoclonal myc antibodies. The anti-annexin XIII-II antibody was used instead at a dilution of 1/300 on transient expressing cells and 1/100 on stable clones in PBS, supplemented with 0.2% gelatin for 1 hour at 37°C. The secondary antibody was a goat anti-rabbit FITC-conjugated antibody (Dianova, Hamburg, Germany). The filters were placed in mounting medium and analyzed using a Leica NTS confocal microscope as described previously (Lafont et al., 1998b).

Membrane fraction analysis

The two-step sucrose gradient was prepared as previously described (Fiedler et al., 1993). Briefly, the MDCKII or MDCKII Lac switchable

cells grown to confluence in 150 cm dishes were homogenized at 4°C in 500 µl of 10 mM Hepes, pH 7.4, 5 mM EGTA, 250 mM sucrose, 1 mM DTT, 25 mg/ml CLAP protease inhibitors. Then, a postnuclear supernatant (PNS) was obtained by 10 minutes centrifugation at 3000 rpm in a microfuge. The PNS was made 1.5 M sucrose, placed in a SW60 centrifuge tubes (Beckman, Munchen, Germany) and overlaid by a 1.2 M and a 0.8 M sucrose layer in Hepes-EGTA. The flotation was carried out at 4°C for 18 hours at 35000 rpm. The membranes float at each sucrose interface. 500 µl fractions were collected starting at the top of the gradient and 30 µl of each fraction was analyzed by SDS-PAGE followed by western blotting.

To prepare the total membrane fraction, MDCKII cells grown to confluence in 15 cm dishes were homogenized in 200 µl of 10 mM Tris-HCl, pH 7.5, 150 mM NaCl, 5 mM EGTA, 1 mM DTT and CLAP. The membranes from 30 µl of the subsequent PNS were collected on a 1 M sucrose cushion by a centrifugation at 100,000 g in a TLA100 rotor (Beckman). The membranes were thereafter treated for 15 minutes with agitation at room temperature (RT) in 30 µl of 10 mM Tris-HCl, pH 7.5, 150 mM NaCl, 5 mM EGTA as a control, or the same buffer supplemented with either 1 M KCl or 0.2% Nonidet P-40 (NP-40), or were treated at 4°C in 30 µl of 0.1 M NaHCO₃, pH 11. For extraction of the cholesterol, the membranes were treated with 10 mM cyclodextrin in 30 µl of buffer for 30 minutes at 37°C. The peripheral-membrane proteins released from the membranes were recovered in the supernatant following a second 100,000 g centrifugation. The samples were directly mixed with 2× loading buffer and analyzed by SDS-PAGE followed by blotting.

Crosslinking of membrane proteins by phospholipids

The synthesis of a C18-stearic acid derivative containing a diazirin ring on the C10 carbon (10-azidostearic acid) is described elsewhere (Thiele et al., 2000). MDCKII cells grown on 2.4 cm size polycarbonate filters for 2.5 days were incubated for 3 hours in medium with 5% FCS. Then cells were incubated in medium supplemented with 1% FCS and 100 µM C18-stearic acid mixed 1:1 with BSA for overnight labeling at 37°C. The fatty acid was then chased for 2 hours with 10% FCS in MEM medium. Cells were washed in PBS⁺, frozen in liquid nitrogen for 5 seconds and subjected, on dry ice, to UV irradiation by a black light lamp equipped with 100-W mercury bulb and a filter cutting wavelengths below 310 nm (Spectroline model B100/F, Spectronics Corporation, Westbury, NY, USA). The cells were 12 cm from the source for 15 minutes of irradiation. Subsequently, cells were scraped from the filters and homogenized. The membranes and the cytosol fractions were separated by a 100,000 g centrifugation, as described above, and the proteins were separated on large SDS-PAGE gels containing 8% polyacrylamide for annexin XIIIb and 13.5% for VIP21/cav1 analysis.

Raft association analysis

MDCKII or the stable MDCKII Lac switchable cells overexpressing annexin XIIIa (MDCK(lac)/55) were grown to confluence in 3 cm dishes and scraped directly after ice-cold PBS washes in 400 µl of 10 mM Tris-HCl, pH 7.5, 150 mM NaCl, 5 mM EGTA or increasing amounts of CaCl₂, 1% Triton X-100 (TX-100), 1 mM DTT, CLAP at 4°C. The cells were incubated for 30 minutes at 4°C to allow the solubilisation of the membranes to occur. Then, the material was adjusted to 40% OptiPrep™ (Nycomed-Pharma, Oslo, Norway) in a final volume of 1 ml and was overlaid with 1.2 ml of 30% OptiPrep™, 1.2 ml 25% OptiPrep™ and 0.8 ml of 5% OptiPrep™ (all in 10 mM Tris-HCl, pH 7.5, 150 mM NaCl, 1% TX-100 plus CaCl₂ as mentioned in the text). The flotation was performed in SW60 tubes at 100,000 g for 4

hours at 4°C. 500 µl fractions were collected starting from the top of the gradient and TCA precipitated. The pellets were washed 3 times with -20°C acetone and all the material was subjected to SDS-PAGE and blot analysis.

Expression and purification of recombinant annexin XIIIa and transport assay

Myristoylated annexin XIIIa was expressed in the *Drosophila* Schneider cells and purified exactly as previously reported for annexin XIIIb (Lafont et al., 1998b). A functional assay reconstituting the transport of exocytic carriers from the TGN to either the apical or the basolateral surface has already been described in detail (Lafont et al., 1998a).

RESULTS

Annexins XIIIa and XIIIb are identical except that annexin XIIIb has a 41-amino-acid insertion in its N-terminal tail. Because of this similarity we were not able to raise an antibody specific for annexin XIIIa, so its expression was analyzed by making use of an antibody directed against a peptide sequence in the N-terminal tail common to both isoforms (Fiedler et al., 1995; Fig. 1A). This affinity-purified antibody recognizes three bands by immunoblotting of an MDCKII lysate (Fig. 1B). By

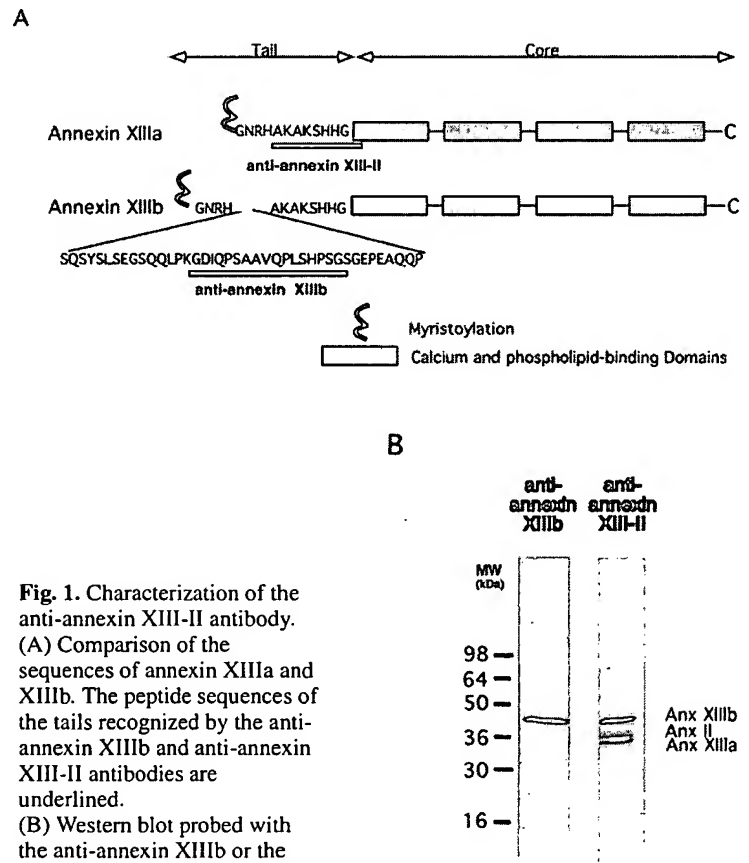


Fig. 1. Characterization of the anti-annexin XIII-II antibody. (A) Comparison of the sequences of annexin XIIIa and XIIIb. The peptide sequences of the tails recognized by the anti-annexin XIIIb and anti-annexin XIII-II antibodies are underlined.

(B) Western blot probed with the anti-annexin XIIIb or the anti-annexin XIII-II antibody on MDCKII cells lysate. The positions of molecular mass markers and annexin XIIIb (40 kDa) and XIIIa (36 kDa) are indicated.

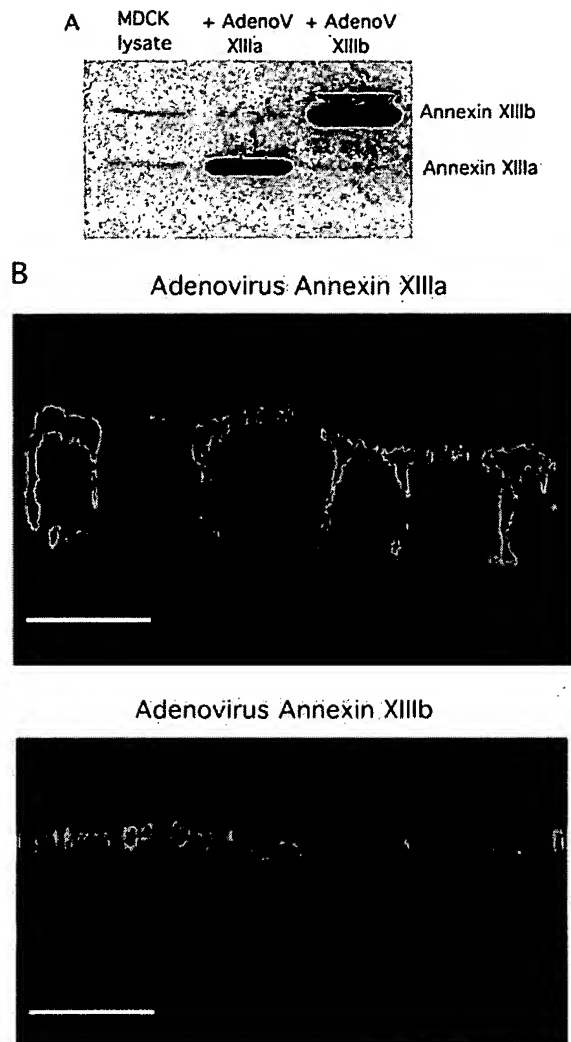


Fig. 2. Immunostaining of annexin XIIIa as compared with that of annexin XIIIb in MDCKII cells. After infection with recombinant adenoviruses overexpressing wild-type annexin XIIIa or XIIIb, MDCKII cells were analyzed by immunoblotting (A) and by immunofluorescence confocal microscopy (B) with the anti-annexin XIII-II antibody. Bar, 10 μ m.

2D-gel analysis and comparison with either overexpressed or purified annexin XIIIa and by microsequencing, we could determine that the upper band corresponds to annexin XIIIb and the lower band corresponds to annexin XIIIa. By microsequencing analysis, the intermediate band was described as being a variant of annexin II (Fiedler et al., 1997), although the amino acid sequence selected to raise the antibody does not show homology to that of annexin II. In this study, this antibody is referred as the anti-annexin XIII-II antibody.

Differential localization of annexin XIIIa versus annexin XIIIb in polarized MDCKII cells

To determine where annexin XIIIa is targeted in MDCKII cells, recombinant annexin XIII adenoviruses were generated and used to infect these cells. We used the anti-annexin XIII-II

antibody at a dilution such that the endogenous annexin XIIIa were not stained, thus allowing detection of adenovirus-expressed annexins by western blotting (Fig. 2A), immunofluorescence (Fig. 2B) and immunoelectron microscopy (Fig. 3). The overexpressed annexin XIIIb was apically localized using both anti-annexin XIIIb and anti-annexin XIII-II antibodies (Figs 2B, 3A). At the same expression level, the overexpressed annexin XIIIa was visible both at the basolateral and at the apical plasma membranes (Figs 2B, 3B). Quantitation by immunoelectron microscopy confirmed that annexin XIIIa was equally distributed between the two plasma membrane domains of MDCKII cells (3.63 ± 0.85 gold particles/ μ m membrane length on apical versus 3.15 ± 0.58 on basolateral membrane).

Calcium-independent binding of the annexin XIIIs to cellular membranes

We reported previously that half of the cellular pool of annexin XIIIb is bound to membranes when calcium ions have been chelated (Lafont et al., 1998b). To characterize the membrane binding features of annexin XIIIa, two membrane pools of high and low buoyant densities were isolated by flotation in a two-step sucrose gradient from an MDCKII cell homogenate. The protein content of the fractions was analyzed by western blotting. Caveolin-1 (VIP21/cav1) was used to follow the presence of membranes in the different peaks (Fig. 4A, fractions 4 and 8). After chelation of calcium ions with EGTA, annexin XIIIa and XIIIb were localized in the top fractions of the gradient containing the light density membranes and also in the soluble pool at the bottom of the gradient.

The myristoyl moiety is necessary for the calcium-independent interaction of annexin XIIIs with membranes

Annexin XIIIa are the only members of this protein family shown to be myristoylated on their N-terminal glycine (Wice and Gordon, 1992). In order to test how this fatty acid modification contributes to membrane linkage, MDCKII cells engineered to express exogenous genes in a regulated manner (MDCKII Lac switchable cells) were stably transfected with a pOPRSV1-1 vector encoding the myristoylated annexin XIIIa or their non-myristoylated mutants. In these cells, the synthesis of the exogenous annexin XIIIa or XIIIb is repressed due to the stable expression of the lac repressor but can be induced by adding IPTG to the cell medium, thereby inhibiting the lac repressor. Two clones of wild-type and non-myristoylated mutants of annexin XIIIa and XIIIb were selected by immunofluorescence microscopy. When membrane association of these exogenous proteins was compared using flotation in the two-step sucrose gradient the non-myristoylated annexin XIIIa were exclusively recovered in the cytosolic fractions (Fig. 4B).

To test whether the myristoyl group was anchoring the annexin XIIIa to the lipid bilayer we performed crosslinking experiments. Polarized MDCKII cells were fed with a modified saturated C18 fatty acid containing a UV-activable diazirine crosslinker. It has been previously shown that such a fatty acid is more than 80% incorporated into phospholipids with a chain length of 18 carbons (Mahoney et al., 1977; Doi et al., 1978). The crosslinker makes covalent amide bonds with the surrounding C-H from lipids or proteins upon UV irradiation.

The proteins crosslinked to additional lipids can subsequently be detected by a mobility shift in SDS-PAGE.

After crosslinking, the membranes were separated from the cytosol by centrifugation at 100,000 *g* and the samples were analysed by immunoblotting. In a typical experiment, the electrophoretic migration of the integral membrane protein VIP21/cav1 was shifted, while in control experiments in which the cells were either fed with fatty acids without crosslinker or were not submitted to UV irradiation, VIP21/cav1 migrated normally (see Fig. Crosslink available at <http://www.unige.ch/sciences/biochimie/Lafont/JCSLecatY2K.html>). The migration of annexin XIIIb was not shifted; however, a shadow trailing the migrating band became visible in the membrane fraction but not in the cytosolic one (see Fig. Crosslink

available at <http://www.unige.ch/sciences/biochimie/Lafont/JCSLecatY2K.html>). The shadow is probably due to the anchoring of the myristoyl group into the bilayer, arising from crosslinking to phospholipids. Because of the presence of the annexin II band overlapping the annexin XIIIa staining, we could not determine unambiguously whether a shadow was associated with annexin XIIIa using the anti-annexin XIII-II antibody. We therefore decided to analyze the membrane association of annexin XIIIa and XIIIb by different approaches.

Hydrophobic interactions are contributing to the membrane binding of annexin XIIIs

A homogenate of MDCKII cells was prepared in the absence of calcium, and membranes were collected on a sucrose

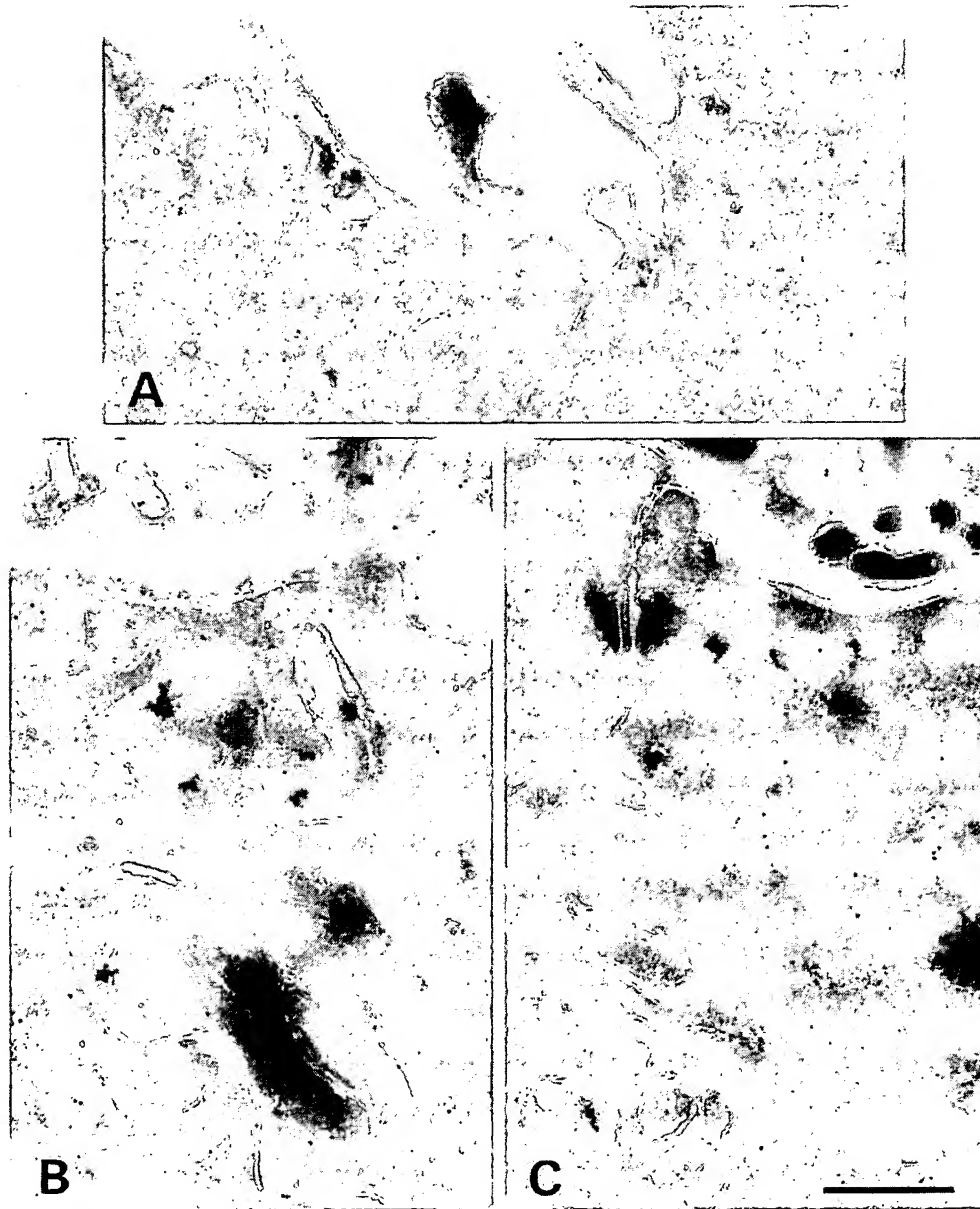


Fig. 3. Immunogold labeling of annexin XIIIa, non-myristoylated annexin XIIIa and annexin XIIIb in MDCKII cells. MDCKII cells infected with recombinant adenoviruses overexpressing annexin XIIIb (A), annexin XIIIa (B) or the non-myristoylated annexin XIIIa (C) were processed for immunoelectron microscopy with the anti-annexin XIII-II antibody (10 nm gold particles). Bar, 500 nm.

cushion by ultracentrifugation at 100,000 *g*. These pelleted membranes were washed with high salt or basic pH buffers and samples were subsequently centrifuged at 100000 *g*. The proteins released from the membrane pool were detected on western blots. The integrity of the membranes was assessed using VIP21/cav1 (Fig. 5A). For both isoforms of annexin XIII, binding to membranes was not abolished by high salt washes (Fig. 5B). Similarly, high pH stripping of the membranes released little protein (Fig. 5B). There are reports that myristoylated or palmitoylated proteins are resistant to pH 11 extraction (Song and Dohman, 1996; Topinka and Bredt, 1998). The resistance of the annexin XIIIs to pH11 treatment shows that hydrophobic interactions are contributing to their membrane association and supports the conclusion of the crosslinking experiment described above.

Since annexin XIIIb has been shown to bind to cholesterol-sphingolipid rafts (Lafont et al., 1998b), we next analyzed whether cholesterol depletion using cyclodextrin was affecting the membrane binding of both annexin XIIIa and XIIIb.

Indeed, this was the only treatment which could significantly, although not entirely, release the annexin XIIIs into the supernatant (Fig. 5C).

A pool of annexin XIIIa is associated with rafts in absence of calcium

To demonstrate raft association of annexin XIIIb, we previously showed the presence of annexin XIIIb in lipid-protein complexes resistant to solubilisation by Triton X-100 at 4°C (Lafont et al., 1998b). These insoluble complexes are separated from solubilised proteins and from cytoskeletal elements by flotation in a density gradient. Insoluble complexes float to low density, unlike cytoskeletally bound elements and soluble proteins, which stay at the bottom of the flotation gradient. When MDCKII cells were lysed with TX-100 at 4°C in a buffer lacking calcium and the material was subsequently subjected to OptiPrep™ gradient centrifugation, part of annexin XIIIa was recovered in the low density fraction (Fig. 6A). This fraction was typically enriched in the

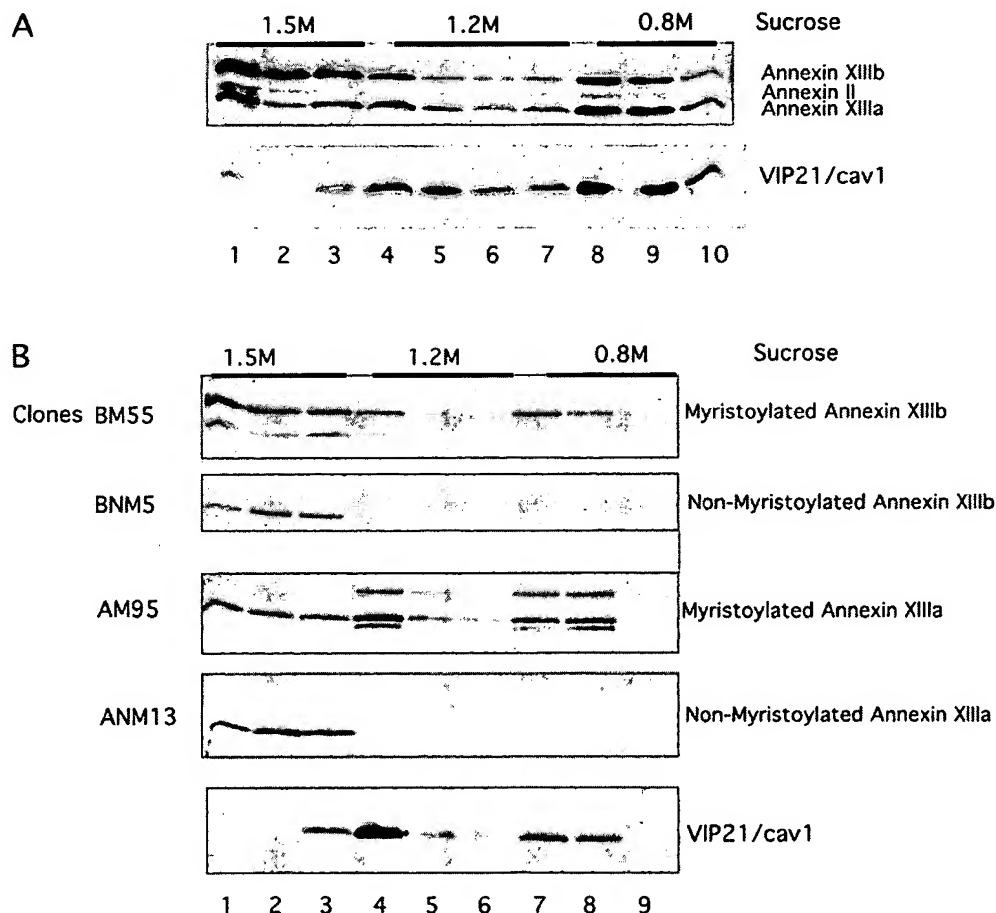


Fig. 4. Calcium-independent binding of annexin XIII to membranes. (A) MDCKII homogenate was prepared with EGTA. The membrane fractions were separated from the cytosolic proteins by a two-step sucrose gradient centrifugation. The partitioning of annexin XIIIa and VIP21/cav1 between the membranes (heavy membranes: fractions 4-5, light membranes: fractions 8-9) and the cytosolic pools (fractions 1-3) was analyzed by western blot using, respectively, anti-annexin XIII-II and anti-VIP21/cav1 antibodies. (B) Stable clones of MDCKII Lac switchable cells overexpressing either the wild-type or the non-myristoylated mutants of the annexin XIIIa were submitted to the two-step sucrose gradient centrifugation and the presence of annexin XIIIa and VIP21/cav1 in each fraction was followed by immunoblotting. Note that a band corresponding to the endogenous annexin II is visible in the immunoblot of the BM55 clone and that two bands corresponding to the endogenous annexin XIIIa (lower) and XIIIb (upper) are visible in the immunoblot of the AM95 clone.

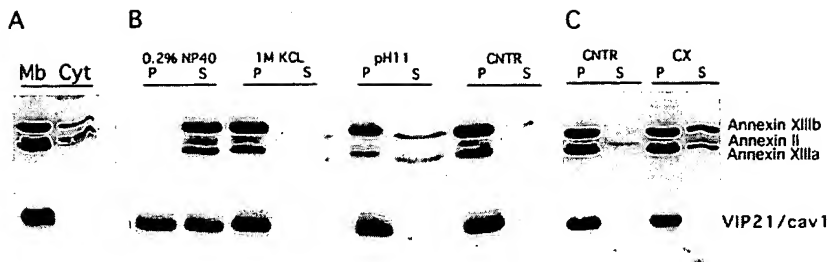


Fig. 5. Cyclodextrin treatment can partially release annexin XIIIa from membranes. (A) The total membrane (Mb) and cytosolic (Cyt) fractions of MDCKII cells were segregated by a 100,000 *g* spin of the PNS in the absence of calcium. (B) Membranes were subsequently subjected to no treatment (CNTR) or extracted for 15 minutes at 4°C with 0.1 M NaHCO₃, pH 11, 1 M KCl or 0.2% NP-40 at RT and then spun at 100,000 *g* and recovered in the pellet (P) while the released proteins were in the supernatant (S). (C) In order to extract cholesterol, membranes were treated with 10 mM cyclodextrin for 30 minutes at 37°C (CX) or left untreated as control (CNTR). The partitioning of annexin XIIIa and VIP21/cav1 between the fractions was analyzed by western blot using the respective antibodies.

cholesterol-binding protein VIP21/cav1. Neither annexin XIIIa nor XIIIb floated anymore after depletion of cholesterol by cyclodextrin (Fig. 6B). A pool of annexin XIIIa thus associates with lipid-rafts independently of calcium. However, we noticed that a fraction of annexin XIIIa was reproducibly associated with the low density fraction. We wondered whether this could reflect a differential behavior of apical versus basolateral annexin XIIIa.

To find out whether the apical and the basolateral pools of

annexin XIIIa differed in their raft-binding properties, we made use of the properties of MDCKII Lac switchable cells. This subclone differs from MDCKII cells by several criteria. For example, MDCKII Lac switchable cells express endogenous annexin XIIIa to a lower extent than MDCKII cells (data not shown) and have a lower capacity for apical delivery (Cheong et al., 1999). Another difference compared to MDCKII cells was that the overexpressed annexin XIIIa exclusively localised to the basolateral plasma membrane of MDCKII Lac switchable cells whereas the overexpressed annexin XIIIb was mostly apical (Fig. 7). This could be observed independently of the expression level by immunofluorescence after expression of annexin XIIIa either stably with pOPRSV1 vector (Fig. 7) or transiently with recombinant adenoviruses

(S. Lecat, unpublished results).

Because of the exclusive basolateral localization of annexin XIIIa in the MDCKII Lac switchable clone, we could analyze biochemically the raft association of the basolateral annexin XIIIa. We prepared detergent-insoluble material with calcium-chelating agents from stable clones expressing annexin XIIIa or XIIIb and performed step density gradient flotation. We found that annexin XIIIa was not floating while VIP21/cav1 (unpublished result) and annexin XIIIb (Fig. 8A) were floating to the same extent as in normal MDCKII cells.

Several annexins have been shown to float after Triton extraction in the presence of calcium (Parkin et al., 1996). This is particularly the case for the basolateral pool of annexin II, which has recently been observed in rafts together with CD44 (Oliferenko et al., 1999). We wanted therefore to compare the effect of calcium on the raft association of annexin XIIIa expressed in MDCKII Lac switchable cells versus that of annexin II. Increasing the calcium concentration to 200 μ M had no effect on VIP21/cav1 (unpublished result) or annexin XIIIb flotation (Fig. 8B). On the other hand, calcium triggered a drastic flotation of annexin II, as previously reported (Fig. 8B; Oliferenko et al., 1999) and a significant and reproducible flotation of a fraction of annexin XIIIa. To verify the specificity of the calcium-dependent raft association of annexin XIIIa, we made use of its non-myristoylated mutant. At a concentration of 1 mM calcium, annexin XIIIa lacking its fatty acid modification was entirely associated with the total membrane fraction recovered from a 100,000 *g* pellet (Fig. 8C). However, despite

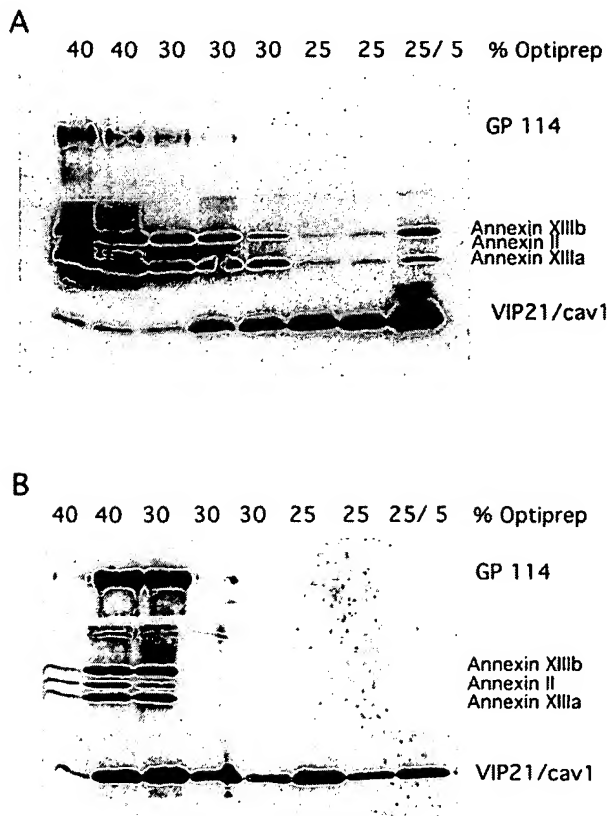


Fig. 6. A fraction of annexin XIIIa binds to detergent-insoluble glycosphingolipid enriched material (DIGs) independently of calcium. MDCKII cells were lysed in 1% TX-100 at 4°C in the absence of calcium and the DIGs were separated from the solubilised fraction by a centrifugation in an Optiprep™ gradient. (A) The presence of GP114 (negative control), annexin XIIIa and VIP21/cav1 (positive control) in the different TCA-precipitated fractions of the gradient was analyzed by western blotting with anti-GP114, anti-annexin XIIIb and anti-VIP21/cav1 antibodies, respectively. (B) Upon extraction of cholesterol from the cell using cyclodextrin, the detergent-insoluble material is drastically reduced.

being bound to membranes, the non-myristoylated annexin XIIIa was not observed in the floating fractions.

Annexin XIIIa is differently implicated in the exocytic pathways of MDCKII cells

We previously reported that, in polarized MDCKII cells, a recombinant myristoylated annexin XIIIb could stimulate the apical delivery of exocytic carriers while the basolateral route was not affected (Lafont et al., 1998b). Here, we followed the transport of viral proteins targeted to either plasma membrane in the same functional assay as was used previously. This assay reconstitutes the trans-Golgi network (TGN)-to-apical or -to-basolateral surface transport steps in Streptolysin-O permeabilized MDCKII cells (Lafont et al., 1995). We found that the purified recombinant myristoylated annexin XIIIa (Fig. 9A), when introduced to permeabilized cells, was localized in both compartments (Fig. 9B) and could stimulate the apical delivery of transport carriers (Fig. 10C). On the contrary, basolateral transport was inhibited (Fig. 9C).

DISCUSSION

In this study, we show that both annexin XIII isoforms bind to membranes independently of calcium. Based on the cytosolic localization of the non-myristoylated mutants, we propose that the N-terminal myristoyl modification present in both isoforms

is necessary for the interaction with the lipid bilayer in the absence of calcium. Calcium-independent membrane binding has also been reported for other annexins. Annexin I interacts with the plasma membrane and with multivesicular bodies of NIH3T3 cells (Futter et al., 1993), annexins VI and II with clathrin coated pits (Turpin et al., 1998), annexin II with the plasma membrane of A549 cells (Liu et al., 1997) and with early endosomes in BHK cells (Jost et al., 1997). In the latter case, the domain important for calcium-independent binding to membrane has been mapped to amino acids 14-25 of the N-terminal tail of annexin II (Jost et al., 1997). A comparison of the known structures of annexins indicates that the N-terminal tail of annexin XIII should protrude out of the core domain on the face opposite to the calcium binding sites (Liemann and Lewit-Bentley, 1995). Our experiments suggest that the myristoyl group at the N terminus is inserted in the lipid bilayer. Thus, due to the shortness of the tail of annexin XIIIa (12 amino acids), the calcium binding sites of the annexin XIIIa core domain might be prevented from facing the membrane, and instead, be exposed towards the cytosol. This opens new perspectives for the function of the annexin core, which could interact in a calcium-dependent manner with proteins in addition to its lipid binding potential. Such a possibility is strengthened by the structural data obtained for the hexameric annexin XII, in which the calcium-binding sites were mediating face-to-face binding of one trimer to another (Luecke et al., 1995). A similar dual binding capacity has been

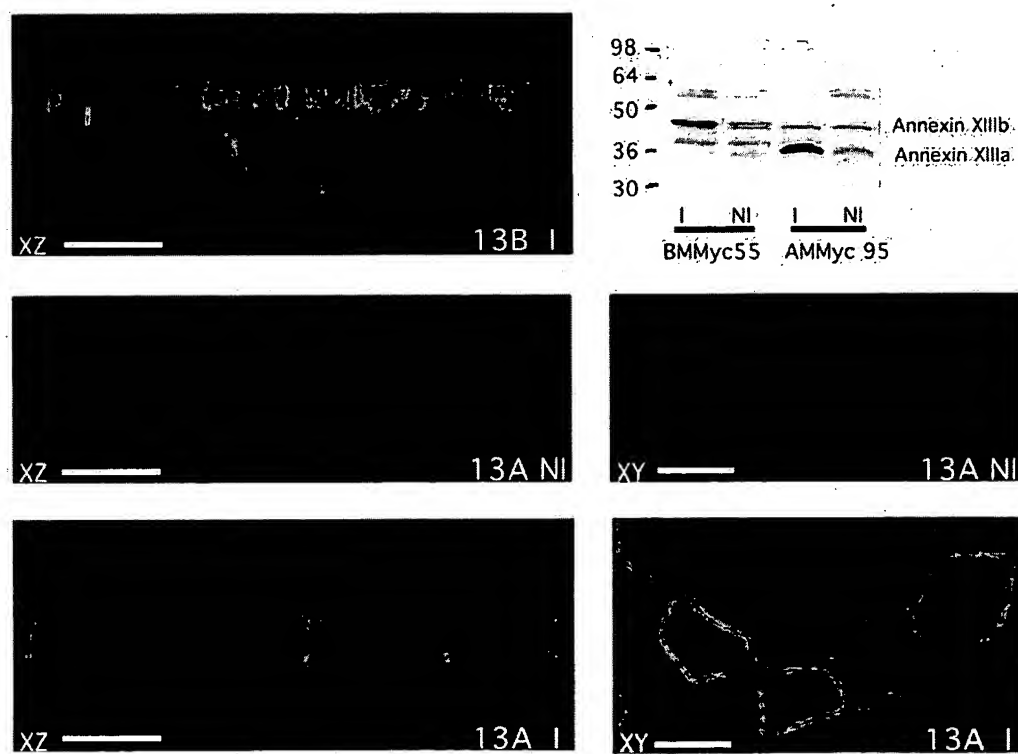


Fig. 7. Basolateral localization of annexin XIIIa in MDCKII Lac switchable cells. Stable clones of MDCKII Lac switchable cells overexpressing either annexin XIIIb (13B) or XIIIa (13A) in an inducible manner were analyzed by immunoblotting and by immunofluorescence confocal microscopy with anti-annexin XIII-II antibody. Confocal xz and xy sections are shown. I, Induced, NI, non-induced. Bar, 10 μ m. Note in the immunoblots (upper right panel) that the overexpressed annexin XIIIa are running slower than the endogenous proteins due to their fusion to the myc-tag. In addition, a band corresponding to the endogenous annexin II is slightly visible in the immunoblot of the BM55 clone and a band corresponding to the endogenous annexin XIIIb is visible in the immunoblot of the AM95 clone.

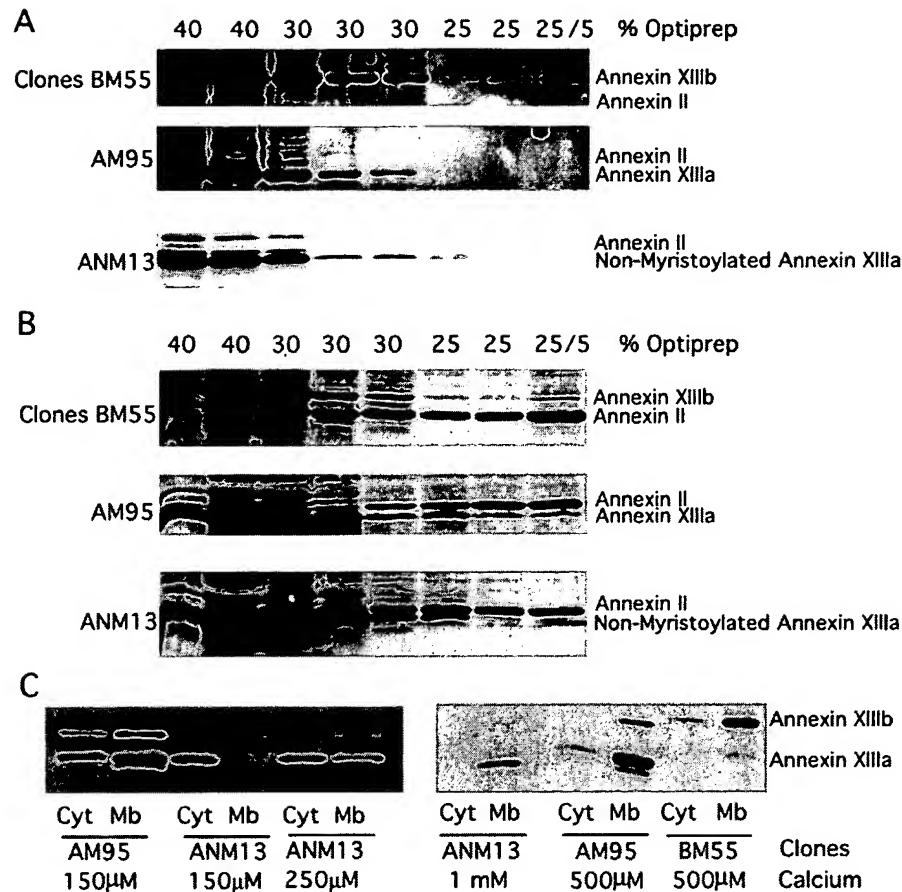


Fig. 8. Raft association of basolateral annexin XIIIa is dependent on calcium and the myristoyl group. Detergent-resistant membranes were prepared from the stable clones of MDCKII Lac switchable cells overexpressing either annexin XIIIb, annexin XIIIa or the non-myristoylated annexin XIIIa in the absence (A) or presence of 1 mM calcium (B). The different TCA-precipitated fractions collected after the OptiPrep™ gradient centrifugation were tested for their content of annexin XIIIa by western blot with the anti-annexin XIII-II antibody. Note that the endogenous annexins are visible in addition to the exogenous annexin XIIIa; in particular, the annexin II staining becomes extremely strong once the sample is prepared in presence of calcium. (C) PNS of MDCKII Lac switchable clones were prepared in presence of increasing amount of calcium. The membrane (Mb) and cytosolic (Cyt) pools were segregated by a 100,000 *g* spin and analyzed for their content of annexin XIIIa, myristoylated or not, by western blotting with anti-annexin XIII-II antibody. The non-myristoylated annexin XIIIa is entirely recovered in the membrane fraction at 1 mM calcium, while at 150 μ M calcium it is still mostly cytosolic. The myristoylated annexin XIIIa are almost completely bound to the membrane fraction at 500 μ M calcium. Note that the endogenous annexin XIIIa (lower band in clone AM95) and XIIIb (upper band in all the clones) are visible in the immunoblot.

demonstrated for the C2 domain (also called CaLB), another calcium-dependent phospholipid binding domain (Davis et al., 1998). For example, the C2A domain of synaptotagmin interacts in a calcium-dependent manner with phospholipids but can also bind to syntaxin or dimerize with itself (Popoli et al., 1997). Interestingly, the C2 domain of p120ras GAP interacts with annexin VI in a calcium-dependent manner (Davis et al., 1996).

With the exception of annexin II and annexin XIIIb, the association of annexins with lipid rafts has not been studied. Here we show by flotation after Triton X-100 solubilization that the apical annexin XIIIa is raft-associated in the absence of calcium while the basolateral annexin XIIIa only associates with rafts in the presence of calcium. Lipid rafts are present both apically and basolaterally but are enriched apically (Simons and van Meer, 1988; Benting et al., 1999). Annexin II and the integral membrane protein CD44 were shown to

partition into rafts at the basolateral plasma membrane of mammary gland epithelial (Oliferenko et al., 1999). This interaction of annexin II with the basolateral rafts was shown to require calcium. How annexin II binds to lipid rafts is not known. In the case of annexin XIIIa, this binding involves the myristoylated N-terminal tail, since in presence of calcium, the non-myristoylated annexin XIIIa was able to bind membranes but not to lipid rafts as assayed by detergent insolubility. The composition of the inner leaflet of rafts is not yet defined. The differential localization of different annexins is difficult to explain without assuming the existence of protein partners for annexin XIIIa. Identifying these putative linkers would help to understand their functions.

We have previously demonstrated that annexin XIIIb is involved functionally in apical transport from the TGN (Lafont et al., 1998b). The data suggested that annexin XIIIb could play a role both during formation of the apical transport containers

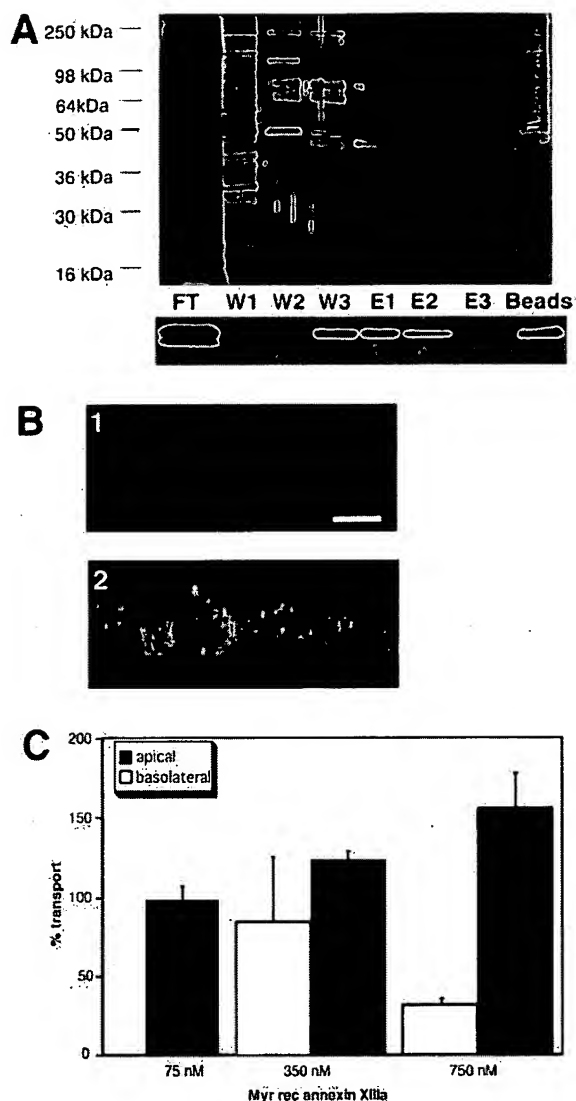


Fig. 9. Annexin XIIIa is differently involved in the exocytic routes in MDCK cells. (A) Upper panel, silver staining of the purified recombinant myristoylated annexin XIIIa expressed in Schneider cells. Lower panel, western blotting using the anti-annexin XIII-II antibody. Samples analyzed are Ni-column flowthrough (FT); imidazole washes 10 mM (W1), 20 mM (W2); 40 mM (W3); elutions 120 mM imidazole (E1-3); Ni beads (B). (B) Immunostaining of recombinant annexin XIIIa (green) in Streptolysin-O permeabilized MDCK cells. Affinity-purified anti-annexin XIII-II was used at 1:200 dilution and nuclei were visualized after DNA staining with propidium iodide. A confocal xz section is shown; bar, 15 μ m. Note that the protein is present in both compartments. (C) Transport assay performed in permeabilized MDCKII cells with the hemagglutinin of influenza virus as an apical reporter and the glycoprotein of vesicular stomatitis virus as a basolateral reporter. Values of duplicate samples from three independent experiments are shown as % transport (mean \pm s.e.m.).

in the TGN and at the docking and the fusion stage of delivery. These results conform with the localization of annexin XIIIb, which has been visualized along the apical pathway from the TGN to the apical membrane. Annexin XIIIa, on the other

hand, was only localized basolaterally in the MDCKII Lac switchable cells, and both apically and basolaterally in the MDCKII cells. Thus the unique 41-amino-acid insertion in the N-terminal tail of annexin XIIIb is likely to contain an apical localization determinant. We attempted to analyze the function of annexin XIIIa using the SLO-permeabilized cell system to investigate its role in apical or in basolateral transport from the TGN. Recombinant myristoylated annexin XIIIa, when added to the permeabilized MDCK cells, was able to enhance apical delivery of influenza virus hemagglutinin as efficiently as annexin XIIIb did. However, contrary to annexin XIIIb, the recombinant annexin XIIIa had an inhibitory effect on the basolateral delivery of VSV-G; recombinant annexin XIIIb had no effect. Thus annexins XIIIb and XIIIa behave identically in the apical compartment. This is perhaps not surprising because apical annexins XIIIb and XIIIa are so similar in their properties. The exact function of annexin XIII in the apical compartment is not yet defined. The protein could help to cluster lipid rafts and associated proteins into apical transport containers, or alternatively could be involved in organizing the docking and fusion stage of the apical delivery. It cannot, however, be excluded that the protein plays its main role in regulating raft-mediated processes at the apical surface. The role of basolateral annexin XIIIa is even more difficult to pinpoint. Does the finding that annexin XIIIa is only basolaterally localized in the MDCK II Lac switchable cell strain suggest that its function is mainly there and that the apical localization in MDCKII cells is due to overexpression? Or do MDCKII Lac switchable cells lack a protein that localizes annexin XIIIa to the apical compartment? In this respect, the random redistribution of the myristoylated apical type II cGMP-dependent protein kinase occurring in the Microvillus Inclusion Disease, presumably because of a sorting deficiency, is of particular interest (Ameen and Salas, 2000). The inhibitory effect on basolateral transport in the SLO-permeabilized MDCKII cells may reflect binding to lipid rafts being transported basolaterally (Benting et al., 1999), and due to steric hindrance this binding inhibits the assembly of the basolateral transport containers. The enigma of the functional roles of the annexins remains. The fact that two very similar isoforms of annexin XIII are so different in their properties is an interesting topic for further research.

Kim Ekroos and Sigrun Brendel are acknowledged for their expert technical assistance. We are extremely thankful to Jeremy Garwood and Ulla Lahtinen for their comments and advice on the manuscript. The TCS-NT confocal laser scan microscope was provided by Leica Lasertechnik (Heidelberg, Germany) as an active participant in the Advanced Light Microscopy Facility at EMBL. This work was supported by the Commission of European Communities and the grant SFB 352 (to K.S.).

REFERENCES

- Ahmed, S. N., Brown, D. A. and London, E. (1997). On the origin of sphingolipid/cholesterol-rich detergent-insoluble cell membranes: Physiological concentrations of cholesterol and sphingolipid induce formation of a detergent-insoluble, liquid-ordered lipid phase in model. *Biochemistry* 36, 10944-10953.
- Ameen, N. A. and Salas, P. J. I. (2000). Microvillus inclusion disease: A genetic defect affecting apical membrane protein traffic in intestinal epithelium. *Traffic* 1, 76-83.

- Arispe, N., Rojas, E., Genge, B. R., Wu, L. N. and Wuthier, R. E. (1996). Similarity in calcium channel activity of annexin V and matrix vesicles in planar lipid bilayers. *Biophys. J.* 71, 1764-1775.
- Balcarova-Ständer, J., Pfeiffer, S.E., Fuller, S.D. and Simons, K. (1984). Development of cell surface polarity in the epithelial Madin-Darby canine kidney (MDCK) cell line. *EMBO J.* 3, 2687-2694.
- Barwise, J. L. and Walker, J. H. (1996). Annexins II, IV, V and VI relocate in response to rises in intracellular calcium in human foreskin fibroblasts. *J. Cell Sci.* 109, 247-255.
- Benting, J. H., Rietveld, A. G. and Simons, K. (1999). N-glycans mediate the apical sorting of a GPI-anchored raft-associated protein in Madin-Darby canine kidney cells. *J. Cell Biol.* 146, 313-320.
- Bitto, E. and Cho, W. (1998). Roles of individual domains of annexin I in its vesicle binding and vesicle aggregation: a comprehensive mutagenesis study. *Biochemistry* 37, 10231-10237.
- Brown, D. A. and London, E. (1997). Structure of detergent-resistant membrane domains: does phase separation occur in biological membranes? *Biochem. Biophys. Res. Commun.* 240, 1-7.
- Brown, D. A. and London, E. (1998). Functions of lipid rafts in biological membranes. *Annu. Rev. Cell. Dev. Biol.* 14, 111-136.
- Brown, R. E. (1998). Sphingolipid organization in biomembranes: what physical studies of model membranes reveal. *J. Cell Sci.* 111, 1-9.
- Burgoyne, R. D. and Clague, M. J. (1994). Annexins in the endocytic pathway. *Trends Biochem. Sci.* 19, 231-232.
- Campos, G. R., Kanemitsu, M. and Boynton, A. L. (1990). Epidermal growth factor induces the accumulation of calpactin II on the cell surface during membrane ruffling. *Cell Motil. Cytoskel.* 15, 34-40.
- Carroll, A. D., Moyen, C., Kesteren, P. V., Tooke, F., Battley, N. H. and Brownlee, C. (1998). Calcium, Annexins, and GTP modulate exocytosis from maize root cap protoplasts. *Plant Cell* 10, 1267-1276.
- Chasserot, G. S., Vitale, N., Sagot, I., Delouche, B., Dirrig, S., Pradel, L. A., Henry, J. P., Aunis, D. and Bader, M. F. (1996). Annexin II in exocytosis: catecholamine secretion requires the translocation of p36 to the subplasmalemmal region in chromaffin cells. *J. Cell Biol.* 133, 1217-1236.
- Chen, J. M., Sheldon, A. and Pincus, M. R. (1993). Structure-function correlations of calcium binding and calcium channel activities based on 3-dimensional models of human annexins I, II, III, V and VII. *J. Biomol. Struct. Dyn.* 10, 1067-1089.
- Cheong, K. H., Zacchetti, D., Schneeberger, E. E. and Simons, K. (1999). VIP17/MAL, a lipid raft-associated protein, is involved in apical transport in MDCK cells. *Proc. Natl. Acad. Sci. USA* 96, 6241-6248.
- Creutz, C. E. (1992). The annexins and exocytosis. *Science* 258, 924-931.
- Davis, A. J., Butt, J. T., Walker, J. H., Moss, S. E. and Gawler, D. J. (1996). The calcium-dependent lipid binding domain of P120GAP mediates protein-protein interaction with calcium-dependent membrane binding proteins. Evidence for a direct interaction between annexin VI and P120GAP. *J. Biol. Chem.* 271, 24333-24336.
- Davis, A. J., Chow, A. H. and Gawler, D. J. (1998). Protein-protein and protein-lipid interactions of the CalB domain. *Biochem. Soc. Trans.* 26, S119.
- Demange, P., Voges, D., Benz, J., Liemann, S., Gottig, P., Berendes, R., Burger, A. and Huber, R. (1994). Annexin V: the key to understanding ion selectivity and voltage regulation? *Trends Biochem. Sci.* 19, 272-276.
- Doi, O., Doi, F., Schroeder, F., Alberts, A. W. and Vagelos, P. R. (1978). Manipulation of fatty acid composition of membrane phospholipid and its effects on cell growth in mouse LM cells. *Biochim. Biophys. Acta.* 509, 239-250.
- Donnelly, S. R. and Moss, S. E. (1997). Annexins in the secretory pathway. *Cell. Mol. Life Sci.* 53, 533-538.
- Emans, N., Gorvel, J. P., Walter, C., Gerke, V., Kellner, R., Griffiths, G. and Gruenberg, J. (1993). Annexin II is a major component of fusogenic endosomal vesicles. *J. Cell Biol.* 120, 1357-1369.
- Ernst, J. D. (1991). Annexin III translocates to the periphagosomal region when neutrophils ingest opsonized yeast. *J. Immunol.* 146, 3110-3114.
- Ernst, J. D., Hoyer, H., Blackwood, R. A. and Mock, T. L. (1991). Identification of a domain that mediates vesicle aggregation reveals functional diversity of annexin repeats. *J. Biol. Chem.* 266, 6670-6673.
- Fiedler, K., Kellner, R. and Simons, K. (1997). Mapping the protein composition of trans-Golgi network (TGN)-derived carrier vesicles from polarized MDCK cells. *Electrophoresis* 18, 2613-2619.
- Fiedler, K., Kobayashi, T., Kurzychalia, T. V. and Simons, K. (1993). Glycosphingolipid-enriched, detergent-insoluble complexes in protein sorting in epithelial cells. *Biochemistry* 32, 6365-6373.
- Fiedler, K., Lafont, F., Parton, R. G. and Simons, K. (1995). Annexin XIIIb: a novel epithelial specific annexin is implicated in vesicular traffic to the apical plasma membrane. *J. Cell Biol.* 128, 1043-1053.
- Futter, C. E., Felder, S., Schlessinger, J., Ullrich, A. and Hopkins, C. R. (1993). Annexin I is phosphorylated in the multivesicular body during the processing of the epidermal growth factor receptor. *J. Cell Biol.* 120, 77-83.
- Harder, T. and Gerke, V. (1993). The subcellular distribution of early endosomes is affected by the annexin IIp11(2) complex. *J. Cell Biol.* 123, 1119-1132.
- He, T. C., Zhou, S., da Costa, L. T., Yu, J., Kinzler, K. W. and Vogelstein, B. (1998). A simplified system for generating recombinant adenoviruses. *Proc. Natl. Acad. Sci.* 95, 3978-3983.
- Hofmann, A., Benz, J., Liemann, S. and Huber, R. (1997). Voltage dependent binding of annexin V, annexin VI and annexin VII-core to acidic phospholipid membranes. *Biochim. Biophys. Acta* 1330, 254-264.
- Jost, M., Zeuschner, D., Seeman, J., Weber, K. and Gerke, V. (1997). Identification and characterization of a novel type of annexin-membrane interaction: Ca²⁺ is not required for the association of annexin II with early endosomes. *J. Cell Sci.* 110, 221-228.
- Kaetzel, M. A., Chan, H. C., Dubinsky, W. P., Dedman, J. R. and Nelson, D. J. (1994). A role for annexin IV in epithelial cell function. Inhibition of calcium-activated chloride conductance. *J. Biol. Chem.* 269, 5297-5302.
- Kamal, A., Ying, Y. and Anderson, R. G. (1998). Annexin VI-mediated loss of spectrin during coated pit budding is coupled to delivery of LDL to lysosomes. *J. Cell Biol.* 142, 937-947.
- Keller, P. and Simons, K. (1998). Cholesterol is required for surface transport of influenza virus hemagglutinin. *J. Cell Biol.* 140, 1357-1367.
- König, J., Prenen, J., Nilius, B. and Gerke, V. (1998). The annexin II-p11 complex is involved in regulated exocytosis in bovine pulmonary artery endothelial cells. *J. Biol. Chem.* 273, 19679-19684.
- Lafont, F., Ikonen, E. and Simons, K. (1998a). Permeabilized epithelial cells to study exocytic membrane transport. In *Cell Biology; A laboratory handbook*, vol. 2 (ed. J. E. Celis) pp. 227-236. San Diego, California: Academic Press.
- Lafont, F., Lecat, S., Verkade, P. and Simons, K. (1998b). Annexin XIIIb associates with lipid microdomain to function in apical delivery. *J. Cell Biol.* 142, 1413-1427.
- Lafont, F., Simons, K. and Ikonen, E. (1995). Dissecting the molecular mechanisms of polarized membrane traffic: reconstitution of three transport steps in epithelial cells using Streptolysin-O permeabilization. *Cold Spring Harbor Symp. Quant. Biol.* LX, 753-762.
- Langen, R., Isas, J. M., Luecke, H., Haigler, H. T. and Hubbell, W. L. (1998). A transmembrane form of annexin XII detected by site-directed spin labeling. *Proc. Natl. Acad. Sci. USA* 95, 14060-14065.
- Lecat, S. and Lafont, F. (1999). Annexins and their interacting proteins in membrane traffic. *Protoplasma* 207, 133-140.
- Liemann, S., Benz, J., Burger, A., Voges, D., Hofmann, A., Huber, R. and Gottig, P. (1996). Structural and functional characterisation of the voltage sensor in the ion channel human annexin V. *J. Mol. Biol.* 258, 555-561.
- Liemann, S. and Huber, R. (1997). Three-dimensional structure of annexins. *Cell. Mol. Life Sci.* 53, 516-521.
- Liemann, S. and Lewit-Bentley, A. (1995). Annexins: a novel family of calcium- and membrane-binding proteins in search of a function. *Structure* 3, 233-237.
- Liu, L., Tao, J. Q. and Zimmerman, U. J. (1997). Annexin II binds to the membrane of A549 cells in a calcium-dependent and calcium-independent manner. *Cell Signal.* 9, 299-304.
- Luecke, H., Chang, B. T., Mailliard, W. S., Schlaepfer, D. D. and Haigler, H. T. (1995). Crystal structure of the annexin XII hexamer and implications for bilayer insertion. *Nature* 378, 512-515.
- Mahoney, E. M., Hamill, A. L., Scott, W. A. and Cohn, Z. A. (1977). Response of endocytosis to altered fatty acyl composition of macrophage phospholipids. *Proc. Natl. Acad. Sci. USA* 74, 4895-4899.
- McCarthy, K. M., Skare, I. B., Stankewich, M. C., Furuse, M., Tsukita, S., Rogers, R. A., Lynch, R. D. and Schneeberger, E. E. (1996). Occludin is a functional component of the tight junction. *J. Cell Sci.* 109, 2287-2298.
- Morgan, R. O. and Fernandez, M. P. (1997). Annexin gene structures and molecular evolutionary genetics. *Cell. Mol. Life Sci.* 53, 508-515.
- Nilius, B., Gerke, V., Prenen, J., Szucs, G., Heinke, S., Weber, K. and Droogmans, G. (1996). Annexin II modulates volume-activated chloride currents in vascular endothelial cells. *J. Biol. Chem.* 271, 30631-30636.
- Oliferenko, S., Pahi, K., Harder, T., Gerke, V., Schwarzer, C., Schwarz, H., Beug, H., Gunthert, U. and Huber, L. A. (1999). Analysis of CD44-

- containing lipid rafts: Recruitment of annexin II and stabilization by the actin cytoskeleton. *J. Cell Biol.* **146**, 843-854.
- Parkin, E. T., Turner, A. J. and Hooper, N. M. (1996). Isolation and characterization of two distinct low-density, triton-insoluble, complexes from porcine lung membranes. *Biochem. J.* **319**, 887-896.
- Pimplikar, S. W., Ikonen, E. and Simons, K. (1994). Basolateral protein transport in streptolysin O-permeabilized MDCK cells. *J. Cell. Biol.* **125**, 1025-1035.
- Popoli, M., Venegoni, A., Buffa, L. and Racagni, G. (1997). Calcium/phospholipid-binding and syntaxin-binding of native synaptotagmin I. *Life Sci.* **61**, 711-721.
- Rietveld, A. and Simons, K. (1998). The differential miscibility of lipids as the basis for the formation of functional membrane rafts. *Biochim. Biophys. Acta* **1376**, 467-479.
- Rosengarth, A., Wintergalen, A., Galla, H. J., Hinz, H. J. and Gerke, V. (1998). Calcium-independent interaction of annexin I with phospholipids monolayers. *FEBS Lett.* **438**, 279-284.
- Selbert, S., Fischer, P., Menke, A., Jockusch, H., Pongratz, D. and Noegel, A. A. (1996). Annexin VII relocalization as a result of dystrophin deficiency. *Exp. Cell Res.* **222**, 199-208.
- Selbert, S., Fischer, P., Pongratz, D., Stewart, M. and Noegel, A. A. (1995). Expression and localization of annexin VII (synexin) in muscle cells. *J. Cell Sci.* **108**, 85-95.
- Simons, K. and Ikonen, E. (1997). Functional rafts in cell membranes. *Nature* **387**, 569-572.
- Simons, K. and van Meer, G. (1988). Lipid sorting in epithelial cells. *Biochemistry* **27**, 6197-6202.
- Song, J. and Dohlman, H. G. (1996). Partial constitutive activation of pheromone responses by a palmitoylation-site mutant of a G protein alpha subunit in yeast. *Biochemistry* **35**, 14806-14817.
- Thiele, C., Hanna, M. J., Fahrenholz, F. and Huttner, W. B. (2000). Cholesterol binds to synaptophysin and is required for biogenesis of synaptic vesicles. *Nature Cell Biol.* **2**, 42-49.
- Topinka, J. R. and Brecht, D. S. (1998). N-terminal palmitoylation of PSD-95 regulates association with cell membranes and interaction with K⁺ channel Kv1.4. *Neuron* **20**, 125-134.
- Trotter, P. J., Orchard, M. A. and Walker, J. H. (1994). Thrombin stimulates the intracellular relocation of annexin V in human platelets. *Biochim. Biophys. Acta* **1222**, 135-140.
- Trotter, P. J., Orchard, M. A. and Walker, J. H. (1995). EGTA-resistant binding of annexin V to platelet membranes can be induced by physiological calcium concentrations. *Biochem. Soc. Trans.* **23**, 375.
- Turpin, E., Russo-Marie, F., Dubois, T., de Paillerets, C., Alfsen, A. and Bomsel, M. (1998). In adrenocortical tissue, annexins II and VI are attached to clathrin coated vesicles in a calcium-independent manner. *Biochim. Biophys. Acta* **1402**, 115-130.
- Wice, B. M. and Gordon, J. I. (1992). A strategy for isolation of cDNAs encoding proteins affecting human intestinal epithelial cell growth and differentiation: Characterization of a novel gut-specific N-myristoylated annexin. *J. Cell Biol.* **116**, 405-422.

In vivo detection and imaging of phosphatidylserine expression during programmed cell death

FRANCIS G. BLANKENBERG*†, PETER D. KATSIKIS‡, JONATHAN F. TAIT§, R. ERIC DAVIS¶, LOUIS NAUMOVSKILL, KATSUICHI OHTSUKI†, SUSAN KOPIWODA†, MICHAEL J. ABRAMS**, MARILYN DARKES**, ROBERT C. ROBBINS††, HOLDEN T. MAECKER‡‡, AND H.W. STRAUSS†

*Department of Radiology, †Department of Genetics, ‡Department of Pathology, §Department of Pediatrics (Hematology/Oncology), ¶Department of Cardiothoracic Surgery, ††Department of Medicine/Oncology, Stanford University School of Medicine, 300 Pasteur Drive, Stanford, CA 94305-5105; §Department of Laboratory Medicine, University of Washington, Health Sciences, Room NW-120, Box 357110, Seattle, WA 98195-7110; and **Anor MED Incorporated, 20353 64th Avenue, Suite #100, Langley, British Columbia, Canada 3A7R3

Communicated by Victor A. McKusick, Johns Hopkins University, Baltimore, MD, March 6, 1998 (Received for review January 27, 1998)

ABSTRACT One of the earliest events in programmed cell death is the externalization of phosphatidylserine, a membrane phospholipid normally restricted to the inner leaflet of the lipid bilayer. Annexin V, an endogenous human protein with a high affinity for membrane bound phosphatidylserine, can be used *in vitro* to detect apoptosis before other well described morphologic or nuclear changes associated with programmed cell death. We tested the ability of exogenously administered radiolabeled annexin V to concentrate at sites of apoptotic cell death *in vivo*. After derivatization with hydrazinonicotinamide, annexin V was radiolabeled with technetium 99m. *In vivo* localization of technetium 99m hydrazinonicotinamide-annexin V was tested in three models: fulminant hepatic apoptosis induced by anti-Fas antibody injection in BALB/c mice; acute rejection in ACI rats with transplanted heterotopic PVG cardiac allografts; and cyclophosphamide treatment of transplanted 38C13 murine B cell lymphomas. External radionuclide imaging showed a two- to sixfold increase in the uptake of radiolabeled annexin V at sites of apoptosis in all three models. Immunohistochemical staining of cardiac allografts for exogenously administered annexin V revealed intense staining of numerous myocytes at the periphery of mononuclear infiltrates of which only a few demonstrated positive apoptotic nuclei by the terminal deoxynucleotidyltransferase-mediated UTP end labeling method. These results suggest that radiolabeled annexin V can be used *in vivo* as a noninvasive means to detect and serially image tissues and organs undergoing programmed cell death.

Programmed cell death (apoptosis) plays a crucial role in the pathogenesis of a number of disorders including AIDS and other viral illnesses, cerebral and myocardial ischemia, autoimmune and neurodegenerative diseases, organ and bone marrow transplant rejection, and tumor response to chemotherapy and radiation (1–3). Since the original description of apoptosis by Wyllie in 1972, its assessment *in vivo* has required direct examination of biopsied or aspirated material (4). An imaging technique capable of localizing and quantifying apoptosis *in vivo* would permit assessment of disease progression or regression and similarly define the efficacy of therapy designed to inhibit or induce cell death (5–6).

Cells undergoing apoptosis redistribute phosphatidylserine (PS) from the inner leaflet of the plasma membrane lipid bilayer to the outer leaflet (7, 8). The externalization of PS is a general feature of apoptosis occurring before membrane bleb formation and DNA degradation (7, 8). Annexin V, a human

protein with a molecular weight of 36,000 has a high affinity for cell or platelet membranes with exposed PS *in vitro* and *in vivo* (9–13). This observation has led to testing radiolabeled annexin V in animal models of acute thrombosis and imaging of atrial thrombi in patients with atrial fibrillation (14, 15). In the current study, annexin V was derivatized with hydrazinonicotinamide (HYNIC) and coupled to technetium 99m (^{99m}Tc) (16) before i.v. administration in animal models of apoptosis. HYNIC, an nicotinic acid analog, is a bifunctional molecule capable of bonding to lysine residues of proteins on one moiety and conjugates of ^{99m}Tc on the other. The agent forms stable complexes with proteins (16) without affecting bioactivity. We performed scintigraphic imaging studies with derivatized annexin V to determine its ability *in vivo* to detect sites of apoptotic cell death occurring in Fas-mediated hepatocyte apoptosis, acute cardiac allograft rejection, and cyclophosphamide treatment of B cell lymphoma. Such *in vivo* imaging may prove useful in the clinical setting for noninvasive diagnosis, monitoring of disease progression or regression, and determining efficacy of treatment.

MATERIALS AND METHODS

Preparation of ^{99m}Tc HYNIC-Annexin V. Human annexin V was produced by expression in *Escherichia coli* as described (13, 17, 18); this material retains PS-binding activity equivalent to that of native annexin V (18). Concentrations were determined using $E_{280} = 0.6 \text{ ml/mg}^{-1} \text{ cm}^{-1}$ and molecular weight was taken as 35, 806. HYNIC-derivatized annexin V was produced by the gentle mixing of 5.6 mg/ml of annexin V in 20 mM Hepes, pH 7.4, and 100 mM NaCl for 3 hr shielded from light with succinimidyl 6-HYNIC (Anor Med, Langley, British Columbia) [222 μg in 18.5 μl (42 mM solution) of *N,N*-dimethyl formamide] at room temperature. The reaction was quenched with 500 μl of 500 mM glycine in PBS, pH 7.4, and then dialyzed at 4°C against 20 mM sodium citrate, pH 5.2, and 100 mM NaCl overnight. Precipitate was then removed by centrifugation at $15,000 \times g$ for 10 min. Then, 100 μl (100 μg) aliquots of HYNIC-annexin V were stored at -70°C . Incorporation of HYNIC into annexin V was found to be 0.9 mol/mol of annexin V by using the methods of King *et al.* (19). Membrane-binding activity of HYNIC-annexin V and decayed ^{99m}Tc HYNIC-annexin V was determined by a modified competition assay in which 5 nmol/liter fluorescein isothiocyanate (FITC)-annexin V was substituted for ¹²⁵I-annexin V (12, 17). After incubation for 15 min at room temperature, cells

The publication costs of this article were defrayed in part by page charge payment. This article must therefore be hereby marked "advertisement" in accordance with 18 U.S.C. §1734 solely to indicate this fact.

© 1998 by The National Academy of Sciences 0027-8424/98/956349-6\$2.00/0 PNAS is available online at <http://www.pnas.org>.

Abbreviations: TUNEL, terminal deoxynucleotidyltransferase-mediated UTP end labeling; PS, phosphatidylserine; HYNIC, hydrazinonicotinamide; ^{99m}Tc, technetium 99m; FITC, fluorescein isothiocyanate; HSA, human serum albumin; ROI, region of interest.

*To whom reprint requests should be addressed. e-mail: MA.FRB@Forsythe.Stanford.Edu.

were centrifuged, the FITC-annexin V bound to the pelleted cells was released with EDTA, and the released FITC-annexin V was measured by fluorometry. In this assay system, unmodified annexin V, HYNIC-annexin V, and decayed ^{99m}Tc HYNIC-annexin V inhibited 50% of the binding of FITC-annexin V at concentrations of 8 nmol/liter, 10.5 nmol/liter, and 12.3 nmol/liter, respectively.

To bind ^{99m}Tc to the HYNIC-annexin conjugate 80 μl of stannous chloride (50 mg/ml in 0.1 M HCl purged for 2 hr with N_2 gas) was first added to 50 ml of a 20 mM tricine solution (pH 7.1, purged for 1 hr with N_2 gas; tricine = *N*-[tris(hydroxymethyl)methyl]glycine). Two hundred microliters of the Sn-tricine solution was then added to 100 μl of ^{99m}Tc O_4 (4–20 mCi (1 Ci = 37 GBq) activity in 0.9% NaCl) previously mixed with a 100 μl (100 μg) aliquot of HYNIC-annexin V according to the methods described by Abrams *et al.* (20). Specific activity was 10–200 $\mu\text{Ci}/\mu\text{g}$ protein (depending on desired activity) with a radiopurity of 92–97% determined with instant thin layer chromatography using 0.9% saline solution as a solvent.

Scintillation Well Counting. Samples were counted in a Packard Cobra II gamma counter (Packard). The energy window was set at a lower level of 120 keV and an upper level of 170 keV for ^{99m}Tc . When ^{125}I was counted, samples were allowed to decay for at least 24 hr. The samples were then recounted using both the technetium window and an ^{125}I setting with a lower level of 20 keV and an upper level of 50 keV. Samples were corrected for any residual cross talk.

Radionuclide Imaging. A Technicare 420 mobile camera (Technicare, Solon, OH) equipped with a low energy high resolution parallel hole collimator was used to record the radionuclide distribution in mice and rats sedated with a mixture of 80 mg/kg ketamine and 4 mg/kg acepromazine injected i.m. Data were recorded by using a 20% window centered on the 140 keV photopeak of technetium into a 128 \times 128 matrix of a dedicated computer system for digital display and analysis (ICON, Siemens, Hoffman Estates, IL). All images were recorded for a preset time of 10–15 min.

Murine Model of Fas-Mediated Apoptosis. Massive hepatic apoptosis can be induced within 1–2 hr in mice following i.v. injection of anti-Fas antibody (21). We used this well described model of *in vivo* programmed cell death to test the specific localization of ^{99m}Tc HYNIC-annexin to an organ undergoing apoptosis *in vivo*. Four- to five-wk-old BALB/c mice were injected i.v. with purified hamster anti-Fas mAb (Jo2, 10 $\mu\text{g}/\text{animal}$, PharMingen, San Diego, CA) using the model proposed by Ogasawara *et al.* (21). Mice were then injected i.v. with 25–50 $\mu\text{g}/\text{kg}$ of ^{99m}Tc HYNIC-annexin V (10–25 $\mu\text{Ci}/\text{animal}$ for biodistribution study and 100–150 $\mu\text{Ci}/\text{animal}$ for imaging studies) 1 or 2 hr after antibody treatment. Animals were killed 1 hr after administration of radiopharmaceutical followed by organ removal for scintillation counting of radioactivity and for histologic and immunohistochemical analyses.

Control studies with ^{99m}Tc labeled human serum albumin (HSA) also were performed in untreated and anti-Fas treated mice. Although other proteins were considered as controls, albumin was selected because distinguishing the potential vascular disruption and protein leakage associated with acute apoptosis was a major goal of this control experiment. The animals were injected with 100–150 μCi of ^{99m}Tc labeled HSA (25 mg/animal) and imaged at 1 and 2 hr, in similar fashion to the mice receiving ^{99m}Tc HYNIC-annexin.

Rodent Model of Cardiac Transplantation. Adult male ACI rats (250–350 g) received heterotopic cardiac allografts from PVG donors (obtained from Harlan-Sprague-Dawley) anastomosed to the hosts' abdominal aorta and inferior vena cava according to a modification of the technique of Ono and Lindsey (22). Syngeneic cardiac isografts from ACI donors also were transplanted to the abdomens of host ACI rats. PVG cardiac allografts in ACI recipients using the model above begin to undergo rejection between 4 and 5 days post-

transplantation as assessed by decreased pulsation to palpation. Five days after transplantation all of the animals received 700–900 μCi of ^{99m}Tc HYNIC-annexin V (10–20 μg protein/kg) via tail vein and were imaged 1 hr later. Animals were then killed, and native and transplanted hearts underwent scintillation counting and histopathologic studies.

Murine Model of Lymphoma. 38C13 murine B cell lymphomas (23) were grown in C3H/HeN mice (Harlan Breeders, Indianapolis) following s.c. injection of 400 tumor cells suspended in 200 μl of RPMI medium 1640 (without serum) into the left flank. Fourteen days after implantation mice underwent treatment with 100 mg/kg of cyclophosphamide injected i.p. Mice were injected i.v. with 25–50 $\mu\text{g}/\text{kg}$ of ^{99m}Tc HYNIC-annexin V (100–150 $\mu\text{Ci}/\text{animal}$) 20 hr after cyclophosphamide administration. Animals were then imaged and killed 1 hr after injection of radiopharmaceutical after tumor removal for scintillation counting and histopathologic studies.

Immunostaining for Bound Human Annexin V and Apoptotic Nuclei. Formalin-fixed paraffin-embedded tissues were sectioned at 5 μm for staining with hematoxylin/eosin or other techniques. Immunostaining for bound human annexin V was performed with a rabbit anti-serum raised against human placental annexin V and affinity purified with recombinant annexin V coupled to Affi-Gel (Bio-Rad). Immunohistochemical detection then was completed by sequential incubations with biotin-labeled goat anti-rabbit antibody and avidin-horseradish peroxidase complex (Jackson Immuno Research), followed by reaction with 3,3'-diaminobenzidine as described by Bindl and Warnke (24).

For the detection of apoptotic nuclei, sections were stained using a modification of the terminal deoxynucleotidyltransferase-mediated UTP end labeling (TUNEL) method described by Gavrieli *et al.* (25). After inhibition of endogenous peroxidase, deparaffinized sections were digested with proteinase K (20 $\mu\text{g}/\text{ml}$) for 15 min at room temperature. Sections were then incubated with λ exonuclease (Life Technologies, Gaithersburg, MD) at 5 unit/ml for 30 min at 37°C followed by equilibration with terminal deoxynucleotidyltransferase reaction buffer (0.2 M potassium cacodylate, 25 mM Tris-HCl, 0.25 mg/ml BSA, 1.5 mM CaCl_2 , 20 mg/ml polyvinylpyrrolidone, and 20 mg/ml Ficoll) and 5 μM dATP. The end-labeling reaction then was performed in terminal deoxynucleotidyltransferase reaction buffer also containing a final concentration of 75 unit/ml of terminal deoxynucleotidyltransferase and 100 μM of 1,N-6-ethenol-dATP (Sigma). After a 60-min incubation at 37°C, the reaction was quenched via rinsing with 1 \times SSC (standard saline citrate). Sections were then incubated with murine 1G4 mAb (gift from Regina Santella, Columbia University), which recognizes the ethenoadenine moiety (26). Subsequent immuno-histochemical detection was as described above, using a biotin-labeled goat anti-mouse antibody.

RESULTS

Biodistribution of Radiolabeled Annexin V in Fulminant Hepatic Apoptosis. There was a 134% and 304% increase in the hepatic uptake of ^{99m}Tc HYNIC-annexin V above controls at 1 and 2 hr after anti-Fas antibody injection, respectively, as determined by biodistribution studies (Table 1). Hepatic uptake was inversely proportional to renal uptake in treated mice with a 75% decrease in renal activity 2 hr after treatment. Of note, there was <5% excretion of administered radiopharmaceutical into the urine in control or treated animals. Splenic uptake was 108% and 54% above control values in the 1- and 2-hr treatment groups, respectively.

Subgroups of mice were co-injected with ^{125}I -HSA to control for nonspecific uptake of inert protein from the circulation caused by hepatic endothelial cell breakdown (27). Hepatic uptake was 120% above control values at 1 hr after anti-Fas antibody injection and remained unchanged in contrast to the

Table 1. Biodistribution study of radiolabeled annexin V after anti-Fas antibody treatment

A)	^{99m} Tc	Controls	1-hr anti-Fas	2-hr anti-Fas
	% ID	(n = 9)	(n = 15)	(n = 12)
	Liver	12.2 ± 1.4	28.6 ± 9.4**	49.3 ± 12.7***
	Kidneys	55.9 ± 8.9	35.2 ± 14.4**	14.0 ± 10.0***
	Spleen	1.6 ± 0.25	3.34 ± 1.42*	2.46 ± 1.22(ns)
B)	¹²⁵ I	Controls	1-hr anti-Fas	2-hr anti-Fas
	% ID	(n = 4)	(n = 6)	(n = 5)
	Liver	3.98 ± 1.09	8.77 ± 3.53*	8.4 ± 1.92*
	Kidneys	1.37 ± 0.35	1.88 ± 0.37(ns)	1.82 ± 0.38(ns)
	Spleen	0.39 ± 0.09	0.47 ± 0.15(ns)	0.37 ± 0.041(ns)
C)	Weight	Controls	1-hr anti-Fas	2-hr anti-Fas
	(grams)	(n = 9)	(n = 15)	(n = 12)
	Liver	1.06 ± 0.097	1.29 ± 0.32(ns)	1.37 ± 0.22*
	Kidneys	0.31 ± 0.061	0.32 ± 0.079(ns)	0.37 ± 0.072(ns)
	Spleen	0.12 ± 0.022	0.12 ± 0.02(ns)	0.11 ± 0.014(ns)

% injected dose (ID) per organ corrected for background, decay, and tail infiltration are listed for mice injected with 100–150 μ Ci (radiopurity >95%, specific activity 150–200 μ Ci/ μ g protein) of ^{99m}Tc HYNIC-annexin co-injected with 0.6 μ Ci (25 mg) of ¹²⁵I radiolabeled HSA. A) Biodistribution of ^{99m}Tc HYNIC-annexin V, B) ¹²⁵I-HSA, and C) Organ weight. Data are expressed as mean \pm standard error of the mean. P-values are shown in parenthesis () for Dunnett's test for multiple comparison of means of the 1- or 2-hr post-treatment groups compared with control. ns, not significant (i.e., P-value > 0.05); *, P < 0.05; **, P < 0.001; ***, P < 0.0001.

progressive rise in annexin V uptake. There was a 29% increase in liver weight at 2 hr. Renal and splenic weight and uptake of ¹²⁵I-HSA did not change significantly after treatment.

Sections of livers from mice treated with anti-Fas antibody showed a spectrum of nuclear changes characteristic of apoptosis (margination of chromatin, pyknosis, and karyorrhexis) as early as 1 hr after injection; changes were more pronounced and focally associated with hemorrhage (peliosis) 2 hr after treatment (Fig. 1A). Immunostaining for ^{99m}Tc HYNIC-annexin V was observed at the cytoplasmic border of apoptotic hepatocytes; although this result was focal, the localization pattern is consistent with PS externalization, and staining never was observed in normal hepatocytes (Fig. 1B) or in anti-Fas antibody-treated mice not injected with ^{99m}Tc HYNIC-annexin V (data not shown).

In Vivo Imaging of Fas-Mediated Fulminant Hepatic Apoptosis. A high concentration of radiolabeled annexin V activity was observed by scintillation camera imaging in the kidneys of control animals with minimal concentration in other organs (Fig. 2). Hepatic uptake in control mice [12% of injected dose (% ID)] did not permit clear delineation of the liver. In mice treated with anti-Fas antibody, there was a diffuse increase in the intensity of hepatic uptake of ^{99m}Tc HYNIC-annexin V observed at 1 hr, which continued to rise at 2 hr after treatment. The transient increase in splenic uptake and the fall in renal activity found in the biodistribution studies both were visualized readily with external imaging following anti-Fas treatment. A total of 19 mice (six control, seven 1-hr, and six 2-hr anti-Fas-treated animals) underwent biodistribution study after imaging with ^{99m}Tc HYNIC-annexin V. The percentage of whole body activity per organ determined by region of interest (ROI) image analysis correlated well with the percentage of injected dose per organ determined by biodistribution (linear correlation coefficients for the liver, kidney, and spleen of $r^2 = 0.853, 0.860,$ and 0.979 , respectively.)

There was no perceptible difference in liver, renal, or splenic uptake on the ^{99m}Tc-HSA images between the treated mice and controls (images not shown). There also was a direct correlation of observed uptake of ^{99m}Tc-HSA as seen by ROI image analysis and the biodistribution of ^{99m}Tc-HSA (data not shown), which mirrored the biodistribution of ¹²⁵I-HSA.

In Vivo Imaging of Cardiac Allograft Rejection. All of the PVG cardiac allografts (n = 4) were visualized easily with ^{99m}Tc HYNIC-annexin V 5 days after transplantation (Fig. 3).

ACI syngeneic cardiac isografts (n = 3) had no visible activity after injection of ^{99m}Tc HYNIC-annexin with uptakes of

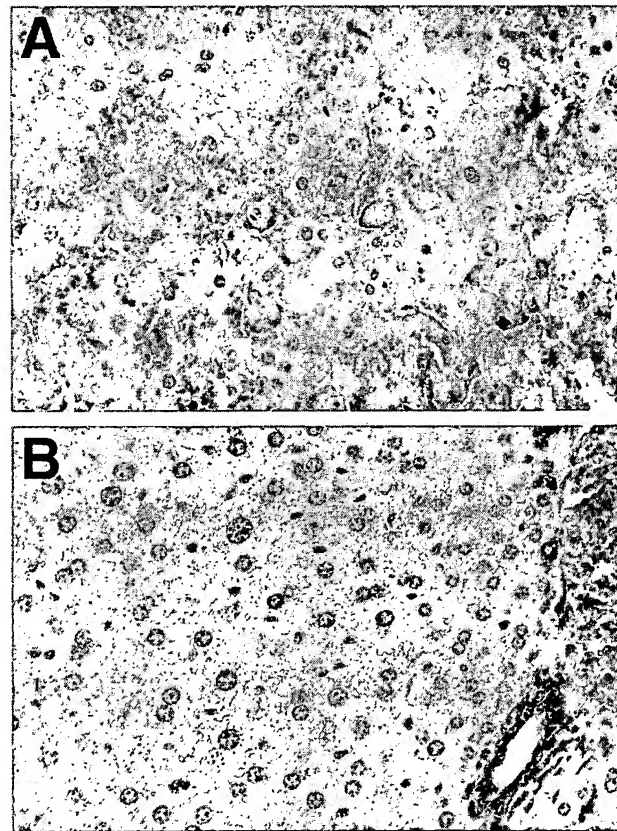


FIG. 1. Histologic sections of murine liver immunostained for exogenously administered human annexin V. (A) Two hours after anti-Fas antibody treatment there is extensive apoptotic nuclear change, slight cytoplasmic retraction, and interstitial hemorrhage. Annexin V staining (brown immunostaining product) is focally present at the cytoplasmic border of apoptotic hepatocytes. (B) No hepatocyte staining was observed in untreated mice. Staining of bile duct epithelium was caused by antibody cross-reactivity because it also was seen in the absence of exogenously administered human annexin V (data not shown). (Diaminobenzidine immunostain with hematoxylin counterstain, $\times 40$ objective magnification.)

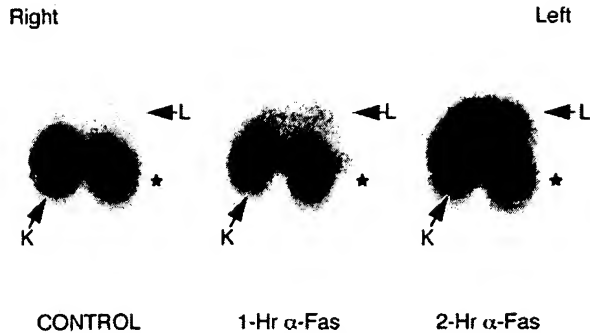


FIG. 2. Imaging Fas-mediated fulminant hepatic apoptosis with radiolabeled annexin V. One hour after injection of 150 μ Ci of radiopharmaceutical (50 μ g/kg of protein) mice were imaged in the prone anterior projection. There was a progressive increase in 99m Tc annexin V uptake of the liver of mice at 1 and 2 hr after anti-Fas antibody injection. Liver activity (L) was 111% and 239% above control values in the 1- and 2-hr mice, respectively, as shown by region of interest image analysis. Kidney activity (K) was 70% and 64% below control values in the 1- and 2-hr mice, respectively. Splenic activity (*) was 168% and 45% above control values in the 1- and 2-hr mice, respectively.

radiopharmaceutical identical to native cardiac activity as confirmed by scintillation well counting (data not shown). The percentage of whole body activity of PVG allografts was 213% above ACI isograft activity ($P < 0.005$; using a two-tailed student's t test) determined by ROI image analysis. Scintillation well-counting assay revealed a >11-fold increase in 99m Tc HYNIC-annexin V uptake in PVG allografts as compared with native heart activity.

Sections of PVG cardiac allografts 5 days after transplantation showed a marked mononuclear inflammatory cell infiltrate in all animals; no infiltrate was observed in syngeneic or native hearts. The infiltrate surrounded areas of myocardial injury and was associated with thrombosis of myocardial vessels. In the center of these areas, there was frank necrosis, with no staining by hematoxylin, but at the periphery, there were nuclei with changes of apoptosis as confirmed by TUNEL

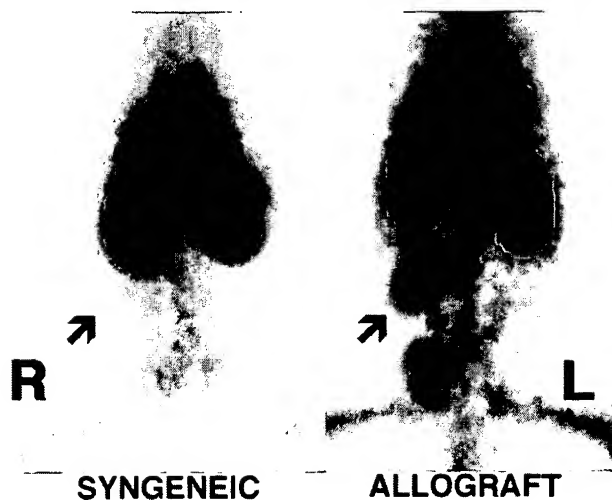


FIG. 3. Imaging cardiac allograft rejection with radiolabeled annexin V. Representative images of abdominal cardiac syngeneic ACI isograft and PVG allograft in ACI host rats 5 days after transplantation. Rats were imaged in the prone anterior projection 1 hr after injection with 900 μ Ci of 99m Tc-annexin V. Location of transplanted hearts are marked by arrows. Intense uptake of 99m Tc HYNIC-annexin V was observed in the cardiac allograft animal (Right) as compared with the lack of visualization of the syngeneic cardiac isograft (Left).

staining (Figs. 4A and B). Immunostaining for 99m Tc HYNIC-annexin V was observed in a granular pattern in cardiac myocytes at the junction of inflamed and necrotic areas; the nuclei of these cells were stained still by hematoxylin, further suggesting that they were apoptotic rather than necrotic (Fig. 5A). Anti-annexin V staining was far more extensive in terms of the number of positive myocytes and intensity compared with TUNEL. Anti-annexin staining was heavy and clumped in frankly necrotic areas as expected (Fig. 5A) but was specific; no staining was observed in syngeneic or native hearts or in staining of allografted hearts in which the primary antibody was omitted (Fig. 5B).

In Vivo Imaging of Treated Murine Lymphoma. Untreated flank tumor implants ($n = 8$) were seen easily by scintillation camera imaging (Fig. 6) and had an annexin V uptake 365% above normal soft tissue activity as shown by ROI image analysis. Treated flank tumors ($n = 6$) showed readily visualizable increases in 99m Tc HYNIC annexin V activity of 78% above control values expressed as whole body activity per gram of tumor ($P < 0.05$ using a two-tailed student's t test for significance). This result was confirmed by scintillation well counting in which treated tumors demonstrated a 132% increase in annexin V uptake expressed as percentage of injected dose per gram of tumor ($P < 0.05$) with a 58% fall in weight ($P < 0.05$) compared with the control. The whole body activity per gram of tumor as seen by ROI image analysis linearly correlated to percentage of injected dose per gram of tumor determined on biodistribution study ($r^2 = 0.831$). Histologic



FIG. 4. Staining for apoptotic nuclei in allografted rodent heart 5 days after transplantation. (A) TUNEL staining showing apoptotic nuclei and fragments in some myocytes bordering areas of necrosis (myocytes without visible nuclei in upper half of field). (B) TUNEL positive nuclei and fragments within inflammatory infiltrate (right half of field) and in some myocytes bordering regions of inflammation. (Diaminobenzidine immunostain with hematoxylin counterstain, $\times 40$ objective magnification.)

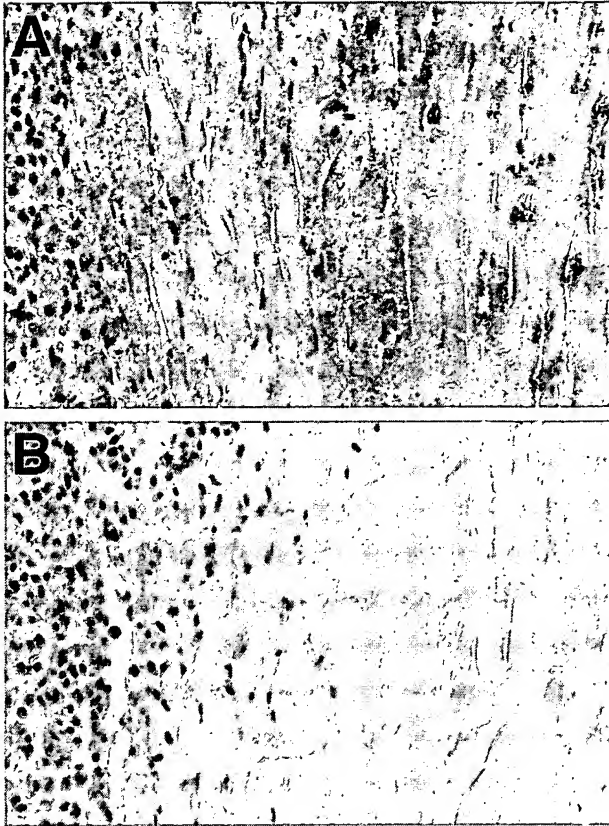


FIG. 5. Immunostaining for exogenously administered human annexin V in allografted rodent heart 5 days after transplantation. (A) Immunostaining with an antibody to human annexin V shows dense, granular staining of apoptotic myocytes at the periphery of the inflammatory infiltrate. Staining of necrotic myocytes (myocytes without visible nuclei) was clumped heavily and central. (B) Immunostaining of area similar to that shown in A omitting the primary antibody, shows no reaction product. (Diaminobenzidine immunostain with hematoxylin counterstain, $\times 40$ objective magnification.)

analysis demonstrated virtually complete ($>95\%$) apoptosis of all lymphoblasts in treated tumors with $<5\%$ apoptotic cells in controls (data not shown).

DISCUSSION

These experiments indicate that exposure of PS on the surface of cells undergoing apoptosis can be detected *in vivo* with radiolabeled annexin V in animal models including Fas-mediated fulminant hepatitis, cardiac allograft rejection, and tumor response to treatment. ^{99m}Tc HYNIC-labeled annexin V radionuclide imaging demonstrated clear and specific localization to regions of apoptotic cell death. As has been shown for annexin V reagents *in vitro*, annexin V radionuclide imaging can provide a tool which can directly assess for early stages of programmed cell death, before membrane vesicle formation and DNA degradation particularly as measured by the TUNEL method (7, 8). Imaging of tissues undergoing apoptosis could be helpful in monitoring the efficacy of therapy of diseases associated with abnormal induction or inhibition of programmed cell death. Apoptosis appears to play an important role in autoimmune and neurodegenerative diseases, cardiomyopathy, myocarditis, cerebral and myocardial ischemia, infectious diseases, cancer, viral induced hepatitis, and organ and bone marrow transplant rejection (1).

The numerous anti-annexin V positive-staining myocytes found in rejecting rodent heart transplants with nuclei which



FIG. 6. Imaging treated murine lymphoma with radiolabeled annexin V. CH3.1HeN mice 14 days after implantation of 38C13 murine B cell lymphoma s.c. into the left flank were treated with 100 mg/kg of cyclophosphamide injected i.p. Twenty hours after treatment mice were injected with 150 μCi of ^{99m}Tc HYNIC annexin V (50 $\mu\text{g}/\text{kg}$ of protein). One hour after administration of ^{99m}Tc HYNIC annexin V mice were imaged in the prone anterior projection. Treated tumor demonstrated uptakes of 363% and 454% above control seen by region of interest analysis and biodistribution assay, respectively. Control tumor weight = 1.29 grams, treated tumor weight = 0.82 grams. L, left; R, right.

were only occasionally TUNEL positive implies that radiolabeled annexin V imaging may be superior to standard histopathologic assessments of apoptosis. These data suggests a far greater role for programmed cell death in cardiac allograft rejection than previously reported (28–32). Anti-annexin V staining of apoptotic myocytes (with or without TUNEL stained nuclei) was diffusely granular in appearance in contrast to the peripheral pattern of apoptotic hepatocytes. This pattern of exogenous annexin V localization may relate to the unique cellular morphology of myocardial tissue; the extensive sarcoplasmic reticulum, which communicates with the extracellular space, also may be capable of externalizing PS during apoptosis.

The ability of annexin V to bind to necrotic cells *in vivo* and bind to PS located in the inner leaflet of the plasma membrane is confirmed by finding heavy and clumped anti-annexin V staining in frankly necrotic areas in cardiac allografts. As a result, annexin V localization *in vivo* does not appear to be entirely specific for apoptosis. In the clinical setting, however, the ability of radiolabeled annexin V to noninvasively image both apoptosis and necrosis may prove useful in reducing the need for routine surveillance through endomyocardial biopsy after cardiac transplantation, which currently is the only reliable clinical means to diagnose acute transplant rejection (33, 34). Furthermore, radiolabeled annexin V imaging of the entire myocardium may provide diagnostic information superior to endomyocardial biopsy, which necessarily can only sample a limited region within the right ventricle.

These studies also demonstrate that radiolabeled annexin V imaging can detect an increase in PS exposure associated with apoptosis of implanted murine flank lymphomas after cyclophosphamide treatment. Estimates of the degree of cell death

during the first week of induction therapy using bone marrow aspirates has been shown to provide prognostic information in childhood leukemia (35, 36). Other investigators have shown a direct relationship between the degree of apoptotic cell death and subsequent tumor growth delay in murine models of lymphoma (37, 38). To date, the only noninvasive imaging method shown to detect apoptosis *in vivo* has been lipid proton NMR spectroscopy (5, 6). Lipid proton NMR spectroscopy, however, has inherent problems with magnetic susceptibility outside the central nervous system and has relatively low sensitivity.

Kidneys in control animals have marked uptake of ^{99m}Tc HYNIC annexin V. The high renal concentration did not preclude the imaging of other major organs undergoing apoptosis. The cellular site of binding is uncertain, but preliminary autoradiographs suggest the renal distribution of annexin V is cortical. The specific mechanism of renal cortical binding is uncertain but may relate to the intrinsic lipid profile of the kidney, in which there is a significantly higher concentration of PS in the cortex as compared with the papillary regions (39).

The initial increase of ^{125}I -HSA hepatic uptake after anti-Fas treatment is most likely caused by an expanded extracellular fluid volume from the early breakdown of hepatic endothelial cells as described by Lacronique *et al.* (27) and is confirmed by an increased hepatic weight of these treated animals. The initial increase of ^{125}I -HSA hepatic uptake, which subsequently remained unchanged, is in marked contrast to the progressive rise of radiolabeled annexin V hepatic uptake, which was specific for increasing numbers of apoptotic hepatocytes.

In summary, this study demonstrates the utility of ^{99m}Tc -radiolabeled annexin V for *in vivo* imaging of PS expression associated with apoptosis. Serial noninvasive assessments of PS externalization with radiolabeled annexin V may provide a more sensitive and rapid means of monitoring disease progression, determining treatment efficacy, and diagnosing a number of human disorders than is currently possible in the clinical setting.

This work was supported in part by the Child Health Research Fund, Lucile Salter Packard Children's Hospital at Stanford, and by the National Institutes of Health Grant HL-47151. The authors also gratefully acknowledge Dr. Regina Santella for the gift of 1G4 antibody.

- Thompson, B. C. (1995) *Science* **267**, 1456–1462.
- Steller, H. (1995) *Science* **267**, 1445–1449.
- Darzynkiewicz, Z. (1995) *J. Cell. Biochem.* **58**, 151–159.
- Kerr, J. F., Wyllie, A. H. & Currie, A. R. (1972) *Brit. J. Cancer* **26**, 239–257.
- Blankenberg, F. G., Storrs, R. W., Naumovski, L., Goralski, T. & Spielman, D. (1996) *Blood* **87**, 1951–1956.
- Blankenberg, F. G., Katsikis, P. D., Storrs, R. W., Bealieu, C., Spielman, D., Chen, J. Y., Naumovski, L. & Tait, J. F. (1997) *Blood* **89**, 3778–3786.
- Martin, S. J., Reutelingsperger, C. P. M., McGahon, A. J., Rader, J. A., van Schie, R. C. A. A., La Face, D. M. & Green, D. R. (1995) *J. Exp. Med.* **182**, 1545–1556.
- Zwaal, R. F. A. & Schroit, A. (1997) *Blood* **89**, 1121–1132.
- Koopman, G., Reutelingsperger, C. P. M., Kuijten, G. A. M., Keehnen, R. M. J., Pals, S. T. & van Oers, M. H. J. (1994) *Blood* **84**, 1415–1420.
- Verhoven, B., Schlegel, R. A. & Williamson, P. (1995) *J. Exp. Med.* **182**, 1597–1601.
- van Heerde, W. L., de Groot, P. G. & Reutelingsperger, C. P. M. (1995) *Thromb. Haemostasis* **73**, 172–179.
- Tait, J. F. & Gibson, D. (1994) *J. Lab. Clin. Med.* **123**, 741–748.
- Wood, B. L., Gibson, D. F. & Tait, J. F. (1996) *Blood* **88**, 1873–1880.
- Tait, J. F., Cerqueira, M. D., Dewhurst, T. A., Fujikawa, K., Ritchie, J. L. & Stratton, J. R. (1994) *Thromb. Res.* **75**, 491–501.
- Stratton, J. R., Dewhurst, T. A., Kasina, S., Reno, J. M., Cerqueira, M. D., Baskin, D. G. & Tait, J. F. (1995) *Circulation* **92**, 3113–3121.
- Abrams, M. J., Juweid, M., tenKate, C. I., Schwartz, D. A., Hauser, M. M., Gaul, F. E., Fuccello, A. J., Rubin, R. H., Strauss, H. W. & Fischman, A. J. (1990) *J. Nucl. Med.* **31**, 2022–2028.
- Tait, J. F., Engelhardt, S., Smith, C. & Fujikawa, K. (1995) *J. Biol. Chem.* **270**, 21594–21599.
- Tait, J. F. & Smith, C. (1991) *Arch. Biochem. Biophys.* **288**, 141–144.
- King, T. P., Zhao, S. W. & Lam, T. (1986) *Biochemistry* **25**, 5774–5779.
- Larsen, S. K., Solomon, H. F., Caldwell, G. & Abrams, M. J. (1995) *Bioconjugate Chem.* **6**, 635–638.
- Ogasawara, J., Watanabe-Fukunaga, R., Adachi, M., Matsuzawa, A., Kasugai, T., Kitamura, Y., Itoh, N., Suda, T. & Nagata, S. (1993) *Nature (London)* **364**, 806–809.
- Woodley, S. L., Gurley, K. E., Hoffman, S. L., Nicolls, M. R., Hagberg, R., Clayberger, C., Holm, B., Wang, X., Hall, B. M. & Strober, S. (1993) *Transplantation* **56**, 1443–1447.
- Maloney, D. G., Kaminski, M. S., Burowski, D., Haimovich, J. & Levy, R. (1985) *Hybridoma* **4**, 191–209.
- Bindl, J. M. & Warnke, R. A. (1986) *Am. J. Clin. Pathol.* **85**, 490–493.
- Gavrieli, Y., Sherman, Y. & Ben-Sasson, S. (1992) *J. Cell Biol.* **119**, 493–501.
- Young, T. L. & Santella, R. M. (1988) *Carcinogenesis* **9**, 589–592.
- Lacronique, V., Mignon, A., Fabre, M., Viollet, B., Rouquet, N., Molina, T., Porteu, A., Henrion, A., Bouscary, D., Varlet, P., *et al.* (1996) *Nat. Med.* **2**, 80–86.
- Seino, K., Nobuhiko, K., Bashuda, H., Okumura, K. & Yagita, H. (1996) *Int. Immunol.* **8**, 1347–1354.
- Laguens, R. P., Cabeza Meckert, P. M., San Martino, J., Perrone, S. & Favaloro, R. (1996) *J. Heart Lung Transplant.* **15**, 911–918.
- Bergese, S. D., Klenotic, S. M., Wakely, M. E., Sedmak, D. D. & Orosz, C. G. (1997) *Transplantation* **63**, 320–325.
- Jollow, K. C., Sundstrom, J. B., Gravanis, M. B., Kanter, K., Herskowitz, A. & Ansari, A. A. (1997) *Transplantation* **63**, 1482–1489.
- Matiba, B., Mariana, S. M. & Krammer, P. H. (1997) *Immunology* **9**, 59–68.
- Mannaerts, H. F., Simoons, M. L., Balk, A. H., Tijssen, J., van der Borden, S. G., Zondervan, P. E., Mochtar, B., Weimer, W. & Roelandt, J. R. (1993) *J. Heart Lung Transplant.* **12**, 411–421.
- Angermann, C. E., Nassau, K., Stempfle, H.-U., Krüger, T. M., Drewello, R., Phys, D., Junge, R., Ing, D., Überfuhr, P., Weib, M., *et al.* (1997) *Circulation* **95**, 140–150.
- Asselin, B. L., Ryan, D., Frantz, C. N., Bernal, S. D., Leavitt, P., Sallan, S. E. & Cohen, H. J. (1989) *Cancer Res.* **49**, 4363–4368.
- Niemeyer, C. M., Gelber, R. D., Tarbell, N. J., Donnelly, M., Clavell, L. A., Blattner, S. R., Donahue, K., Cohen, H. J. & Sallan, S. E. (1991) *Blood* **78**, 2514–2519.
- Stephens, L. C., Hunter, N. R., Ang, K. K., Milas, L. & Meyn, R. E. (1993) *Radiat. Res.* **135**, 75–80.
- Mirkovic, N., Meyn, R. E., Hunter, N. R. & Milas, L. (1994) *Radiother. Oncol.* **33**, 11–16.
- Sterin-Speziale, N., Kahane, V. L., Setton, C. P., del Carmen Fernandez, M. & Speziale, E. H. (1992) *Lipids* **27**, 10–14.

Apoptotic cell death: its implications for imaging in the next millennium

Francis G. Blankenberg¹, Jonathan F. Tait², H. William Strauss^{1,3}

¹ Department of Radiology/Division of Pediatric Radiology, Stanford University School of Medicine, Stanford, Calif., USA

² Department of Laboratory Medicine, University of Washington, Health Sciences, Seattle, Wash., USA

³ Department of Radiology/Division of Nuclear Medicine, Stanford University School of Medicine, Room H0101, 300 Pasteur Drive, Stanford, CA 94305, USA

Abstract. Apoptosis, also known as programmed cell death, is an indispensable component of normal human growth and development, immunoregulation and homeostasis. Apoptosis is nature's primary opponent of cell proliferation and growth. Strict coordination of these two phenomena is essential not only in normal physiology and regulation but in the prevention of disease. Programmed cell death causes susceptible cells to undergo a series of stereotypical enzymatic and morphologic changes governed by ubiquitous endogenous biologic machinery encoded by the human genome. Many of these changes can be readily exploited to create macroscopic images using existing technologies such as lipid proton magnetic resonance (MR) spectroscopy, diffusion-weighted MR imaging and radionuclide receptor imaging with radiolabeled annexin V. In this review the cellular phenomenon of apoptotic cell death and the imaging methods which can detect the process in vitro and in vivo are first discussed. Thereafter an outline is provided of the role of apoptosis in the pathophysiology of clinical disorders including stroke, neurodegenerative diseases, pulmonary inflammatory diseases, myocardial ischemia and inflammation, myelodysplastic disorders, organ transplantation, and oncology, in which imaging may play a critical role in diagnosis and patient management. Objective imaging markers of apoptosis may soon become measures of therapeutic success or failure in both current and future treatment paradigms. Since apoptosis is a major factor in many diseases, quantification and monitoring the process could become important in clinical decision making.

Key words: Apoptosis – Programmed cell death – Imaging methods

Eur J Nucl Med (2000) 27:359–367

Correspondence to: H.W. Strauss, Department of Radiology/Division of Nuclear Medicine, Stanford University School of Medicine, Room H0101, 300 Pasteur Drive, Stanford, CA 94305, USA

Introduction

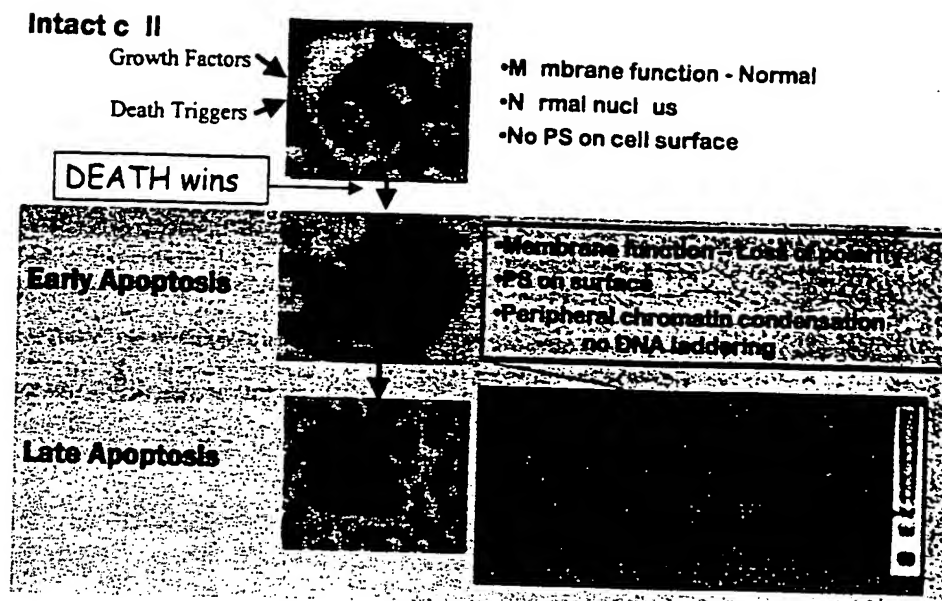
What is apoptosis?

In the yin and yang of existence, it is no surprise that nature has arranged for the orderly demise of cells that have completed their useful function. The programmed disappearance of cells, apoptosis, occurs under both physiologic and pathologic circumstances. Two examples of physiologic programmed cell death are the disappearance of cells when growth factor stimuli are withdrawn (an integral component of the menstrual cycle) and the deletion of activated immune cells when cells have completed their assigned task.

When apoptosis is dysregulated, i.e., there is too little or too much programmed cell death, disease often ensues [1–6]. Diseases associated with excessive apoptosis include AIDS, neurodegenerative disorders (Alzheimer's disease), myelodysplastic syndromes (aplastic anemia, thalassemia), ischemia/reperfusion injury, progression of heart failure in cardiomyopathies, viral infections (chronic hepatitis), toxin-induced liver disease, organ transplant rejection, graft versus host disease, and adult respiratory distress syndrome (particularly when associated with toxic shock). Diseases associated with too little apoptosis include cancer and autoimmune disorders. Successful treatment of neoplasms with drugs or radiation induces apoptosis in the lesion.

Apoptosis is defined as "the dropping of a petal or leaf from a flower or tree." Kerr et al. [7] originally coined this term to define the series of morphologic changes in adrenal tissue when ACTH is withdrawn. The withdrawal of ACTH causes adrenal cells to fragment into small, variably sized vesicles (apoptotic bodies). Neighboring cells or phagocytes then ingest the apoptotic bodies, resulting in the disappearance of the cell without an inflammatory response. The outcome of this process is the controlled removal of senescent, unwanted, or deleterious cells without inciting an inflammatory reaction that might damage adjacent healthy cells and extracellular matrix (Fig. 1). The process of orderly cell auto-

Fig. 1. Sequence of morphologic changes in apoptosis. Initially (*upper panel*) the cell is normal. Following the initiation of apoptosis, chromatin clumping and cytoplasmic condensation occur (*middle panel*). In the late phase of apoptosis (*bottom panel*) the cell begins to form apoptotic bodies and DNA is fragmented with formation for DNA laddering (as indicated on gel electrophoresis)



fragmentation is governed by a cascade of enzymatic activity. Although the original observation suggested that apoptosis is caused by a withdrawal of growth factors, it is now known that a wide array of exogenous or endogenous stimuli [8–12] can trigger the process.

Mechanism of apoptosis

Apoptosis is initiated when there is a disturbance in the local environment of the cell. Cells are constantly bathed in a sea of life-reinforcing stimuli, such as growth factors, and death signals such as tumor necrosis factor. A shift in the balance of these factors with either a decrease in survival factors or a marked increase in death signals can initiate apoptosis. Withdrawal of growth factors, severe mitochondrial damage, attempting mitosis in the presence of irreparable DNA damage, activation of cellular Fas receptors by Fas ligand expressed on activated lymphocytes, hypoxia, heat, cold, chemical injury (chemotherapy), or significant doses of ionizing radiation (causing DNA injury) can result in apoptosis.

Once apoptosis has been triggered, one of several enzymatic cascades is initiated to achieve the orderly destruction of DNA and the dissolution of other cellular elements. A major pathway involves a group of cysteine proteases, the “caspases”. Caspase activation precedes morphologic changes. At the time of caspase activation, cells destined for apoptosis appear to signal their neighbors by expressing phosphatidylserine (PS) on the cell surface [13]. PS, along with phosphatidylethanolamine, sphingomyelin, and phosphatidylcholine, is a normal constituent of the cell membrane. In contrast to the other cell membrane constituents, PS is restricted to the inner leaflet of the cell membrane. This constraint on PS distribution is the result of two enzymes, translocase and

floppase, which actively pump PS to the inner leaflet and the other lipids out. Activation of caspase is associated with inactivation of these membrane pumps, and activation of an enzyme, scramblase, which equilibrates the membrane lipids on the inner and outer leaflet of the cell membrane – resulting in the rapid appearance of PS on the outer leaflet of the membrane [14, 15]. Once the caspases are activated and PS is expressed, the execution phase of apoptosis occurs. Cellular cytoplasm condenses, nuclear DNA is degraded into 180-kDa pieces and the cell fragments into membrane-covered pieces (each expressing PS on the surface) for phagocytosis [16] (Fig. 1, “Late Apoptosis”, bottom panel).

Methods to image apoptosis in vivo

Annexin V

Annexin V [17, 18] is an endogenous human protein which binds to membrane-bound PS with an affinity of about 10^{-9} M. Annexin V, labeled with fluorescein dye, has been used to detect PS expression in studies of apoptosis in hematopoietic cell lines, neurons, fibroblasts, endothelial cells, smooth muscle cells, carcinomas, lymphomas, and all embryonic cell types, as well as non-mammalian plant and insect cells [19]. Annexin V has also been radiolabeled by iodination and coupling to linker molecules such as a diamide dimercaptide (N_2S_2) [20] or hydrazino nicotinamide [20]. The universality of annexin V binding to various cell lines is due to the composition of the phosphoserine head group of PS (the site of annexin V binding), which is identical in all multicellular organisms. In vitro cell binding studies demonstrate a 20-fold increase in annexin concentration in cells undergoing apoptosis compared with control cells.

Table 1. The biodistribution of annexin V in rats

	10 min (n=6)	30 min (n=7)	1 h (n=7)	3 h (n=6)
<i>A) % I.D./organ^a</i>				
Brain	0.0681±0.0202	0.0197±0.0035	0.0149±0.003	0.0093±0.0009
Lungs	2.611±0.367	1.558±0.191	1.000±0.30	0.821±0.085
Heart	0.372±0.0726	0.150±0.048	0.135±0.033	0.134±0.0165
Liver	20.8±1.179	15.8±2.67	21.6±4.12	17.97±1.36
Spleen	4.64±0.459	4.08±1.089	4.75±1.22	4.12±0.571
Kidneys	29.2±6.05	33.5±8.02	45.6±5.48	47.4±2.90
Stomach	0.25±0.056	0.376±0.038	0.51±0.165	0.38±0.138
<i>B) % I.D./gram^b</i>				
Small intestine	0.144±0.066	0.114±0.048	0.128±0.059	0.129±0.011
Colon	0.082±0.066	0.054±0.013	0.052±0.014	0.082±0.039
Skeletal musc.	0.035±0.009	0.024±0.007	0.026±0.008	0.022±0.002
Bone marrow	2.13±0.52	1.55±0.72	2.083±0.57	1.98±0.374
Blood	1.38±0.34	0.306±0.098	0.215±0.090	0.107±0.013

Mean values±standard error for tissue and organ samples from control Sprague-Dawley rats 10 min, 30 min, 1 h and 3 h after injection of 25 µg/kg of ^{99m}Tc-HYNIC-annexin V (500–600 µCi/animal) labeled using a ^{99m}Tc-tricine conjugate method injected via tail vein. Samples were weighed and placed in 3-ml tubes and counted

^a Mean percentage of injected dose (%I.D.) per organ (% I.D./organ)

^b Mean percentage of injected dose per gram of tissue (%I.D./g)

Tait and colleagues utilized radiolabeled annexin V to detect increased PS expression which occurs when platelets are activated in acute thrombosis [21]. Blankenberg and colleagues utilized radiolabeled annexin to detect apoptosis in vivo in animal models of transplant rejection, hypoxic cerebral injury, tumor therapy and Fas induced apoptosis [22, 23].

Following intravenous administration of radiolabeled annexin V, the agent is cleared from the blood with a half-time of less than 5 min, and is concentrated primarily in the kidneys and to a lesser degree in the liver. A summary of annexin biodistribution in rodents is presented in Table 1. Apoptosis induced by stimulation of the Fas/Fas ligand system, transplant rejection, or chemotherapy in tumor-bearing animals has been visualized with technetium-99m labeled annexin imaging.

The minimal cell mass required for successful detection of apoptosis by in vivo imaging is not known. However, in studies of heart transplant rejection by Vriens et al., histologic evidence of apoptosis was present in <10% of cells at the time when annexin imaging demonstrated remarkable focal localization in the transplant (see later discussion of heart transplant rejection). It is likely that single-photon imaging will require significant apoptosis (in at least 10% of cells) to detect the process in a small mass of tissue (~2–3 g). If the extent of the lesion involves a larger mass of tissue, such as the major portion of an organ, less extensive apoptosis will be detectable. It is likely that the contrast of annexin images will be enhanced if the protein is labeled with fluorine-18 and data recorded with positron tomography.

In addition to radionuclide imaging with radiolabeled annexin, other imaging modalities, such as magnetic res-

onance (MR), have been utilized to detect apoptosis in vivo.

MR lipid spectroscopy and diffusion-weighted MR imaging

Since 1982 numerous in vitro and in vivo MR studies have documented the presence of a narrow and intense resonance in the 1.3-ppm region of the lipid proton spectra from cultured tumor, embryonic, and stimulated lymphocyte cell lines and solid, experimental and human tumors [24, 25]. Of note, this resonance has been found to increase in solid tumors following treatment and the induction of apoptotic cell death. A rise in the 1.3-ppm resonance has also been observed acutely after hypoxic-ischemic injury of the cerebrum [26] and cerebral diffuse axonal injury due to child abuse [27] and has been found to be of prognostic significance. This resonance has now been recognized as representing the methylene proton (-CH₂-) of mobile neutral lipid fatty acid chains within the plasma membrane bilayer in vitro [23, 24] and cytoplasmic vesicles in vivo [28, 29].

Coincident with the lipid rearrangements that permit both radiolabeled annexin V and proton lipid MR spectroscopic imaging of apoptotic cells and tissues is the shrinkage of a cell's cytoplasmic volume. There is concurrent increased cytoplasmic microviscosity and restriction of water motion [30]. This apoptotic phenomenon can be imaged by MR using diffusion weighted imaging (DWI), which tags and follows the motion (diffusion or ADC = the average diffusion coefficient) of individual water molecules [31]. The use of DWI to detect and

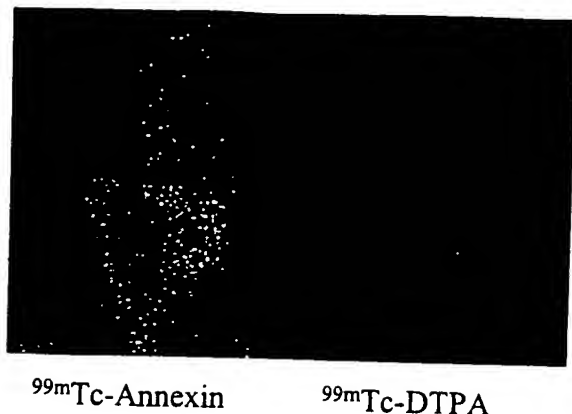


Fig. 2. Hypoxic brain injury due to transient occlusion of the right middle cerebral artery. Seven hours following occlusion/reperfusion, pinhole vertex view images of the head in intact adult rats were obtained after injection of annexin (*left panel*) to identify apoptosis and DTPA (*right panel*) to identify areas of blood-brain barrier breakdown. There is no loss of blood-brain barrier integrity, but annexin uptake is seen in the right hemisphere (*arrow*). The nose is oriented cephalad on images

track apoptotic cell death in vivo is only beginning to be studied and its ultimate clinical applicability, particularly outside the nervous system, remains to be defined.

The following sections describe some specific diseases where apoptosis is known to play a significant role, and where imaging the process may be helpful in clinical decision making.

Central nervous system

Stroke

Hypoxic-ischemic injury (HII) in adults (stroke, multi-infarct dementia) with delayed loss of gray and white matter is due to apoptosis [32]. Blankenberg et al. [33] have shown that moderate to severe injury, without evidence of blood-brain barrier breakdown, is associated with remarkable focal radiolabeled annexin uptake in an adult rat model of ischemic/reperfusion hemispheric injury (Fig. 2). Because the actual cell loss in these patients is gradual (delayed with respect to the insult) there may be a therapeutic window to inhibit (or reverse) early apoptosis with pharmacologic blockade. Imaging with radiolabeled annexin V may be helpful in addressing this clinical problem since annexin V has virtually no background uptake in the brain.

Ischemia/reperfusion injury in preterm/term infants

HII in preterm infants is a major cause of cerebral palsy. Because of the immaturity of the centrifugal cerebrovas-

cular circulation, full-term and preterm neonates manifest HII in a different fashion than adults [34, 35]. Preterm infants tend to suffer watershed ischemic injury in a periventricular distribution (periventricular leukomalacia or PVL) while term infants develop disease of their subcortical white matter. The delayed cell loss of these injuries is mediated by apoptosis [36]. In experimental animals ^{99m}Tc -annexin imaging has clearly delineated these lesions in the absence of blood-brain barrier breakdown.

Traditional imaging techniques do not provide the specificity needed to identify neonates at risk for development of cerebral palsy (which is usually diagnosed at 2–3 years of age) who might benefit from these novel treatments in the first several days (or hours) of life. Reversible abnormalities seen by DWI MR associated with mild transient hemispheric HII resulted in multifocal regions of abnormal annexin V cerebral and cerebellar uptake in a neonatal rabbit model of global hypoxia [37]. Histology of these neonatal rabbit brains demonstrated a correlation between radiolabeled annexin V uptake and subtle scattered ischemic changes in the hippocampus periventricular/subcortical white matter. In the future, neonates who are the products of a difficult labor or delivery could be assessed for suspected HII damage with annexin V imaging to identify patients who might benefit from therapy.

AIDS dementia/Alzheimer's disease

Neuronal and glial cell apoptosis also occurs in acquired immune deficiency syndrome, in encephalitis with or without AIDS-related dementia and in neurodegenerative disorders, such as Alzheimer's and Parkinson's disease [38]. The gradual loss of white and gray matter in Alzheimer's disease is primarily due to apoptosis. Imaging with radiolabeled annexin V could be helpful in the diagnosis and therapeutic management of this diverse group of patients.

Lung disease

High-resolution computed tomography (HRCT) of the chest has enhanced the detection and characterization of disease processes affecting the interstitium of the lung [39]. Diseases such as idiopathic pulmonary fibrosis, desquamative interstitial pneumonitis, *Pneumocystis carinii* pneumonia, lymphocytic interstitial pneumonia, fibrosis in collagen vascular diseases, sarcoidosis, drug or allergic reactions, bronchiolitis obliterans, and bronchiolitis obliterans with organizing pneumonia [40] can be readily identified. These entities, however, all involve cell-mediated inflammation and activation of T lymphocytes, at least in the acute/subacute settings. Although HRCT provides characteristic images, often obviating the need for confirmatory lung biopsy, HRCT cannot

quantify the degree of inflammation. The degree of inflammation is important to define the best management of the process. Without specific information about inflammation, clinicians manage these patients with pulmonary function tests, bronchoalveolar lavage, and serial chest radiography.

Radiolabeled annexin V imaging of the chest may be of value to quantify cell-mediated inflammation and apoptosis in the lungs. In a rat model of cell-mediated lung apoptosis, acute lung transplant rejection, radiolabeled annexin V localization was more sensitive than CT scanning in detecting the process. Other circumstances where apoptosis imaging may play a role include: adult respiratory distress syndrome, which is in part induced by the release of tumor necrosis factor, a potent inducer of apoptotic alveolar cell death; bronchopulmonary dysplasia; neonates with pulmonary oxygen toxicity; cystic fibrosis; and asthma. In each case, the extent of apoptosis will indicate the effectiveness of therapy – if apoptosis is extensive, therapy is not controlling the process.

Heart

Myocardial infarction and reperfusion injury

Like the brain, cardiomyocytes undergo apoptosis in response to hypoxic-ischemic insults that are insufficient to induce frank necrosis [41] [e.g., the peripheral (penumbral) regions of an infarct or following reperfusion of an infarct]. Interestingly, the heart also displays cytoplasmic lipid droplets, the presence of which confers a poorer prognosis in animal models of myocardial ischemia [42]. It is clear that agents which selectively inhibit activation of the apoptotic enzymatic cascade decrease the degree of "infarction" in both the heart and brain in response to an ischemic insult [43, 44]. Preliminary studies of myocardial annexin localization in rats with acute myocardial infarction suggest that apoptosis plays a major role in cell death following acute coronary occlusion (S. Hasegawa and T. Nishimura, personal communication).

Coronary disease and atherosclerosis

Recent biochemical evidence strongly suggests that activated monocytes/macrophages attracted by local vascular endothelial damage and complement activation infiltrate the arterial vascular wall [45]. With continued inflammation there is deposition of lipid at the site of injury, formation of foam cells (lipid-laden macrophages), and formation of an atheroma. Within the plaque there is significant apoptosis involving the monocytes and macrophages infiltrating the lesion, smooth muscle cells at the base of the lesion, and, in unstable plaque, the endothelial cells forming the cap of the plaque. This last

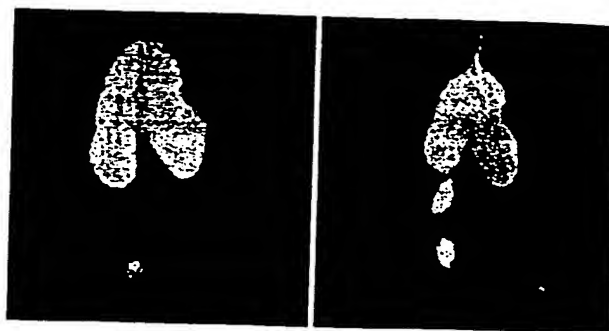


Fig. 3. Two rats with heterotopic hearts transplanted into the abdomen, below the kidneys. One hour following injection of ^{99m}Tc -annexin, anesthetized animals were placed prone on a high-resolution parallel-hole collimator. Images of the syngeneic (left) and allogeneic (right) transplants were recorded on the fourth day after transplant. The bright area in the mid abdomen is the transplant undergoing rejection/apoptosis in the allogeneic animal. Some annexin is seen in the bladder of both animals

event is particularly dangerous as the apoptotic endothelial cells expressing PS on their surface serve as thrombogenic foci.

It is unclear whether external imaging with ^{99m}Tc -annexin V will have sufficient resolution to define these lesions; however, if an intravascular probe were available such lesions might be readily identified. An alternative strategy may involve the use of radiolabeled MCP-1 (monocyte chemotactic peptide), which has a molecular weight of approximately 13,000 [46]. MCP-1 selectively binds to "activated" macrophages and has shown promise in detecting mononuclear infiltration in the subendothelial layers of mechanically traumatized arterial vessels. As activated monocytes/macrophages are intimately involved in chronic inflammation, MCP-1 may be useful as a marker of infectious or noninfectious granulomatous inflammation throughout the body [47].

Myocarditis/cardiomyopathies

Apoptotic cell death plays a major role in viral and autoimmune myocarditis and nonischemic cardiomyopathies [7]. Acute transplant rejection is primarily an immune event mediated by alloreactive T lymphocytes. In a rat model of acute cardiac transplant rejection, serial imaging with ^{99m}Tc -annexin V successfully detected rejection [48] with an accuracy exceeding that of TUNEL staining of biopsy specimens (Fig. 3). Furthermore, when immunosuppressive therapy with cyclosporine was initiated, the decrease in rejection was mirrored by a marked decrease in ^{99m}Tc -annexin localization (Fig. 4). In light of this experience with transplant rejection, annexin V imaging may also be helpful in the detection of apoptosis due to virally induced cardiomyopathies or other autoimmune diseases that affect the heart such as systemic lupus erythematosus, rheumatic fever, and Kawasaki's disease.

Fig. 4. Annexin imaging in acute cardiac transplant rejection before and after cyclosporine therapy. The four panels depict whole body images on days 1, 4, 10, and 18 after transplantation (each image was recorded 1 h after ^{99m}Tc -annexin injection). On day 1 there is no annexin imaging evidence of apoptosis. The image on day 4 demonstrates ^{99m}Tc -annexin localization in the transplanted heart. Treatment with cyclosporin commenced on day 5, and by day 10 the annexin localization has diminished. By day 18, annexin localization has declined further.

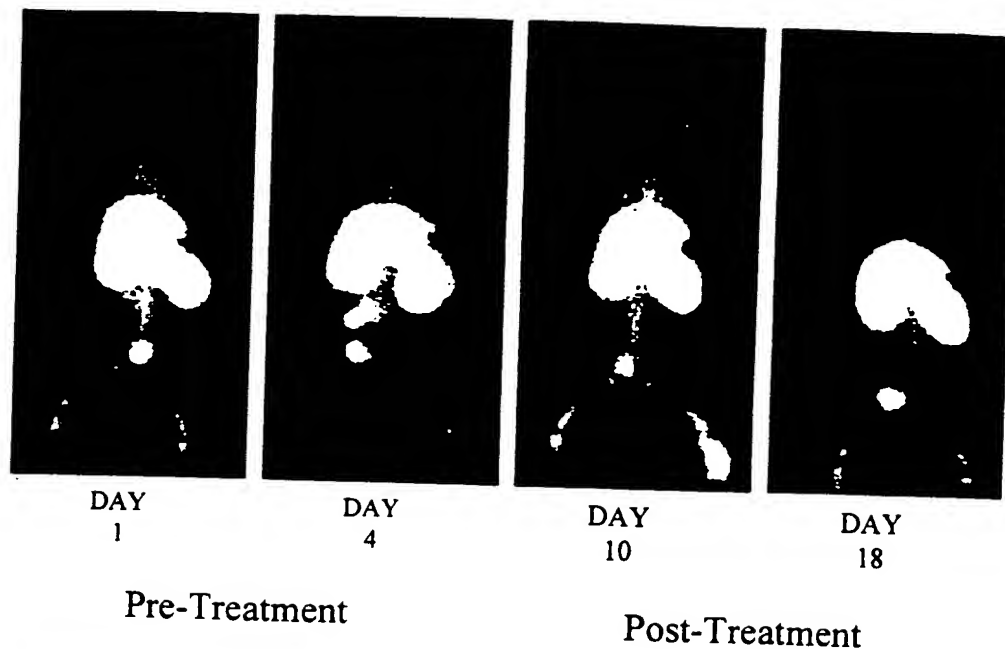
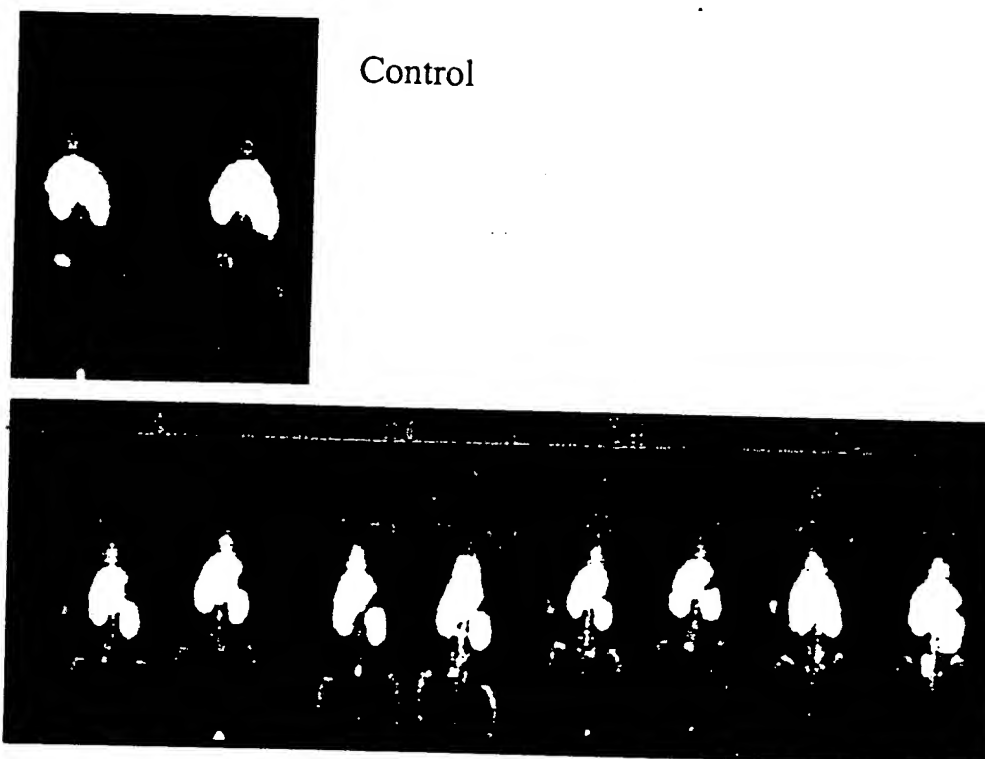


Fig. 5. Whole body posterior images in rats 1 h following tail vein injection of 1 mCi of radiolabeled annexin V before and after treatment with 100 mg/kg of cyclophosphamide administered intraperitoneally to ablate the bone marrow. One day later the animals were imaged. Control animals are shown in the *top panels* and rats that had received cyclophosphamide 8–72 h before annexin imaging are shown in the *bottom panels*. The vertebral and peripheral marrow show increased localization (350%) following cyclophosphamide-induced apoptosis.

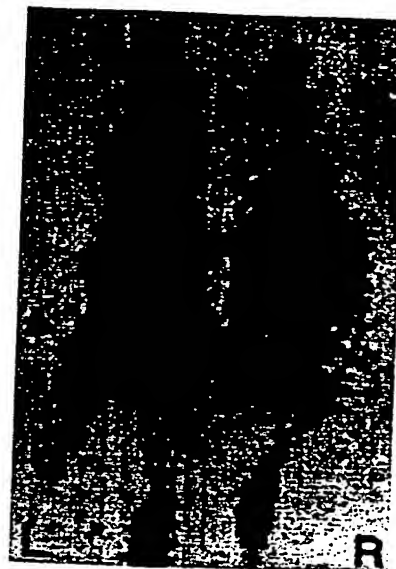


Bone marrow diseases

β -thalassemia, sickle-cell disease, aplastic anemia (myelofibrosis), parvoviral infection (and many other viral infections), autoimmune diseases, toxins, radiation, and chemotherapy cause significant apoptosis in the bone marrow [7]. Bone marrow aspiration is required to determine the degree of disease involvement of the bone marrow [49]. We have shown that cyclophosphamide (a po-

tent bone marrow suppressive and antitumor agent) treatment of otherwise normal adult rats induces a marked increase in bone marrow uptake of annexin V as compared with controls (Fig. 5). Based on this experimental observation, it is likely that ongoing apoptotic bone marrow disease processes such as aplastic anemia may be detected with annexin imaging.

Autoimmune, crystal depositional, and idiopathic arthropathies all appear to be intimately linked to apoptotic cell death of the synovial tissues [7]. Other than symptomatic improvement there are few objective measures with which to guide anti-inflammatory therapy. Efforts are underway to characterize and quantify the quality of hyaline cartilage using a number of MR techniques [50]. Annexin V (and probably MCP-1) imaging may in fact provide an objective measure of disease severity and anti-inflammatory treatment response. Additionally, the gradual loosening and failure of joint prostheses appears to be directly linked to the apoptotic cell death of macrophages which are activated in response to foreign debris [51]. Annexin V imaging may be useful in the management of these patients as well.



Treated
tumor in
left thigh

Fig. 6. Annexin V detection of necrotic versus apoptotic tumor cell death in flank tumors of mice following chemotherapy. The animal on the left demonstrated a greater than 363% increase in left flank 38C13 murine B cell lymphoma annexin V uptake 20 h after treatment with 100 mg/kg of cyclophosphamide (i.p.) compared with untreated flank lymphoma (animal on right)

Organ transplantation

Annexin V can identify acute heart, lung, and liver transplant rejection in vivo [52]. The majority of transplant recipients, however, do not have acute graft rejection, but instead suffer multiple clinically manifest and subclinical episodes of rejection. A combination of smoldering inflammation and a low level of apoptosis are some of the key findings in chronic rejection. The inflammation and apoptosis are primarily manifest as accelerated vascular disease (atherosclerosis) in the graft. Graft vasculopathy is a process that occurs over years, characterized by perivascular mononuclear cell infiltration and apoptotic cell death. The chronicity of the process may be associated with such a low level of apoptosis that the process cannot be detected by annexin V imaging.

Oncology

The degree of cytoreduction in response to antitumor treatment(s) directly correlates with overall disease response, disease-free interval, and ultimate survival in a number of malignancies [53]. Depending on the type of malignancy the only measures of cytoreduction are gross shrinkage or disappearance of tumor as seen by anatomical imaging with ultrasound, CT or MR imaging. Recently, there has been a renewed interest in using proton lipid MR spectroscopy and DWI MR to assess the early treatment response of tumors [26–28]. Unfortunately, these techniques cannot give information except for regional areas of tumor involvement, particularly during induction therapy, when patients can be quite ill. In addition DWI MR detection of tumoral apoptosis relies on the observable shrinkage of the cell cytoplasm during tumor cell death. However, many tumors respond to chemotherapeutic agents which specifically attack DNA, such as doxorubicin (adriamycin), by cell swelling, not

cell shrinkage. Therefore, DWI MR may give misleading results in vivo. This cell swelling is due to a metabolic cell death initiated by massive activation of a normally quiescent nuclear enzyme called poly-ADP-ribose polymerase (PARP or PARS) [54]. PARP is generally activated in the later stages of apoptosis and helps induce fragmentation of a cell's DNA. Direct DNA damage by ionizing radiation, or radical ion formation by agents such as doxorubicin or H₂O₂ [55] in some circumstances can induce massive direct activation of PARP. Activated PARP utilizes NAD to form poly-ADP ribose polymers. To replace lost NAD stores a cell utilizes ATP and if PARP activation is of sufficient intensity, virtually all ATP stores of a cell will be rapidly depleted. A cell depleted of ATP will simply swell and lose membrane integrity (necrosis). In an experimental model of lymphoma treated with cyclophosphamide, therapy-induced apoptosis is readily visible with ^{99m}Tc-annexin V imaging (Fig. 6). Despite these different mechanisms of cell death, annexin V imaging will demonstrate the process because annexin V binds to cells expressing PS on the outer cell surface (apoptosis) or, alternatively, annexin V can gain access to inner plasma membrane leaflet PS after the onset of irreversible membrane failure (PARP-mediated cell death).

19. O'Brien IEW, Reutingsperger CPM, Holdaway KM. Annexin-V and TUNEL use in monitoring the progression of apoptosis in plants. *Cytometry* 1997; 29: 28–33.
20. Abrams MJ, Juweid M, tenKate CI, et al. Technetium-99m-human polyclonal IgG radiolabeled via the hydrazino nicotinamide derivative for imaging focal sites of infection in rats. *J Nucl Med* 1990; 31: 2022–2028.
21. Stratton JR, Dewhurst TA, Kasina S, et al. Selective uptake of radiolabeled annexin V on acute porcine left atrial thrombi. *Circulation* 1995; 92: 3113–3121.
22. Blankenberg FG, Katsikis PD, Tait JF, et al. In vivo detection and imaging of phosphatidylserine expression during programmed cell death. *Proc Natl Acad Sci USA* 1998; 95: 6349–6354.
23. Blankenberg FG, Katsikis PD, Tait JF, et al. Imaging of apoptosis (programmed cell death) with ^{99m}Tc annexin V. *J Nucl Med* 1999; 40: 184–191.
24. Blankenberg FG, Storrs RW, Naumovski L, et al. Detection of apoptotic cell death by proton nuclear magnetic resonance spectroscopy. *Blood* 1996; 87: 1951–1956.
25. Blankenberg FG, Katsikis PD, Storrs RW, et al. Quantitative analysis of apoptotic cell death using proton nuclear magnetic resonance spectroscopy. *Blood* 1997; 89: 3778–3786.
26. Hakumäki JM, Grohn OH, Pirttilä TR, et al. Increased macromolecular resonances in the rat cerebral cortex during severe energy failure as detected by ¹H nuclear magnetic resonance spectroscopy. *Neurosci Lett* 1996; 212: 151–154.
27. Ross BD, Ernst T, Kreis R, et al. ¹H MRS in acute traumatic brain injury. *J Magn Reson Imaging* 1998; 8: 829–840.
28. Remy C, Fouillhe N, Barba I, et al. Evidence that mobile lipids detected in rat brain glioma by ¹H nuclear magnetic resonance correspond to lipid droplets. *Cancer Res* 1997; 57: 407–414.
29. Veale MF, Roberts NJ, King GF, et al. The generation of ¹H-NMR-detectable mobile lipid in stimulated lymphocytes: relationship to cellular activation, the cell cycle, and phosphatidylcholine-specific phospholipase C. *Biochem Biophys Res* 1997; 239: 868–874.
30. Hakumäki JM, Poptani H, Puumalainen AM, et al. Quantitative ¹H NMR diffusion spectroscopy of BT4 C rat glioma during thymidine kinase-mediated gene therapy in vivo: identification of apoptotic response. *Cancer Res* 1998; 58: 3791–3799.
31. D'Arceuil HE, de Crespigny AJ, Rother J, et al. Diffusion and perfusion magnetic resonance imaging of the evolution of hypoxic ischemic encephalopathy in the neonatal rabbit. *J Magn Reson Imaging* 1998; 8: 820–888.
32. Du C, Hu R, Csemansky CA, et al. Very delayed infarction after mild focal cerebral ischemia: a role for apoptosis? *J Cereb Blood Flow Metab* 1996; 16: 195–201.
33. Blankenberg FG, Busch E, Yenari MA, et al. In vivo imaging of apoptotic cell death associated with cerebral hemispheric ischemia using ^{99m}Tc radiolabeled annexin V. *Stroke* 1998; 29: 330.
34. Rutherford MA, Pennock JM, Counsell SJ, et al. Abnormal magnetic resonance signal in the internal capsule predicts poor neurodevelopmental outcome in infants with hypoxic-ischemic encephalopathy. *Pediatrics* 1998; 102: 323–328.
35. Oka A, Belliveau MJ, Rosenberg PA, et al. Vulnerability of oligodendroglia to glutamate: pharmacology, mechanisms, and prevention. *J Neurosci* 1993; 13: 1441–1453.
36. Pulera MR, Adams LM, Liu H, et al. Apoptosis in a neonatal rat model of cerebral hypoxia-ischemia. *Stroke* 1998; 29: 2622–2630.
37. D'Arceuil HE, Blankenberg FG, Tait JF, et al. Radionuclide scanning combined with MR diffusion imaging investigation of apoptosis in neonatal rabbit HIE [abstract]. *Pediatr Res* 1998; 43: 317A.
38. Cotman CW, Anderson AJ. A potential role for apoptosis in neurodegeneration and Alzheimer's disease. *Mol Neurobiol* 1995; 10: 19–45.
39. Lau DM, Siegel MJ, Hildebolt CF, et al. Bronchiolitis blitans syndrome: thin-section CT diagnosis of obstructive changes in infants and young children after lung transplantation. *Radiology* 1998; 208: 783–788.
40. McAdams HP, Rosado-de-Christenson ML, Wehunt WD, et al. The alphabet soup revisited: the chronic interstitial pneumonias in the 1990s. *Radiographics* 1996; 16: 1009–1033.
41. Narula J, Haider N, Virmani R, et al. Apoptosis in myocytes in end-stage heart failure. *N Engl J Med* 1996; 335: 1182–1195.
42. Greve G, Rotevatn S, Svendby K, et al. Early morphologic changes in cat heart muscle cells after acute coronary artery occlusion. *Am J Pathol* 1990; 136: 273–283.
43. Yaoita H, Ogawa K, Maehara K, et al. Attenuation of ischemia/reperfusion injury in rats by a caspase inhibitor [see comments]. *Circulation* 1998; 97: 276–281.
44. Hara H, Friedlander RM, Gagliardini V, et al. Inhibition of interleukin 1beta converting enzyme family proteases reduces ischemic and excitotoxic neuronal damage. *Proc Natl Acad Sci USA* 1997; 94: 2007–2012.
45. Geng Y-J, Holm J, Hygren S, et al. Expression of the macrophage scavenger receptor in atheroma. *Arterioscler Thromb Vasc Biol* 1995; 15: 1995–2002.
46. Torzewski J, Oldroyd R, Lachmann P, et al. Complement-induced release of monocyte chemotactic protein-1 from human smooth muscle cells. A possible initiating event in atherosclerotic lesion formation. *Arterioscler Thromb Vasc Biol* 1996; 16: 673–677.
47. Grandaliano G, Gesualdo L, Ranieri E, et al. Monocyte chemotactic peptide-1 expression and monocyte infiltration in acute renal transplant rejection. *Transplantation* 1997; 63: 414–420.
48. Vriens PW, Blankenberg FG, Stoot JH, et al. The use of Tc ^{99m} annexin V for in vivo imaging of apoptosis during cardiac allograft rejection. *J Thorac Cardiovasc Surg* 1998; 116: 844–853.
49. Niemeyer CM, Gelber RD, Tarbell NJ, et al. Low-dose versus high-dose methotrexate during remission induction in childhood acute lymphoblastic leukemia (protocol 81-01 update). *Blood* 1991; 78: 2514–2519.
50. Uhl M, Allmann KH, Ihling C, et al. Cartilage destruction in small joints by rheumatoid arthritis: assessment of fat-suppressed three-dimensional gradient-echo MR pulse sequences in vitro. *Skeletal Radiol* 1998; 27: 677–682.
51. Nakashima Y, Sun DH, Trainade MC, et al. Induction of macrophage C-C chemokine expression by titanium alloy and bone cement particles. *J Bone Joint Surg [Br]* 1999; 81: 155–162.
52. Blankenberg FG, Strauss HW. Non-invasive diagnosis of acute heart- or lung-transplant rejection using radiolabeled annexin V. *Pediatr Radiol* 1999; 29: 299–305.
53. Lamb JR, Friend SH. Which questimate is the best questimate? Predicting chemotherapeutic outcomes. *Nature Med* 1997; 9: 962–963.
54. Martin DS, Schwartz GK. Chemotherapeutically induced DNA damage, ATP depletion, and the apoptotic biochemical cascade. *Oncol Res* 1997; 9: 1–5.
55. Zhang J, Dawson VL, Dawson TM, et al. Nitric oxide activation of poly(ADP-ribose) synthetase in neurotoxicity. *Science* 1994; 263: 687–689.



ClustalW Results

EXHIBIT A
Docket No.: PF-0733 USN
USSN: 10/018,170

Sequences	Help					
Retrieval	BLAST2	FASTA	ClustalW	GCG Assembly	Phrap	Translation

Confidential -- Property of Incyte Corporation SeqServer Version 4.6 Jan 2002

- ☐ g10436074
- ☐ 2615168CD1

CLUSTAL W (1.7) Multiple Sequence Alignments

Sequence format is Pearson
Sequence 1: g10436074 345 aa
Sequence 2: 2615168CD1 345 aa
Start of Pairwise alignments
Aligning...
Sequences (1:2) Aligned. Score: 99
Start of Multiple Alignment
There are 1 groups
Aligning...
Group 1: Sequences: 2 Score: 4527
Alignment Score 2042
CLUSTAL-Alignment file created [baa4aaqV1.aln]
CLUSTAL W (1.7) multiple sequence alignment

g10436074 2615168CD1	MSVTGGKMAPSLTQEILSHLGLASKTAAWGTLGTLRTFLNFSVDKDAQRLLRAITGQGV MSVTGGKMAPSLTQEILSHLGLASKTAAWGTLGTLRTFLNFSVDKDAQRLLRAITGQGV *****
g10436074 2615168CD1	RSAIVDVLTNRSREQRQLISRNFQERTQQDLMKSLQAALSGNLERIVMALLQPTAQFDAQ RSAIVDVLTNRSREQRQLISRNFQERTQQDLMKSLQAALSGNLERIVMALLQPTAQFDAQ *****
g10436074 2615168CD1	ELRTALKASDSAVIDVAIEILATRTPPQLQECLAVYKHNQVEAVDGITSETSGILQDLLL ELRTALKASDSAVIDVAIEILATRTPPQLQECLAVYKHNQVEAVDDITSETSGILQDLLL *****
g10436074 2615168CD1	ALAKGGRDSYSGIIDYNLAEQDVQALQRAEGPSREETWVPVFTQRNPEHLIRVFDQYQRS ALAKGGRDSYSGIIDYNLAEQDVQALQRAEGPSREETWVPVFTQRNPEHLIRVFDQYQRS *****
g10436074 2615168CD1	TGQEEAEVQNRFHGDAQVALLGLASVIKNTPLYFADKLHQALQETEPNYQVLIRILISR TGQEEAEVQNRFHGDAQVALLGLASVIKNTPLYFADKLHQALQETEPNYQVLIRILISR *****
g10436074 2615168CD1	CETDLLSIRAEFRKKFGKSLYSSLQDAVKGDCQSALLALCRAEDM CETDLLSIRAEFRKKFGKSLYSSLQDAVKGDCQSALLALCRAEDM

Submit sequences to:





Docket No.: PF-0733 USN

Response Under 37 C.F.R. 1.116 - Expedited Procedure
Examining Group 1652

Certificate of Mailing

I hereby certify that this correspondence is being deposited with the United States Postal Service as first class mail in an envelope addressed to:
Mail Stop Appeal Brief Patents, Commissioner for Patents, P.O. Box 1450, Alexandria, VA 22313-1450 on January 27, 2004.

By: 

Printed: Katherine Stog
Lisa McDill

IN THE UNITED STATES PATENT AND TRADEMARK OFFICE
BEFORE THE BOARD OF PATENT APPEALS AND INTERFERENCES

In re Application of: Yue et al.

Title: INTRACELLULAR SIGNALING MOLECULES

Serial No.: 10/018,170

Filing Date:

December 11, 2001

Examiner: Steadman, D

Group Art Unit:

1652

Mail Stop Appeal Brief-Patents
Commissioner for Patents
P.O. Box 1450
Alexandria, VA 22313-1450

BRIEF ON APPEAL

Sir:

Further to the Notice of Appeal filed October 22, 2003, and received by the USPTO on October 27, 2003, herewith are three copies of Appellants' Brief on Appeal. Appellants hereby request a one-month extension of time in order to file this Brief. Authorized fees include the statutory fee of \$110.00 for a one-month extension of time, as well as the \$ 330.00 fee for the filing of this Brief.

This is an appeal from the decision of the Examiner finally rejecting claims 205, 206, 208, 209, 211-215, 217, 224-226, and 228-231 of the above-identified application.

(1) REAL PARTY IN INTEREST

--The above-identified application is assigned of record to **Incyte Pharmaceuticals, Inc.,** (now **Incyte Corporation**, formerly known as **Incyte Genomics, Inc.**) (Reel 012671, Frame 0254) which is the real party in interest herein.

(2) RELATED APPEALS AND INTERFERENCES

Appellants, their legal representative and the assignee are not aware of any related appeals or interferences which will directly affect or be directly affected by or have a bearing on the Board's decision in the instant appeal.

(3) STATUS OF THE CLAIMS

Claims rejected: Claims 205, 206, 208, 209, 211-215, 217, 224-226, and 228-231

Claims allowed: (none)

Claims canceled: Claims 1-204, 207, 210, 216, 218, and 227

Claims withdrawn: Claims 219-223

Claims on Appeal: Claims 205, 206, 208, 209, 211-215, 217, 224-226, and 228-231

(A copy of the claims on appeal, as amended, can be found in the attached Appendix).

(4) STATUS OF AMENDMENTS AFTER FINAL

The Amendment after Final Rejection under 37 C.F.R. §1.116 filed August 27, 2003 has been entered for purposes of this appeal. See the Advisory Action, mailed December 19, 2003, indicating the Amendment would be entered upon filing of an appeal.

(5) SUMMARY OF THE INVENTION

Appellants' invention is directed to polynucleotides and polypeptides, including polynucleotides, comprising the polynucleotide sequence of SEQ ID NO:64, encoding the human annexin (INTRA-12), comprising the amino acid sequence of SEQ ID NO:12, and polypeptides comprising the amino acid sequence of SEQ ID NO:12 (Specification, e.g., at page 7, line 18 through page 8, line 2). Appellants' invention also includes complementary polynucleotides (e.g., at page 9, lines 1-6), recombinant polynucleotides encoding polypeptides comprising SEQ ID NO:12 (e.g., at page 8, lines 9-12), host cells transformed with recombinant polynucleotides, and methods of making polypeptides encoded by the claimed polynucleotides (e.g., at page 8, lines 16-21, pages 31-36 and Example X at pages 67-68). In addition, Appellants' invention comprises polypeptides, including an isolated polypeptide comprising an amino acid sequence of

SEQ ID NO:12 and compositions comprising a polypeptide comprising an amino acid sequence of SEQ ID NO:12 and a pharmaceutically acceptable excipient (Specification, e.g., at page 9, lines 31-33).

INTRA-12 has chemical and structural homology to human annexin 31 (g3688370; Specification, e.g., Table 2). The polynucleotides and polypeptides of the present invention are useful, for example, for toxicology testing, drug discovery, and diagnosis, prevention, and treatment of cancer, immune disorders, neurological disorders, and gastrointestinal disorders.

(6) ISSUES

1. Whether claims 205, 206, 208, 209, 211-215, 217, 224-226, and 228-231 directed to INTRA polypeptide sequences and the polynucleotides that encode them meet the utility requirement of 35 U.S.C. §101.

2. Whether one of ordinary skill in the art would know how to use the claimed sequences, e.g., in toxicology testing, drug development, and the diagnosis of disease, so as to satisfy the enablement requirement of 35 U.S.C. §112, first paragraph.

(7) GROUPING OF THE CLAIMS

As to Issue 1

All of the claims on appeal are grouped together.

As to Issue 2

All of the claims on appeal are grouped together.

(8) APPELLANTS' ARGUMENTS

THE FINAL REJECTION

Claims 205, 206, 208, 209, 211-215, 217, 224-226, and 228-231 stand rejected under 35 U.S.C. §§ 101 and 112, first paragraph, based on the allegation that the claimed invention lacks patentable utility. The rejection alleges in particular that:

- the claimed invention is not supported by either a specific and substantial asserted utility or a well-established utility. The specification discloses no uses for the broadly-claimed polynucleotides and polypeptides. A specific utility is one that is particular to the subject matter claimed, while a substantial utility is one that defines a “real world” use. Utilities that require or constitute carrying out further research to identify or reasonably confirm a “real world” context of use are not substantial utilities.
- there is no well-established, specific and substantial utility for the claimed polynucleotides and polypeptides because the function of the polypeptide of SEQ ID NO:12 has not been empirically determined; therefore, further experimentation would be required to determine the function of the protein.
- the specification does not disclose whether the polynucleotide of SEQ ID NO:64 is differentially expressed in different cells or tissues, and therefore the gene is not a disease marker or an appropriate target for drug discovery or toxicology testing.
- the utility of the claimed polynucleotides in toxicology testing is not specific because if any polynucleotide expressed in a human has utility in toxicology testing, then that polynucleotide has no specific utility as all polynucleotides would have such use.

Issue 1 – Whether the claims meet the utility requirement of 35 U.S.C. § 101

The rejection of claims 205, 206, 208, 209, 211-215, 217, 224-226, and 228-231 is improper, as the inventions of those claims have a patentable utility as set forth in the instant specification, and/or a utility well known to one of ordinary skill in the art.

The invention at issue is a polynucleotide sequence corresponding to a gene that is expressed in reproductive, gastrointestinal, and nervous system tissues (Specification at Table 3). The invention also comprises polypeptides encoded by the claimed polynucleotides. As such, the claimed invention has numerous practical, beneficial uses in toxicology testing, drug development, and the diagnosis of disease, none of which require knowledge of how the polypeptide actually functions.

The similarity of the claimed polypeptide to another polypeptide of known, undisputed utility by itself demonstrates utility beyond the reasonable probability required by law. INTRA-12 is, in that regard, homologous to human annexin 31 (g3688370) (Specification, e.g., at Table 2). In particular, SEQ ID NO:12 shares 98% sequence identity with annexin 31.

This is more than enough homology to demonstrate a reasonable probability that the utility of annexin 31 receptor can be imputed to the claimed invention. It is well-known that the probability that two unrelated polypeptides share more than 40% sequence homology over 70 amino acid residues is exceedingly small. Brenner *et al.*, Proc. Natl. Acad. Sci. U.S.A. 95:6073-78 (1998). Given homology in excess of 40% over many more than 70 amino acid residues, the probability that the claimed polypeptide is related to annexin 31 is, accordingly, very high.

The fact that the claimed polypeptide is a member of the annexin family alone demonstrates utility. Each of the members of this class, regardless of their particular functions, are useful. There is no evidence that any member of this class of polypeptides, let alone a substantial number of them, would not have some patentable utility. It follows that there is a more than substantial likelihood that the claimed polypeptide also has patentable utility, regardless of its actual function. The law has never required a patentee to prove more.

There is, in addition, direct proof of the utility of the claimed invention. Appellants submitted previously the Declarations of Bedilion and Furness describing some of the practical uses of the claimed invention in gene and protein expression monitoring applications as they would have been understood at the time of the patent application.

The Bedilion Declaration describes, in particular, how the claimed expressed polynucleotide can be used in gene expression monitoring applications that were well-known at the time the patent application was filed, and how those applications are useful in developing drugs and monitoring their activity. Dr. Bedilion states that the claimed invention is a useful tool when employed as a highly specific probe in a cDNA microarray:

Persons skilled in the art would appreciate that cDNA microarrays that contained the SEQ ID NO:12-encoding polynucleotides would be a more useful tool than cDNA microarrays that did not contain the polynucleotides in connection with conducting gene expression monitoring studies on proposed (or actual) drugs for treating cancer, immune disorders, neurological disorders, and gastrointestinal disorders for such purposes as evaluating their efficacy and toxicity.

The Patent Examiner does not dispute that the claimed polynucleotide can be used as a probe in cDNA microarrays and used in gene expression monitoring applications. Instead, the Patent Examiner contends that the claimed polynucleotide cannot be useful without precise knowledge of its biological function. But the law never has required knowledge of biological function to prove utility. It is the claimed invention's uses, not its functions, that are the subject of a proper analysis under the utility requirement.

In any event, as demonstrated by the Bedilion Declaration, the person of ordinary skill in the art can achieve beneficial results from the claimed polynucleotide in the absence of any knowledge as to the precise function of the protein encoded by it. The uses of the claimed polynucleotide in gene expression monitoring applications are in fact independent of its precise function.

The Furness Declaration describes, in particular, how the claimed polypeptide can be used in protein expression analysis techniques such as 2-D PAGE gels and western blots. Using the claimed invention with these techniques, persons of ordinary skill in the art can better assess, for example, the potential toxic affect of a drug candidate. (Furness Declaration at ¶ [11]).

The Patent Examiner does not dispute that the claimed polypeptide can be used in 2-D PAGE gels and western blots to perform drug toxicity testing. Instead, the Patent Examiner contends that the claimed polypeptide cannot be useful without precise knowledge of its function. But the law never has required knowledge of biological function to prove utility. It is the claimed invention's uses, not its functions, that are the subject of a proper analysis under the utility requirement.

In any event, as demonstrated by the Furness Declaration, the person of ordinary skill in the art can achieve beneficial results from the claimed polypeptide in the absence of any knowledge as to the precise function of the protein. The uses of the claimed polypeptide for gene expression monitoring applications including toxicology testing are in fact independent of its precise function.

I. The Applicable Legal Standard

To meet the utility requirement of sections 101 and 112 of the Patent Act, the patent applicant need only show that the claimed invention is "practically useful," *Anderson v. Natta*,

480 F.2d 1392, 1397, 178 USPQ 458 (CCPA 1973) and confers a “specific benefit” on the public. *Brenner v. Manson*, 383 U.S. 519, 534-35, 148 USPQ 689 (1966). As discussed in a recent Court of Appeals for the Federal Circuit case, this threshold is not high:

An invention is “useful” under section 101 if it is capable of providing some identifiable benefit. See *Brenner v. Manson*, 383 U.S. 519, 534 [148 USPQ 689] (1966); *Brooktree Corp. v. Advanced Micro Devices, Inc.*, 977 F.2d 1555, 1571 [24 USPQ2d 1401] (Fed. Cir. 1992) (“to violate Section 101 the claimed device must be totally incapable of achieving a useful result”); *Fuller v. Berger*, 120 F. 274, 275 (7th Cir. 1903) (test for utility is whether invention “is incapable of serving any beneficial end”).

Juicy Whip Inc. v. Orange Bang Inc., 51 USPQ2d 1700 (Fed. Cir. 1999).

While an asserted utility must be described with specificity, the patent applicant need not demonstrate utility to a certainty. In *Stiftung v. Renishaw PLC*, 945 F.2d 1173, 1180, 20 USPQ2d 1094 (Fed. Cir. 1991), the United States Court of Appeals for the Federal Circuit explained:

An invention need not be the best or only way to accomplish a certain result, and it need only be useful to some extent and in certain applications: “[T]he fact that an invention has only limited utility and is only operable in certain applications is not grounds for finding lack of utility.” *Envirotech Corp. v. Al George, Inc.*, 730 F.2d 753, 762, 221 USPQ 473, 480 (Fed. Cir. 1984).

The specificity requirement is not, therefore, an onerous one. If the asserted utility is described so that a person of ordinary skill in the art would understand how to use the claimed invention, it is sufficiently specific. See *Standard Oil Co. v. Montedison, S.p.a.*, 212 U.S.P.Q. 327, 343 (3d Cir. 1981). The specificity requirement is met unless the asserted utility amounts to a “nebulous expression” such as “biological activity” or “biological properties” that does not convey meaningful information about the utility of what is being claimed. *Cross v. Iizuka*, 753 F.2d 1040, 1048 (Fed. Cir. 1985).

In addition to conferring a specific benefit on the public, the benefit must also be “substantial.” *Brenner*, 383 U.S. at 534. A “substantial” utility is a practical, “real-world” utility. *Nelson v. Bowler*, 626 F.2d 853, 856, 206 USPQ 881 (CCPA 1980).

If persons of ordinary skill in the art would understand that there is a “well-established” utility for the claimed invention, the threshold is met automatically and the applicant need not make any showing to demonstrate utility. Manual of Patent Examination Procedure at

§ 706.03(a). Only if there is no “well-established” utility for the claimed invention must the applicant demonstrate the practical benefits of the invention. *Id.*

Once the patent applicant identifies a specific utility, the claimed invention is presumed to possess it. *In re Cortright*, 165 F.3d 1353, 1357, 49 USPQ2d 1464 (Fed. Cir. 1999); *In re Brana*, 51 F.3d 1560, 1566; 34 USPQ2d 1436 (Fed. Cir. 1995). In that case, the Patent Office bears the burden of demonstrating that a person of ordinary skill in the art would reasonably doubt that the asserted utility could be achieved by the claimed invention. *Id.* To do so, the Patent Office must provide evidence or sound scientific reasoning. See *In re Langer*, 503 F.2d 1380, 1391-92, 183 USPQ 288 (CCPA 1974). If and only if the Patent Office makes such a showing, the burden shifts to the applicant to provide rebuttal evidence that would convince the person of ordinary skill that there is sufficient proof of utility. *Brana*, 51 F.3d at 1566. The applicant need only prove a “substantial likelihood” of utility; certainty is not required. *Brenner*, 383 U.S. at 532.

II. Uses of the claimed polypeptides and polynucleotides for diagnosis of conditions and disorders characterized by expression of INTRA, for toxicology testing, and for drug discovery are sufficient utilities under 35 U.S.C. §§ 101 and 112, first paragraph

The claimed invention meets all of the necessary requirements for establishing a credible utility under the Patent Law: There are “well-established” uses for the claimed invention known to persons of ordinary skill in the art, and there are specific practical and beneficial uses for the invention disclosed in the patent application’s specification. These uses are explained, in detail, in the Bedilion Declaration and the Furness Declaration accompanying this brief. Objective evidence, not considered by the Patent Office, further corroborates the credibility of the asserted utilities.

A. The use of INTRA for toxicology testing, drug discovery, and disease diagnosis are practical uses that confer "specific benefits" to the public

The claimed invention has specific, substantial, real-world utility by virtue of its use in toxicology testing, drug development and disease diagnosis through gene expression profiling. These uses are explained in detail in the accompanying Bedilion Declaration and Furness Declaration, the substance of which is not rebutted by the Patent Examiner. There is no dispute that the claimed polynucleotide is in fact a useful tool in cDNA microarrays used to perform gene expression analysis and that the claimed polypeptide is a useful tool in two-dimensional polyacrylamide gel electrophoresis ("2-D PAGE") analysis and western blots used to monitor protein expression and assess drug toxicity. These uses are sufficient to establish utilities for the claimed polynucleotide and polypeptide, respectively.

The instant application claims priority to United States Provisional Patent Application Serial No. 60/139,566 filed on June 16, 1999 (hereinafter "the Yue '566 application").

1. The Bedilion Declaration

In his Declaration, Dr. Bedilion explains the many reasons why a person skilled in the art reading the Yue '566 application on June 16, 1999 would have understood that application to disclose the claimed polynucleotide to be useful for a number of gene expression monitoring applications, *e.g.*, as a highly specific probe for the expression of that specific polynucleotide in connection with the development of drugs and the monitoring of the activity of such drugs. (Bedilion Declaration at, *e.g.*, ¶¶ 10-15). Much, but not all, of Dr. Bedilion's explanation concerns the use of the claimed polynucleotide in cDNA microarrays of the type first developed at Stanford University for evaluating the efficacy and toxicity of drugs, as well as for other applications. (Bedilion Declaration, ¶¶ 12 and 15).¹

In connection with his explanations, Dr. Bedilion states that the "Yue '566 specification would have led a person skilled in the art on June 16, 1999 who was using gene expression

¹Dr. Bedilion also explained, for example, why persons skilled in the art would also appreciate, based on the Yue '566 specification, that the claimed polynucleotide would be useful in connection with developing new drugs using technology, such as Northern analysis, that predated by many years the development of the cDNA technology (Bedilion Declaration, ¶ 16).

monitoring in connection with working on developing new drugs for the treatment of cancer, immune disorders, neurological disorders, and gastrointestinal disorders [a] to conclude that a cDNA microarray that contained the SEQ ID NO:12-encoding polynucleotides would be a highly useful tool, and [b] to request specifically that any cDNA microarray that was being used for such purposes contain the SEQ ID NO:12-encoding polynucleotides” (Bedilion Declaration, ¶ 15). For example, as explained by Dr. Bedilion, “[p]ersons skilled in the art would [have appreciated on June 16, 1999] that a cDNA microarray that contained the SEQ ID NO:12-encoding polynucleotides would be a more useful tool than a cDNA microarray that did not contain the polynucleotides in connection with conducting gene expression monitoring studies on proposed (or actual) drugs for treating cancer, immune disorders, neurological disorders, and gastrointestinal disorders for such purposes as evaluating their efficacy and toxicity.” *Id.*

In support of those statements, Dr. Bedilion provided detailed explanations of how cDNA technology can be used to conduct gene expression monitoring evaluations, with extensive citations to pre-June 16, 1999 publications showing the state of the art on June 16, 1999. (Bedilion Declaration, ¶ ¶ 10-14). While Dr. Bedilion’s explanations in paragraph 15 of his Declaration include almost three pages of text and six subparts (a)-(f), he specifically states that his explanations are not “all-inclusive.” *Id.* For example, with respect to toxicity evaluations, Dr. Bedilion had earlier explained how persons skilled in the art who were working on drug development on June 16, 1999 (and for several years prior to June 16, 1999) “without any doubt” appreciated that the toxicity (or lack of toxicity) of any proposed drug was “one of the most important criteria to be evaluated in connection with the development of the drug” and how the teachings of the Yue ‘566 application clearly include using differential gene expression analyses in toxicity studies (Bedilion Declaration, ¶ 10).

Thus, the Bedilion Declaration establishes that persons skilled in the art reading the Yue ‘566 application at the time it was filed “would have wanted their cDNA microarray to have a [SEQ ID NO:12-encoding polynucleotide probe] because a microarray that contained such a probe (as compared to one that did not) would provide more useful results in the kind of gene expression monitoring studies using cDNA microarrays that persons skilled in the art have been doing since well prior to June 16, 1999” (Bedilion Declaration, ¶ 15, item (f)). This, by itself, provides more than sufficient reason to compel the conclusion that the Yue ‘566 application

disclosed to persons skilled in the art at the time of its filing substantial, specific and credible real-world utilities for the claimed polynucleotide.

Nowhere does the Patent Examiner address the fact that, as described on pp. 33-34 of the Yue '566 application, the claimed polynucleotides can be used as highly specific probes in, for example, cDNA microarrays – probes that without question can be used to measure both the existence and amount of complementary RNA sequences known to be the expression products of the claimed polynucleotides. The claimed invention is not, in that regard, some random sequence whose value as a probe is speculative or would require further research to determine.

Given the fact that the claimed polynucleotide is known to be expressed, its utility as a measuring and analyzing instrument for expression levels is as indisputable as a scale's utility for measuring weight. This use as a measuring tool, regardless of how the expression level data ultimately would be used by a person of ordinary skill in the art, by itself demonstrates that the claimed invention provides an identifiable, real-world benefit that meets the utility requirement. *Raytheon v. Roper*, 724 F.2d 951, (Fed. Cir. 1983) (claimed invention need only meet one of its stated objectives to be useful); *In re Cortwright*, 165 F.3d 1353, 1359 (Fed. Cir. 1999) (how the invention works is irrelevant to utility); MPEP § 2107 (“Many research tools such as gas chromatographs, screening assays, and nucleotide sequencing techniques have a clear, specific, and unquestionable utility (e.g., they are useful in analyzing compounds)” (emphasis added)).

Though Applicants need not so prove to demonstrate utility, there can be no reasonable dispute that persons of ordinary skill in the art have numerous uses for information about relative gene expression including, for example, understanding the effects of a potential drug for treating cancer, immune disorders, neurological disorders, and gastrointestinal disorders. Because the patent application states explicitly that the claimed polynucleotide is known to be expressed in reproductive, gastrointestinal, and nervous system tissues and in tissues associated with cancer and inflammation (see the Yue '566 application at Table 3), and expresses a protein that is a member of the annexin family known to be associated with diseases such as cancer, immune disorders, neurological disorders, and gastrointestinal disorders, there can be no reasonable dispute that a person of ordinary skill in the art could put the claimed invention to such use. In other words, the person of ordinary skill in the art can derive more information about a potential cancer, immune disorders, neurological disorders, and gastrointestinal disorders drug candidate

or potential toxin with the claimed invention than without it (see Bedilion Declaration at, e.g., ¶ 15, subparts (e)-(f)).

The Bedilion Declaration shows that a number of pre-June 16, 1999 publications confirm and further establish the utility of cDNA microarrays in a wide range of drug development gene expression monitoring applications at the time the Yue '566 application was filed (Bedilion Declaration ¶¶ 10-14; Bedilion Exhibits A-G). Indeed, Brown and Shalon U.S. Patent No. 5,807,522 (the Brown '522 patent, Bedilion Exhibit D), which issued from a patent application filed in June 1995 and was effectively published on December 29, 1995 as a result of the publication of a PCT counterpart application, shows that the Patent Office recognizes the patentable utility of the cDNA technology developed in the early to mid-1990s. As explained by Dr. Bedilion, among other things (Bedilion Declaration, ¶ 12):

The Brown '522 patent further teaches that the "[m]icroarrays of immobilized nucleic acid sequences prepared in accordance with the invention" can be used in "numerous" genetic applications, including "monitoring of gene expression" applications (see Bedilion Tab D at col. 14, lines 36-42). The Brown '522 patent teaches (a) monitoring gene expression (i) in different tissue types, (ii) in different disease states, and (iii) in response to different drugs, and (b) that arrays disclosed therein may be used in toxicology studies (see Bedilion Tab D at col. 15, lines 13-18 and 52-58 and col. 18, lines 25-30).

Literature reviews published shortly after the filing of the Yue '566 application describing the state of the art further confirm the claimed invention's utility. Rockett et al. confirm, for example, that the claimed invention is useful for differential expression analysis regardless of how expression is regulated:

Despite the development of multiple technological advances which have recently brought the field of gene expression profiling to the forefront of molecular analysis, recognition of the importance of differential gene expression and characterization of differentially expressed genes has existed for many years.

* * *

Although differential expression technologies are applicable to a broad range of models, perhaps their most important advantage is that, in most cases, absolutely no prior knowledge of the specific genes which are up- or down-regulated is required.

* * *

Whereas it would be informative to know the identity and functionality of all genes up/down regulated by . . . toxicants, this would appear a longer term goal However, the current use of gene profiling yields a *pattern* of gene changes for a xenobiotic of unknown toxicity which may be matched to that of well characterized toxins, thus alerting the toxicologist to possible *in vivo* similarities between the unknown and the standard, thereby providing a platform for more extensive toxicological examination. (emphasis added)

Rockett et al., Differential gene expression in drug metabolism and toxicology: practicalities, problems and potential, 29 Xenobiotica No. 7, 655 (1999).

In another pre-June 16, 1999 article, Lashkari et al. state explicitly that sequences that are merely “predicted” to be expressed (predicted Open Reading Frames, or ORFs) – the claimed invention in fact is known to be expressed – have numerous uses:

Efforts have been directed toward the amplification of each predicted ORF or any other region of the genome ranging from a few base pairs to several kilobase pairs. There are many uses for these amplicons– they can be cloned into standard vectors or specialized expression vectors, or can be cloned into other specialized vectors such as those used for two-hybrid analysis. The amplicons can also be used directly by, for example, arraying onto glass for expression analysis, for DNA binding assays, or for any direct DNA assay.

Lashkari et al., Whole genome analysis: Experimental access to all genome sequenced segments through larger-scale efficient oligonucleotide synthesis and PCR, 94 Proc. Nat. Acad. Sci. 8945 (Aug. 1997) (emphasis added).

In his Declaration, Mr. Furness explains the many reasons why a person skilled in the art who read the Yue ‘566 application on June 16, 1999 would have understood that application to disclose the claimed polypeptide to be useful for a number of gene and protein expression monitoring applications, *e.g.*, in 2-D PAGE technologies, in connection with the development of drugs and the monitoring of the activity of such drugs. (Furness Declaration at, *e.g.*, ¶¶ 10-14). Much, but not all, of Mr. Furness’ explanation concerns the use of the claimed polypeptide in the creation of protein expression maps using 2-D PAGE.

2-D PAGE technologies were developed during the 1980’s. Since the early 1990’s, 2-D PAGE has been used to create maps showing the differential expression of proteins in different cell types or in similar cell types in response to drugs and potential toxic agents. Each expression pattern reveals the state of a tissue or cell type in its given environment, *e.g.*, in the presence or

absence of a drug. By comparing a map of cells treated with a potential drug candidate to a map of cells not treated with the candidate, for example, the potential toxicity of a drug can be assessed. (Furness Declaration at ¶ 10.)

The claimed invention makes 2-D PAGE analysis a more powerful tool for toxicology and drug efficacy testing. A person of ordinary skill in the art can derive more information about the state or states or tissue or cell samples from 2-D PAGE analysis with the claimed invention than without it. As Mr. Furness explains:

In view of the Yue '566 application, the Wilkins article, and other related pre-June 1999 publications, persons skilled in the art on June 16, 1999 clearly would have understood the Yue '566 application to disclose the SEQ ID NO:12 polypeptide to be useful in 2-D PAGE analyses for the development of new drugs and monitoring the activities of drugs for such purposes as evaluating their efficacy and toxicity (Furness Declaration, ¶10)

* * *

Persons skilled in the art would appreciate that a 2-D PAGE map that utilized the SEQ ID NO:12 polypeptide sequence would be a more useful tool than a 2-D PAGE map that did not utilize this protein sequence in connection with conducting protein expression monitoring studies on proposed (or actual) drugs for treating cancer, immune disorders, neurological disorders, and gastrointestinal disorders for such purposes as evaluating their efficacy and toxicity. (Furness Declaration, ¶12)

Mr. Furness' observations are confirmed in the literature published before the filing of the patent application. Wilkins, for example, describes how 2-D gels are used to define proteins present in various tissues and measure their levels of expression, the data from which is in turn used in databases:

For proteome projects, the aim of [computer-aided 2-D PAGE] analysis . . . is to catalogue all spots from the 2-D gel in a qualitative and if possible quantitative manner, so as to define the number of proteins present and their levels of expression. Reference gel images, constructed from one or more gels, for the basis of two-dimensional gel databases. (Wilkins, Tab C, p. 26).

B. The use of polynucleotides and polypeptides expressed by humans as tools for toxicology testing, drug discovery, and the diagnosis of disease is now "well-established"

The technologies made possible by expression profiling using polynucleotides and polypeptides are now well-established. The technical literature recognizes not only the prevalence of these technologies, but also their unprecedented advantages in drug development, testing and safety assessment. These technologies include toxicology testing, as described by Bedilion and Furness in their Declarations.

Toxicology testing is now standard practice in the pharmaceutical industry. See, e.g., John C. Rockett et al., *supra*:

Knowledge of toxin-dependent regulation in target tissues is not solely an academic pursuit as much interest has been generated in the pharmaceutical industry to harness this technology in the early identification of toxic drug candidates, thereby shortening the developmental process and contributing substantially to the safety assessment of new drugs.

To the same effect are several other scientific publications, including Emile F. Nuwaysir et al., Microarrays and Toxicology: The Advent of Toxicogenomics, 24 Molecular Carcinogenesis 153 (1999); Sandra Steiner and N. Leigh Anderson, Expression profiling in toxicology -- potentials and limitations, 112-13 Toxicology Letters 467 (2000).

Nucleic acids useful for measuring the expression of whole classes of genes are routinely incorporated for use in toxicology testing. Nuwaysir et al. describes, for example, a Human ToxChip comprising 2089 human clones, which were selected

for their well-documented involvement in basic cellular processes as well as their responses to different types of toxic insult. Included on this list are DNA replication and repair genes, apoptosis genes, and genes responsive to PAHs and dioxin-like compounds, peroxisome proliferators, estrogenic compounds, and oxidant stress. Some of the other categories of genes include transcription factors, oncogenes, tumor suppressor genes, cyclins, kinases, phosphatases, cell adhesion and motility genes, and homeobox genes. Also included in this group are 84 housekeeping genes, whose hybridization intensity is averaged and used for signal normalization of the other genes on the chip.

See also Table 1 of Nuwaysir et al. (listing additional classes of genes deemed to be of special interest in making a human toxicology microarray).

The more genes that are available for use in toxicology testing, the more powerful the technique. "Arrays are at their most powerful when they contain the entire genome of the species they are being used to study." John C. Rockett and David J. Dix, Application of DNA Arrays to Toxicology, 107 Environ. Health Perspec. 681, No. 8 (1999). Control genes are carefully selected for their stability across a large set of array experiments in order to best study the effect of toxicological compounds. See attached email from the primary investigator on the Nuwaysir paper, Dr. Cynthia Afshari, to an Incyte employee, dated July 3, 2000, as well as the original message to which she was responding, indicating that even the expression of carefully selected control genes can be altered. Thus, there is no expressed gene which is irrelevant to screening for toxicological effects, and all expressed genes have a utility for toxicological screening.

In fact, the potential benefit to the public, in terms of lives saved and reduced health care costs, are enormous. Recent developments provide evidence that the benefits of this information are already beginning to manifest themselves. Examples include the following:

- In 1999, CV Therapeutics, an Incyte collaborator, was able to use Incyte gene expression technology, information about the structure of a known transporter gene, and chromosomal mapping location, to identify the key gene associated with Tangiers disease. This discovery took place over a matter of only a few weeks, due to the power of these new genomics technologies. The discovery received an award from the American Heart Association as one of the top 10 discoveries associated with heart disease research in 1999.
- In an April 9, 2000, article published by the Bloomberg news service, an Incyte customer stated that it had reduced the time associated with target discovery and validation from 36 months to 18 months, through use of Incyte's genomic information database. Other Incyte customers have privately reported similar experiences. The implications of this significant saving of time and expense for the number of drugs that may be developed and their cost are obvious.
- In a February 10, 2000, article in the *Wall Street Journal*, one Incyte customer stated that over 50 percent of the drug targets in its current pipeline were derived from the Incyte database. Other Incyte customers have privately reported similar experiences. By doubling the number of targets available to pharmaceutical researchers, Incyte genomic information has demonstrably accelerated the development of new drugs.

C. The similarity of the claimed polypeptide to another of undisputed utility demonstrates utility

Because there is a substantial likelihood that the claimed INTRA-12 is functionally related to annexin 31 and pemphaxin, a polypeptide of undisputed utility, there is by implication a substantial likelihood that the claimed polypeptide and the polynucleotide that encodes it are similarly useful. Appellants need not show any more to demonstrate utility. *In re Brana*, 51 F.3d at 1567.

It is undisputed that the polypeptide encoded for by the claimed polynucleotide shares more than 98% sequence identity over 345 amino acid residues with annexin 31 (g3688370) (Specification, e.g., at Table 2). The presence of multiple annexin domain signatures in SEQ ID NO:12 indicates that INTRA-12 is a member of the annexin family (see specification at Table 2). Members of the annexin family are known to function in phospholipid binding, membrane-cytoskeleton interactions, phospholipase inhibition, anticoagulation, and membrane fusion (Specification at page 4, lines 18-24) and have been implicated in cancer, neurodegenerative diseases, autoimmune diseases, and inflammatory bowel diseases (enclosed references of Bastian (1997) *Cell. Mol. Life Sci.* 53:554-556; Eberhard et al. (1994) *Am. J. Pathol.* 145:640-649; and Gerke and Moss (2002) *Physiol. Rev.* 82:331-371).

CLUSTALW analysis shows that SEQ ID NO:12 is 99.7% identical to pemphaxin (see Exhibit C of the Response to the Final Office Action of June 30, 2003). Although, the Examiner argues that SEQ ID NO:12 is "structurally distinct from pemphaxin" and therefore "cannot be pemphaxin" (Advisory Action, page 6), Applicants note that the sequence of SEQ ID NO:12 and pemphaxin share 344 out of 345 residues in common. Thus, SEQ ID NO:12 is pemphaxin. Pemphaxin acts as a cell surface cholinergic receptor involved in the regulation of keratinocyte cell adhesion and is known to be associated with the autoimmune disorder, pemphigus vulgaris (see article of Nguyen *et al.* *J. Biol. Chem.* (2000) 275:29466-29476, previously submitted as Exhibit B of the Response to the Final Office Action of June 30, 2003). Nguyen et al. identified pemphaxin in a screen for self-antigens recognized by pathogenic autoantibodies associated with the autoimmune disorder pemphigus vulgaris. Pemphaxin is believed to be one of the major proteins targeted by the autoimmune disorder. This corroborates the statement on page 7 of the

Specification that the SEQ ID NO:12 polypeptide and the polynucleotides encoding it may be useful in the diagnosis and treatment of autoimmune disorders.

Members of the annexin class of proteins have been found to be useful cell markers because of their phospholipid binding properties and their association with the plasma membrane (See the response to the Office Action of January 10, 2003 at page 22). Annexin V has been used in radionuclide imaging as a marker of apoptosis to monitor the changes in phospholipid distribution that accompany cell death (enclosed references of Blankenberg et al. (1998) Proc. Natl. Acad. Sci. U.S.A. 95:6349-6354 and Blankenberg et al. (2000) Eur. J. Nucl. Med. 27:359-367). Radionuclide imaging with radiolabeled annexins may be useful for diagnosis of stroke, neurodegenerative diseases, inflammatory diseases, myocardial ischemia, myelodysplastic disorders, organ transplantation, and cancer.

Although, the Examiner has pointed out the absence of type II calcium binding sites in annexin 31, and argues that the SEQ ID NO:12 protein "would not have the phospholipid binding ability of other annexins" (Final Office Acton, page 22), Applicants disagree. Other members of the annexin family display both calcium-dependent and calcium-independent binding to phospholipids. For example, annexin I has a calcium-independent form that associates with membranes in the absence of calcium. Phosphorylation of the calcium-independent form of annexin I by epidermal growth factor kinase converts annexin I to a calcium-dependent form that requires calcium for membrane association (See enclosed reference of Futter et al. (1993) J. Cell Biol. 120:77-83). Annexin II, annexin A11, and annexin XIII also are able to associate with membranes in the absence of calcium. (Also see the enclosed references of Jost et al. (1997) J. Cell Science 110:221-228, Lecona et al. (2003) Biochem. J. 373:437-449, and Lecat et al. (2000) J. Cell Science 113:2607-2618). Thus, the calcium binding site is not required in all annexins to confer phospholipid binding properties. The SEQ ID NO:12 polypeptide, as a member of the annexin family, more likely than not, is a phospholipid binding protein, and as such, is useful like other members of the annexin family.

The Examiner must accept the applicants' assertion that the polypeptide encoded for by the claimed invention is pemphaxin and thus has its utility unless the Examiner can demonstrate through evidence or sound scientific reasoning that a person of ordinary skill in the art would doubt that SEQ ID NO:12 is pemphaxin. See *In re Langer*, 503 F.2d 1380, 1391-92, 183 USPQ

288 (CCPA 1974). The Examiner has not provided sufficient evidence or sound scientific reasoning to the contrary.

While the Examiner has cited literature: Smith et al. (Nat. Biotech 15:1222-1223, 1997); Brenner et al. (Trends in Genetics, 15:132-133, 1999); and Seffernick et al. (J. Bacteriol. 183:2405-2410, 2001, identifying some of the difficulties that may be involved in predicting protein function, none suggests that functional homology cannot be inferred by a reasonable probability in this case. Most important, none contradicts Brenner's basic rule that sequence homology in excess of 40% over 70 or more amino acid residues yields a high probability of functional homology as well. At most, these articles individually and together stand for the proposition that it is difficult to make predictions about function with certainty. The standard applicable in this case is not, however, proof to certainty, but rather proof to reasonable probability.

The Seffernick et al. reference cited by the Examiner does not contradict the findings of Brenner et al. The Seffernick et al. reference describes two enzymes, a melamine deaminase and an atrazine chlorohydrolase, that are 98% identical, yet have different substrate specificities. These two enzymes belong to a class of bacterial amidohydrolases whose members catalyze the hydrolytic displacement of amino groups or chlorine substituents from triazine ring compounds. Notably, the substrates of the two enzymes, melamine and atrazine, have similar structures except that melamine possesses an amino group and atrazine possesses a chlorine substituent. Some other members of the amidohydrolase superfamily catalyze deamination and dechlorination reactions with both triazine ring substrates. Therefore, the 98% sequence homology between melamine deaminase and atrazine chlorohydrolase correctly predicts their functional similarity and their membership in a common enzyme family. As noted by the Examiner, Seffernick et al. recognize that "functional assignments based on >50% sequence identity are considered to be reasonably sound" (Seffernick et al., page 2409, left column, paragraph 2).

Furthermore, the Examiner has not provided evidence that any member of the annexin family, let alone a substantial number of those members, is not useful. In such circumstances, the only reasonable inference is that the polypeptide encoded by the claimed invention, like the other members of the annexin protein family, must be useful.

D. Objective evidence corroborates the utilities of the claimed invention

There is, in fact, no restriction on the kinds of evidence a Patent Examiner may consider in determining whether a “real-world” utility exists. Indeed, “real-world” evidence, such as evidence showing actual use or commercial success of the invention, can demonstrate conclusive proof of utility. *Raytheon v. Roper*, 220 USPQ2d 592 (Fed. Cir. 1983); *Nestle v. Eugene*, 55 F.2d 854, 856, 12 USPQ 335 (6th Cir. 1932). Indeed, proof that the invention is made, used or sold by any person or entity other than the patentee is conclusive proof of utility. *United States Steel Corp. v. Phillips Petroleum Co.*, 865 F.2d 1247, 1252, 9 USPQ2d 1461 (Fed. Cir. 1989).

Over the past several years, a vibrant market has developed for databases containing all expressed genes (along with the polypeptide translations of those genes), in particular genes having medical and pharmaceutical significance such as the instant sequence. (Note that while the value in these databases is enhanced by their completeness, each sequence in them is independently valuable nonetheless.) The databases sold by Appellants’ assignee, Incyte, include exactly the kinds of information made possible by the claimed invention, such as tissue and disease associations. Incyte sells its database containing the claimed sequence and millions of other sequences throughout the scientific community, including to pharmaceutical companies who use the information to develop new pharmaceuticals.

Both Incyte’s customers and the scientific community have acknowledged that Incyte’s databases have proven to be valuable in, for example, the identification and development of drug candidates. As Incyte adds information to its databases, including the information that can be generated only as a result of Incyte’s discovery of the claimed polynucleotide and its use of that polynucleotide on cDNA microarrays, the databases become even more powerful tools. Thus the claimed invention adds more than incremental benefit to the drug discovery and development process.

III. The Patent Examiner’s Rejections Are Without Merit

Rather than responding to the evidence demonstrating utility, the Examiner attempts to dismiss it altogether by arguing that the disclosed and well-established utilities for the claimed

polynucleotide and polypeptide are not "specific and substantial" utilities. (Office Action of January 10, 2003 at p. 4.) The Examiner is incorrect both as a matter of law and as a matter of fact.

A. The Precise Biological Role Or Function Of An Expressed Polynucleotide or Polypeptide Is Not Required To Demonstrate Utility

The Patent Examiner's primary rejection of the claimed invention is based on the ground that, without information as to the precise "biological role" of the claimed invention, the claimed invention's utility is not sufficiently specific. According to the Examiner, it is not enough that a person of ordinary skill in the art could use and, in fact, would want to use the claimed invention either by itself or in a microarray, 2-D gel or western blot to monitor the expression of genes for such applications as the evaluation of a drug's efficacy and toxicity. The Examiner would require, in addition, that the Appellant provide a specific and substantial interpretation of the results generated in any given expression analysis.

It may be that specific and substantial interpretations and detailed information on biological function are necessary to satisfy the requirements for publication in some technical journals, but they are not necessary to satisfy the requirements for obtaining a United States patent. The relevant question is not, as the Examiner would have it, whether it is known how or why the invention works, *In re Cortwright*, 165 F.3d 1353, 1359 (Fed. Cir. 1999), but rather whether the invention provides an "identifiable benefit" in presently available form. *Juicy Whip Inc. v. Orange Bang Inc.*, 185 F.3d 1364, 1366 (Fed. Cir. 1999). If the benefit exists, and there is a substantial likelihood the invention provides the benefit, it is useful. There can be no doubt, particularly in view of the Bedilion Declaration (at, *e.g.*, ¶¶ 10 and 15, Bedilion) and the Furness Declaration (at, *e.g.*, ¶¶ 10-13), that the present invention meets this test.

The threshold for determining whether an invention produces an identifiable benefit is low. *Juicy Whip*, 185 F.3d at 1366. Only those utilities that are so nebulous that a person of ordinary skill in the art would not know how to achieve an identifiable benefit and, at least according to the PTO guidelines, so-called "throwaway" utilities that are not directed to a person

of ordinary skill in the art at all, do not meet the statutory requirement of utility. Utility Examination Guidelines, 66 Fed. Reg. 1092 (Jan. 5, 2001).

Knowledge of the biological function or role of a biological molecule has never been required to show real-world benefit. In its most recent explanation of its own utility guidelines, the PTO acknowledged so much (66 F.R. at 1095):

[T]he utility of a claimed DNA does not necessarily depend on the function of the encoded-gene product. A claimed DNA may have specific and substantial utility because, *e.g.*, it hybridizes near a disease-associated gene or it has gene-regulating activity.

By implicitly requiring knowledge of biological function for any claimed nucleic acid, the Examiner has, contrary to law, elevated what is at most an evidentiary factor into an absolute requirement of utility. Rather than looking to the biological role or function of the claimed invention, the Examiner should have looked first to the benefits it is alleged to provide.

B. Membership in a Class of Useful Products Can Be Proof of Utility

Despite the uncontradicted evidence that the claimed polypeptide is related to pemphaxin, a member of the annexin family, whose members indisputably are useful, the Examiner refused to impute the utility of pemphaxin to INTRA-12. In the Office Action of January 10, 2003, the Patent Examiner takes the position that unless Appellants can identify which particular annexin function is possessed by INTRA-12, utility cannot be imputed.

In order to demonstrate utility by membership in a class, the law requires only that the class not contain a substantial number of useless members. So long as the class does not contain a substantial number of useless members, there is sufficient likelihood that the claimed invention will have utility, and a rejection under 35 U.S.C. § 101 is improper. That is true regardless of how the claimed invention ultimately is used and whether or not the members of the class possess one utility or many. *See Brenner v. Manson*, 383 U.S. 519, 532 (1966); *Application of Kirk*, 376 F.2d 936, 943 (CCPA 1967).

Membership in a “general” class is insufficient to demonstrate utility only if the class contains a sufficient number of useless members such that a person of ordinary skill in the art

could not impute utility by a substantial likelihood. There would be, in that case, a substantial likelihood that the claimed invention is one of the useless members of the class. In the few cases in which class membership did not prove utility by substantial likelihood, the classes did in fact include predominately useless members. *E.g.*, *Brenner* (man-made steroids); *Kirk* (same); *Natta* (man-made polyethylene polymers).

The Examiner addresses INTRA-12 as if the general class in which it is included is not the annexin family, but rather all polynucleotides or all polypeptides, including the vast majority of useless theoretical molecules not occurring in nature, and thus not pre-selected by nature to be useful. While these “general classes” may contain a substantial number of useless members, the annexin family does not. The annexin family is sufficiently specific to rule out any reasonable possibility that INTRA-12 would not also be useful like the other members of the family.

Because the Examiner has not presented any evidence that the annexin class of proteins has any, let alone a substantial number, of useless members, the Examiner must conclude that there is a “substantial likelihood” that the INTRA-12 encoded by the claimed polynucleotides is useful. It follows that SEQ ID NO:12 and SEQ ID NO:64 also are useful.

Even if the Examiner's “common utility” criterion were correct – and it is not – the annexin family would meet it. It is undisputed that known members of the annexin family function in phospholipid binding, membrane-cytoskeleton interactions, phospholipase inhibition, anticoagulation, and membrane fusion. A person of ordinary skill in the art need not know any more about how the claimed invention functions to use it, and the Examiner presents no evidence to the contrary. Instead, the Examiner makes the conclusory observation that a person of ordinary skill in the art would need to know whether, for example, any given annexin functions in phospholipid binding, membrane-cytoskeleton interactions, or phospholipase inhibition. The Examiner then goes on to assume that the only use for INTRA-12 absent knowledge as to how INTRA-12 actually works is further study of INTRA-12 itself.

Not so. As demonstrated by Appellants, knowledge that INTRA-12 is an annexin related to annexin 31 is more than sufficient to make it useful for the diagnosis and treatment of cancer, immune disorders, neurological disorders, and gastrointestinal disorders. The Examiner must accept these facts to be true unless the Examiner can provide evidence or sound scientific reasoning to the contrary. But the Examiner has not done so.

C. Because the uses of polynucleotides encoding INTRA in toxicology testing, drug discovery, and disease diagnosis are practical uses beyond mere study of the invention itself, the claimed invention has substantial utility.

The Examiner rejected the claims at issue on the ground that the use of an invention as tool for research is not a “substantial” use. Because the Examiner’s rejection assumes a substantial overstatement of the law, and is incorrect in fact, it must be overturned.

There is no authority for the proposition that use as a tool for research is not a substantial utility. Indeed, the Patent Office has recognized that just because an invention is used in a research setting does not mean that it lacks utility (MPEP § 2107):

Many research tools such as gas chromatographs, screening assays, and nucleotide sequencing techniques have a clear, specific and unquestionable utility (e.g., they are useful in analyzing compounds). An assessment that focuses on whether an invention is useful only in a research setting thus does not address whether the specific invention is in fact “useful” in a patent sense. Instead, Office personnel must distinguish between inventions that have a specifically identified utility and inventions whose specific utility requires further research to identify or reasonably confirm.

The Patent Office’s actual practice has been, at least until the present, consistent with that approach. It has routinely issued patents for inventions whose only use is to facilitate research, such as DNA ligases. These are acknowledged by the PTO’s Training Materials themselves to be useful, as well as DNA sequences used, for example, as markers.

Only a limited subset of research uses are not “substantial” utilities: those in which the only known use for the claimed invention is to be an **object** of further study, thus merely inviting further research. This follows from *Brenner*, in which the U.S. Supreme Court held that a process for making a compound does not confer a substantial benefit where the only known use of the compound was to be the object of further research to determine its use. *Id.* at 535. Similarly, in *Kirk*, the Court held that a compound would not confer substantial benefit on the public merely because it might be used to synthesize some other, unknown compound that would confer substantial benefit. *Kirk*, 376 F.2d at 940, 945 (“What Appellants are really saying to those in the art is take these steroids, experiment, and find what use they do have as medicines.”).

Nowhere do those cases state or imply, however, that a material cannot be patentable if it has some other beneficial use in research.

Such beneficial uses beyond studying the claimed invention itself have been demonstrated, in particular those described in the Bedilion and Furness Declarations. The claimed invention is a tool, rather than an object, of research. The data generated in gene expression monitoring using the claimed invention as a tool is **not** used merely to study the claimed polynucleotide itself, but rather to study properties of tissues, cells, and potential drug candidates and toxins. Without the claimed invention, the information regarding the properties of tissues, cells, drug candidates and toxins is less complete.

Moreover, as discussed above in section II D., SEQ ID NO:12 shares homology with other members of the annexin family. Therefore, the skilled artisan would have considered INTRA to be an important and valuable tool, in particular, for use in research on cancer, immune disorders, neurological disorders, and gastrointestinal disorders. The claimed invention has numerous other uses as a research tool, each of which alone is a "substantial utility." These include uses such as diagnostic assays (e.g., pages 51-56), chromosomal markers (e.g., pages 56-57), and ligand screening assays (e.g., page 36).

IV. By Requiring the Patent Applicant to Assert a Particular or Unique Utility, the Patent Examination Utility Guidelines and Training Materials Applied by the Patent Examiner Misstate the Law

There is an additional, independent reason to overturn the rejections: to the extent the rejections are based on Revised Interim Utility Examination Guidelines (64 FR 71427, December 21, 1999), the final Utility Examination Guidelines (66 FR 1092, January 5, 2001) and/or the Revised Interim Utility Guidelines Training Materials (USPTO Website www.uspto.gov, March 1, 2000), the Guidelines and Training Materials are themselves inconsistent with the law.

The Training Materials, which direct the Examiners regarding how to apply the Utility Guidelines, address the issue of specificity with reference to two kinds of asserted utilities:

“specific” utilities which meet the statutory requirements, and “general” utilities which do not. The Training Materials define a “specific utility” as follows:

A [specific utility] is *specific* to the subject matter claimed. This contrasts to *general* utility that would be applicable to the broad class of invention. For example, a claim to a polynucleotide whose use is disclosed simply as “gene probe” or “chromosome marker” would not be considered to be specific in the absence of a disclosure of a specific DNA target. Similarly, a general statement of diagnostic utility, such as diagnosing an unspecified disease, would ordinarily be insufficient absent a disclosure of what condition can be diagnosed.

The Training Materials distinguish between “specific” and “general” utilities by assessing whether the asserted utility is sufficiently “particular,” *i.e.*, unique (Training Materials at p.52) as compared to the “broad class of invention.” (In this regard, the Training Materials appear to parallel the view set forth in Stephen G. Kunin, Written Description Guidelines and Utility Guidelines, 82 J.P.T.O.S. 77, 97 (Feb. 2000) (“With regard to the issue of specific utility the question to ask is whether or not a utility set forth in the specification is *particular* to the claimed invention.”)).

Such “unique” or “particular” utilities never have been required by the law. To meet the utility requirement, the invention need only be “practically useful,” *Natta*, 480 F.2d 1 at 1397, and confer a “specific benefit” on the public. *Brenner*, 383 U.S. at 534. Thus, incredible “throw-away” utilities, such as trying to “patent a transgenic mouse by saying it makes great snake food,” do not meet this standard. Karen Hall, Genomic Warfare, *The American Lawyer* 68 (June 2000) (quoting John Doll, Chief of the Biotech Section of USPTO).

This does not preclude, however, a general utility, contrary to the statement in the Training Materials where “specific utility” is defined (page 5). Practical real-world uses are not limited to uses that are unique to an invention. The law requires that the practical utility be “definite,” not particular. *Montedison*, 664 F.2d at 375. Appellant is not aware of any court that has rejected an assertion of utility on the grounds that it is not “particular” or “unique” to the specific invention. Where courts have found utility to be too “general,” it has been in those cases in which the asserted utility in the patent disclosure was not a practical use that conferred a specific benefit. That is, a person of ordinary skill in the art would have been left to guess as to

how to benefit at all from the invention. In *Kirk*, for example, the CCPA held the assertion that a man-made steroid had “useful biological activity” was insufficient where there was no information in the specification as to how that biological activity could be practically used. *Kirk*, 376 F.2d at 941.

The fact that an invention can have a particular use does not provide a basis for requiring a particular use. See *Brana, supra* (disclosure describing a claimed antitumor compound as being homologous to an antitumor compound having activity against a “particular” type of cancer was determined to satisfy the specificity requirement). “Particularity” is not and never has been the *sine qua non* of utility; it is, at most, one of many factors to be considered.

As described *supra*, broad classes of inventions can satisfy the utility requirement so long as a person of ordinary skill in the art would understand how to achieve a practical benefit from knowledge of the class. Only classes that encompass a significant portion of nonuseful members would fail to meet the utility requirement. *Supra* § II.B.2 (*Montedison*, 664 F.2d at 374-75).

The Training Materials fail to distinguish between broad classes that convey information of practical utility and those that do not, lumping all of them into the latter, unpatentable category of “general” utilities. As a result, the Training Materials paint with too broad a brush. Rigorously applied, they would render unpatentable whole categories of inventions that heretofore have been considered to be patentable and that have indisputably benefitted the public, including the claimed invention. See *supra* § II.B. Thus the Training Materials cannot be applied consistently with the law.

Issue 2 – Whether claims 205, 206, 208, 209, 211-215, 217, 224-226, and 228-231 meet the enablement requirement of 35 U.S.C. § 112, first paragraph

To the extent the rejection of the claimed invention under 35 U.S.C. § 112, first paragraph, is based on the improper rejection for lack of utility under 35 U.S.C. § 101, it must be reversed.

The rejection set forth in the Office Action is based on the assertions discussed above, i.e., that the claimed invention lacks patentable utility. To the extent that the rejection under § 112, first paragraph, is based on the improper allegation of lack of patentable utility under § 101, it fails for the same reasons.

CONCLUSION

Appellants respectfully submit that rejections for lack of utility based, *inter alia*, on an allegation of "lack of specificity," as set forth in the Office Action and as justified in the Revised Interim and final Utility Guidelines and Training Materials, are not supported in the law. Neither are they scientifically correct, nor supported by any evidence or sound scientific reasoning. These rejections are alleged to be founded on facts in court cases such as *Brenner* and *Kirk*, yet those facts are clearly distinguishable from the facts of the instant application, and indeed most if not all nucleotide and protein sequence applications. Nevertheless, the PTO is attempting to mold the facts and holdings of these prior cases, "like a nose of wax,"² to target rejections of claims to polypeptide and polynucleotide sequences, as well as to claims to methods of detecting said polynucleotide sequences, where biological activity information has not been proven by laboratory experimentation, and they have done so by ignoring perfectly acceptable utilities fully disclosed in the specifications as well as well-established utilities known to those of skill in the art. As is disclosed in the specification, and even more clearly, as one of ordinary skill in the art would understand, the claimed invention has well-established, specific, substantial and credible utilities. The rejections are, therefore, improper and should be reversed.

Moreover, to the extent the above rejections were based on the Revised Interim and final Examination Guidelines and Training Materials, those portions of the Guidelines and Training Materials that form the basis for the rejections should be determined to be inconsistent with the law.

Due to the urgency of this matter, including its economic and public health implications, an expedited review of this appeal is earnestly solicited.

If the USPTO determines that any additional fees are due, the Commissioner is hereby authorized to charge Deposit Account No. **09-0108**.

This brief is enclosed in triplicate

²"The concept of patentable subject matter under §101 is not 'like a nose of wax which may be turned and twisted in any direction * * *.' *White v. Dunbar*, 119 U.S. 47, 51." (*Parker v. Flook*, 198 USPQ 193 (US SupCt 1978))

Respectfully submitted,
INCYTE CORPORATION

Date: January 27, 2004




James M. Verna, Ph.D.

Reg. No. 33,287

Direct Dial Telephone: (650) 845 -5415

Date: January 27, 2004



Jenny Buchbinder

Reg. No. 48,588

Direct Dial Telephone: (650) 843-7212

Customer No.: 27904

3160 Porter Drive

Palo Alto, California 94304

Phone: (650) 855-0555

Fax: (650) 849-8886

Enclosures:

1. Rockett et al., Differential gene expression in drug metabolism and toxicology: practicalities, problems and potential, 29 Xenobiotica No. 7, 655 (1999)
2. Lashkari et al., Whole genome analysis: Experimental access to all genome sequenced segments through larger-scale efficient oligonucleotide synthesis and PCR, 94 Proc. Nat. Acad. Sci. 8945 (Aug. 1997).
3. Emile F. Nuwaysir et al., Microarrays and Toxicology: The Advent of Toxicogenomics, 24 Molecular Carcinogenesis 153 (1999);
4. Sandra Steiner and N. Leigh Anderson, Expression profiling in toxicology -- potentials and limitations, 112-13 Toxicology Letters 467 (2000).
5. John C. Rockett and David J. Dix, Application of DNA Arrays to Toxicology, 107 Environ. Health Perspec. 681, No. 8 (1999).
6. Email from the primary investigator on the Nuwaysir paper, Dr. Cynthia Afshari, to an Incyte employee, dated July 3, 2000, as well as the original message to which she was responding.
7. Brenner et al., Proc. Natl. Acad. Sci. 95:6073-78 (1998).
8. Bastian Cell. Mol. Life Sci. 53:554-556 (1997).
9. Eberhard et al. Am. J. Pathol. 145:640-649 (1994).
10. Gerke and Moss Physiol. Rev. 82:331-371 (2002).
11. Nguyen et al., J. Biol. Chem. 275:29466-29476 (2000).
12. Futter et al. J. Cell Biol. 120:77-83 (1993).

13. Jost et al. J. Cell Science 110:221-228 (1997).
14. Lecona et al. Biochem. J. 373:437-449 (2003).
15. Lecat et al., J. Cell Science 113:2607-2618 (2000).
16. Blankenberg et al. Proc. Natl. Acad. Sci. U.S.A. 95:6349-6354 (1998).
17. Blankenberg et al. Eur. J. Nucl. Med. 27:359-367 (2000).
18. Declaration of Mr. Furness, under 37 C.F.R. § 1.132.
19. Declaration of Dr. Bedilion, under 37 C.F.R. § 1.132.
20. CLUSTALW alignment

APPENDIX - CLAIMS ON APPEAL

205. An isolated polypeptide comprising an amino acid sequence of SEQ ID NO:12.
206. A composition comprising a polypeptide of claim 205 and a pharmaceutically acceptable excipient.
208. A method for treating a disease or condition associated with decreased expression of functional INTRA, comprising administering to a patient in need of such treatment the composition of claim 206.
209. A method of screening for a compound that specifically binds to the polypeptide of claim 205, the method comprising:
- a) combining the polypeptide of claim 205 with at least one test compound under suitable conditions, and
 - b) detecting binding of the polypeptide of claim 205 to the test compound, thereby identifying a compound that specifically binds to the polypeptide of claim 205.
211. An isolated polynucleotide encoding a polypeptide comprising an amino acid sequence of SEQ ID NO:12.
212. An isolated polynucleotide of claim 211 comprising a polynucleotide sequence of SEQ ID NO:64.
213. A recombinant polynucleotide comprising a promoter sequence operably linked to a polynucleotide of claim 211.
214. A cell transformed with a recombinant polynucleotide of claim 213.

215. A method of producing a polypeptide comprising an amino acid sequence of SEQ ID NO:12, the method comprising:

- a) culturing a cell under conditions suitable for expression of the polypeptide, wherein said cell is transformed with a recombinant polynucleotide, and said recombinant polynucleotide comprises a promoter sequence operably linked to a polynucleotide of claim 211, and
- b) recovering the polypeptide so expressed.

217. An isolated polynucleotide selected from the group consisting of:

- a) a polynucleotide comprising a polynucleotide sequence of SEQ ID NO:64,
- b) a polynucleotide completely complementary to a polynucleotide of a), and
- c) an RNA equivalent of a)-b).

224. A microarray wherein at least one element of the microarray is a polynucleotide of claim 217.

225. A method of generating an expression profile of a sample which contains polynucleotides, the method comprising:

- a) labeling the polynucleotides of the sample,
- b) contacting the microarray of claim 224 with the labeled polynucleotides of the sample under conditions suitable for the formation of a hybridization complex, and
- c) quantifying the expression of the polynucleotides in the sample.

226. An array comprising different nucleic acids affixed in distinct physical locations on a solid substrate, wherein at least one of said nucleic acids comprises a first polynucleotide sequence completely complementary to a target polynucleotide, and wherein said target polynucleotide is a polynucleotide of claim 217.

228. An array of claim 226, which is a microarray.

229. An array of claim 226, further comprising said target polynucleotide hybridized to a nucleic acid comprising said first polynucleotide sequence.

230. An array of claim 226, wherein a linker joins at least one of said nucleic acids to said solid substrate.

231. An array of claim 226, wherein each distinct physical location on the substrate contains multiple nucleic acids, and the multiple nucleic acids at any single distinct physical location have the same sequence, and each distinct physical location on the substrate contains nucleic acids having a sequence which differs from the sequence of nucleic acids at another distinct physical location on the substrate.

Differential gene expression in drug metabolism and toxicology: practicalities, problems and potential

JOHN C. ROCKETT†, DAVID J. ESDAILE‡
and G. GORDON GIBSON*

Molecular Toxicology Laboratory, School of Biological Sciences, University of Surrey,
Guildford, Surrey, GU2 5XH, UK

Received January 8, 1999

1. An important feature of the work of many molecular biologists is identifying which genes are switched on and off in a cell under different environmental conditions or subsequent to xenobiotic challenge. Such information has many uses, including the deciphering of molecular pathways and facilitating the development of new experimental and diagnostic procedures. However, the student of gene hunting should be forgiven for perhaps becoming confused by the mountain of information available as there appears to be almost as many methods of discovering differentially expressed genes as there are research groups using the technique.

2. The aim of this review was to clarify the main methods of differential gene expression analysis and the mechanistic principles underlying them. Also included is a discussion on some of the practical aspects of using this technique. Emphasis is placed on the so-called 'open' systems, which require no prior knowledge of the genes contained within the study model. Whilst these will eventually be replaced by 'closed' systems in the study of human, mouse and other commonly studied laboratory animals, they will remain a powerful tool for those examining less fashionable models.

3. The use of suppression-PCR subtractive hybridization is exemplified in the identification of up- and down-regulated genes in rat liver following exposure to phenobarbital, a well-known inducer of the drug metabolizing enzymes.

4. Differential gene display provides a coherent platform for building libraries and microchip arrays of 'gene fingerprints' characteristic of known enzyme inducers and xenobiotic toxicants, which may be interrogated subsequently for the identification and characterization of xenobiotics of unknown biological properties.

Introduction

It is now apparent that the development of almost all cancers and many non-neoplastic diseases are accompanied by altered gene expression in the affected cells compared to their normal state (Hunter 1991, Wynford-Thomas 1991, Vogelstein and Kinzler 1993, Semenza 1994, Cassidy 1995, Kleinjan and Van Hegningen 1998). Such changes also occur in response to external stimuli such as pathogenic micro-organisms (Rohn *et al.* 1996, Singh *et al.* 1997, Griffin and Krishna 1998, Lunney 1998) and xenobiotics (Sewall *et al.* 1995, Dogra *et al.* 1998, Ramana and Kohli 1998), as well as during the development of undifferentiated cells (Hecht 1998, Rudin and Thompson 1998, Schneider-Maunoury *et al.* 1998). The potential medical and therapeutic benefits of understanding the molecular changes which occur in any given cell in progressing from the normal to the 'altered' state are enormous. Such profiling essentially provides a 'fingerprint' of each step of a

* Author for correspondence; e-mail: g.gibson@surrey.ac.uk

† Current Address: US Environmental Protection Agency, National Health and Environmental Effects, Research Laboratory, Reproductive Toxicology Division, Research Triangle Park, NC 27711, USA.

‡ Rhone-Poulenc Agrochemicals, Toxicology Department, Sophia-Antipolis, Nice, France.

cell's development or response and should help in the elucidation of specific and sensitive biomarkers representing, for example, different types of cancer or previous exposure to certain classes of chemicals that are enzyme inducers.

In drug metabolism, many of the xenobiotic-metabolizing enzymes (including the well-characterized isoforms of cytochrome P450) are inducible by drugs and chemicals in man (Pelkonen *et al.* 1998), predominantly involving transcriptional activation of not only the cognate cytochrome P450 genes, but additional cellular proteins which may be crucial to the phenomenon of induction. Accordingly, the development of methodology to identify and assess the full complement of genes that are either up- or down-regulated by inducers are crucial in the development of knowledge to understand the precise molecular mechanisms of enzyme induction and how this relates to drug action. Similarly, in the field of chemical-induced toxicity, it is now becoming increasingly obvious that most adverse reactions to drugs and chemicals are the result of multiple gene regulation, some of which are causal and some of which are casually-related to the toxicological phenomenon *per se*. This observation has led to an upsurge in interest in gene-profiling technologies which differentiate between the control and toxin-treated gene pools in target tissues and is, therefore, of value in rationalizing the molecular mechanisms of xenobiotic-induced toxicity. Knowledge of toxin-dependent gene regulation in target tissues is not solely an academic pursuit as much interest has been generated in the pharmaceutical industry to harness this technology in the early identification of toxic drug candidates, thereby shortening the developmental process and contributing substantially to the safety assessment of new drugs. For example, if the gene profile in response to say a testicular toxin that has been well-characterized *in vivo* could be determined in the testis, then this profile would be representative of all new drug candidates which act via this specific molecular mechanism of toxicity, thereby providing a useful and coherent approach to the early detection of such toxicants. Whereas it would be informative to know the identity and functionality of all genes up/down regulated by such toxicants, this would appear a longer term goal, as the majority of human genes have not yet been sequenced, far less their functionality determined. However, the current use of gene profiling yields a *pattern* of gene changes for a xenobiotic of unknown toxicity which may be matched to that of well-characterized toxins, thus alerting the toxicologist to possible *in vivo* similarities between the unknown and the standard, thereby providing a platform for more extensive toxicological examination. Such approaches are beginning to gain momentum, in that several biotechnology companies are commercially producing 'gene chips' or 'gene arrays' that may be interrogated for toxicity assessment of xenobiotics. These chips consist of hundreds/thousands of genes, some of which are degenerate in the sense that not all of the genes are mechanistically-related to any one toxicological phenomenon. Whereas these chips are useful in broad-spectrum screening, they are maturing at a substantial rate, in that gene arrays are now becoming more specific, e.g. chips for the identification of changes in growth factor families that contribute to the aetiology and development of chemically-induced neoplasias.

Although documenting and explaining these genetic changes presents a formidable obstacle to understanding the different mechanisms of development and disease progression, the technology is now available to begin attempting this difficult challenge. Indeed, several 'differential expression analysis' methods have been developed which facilitate the identification of gene products that demonstrate

altered expression in cells of one population compared to another. These methods have been used to identify differential gene expression in many situations, including invading pathogenic microbes (Zhao *et al.* 1998), in cells responding to extracellular and intracellular microbial invasion (Duguid and Dinauer 1990, Ragno *et al.* 1997, Maldarelli *et al.* 1998), in chemically treated cells (Syed *et al.* 1997, Rockett *et al.* 1999), neoplastic cells (Liang *et al.* 1992, Chang and Terzaghi-Howe 1998), activated cells (Gurskaya *et al.* 1996, Wan *et al.* 1996), differentiated cells (Hara *et al.* 1991, Guimaraes *et al.* 1995a, b), and different cell types (Davis *et al.* 1984, Hedrick *et al.* 1984, Xhu *et al.* 1998). Although differential expression analysis technologies are applicable to a broad range of models, perhaps their most important advantage is that, in most cases, absolutely no prior knowledge of the specific genes which are up- or down-regulated is required.

The field of differential expression analysis is a large and complex one, with many techniques available to the potential user. These can be categorized into several methodological approaches, including:

- (1) Differential screening,
- (2) Subtractive hybridization (SH) (includes methods such as chemical cross-linking subtraction—CCLS, suppression-PCR subtractive hybridization—SSH, and representational difference analysis—RDA),
- (3) Differential display (DD),
- (4) Restriction endonuclease facilitated analysis (including serial analysis of gene expression—SAGE—and gene expression fingerprinting—GEF),
- (5) Gene expression arrays, and
- (6) Expressed sequence tag (EST) analysis.

The above approaches have been used successfully to isolate differentially expressed genes in different model systems. However, each method has its own subtle (and sometimes not so subtle) characteristics which incur various advantages and disadvantages. Accordingly, it is the purpose of this review to clarify the mechanistic principles underlying the main differential expression methods and to highlight some of the broader considerations and implications of this very powerful and increasingly popular technique. Specifically, we will concentrate on the so-called 'open' systems, namely those which do not require any knowledge of gene sequences and, therefore, are useful for isolating unknown genes. Two 'closed' systems (those utilising previously identified gene sequences), EST analysis and the use of DNA arrays, will also be considered briefly for completeness. Whilst emphasis will often be placed on suppression PCR subtractive hybridization (SSH, the approach employed in this laboratory), it is the aim of the authors to highlight, wherever possible, those areas of common interest to those who use, or intend to use, differential gene expression analysis.

Differential cDNA library screening (DS)

Despite the development of multiple technological advances which have recently brought the field of gene expression profiling to the forefront of molecular analysis, recognition of the importance of differential gene expression and characterization of differentially expressed genes has existed for many years. One of the original approaches used to identify such genes was described 20 years ago by St John and Davis (1979). These authors developed a method, termed 'differential plaque filter

hybridization', which was used to isolate galactose-inducible DNA sequences from yeast. The theory is simple: a genomic DNA library is prepared from normal, unstimulated cells of the test organism/tissue and multiple filter replicas are prepared. These replica blots are probed with radioactively (or otherwise) labelled complex cDNA probes prepared from the control and test cell mRNA populations. Those mRNAs which are differentially expressed in the treated cell population will show a positive signal only on the filter probed with cDNA from the treated cells. Furthermore, labelled cDNA from different test conditions can be used to probe multiple blots, thereby enabling the identification of mRNAs which are only up-regulated under certain conditions. For example, St John and Davis (1979) screened replica filters with acetate-, glucose- and galactose-derived probes in order to obtain genes induced specifically by galactose metabolism. Although groundbreaking in its time this method is now considered insensitive and time-consuming, as up to 2 months are required to complete the identification of genes which are differentially expressed in the test population. In addition, there is no convenient way to check that the procedure has worked until the whole process has been completed.

Subtractive Hybridization (SH)

The developing concept of differential gene expression and the success of early approaches such as that described by St John and Davis (1979) soon gave rise to a search for more convenient methods of analysis. One of the first to be developed was SH, numerous variations of which have since been reported (see below). In general, this approach involves hybridization of mRNA/cDNA from one population (tester) to excess mRNA/cDNA from another (driver), followed by separation of the unhybridized tester fraction (differentially expressed) from the hybridized common sequences. This step has been achieved physically, chemically and through the use of selective polymerase chain reaction (PCR) techniques.

Physical separation

Original subtractive hybridization technology involved the physical separation of hybridized common species from unique single stranded species. Several methods of achieving this have been described, including hydroxyapatite chromatography (Sargent and Dawid 1983), avidin-biotin technology (Duguid and Dinauer 1990) and oligodT-latex separation (Hara *et al.* 1991). In the first approach, common mRNA species are removed by cDNA (from test cells)-mRNA (from control cells) subtractive hybridization followed by hydroxyapatite chromatography, as hydroxyapatite specifically adsorbs the cDNA-mRNA hybrids. The unabsorbed cDNA is then used either for the construction of a cDNA library of differentially expressed genes (Sargent and Dawid 1983, Schneider *et al.* 1988) or directly as a probe to screen a preselected library (Zimmerman *et al.* 1980, Davis *et al.* 1984, Hedrick *et al.* 1984). A schematic diagram of the procedure is shown in figure 1.

Less rigorous physical separation procedures coupled with sensitivity enhancing PCR steps were later developed as a means to overcome some of the problems encountered with the hydroxyapatite procedure. For example, Duguid and Dinauer (1990) described a method of subtraction utilizing biotin-affinity systems as a means to remove hybridized common sequences. In this process, both the control and tester mRNA populations are first converted to cDNA and an adaptor ('oligovector',

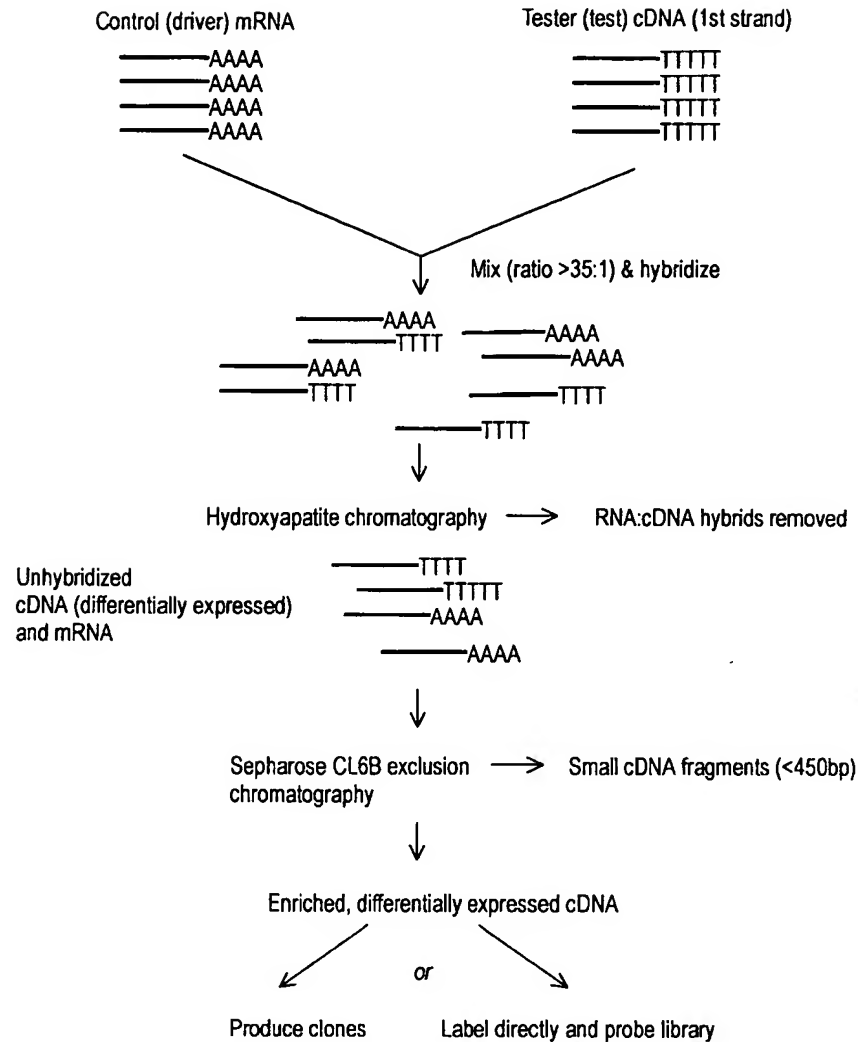


Figure 1. The hydroxyapatite method of subtractive hybridization. cDNA derived from the treated/alterd (tester) population is mixed with a large excess of mRNA from the control (driver) population. Following hybridization, mRNA-cDNA hybrids are removed by hydroxyapatite chromatography. The only cDNAs which remain are those which are differentially expressed in the treated/alterd population. In order to facilitate the recovery of full length clones, small cDNA fragments are removed by exclusion chromatography. The remaining cDNAs are then cloned into a vector for sequencing, or labelled and used directly to probe a library, as described by Sargent and Dawid (1983).

containing a restriction site) ligated to both sides. Both populations are then amplified by PCR, but the driver cDNA population is subsequently digested with the adaptor-containing restriction endonuclease. This serves to cleave the oligo-vector and reduce the amplification potential of the control population. The digested control population is then biotinylated and an excess mixed with tester cDNA. Following denaturation and hybridization, the mix is applied to a biocytin column (streptavidin may also be used) to remove the control population, including heteroduplexes formed by annealing of common sequences from the tester population. The procedure is repeated several times following the addition of fresh

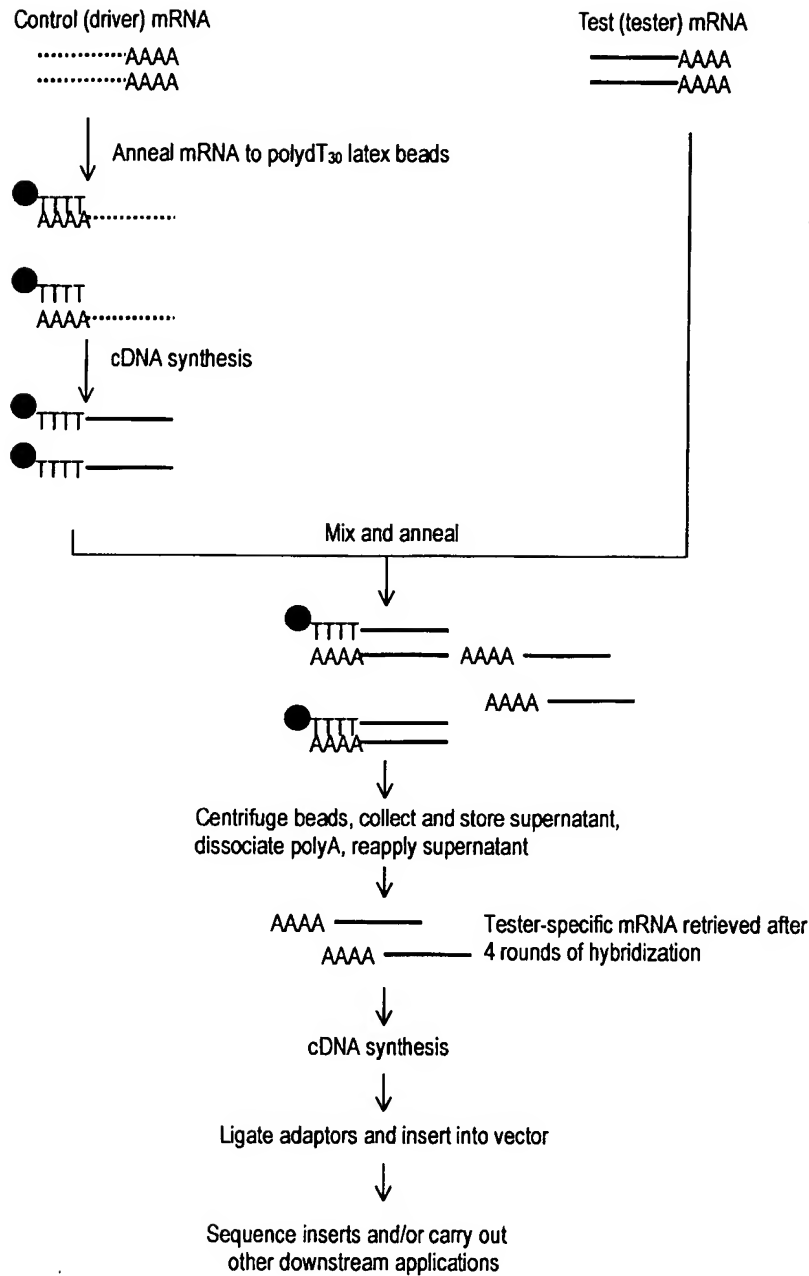


Figure 2. The use of oligodT₃₀ latex to perform subtractive hybridization. mRNA extracted from the control (driver) population is converted to anchored cDNA using polydT oligonucleotides attached to latex beads. mRNA from the treated/alterd (tester) population is repeatedly hybridized against an excess of the anchored driver cDNA. The final population of mRNA is tester specific and can be converted into cDNA for cloning and other downstream applications, as described by Hara *et al.* (1991).

control cDNA. In order to further enrich those species differentially expressed in the tester cDNA, the subtracted tester population is amplified by PCR following every second subtraction cycle. After six cycles of subtraction (three reamplification steps) the reaction mix is ligated into a vector for further analysis.

In a slightly different approach, Hara *et al.* (1991) utilized a method whereby oligo(dT₃₀) primers attached to a latex substrate are used to first capture mRNA extracted from the control population. Following 1st strand cDNA synthesis, the RNA strand of the heteroduplexes is removed by heat denaturation and centrifugation (the cDNA-oligotex-dT₃₀ forms a pellet and the supernatant is removed). A quantity of tester mRNA is then repeatedly hybridized to the immobilized control (driver) cDNA (which is present in 20-fold excess). After several rounds of hybridization the only mRNA molecules left in the tester mRNA population are those which are not found in the driver cDNA-oligotex-dT₃₀ population. These tester-specific mRNA species are then converted to cDNA and, following the addition of adaptor sequences, amplified by PCR. The PCR products are then ligated into a vector for further analysis using restriction sites incorporated into the PCR primers. A schematic illustration of this subtraction process is shown in figure 2.

However, all these methods utilising physical separation have been described as inefficient due to the requirement for large starting amounts of mRNA, significant loss of material during the separation process and a need for several rounds of hybridization. Hence, new methods of differential expression analysis have recently been designed to eliminate these problems.

Chemical Cross-Linking Subtraction (CCLS)

In this technique, originally described by Hampson *et al.* (1992), driver mRNA is mixed with tester cDNA (1st strand only) in a ratio of > 20:1. The common sequences form cDNA:mRNA hybrids, leaving the tester specific species as single stranded cDNA. Instead of physically separating these hybrids, they are inactivated chemically using 2,5 diaziridinyl-1,4-benzoquinone (DZQ). Labelled probes are then synthesized from the remaining single stranded cDNA species (unreacted mRNA species remaining from the driver are not converted into probe material due to specificity of Sequenase T7 DNA polymerase used to make the probe) and used to screen a cDNA library made from the tester cell population. A schematic diagram of the system is shown in figure 3.

It has been shown that the differentially expressed sequences can be enriched at least 300-fold with one round of subtraction (Hampson *et al.* 1992), and that the technique should allow isolation of cDNAs derived from transcripts that are present at less than 50 copies per cell. This equates to genes at the low end of intermediate abundance (see table 1). The main advantages of the CCLS approach are that it is rapid, technically simple and also produces fewer false positives than other differential expression analysis methods. However, like the physical separation protocols, a major drawback with CCLS is the large amount of starting material required (at least 10 µg RNA). Consequently, the technique has recently been refined so that a renewable source of RNA can be generated. The degenerate random oligonucleotide primed (DROP) adaptation (Hampson *et al.* 1996, Hampson and Hampson 1997) uses random hexanucleotide sequences to prime solid phase-synthesized cDNA. Since each primer includes a T7 polymerase promoter sequence

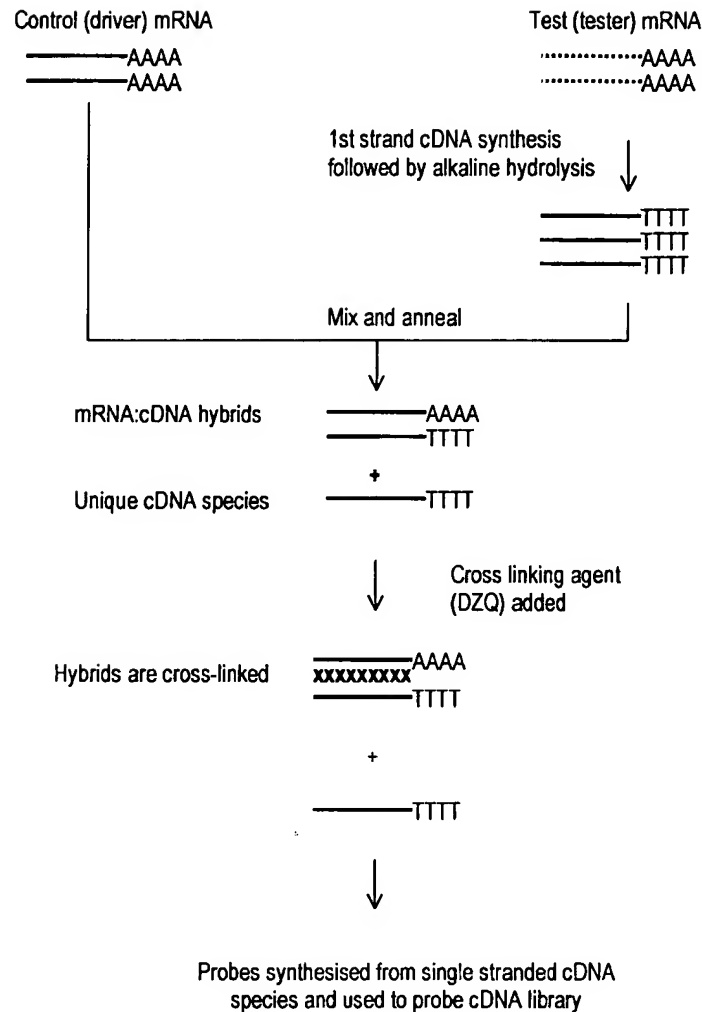


Figure 3. Chemical cross-linking subtraction. Excess driver mRNA is mixed with 1st strand tester cDNA. The common sequences form mRNA:cDNA hybrids which are cross linked with 2,5 diaziridinyl-1,4-benzoquinone (DZQ) and the remaining cDNA sequences are differentially expressed in the tester population. Probes are made from these sequences using Sequenase 2.0 DNA polymerase, which lacks reverse transcriptase activity and, therefore, does not react with the remaining mRNA molecules from the driver. The labelled probes are then used to screen a cDNA library for clones of differentially expressed sequences. Adapted from Walter *et al.* (1996), with permission.

Table 1. The abundance of mRNA species and classes in a typical mammalian cell.

mRNA class	Copies of each species/cell	No. of mRNA species in class	Mean % of each species in class	Mean mass (ng) of each species/ μ g total RNA
Abundant	12000	4	3.3	1.65
Intermediate	300	500	0.08	0.04
Rare	15	11000	0.004	0.002

Modified from Bertoli *et al.* (1995).

at the 5' end, the final pool of random cDNA fragments is a PCR-renewable cDNA population which is representative of the expressed gene pool and can be used to synthesize sense RNA for use as driver material. Furthermore, if the final pool of random cDNA fragments is reamplified using biotinylated T7 primer and random hexamer, the product can be captured with streptavidin beads and the antisense strand eluted for use as tester. Since both target and driver can be generated from the same DROP product, subtraction can be performed in both directions (i.e. for up- and down-regulated species) between two different DROP products.

Representational Difference Analysis (RDA)

RDA of cDNA (Hubank and Schatz 1994) is an extension of the technique originally applied to genomic DNA as a means of identifying differences between two complex genomes (Lisitsyn *et al.* 1993). It is a process of subtraction and amplification involving subtractive hybridization of the tester in the presence of excess driver. Sequences in the tester that have homologues in the driver are rendered unamplifiable, whereas those genes expressed only in the tester retain the ability to be amplified by PCR. The procedure is shown schematically in figure 4.

In essence, the driver and tester mRNA populations are first converted to cDNA and amplified by PCR following the ligation of an adaptor. The adaptors are then removed from both populations and a new (different) adaptor ligated to the amplified tester population only. Driver and tester populations are next melted and hybridized together in a ratio of 100:1. Following hybridization, only tester:tester homohybrids have 5' adaptors at each end of the DNA duplex and can, thus, be filled in at both 3' ends. Hence, only these molecules are amplified exponentially during the subsequent PCR step. Although tester:driver heterohybrids are present, they only amplify in a linear fashion, since the strand derived from the driver has no adaptor to which the primer can bind. Driver:driver heterohybrids have no adaptors and, therefore, are not amplified. Single stranded molecules are digested with mung bean nuclease before a further PCR-enrichment of the tester:tester homohybrids. The adaptors on the amplified tester population are then replaced and the whole process repeated a further two or three times using an increasing excess of driver (Hubank and Schatz used a tester:driver ratio of 1:400, 1:80000 and 1:800000 for the second, third and fourth hybridizations, respectively). Different adaptors are ligated to the tester between successive rounds of hybridization and amplification to prevent the accumulation of PCR products that might interfere with subsequent amplifications. The final display is a series of differentially expressed gene products easily observable on an ethidium bromide gel.

The main advantages of RDA are that it offers a reproducible and sensitive approach to the analysis of differentially expressed genes. Hubank and Schatz (1994) reported that they were able to isolate genes that were differentially expressed in substantially less than 1% of the cells from which the tester is derived. Perhaps the main drawback is that multiple rounds of ligation, hybridization, amplification and digestion are required. The procedure is, therefore, lengthier than many other differential display approaches and provides more opportunity for operator-induced error to occur. Although the generation of false positives has been noted, this has been solved to some degree by O'Neill and Sinclair (1997) through the use of HPLC-purified adaptors. These are free of the truncated adaptors which appear to be a major source of the false positive bands. A very similar technique to RDA, termed linker capture subtraction (LCS) was described by Yang and Sytowski (1996).

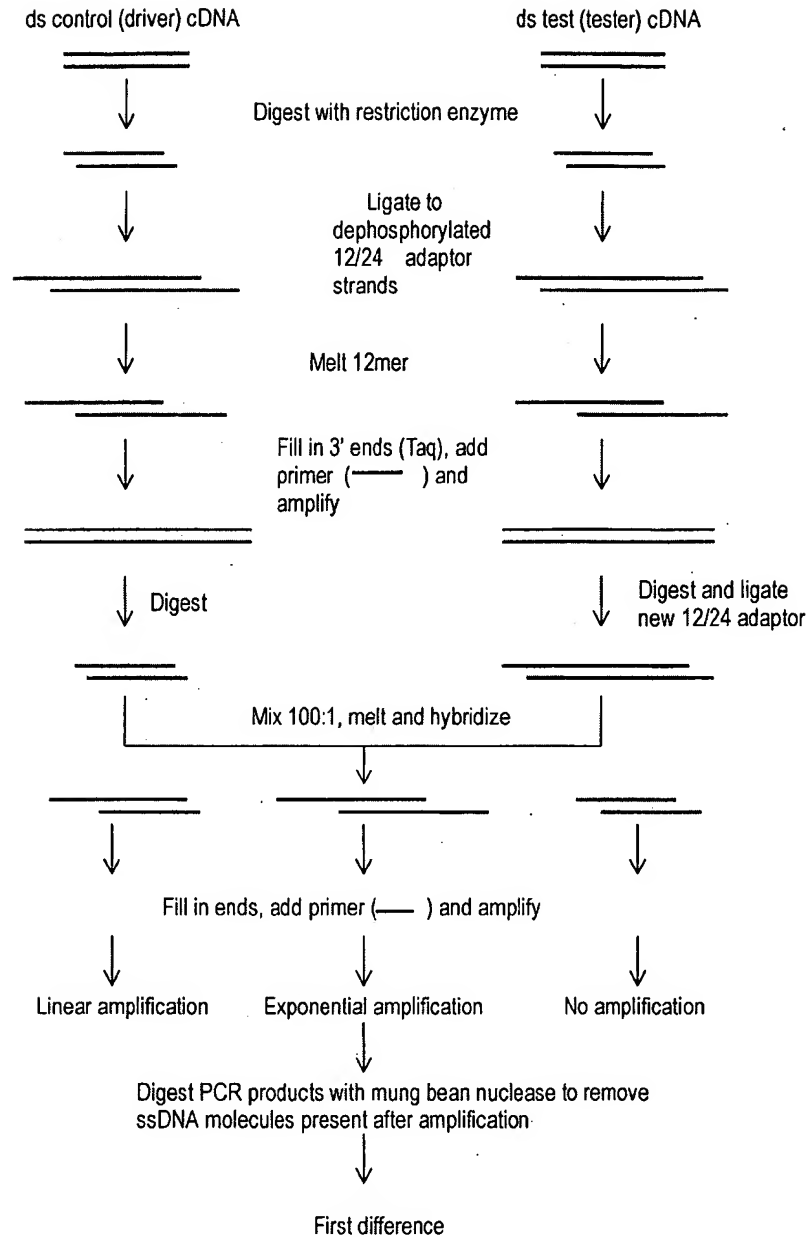


Figure 4. The representational difference analysis (RDA) technique. Driver and tester cDNA are digested with a 4-cutter restriction enzyme such as *DpnII*. The 1st set of 12/24 adaptor strands (oligonucleotides) are ligated to each other and the digested cDNA products. The 12mer is subsequently melted away and the 3' ends filled in using Taq DNA polymerase. Each cDNA population is then amplified using PCR, following which the 1st set of adaptors is removed with *DpnII*. A second set of 12/24 adaptor strands is then added to the amplified tester cDNA population, after which the tester is hybridized against a large excess of driver. The 12mer adaptors are melted and the 3' ends filled in as before. PCR is carried out with primers identical to the new 24mer adaptor. Thus, the only hybridization products which are exponentially amplified are those which are tester:tester combinations. Following PCR, ssDNA products are removed with mung bean nuclease, leaving the 'first difference product'. This is digested and a third set of 12/24 adaptors added before repeating the subtraction process from the hybridization stage. The process is repeated to the 3rd or 4th difference product, as described by Lisitsyn *et al.* (1993) and Hubank and Schatz (1994).

Suppression PCR Subtractive Hybridization (SSH)

The most recent adaptation of the SH approach to differential expression analysis was first described by Diatchenko *et al.* (1996) and Gurskaya *et al.* (1996). They reported that a 1000–5000 fold enrichment of rare cDNAs (equivalent to isolating mRNAs present at only a few copies per cell) can be obtained without the need for multiple hybridizations/subtractions. Instead of physical or chemical removal of the common sequences, a PCR-based suppression system is used (see figure 5).

In SSH, excess driver cDNA is added to two portions of the tester cDNA which have been ligated with different adaptors. A first round of hybridization serves to enrich differentially expressed genes and equalize rare and abundant messages. Equalization occurs since reannealing is more rapid for abundant molecules than for rarer molecules due to the second order kinetics of hybridization (James and Higgins 1985). The two primary hybridization mixes are then mixed together in the presence of excess driver and allowed to hybridize further. This step permits the annealing of single stranded complementary sequences which did not hybridize in the primary hybridization, and in doing so generates templates for PCR amplification. Although there are several possible combinations of the single stranded molecules present in the secondary hybridization mix, only one particular combination (differentially expressed in the tester cDNA composed of complimentary strands having different adaptors) can amplify exponentially.

Having obtained the final differential display, two options are available if cloning of cDNAs is desired. One is to transform the whole of the final PCR reaction into competent cells. Transformed colonies can then be isolated and their inserts characterized by sequencing, restriction analysis or PCR. Alternatively, the final PCR products can be resolved on a gel and the individual bands excised, reamplified and cloned. The first approach is technically simpler and less time consuming. However, ligation/transformation reactions are known to be biased towards the cloning of smaller molecules, and so the final population of clones will probably not contain a representative selection of the larger products. In addition, although equalization theoretically occurs, observations in this laboratory suggest that this is by no means perfectly accomplished. Consequently, some gene species are present in a higher number than others and this will be represented in the final population of clones. Thus, in order to obtain a substantial proportion of those gene species that actually demonstrate differential expression in the tester population, the number of clones that will have to be screened after this step may be substantial. The second approach is initially more time consuming and technically demanding. However, it would appear to offer better prospects for cloning larger and low abundance gel products. In addition, one can incorporate a screening step that differentiates different products of different sequences but of the same size (HA-staining, see later). In this way, a good idea of the final number of clones to be isolated and identified can be achieved.

An alternative (or even complementary) approach is to use the final differential display reaction to screen a cDNA library to isolate full length clones for further characterization, or a DNA array (see later) to quickly identify known genes. SSH has been used in this laboratory to begin characterization of the short-term gene expression profiles of enzyme-inducers such as phenobarbital (Rockett *et al.* 1997) and Wy-14,643 (Rockett *et al.* unpublished observations). The isolation of differentially expressed genes in this manner enables the construction of a fingerprint

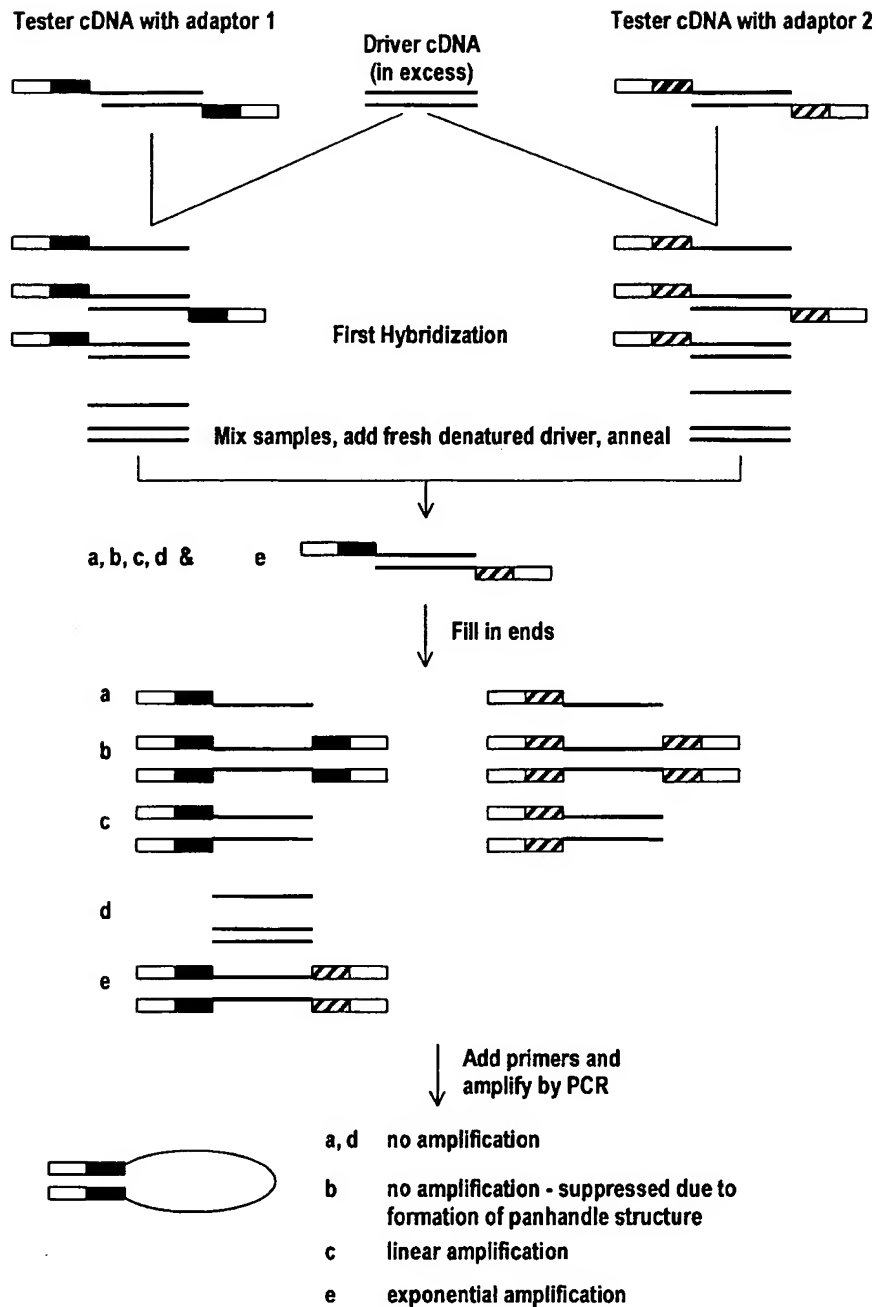


Figure 5. PCR-select cDNA subtraction. In the primary hybridization, an excess of driver cDNA is added to each tester cDNA population. The samples are heat denatured and allowed to hybridize for between 3 and 8 h. This serves two purposes: (1) to equalize rare and abundant molecules; and (2) to enrich for differentially expressed sequences—cDNAs that are not differentially expressed form type c molecules with the driver. In the secondary hybridization, the two primary hybridizations are mixed together without denaturing. Fresh denatured driver can also be added at this point to allow further enrichment of differentially expressed sequences. Type e molecules are formed in this secondary hybridization which are subsequently amplified using two rounds of PCR. The final products can be visualized on an agarose gel, labelled directly or cloned into a vector for downstream manipulation. As described by Diatchenko *et al.* (1996) and Gurskaya *et al.* (1996), with permission.

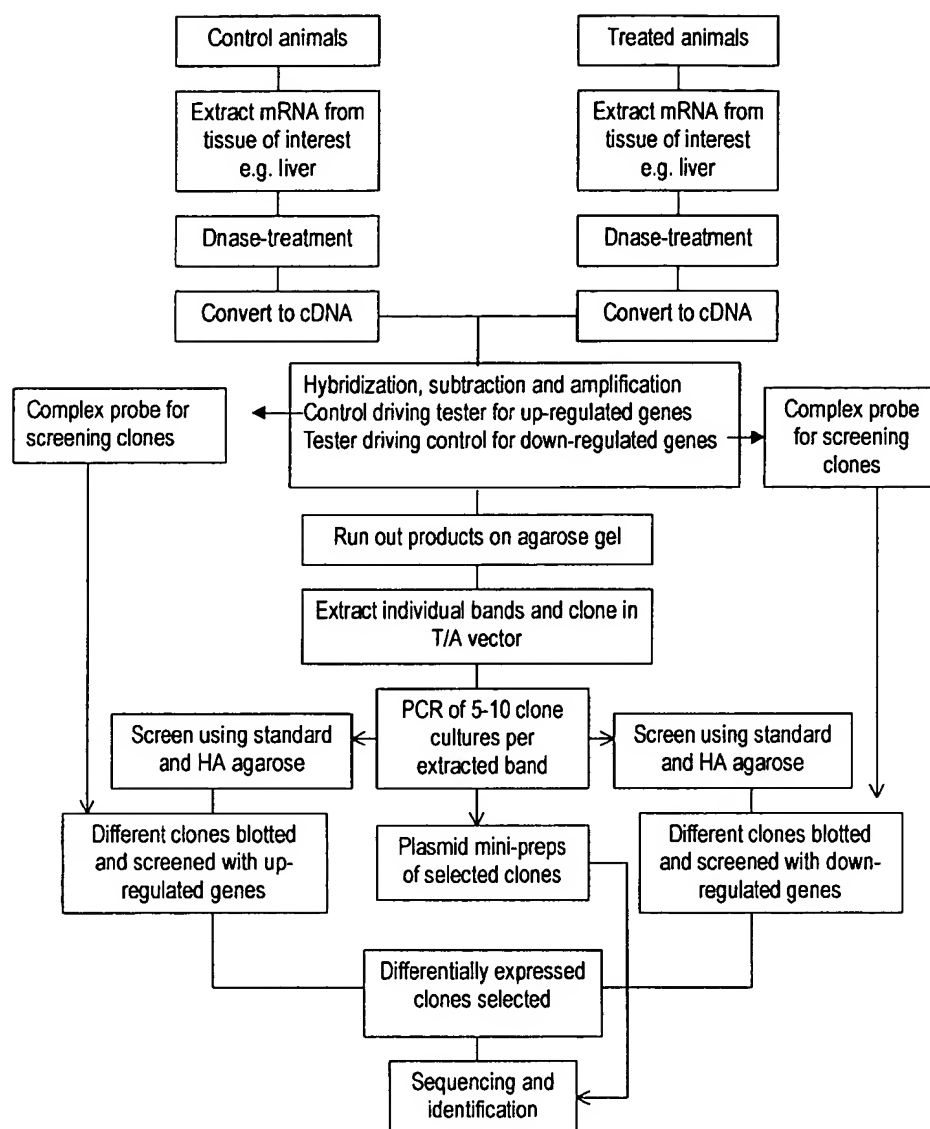


Figure 6. Flow diagram showing method used in this laboratory to isolate and identify clones of genes which are differentially expressed in rat liver following short term exposure to the enzyme inducers, phenobarbital and Wy-14,643.

of expressed genes which are unique to each compound and time/dose point. Such information could be useful in short-term characterization of the toxic potential of new compounds by comparing the gene-expression profiles they elicit with those produced by known inducers. Figure 6 shows a flow diagram of the method used to isolate, verify and clone differentially expressed genes, and figure 7 shows expression profiles obtained from a typical SSH experiment. Subsequent sub-cloning of the individual bands, sequencing and gene data base interrogation reveals many genes which are either up- or down-regulated by phenobarbital in the rat (tables 2 and 3).

One of the advantages in using the SSH approach is that no prior knowledge is required of which specific genes are up/down-regulated subsequent to xenobiotic

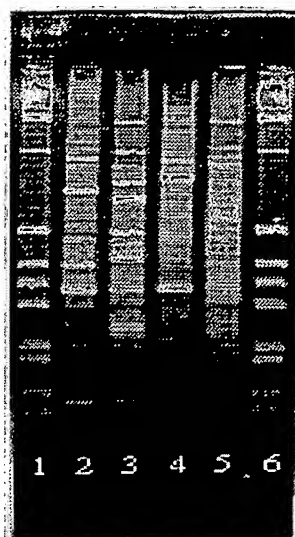


Figure 7. SSH display patterns obtained from rat liver following 3-day treatment with WY-14,643 or phenobarbital. mRNA extracted from control and treated livers was used to generate the differential displays using the PCR-Select cDNA subtraction kit (Clontech). Lane: 1—1kb ladder; 2—genes upregulated following Wy,14-643 treatment; 3—genes downregulated following Wy,14-643 treatment; 4—genes upregulated following phenobarbital treatment; 5—genes downregulated following phenobarbital treatment; 6—1kb ladder. Reproduced from Rockett *et al.* (1997), with permission.

exposure, and an almost complete complement of genes are obtained. For example, the peroxisome proliferator and non-genotoxic hepatocarcinogen Wy,14,643, up-regulates at least 28 genes and down-regulates at least 15 in the rat (a sensitive species) and produces 48 up- and 37 down-regulated genes in the guinea pig, a resistant species (Rockett, Swales, Esda and Gibson, unpublished observations). One of these genes, CD81, was up-regulated in the rat and down-regulated in the guinea pig following Wy-14,643 treatment. CD81 (alternatively named TAPA-1) is a widely expressed cell surface protein which is involved in a large number of cellular processes including adhesion, activation, proliferation and differentiation (Levy *et al.* 1998). Since all of these functions are altered to some extent in the phenomena of hepatomegaly and non-genotoxic hepatocarcinogenesis, it is intriguing, and probably mechanistically-relevant, that CD81 expression is differentially regulated in a resistant and susceptible species. However, the down-side of this approach is that the majority of genes can be sequenced and matched to database sequences, but the latter are predominantly expressed sequence tags or genes of completely unknown function, thus partially obscuring a realistic overall assessment of the critical genes of genuine biological interest. Notwithstanding the lack of complete functional identification of altered gene expression, such gene profiling studies essentially provides a 'molecular fingerprint' in response to xenobiotic challenge, thereby serving as a mechanistically-relevant platform for further detailed investigations.

Differential Display (DD)

Originally described as 'RNA fingerprinting by arbitrarily primed PCR' (Liang and Pardee 1992) this method is now more commonly referred to as 'differential

Table 2. Genes up-regulated in rat liver following 3-day exposure to phenobarbital.

Band number (approximate size in bp)	Highest sequence similarity	FASTA-EMBL gene identification
5 (1300)	93.5%	CYP2B1
7 (1000)	95.1%	Preproalbumin Serum albumin mRNA
8 (950)	98.3%	NCI-CGAP-Pr1 <i>H. sapiens</i> (EST)
10 (850)	95.7%	CYP2B1
11 (800)	Clone 1 94.9%	CYP2B1
	Clone 2 75.3%	CYP2B2
12 (750)	93.8%	TRPM-2 mRNA
15 (600)	92.9%	Sulfated glycoprotein Preproalbumin Serum albumin mRNA
16 (55)	Clone 1 95.2%	CYP2B1
	Clone 2 93.6%	Haptoglobulin mRNA partial alpha
21 (350)	99.3%	18S, 5.8S & 28S rRNA

Bands 1–4, 6, 9, 13, 14, and 17–20 are shown to be false positives by dot blot analysis and, therefore, are not sequenced. Derived from Rockett *et al.* (1997). It should be noted that the above genes do not represent the complete spectrum of genes which are up-regulated in rat liver by phenobarbital, but simply represents the genes sequenced and identified to date.

Table 3. Genes down-regulated in rat liver following 3-day exposure to phenobarbital.

Band number (approximate size in bp)	Highest sequence similarity	FASTA-EMBL gene identification
1 (1500)	95.3%	3-oxoacyl-CoA thiolase
2 (1200)	92.3%	Hemopoxin mRNA
3 (1000)	91.7%	Alpha-2u-globulin mRNA
7 (700)	Clone 1 77.2%	<i>M. musculus</i> Cl inhibitor
	Clone 2 94.5%	Electron transfer flavoprotein
	Clone 3 91.0%	<i>M. musculus</i> Topoisomerase 1 (Topo 1)
8 (650)	Clone 1 86.9%	Soares 2NbMT <i>M. musculus</i> (EST)
	Clone 2 96.2%	Alpha-2u-globulin (s-type) mRNA
9 (600)	Clone 1 86.9%	Soares mouse NML <i>M. musculus</i> (EST)
	Clone 2 82.0%	Soares p3NMF 19.5 <i>M. musculus</i> (EST)
10 (550)	73.8%	Soares mouse NML <i>M. musculus</i> (EST)
11 (525)	95.7%	NCI-CGAP-Pr1 <i>H. sapiens</i> (EST)
12 (375)	100.0%	Ribosomal protein
13 (23)	Clone 1 97.2%	Soares mouse embryo NbME135 (EST)
	Clone 2 100.0%	Fibrinogen B-beta-chain
	Clone 3 100.0%	Apolipoprotein E gene
14 (170)	96.0%	Soares p3NMF19.5 <i>M. musculus</i> (EST)
15 (140)	97.3%	Stratagene mouse testis (EST)
Others: (300)	96.7%	<i>R. norvegicus</i> RASP 1 mRNA
(275)	93.1%	Soares mouse mammary gland (EST)

EST = Expressed sequence tag. Bands 4–6 were shown to be false positives by dot blot analysis and, therefore, were not sequenced. Derived from Rockett *et al.* (1997). It should be noted that the above genes do not represent the complete spectrum of genes which are down-regulated in rat liver by phenobarbital, but simply represents the genes sequenced and identified to date.

display' (DD). In this method, all the mRNA species in the control and treated cell populations are amplified in separate reactions using reverse transcriptase-PCR (RT-PCR). The products are then run side-by-side on sequencing gels. Those bands which are present in one display only, or which are much more intense in one

display compared to the other, are differentially expressed and may be recovered for further characterization. One advantage of this system is the speed with which it can be carried out—2 days to obtain a display and as little as a week to make and identify clones.

Two commonly used variations are based on different methods of priming the reverse transcription step (figure 8). One is to use an oligo dT with a 2-base 'anchor' at the 3'-end, e.g. 5' (dT_n)CA 3' (Liang and Pardee 1992). Alternatively, an arbitrary primer may be used for 1st strand cDNA synthesis (Welsh *et al.* 1992). This variant of RNA fingerprinting has also been called 'RAP' (RNA Arbitrarily Primed)-PCR. One advantage of this second approach is that PCR products may be derived from anywhere in the RNA, including open reading frames. In addition, it can be used for mRNAs that are not polyadenylated, such as many bacterial mRNAs (Wong and McClelland 1994). In both cases, following reverse transcription and denaturation, second strand cDNA synthesis is carried out with an arbitrary primer (*arbitrary* primers have a single base at each position, as compared to *random* primers, which contain a mixture of all four bases at each position). The resulting PCR, thus, produces a series of products which, depending on the system (primer length and composition, polymerase and gel system), usually includes 50–100 products per primer set (Band and Sager 1989). When a combination of different dT-anchors and arbitrary primers are used, almost all mRNA species from a cell can be amplified. When the cDNA products from two different populations are analysed side by side on a polyacrylamide gel, differences in expression can be identified and the appropriate bands recovered for cloning and further analysis.

Although DD is perhaps the most popular approach used today for identifying differentially expressed genes, it does suffer from several perceived disadvantages:

- (1) It may have a strong bias towards high copy number mRNAs (Bertioli *et al.* 1995), although this has been disputed (Wan *et al.* 1996) and the isolation of very low abundance genes may be achieved in certain circumstances (Guimeraes *et al.* 1995a).
- (2) The cDNAs obtained often only represent the extreme 3' end of the mRNA (often the 3'-untranslated region), although this may not always be the case (Guimeraes *et al.* 1995a). Since the 3' end is often not included in Genbank and shows variation between organisms, cDNAs identified by DD cannot always be matched with their genes, even if they have been identified.
- (3) The pattern of differential expression seen on the display often cannot be reproduced on Northern blots, with false positives arising in up to 70% of cases (Sun *et al.* 1994). Some adaptations have been shown to reduce false positives, including the use of two reverse transcriptases (Sung and Denman 1997), comparison of uninduced and induced cells over a time course (Burn *et al.* 1994) and comparison of DDPCR-products from two uninduced and two induced lines (Sompayrac *et al.* 1995). The latter authors also reported that the use of cytoplasmic RNA rather than total RNA reduces false positives arising from nuclear RNA that is not transported to the cytoplasm.

Further details of the background, strengths and weaknesses of the DD technique can be obtained from a review by McClelland *et al.* (1996) and from articles by Liang *et al.* (1995) and Wan *et al.* (1996).

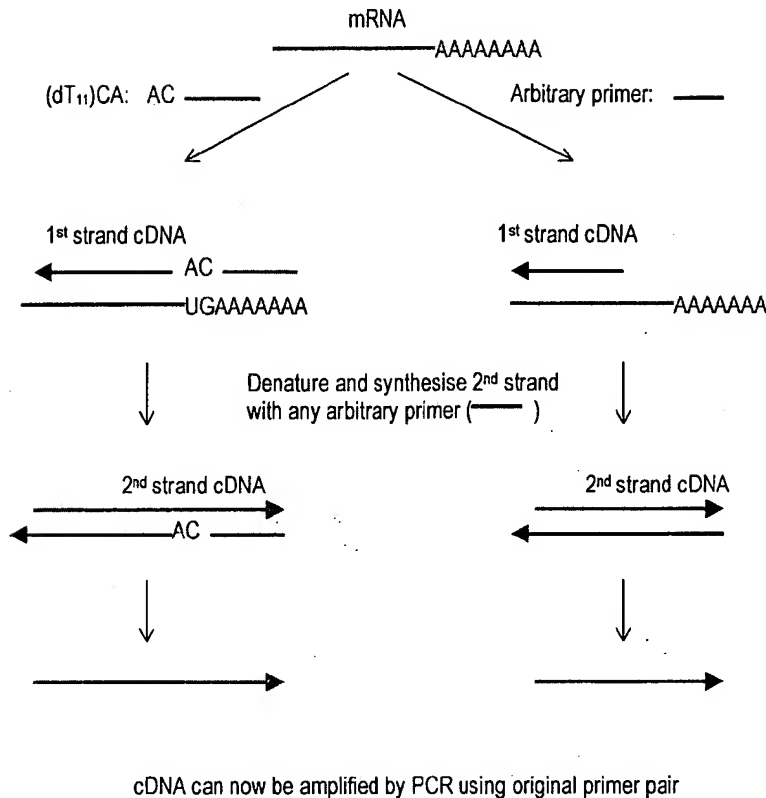


Figure 8. Two approaches to differential display (DD) analysis. 1st strand synthesis can be carried out either with a polydT₁₁NN primer (where N = G, C or A) or with an arbitrary primer. The use of different combinations of G, C and A to anchor the first strand polydT primer enables the priming of the majority of polyadenylated mRNAs. Arbitrary primers may hybridize at none, one or more places along the length of the mRNA, allowing 1st strand cDNA synthesis to occur at none, one or more points in the same gene. In both cases, 2nd strand synthesis is carried out with an arbitrary primer. Since these arbitrary primers for the 2nd strand may also hybridize to the 1st strand cDNA in a number of different places, several different 2nd strand products may be obtained from one binding point of the 1st strand primer. Following 2nd strand synthesis, the original set of primers is used to amplify the second strand products, with the result that numerous gene sequences are amplified.

Restriction endonuclease-facilitated analysis of gene expression

Serial Analysis of Gene Expression (SAGE)

A more recent development in the field of differential display is SAGE analysis (Velculescu *et al.* 1995). This method uses a different approach to those discussed so far and is based on two principles. Firstly, in more than 95% of cases, short nucleotide sequences ('tags') of only nine or 10 base pairs provide sufficient information to identify their gene of origin. Secondly, concatenation (linking together in a series) of these tags allows sequencing of multiple cDNAs within a single clone. Figure 9 shows a schematic representation of the SAGE process. In this procedure, double stranded cDNA from the test cells is synthesized with a biotinylated polydT primer. Following digestion with a commonly cutting (4bp recognition sequence) restriction enzyme ('anchoring enzyme'), the 3' ends of the cDNA population are captured with streptavidin beads. The captured population is

split into two and different adaptors ligated to the 5' ends of each group. Incorporated into the adaptors is a recognition sequence for a type IIS restriction enzyme—one which cuts DNA at a defined distance (< 20 bp) from its recognition sequence. Hence, following digestion of each captured cDNA population with the IIS enzyme, the adaptors plus a short piece of the captured cDNA are released. The two populations are then ligated and the products amplified. The amplified products are cleaved with the original anchoring enzyme, religated (concatomers are formed in the process) and cloned. The advantage of this system is that hundreds of gene tags can be identified by sequencing only a few clones. Furthermore, the number of times a given transcript is identified is a quantitative measurement of that gene's abundance in the original population, a feature which facilitates identification of differentially expressed genes in different cell populations.

Some disadvantages of SAGE analysis include the technical difficulty of the method, a large amount of accurate sequencing is required, biased towards abundant mRNAs, has not been validated in the pharmaco/toxicogenomic setting and has only been used to examine well known tissue differences to date.

Gene Expression Fingerprinting (GEF)

A different capture/restriction digest approach for isolating differentially expressed genes has been described by Ivanova and Belyavsky (1995). In this method, RNA is converted to cDNA using biotinylated oligo(dT) primers. The cDNA population is then digested with a specific endonuclease and captured with magnetic streptavidin microbeads to facilitate removal of the unwanted 5' digestion products. The use of restricted 3'-ends alone serves to reduce the complexity of the cDNA fragment pool and helps to ensure that each RNA species is represented by not more than one restriction product. An adaptor is ligated to facilitate subsequent amplification of the captured population. PCR is carried out with one adaptor-specific and one biotinylated polydT primer. The reamplified population is recaptured and the non-biotinylated strands removed by alkaline dissociation. The non-biotinylated strand is then resynthesized using a different adaptor-specific primer in the presence of a radiolabelled dNTP. The labelled immobilized 3' cDNA ends are next sequentially treated with a series of different restriction endonucleases and the products from each digestion analysed by PAGE. The result is a fingerprint composed of a number of ladders (equal to the number of sequential digests used). By comparing test versus control fingerprints, it is possible to identify differentially expressed products which can then be isolated from the gel and cloned. The advantages of this procedure are that it is very robust and reproducible, and the authors estimate that 80–93% of cDNA molecules are involved in the final fingerprint. The disadvantage is that polyacrylamide gels can rarely resolve more than 300–400 bands, which compares poorly to the 1000 or more which are estimated to be produced in an average experiment. The use of 2-D gels such as those described by Uitterlinden *et al.* (1989) and Hatada *et al.* (1991) may help to overcome this problem.

A similar method for displaying restriction endonuclease fragments was later described by Prashar and Weissman (1996). However, instead of sequential digestion of the immobilized 3'-terminal cDNA fragments, these authors simply compared the profiles of the control and treated populations without further manipulation.

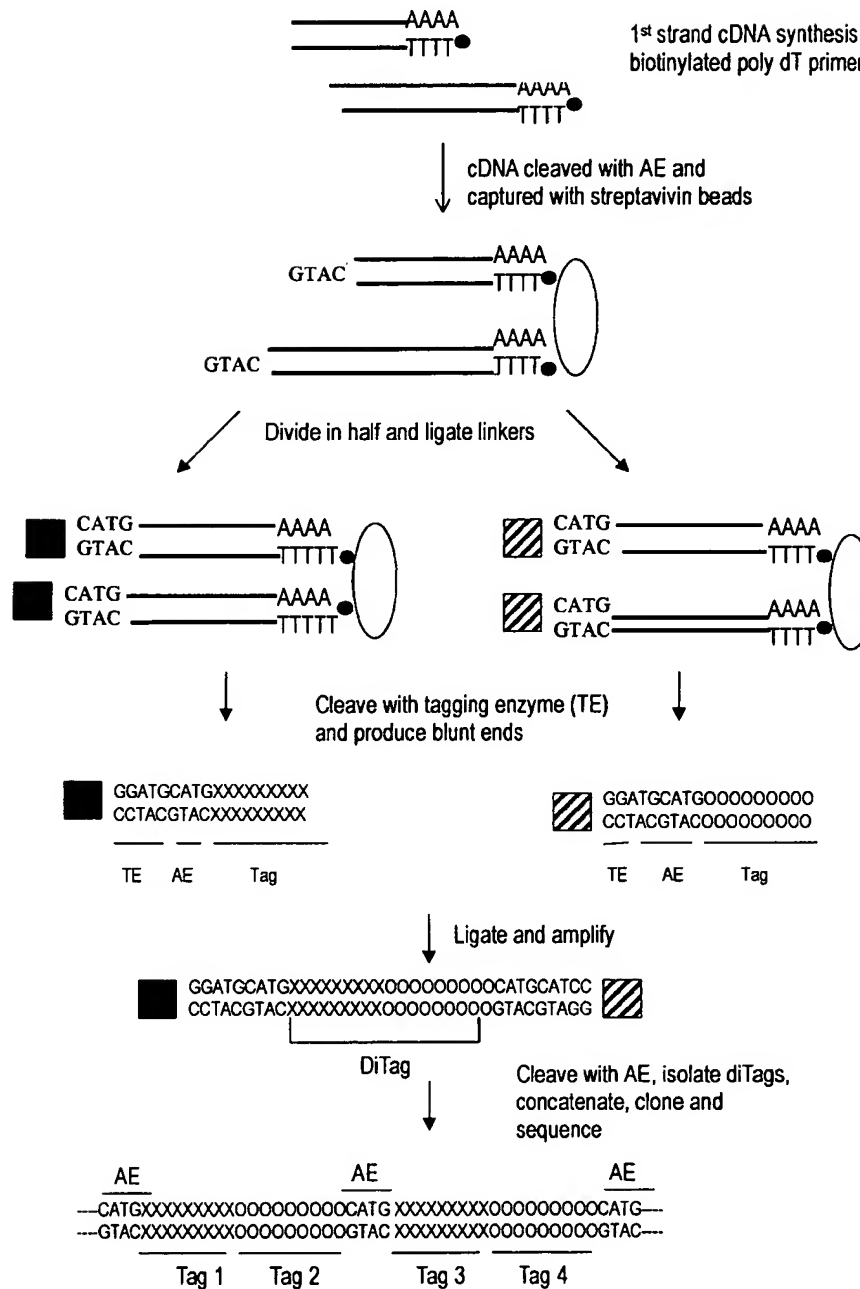


Figure 9. Serial analysis of gene expression (SAGE) analysis. cDNA is cleaved with an anchoring enzyme (AE) and the 3' ends captured using streptavidin beads. The cDNA pool is divided in half and each portion ligated to a different linker, each containing a type IIS restriction site (tagging enzyme, TE). Restriction with the type IIS enzyme releases the linker plus a short length of cDNA (XXXXXX and OOOOO indicate nucleotides of different tags). The two pools of tags are then ligated and amplified using linker-specific primers. Following PCR, the products are cleaved with the AE and the ditags isolated from the linkers using PAGE. The ditags are then ligated (during which process, concatenization occurs) and cloned into a vector of choice for sequencing. After Velculescu *et al.* (1995), with permission.

DNA arrays

'Open' differential display systems are cumbersome in that it takes a great deal of time to extract and identify candidate genes and then confirm that they are indeed up- or down-regulated in the treated compared to the control tissue. Normally, the latter process is carried out using Northern blotting or RT-PCR. Even so, each of the aforementioned steps produce a bottleneck to the ultimate goal of rapid analysis of gene expression. These problems will likely be addressed by the development of so-called DNA arrays (e.g. Gress *et al.* 1992, Zhao *et al.* 1995, Schena *et al.* 1996), the introduction of which has signalled the next era in differential gene expression analysis. DNA arrays consist of a gridded membrane or glass 'chips' containing hundreds or thousands of DNA spots, each consisting of multiple copies of part of a known gene. The genes are often selected based on previously proven involvement in oncogenesis, cell cycling, DNA repair, development and other cellular processes. They are usually chosen to be as specific as possible for each gene and animal species. Human and mouse arrays are already commercially available and a few companies will construct a personalized array to order, for example Clontech Laboratories and Research Genetics Inc. The technique is rapid in that hundreds or even thousands of genes can be spotted on a single array, and that mRNA/cDNA from the test populations can be labelled and used directly as probe. When analysed with appropriate hardware and software, arrays offer a rapid and quantitative means to assess differences in gene expression between two cell populations. Of course, there can only be identification and quantitation of those genes which are in the array (hence the term 'closed' system). Therefore, one approach to elucidating the molecular mechanisms involved in a particular disease/development system may be to combine an open and closed system—a DNA array to directly identify and quantitate the expression of known genes in mRNA populations, and an open system such as SSH to isolate unknown genes which are differentially expressed.

One of the main advantages of DNA arrays is the huge number of gene fragments which can be put on a membrane—some companies have reported gridding up to 60 000 spots on a single glass 'chip' (microscope slide). These high density chip-based micro-arrays will probably become available as mass-produced off-the-shelf items in the near future. This should facilitate the more rapid determination of differential expression in time and dose-response experiments. Aside from their high cost and the technical complexities involved in producing and probing DNA arrays, the main problem which remains, especially with the newer micro-array (gene-chip) technologies, is that results are often not wholly reproducible between arrays. However, this problem is being addressed and should be resolved within the next few years.

EST databases as a means to identify differentially expressed genes

Expressed sequence tags (ESTs) are partial sequences of clones obtained from cDNA libraries. Even though most ESTs have no formal identity (putative identification is the best to be hoped for), they have proven to be a rapid and efficient means of discovering new genes and can be used to generate profiles of gene-expression in specific cells. Since they were first described by Adams *et al.* (1991), there has been a huge explosion in EST production and it is estimated that there are now well over a million such sequences in the public domain, representing over half

of all human genes (Hillier *et al.* 1996). This large number of freely available sequences (both sequence information and clones are normally available royalty-free from the originators) has enabled the development of a new approach towards differential gene expression analysis as described by Vasmatazis *et al.* (1998). The approach is simple in theory: EST databases are first searched for genes that have a number of related EST sequences from the target tissue of choice, but none or few from non-target tissue libraries. Programmes to assist in the assembly of such sets of overlapping data may be developed in-house or obtained privately or from the internet. For example, the Institute for Genomic Research (TIGR, found at <http://www.tigr.org>) provides many software tools free of charge to the scientific community. Included amongst these is the TIGR assembler (Sutton *et al.* 1995), a tool for the assembly of large sets of overlapping data such as ESTs, bacterial artificial chromosomes (BAC)s, or small genomes. Candidate EST clones representing different genes are then analysed using RNA blot methods for size and tissue specificity and, if required, used as probes to isolate and identify the full length cDNA clone for further characterization. In practice however, the method is rather more involved, requiring bioinformatic and computer analysis coupled with confirmatory molecular studies. Vasmatazis *et al.* (1998) have described several problems in this fledgling approach, such as separating highly homologous sequences derived from different genes and an overemphasis of specificity for some EST sequences. However, since these problems will largely be addressed by the development of more suitable computer algorithms and an increased completeness of the EST database, it is likely that this approach to identifying differentially expressed genes may enjoy more patronage in the future.

Problems and potential of differential expression techniques

The holistic or single cell approach?

When working with *in vivo* models of differential expression, one of the first issues to consider must be the presence of multiple cell types in any given specimen. For example, a liver sample is likely to contain not only hepatocytes, but also (potentially) Ito cells, bile ductule cells, endothelial cells, various immune cells (e.g. lymphocytes, macrophages and Kupffer cells) and fibroblasts. Other tissues will each have their own distinctive cell populations. Also, in the case of neoplastic tissue, there are almost always normal, hyperplastic and/or dysplastic cells present in a sample. One must, therefore, be aware that genes obtained from a differential display experiment performed on an animal tissue model may not necessarily arise exclusively from the intended 'target' cells, e.g. hepatocytes/neoplastic cells. If appropriate, further analyses using immunohistochemistry, *in situ* hybridization or *in situ* RT-PCR should be used to confirm which cell types are expressing the gene(s) of interest. This problem is probably most acute for those studying the differential expression of genes in the development of different cell types, where there is a need to examine homologous cell populations. The problem is now being addressed at the National Cancer Institute (Bethesda, MD, USA) where new microdissection techniques have been employed to assist in their gene analysis programme, the Cancer Genome Anatomy Project (CGAP) (For more information see web site: <http://www.ncbi.nlm.nih.gov/ncicgap/intro.html>). There are also separation techniques available that utilise cell-specific antigens as a means to isolate target cells,

e.g. fluorescence activated cell sorting (FACS) (Dunbar *et al.* 1998, Kas-Deelen *et al.* 1998) and magnetic bead technology (Richard *et al.* 1998, Rogler *et al.* 1998).

However, those taking a holistic approach may consider this issue unimportant. There is an equally appropriate view that all those genes showing altered expression within a compromised tissue should be taken into consideration. After all, since all tissues are complex mixes of different, interacting cell types which intimately regulate each other's growth and development, it is clear that each cell type could in some way contribute (positively or negatively) towards the molecular mechanisms which lie behind responses to external stimuli or neoplastic growth. It is perhaps then more informative to carry out differential display experiments using *in vivo* as opposed to *in vitro* models, where uniform populations of identical cells probably represent a partial, skewed or even inaccurate picture of the molecular changes that occur.

The incidence and possible implications of inter-individual biological variation should be considered in any approach where whole animal models are being used. It is clear that individuals (humans and animals) respond in different ways to identical stimuli. One of the best characterized examples is the debrisoquine oxidation polymorphism, which is mediated by cytochrome CYP2D6 and determines the pharmacokinetics of many commonly prescribed drugs (Lennard 1993, Meyer and Zanger 1997). The reasons for such differences are varied and complex, but allelic variations, regulatory region polymorphisms and even physical and mental health can all contribute to observed differences in individual responses. Careful thought should, therefore, be given to the specific objectives of the study and to the possible value of pooling starting material (tissue/mRNA). The effect of this can be beneficial through the ironing out of exaggerated responses and unimportant minor fluctuations of (mechanistically) irrelevant genes in individual animals, thus providing a clearer overall picture of the general molecular mechanisms of the response. However, at the same time such minor variations may be of utmost importance in deciding the ability of individual animals to succumb to or resist the effects of a given chemical/disease.

How efficient are differential expression techniques at recovering a high percentage of differentially expressed genes?

A number of groups have produced experimental data suggesting that mammalian cells produce between 8000–15000 different mRNA species at any one time (Mechler and Rabbitts 1981, Hedrick *et al.* 1984, Bravo 1990), although figures as high as 20–30000 have also been quoted (Axel *et al.* 1976). Hedrick *et al.* (1984) provided evidence suggesting that the majority of these belong to the rare abundance class. A breakdown of this abundance distribution is shown in table 1.

When the results of differential display experiments have been compared with data obtained previously using other methods, it is apparent that not all differentially expressed mRNAs are represented in the final display. In particular, rare messages (which, importantly, often include regulatory proteins) are not easily recovered using differential display systems. This is a major shortcoming, as the majority of mRNA species exist at levels of less than 0.005% of the total population (table 1). Bertoli *et al.* (1995) examined the efficiency of DD templates (heterogeneous mRNA populations) for recovering rare messages and were unable to detect mRNA

species present at less than 1.2% of the total mRNA population—equivalent to an intermediate or abundant species. Interestingly, when simple model systems (single target only) were used instead of a heterogeneous mRNA population, the same primers could detect levels of target mRNA down to 10000× smaller. These results are probably best explained by competition for substrates from the many PCR products produced in a DD reaction.

The numbers of differentially expressed mRNAs reported in the literature using various model systems provides further evidence that many differentially expressed mRNAs are not recovered. For example, DeRisi *et al.* (1997) used DNA array technology to examine gene expression in yeast following exhaustion of sugar in the medium, and found that more than 1700 genes showed a change in expression of at least 2-fold. In light of such a finding, it would not be unreasonable to suggest that of the 8000–15 000 different mRNA species produced by any given mammalian cell, up to 1000 or more may show altered expression following chemical stimulation. Whilst this may be an extreme figure, it is known that at least 100 genes are activated/upregulated in Jurkat (T-) cells following IL-2 stimulation (Ullman *et al.* 1990). In addition, Wan *et al.* (1996) estimated that interferon- γ -stimulated HeLa cells differentially express up to 433 genes (assuming 24000 distinct mRNAs expressed by the cells). However, there have been few publications documenting anywhere near the recovery of these numbers. For example, in using DD to compare normal and regenerating mouse liver, Bauer *et al.* (1993) found only 70 of 38000 total bands to be different. Of these, 50% (35 genes) were shown to correspond to differentially expressed bands. Chen *et al.* (1996) reported 10 genes upregulated in female rat liver following ethinyl estradiol treatment. McKenzie and Drake (1997) identified 14 different gene products whose expression was altered by phorbol myristate acetate (PMA, a tumour promoter agent) stimulation of a human myelomonocytic cell line. Kilty and Vickers (1997) identified 10 different gene products whose expression was upregulated in the peripheral blood leukocytes of allergic disease sufferers. Linskens *et al.* (1995) found 23 genes differentially expressed between young and senescent fibroblasts. Techniques other than DD have also provided an apparent paucity of differentially expressed genes. Using SH for example, Cao *et al.* (1997) found 15 genes differentially expressed in colorectal cancer compared to normal mucosal epithelium. Fitzpatrick *et al.* (1995) isolated 17 genes upregulated in rat liver following treatment with the peroxisome proliferator, clofibrate; Philips *et al.* (1990) isolated 12 cDNA clones which were upregulated in highly metastatic mammary adenocarcinoma cell lines compared to poorly metastatic ones. Prashar and Weissman (1996) used 3' restriction fragment analysis and identified approximately 40 genes showing altered expression within 4 h of activation of Jurkat T-cells. Groenink and Leegwater (1996) analysed 27 gene fragments isolated using SSH of delayed early response phase of liver regeneration and found only 12 to be upregulated.

In the laboratory, SSH was used to isolate up to 70 candidate genes which appear to show altered expression in guinea pig liver following short-term treatment with the peroxisome proliferator, WY-14,643 (Rockett, Swales, Esdaile and Gibson, unpublished observations). However, these findings have still to be confirmed by analysis of the extracted tissue mRNA for differential expression of these sequences.

Whilst the latest differential display technologies are purported to include design and experimental modifications to overcome this lack of efficiency (in both the total number of differentially expressed genes recovered and the percentage that are true

positives), it is still not clear if such adaptations are practically effective—proving efficiency by spiking with a known amount of limited numbers of artificial construct(s) is one thing, but isolating a high percentage of the rare messages already present in an mRNA population is another. Of course, some models will genuinely produce only a small number of differentially expressed genes. In addition, there are also technical problems that can reduce efficiency. For example, mRNAs may have an unusual primary structure that effectively prevents their amplification by PCR-based systems. In addition, it is known that under certain circumstances not all mRNAs have 3' polyA sites. For example, during *Xenopus* development, deadenylation is used as a means to stabilize RNAs (Voeltz and Steitz 1998), whilst preferential deadenylation may play a role in regulating Hsp70 (and perhaps, therefore, other stress protein) expression in *Drosophila* (Dellavalle *et al.* 1994). The presence of deadenylated mRNAs would clearly reduce the efficiency of systems utilizing a polydT reverse transcription step. The efficiency of any system also depends on the quality of the starting material. All differential display techniques use mRNA as their target material. However, it is difficult to isolate mRNA that is completely free of ribosomal RNA. Even if polydT primers are used to prime first strand cDNA synthesis, ribosomal RNA is often transcribed to some degree (Clontech PCR-Select cDNA Subtraction kit user manual). It has been shown, at least in the case of SSH, that a high rRNA:mRNA ratio can lead to inefficient subtractive hybridization (Clontech PCR-Select cDNA Subtraction kit user manual), and there is no reason to suppose that it will not do likewise in other SH approaches. Finally, those techniques that utilise a presubtraction amplification step (e.g. RDA) may present a skewed representation since some sequences amplify better than others.

Of course, probably the most important consideration is the temporal factor. It is clear that any given differential display experiment can only interrogate a cell at one point in time. It may well be that a high percentage of the genes showing altered expression at that time are obtained. However, given that disease processes and responses to environmental stimuli involve dynamic cascades of signalling, regulation, production and action, it is clear that all those genes which are switched on/off at different times will not be recovered and, therefore, vital information may well be missed. It is, therefore, imperative to obtain as much information about the model system beforehand as possible, from which a strategy can be derived for targeting specific time points or events that are of particular interest to the investigator. One way of getting round this problem of single time point analysis is to conduct the experiment over a suitable time course which, of course, adds substantially to the amount of work involved.

How sensitive are differential expression technologies?

There has been little published data that addresses the issue of how large the change in expression must be for it to permit isolation of the gene in question with the various differential expression technologies. Although the isolation of genes whose expression is changed as little as 1.5-fold has been reported using SSH (Groenink and Leegwater 1996), it appears that those demonstrating a change in excess of 5-fold are more likely to be picked up. Thus, there is a 'grey zone' in between where small changes could fade in and out of isolation between

experiments and animals. DD, on the other hand, is not subject to this grey zone since, unlike SH approaches, it does not amplify the difference in expression between two samples. Wan *et al.* (1996) reported that differences in expression of twofold or more are detectable using DD.

Resolution and visualization of differential expression products

It seems highly improbable with current technology that a gel system could be developed that is able to resolve all gene species showing altered expression in any given test system (be it SH- or DD-based). Polyacrylamide gel electrophoresis (PAGE) can resolve size differences down to 0.2% (Sambrook *et al.* 1989) and are used as standard in DD experiments. Even so, it is clear that a complex series of gene products such as those seen in a DD will contain unresolvable components. Thus, what appears to be one band in a gel may in fact turn out to be several. Indeed, it has been well documented (Mathieu-Daude *et al.* 1996, Smith *et al.* 1997) that a single band extracted from a DD often represents a composite of heterogeneous products, and the same has been found for SSH displays in this laboratory (Rockett *et al.* 1997). One possible solution was offered by Mathieu-Daude *et al.* (1996), who extracted and reamplified candidate bands from a DD display and used single strand conformation polymorphism (SSCP) analysis to confirm which components represented the truly differentially expressed product.

Many scientists often try to avoid the use of PAGE where possible because it is technically more demanding than agarose gel electrophoresis (AGE). Unfortunately, high resolution agarose gels such as Metaphor (FMC, Lichfield, UK) and AquaPor HR (National Diagnostics, Hessle, UK), whilst easier to prepare and manipulate than PAGE, can only separate DNA sequences which differ in size by around 1.5–2% (15–20 base pairs for a 1Kb fragment). Thus, SSH, RDA or other such products which differ in size by less than this amount are normally not resolvable. However, a simple technique does in fact exist for increasing the resolving power of AGE—the inclusion of HA-red (10-phenyl neutral red-PEG ligand) or HA-yellow (bisbenzamide-PEG ligand) (Hanse Analytik GmbH, Bremen, Germany) in a gel separates identical or closely sized products on base content. Specifically, HA-red and -yellow selectively bind to GC and AT DNA motifs, respectively (Wawer *et al.* 1995, Hanse Analytik 1997, personal communication). Since both HA-stains possess an overall positive charge, they migrate towards the cathode when an electric field is applied. This is in direct opposition to DNA, which is negatively charged and, therefore, migrates towards the anode. Thus, if two DNA clones are identical in size (as perceived on a standard high resolution agarose gel), but differ in AT/GC content, inclusion of a HA-dye in the gel will effectively retard the migration of one of the sequences compared to the other, effectively making it apparently larger and, thus, providing a means of differentiating between the two. The use of HA-red has been shown to resolve sequences with an AT variation of less than 1% (Wawer *et al.* 1995), whilst Hanse Analytik have reported that HA staining is so sensitive that in one case it was used to distinguish two 567bp sequences which differed by only a single point mutation (Hanse Analytik 1996, personal communication). Therefore, if one wishes to check whether all the clones produced from a specific band in a differential display experiment are derived from the same gene species, a small amount of reamplified or digested clone can be run on a standard high resolution gel, and a second aliquot

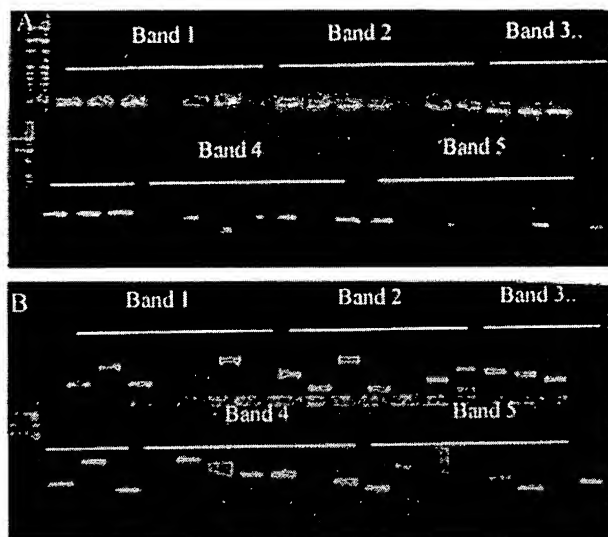


Figure 10. Discrimination of clones of identical/nearly identical size using HA-red. Bands of decreasing size (1–5) were extracted from the final display of a suppression subtractive hybridization experiment and cloned. Seven colonies were picked at random from each cloned band and their inserts amplified using PCR. The products were run on two gels, (A) a high resolution 2% agarose gel, and (B) a high resolution 2% agarose gel containing 1 U/ml HA-red. With few exceptions, all the clones from each band appear to be the same size (gel A). However, the presence of HA-red (gel B), which separates identically-sized DNA fragments based on the percentage of GC within the sequence, clearly indicates the presence of different gene species within each band. For example, even though all five re-amplified clones of band 1 appear to be the same size, at least four different gene species are represented.

in a similar gel containing one of the HA-stains. The standard gel should indicate any gross size differences, whilst the HA-stained gel should separate otherwise unresolvable species (on standard AGE) according to their base content. Geisinger *et al.* (1997) reported successful use of this approach for identifying DD-derived clones. Figure 10 shows such an experiment carried out in this laboratory on clones obtained from a band extracted from an SSH display.

An alternative approach is to carry out a 2-D analysis of the differential display products. In this approach, size-based separation is first carried out in a standard agarose gel. The gel slice containing the display is then extracted and incorporated in to a HA gel for resolution based on AT/GC content.

Of course, one should always consider the possibility of there being different gene species which are the same size and have the same GC/AT content. However, even these species are not unresolvable given some effort—again, one might use SSCP, or perhaps a denaturing gradient gel electrophoresis (DGGE) or temperature gradient field electrophoresis (TGGE) approach to resolve the contents of a band, either directly on the extracted band (Suzuki *et al.* 1991) or on the reamplified product.

The requirement of some differential display techniques to visualize large numbers of products (e.g. DD and GEF) can also present a problem in that, in terms of numbers, the resolution of PAGE rarely exceeds 300–400 bands. One approach to overcoming this might be to use 2-D gels such as those described by Uitterlinden *et al.* (1989) and Hatada *et al.* (1991).

Extraction of differentially expressed bands from a gel can be complex since, in some cases (e.g. DD, GEF), the results are visualized by autoradiographic means, such that precise overlay of the developed film on the gel must occur if the correct band is to be extracted for further analysis. Clearly, a misjudged extraction can account for many man-hours lost. This problem, and that of the use of radioisotopes, has been addressed by several groups. For example, Lohmann *et al.* (1995) demonstrated that silver staining can be used directly to visualize DD bands in horizontal PAGs. An *et al.* (1996) avoided the use of radioisotopes by transferring a small amount (20–30%) of the DNA from their DD to a nylon membrane, and visualizing the bands using chemiluminescent staining before going back to extract the remaining DNA from the gel. Chen and Peck (1996) went one step further and transferred the entire DD to a nylon membrane. The DNA bands were then visualized using a digoxigenin (DIG) system (DIG was attached to the polydT primers used in the differential display procedure). Differentially expressed bands were cut from the membrane and the DNA eluted by washing with PCR buffer prior to reamplification.

One of the advantages of using techniques such as SSH and RDA is that the final display can be run on an agarose gel and the bands visualized with simple ethidium bromide staining. Whilst this approach can provide acceptable results, overstaining with SYBR Green I or SYBR Gold nucleic acid stains (FMC) effectively enhances the intensity and sharpness of the bands. This greatly aids in their precise extraction and often reveals some faint products that may otherwise be overlooked. Whilst differential displays stained with SYBR Green I are better visualized using short wavelength UV (254 nm) rather than medium wavelength (306 nm), the shorter wavelength is much more DNA damaging. In practice, it takes only a few seconds to damage DNA extracted under 254 nm irradiation, effectively preventing reamplification and cloning. The best approach is to over stain with SYBR Green I and extract bands under a medium wavelength UV transillumination.

The possible use of 'microfingerprinting' to reduce complexity

Given the sheer number of gene products and the possible complexity of each band, an alternative approach to rapid characterization may be to use an enhanced analysis of a small section of a differential display—a 'sub-fingerprint' or 'micro-fingerprint'. In this case, one could concentrate on those bands which only appear in a particular chosen size region. Reducing the fingerprint in this way has at least two advantages. One is that it should be possible to use different gel types, concentrations and run times tailored exactly to that region. Currently, one might run products from 100–3000 + bp on the same gel, which leads to compromise in the gel system being used and consequently to suboptimal resolution, both in terms of size and numbers, and can lead to problems in the accurate excision of individual bands. Secondly, it may be possible to enhance resolution by using a 2-D analysis using a HA-stain, as described earlier. In summary, if a range of gene product sizes is carefully chosen to include certain 'relevant' genes, the 2-D system standardized, and appropriate gene analysis used, it may be possible to develop a method for the early and rapid identification of compounds which have similar or widely different cellular effects. If the prognosis for exposure to one or more other chemicals which display a similar profile is already known, then one could perhaps predict similar effects for any new compounds which show a similar micro-fingerprint.

An alternative approach to microfingerprinting is to examine altered expression in specific families of genes through careful selection of PCR primers and/or post-reaction analysis. Stress genes, growth factors and/or their receptors, cell cycling genes, cytochromes P450 and regulatory proteins might be considered as candidates for analysis in this way. Indeed, some off-the-shelf DNA arrays (e.g. Clontech's Atlas cDNA Expression Array series) already anticipated this to some degree by grouping together genes involved in different responses e.g. apoptosis, stress, DNA-damage response etc.

Screening

False positives

The generation of false positives has been discussed at length amongst the differential display community (Liang *et al.* 1993, 1995, Nishio *et al.* 1994, Sun *et al.* 1994, Sompayrac *et al.* 1995). The reason for false positives varies with the technique being used. For instance, in RDA, the use of adaptors which have not been HPLC purified can lead to the production of false positives through illegitimate ligation events (O'Neill and Sinclair 1997), whilst in DD they can arise through PCR artifacts and illegitimate transcription of rRNA. In SH, false positives appear to be derived largely from abundant gene species, although some may arise from cDNA/mRNA species which do not undergo hybridization for technical reasons.

A quick screening of putative differentially expressed clones can be carried out using a simple dot blot approach, in which labelled first strand probes synthesized from tester and driver mRNA are hybridized to an array of said clones (Hedrick *et al.* 1984, Sakaguchi *et al.* 1986). Differentially expressed clones will hybridize to tester probe, but not driver. The disadvantage of this approach is that rare species may not generate detectable hybridization signals. One option for those using SSH is to screen the clones using a labelled probe generated from the subtracted cDNA from which it was derived, and with a probe made from the reverse subtraction reaction (ClonTechniques 1997a). Since the SSH method enriches rare sequences, it should be possible to confirm the presence of clones representing low abundance genes. Despite this quick screening step, there is still the need to go back to the original mRNA and confirm the altered expression using a more quantitative approach. Although this may be achieved using Northern blots, the sensitivity is poor by today's high standards and one must rely on PCR methods for accurate and sensitive determinations (see below).

Sequence analysis

The majority of differential display procedures produce final products which are between 100 and 1000bp in size. However, this may considerably reduce the size of the sequence for analysis of the DNA databases. This in turn leads to a reduced confidence in the result—several families of genes have members whose DNA sequences are almost identical except in a few key stretches, e.g. the cytochrome P450 gene superfamily (Nelson *et al.* 1996). Thus, does the clone identified as being almost identical to gene X_0 really come from that gene, or its brother gene X_1 or its as yet undiscovered sister X_2 ? For example, using SSH, part of a gene was isolated,

which was up-regulated in the liver of rats exposed to Wy-14,643 and was identified by a FASTA search as being transferrin (data not shown). However, transferrin is known to be downregulated by hypolipidemic peroxisome proliferators such as Wy-14,643 (Hertz *et al.* 1996), and this was confirmed with subsequent RT-PCR analysis. This suggests that the gene sequence isolated may belong to a gene which is closely related to transferrin, but is regulated by a different mechanism.

A further problem associated with SH technology is redundancy. In most cases before SH is carried out, the cDNA population must first be simplified by restriction digestion. This is important for at least two reasons:

- (1) To reduce complexity—long cDNA fragments may form complex networks which prevent the formation of appropriate hybrids, especially at the high concentrations required for efficient hybridization.
- (2) Cutting the cDNAs into small fragments provides better representation of individual genes. This is because genes derived from related but distinct members of gene families often have similar coding sequences that may cross-hybridize and be eliminated during the subtraction procedure (Ko 1990). Furthermore, different fragments from the same cDNA may differ considerably in terms of hybridization and amplification and, thus, may not efficiently do one or the other (Wang and Brown 1991). Thus, some fragments from differentially expressed cDNAs may be eliminated during subtractive hybridization procedures. However, other fragments may be enriched and isolated. As a consequence of this, some genes will be cut one or more times, giving rise to two or more fragments of different sizes. If those same genes are differentially expressed, then two or more of the different size fragments may come through as separate bands on the final differential display, increasing the observed redundancy and increasing the number of redundant sequencing reactions.

Sequence comparisons also throw up another important point—at what degree of sequence similarity does one accept a result. Is 90% identity between a gene derived from your model species and another acceptably close? Is 95% between your sequence and one from the same species also acceptable? This problem is particularly relevant when the forward and reverse sequence comparisons give similar sequences with completely different gene species! An arbitrary decision seems to be to allocate genes that are definite (95% and above similarity) and then group those between 60 and 95% as being related or possible homologues.

Quantitative analysis

At some point, one must give consideration to the quantitative analysis of the candidate genes, either as a means of confirming that they are truly differentially expressed, or in order to establish just what the differences are. Northern blot analysis is a popular approach as it is relatively easy and quick to perform. However, the major drawback with Northern blots is that they are often not sensitive enough to detect rare sequences. Since the majority of messages expressed in a cell are of low abundance (see table 1), this is a major problem. Consequently, RT-PCR may be the method of choice for confirming differential expression. Although the procedure is somewhat more complex than Northern analysis, requiring synthesis of primers and optimization of reaction conditions for each gene species, it is now possible to set up high throughput PCR systems using multichannel pipettes, 96 +well plates and

appropriate thermal cycling technology. Whilst quantitative analysis is more desirable, being more accurate and without reliance on an internal standard, the money and time needed to develop a competitor molecule is often excessive, especially when one might be examining tens or even hundreds of gene species. The use of semi-quantitative analysis is simpler, although still relatively involved. One must first of all choose an internal standard that does not change in the test cells compared to the controls. Numerous reference genes have been tried in the past, for example interferon-gamma (IFN- γ , Frye *et al.* 1989), β -actin (Heuval *et al.* 1994), glyceraldehyde-3-phosphate dehydrogenase (GAPDH, Wong *et al.* 1994), dihydrofolate reductase (DHFR, Mohler and Butler 1991), β -2-microglobulin (β -2-m, Murphy *et al.* 1990), hypoxanthine phosphoribosyl transferase (HPRT, Foss *et al.* 1998) and a number of others (ClonTechniques 1997b). Ideally, an internal standard should not change its level of expression in the cell regardless of cell age, stage in the cell cycle or through the effects of external stimuli. However, it has been shown on numerous occasions that the levels of most housekeeping genes currently used by the research community do in fact change under certain conditions and in different tissues (ClonTechniques 1997b). It is imperative, therefore, that preliminary experiments be carried out on a panel of housekeeping genes to establish their suitability for use in the model system.

Interpretation of quantitative data must also be treated with caution. By comparing the lists of genes identified by differential expression one can perhaps gain insight into why two different species react in different ways to external stimuli. For example, rats and mice appear sensitive to the non-genotoxic effects of a wide range of peroxisome proliferators whilst Syrian hamsters and guinea pigs are largely resistant (Orton *et al.* 1984, Rodricks and Turnbull 1987, Lake *et al.* 1989, 1993, Makowska *et al.* 1992). A simplified approach to resolving the reason(s) why is to compare lists of up- and down-regulated genes in order to identify those which are expressed in only one species and, through background knowledge of the effects of the said gene, might suggest a mechanism of facilitated non-genotoxic carcinogenesis or protection. Of course, the situation is likely to be far more complex. Perhaps if there were one key gene protecting guinea pig from non-genotoxic effects and it was upregulated 50 times by PPs, the same gene might only be up-regulated five times in the rat. However, since both were noted to be upregulated, the importance of the gene may be overlooked. Just to complicate matters, a large change in expression does not necessarily mean a biologically important change. For example, what is the true relevance of gene Y which shows a 50-fold increase after a particular treatment, and gene Z which shows only a 5-fold increase? If one examines the literature one may find that historically, gene Y has often been shown to be up-regulated 40–60-fold by a number of unrelated stimuli—in light of this the 50-fold increase would appear less significant. However, the literature may show that gene Z has never been recorded as having more than doubled in expression—which makes your 5-fold increase all the more exciting. Perhaps even more interesting is if that same 5-fold increase has only been seen in related neoplasms or following treatment with related chemicals.

Problems in using the differential display approach

Differential display technology originally held promise of an easily obtainable 'fingerprint' of those genes which are up- or down-regulated in test animals/cells in a developmental process or following exposure to given stimuli. However, it has

become clear that the fingerprinting process, whilst still valid, is much too complex to be represented by a single technique profile. This is because all differential display techniques have common and/or unique technical problems which preclude the isolation and identification of all those genes which show changes in expression. Furthermore, there are important genetic changes related to disease development which differential expression analysis is simply not designed to address. An example of this is the presence of small deletions, insertions, or point mutations such as those seen in activated oncogenes, tumour suppressor genes and individual polymorphisms. Polymorphic variations, small though they usually are, are often regarded as being of paramount importance in explaining why some patients respond better than others to certain drug treatments (and, in logical extension, why some people are less affected by potentially dangerous xenobiotics/carcinogens than others). The identification of such point mutations and naturally occurring polymorphisms requires the subsequent application of sequencing, SSCP, DGGE or TGGE to the gene of interest. Furthermore, differential display is not designed to address issues such as alternatively spliced gene species or whether an increased abundance of mRNA is a result of increased transcription or increased mRNA stability.

Conclusions

Perhaps the main advantage of open system differential display techniques is that they are not limited by extant theories or researcher bias in revealing genes which are differentially expressed, since they are designed to amplify all genes which demonstrate altered expression. This means that they are useful for the isolation of previously unknown genes which may turn out be useful biomarkers of a particular state or condition. At least one open system (SAGE) is also quantitative, thus eliminating the need to return to the original mRNA and carry out Northern/PCR analysis to confirm the result. However, the rapid progress of genome mapping projects means that over the next 5–10 years or so, the balance of experimental use will switch from open to closed differential display systems, particularly DNA arrays. Arrays are easier and faster to prepare and use, provide quantitative data, are suitable for high throughput analysis and can be tailored to look at specific signalling pathways or families of genes. Identification of all the gene sequences in human and common laboratory animals combined with improved DNA array technology, means that it will soon no longer be necessary to try to isolate differentially expressed genes using the technically more demanding open system approach. Thus, their main advantage (that of identifying unknown genes) will be largely eradicated. It is likely, therefore, that their sphere of application will be reduced to analysis of the less common laboratory species, since it will be some time yet before the genomes of such animals as zebrafish, electric eels, gerbils, crayfish and squid, for example, will be sequenced.

Of course, in the end the question will always remain: What is the functional/biological significance of the identified, differentially expressed genes? One persistent problem is understanding whether differentially expressed genes are a cause or consequence of the altered state. Furthermore, many chemicals, such as non-genotoxic carcinogens, are also mitogens and so genes associated with replication will also be upregulated but may have little or nothing to do with the

carcinogenic effect. Whilst differential display technology cannot hope to answer these questions, it does provide a springboard from which identification, regulatory and functional studies can be launched. Understanding the molecular mechanism of cellular responses is almost impossible without knowing the regulation and function of those genes and their condition (e.g. mutated). In an abstract sense, differential display can be likened to a still photograph, showing details of a fixed moment in time. Consider the Historian who knows the outcome of a battle and the placement and condition of the troops before the battle commenced, but is asked to try and deduce how the battle progressed and why it ended as it did from a few still photographs—an impossible task. In order to understand the battle, the Historian must find out the capabilities and motivation of the soldiers and their commanding officers, what the orders were and whether they were obeyed. He must examine the terrain, the remains of the battle and consider the effects the prevailing weather conditions exerted. Likewise, if mechanistic answers are to be forthcoming, the scientist must use differential display in combination with other techniques, such as knockout technology, the analysis of cell signalling pathways, mutation analysis and time and dose response analyses. Although this review has emphasized the importance of differential gene profiling, it should not be considered in isolation and the full impact of this approach will be strengthened if used in combination with functional genomics and proteomics (2-dimensional protein gels from isoelectric focusing and subsequent SDS electrophoresis and virtual 2D-maps using capillary electrophoresis). Proteomics is attracting much recent attention as many of the changes resulting in differential gene expression do not involve changes in mRNA levels, as described extensively herein, but rather protein-protein, protein-DNA and protein phosphorylation events which would require functional genomics or proteomic technologies for investigation.

Despite the limitations of differential display technology, it is clear that many potential applications and benefits can be obtained from characterizing the genetic changes that occur in a cell during normal and disease development and in response to chemical or biological insult. In light of functional data, such profiling will provide a 'fingerprint' of each stage of development or response, and in the long term should help in the elucidation of specific and sensitive biomarkers for different types of chemical/biological exposure and disease states. The potential medical and therapeutic benefits of understanding such molecular changes are almost immeasurable. Amongst other things, such fingerprints could indicate the family or even specific type of chemical an individual has been exposed to plus the length and/or acuteness of that exposure, thus indicating the most prudent treatment. They may also help uncover differences in histologically identical cancers, provide diagnostic tests for the earliest stages of neoplasia and, again, perhaps indicate the most efficacious treatment.

The Human Genome Project will be completed early in the next century and the DNA sequence of all the human genes will be known. The continuing development and evolution of differential gene expression technology will ensure that this knowledge contributes fully to the understanding of human disease processes.

Acknowledgements

We acknowledge Drs Nick Plant (University of Surrey), Sally Darney and Chris Luft (US EPA at RTP) for their critical analysis of the manuscript prior to submission. This manuscript has been reviewed in accordance with the policy of the

US Environmental Protection Agency and approved for publication. Approval does not signify that the contents reflect the views and policies of the Agency, nor does mention of trade names constitute endorsement or recommendation for use.

References

- ADAMS, M. D., KELLEY, J. M., GOCAYNE, J. D., DUBNICK, M., POLYMERPOULOS, M. H., XIAO, H., MERRIL, C. R., WU, A., OLDE, B., MORENO, R. F., KERLAVAGE, A. R., McCOMBIE, W. R. and VENTOR, J. C., 1991, Complementary DNA sequencing: expressed sequence tags and human genome project. *Science*, **252**, 1651–1656.
- AN, G., LUO, G., VELTRI, R. W. and O'HARA, S. M., 1996, Sensitive non-radioactive differential display method using chemiluminescent detection. *Biotechniques*, **20**, 342–346.
- AXEL, R., FEIGELSON, P. and SCHULTZ, G., 1976, Analysis of the complexity and diversity of mRNA from chicken liver and oviduct. *Cell*, **7**, 247–254.
- BAND, V. and SAGER, R., 1989, Distinctive traits of normal and tumor-derived human mammary epithelial cells expressed in a medium that supports long-term growth of both cell types. *Proceedings of the National Academy of Sciences, USA*, **86**, 1249–1253.
- BAUER, D., MULLER, H., REICH, J., RIEDEL, H., AHRENKIEL, V., WARTHOF, P. and STRAUSS, M., 1993, Identification of differentially expressed mRNA species by an improved display technique (DDRT-PCR). *Nucleic Acids Research*, **21**, 4272–4280.
- BERTIOLI, D. J., SCHLICHTER, U. H. A., ADAMS, M. J., BURROWS, P. R., STEINBISS, H.-H. and ANTONIW, J. F., 1995, An analysis of differential display shows a strong bias towards high copy number mRNAs. *Nucleic Acids Research*, **23**, 4520–4523.
- BRAVO, R., 1990, Genes induced during the G0/G1 transition in mouse fibroblasts. *Seminars in Cancer Biology*, **1**, 37–46.
- BURN, T. C., PETROVICK, M. S., HOHAUS, S., ROLLINS, B. J. and TENEN, D. G., 1994, Monocyte chemoattractant protein-1 gene is expressed in activated neutrophils and retinoic acid-induced human myeloid cell lines. *Blood*, **84**, 2776–2783.
- CAO, J., CAI, X., ZHENG, L., GENG, L., SHI, Z., PAO, C. C. and ZHENG, S., 1997, Characterisation of colorectal cancer-related cDNA clones obtained by subtractive hybridisation screening. *Journal of Cancer Research and Clinical Oncology*, **123**, 447–451.
- CASSIDY, S. B., 1995, Uniparental disomy and genomic imprinting as causes of human genetic disease. *Environmental and Molecular Mutagenesis*, **25** (Suppl 26), 13–20.
- CHANG, G. W. and TERZAGHI-HOWE, M., 1998, Multiple changes in gene expression are associated with normal cell-induced modulation of the neoplastic phenotype. *Cancer Research*, **58**, 4445–4452.
- CHEN, J., SCHWARTZ, D. A., YOUNG, T. A., NORRIS, J. S. and YAGER, J. D., 1996, Identification of genes whose expression is altered during mitosisuppression in livers of ethinyl estradiol-treated female rats. *Carcinogenesis*, **17**, 2783–2786.
- CHEN, J. J. W. and PECK, K., 1996, Non-radioactive differential display method to directly visualise and amplify differential bands on nylon membrane. *Nucleic Acid Research*, **24**, 793–794.
- CLON TECHNIQUES, 1997a, PCR-Select Differential Screening Kit—the nextstep after Clontech PCR-Select cDNA subtraction. *ClonTechniques*, **XII**, 18–19.
- CLON TECHNIQUES, 1997b, Housekeeping RT-PCR amplimers and cDNA probes. *ClonTechniques*, **XII**, 15–16.
- DAVIS, M. M., COHEN, D. I., NIELSEN, E. A., STEINMETZ, M., PAUL, W. E. and HOOD, L., 1984, Cell-type-specific cDNA probes and the murine I region: the localization and orientation of Ad alpha. *Proceedings of the National Academy of Sciences (USA)*, **81**, 2194–2198.
- DELLAVALLE, R. P., PETERSON, R. and LINDQUIST, S., 1994, Preferential deadenylation of HSP70 mRNA plays a key role in regulating Hsp70 expression in *Drosophila melanogaster*. *Molecular and Cell Biology*, **14**, 3646–3659.
- DERISI, J. L., VASHWANATH, R. L. and BROWN, P., 1997, Exploring the metabolic and genetic control of gene expression on a genomic scale. *Science*, **278**, 680–686.
- DIATCHENKO, L., LAU, Y.-F. C., CAMPBELL, A. P., CHENCHIK, A., MOQADAM, F., HUANG, B., LUKYANOV, K., GURSKAYA, N., SVERDLOV, E. D. and SIEBERT, P. D., 1996, Suppression subtractive hybridisation: A method for generating differentially regulated or tissue-specific cDNA probes and libraries. *Proceedings of the National Academy of Sciences (USA)*, **93**, 6025–6030.
- DOGRA, S. C., WHITELAW, M. L. and MAY, B. K., 1998, Transcriptional activation of cytochrome P450 genes by different classes of chemical inducers. *Clinical and Experimental Pharmacology and Physiology*, **25**, 1–9.
- DUGUID, J. R. and DINAUER, M. C., 1990, Library subtraction of *in vitro* cDNA libraries to identify differentially expressed genes in scrapie infection. *Nucleic Acids Research*, **18**, 2789–2792.
- DUNBAR, P. R., OGG, G. S., CHEN, J., RUST, N., VAN DER BRUGGEN, P. and CERUNDOLO, V., 1998, Direct isolation, phenotyping and cloning of low-frequency antigen-specific cytotoxic T lymphocytes from peripheral blood. *Current Biology*, **26**, 413–416.

- FITZPATRICK, D. R., GERMAIN -LEE, E. and VALLE, D., 1995, Isolation and characterisation of rat and human cDNAs encoding a novel putative peroxisomal enoyl-CoA hydratase. *Genomics*, **27**, 457-466.
- FOSS, D. L., BAARSCH, M. J. and MURTAUGH, M. P., 1998, Regulation of hypoxanthine phosphoribosyltransferase, glyceraldehyde-3-phosphate dehydrogenase and beta-actin mRNA expression in porcine immune cells and tissues. *Animal Biotechnology*, **9**, 67-78.
- FRYE, R. A., BENZ, C. C. and LIU, E., 1989, Detection of amplified oncogenes by differential polymerase chain reaction. *Oncogene*, **4**, 1153-1157.
- GEISINGER, A., RODRIGUEZ, R., ROMERO, V. and WETTSTEIN, R., 1997, A simple method for screening cDNAs arising from the cloning of RNA differential display bands. *Elsevier Trends Journals Technical Tips Online*, <http://tto.trends.com>, document T01110.
- GRESS, T. M., HOHEISEL, J. D., LENNON, G. G., ZEHETNER, G. and LEHRACH, H., 1992, Hybridisation fingerprinting of high density cDNA filter arrays with cDNA pools derived from whole tissues. *Mammalian Genome*, **3**, 609-619.
- GRIFFIN, G. and KRISHNA, S., 1998, Cytokines in infectious diseases. *Journal of the Royal College of Physicians, London*, **32**, 195-198.
- GROENINK, M. and LEEGWATER, A. C. J., 1996, Isolation of delayed early genes associated with liver regeneration using Clontech PCR-select subtraction technique. *Clontechniques*, **XI**, 23-24.
- GUIMARAES, M. J., BAZAN, J. F., ZLOTNIK, A., WILES, M. V., GRIMALDI, J. C., LEE, F. and MCCLANAHAN, T., 1995b, A new approach to the study of haematopoietic development in the yolk sac and embryoid bodies. *Development*, **121**, 3335-3346.
- GUIMARAES, M. J., LEE, F., ZLOTNIK, A. and MCCLANAHAN, T., 1995a, Differential display by PCR: novel findings and applications. *Nucleic Acids Research*, **23**, 1832-1833.
- GURSKAYA, N. G., DIATCHENKO, L., CHENCHIK, P. D., SIEBERT, P. D., KHASPEKOV, G. L., LUKYANOV, K. A., VAGNER, L. L., ERMOLAEVA, O. D., LUKYANOV, S. A. and SVERDLOV, E. D., 1996, Equalising cDNA subtraction based on selective suppression of polymerase chain reaction: Cloning of Jurkat cell transcripts induced by phytohemagglutinin and phorbol 12-Myristate 13-Acetate. *Analytical Biochemistry*, **240**, 90-97.
- HAMPSON, I. N. and HAMPSON, L., 1997, CCLS and DROP—subtractive cloning made easy. *Life Science News* (A publication of Amersham Life Science), **23**, 22-24.
- HAMPSON, I. N., HAMPSON, L. and DEXTER, T. M., 1996, Directional random oligonucleotide primed (DROP) global amplification of cDNA: its application to subtractive cDNA cloning. *Nucleic Acids Research*, **24**, 4832-4835.
- HAMPSON, I. N., POPE, L., COWLING, G. J. and DEXTER, T. M., 1992, Chemical cross linking subtraction (CCLS): a new method for the generation of subtractive hybridisation probes. *Nucleic Acids Research*, **20**, 2899.
- HARA, E., KATO, T., NAKADA, S., SEKIYA, S. and ODA, K., 1991, Subtractive cDNA cloning using oligo(dT)30-latex and PCR: isolation of cDNA clones specific to undifferentiated human embryonal carcinoma cells. *Nucleic Acids Research*, **19**, 7097-7104.
- HATADA, I., HAYASHIZAKE, Y., HIROTSUNE, S., KOMATSUBARA, H. and MUKAI, T., 1991, A genomic scanning method for higher organisms using restriction sites as landmarks. *Proceedings of the National Academy of Sciences (USA)*, **88**, 9523-9527.
- HECHT, N., 1998, Molecular mechanisms of male sperm cell differentiation. *Bioessays*, **20**, 555-561.
- HEDRICK, S., COHEN, D. I., NIELSEN, E. A. and DAVIS, M. E., 1984, Isolation of T cell-specific membrane-associated proteins. *Nature*, **308**, 149-153.
- HERTZ, R., SECKBACH, M., ZAKIN, M. M. and BAR-TANA, J., 1996, Transcriptional suppression of the transferrin gene by hypolipidemic peroxisome proliferators. *Journal of Biological Chemistry*, **271**, 218-224.
- HEUVAL, J. P. V., CLARK, G. C., KOHN, M. C., TRITSCHER, A. M., GREENLEE, W. F., LUCIER, G. W. and BELL, D. A., 1994, Dioxin-responsive genes: Examination of dose-response relationships using quantitative reverse transcriptase-polymerase chain reaction. *Cancer Research*, **54**, 62-68.
- HILLIER, L. D., LENNON, G., BECKER, M., BONALDO, M. F., CHIAPELLI, B., CHISSOE, S., DIETRICH, N., DUBUQUE, T., FAVELLO, A., GISH, W., HAWKINS, M., HULTMAN, M., KUCABA, T., LACY, M., LE, M., LE, N., MARDIS, E., MOORE, B., MORRIS, M., PARSONS, J., PRANGE, C., RIFKIN, L., ROHLFING, T., SCHELLENBERG, K., SOARES, M. B., TAN, F., THIERRY -MEG, J., TREVASKIS, E., UNDERWOOD, K., WOHLDMAN, P., WATERSTON, R., WILSON, R. and MARRA, M., 1996, Generation and analysis of 280,000 human expressed sequence tags. *Genome Research*, **6**, 807-828.
- HUBANK, M. and SCHATZ, D. G., 1994, Identifying differences in mRNA expression by representational difference analysis. *Nucleic Acids Research*, **22**, 5640-5648.
- HUNTER, T., 1991, Cooperation between oncogenes. *Cell*, **64**, 249-270.
- IVANOVA, N. B. and BELYAVSKY, A. V., 1995, Identification of differentially expressed genes by restriction endonuclease-based gene expression fingerprinting. *Nucleic Acids Research*, **23**, 2954-2958.
- JAMES, B. D. and HIGGINS, S. J., 1985, *Nucleic Acid Hybridisation* (Oxford: IRL Press Ltd).
- KAS-DEELEN, A. M., HARMSSEN, M. C., DE MAAR, E. F. and VAN SON, W. J., 1998, A sensitive method for

- quantifying cytomegalic endothelial cells in peripheral blood from cytomegalovirus-infected patients. *Clinical Diagnostic and Laboratory Immunology*, 5, 622-626.
- KILTY, I. and VICKERS, P., 1997, Fractionating DNA fragments generated by differential display PCR. *Strategies Newsletter* (Stratagene), 10, 50-51.
- KLEINJAN, D.-J. and VAN HEYNINGEN, V., 1998, Position effect in human genetic disease. *Human and Molecular Genetics*, 7, 1611-1618.
- KO, M. S., 1990, An 'equalized cDNA library' by the reassociation of short double-stranded cDNAs. *Nucleic Acids Research*, 18, 5705-5711.
- LAKE, B. G., EVANS, J. G., CUNNINGHAME, M. E. and PRICE, R. J., 1993, Comparison of the hepatic effects of Wy-14,643 on peroxisome proliferation and cell replication in the rat and Syrian hamster. *Environmental Health Perspectives*, 101, 241-248.
- LAKE, B. G., EVANS, J. G., GRAY, T. J. B., KOROSI, S. A. and NORTH, C. J., 1989, Comparative studies of nafenopin-induced hepatic peroxisome proliferation in the rat, Syrian hamster, guinea pig and marmoset. *Toxicology and Applied Pharmacology*, 99, 148-160.
- LENNARD, M. S., 1993, Genetically determined adverse drug reactions involving metabolism. *Drug Safety*, 9, 60-77.
- LEVY, S., TODD, S. C. and MAECKER, H. T., 1998, CD81(TAPA-1): a molecule involved in signal transduction and cell adhesion in the immune system. *Annual Review of Immunology*, 16, 89-109.
- LIANG, P. and PARDEE, A. B., 1992, Differential display of eukaryotic messenger RNA by means of the polymerase chain reaction. *Science*, 257, 967-971.
- LIANG, P., AVERBOUKH, L., KEYOMARSI, K., SAGER, R. and PARDEE, A., 1992, Differential display and cloning of messenger RNAs from human breast cancer versus mammary epithelial cells. *Cancer Research*, 52, 6966-6968.
- LIANG, P., AVERBOUKH, L. and PARDEE, A. B., 1993, Distribution & cloning of eukaryotic mRNAs by means of differential display refinements and optimisation. *Nucleic Acids Research*, 21, 3269-3275.
- LIANG, P., BAUER, D., AVERBOUKH, L., WARTHOF, P., ROHRWILD, M., MULLER, H., STRAUSS, M. and PARDEE, A. B., 1995, Analysis of altered gene expression by differential display. *Methods in Enzymology*, 254, 304-321.
- LINSKENS, M. H., FENG, J., ANDREWS, W. H., ENLOW, B. E., SAATI, S. M., TONKIN, L. A., FUNK, W. D. and VILLEPONTEAU, B., 1995, Cataloging altered gene expression in young and senescent cells using enhanced differential display. *Nucleic Acids Research*, 23, 3244-3251.
- LISITSYN, N., LISITSYN, N. and WIGLER, M., 1993, Cloning the differences between two complex genomes. *Science*, 259, 946-951.
- LOHMANN, J., SCHICKLE, H. and BOSCH, T. C. G., 1995, REN Display, a rapid and efficient method for non-radioactive differential display and mRNA isolation. *Biotechniques*, 18, 200-202.
- LUNNEY, J. K., 1998, Cytokines orchestrating the immune response. *Reviews in Science and Technology*, 17, 84-94.
- MAKOWSKA, J. M., GIBSON, G. G. and BONNER, F. W., 1992, Species differences in ciprofibrate-induction of hepatic cytochrome P450A1 and peroxisome proliferation. *Journal of Biochemical Toxicology*, 7, 183-191.
- MALDARELLI, F., XIANG, C., CHAMOUN, G. and ZEICHNER, S. L., 1998, The expression of the essential nuclear splicing factor SC35 is altered by human immunodeficiency virus infection. *Virus Research*, 53, 39-51.
- MATHIEU-DAUDE, F., CHENG, R., WELSH, J. and McCLELLAND, M., 1996, Screening of differentially amplified cDNA products from RNA arbitrarily primed PCR fingerprints using single strand conformation polymorphism (SSCP) gels. *Nucleic Acids Research*, 24, 1504-1507.
- McKENZIE, D. and DRAKE, D., 1997, Identification of differentially expressed gene products with the castaway system. *Strategies Newsletter* (Stratagene), 10, 19-20.
- McCLELLAND, M., MATHIEU-DAUDE, F. and WELSH, J., 1996, RNA fingerprinting and differential display using arbitrarily primed PCR. *Trends in Genetics*, 11, 242-246.
- MECHLER, B. and RABBITTS, T. H., 1981, Membrane-bound ribosomes of myeloma cells. IV. mRNA complexity of free and membrane-bound polysomes. *Journal of Cell Biology*, 88, 29-36.
- MEYER, U. A. and ZANGER, U. M., 1997, Molecular mechanisms of genetic polymorphisms of drug metabolism. *Annual Review of Pharmacology and Toxicology*, 37, 269-296.
- MOHLER, K. M. and BUTLER, L. D., 1991, Quantitation of cytokine mRNA levels utilizing the reverse transcriptase-polymerase chain reaction following primary antigen-specific sensitization in vivo—I. Verification of linearity, reproducibility and specificity. *Molecular Immunology*, 28, 437-447.
- MURPHY, L. D., HERZOG, C. E., RUDICK, J. B., TITO FOJO, A. and BATES, S. E., 1990, Use of the polymerase chain reaction in the quantitation of the *mdr-1* gene expression. *Biochemistry*, 29, 10351-10356.
- NELSON, D. R., KOYMANS, L., KAMATAKI, T., STEGEMAN, J. J., FEYEREISEN, R., WAXMAN, D. J., WATERMAN, M. R., GOTOH, O., COON, M. J., ESTABROOK, R. W., GUNSALUS, I. C. and NEBERT, D. W., 1996, Update on new sequences, gene mapping, accession numbers and nomenclature. *Pharmacogenetics*, 6, 1-42.

- NISHIO, Y., AIELLO, L. P. and KING, G. L., 1994, Glucose induced genes in bovine aortic smooth muscle cells identified by mRNA differential display. *FASEB Journal*, **8**, 103-106.
- O'NEILL, M. J. and SINCLAIR, A. H., 1997, Isolation of rare transcripts by representational difference analysis. *Nucleic Acids Research*, **25**, 2681-2682.
- ORTON, T. C., ADAM, H. K., BENTLEY, M., HOLLOWAY, B. and TUCKER, M. J., 1984, Clobazart: species differences in the morphological and biochemical response of the liver following chronic administration. *Toxicology and Applied Pharmacology*, **73**, 138-151.
- PELKONEN, O., MAENPAA, J., TAAVITSAINEN, P., RAUTIO, A. and RAUNIO, H., 1998, Inhibition and Induction of human cytochrome P450 (CYP) enzymes. *Xenobiotica*, **28**, 1203-1253.
- PHILIPS, S. M., BENDALL, A. J. and RAMSHAW, I. A., 1990, Isolation of genes associated with high metastatic potential in rat mammary adenocarcinomas. *Journal of the National Cancer Institute*, **82**, 199-203.
- PRASHAR, Y. and WEISSMAN, S. M., 1996, Analysis of differential gene expression by display of 3' end restriction fragments of cDNAs. *Proceedings of the National Academy of Sciences (USA)*, **93**, 659-663.
- RAGNO, S., ESTRADA, I., BUTLER, R. and COLSTON, M. J., 1997, Regulation of macrophage gene expression following invasion by *Mycobacterium tuberculosis*. *Immunology Letters*, **57**, 143-146.
- RAMANA, K. V. and KOHLI, K. K., 1998, Gene regulation of cytochrome P450—an overview. *Indian Journal of Experimental Biology*, **36**, 437-446.
- RICHARD, L., VELASCO, P. and DETMAR, M., 1998, A simple immunomagnetic protocol for the selective isolation and long-term culture of human dermal microvascular endothelial cells. *Experimental Cell Research*, **240**, 1-6.
- ROCKETT, J. C., ESDAILE, D. J. and GIBSON, G. G., 1997, Molecular profiling of non-genotoxic hepatocarcinogenesis using differential display reverse transcription-polymerase chain reaction (ddRT-PCR). *European Journal of Drug Metabolism and Pharmacokinetics*, **22**, 329-333.
- RODRICKS, J. V. and TURNBULL, D., 1987, Inter-species differences in peroxisomes and peroxisome proliferation. *Toxicology and Industrial Health*, **3**, 197-212.
- ROGLER, G., HAUSMANN, M., VOGL, D., ASCHENBRENNER, E., ANDUS, T., FALK, W., ANDRESEN, R., SCHOLMERICH, J. and GROSS, V., 1998, Isolation and phenotypic characterization of colonic macrophages. *Clinical and Experimental Immunology*, **112**, 205-215.
- ROHN, W. M., LEE, Y. J. and BENVENISTE, E. N., 1996, Regulation of class II MHC expression. *Critical Reviews in Immunology*, **16**, 311-330.
- RUDIN, C. M. and THOMPSON, C. B., 1998, B-cell development and maturation. *Seminars in Oncology*, **25**, 435-446.
- SAKAGUCHI, N., BERGER, C. N. and MELCHERS, F., 1986, Isolation of a cDNA copy of an RNA species expressed in murine pre-B cells. *EMBO Journal*, **5**, 2139-2147.
- SAMBROOK, J., FRITSCH, E. F. and MANIATIS, T., 1989, Gel electrophoresis of DNA. In N. Ford, M. Nolan and M. Ferguson (eds), *Molecular Cloning—A laboratory manual*, 2nd edition (New York: Cold Spring Harbour Laboratory Press), Volume 1, pp. 6-37.
- SARGENT, T. D. and DAWID, I. B., 1983, Differential gene expression in the gastrula of *Xenopus laevis*. *Science*, **222**, 135-139.
- SCHENA, M., SHALON, D., HELLER, R., CHAI, A., BROWN, P. O. and DAVIS, R. W., 1996, Parallel human genome analysis: Microarray-based expression monitoring of 1000 genes. *Proceedings of the National Academy of Sciences (USA)*, **93**, 10614-10619.
- SCHNEIDER, C., KING, R. M. and PHILIPSON, L., 1988, Genes specifically expressed at growth arrest of mammalian cells. *Cell*, **54**, 787-793.
- SCHNEIDER-MAUNOURY, S., GILARDI-HEBENSTREIT, P. and CHARNAY, P., 1998, How to build a vertebrate hindbrain. Lessons from genetics. *C R Academy of Science III*, **321**, 819-834.
- SEMENZA, G. L., 1994, Transcriptional regulation of gene expression: mechanisms and pathophysiology. *Human Mutations*, **3**, 180-199.
- SEWALL, C. H., BELL, D. A., CLARK, G. C., TRITSCHER, A. M., TULLY, D. B., VANDEN HEUVEL, J. and LUCIER, G. W., 1995, Induced gene transcription: implications for biomarkers. *Clinical Chemistry*, **41**, 1829-1834.
- SINGH, N., AGRAWAL, S. and RASTOGI, A. K., 1997, Infectious diseases and immunity: special reference to major histocompatibility complex. *Emerging Infectious Diseases*, **3**, 41-49.
- SMITH, N. R., LI, A., ALDERSLEY, M., HIGH, A. S., MARKHAM, A. F. and ROBINSON, P. A., 1997, Rapid determination of the complexity of cDNA bands extracted from DDRT-PCR polyacrylamide gels. *Nucleic Acids Research*, **25**, 3552-3554.
- SOMPAYRAC, L., JANE, S., BURN, T. C., TENEN, D. G. and DANNA, K. J., 1995, Overcoming limitations of the mRNA differential display technique. *Nucleic Acids Research*, **23**, 4738-4739.
- ST JOHN, T. P. and DAVIS, R. W., 1979, Isolation of galactose-inducible DNA sequences from *Saccharomyces cerevisiae* by differential plaque filter hybridisation. *Cell*, **16**, 443-452.
- SUN, Y., HEGAMYER, G. and COLBURN, N. H., 1994, Molecular cloning of five messenger RNAs differentially expressed in preneoplastic or neoplastic JB6 mouse epidermal cells: one is homologous to human tissue inhibitor of metalloproteinases-3. *Cancer Research*, **54**, 1139-1144.

- SUNG, Y. J. and DENMAN, R. B., 1997, Use of two reverse transcriptases eliminates false-positive results in differential display. *Biotechniques*, **23**, 462–464.
- SUTTON, G., WHITE, O., ADAMS, M. and KERLAVAGE, A., 1995, TIGR Assembler; A new tool for assembling large shotgun sequencing projects. *Genome Science and Technology*, **1**, 9–19.
- SUZUKI, Y., SEKIYA, T. and HAYASHI, K., 1991, Allele-specific polymerase chain reaction: a method for amplification and sequence determination of a single component among a mixture of sequence variants. *Analytical Biochemistry*, **192**, 82–84.
- SYED, V., GU, W. and HECHT, N. B., 1997, Sertoli cells in culture and mRNA differential display provide a sensitive early warning assay system to detect changes induced by xenobiotics. *Journal of Andrology*, **18**, 264–273.
- UITTERLINDEN, A. G., SLAGBOOM, P., KNOOK, D. L. and VUJL, J., 1989, Two-dimensional DNA fingerprinting of human individuals. *Proceedings of the National Academy of Sciences (USA)*, **86**, 2742–2746.
- ULLMAN, K. S., NORTHROP, J. P., VERWEIJ, C. L. and CRABTREE, G. R., 1990, Transmission of signals from the T lymphocyte antigen receptor to the genes responsible for cell proliferation and immune function: the missing link. *Annual Review of Immunology*, **8**, 421–452.
- VASMATZIS, G., ESSAND, M., BRINKMANN, U., LEE, B. and PASTON, I., 1998, Discovery of three genes specifically expressed in human prostate by expressed sequence tag database analysis. *Proceedings of the National Academy of Sciences (USA)*, **95**, 300–304.
- VELCULESCU, V. E., ZHANG, L., VOGELSTEIN, B. and KINZLER, K. W., 1995, Serial analysis of gene expression. *Science*, **270**, 484–487.
- VOELTZ, G. K. and STEITZ, J. A., 1998, AuuuA sequences direct mRNA deadenylation uncoupled from decay during *Xenopus* early development. *Molecular and Cell Biology*, **18**, 7537–7545.
- VOGELSTEIN, B. and KINZLER, K. W., 1993, The multistep nature of cancer. *Trends in Genetics*, **9**, 138–141.
- WALTER, J., BELFIELD, M., HAMPSON, I. and READ, C., 1997, A novel approach for generating subtractive probes for differential screening by CCLS. *Life Science News*, **21**, 13–14.
- WAN, J. S., SHARP, S. J., POIRIER, G. M.-C., WAGAMAN, P. C., CHAMBERS, J., PYATI, J., HOM, Y.-L., GALINDO, J. E., HUVAR, A., PETERSON, P. A., JACKSON, M. R. and ERLANDER, M. G., 1996, Cloning differentially expressed mRNAs. *Nature Biotechnology*, **14**, 1685–1691.
- WALTER, J., BELFIELD, M., HAMPSON, I. and READ, C., 1997, A novel approach for generating subtractive probes for differential screening by CCLS. *Life Science News*, **21**, 13–14.
- WANG, Z. and BROWN, D. D., 1991, A gene expression screen. *Proceedings of the National Academy of Sciences (USA)*, **88**, 11505–11509.
- WAWER, C., RUGGEBERG, H., MEYER, G. and MUYZER, G., 1995, A simple and rapid electrophoresis method to detect sequence variation in PCR-amplified DNA fragments. *Nucleic Acids Research*, **23**, 4928–4929.
- WELSH, J., CHADA, K., DALAL, S. S., CHENG, R., RALPH, D. and MCCLELLAND, M., 1992, Arbitrarily primed PCR fingerprinting of RNA. *Nucleic Acids Research*, **20**, 4965–4970.
- WONG, H., ANDERSON, W. D., CHENG, T. and RIABOWOL, K. T., 1994, Monitoring mRNA expression by polymerase chain reaction: the 'primer-dropping' method. *Analytical Biochemistry*, **223**, 251–258.
- WONG, K. K. and MCCLELLAND, M., 1994, Stress-inducible gene of *Salmonella typhimurium* identified by arbitrarily primed PCR of RNA. *Proceedings of the National Academy of Sciences (USA)*, **91**, 639–643.
- WYNFORD-THOMAS, D., 1991, Oncogenes and anti-oncogenes; the molecular basis of tumour behaviour. *Journal of Pathology*, **165**, 187–201.
- XHU, D., CHAN, W. L., LEUNG, B. P., HUANG, F. P., WHEELER, R., PIEDRAFITA, D., ROBINSON, J. H. and LIEW, F. Y., 1998, Selective expression of a stable cell surface molecule on type 2 but not type 1 helper T cells. *Journal of Experimental Medicine*, **187**, 787–794.
- YANG, M. and SYTOWSKI, A. J., 1996, Cloning differentially expressed genes by linker capture subtraction. *Analytical Biochemistry*, **237**, 109–114.
- ZHAO, N., HASHIDA, H., TAKAHASHI, N., MISUMI, Y. and SAKAKI, Y., 1995, High-density cDNA filter analysis: a novel approach for large scale quantitative analysis of gene expression. *Gene*, **156**, 207–213.
- ZHAO, X. J., NEWSOME, J. T. and CIHLAR, R. L., 1998, Up-regulation of two *Candida albicans* genes in the rat model of oral candidiasis detected by differential display. *Microbial Pathogenesis*, **25**, 121–129.
- ZIMMERMANN, C. R., ORR, W. C., LECLERC, R. F., BARNARD, C. and TIMBERLAKE, W. E., 1980, Molecular cloning and selection of genes regulated in *Aspergillus* development. *Cell*, **21**, 709–715.

Whole genome analysis: Experimental access to all genome sequenced segments through larger-scale efficient oligonucleotide synthesis and PCR

DEVAL A. LASHKARI*†, JOHN H. MCCUSKER‡, AND RONALD W. DAVIS*§

*Departments of Genetics and Biochemistry, Beckman Center, Stanford University, Stanford, CA 94305; and ‡Department of Microbiology, 3020 Duke University Medical Center, Durham, NC 27710

Contributed by Ronald W. Davis, May 20, 1997

ABSTRACT The recent ability to sequence whole genomes allows ready access to all genetic material. The approaches outlined here allow automated analysis of sequence for the synthesis of optimal primers in an automated multiplex oligonucleotide synthesizer (AMOS). The efficiency is such that all ORFs for an organism can be amplified by PCR. The resulting amplicons can be used directly in the construction of DNA arrays or can be cloned for a large variety of functional analyses. These tools allow a replacement of single-gene analysis with a highly efficient whole-genome analysis.

The genome sequencing projects have generated and will continue to generate enormous amounts of sequence data. The genomes of *Saccharomyces cerevisiae*, *Escherichia coli*, *Haemophilus influenzae* (1), *Mycoplasma genitalium* (2), and *Methanococcus jannaschii* (3) have been completely sequenced. Other model organisms have had substantial portions of their genomes sequenced as well, including the nematode *Caenorhabditis elegans* (4) and the small flowering plant *Arabidopsis thaliana* (5). This massive and increasing amount of sequence information allows the development of novel experimental approaches to identify gene function.

One standard use of genome sequence data is to attempt to identify the functions of predicted open reading frames (ORFs) within the genome by comparison to genes of known function. Such a comparative analysis of all ORFs to existing sequence data is fast, simple, and requires no experimentation and is therefore a reasonable first step. While finding sequence homologies/motifs is not a substitute for experimentation, noting the presence of sequence homology and/or sequence motifs can be a useful first step in finding interesting genes, in designing experiments and, in some cases, predicting function. However, this type of analysis is frequently uninformative. For example, over one-half of new ORFs in *S. cerevisiae* have no known function (6). If this is the case in a well studied organism such as yeast, the problem will be even worse in organisms that are less well studied or less manipulable. A large, experimentally determined gene function database would make homology/motif searches much more useful.

Experimental analysis must be performed to thoroughly understand the biological function of a gene product. Scaling up from classical "cottage industry" one-gene-oriented approaches to whole-genome analysis would be very expensive and laborious. It is clear that novel strategies are necessary to efficiently pursue the next phase of the genome projects—whole-genome experimental analysis to explore gene expression, gene product function, and other genome functions. Model organisms, such as *S. cerevisiae*, will be extremely

important in the development of novel whole-genome analysis techniques and, subsequently, in improving our understanding of other more complex and less manipulable organisms.

The genome sequence can be systematically used as a tool to understand ORFs, gene product function, and other genome regions. Toward this end, a directed strategy has been developed for exploiting sequence information as a means of providing information about biological function (Fig. 1). Efforts have been directed toward the amplification of each predicted ORF or any other region of the genome ranging from a few base pairs to several kilobase pairs. There are many uses for these amplicons—they can be cloned into standard vectors or specialized expression vectors, or can be cloned into other specialized vectors such as those used for two-hybrid analysis. The amplicons can also be used directly by, for example, arraying onto glass for expression analysis, for DNA binding assays, or for any direct DNA assay (7). As a pilot study, synthetic primers were made on the 96-well automated multiplex oligonucleotide synthesizer (AMOS) instrument (8) (Fig. 2). These oligonucleotides were used to amplify each ORF on yeast chromosome V. The current version of this instrument can synthesize three plates of 96 oligonucleotides each (25 bases) in an 8-hr day. The amplification of the entire set of PCR products was then analyzed by gel electrophoresis (Fig. 3). Successful amplification of the proper length product on the first attempt was 95%. This project demonstrates that one can go directly from sequence information to biological analysis in a truly automated, totally directed manner.

These amplicons can be incorporated directly in arrays or the amplicons can be cloned. If the amplicons are to be cloned, novel sequences can be incorporated at the 5' end of the oligonucleotide to facilitate cloning. One potential problem with cloning PCR products is that the cloned amplicons may contain sequence alterations that diminish their utility. One option would be to resequence each individual amplicon. However, this is expensive, inefficient, and time consuming. A faster, more cost-effective, and more accurate approach is to apply comparative sequencing by denaturing HPLC (9). This method is capable of detecting a single base change in a 2-kb heteroduplex. Longer amplicons can be analyzed by use of appropriate restriction fragments. If any change is detected in a clone, an alternate clone of the same region can be analyzed. Modifying the system to allow high throughput analysis by denaturing HPLC is also relatively simple and straightforward.

If amplicons are used directly on arrays without cloning, it is important to note that, even if single PCR product bands are observed on gels, the PCR products will be contaminated with various amounts of other sequences. This contamination has the potential to affect the results in, for example, expression

The publication costs of this article were defrayed in part by page charge payment. This article must therefore be hereby marked "advertisement" in accordance with 18 U.S.C. §1734 solely to indicate this fact.

© 1997 by The National Academy of Sciences 0027-8424/97/948945-3\$2.00/0
PNAS is available online at <http://www.pnas.org>.

†Present address: Synteni, Inc., 6519 Dumbarton Circle, Fremont, CA 94555.

§To whom reprint requests should be addressed at: Department of Biochemistry, Beckman Center, B400, Stanford University, Stanford, CA 94305-5307. e-mail: gilbert@cmgm.stanford.edu.

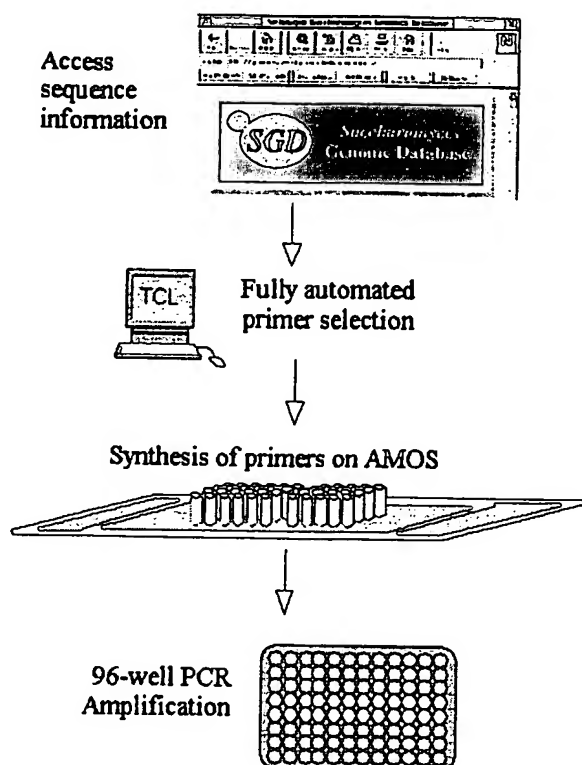


FIG. 1. Overview of systematic method for isolating individual genes. Sequence information is obtained automatically from sequence databases. The data are input into primer selection software specifically designed to target ORFs as designated by database annotations. The output file containing the primer information is directly read by a high-throughput oligonucleotide synthesizer, which makes the oligonucleotides in 96-well plates (AMOS, automated multiplex oligonucleotide synthesizer). The forward and reverse primers are synthesized in the same location on separate plates to facilitate the downstream handling of primers. The amplicons are generated by PCR in 96-well plates as well.

analysis. On the other hand, direct use of the amplicons is much less labor intensive and greatly decreases the occurrence of mistakes in clone identification, a ubiquitous problem associated with large clone set archiving and retrieving.

Any large-scale effort to capture each ORF within a genome must rely on automation if cost is to be minimized while efficiency is maximized. Toward that end, primers targeting ORFs were designed automatically using simple new scripts and existing primer selection software. These script-selected primer sequences were directly read by the high-throughput synthesizer and the forward and reverse primers were synthesized in separate plates in corresponding wells to facilitate automated pipetting and PCR amplifications. Each of the resulting PCR products, generated with minimum labor, contains a known, unique ORF.

Large-scale genome analysis projects are dependent on newly emerging technologies to make the studies practical and economically feasible. For example, the cost of the primers, a significant issue in the past, has been reduced dramatically to make feasible this and other projects that require tens of thousands of oligonucleotides. Other methods of high-throughput analysis are also vital to the success of functional analysis projects, such as microarraying and oligonucleotide chip methods (10–14).

Changes in attitude are also required. One of the major costs of commercial oligonucleotides is extensive quality control such that virtually 100% of the supplied oligonucleotides are successfully synthesized and work for their intended purpose.

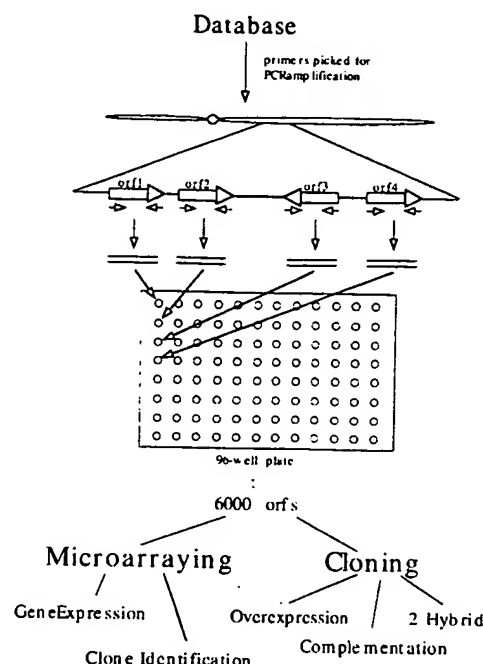


FIG. 2. Overall approach for using database of a genome to direct biological analysis. The synthesis of the 6,000 ORFs (orfs) for each gene of *S. cerevisiae* can be used in many applications utilizing both cloning and microarraying technology.

Considerable cost reduction can be obtained by simply decreasing the expected successful synthesis rate to 95–97%. One can then achieve faster and cheaper whole genome coverage by simply adding a single quality control at the end of the experiment and batching the failures for resynthesis.

The directed nature of the amplicon approach is of clear advantage. The sequence of each ORF is analyzed automatically, and unique specific primers are made to target each ORF. Thus, there is relatively little time or labor involved—for example, no random cloning and subsequent screening is required because each product is known. In the test system, primers for 240 ORFs from chromosome V were systematically synthesized, beginning from the left arm and continuing through to the right arm. At no point was there any manual analysis of sequence information to generate the collection. In many ways, now that the sequence is known, there is no need for the researcher to examine it.

These amplicons can be arrayed and expression analysis can be done on all arrayed ORFs with a single hybridization (10). Those ORFs that display significant differential expression patterns under a given selection are easily identified without the laborious task of searching for and then sequencing a clone. Once scaled up, the procedure provides even greater returns on effort, because a single hybridization will ultimately provide a "snapshot" of the expression of all genes in the yeast genome. Thus, the limiting factor in whole genome analysis will not be the analysis process itself, but will instead be the ability of researchers to design and carry out experimental selections.

Current expression and genetic analysis technologies are geared toward the analysis of single genes and are ill suited to analyze numerous genes under many conditions. Additional difficulties with current technologies include: the effort and expense required to analyze expression and make mutants, the potential duplication of effort if done by different laboratories, and the possibility of conflicting results obtained from different laboratories. In contrast, whole genome analysis not only is more efficient, it also provides data of much higher quality; all genes are assayed and compared in parallel under exactly

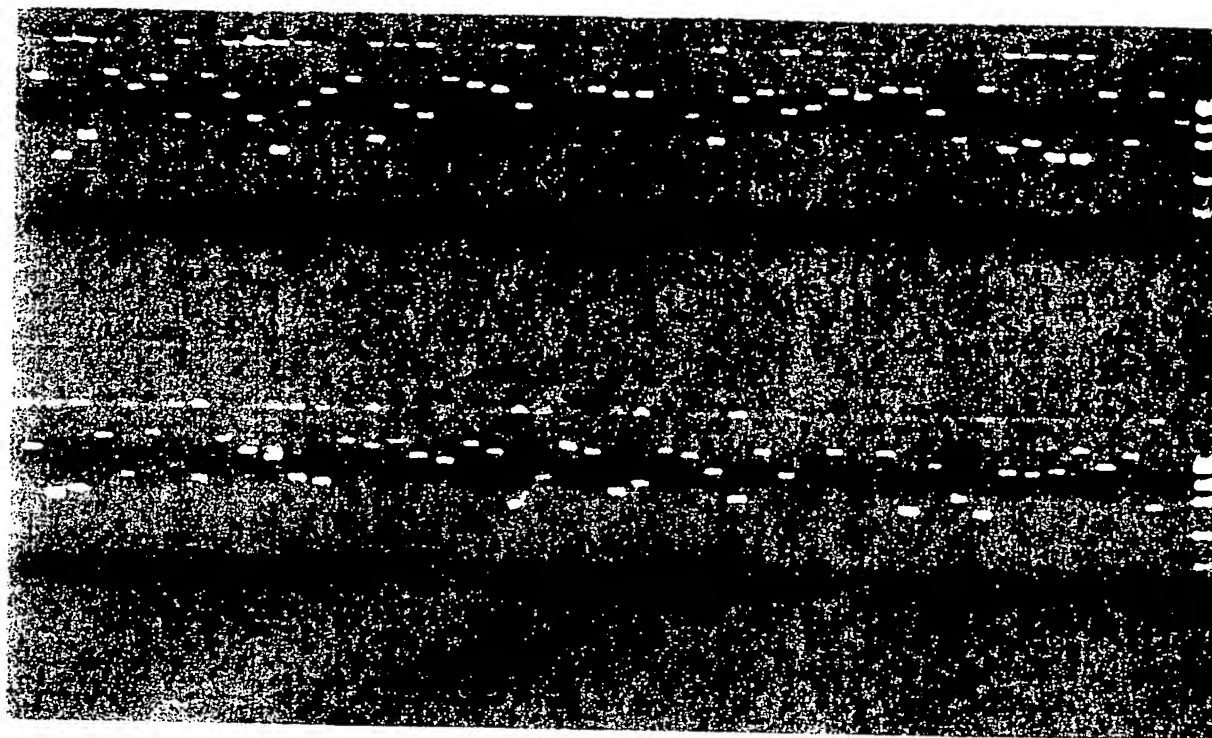


FIG. 3. Gel image of amplifications. Using the method described in Fig. 1, amplicons were generated for ORFs of *S. cerevisiae* chromosome V. One plate of 96 amplification reactions is shown.

the same conditions. In addition, amplicons have many applications beyond gene expression. For example, one recent approach is to incorporate a unique DNA sequence tag, synthesized as part of each gene specific primer, during amplification. The tags or molecular bar codes, when reintroduced into the organism as a gene deletion or as a gene clone, can be used much more efficiently than individual mutations or clones because pools of tagged mutants or transformants can be analyzed in parallel. This parallel analysis is possible because the tags are readily and quantitatively amplified even in complex mixtures of tags (13).

These ORF genome arrays and oligonucleotide tagged libraries can be used for many applications. Any conventional selection applied to a library that gives discrete or multiple products can use these technologies for a simple direct read-out. These include screens and selections for mutant complementation, overexpression suppression (15, 16), second-site suppressors, synthetic lethality, drug target overexpression (17), two-hybrid screens (18), genome mismatch scanning (19), or recombination mapping.

The genome projects have provided researchers with a vast amount of information. These data must be used efficiently and systematically to gain a truly comprehensive understanding of gene function and, more broadly, of the entire genome which can then be applied to other organisms. Such global approaches are essential if we are to gain an understanding of the living cell. This understanding should come from the viewpoint of the integration of complex regulatory networks, the individual roles and interactions of thousands of functional gene products, and the effect of environmental changes on both gene regulatory networks and the roles of all gene products. The time has come to switch from the analysis of a single gene to the analysis of the whole genome.

Support was provided by National Institutes of Health Grants R37H60198 and P01H600205.

1. Fleischmann, R. D., Adams, M. D., White, O., Clayton, R. A., Kirkness, E. F., *et al.* (1995) *Science* **269**, 496–512.
2. Fraser, C. M., Gocayne, J. D., White, O., Adams, M. D., Clayton, R. A., *et al.* (1995) *Science* **270**, 397–403.
3. Bult, C. J., White, O., Olsen, G. J., Zhou, L., Fleischmann, R. D., *et al.* (1996) *Science* **273**, 1058–1073.
4. Sulston, J., Du, Z., Thomas, K., Wilson, R., Hillier, L., Staden, R., Halloran, N., Green, P., Thierry-Mieg, J., Qiu, L., Dear, S., Coulson, A., Craxton, M., Durbin, R., Berks, M., Metzstein, M., Hawkins, T., Ainscough, R. & Waterston, R. (1992) *Nature (London)* **356**, 37–41.
5. Newman, T., de Bruijn, F. J., Green, P., Keegstra, K., Kende, H., *et al.* (1994) *Plant Physiol.* **106**, 1241–1255.
6. Oliver, S. (1996) *Nature (London)* **379**, 597–600.
7. Lashkari, D. A. (1996) Ph.D. dissertation (Stanford Univ., Stanford, CA).
8. Lashkari, D. A., Hunnicke-Smith, S. P., Norgren, R. M., Davis, R. W. & Brennan, T. (1995) *Proc. Natl. Acad. Sci. USA* **92**, 7912–7915.
9. Oefner, P. J. & Underhill, P. A. (1995) *Am. J. Hum. Genet.* **57**, A266.
10. Schena, M., Shalon, D., Davis, R. W. & Brown, P. O. (1995) *Science* **270**, 467–470.
11. Fodor, S. P., Read, J. L., Pirrung, M. C., Stryer, L., Lu, A. T. & Solas, D. (1991) *Science* **251**, 767–773.
12. Chee, M., Yang, R., Hubbell, E., Berno, A., Huang, X. C., Stern, D., Winkler, J., Lockhart, D. J., Morris, M. S. & Fodor, S. P. (1996) *Science* **274**, 610–614.
13. Shoemaker, D. D., Lashkari, D. A., Morris, D., Mittmann, M. & Davis, R. W. (1996) *Nat. Genet.* **14**, 450–456.
14. Smith, V., Chou, K., Lashkari, D., Botstein, D. & Brown, P. O. (1996) *Science* **274**, 2069–2074.
15. Magdolen, V., Drubin, D. G., Mages, G. & Bandlow, W. (1993) *FEBS Lett.* **316**, 41–47.
16. Ramer, S. W., Elledge, S. J. & Davis, R. W. (1992) *Proc. Natl. Acad. Sci. USA* **89**, 11589–11593.
17. Rine, J., Hansen, W., Hardeman, E. & Davis, R. W. (1983) *Proc. Natl. Acad. Sci. USA* **80**, 6750–6754.
18. Fields, S. & Song, O. (1989) *Nature (London)* **340**, 245–246.
19. Nelson, S. F., McCusker, J. H., Sander, M. A., Kee, Y., Modrich, P. & Brown, P. O. (1994) *Nat. Genet.* **4**, 11–18.

Microarrays and Toxicology: The Advent of Toxicogenomics

Emile F. Nuwaysir,¹ Michael Bittner,² Jeffrey Trent,² J. Carl Barrett,¹ and Cynthia A. Afshari¹

¹Laboratory of Molecular Carcinogenesis, National Institute of Environmental Health Sciences, Research Triangle Park, North Carolina

²Laboratory of Cancer Genetics, National Human Genome Research Institute, Bethesda, Maryland

The availability of genome-scale DNA sequence information and reagents has radically altered life-science research. This revolution has led to the development of a new scientific subdiscipline derived from a combination of the fields of toxicology and genomics. This subdiscipline, termed toxicogenomics, is concerned with the identification of potential human and environmental toxicants, and their putative mechanisms of action, through the use of genomics resources. One such resource is DNA microarrays or "chips," which allow the monitoring of the expression levels of thousands of genes simultaneously. Here we propose a general method by which gene expression, as measured by cDNA microarrays, can be used as a highly sensitive and informative marker for toxicity. Our purpose is to acquaint the reader with the development and current state of microarray technology and to present our view of the usefulness of microarrays to the field of toxicology. *Mol. Carcinog.* 24:153-159, 1999. © 1999 Wiley-Liss, Inc.

Key words: toxicology; gene expression; animal bioassay

INTRODUCTION

Technological advancements combined with intensive DNA sequencing efforts have generated an enormous database of sequence information over the past decade. To date, more than 3 million sequences, totaling over 2.2 billion bases [1], are contained within the GenBank database, which includes the complete sequences of 19 different organisms [2]. The first complete sequence of a free-living organism, *Haemophilus influenzae*, was reported in 1995 [3] and was followed shortly thereafter by the first complete sequence of a eukaryote, *Saccharomyces cerevisiae* [4]. The development of dramatically improved sequencing methodologies promises that complete elucidation of the *Homo sapiens* DNA sequence is not far behind [5].

To exploit more fully the wealth of new sequence information, it was necessary to develop novel methods for the high-throughput or parallel monitoring of gene expression. Established methods such as northern blotting, RNase protection assays, S1 nuclease analysis, plaque hybridization, and slot blots do not provide sufficient throughput to effectively utilize the new genomics resources. Newer methods such as differential display [6], high-density filter hybridization [7,8], serial analysis of gene expression [9], and cDNA- and oligonucleotide-based microarray "chip" hybridization [10-12] are possible solutions to this bottleneck. It is our belief that the microarray approach, which allows the monitoring of expression levels of thousands of genes simultaneously, is a tool of unprecedented power for use in toxicology studies.

Almost without exception, gene expression is altered during toxicity, as either a direct or indirect result of toxicant exposure. The challenge facing toxicologists is to define, under a given set of experimental conditions, the characteristic and specific pattern of gene expression elicited by a given toxicant. Microarray technology offers an ideal platform for this type of analysis and could be the foundation for a fundamentally new approach to toxicology testing.

MICROARRAY DEVELOPMENT AND APPLICATIONS

cDNA Microarrays

In the past several years, numerous systems were developed for the construction of large-scale DNA arrays. All of these platforms are based on cDNAs or oligonucleotides immobilized to a solid support. In the cDNA approach, cDNA (or genomic) clones of interest are arrayed in a multi-well format and amplified by polymerase chain reaction. The products of this amplification, which are usually 500- to 2000-bp clones from the 3' regions of the genes of interest, are then spotted onto solid support by using high-speed robotics. By using this method, microarrays of up to 10 000 clones can be generated by spotting onto a glass substrate

*Correspondence to: Laboratory of Molecular Carcinogenesis, National Institute of Environmental Health Sciences, 111 Alexander Drive, Research Triangle Park, NC 27709.

Received 8 December 1998; Accepted 5 January 1999

Abbreviations: PAH, polycyclic aromatic hydrocarbon; NIEHS, National Institute of Environmental Health Sciences.

[13,14]. Sample detection for microarrays on glass involves the use of probes labeled with fluorescent or radioactive nucleotides.

Fluorescent cDNA probes are generated from control and test RNA samples in single-round reverse-transcription reactions in the presence of fluorescently tagged dUTP (e.g., Cy3-dUTP and Cy5-dUTP), which produces control and test products labeled with different fluors. The cDNAs generated from these two populations, collectively termed the "probe," are then mixed and hybridized to the array under a glass coverslip [10,11,15]. The fluorescent signal is detected by using a custom-designed scanning confocal microscope equipped with a motorized stage and lasers for fluor excitation [10,11,15]. The data are analyzed with custom digital image analysis software that determines for each DNA feature the ratio of fluor 1 to fluor 2, corrected for local background [16,17]. The strength of this approach lies in the ability to label RNAs from control and treated samples with different fluorescent nucleotides, allowing for the simultaneous hybridization and detection of both populations on one microarray. This method eliminates the need to control for hybridization between arrays. The research groups of Drs. Patrick Brown and Ron Davis at Stanford University spearheaded the effort to develop this approach, which has been successfully applied to studies of *Arabidopsis thaliana* RNA [10], yeast genomic DNA [15], tumorigenic versus non-tumorigenic human tumor cell lines [11], human T-cells [18], yeast RNA [19], and human inflammatory disease-related genes [20]. The most dramatic result of this effort was the first published account of gene expression of an entire genome, that of the yeast *Saccharomyces cerevisiae* [21].

In an alternative approach, large numbers of cDNA clones can be spotted onto a membrane support, albeit at a lower density [7,22]. This method is useful for expression profiling and large-scale screening and mapping of genomic or cDNA clones [7,22–24]. In expression profiling on filter membranes, two different membranes are used simultaneously for control and test RNA hybridizations, or a single membrane is stripped and reprobed. The signal is detected by using radioactive nucleotides and visualized by phosphorimager analysis or autoradiography. Numerous companies now sell such cDNA membranes and software to analyze the image data [25–27].

Oligonucleotide Microarrays

Oligonucleotide microarrays are constructed either by spotting prefabricated oligos on a glass support [13] or by the more elegant method of direct in situ oligo synthesis on the glass surface by photolithography [28–30]. The strength of this approach lies in its ability to discriminate DNA molecules based on single base-pair difference. This allows the application of this method to the fields of medical diagnos-

tics, pharmacogenetics, and sequencing by hybridization as well as gene-expression analysis.

Fabrication of oligonucleotide chips by photolithography is theoretically simple but technically complex [29,30]. The light from a high-intensity mercury lamp is directed through a photolithographic mask onto the silica surface, resulting in deprotection of the terminal nucleotides in the illuminated regions. The entire chip is then reacted with the desired free nucleotide, resulting in selected chain elongation. This process requires only 4n cycles (where n = oligonucleotide length in bases) to synthesize a vast number of unique oligos, the total number of which is limited only by the complexity of the photolithographic mask and the chip size [29,31,32].

Sample preparation involves the generation of double-stranded cDNA from cellular poly(A)⁺ RNA followed by antisense RNA synthesis in an in vitro transcription reaction with biotinylated or fluor-tagged nucleotides. The RNA probe is then fragmented to facilitate hybridization. If the indirect visualization method is used, the chips are incubated with fluor-linked streptavidin (e.g., phycoerythrin) after hybridization [12,33]. The signal is detected with a custom confocal scanner [34]. This method has been applied successfully to the mapping of genomic library clones [35], to de novo sequencing by hybridization [28,36], and to evolutionary sequence comparison of the *BRCA1* gene [37]. In addition, mutations in the cystic fibrosis [38] and *BRCA1* [39] gene products and polymorphisms in the human immunodeficiency virus-1 clade B protease gene [40] have been detected by this method. Oligonucleotide chips are also useful for expression monitoring [33] as has been demonstrated by the simultaneous evaluation of gene-expression patterns in nearly all open reading frames of the yeast strain *S. cerevisiae* [12]. More recently, oligonucleotide chips have been used to help identify single nucleotide polymorphisms in the human [41] and yeast [42] genomes.

THE USE OF MICROARRAYS IN TOXICOLOGY

Screening for Mechanism of Action

The field of toxicology uses numerous in vivo model systems, including the rat, mouse, and rabbit, to assess potential toxicity and these bioassays are the mainstay of toxicology testing. However, in the past several decades, a plethora of in vitro techniques have been developed to measure toxicity, many of which measure toxicant-induced DNA damage. Examples of these assays include the Ames test, the Syrian hamster embryo cell transformation assay, micronucleus assays, measurements of sister chromatid exchange and unscheduled DNA synthesis, and many others. Fundamental to all of these methods is the fact that toxicity is often preceded by, and results in, alterations in gene expression. In many cases, these changes in gene expression are a

far more sensitive, characteristic, and measurable endpoint than the toxicity itself. We therefore propose that a method based on measurements of the genome-wide gene expression pattern of an organism after toxicant exposure is fundamentally informative and complements the established methods described above.

We are developing a method by which toxicants can be identified and their putative mechanisms of action determined by using toxicant-induced gene expression profiles. In this method, in one or more defined model systems, dose and time-course parameters are established for a series of toxicants within a given prototypic class (e.g., polycyclic aromatic hydrocarbons (PAHs)). Cells are then treated with these agents at a fixed toxicity level (as measured by cell survival), RNA is harvested, and toxicant-induced gene expression changes are assessed by hybridization to a cDNA microarray chip (Figure 1). We have developed a custom DNA chip, called ToxChip v1.0, specifically for this purpose and will discuss it in more detail below. The changes in gene expression induced by the test agents in the model systems are analyzed, and the common set of changes unique to that class of toxicants, termed a toxicant signature, is determined.

This signature is derived by ranking across all experiments the gene-expression data based on rela-

tive fold induction or suppression of genes in treated samples versus untreated controls and selecting the most consistently different signals across the sample set. A different signature may be established for each prototypic toxicant class. Once the signatures are determined, gene-expression profiles induced by unknown agents in these same model systems can then be compared with the established signatures. A match assigns a putative mechanism of action to the test compound. Figure 2 illustrates this signature method for different types of oxidant stressors, PAHs, and peroxisome proliferators. In this example, the unknown compound in question had a gene-expression profile similar to that of the oxidant stressors in the database. We anticipate that this general method will also reveal cross talk between different pathways induced by a single agent (e.g., reveal that a compound has both PAH-like and oxidant-like properties). In the future, it may be necessary to distinguish very subtle differences between compounds within a very large sample set (e.g., thousands of highly similar structural isomers in a combinatorial chemistry library or peptide library). To generate these highly refined signatures, standard statistical clustering techniques or principal-component analysis can be used.

For the studies outlined in Figure 2, we developed the custom cDNA microarray chip ToxChip v1.0.

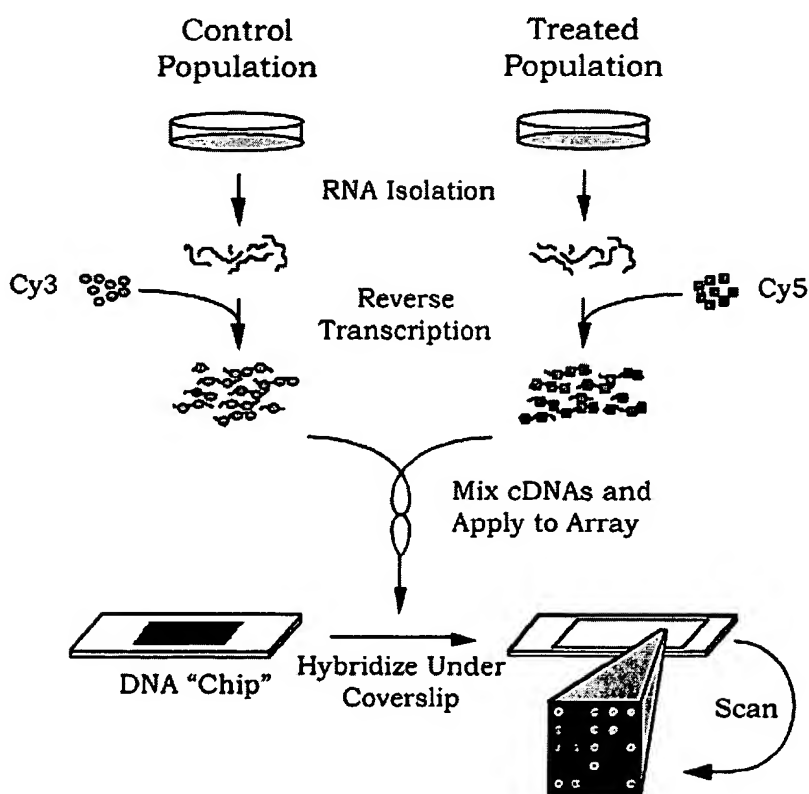


Figure 1. Simplified overview of the method for sample preparation and hybridization to cDNA microarrays. For illus-

trative purposes, samples derived from cell culture are depicted, although other sample types are amenable to this analysis.

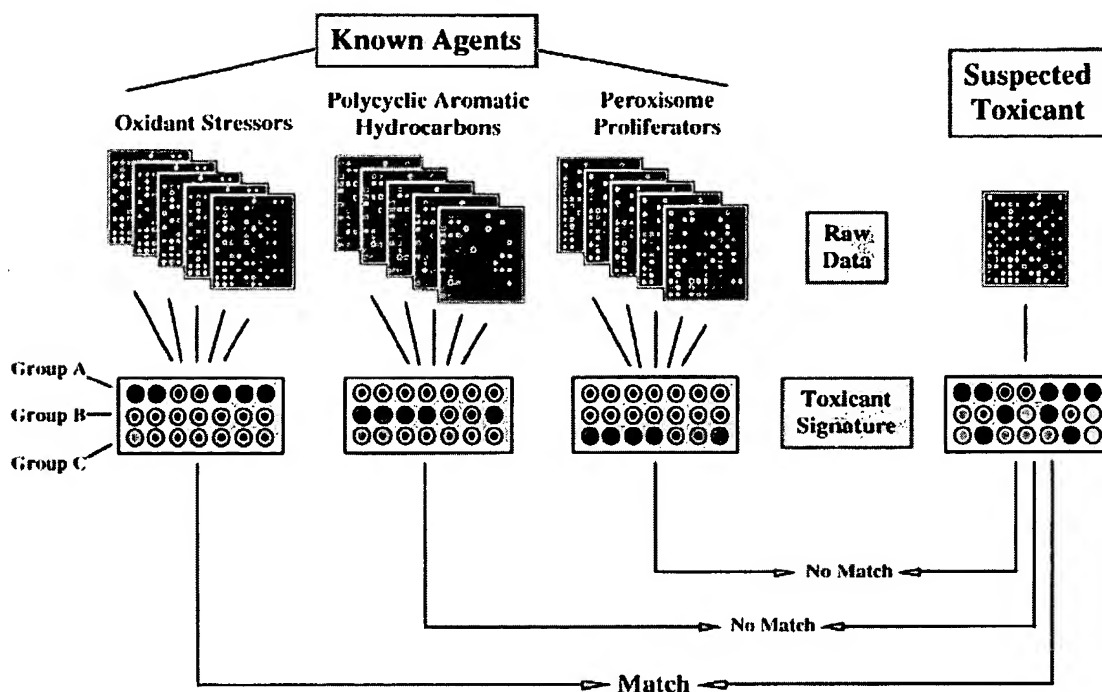


Figure 2. Schematic representation of the method for identification of a toxicant's mechanism of action. In this method, gene-expression data derived from exposure of model systems to known toxicants are analyzed, and a set of changes characteristic to that type of toxicant (termed the toxicant signature) is identified. As depicted, oxidant stressors produce

consistent changes in group A genes (indicated by red and green circles), but not group B or C genes (indicated by gray circles). The set of gene-expression changes elicited by the suspected toxicant is then compared with these characteristic patterns, and a putative mechanism of action is assigned to the unknown agent.

The 2090 human genes that comprise this subarray were selected for their well-documented involvement in basic cellular processes as well as their responses to different types of toxic insult. Included on this list are DNA replication and repair genes, apoptosis genes, and genes responsive to PAHs and dioxin-like compounds, peroxisome proliferators, estrogenic compounds, and oxidant stress. Some of the other categories of genes include transcription factors, oncogenes, tumor suppressor genes, cyclins, kinases, phosphatases, cell adhesion and motility genes, and homeobox genes. Also included in this group are 84 housekeeping genes, whose hybridization intensity is averaged and used for signal normalization of the other genes on the chip. To date, very few toxicants have been shown to have appreciable effects on the expression of these housekeeping genes. However, this housekeeping list will be revised if new data warrant the addition or deletion of a particular gene. Table 1 contains a general description of some of the different classes of genes that comprise ToxChip v1.0.

When a toxicant signature is determined, the genes within this signature are flagged within the database. When uncharacterized toxicants are then screened, the data can be quickly reformatted so that blocks of genes representing the different signatures

are displayed [11]. This facilitates rapid, visual interpretation of data. We are also developing ToxChip v2.0 and chips for other model systems, including rat, mouse, *Xenopus*, and yeast, for use in toxicology studies.

Animal Models in Toxicology Testing

The toxicology community relies heavily on the use of animals as model systems for toxicology testing. Unfortunately, these assays are inherently expensive, require large numbers of animals and take a long time to complete and analyze. Therefore, the National Institute of Environmental Health Sciences (NIEHS), the National Toxicology Program, and the toxicology community at large are committed to reducing the number of animals used, by developing more efficient and alternative testing methodologies. Although substantial progress has been made in the development of alternative methods, bioassays are still used for testing endpoints such as neurotoxicity, immunotoxicity, reproductive and developmental toxicology, and genetic toxicology. The rodent cancer bioassay is a particularly expensive and time-consuming assay, as it requires almost 4 yr, 1200 animals, and millions of dollars to execute and analyze [43]. In vitro experiments of the type outlined in Figure 2 might provide evidence that an unknown

Table 1. ToxChip v1.0: A Human cDNA Microarray Chip Designed to Detect Responses to Toxic Insult

Gene category	No. of genes on chip
Apoptosis	72
DNA replication and repair	99
Oxidative stress/redox homeostasis	90
Peroxisome proliferator responsive	22
Dioxin/PAH responsive	12
Estrogen responsive	63
Housekeeping	84
Oncogenes and tumor suppressor genes	76
Cell-cycle control	51
Transcription factors	131
Kinases	276
Phosphatases	88
Heat-shock proteins	23
Receptors	349
Cytochrome P450s	30

*This list is intended as a general guide. The gene categories are not unique, and some genes are listed in multiple categories.

agent is (or is not) responsible for eliciting a given biological response. This information would help to select a bioassay more specifically suited to the agent in question or perhaps suggest that a bioassay is not necessary, which would dramatically reduce cost, animal use, and time.

The addition of microarray techniques to standard bioassays may dramatically enhance the sensitivity and interpretability of the bioassay and possibly reduce its cost. Gene-expression signatures could be determined for various types of tissue-specific toxicants, and new compounds could be screened for these characteristic signatures, providing a rapid and sensitive *in vivo* test. Also, because gene expression is often exquisitely sensitive to low doses of a toxicant, the combination of gene-expression screening and the bioassay might allow the use of lower toxicant doses, which are more relevant to human exposure levels, and the use of fewer animals. In addition, gene-expression changes are normally measured in hours or days, not in the months to years required for tumor development. Furthermore, microarrays might be particularly useful for investigating the relationship between acute and chronic toxicity and identifying secondary effects of a given toxicant by studying the relationship between the duration of exposure to a toxicant and the gene-expression profile produced. Thus, a bioassay that incorporates gene-expression signatures with traditional endpoints might be substantially shorter, use more realistic dose regimens, and cost substantially less than the current assays do.

These considerations are also relevant for branches of toxicology not related to human health and not using rodents as model systems, such as aquatic toxicology and plant pathology. Bioassays based on the flathead minnow, *Daphnia*, and *Arabidopsis* could

also be improved by the addition of microarray analysis. The combination of microarrays with traditional bioassays might also be useful for investigating some of the more intractable problems in toxicology research, such as the effects of complex mixtures and the difficulties in cross-species extrapolation.

Exposure Assessment, Environmental Monitoring, and Drug Safety

The currently used methods for assessment of exposure to chemical toxicants are based on measurement of tissue toxin levels or on surrogate markers of toxicity, termed biomarkers (e.g., peripheral blood levels of hepatic enzymes or DNA adducts). Because gene expression is a sensitive endpoint, gene expression as measured with microarray technology may be useful as a new biomarker to more precisely identify hazards and to assess exposure. Similarly, microarrays could be used in an environmental-monitoring capacity to measure the effect of potential contaminants on the gene-expression profiles of resident organisms. In an analogous fashion, microarrays could be used to measure gene-expression endpoints in subjects in clinical trials. The combination of these gene-expression data and more established toxic endpoints in these trials could be used to define highly precise surrogates of safety.

Gene-expression profiles in samples from exposed individuals could be compared to the profiles of the same individuals before exposure. From this information, the nature of the toxic exposure can be determined or a relative clinical safety factor estimated. In the future it may also be possible to estimate not only the nature but the dose of the toxicant for a given exposure, based on relative gene-expression levels. This general approach may be particularly appropriate for occupational-health applications, in which unexposed and exposed samples from the same individuals may be obtainable. For example, a pilot study of gene expression in peripheral-blood lymphocytes of Polish coke-oven workers exposed to PAHs (and many other compounds) is under consideration at the NIEHS. An important consideration for these types of studies is that gene expression can be affected by numerous factors, including diet, health, and personal habits. To reduce the effects of these confounding factors, it may be necessary to compare pools of control samples with pools of treated samples. In the future it may be possible to compare exposed sample sets to a national database of human-expression data, thus eliminating the need to provide an unexposed sample from the same individual. Efforts to develop such a national gene-expression database are currently under way [44,45]. However, this national database approach will require a better understanding of genome-wide gene expression across the highly diverse human population and of the effects of environmental factors on this expression.

Alleles, Oligo Arrays, and Toxicogenetics

Gene sequences vary between individuals, and this variability can be a causative factor in human diseases of environmental origin [46,47]. A new area of toxicology, termed toxicogenetics, was recently developed to study the relationship between genetic variability and toxicant susceptibility. This field is not the subject of this discussion, but it is worthwhile to note that the ability of oligonucleotide arrays to discriminate DNA molecules based on single base-pair differences makes these arrays uniquely useful for this type of analysis. Recent reports demonstrated the feasibility of this approach [41,42]. The NIEHS has initiated the Environmental Genome Project to identify common sequence polymorphisms in 200 genes thought to be involved in environmental diseases [48]. In a pilot study on the feasibility of this application to the Environmental Genome Project, oligonucleotide arrays will be used to resequence 20 candidate genes. This toxicogenetic approach promises to dramatically improve our understanding of interindividual variability in disease susceptibility.

FUTURE PRIORITIES

There are many issues that must be addressed before the full potential of microarrays in toxicology research can be realized. Among these are model system selection, dose selection, and the temporal nature of gene expression. In other words, in which species, at what dose, and at what time do we look for toxicant-induced gene expression? If human samples are analyzed, how variable is global gene expression between individuals, before and after toxicant exposure? What are the effects of age, diet, and other factors on this expression? Experience, in the form of large data sets of toxicant exposures, will answer these questions.

One of the most pressing issues for array scientists is the construction of a national public database (linked to the existing public databases) to serve as a repository for gene-expression data. This relational database must be made available for public use, and researchers must be encouraged to submit their expression data so that others may view and query the information. Researchers at the National Institutes of Health have made laudable progress in developing the first generation of such a database [44,45]. In addition, improved statistical methods for gene clustering and pattern recognition are needed to analyze the data in such a public database.

The proliferation of different platforms and methods for microarray hybridizations will improve sample handling and data collection and analysis and reduce costs. However, the variety of microarray methods available will create problems of data compatibility between platforms. In addition, the near-infinite variety of experimental conditions under

which data will be collected by different laboratories will make large-scale data analysis extremely difficult. To help circumvent these future problems, a set of standards to be included on all platforms should be established. These standards would facilitate data entry into the national database and serve as reference points for cross-platform and inter-laboratory data analysis.

Many issues remain to be resolved, but it is clear that new molecular techniques such as microarray hybridization will have a dramatic impact on toxicology research. In the future, the information gathered from microarray-based hybridization experiments will form the basis for an improved method to assess the impact of chemicals on human and environmental health.

ACKNOWLEDGMENTS

The authors would like to thank Drs. Robert Maronpot, George Lucier, Scott Masten, Nigel Walker, Raymond Tennant, and Ms. Theodora Deverenux for critical review of this manuscript. EFN was supported in part by NIEHS Training Grant #ES07017-24.

REFERENCES

1. <http://www.ncbi.nlm.nih.gov/Web/Genbank/index.html>
2. <http://www.ncbi.nlm.nih.gov/Entrez/Genome/org.html>
3. Fleischmann RD, Adams MD, White O, et al. Whole-genome random sequencing and assembly of *Haemophilus influenzae* Rd. *Science* 1995;269:496-512.
4. Goffeau A, Barrell BG, Bussey H, et al. Life with 6000 genes. *Science* 1996;274:546, 563-567.
5. <http://www.perkin-elmer.com/press/prc5448.html>
6. Liang P, Pardee AB. Differential display of eukaryotic messenger RNA by means of the polymerase chain reaction. *Science* 1992;257:967-971.
7. Pietu G, Alibert O, Guichard V, et al. Novel gene transcripts preferentially expressed in human muscles revealed by quantitative hybridization of a high density cDNA array. *Genome Res* 1996;6:492-503.
8. Zhao ND, Hashida H, Takahashi N, Misumi Y, Sakaki Y. High-density cDNA filter analysis—A novel approach for large-scale, quantitative analysis of gene expression. *Gene* 1995;156:207-213.
9. Velculescu VE, Zhang L, Vogelstein B, Kinzler KW. Serial analysis of gene expression. *Science* 1995;270:484-487.
10. Schena M, Shalon D, Davis RW, Brown PO. Quantitative monitoring of gene-expression patterns with a complementary DNA microarray. *Science* 1995;270:467-470.
11. DeRisi J, Penland L, Brown PO, et al. use of a cDNA microarray to analyse gene expression patterns in human cancer. *Nat Genet* 1996;14:457-460.
12. Wodicka L, Dong HL, Mittmann M, Ho MH, Lockhart DJ. Genome-wide expression monitoring in *Saccharomyces cerevisiae*. *Nat Biotechnol* 1997;15:1359-1367.
13. Marshall A, Hodgson J. DNA chips: An array of possibilities. *Nat Biotechnol* 1998;16:27-31.
14. <http://www.synteni.com>
15. Shalon D, Smith SJ, Brown PO. A DNA microarray system for analyzing complex DNA samples using two-color fluorescent probe hybridization. *Genome Res* 1996;6:639-645.
16. Chen Y, Dougherty ER, Bittner ML. Ratio-based decisions and the quantitative analysis of cDNA microarray images. *Biomedical Optics* 1997;2:364-374.
17. Khan J, Simon R, Bittner M, et al. Gene expression profiling of alveolar rhabdomyosarcoma with cDNA microarrays. *Cancer Res* 1998;58:5009-5013.
18. Schena M, Shalon D, Heller R, Chai A, Brown PO, Davis RW. Parallel human genome analysis: Microarray-based expression monitoring of 1000 genes. *Proc Natl Acad Sci USA* 1996; 93:10614-10619.

19. Lashkari DA, DeRisi JL, McCusker JH, et al. Yeast microarrays for genome wide parallel genetic and gene expression analysis. *Proc Natl Acad Sci USA* 1997;94:13057-13062.
20. Heller RA, Schena M, Chai A, et al. Discovery and analysis of inflammatory disease-related genes using cDNA microarrays. *Proc Natl Acad Sci USA* 1997;94:2150-2155.
21. DeRisi JL, Iyer VR, Brown PO. Exploring the metabolic and genetic control of gene expression on a genomic scale. *Science* 1997;278:680-686.
22. Drmanac S, Stavropoulos NA, Labat I, et al. Gene-representing cDNA clusters defined by hybridization of 57,419 clones from infant brain libraries with short oligonucleotide probes. *Genomics* 1996;37:29-40.
23. Milosavljevic A, Savkovic S, Crkvenjakov R, et al. DNA sequence recognition by hybridization to short oligomers: Experimental verification of the method on the *E. coli* genome. *Genomics* 1996;37:77-86.
24. Drmanac S, Drmanac R. Processing of cDNA and genomic kilobase-size clones for massive screening, mapping and sequencing by hybridization. *Biotechniques* 1994;17:328-329, 332-336.
25. <http://www.resgen.com/>
26. <http://www.genomesystems.com/>
27. <http://www.clontech.com/>
28. Pease AC, Solas DA, Fodor SPA. Parallel synthesis of spatially addressable oligonucleotide probe matrices. Abstract. Abstracts of Papers of the American Chemical Society 1992;203:34.
29. Pease AC, Solas D, Sullivan EJ, Cronin MT, Holmes CP, Fodor SPA. Light-generated oligonucleotide arrays for rapid DNA sequence analysis. *Proc Natl Acad Sci USA* 1994;91:5022-5026.
30. Fodor SPA, Read JL, Pirrung MC, Stryer L, Lu AT, Solas D. Light-directed, spatially addressable parallel chemical synthesis. *Science* 1991;251:767-773.
31. McGall G, Labadie J, Brock P, Wallraff G, Nguyen T, Hinsberg W. Light-directed synthesis of high-density oligonucleotide arrays using semiconductor photoresists. *Proc Natl Acad Sci USA* 1996;93:13555-13560.
32. Lipshutz RJ, Morris D, Chee M, et al. Using oligonucleotide probe arrays to access genetic diversity. *Biotechniques* 1995;19:442-447.
33. Lockhart DJ, Dong HL, Byrne MC, et al. Expression monitoring by hybridization to high-density oligonucleotide arrays. *Nat Biotechnol* 1996;14:1675-1680.
34. <http://www.mdyn.com/>
35. Sapolsky RJ, Lipshutz RJ. Mapping genomic library clones using oligonucleotide arrays. *Genomics* 1996;33:445-456.
36. Chee M, Yang R, Hubbell E, et al. Accessing genetic information with high-density DNA arrays. *Science* 1996;274:610-614.
37. Hacia JG, Makalowski W, Edgemon K, et al. Evolutionary sequence comparisons using high-density oligonucleotide arrays. *Nat Genet* 1998;18:155-158.
38. Cronin MT, Fucini RV, Kim SM, Masino RS, Wespi RM, Miyada CG. Cystic fibrosis mutation detection by hybridization to light-generated DNA probe arrays. *Hum Mutat* 1996;7:244-255.
39. Hacia JG, Brody LC, Chee MS, Fodor SPA, Collins FS. Detection of heterozygous mutations in BRCA1 using high density oligonucleotide arrays and two-colour fluorescence analysis. *Nat Genet* 1996;14:441-447.
40. Kozal MJ, Shah N, Shen NP, et al. Extensive polymorphisms observed in HIV-1 clade B protease gene using high-density oligonucleotide arrays. *Nat Med* 1996;2:753-759.
41. Wang DG, Fan JB, Siao CJ, et al. Large-scale identification, mapping, and genotyping of single-nucleotide polymorphisms in the human genome. *Science* 1998;280:1077-1082.
42. Winzeler EA, Richards DR, Conway AR, et al. Direct allelic variation scanning of the yeast genome. *Science* 1998;281:1194-1197.
43. Chhabra RS, Huff JE, Schwetz BS, Selkirk J. An overview of prechronic and chronic toxicity carcinogenicity experimental-study designs and criteria used by the National Toxicology Program. *Environ Health Perspect* 1990;86:313-321.
44. Ermolaeva O, Rastogi M, Pruitt KD, et al. Data management and analysis for gene expression arrays. *Nat Genet* 1998;20:19-23.
45. <http://www.nhgri.nih.gov/DIR/LCG/15K/HTML/dbase.html>
46. Samson M, Libert F, Doranz BJ, et al. Resistance to HIV-1 infection in Caucasian individuals bearing mutant alleles of the CCR-5 chemokine receptor gene. *Nature* 1996;382:722-725.
47. Bell DA, Taylor JA, Paulson DF, Robertson CN, Mohler JL, Lucier GW. Genetic risk and carcinogen exposure—A common inherited defect of the carcinogen-metabolism gene glutathione-S-transferase M1 (Gstm1) that increases susceptibility to bladder cancer. *J Natl Cancer Inst* 1993;85:1159-1164.
48. <http://www.niehs.nih.gov/envgenom/home.html>



Toxicology Letters 112–113 (2000) 467–471

**Toxicology
Letters**

www.elsevier.com/locate/toxlet

Expression profiling in toxicology — potentials and limitations

Sandra Steiner *, N. Leigh Anderson

Large Scale Biology Corporation, 9620 Medical Center Drive, Rockville, MD 20850-3338, USA

Abstract

Recent progress in genomics and proteomics technologies has created a unique opportunity to significantly impact the pharmaceutical drug development processes. The perception that cells and whole organisms express specific inducible responses to stimuli such as drug treatment implies that unique expression patterns, molecular fingerprints, indicative of a drug's efficacy and potential toxicity are accessible. The integration into state-of-the-art toxicology of assays allowing one to profile treatment-related changes in gene expression patterns promises new insights into mechanisms of drug action and toxicity. The benefits will be improved lead selection, and optimized monitoring of drug efficacy and safety in pre-clinical and clinical studies based on biologically relevant tissue and surrogate markers. © 2000 Elsevier Science Ireland Ltd. All rights reserved.

Keywords: Proteomics; Genomics; Toxicology

1. Introduction

The majority of drugs act by binding to protein targets, most to known proteins representing enzymes, receptors and channels, resulting in effects such as enzyme inhibition and impairment of signal transduction. The treatment-induced perturbations provoke feedback reactions aiming to compensate for the stimulus, which almost always are associated with signals to the nucleus, resulting in altered gene expression. Such gene expression regulations account for both the

pharmacological action and the toxicity of a drug and can be visualized by either global mRNA or global protein expression profiling. Hence, for each individual drug, a characteristic gene regulation pattern, its molecular fingerprint, exists which bears valuable information on its mode of action and its mechanism of toxicity.

Gene expression is a multistep process that results in an active protein (Fig. 1). There exist numerous regulation systems that exert control at and after the transcription and the translation step. Genomics, by definition, encompasses the quantitative analysis of transcripts at the mRNA level, while the aim of proteomics is to quantify gene expression further down-stream, creating a snapshot of gene regulation closer to ultimate cell function control.

* Corresponding author. Tel.: +1-301-4245989; fax: +1-301-7624892.

E-mail address: steiner@lsbc.com (S. Steiner)

2. Global mRNA profiling

Expression data at the mRNA level can be produced using a set of different technologies such as DNA microarrays, reverse transcript imaging, amplified fragment length polymorphism (AFLP), serial analysis of gene expression (SAGE) and others. Currently, DNA microarrays are very popular and promise a great potential. On a typical array, each gene of interest is represented either by a long DNA fragment (200–2400 bp) typically generated by polymerase chain reaction (PCR) and spotted on a suitable substrate using robotics (Schena et al., 1995; Shalon et al., 1996) or by several short oligonucleotides (20–30 bp) synthesized directly onto a solid support using photolabile nucleotide chemistry (Fodor et al., 1991; Chee et al., 1996). From control and treated tissues, total RNA or mRNA is isolated and reverse transcribed in the presence of radioactive or fluorescent labeled nucleotides, and the labeled probes are then hybridized to the arrays. The intensity of the array signal is measured for each gene transcript by either autoradiography or laser scanning confocal microscopy. The ratio between the signals of control and treated samples reflect the relative drug-induced change in transcript abundance.

3. Global protein profiling

Global quantitative expression analysis at the protein level is currently restricted to the use of two-dimensional gel electrophoresis. This technique combines separation of tissue proteins by isoelectric focusing in the first dimension and by sodium dodecyl sulfate slab gel electrophoresis-based molecular weight separation on the second, orthogonal dimension (Anderson et al., 1991). The product is a rectangular pattern of protein spots that are typically revealed by Coomassie Blue, silver or fluorescent staining (Fig. 2). Protein spots are identified by mass spectrometry following generation of peptide mass fingerprints (Mann et al., 1993) and sequence tags (Wilkins et al., 1996). Similar to the mRNA approach, the ratio between the optical density of spots from control and treated samples are compared to search for treatment-related changes.

4. Expression data analysis

Bioinformatics forms a key element required to organize, analyze and store expression data from either source, the mRNA or the protein level. The overall objective, once a mass of high-quality

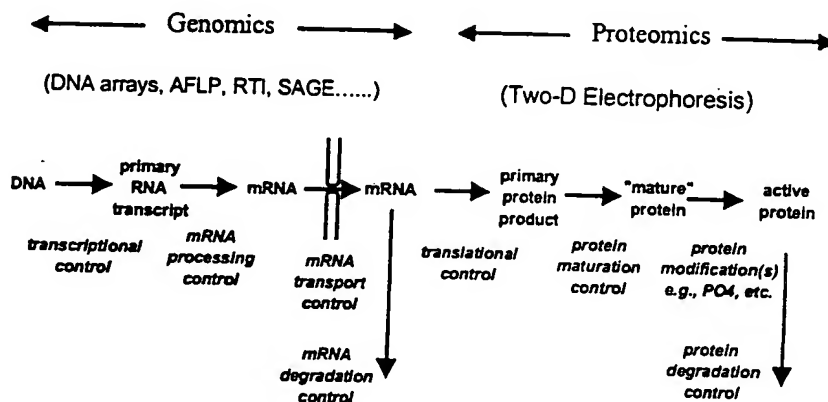


Fig. 1. Production of an active protein is a multistep process in which numerous regulation systems exert control at various stages of expression. Molecular fingerprints of drugs can be visualized through expression profiling at the mRNA level (genomics) using a variety of technologies and at the protein level (proteomics) using two-dimensional gel electrophoresis.

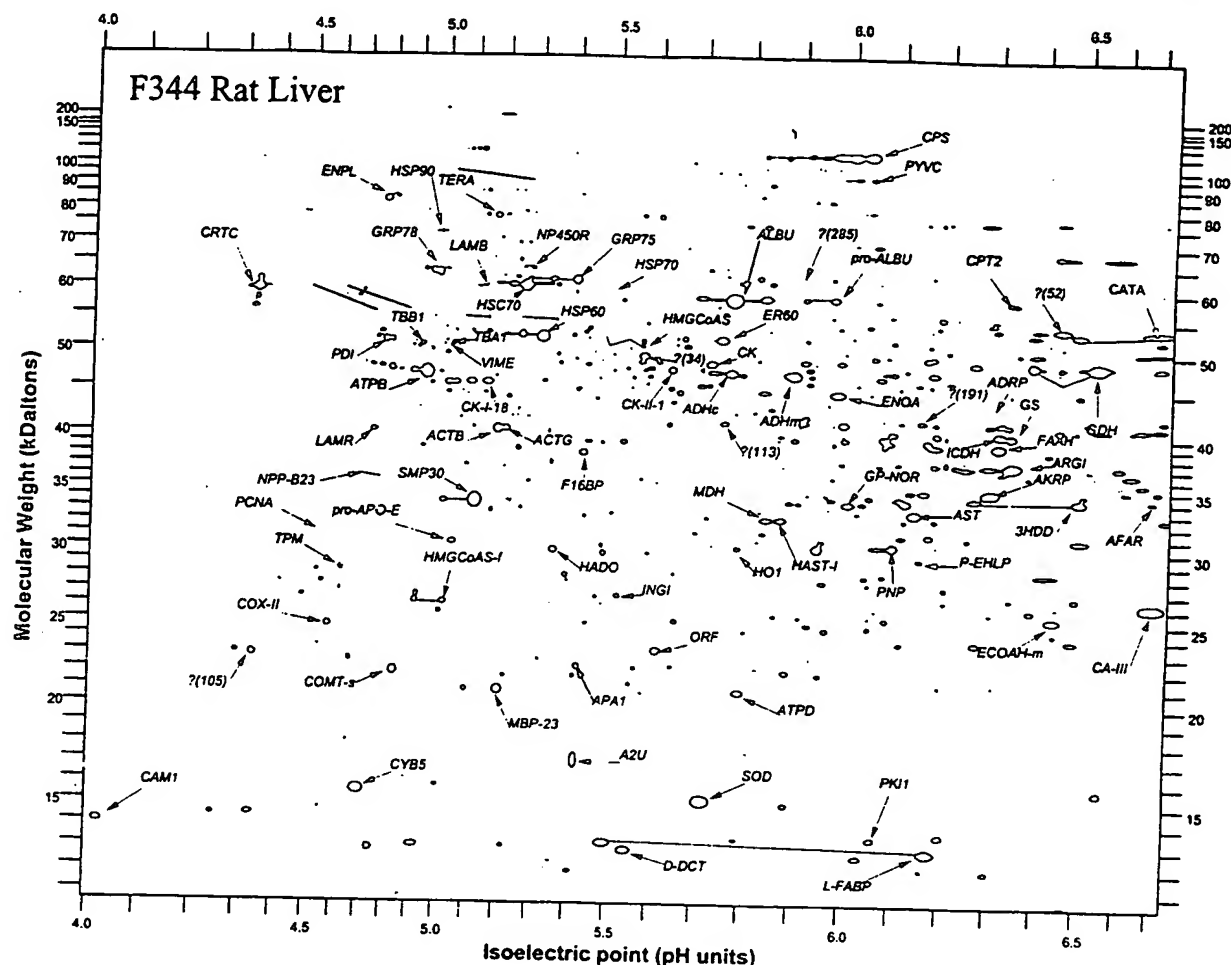


Fig. 2. Computerized representation of a Coomassie Blue stained two-dimensional gel electrophoresis pattern of Fischer F344 rat liver homogenate.

quantitative expression data has been collected, is to visualize complex patterns of gene expression changes, to detect pathways and sets of genes tightly correlated with treatment efficacy and toxicity, and to compare the effects of different sets of treatment (Anderson et al., 1996). As the drug effect database is growing, one may detect similarities and differences between the molecular fingerprints produced by various drugs, information that may be crucial to make a decision whether to refocus or extend the therapeutic spectrum of a drug candidate.

5. Comparison of global mRNA and protein expression profiling

There are several synergies and overlaps of data obtained by mRNA and protein expression analysis. Low abundant transcripts may not be easily quantified at the protein level using standard two-dimensional gel electrophoresis analysis and their detection may require prefractionation of samples. The expression of such genes may be preferably quantified at the mRNA level using techniques allowing PCR-mediated target amplifi-

cation. Tissue biopsy samples typically yield good quality of both mRNA and proteins; however, the quality of mRNA isolated from body fluids is often poor due to the faster degradation of mRNA when compared with proteins. RNA samples from body fluids such as serum or urine are often not very 'meaningful', and secreted proteins are likely more reliable surrogate markers for treatment efficacy and safety. Detection of post-translational modifications, events often related to function or nonfunction of a protein, is restricted to protein expression analysis and rarely can be predicted by mRNA profiling. Information on subcellular localization and translocation of proteins has to be acquired at the level of the protein in combination with sample prefractionation procedures. The growing evidence of a poor correlation between mRNA and protein abundance (Anderson and Seilhamer, 1997) further suggests that the two approaches, mRNA and protein profiling, are complementary and should be applied in parallel.

6. Expression profiling and drug development

Understanding the mechanisms of action and toxicity, and being able to monitor treatment efficacy and safety during trials is crucial for the successful development of a drug. Mechanistic insights are essential for the interpretation of drug effects and enhance the chances of recognizing potential species specificities contributing to an improved risk profile in humans (Richardson et al., 1993; Steiner et al., 1996b; Aicher et al., 1998). The value of expression profiling further increases when links between treatment-induced expression profiles and specific pharmacological and toxic endpoints are established (Anderson et al., 1991, 1995, 1996; Steiner et al. 1996a). Changes in gene expression are known to precede the manifestation of morphological alterations, giving expression profiling a great potential for early compound screening, enabling one to select drug candidates with wide therapeutic windows reflected by molecular fingerprints indicative of high pharmacological potency and low toxicity (Arce et al., 1998). In later phases of drug devel-

opment, surrogate markers of treatment efficacy and toxicity can be applied to optimize the monitoring of pre-clinical and clinical studies (Doherty et al., 1998).

7. Perspectives

The basic methodology of safety evaluation has changed little during the past decades. Toxicity in laboratory animals has been evaluated primarily by using hematological, clinical chemistry and histological parameters as indicators of organ damage. The rapid progress in genomics and proteomics technologies creates a unique opportunity to dramatically improve the predictive power of safety assessment and to accelerate the drug development process. Application of gene and protein expression profiling promises to improve lead selection, resulting in the development of drug candidates with higher efficacy and lower toxicity. The identification of biologically relevant surrogate markers correlated with treatment efficacy and safety bears a great potential to optimize the monitoring of pre-clinical and clinical trials.

References

- Aicher, L., Wahl, D., Arce, A., Grenet, O., Steiner, S., 1998. New insights into cyclosporine A nephrotoxicity by proteome analysis. *Electrophoresis* 19, 1998–2003.
- Anderson, N.L., Seilhamer, J., 1997. A comparison of selected mRNA and protein abundances in human liver. *Electrophoresis* 18, 533–537.
- Anderson, N.L., Esquer-Blasco, R., Hofmann, J.P., Anderson, N.G., 1991. A two-dimensional gel database of rat liver proteins useful in gene regulation and drug effects studies. *Electrophoresis* 12, 907–930.
- Anderson, L., Steele, V.K., Kelloff, G.J., Sharma, S., 1995. Effects of oltipraz and related chemoprevention compounds on gene expression in rat liver. *J. Cell. Biochem. Suppl.* 22, 108–116.
- Anderson, N.L., Esquer-Blasco, R., Richardson, F., Foxworthy, P., Eacho, P., 1996. The effects of peroxisome proliferators on protein abundances in mouse liver. *Toxicol. Appl. Pharmacol.* 137, 75–89.
- Arce, A., Aicher, L., Wahl, D., Esquer-Blasco, R., Anderson, N.L., Cordier, A., Steiner, S., 1998. Changes in the liver proteome of female Wistar rats treated with the hypoglycemic agent SDZ PGU 693. *Life Sci.* 63, 2243–2250.

- Chee, M., Yang, R., Hubbell, E., Berno, A., Huang, X.C., Stern, D., Winkler, J., Lockhart, D.J., Morris, M.S., Fodor, S.P., 1996. Accessing genetic information with high-density DNA arrays. *Science* 274, 610-614.
- Doherty, N.S., Littman, B.H., Reilly, K., Swindell, A.C., Buss, J., Anderson, N.L., 1998. Analysis of changes in acute-phase plasma proteins in an acute inflammatory response and in rheumatoid arthritis using two-dimensional gel electrophoresis. *Electrophoresis* 19, 355-363.
- Fodor, S.P., Read, J.L., Pirrung, M.C., Stryer, L., Lu, A.T., Solas, D., 1991. Light-directed, spatially addressable parallel chemical synthesis. *Science* 251, 767-773.
- Mann, M., Hojrup, P., Roepstorff, P., 1993. Use of mass spectrometric molecular weight information to identify proteins in sequence databases. *Biol. Mass Spectrom.* 22, 338-345.
- Richardson, F.C., Strom, S.C., Copple, D.M., Bendele, R.A., Probst, G.S., Anderson, N.L., 1993. Comparisons of protein changes in human and rodent hepatocytes induced by the rat-specific carcinogen, methapyrilene. *Electrophoresis* 14, 157-161.
- Schena, M., Shalon, D., Davis, R.W., Brown, P.O., 1995. Quantitative monitoring of gene expression patterns with a complementary DNA microarray. *Science* 251, 467-470.
- Shalon, D., Smith, S.J., Brown, P.O., 1996. A DNA microarray system for analyzing complex DNA samples using two-color fluorescent probe hybridization. *Genome Res.* 6, 639-645.
- Steiner, S., Wahl, D., Mangold, B.L.K., Robison, R., Raymackers, J., Meheus, L., Anderson, N.L., Cordier, A., 1996a. Induction of the adipose differentiation-related protein in liver of etomoxir treated rats. *Biochem. Biophys. Res. Commun.* 218, 777-782.
- Steiner, S., Aicher, L., Raymackers, J., Meheus, L., Esquer-Blasco, R., Anderson, L., Cordier, A., 1996b. Cyclosporine A mediated decrease in the rat renal calcium binding protein calbindin-D 28 kDa. *Biochem. Pharmacol.* 51, 253-258.
- Wilkins, M.R., Gasteiger, E., Sanchez, J.C., Appel, R.D., Hochstrasser, D.F., 1996. Protein identification with sequence tags. *Curr. Biol.* 6, 1543-1544.

Application of DNA Arrays to Toxicology

John C. Rockett and David J. Dix

Reproductive Toxicology Division, National Health and Environmental Effects Research Laboratory, U.S. Environmental Protection Agency, Research Triangle Park, North Carolina, USA

DNA array technology makes it possible to rapidly genotype individuals or quantify the expression of thousands of genes on a single filter or glass slide, and holds enormous potential in toxicologic applications. This potential led to a U.S. Environmental Protection Agency-sponsored workshop titled "Application of Microarrays to Toxicology" on 7-8 January 1999 in Research Triangle Park, North Carolina. In addition to providing state-of-the-art information on the application of DNA or gene microarrays, the workshop catalyzed the formation of several collaborations, committees, and user's groups throughout the Research Triangle Park area and beyond. Potential application of microarrays to toxicologic research and risk assessment include genome-wide expression analyses to identify gene-expression networks and toxicant-specific signatures that can be used to define mode of action, for exposure assessment, and for environmental monitoring. Arrays may also prove useful for monitoring genetic variability and its relationship to toxicant susceptibility in human populations. **Key words:** DNA arrays, gene arrays, microarrays, toxicology. *Environ Health Perspect* 107:681-685 (1999). [Online 6 July 1999]
<http://ehpnet1.niehs.nih.gov/docs/1999/107p681-685rockett/abstract.html>

Decoding the genetic blueprint is a dream that offers manifold returns in terms of understanding how organisms develop and function in an often hostile environment. With the rapid advances in molecular biology over the last 30 years, the dream has come a step closer to reality. Molecular biologists now have the ability to elucidate the composition of any genome. Indeed, almost 20 genomes have already been sequenced and more than 60 are currently under way. Foremost among these is the Human Genome Mapping Project. However, the genomes of a number of commonly used laboratory species are also under intensive investigation, including yeast, *Arabidopsis*, maize, rice, zebra fish, mouse, rat, and dog. It is widely expected that the completion of such programs will facilitate the development of many powerful new techniques and approaches to diagnosing and treating genetically and environmentally induced diseases which afflict mankind. However, the vast amount of data being generated by genome mapping will require new high-throughput technologies to investigate the function of the millions of new genes that are being reported. Among the most widely heralded of the new functional genomics technologies are DNA arrays, which represent perhaps the most anticipated new molecular biology technique since polymerase chain reaction (PCR).

Arrays enable the study of literally thousands of genes in a single experiment. The potential importance of arrays is enormous and has been highlighted by the recent publication of an entire *Nature Genetics* supplement dedicated to the technology (1). Despite this huge surge of interest, DNA arrays are still little used and largely unproven, as demonstrated by the high ratio of review and press articles to actual data papers. Even so, the potential they offer

has driven venture capitalists into a frenzy of investment and many new companies are springing up to claim a share of this rapidly developing market.

The U.S. Environmental Protection Agency (EPA) is interested in applying DNA array technology to ongoing toxicologic studies. To learn more about the current state of the technology, the Reproductive Toxicology Division (RTD) of the National Health and Environmental Effects Research Laboratory (NHEERL; Research Triangle Park, NC) hosted a workshop on "Application of Microarrays to Toxicology" on 7-8 January 1999 in Research Triangle Park, North Carolina. The workshop was organized by David Dix, Robert Kavlock, and John Rockett of the RTD/NHEERL. Twenty-two intramural and extramural scientists from government, academia, and industry shared information, data, and opinions on the current and future applications for this exciting new technology. The workshop had more than 150 attendees, including researchers, students, and administrators from the EPA, the National Institute of Environmental Health Sciences (NIEHS), and a number of other establishments from Research Triangle Park and beyond. Presentations ranged from the technology behind array production through the sharing of actual experimental data and projections on the future importance and applications of arrays. The information contained in the workshop presentations should provide aid and insight into arrays in general and their application to toxicology in particular.

Array Elements

In the context of molecular biology, the word "array" is normally used to refer to a series of DNA or protein elements firmly attached in

a regular pattern to some kind of supportive medium. DNA array is often used interchangeably with gene array or microarray. Although not formally defined, microarray is generally used to describe the higher density arrays typically printed on glass chips. The DNA elements that make up DNA arrays can be oligonucleotides, partial gene sequences, or full-length cDNAs. Companies offering pre-made arrays that contain less than full-length clones normally use regions of the genes which are specific to that gene to prevent false positives arising through cross-hybridization. Sequence verification of cDNA clone identity is necessary because of errors in identifying specific clones from cDNA libraries and databases. Premade DNA arrays printed on membranes are currently or imminently available for human, mouse, and rat. In most cases they contain DNA sequences representing several thousand different sequence clusters or genes as delineated through the National Center for Biotechnology Information UniGene Project (2). Many of these different UniGene clusters (putative genes) are represented only by expressed sequence tags (ESTs).

Array Printing

Arrays are typically printed on one of two types of support matrix. Nylon membranes are used by most off-the-shelf array providers such as Clontech Laboratories, Inc. (Palo Alto, CA), Genome Systems, Inc. (St. Louis, MO), and Research Genetics, Inc. (Huntsville, AL). Microarrays such as those produced by Affymetrix, Inc. (Santa Clara, CA), Incyte Pharmaceuticals, Inc. (Palo Alto, CA), and many do-it-yourself (DIY) arraying groups use glass wafers or slides. Although standard microscope slides may be used, they must be preprepared to facilitate sticking of the DNA to the glass. Several different

Address correspondence to J. Rockett, Reproductive Toxicology Division (MD-72), National Health and Environmental Effects Research Laboratory, U.S. EPA, Research Triangle Park, NC 27711 USA. Telephone: (919) 541-2678. Fax: (919) 541-4017. E-mail: rockett.john@epa.gov

The authors thank R. Kavlock for envisioning the application of array technology to toxicology at the U.S. Environmental Protection Agency. We also thank T. Wall and B. Deitz for administrative assistance.

This document has been reviewed in accordance with EPA policy and approved for publication. Mention of companies, trade names, or products does not signify endorsement of such by the EPA.

Received 23 March 1999; accepted 22 April 1999.

coatings have been successfully used, including silane and lysine. The coating of slides can easily be carried out in the laboratory, but many prefer the convenience of precoated slides available from suppliers.

Once the support matrix has been prepared, the DNA elements can be applied by several methods. Affymetrix, Inc., has developed a unique photolithographic technology for attaching oligonucleotides to glass wafers. More commonly, DNA is applied by either noncontact or contact printing. Noncontact printers can use thermal, solenoid, or piezoelectric technology to spray aliquots of solution onto the support matrix and may be used to produce slide or membrane-based arrays. Cartesian Technologies, Inc. (Irvine, CA) has developed nQUAD technology for use in its PixSys printers. The system couples a syringe pump with the microsolenoid valve, a combination that provides rapid quantitative dispensing of nanoliter volumes (down to 4.2 nL) over a variable volume range. A different approach to noncontact printing uses a solid pin and ring combination (Genetic MicroSystems, Inc., Woburn, MA). This system (Figure 1) allows a broader range of sample, including cell suspensions and particulates, because the printing head cannot be blocked up in the same way as a spray nozzle. Fluid transfer is controlled in this system primarily by the pin dimensions and the force of deposition, although the nature of the support matrix and the sample will also affect transfer to some degree.

In contact printing, the pin head is dipped in the sample and then touched to the support matrix to deposit a small aliquot. Split pins were one of the first contact-printing devices to be reported and are the suggested format for DIY arrayers, as described by Brown (3). Split pins are small metal pins with a precise groove cut vertically in the middle of the pin tip. In this system, 1–48 split pins are positioned in the pin-head. The split pins work by simple capillary action, not unlike a fountain pen—when the pin heads are dipped in the sample, liquid is drawn into the pin groove. A small (fixed) volume is then deposited each time the split pins are gently touched to the support matrix. Sample (100–500 pL depending on a variety of parameters) can be deposited on multiple slides before refilling is required, and array densities of $> 2,500$ spots/cm² may be produced. The deposit volume depends on the split size, sample fluidity, and the speed of printing. Split pins are relatively simple to produce and can be made in-house if a suitable machine shop is available. Alternatively, they can be obtained directly from companies such as TeleChem International, Inc. (Sunnyvale, CA).

Irrespective of their source, printers should be run through a preprint sequence prior to producing the actual experimental

arrays: the first 100 or so spots of a new run tend to be somewhat variable. Factors affecting spot reproducibility include slide treatment homogeneity, sample differences, and instrument errors. Other factors that come into play include clean ejection of the drop and clogging (nQUAD printing) and mechanical variations and long-term alteration in print-head surface of solid and split pins. However, with careful preparation it is possible to get a coefficient of variance for spot reproducibility below 10%.

One potential printing problem is sample carryover. Repeated washing, blotting, and drying (vacuum) of print pins between samples is normally effective at reducing sample carryover to negligible amounts. Printing should also be carried out in a controlled environment. Humidified chambers are available in which to place printers. These help prevent dust contamination and produce a uniform drying rate, which is important in determining spot size, quality, and reproducibility.

In summary, although several printing technologies are available, none are particularly outstanding and the bottom line is that they are still in a relatively early stage of evolution.

Array Hybridization

The hybridization protocol is, practically speaking, relatively straightforward and those with previous experience in blotting should have little difficulty. Array hybridizations are, in essence, reverse Southern/Northern blots—instead of applying a labeled probe to the target population of DNA/RNA, the labeled population is applied to the probe(s). With membrane-based arrays, the control and treated mRNA populations are normally converted to cDNA and labeled with isotope (e.g., ³²P) in the process. These labeled populations are then hybridized independently to parallel or serial arrays and the hybridization signal is detected with a phosphorimager. A less commonly used alternative to radioactive probes is enzymatic detection. The probe may be biotinylated, haptenylated, or have alkaline phosphatase/horseradish peroxidase attached. Hybridization is detected by enzymatic reaction yielding a color reaction (4). Differences in hybridization signals can be detected by eye or, more accurately, with the help of digital imaging and commercially available software. The labeling of the test populations for slide-based microarrays uses a slightly different approach. The probe typically consists of two samples of polyA⁺ RNA (usually from a treated and a control population) that are converted to cDNA; in the process each is labeled with a different fluor. The independently labeled probes are then mixed together and hybridized to a single microarray slide and the resulting combined fluorescent signal is scanned. After

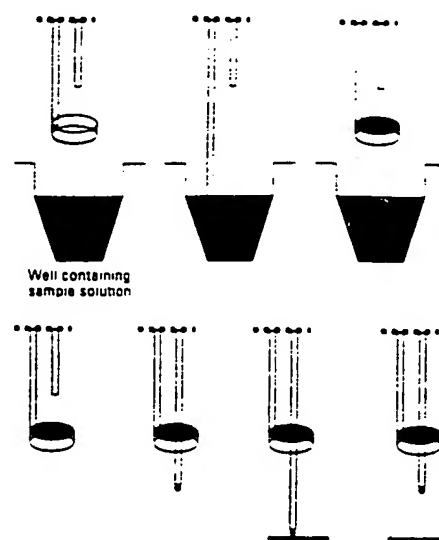


Figure 1. Genetic MicroSystems (Woburn, MA) pin ring system for printing arrays. The pin ring combination consists of a circular open ring oriented parallel to the sample solution, with a vertical pin centered over the ring. When the ring is dipped into a solution and lifted, it withdraws an aliquot of sample held by surface tension. To spot the sample, the pin is driven down through the ring and a portion of the solution is transferred to the bottom of the pin. The pin continues to move downward until the pendant drop of solution makes contact with the underlying surface. The pin is then lifted, and gravity and surface tension cause deposition of the spot onto the array. Figure from Flowers et al. (14), with permission from Genetic MicroSystems.

normalization, it is possible to determine the ratio of fluorescent signals from a single hybridization of a slide-based microarray.

cDNA derived from control and treated populations of RNA is most commonly hybridized to arrays, although subtractive hybridization or differential display reactions may also be used. Fluorophore- or radiolabeled nucleotides are directly incorporated into the cDNA in the process of converting RNA to cDNA. Alternatively, 5' end-labeled primers may be used for cDNA synthesis. These are labeled with a fluorophore for direct visualization of the hybridized array. Alternatively, biotin or a hapten may be attached to the primer, in which case fluor-labeled streptavidin or antibody must be applied before a signal can be generated. The most commonly used fluorophores at present are cyanine (Cy)3 and Cy5 (Amersham Pharmacia Biotech AB, Uppsala, Sweden). However, the relative expense of these fluorescent conjugates has driven a search for cheaper alternatives. Fluorescein, rhodamine, and Texas red have all been used, and companies such as Molecular Probes, Inc. (Eugene, OR) are developing a series of labeled nucleotides with a wide range of excitation and emission spectra which may prove to function as well as the Cy dyes.

Analysis of DNA Microarrays

Membrane-based arrays are normally analyzed on film or with a phosphorimager, whereas chip-based arrays require more specialized scanning devices. These can be divided into three main groups: the charge-coupled device camera systems, the nonconfocal laser scanners, and the confocal laser scanners. The advantages and disadvantages of each system are listed in Table 1.

Because a typical spot on a microarray can contain $> 10^8$ molecules, it is clear that a large variation in signal strength may occur. Current scanners cannot work across this many orders of magnitude (4 or 5 is more typical). However, the scanning parameters can normally be adjusted to collect more or less signal, such that two or three scans of the same array should permit the detection of rare and abundant genes.

When a microarray is scanned, the fluorescent images are captured by software normally included with the scanner. Several commercial suppliers provide additional software for quantifying array images, but the software tools are constantly evolving to meet the developing needs of researchers, and it is prudent to define one's own needs and clarify the exact capabilities of the software before its purchase. Issues that should be considered include the following:

- Can the software locate offset spots?
- Can it quantitate across irregular hybridization signals?
- Can the arrayed genes be programmed in for easy identification and location?
- Can the software connect via the Internet to databases containing further information on the gene(s) of interest?

One of the key issues raised at the workshop was the sensitivity of microarray technology. Experiments by General Scanning, Inc. (Watertown, MA), have shown that by using the Cy dyes and their scanner, signal can be detected down to levels of < 1 fluor molecule per square micrometer, which translates to detecting a rare message at approximately one copy per cell or less.

Array Applications

Although arrays are an emerging technology certain to undergo improvement and alteration, they have already been applied usefully to a number of model systems. Arrays are at their most powerful when they contain the entire genome of the species they are being used to study. For this reason, they have strong support among researchers utilizing yeast and *Caenorhabditis elegans* (5). The genomes of both of these species have been sequenced and, in the case of yeast, deposited onto arrays for examination of gene expression (6,7). With both of these species, it is relatively easy to perturb individual gene expression. Indeed, *C.*

Table 1. Advantages and disadvantages of different microarray scanning systems.

	CCD camera system	Nonconfocal laser scanner	Confocal laser scanner
Advantages	Few moving parts	Relatively simple optics	Small depth of focus reduces artifacts
	Fast scanning of bright samples	—	May have high light collection efficiency
Disadvantages	Less appropriate for dim samples	Low light collection efficiency	Small depth of focus requires scanning precision
	Optical scatter can limit performance	Background artifacts not rejected	
		Resolution typically low	

CCD, charge-coupled device.
From Kawasaki (13).

elegans knockouts can be made simply by soaking the worms in an antisense solution of the gene to be knocked out.

By a process of systematic gene disruption, it is now possible to examine the cause and effect relationships between different genes in these simple organisms. This kind of approach should help elucidate biochemical pathways and genetic control processes, deconvolute polygenic interactions, and define the architecture of the cellular network. A simple case study of how this can be achieved was presented by Butow [University of Texas Southwestern Medical Center, Dallas, TX (Figure 2)]. Although it is the phenotypic result of a single gene knockout that is being examined, the effect of such perturbation will almost always be polygenic. Polygenic interactions will become increasingly important as researchers begin to move away from single gene systems when examining the nature of toxicologic responses to external stimuli. This is especially important in toxicology because the phenotype produced by a given environmental insult is never the result of the action of a single gene; rather, it is a complex interaction of one or multiple cellular pathways. Phenomena such as quantitative trait (the continuous variation of phenotype), epistasis (the effect of alleles of one or more genes on the expression of other genes), and penetrance (proportion of individuals of a given genotype that display a particular phenotype) will become increasingly evident and important as toxicologists push toward the ultimate goal of matching the responses of individuals to different environmental stimuli.

Analysis of the transcriptome (the expression level of all the genes in a given cell population) was a use of arrays addressed by several speakers. Unfortunately, current gene nomenclature is often confusing in that single genes are allocated multiple names (usually as a result of independent discovery by different laboratories), and there was a call for standardization of gene nomenclature. Nevertheless, once a transcriptome has been assembled it can then be transferred onto arrays and used to screen any chosen system. The EPA MicroArray Consortium (EPAMAC) is assembling testes

transcriptomes for human, rat, and mouse. In a slightly different approach, Nuwaysir et al. (8) describes how the NIEHS assembled what is effectively a "toxicological transcriptome"—a library of human and mouse genes that have previously been proven or implicated in responses to toxicologic insults. Clontech Laboratories, Inc. (Palo Alto, CA), has begun a similar process by developing stress/toxicology filter arrays of rat, mouse, and human genes. Thus, rather than being tissue or cell specific, these stress/toxicology arrays can be used across a variety of model systems to look for alterations in the expression of toxicologically important genes and define the new field of toxicogenomics. The potential to identify toxicant families based on tissue- or cell-specific gene expression could revolutionize drug testing. These molecular signatures or fingerprints could not only point to the possible toxicity/carcinogenicity of newly discovered compounds (Figure 3), but also aid in elucidating their mechanism of action through identification of gene expression networks. By extension, such signatures could provide easily identifiable biomarkers to assess the degree, time, and nature of exposure.

DNA arrays are primarily a tool for examining differential gene expression in a given model. In this context they are referred to as closed systems because they lack the ability of other differential expression technologies, e.g., differential display and subtractive hybridization, to detect previously unknown genes not present on the array. This would appear to limit the power of DNA arrays to the imaginations and preconceptions of the researcher in selecting genes previously characterized and thought to be involved in the model system. However, the various genome sequencing projects have created a new category of sequence—the EST—that has partially mollified this deficiency. ESTs are cDNAs expressed in a given tissue that, although they may share some degree of sequence similarity to previously characterized genes, have not been assigned specific genetic identity. By incorporating EST clones into an array, it is possible to monitor the expression of these unknown genes. This can enable the identification of previously uncharacterized genes that may have biologic

significance in the model system. Filter arrays from Research Genetics and slide arrays from Incyte Pharmaceuticals both incorporate large numbers of ESTs from a variety of species.

A further use of microarrays is the identification of single nucleotide polymorphisms (SNPs). These genomic variations are abundant—they occur approximately every 1 kb or so—and are the basis of restriction fragment length polymorphism analysis used in forensic analysis. Affymetrix, Inc., designed chips that contain multiple repeats of the same gene sequence. Each position is present with all four possible bases. After the hybridization of the sample, the degree of hybridization to the different sequences can be measured and the exact sequence of the target gene deduced. SNPs are thought to be of vital importance in drug metabolism and toxicology. For example, single base differences in the regulatory region or active site of some genes can account for huge differences in the activity of that gene. Such SNPs are thought to explain why some people are able to metabolize certain xenobiotics better than others. Thus, arrays provide a further tool for the toxicologist investigating the nature of susceptible subpopulations and toxicologic response.

There are still many wrinkles to be ironed out before arrays become a standard tool for toxicologists. The main issues raised at the workshop by those with hands-on experience were the following:

- **Expense:** the cost of purchasing/contracting this technology is still too great for many individual laboratories.

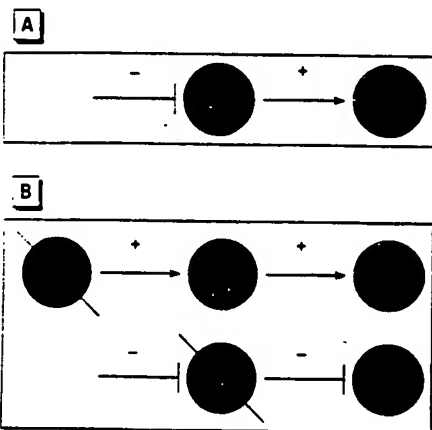


Figure 2. Potential effects of gene knockout within positively and negatively regulated gene expression networks. i_1 is limiting in wild type for expression of i_2 . (A) A simple, two-component, linear regulatory network operating on gene i_2 , where i_1 is a positive effector of i_2 and j_n is either a positive or negative effector of i_1 . This network could be deduced by examining the consequence of (B) deleting j_n on the expression of i_1 and i_2 , where the expression of i_2 would be decreased or increased depending on whether j_n was a positive or negative regulator. These and other connected components of even greater complexity could be revealed by genome-wide expression analysis. From Butow (15).

- **Clones:** the logistics of identifying, obtaining, and maintaining a set of nonredundant, non-contaminated, sequence-verified, species/cell/tissue/field-specific clones.
- **Use of inbred strains:** where whole-organism models are being used, the use of inbred strains is important to reduce the potentially confusing effects of the individual variation typically seen in outbred populations.
- **Probe:** the need for relatively large amounts of RNA, which limits the type of sample (e.g., biopsy) that can be used. Also, different RNA extraction methods can give different results.
- **Specificity:** the ability to discriminate accurately between closely related genes (e.g., the cytochrome p450 family) and splice variants.
- **Quantitation:** the quantitation of gene expression using gene arrays is still open to debate. One reason for this is the different incorporation of the labeling dyes. However, the main difficulty lies in knowing what to normalize against. One option is to include a large number of so-called housekeeping genes in the array. However, the expression of these genes often change depending on the tissue and the toxicant, so it is necessary to characterize the expression of these genes in the model system before utilizing them. This is clearly not a viable option when screening multiple new compounds. A second option is to include on the array genes from a non-related species (e.g., a plant gene on an animal array) and to spike the probe with synthetic RNA(s) complementary to the gene(s).
- **Reproducibility:** this is sometimes questionable, and a figure of approximately two or three repeats was used as the minimum number required to confirm initial findings.

Again, however, most people advocated the use of Northern blots or reverse transcriptase PCR to confirm findings.

- **Sensitivity:** concerns were voiced about the number of target molecules that must be present in a sample for them to be detected on the array.
- **Efficiency:** reproducible identification of 1.5- to 2-fold differences in expression was reported, although the number of genes that undergo this level of change and remain undetected is open to debate. It is important that this level of detection be ultimately achieved because it is commonly perceived that some important transcription factors and their regulators respond at such low levels. In most cases, 3- to 5-fold was the minimum change that most were happy to accept.
- **Bioinformatics:** perhaps the greatest concern was how to accurately interpret the data with the greatest accuracy and efficiency. The biggest headache is trying to identify networks of gene expression that are common to different treatments or doses. The amount of data from a single experiment is huge. It may be that, in the future, several groups individually equipped with specialized software algorithms for studying their favorite genes or gene systems will be able to share the same hybridized chips. Thus, arrays could usher in a new perspective on collaboration and the sharing of data.

EPAMAC

Perhaps the main reason most scientists are unable to use array technology is the high cost involved, whether buying off-the-shelf membranes, using contract printing services, or

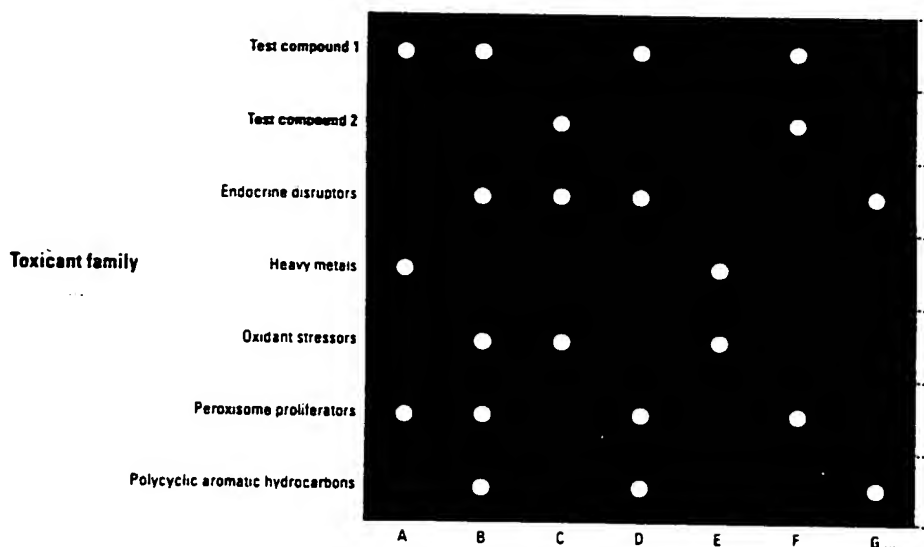


Figure 3. Gene expression profiles—also called fingerprints or signatures—of known toxicants or toxicant families may, in the future, be used to identify the potential toxicity of new drugs, etc. In this example, the genetic signature of test compound 1 is identical to that of known peroxisome proliferators, whereas that of test compound 2 does not match any known toxicant family. Based on these results, test compound 2 would be retained for further testing and test compound 1 would be eliminated.

producing chips in-house. In view of this, researchers at the RTD/NHEERL initiated the EPAMAC. This consortium brings together scientists from the EPA and a number of extramural labs with the aim of developing microarray capability through the sharing of resources and data. EPAMAC researchers are primarily interested in the developmental and toxicologic changes seen in testicular and breast tissue, and a portion of the workshop was set aside for EPAMAC members to share their ideas on how the experimental application of microarrays could facilitate their research. One of the central areas of interest to EPAMAC members is the effect of xenobiotics on male fertility and reproductive health. Of greatest concern is the effect of exposure during critical periods of development and germ cell differentiation (9), and how this may compromise sperm counts and quality following sexual maturation (10). As well as spermatogenic tissue, there is also interest in how residual mRNA found in mature sperm (11) could be used as an indicator of previous xenobiotic effects (it is easier to obtain a semen sample than a testicular biopsy). Arrays will be used to examine and compare the effect of exposure to heat and chemicals in testicular and epididymal gene expression profiles, with the aim of establishing relationships/associations between changes in developmental landmarks and the effects on sperm count and quality. Cluster, pattern, and other analysis of such data should help identify hidden relationships between genes that may reveal potential mechanisms of action and uncover roles for genes with unknown functions.

Summary

The full impact of DNA arrays may not be seen for several years, but the interest shown at this regional workshop indicates the high level of interest that they foster. Apart from educating and advertising the various technologies in this field, this workshop brought together a number of researchers from the Research Triangle Park area who are already using DNA arrays. The interest in sharing ideas and experiences led to the initiation of a Triangle array user's group.

Array technology is still in its infancy. This means that the hardware is still improving and there is no current consensus for standard procedures, quantitation, and interpretation. Consistency in spotting and scanning arrays is not yet optimized, and this is one of the most critical requirements of any experiment. In addition, one of the dark regions of array technology—strife in the courts over who owns what portions of it—has further muddled the future and is a potential barrier toward the development of consensus procedures.

Perhaps the greatest hurdle for the application of arrays is the actual interpretation of data. No specialists in bioinformatics attended the workshop, largely because they are rare and because as yet no one seems clear on the best method of approaching data analysis and interpretation. Cross-referencing results from multiple experiments (time, dose, repeats, different animals, different species) to identify commonly expressed genes is a great challenge. In most cases, we are still a long way from understanding how the expression of gene *X* is related to the expression of gene *Y*, and ordering gene expression to delineate causal relationships.

To the ordinary scientist in the typical laboratory, however, the most immediate problem is a lack of affordable instrumentation. One can purchase premade membranes at relatively affordable prices. Although these may be useful in identifying individual genes to pursue in more detail using other methods, the numbers that would be required for even a small routine toxicology experiment prohibit this as a truly viable approach. For the toxicologist, there is a need to carry out multiple experiments—dose responses, time curves, multiple animals, and repeats. Glass-based DNA arrays are most attractive in this context because they can be prepared in large batches from the same DNA source and accommodate control and treated samples on the same chip. Another problem with current off-the-shelf arrays is that they often do not contain one or more of the particular genes a group is interested in. One alternative is to obtain and/or produce a set of custom clones and have contract printing of membranes or slides carried out by a company such as Genomic Solutions, Inc. (Ann Arbor, MI). This approach

is less expensive than laying out capital for one's own entire system, although at some point it might make economic sense to print one's own arrays.

Finally, DNA arrays are currently a team effort. They are a technology that uses a wide range of skills including engineering, statistics, molecular biology, chemistry, and bioinformatics. Because most individuals are skilled in only one or perhaps two of these areas, it appears that success with arrays may be best expected by teams of collaborators consisting of individuals having each of these skills.

Those considering array applications may be amused or goaded on by the following quote from *Fortune* magazine (12):

Microprocessors have reshaped our economy, spawned vast fortunes and changed the way we live. Gene chips could be even bigger.

Although this comment may have been designed to excite the imagination rather than accurately reflect the truth, it is fair to say that the age of functional genomics is upon us. DNA arrays look set to be an important tool in this new age of biotechnology and will likely contribute answers to some of toxicology's most fundamental questions.

REFERENCES AND NOTES

1. The chipping forecast. *Nat Genet* 21(Suppl 1):3-60 (1999).
2. National Center for Biotechnology Information. The Unigene System. Available: www.ncbi.nlm.nih.gov/Schuler/UniGene [cited 22 March 1999].
3. Brown PO. The Brown Lab. Available: <http://cmgm.Stanford.edu/pbrown> [cited 22 March 1999].
4. Chen JJ, Wu R, Yang PC, Huang JY, Sher YP, Han MH, Kao WC, Lee PJ, Chiu TF, Chang F, et al. Profiling expression patterns and isolating differentially expressed genes by cDNA microarray system with colony-metry detection. *Genomics* 51:313-324 (1998).
5. Ward S. DNA Microarray Technology to Identify Genes Controlling Spermatogenesis. Available: www.mcb.arizona.edu/wardlab/microarray.html [cited 22 March 1999].
6. Marton MJ, DeRisi JL, Bennett HA, Iyer VR, Meyer MR, Roberts CJ, Stoughton R, Burdick J, Slade D, Dai H, et al. Drug target validation and identification of secondary drug target effects using DNA microarrays. *Nat Med* 4:1293-1301 (1998).
7. Brown PO. The Full Yeast Genome on a Chip. Available: <http://cmgm.Stanford.edu/pbrown/yeastchip.html> [cited 22 March 1999].
8. Nuwaysir EF, Bittner M, Trent J, Barrett JC, Alshari CA. Microarrays and toxicology: the advent of toxicogenomics. *Mol Carcinog* 24(3):153-159 (1999).
9. Hecht NB. Molecular mechanisms of male germ cell differentiation. *Bioessays* 20:555-561 (1998).
10. Zacharewski TR, Timothy R. Zacharewski. Available: www.bch.msu.edu/faculty/zachar.htm [cited 22 March 1999].
11. Kramer JA, Krawetz SA. RNA in spermatozoa: implications for the alternative haploid genome. *Mol Hum Reprod* 3:473-478 (1997).
12. Stipp D. Gene chip breakthrough. *Fortune*, March 31:56-73 (1997).
13. Kawesaki E (General Scanning Instruments, Inc., Watertown, MA). Unpublished data.
14. Flowers P, Overbeck J, Mace ML Jr, Pagliughi FM, Eggers WJE, Yonkers H, Honkanen P, Montagu J, Rose SD. Development and Performance of a Novel Microarraying System Based on Surface Tension Forces. Available: <http://www.geneticmicro.com/resources/html/coldspring.html> [cited 22 March 1999].
15. Butow R (University of Texas Medical Center, Dallas, TX). Unpublished data.

SPEAKERS

Cindy Alshari	Abdel Elkahoulou
NIHES	Research Genetics, Inc.
Linda Birnbaum	Sue Fenton
U.S. EPA	U.S. EPA
Ron Butow	Norman Hecht
University of Texas	University of Pennsylvania
Southwestern Medical	Pat Hurban
Center	Paradigm Genetics, Inc.
Alex Chenchik	Bob Kavlock
Clontech Laboratories, Inc.	U.S. EPA
David Dix	Ernie Kawasaki
U.S. EPA	General Scanning, Inc.

Steve Krawetz	Jim Samet
Wayne State University	U.S. EPA
Nick Mace	Sam Ward
Genetic Microsystems, Inc.	University of Arizona
Scott Mordacai	Jeff Welch
Affymetrix, Inc.	U.S. EPA
Kevin Morgan	Reen Wu
Glaxo Wellcome, Inc.	University of California
Elaine Poplin	at Davis
Research Genetics, Inc.	Tim Zacharewski
Don Rose	Michigan State University
Cartesian Technologies, Inc.	

Subject: RE: [Fwd: Toxicology Chip]

Date: Mon. 3 Jul 2000 08:09:45 -0400

From: "Afshari.Cynthia" <afshari@niehs.nih.gov>

To: "Diana Hamlet-Cox" <dianahc@incyte.com>

You can see the list of clones that we have on our 12K chip at:

<http://manuel.niehs.nih.gov/maps/guest/clonesrch.cfm>

We selected a subset of genes (2000K) that we believed critical to tox response and basic cellular processes and added a set of clones and ESTs to this. We have included a set of control genes (80-) that were selected by the NHGRI because they did not change across a large set of array experiments. However, we have found that some of these genes change significantly after tox treatments and are in the process of looking at the variation of each of these 80- genes across our experiments.

Our chips are constantly changing and being updated and we hope that our data will lead us to what the toxchip should really be.

I hope this answers your question.

Cindy Afshari

> -----

> From: Diana Hamlet-Cox
> Sent: Monday, June 26, 2000 8:52 PM
> To: afshari@niehs.nih.gov
> Subject: [Fwd: Toxicology Chip]

> Dear Dr. Afshari,

> Since I have not yet had a response from Bill Grigg, perhaps he was not the right person to contact.

> Can you help me in this matter? I don't need to know the sequences, necessarily, but I would like very much to know what types of sequences are being used, e.g., GPCRs (more specific?), ion channels, etc.

> Diana Hamlet-Cox

> ----- Original Message -----

> Subject: Toxicology Chip
> Date: Mon. 19 Jun 2000 18:31:48 -0700
> From: Diana Hamlet-Cox <dianahc@incyte.com>
> Organization: Incyte Pharmaceuticals
> To: grigg@niehs.nih.gov

> Dear Colleague:

> I am doing literature research on the use of expressed genes as pharmacotoxicology markers, and found the Press Release dated February 29, 2000 regarding the work of the NIEHS in this area. I would like to know if there is a resource I can access (or you could provide?) that would give me a list of the 12,000 genes that are on your Human ToxChip Microarray. In particular, I am interested in the criteria used to select sequences for the ToxChip, including any control sequences included in the microarray.

> Thank you for your assistance in this request.

> Diana Hamlet-Cox, Ph.D.
> Incyte Genomics, Inc.

> --

> =====

> This email message is for the sole use of the intended recipient(s) and
> may contain confidential and privileged information subject to
> attorney-client privilege. Any unauthorized review, use, disclosure or
> distribution is prohibited. If you are not the intended recipient,
> please contact the sender by reply email and destroy all copies of the
> original message.

> *****

>
>

Assessing sequence comparison methods with reliable structurally identified distant evolutionary relationships

STEVEN E. BRENNER^{*†‡}, CYRUS CHOTHIA^{*}, AND TIM J. P. HUBBARD[§]

^{*}MRC Laboratory of Molecular Biology, Hills Road, Cambridge CB2 2QH, United Kingdom; and [§]Sanger Centre, Wellcome Trust Genome Campus, Hinxton, Cambs CB10 1SA, United Kingdom

Communicated by David R. Davies, National Institute of Diabetes, Bethesda, MD, March 16, 1998 (received for review November 12, 1997)

ABSTRACT Pairwise sequence comparison methods have been assessed using proteins whose relationships are known reliably from their structures and functions, as described in the SCOP database [Murzin, A. G., Brenner, S. E., Hubbard, T. & Chothia C. (1995) *J. Mol. Biol.* 247, 536-540]. The evaluation tested the programs BLAST [Altschul, S. F., Gish, W., Miller, W., Myers, E. W. & Lipman, D. J. (1990) *J. Mol. Biol.* 215, 403-410], WU-BLAST2 [Altschul, S. F. & Gish, W. (1996) *Methods Enzymol.* 266, 460-480], FASTA [Pearson, W. R. & Lipman, D. J. (1988) *Proc. Natl. Acad. Sci. USA* 85, 2444-2448], and SSEARCH [Smith, T. F. & Waterman, M. S. (1981) *J. Mol. Biol.* 147, 195-197] and their scoring schemes. The error rate of all algorithms is greatly reduced by using statistical scores to evaluate matches rather than percentage identity or raw scores. The E-value statistical scores of SSEARCH and FASTA are reliable: the number of false positives found in our tests agrees well with the scores reported. However, the P-values reported by BLAST and WU-BLAST2 exaggerate significance by orders of magnitude. SSEARCH, FASTA $ktup = 1$, and WU-BLAST2 perform best, and they are capable of detecting almost all relationships between proteins whose sequence identities are >30%. For more distantly related proteins, they do much less well; only one-half of the relationships between proteins with 20-30% identity are found. Because many homologs have low sequence similarity, most distant relationships cannot be detected by any pairwise comparison method; however, those which are identified may be used with confidence.

Sequence database searching plays a role in virtually every branch of molecular biology and is crucial for interpreting the sequences issuing forth from genome projects. Given the method's central role, it is surprising that overall and relative capabilities of different procedures are largely unknown. It is difficult to verify algorithms on sample data because this requires large data sets of proteins whose evolutionary relationships are known unambiguously and independently of the methods being evaluated. However, nearly all known homologs have been identified by sequence analysis (the method to be tested). Also, it is generally very difficult to know, in the absence of structural data, whether two proteins that lack clear sequence similarity are unrelated. This has meant that although previous evaluations have helped improve sequence comparison, they have suffered from insufficient, imperfectly characterized, or artificial test data. Assessment also has been problematic because high quality database sequence searching attempts to have both sensitivity (detection of homologs) and specificity (rejection of unrelated proteins); however, these complementary goals are linked such that increasing one causes the other to be reduced.

Sequence comparison methodologies have evolved rapidly, so no previously published tests have evaluated modern versions of programs commonly used. For example, parameters in BLAST (1) have changed, and WU-BLAST2 (2)—which produces gapped alignments—has become available. The latest version of FASTA (3) previously tested was 1.6, but the current release (version 3.0) provides fundamentally different results in the form of statistical scoring.

The previous reports also have left gaps in our knowledge. For example, there has been no published assessment of thresholds for scoring schemes more sophisticated than percentage identity. Thus, the widely discussed statistical scoring measures have never actually been evaluated on large databases of real proteins. Moreover, the different scoring schemes commonly in use have not been compared.

Beyond these issues, there is a more fundamental question: in an absolute sense, how well does pairwise sequence comparison work? That is, what fraction of homologous proteins can be detected using modern database searching methods?

In this work, we attempt to answer these questions and to overcome both of the fundamental difficulties that have hindered assessment of sequence comparison methodologies. First, we use the set of distant evolutionary relationships in the SCOP: Structural Classification of Proteins database (4), which is derived from structural and functional characteristics (5). The SCOP database provides a uniquely reliable set of homologs, which are known independently of sequence comparison. Second, we use an assessment method that jointly measures both sensitivity and specificity. This method allows straightforward comparison of different sequence searching procedures. Further, it can be used to aid interpretation of real database searches and thus provide optimal and reliable results.

Previous Assessments of Sequence Comparison. Several previous studies have examined the relative performance of different sequence comparison methods. The most encompassing analyses have been by Pearson (6, 7), who compared the three most commonly used programs. Of these, the Smith-Waterman algorithm (8) implemented in SSEARCH (3) is the oldest and slowest but the most rigorous. Modern heuristics have provided BLAST (1) the speed and convenience to make it the most popular program. Intermediate between these two is FASTA (3), which may be run in two modes offering either greater speed ($ktup = 2$) or greater effectiveness ($ktup = 1$). Pearson also considered different parameters for each of these programs.

To test the methods, Pearson selected two representative proteins from each of 67 protein superfamilies defined by the PIR database (9). Each was used as a query to search the database, and the matched proteins were marked as being homologous or unrelated according to their membership of PIR.

Abbreviation: EPO, errors per query.

[†]Present address: Department of Structural Biology, Stanford University, Farchild Building D-109, Stanford, CA 94305-5126

[‡]To whom reprints requests should be addressed. e-mail: brenner@hyper.stanford.edu.

The publication costs of this article were defrayed in part by page charge payment. This article must therefore be hereby marked "advertisement" in accordance with 18 U.S.C. §1734 solely to indicate this fact.

© 1998 by The National Academy of Sciences 0027-8424/98/956073-6\$2.00/0 PNAS is available online at <http://www.pnas.org>.

superfamilies. Pearson found that modern matrices and "in-scaling" of raw scores improve results considerably. He also reported that the rigorous Smith-Waterman algorithm worked slightly better than FASTA, which was in turn more effective than BLAST.

Very large scale analyses of matrices have been performed (10), and Henikoff and Henikoff (11) also evaluated the effectiveness of BLAST and FASTA. Their test with BLAST considered the ability to detect homologs above a predetermined score but had no penalty for methods which also reported large numbers of spurious matches. The Henikoffs searched the SWISS-PROT database (12) and used PROSITE (13) to define homologous families. Their results showed that the BLOSUM62 matrix (14) performed markedly better than the extrapolated PAM-series matrices (15), which previously had been popular.

A crucial aspect of any assessment is the data that are used to test the ability of the program to find homologs. But in Pearson's and the Henikoffs' evaluations of sequence comparison, the correct results were effectively unknown. This is because the superfamilies in PIR and PROSITE are principally created by using the same sequence comparison methods which are being evaluated. Interdependency of data and methods creates a "chicken and egg" problem, and means for example, that new methods would be penalized for correctly identifying homologs missed by older programs. For instance, immunoglobulin variable and constant domains are clearly homologous, but PIR places them in different superfamilies. The problem is widespread: each superfamily in PIR 48.00 with a structural homolog is itself homologous to an average of 1.6 other PIR superfamilies (16).

To surmount these sorts of difficulties, Sander and Schneider (17) used protein structures to evaluate sequence comparison. Rather than comparing different sequence comparison algorithms, their work focused on determining a length-dependent threshold of percentage identity, above which all proteins would be of similar structure. A result of this analysis was the HSSP equation; it states that proteins with 25% identity over 80 residues will have similar structures, whereas shorter alignments require higher identity. (Other studies also have used structures (18-20), but these focused on a small number of model proteins and were principally oriented toward evaluating alignment accuracy rather than homology detection.)

A general solution to the problem of scoring comes from statistical measures (i.e., E-values and P-values) based on the extreme value distribution (21). Extreme value scoring was implemented analytically in the BLAST program using the Karlin and Altschul statistics (22, 23) and empirical approaches have been recently added to FASTA and SSEARCH. In addition to being heralded as a reliable means of recognizing significantly similar proteins (24, 25), the mathematical tractability of statistical scores "is a crucial feature of the BLAST algorithm" (1). The validity of this scoring procedure has been tested analytically and empirically (see ref. 2 and references in ref. 24). However, all large empirical tests used random sequences that may lack the subtle structure found within biological sequences (26, 27) and obviously do not contain any real homologs. Thus, although many researchers have suggested that statistical scores be used to rank matches (24, 25, 28), there have been no large rigorous experiments on biological data to determine the degree to which such rankings are superior.

A Database for Testing Homology Detection. Since the discovery that the structures of hemoglobin and myoglobin are very similar though their sequences are not (29), it has been apparent that comparing structures is a more powerful (if less convenient) way to recognize distant evolutionary relationships than comparing sequences. If two proteins show a high degree of similarity in their structural details and function, it

is very probable that they have an evolutionary relationship though their sequence similarity may be low.

The recent growth of protein structure information combined with the comprehensive evolutionary classification in the SCOP database (4, 5) have allowed us to overcome previous limitations. With these data, we can evaluate the performance of sequence comparison methods on real protein sequences whose relationships are known confidently. The SCOP database uses structural information to recognize distant homologs, the large majority of which can be determined unambiguously. These superfamilies, such as the globins or the immunoglobulins, would be recognized as related by the vast majority of the biological community despite the lack of high sequence similarity.

From SCOP, we extracted the sequences of domains of proteins in the Protein Data Bank (PDB) (30) and created two databases. One (PDB90D-B) has domains, which were all <90% identical to any other, whereas (PDB40D-B) had those <40% identical. The databases were created by first sorting all protein domains in SCOP by their quality and making a list. The highest quality domain was selected for inclusion in the database and removed from the list. Also removed from the list (and discarded) were all other domains above the threshold level of identity to the selected domain. This process was repeated until the list was empty. The PDB40D-B database contains 1,323 domains, which have 9,044 ordered pairs of distant relationships, or ~0.5% of the total 1,749,006 ordered pairs. In PDB90D-B, the 2,079 domains have 53,988 relationships, representing 1.2% of all pairs. Low complexity regions of sequence can achieve spurious high scores, so these were masked in both databases by processing with the SEG program (27) using recommended parameters: 12 1.8 2.0. The databases used in this paper are available from <http://sss.stanford.edu/sss/>, and databases derived from the current version of SCOP may be found at <http://scop.mrc-lmb.cam.ac.uk/scop/>.

Analyses from both databases were generally consistent, but PDB40D-B focuses on distantly related proteins and reduces the heavy overrepresentation in the PDB of a small number of families (31, 32), whereas PDB90D-B (with more sequences) improves evaluations of statistics. Except where noted otherwise, the distant homolog results here are from PDB40D-B. Although the precise numbers reported here are specific to the structural domain databases used, we expect the trends to be general.

Assessment Data and Procedure. Our assessment of sequence comparison may be divided into four different major categories of tests. First, using just a single sequence comparison algorithm at a time, we evaluated the effectiveness of different scoring schemes. Second, we assessed the reliability of scoring procedures, including an evaluation of the validity of statistical scoring. Third, we compared sequence comparison algorithms (using the optimal scoring scheme) to determine their relative performance. Fourth, we examined the distribution of homologs and considered the power of pairwise sequence comparison to recognize them. All of the analyses used the databases of structurally identified homologs and a new assessment criterion.

The analyses tested BLAST (1), version 1.4.9MP, and WU-BLAST2 (2), version 2.0a13MP. Also assessed was the FASTA package, version 3.0i76 (3), which provided FASTA and the SSEARCH implementation of Smith-Waterman (8). For SSEARCH and FASTA, we used BLOSUM45 with gap penalties -12/-1 (7, 16). The default parameters and matrix (BLOSUM62) were used for BLAST and WU-BLAST2.

The "Coverage Vs. Error" Plot. To test a particular protocol (comprising a program and scoring scheme), each sequence from the database was used as a query to search the database. This yielded ordered pairs of query and target sequences with associated scores, which were sorted, on the basis of their scores, from best to worst. The ideal method would have

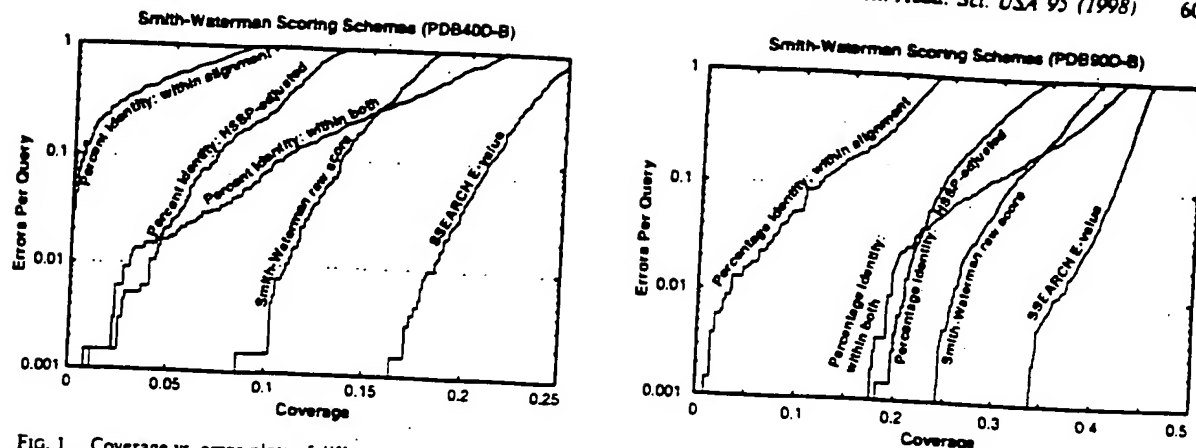


FIG. 1. Coverage vs. error plots of different scoring schemes for SSEARCH Smith-Waterman. (A) Analysis of PDB400-B database. (B) Analysis of PDB900-B database. All of the proteins in the database were compared with each other using the SSEARCH program. The results of this single set of comparisons were considered using five different scoring schemes and assessed. The graphs show the coverage and errors per query (EPQ) for statistical scores, raw scores, and three measures using percentage identity. In the coverage vs. error plot, the x axis indicates the fraction of all homologs in the database (known from structure) which have been detected. Precisely, it is the number of detected pairs of proteins with the same fold divided by the total number of pairs from a common superfamily. PDB400-B contains a total of 9,044 homologs, so a score of 10% indicates identification of 904 relationships. The y axis reports the number of EPQ. Because there are 1,323 queries made in the PDB400-B all-vs.-all comparison, 13 errors corresponds to 0.01, or 1% EPQ. The y axis is presented on a log scale to show results over the widely varying degrees of accuracy which may be desired. The scores that correspond to the levels of EPQ and coverage are shown in Fig. 4 and Table 1. The graph demonstrates the trade-off between sensitivity and selectivity. As more homologs are found (moving to the right), more errors are made (moving up). The ideal method would be in the lower right corner of the graph, which corresponds to identifying many evolutionary relationships without selecting unrelated proteins. Three measures of percentage identity are plotted. Percentage identity within alignment is the degree of identity within the aligned region of the proteins, without consideration of the alignment length. Percentage identity within both is the number of identical residues in the aligned region as a percentage of the average length of the query and target proteins. The HSSP equation (17) is $H = 290.15 / (l - 0.56)$ where l is length for $10 < l < 80$; $H > 100$ for $l < 10$; $H = 24.7$ for $l > 80$. The percentage identity HSSP-adjusted score is the percent identity within the alignment minus H . Smith-Waterman raw scores and E-values were taken directly from the sequence comparison program.

perfect separation, with all of the homologs at the top of the list and unrelated proteins below. In practice, perfect separation is impossible to achieve so instead one is interested in drawing a threshold above which there are the largest number of related pairs of sequences consistent with an acceptable error rate.

Our procedure involved measuring the coverage and error for every threshold. Coverage was defined as the fraction of structurally determined homologs that have scores above the selected threshold; this reflects the sensitivity of a method. Errors per query (EPQ), an indicator of selectivity, is the number of nonhomologous pairs above the threshold divided by the number of queries. Graphs of these data, called coverage vs. error plots, were devised to understand how

protocols compare at different levels of accuracy. These graphs share effectively all of the beneficial features of Receiver Operating Characteristic (ROC) plots (33, 34) but better represent the high degrees of accuracy required in sequence comparison and the huge background of nonhomologs.

This assessment procedure is directly relevant to practical sequence database searching, for it provides precisely the information necessary to perform a reliable sequence database search. The EPQ measure places a premium on score consistency; that is, it requires scores to be comparable for different queries. Consistency is an aspect which has been largely

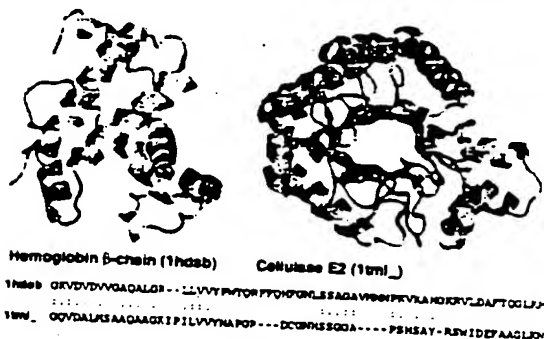


FIG. 2. Unrelated proteins with high percentage identity. Hemoglobin β -chain (PDB code 1hds chain b, ref. 38, Left) and cellulase E2 (PDB code 1tml, ref. 39, Right) have 39% identity over 64 residues, a level which is often believed to be indicative of homology. Despite this high degree of identity, their structures strongly suggest that these proteins are not related. Appropriately, neither the raw alignment score of 85 nor the E-value of 1.3 is significant. Proteins rendered by RASMOL (40).

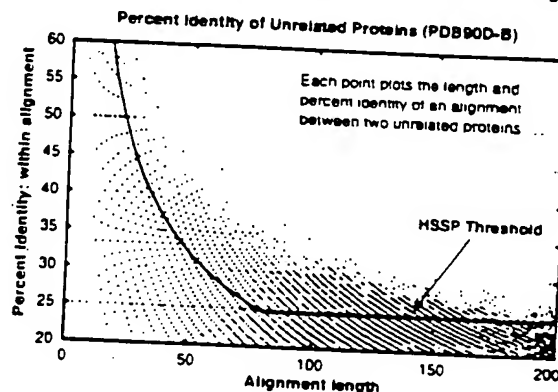


FIG. 3. Length and percentage identity of alignments of unrelated proteins in PDB900-B: Each pair of nonhomologous proteins found with SSEARCH is plotted as a point whose position indicates the length and the percentage identity within the alignment. Because alignment length and percentage identity are quantized, many pairs of proteins may have exactly the same alignment length and percentage identity. The line shows the HSSP threshold (though it is intended to be applied with a different matrix and parameters).

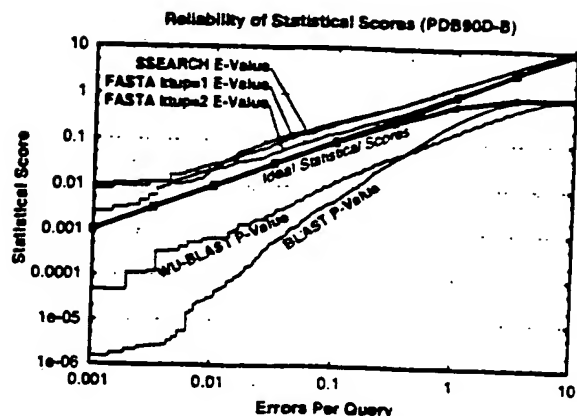


FIG. 4. Reliability of statistical scores in PDB90D-B: Each line shows the relationship between reported statistical score and actual error rate for a different program. E-values are reported for SSEARCH and FASTA, whereas P-values are shown for BLAST and WU-BLAST. If the scoring were perfect, then the number of errors per query and the E-values would be the same, as indicated by the upper bold line. (P-values should be the same as EPQ for small numbers, and diverges at higher values, as indicated by the lower bold line.) E-values from SSEARCH and FASTA are shown to have good agreement with EPQ but underestimate the significance slightly. BLAST and WU-BLAST are overconfident, with the degree of exaggeration dependent upon the score. The results for PDB40D-B were similar to those for PDB90D-B despite the difference in number of homologs detected. This graph could be used to roughly calibrate the reliability of a given statistical score.

ignored in previous tests but is essential for the straightforward or automatic interpretation of sequence comparison results. Further, it provides a clear indication of the confidence that should be ascribed to each match. Indeed, the EPQ measure should approximate the expectation value reported by database searching programs, if the programs' estimates are accurate.

The Performance of Scoring Schemes. All of the programs tested could provide three fundamental types of scores. The first score is the percentage identity, which may be computed in several ways based on either the length of the alignment or the lengths of the sequences. The second is a "raw" or "Smith-Waterman" score, which is the measure optimized by the Smith-Waterman algorithm and is computed by summing the substitution matrix scores for each position in the alignment and subtracting gap penalties. In BLAST, a measure

related to this score is scaled into bits. Third is a statistical score based on the extreme value distribution. These results are summarized in Fig. 1.

Sequence Identity. Though it has been long established that percentage identity is a poor measure (35), there is a common rule-of-thumb stating that 30% identity signifies homology. Moreover, publications have indicated that 25% identity can be used as a threshold (17, 36). We find that these thresholds, originally derived years ago, are not supported by present results. As databases have grown, so have the possibilities for chance alignments with high identity; thus, the reported cutoffs lead to frequent errors. Fig. 2 shows one of the many pairs of proteins with very different structures that nonetheless have high levels of identity over considerable aligned regions. Despite the high identity, the raw and the statistical scores for such incorrect matches are typically not significant. The principal reasons percentage identity does so poorly seem to be that it ignores information about gaps and about the conservative or radical nature of residue substitutions.

From the PDB90D-B analysis in Fig. 3, we learn that 30% identity is a reliable threshold for this database only for sequence alignments of at least 150 residues. Because one unrelated pair of proteins has 43.5% identity over 62 residues, it is probably necessary for alignments to be at least 70 residues in length before 40% is a reasonable threshold, for a database of this particular size and composition.

At a given reliability, scores based on percentage identity detect just a fraction of the distant homologs found by statistical scoring. If one measures the percentage identity in the aligned regions without consideration of alignment length, then a negligible number of distant homologs are detected. Use of the HSP equation improves the value of percentage identity, but even this measure can find only 4% of all known homologs at 1% EPQ. In short, percentage identity discards most of the information measured in a sequence comparison.

Raw Scores. Smith-Waterman raw scores perform better than percentage identity (Fig. 1), but ln-scaling (7) provided no notable benefit in our analysis. It is necessary to be very precise when using either raw or bit scores because a 20% change in cutoff score could yield a tenfold difference in EPQ. However, it is difficult to choose appropriate thresholds because the reliability of a bit score depends on the lengths of the proteins matched and the size of the database. Raw score thresholds also are affected by matrix and gap parameters.

Statistical Scores. Statistical scores were introduced partly to overcome the problems that arise from raw scores. This scoring scheme provides the best discrimination between homologous proteins and those which are unrelated. Most

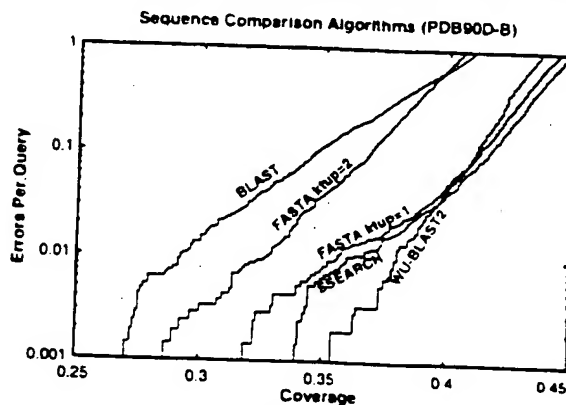
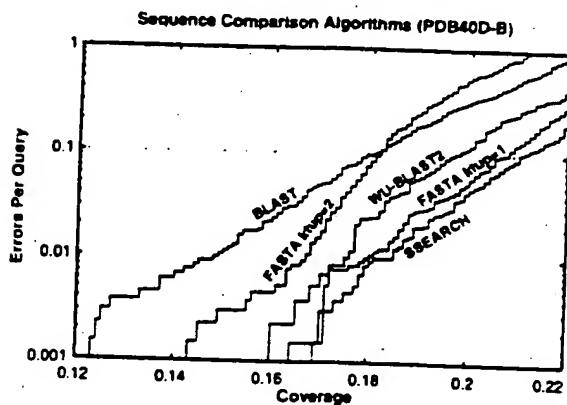


FIG. 5. Coverage vs. error plots of different sequence comparison methods: Five different sequence comparison methods are evaluated, each using statistical scores (E- or P-values). (A) PDB40D-B database. In this analysis, the best method is the slow SSEARCH, which finds 18% of relationships at 1% EPQ. FASTA ktup = 1 and WU-BLAST2 are almost as good. (B) PDB90D-B database. The quick WU-BLAST2 program provides the best coverage at 1% EPQ on this database, although at higher levels of error it becomes slightly worse than FASTA ktup = 1 and SSEARCH.

likely, its power can be attributed to its incorporation of more information than any other measure; it takes account of the full substitution and gap data (like raw scores) but also has details about the sequence lengths and composition and is scaled appropriately.

We find that statistical scores are not only powerful, but also easy to interpret. SSEARCH and FASTA show close agreement between statistical scores and actual number of errors per query (Fig. 4). The expectation value score gives a good, slightly conservative estimate of the chances of the two sequences being found at random in a given query. Thus, an E-value of 0.01 indicates that roughly one pair of nonhomologs of this similarity should be found in every 100 different queries. Neither raw scores nor percentage identity can be interpreted in this way, and these results validate the suitability of the extreme value distribution for describing the scores from a database search.

The P-values from BLAST also should be directly interpretable but were found to overstate significance by more than two orders of magnitude for 1% EPO for this database. Nonetheless, these results strongly suggest that the analytic theory is fundamentally appropriate. WU-BLAST2 scores were more reliable than those from BLAST, but also exaggerate expected confidence by more than an order of magnitude at 1% EPO.

Overall Detection of Homologs and Comparison of Algorithms. The results in Fig. 5A and Table 1 show that pairwise sequence comparison is capable of identifying only a small fraction of the homologous pairs of sequences in PDB40D-B. Even SSEARCH with E-values, the best protocol tested, could find only 18% of all relationships at a 1% EPO. BLAST, which identifies 15%, was the worst performer, whereas FASTA ktup = 1 is nearly as effective as SSEARCH. FASTA ktup = 2 and WU-BLAST2 are intermediate in their ability to detect homologs. Comparison of different algorithms indicates that those capable of identifying more homologs are generally slower. SSEARCH is 25 times slower than BLAST and 6.5 times slower than FASTA ktup = 1. WU-BLAST2 is slightly faster than FASTA ktup = 2, but the latter has more interpretable scores.

In PDB90D-B, where there are many close relationships, the best method can identify only 38% of structurally known homologs (Fig. 5B). The method which finds that many relationships is WU-BLAST2. Consequently, we infer that the differences between FASTA ktup = 1, SSEARCH, and WU-BLAST2 programs are unlikely to be significant when compared with variation in database composition and scoring reliability.

Fig. 6 helps to explain why most distant homologs cannot be found by sequence comparison: a great many such relationships have no more sequence identity than would be expected by chance. SSEARCH with E-values can recognize >90% of the homologous pairs with 30–40% identity. In this region, there are 30 pairs of homologous proteins that do not have significant E-values, but 26 of these involve sequences with <50 residues. Of sequences having 25–30% identity, 75% are identified by SSEARCH E-values. However, although the number of homologs grows at lower levels of identity, the detection falls off sharply: only 40% of homologs with 20–25% identity

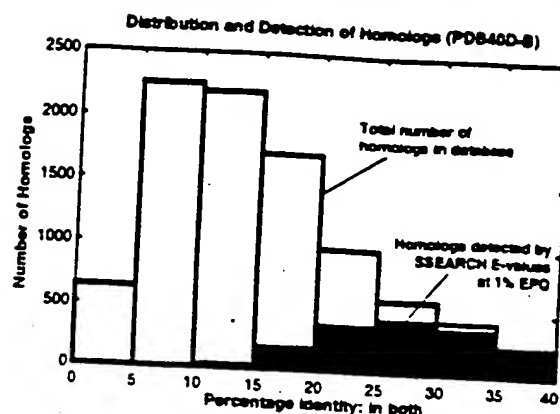


FIG. 6. Distribution and detection of homologs in PDB40D-B. Bars show the distribution of homologous pairs PDB40D-B according to their identity (using the measure of identity in both). Filled regions indicate the number of these pairs found by the best database searching method (SSEARCH with E-values) at 1% EPO. The PDB40D-B database contains proteins with <40% identity, and as shown on this graph, most structurally identified homologs in the database have diverged extremely far in sequence and have <20% identity. Note that the alignments may be inaccurate, especially at low levels of identity. Filled regions show that SSEARCH can identify most relationships that have 25% or more identity, but its detection wanes sharply below 25%. Consequently, the great sequence divergence of most structurally identified evolutionary relationships effectively defeats the ability of pairwise sequence comparison to detect them.

are detected and only 10% of those with 15–20% can be found. These results show that statistical scores can find related proteins whose identity is remarkably low; however, the power of the method is restricted by the great divergence of many protein sequences.

After completion of this work, a new version of pairwise BLAST was released: BLASTGP (37). It supports gapped alignments, like WU-BLAST2, and dispenses with sum statistics. Our initial tests on BLASTGP using default parameters show that its E-values are reliable and that its overall detection of homologs was substantially better than that of ungapped BLAST, but not quite equal to that of WU-BLAST2.

CONCLUSION

The general consensus amongst experts (see refs. 7, 24, 25, 27 and references therein) suggests that the most effective sequence searches are made by (i) using a large current database in which the protein sequences have been complexity masked and (ii) using statistical scores to interpret the results. Our experiments fully support this view.

Our results also suggest two further points. First, the E-values reported by FASTA and SSEARCH give fairly accurate estimates of the significance of each match, but the P-values provided by BLAST and WU-BLAST2 underestimate the true

Table 1. Summary of sequence comparison methods with PDB40D-B

Method	Relative Time*	1% EPO Cutoff	Coverage at 1% EPO
SSEARCH % identity: within alignment	25.5	>70%	<0.1
SSEARCH % identity: within both	25.5	34%	3.0
SSEARCH % identity: HSSP-scaled	25.5	35% (HSSP = 9.8)	4.0
SSEARCH Smith-Waterman raw scores	25.5	142	10.5
SSEARCH E-values	25.5	0.03	16.4
FASTA ktup = 1 E-values	3.9	0.03	17.9
FASTA ktup = 2 E-values	1.4	0.03	16.7
WU-BLAST2 P-values	1.1	0.003	17.5
BLAST P-values	1.0	0.00016	14.8

*Times are from large database searches with genome proteins.

extent of errors. Second, SSEARCH, WU-BLAST2, and FASTA ktup = 1 perform best, though BLAST and FASTA ktup = 2 detect most of the relationships found by the best procedures and are appropriate for rapid initial searches.

The homologous proteins that are found by sequence comparison can be distinguished with high reliability from the huge number of unrelated pairs. However, even the best database searching procedures tested fail to find the large majority of distant evolutionary relationships at an acceptable error rate. Thus, if the procedures assessed here fail to find a reliable match, it does not imply that the sequence is unique; rather, it indicates that any relatives it might have are distant ones.**

**Additional and updated information about this work, including supplementary figures, may be found at <http://sss.stanford.edu/sss/>.

The authors are grateful to Drs. A. G. Murzin, M. Levitt, S. R. Eddy, and G. Mitchison for valuable discussion. S.E.B. was principally supported by a St. John's College (Cambridge, UK) Benefactors' Scholarship and by the American Friends of Cambridge University. S.E.B. dedicates his contribution to the memory of Rabbi Albert T. and Clara S. Bilgray.

1. Altschul, S. F., Gish, W., Miller, W., Myers, E. W. & Lipman, D. J. (1990) *J. Mol. Biol.* 215, 403-410.
2. Altschul, S. F. & Gish, W. (1996) *Methods Enzymol.* 266, 460-480.
3. Pearson, W. R. & Lipman, D. J. (1988) *Proc. Natl. Acad. Sci. USA* 85, 2444-2448.
4. Murzin, A. G., Brenner, S. E., Hubbard, T. & Chothia, C. (1995) *J. Mol. Biol.* 247, 536-540.
5. Brenner, S. E., Chothia, C., Hubbard, T. J. P. & Murzin, A. G. (1996) *Methods Enzymol.* 266, 635-643.
6. Pearson, W. R. (1991) *Genomics* 11, 635-650.
7. Pearson, W. R. (1995) *Protein Sci.* 4, 1145-1160.
8. Smith, T. F. & Waterman, M. S. (1981) *J. Mol. Biol.* 147, 195-197.
9. George, D. G., Hunt, L. T. & Barker, W. C. (1996) *Methods Enzymol.* 266, 41-59.
10. Vogt, G., Etzold, T. & Argos, P. (1995) *J. Mol. Biol.* 249, 816-831.
11. Henikoff, S. & Henikoff, J. G. (1993) *Proteins* 17, 49-61.
12. Bairoch, A. & Apweiler, R. (1996) *Nucleic Acids Res.* 24, 21-25.
13. Bairoch, A., Bucher, P. & Hofmann, K. (1996) *Nucleic Acids Res.* 24, 189-196.
14. Henikoff, S. & Henikoff, J. G. (1992) *Proc. Natl. Acad. Sci. USA* 89, 10915-10919.
15. Dayhoff, M., Schwartz, R. M. & Orcutt, B. C. (1978) in *Atlas of Protein Sequence and Structure*, ed. Dayhoff, M. (National Biochemical Research Foundation, Silver Spring, MD), Vol. 5, Suppl. 3, pp. 345-352.
16. Brenner, S. E. (1996) Ph.D. thesis (University of Cambridge, UK).
17. Sander, C. & Schneider, R. (1991) *Proteins* 9, 56-68.
18. Johnson, M. S. & Overington, J. P. (1993) *J. Mol. Biol.* 233, 716-738.
19. Barton, G. J. & Sternberg, M. J. E. (1987) *Protein Eng.* 1, 89-94.
20. Lesk, A. M., Levitt, M. & Chothia, C. (1986) *Protein Eng.* 1, 77-78.
21. Arratia, R., Gordon, L. & M. W. (1986) *Ann. Stat.* 14, 971-993.
22. Karlin, S. & Altschul, S. F. (1990) *Proc. Natl. Acad. Sci. USA* 87, 2264-2268.
23. Karlin, S. & Altschul, S. F. (1993) *Proc. Natl. Acad. Sci. USA* 90, 5873-5877.
24. Altschul, S. F., Boguski, M. S., Gish, W. & Wootton, J. C. (1994) *Nat. Genet.* 6, 119-129.
25. Pearson, W. R. (1996) *Methods Enzymol.* 266, 227-258.
26. Lipman, D. J., Wilbur, W. J., Smith, T. F. & Waterman, M. S. (1984) *Nucleic Acids Res.* 12, 215-226.
27. Wootton, J. C. & Federhen, S. (1996) *Methods Enzymol.* 266, 554-571.
28. Waterman, M. S. & Vingron, M. (1994) *Stat. Science* 9, 367-381.
29. Perutz, M. F., Kendrew, J. C. & Watson, H. C. (1965) *J. Mol. Biol.* 13, 669-678.
30. Abola, E. E., Bernstein, F. C., Bryant, S. H., Koetzle, T. F. & Weng, J. (1987) in *Crystallographic Databases: Information Content, Software Systems, Scientific Applications*, eds. Allen, F. H., Bergerhoff, G. & Sievers, R. (Data Comm. Intl. Union Crystallogr., Cambridge, UK), pp. 107-132.
31. Brenner, S. E., Chothia, C. & Hubbard, T. J. P. (1997) *Curr. Opin. Struct. Biol.* 7, 369-376.
32. Orengo, C., Michie, A., Jones, S., Jones, D. T., Swindells, M. B. & Thornton, J. (1997) *Structure (London)* 5, 1093-1108.
33. Zweig, M. H. & Campbell, G. (1993) *Clin. Chem.* 39, 561-577.
34. Gribskov, M. & Robinson, N. L. (1996) *Comput. Chem.* 20, 25-33.
35. Fitch, W. M. (1966) *J. Mol. Biol.* 16, 9-16.
36. Chung, S. Y. & Subbiah, S. (1996) *Structure (London)* 4, 1123-1127.
37. Altschul, S. F., Madden, T. L., Schaffer, A. A., Zhang, J., Zhang, Z., Miller, W. & Lipman, D. J. (1997) *Nucleic Acids Res.* 25, 3389-3402.
38. Gilling, R., Schmidt, W., Jr., Houston, T., Amma, E. & Huisman, T. (1979) *J. Mol. Biol.* 131, 417-433.
39. Spezio, M., Wilson, D. & Karplus, P. (1993) *Biochemistry* 32, 9906-9916.
40. Sayle, R. A. & Milner-White, E. J. (1995) *Trends Biochem. Sci.* 20, 374-376.

Annexins in cancer and autoimmune diseases

B. C. Bastian

Klinik und Poliklinik für Hautkrankheiten, Julius-Maximilians Universität Würzburg, Josef-Schneider-Str. 2, D-97080 Würzburg (Germany)

Abstract. Several annexins have been implicated in the pathogenesis of benign and malignant neoplasms of different origins. In some tumours a suppressive action of annexins has been shown, whereas studies of other tumours indicate an involvement of annexins in tumour progression. In the light of the expression of annexins at distinct episodes of fetal development these observations point towards a functional role of annexins in cellular development and differentiation. This view is supported by data that link certain annexins to distinct pathways of signal transduction. Auto-antibodies against several annexins have been detected in patients with autoimmune diseases such as systemic lupus erythematosus, rheumatoid arthritis and inflammatory bowel disease. Until now it is unclear whether their presence reflects a relevant pathogenetic mechanism or merely represents an unspecific expression of a raised autoimmunity in these patients.

Key words. Annexins; neoplasms; pathology; autoimmune diseases; auto-antibodies; differentiation.

Expression of annexins in tumours

The finding that several annexins are subject to growth-dependent regulation of expression, together with their participation in signalling pathways and cell-cell adhesion, has awoken interest in their role in the pathogenesis of cancer. Considering the related structural properties of the annexins it is of interest that tumour suppressing and promoting attributes have also been demonstrated for different annexins.

In 1983 Hattori et al. reported that AX-1 can induce differentiation in the human histiocytic lymphoma cell line U937 [1]. In their experiments a similar effect could be obtained by treatment of the cells for 6 days with dexamethasone. This dexamethasone-inducible differentiation could be blocked by a monoclonal anti-AX-1 antibody, suggesting that the dexamethasone effect was mediated by AX-1. However, other investigators failed to confirm AX-1 mRNA and protein induction by dexamethasone in U937 cells [2] as well as in primary human macrophages [3]. That these discrepancies might be a reflection of different culture conditions has been shown by Schlaepfer et al. [4]. The cellular level of AX-1 varies with the growth state of cells, with proliferating cells having significantly higher cellular levels and synthesis rates than quiescent cells. Differentiation induction by AX-1 was also reported for the human lung cell adenocarcinoma cell line A549 [5, 6] and the human squamous cell carcinoma cell line SqCC/Y1 [7]. Immunohistochemical analyses have revealed increased

expression of AX-1 in a variety of central and peripheral nervous system tumours [8] and squamous cell carcinoma of the skin [9].

AX-2 has also been shown to underlie a growth-dependent regulation and to be inducible by mitogenic substances [10, 11]. In contrast to the described tumour suppressive effects assigned to AX-1 the association of AX-2 phosphorylation with retroviral transformation has raised the suspicion that AX-2 could be involved in the pathogenesis of cancer [12–14]. AX-2 has been shown to be highly abundant in human hepatocellular carcinoma but not in normal liver, human fetal tissue or regenerating rat liver after injury [15]. Overexpression of AX-2 mRNA and protein have further been demonstrated in human pancreatic cancer and pancreatic cancer derived cell lines [16, 17], multi-drug resistant small cell lung cancer [18], and high but not low grade gliomas [19, 20]. In the Eker rat hereditary renal carcinoma model, a dominant disorder with a defect in the rat analogue of the human tuberous sclerosis (*TSC2*) gene, a differential analysis showed the AX-2 heavy chain to be one of four genes with increased expression compared to normal animals [21]. Low baseline AX-2 expressions and strong increases after induction of differentiation are found in the PC12 rat adrenal pheochromocytoma and the F9 murine teratocarcinoma cell lines [22, 23]. Tressler et al. have demonstrated that AX-2 and AX-6 expressed on murine RAW117 lymphoma cells serve as adhesion molecules for tumour cell-endothelial cell binding [24, 25]. They showed that AX-2 and AX-6 are present on the external plasma membrane and that the binding of tumour cells could be significantly reduced by antibodies against AX-2 or AX-6. These findings indicate a pivotal role of certain AXs in cell-cell interaction.

Current address: Cancer Genetics Program, University of California San Francisco, Cancer Center, Box 0808, San Francisco (California 94143-0808, USA), Fax +1 415 476 8218, e-mail: bastian@cc.ucsf.edu

AXs-1, 2, 4, 5 and 6 were also shown to be expressed by cultured osteoblasts and the human osteosarcoma cell line MG-63 [26]. In this study the amount of AX-5 found in MG-63 cells was three times higher than in the primary osteoblast cultures. The authors also noted an influence on AX-5 levels on the state of growth of the culture. Karube et al. found a decrease of AX-5 mRNA and protein in carcinomas of the uterine cervix and endometrium when compared to normal tissues [27]. As AX-5 has been shown to exert an inhibitory action on protein kinase C [28, 29] the decreased levels of AX-5 might lead to a dysregulated activation of protein kinase C.

In contrast to AX-1 and -2 which are regulated during normal cell growth, the expression of AX-6 appears to be constitutive in most cell lines [30]. Tumour suppressive effects have been assigned to AX-6 in certain model systems. AX-6 is not expressed in the human squamous cell carcinoma line A431 which is characterized by a lack of contact inhibition and reduced growth factor requirement. After transfection with the AX-6 gene A431 cells stopped proliferating after reaching confluence [31] and grew smaller tumours than the non-transfected cells in mice [32]. Recently, AX-6 has been demonstrated to be differentially expressed in a murine melanoma cell line when compared to a syngeneic Melan-a-immortalized melanocyte cell line [33].

Acute promyelocytic leukemia (APL) is a disorder characterized by a balanced t(15;17) translocation in which the breakpoint involves the retinoic acid receptor- α and the *PML* gene [34]. AX-8 was shown to be overexpressed in APL cells in the majority of cases [35, 36]. As the AX-8 gene is located on chromosome 10 its overexpression cannot be directly related to the translocation. Interestingly, all-trans-retinoic acid, a strikingly effective drug to induce remissions in APL patients, is able to reduce the AX-8 expression in the APL-derived cell line NB4 [35]. This has been shown to be due to transcriptional regulation of the AX-8 gene [36]. The negative response of AX-8 expression to all-trans-retinoic acid supports the notion that AX-8 might act as a signal transducer involved in regulation of cell growth and differentiation.

Annexins as potential auto-antigens in autoimmune diseases

Auto-antibodies against AX-1 in patients with rheumatic diseases such as systemic lupus erythematosus (SLE) and rheumatoid arthritis (RA) were first described by Hirata et al. in 1981 [37]. These investigators found that patients' sera were able to abrogate the inhibitory action of a partly purified rabbit lipocortin on phospholipase A₂. This effect was decreased after absorption of the IgM fraction but not the IgG fraction of the sera, which suggests that circulating IgM antibodies

against AX-1 were present in those patients. Later, AX-1 of the IgM and to a lesser extent of the IgG-type were found in patients with RA and SLE using a recombinant human AX-1 and a correlation with disease activity was claimed [38]. Initially, it was suggested that corticosteroids might, by the induction of AX-1, induce the formation of AX-1 auto-antibodies, and that their presence might impair the inhibitory action of corticosteroids on phospholipase A₂ [38]. However, a causal role of corticosteroids in the induction of AX-1 auto-antibodies seems unlikely, because asthma patients treated with corticosteroids do not show AX-1 auto-antibodies [39]. Furthermore, no association of AX-1 auto-antibodies with either serum phospholipase A₂ levels or activity could be shown [40]. Patients with SLE were also reported to have auto-antibodies against AX-5 [41]. In this study the auto-antibodies were more common in patients who additionally had positive anti-cardiolipin antibodies or lupus anticoagulant. AX-1 auto-antibodies have also been demonstrated in patients with inflammatory bowel diseases, such as Crohn's disease or ulcerative colitis, who lack any association with corticosteroid treatment [42]. Interestingly, in this study patients with active confirmed bacterial diarrhoea had the highest titres of AX-1 auto-antibodies, suggesting that their presence might not be confined to autoimmune diseases but might reflect a nonspecific reaction to inflammation. This view is supported by studies demonstrating auto-antibodies against AX-1, AX-2, AX-3, AX-4, AX-5, and AX-6 in a plethora of inflammatory and neoplastic skin diseases without a clear correlation to any disease group including autoimmune diseases [43, 44]. For obvious reasons, a final judgement on the relevance of AX auto-antibodies requires the elucidation of the functions of AXs.

- 1 Hattori T., Hoffman T. and Hirata F. (1983) Differentiation of a histiocytic lymphoma cell line by lipomodulin a phospholipase inhibitory protein. *Biochem. Biophys. Res. Commun.* 111: 551-559
- 2 Isacke C. M., Lindberg R. A. and Hunter T. (1989) Synthesis of p36 and p35 is increased when U-937 cells differentiate in culture but expression is not inducible by glucocorticoids. *Molec. Cell Biol.* 9: 232-240
- 3 Bronnegard M. O., Andersson O., Edwall J., Lund G., Norstedt G. and Carlstedt-Duke J. (1988) Human calpactin II (lipocortin I) messenger ribonucleic acid is not induced by glucocorticoids. *Molec. Endocrinol.* 2: 732-739
- 4 Schlaepfer D. D. and Haigler H. T. (1990) Expression of annexins as a function of cellular growth state. *J. Cell Biol.* 111: 19685-21061
- 5 Croxtall J. D., Waheed S., Choudhury Q., Anand R. and Flower R. J. (1993) N-terminal peptide fragments of lipocortin-1 inhibit A549 cell growth and block EGF-induced stimulation of proliferation. *Int. J. Cancer* 54: 153-158
- 6 Croxtall J. D. and Flower R. J. (1992) Lipocortin 1 mediates dexamethasone-induced growth arrest of the A549 lung adenocarcinoma cell line. *Proc. Natl Acad. Sci. USA* 89: 3571-3575
- 7 Violette S. M., King I., Browning J. L., Pepinsky R. B., Wallner B. P. and Sartorelli A. C. (1990) Role of lipocortin I in the glucocorticoid induction of the terminal differentiation of a human squamous carcinoma. *J. Cell Physiol.* 142: 70-77

- 8 Johnson M. D., Kamso-Pratt J., Pepinsky R. B. and Whetsell W. O. J. (1989) Lipocortin-I immunoreactivity in central and peripheral nervous system glial tumours. *Hum. Pathol.* 20: 772-776
- 9 Bastian B. C., van der Piepen U., Römisch J., Pâques E. P. and Bröcker E. B. (1993) Localization of annexins in normal and diseased human skin. *J. Dermatol. Sci.* 6: 225-234
- 10 Chiang Y., Schneiderman M. H. and Vishwanatha J. K. (1993) Annexin II expression is regulated during mammalian cell cycle. *Cancer Res.* 53: 6017-6021
- 11 Kreutzer J. C. and Hirschhorn R. R. (1990) The growth-regulated gene *IB6* is identified as the heavy chain of calpactin I. *Exp. Cell Res.* 188: 153-159
- 12 Radke K., Gilmore T. and Martin G. S. (1980) Transformation by Rous sarcoma virus: a cellular substrate for transformation-specific protein phosphorylation contains phosphotyrosine. *Cell* 21: 821-828
- 13 Erikson E. and Erikson R. L. (1980) Identification of a cellular protein substrate phosphorylated by the avian sarcoma virus-transforming gene product. *Cell* 21: 829-836
- 14 Ozaki T. and Sakiyama S. (1993) Molecular cloning of rat calpactin I heavy-chain cDNA whose expression is induced in v-src-transformed rat culture cell lines. *Oncogene* 8: 1707-1710
- 15 Frohlich M., Motte P., Galvin K., Takahashi H., Wands J. and Ozturk M. (1990) Enhanced expression of the protein kinase substrate p36 in human hepatocellular carcinoma. *Molec. Cell Biol.* 10: 3216-3223
- 16 Vishwanatha J. K., Chiang Y., Kumble K. D., Hollingsworth M. A. and Pour P. M. (1993) Enhanced expression of annexin II in human pancreatic carcinoma cells and primary pancreatic cancers. *Carcinogenesis* 14: 2575-2579
- 17 Kumble K. D., Hirota M., Pour P. M. and Vishwanatha J. K. (1992) Enhanced levels of annexins in pancreatic carcinoma cells of Syrian hamsters and their intrapancreatic allografts. *Cancer Res.* 52: 163-167
- 18 Cole S. P., Pinkoski M. J., Bhardwaj G. and Deeley R. G. (1992) Elevated expression of annexin II (lipocortin II, p36) in a multidrug resistant small cell lung cancer cell line. *Br. J. Cancer* 65: 498-502
- 19 Reeves S. A., Chavez-Kappel C., Davis R., Rosenblum M. and Israel M. A. (1992) Developmental regulation of annexin II (Lipocortin 2) in human brain and expression in high grade glioma. *Cancer Res.* 52: 6871-6876
- 20 Roseman B. J., Bollen A., Hsu J., Lamborn K. and Israel M. A. (1994) Annexin II marks astrocytic brain tumours of high histologic grade. *Oncol. Res.* 6: 561-567
- 21 Hino O., Kobayashi E., Nishizawa M., Kubo Y., Kobayashi T., Hirayama Y. et al. (1995) Renal carcinogenesis in the Eker rat. *J. Cancer Res. Clin. Oncol.* 121: 602-605
- 22 Fox M. T., Prentice D. A. and Hughes J. P. (1991) Increases in p11 and annexin II proteins correlate with differentiation in the PC12 pheochromocytoma. *Biochem. Biophys. Res. Commun.* 177: 1188-93
- 23 Harder T., Thiel C. and Gerke V. (1993) Formation of the annexin IIp112 complex upon differentiation of F9 teratocarcinoma cells. *J. Cell Sci.* 104: 1109-1117
- 24 Tressler R. J., Yeatman T. and Nicolson G. L. (1994) Extracellular annexin VI expression is associated with divalent cation-dependent endothelial cell adhesion of metastatic RAW117 large-cell lymphoma cells. *Exp. Cell Res.* 215: 395-400
- 25 Tressler R. J., Updyke T. V., Yeatman T. and Nicolson G. L. (1993) Extracellular annexin II is associated with divalent cation-dependent tumour cell-endothelial cell adhesion of metastatic RAW117 large-cell lymphoma cells. *J. Cell Biochem.* 53: 265-276
- 26 Mohiti J., Walker J. H. and Caswell A. M. (1995) Studies on annexins in primary cultures of human osteoblasts and in the human osteosarcoma cell line MG-63. *Biochem. Soc. Trans.* 23: 36S
- 27 Karube A., Shidara Y., Hayasaka K., Maki M. and Tanaka T. (1995) Suppression of calphobindin I (CPB I) production in carcinoma of uterine cervix and endometrium. *Gynecol. Oncol.* 58: 295-300
- 28 Shibata S., Sato H. and Maki M. (1992) Calphobindins (placental annexins) inhibit protein kinase C. *J. Biochem.* 112: 552-556
- 29 Schlaepfer D. D., Jones J. J. and Haigler H. T. (1992) Inhibition of protein kinase C by annexin V. *Biochemistry* 31: 1886-1891
- 30 Moss S. E., Jacob S. M., Davies A. A. and Crumpton M. J. (1992) A growth-dependent post-translational modification of annexin VI. *Biochim. Biophys. Acta* 1160: 120-126
- 31 Theobald J., Smith P. D., Jacob S. M. and Moss S. E. (1994) Expression of annexin VI in A431 carcinoma cells suppresses proliferation: a possible role for annexin VI in cell growth regulation. *Biochim. Biophys. Acta* 1223: 383-390
- 32 Theobald J., Hanby A., Patel K. and Moss S. E. (1995) Annexin VI has tumour-suppressor activity in human A431 squamous epithelial carcinoma cells. *Br. J. Cancer* 71: 786-788
- 33 Francia G., Mitchell S. D., Moss S. E., Hanby A. M., Marshall J. F. and Hart I. R. (1996) Identification by differential display of annexin-VI, a gene differentially expressed during melanoma progression. *Cancer Res.* 56: 3855-3858
- 34 Warrell R. P., de Thé, H., Wang Z. Y. and Degos L. (1993) Acute promyelocytic leukemia. *New Engl. J. Med.* 329: 177-189
- 35 Chang K. S., Wang G., Freireich E. J., Daly M., Naylor S. L., Trujillo J. M. et al. (1992) Specific expression of the annexin VIII gene in acute promyelocytic leukemia. *Blood* 79: 1802-1810
- 36 Sarkar A., Yang P., Fan Y. H., Mu Z. M., Hauptmann R., Adolf G. R. et al. (1994) Regulation of the expression of annexin VIII in acute promyelocytic leukemia. *Blood* 84: 279-286
- 37 Hirata F., del Carmine R., Nelson C. A., Axelrod, J., Schiffmann E., Warabi A. et al. (1981) Presence of autoantibody for phospholipase inhibitory protein, lipomodulin, in patients with rheumatic diseases. *Proc. Natl Acad. Sci. USA* 78: 3190-3194
- 38 Goulding N. J., Podgorski M. R., Hall N. D., Flower R. J., Browning J. L., Pepinsky R. B. et al. (1989) Autoantibodies to recombinant lipocortin-I in rheumatoid arthritis and systemic lupus erythematosus. *Ann. Rheum. Dis.* 48: 843-850
- 39 Wilkinson J. R., Podgorski M. R., Godolphin J. L., Goulding N. J. and Lee T. H. (1990) Bronchial asthma is not associated with auto-antibodies to lipocortin-I. *Clin. Exp. Allergy* 20: 189-192
- 40 Pruzanski W., Goulding N. J., Flower R. J., Gladman D. D., Urowitz M. B., Goodman P. J. et al. (1994) Circulating group II phospholipase A2 activity and antilipocortin antibodies in systemic lupus erythematosus. Correlative study with disease activity. *J. Rheumatol.* 21: 252-257
- 41 Matsuda J., Saitoh N., Gohchi K., Gotoh M. and Tsukamoto M. (1994) Anti-annexin V antibody in systemic lupus erythematosus patients with lupus anticoagulant and/or anticardiolipin antibody. *Am. J. Hematol.* 47: 56-58
- 42 Stevens T. R., Smith S. F. and Rampton D. S. (1993) Antibodies to human recombinant lipocortin-I in inflammatory bowel disease. *Clin. Sci.* 84: 381-386
- 43 Kraus M., Römisch J., Bastian B. C., Pâques E. P. and Hartmann A. A. (1992) Detection of human anti-annexin autoantibodies by enzyme immunoassays. *J. Immunoassay* 13: 411-439
- 44 Bastian B. C., Nuss B., Römisch J., Kraus M. and Bröcker E. B. (1994) Autoantibodies to annexins: a diagnostic marker for cutaneous disorders? *J. Dermatol. Sci.* 8: 194-202

Alterations of Annexin Expression in Pathological Neuronal and Glial Reactions

Immunohistochemical Localization of Annexins I, II (p36 and p11 Subunits), IV, and VI in the Human Hippocampus

David A. Eberhard, Morry D. Brown, and
Scott R. VandenBerg

From the Department of Pathology (Neuropathology),
University of Virginia Health Sciences Center,
Charlottesville, Virginia

Annexins are Ca^{2+} -dependent membrane-binding proteins that are potentially important in Ca^{2+} -induced neurotoxicity or neuroprotection. To address the possible involvement of annexins in cellular reactions to brain injury and neurodegenerative disease, we studied the immunohistochemical localization of annexins I, II (p36 and p11), IV, and VI in the adult human hippocampus. Formalin-fixed, paraffin-embedded tissue from autopsy cases representing hypoxic-ischemic injury, seizure disorders, Alzheimer's disease, and age-related controls were examined. Neurons showed cytoplasmic immunoreactivity for annexin I, whereas annexin VI was distributed in patterns suggesting plasma membrane and perisynaptic locations. The cytoarchitectural distribution of annexin VI within neurons was altered in pathological states and annexin VI was strongly associated with neuronal granulovacuolar bodies in Alzheimer's disease. Reactive astrocytes expressed annexins I, II (p36 and p11), and IV, whereas quiescent astrocytes were minimally immunoreactive. Significant annexin immunoreactivity was also detected in oligodendrocytes (annexin IV), ependymocytes (I, II, and IV), choroid plexus (I, IV, and VI), meningeal epithelium (I, II, IV, and VI), and vascular endothelium (II and IV) and smooth muscle (I, IV, and VI). This is the first comparative study of immunoreactivities for multiple annexins in human brain. Neurons and

glia display selective and different profiles of annexin protein expression and show immunohistochemical changes in pathological conditions, which suggest involvement of annexins in neuronal and glial reactions to injury. (Am J Pathol 1994, 145:640-649)

The annexins are a family of proteins that are defined by a conserved COOH-terminal domain that confers Ca^{2+} -dependent binding to membranes containing acidic phospholipids. The NH₂-terminal sequence of each annexin is unique and presumably confers functional specificity to the protein. A variety of roles for annexins in cellular physiology have been proposed, such as mediation of membrane trafficking events and membrane-cytoskeleton interactions, regulation of phospholipase activity and eicosanoid release, receptor signal transduction, modulation, or formation of Ca^{2+} channels, and control of cellular proliferation and differentiation.^{1,2} However, at present there is little understanding of the specific functions of particular annexins *in vivo*.

Annexins are widely distributed among species and tissues. In the mammalian nervous system, different annexins are expressed in various cell types.³⁻⁶ The patterns of annexin expression in the brain may change during development^{3,7} and in pathological states.^{8,9} To better define the relationship of annexins to cellular reactions to injury and de-

generation in the have compared t and p36 subunits a variety of cond and neuronal dar damage, chronic mer's disease w ations in both the tectural patterns changes occurrence tion of annexin V ins I, II, and IV ir gest that the an and glial respor

Materials and

Case Materie

Hippocampal s cases (13 male tients (ages 35 acute or chror garded as cont zure disorders scleriosis and fc trogliosis witho tients with histic logical findings Four patients events that occ three showed n gliosis and one patients were and showed a Postmortem int hours (median were used as mortem fixation istry. These co cerebral neoc sented a varie processes, inl mer's disease.

Tissue Proc Immunohisti

In most cases in 10 to 20% temperature fc embedding in freshly dissec

DAE was supported by grant T32 NS 7236 from NINCDS and MDB was supported by a GEM fellowship of the National Consortium for Graduate Degrees for Minorities in Engineering and Science, Inc.

Accepted for publication June 12, 1994

Address reprint requests to Dr. Scott R. VandenBerg, Department of Pathology (Neuropathology), Box 214, University of Virginia Health Sciences Center, Charlottesville, VA 22908

generation in the human central nervous system, we have compared the distributions of annexins I, II (p11 and p36 subunits), IV, and VI in the hippocampus after a variety of conditions associated with glial reactions and neuronal damage. In this study, hypoxic ischemic damage, chronic seizure-related injury, and Alzheimer's disease were accompanied by specific alterations in both the cellular distributions and cytoarchitectural patterns of the annexins. The most prominent changes occurred with the cytoarchitectural distribution of annexin VI in neurons and increases of annexins I, II, and IV in reactive astroglia. These data suggest that the annexins may be involved in neuronal and glial responses to acute and chronic injury.

Materials and Methods

Case Material

Hippocampal sections from a total of 20 postmortem cases (13 male, 7 female) were examined. Four patients (ages 35 to 66 years) with no history of either acute or chronic neurological disorders were regarded as controls. Six patients had histories of seizure disorders; two had asymmetric hippocampal sclerosis and four showed mild to moderate hilar astrogliosis without significant neuronal loss. Four patients with histories of chronic dementia had pathological findings diagnostic of Alzheimer's disease.¹⁰ Four patients had significant hypoxic/ischemic events that occurred 4 days to 2 weeks before death: three showed neuronal loss in hippocampal CA1 with gliosis and one had a subacute infarct in CA1. Two patients were terminally unresponsive after shock and showed acute neuronal injury without gliosis. Postmortem intervals for all cases ranged from 2 to 24 hours (median, 12 hours). Neurosurgical specimens were used as controls to assess the effects of postmortem fixation delay on annexin immunohistochemistry. These consisted of gray and white matter from cerebral neocortex and hippocampus and represented a variety of diseases, including inflammatory processes, infarcts, seizure disorders, and Alzheimer's disease.

Tissue Processing and Immunohistochemistry

In most cases the entire brain was fixed by immersion in 10 to 20% phosphate-buffered formalin at room temperature for 2 weeks before dissection and routine embedding in paraffin. In three cases, the brains were freshly dissected and hippocampal slices were fixed

for 3 to 4 days at 4 C in phosphate-buffered 10% formalin before paraffin embedding. The control neurosurgical specimens were fixed and processed under a variety of conditions, ranging from rapid immersion and fixation of fresh tissue in 10% buffered zinc formalin for 48 hours at 4 C to routine fixation for 8 to 24 hours at room temperature. Fixed tissue was embedded in either regular temperature or low melting point paraffin (42 C). Variations in tissue processing did not affect the cellular and cytoarchitectural localizations of specific annexin immunoreactivities related to either normal or disease states. The overall intensity of immunostaining was somewhat less robust in deeper regions of the postmortem brains fixed by whole immersion compared with fresh tissue sections that were more rapidly fixed.

Immunohistochemistry was performed for annexins I, II (p11 and p36), IV, and VI and for glial fibrillary acidic protein (GFAP) in all cases; for S100 β and β A4-amyloid in Alzheimer's disease cases; and for synaptophysin, HAM 56, and factor VIII in selected other cases. Primary antibodies were obtained from the following sources and used at the indicated concentrations in phosphate-buffered saline (PBS): 1) monoclonal mouse IgG antibodies directed to annexin I, annexin II (p36 monomer), annexin II (p11 subunit), annexin IV, and annexin VI (each at 1:500; Zymed Laboratories, Inc., South San Francisco, CA); 2) rabbit polyclonal antibodies directed to GFAP (1:1400; Dako Corp., Carpinteria, CA); 3) monoclonal mouse IgG directed to synaptophysin (SY38, 1:10; Boehringer Mannheim Corp., Indianapolis, IN); 4) rabbit polyclonal antibodies directed to β 4-amyloid (1:10; Boehringer Mannheim Corp.); 5) rabbit polyclonal antibodies directed to S100 β (1:2000; Chemicon International, Inc., Temecula, CA); 6) monoclonal mouse IgG antibodies directed to human macrophage antigen (HAM 56, 1:100; Dako Corp.); and 7) monoclonal mouse IgG antibodies directed to factor VIII (1:10; Dako Corp.). The specificities of the antiannexin antibodies were confirmed by Western blotting of normal and neoplastic human brain tissues and of cultured U251 human glioma cells.

Paraffin sections, 5 μ thick, were prepared for immunohistochemistry by deparaffinization in xylene, preincubation for 30 minutes at 22 C with methanolic H₂O₂ (1.75%), and hydration in graded alcohols. For annexin II (p11 subunit or p36) immunohistochemistry sections were then treated either with pepsin (Sigma Chemical Co., St. Louis, MO) 4 mg/ml in 0.01 N HCl for 15 to 30 minutes at 37 C or by microwaving at 750 W in 10 mmol/L sodium citrate buffer (pH 6) for three to four consecutive 5-minute intervals, replacing evaporated buffer volume with H₂O after each inter-

val. The patterns of p11 immunoreactivity produced after each of these treatments were identical. For p36, microwave pretreatment allowed detection of immunoreactivity but pepsin pretreatment did not. For detection of β A4 epitopes, sections were incubated with 88% formic acid for 5 minutes at 22 C. All sections were then rinsed in PBS, blocked with 1.5% nonimmune serum in PBS (horse serum for monoclonal antibodies or goat serum for polyclonal antibodies), and incubated with the primary antibodies for 18 to 24 hours at 4 C. Primary antibody was labeled by the avidin-biotin complex method¹¹ using the Vectastain Elite kit (Vector Laboratories Inc., Burlingame, CA) and visualized with peroxidase-coupled anti-mouse or anti-rabbit antibodies using diaminobenzidine (DAB) as the chromogen. The sections were counterstained with hematoxylin.

Dual-label immunohistochemistry for p11 and GFAP was performed by first visualizing p11 with microwave pretreatment as described above using aminoethylcarbazole (AEC) as chromogen. The sections were then incubated with pepsin (4 mg/ml in 0.01 N HCl, 15 minutes at 37 C), rinsed in PBS, and blocked with nonimmune goat serum. GFAP was then visualized as described above, using DAB-Ni complex as chromogen. Dual labeling for β A4 and p11 was performed by first visualizing β A4 with formic acid pretreatment as described above using AEC as chromogen; p11 was then visualized with pepsin or microwave pretreatment as described above using DAB-Ni complex as chromogen.

Annexin Nomenclature

Studies cited herein have used a variety of designations for the annexin proteins. The system used here is that of Crumpton and Dedman:¹² p37, annexin I; p36, annexin II monomer; p32, annexin IV; p67/68, annexin VI.

Results

Normal Hippocampus

The cellular localizations of annexins I, II (p36 and p11), IV, and VI are summarized in Table 1.

Annexin I

Moderate to strong immunoreactivity for annexin I was present in neurons, subependymal and subpial astrocytes, choroid plexus epithelium, ependyma, and vascular smooth muscle (Figure 1A). In neurons,

Table 1. Cellular Localization of Annexins in Human Hippocampus and Associated Structures

	Annexin			
	I	II	IV	VI
Neurons	++	-	-	+++
Subependymal/subpial astrocytes	++	+++	++	-
Parenchymal astrocytes	-	-	+	-
Oligodendrocytes	-	-	++	-
Ependyma	+++	+++	+++	+
Choroid plexus	+++	+	+++	+++
Meningothelium	+++	+++	+++	++
Endothelium	+	+++	+++	+
Smooth muscle	++	-	++	++

annexin I was primarily confined to the soma in a diffuse to granular cytoplasmic pattern (Figure 3F), sometimes with a perinuclear distribution. The intensity of the annexin I immunoreactivity of the hippocampal neurons ranged from most intense in bipolar neurons of the stratum oriens, to moderate in the pyramidal neurons of the cornu ammonis, and to only mild in the granular cells of the dentate gyrus. Immunoreactivity in other cell types generally showed a diffuse cytoplasmic pattern. Subependymal and subpial astrocytes exhibited moderate immunoreactivity in cell bodies and larger processes. In contrast, annexin I was not detected in nonreactive parenchymal astrocytes and oligodendroglia. The neuropil showed a faint to mild diffuse staining, somewhat less in white matter compared with gray matter. Immunoreactivity in vascular endothelium was mild and variable.

Annexin II (p36 and p11)

Immunoreactivities for annexin II (p36 and p11) showed similar cellular and cytoarchitectural distributions (Figure 1B). In ependymocytes and subependymal and subpial astrocytes, immunoreactivity was usually most intense at the cell periphery but was sometimes cytoplasmic. Immunostaining in deep white matter was variable and when present was associated with perivascular astroglia. Annexin II p36 and p11 were absent in neurons, nonreactive parenchymal astrocytes, oligodendrocytes, and neuropil. In other cell types, p11 and p36 immunoreactivities were strong in arachnoid meningotheilium and vascular endothelium, whereas staining of the choroid plexus epithelium and vascular smooth muscle was variable and mild.

Annexin IV

Moderate to strong cytoplasmic immunoreactivity for annexin IV was present in subependymal and subpial

Figure 1. (A) ...
bulla
norea
A' in
assoc.
prim.
temp

astr
eper
smo
sub
fuse
larg
nexi
cyto
tion,
cell
app
per
per
mer
tect
Ar
eper
end
was
type

Anr.

Mod
pre

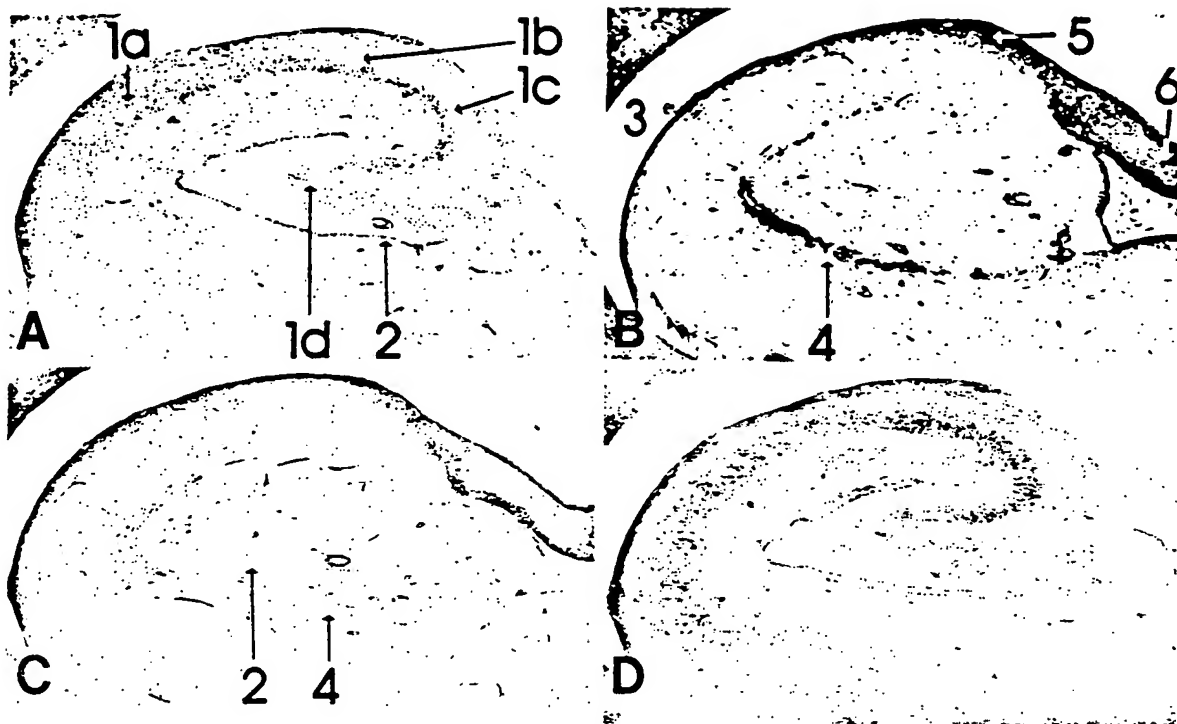


Figure 1. Annexin immunohistochemistry of normal hippocampus. Adjacent tissue sections were processed for annexin I (A), p11 (B), annexin IV (C), and annexin VI (D) using biotin-avidin immunohistochemistry with hematoxylin counterstain. A: Annexin I was present in neuronal cell bodies in the dentate gyrus and Ammon's horn, glia in hippocampal fissure, fimbria, and alveus, and ependyma and vessels. B: Dense p11 immunoreactivity was associated with glia in fimbria, alveus, and hippocampal fissure, and with vessels and ependyma. C: The distribution of annexin IV immunoreactivity resembled that of p11 but the staining was less dense and more diffuse. Immunoreactivity in dentate granule cell layer was associated with glia. D: Annexin VI was prominent in pyramidal and granule cell layers and dendritic fields. Staining in fimbria and alveus was primarily axonal. Original magnification, $\times 175$. 1, Ammon's horn; 2, CA1; 3, CA2; 4, CA3; 5, CA4; 6, CA5. 2, granule cell layer of dentate gyrus; 3, temporal horn of lateral ventricle; 4, hippocampal fissure; 5, alveus; 6, fimbria.

astrocytes, oligodendroglia, choroid plexus, ependyma, arachnoid meningotheilium, vascular smooth muscle, and endothelium (Figure 1C). The subependymal and subpial astrocytes contained diffuse or granular staining patterns in cytoplasm and larger processes. In choroid plexus epithelium, annexin IV was distributed in a relatively coarse granular cytoplasmic pattern, often with subapical accumulation, and in ependymocytes was usually localized to cell borders. Annexin IV in oligodendroglia was most apparent in populations exhibiting perineuronal and perivascular satellitosis where it was present as a thin perinuclear cytoplasmic rim or outlining the plasma membrane (Figure 3H). Annexin IV was never detected in neurons.

Annexin IV was also detected in the nuclei of some ependymocytes, astrocytes, oligodendrocytes, and endothelial cells. The presence of nuclear staining was not correlated with cytoplasmic staining or the type of lesion, clinical history, or patient age.

Annexin VI

Moderate to strong annexin VI immunoreactivity was present in neurons, choroid plexus epithelium, arach-

noid meningotheilium, and vascular smooth muscle (Figure 1D). In pyramidal neurons, annexin VI was primarily localized to the plasma membranes of dendritic processes and perikarya and in neuropil in a granular or punctate pattern similar to that of synaptophysin (Figure 3, A and B). Bipolar neurons in the stratum oriens displayed dense cytoplasmic staining of soma and proximal processes, whereas the immunoreactivity in granule cells was less prominent. The only immunoreactivity in the white matter was confined to axonal fibers. Annexin VI in the choroid plexus epithelium was concentrated in the apical and basal regions, whereas ependyma displayed negligible immunoreactivity. Annexin VI was not detected in non-reactive astrocytes, oligodendroglia, and endothelial cells.

Pathological States

All the types of acute central nervous system damage and chronic degeneration were associated with alterations of the cytoarchitectural distribution of annexin VI in affected neurons and increased expression of annexins I, II, and IV in reactive astrocytes.

However, the intraneuronal distribution of annexin VI and the relative degree of expression for the annexins showed some differences in the various pathological processes.

Neuronal Annexins

In subacute hypoxic ischemic injury, seizure damage, and Alzheimer's disease, the surviving CA2 pyramidal neurons displayed increased annexin VI immunoreactivity within the somal cytoplasm (Figure 3E). The differences in staining intensities of the CA2 neurons compared with those in other areas was often quite marked. Similar but more variable changes were present in the CA3 and CA4 neurons. In Alzheimer's disease, the granulovacuolar bodies within degenerating pyramidal neurons were strongly immunoreactive for annexin VI. The vacuolar membranes of these bodies were consistently labeled, whereas the granular bodies were more variably stained (Figure 3E). In contrast, annexin VI was never detected in neurofibrillary tangles or neuritic plaques.

Each case of acute hypoxic ischemic injury displayed a unique pattern of annexin VI immunoreactivity within neurons. The first was a concentration of immunoreactivity within proximal dendritic segments in CA2-4 (Figure 3C) or within the somal cytoplasm in CA1-2 (Figure 3D). The other was a markedly heterogeneous distribution of immunoreactivity within pyramidal neurons, including focal staining of plasma membrane and vesicular structures within the cytoplasm.

In contrast to annexin VI, annexin I immunoreactivity in neurons showed no consistent pattern of alteration in the various disease states. In Alzheimer's disease, staining within neurons was excluded from intracellular neurofibrillary tangles and granulovacuolar bodies in degenerating neurons.

Glial Annexins

Reactive astrocytes were identified by prominent cytoplasm and processes with strong GFAP immunoreactivity. Astrocytes in the endfolium region adjacent to the granular cell layer appeared to be the most sensitive to developing reactive changes in response to hypoxic ischemic injury and seizures. In more severe cases reactive astrocytes were more widely distributed, particularly in areas of neuronal loss or infarction. In Alzheimer's disease, reactive astrocytes were diffusely distributed, often in association with senile plaques and degenerating neurons.

Reactive astrocyte populations displayed variable expression of annexins I, II, and IV. In general, annexin immunoreactivity was most prominent within cells and the surrounding neuropil in regions of more severe gliosis, eg, adjacent to an infarct (Figure 2A). The intracellular pattern of annexin I immunoreactivity was always diffuse (Figure 3F). Annexin IV was diffusely distributed within gemistocytic astrocytes (Figure 3, H) or in punctate, granular, or vesicular patterns within fibrillary astrocytes. In contrast, annexin II p11 and p36 were usually most strongly localized at the cell periphery. In Alzheimer's disease, astrocytic p11/p36 was also localized to discrete plaque-like areas (Figure 2B). Dual-label immunohistochemistry showed that p11 immunoreactive astrocytes, when present, were only in close proximity to diffuse and mature β -amyloid plaques and were not associated with either dystrophic neurites or extracellular neurofibrillary tangles. However, many β -amyloid plaques were not associated with p11/p36 immunoreactivity. In contrast to the focal pattern of p11/p36 expression, GFAP and S100 β immunoreactive astrocytes were more widely distributed (Figure 3G). Annexin I or IV immunoreactive astrocytes did not show a plaque-like pattern and were distributed without any specific relationship to neuritic plaques, neurofibrillary tangles, or degenerating neurons.

Only annexin IV could be consistently identified in activated microglia with ramified, rod, and amoeboid morphologies. These cell populations were also immunoreactive for the HAM-56 macrophage antigen but not GFAP or factor VIII. Annexin IV immunoreactivity was distributed in granular or vesicular patterns within the cytoplasm and processes.

Discussion

Previous studies have described the isolation and biochemical characterization of the major species of annexins in mammalian brain, which include annexins I, II, IV, and VI.^{4,13} Little is known, however, about the specific cellular distribution or physiological roles of this family of proteins in the human nervous system. This study examined the comparative cellular localization of the major annexins in the human hippocampus, which contains physiologically distinct neuronal cell types and undergoes well-characterized pathological changes in response to injury and degenerative processes. Annexin VI was selectively distributed in neurons and annexins II and IV in glia, whereas annexin I was present in both neurons and astroglia. These data concur with previous findings in non-

Fig-
ure
x 15
orig:

hur
plic
spe
cor

sub
has
dog
of a
am
ast
res
Lik
rea
The
cor
of E
prc
lan
twr

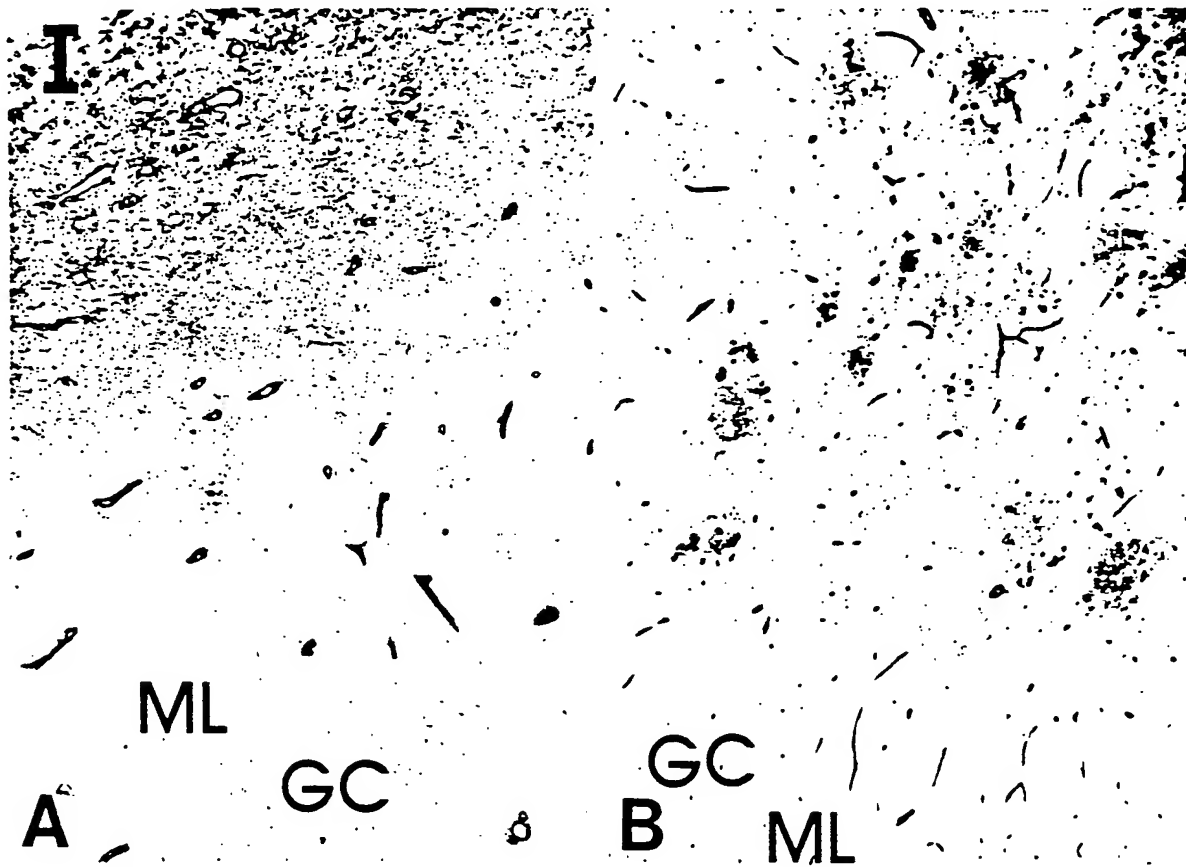


Figure 2. Pathological patterns of p11 immunoreactivity. **A:** Subacute infarct in CA1. The region adjacent to the infarct was densely stained. Annexins I, II (p36), and IV showed similar patterns. (Biotin-avidin immunoperoxidase with hematoxylin counterstain, original magnification $\times 150$.) **B:** Alzheimer's disease. Staining was associated with plaques in CA4. (Biotin-avidin immunoperoxidase with hematoxylin counterstain, original magnification $\times 60$.) I, infarct; GC, granule cell layer of dentate gyrus; ML, molecular layer of dentate gyrus.

human mammalian brain.^{3-5,13} Our findings also implicate the annexins in neuronal and astroglial responses to acute and chronic neurodegenerative conditions.

Annexin I has been shown to be a major cellular substrate for the EGF receptor tyrosine kinase¹⁴ and has also received much attention as a putative endogenous anti-inflammatory agent.¹⁵ The localization of annexin I immunoreactivity in neurons of the cornu ammonis and dentate gyrus and in subependymal astrocytes, ependymocytes, and choroid plexus corresponds to the localization of the EGF receptor.¹⁶ Like annexin I, the EGF receptor is also expressed in reactive astrocytes but not in quiescent astrocytes.¹⁷ The parallel distributions of these proteins are thus consistent with a role for annexin I in mediating effects of EGF on neurons and glia. Annexin I has also been proposed to play a role in regulating glial prostaglandin production, based on the relationships between annexin I expression, phospholipase A₂ activ-

ity, and eicosanoid release in cultured astrocytes.¹⁸ Annexin I in rat hippocampus has a neuronal and glial distribution like that described here⁵ and is present in synaptic plasma membrane fractions as a covalent dimer,¹⁹ presumably due to cross-linking by transglutaminase.²⁰ In human brain, Johnson et al⁶ detected annexin I immunoreactivity in ependyma, subependymal astrocytes, choroid plexus, and reactive astrocytes associated with brain injury, but unlike this study, not in neurons. The most obvious explanation for this variance would be differences in the epitopes recognized by the antibodies used in these studies; it is possible that posttranslational modifications of annexin I in neurons, such as cross-linking, could mask immunoreactive epitopes.

Annexin VI immunoreactivity was associated with neuronal cell membranes and processes in a pattern suggestive of terminal and perisynaptic locations and was the only annexin that was not detected in

1144-1149



reactive o
 secretory
 ing conce
 One poter
 and chorc
 membran
 involved
 granules
 totic recy
 VI is requ
 dicytotic
 chain do
 binding
 and IV, I
 suggesti
 teins.⁴ A
 the activ
 sarcopla
 been id
 that an
 naling n
 Expre
 cells wa
 lations e
 tectural
 were qu
 p36 we
 branes
 wherea
 active i
 godenc
 someti
 These
 likely r
 as pro
 toplas
 IV in r
 blasts.
 gester
 ponon
 proteir
 with c
 Two
 teristic
 nexin
 pyran
 p36

Figure
 memb
 bodies
 per left
 reacti
 plaqu
 oligod.
 x52

reactive or quiescent macroglia. The choroid plexus secretory epithelium showed strong annexin VI staining concentrated in the subplasmalemmal region. One potential role for annexin VI in synaptic terminals and choroid plexus is regulation of clathrin-mediated membrane trafficking. Clathrin-coated vesicles are involved in the biogenesis of dense-core secretory granules and synaptic vesicles, and in the endocytotic recycling of vesicles after exocytosis.²¹ Annexin VI is required for the budding of clathrin-coated endocytotic pits *in vitro*.²² Although the clathrin heavy chain does not exhibit Ca^{2+} -dependent membrane binding properties, it co-purifies with annexins VI and IV prepared from brain using this technique, suggesting an association with the annexin proteins.⁴ Annexin VI has also been shown to modulate the activity of a ryanodine-sensitive Ca^{2+} channel in sarcoplasmic reticulum.²³ Ryanodine receptors have been identified in neurons,²⁴ raising the possibility that annexin VI might modulate neuronal Ca^{2+} signaling mechanisms.

Expression of annexins II (p11/p36) and IV in neural cells was limited to glia. However, the glial cell populations expressing these annexins and the cytoarchitectural distribution of immunoreactivity within cells were quite different. Immunoreactivities for p11 and p36 were associated primarily with plasma membranes and processes of reactive astrocytes, whereas annexin IV staining was cytoplasmic in reactive astrocytes and was also present in some oligodendrocyte populations, activated microglia, and sometimes in the nuclei of glial (and endothelial) cells. These different patterns of annexin localization most likely reflect roles in different cellular activities, such as proliferation,²⁵ migration,²⁶ and extension of cytoplasmic processes.^{25,27} The localization of annexin IV in nuclei has been previously reported in fibroblasts.²⁸ Intracellular functions of annexins are suggested by the discoveries that annexin II is a component of the DNA polymerase α -primer recognition protein complex,²⁹ and of a novel annexin associated with calyculin.³⁰

Two patterns of annexin localization were characteristic of Alzheimer's disease: the association of annexin VI with granulovacuolar bodies in degenerating pyramidal neurons and expression of annexin II (p11/p36) by astrocytes closely associated with some

β -amyloid plaques. Granulovacuolar bodies contain immunoreactivities for cytoskeletal epitopes similar to those found in neurofibrillary tangles and neuritic plaques, and thus seem to be related to neurofibrillary degeneration.³¹ The presence of strong annexin VI immunoreactivity associated with the membranes of granulovacuolar bodies (but not with neurofibrillary tangles or neuritic plaques) suggests that annexin VI could be important in their formation, perhaps involving an aberrant vesicular trafficking pathway. The occasional association of p11/p36 immunoreactive astrocytes with extracellular β -amyloid deposits in Alzheimer's hippocampus suggests that some amyloid plaques may contain a component that stimulates annexin II expression. Plaques are heterogeneous in composition, containing variable amounts of amyloid precursor derivatives, neuritic components, microglia, and secondary substances such as immunoglobulins and complement factors.³² It seems likely that plaque components other than amyloid and neurites are related to annexin II expression in plaque-associated astrocytes, because p11/p36 immunoreactivity was inconstantly present in mature or immature plaques and was not seen in reactive astrocytes associated with extracellular neurofibrillary tangles, which, like neuritic plaques, contain paired helical filaments.

The increased expression of annexins in pathological states may represent a neural tissue response that serves to limit damage. Membrane degradation by phospholipases represents one mechanism underlying neuronal injury after hypoxia ischemia, excitotoxic exposure, seizures, and in chronic neurodegenerative diseases.³³ Annexins, which inhibit phospholipase activity *in vitro*, could thus act as endogenous neuroprotective agents. In subacute and chronic states (posthypoxic, seizures, and Alzheimer's disease) annexin VI immunoreactivity was consistently increased within the cytoplasm of pyramidal neuronal soma in CA2. Neurons in this region are more resistant to injury than those in other regions of the hippocampus, raising the possibility that an increase in annexin VI expression could represent a response promoting neuronal survival or recovery from injury. An alternative explanation is that annexin VI may accumulate in neuronal soma because of disruption of normal axonal-dendritic transport mechanisms, because an-

Figure 3. Cellular localization of annexins. **A–E:** Annexin VI immunoreactivity in normal CA2 (**A**) and CA1 (**B**) was associated with neuronal membranes and neuropil. In acute hypoxic ischemic injury, annexin VI was concentrated within dendritic segments in CA2 (**C**) and neuronal cell bodies in CA1 (**D**). In Alzheimer's disease (**E**), annexin VI was selectively increased within CA2 neurons (lower right) but not in CA1 neurons (upper left) and was also associated with granulovacuolar bodies (inset). **F:** Annexin I immunoreactivity was present in both pyramidal neurons and reactive astrocytes (inset). **G:** Dual-labeling for p11 (AEC, red) and GFAP (DAB-Ni, black) demonstrated p11 immunoreactivity in an Alzheimer's plaque-associated astrocyte (arrowhead) and capillaries, whereas other astrocytes stained only for GFAP (arrows). **H:** Annexin IV was present in oligodendrocytes and reactive astrocytes (inset). Biotin-avidin immunoperoxidase with hematoxylin counterstain, magnifications: **A–D**, $\times 338$; **E**, $\times 52$; inset, $\times 676$; **F**, $\times 180$; inset, $\times 541$; **G**, $\times 226$; **H**, $\times 541$; inset, $\times 609$.

nexin VI has been identified in the slow component of axonal transport in rat peripheral nerve.³⁴

The presence of annexin I immunoreactivity in neurons is also compatible with the hypothesis that neuronal annexins could confer resistance to Ca^{2+} -induced neuronal injury. Although annexin I did not show patterns of expression in neuronal populations which clearly corresponded with their relative degrees of resistance or susceptibility to injury, recent studies have directly demonstrated neuroprotective properties of endogenous annexin I. Surprisingly, the active protein appears to reside in the extracellular space, because intraventricular administration of annexin I in live rats decreased the sizes of cerebral lesions induced by ischemia⁹ or glutamate receptor agonist,³⁵ whereas injection of neutralizing antibody had the opposite effect. Potential sources of endogenous extracellular annexin I could include local release by neurons and reactive astrocytes or secretion into the cerebrospinal fluid by choroid plexus, because annexin I has been shown to be selectively secreted by other cell types.^{36,37} Annexin I could also be released from damaged tissue or inflammatory cells. Although this study confirms previous observations that annexin I is increased in injured brain tissue,^{8,9} we found that annexins II and IV were also increased. The role(s) of these annexins in neuroprotection has yet to be studied.

Annexins in the cerebral vascular endothelium are probably not related to special physiological functions, such as the blood-brain barrier, because relatively high levels of annexins I, II, IV, and VI are present in cultured human umbilical vein endothelial cells.³⁸ It is quite possible that we did not detect significant annexin VI immunoreactivity in the endothelium because of the relatively strong reaction in adjacent vascular smooth muscle and neuropil. Our data regarding annexin expression in cerebrovascular smooth muscle agree with a previous report that smooth muscle cells express annexin VI but not annexin II.³⁹

Annexins are widely distributed throughout the body and therefore could be involved in pathophysiological processes in nonneural tissues and brain. Annexin I expression is increased in rat renal tubules during recovery from ischemia,⁴⁰ supporting a hypothesis that annexins may participate in general cellular and tissue mechanisms for limiting injury and promoting repair. Further studies of multiple annexins, as described here in the human hippocampus, may define patterns of expression that are unique or common to various types of cells and pathological states, suggesting links between specific annexins and cellular functions.

Acknowledgments

We thank Dr. C. Creutz for helpful discussions.

References

1. Klee CB: Ca^{2+} -dependent phospholipid- (and membrane-) binding proteins. *Biochemistry* 1988, 27:6645-6653
2. Burgoyne RD, Geisow MJ: The annexin family of calcium-binding proteins. *Cell Calcium* 1989, 10:1-10
3. Burgoyne RD, Cambray-Deakin MA, Norman K-M: Developmental regulation of tyrosine kinase substrate p36 (calpactin heavy chain) in rat cerebellum. *J Mol Neurosci* 1989, 1:47-54
4. Woolgar JA, Boustead CM, Walker JH: Characterization of annexins in mammalian brain. *J Neurochem* 1990, 54:62-71
5. Strijbos PJLM, Tilders FJH, Carey F, Forder R, Rothwell NJ: Localization of immunoreactive lipocortin-1 in the brain and pituitary gland of the rat: effects of adrenalectomy, dexamethasone, and colchicine treatment. *Brain Res* 1991, 553:249-260
6. Spreca A, Rambotti MG, Giambanco I, Pula G, Bianchi R, Ceccarelli P, Donato R: Immunocytochemical localization of annexin V (CaBP33), a Ca^{2+} -dependent phospholipid- and membrane-binding protein, in the rat nervous system and skeletal muscles and in the porcine heart. *J Cell Physiol* 1992, 152:587-598
7. Reeves SA, Chavez-Kappel C, Davis R, Rosenblum M, Israel MA: Developmental regulation of annexin II (lipocortin-2) in human brain and expression in high grade glioma. *Cancer Res* 1992, 52:6871-6876
8. Johnson MD, Kamso-Pratt JM, Whetsell WO, Pepinsky RB: Lipocortin-1 immunoreactivity in the normal human central nervous system and lesions with astrocytosis. *Am J Clin Pathol* 1989, 92:424-429
9. Relton JK, Strijbos PJ, O'Shaughnessy CT, Carey F, Forder RA, Tilders FJ, Rothwell NJ: Lipocortin-1 is an endogenous inhibitor of ischemic damage in the rat brain. *J Exp Med* 1991, 174:305-310
10. Khachaturian ZS: Diagnosis of Alzheimer's disease. *Arch Neurol* 1995, 42:1097-1104
11. Hsu S, Raine L, Fanger H: Use of avidin-biotin-peroxidase complex (ABC) in immunoperoxidase techniques: a comparison between ABC and unlabeled antibody (PAP) procedures. *J Histochem Cytochem* 1981, 29:577-580
12. Crumpton MJ, Dedman JR: Protein terminology tangle. *Nature* 1990, 345:212
13. Regnoul F, Rendon A, Pradel RA: Biochemical characterization of annexins I and II isolated from pig nervous tissue. *J Neurochem* 1991, 56:1985-1996
14. Fava RA, Cohen S: Isolation of a calcium-dependent 35-kilodalton substrate for the epidermal growth factor receptor/kinase from A431 cells. *J Biol Chem* 1984, 259:2636-2645

15. Fic
the
16. We
ca
rec
toc
17. Bir
LB
in :
ea:
18. Ge
P,
inc
cy:
19. Pr:
mc
19
20. An
inc
su-
mc
11
21. Ja
rin
65
22. Lir
qu
19
23. Di:
De
tiv.
kD
24. So
ma
14
25. Sc
a :
11
26. Br.
ca-
ma
Ce
27. Fo
an
the
Cc
28. We
tor
ex:
teir

15. Flow RJJ: Lipocortin and the mechanisms of action of the glucocorticoids. *Br J Pharmacol* 1988, 94:987-1015
16. Werner MH, Nanney LB, Stoscheck CM, King LE: Localization of immunoreactive epidermal growth factor receptors in human nervous system. *J Histochem Cytochem* 1988, 36:81-86
17. Birecree E, Whetsell WO, Stoscheck C, King LE, Nanney LB: Immunoreactive epidermal growth factor receptors in neuritic plaques from patients with Alzheimer's disease. *J Neuropathol Exp Neurol* 1988, 47:549-560
18. Gebicke-Haerter PJ, Schober A, Dieter P, Honegger P, Hertting G: Regulation and glucocorticoid-independent induction of lipocortin I in cultured astrocytes. *J Neurochem* 1991, 57:175-183
19. Pradel LA, Rendon A: Annexin I is present in different molecular forms in rat cerebral cortex. *FEBS Lett* 1993, 327:41-44
20. Ando Y, Imamura S, Owada MK, Kannagi R: Calcium-induced intracellular cross-linking of lipocortin I by tissue transglutaminase in A431 cells: augmentation by membrane phospholipids. *J Biol Chem* 1991, 266:1101-1108
21. Jackson AP: Endocytosis in the brain: the role of clathrin light-chains. *Biochem Soc Transact* 1992, 20:653-655
22. Lin HC, Sudhof TC, Anderson RGW: Annexin I is required for the budding of clathrin-coated pits. *Cell* 1992, 70:283-291
23. Diaz-Munoz M, Hamilton S, Kaetzel MA, Hazarika P, Dedman JR: Modulation of Ca^{2+} release channel activity from sarcoplasmic reticulum by annexin VI (67-kDa calcimedlin). *J Biol Chem* 1990, 265:15894-15899
24. Sorrentino V, Volpe P: Ryanodine receptors: how many, where, and why? *Trends Pharmacol Sci* 1993, 14:98-103
25. Schlaepfer DD, Haigler HT: Expression of annexins as a function of cellular growth state. *J Cell Biol* 1990, 111:229-238
26. Braslau DL, Ringo DL, Rocha V: Synthesis of novel calcium-dependent proteins associated with mammary epithelial cell migration and differentiation. *Exp Cell Res* 1984, 155:213-21
27. Fox MT, Prentice DA, Hughes JP: Increases in p11 and annexin II proteins correlate with differentiation in the PC12 pheochromocytoma. *Biochem Biophys Res Commun* 1991, 177:1188-1193
28. Walker JH, Boustead CM, Brown R, Koster JJ, Middleton CA: Tissue and subcellular distribution of endonexin, a calcium-dependent phospholipid-binding protein. *Biochem Soc Trans* 1990, 18:1235-1236
29. Jindal HK, Chaney WG, Anderson CW, Davis RG, Vishwanatha JK: The protein-tyrosine kinase substrate, calpactin I heavy chain (p36), is part of the primer recognition protein complex that interacts with DNA polymerase α . *J Biol Chem* 1991, 266:5169-5176
30. Mizutani A, Usuda N, Tokumitsu H, Minami H, Yasui K, Kobayashi R, Hidaka H: CAP-50, a newly identified annexin, localizes in the nuclei of cultured fibroblast 3Y1 cells. *J Biol Chem* 1992, 267:13498-13504
31. Bondareff W, Wischik CM, Novak M, Roth M: Sequestration of tau by granulovacuolar degeneration in Alzheimer's disease. *Am J Pathol* 1991, 139:641-648
32. Alafuzoff I, Adolfsson R, Grundke-Iqbal I, Winblad B: Blood-brain barrier in Alzheimer dementia and in nondemented elderly: an immunocytochemical study. *Acta Neuropathol* 1987, 73:160-166
33. Choi DW: Glutamate neurotoxicity and diseases of the nervous system. *Neuron* 1988, 1:623-634
34. Sekimoto S, Tashiro T, Komiya Y: Two 68-kDa proteins in slow axonal transport belong to the 70-kDa heat shock protein family and the annexin family. *J Neurochem* 1991, 56:1774-1782
35. Black MD, Carey F, Crossman AR, Relton JK, Rothwell NJ: Lipocortin-1 inhibits NMDA receptor-mediated neuronal damage in the striatum of the rat. *Brain Res* 1992, 585:135-140
36. Solito E, Rauger G, Melli M, Parenti L: Dexamethasone induces the expression of the mRNA of lipocortin 1 and 2 and the release of lipocortin 1 and 5 in differentiated, but not undifferentiated U-937 Cells. *FEBS Lett* 1991, 291:236-244
37. Christmas F, Callaway J, Fallon J, Jones J, Haigler HT: Selective secretion of annexin I, a protein without a signal sequence, by the human prostate gland. *J Biol Chem* 1991, 266:2499-507
38. Romisch J, Schuler E, Bastian B, Burger T, Dunkel FG, Schwinn A, Hartmann AA, Paques EP: Annexins I to VI: quantitative determination in different human cell types and in plasma after myocardial infarction. *Blood Coagul Fibrinol* 1992, 3:11-17
39. Iida H, Hatae T, Shibata Y: Immunocytochemical localization of 67 kD Ca^{2+} binding protein (p67) in ventricular, skeletal, and smooth muscle cells. *J Histochem Cytochem* 1992, 40:1899-1907
40. McKanna JA, Chuncharunee A, Munger KA, Breyer JA, Cohen S, Harris RC: Localization of p35 (annexin I, lipocortin 1) in normal adult rat kidney and during recovery from ischemia. *J Cell Physiol* 1992, 153:467-476

Annexins: From Structure to Function

VOLKER GERKE AND STEPHEN E. MOSS

Institute for Medical Biochemistry, Center for Molecular Biology of Inflammation, University of Münster, Münster, Germany; and Department of Cell Biology, Institute of Ophthalmology, University College London, London, United Kingdom

I. Introduction: Overview of the Annexin Family	331
II. Biochemical Properties of Annexins and Their Three-Dimensional Structure	332
A. Molecular structures	332
B. Annexins as membrane binding proteins: canonical and atypical properties	336
C. Nonlipid annexin ligands	338
D. Modulation of annexin properties by posttranslational modifications	342
III. Molecular Evolution of the Annexin Family and Regulation of Annexin Gene Expression	343
A. Molecular phylogeny of annexins	343
B. Gene structures	344
C. Regulation of gene expression	345
IV. Functional Diversity Within the Annexin Family	347
A. Annexins in membrane traffic and organization	347
B. Annexins and ion channels	353
C. Extracellular annexin activities	356
D. Annexin transgenesis and targeted gene disruption	358
V. Annexins and Human Disease	359
A. Disorders of the heart and circulation	359
B. Annexins and physiological stress	361
C. Annexins and cancer	361
VI. Conclusion	362

Gerke, Volker, and Stephen E. Moss. Annexins: From Structure to Function. *Physiol Rev* 82: 331–371, 2002; 10.1152/physrev.00030.2001.—Annexins are Ca^{2+} and phospholipid binding proteins forming an evolutionary conserved multigene family with members of the family being expressed throughout animal and plant kingdoms. Structurally, annexins are characterized by a highly α -helical and tightly packed protein core domain considered to represent a Ca^{2+} -regulated membrane binding module. Many of the annexin cores have been crystallized, and their molecular structures reveal interesting features that include the architecture of the annexin-type Ca^{2+} binding sites and a central hydrophilic pore proposed to function as a Ca^{2+} channel. In addition to the conserved core, all annexins contain a second principal domain. This domain, which NH_2 -terminally precedes the core, is unique for a given member of the family and most likely specifies individual annexin properties in vivo. Cellular and animal knock-out models as well as dominant-negative mutants have recently been established for a number of annexins, and the effects of such manipulations are strikingly different for different members of the family. At least for some annexins, it appears that they participate in the regulation of membrane organization and membrane traffic and the regulation of ion (Ca^{2+}) currents across membranes or Ca^{2+} concentrations within cells. Although annexins lack signal sequences for secretion, some members of the family have also been identified extracellularly where they can act as receptors for serum proteases on the endothelium as well as inhibitors of neutrophil migration and blood coagulation. Finally, deregulations in annexin expression and activity have been correlated with human diseases, e.g., in acute promyelocytic leukemia and the antiphospholipid antibody syndrome, and the term *annexinopathies* has been coined.

I. INTRODUCTION: OVERVIEW OF THE ANNEXIN FAMILY

Nature has achieved the means to tightly control intracellular Ca^{2+} concentrations, thereby enabling the

ion to serve second messenger functions in a variety of processes which couple extracellular signals to cellular responses. Systems regulating intracellular Ca^{2+} levels thus are considered part of the intricate Ca^{2+} signaling network. They include gated Ca^{2+} channels and energy-

dependent pumps, which are located in organelle membranes and the plasma membrane, as well as intracellular Ca^{2+} binding proteins serving as regulated Ca^{2+} buffers. Other classes of Ca^{2+} binding proteins participate more directly in Ca^{2+} signaling as they display altered properties in response to Ca^{2+} binding. Annexins can be considered a subgroup of the latter, although their precise position within Ca^{2+} signaling chains remains elusive. Moreover, a growing body of evidence suggests that annexins can also function in their Ca^{2+} -free conformation in a hitherto unknown fashion, thereby increasing the functional diversity among these proteins.

The name annexin is derived from the Greek *annex* meaning "bring/hold together" and was chosen to describe the principal property of all or at least nearly all annexins, i.e., the binding to and possibly holding together of certain biological structures, in particular membranes. The name also has a somewhat historical flavor as it takes into account the point that a number of the groups who independently of one another discovered annexins were in search for such scaffolding or bridging proteins. However, initially, i.e., at the date of their discoveries in the late 1970s and early 1980s, annexins received diverse and unrelated names referring to their biochemical properties. These included synexin (for granule aggregating protein, Ref. 52), chromobindins (proteins binding to chromaffin granules, Ref. 54), calcimodins (proteins mediating Ca^{2+} signals, Ref. 199), lipocortins (steroid-inducible lipase inhibitors, Ref. 85), and calpactins (proteins binding Ca^{2+} , phospholipid, and actin, Ref. 101). Intensive biochemical work, protein and cDNA sequencing, as well as gene cloning led to the realization that all such proteins identified shared key biochemical properties as well as gene structure and sequence features. Hence, the concept of a novel multigene family arisen by gene duplication was developed and the common name annexin was introduced to solve the terminology tangle (55).

By definition, an annexin protein has to fulfill two major criteria. First, it must be capable of binding in a Ca^{2+} -dependent manner to negatively charged phospholipids. Second, it has to contain as a conserved structural element the so-called annexin repeat, a segment of some 70 amino acid residues. Molecular structures obtained for a number of annexins over the past decade helped to extend the similarities to the three-dimensional level. Moreover, they defined a hitherto unknown structural fold, the conserved annexin domain, which is built of four annexin repeats packed into a highly α -helical disk, and which now is considered to be a general membrane binding module. Once clearly defined and advanced by genome sequencing work, the annexin family has grown steadily in the 1990s, and with the turn of the century, now amounts to more than 160 unique annexin proteins present in more than 65 different species ranging from fungi and protists to plants and higher vertebrates (Fig. 1)

(202, 204). In this review we summarize the biochemical and structural properties of annexins, putting a particular emphasis on novel aspects of annexin interactions with lipids and other biological ligands. For a detailed discussion of the canonical annexin properties, their structural organization, and intracellular as well as tissue distribution, the interested reader is referred to previous reviews (51, 97, 244).

Having accumulated a wealth of biochemical and structural knowledge, we are still in need of assigning a physiological function to the annexin family as a whole, or better, because they are likely to differ, to individual annexins. Recent knock-out models, both at the cellular and the animal level, as well as the development and use of dominant-negative mutant proteins have introduced the first direct approaches for analyzing annexin function. They underscore the concept of functional diversity within the family. Moreover, it has recently become clear that certain dysregulations in annexin expression and activity can be correlated with human diseases and that this has led to the introduction of the term *annexinopathies*. Although we still have to await final proof of a direct correlation, we decided to concentrate our review on such recent developments leading to the proposal of some models concerning annexin function.

II. BIOCHEMICAL PROPERTIES OF ANNEXINS AND THEIR THREE-DIMENSIONAL STRUCTURE

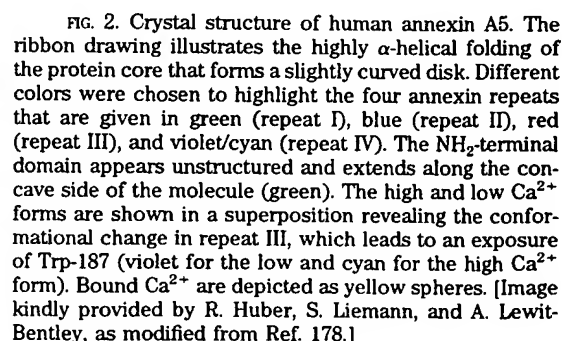
A. Molecular Structures

1. Structures of annexin protein cores: the conserved membrane binding modules

Each annexin is composed of two principal domains: the divergent NH_2 -terminal "head" and the conserved COOH-terminal protein core. The latter harbors the Ca^{2+} and membrane binding sites and is responsible for mediating the canonical membrane binding properties. An annexin core comprises four (in annexin A6 eight) segments of internal and interannexin homology that are easily identified in a linear sequence alignment (for review, see Ref. 244). It forms a highly α -helical and tightly packed disk with a slight curvature and two principle sides. The more convex side contains novel types of Ca^{2+} binding sites, the so-called type II and type III sites (335), and faces the membrane when an annexin is associated peripherally with phospholipids. The more concave side points away from the membrane and thus appears accessible for interactions with the NH_2 -terminal domain and/or possibly cytoplasmic binding partners (Fig. 2). The first structure known for an annexin core was that solved by Huber et al. (134) for annexin A5 in 1990. In the

FIG. 1. The new annexin nomenclature. The five major annexin groups (A–E) are shown, with details of the most extensively studied family members. The nomenclature is that proposed by Reg Morgan and Pilar Fernandez and endorsed by participants at the 50th Harden Conference on Annexins held at Wye College, UK, September 1–5, 1999. A more extensive list of annexin subfamilies and species is posted at the European annexin web site (<http://www24.brinkster.com/annexins/>). There are several important points to note. The vertebrate annexins (A1–A13) are unlikely to be widely represented in invertebrate species. The oldest of this group, namely, annexins A7, A11, and A13, are possible exceptions, and an annexin A11 ortholog has been described in the mollusk *Aplysia*. Within the B group, the *Caenorhabditis elegans* annexins have yet to be assigned numbers. In the C group, the *Dictyostelium* annexin, originally described incorrectly as annexin VII (synexin), is now established as being orthologous to the *Neurospora* annexin.

Recent findings include the elucidation of the first structures of annexins from lower eukaryotes and plants. Liemann et al. (177) crystallized the core of annexin C1



from *Dictyostelium discoideum*, whereas Hofmann et al. (127) elucidated the structure of a plant annexin, annexin D11 from *Capsicum annuum*, which revealed not only the typical annexin fold but also differences to nonplant annexins in annexin repeats I and III and in the membrane binding loops. Another recent advance is the introduction of benzodiazepine and benzothiazepine derivatives as annexin ligands and their cocrystallization with annexins. The benzothiazepine K201 was first described to bind to annexin A5 and inhibit its Ca^{2+} channel activity, most likely by restraining a hinge movement of the two annexin A5 modules formed by annexin repeats I/IV and II/III, respectively (149, 150). Other structurally related benzodiazepine compounds have subsequently been identified as ligands for various annexins with the interaction being based on similar structural principles (126). However, a possible pharmacological role of these interactions remains to be shown. Crystal structure determination and biochemical characterization in combination with site-directed mutagenesis have also proven powerful in recent years in characterizing the contribution of certain residues to the overall fold of annexin cores and/or their biochemical properties. Conserved arginine residues present in the so-called endonexin fold of each homology segment, for example, were shown to be crucial for stabilizing the tertiary structure of annexin A5. On the other hand, substitution by alanine of different serine and threonine residues and the unique tryptophan in the same annexin results in altered membrane binding underscoring the importance of these residues in mediating intermolecular, i.e., annexin-phospholipid, contacts (31, 32). Moreover, mutational analysis revealed that the aspartate residue at position 226 of annexin A5 participates as a molecular switch in a Ca^{2+} - and pH-dependent conformational change (294). Like many other annexins, annexin A4 is a substrate of protein kinase C (PKC), at least in *in vitro* reactions, and Kaetzel et al. (147) have attempted to monitor structural changes resulting from this phosphorylation. They show that replacement by glutamate of the PKC acceptor site, threonine-6, causes a release of the NH_2 -terminal domain from the protein core indicative of a regulatory role in the membrane aggregation displayed by this annexin. Annexin B12 has also been subjected to detailed scrutiny by mutagenesis involving cysteine substitutions for spin labeling purposes (see below) and the glutamate at position 105. This residue has been found to participate in the formation of intermolecular Ca^{2+} binding sites in a hexameric form of the molecule (185), and replacement of Glu-105 by lysine stabilizes this hexamer by favoring extensive hydrogen bonding (35).

Recently, techniques other than crystallization of the soluble proteins have been introduced to study in detail structural properties of annexins, in particular when

bound to membrane or phospholipid surfaces. They include cryoelectron microscopy, which led to the identification of highly structured junctions formed by different annexins between opposing membranes (167), and atomic force microscopy (AFM), which enabled the high-resolution analysis of two-dimensional crystals of annexin A5 formed on planar lipid bilayers (248, 249). Two-dimensional crystals of annexin A6 formed on artificial lipid monolayers were also obtained and characterized recently, revealing an intrinsic flexibility of this eight-annexin repeat-containing molecule. Here the two lobes of annexin A6, i.e., repeats I-IV and V-VIII, respectively, were found to bind to the phospholipid in both parallel or antiparallel orientation, with the latter providing a structural basis for membrane cross-linking (6). Evidence for conformational changes occurring in annexins upon membrane binding was obtained by analyzing membrane-bound annexin A5 with transmission and internal reflection infrared spectroscopy. Interestingly, it was inferred from these studies that a new β -structure with interstrand hydrogen bonds oriented parallel to the membrane surface is formed upon interaction with a lipid monolayer. On the other hand, analyses of two-dimensional crystals of the same annexin on membrane surfaces by high-resolution electron microscopy and AFM, and crystal structure analysis of a cross-linked form of annexin A2 capable of binding membranes, do not provide evidence for substantial conformational alterations accompanying the canonical Ca^{2+} -dependent membrane binding (26, 29, 229, 248). Relatively subtle changes, however, might occur. These include the exposure of the unique tryptophan in repeat 3 of annexin A5 observed in high Ca^{2+} (47, 174). Thus, despite the wealth of structural information on soluble as well as membrane-bound annexins, it is not clear whether the peripheral and Ca^{2+} -dependent membrane binding of annexins as a whole, or individual annexins, requires or is accompanied by conformational changes. Moreover, the structural basis of (possible) membrane insertions of annexins triggered by certain environmental changes like hydrogen ion concentration (see below) need to be described in more detail, possibly also by integrating into such analyses the characterization of folding properties of individual annexin repeats such as the first repeat of annexin A1 (49, 94).

2. Structures of the unique NH_2 -terminal annexin domains and their complexes with protein ligands

Molecular details of the three-dimensional folds of annexin molecules are mostly restricted to the protein core domains (see above) and unique NH_2 -terminal regions of the smaller annexins containing NH_2 -terminal sequences of 16 or fewer residues. In these structures, the NH_2 -terminal sequences extend along the concave side of

the molecule partially engaged in hydrophobic interactions with the protein core. In annexin A3, a direct effect of the NH₂-terminal domain on properties displayed by the core has been shown by replacing Trp-5 (in the unique NH₂-terminal sequence) by alanine. The W5A mutant protein shows a much stronger phospholipid binding, and although having a similar overall structure has a more disordered NH₂-terminal domain. Interestingly, through urea-induced denaturation analysis, it became apparent that the NH₂-terminal domain, even though comprising only 16 residues, unfolds separately from the protein core (128). Thus it appears that the short NH₂-terminal domains of the smaller annexins, located on the concave side of the folded molecule, affect the Ca²⁺-dependent phospholipid binding executed by the convex, or opposite, side possibly through stabilizing or destabilizing slightly different conformations of the molecule. This underscores the regulatory importance of even the small NH₂-terminal domains, a notion that had previously been postulated due to the presence of sites for posttranslational modifications in these regions (see below). Moreover, the finding that subtle differences in the NH₂-terminal sequence, which do not affect the overall structure, result in significantly altered properties could at least in part explain functional diversity among otherwise highly conserved annexins.

Recently, the first complete structure of a longer annexin, annexin A1, has been determined at high resolution (255). Annexin A1 has an NH₂-terminal domain of 40 residues, the first 10–14 of which represent the binding site for a protein ligand of the S100 family, S100A11 (188, 273). Interestingly, in the Ca²⁺-free crystals of annexin A1, this NH₂-terminal sequence forms an amphipathic α -helix and replaces a helix in the tightly packed core domain (helix D of repeat III), which in turn is unwound and partially extrudes from the protein surface (255). Such a structure could have interesting mechanistic and regulatory consequences. Given the tight internal packing of the NH₂-terminal helix, one would assume that this sequence is not available for S100A11 binding in Ca²⁺-free annexin A1. However, upon Ca²⁺-dependent membrane binding, the D helix of repeat III could be forced back into the position described for the Ca²⁺-loaded annexin A1 core (335), thereby freeing the NH₂-terminal helix and enabling this sequence to interact with S100A11. Moreover, such movement could be the prerequisite for the membrane aggregation activity described for annexin A1, e.g., by making accessible a second membrane binding site or a site for homophilic annexin 1 interaction (for a hypothetical model see Fig. 3). Thus, in the case of annexin A1, Ca²⁺ could have a dual regulatory function. First, it could trigger membrane attachment through the convex side of the molecule, and second, by inducing the switch of helix D, it would enable the membrane-bound

protein to interact with cellular protein ligands (S100A11) and/or a second membrane surface. In this respect, it is interesting to note that thermodynamic analyses revealed cooperativity in the binding of Ca²⁺ to annexin A1 (257). Finally, the conformational switch postulated by Rosengarth et al. (255) could also modulate the accessibility of phosphorylatable residues in the NH₂-terminal domain of annexin A1 for their respective kinases (see below), thereby guaranteeing a spatially restricted, probably membrane-dependent, regulation of annexin A1 activities.

The structure of the very same NH₂-terminal domain of annexin A1 comprising residues 1–14 has also been solved in complex with its S100A11 ligand. Cocrystals of S100A11, a homodimeric protein containing two EF hand-type Ca²⁺ binding sites, with the NH₂-terminal annexin A1 peptide revealed a 1:1 stoichiometry, with the two peptides occupying hydrophobic pockets on two opposite sides of the S100A11 dimer (246). The structure of the complex proved to be very similar to that of the NH₂-terminal sequence of annexin A2 bound to a related S100 protein, S100A10 (247). In both annexins (A1 and A2), the first 14 residues form amphipathic α -helices providing the binding sites for two ligands of the S100 protein family (15, 142, 188, 273). At least in the case of annexin A2, it has been shown that the formation of a heterotetrameric complex containing the S100A10 dimer and two annexin A2 chains significantly alters the properties of this annexin in vitro and also within cells (for reviews, see Refs. 97, 330). Importantly, the annexin A2-S100A10 complex can aggregate membrane vesicles at micromolar Ca²⁺ levels, a property not shared with monomeric annexin A2 or, as a matter of fact, any other annexin. The structure of the NH₂-terminal annexin A2 peptide in complex with S100A10, in combination with high-resolution images of junctions formed between adjacent membranes by the annexin A2-S100A10 complex, now provides the first detailed structural explanation of this aggregation activity. It appears that due to the highly symmetric nature of the structures, the complex links annexin A2-bound membrane surfaces through the dimerization of S100A10, i.e., the two annexin A2 subunits of the membrane-linking complex are bound to two separate bilayers with the S100A10 dimer connecting them through binding to the NH₂-terminal domains (167, 175, 247). A similar scenario could hold true for the annexin A1-S100A11 complex, which in contrast to annexin A2-S100A10 requires Ca²⁺ binding to the S100 protein and probably Ca²⁺/membrane-bound annexin (see above) for complex formation. Nevertheless, we are still in need of high-resolution structures of complete annexin A2-S100A10 and annexin A1-S100A11 complexes to prove or disprove this attractive model, as well as some evidence that the annexin A1-S100A11 exists in vivo.

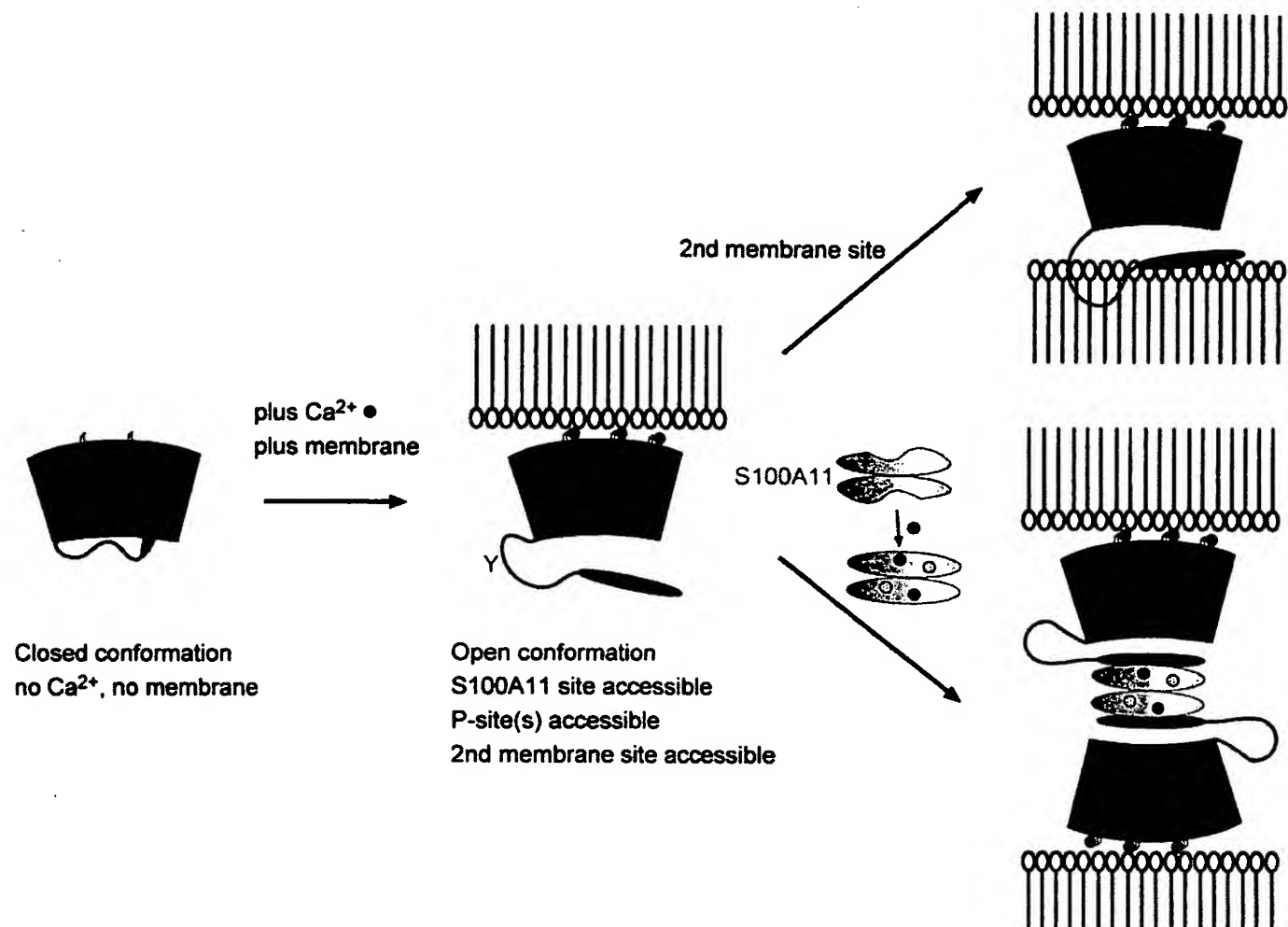


FIG. 3. Model describing the switch of helix D in the annexin A1 structure and its implications for membrane aggregation. In the crystal structure of Ca²⁺-free annexin A1 (red), the NH₂-terminal α -helix, which contains the S100A11 binding site (brown), is replacing helix D of the third repeat (255). Ca²⁺-dependent membrane binding could be accompanied by a conformational change establishing the Ca²⁺-bound crystal structure of the annexin A1 core (335) and, most likely, a more accessible NH₂-terminal domain. As a result, the NH₂-terminal domain can interact with a second membrane surface or the S100A11 dimer, which itself requires Ca²⁺ binding to establish an interaction-competent conformation. An as of yet hypothetical annexin A1/S100A11 heterotetramer would represent an entity capable of linking membrane surfaces (see text and Ref. 255 for details).

B. Annexins as Membrane Binding Proteins: Canonical and Atypical Properties

1. Ca²⁺-dependent phospholipid binding and vesicle aggregation

Biochemically, annexins are defined as soluble, hydrophilic proteins that bind to negatively charged phospholipids in a Ca²⁺-dependent manner (they are Ca²⁺/phospholipid binding proteins). This binding is reversible, and removal of Ca²⁺ by Ca²⁺ chelating agents will lead to a liberation of annexins from the phospholipid matrix. The interaction of annexins with negatively charged phospholipids observed *in vitro* is thought to reflect in a more physiological scenario the binding to cellular membranes, in particular, the cytosolic leaflets of the plasma mem-

brane and various organelle membranes. This canonical annexin property is retained within the annexin cores, the conserved annexin modules most likely representing building blocks designed for peripheral membrane association. However, although Ca²⁺-dependent phospholipid binding is shared by all annexins, individual members differ significantly in their Ca²⁺ sensitivity and phospholipid headgroup specificity. A large number of reports analyzing the Ca²⁺-regulated phospholipid binding of annexins *in vitro* have been published, and a comprehensive overview has been given by Raynal and Pollard (244).

Although differences in the binding to phospholipids with different headgroups (e.g., phosphatidic acid, phosphatidylserine, phosphatidylinositol) have long been recognized in *in vitro* studies, it has only recently become

clear that annexin cores also show specificity with respect to their membrane binding in living cells. Through expression of chimeric proteins containing different annexin cores fused to the green fluorescent protein (GFP), it was possible to visualize the distribution of such annexin cores in living cells. Strikingly different distributions were observed within a given cell type showing, e.g., an endosomal localization for the annexin A1 core, an association with certain plasma membrane structures for the annexin A4 core, and a nonmembranous, cytosolic distribution for the annexin A2 core (245). Such live cell experiments have to be extended to reveal annexin dynamics and to circumvent the potential problem that in fixed cells annexin distributions could be subjected to artifacts due to the presence or absence of Ca^{2+} in the fixation/permeabilization buffers. Although the annexin cores carry specificity with respect to membrane binding, an additional layer of such specificity is most likely added by the unique NH_2 -terminal domains of the annexins as in live cells full-length proteins show distributions often differing from the respective cores (73, 196, 245). Moreover, it remains to be seen how interactions with other protein ligands and posttranslational modifications (see below) affect the specific localizations of annexins to certain cellular sites.

Although well described *in vitro*, the physiological importance of Ca^{2+} -dependent phospholipid (and membrane) binding is not understood. However, interesting models have been put forward to assign functions to a peripherally associated and abundant membrane binding protein like, e.g., annexin A5. *In situ*, annexin A5 can form two-dimensional crystals on planar lipid bilayers containing negatively charged phospholipids (26, 229, 248, 249). Such crystalline or semi-crystalline arrangement will most likely affect membrane properties including rigidity, fluidity, and lipid segregation and can therefore participate in the regulation and/or stabilization of membrane domains. Indeed, electron paramagnetic resonance (EPR) spectroscopy reveals that Ca^{2+} -dependent binding of annexin A5 to phospholipid vesicles parallels a rigidification of the membrane (193). Moreover, it was shown that binding of this annexin to the surface of T cells (by an as yet unknown mechanism) delays programmed cell death most likely by generating a certain (in this case extracellular) membrane constraint which in turn interferes with the release of CD4^+ membrane particles (99). On the other hand, membrane binding also affects the annexin protein, as annexin A5, thermodynamically a marginally stable protein (like annexin A1; Refs. 256, 328) is protected to a significant degree from thermal denaturation by Ca^{2+} /phospholipid binding (338).

Annexins are not only capable of binding phospholipid-containing membranes but at least in some cases, e.g., annexins A1, A2, A4, A6 and A7, also mediate membrane vesicle aggregation. Again, phospholipid composi-

tion and Ca^{2+} sensitivity for this aggregation activity differ for individual members (for review, see Ref. 244). As molecular structures of annexins reveal one Ca^{2+} /lipid-binding surface (see above), several models have been put forward to explain an aggregation activity based on the linking of membrane surfaces (see also Ref. 97). One proposal, based on the self-association properties of several annexins, is a protein-protein interaction of annexin molecules bound to two separate membranes (for reviews, see Refs. 51, 244; recent example in Ref. 180). A second explanation is based on the identification of a second membrane binding site in annexin A1 (for review, see Ref. 97 and also discussion in Ref. 23). A sequence in the unique NH_2 -terminal domain of annexin A1, residues 24–35, constitutes a crucial part of this second binding domain and when fused to the core of annexin A5 can confer membrane aggregation activity to this otherwise inactive annexin (40). In contrast to the Ca^{2+} -dependent primary membrane binding via the annexin A1 core, the secondary binding is mainly hydrophobic in nature, and it appears that lateral aggregation of annexin A1 molecules bound to one membrane surface precedes the aggregation mediated through the secondary binding site (24). Interestingly, recent crystal structure determination of full-length annexin A1 suggests that the NH_2 -terminal domain of this annexin only becomes fully accessible when the protein core is linked to a membrane surface via its Ca^{2+} /phospholipid binding sites (255). This could indicate that the second (NH_2 -terminal) membrane binding site in annexin A1 is dormant in the cytosolic protein and only becomes activated when the protein associates with membranes. A third alternative of aggregation activity is probably realized in annexin A6, the only member of the family identified so far with eight instead of four annexin repeats. Here a duplication of the core domain has generated a second Ca^{2+} -dependent phospholipid-binding module, thus allowing for two spatially separated membrane interactions (6). Yet another route is taken by annexin A2 and possibly also other annexins capable of interacting with dimeric protein ligands of the S100 family (see below). The NH_2 -terminal domain of annexin A2 harbors a highly specific binding site for the small dimeric S100 protein S100A10, with protein-protein interaction leading to the formation of a heterotetrameric complex. In this complex, two annexin A2 molecules are noncovalently linked via a S100A10 dimer bound to their NH_2 -terminal domains, thereby generating an entity capable of binding simultaneously to two membrane surfaces through the two annexin A2 cores (175). Thus it appears that although several annexins mediate membrane-membrane contacts, the way this is achieved differs from member to member. This could explain the different Ca^{2+} concentrations required by different annexins for half-maximal vesicle aggregation (for review, see Ref. 244) and also the differing dimensions of annexin-dependent junc-

tions observed in high-resolution cryoelectron microscopy of lipid vesicles aggregated by different annexins in the presence of Ca^{2+} (167).

2. Ca^{2+} -independent lipid binding

Although Ca^{2+} -dependent phospholipid binding remains the criterion of choice for defining an annexin protein biochemically, additional "atypical" lipid binding properties have begun to emerge in recent years. These properties again vary between the different annexins analyzed so far, but it appears that the single most important parameter regulating Ca^{2+} -independent membrane binding is the pH value chosen to analyze the interaction. Annexin A5, for example, binds to and apparently penetrates the bilayer of phosphatidylserine (PS) vesicles at pH 4 (158), and at pH 5 was shown to induce a leakage of PS vesicles (124). Both activities are observed in the absence of Ca^{2+} , whereas at neutral pH Ca^{2+} binding to the protein appears to be a prerequisite for the lipid interaction (158). Most likely, this switch in properties is accompanied by a conformational change in the annexin A5 molecule, which has been shown to occur between pH 4.6 and 4 when the acid-induced unfolding of the protein was analyzed (16). This change is characterized by solvent exposure of a unique tryptophan residue in annexin A5 (Trp-187), and thus is reminiscent of a Ca^{2+} -induced exposure of the same tryptophan at neutral pH (192, 293–296). Conformational changes leading to Ca^{2+} -independent phospholipid binding *in vitro* have also been proposed to occur when Ca^{2+} sites in annexin 2 were inactivated by mutagenesis (79), although such mutations interfere with the intracellular membrane localization of this and other annexins (145, 245).

Considerable progress in analyzing Ca^{2+} -independent annexin-membrane interactions occurring at lower pH has come recently through the introduction of site-directed spin labeling. By engineering protein mutants with unique cysteines and specifically derivatizing these cysteines with a paramagnetic nitroxide side chain, the groups of Haigler, Langen, and Hubbell (168, 169) were able to probe the structure of annexin B12 bound to membranes at lower pH. Combined with the use of reagents that selectively and photoactivatably label amino acid side chains exposed to the hydrophobic domain of the bilayer, they could show that annexin B12 inserts into the bilayer of PS/phosphatidylcholine (PC)-containing vesicles. This insertion is likely to be accompanied by the formation of a continuous transmembrane α -helix. In the solution structure of the molecule, this part forms a helix-loop-helix motif, and it is tempting to speculate that the switch from the helix-loop-helix motif to the transmembrane helix drives a reversible membrane insertion (138, 168, 169). Based on these observations, Langen et al. (168) propose concerted conformational changes in all four

annexin repeats of annexin B12, which are triggered by low pH and involve the formation of several elongated transmembrane helices from helix-loop(turn)-helix structures found in solution (Fig. 4). As a consequence, the entire molecule can assume a transmembrane topology as defined by accessibility to proteases present on either side of the membrane (289). The pH-dependent switch in conformation could be induced by the protonation of certain carboxylate residues found in or close to the loop of the helix-loop-helix motif, which upon deprotonation could drive the protein back to the solution conformation (168). Such a model could also hold true for other annexins, as all have similar solution structures, and its reversibility could perhaps explain why and how certain annexins under certain circumstances can span a lipid bilayer. The latter could be of particular importance in the case of annexins A1 and A2, which also appear to have extracellular activities and for which cell surface receptors have been described (see below). At least in the case of annexins A1 and A6, pH-driven membrane insertion has been identified (103, 258), although it is not clear whether this could lead to membrane translocation.

In addition to the points discussed above, Ca^{2+} -independent membrane associations have also been observed for several annexins at neutral pH. Examples for these types of Ca^{2+} -independent interactions are the association of annexins A2 and A6 with endosomal membranes (120, 145, 160, 275), the binding of annexin A2 to A549 cell membranes (182), and the interaction of annexin A5 with the plasma membrane of platelets (for review, see Ref. 322). At least in part it appears that such interactions are mediated through a binding of the respective annexin to a protein ligand that is itself associated with or embedded in the cellular membrane.

C. Nonlipid Annexin Ligands

1. Annexin complexes with EF hand-type Ca^{2+} binding proteins

The EF hand denotes a helix-loop-helix Ca^{2+} binding motif that is present in a large number of proteins comprising the EF hand superfamily with its distinct subfamilies (for review, see Ref. 154). Several EF hand proteins, in particular those of the S100 subfamily, form complexes with members of the annexin family. S100 proteins are small (~10 kDa) proteins characterized by two consecutive EF hands connected by a flexible linker region and flanked by unique NH_2 - and COOH -terminal extensions. Similar to calmodulin, they are thought to interact with and thereby regulate cellular target proteins in a Ca^{2+} -dependent manner (for reviews, see Refs. 68, 267). Three S100 proteins, S100A6, S100A10, and S100A11, were shown to bind specifically to three different annexins, annexins A11, A2, and A1, respectively. The best charac-

Membrane destabilization

Membrane insertion

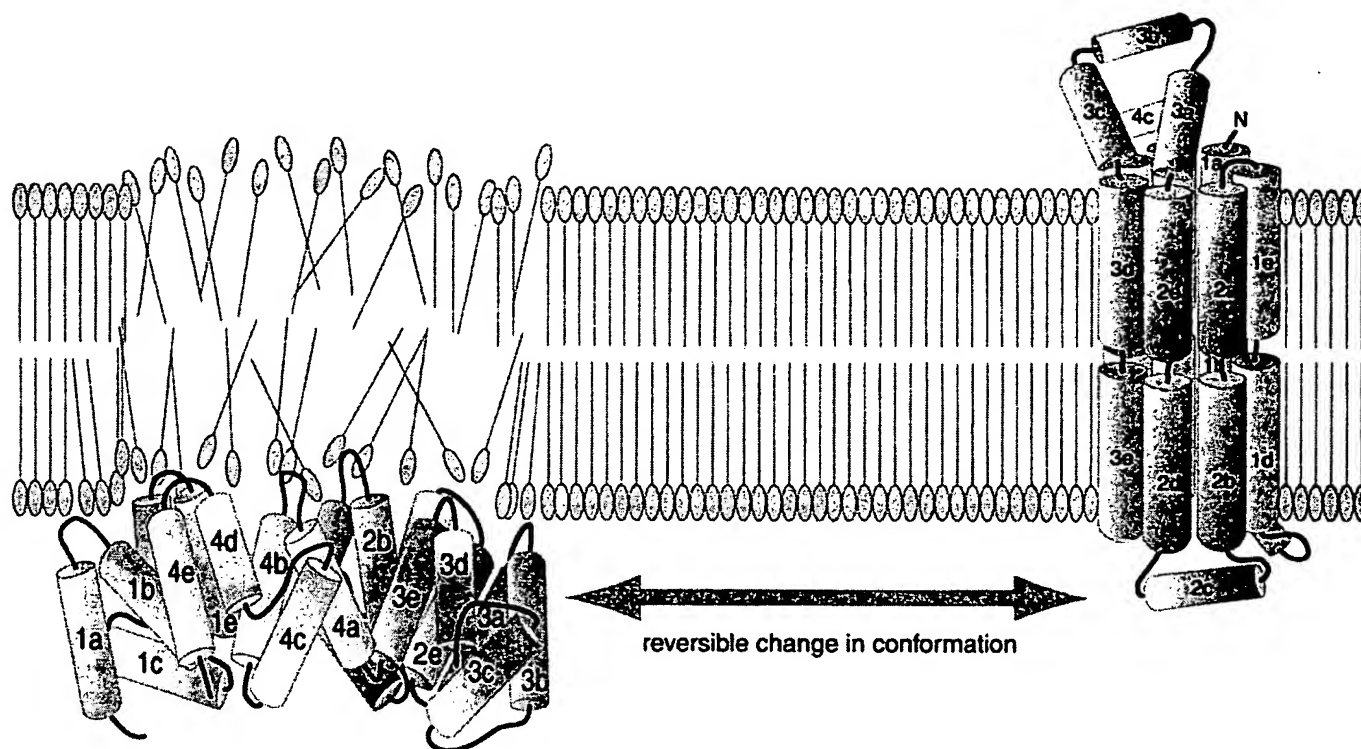


FIG. 4. Peripheral membrane binding and insertion by an annexin. Two potential interaction states for a monomeric annexin molecule with the cytoplasmic leaflet of a hypothetical membrane are shown. The peripherally bound annexin on the *left* assumes the tertiary structure depicted in Figure 2 and has been postulated to increase membrane permeability by apposition of its convex upper surface with the lipid bilayer, which in turn has been suggested to lead to ion flow. The fully membrane integrated structure on the *right* is based on that proposed by Langen and co-workers (168, 169), after protonation at acidic pH, destabilization of the native α -helical structure, and refolding into the seven-transmembrane spanning configuration. Although the proposed structure is obliged to have NH_2 and COOH termini on opposing sides of the bilayer, the orientation shown in the figure is arbitrary.

terized of these annexin-S100 complexes is the annexin A2-S100A10 (p11) heterotetramer. Here it was clearly established that complex formation is highly specific, occurs *in vivo*, can be regulated by posttranslational modifications in the annexin, and modulates properties displayed by the isolated subunits (for review, see Ref. 97). S100A10 is the only member of the S100 family that has suffered deletions and mutations in its two EF hand loops, rendering the Ca^{2+} sites nonfunctional. However, it appears that the resulting conformation of the protein represents a permanently active state with respect to its capacity to bind the annexin A2 target (143, 246, 247). The S100A10 binding site on annexin A2 is restricted to the NH_2 -terminal 14 residues and peptides corresponding to this sequence bind to S100A10 with high specificity and affinity. Moreover, such peptides disrupt by competition preformed annexin A2-S100A10 complexes and therefore

can be used as tools for studying complex function (161). At least in studies with synthetic peptides, an important feature of this binding site is the NH_2 -terminal acetylation of the NH_2 -terminal serine residue of annexin A2, a post-translational modification occurring with high efficiency in eukaryotic cells (15). On the other hand, annexin A2, expressed recombinantly in bacteria and lacking the *N*-acetyl group, is also capable of binding p11, although the affinity of this interaction has not been compared with that of the acetylated protein (151). The apparent discrepancy in these results remains to be resolved, in particular since only an acetylated NH_2 -terminal annexin peptide is capable of disrupting the annexin A2-S100A10 heterotetramer (161).

Complex formation between annexin A1 and S100A11 is based on very similar principles, although in this case Ca^{2+} binding to the S100 protein is required to

establish the interaction-competent form of S100A11 (188, 246, 273). Moreover, it remains to be established if and when this interaction occurs *in vivo*. In contrast to the heterotetrameric annexin A2-S100A10 complexes, standard isolation protocols do not yield annexin A1-S100A11 complexes but only the separated subunits. Likewise, a strong colocalization has not been reported so far, although ectopic expression studies using mutant proteins indicate that annexin A1 can target S100A11 to endosomal membranes in baby hamster kidney (BHK) cells (274). It appears likely that the strict Ca^{2+} dependence of the annexin A1-S100A11 interaction interferes with the visualization or isolation of complexes once Ca^{2+} drops below a certain threshold within the cells or during isolation. On the basis of the high structural similarity of the annexin A2-S100A10 and annexin A1-S100A11 complexes, it is likely that both are heterotetrameric entities with the capacity of linking membrane surfaces in a symmetric manner (see Fig. 3 for annexin A1). While the former complex is known to exist in resting cells irrespective of cellular Ca^{2+} transients (but perhaps regulated by PKC phosphorylation in the NH_2 -terminal sequence of annexin A2; Ref. 144), the latter is probably dependent on (perhaps locally restricted) Ca^{2+} rises and could be of importance during Ca^{2+} -regulated membrane transport events.

The third annexin-S100 protein interaction described to date is that between annexin A11 and S100A6 (312). Although the S100 binding site in annexin A11 is also located in the NH_2 -terminal domain (303, 311), the mode of complex formation is likely to be different. Annexin A11 contains a long NH_2 -terminal domain of almost 200 residues rich in glycine, tyrosine, and proline residues, which resembles that of annexin A7 and possibly lacks a well-ordered three-dimensional fold (177), or contains segments with pro- β -helices (190). However, sequences within the NH_2 -terminal domain of annexin A11 do not resemble the amphipathic helices found in annexins A1 and A2 and thus are unlikely to fit in a homologous manner in a binding pocket formed by the S100 dimer. The physiological consequences of the annexin A11-S100A6 interaction remain to be established, although it is interesting to note that only one NH_2 -terminal splice form of annexin A11 can interact with S100A6 at least *in vitro* (302). Other annexin-S100 interactions have been described, e.g., that of annexin A6 with S100A1 and S100B (96), but the structural basis and physiological significance of such complexes is less well defined. The reader is referred to the S100 literature for further detail (e.g., Ref. 68).

In contrast to S100 proteins, sorcin is a member of the EF hand superfamily containing four and not two of the helix-loop-helix motifs. It binds in a Ca^{2+} -dependent manner to the GYP-rich NH_2 -terminal domain of annexin A7 (28) with the NH_2 -terminal domain of sorcin being required for the interaction (327). Complex formation can

recruit sorcin to the membrane of chromaffin granules, which are a prime site of annexin A7 localization. Moreover, binding of sorcin inhibits the chromaffin granule aggregation mediated by annexin A7 (28), thus underscoring the regulatory importance of complex formation. The common picture emerging from the interaction analyses is that it is most likely to be the annexins that are affected in their properties by EF hand protein binding, rather than the other way round. Although the structural basis of the interaction probably differs between the different complexes, a common feature is the importance of the NH_2 -terminal annexin domain for binding. Protein binding to this unique domain in the respective annexin can have a number of consequences ranging from the establishment of a different physical entity capable of interconnecting membranes (see, for example, Fig. 3) to a protein complex with altered biochemical properties.

2. Annexin interactions with cytoskeletal proteins

A number of annexins have been described as cytoskeleton, in particular F-actin, binding proteins, and it has been suggested that at least some members of the family could participate in regulating membrane-cytoskeleton dynamics. Here we do not survey the entire literature in this area but only focus on recent developments. For an overview of the earlier literature, the reader is referred to previous reviews (97, 244).

Annexin A1 binds to F-actin and also interacts with profilin, a G-actin binding protein and regulator of actin polymerization. Complex formation between annexin A1 and profilin modifies the profilin effect on actin polymerization. Because of the partially overlapping intracellular localization of the two proteins, it is tempting to speculate that the annexin A1-profilin interaction participates in regulating the membrane-associated cytoskeleton (2). In addition to this interaction with a protein involved in actin cytoskeleton dynamics, some colocalization of annexin A1 with tubulin and cytokeratin-8 has also been reported. In A549 human lung adenocarcinoma cells, striking patches of annexin A1 immunolabeling are found at the plasma membrane, which are also positive for these two cytoskeletal proteins (313). It is not clear, however, whether this colocalization reflects a functional interaction.

Annexin A2 is another F-actin binding annexin that also has a Ca^{2+} -dependent filament bundling activity. This bundling activity is particularly pronounced in the case of the heterotetrameric annexin A2-S100A10 complex (for review, see Refs. 97, 330). Recently, the F-actin binding site has been mapped to the COOH terminus of annexin A2, underscoring the specificity of the interaction (80). Annexin A2 is not associated with stress fibers or cytoplasmic actin filaments but appears to play a role in the organization of membrane-associated actin at sites of cho-

lesterol-rich membrane domains. Evidence for this view is severalfold. In the presence of Ca^{2+} , annexin A2 binds to and possibly promotes the lateral association of glycosphingolipid- and cholesterol-rich lipid microdomains (rafts) (8, 119). It has been proposed that in smooth muscle cells this association promotes the binding of annexin A6, which itself mediates the formation of a reversible membrane contact with the actin cytoskeleton (8, 9). On the other hand, annexin A2 could also carry out this task by itself or in conjunction with other actin binding proteins, since cholesterol-sequestering agents specifically release annexin A2 together with the cortical cytoskeletal proteins α -actinin, ezrin, and actin from membranes of BHK and endothelial cells (120; J. König and V. Gerke, unpublished observations). Moreover, expression in epithelial cells of a mutant annexin A2 protein causing the submembrane aggregation of annexin A2 and its ligand S100A10 results in the simultaneous aggregation of a transmembrane raft protein (CD44) and a redirection of actin bundles toward these clusters (216). Thus, due to its Ca^{2+} -dependent membrane and F-actin binding and its intracellular location at sites of membrane rafts, annexin A2 could serve as an organizer of these membrane microdomains and their connection to the actin cytoskeleton.

Annexin A5 has been observed to relocate to the cortical membrane cytoskeleton after activation of platelets. This relocation appears to involve both binding to the plasma membrane and to a specific actin isoform, γ -actin, and is paralleled by an association with the platelet membrane of cytosolic phospholipase A_2 , suggesting an interaction between this phospholipase and annexin A5 (319–321). Annexin A6, another actin-binding annexin, has been implicated in mediating in a Ca^{2+} -dependent manner membrane-cytoskeleton contacts in smooth muscle cells (9). Spectrin is another binding partner of annexin A6 in the cortical cytoskeleton. Because annexin A6 promotes a cysteine protease-dependent type of budding of clathrin-coated vesicles at the plasma membrane, it has been proposed that the protein participates in disconnecting the clathrin lattice from the spectrin membrane cytoskeleton during the final stages of coated pit budding (148). With the exception of annexin A2 (98), it is not known whether other annexins share this spectrin binding property. In addition to the family members mentioned above, F-actin binding annexins have recently also been identified in the killifish medaka (297) and in plants (131), although their functional roles in these organisms have not been addressed so far.

3. Other ligands

In addition to Ca^{2+} , phospholipid, EF hand type proteins, and cytoskeleton-associated proteins, a number of other annexin ligands ranging from proteins to RNA and

smaller molecules have been described. An account of such binding partners is given in previous reviews (97, 244), and only the most recent findings are summarized here. Moreover, this section primarily focuses on intracellular binding partners, whereas extracellular protein ligands are discussed when we review extracellular activities of annexins (see sect. IV C).

Annexin protein ligands other than the ones summarized above include the cytosolic phospholipase A_2 , which interacts with annexin A1 (156) and the p120 Ras GTPase activating protein (GAP), which through its C2 domain binds to annexin A6 (60). Within annexin A6, the binding site has been mapped to the unique linker region connecting the two four-repeat lobes of the protein (44). This region is not found in other annexins, thus emphasizing the specificity of the interaction. Recently, two protein kinases, Fyn (a src kinase family member) and Pyk2 (a member of the focal adhesion kinase family), have also been found in the annexin A6-p120GAP complex, indicating that annexins could also participate in certain signaling events (43). A link between annexin A6 and signaling has also been inferred from its association with activated PKC- α , which was described in skeletal muscle (272). Another binding partner for annexin A6 was identified in clathrin-coated vesicles isolated from adrenocortical tissue. In a subpopulation of these vesicles, which also contain the transferrin receptor, annexin A6 tightly associates with the GTPase dynamin known to participate in the pinching off of clathrin-coated endocytic vesicles (318). In the vesicle preparations, annexin A2 was shown to bind to a yet unidentified 200-kDa protein, suggesting that these two annexins could participate in defining specific protein-lipid interaction domains during endocytosis (see also below). A similar function has been suggested for annexin A13, which interacts with the C2 domain of the Nedd4 ubiquitin protein ligase, thereby participating in the apical membrane targeting of Nedd4 in polarized epithelial cells (231). Annexin A13 exists in two NH_2 -terminal splice variants, a and b, with 13b being specifically targeted to the apical transport vesicles also containing raft components (see below). The binding of annexin A13 to Nedd4 was initially identified in a yeast two-hybrid screen and a number of annexin-protein interactions, e.g., that of annexin A5 with the intracellular domain of the vascular endothelial growth factor (VEGF) receptor Flk-1 (334), have been reported using similar approaches. Interestingly, in all cases reported it has been the protein ligand and never the annexin that was used as the bait in the initial screen.

Some annexins have also been shown to bind to other cellular macromolecules. Annexins A2, A4, A5, A6, and the *Caenorhabditis elegans* protein annexin B7 interact with carbohydrates, in particular glycosaminoglycans, and in some cases the binding sites have been mapped to certain regions within the respective annexin molecule

(83, 139, 152, 159, 265). These interactions are likely to come into play when annexins are present extracellularly, but their functional significance remains to be proven. Nucleic acids comprise yet another class of macromolecules reported to bind to annexins in a Ca^{2+} -dependent manner. Whereas annexin A1 interacts with purine-rich RNA and pyrimidine-rich DNA, annexin A2 has been found associated with mRNA of a distinct polysomal subpopulation (123, 326). It is not known whether and how annexin binding affects stability or functional state of the mRNAs, e.g., in terms of translation efficiency. However, because of the sequence specific binding (A. Vedeler, personal communication) and the fact that annexins A1 and A2 are also actin binding proteins, it has been speculated that the annexin proteins participate in the intracellular positioning of certain mRNAs via an interaction with both the mRNA and the actin cytoskeleton. Single nucleotides binding to certain annexin proteins have also been described in recent reports. While ATP binds to annexins A1 (118) and A6 (for review, see Ref. 11), annexin A7 not only interacts with but also catalyzes the hydrolysis of GTP (34). This latter observation led to the suggestion that annexin A7 acts as an atypical G protein involved in mediating the Ca^{2+} /GTP signal during exocytotic membrane fusion (34). However, although GTP and GDP were present in immunoprecipitates of annexin A7 from permeabilized chromaffin cells, the ratio of GTP to GDP was apparently not influenced by Ca^{2+} , raising questions as to how the GTPase activity might be regulated in vivo. Clearly, further work is required to improve our understanding of how annexins interact with nucleotides, especially as annexins lack a consensus nucleotide binding site. In this context, the three-dimensional structures of annexins complexed to nucleotides will be particularly informative, together with the identification of proteins that might modulate any catalytic activity ascribed to annexins, such as the activator proteins, dissociation inhibitors, and exchange factors that collectively regulate other GTPases.

D. Modulation of Annexin Properties by Posttranslational Modifications

Annexins are long known to be targets for posttranslational modifications. In fact, annexin A2 was initially isolated as a major v-src protein kinase substrate, and the tyrosine kinase activity of the epidermal growth factor (EGF) receptor has long been known to phosphorylate annexin A1 (see previous reviews, Refs. 51, 97, 111 and also Ref. 259 for an overview). More recently, additional phosphorylations by signal transducing kinases of these and other annexins have been reported with at least some of them affecting annexin properties. Other tyrosine kinases recognizing annexins A1 and A2 as substrates are

those associated with the platelet-derived growth factor (PDGF) receptor, the hepatocyte growth factor/scatter factor, and the insulin receptor (for review, see Ref. 259). In the latter case, annexin A2 only undergoes insulin-triggered tyrosine phosphorylation when receptor internalization is occurring (22). To some extent, this mimics the tyrosine phosphorylation of annexin A1 upon activation and internalization of the EGF receptor and indicates that both annexins and their phosphorylation are mechanistically linked to the internalization/endocytic sorting of certain ligand bound receptors (see also below). Although these phosphorylations are known to occur in vivo, their physiological consequences have not been established. In vitro or in situ studies, however, have revealed alterations in the Ca^{2+} /membrane binding of annexins A1 and A2 phosphorylated at Tyr-20 (by the EGF receptor kinase, Ref. 61) and Tyr-23 (by the src kinase, Ref. 102), respectively. Tyrosine phosphorylated annexin A1 is more susceptible to NH_2 -terminal proteolysis, thus showing altered phospholipid vesicle binding and aggregation activities (for review, see Ref. 111). Moreover, in contrast to the nonphosphorylated form, it requires Ca^{2+} for the association with the membrane of multivesicular endosomes (92). In the case of annexin A2, tyrosine phosphorylation decreases its affinity for phospholipids and interferes with capability of the annexin A2-S100A10 complex to aggregate chromaffin granules at micromolar Ca^{2+} concentrations (132, 236). A mutual influence of Tyr-23 phosphorylation and phospholipid binding is also corroborated by the finding that phosphorylation of annexin A2 by pp60^{src} is significantly enhanced when the protein is bound to PS containing vesicle (17). Recently, annexins A7 and A11 were also described to be phosphorylated on tyrosine residues, in this case in rat vascular smooth muscle cells in response to PDGF. In vitro both annexins are also phosphorylated by the Ca^{2+} -dependent tyrosine kinase Pyk-2, the src tyrosine kinase, and the EGF receptor kinase, but the physiological consequences of these phosphorylations have not yet been described (91).

A number of serine/threonine kinases that phosphorylate annexins have also been described. Phosphorylation sites again reside in the unique NH_2 -terminal domains of the annexins, and the modifications in some cases have been shown to affect biochemical properties of the annexins, in particular their affinity for Ca^{2+} /phospholipid (already reviewed in Refs. 97, 244). PKC, for example, has long been known to phosphorylate a number of annexins, with annexin A5 being a remarkable exception as it can serve as a PKC inhibitor (261). The strongest evidence for PKC phosphorylation regulating annexin activities in cells has accumulated in the case of annexin A2 and its involvement in Ca^{2+} -regulated exocytosis in adrenal chromaffin cells. Here, nicotine stimulation leads to annexin A2 phosphorylation by PKC with activation of PKC being a prerequisite for regulated exocytosis (63, 263). A link be-

tween secretion and PKC phosphorylation has also been obtained recently in the case of annexin A7, with PKC phosphorylation activating the Ca^{2+} -dependent membrane fusion displayed by this annexin (33). Other kinases acting on annexins are casein kinase I, which phosphorylates annexin A2, and a yet to be defined histidine-specific kinase which phosphorylates annexin A1 (95, 208). Recent evidence for a participation in intracellular signaling has been obtained for annexin A1, whose expression levels have been coupled to regulation of the extracellular signal-regulated kinase (ERK) pathway in RAW macrophages (1).

As pointed out above, annexin phosphorylation often results in an altered susceptibility toward proteolysis. Although this could be considered a mere indication of a conformational change, it could also reflect an important intracellular consequence of the posttranslational modification directly linked to altered properties displayed by the modified annexin. Cleavage generally occurs in the unique NH_2 -terminal annexin domain with the resulting NH_2 -terminally truncated molecule showing, as revealed in particular for annexins A1 and A2, an altered sensitivity toward Ca^{2+} /phospholipid (for review see Refs. 111, 244) and a different intracellular location (245, 275). In addition, it appears at least in the case of annexin A1 that NH_2 -terminal cleavage by an intracellular protease can occur without prior phosphorylation and can thus itself be considered the regulatory event. This has been shown in human neutrophils where removal by a membrane localized metalloprotease of the NH_2 -terminal eight residues of annexin A1 results in a protein species with a decreased Ca^{2+} requirement for binding to secretory vesicles and the plasma membrane, an event possibly linked to the exocytosis of different vesicle populations (206, 207). In annexin A2, another recently observed modification is a *S*-glutathiolation of Cys-8 in the NH_2 -terminal domain, which is observed after oxidative stress, e.g., in tumor necrosis factor (TNF)- α -treated cells (304). Modification of this cysteine, which is located in the S100A10 binding sequence, does not affect the interaction with S100A10 (143). On the other hand, a general cysteine modification of the annexin A2-S100A10 complex by *N*-ethylmaleimide (NEM), which most likely also affects Cys-8, strongly inhibits the ability of the complex to aggregate lipid vesicles (282). It is not clear whether cysteine residues participate directly in the aggregation activity or whether their derivatization interferes with certain conformational changes in the molecule required for the activity. However, as annexin A2 has been implicated in membrane trafficking events possibly requiring its aggregation activity (see below), NEM, which is frequently used as an inhibitor of membrane fusion, could also affect annexin A2.

Hence, a variety of posttranslational modifications on annexins which also include the *N*-myristoylation of an-

nexin A13a and -b (77, 336) have been described, with most of them affecting the Ca^{2+} and/or membrane binding properties of the molecules and thus their most probable intracellular activity. Future analyses have to reveal how these modifications are mechanistically linked to the different annexin functions.

III. MOLECULAR EVOLUTION OF THE ANNEXIN FAMILY AND REGULATION OF ANNEXIN GENE EXPRESSION

Ever since annexins were first reported in the literature they have been categorized as a structurally conserved family of Ca^{2+} binding proteins. The structural conservation remains a defining characteristic, but the discovery of human annexins A9 and A10 (201, 204) provides what appear to be exceptions to the unifying ability of annexins to bind Ca^{2+} . Nevertheless, the conservation of annexin primary structures extends throughout multicellular eukaryotic species, and the abundance of annexin sequences provides unique insights not only into the evolution of the annexin gene family, but also genetic molecular evolution in a broader sense. For readers seeking detailed accounts of annexin evolution, there are several excellent recent articles (203, 200, 204); here we focus on the major features of annexin phylogeny and ask whether or not functional insight can be gained by examination of molecular relationships between annexins.

A. Molecular Phylogeny of Annexins

Annexins have been described in most eukaryotic organisms, with the exception of those yeasts for which genomic sequences are available. The absence of recognizable annexin-like sequences in *Saccharomyces cerevisiae* had been anticipated by a number of investigators in the field who had used both biochemical and molecular genetic screens in what ultimately proved to be unfruitful searches for yeast annexins. Nevertheless, given the genetic diversity of yeasts, it remains possible that an ancestral eukaryotic annexin will be discovered in certain yeast species.

The simplest organisms known to express annexins are the protist *Giardia lamblia* and the fungus *Neurospora crassa*. The existence of at least three annexins in the protist is surprising given the simplicity of the organism and that more sophisticated multicellular eukaryotes such as *Hydra vulgaris* and *Dictyostelium discoideum* have at most one or two annexins. A long-running question in annexin evolution is whether any of the annexins discovered in these primitive organisms represents the ancestor of the modern vertebrate annexins. Early studies describing the *D. discoideum* annexin as a direct ortholog of vertebrate annexin A7 (106) now appear to be incor-

rect. However, the *D. discoideum* annexin does occupy an interesting niche in annexin evolution. The *D. discoideum* and *N. crassa* annexins share ~40% amino acid sequence identity, which given their evolutionary distance suggests they may be orthologs. Indeed, this annexin has now been discovered in the oyster mushroom and potato fungus (R. Morgan and M. Fernandez, personal communication), suggesting the evolutionary segregation of this annexin to this group of organisms.

A second major group of annexins distinct from the vertebrate cohort have been described in plants (64). Plant annexins are characterized by their lack of variable NH₂-terminal domains and, at least in modern flowering plants, by the absence of type II Ca²⁺ binding sites in repeats 2 and 3. Thus, from an evolutionary viewpoint, plant annexins have evolved in quite distinct ways to those in the animal phyla. The position of the fungal and mold annexins relative to either the animal or plant kingdoms is unclear, but sequence identity of ~40% between *D. discoideum* annexin C1 and human annexin A11 raises the possibility that the former is a direct ancestor of the latter. Analysis of the structure of the annexin A11 gene (10) revealed it to be the common ancestor of up to nine descendant annexins (A1, A2, A3, A4, A5, A6, A8, A9, and A10), indicating that at the time of the early chordate radiation 500–600 million years ago the first vertebrate genomes probably contained the genes for only three annexins, namely, annexins A13, A7, and A11. Exon splicing patterns within the core tetrads of annexins A13, A7, and A11 support the idea that A11 is a descendent of A7 and that this in turn evolved from A13. However, orthologs of annexins A7, A11, and A13 have not been formally identified in any nonvertebrate species, and any direct lineage between annexins in organisms such as *D. discoideum* and vertebrates remains conjectural.

A final point of interest to emerge from studies on the molecular evolution of the annexins concerns the origins of annexin A6. This annexin is unique within the family in that it comprises two of the tetrad repeats found in all other annexins. The two tetrads are joined by a short linking sequence, and it was previously hypothesized that annexin A6 was formed by tandem duplication and fusion of a single tetrad (285, 286). Because the 5'-tetrad of annexin A6 is most closely related to annexin A5, it was proposed that the progenitor of this duplication event was the 5'-tetrad. However, the recent discovery and analysis of the annexin A10 gene provides an alternative and much more persuasive explanation for the origins of annexin A6 (204). First, annexin A10 has greater similarity to the 3'-tetrad of annexin A6 than the two halves of annexin A6 have to one another, and significantly, an unusual single codon deletion near the start of repeat three is present in both annexin A10 and the 3'-tetrad of annexin A6. These and other phylogenetic data suggest that the two four-repeat annexins A5 and A10, which are located on human

chromosome 4q26 and 4q33, respectively, may have duplicated and fused to form the 5'- and 3'-lobes of annexin A6 early in chordate evolution.

Collectively, these phylogenetic studies enable us to put the annexins into a meaningful evolutionary context, but they tell us little about annexin function. Because the invertebrate and plant annexins do not have mammalian orthologs, analysis of annexin function in these simpler organisms may yield little information about the functions of the vertebrate family. Despite the difficulty in extracting functional insight from phylogenetic analysis, the fact that the family of 12 mammalian annexins have been tightly conserved over several 100 million years suggests that these proteins do indeed have important physiological roles.

B. Gene Structures

1. Conservation of genomic structure in the annexins

The structural organization of annexin genes is highly conserved, at least with regard to the positions of intron-exon boundaries (286). Most four-repeat annexins comprise 12–15 exons, the variation depending in large part on the length of the NH₂-terminal domains. Thus annexins A7 and A11 have long NH₂ termini encoded by up to six exons, whereas annexin A5 has a short NH₂ terminus encoded by two exons. For several annexins, particularly those with long NH₂ termini, alternative splicing adds to the diversity of annexin isoforms, which may in turn amplify functional variability within the family as a whole. Annexin A6, which has a duplicated tetrad core and therefore 8 conserved repeats, comprises 26 exons and is the largest annexin gene extending over ~60 kb (285). Within the conserved repeats, the tendency is for intron sizes to be considerably smaller than for those introns that lie between the first two or three exons. In many mammalian annexin genes, the first two or three introns are frequently 10 kb or more, whereas introns within the tetrad core are often <1 kb. Almost all alternative splicing of annexin RNA transcripts occurs within exons that encode the variable NH₂ termini. Given that annexin NH₂ termini contain binding motifs for protein partners and sites for posttranslational modifications, alternative splicing in these domains may contribute to the regulation of annexin function. Perhaps the best-characterized exception to this general rule is the alternative splicing of exon 21 in the seventh repeat of ANXA6. Exclusion of this 18-nucleotide exon gives rise to the characteristic appearance of annexin A6 on gel electrophoresis or Western blotting as a closely spaced polypeptide doublet (205).

Cladistic analysis of the mammalian annexin gene family reveals that annexins fall into three major groups. One group comprises the earliest vertebrate annexins,

these being A7, A11, and A13. A second group includes annexins A4, A5, and A8, and the third group comprises annexins A1, A2, and A3, with annexins A9 and A10 as somewhat distant members. Annexin A6 is more difficult to categorize, because the 5'-tetrad is most closely related to the A4,A5,A8 group and the 3'-tetrad to the A1,A2,A3 group. Nevertheless, the cladistic demarcation of these groups raises the question of whether or not they correspond to functional groupings. Despite the lack of clear functional data for most annexins, it is certainly possible to identify some cohesion within these groups. For example, annexins A1 and A2 both bind proteins of the S100 family, both are physiological substrates for protein serine/threonine and tyrosine kinases, and both are suggested to function in the endocytic pathway. In contrast, annexins A4 and A5 are more closely linked with regulation of ion flow (see sect. IVB), and annexin A6, which arguably belongs in both groups, has been proposed to have roles that impinge on both the endocytic pathway and regulation of Ca^{2+} signaling. Although such notions are purely speculative, the possibility that annexin clades may represent functional groupings might be relevant to the issue of functional redundancy and therefore the design of gene knock-out experiments.

2. Structural and regulatory features

The completion of the human genome sequencing project, together with increasingly sophisticated algorithms for detecting and analyzing DNA sequences, has led to the identification of unusual and interesting elements within certain annexin genes. The most detailed analyses have been conducted for the annexin A5 and A11 genes (10, 137, 251). The rat and mouse annexin A5 genes are unusual in having two promoters. In both species, the promoter proximal to the gene has a high GC content and lacks a TATA box; this is also true for the human and chick annexin A5 genes (48, 76, 227), and all have an abundance of binding sites for the ubiquitous SP1 transcription factor. In contrast, the distal promoter in the rat and mouse annexin A5 genes has a TATA box and conserved binding sites for transcription factors such as AP1, the glucocorticoid receptor, and MyoD. The significance of these observations is not clear, but the possibility exists that under certain conditions, perhaps during cell differentiation, proliferation, or transformation, transcription from the distal promoter results in an annexin A5 transcript that omits exon 2 in which the start methionine is located. Such a transcript would initiate translation within the first conserved repeat, and the protein thus generated would be predicted to lack the NH_2 terminus and have a molecular mass ~ 3 kDa smaller than the full-length protein. Although there are no reports of the natural occurrence of such an annexin A5 splice variant, in vitro studies of recombinant annexin A5 showed that a

mutant lacking the NH_2 terminus was unable to mediate a Ca^{2+} influx into phospholipid vesicles (20). Further investigation of these annexin A5 splice forms supported by a clearer understanding of annexin A5 function could reveal the significance of the two promoters for this gene.

The mouse annexin A5 gene also contains an endogenous retrovirus (251) located in intron 4. The MuERV-L sequence is believed to exist in only 100–200 copies in the mouse genome, although there is no evidence that its presence has any impact on the regulation of annexin A5 expression. The same gene also contains a region of Z-DNA (alternating purine-pyrimidine tract) in intron 6, and other Z-DNA sequences have been identified in the annexin A6 (287) and A11 genes (10). Given the abundance of repetitive elements in mammalian genomes, it is not surprising that *Alu* sequences, long interspersed nuclear elements (LINEs), mammalian-wide interspersed repeats (MIRs), and other less common elements have all been described in various annexin genes. For the most part, these appear to be no more than genomic landmarks, but in the case of annexin A6, a LINE-2 element named ALF (for annexin A6 LINE-2 fragment) was shown to function as a potent and highly specific T-cell silencer that may play a role in the downregulation of annexin A6 in T cells exposed to phorbol ester and calcium ionophore (69). This sequence was also shown to be present in other genes including interleukin-4 and PKC- β , both of which are similarly downregulated by this combination of agonists in T cells.

C. Regulation of Gene Expression

Annexins are frequently described as being ubiquitous. This is true in the sense that any single cell type appears to express a range of annexins, or an "annexin fingerprint," but no single annexin is expressed in all cells, implying that regulation of annexin gene expression is tightly controlled. Insight into the mechanisms of annexin gene regulation can be gained by direct investigation of the relevant gene promoters or by indirect analysis of annexin expression.

1. Annexin gene promoters

Relatively few vertebrate annexins have been subjected to detailed promoter analysis. Two annexin A1 genes have been investigated in pigeons, one of which is strongly inducible by prolactin, and both of which bind Y-box factors (237, 323). The promoters for these genes have been partially characterized, but the most detailed analyses have been performed on the human annexin A1 (70, 290), A6 (70), and A7 (301) gene promoters. The annexin A1 gene promoter contains CAAT and TATA boxes that were shown in deletion studies to be essential for minimal promoter activity. Analysis of the annexin A1

promoter also permitted investigation of the sensitivity to dexamethasone, a glucocorticoid analog. Although one study found the promoter to be unresponsive to treatment with dexamethasone (70), the other reported some level of induction (290). The different results may correspond to the use of different cell lines in each report or may reflect the exposure times used which in the former case extended to 8 h, and in the latter to 24 h. Despite these differences, both studies support the notion that annexin A1 is not a glucocorticoid primary response gene. Interestingly, studies on the cytokine responsiveness of the annexin A1 promoter showed the gene to be induced by interleukin-6 (290). This result is consistent with a role for annexin A1 in the acute phase response to inflammation.

The human annexin A6 gene promoter also contains CAAT and TATA boxes, although these are somewhat distal to the transcription start site and in this case the minimal promoter lies downstream of and does not include these elements (70). The most unusual feature of the annexin A6 promoter is a potent T cell-specific silencer located ~600 bases 5' to the transcription start site (69). This element was discussed in section mB2. The human annexin A7 gene promoter has also been serially dissected, and it lacks CAAT and TATA boxes but is GC rich and contains many SP1 binding sites (301). The phylogenetically related annexin A11 gene promoter also lacks CAAT and TATA boxes, and it too is GC rich (10). The presence of SP1 binding sites in most, if not all, annexin promoters so far examined, is consistent with their broad patterns of expression, but the existence of other regulatory elements, or in the case of annexin A5 an alternative promoter, suggests that under certain circumstances tight transcriptional control may be exerted.

2. Annexin expression in development and differentiation

The annexin literature contains many reports in which the expression of individual annexins is correlated with cell proliferation, differentiation, or transformation. For the most part, these studies do not reveal any great insight into annexin function, so in this review we focus on instances where annexin expression is developmentally regulated and in which the annexin exhibits a particularly striking and suggestive association with a certain cell type or cellular localization. Many of the clearest examples of potential functional correlates are to be found in the simple eukaryotes. In these cases, the presence of only a few annexins together with fewer cell types allows a more straightforward interpretation of the observations.

Hydra vulgaris expresses at least two annexins, of which annexin B12 (formerly annexin XII) is the best characterized. Annexin B12 was discovered first (270) and is clearly the major annexin in *Hydra*, being expressed at

an estimated 100-fold excess of a second as yet uncharacterized annexin. Immunofluorescence analysis of whole *Hydra* revealed the staining pattern of the two annexins to be segregated, with annexin B12 being largely confined to epithelial battery cells throughout the tentacles, with the second *Hydra* annexin being maximally located in the cytoplasm of nematocytes (269). The epithelial battery cells differentiate from gastric ectodermal epithelial stem cells, whereas nematocytes differentiate from interstitial cells. The battery epithelial cells and nematocytes are closely aligned in *Hydra* tentacles; both are motile and both are actively turned over. The presence of annexins in these cells therefore fits with current models of annexin function in cell matrix adhesion and cell membrane plasticity and remodeling. The nematode worm *C. elegans* is somewhat more complex in that it expresses four annexins (annexins B5 to B8), of which annexin B7 is the best characterized. Annexin B7 (originally nex-1) was discovered using classical protein biochemical techniques as a major 32-kDa polypeptide exhibiting reversible Ca^{2+} -dependent binding to phospholipids (53). Immunocytochemical and electron microscopic investigation of this protein revealed it to be associated with a well-defined subset of cell types and structures including the membrane systems of the secretory glands in the pharynx and the uterine wall and vulva. However, the most striking and most intense localization was to the convoluted membranes of the spermathecal valve. These membranes undergo major conformational changes as eggs pass through the valve, suggesting a possible role for annexin B7 in the regulation of membrane fluidity or membrane-membrane and membrane-cytoskeleton interactions. So far, only annexin B7 has been isolated and biochemically characterized, although annexins B6 and B8 (nex-2 and nex-3, respectively) have been shown by RT-PCR to be actively transcribed (57). Of these, annexin B6 has an unusually long NH_2 terminus similar to those that characterize annexins A7 and A11, indicating possible evolutionary linkage with the modern annexins. Although genetic studies have not yet been reported for these annexins, the emergence of RNA interference as a particularly effective technique for preventing gene expression in *C. elegans* (81) opens the way for a detailed and potentially highly informative analysis of annexin function in this organism.

Despite the prevalence of annexins in most eukaryotic species, relatively little is known about developmental regulation of annexin gene expression. A few studies have focused on mammalian annexin gene expression in the developing mouse brain (115, 116), the results of which revealed distinct patterns of temporal and spatial regulation of individual annexins. Other investigators reported developmental regulation of expression of at least four annexins in the loach *Misgurnus fossilis* (140) and the medaka fish *Oryzias latipes* (219). The latter study extended to whole mount RNA in situ hybridization to

examine the localization of four annexins during embryogenesis. As with the investigation of nematode annexins, this work identified tightly controlled annexin expression associated with specific organs or cell types. The annexin expressed earliest in medaka embryogenesis is a likely ortholog of annexin A11, which appears transiently in the prechordal mesendoderm and hindbrain. The three other medaka annexins, which may be orthologs of annexins A1, A4, and A5, all appear later in embryogenesis but in a range of tissues including liver, floor plate, and skin.

These studies represent only a small part of a large and fragmentary literature relating to the developmental, cell growth, and differentiation-dependent regulation of annexin expression. The picture that emerges from these studies is that for many annexins expression patterns are broad, which might imply fundamental roles in cell physiology for most members of the family. For the majority of annexins, functions suggested on the basis of observations made in a single cell type may therefore be incorrect. However, other annexins are undoubtedly restricted in their patterns of expression, sometimes with regard to cell and tissue development and sometimes in terminally differentiated cells. In these cases, exemplified by annexin A13, which is clearly involved in apical vesicle transport in certain polarized epithelial cells, it is more reasonable to predict a specialized cell type-specific function. In simpler eukaryotes with fewer annexins, of which several examples have been described here, there is now the prospect of combining genetics with developmental analysis to provide new information about function. Even if the absence of orthologous annexins in vertebrates presents a bar to direct extrapolation of function, the knowledge will impinge on the experimental design of genetic approaches to annexin function in species such as the mouse.

IV. FUNCTIONAL DIVERSITY WITHIN THE ANNEXIN FAMILY

A. Annexins in Membrane Traffic and Organization

A priori, annexins are intracellular proteins, and their denominating property, i.e., binding in a Ca^{2+} -regulated manner to negatively charged phospholipid surfaces, strongly argues for their functioning in conjunction with such phospholipids that are enriched in the cytoplasmic leaflets of cellular membranes. Exceptions are, however, disturbed cells undergoing apoptosis which display negatively charged phospholipids on their surface. In fact, it is the canonical annexin property of Ca^{2+} -dependent binding to acidic phospholipids which led to the introduction of annexin A5 as a diagnostic tool for labeling the surface of apoptotic cells. It has to be emphasized here that this diagnostic binding, albeit very useful, does not necessar-

ily have any implications for the *in vivo* function of annexin A5.

A large number of reports have provided circumstantial and also more direct evidence for annexins functioning in intracellular membrane organization. These include the detailed analyses of annexin distributions within different types of mostly cultured cells. A survey of these localization studies has been presented before (97). As a whole it appears that different annexins show strikingly different subcellular distributions and often reside in both a cytosolic and a membrane-associated pool, with a switch between the two typically being regulated by Ca^{2+} . The respective target membranes identified for different annexins are in most cases the plasma membrane and membranes of the biosynthetic or the endocytic pathway, and it has therefore been concluded that annexins function in these membrane trafficking steps.

More recently, studies on the intracellular location of annexins have been extended to live cells in approaches using GFP fusions. Such analyses revealed that annexin A1 associates with membranes of the endosomal, transferrin-accessible system of HeLa cells in a manner dependent on active Ca^{2+} binding sites being present in the protein. Moreover, it was shown that removal of the unique NH_2 -terminal domain of the protein results in a change in intracellular localization with the annexin A1-core being targeted to late endosomal membranes. Interestingly, this also appears to be specific since protein cores of other annexins (annexins A2 and A4) show different distributions in live HeLa cells (245). In light of the finding that proteolytic cleavage within the NH_2 -terminal domain of annexin A1 is likely to occur within cells (possibly triggered by phosphorylation, see above), the distinct localizations of full-length and NH_2 -terminally truncated annexin A1 could reflect distinct functions of the two species. Full-length annexin A2 localizes to the plasma membrane in living HeLa and HepG2 cells and also to membranes of the endosomal system in living BHK and rat basophilic leukemia cells (196, 245, 342). In the latter case, inspection by evanescent field microscopy of pinocytic vesicles formed under mildly hyperosmotic conditions revealed the presence of annexin A2-GFP in actin tails propelling these pinosomes. Moreover, formation of such pinocytic rockets is inhibited by overexpression of a mutant protein dominantly interfering with the annexin A2 localization, thus suggesting an important role of this annexin in organizing interfaces between certain membranes or membrane domains and the actin cytoskeleton (196). An annexin A7-GFP chimera was also localized recently to discrete intracellular structures, in this case in differentiated myoblasts (45). Upon subcellular fractionation, the annexin A7-containing membranes copurify with caveolin-3, but a role of annexin A7 in, e.g., the establishment or stabilization of tubules during myogen-

esis, remains to be shown and is not as yet evident in annexin A7-deficient mice (see sect. IV D).

1. Annexins in the biosynthetic pathway

A number of annexin proteins, including annexins A1, A2, A3, A6, A7, A11, A13, and B7, have been linked to exocytotic processes, more specifically post-*trans*-Golgi network events in the biosynthetic pathway (for reviews, see Refs. 30, 51, 97, 244). The most compelling evidence for such an involvement which go beyond the mere localization of the protein to secretory organelle membranes and/or the plasma membrane has been reported for annexins A2 and A13. Annexin A2 has been identified as a cytosolic protein that can retard the rundown of secretory responsiveness to Ca^{2+} stimulation of permeabilized chromaffin cells when added exogenously as a purified protein. In this assay, the annexin A2-S100A10 complex, which is localized in several cell types to the sites of plasma membrane/secretory granule membrane contact and/or intergranule contact (212, 276, 277) and which is capable of aggregating vesicles (see above), is more efficient than the monomeric annexin protein. Moreover, PKC phosphorylation of annexin A2 is required for the activity (263) (recall that PKC is activated upon nicotinic stimulation of chromaffin cells), and a peptide corresponding to an NH_2 -terminal annexin A2 sequence containing the PKC site inhibits catecholamine secretion in nicotine-stimulated chromaffin cells. Interestingly, it appears that the function of the annexin A2-S100A10 complex in chromaffin granule exocytosis is restricted to adrenergic cells as the S100A10 subunit is not expressed in the noradrenergic cell type (38) (for review, see Ref. 5). By correlation, it was also inferred that the annexin A2-S100A10 complex participates in lung surfactant secretion from alveolar type II cells as phenothiazines inhibited this secretion in a manner similar to their inhibition of annexin A2-S100A10-mediated vesicle aggregation (181). Yet another Ca^{2+} -triggered exocytosis event is the regulated secretion of different granule contents from endothelial cells, the most prominent being the von Willebrand factor stored in Weibel-Palade bodies. With the use of a whole cell patch-clamp approach combined with membrane capacitance recordings, it was shown that disruption of the annexin A2-S100A10 complex by a competitor peptide corresponding to the S100A10 binding site on annexin A2 markedly inhibits the Ca^{2+} -dependent exocytotic membrane fusion (161). Annexin A2 and S100A10 in endothelial cells are located at the plasma membrane and not found on Weibel-Palade bodies. Hence, it has been proposed that the complex indirectly functions in endothelial granule exocytosis by organizing the plasma membrane in a manner supporting the granule-plasma membrane fusion event (161, 213). In line with this proposal, annexin A2 is found concentrated at certain subdomains

of the plasma membrane and seems to provide a link between such subdomains and the actin cytoskeleton (see below).

Annexin A13, a myristoylated member of the family occurring in two NH_2 -terminal splice variants (a and b), is only expressed in a limited subset of polarized epithelial cells. Here, the 13b variant is localized specifically to the TGN, post-TGN carrier vesicles, and the apical plasma membrane. Antibodies directed against the unique exon encoded sequence in the annexin A13b splice form interfere with carrier vesicle transport to the apical but not the basolateral membrane domain of permeabilized Madin-Darby canine kidney (MDCK) cells, suggesting a very specific role of the protein in this transport step (77). Annexin A13b binds to sphingolipid- and cholesterol-rich domains (rafts) that bud off the TGN and that are destined for the apical plasma membrane in a transport step requiring a microtubule minus end-directed motor (214). The TGN budding is inhibited by annexin A13b antibodies and stimulated by myristoylated but not unmyristoylated annexin A13b (165). The other splice variant, annexin A13a, also stimulates apical biosynthetic transport but, in contrast to annexin A13b, also appears to be involved in the basolateral delivery in polarized cells (172). Due to their specific and in some cases regulated association with raft domains, the involvement of annexin A13 isoforms in post-TGN transport to the plasma membrane could be based on a membrane-organizing effect and thus could mirror the situation discussed for annexin A2 in Ca^{2+} -regulated exocytosis in endothelial cells. Thus the membrane-organizing capacity of annexins, which differs in extent, regulation, and target membrane between different members of the family, could represent the mechanistic basis of annexin effects in membrane transport events.

Other biosynthetic membrane transport steps affected by annexins include Ca^{2+} -dependent secretion in neutrophils, which in a streptolysin-O (SLO)-permeabilized cell system is stimulated by annexins A1 and A3 (254), and Ca^{2+} -induced insulin secretion in pancreatic β -cells, which in SLO-permeabilized cells is inhibited by annexin A11 antibodies (135). However, in all cases, live cell experiments, e.g., the injection of antibodies or interfering peptides/proteins or the generation of cells deficient in specific annexins combined with a subsequent characterization of transport steps in the modified cells, are required to corroborate and more specifically define the role of annexins in exocytosis.

2. Annexins in the endocytic pathway

Membranes of the endosomal system have also been identified as target structures for several annexins, and the mode of membrane binding has been studied extensively, both in terms of the specific target membrane

selected by the individual annexins and in terms of the structural requirements for membrane binding within the annexin molecule. Some of the literature describing annexin-endosome interactions has been reviewed before (97, 108). More recently, the specificity and thus most likely functional importance of such interactions has received support by a number of observations regarding annexins A1, A2, and A6. Live cell experiments analyzing the intracellular distribution of annexin-GFP chimeras have underscored the importance of the unique NH₂-terminal domain in positioning the individual annexin at certain target membranes (see above). Annexin A1, for example, is found on early, transferrin-accessible endosomes in BHK and HeLa cells, although some protein is also present on multivesicular endosomes, at least in mouse fibroblasts (92, 245, 275). Upon removal of the NH₂-terminal domain, the resulting annexin 1 core domain redistributes to late endosomes with the interaction still being Ca²⁺ dependent and specific, i.e., not observed with other highly homologous annexin cores (245, 275). This switch could also occur under certain cellular con-

ditions, e.g., when upon internalization of the EGF receptor annexin A1 becomes phosphorylated on Tyr-20 and thus more susceptible to NH₂-terminal proteolysis (see above). The proteolysis removes at least part of the NH₂-terminal domain and thus not only the sequence required for localizing the protein to early endosomes but also the binding site for the annexin A1 ligand S100A11. As a result, a putative heterotetrameric annexin A1-S100A11 complex capable of linking membrane surfaces would be disrupted. Together with the finding that the association of annexin 1 with multivesicular endosomes is regulated through phosphorylation by internalized EGF receptors, the proposed role of the protein in mediating the inward vesiculation in multivesicular endosomes (92) could be envisaged as depicted in Figure 5. Annexin A1 in its Ca²⁺-regulated complex with S100A11 (which is targeted to early endosomes by annexin A1, Ref. 274) could organize the limiting membrane of multivesicular endosomes *in statu nascendi*, i.e., early endosomes or budding endosomal carrier vesicles in the process of becoming multivesicular, in a way that supports the inward vesiculation.

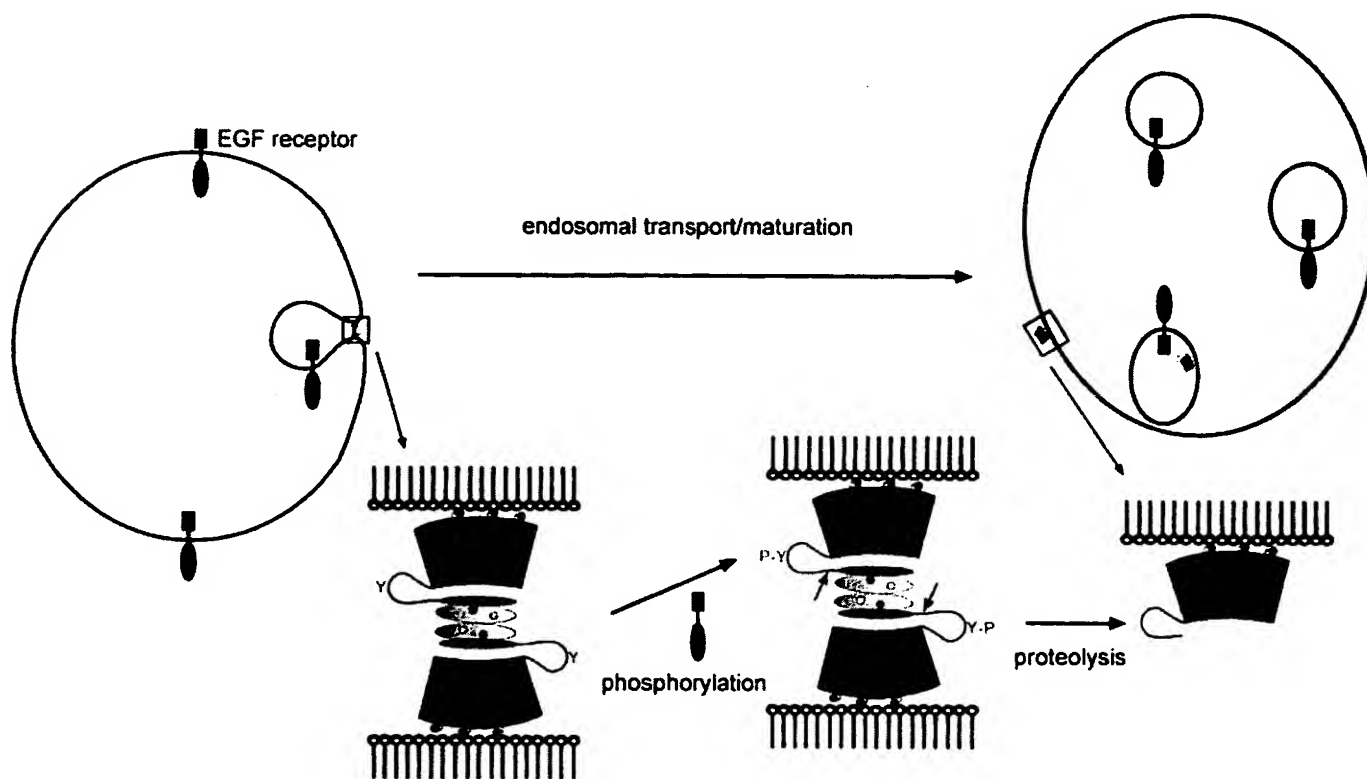


FIG. 5. Model describing a potential participation of annexin A1-S100A11 in the inward vesiculation process generating multivesicular endosomes. Owing to its potential membrane linking properties, the as of yet hypothetical heterotetramer of annexin A1 (red) and S100A11 (orange) could stabilize membrane interactions required for inward budding. Phosphorylation of Tyr-20 of annexin A1 by the internalized epidermal growth factor (EGF) receptor (92) renders the protein more susceptible for proteolysis occurring in the NH₂-terminal domain. Proteolytic cleavage would release the S100A11 dimer (together with the NH₂-terminal annexin A1 sequence) in a process that could accompany the actual membrane fission and internal vesicle release. As a result, an NH₂-terminal foreshortened annexin A1 would be present on multivesicular/late endosomal membranes, a localization in line with that of ectopically expressed annexin A1 core-green fluorescent protein (245).

Once the inward budding is about to be completed with the final fusion process, annexin A1 becomes phosphorylated by internalized receptors destined for degradation. This leads to limited proteolysis and thus disruption of the complex between annexin 1 and S100A11 in a process which might be coupled to the actual fusion. This activity might not be essential for endosome maturation/transport to occur but might facilitate the kinetics by providing a supporting membrane scaffold. Whether and how this model relates to observed stimulatory effects of annexin A1 on cell proliferation, EGF receptor synthesis, and phosphorylation remains to be established (62).

Annexin A2 was also identified on early endosomes (in addition to its localization at the plasma membrane and on certain secretory granules). Interestingly, its interaction with endosomal membranes occurs in the absence of Ca^{2+} and is primarily mediated by the NH_2 -terminal domain, which upon fusion to an annexin A1 core can transfer this unique property to the otherwise Ca^{2+} -sensitive annexin A1 (120, 145, 160). It is not clear whether the NH_2 -terminal annexin A2 sequence in question interacts with a protein receptor, e.g., a 200-kDa protein identified in ligand blotting experiments in certain clathrin-coated vesicle preparations (318), or specifically associates with a unique lipid structure, e.g., cholesterol-rich membrane domains that are required for this atypical annexin-membrane interaction (120, 160). Annexin A2 is not distributed evenly over the early endosomal compartment. Immunoaffinity approaches reveal that it is enriched on Rab11- (and also transferrin receptor-) but not Rab5-positive endosomes of Chinese hamster ovary (CHO) cells, whereas it is not found in transferrin receptor-positive recycling endosomes of polarized MDCK cells (93, 315). In BHK cells, on the other hand, endosomes isolated on immobilized annexin A2 antibodies are positive for the transferrin receptor but not the early endosomal antigen EEA1. This correlates with the ultrastructural colocalization of annexin A2 and the transferrin receptor on endosomes of BHK cells (341). Thus it appears that the fine tuning of annexin A2 localization within the early endosomal compartment is handled differently in different cells, possibly in conjunction with its proposed function as a scaffolding protein organizing and/or stabilizing rafts (see below).

A similar scenario could hold true for annexin A6, which has been localized to different endosomal membranes in different cells. In rat liver hepatocytes, it is found on an apical endocytic compartment, whereas it is present on late endosomes/prelysosomes of NRK fibroblasts (218, 235). Furthermore, some annexin A6 is also associated with the plasma membrane and clathrin-coated vesicles (179, 318), where it could function in facilitating coated pit budding. Earlier experiments employing immobilized plasma membranes and taking the loss of clathrin from such membranes as a measure for

coated pit budding reported an inhibitory effect when the cytosol required in this Ca^{2+} - and ATP-dependent reaction was depleted of annexin A6 (179). More recently, with the use of the same assay, it was shown that annexin A6 is only required for a certain type of coated pit budding, one sensitive to the cysteine protease inhibitor ALLN. The involvement of annexin A6 depended on its association with spectrin indicative of a function of the protein in remodeling the spectrin lattice as a prerequisite for efficient budding (148). Moreover, the same study revealed that microinjection of a truncated annexin A6 mutant inhibited low-density lipoprotein (LDL) uptake, thus paralleling the inhibitory effect of the mutant on coated pit budding in the *in vitro* assay. Other coated pit budding events (those not affected by ALLN) do not require annexin A6, thus providing a possible explanation for the finding that receptor-mediated endocytosis in annexin A6-negative A 431 cells is not stimulated by ectopic overexpression of the protein (288). On the other hand, ectopic overexpression of annexin A6 in CHO cells has a stimulatory effect on LDL receptor endocytosis, however, only when the receptor itself is overexpressed as well. In these experiments, annexin A6 remained associated with LDL-containing vesicles also at later stages of the endocytic pathway, possibly suggesting additional functions of the protein in late endocytic events (107). Such functions are likely to include trafficking events leading to LDL degradation, since microinjection of a mutated annexin A6 into NRK cells causes a retention of LDL in the prelysosomal compartment (234).

3. Annexins and phagocytosis

A translocation of different annexins to the membrane of maturing phagosomes has been observed in a number of phagocytic cells and has been taken as an indication for the involvement of the proteins in phagocytosis (previously reviewed in Ref. 97). Such observations have been extended in the recent past showing, for example, that annexins A1–A5 are present on isolated phagosomes from J774 macrophages, with the levels of annexin A4 (but not those of the other annexins) increasing with age of the maturing phagosomes (66). In another study using macrophage-like cells and analyzing Fc receptor-mediated phagocytosis, annexins A7 and A11 in addition to the members mentioned above were found to translocate to the phagosomes upon particle ingestion (230). In differentiated human monocytes, phagocytic uptake of *Brucella* bacteria (opsonized or nonopsonized) is accompanied by a recruitment of annexin A1-positive structures to the site of entry (164), whereas neutrophils phagocytosing yeast cells show a translocation of annexin A11 to the periphagosomal region (284). When the same cells take up an attenuated strain of *Mycobacterium tuberculosis*, the intracellular distribution of annexins A1

and A5 remains unchanged while annexins A3, A4, and A6 are translocated from the cytoplasm to the proximity of the bacteria containing phagosomes. In the case of annexin A4, this even occurs in Ca^{2+} -depleted neutrophils (189). Similar observations have also been made in human dendritic cells phagocytosing *M. tuberculosis* (170). Although these reports point to a role of the respective annexins in phagosome maturation, e.g., by facilitating certain transport or phagosome-endosome fusion steps, they so far only represent circumstantial evidence. We are still in need of functional approaches, e.g., analysis of phagocytosis in cells with an altered annexin expression or in the presence of dominantly interfering compounds, to make a conclusive connection between annexins and phagocytosis.

4. Annexins and the establishment/stabilization of membrane domains

Recent years have seen a formulation of the concept of membrane microdomains (rafts) being involved in aspects of membrane transport and also representing platforms for signaling events (for review, see Refs. 27, 281). Rafts are lateral assemblies of membrane patches rich in sphingolipids and cholesterol, which due to their high content of saturated hydrocarbon chains form a liquid-ordered phase in the more disordered background of glycerolipids containing unsaturated fatty acid chains. Biochemically, rafts (or detergent-resistant membrane complexes, DRMs) are defined by their resistance toward treatment with nonionic detergent in the cold and their ability to float to low density in sucrose density gradients. A number of membrane proteins have been described as raft associated. Typically, these proteins contain a certain fatty acid, isoprene or lipid moiety (e.g., glycosylphosphatidylinositol or GPI) which helps anchor them in the membrane raft. Most of the typical lipid and also protein components of rafts described to date are those found in the exoplasmic leaflet of the bilayer. The inner leaflet of these microdomains is less well characterized, although it appears to contain glycerophospholipids with a higher degree of saturation than the total plasma membrane (88) and also is likely to be enriched in cholesterol (281). Moreover, information on proteins associating specifically with the cytoplasmic side of rafts and thereby possibly regulating their assembly and dynamics is rather scarce. It is here where annexins could come into play as several members of the family have been identified in raft preparations and seem to associate with rafts in a manner which is in some cases but not strictly regulated by Ca^{2+} . Recent evidence in support of this view is summarized below for different annexins.

Rafts and membrane microdomains are not restricted to the plasma membrane but are also found in membranes of the biosynthetic (Golgi) and the endoso-

mal system (209, 279, 280). Annexin A1, a substrate of the EGF receptor kinase implicated in endosomal sorting of the receptor (see above), is also a substrate of PKC and localizes with the active enzyme to the endosomal compartment. After PKC activation initiated by exposure of cells to phorbol esters, downregulation of the enzyme appears to occur via translocation from the plasma membrane to endosomes, a process which is inhibited by caveolin binding drugs. Because PKC translocation and thus its colocalization with annexin A1 does not depend on the endosomal GTPase Rab5, it has been proposed that the transport is mediated through caveolae, cell surface invaginations containing a subset of lipid rafts which are formed by polymerization of the cholesterol-binding caveolin proteins (238; for review on caveolae, see Refs. 3, 136). Thus it appears that annexin A1 could also be involved in the downregulation of membrane-bound PKC through caveolae-mediated traffic to endosomes. Although evidence in support of this hypothesis is vague and circumstantial, several lines of research have strongly and more directly implicated annexin A2 in the organization and dynamics of membrane rafts. In several types of cells, annexin A2 associates with membrane rafts (biochemically defined as described above) in both a Ca^{2+} -dependent and a Ca^{2+} -independent manner. These include adrenal chromaffin cells where, after nicotine stimulation and in the presence of $1\ \mu\text{M}\ \text{Ca}^{2+}$, the protein translocates to Triton X-100 (TX-100)-insoluble membrane subdomains (262) as well as MDCK, polarized mammary epithelial, and smooth muscle cells where raft association is also Ca^{2+} dependent (8, 119, 216). On the other hand, BHK as well as bovine endothelial cells contain annexin A2, whose association with rafts is not sensitive to Ca^{2+} chelation but correlates with the amount of membrane cholesterol (50, 120). Interestingly, annexin A2 associated Ca^{2+} independently with BHK or endothelial cell membranes can be specifically released together with a subset of cortical cytoskeletal elements (actin, α -actinin, ezrin, and moesin) by sequestration of membrane cholesterol, suggesting a link between raft-associated annexin A2 and the membrane underlying actin cytoskeleton (120; König and Gerke, unpublished observations).

A role of annexin A2 as an organizer of membrane domains has gained further support in the case of the Ca^{2+} -dependently raft-associated protein. In the sarcolemma of smooth muscle cells, the dynamics of rafts, their lateral assembly, and association with the actin cytoskeleton appear to be regulated by changes in intracellular Ca^{2+} concentrations occurring during smooth muscle contraction. These changes correlate with the Ca^{2+} -dependent association of annexin A2 with membrane rafts and the translocation of annexin A6 to a membrane-cytoskeleton complex. Hence, it was proposed that an initial Ca^{2+} rise in smooth muscle cells triggers the binding of annexin A2 to lipid rafts and a clustering of these rafts

which is promoted by lateral annexin assembly. As a consequence, the spatial organization of, e.g., membrane receptors, is altered leading to a second Ca^{2+} transient further elevating intracellular Ca^{2+} . This is proposed to trigger a translocation of annexin A6 to the sarcolemma where it could be involved in the formation of bonds between the plasma membrane and the actin cytoskeleton (8). Annexin A2 is a F-actin binding protein itself (98) and thus could also participate more directly in the formation of membrane-cytoskeleton links. In a recent study it was shown to colocalize in basolateral lipid rafts of mammary epithelial cells with the hyaluronic acid receptor CD44. Antibody-induced clustering of CD44 leads to a similar clustering of annexin A2. Even more interestingly, clustering of annexin A2 at the cytoplasmic side of the membrane, which was achieved through ectopic expression of a *trans*-dominant annexin A2 mutant protein, led to the enrichment of CD44 in the annexin A2-positive patches. Moreover, a reorientation of F-actin toward the annexin A2 clusters was observed (216). A rearrangement of cortical actin can also be induced by certain pathogens, e.g., enteropathogenic *Escherichia coli* (EPEC), which induce the formation of actin-rich pedestals underneath their site of host cell attachment. Interestingly, bacterial attachment triggers a clustering of membrane raft components and a recruitment of annexin A2 to the attachment sites, suggesting that annexin A2 could participate in this process by stabilizing raft patches and their linkage to the actin cytoskeleton beneath adhering EPEC (343).

Collectively, these findings indicate that annexin A2 could represent a cytoplasmic protein peripherally associating with the cytoplasmic leaflet of membrane rafts, thereby stabilizing these domains and providing a link with the cortical actin cytoskeleton. Such a function would depend crucially on the membrane association of annexin A2 and therefore could be regulated in two ways, by membrane cholesterol content and local Ca^{2+} concentration, as indeed shown recently for annexin A2 associated with endosomal membranes (279, 341) or artificial liposomes containing cholesterol (7). This dual regulation mode reflects itself in the structure of the molecule as the NH_2 -terminal domain mediates a Ca^{2+} -independent interaction with cholesterol-rich membrane domains (160) and the COOH-terminal protein core harbors the Ca^{2+} -regulated binding site. As depicted in Figure 6, this could mean that some annexin A2 binds to cholesterol-containing membrane domains or specific receptors therein, already in the absence of Ca^{2+} . Once Ca^{2+} rises, e.g., during regulated exocytosis, at the sarcolemma upon smooth muscle cell activation or during certain types of endosomal fusion (129), additional annexin A2 molecules are recruited to the same sites providing a sort of membrane scaffold and, given they reside in complex with the S100A10 dimer, contact sites to other membranes or the cytoskeleton. In this view the annexin serves a more

structural role in the membrane periphery affecting indirectly a number of membrane transport events, thus functioning in a manner similar to that discussed for membrane skeleton proteins, e.g., spectrin or spectrin-associated proteins present on intracellular membranes (14, 197, 340).

As already mentioned, annexin A6 has also been implicated in the organization of membrane domains, in particular their association with the cytoskeleton in smooth muscle cells (8, 9). It could serve a similar function in mammary epithelial cells as a fraction of annexin A6 is recovered from the TX-100-insoluble fraction from these cells in a manner which appears to be regulated during polarization of the cells (171). Moreover, annexin A6 associates with raft fractions from synaptic plasma membranes in a Ca^{2+} -dependent manner (217). Whether and how this relates to the spectrin binding of annexin A6 and its proposed function in clathrin-coated pit budding remains to be shown. The sole annexin whose association with lipid rafts was shown to be functionally important for membrane trafficking events is annexin A13b (see also above). Together with its NH_2 -terminal splice variant, annexin A13a, it is the only member of the family that can be NH_2 -terminally myristoylated (77, 336). Annexin A13b is located in the apical compartment of polarized MDCK cells and found on the *trans*-Golgi network, at the apical cell surface and on exocytic apical carrier vesicles whose formation is inhibited by anti-annexin A13b antibody (165). As judged by several criteria including flotation in Optiprep gradients of TX-100-insoluble fractions obtained from apical carrier vesicles, annexin A13b clearly is a raft-associated protein, and it was proposed to function by binding to apical rafts that bud off the *trans*-Golgi network (165). Recently, it was also shown that annexin A13b participates in mediating the apical membrane targeting of the ubiquitin ligase Nedd4. The enzyme contains a C2 domain and associates with lipid rafts in a Ca^{2+} -dependent manner, most likely through an interaction of this Ca^{2+} -sensitive C2 domain with the raft-associating annexin A13b (231). Annexin A13a differs from the 13b variant by a deletion of 41 amino acid residues from the unique NH_2 -terminal domain and a somewhat broader intracellular distribution as it is also found at the basolateral membrane. Interestingly, its association with lipid rafts differs between the apical and the basolateral compartment of polarized epithelial cells with only the latter requiring Ca^{2+} . Moreover, and in contrast to annexin A13b, the 13a variant appears to be involved in the basolateral transport route (172). Thus different annexins seem to participate to differing extents in the organization of membrane domains (e.g., lipid rafts) with their association with these domains and thus their role in the process being regulated by changes in cytosol conditions (Ca^{2+} , pH?) and membrane lipid content (cholesterol, acidic phospholipids).

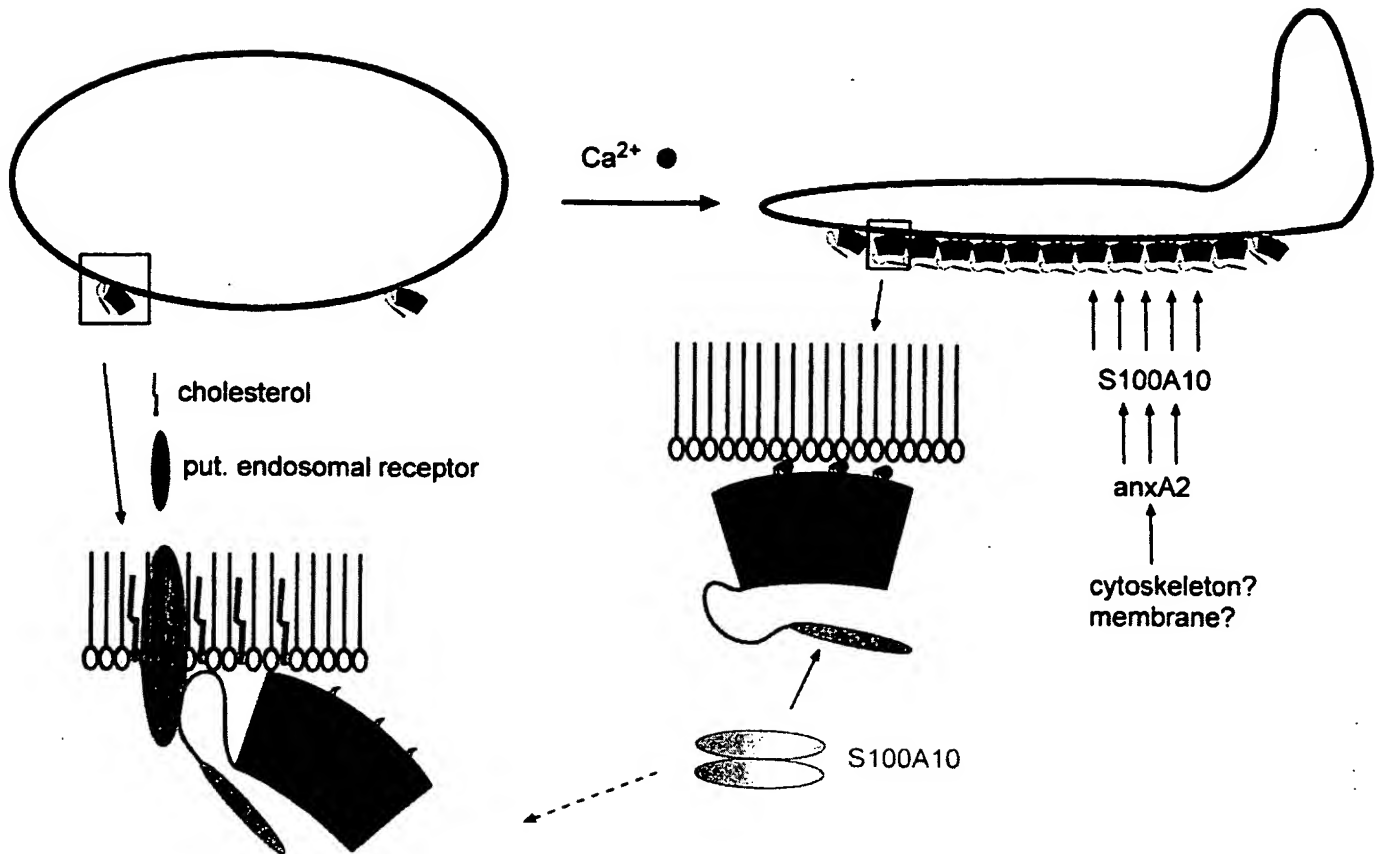


FIG. 6. Ca^{2+} -independent and Ca^{2+} -dependent interactions of annexin A2 with endosomal membranes. In the absence of Ca^{2+} , annexin A2 (blue) binds to endosomes in a manner requiring membrane cholesterol and a unique sequence in the NH_2 -terminal domain of the protein. The amount of endosome-associated annexin A2 increases significantly in the presence of Ca^{2+} , with the membrane binding now being driven by the canonical and Ca^{2+} -dependent membrane interaction. A high-density packing of annexin A2 molecules could be envisaged, which is in line with cryoelectron microscopy studies of annexin A2 bound to artificial bilayers (167). Such annexin A2 assemblies could stabilize certain membrane domains/organizations, and after S100A10-dependent formation of the annexin A2-S100A10 heterotetramer, these domains could be linked to a second membrane or cytoskeleton surface.

B. Annexins and Ion Channels

In section 11B we discussed the Ca^{2+} -dependent and Ca^{2+} -independent interactions between annexins and phospholipid membranes. In the former case, such interactions depend largely on the conserved annexin core and the Ca^{2+} -binding sites therein, and in both cases a degree of reversibility is a characteristic of membrane binding for most members of the annexin family. A major challenge in the annexin field has been to understand what annexins do once membrane bound. For some annexins there is increasingly persuasive evidence for roles in vesicle trafficking and/or membrane organization, but for most annexins, the functional significance of reversible membrane binding remains elusive. However, one intriguing possibility to have emerged in the last decade is that membrane-associated annexins might function either as ion channels and/or ion channel regulators. If correct, such activities would point to annexins as both effectors

and regulators of ion fluxes and place these proteins as key mediators in the control of cellular Ca^{2+} homeostasis.

1. Regulation of ion channel activity by annexins

The first study to implicate any annexin in the regulation of ion flow demonstrated that purified annexin A6 increased the mean open time and opening frequency of the sarcoplasmic reticulum ryanodine-sensitive Ca^{2+} channel (67). This modulatory activity appeared to be specific because there was no effect of annexin A6 on sarcoplasmic K^+ or Cl^- currents. These findings suggested that annexin A6 might have a role in the regulation of intracellular Ca^{2+} signaling in cardiomyocytes and skeletal muscle cells, cell types in which annexin A6 is known to be expressed at high levels. However, annexin A6 only exhibited this property when added to the luminal side of the membrane, and annexin A6 is generally considered to be a cytosolic protein. The problem of under-

standing the effect of annexin A6 in this system was further compounded by the subsequent observation that purified annexin A6 exhibits Ca^{2+} channel activity in artificial phospholipid membranes (19). This raises the possibility that changes in the Ca^{2+} permeability observed in sarcoplasmic reticulum membranes attributed to the ryanodine receptor may have been partly or wholly due to annexin A6 itself. Another study, this time demonstrating a cytosolic effect of annexin A6, showed that the introduction of a neutralizing antibody to annexin A6 led to an increase in K^+ currents in dorsal root ganglia (DRG) and spinal cord neurons, and to an increase in Ca^{2+} currents in DRG (211). A model in which displacement of annexin A6 from intracellular membranes leads to amplification of the Ca^{2+} signal is consistent with work showing that elevation of cytosolic Ca^{2+} induced by hydroperoxide is associated with translocation of annexin A6 from the cytoplasmic face of the plasma membrane (130). Another study, again supporting a role for annexin A6 in the regulation of Ca^{2+} influx, showed that ectopic expression of annexin A6 in epithelial A431 cells leads to attenuation of Ca^{2+} influx stimulated by EGF (84). A431 cells normally lack annexin A6 and exhibit a sustained elevation of intracellular Ca^{2+} after exposure to EGF. This work showed that whereas Ca^{2+} release from intracellular stores was unaffected by annexin A6, membrane hyperpolarization and consequent Ca^{2+} influx was inhibited. Interestingly, this inhibitory activity was only observed for the larger of the two splice forms of annexin A6, an effect that also directly correlated with splice variant-specific growth suppression in these cells.

Annexins A2 and A4 have also been demonstrated to modulate the activity of ion channels, although in both cases the effects were observed on Cl^- rather than Ca^{2+} channels. Annexin A4 is located at the apical cell plasma membrane in polarized colonic T84 cells, and in electrophysiological experiments it was found that introduction of purified recombinant annexin A4 into T84 cells through the patch electrode led to inhibition of the Ca^{2+} -induced Cl^- current (146). Consistent with this, an antibody to annexin A4 and also an antisense oligonucleotide to annexin A4 mRNA, both reduced the threshold for Cl^- current activation. Activation of the Ca^{2+} -dependent Cl^- conductance occurs in response to mobilization of Ca^{2+} from intracellular stores or, in patched cell experiments, by introduction of calmodulin-dependent protein kinase II (CaMKII). Inhibition of CaMKII using a specific peptide blocked the activation of the Ca^{2+} -dependent Cl^- channel observed with the antibody to annexin A4 (37). Annexin A4 is not believed to activate or inhibit CaMKII, nor to act as a substrate for the kinase, suggesting that it may inhibit the Cl^- channel through a direct protein-protein interaction. Regulation of the Cl^- channel by annexin A4 might also involve inositol 3,4,5,6-tetrakisphosphate [$\text{Ins}(3,4,5,6)\text{P}_4$]. In electrophysiological experiments in

T84 cells, the potency of $\text{Ins}(3,4,5,6)\text{P}_4$ as an inhibitor of the Ca^{2+} -dependent Cl^- channel was doubled in the presence of annexin A4, when annexin A4 was added at a concentration at which it has no inhibitory effect when used alone (339). These observations suggest a function for annexin A4 as part of a complex signaling pathway involving both protein kinases and intracellular Ca^{2+} . The involvement of annexin A2 in Cl^- channel regulation is less well characterized but no less intriguing. A single study reported that introduction of a synthetic peptide corresponding to the NH_2 -terminal domain of annexin A2 into endothelial cells via a patch electrode led to rundown of the osmotic-regulated Cl^- channel (213). In a control experiment, a similar peptide with a single amino acid substitution that eliminated S100A10 binding was shown to be without effect. These results imply that correct assembly of the annexin A2/S100A10 heterotetramer is required for the integrity of this current. The reason for this is unclear, but in many cells the annexin A2/S100A10 complex is stably associated with the submembraneous actin cytoskeleton, which in turn may have a functional interface with volume-sensitive Cl^- channels (VSCC). Indeed, specialized membrane-cytoskeleton compartments rich in cholesterol, caveolin, and ERM (ezrin, radixin, moesin) proteins are implicated in VSCC function and also contain annexin A2 (316). Furthermore, chicken DT40 cells containing a targeted disruption of the annexin A2 gene exhibit a more hyperpolarized resting membrane potential, consistent with dysregulation of chloride homeostasis (163). Collectively, these studies suggest that whereas annexin A4 may be involved in a direct molecular interplay with the Ca^{2+} -dependent Cl^- channel, the effect of annexin A2 on VSCCs might be an indirect consequence of a possible role in the regulation of membrane cytoskeleton interactions.

2. Annexin-dependent ion fluxes

The problem of defining specific functions for individual annexins is a recurring theme in annexin research. When annexin A1 (lipocortin) was first described as an inhibitor of phospholipase A_2 (PLA_2), this was widely accepted as an explanation for the apparent anti-inflammatory activity of annexin A1. However, as the family expanded, it rapidly became clear that all annexins can inhibit PLA_2 by Ca^{2+} -dependent sequestration of the phospholipid substrate (59). Although the inhibition of PLA_2 is therefore now believed to be nonspecific and probably nonphysiological, the anti-inflammatory activity of annexin A1 is nevertheless specific to this protein, and recently a more convincing mechanism has emerged to explain its activity (see sect. IV C1). A similar history surrounds the idea that annexins might function as ion channels. The first annexin to be shown to have Ca^{2+} channel activity was annexin A7 (233, 252), but this was soon

extended to annexin A5 (253), and in conjunction with X-ray crystallographic studies, most annexins have now been demonstrated to have Ca^{2+} channel activity (19, 29, 134, 232). Just as PLA_2 inhibition by annexins was shown to be the consequence of a shared biochemical property, so it appears that the Ca^{2+} channel activity of annexins may be due to a common structural feature, namely, the central hydrophilic pore in the annexin core (see sect. 1A1). However, in contrast to the anti-inflammatory activity of annexin A1, no annexin has ever been shown to exhibit Ca^{2+} channel activity in a living cell. Moreover, the general view of annexins as peripheral membrane binding proteins presents a conceptual obstacle to the idea that these proteins could function as ion channels. Despite this, the selectivity of the annexin ion channel for Ca^{2+} , together with pharmacological and electrophysiological properties that correspond to those of as yet uncharacterized Ca^{2+} channels in nonexcitable cells, ensures continuing interest in this subject.

To understand how annexins might function as Ca^{2+} channels, it is necessary to examine the way in which annexins interact with phospholipid membranes. In experiments using artificial lipid bilayers, the interaction between annexins and membranes depends on four key variables; these are the phospholipid composition of the bilayer, the concentration of the annexin, the concentration of Ca^{2+} , and the transmembrane voltage (125). For ion channel activity to occur, the annexin must first bind to the membrane, and then some poorly understood gating process must follow that leads to Ca^{2+} flux. Because the first step depends on the availability of free Ca^{2+} , the observation that as Ca^{2+} concentration increases the Ca^{2+} channel activity decreases may appear counterintuitive. However, a Ca^{2+} binding site in the proposed channel makes the current-voltage curve for annexin A5 nonlinear (253), and it is established that annexin A5 becomes more tightly membrane bound at elevated Ca^{2+} levels and that this has the effect of stabilizing the membrane (104, 210). For Ca^{2+} channel activity to occur, membrane destabilization is required. In addition, several annexins display anticooperativity of binding, such that as the protein concentration increases, so membrane binding decreases (125). Annexins also bind to membranes with higher affinity at increasingly negative resting membrane potentials, although in the absence of Ca^{2+} the membrane potential negativity required for annexin binding extends well out of the accepted physiological range. However, the requirement for a negative potential difference is reduced as the free Ca^{2+} concentration increases. In applying a reductionist approach to the analysis of annexin ion channel activity and membrane binding, one should keep in mind that some of these variables may have little influence *in vivo*, whereas other factors (such as other divalent cations, posttranslational modifications, and cofactors) could well come into play. Also, when one con-

siders the issue of annexin-specific channel activity, it is important to note that with regard to these four variables annexins behave quite differently. For example, whereas high free Ca^{2+} concentration leads to tight binding of annexin A5 to membranes, this is not the case for either annexins A6 or A7. Thus, under conditions of high free Ca^{2+} , annexins A6 and A7 display more Ca^{2+} channel activity than annexin A5 (125).

Recent studies have added a fifth key variable, namely, pH, to the parameters that govern the interactions between annexins and phospholipid membranes (see sect. 1B). Several investigators have reported that mildly acidic pH favors the Ca^{2+} -independent binding of annexins to phospholipid membranes (158, 168), and spin labeling experiments using derivatized recombinant *Hydra* annexin B12 showed that protonation led to gross changes in the structure of the protein, proposed to correspond to the assembly of transmembrane α -helices which form a new membrane-spanning molecule with a central hydrophilic pore (168) (Fig. 4). Subsequent experiments showed that at pH 5.0 and below, annexins A5 and B12 both label with a photoactivatable agent that partitions into the hydrophobic domain of a lipid bilayer and that both proteins form ion channels at low pH but not at neutral pH (138). Further studies supporting the idea that annexin B12 forms a transmembrane structure showed that when added to the opposite side of the bilayer to the purified annexin, pronase caused an increase to preannexin values in the conductance of the probe nonactin (289). The conclusion of these carefully controlled studies is that the pronase effect can only be explained if annexin B12 forms a structure that spans the lipid bilayer. The key points to emerge from these studies is that the pH-dependent insertion of annexins into lipid bilayers is reversible and that it is inhibited by free Ca^{2+} . The reversibility is significant because it suggests that a dynamic equilibrium may exist between the soluble cytosolic annexin, the peripherally membrane-bound form, and the membrane-inserted form. At neutral pH it can be argued that the equilibrium is heavily biased away from the membrane-inserted form, which is consistent with reports that channel activity for annexins, despite being widely reported at neutral pH, is actually exceedingly rare (125, 138). Despite the topographical appeal of this model, there is resistance to the idea that the tightly folded α -helical annexin core could unfold and insert into membranes. Nevertheless, molecular rearrangements of this sort are not unprecedented because members of the Bcl family of pro- and antiapoptotic proteins undergo similar pH-dependent insertion into acidic phospholipid bilayers (198, 268, 271). A second problem concerns the requirement for a pH < 6.0 to induce annexin membrane insertion, given that in healthy living cells the intracellular pH probably never falls below 6.5.

In considering these problems there is a need to

interpret the findings of *in vitro* studies in terms of how annexins might function as ion channels in living cells. Thus, if annexin A5 does function as a Ca^{2+} channel, the expectation might be that such an activity would be favored under conditions of intracellular acidification and membrane hyperpolarization. In B lymphocytes, exposure to physiological concentrations of peroxide leads to a Ca^{2+} influx accompanied by membrane hyperpolarization and intracellular acidification from pH 7.3 to pH 7.0. Other Ca^{2+} mobilizing agonists such as thapsigargin or antibody to the B cell receptor do not change membrane polarity or cytosolic pH. Targeted disruption of the annexin A5 gene in B cells leads to loss of the Ca^{2+} influx component of the peroxide response, but Ca^{2+} responses to other agonists are unaffected in such cells (163). Significantly, this study also showed that in experiments using a photoactivatable agent to label annexin A5 in synthetic lipid bilayers, exposure of the protein to peroxide led to membrane insertion independently of any requirement for acidification. These results support a role for annexin A5 either as a Ca^{2+} channel or as an essential signaling intermediate in a Ca^{2+} influx pathway. Further cellular evidence for a Ca^{2+} channel role for annexin A5 comes from studies on mineralizing chondrocytes (157). The deposition of new bone by chondrocytes is mediated by matrix vesicles, PS-rich structures with a proteinaceous core that binds Ca^{2+} upon entry, to form calcium phosphate crystals. The Ca^{2+} influx channels in matrix vesicles share many properties with annexin A5 Ca^{2+} channels *in vitro*. Thus both are blocked by Zn^{2+} , activated by ATP, and inhibited by GTP, and maximal Ca^{2+} influx is observed when annexin A5 is associated Ca^{2+} -independently with the vesicles (4). These studies, together with those in B cells, provide evidence that annexin A5 may indeed function as a Ca^{2+} channel under certain conditions. However, definitive proof may be difficult to obtain, and even if this is eventually established, the question of whether or not annexin A5 functions as a peripherally bound or integral membrane protein may take longer to answer.

C. Extracellular Annexin Activities

Although annexins *per se* are intracellular proteins, i.e., they localize to the cytoplasm and/or intracellular organelles and lack signal sequences guiding them to the canonical secretory pathway, a number of properties have been attributed to extracellular annexins. Although it is still a mystery whether and to what extent regulated secretion of annexins can occur, the recent description of cell or extracellular matrix receptors for different annexins supports the physiological (or pathophysiological) meaning of such extracellular properties. The more recent findings along these lines will be summarized below. For a detailed and more complete account of extracellular

annexin activities described in the past, the reader is referred to the review by Raynal and Pollard (244).

1. Annexin A1 and the control of inflammatory responses

Annexin A1 (lipocortin I) has long been suggested to function as a cellular mediator of anti-inflammatory glucocorticoids since its expression and secretion in several cell types is induced by glucocorticoids (see, for example, Refs. 46, 228, 308) and since exogenously administered protein exhibits anti-inflammatory activities in several animal models of inflammation (for reviews, see Refs. 85, 86, 260). Although this effect has initially been attributed to the capability of annexin A1 to inhibit PLA_2 and thus the production of eicosanoids, it has become clear more recently that the anti-inflammatory activity of the protein is most likely due to interference with granulocyte recruitment, migration, and/or activation at sites of inflammation (for reviews, see Refs. 105, 221, 222).

Inflammatory processes are characterized by a localized emigration of neutrophils and other leukocytes from the blood into the inflamed tissue. This process crucially depends on strictly regulated interactions between the leukocytes and the endothelial lining of the vessels ranging from leukocyte rolling on the endothelium to firm adhesion of the blood cells and finally their transendothelial migration (for reviews, see Refs. 176, 298). The transition from rolling to firm adhesion of neutrophils requires their activation by soluble or surface-bound mediators like chemokines and other chemoattractants that also provide a gradient along which neutrophils navigate toward the site of inflammation. Glucocorticoids delay this extravasation of leukocytes, and several lines of evidence have implicated annexin A1 as a central mediator of this glucocorticoid effect. In neutrophils adhering to activated endothelium, annexin A1 is mobilized and externalized through an as yet unknown mechanism resulting in a downregulation of neutrophil transmigration (224). Most likely this is due to an inhibitory effect on transmigration of the released annexin A1, which has been described *in vitro* and *in vivo* with exogenously applied protein as well as peptides derived from the unique NH_2 -terminal domain of annexin A1 (for reviews, see Refs. 105, 221, 222). Such NH_2 -terminal peptides typically covering residues 1–25 of the annexin A1 sequence in their NH_2 -terminally acetylated form (Ac1–25), as well as the entire molecule, are also capable of restricting leukocyte migration and thus tissue damage in animal models of splanchnic artery occlusion/reperfusion and myocardial ischemia/reperfusion injury (56, 58). Thus *in vitro* systems as well as a number of animal models have proven the antimigratory effect of annexin A1 (and the unique NH_2 -terminal peptides) on leukocyte extravasation, and the protective influence of the protein/peptides in several pathophysiological situa-

tions has sparked interest in their pharmacological potential.

Given these well-established effects of annexin A1 on neutrophil extravasation, two questions arise. First, what is the mechanistic basis of the effect, and second, can endogenous annexin A1 function as a modulator of leukocyte extravasation, e.g., by downregulating inflammatory responses to prevent chronic inflammation? To explain the antimigratory effects, a direct action of extracellular annexin A1 on leukocytes had long been postulated and indeed been proven in a number of studies. Among other things, the NH₂-terminal annexin A1 peptide Ac1–25 was shown to affect directly a number of neutrophil functions, and preincubation of neutrophils with the annexin A1 peptide resulted in decreased migration of these cells through untreated endothelial monolayers (226, 331). Proteinaceous binding sites for annexin A1 have been shown to exist on human monocytes and neutrophils as well as on monocytic U937 cells, with bound annexin A1 in the latter case being colocalized and coimmunoprecipitated with $\alpha_4\beta_1$ -integrins (75, 291). Compelling evidence has been obtained recently for a specific binding of annexin A1 (and its NH₂-terminal peptides) to the formyl peptide receptor (FPR) on neutrophils. FPR is a heptahelical, G protein-coupled receptor recognized by bacterial peptides of the prototype formyl-Met-Leu-Phe (fMLP) which are thought to provide the chemoattractant gradient for guiding neutrophils toward the site of bacterial infection. When employed in an *in vitro* transmigration model, antagonistic fMLP peptides were shown to reverse the inhibitory effect of annexin A1 (and its NH₂-terminal peptide) on neutrophil transmigration, and ectopically expressed FPR was specifically triggered by the annexin A1 peptides (331). As the annexin A1 peptides can also desensitize the FPR on neutrophils toward fMLP challenge, it appears that their inhibitory action on neutrophil extravasation is based on their binding to and activation/desensitization of the FPR. Such a role of the FPR in mediating the anti-inflammatory effect of annexin A1 has been corroborated by *in vivo* experiments employing FPR knockout mice (225). FPR activation by annexin A1 peptides can occur also in nonmyeloid cells leading, e.g., in human lung A549 cells, to the induction of acute phase protein expression, thus arguing for a more widespread role of the annexin A1-FPR interaction (U. Rescher, A. Danielczyk, A. Markoff, and V. Gerke, unpublished observations).

Although this provides a mechanistic explanation for the pharmacological action of exogenously applied annexin A1 (or NH₂-terminal annexin A1 peptides), it is not clear whether such scenarios could also hold true for endogenously released annexin A1. Regulated externalization of annexin A1 has been described for endothelium-adherent leukocytes (224, 291), but it is not clear whether the amounts released are sufficient to trigger the

FPR. Moreover, with the mechanism of secretion unknown, it remains possible that the extracellular annexin A1 stems at least in part from lysed cells. Thus we are in need of identifying in molecular terms a system promoting regulated annexin A1 release. The protein does not follow the classical secretory pathway because its release is not inhibited by brefeldin A, monensin, or nocodazole (228). However, in neutrophils, some annexin A1 colocalizes with gelatinase in gelatinase storage granules, and this appears to be released to the cell surface upon adhesion of the neutrophils to endothelial monolayers (223). Nonetheless, it is not clear how the protein reaches the lumen of the granules and whether this relates to the Ca²⁺-dependent secretion of annexin A1 in activated human neutrophils, which was described recently in a proteomic approach (25). Whatever model is favored, for active secretion to occur the transport of annexin A1 across the bilayer (that of the plasma membrane or of internal membranes of secretory organelles) is required, and it is not yet clear how that can happen. In this context, the pH-induced conformational change allowing annexin A1 to insert into the bilayer (see above) might be hypothesized, but it remains to be shown whether such insertion (possibly followed by a release at the other side of the bilayer) can occur under physiological conditions met in cells.

2. Extracellular activities of other annexins

This section focuses on recent developments relating to extracellular activities of annexins A2 and A5. Extracellular annexin A2 has been described as a surface-bound receptor for a number of different molecules, indicating that it might act as a more general surface anchor and not as a specific receptor of a given ligand. Best studied is probably the interaction of elements of the plasmin/plasminogen activator system with annexin A2 present on the surface of endothelial cells. Annexin A2 binds both plasminogen and the tissue plasminogen activator (tPA), with the former interaction being inhibited by the atherogenic lipoprotein A and the latter being blocked by homocysteine (for review, see Ref. 114). The tPA binding site on annexin A2 has been mapped to the NH₂-terminal domain and encompasses residues 7–12. This sequence contains an accessible cysteine residue at position 8 (142), and it is this cysteine that is derivatized by homocysteine leading to the reduction in tPA binding (112). Thus annexin A2 present on the surface of endothelial cells could play a role in fibrinolytic surveillance by anchoring key components of the fibrinolytic cascade. Increased homocysteine levels would interfere with this annexin A2 action, thus providing a possible explanation for a link between increased homocysteine levels and the risk of atherogenesis (113). The antithrombogenic action of annexin A2 could also be directly associated with the

hemorrhagic disorder in patients suffering from acute promyelocytic leukemia, as will be discussed below. However, we have to take into account that annexin A2 is probably not the only cell surface receptor for tPA on the endothelium (90). Moreover, in addition to binding to tPA and stimulating the conversion of plasminogen to plasmin, annexin A2 (in complex with its S100A10 ligand) can also inhibit the plasmin-mediated lysis of fibrin polymers and can inhibit plasmin activity by stimulating its autolytic digestion (41, 42, 82). Thus the relation between extracellular annexin A2 and the regulation of thrombogenesis is likely to be complex.

Annexin A2 present on the surface of endothelial cells has also been described to represent the binding site for β_2 -glycoprotein I, a phospholipid-binding protein from plasma known as an autoantigen in the antiphospholipid antibody syndrome. This interaction indicates that the association of β_2 -glycoprotein I with endothelial cells is not mediated directly by phospholipids but depends on annexin A2 (186). Other ligands for cell-surface bound annexin A2 are procathepsin B (on human breast carcinoma and glioma cells) (187) and a vitamin D analog that appears to use annexin A2 as a receptor on rat osteoblast-like cells with the interaction being inhibited by Ca^{2+} (12, 13). It is not clear whether and how this relates to the finding that gene expression of annexin A2 itself is up-regulated by 1,25-dihydroxyvitamin D_3 and that extracellular annexin A2 stimulates the proliferation of osteoclast precursors by activating T cells to secrete granulocyte-macrophage colony stimulating factor (194). However, as already discussed above for annexin A1, it remains to be shown whether, how, and to what extent annexin A2 is actively exported from, for example, endothelial cells and whether such export can be regulated under physiological conditions. Moreover, for annexin A2 acting as a cell surface receptor, it requires anchoring on or in the cell membrane, the mechanism for which has so far not been elucidated.

Several functions have also been proposed for extracellular annexin A5. It was originally described as an anticoagulant protein, and this activity most likely depends on its Ca^{2+} -regulated binding to anionic phospholipids, possibly those exposed on the surface of activated platelets or endothelial cells. This binding could interfere with the accessibility of such sites for coagulation factors, thereby preventing their local accumulation/activation (for review, see Ref. 244). More recently, antibody-mediated inhibition of an anticoagulant property of annexin A5 has been proposed to occur in recurrent pregnancy losses observed in patients with antiphospholipid syndrome (for review, see Ref. 240). As discussed in detail in section v, annexin A5 binds to the apical surface of placental syncytiotrophoblasts and by shielding these coagulation-promoting surfaces could be important for the maintenance of blood flow through the placenta. Anti-annexin A5 anti-

bodies that are found in patients with antiphospholipid syndrome (and also in the sera of patients suffering from systemic lupus erythematosus, Ref. 266) decrease the ability of annexin A5 to form a shield on the trophoblast surface and could thus cause placental thrombosis (240, 241, 243, 333). In vitro annexin A5 was also shown to interact with the NH_2 -terminal (extracellular) domain of polycystin 1, the major protein affected in autosomal dominant polycystic kidney disease, although the in vivo relevance of this interaction remains to be established (A. Markoff, N. Bogdanova, U. Rescher, F. Qian, B. Dworniczak, G. Germino, Y. Horst, and V. Gerke, unpublished observations). Moreover, the protein is capable of binding to components of the extracellular matrix, in particular types II and X collagens. Such binding could relate to the finding that annexin A5 (as a Ca^{2+} channel, see above) affects the Ca^{2+} uptake in chondrocyte-derived matrix vesicles in a manner depending on the binding to collagens types II and X (for review, see Ref. 329). The annexin A5 knock-out models underway should answer the question whether annexin A5 has a crucial role to play in such processes.

D. Annexin Transgenesis and Targeted Gene Disruption

Modulation of gene expression by either transgenic expression or targeted gene disruption has been used in many species to gain insight into protein function. Given the historical difficulty of assigning functions to annexins, it is perhaps surprising that such studies appeared relatively recently in the annexin literature. This might have been partly due to the expectation that annexins would be discovered in yeast, in which genetic manipulation is facile, or could reflect an unwillingness by funding agencies to support what are seen to be risky projects. Despite the absence of annexins in yeast, the presence of annexins in roundworms and insects leads one to hope that eventually mutants will be established in these organisms that might give clues to function. Indeed, the first genetic experiment involving annexins reported that disruption of annexin C1 in *Dictyostelium* did not lead to any adverse effects when cells were cultured under normal conditions (71). However, the cells were significantly disadvantaged when cultured in low external Ca^{2+} , exhibiting defects in growth, motility, and chemotaxis, observations that support a role for annexin C1 either as a Ca^{2+} mediator or as a regulator of Ca^{2+} homeostasis (72). The only transgenic studies reported to date describe the effects of overexpression of annexin A6 targeted to cardiomyocytes. These animals display left ventricular dilation and cardiomyopathy and die of heart failure at a relatively young age. Studies on isolated cardiomyocytes from young animals revealed that overexpression of annexin A6 was associ-

ated with a lower resting level of cytosolic Ca^{2+} and smaller Ca^{2+} spikes associated with attenuation of contractility when the cardiomyocytes were electronically paced (109). These results correlate inversely with studies on annexin A6 expression in failing human hearts (described in sect. vA2). Perhaps unexpectedly in view of these results, annexin A6 null mutant mice are healthy and fertile and fail to exhibit any cardiovascular defects with regard to heart rate, blood pressure, and circulatory collapse in response to endotoxic shock (121). However, in certain respects, the mouse is not an ideal model for human cardiovascular function, partly because the mouse heart beats almost maximally so that any "enhancement" in cardiomyocyte contractility would be difficult to detect. Indeed, in isolated cardiomyocytes from annexin A6 knock-out mice in which contraction rate can be regulated, significantly increased mechanical properties linked to altered Ca^{2+} handling are observed, when compared with cells from wild-type littermates (G. Song, S. E. Moss, and M. Duchen, unpublished observations).

The lack of an overt phenotype in annexin A6 knock-out mice contrasts with studies on annexin A7. Targeted disruption of annexin A7 in mice led to embryonic lethality at day 10 due to cerebral hemorrhage. Mice heterozygous for the mutation are viable and fertile but have defects in insulin secretion, although the insulin content of islet cells is considerably higher than in wild-type mice (299). Investigation of this phenotype revealed that expression of the inositol 1,4,5-trisphosphate (InsP_3) receptor was also reduced, leading to the failure of InsP_3 to release intracellular calcium. Although this observation explains the phenotype and establishes a potential link between annexin A7 and Ca^{2+} signaling, it is not clear why a partial reduction in annexin A7 expression levels should be accompanied by a parallel loss of InsP_3 receptor expression. In a separate annexin A7 gene knock-out project, the null mutant mice were found to be healthy and viable and no different from control mice with regard to glucose-stimulated insulin secretion, although cardiomyocytes isolated from these mice showed alterations in their frequency-induced shortening (122). However, as observed with annexin A6 knock-out mice, cardiomyocytes lacking annexin A7 manifested disturbances in power-contraction frequency. Although there are other examples of gene disruption studies in which different groups reported distinct phenotypes, and in the case of annexin A7 there were differences in design of targeting constructs and disruption sites, reconciliation of the embryonic lethality and minimal phenotype reported by these two groups represents a considerable challenge. In other ongoing studies, mice containing a targeted disruption of the annexin A1 gene are reported to be viable and healthy (R. Flower, personal communication), and matings between mice heterozygous for a disrupting mutation of the annexin A5 gene yield viable pups (K. von der Mark and E.

Pöschl, personal communication). Although systematic analysis of annexin null mutant mice is therefore still at an early stage, these preliminary observations exemplify not only the potential value of gene knockout in exploring annexin function, but also the need to keep an open mind with regard to the interpretation of phenotype.

V. ANNEXINS AND HUMAN DISEASE

A. Disorders of the Heart and Circulation

1. Annexins and cardiovascular biology

As yet, no human diseases have been described in which a mutation in an annexin gene is a primary cause. However, there is evidence that through changes in expression, properties, or localization, annexins may contribute to the pathophysiology of disease phenotypes. The most striking examples of these secondary effects have been termed "annexinopathies" (239) and are characterized by dysregulation of what may be the normal anti-thrombotic properties of extracellular annexins. As discussed earlier, annexin A2 on the surface of vascular endothelial cells can act as a receptor for tPA, so its presence would favor a thrombolytic environment and might therefore make a positive contribution to the overall health of the vasculature. Conversely, changes in endothelial cell behavior leading to reduced cell surface expression of annexin A2 or metabolic changes that chemically modify annexin A2 could be hypothesized to lead to predisposition to cardiovascular disease. Of numerous risk factors implicated in atherothrombotic vascular disease, elevated plasma homocysteine is of particular relevance. Homocysteine is a metabolic derivative of dietary methionine and was shown to incorporate into the NH_2 terminus of annexin A2 replacing Cys-8, a key residue in mediating the tPA processive activity of annexin A2 (113). In this study, substitution of Cys-8 with homocysteine led to a ~65% loss in tPA binding capacity, consistent with the development of reduced thromboresistance in homocysteinemic individuals. A second risk factor with a well-established link to cardiovascular disease is oxidative stress. In a recent study, annexin A2 was identified as a major cellular target for glutathiolation in response to oxidative stress induced by hydrogen peroxide or $\text{TNF-}\alpha$. Interestingly, the reactive cysteine identified as the target for glutathione in this study was again Cys-8 in the annexin A2 NH_2 terminus (304). A third risk factor shown in epidemiological studies to be linked to cardiovascular disease is alcohol consumption, although the effect of moderate intake is protective rather than deleterious. One recent study reported that vascular endothelial cells cultured in the presence of low concentrations of ethanol exhibited a doubling of cell surface fibrinolytic activity

that correlated with a sustained increase in annexin A2 mRNA and protein (306). Although these studies do not prove that annexin A2 is directly involved in the development of or susceptibility to cardiovascular disease, they support the idea that metabolic changes known to influence risk could be mediated at least in part by chemical modifications in and transcriptional regulation of annexin A2.

2. Heart disease

Because of the importance of Ca^{2+} homeostasis in the heart, and the abundance of annexins A2, A5, and A6 in cardiomyocytes and the supporting cellular infrastructure, there is considerable interest in elucidating the roles of cardiac annexins. Immunocytochemical studies identified annexins A5 and A6 in both myocytes and nonmyocytes in a variety of species, and most of these reported a concentration of annexin A5 with the sarcolemma and Z line in cardiomyocytes (141, 183, 191, 317, 332) and a preferential localization of annexin A6 with the sarcolemma and intercalated disks (184, 191, 317). In addition, annexin A5 has been reported to be localized to the nucleus and nuclear membrane in neonatal differentiating myocytes and becomes associated with the sarcolemma only in terminally differentiated adult cells (183). In a parallel study, annexin A6 was found colocalized with uncharacterized subcellular structures in neonatal myocytes and was only associated with the sarcolemma in adult cells (184). Although the function of cardiac annexin A5 is not known, the benzothiazepine derivative K201, which blocks the Ca^{2+} channel activity of annexin A5 in vitro (150), has been shown to protect the myocardium against the cytotoxic effects of Ca^{2+} associated with ischemia/reperfusion injury (110).

Several other lines of evidence suggest that annexins have important functions in the heart. The most striking of these is the demonstration that cardiomyocyte-specific overexpression of annexin A6 in transgenic mice leads to hypertrophy and heart failure (109) (see also sect. IV D). This study prompted several investigations into annexin expression in heart disease, both in a variety of animal models and also in humans with end-stage heart failure. The picture that emerges from these studies is that the expression levels of annexins A2, A5, and A6 are largely unaffected during ventricular hypertrophy (141), but that during end-stage heart failure the levels of annexin A6 fall in cardiomyocytes whereas those of annexins A2 and A5 rise (292). Other investigators reported similar rises in annexins A2 and A5 during heart failure, but restricted to nonmuscle cells (18), and also elevation of annexin A6 in interstitial tissue (317). The significance of these changes is not clear, but given that overexpression of annexin A6 reduces the contractility of cardiomyocytes (109) and that the opposite effect is observed in annexin A6 null mutant

mice (Song et al., unpublished observations), it is possible that downregulation of annexin A6 during heart failure is a form of molecular compensation that favors improved cardiomyocyte function.

3. Annexins as anticoagulants

As discussed in section VA1, there is growing evidence that annexin A2 has an antithrombotic role at the endothelial cell surface. More direct evidence for the involvement of annexin A2 in disease pathology emerged from studies on leukemic cells from patients with acute promyelocytic leukemia (APL). Patients with APL exhibit an increased tendency to hemorrhagic diathesis and respond well to treatment with all-*trans*-retinoic acid. APL leukocytes were found to strongly overexpress annexin A2 at the cell surface and also to stimulate the generation of plasmin from tPA twice as efficiently as other leukemic cells (195). Plasmin generation was blocked by anti-annexin A2 antibodies and could be induced in non-APL cells by ectopic expression of annexin A2. Moreover, exposure of APL cells to all-*trans*-retinoic acid led to a marked reduction in annexin A2 mRNA and protein which correlated with diminished tPA binding. This study provides the clearest evidence so far for any member of the annexin family having a direct role in the pathophysiology of a human disease.

Like annexin A2, annexin A5 has also been suggested to have an antithrombotic role that becomes compromised in disease. However, whereas annexin A2 appears to function as an intermediary in the fibrinolytic cascade, annexin A5 has been proposed to have a more direct role, by forming a molecular shield that insulates the apical surfaces of placental villi from the activities of circulating coagulant proteins. Anticoagulant activity is a feature of all Ca^{2+} binding annexins and can be explained by simple Ca^{2+} -dependent sequestration of the phospholipid matrix with which procoagulant factors interact. In this respect, annexins behave in exactly the same way as when first described as inhibitors of PLA_2 , since the enzyme also requires both Ca^{2+} and phospholipid as cofactor and substrate, respectively. Although this type of anticoagulant activity and PLA_2 inhibition have long been viewed as purely in vitro properties of annexins, there is now evidence that the anticoagulant activity of annexin A5 might be of biological importance in the recurrent pregnancy losses associated with antiphospholipid syndrome (240). A diagnostic observation in patients with antiphospholipid syndrome is the presence in the serum of antibodies against a range of proteins or phospholipids, including annexin A5, prothrombin, cardiolipin, β_2 -glycoprotein-I, and phosphatidylethanolamine (78, 314), and a number of studies suggest that displacement of the annexin A5 shield by anti-annexin A5 antibodies is causative in the generation of a thrombogenic environment and consequent fetal loss. For example, displacement of annexin A5

from the syncytiotrophoblast surface with either specific antisera or Ca^{2+} chelator (242) leads to accelerated coagulation of plasma, and in a mouse model, infusion of anti-annexin A5 antibodies led to placental infarction and pregnancy wastage (333). However, not all investigators take the same view. Several clinical studies failed to detect either anti-annexin A5 antibodies (278) or any changes in expression or localization of annexin A5 (166) in women with pregnancy loss associated with antiphospholipid syndrome. Another study found no evidence that displacement of annexin A5 using antiphospholipid antibodies increased the thrombogenicity of the cell surface (21). If annexin A5 really does have a protective function in the placenta as an anticoagulant, the mechanism of its activity is likely to be considerably more complex than proposed in current models, suggesting that the protein forms an antithrombotic shield in two-dimensional crystalline arrays on the exposed phospholipid surface.

B. Annexins and Physiological Stress

Physiological stress occurs at the cellular level in many disease states and is typically associated with the activation of certain signaling pathways, changes in cell morphology and activity, and modulation of gene expression. Many of these changes can be induced in normal cells by using osmotic, temperature, and oxidative shock, and new research suggests that members of the annexin family may be involved in the cellular response to stress. Annexin A1 was reported to have chaperone activity in *in vitro* experiments in which the purified protein was demonstrated to protect the enzymes citrate synthase and glutamate dehydrogenase from heat inactivation (155). Furthermore, heat shock, hydrogen peroxide, and sodium arsenite were all demonstrated to induce expression of annexin A1 and also translocation of the protein from the cytosol to the nucleus in A549 and HeLa cells (250). The same set of agonists also activated the annexin A1 gene promoter in experiments using a reporter gene. Other annexins have also been shown to be regulated by cytotoxic stress. For example, annexin A4 was shown to be induced in human non-small-cell lung carcinoma cells by the antimitotic drug paclitaxel and to concentrate in the nuclei of stressed cells (117). The correlation between annexin translocation to the nucleus and cellular stress extends to annexin A5, which exhibits the same behavior in primary cultures of vascular endothelial cells grown under conditions of mild hyperoxidative stress (S. M. Saire and S. E. Moss, unpublished observations). Annexin A5 has also been identified in a screen for proteins induced by hypoxic stress in cultured human cervical epithelial cells (65). Annexin A2 was also found to be induced by hypoxia in this study and by hyperoxidative stress in a model of renal cell carcinoma (307). Thus, at

least in certain cell types, annexins A2 and A5 appear to be upregulated by changes in cellular redox state, irrespective of whether these tend toward a more reducing or a more oxidative environment. The idea that members of the annexin family might have stress-related functions is also supported by studies in plants (100, 162, 310). One of these studies reported that an annexin from *Arabidopsis thaliana* possesses catalase activity and that expression of this annexin restored the ability of a delta oxyR mutant strain of *E. coli* to grow in the presence of peroxide (100). Although such enzyme activity has never been convincingly demonstrated for any animal annexin, there is growing evidence that annexin function may be directly influenced by oxidative and perhaps other stresses. Annexin A2 is glutathiolated in HeLa cells exposed to peroxide (304), annexin A6 has been reported to contribute to the Ca^{2+} signal in macrophages exposed to peroxide by dissociation from the plasma membrane (130), and targeted disruption of the annexin A5 gene in B cells leads to loss of the Ca^{2+} influx response to peroxide (163). Mechanical stress has also been shown to influence annexin behavior. Relaxation of human foreskin fibroblasts grown on collagen matrices led to the enrichment of annexins A2 and A6 with shed membrane vesicles (173), and mild hyperosmolar shock leads to the association of GFP-tagged annexin A2 with mobile endocytic vesicles in rat basophilic leukemia cells (196). Collectively, these studies suggest that physiological stress may be important in the regulation not only of annexin gene expression but also the activities and intracellular localization of at least some annexins.

C. Annexins and Cancer

Annexins A1 and A2 were first discovered as major cellular substrates for phosphorylation on tyrosine by the EGF receptor and the transforming gene product of the Rous sarcoma virus, respectively, implicating these proteins in signaling pathways known to be subverted or involved in cancer. Nevertheless, evidence in support of causative roles for any annexin in the development of cancer or in cell transformation is still mainly circumstantial. Recent studies have reported a correlation between the level of annexin A1 expression in RAW 264.7 macrophages and the cellular responsiveness to lipopolysaccharide (LPS) of components of the mitogen-activated protein (MAP) kinase pathway (1). Cells expressing reduced levels of annexin A1 exhibited potentiation of LPS-induced MAP kinase activation, with elevated annexin A1 expression having the inverse correlation. A similar investigation reported a correlation between annexin A1 expression and mobilization of intracellular Ca^{2+} in MCF-7 breast carcinoma cells (89). In this case, overexpression of annexin A1 led to abrogation of Ca^{2+} release after activation of purinergic or bradykinin receptors, whereas

downregulation of annexin A1 using antisense had the converse effect. Another recent study provided evidence that annexin A1 overexpression in rat 2 fibroblasts leads to direct inhibition of cytosolic PLA₂, which in turn depresses the serum response element of *c-fos* (215). These authors also used deletion mutants to map the functional site in annexin A1 to a domain comprising the first conserved annexin repeat. Collectively, these studies all imply a growth-suppressive role for annexin A1 despite the apparent mechanistic diversity underlying each case. The difficulty comes in reconciling the reported effects of annexin A1 on MAP kinase signaling, *c-fos* induction, and Ca²⁺ mobilization to a single function. Does annexin A1 really regulate signal transduction pathways via interactions with multiple cellular targets, or can these observations be explained by a more general effect of annexin A1 on Ca²⁺ signaling or endocytosis? And, the conclusions of these studies are not supported by work showing that annexin A1 is strongly upregulated in a prostate cancer cell line (324), esophageal cancer (74), a stomach cancer cell line (283), mammary adenocarcinoma (220), and hepatocarcinoma (62). Interestingly, the latter study also showed that annexin A1 is upregulated during normal hepatocyte proliferation after partial hepatectomy and that the proliferative rate of both normal and malignant hepatocytes was attenuated by antisense to annexin A1. These results suggest a link between annexin A1 and cell proliferation, rather than malignant transformation per se, and they suggest that cell growth is associated with elevated rather than reduced levels of annexin A1. It must be hoped that clarification of these apparently contradictory lines of evidence will come from analysis of annexin A1 null mutant mice.

Other annexins have also been linked with cell growth and transformation, frequently in studies using similar experimental designs to those described above for annexin A1. For example, overexpression of annexin A5 in MCF-7 cells leads to inhibition of phorbol ester-mediated activation of the MAP kinase pathway (264), and heterologous expression of annexin A6 at physiological levels in human A431 carcinoma cells leads to inhibition of growth factor-mediated Ca²⁺ influx (84) and slower tumor growth in mice (309). Interestingly, the correlation between expression of annexin A6 and growth suppression extends to melanoma, where a genetic screen identified annexin A6 as a protein downregulated in the transition from a nonmetastatic to a metastatic phenotype (87). A similar result was recently obtained for annexin 2, which appears to be downregulated in prostate cancer (39), and annexin A7, which is expressed at low levels in the most metastatic malignant melanomas (153). Interestingly, a recent study examining loss of heterozygosity (LOH) at the annexin A7 locus in prostate cancer specimens identified this LOH in 35% of the primary prostate tumors. Analysis of annexin A7 expression in prostate

tumor microarrays revealed low levels of expression in metastatic and local recurrences of hormone refractory prostate cancer compared with primary tumors. Moreover, the same study showed that ectopic expression of annexin A7 in two prostate tumor cell lines reduced cell proliferation and that heterozygous annexin A7 knock-out mice (+/-) have a more cancer-prone phenotype (300). A potential role of an annexin as tumor suppressor gene is not without precedent, since Theobald et al. (309) had reported that annexin A6 has tumor suppressor activity in human A 431 cells.

The advent of global gene expression analysis using proteomics and DNA chip technology has also revealed changes in annexin gene expression in numerous cancers and other diseased or stressed cell states (36, 74, 283, 325, 337). There are several searchable web sites reporting these findings, and for one of the most informative, interested readers are referred to <http://genome-www.stanford.edu/> for the results of the NC160 Cancer Microarray Project. Some of the most striking findings here include upregulation of annexin A5 in melanomas and annexin A9 in prostate and colon cancers and downregulation of annexin A5 in leukemias and annexin A1 in prostate cancers. Correlations of this type are intriguing and suggest that changes in the levels of expression of certain annexins may influence patterns of cellular behavior, such as motility, invasiveness, and proliferative rate, without actually initiating the transformation process. As such, annexins may yet prove to have therapeutic potential in the treatment of malignant disease.

VI. CONCLUSION

Annexins comprise a multigene family of Ca²⁺-regulated membrane binding proteins that has evolved into different branches with members expressed widely throughout the animal and plant kingdoms. The conserved Ca²⁺/membrane binding unit present in all annexins (the core domain) can be viewed as a tool invented by nature to peripherally dock proteins to membranes. Such docking can occur at high density, possibly enabling the annexins to organize membranes, e.g., by assembling interacting phospholipids into certain domains, or at low density, under which circumstances annexins may increase membrane permeability. Membrane insertion shown for some annexins to occur in vitro at lower pH might follow such peripheral association, but conditions possibly inducing this in vivo and potential physiological consequences still need to be established. The second principal annexin domain located at the NH₂-terminal end is unique for a given member and specifies or fine-tunes its intracellular (in some cases also extracellular) interactions with certain target membranes or protein ligands. Such interactions may either affect annexin properties or

may be affected by annexin binding. The basis of annexin function as a whole most likely resides in their unique mode of membrane interaction, which in turn can influence a number of membrane-related events, e.g., membrane traffic and the organization of compartment membranes and the plasma membrane. Through their apparent ability to organize, perturb, or integrate into membranes with which they interact, annexins may therefore have roles as effectors, regulators, and mediators of Ca^{2+} signals. Such biological activities have now been shown for some annexins, and further knockout as well as mutant models are under development to decipher the roles of other members of the family. However, we still have a long way to go to understand the precise functions of individual annexins. Redundancy in the family coupled to the problem of dealing with scaffolding or structural functions for many annexins will demand imaginative experimental approaches and rigorous objectivity in the interpretation of the results.

We owe a major debt of thanks to the many annexin workers who provided prepublication information, including Rod Flower, Klaus von der Mark, Ernst Pöschl, Angelika Noegel, Annie Vedeler, and Thorsten Kirsch. We also thank Reg Morgan, Pilar Fernandez, and Harry Haigler as well as members of our laboratories for proofreading the manuscript or parts thereof.

Work in the Moss laboratory is funded by the Wellcome Trust, Medical Research Council, Leukemia Research Fund, Arthritis Research Campaign, British Heart Foundation, Fight for Sight, and Guide Dogs for the Blind. Work in the Gerke laboratory is funded by the Deutsche Forschungsgemeinschaft, the European Union, and the Interdisciplinary Center for Clinical Research of the University of Münster.

Address for reprint requests and other correspondence: V. Gerke, Institute for Medical Biochemistry, ZMBE, Univ. of Münster, von-Esmarch-Str. 56, D-48149 Münster, Germany.

REFERENCES

- ALLDRIDGE LC, HARRIS HJ, PLEVIN R, HANNON R, AND BRYANT, CE. The annexin protein lipocortin 1 regulates the MAPK/ERK pathway. *J Biol Chem* 274: 37620–37628, 1999.
- ALVAREZ-MARTINEZ MT, PORTE F, LIAUTARD JP, AND SRI-WIDADA J. Effects of profilin-annexin I association on some properties of both profilin and annexin I. *Biochim Biophys Acta* 1399: 331–340, 1997.
- ANDERSON RG. The caveolae membrane system. *Annu Rev Biochem* 67: 199–225, 1998.
- ARISPE N, ROJAS E, GENGGE BR, WU LNY, AND WUTHIER RE. Similarity in calcium channel activity of annexin V and matrix vesicles in planar lipid bilayers. *Biophys J* 71: 1764–1775, 1996.
- AUNIS D AND LANGLEY K. Physiological aspects of exocytosis in chromaffin cells of the adrenal medulla. *Acta Physiol Scand* 167: 89–97, 1999.
- AVILA-SAKAR AJ, KRETSINGER RH, AND CREUTZ CE. Membrane-bound 3D structures reveal the intrinsic flexibility of annexin VI. *J Struct Biol* 130: 54–62, 2000.
- AYALA-SANMARTIN J, HENRY J, AND PRADEL L. Cholesterol regulates membrane binding and aggregation by annexin 2 at submicromolar $\text{Ca}(2+)$ concentrations. *Biochim Biophys Acta* 1510: 18–28, 2001.
- BABIYCHUK EB AND DRAEGER A. Annexins in cell membrane dynamics: $\text{Ca}(2+)$ -regulated association of lipid microdomains. *J Cell Biol* 150: 1113–1124, 2000.
- BABIYCHUK EB, PALSTRA RJ, SCHALLER J, KAMPFER U, AND DRAEGER A. Annexin VI participates in the formation of a reversible, membrane cytoskeleton complex in smooth muscle cells. *J Biol Chem* 274: 35191–35195, 1999.
- BANCES P, FERNANDEZ M-R, RODRIGUEZ-GARCIA M-I, MORGAN RO, AND FERNANDEZ M-P. Annexin A11 (ANXA11) gene structure as the progenitor of paralogous annexins and source of orthologous cDNA isoforms. *Genomics* 69: 95–103, 2000.
- BANDOROWICZ-PIKULA S, DANIELUK M, WRZOSEK A, BUS R, BUCHET R, AND PIKULA S. Annexin VI: an intracellular target for ATP. *Acta Biochim Pol* 46: 810–812, 1999.
- BARAN DT, QUAIL JM, RAY R, AND HONEYMAN T. Binding of $1\alpha,25$ -dihydroxyvitamin D(3) to annexin II: effect of vitamin D metabolites and calcium. *J Cell Biochem* 80: 259–265, 2001.
- BARAN DT, QUAIL JM, RAY R, LESZYK L, AND HONEYMAN T. Annexin II is the membrane receptor that mediates the rapid actions of $1\alpha,25$ -dihydroxyvitamin D(3). *J Cell Biochem* 78: 34–46, 2000.
- BECK KA, BUCHANAN JA, MALHOTRA V, AND NELSON WJ. Golgi spectrin: identification of an erythroid alpha spectrin homolog associated with the Golgi complex. *J Cell Biol* 127: 707–723, 1994.
- BECKER T, WEBER K, AND JOHNSON N. Protein-protein recognition via short amphiphilic helices: a mutational analysis of the binding site of annexin II for p11. *EMBO J* 9: 4207–4213, 1990.
- BEERMANN B, HINZ H-J, HOFMANN A, AND HUBER R. Acid induced unfolding of annexin V wild type shows two intermediate states. *FEBS Lett* 423: 265–269, 1998.
- BELLAGAMBA C, HUBAISHY I, BJORGE JD, FITZPATRICK SL, FUJITA DJ, AND WAISMAN DM. Tyrosine phosphorylation of annexin II tetramer is stimulated by membrane binding. *J Biol Chem* 272: 3195–3199, 1997.
- BENEVOLENSKY D, BELIKOVA Y, MOHAMMADZADEH R, TROUVE P, MAROTTE F, RUSSO-MARIE F, SAMUEL JL, AND CHARLEMAGNE D. Expression and localization of the annexins II, V, and VI in myocardium from patients with end-stage heart failure. *Lab Invest* 80: 123–133, 2000.
- BENZ J, BERGNER A, HOFMANN A, DEMANGE P, GÖTTIG P, LIEMANN S, HUBER R, AND VOGES D. The structure of recombinant human annexin VI in crystals and membrane-bound. *J Mol Biol* 260: 638–643, 1996.
- BERENDES R, BURGER A, VOGES D, DEMANGE P, AND HUBER R. Calcium influx through annexin V ion channels into large unilamellar vesicles measured with fura-2. *FEBS Lett* 317: 131–134, 1993.
- BEVERS EM, JANSSEN MP, WILLEMS GM, AND ZWAAL FA. No evidence for enhanced thrombin formation through displacement of annexin V by antiphospholipid antibodies. *Thromb Haemostasis* 83: 792–794, 2000.
- BIENER Y, FEINSTEIN R, MAYAK M, KABURAGI Y, KADOWAKI T, AND ZICK Y. Annexin II is a novel player in insulin signal transduction. *J Biol Chem* 271: 29489–29496, 1996.
- BITTO E AND CHO W. Roles of individual domains of annexin I in its vesicle binding and vesicle aggregation: a comprehensive mutagenesis study. *Biochemistry* 37: 10231–10237, 1998.
- BITTO E, LI M, TIKHONOV AM, SCHLOSSMANN ML, AND CHO W. Mechanism of annexin I-mediated membrane aggregation. *Biochemistry* 39: 13469–13477, 2000.
- BOUSSAC M AND GARIN J. Calcium-dependent secretion in human neutrophils: a proteomic approach. *Electrophoresis* 21: 665–672, 2000.
- BRISSEN A, MOSSER G, AND HUBER R. Structure of soluble and membrane-bound annexin V. *J Mol Biol* 220: 199–203, 1991.
- BROWN DA AND LONDON E. Functions of lipid rafts in biological membranes. *Annu Rev Cell Dev Biol* 14: 111–136, 1998.
- BROWNAWELL A AND CREUTZ C. Calcium-dependent binding of sorcin to the N-terminal domain of synexin (annexin VII). *J Biol Chem* 272: 22182–22190, 1997.
- BURGER A, BERENDES R, LIEMANN S, BENZ J, HOFMANN A, GÖTTIG P, HUBER R, GERKE V, THIEL C, RÖMISCH J, AND WEBER K. The crystal structure and ion channel activity of human annexin II, a peripheral membrane protein. *J Mol Biol* 257: 839–847, 1996.
- BURGOYNE RD. Calpactin in exocytosis. *Nature* 331: 20, 1988.
- CAMPOS B, MO YD, MEALY TR, LI CW, SWAIRJO MA, BALCH C, HEAD JF, RETZINGER G, DEDMAN JR, AND SEATON BA. Mutational and crystallographic analyses of interfacial residues suggest direct interac-

- tions with phospholipid membrane components. *Biochemistry* 37: 8004–8010, 1998.
32. CAMPOS B, WANG S, RETZINGER GS, KAETZEL MA, SEATON BA, KARIN NJ, JOHNSON JD, AND DEDMAN JR. Mutation of highly conserved arginine residues disrupts the structure and function of annexin V. *Arch Med Res* 30: 360–367, 1999.
 33. CAO HUY H AND POLLARD HB. Activation of annexin 7 by protein kinase C in vitro and in vivo. *J Biol Chem* 276: 12813–12821, 2001.
 34. CAO HUY H, SRIVASTAVA M, AND POLLARD HB. Membrane fusion protein synexin (annexin VII) as a Ca^{2+} /GTP sensor in exocytotic secretion. *Proc Natl Acad Sci USA* 93: 10797–10802, 1996.
 35. CARTAILLER J, HAIGLER HT, AND LUECKE H. Annexin XII E105K crystal structure: identification of a pH-dependent switch for mutant hexamerization. *Biochemistry* 39: 2475–2483, 2000.
 36. CELIS A, RASMUSSEN HH, CELIS P, BASSE B, LAURIDSEN JB, RATZ G, HEIN B, OSTERGAARD M, WOLF H, ORNSTOFT T, AND CELIS JE. Short-term culturing of low-grade superficial bladder transitional cell carcinomas leads to changes in the expression levels of several proteins involved in key cellular activities. *Electrophoresis* 20: 355–361, 1999.
 37. CHAN HC, KAETZEL MA, GOTTER AL, DEDMAN JR, AND NELSON DJ. Annexin IV inhibits calmodulin-dependent protein kinase II-activated chloride conductance. A novel mechanism for ion channel regulation. *J Biol Chem* 269: 32464–32468, 1994.
 38. CHASSEROT-GOLAZ S, VITALE N, SAGOT I, DELOUCHE B, DIRRIG S, PRADEL LA, HENRY JP, AUNIS D, AND BADER M-F. Annexin II in exocytosis: catecholamine secretion requires the translocation of p36 to the subplasmalemmal region in chromaffin cells. *J Cell Biol* 133: 1217–1236, 1996.
 39. CHETCUTI A, MARGAN SH, RUSSELL P, MANN S, MILLAR DS, CLARK SJ, ROGERS J, HANDELSMANN DJ, AND DONG Q. Loss of annexin II heavy and light chains in prostate cancer and its precursors. *Cancer Res* 61: 6331–6334, 2001.
 40. CHO W AND BITTO E. Structural determination of the vesicle aggregation activity of annexin I. *Biochemistry* 38: 14094–14100, 1999.
 41. CHOI K-S, FITZPATRICK SL, FILIPENKO NR, FOGG DK, KASSAM G, MAGLIOCCO AM, AND WAISMAN DM. Regulation of plasmin-dependent fibrin clot lysis by annexin II heterotetramer. *J Biol Chem* 276: 25212–25221, 2001.
 42. CHOI K-S, GHUMAN J, KASSAM G, KANG H-M, FITZPATRICK SL, AND WAISMAN DM. Annexin II tetramer inhibits plasmin-dependent fibrinolysis. *Biochemistry* 37: 648–655, 1998.
 43. CHOW A, DAVIS AJ, AND GAWLER DJ. Identification of a novel protein complex containing annexin VI, Fyn, Pyk2, and the P120(GAP) C2 domain. *FEBS Lett* 469: 88–92, 2000.
 44. CHOW A AND GAWLER DJ. Mapping the site of interaction between annexin VI and the p120GAP C2 domain. *FEBS Lett* 460: 166–172, 1999.
 45. CLEMEN CS, HOFMANN A, ZAMPARELLI C, AND NOEGEL AA. Expression and localization of annexin VII (synexin) isoforms in differentiating myoblasts. *J Muscle Res Cell Motil* 20: 669–679, 1999.
 46. COMERA C AND RUSSO-MARIE F. Glucocorticoid induced annexin I secretion by monocytes and peritoneal leukocytes. *Br J Pharmacol* 115: 1043–1047, 1995.
 47. CONCHA NO, HEAD JF, KAETZEL MA, DEDMAN JR, AND SEATON BA. Rat annexin V crystal structure: Ca^{2+} -induced conformational changes. *Science* 261: 1321–1324, 1993.
 48. COOKSON BT, ENGELHARDT S, SMITH C, BAMFORD HA, PROCHAZKA M, AND TAIT JF. Organization of the human annexin V (ANX5) gene. *Genomics* 20: 463–467, 1994.
 49. CORDIER-OSCHENBEIN F, GUEROIS R, BALEUX F, HUYNH-DINH T, CHAFOTTE A, NEUMANN J-M, AND SANSON A. Folding properties of an annexin I domain: a (1)H-(15)N NMR and CD study. *Biochemistry* 35: 10347–10357, 1996.
 50. CORVERA S, DIBONAVENTURE C, AND SHPETNER HS. Cell confluence-dependent remodeling of endothelial membranes mediated by cholesterol. *J Biol Chem* 275: 31414–31421, 2000.
 51. CREUTZ CE. The annexins and exocytosis. *Science* 258: 924–931, 1992.
 52. CREUTZ CE, PAZOLES CJ, AND POLLARD HB. Identification and purification of an adrenal medullary protein (synexin) that causes calcium-dependent aggregation of chromaffin granules. *J Biol Chem* 253: 2858–2866, 1978.
 53. CREUTZ CE, SNYDER SL, DAIGLE SN, AND REDICK J. Identification, localization, and functional implications of an abundant nematode annexin. *J Cell Biol* 132: 1079–1092, 1996.
 54. CREUTZ CE, ZAKS WJ, HAMMAN HC, CRANE S, MARTIN WH, GOULD KL, ODDIE KM, AND PARSONS SJ. Identification of chromaffin granule-binding proteins. *J Biol Chem* 262: 1860–1868, 1987.
 55. CRUMPTON MJ AND DEDMAN JR. Protein terminology tangle. *Nature* 345: 212, 1990.
 56. CUZZOCREA S, TAILOR A, ZINGARELLI B, SALZMAN AL, FLOWER RJ, SZABO C, AND PERRETTI M. Lipocortin 1 protects against splanchnic artery occlusion and reperfusion injury by affecting neutrophil migration. *J Immunol* 159: 5089–5097, 1997.
 57. DAIGLE SN AND CREUTZ CE. Transcription, biochemistry and localization of nematode annexins. *J Cell Sci* 112: 1901–1913, 1999.
 58. D'AMICO M, DI FILIPPO C, LA M, SOLITO E, MCLEAN PG, FLOWER RJ, OLIANI SM, AND PERRETTI M. Lipocortin 1 reduces myocardial ischemia-reperfusion injury by affecting local leukocyte recruitment. *FASEB J* 14: 1867–1869, 2000.
 59. DAVIDSON FF, DENNIS EA, POWELL M, AND GLENNEY JR. Inhibition of phospholipase A_2 by "lipocortins" and calpactins. *J Biol Chem* 262: 1698–1705, 1987.
 60. DAVIS AJ, BUTT JT, WALKER JH, MOSS SE, AND GAWLER DJ. The CalB domain of p120(GAP) mediates protein-protein interactions with Ca^{2+} -dependent membrane binding proteins: evidence for a direct interaction between annexin VI and p120(GAP). *J Biol Chem* 271: 24333–24336, 1996.
 61. DE BK, MISONO KS, LUKAS TJ, MROCKOWSKI B, AND COHEN S. A calcium-dependent 35-kilodalton substrate for epidermal growth factor receptor/kinase isolated from normal tissue. *J Biol Chem* 261: 13784–13792, 1986.
 62. DE COUPADE C, GILLET R, BENNOUN M, BRIAND P, RUSSO-MARIE F, AND SOLITO E. Annexin I expression and phosphorylation are upregulated during liver regeneration and transformation in antithrombin III SV40 large T antigen transgenic mice. *Hepatology* 31: 371–380, 2000.
 63. DELOUCHE B, PRADEL LA, AND HENRY JP. Phosphorylation by protein kinase C of annexin 2 in chromaffin cells stimulated by nicotine. *J Neurochem* 68: 1720–1727, 1997.
 64. DELMER DP AND POTIKHA TS. Structures and functions of annexins in plants. *Cell Mol Life Sci* 53: 546–553, 1997.
 65. DENKO N, SCHINDLER C, KOONG A, LADEROUTE K, GREEN C, AND GIACCIA A. Epigenetic regulation of gene expression in cervical cancer cells by the tumor microenvironment. *Clin Cancer Res* 6: 480–487, 2000.
 66. DIAKONOVA M, GERKE V, ERNST J, LAUTARD J-P, VAN DER VUSSE G, AND GRIFFITHS G. Localization of five annexins in J774 macrophages and on isolated phagosomes. *J Cell Sci* 110: 1199–1213, 1997.
 67. DIAZ-MUNOZ M, HAMILTON SL, KAETZEL MA, HAZARIKA P, AND DEDMAN JR. Modulation of calcium release channel activity from sarcoplasmic reticulum by annexin VI (67 kDa-calcimedlin). *J Biol Chem* 265: 15894–15899, 1990.
 68. DONATO R. Functional roles of S100 proteins, calcium-binding proteins of the EF-hand type. *Biochim Biophys Acta* 1450: 191–231, 1999.
 69. DONNELLY SR, HAWKINS TE, AND MOSS SE. A conserved nuclear element with a role in mammalian gene regulation. *Hum Mol Genet* 8: 1723–1728, 1999.
 70. DONNELLY SR AND MOSS SE. Functional analysis of the human annexin I and VI gene promoters. *Biochem J* 332: 681–687, 1998.
 71. DÖRING V, SCHLEICHER M, AND NOEGEL AA. *Dictyostelium* annexin VII (synexin). cDNA sequence and isolation of a gene disruption mutant. *J Biol Chem* 266: 17509–17515, 1991.
 72. DÖRING V, VERETOUT F, ALBRECHT R, MÜHLBAUER B, SCHLATTERER C, SCHLEICHER M, AND NOEGEL AA. The in vivo role of annexin VII (synexin): characterization of an annexin VII-deficient *Dictyostelium* mutant indicates an involvement in Ca^{2+} -regulated processes. *J Cell Sci* 108: 2065–2076, 1995.
 73. EBERHARD D, KARNS LR, VANDENBERG SR, AND CREUTZ CE. Control of the nucleo-cytoplasmic partitioning of annexin II by a nuclear export signal and by p11 binding. *J Cell Sci* 114: 3155–3166, 2001.
 74. EMMERT-BUCK MR, GILLESPIE JW, PAWELETZ CP, ORNSTEIN DK, BASRUR V, APPELLA E, WANG QH, HUANG J, HU N, TAYLOR P, AND PETRICORN EF. An approach to proteomic analysis of human tumors. *Mol Carcinog* 27: 158–165, 2000.

75. EUZGER HS, FLOWER RJ, GOULDING NJ, AND PERRETTI M. Differential modulation of annexin I binding sites on monocytes and neutrophils. *Mediators Inflamm* 8: 53–62, 1999.
76. FERNÁNDEZ M-P, MORGAN RO, FERNÁNDEZ M-R, AND CARCEDO M-T. The gene encoding human annexin V has a TATA-less promoter with a high G+C content. *Gene* 149: 253–260, 1994.
77. FIEDLER K, LAFONT F, PARTON RG, AND SIMONS K. Annexin XIIIb: a novel epithelial specific annexin is implicated in vesicular traffic to the apical plasma membrane. *J Cell Biol* 128: 1043–1053, 1995.
78. FIELD SL, BRIGHTON TA, MCNEIL HP, AND CHESTERMAN CN. Recent insights into antiphospholipid antibody-mediated thrombosis. *Baillieres Best Pract Res Clin Haematol* 12: 407–422, 1999.
79. FILIPENKO NR AND WAISMAN DM. Characterization of Ca^{2+} -binding sites of annexin II tetramer. *J Biol Chem* 275: 38877–38884, 2000.
80. FILIPENKO NR AND WAISMAN DM. The C-terminus of annexin II mediates binding to F-actin. *J Biol Chem* 276: 5310–5315, 2001.
81. FIRE A, XU S, MONTGOMERY MK, KOSTAS SA, DRIVER SE, AND MELLO CC. Potent and specific genetic interference by double-stranded RNA in *Caenorhabditis elegans*. *Nature* 391: 806–811, 1998.
82. FITZPATRICK SL, KASSAM G, CHOI KS, KANG HM, FOGG DK, AND WAISMAN DM. Regulation of plasmin activity by annexin II tetramer. *Biochemistry* 39: 1021–1028, 2000.
83. FITZPATRICK SL, KASSAM G, MANRO A, BRAAT CE, LOUIE P, AND WAISMAN DM. Fucoidan-dependent conformational changes in annexin II tetramer. *Biochemistry* 39: 2140–2148, 2000.
84. FLEET A, ASHWORTH R, KUBISTA H, EDWARDS H, BOLSOVER S, MOBBS P, AND MOSS SE. Inhibition of EGF-dependent calcium influx by annexin VI is splice form-specific. *Biochem Biophys Res Commun* 260: 540–546, 1999.
85. FLOWER RJ. Background and discovery of lipocortins. *Agents Actions* 17: 255–262, 1986.
86. FLOWER RJ AND ROTHWELL NJ. Lipocortin-1: cellular mechanisms and clinical relevance. *Trends Pharmacol Sci* 15: 71–76, 1994.
87. FRANCIA G, MITCHELL SD, MOSS SE, HANBY AM, MARSHALL JF, AND HART IR. Identification by differential display of annexin-VI, a gene differentially expressed during melanoma progression. *Cancer Res* 56: 3855–3858, 1996.
88. FREDRIKSSON EK, SHIPKOVA PA, SHEETS ED, HOLOWKA D, BAIRD B, AND McLAFFERTY FW. Quantitative analysis of phospholipids in functionally important membrane domains from RBL-2H3 mast cells using tandem high-resolution mass spectrometry. *Biochemistry* 38: 8056–8063, 1999.
89. FREY BM, REBER BF, VISHWANATH BS, ESCHER G, AND FREY FJ. Annexin I modulates cell functions by controlling intracellular calcium release. *FASEB J* 13: 2235–2245, 1999.
90. FUKAO H, UESHIMA S, TAKAISHI T, OKADO K, AND MATSUO O. Enhancement of tissue type plasminogen activator (tPA) activity by purified tPA receptor expressed in human endothelial cells. *Biochim Biophys Acta* 1356: 111–120, 1997.
91. FURGE LL, CHEN K, AND COHEN S. Annexin VII and annexin XI are tyrosine phosphorylated in peroxyvanadate-treated dogs and in platelet derived growth factor-treated rat vascular smooth muscle cells. *J Biol Chem* 274: 33504–33509, 1999.
92. FUTTER CE, FELDER S, SCHLESSINGER J, ULLRICH A, AND HOPKINS CR. Annexin I is phosphorylated in the multivesicular body during the processing of the epidermal growth factor receptor. *J Cell Biol* 120: 77–83, 1993.
93. GAGESCU R, DEMAUREX N, PARTON RG, HUNZIKER W, HUBER L, AND GRUENBERG J. The recycling endosome of Madin-Darby canine kidney cells is a mildly acidic compartment rich in raft components. *Mol Biol Cell* 11: 2775–2791, 2000.
94. GAO J, LI Y, AND YAN H. NMR solution structure of domain 1 of human annexin I shows an autonomous folding unit. *J Biol Chem* 274: 2971–2977, 1999.
95. GAO ZH, METHERRALL J, AND VIRSHUP DM. Identification of casein kinase I substrates by in vitro expression cloning screening. *Biochem Biophys Res Commun* 268: 562–566, 2000.
96. GARBUGLIA M, VERZINI M, AND DONATO R. Annexin VI binds S100A1 and S100B and blocks the ability of S100A1 and S100B to inhibit desmin and GFAP assemblies into intermediate filaments. *Cell Calcium* 24: 177–191, 1998.
97. GERKE V AND MOSS SE. Annexins and membrane dynamics. *Biochim Biophys Acta* 1357: 129–154, 1997.
98. GERKE V AND WEBER K. Identity of p36K phosphorylated upon Rous sarcoma virus transformation with a protein from brush borders: calcium-dependent binding to nonerythroid spectrin and F-actin. *EMBO J* 3: 227–233, 1984.
99. GIDON-JEANGIRARD C, HUGEL B, HOLL V, TOTI F, LAPLANCHE JL, MEYER D, AND FREYSSINET JM. Annexin V delays apoptosis while exerting an external constraint preventing the release of CD4+ and PrPc+ membrane particles in a human T lymphocyte model. *J Immunol* 162: 5712–5718, 1999.
100. GIDROL X, SABELLI PA, FERN YS, AND KUSH AK. Annexin-like protein from *Arabidopsis thaliana* rescues DeltaoxyR mutant of *Escherichia coli* from H_2O_2 stress. *Proc Natl Acad Sci USA* 93: 11268–11273, 1996.
101. GLENNEY JR, TACK B, AND POWELL MA. Calpactins: two distinct Ca^{2+} -regulated phospholipid and actin-binding proteins isolated from bovine lung and placenta. *J Biol Chem* 263: 503–511, 1987.
102. GLENNEY JR AND TACK BF. Amino-terminal sequence of p36 and associated p11: identification of the site of tyrosine phosphorylation and homology with S-100. *Proc Natl Acad Sci USA* 82: 7884–7888, 1985.
103. GOLCZAK M, KICINSKA A, BANDOROWICZ J, BUCHET R, SZEWczyk A, AND PIKULA S. Acidic pH-induced folding of annexin VI is a prerequisite for its insertion into lipid bilayers and formation of ion channels by the protein molecule. *FASEB J* 15: 1083–1085, 2001.
104. GOOSSENS ELJ, REUTELINGSPEERGER CPM, JONGSMA FHM, KRAAYENHOF R, AND HERMENS WT. Annexin V perturbs or stabilises phospholipid membranes in a calcium-dependent manner. *FEBS Lett* 359: 155–158, 1995.
105. GOULDING NJ, EUZGER HS, BUTT SK, AND PERRETTI M. Novel pathways for glucocorticoid effects on neutrophils in chronic inflammation. *Inflamm Res* 47: S158–S165, 1998.
106. GREENWOOD M AND TSANG A. Sequence and expression of annexin VII of *Dictyostelium discoideum*. *Biochim Biophys Acta* 1088: 429–432, 1991.
107. GREWAL T, HEEREN J, MEWAWALA D, SCHNITGERHANS T, WENDT D, SALOMON G, ENRICH C, BEISIEGEL U, AND JÄCKLE S. Annexin VI stimulates endocytosis and is involved in the trafficking of LDL to the prelysosomal compartment. *J Biol Chem* 275: 33806–33813, 2000.
108. GRUENBERG J AND EMANS N. Annexins in membrane traffic. *Trends Cell Biol* 3: 224–227, 1993.
109. GUNTESKI-HAMBLIN AM, SONG GJ, WALSH RA, FRENZKE M, BOVIN GP, DORN GW II, KAETZEL MA, HORSEMAN ND, AND DEDMAN JR. Annexin VI overexpression targeted to heart alters cardiomyocyte function in transgenic mice. *Am J Physiol Heart Circ Physiol* 270: H1091–H1100, 1996.
110. HACHIDA M, LU H, KANEKO N, HORIKAWA Y, OHKADO A, GU H, ZHANG XL, HOSHI H, NONOYAMA M, NAKANISHI T, AND KOYANAGI H. Protective effect of JTV519 (K201), a new 1,4-benzothiazepine derivative, on prolonged myocardial preservation. *Transplant Proc* 31: 996–1000, 1999.
111. HAIGLER HT AND SCHLAEPFER DD. Annexin I phosphorylation and secretion. In: *The Annexins*, edited by Moss SE. London: Portland, 1992, p. 11–34.
112. HAJJAR K, MAURI L, JACOVINA AT, ZHONG F, MIRZA UA, PADOVAN JC, AND CHAIT BT. Tissue plasminogen activator binding to the annexin II tail domain. Direct modulation by homocysteine. *J Biol Chem* 273: 9987–9993, 1998.
113. HAJJAR KA AND JACOVINA AT. Modulation of annexin II by homocysteine: implications for atherothrombosis. *J Invest Med* 46: 364–369, 1998.
114. HAJJAR KA AND KRISHNAN S. Annexin II: a mediator of the plasmin/plasminogen activator system. *Trends Cardiovasc Med* 9: 128–138, 1999.
115. HAMRE KM, CHEPENIK KP, AND GOLDOWITZ D. The annexins: specific markers of midline structures and sensory neurons in the developing murine central nervous system. *J Comp Neurol* 352: 421–435, 1995.
116. HAMRE KM, KELLER-PECK CR, CAMPBELL RM, PETERSON AC, MULLEN RJ, AND GOLDOWITZ D. Annexin IV is a marker of roof and floor plate development in the murine CNS. *J Comp Neurol* 368: 527–537, 1996.
117. HAN EK, TAHIR SK, CHERIAN SP, COLLINS N, AND NG SC. Modulation of paclitaxel resistance by annexin IV in human cancer cell lines. *Br J Cancer* 83: 83–88, 2000.

118. HAN H-Y, LEE Y-H, OH J-Y, NA D-S, AND LEE B-J. NMR analysis of the interaction of human annexin I with ATP, Ca(2+), and Mg(2+). *FEBS Lett* 425: 523-527, 1998.
119. HARDER T AND GERKE V. The annexin II(2)p11(2) complex is the major component of the Triton X-100 insoluble low-density fraction prepared from MDCK cells in the presence of Ca(2+). *Biochim Biophys Acta* 1223: 375-382, 1994.
120. HARDER T, KELLNER R, PARTON RG, AND GRUENBERG J. Specific release of membrane-bound annexin II and cortical cytoskeletal elements by sequestration of membrane cholesterol. *Mol Biol Cell* 8: 533-545, 1997.
121. HAWKINS TE, ROES J, REES D, MONKHOUSE J, AND MOSS SE. Immunological development and cardiovascular function are normal in annexin VI null mutant mice. *Mol Cell Biol* 19: 8028-8032, 1999.
122. HERR C, SMYTH N, ULLRICH S, YUN F, SASSE P, HESCHELER J, FLEISCHMANN B, LASEK K, BRIJUS K, SCHWINGER RH, FÄSSLER R, SCHRODER R, AND NOEGEL AA. Loss of annexin A7 leads to alterations in frequency-induced shortening of isolated murine cardiomyocytes. *Mol Cell Biol* 21: 4119-4128, 2001.
123. HIRATA A AND HIRATA F. Lipocortin (annexin) I heterotetramer binds to purine RNA and pyrimidine DNA. *Biochem Biophys Res Commun* 265: 200-204, 1999.
124. HOEKSTRA D, BUIST AR, Klappe K, AND REUTELINGS-SPERGER CP. Interaction of annexins with membranes: the N-terminus as a governing parameter as revealed with a chimeric annexin. *Biochemistry* 32: 14194-14202, 1993.
125. HOFMANN A, BENZ J, LIEMANN S, AND HUBER R. Voltage dependent binding of annexin V, annexin VI and annexin VII core to acidic phospholipid membranes. *Biochim Biophys Acta* 1330: 254-264, 1997.
126. HOFMANN A, ESCHERICH A, LEWIT-BENTLEY A, BENZ J, RAGUENES-NICOL C, RUSSO-MARIE F, GERKE V, MARODER L, AND HUBER R. Interactions of benzodiazepine derivatives with annexins. *J Biol Chem* 273: 2885-2894, 1998.
127. HOFMANN A, PROUST J, DOROWSKI A, SCHANTZ R, AND HUBER R. Annexin 24 from *Capsicum annuum*: X-ray structure and biochemical characterization. *J Biol Chem* 275: 8072-8082, 2000.
128. HOFMANN A, RAGUENES-NICOL C, FAVIER-PERRON B, MESONERO J, HUBER R, RUSSO-MARIE F, AND LEWIT-BENTLEY A. The annexin A3-membrane interaction is modulated by an N-terminal tryptophan. *Biochemistry* 39: 7712-7721, 2000.
129. HOLROYD C, KISTNER U, ANNAERT W, AND JAHN R. Fusion of endosomes involved in synaptic vesicle recycling. *Mol Biol Cell* 10: 3035-3044, 1999.
130. HOYAL CR, THOMAS AP, AND FORMAN HJ. Hydroperoxide-induced increases in intracellular calcium due to annexin VI translocation and inactivation of plasma membrane Ca²⁺-ATPase. *J Biol Chem* 271: 29205-29210, 1996.
131. HU S, BRADY SR, KOVAR DR, STAIGER CJ, CLARK GB, ROUX SJ, AND MUDAY GK. Technical advance: identification of plant actin-binding proteins by F-actin affinity chromatography. *Plant J* 24: 127-137, 2000.
132. HUBAISHY I, JONES PG, BJORGE J, BELLAGAMBA C, FITZPATRICK S, FUJITA DJ, AND WAISMAN DM. Modulation of annexin II tetramer by tyrosine phosphorylation. *Biochemistry* 34: 14527-14534, 1995.
133. HUBER R, BERENDES R, BURGER A, LUECKE H, AND KARSHIKOV A. Annexin V: crystal structure and its implication on function. In: *The Annexins*, edited by Moss SE. London: Portland, 1992, p. 105-124.
134. HUBER R, RÖMISCH J, AND PAQUES EP. The crystal and molecular structure of human annexin V, an anticoagulant calcium, membrane binding protein. *EMBO J* 9: 3867-3874, 1990.
135. IINO S, SUDO T, NIWA T, FUKUSAWA T, HIDAKA H, AND NIKI I. Annexin XI may be involved in Ca(2+) or GTP-gammaS-induced insulin secretion in the pancreatic beta-cell. *FEBS Lett* 479: 46-50, 2000.
136. IKONEN E AND PARTON RG. Caveolins and cellular cholesterol balance. *Traffic* 1: 212-217, 2000.
137. IMAI Y AND KOHSAKA S. Structure of rat annexin V gene and molecular diversity of its transcripts. *Eur J Biochem* 232: 327-334, 1995.
138. ISAS JM, CARTAILLER JP, SOKOLOV Y, PATEL DR, LANGEN R, LUECKE H, HALL JE, AND HAIGLER HT. Annexins V and XII insert into bilayers at mildly acidic pH and form ion channels. *Biochemistry* 39: 3015-3022, 2000.
139. ISHITSUKA R, KOJIMA K, UTSUMI H, OGAWA H, AND MATSUMOTO I. Glycosaminoglycan binding properties of annexin IV, V, and VI. *J Biol Chem* 273: 9935-9941, 1998.
140. IVANENKOV VV, WEBER K, AND GERKE V. The expression of different annexins in the fish embryo is developmentally regulated. *FEBS Lett* 352: 227-230, 1994.
141. JANS SW, DE JONG YF, REUTELINGS-SPERGER CP, VAN DER VUSSE GJ, AND VAN BILSEN M. Differential expression and localization of annexin V in cardiac myocytes during growth and hypertrophy. *Mol Cell Biochem* 178: 229-236, 1998.
142. JOHNSON N, MARRIOTT G, AND WEBER K. p36, the major cytoplasmic substrate of src tyrosine protein kinase, binds to its p11 subunit via a short amino-terminal amphipathic helix. *EMBO J* 7: 2435-2442, 1988.
143. JOHNSON N AND WEBER K. Alkylation of cysteine 82 of p11 abolishes the complex formation with the tyrosine protein kinase substrate p36 (annexin 2, calpactin 2, lipocortin 2). *J Biol Chem* 265: 14464-14468, 1990.
144. JOST M AND GERKE V. Mapping of a regulatory important site for protein kinase C phosphorylation in the N-terminal domain of annexin II. *Biochim Biophys Acta* 1313: 283-289, 1996.
145. JOST M, ZEUSCHNER D, SEEMANN J, WEBER K, AND GERKE V. Identification and characterization of a novel type of annexin-membrane interaction: Ca²⁺ is not required for the association of annexin II with endosomal membranes. *J Cell Sci* 110: 221-228, 1997.
146. KAETZEL MA, CHANG CHAN H, DUBINSKY WP, DEDMAN JR, AND NELSON DJ. A role for annexin IV in epithelial cell function. Inhibition of calcium-activated chloride conductance. *J Biol Chem* 269: 5297-5302, 1994.
147. KAETZEL MA, MO YD, MEALY TR, CAMPOS B, BERGSMAN-SCHUTTER W, BRISSON A, DEDMAN JR, AND SEATON BA. Phosphorylation mutants elucidate the mechanism of annexin IV-mediated membrane aggregation. *Biochemistry* 40: 4192-4199, 2001.
148. KAMAL A, YING Y, AND ANDERSON RG. Annexin VI-mediated loss of spectrin during coated pit budding is coupled to delivery of LDL to lysosomes. *J Cell Biol* 142: 937-947, 1998.
149. KANEKO N, AGO H, MATSUDA R, INAGAKI E, AND MIYANO M. Crystal structure of annexin V with its ligand K-201 as a calcium channel activity inhibitor. *J Mol Biol* 274: 16-20, 1997.
150. KANEKO N, MATSUDA R, TODA M, AND SHIMAMOTO K. Inhibition of annexin V-dependent Ca(2+) movement in large unilamellar vesicles by K201, a new 1,4-benzothiazepine derivative. *Biochim Biophys Acta* 1330: 1-7, 1997.
151. KANG H-M, KASSAM G, JARVIS SE, FITZPATRICK SL, AND WAISMAN DM. Characterization of human recombinant annexin II tetramer purified from bacteria: role of N-terminal acetylation. *Biochemistry* 36: 2041-2050, 1997.
152. KASSAM G, MANRO A, BRAAT CE, LOUIE P, FITZPATRICK SL, AND WAISMAN DM. Characterization of the heparin binding properties of annexin II tetramer. *J Biol Chem* 272: 15093-15100, 1997.
153. KATAOKA TR, ITO A, ASADA H, WATABE K, NISHIYAMA K, NAKAMOTO K, ITAMI S, YOSHIKAWA K, ITO M, NOJIMA H, AND KITAMURA Y. Annexin VII as a novel marker for invasive phenotype of malignant melanoma. *Jpn J Cancer Res* 91: 75-83, 2000.
154. KAWASAKI H AND KRETSINGER RH. Calcium-binding proteins 1: EF-hands. *Protein Profile* 2: 297-490, 1995.
155. KIM GY, LEE HB, LEE SO, RHEE HJ, AND NA DS. Chaperone-like function of lipocortin 1. *Biochem Mol Biol Int* 43: 521-528, 1997.
156. KIM SW, RHEE HJ, KO J, KIM YJ, KIM HG, YANG JM, CHOI EC, AND NA DS. Inhibition of cytosolic phospholipase A₂ by annexin I. Specific interaction model and mapping of interaction site. *J Biol Chem* 276: 15712-15719, 2001.
157. KIRSCH T, NAH HD, DEMUTH DR, HARRISON G, GOLUB EE, ADAMS SL, AND PACIFICI M. Annexin V-mediated calcium flux across membranes is dependent on the lipid composition: implications for cartilage mineralization. *Biochemistry* 36: 3359-3367, 1997.
158. KÖHLER G, HERING U, ZSCHÖRNIG O, AND ARNOLD K. Annexin V interaction with phosphatidylserine-containing vesicles at low and neutral pH. *Biochemistry* 36: 8189-8194, 1997.
159. KOJIMA K, YAMAMOTO K, IRIMURA T, OSAWA T, OGAWA H, AND MATSUMOTO I. Characterization of carbohydrate binding protein p33/41: relation with annexin IV, molecular basis of the doublet forms (p33 and p41), and modulation for the carbohydrate binding activity phospholipids. *J Biol Chem* 271: 7679-7685, 1996.

160. KÖNIG J AND GERKE V. Modes of annexin-membrane interactions analyzed by employing chimeric annexin proteins. *Biochim Biophys Acta*. In press.
161. KÖNIG J, PRENEN J, NILIUS B, AND GERKE V. The annexin II-p11 complex is involved in regulated exocytosis in bovine pulmonary artery endothelial cells. *J Biol Chem* 273: 19679–19684, 1998.
162. KOVACS I, AYAYDIN F, OBERSCHALL A, IPACS I, BOTTKA S, PONGOR S, DUDITS D, AND TOTTH EC. Immunolocalization of a novel annexin-like protein encoded by a stress and abscisic acid responsive gene in alfalfa. *Plant J* 15: 185–197, 1998.
163. KUBISTA H, HAWKINS TE, PATEL DR, HAIGLER HT, AND MOSS SE. Annexin 5 mediates a peroxide-induced Ca^{2+} influx in B cells. *Curr Biol* 9: 1403–1406, 1999.
164. KUSUMAWATI A, CAZAVIEILLE C, PORTE F, BETTACHE S, LIAUTAUD J-P, AND SRI WIDADA J. Early events and implication of F-actin and annexin I associated structures in the phagocytic uptake of *Brucella suis* by the J774A.1 murine cell line and human monocytes. *Microb Pathog* 28: 343–352, 2000.
165. LAFONT F, LECAT S, VERKANDÉ P, AND SIMONS K. Annexin XIIIb associates with lipid microdomains to function in apical delivery. *J Cell Biol* 142: 1413–1427, 1998.
166. LAKASING L, CAMPA JS, POSTON R, KHAMASHTA MA, AND POSTON L. Normal expression of tissue factor, thrombomodulin, and annexin V in placentas from women with antiphospholipid syndrome. *Am J Obstet Gynecol* 181: 180–189, 1999.
167. LAMBERT O, GERKE V, BADER MF, PORTE F, AND BRISSON A. Structural analysis of junctions formed between lipid membranes and several annexins by cryoelectron microscopy. *J Mol Biol* 272: 42–55, 1997.
168. LANGEN R, ISAS JM, HUBBEL WL, AND HAIGLER HT. A transmembrane form of annexin XII detected by site-directed spin labeling. *Proc Natl Acad Sci USA* 95: 14060–14065, 1998.
169. LANGEN R, ISAS JM, LUECKE H, HAIGLER HT, AND HUBBEL WL. Membrane-mediated assembly of annexins studied by site-directed spin labeling. *J Biol Chem* 273: 22453–22458, 1998.
170. LARSSON M, MAJEED M, ERNST JD, MAGNUSSON KE, STENDAHL O, AND FORSUM U. Role of annexins in endocytosis of antigens in immature human dendritic cells. *Immunology* 92: 501–511, 1997.
171. LAVIALLE F, RAINTEAU D, MASSEY-HARROUCHE D, AND METZ F. Establishment of plasma membrane polarity in mammary epithelial cells correlates with changes in prolactin trafficking and in annexin VI recruitment to membranes. *Biochim Biophys Acta* 1464: 83–94, 2000.
172. LECAT S, VERKANDÉ P, THIELE C, FIEDLER K, SIMONS K, AND LAFONT F. Different properties of two isoforms of annexin XIII in MDCK cells. *J Cell Sci* 113: 2607–2618, 2000.
173. LEE T-L, LIN Y-C, MOCHITATE K, AND GRINNELL F. Stress-relaxation of fibroblasts in collagen matrices triggers ectocytosis of plasma membrane vesicles containing actin, annexins II and VI, and β_1 integrin receptors. *J Cell Sci* 105: 167–177, 1993.
174. LEWITT-BENTLEY A, MORERA S, HUBER R, AND BODO G. The effect of metal binding on the structure of annexin V and implications for membrane binding. *Eur J Biochem* 210: 73–77, 1992.
175. LEWITT-BENTLEY A, RETY S, SOPKOVA-DE OLIVEIRA SANTOS J, AND GERKE V. S100-annexin complexes: some insights from structural studies. *Cell Biol Int* 24: 799–802, 2000.
176. LEY K. Molecular mechanisms of leukocyte recruitment in the inflammatory process. *Cardiovasc Res* 32: 733–742, 1996.
177. LIEMANN S, BRINGEMEIER I, BENZ J, GÖTTIG P, HOFMANN A, HUBER R, NOEGEL AA, AND JACOB U. Crystal structure of the C-terminal tetrad repeat from synexin (annexin VII) of *Dictyostelium discoideum*. *J Mol Biol* 270: 79–88, 1997.
178. LIEMANN S AND LEWITT-BENTLEY A. Annexins: a novel family of calcium- and membrane-binding proteins in search of a function. *Structure* 3: 233–237, 1995.
179. LIN HC, SUDHOF TC, AND ANDERSON RG. Annexin VI is required for budding of clathrin-coated pits. *Cell* 70: 283–291, 1992.
180. LIU L. Calcium-dependent self-association of annexin II: a possible implication in exocytosis. *Cell Signal* 11: 317–324, 1999.
181. LIU L, TAO JQ, LI HL, AND ZIMMERMAN UJ. Inhibition of lung surfactant secretion from alveolar type II cells and annexin II tetramer-mediated membrane fusion by phenothiazines. *Arch Biochem Biophys* 342: 322–328, 1997.
182. LIU L, TAO J-Q, AND ZIMMERMAN U-JP. Annexin II binds to the membrane of A549 cells in a calcium-dependent and calcium-independent manner. *Cell Signal* 9: 299–304, 1997.
183. LUCKCUCK T, TROTTER PJ, AND WALKER JH. Localization of annexin V in the adult and neonatal heart. *Biochem Biophys Res Commun* 238: 622–628, 1997.
184. LUCKCUCK T, TROTTER PJ, AND WALKER JH. Localization of annexin VI in the adult and neonatal heart. *Cell Biol Int* 22: 199–205, 1998.
185. LUECKE H, CHANG BT, MAILLIARD WS, SCHLAEFFER DD, AND HAIGLER HT. Crystal structure of the annexin XII hexamer and implications for bilayer insertion. *Nature* 378: 512–515, 1995.
186. MA K, SIMANTOV R, ZHANG JC, SILVERSTEIN R, HAJJAR KA, AND MCCRAE KR. High affinity binding of beta 2-glycoprotein I to human endothelial cells is mediated by annexin 2. *J Biol Chem* 275: 15541–15548, 2000.
187. MAI J, FINLEY RL, WAISMAN DM, AND SLOANE BF. Human procathepsin B interacts with the annexin II tetramer on the surface of tumor cells. *J Biol Chem* 275: 12806–12812, 2000.
188. MAILLIARD WS, HAIGLER HT, AND SCHLAEFFER DD. Calcium dependent binding of S100C to the N-terminal domain of annexin I. *J Biol Chem* 271: 719–725, 1996.
189. MAJEED M, PERSKVIST N, ERNST JD, ORSELTUS K, AND STENDAHL O. Roles of calcium and annexins in phagocytosis and elimination of an attenuated strain of *Mycobacterium tuberculosis* in human neutrophils. *Microb Pathog* 24: 309–320, 1998.
190. MATSUSHIMA N, CREUTZ CE, AND KRETSINGER RH. Polyproline, beta-turn helices. Novel secondary structures proposed for the tandem repeats within rhodopsin, synaptophysin, synexin, gliadin, RNA polymerase II, hordein, and gluten. *Proteins* 7: 125–155, 1990.
191. MATTEO RG AND MORAVEC CS. Immunolocalization of annexins IV, V and VI in the failing and non-failing human heart. *Cardiovasc Res* 45: 961–970, 2000.
192. MEERS P AND MEALY T. Relationship between annexin V tryptophan exposure, calcium, and phospholipid binding. *Biochemistry* 32: 5411–5418, 1993.
193. MEGLI FM, SELVAGGI M, LIEMANN S, QUAGLIARIELLO E, AND HUBER R. The calcium-dependent binding of annexin V to phospholipid vesicles influences the bilayer inner fluidity. *Biochemistry* 37: 10540–10546, 1998.
194. MENAA C, DEVLIN RD, REDDY SV, GAZIT Y, CHOI SJ, AND ROODMAN GD. Annexin II increases osteoclast formation by stimulating the proliferation of osteoclast precursors in human marrow cultures. *J Clin Invest* 103: 1605–1613, 1999.
195. MENELL JS, CESARMAN GM, JACOVINA TA, MCLAUGHLIN MA, LEV AE, AND HAJJAR KA. Annexin II and bleeding in acute promyelocytic leukemia. *N Engl Med* 340: 994–1004, 1999.
196. MERRIFIELD CJ, RESCHER U, ALMERS W, PROUST J, GERKE V, SECHI AS, AND MOSS SE. Annexin 2 has an essential role in actin-based macropinoscytic rocketing. *Curr Biol* 11: 1136–1141, 2001.
197. MICHAELY P, KAMAL A, ANDERSON RGW, AND BENNETT V. A requirement for ankyrin to clathrin coated pit budding. *J Biol Chem* 274: 35908–35913, 1999.
198. MINN AJ, VELEZ P, SCHENDEL SL, LIANG H, MUCHMORE SW, FESIK SW, FILL M, AND THOMPSON CB. Bcl-x(L) forms an ion channel in synthetic lipid membranes. *Nature* 385: 353–357, 1997.
199. MOORE PB, KRAUS FRIEDMANN N, AND DEDMAN JR. Unique calcium-dependent hydrophobic binding proteins: possible independent mediators of intracellular calcium distinct from calmodulin. *J Cell Sci* 72: 121–133, 1984.
200. MORGAN RO, BELL DW, TESTA JR, AND FERNANDEZ MP. Genomic locations of *ANX11* and *ANX13* and the evolutionary genetics of human annexins. *Genomics* 48: 100–110, 1998.
201. MORGAN RO, BELL DW, TESTA JR, AND FERNANDEZ M-P. Human annexin 31 genetic mapping and origin. *Gene* 227: 33–38, 1999.
202. MORGAN RO AND FERNANDEZ MP. Distinct annexin subfamilies in plants and protists diverged prior to animal annexins and from a common ancestor. *J Mol Evol* 44: 178–188, 1997.
203. MORGAN RO AND FERNANDEZ MP. Annexin gene structures and molecular evolutionary genetics. *Cell Mol Life Sci* 53: 508–515, 1997.
204. MORGAN RO, JENKINS NA, GILBERT DJ, COPELAND NG, BALSARA BR, TESTA JR, AND FERNANDEZ MP. Novel human and mouse annexin A10 are linked to the genome duplications during early chordate evolution. *Genomics* 60: 40–49, 1999.
205. MOSS SE AND CRUMPTON MJ. Alternative splicing gives rise to two

- forms of the p68 calcium-binding protein. *FEBS Lett* 261: 299–302, 1990.
206. MOVITZ C AND DAHLGREN C. Endogenous cleavage of annexin I generates a truncated protein with a reduced calcium requirement for binding to neutrophil secretory vesicles and plasma membrane. *Biochim Biophys Acta* 1468: 231–238, 2000.
 207. MOVITZ C, SJOLIN C, AND DAHLGREN C. Cleavage of annexin I in human neutrophils by a membrane-localized metalloprotease. *Biochim Biophys Acta* 1416: 101–108, 1999.
 208. MUIMO R, HORNICKOVA Z, RIEMEN C, GERKE V, MATTHEWS H, AND MEHTA A. Histidine phosphorylation of annexin I in airway epithelia. *J Biol Chem* 275: 36632–36636, 2000.
 209. MUKHERJEE S AND MAXFIELD FR. Role of membrane organization and membrane domains in endocytic lipid trafficking. *Traffic* 1: 203–211, 2000.
 210. MUKHOPADHYAY S AND CHO WH. Interactions of annexin V with phospholipid monolayers. *Biochim Biophys Acta* 1279: 58–62, 1996.
 211. NACIFF JM, BEHBEHANI MM, KAETZEL MA, AND DEDMAN JR. Annexin VI modulates Ca^{2+} and K^{+} conductances of spinal cord and dorsal root ganglion neurons. *Am J Physiol Cell Physiol* 271: C2004–C2015, 1996.
 212. NAKATA T, SOBUE K, AND HIROKAWA N. Conformational change and localization of calpactin I complex involved in exocytosis as revealed by quick-freeze deep-etch electron microscopy and immunocytochemistry. *J Cell Biol* 110: 13–25, 1990.
 213. NILIUS B, GERKE V, PRENEN J, SZÜCS G, HEINKE S, WEBER K, AND DROGMANS G. Annexin II modulates volume-activated chloride currents in vascular endothelial cells. *J Biol Chem* 271: 30631–30636, 1996.
 214. NODA Y, OKADA Y, SAITO N, SETOU M, XU Y, ZHANG Z, AND HIROKAWA N. Kifc3, a microtubule minus end-directed motor for the apical transport of annexin XIIIb-associated Triton-insoluble membranes. *J Cell Biol* 155: 77–88, 2001.
 215. OH J, RHEE HJ, KIM S, KIM SB, YOU H, KIM JH, AND NA DS. Annexin-I inhibits PMA-induced c-fos SRE activation by suppressing cytosolic phospholipase A_2 signal. *FEBS Lett* 477: 244–248, 2000.
 216. OLIFERENKO S, PAIHA K, HARDER T, GERKE V, SCHWARZLER C, SCHWARZ H, BEUG H, GÜNTHER T, AND HUBER L. Analysis of CD44-containing lipid rafts: recruitment of annexin II and stabilization by the actin cytoskeleton. *J Cell Biol* 146: 843–854, 1999.
 217. ORITO A, KUMANOGOH H, YASAKA K, SOKAWA J, HIDAKA H, SOKAWA Y, AND MAEKAWA S. Calcium-dependent association of annexin VI, protein kinase C alpha, and neurocalcin alpha on the raft fraction derived from the synaptic plasma membrane. *J Neurosci Res* 64: 235–241, 2001.
 218. ORTEGA D, POL A, BIERMER M, JÄCKLE S, AND ENRICH C. Annexin VI defines an apical endocytic compartment in rat liver hepatocytes. *J Cell Sci* 111: 261–269, 1998.
 219. OSTERLOH D, WITTBRODT J, AND GERKE V. Characterization and developmentally regulated expression of four annexins in the killifish medaka. *DNA Cell Biol* 17: 835–847, 1998.
 220. PENCIL SD AND TOTH M. Elevated levels of annexin I protein in vitro and in vivo in rat and human mammary adenocarcinoma. *Clin Exp Metastasis* 16: 113–121, 1998.
 221. PERRETTI M. Endogenous mediators that inhibit the leukocyte-endothelium interaction. *Trends Pharmacol Sci* 18: 418–425, 1997.
 222. PERRETTI M. Lipocortin 1 and chemokine modulation of granulocyte and monocyte accumulation in experimental inflammation. *Gen Pharmacol* 31: 545–552, 1998.
 223. PERRETTI M, CHRISTIAN H, WHEELER SK, AIELLO I, MUGRIDGE KG, MORRIS JF, FLOWER RJ, AND GOULDING NJ. Annexin I is stored within gelatinase granules of human neutrophil and mobilized on the cell surface upon adhesion but not phagocytosis. *Cell Biol Int* 24: 163–174, 2000.
 224. PERRETTI M, CROXTALL JD, WHEELER SK, GOULDING NJ, HANNON R, AND FLOWER RJ. Mobilizing lipocortin 1 in adherent human leukocytes downregulates their transmigration. *Nature Med* 2: 1259–1262, 1996.
 225. PERRETTI M, GETTING SJ, SOLITO E, MURPHY PM, AND GAO JL. Involvement of the receptor for formylated peptides in the in vivo antimigratory actions of annexin I and its mimetics. *Am J Pathol* 158: 1969–1973, 2001.
 226. PERRETTI M, WHEELER SK, CHOUDHURY Q, CROXTALL JD, AND FLOWER RJ. Selective inhibition of neutrophil function by a peptide derived from lipocortin 1 N-terminus. *Biochem Pharmacol* 50: 1037–1042, 1995.
 227. PFANNMÜLLER E, TURNAY J, BERTLING W, AND VON DER MARK K. Organisation of the chicken annexin V gene and its correlation with the tertiary structure of the protein. *FEBS Lett* 336: 467–471, 1993.
 228. PHILIP JG, FLOWER RJ, AND BUCKINGHAM JC. Blockade of the classical pathway of protein secretion does not affect the cellular exportation of lipocortin I. *Regul Peptides* 73: 133–139, 1998.
 229. PIGAULT C, FOLLENIUS WA, SCHMUTZ M, FREYSSINET JM, AND BRISSON A. Formation of two-dimensional arrays of annexin V on phosphatidylserine-containing liposomes. *J Mol Biol* 236: 199–208, 1994.
 230. PITTIS MG AND GARCIA RC. Annexin VII and XI are present in a human macrophage-like cells line. Differential translocation on FcR-mediated phagocytosis. *J Leukoc Biol* 66: 845–850, 1999.
 231. PLANT PJ, LAFONT F, LECAT S, VERKADE P, SIMONS K, AND ROTIN D. Apical membrane targeting of Nedd 4 is mediated by an association of its C2 domain with annexin XIIIb. *J Cell Biol* 149: 1473–1483, 2000.
 232. POLLARD HB, GUY HR, ARISPE N, DE LA FUENTE M, LEE G, ROJAS EM, POLLARD JR, SRIVASTAVA M, ZHANG-KECK Z-Y, MEREZHINSKAYA N, CAO-HUY H, BURNS AL, AND ROJAS E. Calcium channel and membrane fusion activity of synexin and other members of the annexin gene family. *Biophys J* 62: 15–18, 1992.
 233. POLLARD HB AND ROJAS E. Ca^{2+} -activated synexin forms highly selective, voltage-gated Ca^{2+} channels in phosphatidylserine bilayer membranes. *Proc Natl Acad Sci USA* 85: 2974–2978, 1988.
 234. PONS M, GREWAL T, RIUS E, SCHNITGERHANS T, JACKLE S, AND ENRICH C. Evidence for the involvement of annexin 6 in the trafficking between the endocytic compartment and lysosomes. *Exp Cell Res* 269: 13–22, 2001.
 235. PONS M, IHRKE G, KOCH S, BIERMER M, POL A, JÄCKLE S, AND ENRICH C. Late endocytic compartments are major sites of annexin VI localization in NRK fibroblasts and polarized WIF-B hepatoma cells. *Exp Cell Res* 257: 33–47, 2000.
 236. POWELL MA AND GLENNEY JR JR. Regulation of calpactin I phospholipid binding by calpactin I light-chain binding and phosphorylation by p60^{v-src}. *Biochem J* 247: 321–328, 1987.
 237. PRATT SL AND HORSEMAN ND. Identification of two Y-Box binding proteins that interact with the promoters of columbid annexin I genes. *Gene* 214: 147–156, 1998.
 238. PREVOSTEL C, ALICE V, JOUBERT D, AND PARKER PJ. Protein kinase C actively downregulates through caveolae-dependent traffic to an endosomal compartment. *J Cell Sci* 113: 2575–2584, 2000.
 239. RAND JH. “Annexinopathies”—a new class of diseases. *N Engl J Med* 340: 1035–1036, 1999.
 240. RAND JH. Antiphospholipid antibody-mediated disruption of the annexin V antithrombotic shield: a thrombogenic mechanism for the antiphospholipid syndrome. *J Autoimmun* 15: 107–111, 2000.
 241. RAND JH AND WU XX. Antibody-mediated disruption of the annexin V antithrombotic shield: a new mechanism for thrombosis in the antiphospholipid syndrome. *Thromb Haemostasis* 82: 649–655, 1999.
 242. RAND JH, WU XX, ANDREE HA, LOCKWOOD CJ, GULLER S, SCHER J, AND HARPEL PC. Pregnancy loss in the antiphospholipid-antibody syndrome—a possible thrombogenic mechanism. *N Engl J Med* 337: 154–160, 1997.
 243. RAND JH, WU XX, GULLER S, GIL J, GUHA A, SCHER J, AND LOCKWOOD CJ. Reduction of annexin-V (placental anticoagulant protein-I) on placental villi of women with antiphospholipid antibodies and recurrent spontaneous abortion. *Am J Obstet Gynecol* 171: 1566–1572, 1994.
 244. RAYNAL P AND POLLARD HB. Annexins: the problem of assessing the biological role for a gene family of multifunctional calcium- and phospholipid-binding proteins. *Biochim Biophys Acta* 1197: 63–93, 1994.
 245. RESCHER U, ZOBIAK N, AND GERKE V. Intact Ca^{2+} binding sites are required for targeting annexin I to endosomal membranes in living HeLa cells. *J Cell Sci* 113: 3931–3938, 2000.
 246. RETY S, OSTERLOH D, ARIE J-P, TABARIES S, SEEMANN J, RUSSO-MARIE F, GERKE V, AND LEWIT-BENTLEY A. Structural basis of the $Ca(2+)$ -

- dependent association between S100C (S100A11) and its target, the N-terminal part of annexin I. *Structure* 8: 175–184, 2000.
247. RETY S, SOKOVA J, RENOARD M, OSTERLOH D, TABARIES S, RUSSO-MARIE F, AND LEWIT-BENTLEY A. The crystal structure of a complex of p11 with the annexin II N-terminal peptide. *Nature Struct Biol* 6: 89–95, 1999.
 248. REVIKINE I, BERGSMAS-SCHUTTER W, AND BRISSON A. Growth of protein 2-D crystals on supported planar lipid bilayers imaged in situ by AFM. *J Struct Biol* 121: 356–361, 1998.
 249. REVIKINE I, BERGSMAS-SCHUTTER W, MAZERES-DUBUT C, GOVORUKHINA N, AND BRISSON A. Surface topography of the p3 and p6 annexin V crystal forms determined by atomic force microscopy. *J Struct Biol* 131: 234–239, 2000.
 250. RHEE HJ, KIM GY, HUH JW, KIM SW, AND NA DS. Annexin I is a stress protein induced by heat, oxidative stress and a sulfhydryl-reactive agent. *Eur J Biochem* 267: 3220–3225, 2000.
 251. RODRIGUEZ-GARCIA M-I, MORGAN RO, FERNANDEZ M-R, BANCES P, AND FERNANDEZ M-P. Mouse annexin V genomic organization includes an endogenous retrovirus. *Biochem J* 337: 125–131, 1999.
 252. ROJAS E AND POLLARD HB. Membrane capacity measurements suggest a calcium-dependent insertion of synexin into phosphatidylserine bilayers. *FEBS Lett* 217: 25–31, 1987.
 253. ROJAS E, POLLARD HB, HAIGLER HT, PARRA C, AND BURNS AL. Calcium-activated endonexin II forms calcium channels across acidic phospholipid bilayer membranes. *J Biol Chem* 265: 21207–21215, 1990.
 254. ROSALES JL AND ERNST JD. Calcium-dependent neutrophil secretion: characterization and regulation by annexins. *J Immunol* 159: 6195–6202, 1997.
 255. ROSENGARTH A, GERKE V, AND LUECKE H. X-ray structure of full-length annexin I and implications for membrane aggregation. *J Mol Biol* 306: 489–498, 2001.
 256. ROSENGARTH A, RÖSGEN J, HINZ H-J, AND GERKE V. A comparison of the energetics of annexin I and annexin V. *J Mol Biol* 288: 1013–1025, 1999.
 257. ROSENGARTH A, RÖSGEN J, HINZ H-J, AND GERKE V. Folding energetics of ligand binding proteins. II. Cooperative binding of $\text{Ca}(2+)$ ions to annexin I. *J Mol Biol* 306: 825–835, 2001.
 258. ROSENGARTH A, WINTERGALEN A, GALLA H-J, HINZ H-J, AND GERKE V. $\text{Ca}(2+)$ independent interaction of annexin I with phospholipid membranes. *FEBS Lett* 438: 279–284, 1998.
 259. ROTHHUT B. Participation of annexins in protein phosphorylation. *Cell Mol Life Sci* 53: 522–526, 1997.
 260. RUSSO-MARIE F. Lipocortins as antiphospholipase A_2 and anti-inflammatory proteins. In: *Biochemistry, Molecular Biology and Physiology of Phospholipase A_2 and Its Regulatory Factors*, edited by Mukherjee AB. New York: Plenum, 1990, p. 197–210.
 261. RUSSO-MARIE F. Annexin V and phospholipid metabolism. *Clin Chem Lab Med* 37: 287–291, 1999.
 262. SAGOT I, REGNOUF F, HENRY JP, AND PRADEL LA. Translocation of cytosolic annexin 2 to a Triton-insoluble membrane subdomain upon nicotine stimulation of chromaffin cultured cells. *FEBS Lett* 410: 229–234, 1997.
 263. SARAFIAN T, PRADEL L-A, HENRY J-P, AUNIS D, AND BADER M-F. The participation of annexin II (Calpactin I) in calcium-evoked exocytosis requires protein kinase C. *J Cell Biol* 114: 1135–1147, 1991.
 264. SATO H, OGATA H, AND DE LUCA LM. Annexin V inhibits the 12-O-tetradecanoylphorbol-13-acetate-induced activation of Ras/extracellular signal-regulated kinase (ERK) signaling pathway upstream of Shc in MCF-7 cells. *Oncogene* 19: 2904–2912, 2000.
 265. SATOH A, HAZUKI H, KOJIMA K, HIRABAYASHI J, AND MATSUMOTO I. Ligand-binding properties of annexin from *Caenorhabditis elegans* (annexin 16, Nex-1). *J Biochem (Tokyo)* 128: 377–381, 2000.
 266. SATOH A, SUZUKI K, TAKAYAMA E, KOJIMA K, HIRAKA T, KAWAKAMI M, MATSUMOTO I, AND OHSUZU F. Detection of anti-annexin IV and V antibodies in patients with antiphospholipid syndrome and systemic lupus erythematosus. *J Rheumatol* 26: 1715–1720, 1999.
 267. SCHAFER BW AND HEIZMANN CW. The S100 family of EF-hand calcium-binding proteins: functions and pathology. *Trends Biochem Sci* 21: 134–140, 1996.
 268. SCHENDEL SL, XIE Z, MONTAL MO, MATSUYAMA S, MONTAL M, AND REED JC. Channel formation by antiapoptotic protein Bcl-2. *Proc Natl Acad Sci USA* 94: 5113–5118, 1997.
 269. SCHLAEPFER DD, BODE HR, AND HAIGLER HT. Distinct cellular expression pattern of annexins in *Hydra vulgaris*. *J Cell Biol* 118: 911–928, 1992.
 270. SCHLAEPFER DD, FISHER DA, BRANDT ME, BODE HR, JONES JM, AND HAIGLER HT. Identification of a novel annexin in *Hydra vulgaris*. *J Biol Chem* 267: 9529–9539, 1992.
 271. SCHLESINGER PH, GROSS A, YIN XM, YAMAMOTO K, SATTO M, WAKSMAN G, AND KORSMEYER SJ. Comparison of the ion channel characteristics of proapoptotic BAX and antiapoptotic BCL-2. *Proc Natl Acad Sci USA* 94: 11357–11362, 1997.
 272. SCHMITZ-PFEIFFER C, BROWNE CL, WALKER J, AND BIDEN TJ. Activated protein kinase C α associates with annexin VI from skeletal muscle. *Biochem J* 330: 675–681, 1998.
 273. SEEMANN J, WEBER K, AND GERKE V. Structural requirements for annexin I-S100C complex formation. *Biochem J* 319: 123–129, 1996.
 274. SEEMANN J, WEBER K, AND GERKE V. Annexin I targets S100C to early endosomes. *FEBS Lett* 413: 185–190, 1997.
 275. SEEMANN J, WEBER K, OSBORN M, PARTON RG, AND GERKE V. The association of annexin I with early endosomes is regulated by Ca^{2+} and requires an intact N-terminal domain. *Mol Biol Cell* 7: 1359–1374, 1996.
 276. SENDA T, OKABE T, MATSUDA M, AND FUJITA H. Quick-freeze, deep-etch visualization of exocytosis in anterior pituitary secretory cells: localization and possible roles of actin and annexin II. *Cell Tissue Res* 277: 51–60, 1994.
 277. SENDA T, YAMASHITA K, OKABE T, SUGIMOTO N, AND MATSUDA M. Intergranule bridges in the anterior pituitary cell and their possible involvement in $\text{Ca}(2+)$ -induced granule-granule fusion. *Cell Tissue Res* 292: 513–519, 1998.
 278. SIAKA C, LAMBERT M, CARON C, AMIRAL J, HACHULLA E, HATRON PY, AND GOUDEMAND J. Low prevalence of anti-annexin V antibodies in antiphospholipid syndrome with fetal loss. *Rev Med Intern* 20: 762–765, 1999.
 279. SIMONS K AND GRUENBERG J. Jamming the endosomal system: lipid rafts and lysosomal storage diseases. *Trends Cell Biol* 10: 459–462, 2000.
 280. SIMONS K AND IKONEN E. Functional rafts in cell membranes. *Nature* 387: 569–572, 1997.
 281. SIMONS K AND TOOMRE D. Lipid rafts and signal transduction. *Nature Rev* 1: 31–39, 2000.
 282. SINGH TK AND LIU L. Modification of cysteine residues by N-ethylmaleimide inhibits annexin II tetramer mediated liposome aggregation. *Arch Biochem Biophys* 381: 135–140, 2000.
 283. SINHA P, HUTTER G, KOTTGEN E, DIETEL M, SCHADENDORF D, AND LAGE H. Increased expression of annexin I and thioredoxin detected by two-dimensional gel electrophoresis of drug resistant human stomach cancer cells. *J Biochem Biophys Methods* 37: 105–116, 1998.
 284. SJOLIN C, MOVITZ C, LUNDQVIST H, AND DAHLGREN C. Translocation of annexin XI to neutrophil subcellular organelles. *Biochim Biophys Acta* 1326: 149–156, 1997.
 285. SMITH PD, DAVIES A, CRUMPTON MJ, AND MOSS SE. Structure of the human annexin VI gene. *Proc Natl Acad Sci USA* 91: 2713–2717, 1994.
 286. SMITH PD AND MOSS SE. Structural evolution of the annexin supergene family. *Trends Genet* 10: 241–246, 1994.
 287. SMITH PD AND MOSS SE. Z-DNA-forming sequences at a putative duplication site in the human annexin VI-encoding gene. *Gene* 138: 239–242, 1994.
 288. SMYTHE E, SMITH PD, JACOB SM, THEOBALD J, AND MOSS SE. Endocytosis occurs independently of annexin VI in human A431 cells. *J Cell Biol* 124: 301–306, 1994.
 289. SOKOLOV Y, MAILLIARD WS, TRANNGO N, ISAS M, LUECKE H, HAIGLER HT, AND HALL JE. Annexins V and XII alter the properties of planar lipid bilayers seen by conductance probes. *J Gen Physiol* 115: 571–582, 2000.
 290. SOLITO E, DE COUPADE C, PARENTE L, FLOWER RJ, AND RUSSO-MARIE F. IL-6 stimulates annexin 1 expression and translocation and suggests a new biological role as class II acute phase protein. *Cytokine* 10: 514–521, 1998.
 291. SOLITO E, ROMERO IA, MARULLO S, RUSSO-MARIE F, AND WEKSLER BB. Annexin I binds to U937 monocytic cells and inhibits their adhesion to microvascular endothelium. *J Immunol* 165: 1573–1581, 2000.
 292. SONG GJ, CAMPOS B, WAGONER LE, DEDMAN JR, AND WALSH RA.

- Altered cardiac annexin mRNA and protein levels in the left ventricle of patients with end-stage heart failure. *J Mol Cell Cardiol* 30: 443–451, 1998.
293. SOPKOVA J, RENOARD M, AND LEWITT BA. The crystal structure of a new high-calcium form of annexin V. *J Mol Biol* 234: 816–825, 1993.
 294. SOPKOVA-DE OLIVEIRA SANTOS J, VINCENT M, TABARIES S, CHEVALIER A, KERBOEUF D, RUSSO-MARIE F, LEWITT-BENTLEY A, AND GALLAY J. Annexin A5 D226K structure and dynamics: identification of a molecular switch for the large scale conformational change of domain III. *FEBS Lett* 493: 122–128, 2001.
 295. SOPKOVA J, VINCENT M, TAKAHASHI M, LEWITT-BENTLEY A, AND GALLAY J. Conformational flexibility of domain III of annexin V studied by fluorescence of tryptophan 187 and circular dichroism: the effect of pH. *Biochemistry* 37: 11962–11970, 1998.
 296. SOPKOVA J, VINCENT M, TAKAHASHI M, LEWITT-BENTLEY A, AND GALLAY J. Conformational flexibility of domain II of annexin V at membrane/water interfaces. *Biochemistry* 38: 5447–5458, 1999.
 297. SPENNEBERG R, OSTERLOH D, AND GERKE V. Phospholipid vesicle binding and aggregation by four novel fish annexins are differently regulated by Ca^{2+} . *Biochim Biophys Acta* 1448: 311–319, 1998.
 298. SPRINGER TA. Traffic signals for lymphocyte recirculation and leukocyte emigration: the multistep paradigm. *Cell* 76: 301–314, 1994.
 299. SRIVASTAVA M, ATWATER I, GLASMAN M, LEIGHTON X, GOPING G, CAO HUY H, MILLER G, PICHEL J, WESTPHAL H, MEARS D, ROJAS E, AND POLLARD HB. Defects in inositol 1,4,5-trisphosphate receptor expression, Ca^{2+} signaling, and insulin secretion in the *anx7*(+/-) knockout mouse. *Proc Natl Acad Sci USA* 96: 13783–13788, 1999.
 300. SRIVASTAVA M, BUBENDORF L, SRIKANTAN V, FOSSOM L, NOLAN L, GLASMAN M, LEIGHTON X, FEHRLE W, PITTALUGA S, RAFFELD M, KOIVISTO P, WILLI N, GASSER TC, KONONEN J, SAUTER G, KALLIONIEMI OP, SRIVASTAVA S, AND POLLARD HP. *Anx7*, a candidate tumor suppressor gene for prostate cancer. *Proc Natl Acad Sci USA* 98: 4575–4580, 2001.
 301. SRIVASTAVA M AND POLLARD HB. Low in vivo levels of human *anx7* (annexin vii) gene expression are due to endogenous inhibitory promoter sequences. *Cell Biol Int* 24: 475–481, 2000.
 302. SUDO T AND HIDAKA H. Regulation of calyculin (S100A6) binding by alternative splicing in the N-terminal regulatory domain of annexin XI isoforms. *J Biol Chem* 273: 6351–6357, 1998.
 303. SUDO T AND HIDAKA H. Characterization of the calyculin (S100A6) binding site of annexin XI-A by site-directed mutagenesis. *FEBS Lett* 444: 11–14, 1999.
 304. SULLIVAN DM, WEHR NB, FERGUSON MM, LEVINE RL, AND FINKEL T. Identification of oxidant-sensitive proteins: TNF- α induces protein glutathiolation. *Biochemistry* 39: 11121–11128, 2000.
 305. SWAIRJO MA AND SEATON BA. Annexin structure and membrane interactions: a molecular perspective. *Annu Rev Biophys Biomol Struct* 23: 193–213, 1994.
 306. TABENGWA EM, ABOU-AGAG LH, BENZA RL, TORRES JA, AIKENS ML, AND BOOYSE FM. Ethanol-induced up-regulation of candidate plasminogen receptor annexin II in cultured human endothelial cells. *Alcohol Clin Exp Res* 24: 754–761, 2000.
 307. TANAKA T, KONDO S, IWASA Y, HIAI H, AND TOYOKUNI S. Expression of stress-response and cell proliferation genes in renal cell carcinoma induced by oxidative stress. *Am J Pathol* 156: 2149–2157, 2000.
 308. TAYLOR AD, PHILIP JG, JOHN CD, COVER PO, MORRIS JF, FLOWER RJ, AND BUCKINGHAM JC. Annexin I (lipocortin 1) mediates the glucocorticoid inhibition of cyclic adenosine 3',5'-monophosphate-stimulated prolactin secretion. *Endocrinology* 141: 2209–2219, 2000.
 309. THEOBALD J, HANBY A, PATEL K, AND MOSS SE. Annexin VI has tumour-suppressor activity in human A431 squamous epithelial carcinoma cells. *Br J Cancer* 71: 786–788, 1995.
 310. THONAT C, MATHIEU C, CREVECOEUR M, PENEL C, GASPAR T, AND BOYER N. Effects of a mechanical stimulation on localization of annexin-like proteins in *Bryonia dioica* internodes. *Plant Physiol* 114: 981–988, 1997.
 311. TOKUMITSU H, MIZUTANI A, AND HIDAKA H. Calyculin-binding site located on the NH_2 -terminal domain of rabbit CAP-50 (annexin XI): functional expression of CAP-50 in *Escherichia coli*. *Arch Biochem Biophys* 303: 302–306, 1993.
 312. TOKUMITSU H, MIZUTANI A, MINAMI H, KOBAYASHI R, AND HIDAKA H. A calyculin-associated protein is a newly identified member of the Ca^{2+} /phospholipid-binding proteins, annexin family. *J Biol Chem* 267: 8919–8924, 1992.
 313. TRAVERSO V, MORRIS JF, FLOWER RJ, AND BUCKINGHAM J. Lipocortin 1 (annexin I) in patches associated with the membrane of a lung adenocarcinoma cell line and in the cytoplasm. *J Cell Sci* 111: 1405–1418, 1998.
 314. TRIPLETT DA AND ASHERSON RA. Pathophysiology of the catastrophic antiphospholipid syndrome (CAPS). *Am J Hematol* 65: 154–159, 2000.
 315. TRISCHLER M, STOOBVOGEL W, AND ULLRICH O. Biochemical analysis of distinct Rab5- and Rab11-positive endosomes along the transferrin pathway. *J Cell Sci* 112: 4773–4783, 1999.
 316. TROUET D, NILIUS B, JACOBS A, REMACLE C, DROOGMANS G, AND EGGERMONT J. Caveolin-1 modulates the activity of the volume-regulated chloride channel. *J Physiol (Lond)* 520: 113–119, 1999.
 317. TROUVE P, LEGOT S, BELIKOVA I, MAROTTE F, BENEVOLENSKY D, RUSSO-MARIE F, SAMUEL JL, AND CHARLEMAGNE D. Localization and quantitation of cardiac annexins II, V, and VI in hypertensive guinea pigs. *Am J Physiol Heart Circ Physiol* 276: H1159–H1166, 1999.
 318. TURPIN E, RUSSO-MARIE F, DUBOIS T, DE PAILLERETS C, ALFSEN A, AND BOMSEL M. In adrenocortical tissue, annexins II and VI are attached to clathrin coated vesicles in a calcium-independent manner. *Biochim Biophys Acta* 1402: 115–130, 1998.
 319. TZIMA E, TROTTER PJ, HASTINGS AD, ORCHARD MA, AND WALKER JH. Investigation of the relocation of cytosolic phospholipase A_2 and annexin V in activated platelets. *Thromb Res* 97: 421–429, 2000.
 320. TZIMA E, TROTTER PJ, ORCHARD MA, AND WALKER JH. Annexin V binds to the actin-based cytoskeleton at the plasma membrane of activated platelets. *Exp Cell Res* 251: 185–193, 1999.
 321. TZIMA E, TROTTER PJ, ORCHARD MA, AND WALKER JH. Annexin V relocates to the platelet cytoskeleton upon activation and binds to a specific isoform of actin. *Eur J Biochem* 267: 4720–4730, 2000.
 322. TZIMA E AND WALKER JH. Platelet annexin V: the ins and outs. *Platelets* 11: 245–251, 2000.
 323. UHRIN P AND HORSEMAN ND. Regulation of the annexin Icp35 gene in transfected mammary gland cell lines. *Biochem Mol Biol Int* 30: 305–310, 1993.
 324. VAARALA MH, PORVARI K, KYLLONEN A, AND VIHKO P. Differentially expressed genes in two LNCaP prostate cancer cell lines reflecting changes during prostate cancer progression. *Lab Invest* 80: 1259–1268, 2000.
 325. VAN GINKEL PR, GEE RL, WALKER TM, HU DN, HEIZMANN CW, AND POLANS AS. The identification and differential expression of calcium-binding proteins associated with ocular melanoma. *Biochim Biophys Acta* 1448: 290–297, 1998.
 326. VEDELER A AND HOLLAS H. Annexin II is associated with mRNA which may constitute a distinct subpopulation. *Biochem J* 348: 565–572, 2000.
 327. VERZILI D, ZAMPARELLI C, MATTEI B, NOEGEL AA, AND CHIANCONE E. The sorcin-annexin VII calcium-dependent interaction requires the sorcin N-terminal domain. *FEBS Lett* 471: 197–200, 2000.
 328. VOGL T, JATZKE C, HINZ H-J, BENZ J, AND HUBER R. Thermodynamic stability of annexin V E17G: equilibrium parameters from an irreversible unfolding reaction. *Biochemistry* 36: 1657–1668, 1997.
 329. VON DER MARK K AND MOLLENHAUER J. Annexin V interactions with collagen. *Cell Mol Life Sci* 53: 539–545, 1997.
 330. WAISMAN DM. Annexin II tetramer: structure and function. *Mol Cell Biochem* 149/150: 301–322, 1995.
 331. WALTHER A, RIEHEMANN K, AND GERKE V. A novel ligand of the formyl peptide receptor: annexin I regulates neutrophil extravasation by interacting with the FPR. *Mol Cell* 5: 831–840, 2000.
 332. WANG LM, RAHMAN MM, IIDA H, INAI T, KAWABATA S, IWANAGA S, AND SHIBATA Y. Annexin V is localized in association with Z-line of rat cardiac myocytes. *Cardiovasc Res* 30: 363–371, 1995.
 333. WANG X, CAMPOS B, KAETZEL MA, AND DEDMAN JR. Annexin V is critical in the maintenance of murine placental integrity. *Am J Obstet Gynecol* 180: 1008–1016, 1999.
 334. WEN Y, EDELMAN JL, KANG T, AND SACHS G. Lipocortin V may function as a signaling protein for vascular endothelial growth factor receptor-2/Flk-1. *Biochem Biophys Res Commun* 258: 713–721, 1999.
 335. WENG X, LUECKE H, SONG IS, KANG DS, KIM SH, AND HUBER R. Crystal

- structure of human annexin I at 2.5 Å resolution. *Protein Sci* 2: 448–458, 1993.
336. WICE BM AND GORDON JL. A strategy for isolation of cDNAs encoding proteins affecting human intestinal epithelial cell growth and differentiation: characterization of a novel gut-specific N-myristoylated annexin. *J Cell Biol* 116: 405–422, 1992.
337. WILLIAMS K, CHUBB C, HUBERMAN E, AND GIOMETTI CS. Analysis of differential protein expression in normal and neoplastic human breast epithelial cell lines. *Electrophoresis* 19: 333–343, 1998.
338. WU F, FLACH CR, SEATON BA, MEALY TR, AND MENDELSON R. Stability of annexin V in ternary complex with Ca^{2+} and anionic phospholipids: IR studies of monolayers and bulk phases. *Biochemistry* 38: 792–799, 1999.
339. XIE W, KAETZEL MA, BRUZIK KS, DEDMAN JR, SHEARS SB, AND NELSON DJ. Inositol 3,4,5,6-tetrakisphosphate inhibits the calmodulin-dependent protein kinase II-activated chloride conductance in T84 colonic epithelial cells. *J Biol Chem* 271: 14092–14097, 1996.
340. XU J, ZIEMNICKA D, MERZ GS, AND KOTULA L. Human spectrin src homology 3 domain binding protein 1 regulates macropinocytosis in NIH 3T3 cells. *J Cell Sci* 113: 3805–3814, 2000.
341. ZEUSCHNER D, STOORVOGEL W, AND GERKE V. Association of annexin 2 with recycling endosomes requires either calcium or cholesterol-stabilized membrane domains. *Eur J Cell Biol* 80: 499–507, 2001.
342. ZOBIACK N, GERKE V, AND RESCHER U. Complex formation and submembranous localization of annexin 2 and S100A10 in live HepG2 cells. *FEBS Lett* 500: 137–140, 2001.
343. ZOBIACK N, RESCHER U, LAARMANN S, MICHGEHL S, SCHMIDT MA, AND GERKE V. Cell surface attachment of pedestal-forming enteropathogenic *E. coli* induces a clustering of raft components and a recruitment of annexin 2. *J Cell Sci*. In press.

Pemphigus Vulgaris Antibody Identifies Pemphaxin

A NOVEL KERATINOCYTE ANNEXIN-LIKE MOLECULE BINDING ACETYLCHOLINE*

Received for publication, April 13, 2000, and in revised form, July 3, 2000
Published, JBC Papers in Press, July 17, 2000, DOI 10.1074/jbc.M003174200

Vu Thuong Nguyen, Assane Ndoeye, and Sergei A. Grandt†

From the Department of Dermatology, University of California at Davis, Sacramento, California 95817

Because pemphigus vulgaris (PV) IgGs adsorbed on the rDsg3-Ig-His baculoprotein induced blisters in neonatal mice, it was proposed that anti-desmoglein 3 (Dsg 3) autoantibody causes PV. However, we found that rDsg3-Ig-His absorbs autoantibodies to different antigens, including a non-Dsg 3 keratinocyte protein of 130 kDa. This prompted our search for novel targets of PV autoimmunity. The PV IgG eluted from a 75-kDa keratinocyte protein band both stained epidermis in a pemphigus-like pattern and induced acantholysis in keratinocyte monolayers. Screening of a keratinocyte λ gt11 cDNA library with this antibody identified clones carrying cDNA inserts encoding a novel molecule exhibiting ~40% similarity with annexin-2, named pemphaxin (PX). Recombinant PX (rPX-His) was produced in *Escherichia coli* M15 cells, and, because annexins can act as cholinergic receptors, its conformation was tested in a cholinergic radioligand binding assay. rPX-His specifically bound [3 H]acetylcholine, suggesting that PX is one of the keratinocyte cholinergic receptors known to be targeted by disease-causing PV antibodies. Preabsorption of PV sera with rPX-His eliminated acantholytic activity, and eluted antibody immunoprecipitated native PX. This antibody alone did not cause skin blisters *in vivo*, but its addition to the preabsorbed PV IgG fraction restored acantholytic activity, indicating that acantholysis in PV results from synergistic action of antibodies to different keratinocyte self-antigens, including both acetylcholine receptors and desmosomal cadherins.

skin adhesion in which keratinocytes (KC), the stratified epithelial cells comprising the epidermis, lose their ability to adhere to one another (acantholysis) (1). Acantholysis leads to an intra-epidermal split and separation of the suprabasal epidermal layer, which is clinically manifested by blistering that denudes skin and oral mucosa. Introduction of glucocorticosteroids into the treatment of PV patients decreased mortality from 90 to 10% (reviewed in Ref. 2). Long-term corticosteroid therapy of PV patients is life-saving but causes severe side effects, including death (3, 4). This urges development of non-hormonal therapy of pemphigus acantholysis. The pathophysiology of PV includes an array of IgG autoantibodies reacting with keratinocyte self-antigens with the apparent molecular mass ranging from 12 to 190 kDa (reviewed in Ref. 5), including a 130-kDa keratinocyte polypeptide (6, 7). The notion that autoantibodies are the main cause of PV stems from the fact that passive transfer of pemphigus, but not normal, IgGs to neonatal mice can induce skin lesions characteristic of PV (8). Using pemphigus antibodies eluted from the 130-kDa band as a probe, Amagai *et al.* (9) screened the human keratinocyte λ gt11 cDNA library and found that two of the clones recognized by these PV antibodies represented a novel desmosomal cadherin termed desmoglein (Dsg) 3. The hypothesis that PV, a disease of skin adhesion, is caused by an antibody to Dsg 3, an adhesion molecule, prompted experiments toward elucidation of the biological effects of anti-Dsg 3 antibody. However, acantholysis could not be documented in keratinocyte monolayers treated with anti-Dsg 3 antibody. Several recombinant Dsg 3 (rDsg3) proteins were produced and used to test if adsorbed antibodies can elicit skin blistering in neonatal mice upon passive transfer (10, 11). Although rDsg3 could absorb PV antibodies to Dsg 3, it failed to absorb all disease-causing antibody, and PV IgGs depleted of antibodies to Dsg 3 kept binding to KC in murine epidermis and inducing gross skin blisters (10, 12). Only creation of a chimeric baculoprotein that included both the extracellular epitope of Dsg 3 and an Fc portion of human IgG₁ could fulfill both goals: elimination of all disease-causing antibodies from pemphigus serum and induction of gross skin blisters in neonatal mice injected with concentrated eluants (13, 14). Explanations of this phenomenon include: 1) a possibility that the IgG portion rendered the rDsg3 with appropriate conformational epitope, which could be tested by crystallography; and 2) a possibility that the tertiary structure of the chimera mimicked non-Dsg 3 targets of pemphigus autoimmunity, which could be tested by characterizing the antigenic profile of the eluted IgG. Neither possibility was tested. Recently, it has become evident that anti-Dsg 3 antibody alone is not sufficient to cause skin blisters (15). A role for an autoantibody to another desmosomal cadherin, Dsg1, was

Pemphigus vulgaris (PV¹) is a potentially lethal disease of

* This work was supported by the International Pemphigus Research Fund. Preliminary reports of these findings were presented at the Third Tricontinental Meeting of the Society for Investigative Dermatology, the European Society for Dermatological Research, and the Japanese Society for Investigative Dermatology, Cologne, Germany, May 9, 1998, and at the 60th Annual Meeting of the Society for Investigative Dermatology, Chicago, Illinois, May 7, 1999, and May 12, 2000, and published in abstract form in the *Journal of Investigative Dermatology* 110:486, 1998, and *Journal of Investigative Dermatology* 112:250, 1999, respectively. The costs of publication of this article were defrayed in part by the payment of page charges. This article must therefore be hereby marked "advertisement" in accordance with 18 U.S.C. Section 1734 solely to indicate this fact.

The nucleotide sequence(s) reported in this paper has been submitted to the GenBank™/EBI Data Bank with accession number(s) AF230929.

† To whom correspondence should be addressed: Dept. of Dermatology, University of California, Davis, UC Davis Medical Center, 4860 Y St., Suite 3400, Sacramento, CA 95817. Tel.: 916-734-6057; Fax: 916-734-6793; E-mail: sagrandt@ucdavis.edu.

¹ The abbreviations used are: PV, pemphigus vulgaris; PX, pemphaxin; ACh, acetylcholine; DIF, direct immunofluorescence; Dsg, desmoglein; FITC, fluorescein isothiocyanate; IIF, indirect immunofluorescence; IPTG, isopropyl-D-thiogalactoside; KC, keratinocytes; KGM, serum-free keratinocyte growth medium; PBS, phosphate-buffered saline; PCR, polymerase chain reaction; PrBCM, propylbenzylcholine

mustard; rDsg, recombinant Dsg; rPX-His, recombinant PX; PAGE, polyacrylamide gel electrophoresis; TBS, Tris-buffered saline; bp, base pair(s); kb, kilobase(s); kbp, kilobase pair(s).

proposed to explain skin blisters in PV patients (16). However, well-documented cases of generalized disease in PV patients lacking Dsg1 antibody (17) argued in favor of the existence of a yet unidentified disease-causing non-Dsg1/Dsg 3 antibody that could have been nonspecifically preabsorbed with rDsg3-Ig constructs. Furthermore, intraperitoneal injection of the PV IgG, which did not have anti-Dsg1 activity, into neonatal *Dsg3* knockout mice (*i.e.* *Dsg3*^{null} mice) resulted in gross skin blisters (5). It should be mentioned that neonatal *Dsg3*^{null} mice lack the true PV phenotype, in that they do not develop spontaneous skin blisters (5, 18), which has already justified their use in passive transfer experiments by different research groups studying the nature of disease-causing PV antibodies (5, 15).

Recently, we have compared antibodies eluted from rDsg3 (rDsg3-His) and rDsg3-Ig (rDsg3-Ig-His), which were used in the original preabsorption experiments (10, 13, 14), and demonstrated that the two Dsg 3 constructs adsorb antibodies with different antigenic specificities (19). The PV IgGs eluted from rDsg3-His reacted predominantly with the 130-kDa protein band present in normal human KC in addition to a few weakly stained bands that varied among test PV sera. In marked contrast, the antibodies eluted from rDsg3-Ig-His recognized several different protein bands, including a non-Dsg 3 130-kDa band in the immunoblot of Dsg 3^{-/-} keratinocyte proteins. Thus, crossreactivity of *Dsg3-Ig-His* with non-Dsg 3 antibodies explains how this chimeric baculoprotein could absorb all disease-causing PV IgG.

The vast majority of pemphigus patients develop antibodies that immunoprecipitate keratinocyte membrane proteins binding the covalent cholinergic radioligand [³H]propylbenzilylcholine mustard ([³H]PrBCM) (5) and compete with a cholinergic radioligand, [³H]atropine, for binding to the cell membrane of intact human KC in culture (20). The nature of the acetylcholine (ACh) receptor(s) targeted by PV autoimmunity remains to be determined. Addition to either muscarinic or nicotinic antagonists to keratinocyte monolayers in both cases results in acantholysis (reviewed in Refs. 21, 22), whereas cholinergic agonists stimulate cell-to-cell adhesion of KC, and can reverse, attenuate, or prevent acantholysis in keratinocyte monolayers when added to culture after, simultaneously with, or prior to PV IgG, respectively (20). The anti-acantholytic activity of cholinergic agonists suggests a novel avenue for development of non-hormonal treatment of pemphigus.

In this study, we demonstrate the nature of a novel target for non-Dsg 3 disease-causing PV IgG. Screening of the keratinocyte cDNA expression library with PV IgG immunoaffinity-purified on a 75-kDa area of the immunoblotting membrane revealed a novel human annexin-like molecule, which we named pemphaxin (PX). We produced recombinant PX (rPX-His) and demonstrated that this protein acts as a cholinergic receptor in the radioligand binding assay with [³H]ACh. PV IgG specifically recognized rPX-His, and preabsorption of PV sera with rPX-His eliminated the acantholytic activity that could be restored by adding back the anti-PX antibody eluted from the affinity column. Thus, disease-causing PV antibody identified PX, a novel human annexin that acts as a keratinocyte cell surface receptor for ACh, and, therefore, may mediate known biological effects of this cytotransmitter on adhesion and motility of KC.

EXPERIMENTAL PROCEDURES

Sources of Sera and Tissue—The sera and IgG fractions were from well-established PV patients, and from healthy volunteers. This study had been approved by the University of California Davis Human Subjects Review Committee. The diagnosis of PV was made based on the results of both comprehensive clinical and histological examinations together with immunological studies, which included direct immunofluorescence (DIF), indirect immunofluorescence (IIF) on various epi-

thelial substrates, immunoblotting, and immunoprecipitation, following standard protocols (23). The serum samples were stored frozen at -80 °C until use in experiments. The serum IgG fractions were isolated using 40% ammonium sulfate followed by dialysis with Ca²⁺- and Mg²⁺-free phosphate-buffered saline (PBS; Life Technologies, Inc., Gaithersburg, MD), lyophilized, and reconstituted in PBS as detailed elsewhere (5). The protein concentration was determined using the Micro BCA kit (Pierce). The samples of normal human neonatal foreskins that were used to start keratinocyte cell cultures were transported to the laboratory in culture medium, and the samples of normal human abdominoplasty skin that served as a source of keratinocyte membrane protein for immunoblotting were frozen immediately after harvesting.

Immunoaffinity Purification of Acantholytic Anti-keratinocyte PV Antibody—The enriched fraction of human keratinocyte membrane protein (5) was used as a substrate in immunoblotting experiments aimed at characterizing novel PV antigens. The epidermis was separated from the dermis by incubation in RPMI 1640 medium (Sigma), supplemented to contain 200 mM EDTA for 90 min at 37 °C and 5% CO₂ (24), and harvested into a 50-ml polyethylene centrifuge tube filled with ice-cold Tris-buffered saline (TBS), pH 7.4, that contained the following protease inhibitors: 2 mM phenylmethylsulfonyl fluoride, 0.1 mg/ml bacitracin, 10 µg/ml leupeptin, 10 µg/ml soybean trypsin inhibitor, 10 µg/ml pepstatin A, and 10 µg/ml chymostatin (all from Sigma). The epidermis was then washed three times by centrifugation, put on ice, and homogenized with a PowerGen tissue-and-cell disrupter (Fisher Scientific, Santa Clara, CA) in the same buffer containing 20 mM Ca²⁺. Large organelles and epidermal debris were removed by centrifugation at 2000 × *g* for 45 min at 4 °C, and the cell membrane fraction was pelleted from the supernatant by centrifugation at 80,000 × *g* for 1 h at 4 °C. The pellet was solubilized in sodium dodecyl sulfate-polyacrylamide gel electrophoresis (SDS-PAGE) buffer containing 2% SDS and 5% β-mercaptoethanol, boiled for 5 min, and cleared by centrifugation at 40,000 × *g* for 1 h at 4 °C. Western blotting of SDS-PAGE-resolved proteins was performed as reported previously (5) with minor modifications. Briefly, the proteins were separated on a 7.5% SDS-PAGE gel and transferred to an Immobilon-P membrane (Millipore Corp., Bedford, MA), which was blocked, first with 5% milk in TBS for 1 h at 37 °C and then with TBS containing 1% normal goat serum, 3% dried milk, and 0.05% Tween 20 (Sigma) overnight at 4 °C, and cut into 4-mm wide vertical strips. Each strip was exposed to a primary antibody, *i.e.* PV or normal human serum, for 1 h at room temperature and then washed thoroughly. The protein bands recognized by PV and normal human IgGs were visualized by biotinylated goat anti-human IgG antibody (Pierce) and developed using a biotin/avidin system (Vectastain ABC system; Vector Laboratories, Burlingame, CA). The specificity of binding was determined in negative control experiments, in which the primary antibodies were omitted. The PV IgG fractions were isolated from the immunoblotting membrane areas that were recognized uniquely by PV IgG, but not normal human IgG, following a procedure described previously (25). Briefly, approximately 3-mm wide horizontal strips carrying a keratinocyte membrane protein with a particular molecular mass of ±3 kDa were cut out from the immunoblotting membrane and incubated overnight with PV serum diluted 1:5 in TBS containing 20 mM CaCl₂, 0.05% Tween 20 (Sigma), and 1% non-fat skim milk to allow antibody binding. The strips were then washed thoroughly, and the antibodies were eluted by a 3-min incubation at 37 °C in a solution containing 500 µl of 20 mM sodium citrate, 1% milk, and 0.05% Tween 20 (pH 3.2) and immediately neutralized by adjusting the pH to 7.4 with the 2 M Tris base.

Immunofluorescence Screening Experiments—The IIF experiments testing the ability of PV IgG eluted from the strips of immunoblotting membranes to specifically stain KC in the tissue samples were performed as described previously (5) with minor modifications. Briefly, 4- to 8-mm cryostat sections of freshly frozen normal human skin, monkey esophagus, or murine skin were incubated overnight at 4 °C with the immunoaffinity-purified PV IgG fractions, after which the tissue sections were washed and binding of primary antibody was visualized by incubating the tissue section with fluorescein isothiocyanate (FITC)-labeled goat anti-human IgG antibody (Pierce) for 1 h at room temperature. The specificity of antibody binding was demonstrated by omitting the primary antibody, which abolished the staining. The immunofluorescence images were obtained using a fluorescence microscope (Axiovert 135, Carl Zeiss Inc., Thornwood, NY) with a charge-coupled device video camera (Photon Technology International, Monmouth Junction, NJ) attached.

Cell Culture Screening Experiments—Acantholytic activity of the eluted PV IgGs, which stained the stratified epithelial substrate in a

pemphigus-like, "intercellular" pattern, were tested in the monolayers of normal human foreskin KC isolated from the epidermis and grown at 37 °C in serum-free keratinocyte growth medium (KGM; Life Technologies, Inc.) containing 0.09 mM Ca^{2+} in a humid 5% CO_2 incubator, as detailed elsewhere (26). To observe changes in cell morphology, second passage KC were seeded into 6-well tissue culture plates at a cell density of 1×10^5 /well and grown to confluence (i.e. for 5–7 days) in 2 ml of KGM per well. The monolayers were then fed with equal amounts of test PV (experiment) or normal human serum (control) IgG fractions, 10 $\mu\text{g}/\text{ml}$ KGM, and returned to a 5% CO_2 incubator for a 12-h incubation at 37 °C. After incubation, the cells were fixed with 3% glutaraldehyde and stained with the trypan blue dye solution (Sigma), and the images of the experimental and control keratinocyte monolayers were captured using a camera-adapted light microscope (Olympus Corp., Lake Success, NY).

Screening of cDNA Library—Following standard procedures (27), the human keratinocyte $\lambda\text{gt}11$ cDNA library (CLONTECH, Palo Alto, CA) was screened with PV antibody that was immunoaffinity-purified from a 75-kDa keratinocyte membrane protein band. Briefly, the host bacteria Y1090r- were grown overnight, infected with phages from the library for 30 min, plated on Mg^{2+} -containing agar plates, and grown overnight at 37 °C. Over 3 million plaques formed on the bacterial lawns were screened by lifting isopropyl-D-thiogalactoside (IPTG; Sigma) containing nitrocellulose filters (Millipore Corp.). After blocking with 3% dry milk (Sigma) in TBS, the filters were incubated for 2 h at room temperature with the immunoaffinity-purified antibody. The plaques specifically recognized by the antibody were visualized using horseradish peroxidase-conjugated goat anti-human IgG (Bio-Rad, Hercules, CA). The positive plaques were isolated and rescreened until a single clone was isolated. The insert from isolated clones were amplified using a pair of cloning primers specific for the $\lambda\text{gt}11$ vector: 5'-ggggggggtaccggatcccggtcgacgggtttccatattg-3' (forward) and 5'-cccgggatccatattggtaccagcttattttgacaccagacca-3' (reverse). The polymerase chain reaction (PCR) products were purified from the gel using the silica membrane spin-column technology (QIAquick Spin, Qiagen, Santa Clarita, CA) and sequenced in both directions with a pair of specific sequence primers: 5'-gactctggagcccg-3' (forward) and 5'-ggtagcgaccggcg-3' (reverse) using an automated DNA sequencing system (ABI Prism 377, Perkin-Elmer). Homology searches were run against the GenBank® nucleotide and protein sequence data bases using the BLAST search program from the National Center of Biological Information web site. The amino acid multiple sequence alignment was performed using Gene Jockey III software (Biosoft, Cambridge, UK). The cDNA insert was removed from the purified $\lambda\text{gt}11$ phagemid and subcloned into pBluescript vector (Stratagene, La Jolla, CA) for further characterization.

PCR Experiments—PCR was performed as described by us elsewhere (5). Briefly, each reaction had a final volume of 50 μl containing the DNA templates, $1 \times$ PCR buffer (Promega, Madison, WI); 0.2 mM each of dATP, dCTP, dGTP, dTTP; 2 units of *Taq* DNA polymerase (Promega); and 1 μM each of the sense and antisense primers. The reaction mixture was first heated at 95 °C for 5 min and hot-started with 2 units of DNA *Taq*-polymerase (Life Technologies, Inc.) followed by 35 cycles (or 15 cycles for cloning experiments) of denaturing at 95 °C for 60 s, annealing at an appropriate temperature (optimized for primers used in each PCR) for 60 s, and extension at 72 °C for 120 s. In the final cycle, the extension was increased to 8 min. The PCR products were electrophoresed on 2% agarose gels containing 1 $\mu\text{g}/\text{ml}$ ethidium bromide and photographed under fluorescent UV illumination (AlphaImager 2000, Alpha Innotech Corp., San Leandro, CA). The size of the PCR product was estimated by using a 100- or a 250-bp DNA ladder standard (Life Technologies, Inc.).

Expression of rPX-His in Escherichia coli—The expression vector pQE-30 (Qiagen), which is designed to express proteins containing a 6xHis-tag at the N-terminal, was used to express rPX-His. The vector was linearized by digestion with the *Sph*I and *Kpn*I restriction enzymes for 1 h at 37 °C, then purified from an agarose gel, and incubated at 37 °C with 5 units of alkaline phosphatase (Promega) to enhance the efficiency of ligation. cDNA from the PX $\lambda\text{gt}11$ clone was amplified by PCR with the following primers: 5'-ccgcatgcgatgacgatgacaaatgtctgtgactggcggaagatggc-3' (forward) and 5'-cccgggatccatattggtaccagcttattttgacaccagacca-3' (reverse). The forward primer was designed to have an additional *Sph*I restriction site, which allows the insert to be ligated in-frame with the 6xHis gene of the pQE-30 vector. The PCR product was double digested with *Sph*I and *Kpn*I restriction enzymes and purified. Digested product was directionally cloned into unique *Sph*I and *Kpn*I sites in the multiple cloning site of the pQE-30 vector. The ligated vector was used to transform *E. coli* expression

strain M15 (Qiagen). Transformed cells were plated on a NYZ agar plate containing 25 $\mu\text{g}/\text{ml}$ kanamycin and 100 $\mu\text{g}/\text{ml}$ ampicillin and grown overnight. To verify the clone that produced the rPX-His protein, transformed bacterial colonies were blotted to a marked nitrocellulose filter and inversely placed on an IPTG-containing NYZ agar plate and grown for 4 h. The filter was then treated with denaturing buffer, neutralized, blocked with 3% non-fat milk in TBS and screened for colonies that produced rPX-His using anti-RGS-His monoclonal antibody (Qiagen). Positive clones were selected from the original plate, and their plasmids were sequenced with a specific primer to confirm that the correct PX cDNA had proper frame and orientation. A representative clone was inoculated into NYZ medium containing 25 $\mu\text{g}/\text{ml}$ kanamycin and 100 $\mu\text{g}/\text{ml}$ ampicillin. The culture was incubated, with shaking, at 37 °C until an A_{600} of 0.6 was reached, and IPTG was added to a final concentration of 2 mM. Culture samples (2 ml each) were collected every hour during 4 h and centrifuged, and the bacterial pellets were dissolved in sample buffer and analyzed by SDS-PAGE with Coomassie Blue staining.

Production and Purification of rPX-His—Large scale rPX-His production was performed in 1 liter of medium, as described above. The cell pellet was lysed at room temperature by stirring the pellet in a buffered solution containing 8 M urea, pH 8.0 (lysis solution). Once the solution became translucent, the cellular debris was removed by centrifugation at $40,000 \times g$ for 1 h at 4 °C. The clarified supernatant was incubated with nickel-nitrilotriacetic acid-agarose resin (Ni-NTA, Qiagen) to capture the His-tagged protein. The resin was washed with several volumes of buffered 8 M urea, pH 6.3, until a A_{280} of about 0.001 was achieved, and loaded into a column. The rPX-His protein was eluted from the column using either denaturing or non-denaturing condition. The denatured rPX-His was eluted with a buffer containing 8 M urea, pH 5.9 and 4.5, resolved by SDS-PAGE, and analyzed by immunoblotting with PV IgG. Or, the immobilized rPX-His was first renatured over a period of 1.5 h in a linear 6 to 1 M urea gradient in 500 mM NaCl, 20% glycerol, 20 mM Tris-Cl, pH 7.4, containing protease inhibitors, and then eluted with a non-denaturing buffer containing 50 mM NaH_2PO_4 , 300 mM NaCl, and 250 mM imidazole, pH 8.0. The purified renatured rPX-His was used in the radioligand binding assays as well as for immunoaffinity purification of anti-PX PV antibody.

Radioligand Binding Assays with rPX-His—Nitrocellulose filters (13-mm diameter, catalog no. HAWPO1300, Millipore Corp.) with a total protein capacity of 160 $\mu\text{g}/\text{cm}^2$ were placed into the bottom of each well of a bovine serum albumin-pretreated 24-well standard cell-and-tissue culture plate (Nalco Nunc International, Denmark). One μg of the affinity-purified rPX-His was diluted in 300 μl of PBS and loaded into each filter for overnight incubation at 4 °C to allow complete absorption of rPX-His by the filter (determined in a series of preliminary experiments by measuring the optical density at 280 nm of free rPX-His remaining in the solution). The membranes carrying rPX-His were blocked with 2% bovine serum albumin for 1 h at room temperature, after which the plates were put on ice, washed three times with ice-cold PBS, and exposed in triplicate for 1 h to increasing, from 0 to 1000 nM, concentrations of [^3H]ACh iodide (82.0 mCi/mmol, NEN Life Science Products, Boston, MA). Nonspecific binding was measured in parallel wells, in which the filters were exposed to the same increasing doses [^3H]ACh in the presence of 100-fold concentrations of non-labeled ACh iodide (Sigma). The filters were then washed thoroughly with ice-cold PBS, placed in 6-ml vials containing 5 ml of liquid scintillation mixture (Ecolite, ICN, Costa Mesa, CA), and their radioactivity was counted in the liquid scintillation counter (model 1409, Wallac Inc., Gaithersburg, MD). The specific binding was computed by subtracting the nonspecific binding from total binding, and the binding capacity (B_{max}) and dissociation constant (K_d) were calculated using the ligand binding analysis software Prism (GraphPad, San Diego, CA). In a separate set of radioligand binding experiments, we investigated the ability of the cholinergic radioligand [^3H]PrBCM (5 mCi/mmol of the customized [^3H]PrBCM; NEN Life Products) to label rPX-His and the ability of the nicotinic agonist nicotine and the muscarinic agonist muscarine (both from Sigma) to abolish rPX-His labeling with [^3H]PrBCM. Prior to the assay, [^3H]PrBCM was cyclized in 10 mM PBS at 30 °C for 20 min to activate the aziridinium ions (28).

Immunoaffinity Purification and Characterization of Anti-PX PV IgG—PV sera were diluted 1:5 in Immunosorbent Gentle binding buffer (Pierce) and incubated overnight at 4 °C with rPX-His immobilized on Ni-NTA resin. The pass-through serum fraction was collected, and the IgGs were isolated using 40% ammonium sulfate precipitation followed by dialysis against Ca^{2+} - and Mg^{2+} -free PBS. The rPX-His column with bound PV antibody was washed 10 times with TBS containing 300 mM NaCl, and the immunoaffinity-purified anti-PX IgG fraction was eluted

from the column by Immunopure Gentle elution buffer and desalted on a D-Salt Exellulose plastic desalting column (both from Pierce). The pattern of specific binding of the eluted antibody was examined by IIF on human skin and monkey esophagus. The antigenic profile of the eluted PV IgG was identified by immunoprecipitation of metabolically labeled human keratinocyte proteins (see below), which is considered the most sensitive and specific approach to characterize the antigenic specificity pemphigus antibodies (7).

Metabolic Labeling of Cultured KC and Immunoprecipitation Assay—Second passage human foreskin KC were grown to approximately 90% confluence, washed thoroughly with prewarmed (37 °C) PBS, incubated for 15 min at 37 °C in methionine-free Dulbecco's modified Eagle's medium (Life Technologies, Inc.) containing 15% newborn calf serum, and then exposed to 100 μ Ci/ml [35 S]methionine (1000 Ci/mmol, Amersham Pharmacia Biotech, Arlington Heights, IL) in 1.8 mM Ca^{2+} labeling medium for 16 h in a humid, 5% CO_2 incubator at 37 °C. The keratinocyte monolayers were then washed thoroughly, and the cells were scraped with a rubber policeman; pelleted by centrifugation at $300 \times g$ for 5 min at 4 °C; resuspended in ice-cold 10 mM TBS containing 0.025% NaN_3 , 20 mM Ca^{2+} , 1% Nonidet P-40 (Amersham Pharmacia Biotech) and the protease inhibitors 1 mM iodoacetamide, 2 mM phenylmethylsulfonyl fluoride, 5 μ g/ml leupeptin, 5 μ g/ml pepstatin A, and 5 μ g/ml chymostatin; put on ice; and homogenized. Solubilized [35 S]methionine-labeled proteins were separated by centrifugation at $40,000 \times g$ for 60 min at 4 °C and used as a source of naturally folded keratinocyte proteins. The radiolabeled keratinocyte protein solution was incubated with immunoaffinity-purified anti-PX PV IgG overnight at 4 °C with gentle shaking. The immune complexes were precipitated with slurry protein A-Sepharose suspension, washed, and resolved by 7.5% SDS-PAGE. The gels were fixed and enhanced with 1 M sodium salicylate, and the radioactivity was analyzed using the storage phosphor autoradiography feature of the Storm system (Molecular Dynamics, Mountain View, CA).

Antibody Transfer to Neonatal Mice—The PV phenotype was induced in neonatal mice by passive transfer of PV patients' serum IgG fractions to normal Balb/c mice (8). The IgGs were injected intraperitoneally through a 30-gauge needle at a dose of 20 mg/g of body weight per day into 10- to 12-h-old pups. The neonates always received the same amounts of PV IgG (experiment) and normal human IgG (control). The latter was isolated from normal human serum purchased from Sigma Chemical Co. The mice were sacrificed when fully developed skin lesions could be seen or, if no gross lesions could be observed, approximately 24 h after the last injection. The lesional and perilesional skin samples were collected and examined by staining with hematoxylin and eosin and by DIF with FITC-conjugated goat anti-human IgG antibody (Pierce).

Statistics—The results of quantitative experiments were expressed as mean \pm S.D. Significance was determined using the Student's *t* test.

RESULTS

Selection of an Immunoaffinity-purified Acantholytic Anti-keratinocyte PV IgG as a Candidate for cDNA Library Screening—In an attempt to identify the pathogenic PV antibody, we investigated the ability of different fractions of immunoaffinity-purified anti-keratinocyte PV IgGs to: 1) stain the stratified epithelial substrates in a fishnet-like, "intercellular" pattern, which is diagnostic of PV (1); and 2) induce acantholysis in keratinocyte monolayers, which has become a standard approach to test disease-causing ability of PV antibodies (29, 30). Among tested PV IgG fractions, the antibody eluted from the horizontal strip excised from the 75-kDa area of the immunoblotting membrane produced intercellular epithelial staining of both normal human skin and monkey esophagus in IIF experiments (Fig. 1, A and B). Treatment of confluent monolayers of normal human KC with this immunoaffinity-purified PV IgG fraction, but not with normal human IgG, produced changes of the cell morphology characteristic of pemphigus acantholysis (Fig. 1, C and D). No acantholysis could be seen in cultures treated with equal amounts of PV IgG eluted from the 130-kDa area of immunoblots of normal human keratinocyte proteins (data not shown). Therefore, PV IgG immunoaffinity-purified on a 75-kDa band was selected to probe the λ gt11 human keratinocyte cDNA expression library.

Isolation of cDNA Clones Encoding PX and Sequence Anal-

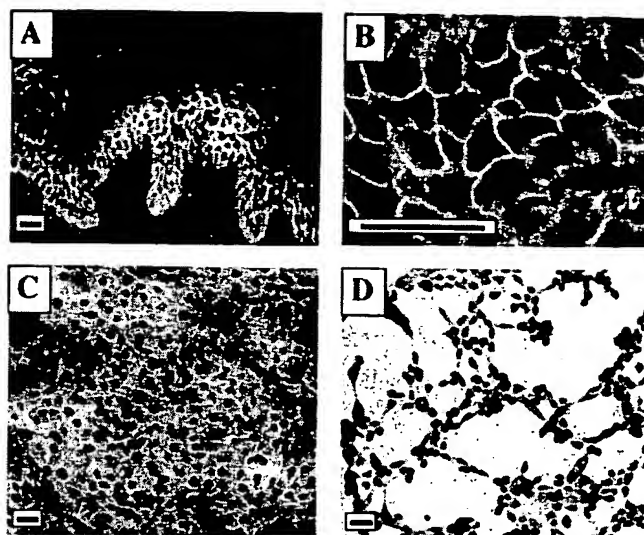
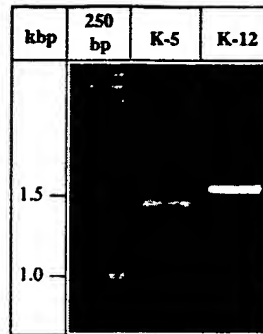


FIG. 1. Selection of the acantholytic anti-keratinocyte PV IgG fraction for screening human keratinocyte λ gt11 cDNA library. A and B, the PV IgG immunoaffinity-purified on the horizontal strip excised from the 75-kDa area of the immunoblotting membrane produced intercellular epithelial staining of both normal human skin (A) and monkey esophagus (B) in IIF experiments. FITC-labeled rabbit anti-human IgG was used as a secondary antibody. No staining was seen when the PV IgG was omitted or replaced with an irrelevant antibody (not shown). Scale bars, 50 μ m. C and D, A confluent monolayer of second passage normal human foreskin KC was incubated with either normal human IgG (C; negative control) of equal amount of the PV IgG that was immunoaffinity-purified on a 75-kDa band (D) for 12 h, and then fixed and stained with the trypan blue dye. The cell morphology is characteristic of pemphigus acantholysis was induced by anti-75 kDa PV antibody (D). No such changes could be observed in a parallel control experiment in which a confluent keratinocyte monolayer was treated with PV IgG immunoaffinity-purified on the 130-kDa horizontal strip (not shown). Scale bars, 50 μ m.

ysis—Approximately 3×10^6 plaques of λ gt11 human keratinocyte cDNA expression library were screened with the affinity-purified antibody from three PV sera (codes: PRC-45, PRC-46, and PRC-47), which contained the anti-75-kDa band acantholytic PV IgG that stained the stratified epithelium in a pemphigus-like pattern. In the first round of screening, four plaques were found to be positive for antibody binding. However, only two clones, designated as K5 and K12, remained immunoreactive after subsequent rescreeing. Because PV IgG eluted from the filter blotted with both K5 and K12 clones stained monkey esophagus in a pemphigus-like pattern (data not shown), both clones were selected for further characterization. PCR amplification of the cDNA insert using a pair of λ gt11 cloning primer revealed that K5 and K12 clones carried the 1.3- and 1.4-kb cDNA inserts, respectively (Fig. 2A). Unexpectedly, sequence analysis of the cDNA inserts from both clones predicted the same open reading frame of 1035 bp, encoding a full-length protein comprised of 345 amino acids (Fig. 2B) with a calculated molecular mass of 38.3 kDa. Examination of the nucleotide sequence revealed an in-frame stop codon situated upstream of the first ATG codon, which indicated that a complete coding region was identified. There were two tandem ATG potential translation initiation codons after the upstream in-frame stop codon. The first one most likely represented the initiation codon, because it was preceded with the Kozak consensus sequence (31). No poly(A) tail was detected. A BLAST search of the GenBank[®] data base at the NCBI web site showed that the nucleotide sequence encoded a previously unknown molecule. The deduced amino acid sequence revealed a high degree of homology to the members of the Ca^{2+} -dependent annexin protein gene family. The strong-

A



B

-226 ATCGGCGGAATTCGCCCCACTTTCCTCTACCAGGCCACACCGGAGGCAGTG -175
 -174 CTCACACAGGCAAGCTACCAGGCCACAACAAGCACCCACCTCACCTCTGGCACCTCTGAGCATCCACGTACTTGCAAGAACTCTT -88
 -87 GCTCACATCAGCTAAGAGATTGCACCTGCTGACCTAGAGATTCCGGCCTGTGCTCTGTGCTGCTGAGCAGGGCAACCAAGTAGCACC -1

1 ATG TCT GTG ACT GGC GGG AAG ATG GCA CCG TCC CTC ACC CAG GAG ATC CTC AGC CAC CTG GGC CTG 66
 1 Met Ser Val Thr Gly Gly Lys Met Ala Pro Ser Leu Thr Gln Glu Ile Leu Ser His Leu Gly Leu 22

67 GCC AGC AAG ACT GCA GCG TGG GGG ACC CTG GGC ACC CTC AGG ACC TTC TTG AAC TTC AGC GTG GAC 132
 23 Ala Ser Lys Thr ala Ala Trp Gly Thr Leu Gly Thr Leu Arg Thr Phe Leu Asn Phe Ser Val Asp 44

133 AAG GAT GCG CAG AGG CTA CTG AGG GCC ATT ACT GGC CAA GGC GTG GAC CGC AGT GCC ATT GTG GAC 198
 45 Lys Asp Ala Gln Arg Leu Leu Arg Ala Ile Thr Gly Gln Gly Val Asp Arg Ser Ala Ile Val Asp 66

199 GTG CTG ACC AAC CGG AGC AGA GAG CAA AGG CAG CTC ATC TCA CGA AAC TTC CAG GAG CGC ACC CAA 264
 67 Val Leu Thr Asn Arg Ser Arg Glu Gln Arg Gln Leu Ile Ser Arg Asn Phe Gln Glu Arg Thr Gln 88

265 CAG GAC CTG ATG AAG TCT CTA CAG GCA GCA CTT TCC GGC AAC CTG GAG AGG ATT GTG ATG GCT CTG 330
 89 Gln Asp Leu Met Lys Ser Leu Gln Ala Ala Leu Ser Gly Asn Leu Glu Arg Ile Val Met Ala Leu 110

331 CTG CAG CCC ACA GCC CAG TTT GAC GCC CAG GAA TTG AGG ACA GCT CTG AAG GCC TCA GAT TCT GCT 396
 111 Leu Gln Pro Thr Ala Gln Phe Asp Ala Gln Glu Leu Arg Thr Ala Leu Lys Ala Ser Asp Ser Ala 132

397 GTG GAC GTG GCC ATT GAA ATT CTT GCC ACT CGA ACC CCA CCC CAG CTG CAG GAG TGC TTG GCA GTC 462
 133 Val Asp Val Ala Ile Glu Ile Leu Ala Thr Arg Thr Pro Pro Gln Leu Gln Glu Cys Leu Ala Val 154

463 TAC AAA CAC AAT TTC CAG GTG GAG GCT GTG GAT GGC ATC ACA TCT GAG ACC AGT GGC ATC TTG CAG 528
 155 Tyr Lys His Asn Phe Gln Val Glu Ala Val Asp Gly Ile Thr Ser Glu Thr Ser Gly Ile Leu Gln 176

529 GAC CTG CTG TTG GCC CTG GCC AAG GGG GGC CGT GAC AGC TAC TCT GGA ATC ATT GAC TAT AAT CTG 594
 177 Asp Leu Leu Leu Ala Leu Ala Lys Gly Gly Arg Asp Ser Tyr Ser Gly Ile Ile Asp Tyr Asn Leu 198

595 GCA GAA CAA GAT GTC CAG GCA CTG CAG CGG GCA GAA GGA CCT AGC AGA GAG GAA ACA TGG GTC CCA 660
 199 Ala Glu Gln Asp Val Gln Ala Leu Gln Arg Ala Glu Gly Pro Ser Arg Glu Glu Thr Trp Val Pro 220

661 GTC TTC ACC CAG CGA AAT CCT GAA CAC CTC ATC CGA GTG TTT GAT CAG TAC CAG CGG AGC ACT GGG 726
 221 Val Phe Thr Gln Arg Asn Pro Glu His Leu Ile Arg Val Phe Asp Gln Tyr Gln Arg Ser Thr Gly 242

727 CAA GAG CTG GAG GAG GCT GTC CAG AAC CGT TTC CAT GGA GAT GCT CAG GTG GCT CTG CTC GGC CTA 792
 243 Leu Glu Gln Glu Glu Ala Val Gln Asn Arg Phe His Gly Asp Ala Gln Val Ala Leu Leu Gly Leu 264

793 GCT TCG GTG ATC AAG AAC ACA CCG CTG TAC TTT GCT GAC AAA CTT CAT CAA GCC CTC CAG GAA ACT 858
 265 Ala Ser Val Ile Lys Asn Thr Pro Leu Tyr Phe Ala Asp Lys Leu His Gln Ala Leu Gln Glu Thr 286

859 GAG CCC AAT TAC CAA GTC CTG ATT CGC ATC CTT ATC TCT CGA TGT GAG ACT GAC CTT CTG AGT ATC 924
 287 Glu Pro Asn Tyr Gln Val Leu Ile Arg Ile Leu Ile Ser Arg Cys Glu Thr Asp Leu Leu Ser Ile 308

925 AGA GCT GAG TTC AGG AAG AAA TTT GGG AAG TCC CTC TAC TCT TCT CTC CAG GAT GCA GTG AAA GGG 990
 309 Arg Ala Glu Phe Arg Lys Lys Phe Gly Lys Ser Leu Tyr Ser Ser Leu Gln Asp Ala Val Lys Gly 330

991 GAT TGC CAG TCA GCC CTC CTG GCC TTG TGC AGG GCT GAA GAC ATG TGAGACTTCCTGCCCCACCCACATG 1062
 331 Asp Cys Gln Ser Ala Leu Leu Ala Leu Cys Arg Ala Glu Asp Met 345

1063 ACATCCGAGGATCTGAGATTCCGTGTTTGGCTGAACCTGGGAGACCAGCTGGGCCTCCAAGTAGGATAACCCCTCACTGAGCACCC 1156
 1150 GGATTCC

FIG. 2. Identification of pemphaxin (PX)—a novel human annexin-like molecule—using the anti-75-kDa band immunoaffinity-purified PV IgG as a probe. A, PCR amplification of cDNA inserts from λ gt11 phages isolated from the clones K5 and K12 using specific λ gt11 forward and reverse cloning primers. The 1.5- and 1.6-kbp PCR products carried copies of 1.3- and 1.4-kbp cDNA inserts, respectively, from the two clones that were specifically recognized by affinity-purified PV IgG as a result of screening of 3 million plaques of a λ gt11 human keratinocyte cDNA expression library. Sequence analysis of both cDNA inserts revealed that both encoded for the same novel molecule, PX. B, the nucleotide sequence and the predicted amino acid sequence of PX. The in-frame upstream and downstream stop codons are underlined. The Kozak sequence that precedes the potential initiation ATG codon is double underlined. C, multiple amino acid sequence alignment of PX with the annexin-2 sequences reported for different species showing that PX shares the same amino acids in most of the conserved regions. Shaded regions indicate the identical amino acid residues among all compared sequences. The arrow denotes potential glycosylation site. The asterisks denote the potential type II Ca^{2+} binding sites. The potential actin bundling site is underlined. Anx-2, annexin-2.

C

Pemphaxin	MSVTGGKMAPSLTQHTSSHCGLASK-TAAMGTLGLTRTLPLNSVDKDAQRLLRLATGGGVSATVDVLTSSRECRQY
Human Anx-2	HSITV-----HETTCISLEGDHSTPPSAYGVSVKAYTTFDAERDALNIETALTKGVDEVTIVNLLTNRNAGRODI
Bovine Anx-2	HSITV-----HETTCISLEGDHSTPPSAYGVSVKAYTTFDAERDALNIETALTKGVDEVTIVNLLTNRNAGRODI
Rat Anx-2	HSITV-----HETTCISLEGDHSTPPSAYGVSVKAYTTFDAERDALNIETALTKGVDEVTIVNLLTNRNAGRODI
Chick Anx-2	HSITV-----HETTCISLEGDHSTPPSAYGVSVKAYTTFDAERDALNIETALTKGVDEVTIVNLLTNRNAGRODI
Pemphaxin	SRNFOKFTQODYHKSLOALSCHLIRIVHALLQPTAOPDAORLTALKASDSAVIVAFELATETPPQLURCLAYRNF
Human Anx-2	AFAYGRRTKKELASAKSALSCHLETIVILGLKTPAQYDASRLKASMKGLCTDESLIETICRTNOELQINRYKREY
Bovine Anx-2	AFAYGRRTKKELASAKSALSCHLETIVILGLKTPAQYDASRLKASMKGLCTDESLIETICRTNOELQINRYKREY
Rat Anx-2	AFAYGRRTKKELASAKSALSCHLETIVILGLKTPAQYDASRLKASMKGLCTDESLIETICRTNOELQINRYKREY
Chick Anx-2	AFAYGRRTKKELASAKSALSCHLETIVILGLKTPAQYDASRLKASMKGLCTDESLIETICRTNOELQINRYKREY
Pemphaxin	QVEAVDGLTSETGIIQDILLALAGGRDSYSGIIDYNLAQVQALQARAGPSREE---TWVPVPTQKNPEELIRVFDQ
Human Anx-2	KTDLEKDIISDTSGDFPKLHVALANGRAEDGSVIDYELIDQARDLYDAGVKKRGTDVFKNISINTERSVPHLOKVFDR
Bovine Anx-2	KTDLEKDIISDTSGDFPKLHVALANGRAEDGSVIDYELIDQARDLYDAGVKKRGTDVFKNISINTERSVCHLOKVFDR
Rat Anx-2	KTDLEKDIISDTSGDFPKLHVALANGRAEDGSVIDYELIDQARDLYDAGVKKRGTDVFKNISINTERSVCHLOKVFDR
Chick Anx-2	KTDLEKDIISDTSGDFPKLHVALANGRAEDGSVIDYELIDQARDLYDAGVKKRGTDVFKNISINTERSVPHLOKVFDR
Pemphaxin	YQRSTGQELEKAVQNRPHGLAQVALLGLASVTKRIFLYADKLEHQAQLOSTEPNYQV-----CETULSIRAEFRKY
Human Anx-2	YKSYSPYDMLSIKKEVKGDLENAPENLVQCIQNKFLYADRLYDSMKGKGTDRK-----VASEVDMLKIRSEFKRY
Bovine Anx-2	YKSYSPYDMLSIKKEVKGDLENAPENLVQCIQNKFLYADRLYDSMKGKGTDRK-----VASEVDMLKIRSEFKRY
Rat Anx-2	YKSYSPYDMLSIKKEVKGDLENAPENLVQCIQNKFLYADRLYDSMKGKGTDRK-----VASEVDMLKIRSEFKRY
Chick Anx-2	YKSYSPYDMLSIKKEVKGDLENAPENLVQCIQNKFLYADRLYDSMKGKGTDRK-----VASEVDMLKIRSEFKRY
Pemphaxin	GRSLYSSIRIDAVKGDQCSALLALCARADM
Human Anx-2	GRSLYTFYIQDTRGDIYQKALLYLGGDD
Bovine Anx-2	GRSLYTFYIQDTRGDIYQKALLYLGGDD
Rat Anx-2	GRSLYTFYIQDTRGDIYQKALLYLGGDD
Chick Anx-2	GRSLYTFYIQDTRGDIYQKALLYLGGDD

FIG. 2—continued

est similarity, approximately 40%, was observed with annexin-2 present in chicken (GenBank[®] accession number P17785), cow (P04272), rat (Q07936) and humans (NP004030). The amino acid sequence alignment (Fig. 2C) revealed several conserved regions, including the type II Ca^{2+} binding sites (32, 33) and the actin bundling site that plays a role in Ca^{2+} -dependent bundling of actin microfilaments by annexins (34). Because of its homology to the members of the annexin protein gene family, we tentatively named this newly discovered PV antigen pemphaxin (*i.e.* pemphigus + annexin = pemphaxin).

Expression of the rPX-His Fusion Protein in *E. coli* and Its Affinity Purification.—To allow experiments with immunoaffinity-purified anti-PX PV antibody, we produced a full-length recombinant PX. Because both K5 and K12 clones carried full-length cDNAs encoding the complete open reading frame of PX, we chose to directionally clone the K5 cDNA to the pQE-30 expression vector, which was designed to express PX protein carrying a poly-His tag at its N terminus. The cloned pQE-30-PX was transformed into *E. coli* M15 cells, and the colonies expressing rPX-His were selected by screening with anti-RGS-His monoclonal antibody. Antibody staining revealed six strongly positive colonies that contained correct PX inserts, as confirmed by subsequent sequencing. Clone 1 was selected for a time course characterization of PX expression. As seen in Fig. 3A, the transfected bacteria began to produce rPX-His after induction with 2 mM IPTG, and the amount of this fusion protein, estimated by the time course study with the time points of 1, 2, 3, and 4 h, gradually increased and reached saturation at 4 h after induction. As expected from the deduced molecular mass of PX, the newly produced rPX-His migrated with a 40-kDa protein band on the 12% SDS-PAGE gel. No proteins were induced by IPTG in control, non-transfected *E. coli* M15 cells (data not shown). The rPX-His was isolated from the mixture of *E. coli* proteins on the Ni-NTA column via its His residues. The rPX-His fusion protein was eluted from the column, and its purity was confirmed by finding a single band in 12% SDS-PAGE-resolved eluant (Fig. 3A, lane PX). The ability of rPX-His to exhibit PX conformational epitope(s) recognized by PV antibody was confirmed by immunoblotting of affinity-

purified rPX-His with the three PV sera that were used in the cDNA library screening experiments (Fig. 3B).

Cholinergic Radioligand Binding by rPX-His.—Cholinergic ligand binding properties of annexins-1, -2, and -3 (35) suggested that PX also acts as a cholinergic receptor binding ACh on the cell surface of KC. To test this hypothesis, rPX-His was used in a standard radioligand binding assay. The saturable specific binding was achieved with the reversible cholinergic radioligand [³H]ACh (Fig. 4A). The analysis of binding kinetics revealed the K_d value of 909 nM and a B_{max} of 176 pmol/mg of protein, indicating that, on the cell membrane of KC, PX may act as a low affinity receptor for endogenously produced and secreted ACh.

Because we demonstrated in a previous study (5) that 85% of pemphigus patients develop autoantibodies, which immunoprecipitate a keratinocyte membrane protein covalently labeled with the cholinergic radioligand [³H]PrBCM, we further asked whether [³H]PrBCM can specifically label rPX-His. The specificity of [³H]PrBCM binding to rPX-His was demonstrated in the binding inhibition experiment using non-labeled cholinergic ligands ACh, nicotine, and muscarine as competitors (Fig. 4B). As expected, ACh as well as its nicotinic and muscarinic congeners decreased significantly ($p < 0.05$) the amount of [³H]PrBCM bound to rPX-His, indicating that PX exhibits dual, muscarinic and nicotinic pharmacology. The dose-dependent radioligand binding inhibition assay with [³H]PrBCM could not be performed because of the irreversible nature of its binding to a receptor molecule, via an alkylation reaction (36).

Characterization of Immunoaffinity-purified Anti-PX PV Antibody.—The anti-PX PV IgG was immunoaffinity-purified on rPX-His immobilized on the Ni-NTA column via its His tags, and the PV IgG fraction eluted from the resin was characterized by: 1) IIF assay using human skin and monkey esophagus as substrates; and 2) immunoprecipitation assay with metabolically radiolabeled keratinocyte proteins. In the IIF assays, the immunoaffinity-purified anti-PX PV IgG stained, in a distinct fishnet-like, pemphigus pattern, the stratified squamous epithelium in human skin and monkey esophagus (Fig. 5, A and

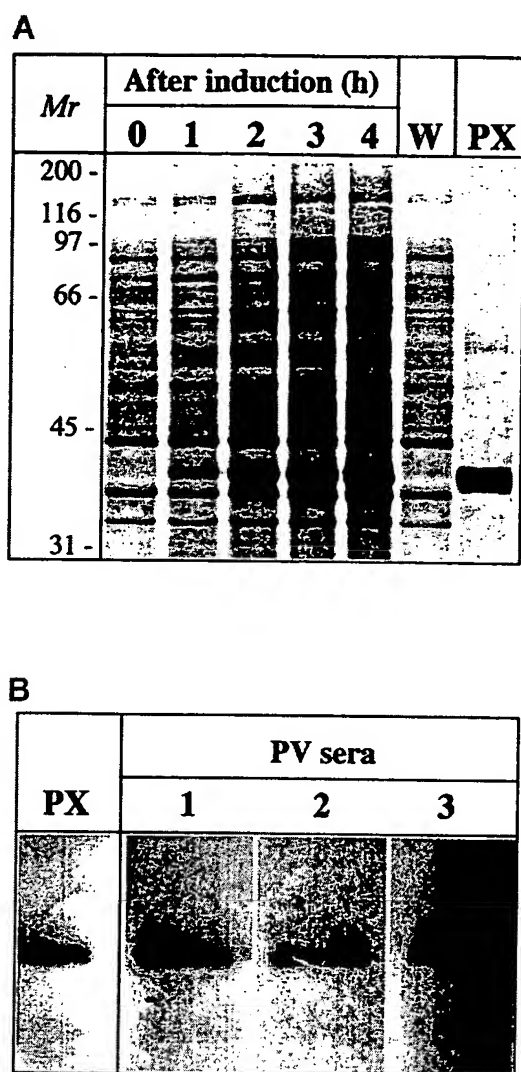


FIG. 3. Expression of the rPX-His fusion protein in *E. coli* and its affinity purification. A, the time-course study of the expression of rPX-His. The selected *E. coli* M15 cells transformed with pQE30-PX were grown in NYZ medium to an optical density of 0.6. at 600 nm and induced with 2 mM IPTG. 1-ml samples of bacterial culture were collected before induction and at 1, 2, 3, and 4 h post induction. The protein extracts of these samples were analyzed on 12% SDS-PAGE gel stained with Coomassie Blue. A sample of rPX-His purified on a Ni-NTA column is designated as PX, and the wash-through fraction is designated as W. No additional proteins were produced in the control experiments in which non-transformed *E. coli* M15 cells were induced with IPTG (not shown). B, the conformational epitope of rPX-His allows its immunorecognition by PV IgG. Western blots of affinity-purified rPX-His were stained with sera from the three PV patients whose IgG fraction was used to screen λ gt11 human keratinocyte cDNA expression libraries. Binding of anti-PX PV IgG was visualized using horseradish peroxidase-conjugated goat anti-human IgG antibody. No staining could be seen in the negative control experiment in which the primary antibody was omitted (not shown). In the reference lane, denoted PX, the rPX-His fusion protein is visualized by staining with Coomassie Blue.

B). The epithelia of other types, such as those lining human bronchi, lung alveoli, small and large intestine, and renal glomeruli, did not exhibit specific staining (data not shown), indicating that the stratified epithelium is a major site of the epithelial expression of PX in human beings. We did not test non-epithelial tissues in this study.

Although addition of a 6xHis-tag to PX should not alter its conformational epitope, we sought to rule out even a remote possibility that, in addition to anti-PX, the rPX-His fusion protein absorbs antibodies of other specificities. The purity of

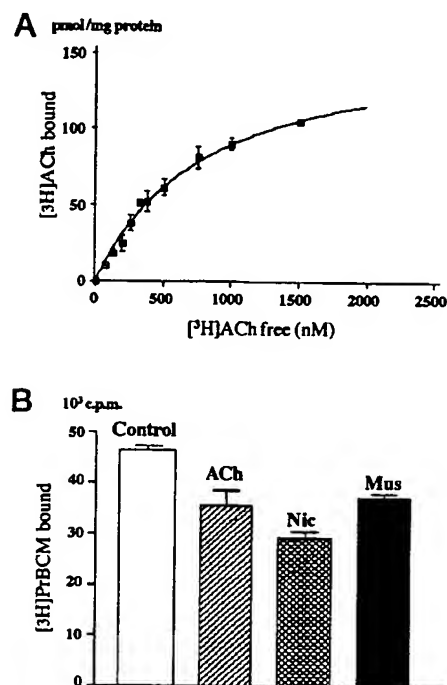


FIG. 4. Cholinergic radioligand-binding to rPX-His. A, saturable binding of the reversible cholinergic radioligand [3 H]ACh to rPX-His in a standard radioligand binding assay detailed under "Experimental Procedures." The analysis of the specific binding revealed a B_{max} of 176 pmol/mg of protein with a K_d of 909 nM. B, blocking of rPX-His labeling by [3 H]PrBCM in the presence of ACh, the nicotinic ligand nicotine (Nic) or the muscarinic ligand muscarine (Mus). The data are mean \pm S.D. of triplicate measurements of [3 H]PrBCM radioactivity (in cpm) associated with rPX-His after its 30-min incubation with 5 nM [3 H]PrBCM at room temperature in the presence or absence of 10 μ M of non-labeled cholinergic drugs ACh, Nic, or Mus.

PV IgG eluted from rPX-His was tested in an immunoprecipitation assay, which allows an antibody to recognize its antigen in the native form, to increase the sensitivity and specificity of antibody characterization. The immunoprecipitation assay showed that the affinity-purified anti-PX PV IgG precipitated keratinocyte proteins with apparent molecular masses of 40 and 80 kDa (Fig. 5C). Because the deduced molecular mass of PX is 38.3 kDa, these results suggested that PX exists as a monomer and a homodimer in KC. This hypothesis was further supported by demonstration of the predicted reciprocal changes in the relative amounts of the 40- and 80-kDa products depending on the presence or absence of the reducing agent β -mercaptoethanol in the SDS-PAGE buffer (Fig. 5C). Indeed, the covalent linkage of two annexins in a dimer is common for certain annexins (reviewed in Ref. 37).

Absorption of Disease-causing PV Antibodies with rPX-His.—To determine the pathophysiological significance of anti-PX antibody in pemphigus, we next asked if depletion of the PV IgG fraction of anti-PX antibody could affect the ability of PV IgG to cause gross skin blisters in neonatal mice. Equal amounts of the intact whole PV IgG fraction (positive control) and the PV IgGs that either passed through the Ni-NTA column containing immobilized rPX-His or were eluted from the column were injected intraperitoneally into 10- to 12-h-old Balb/c mice at a concentration of 20 mg of IgG/g of body weight per day. Only the mice that received non-absorbed PV IgGs reproducibly developed pemphigus-like gross skin lesions between the 16th and 24th h after a single injection. The mice injected repeatedly with either the pass-through (Fig. 5D) or the immunoaffinity-purified anti-PX IgGs (not shown) did not develop any macro- or microscopic skin changes, despite deposition of injected IgGs in mouse epidermis in both cases (Fig.

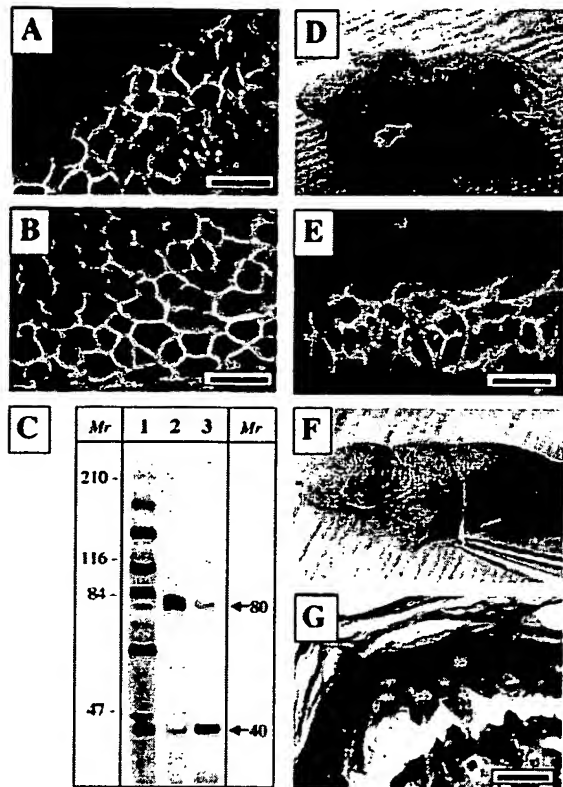


FIG. 5. Characterization of immunoaffinity-purified anti-PX PV antibody. A and B, characterization of immunoaffinity-purified anti-PX PV IgG by IIF. Typical pemphigus-like, "intercellular" staining pattern produced due to binding of the PV IgG fraction eluted from rPX-His to normal human epidermis (A) and monkey esophagus (B). No staining could be seen in negative control experiments stained by a secondary antibody without anti-PX PV IgG (not shown). Scale bars, 50 μ m. C, characterization of immunoaffinity-purified anti-PX PV IgG by immunoprecipitation. The whole PV serum (lane 1) or PV IgG eluted from rPX-His (lanes 2 and 3) were used to immunoprecipitate 35 S-metabolically labeled human keratinocyte protein extract, as detailed under "Experimental Procedures." The immunoprecipitate in lanes 1 and 3 was diluted in SDS-PAGE buffer containing both 2% SDS and 5% β -mercaptoethanol, which allowed predominant visualization of rPX-His in the form of a 40-kDa monomer. The immunoprecipitate resolved in lane 2 was treated without the reducing agent β -mercaptoethanol, which produced a reciprocal staining picture, because omission of β -mercaptoethanol allowed predominant visualization of rPX-His in a form of a naturally assembled homodimer with an apparent molecular mass of 80 kDa. D and E, results of passive transfer of PV IgG preabsorbed with rPX-His to a neonatal Balb/c mouse. Lack of any visible alteration of skin integrity in a pup injected intraperitoneally during 2 days with the pass-through PV IgG fraction in a total dose of 40 mg/g body weight. Demonstration of the deposits of injected pass-through PV IgGs in the epidermis of this mouse by DIF (E). Scale bar, 50 μ m. F and G, results of the passive transfer experiment using the pass-through PV IgG fraction that was supplemented with the immunoaffinity-purified anti-rPX-His IgG. An extensive blister with a loosely attached peripheral skin (positive Nikolsky sign) in a neonate approximately 16 h after a single intraperitoneal injection of 20 mg/g PV IgG (F). The skin blister in this pup resulted from a typical PV-like suprabasilar acantholysis observed by hematoxylin and eosin examination of the perilesional skin (G). The fishnet-like deposits of injected IgG in the epidermis of this mouse were confirmed by DIF (not shown). Scale bar, 50 μ m.

5E). These results indicated that, although absorption with rPX-His eliminates the acantholytic activity of PV serum, the anti-PX antibody alone is not sufficient to induce acantholysis and gross skin blisters in neonatal mice. Therefore, we hypothesized that, although anti-PX antibody is essential for acantholysis development, it is not the only one in the pool of disease-causing PV antibodies that are required to break the integrity of live epidermis.

To test this hypothesis, we sought to determine if acantho-

lytic activity of preabsorbed PV IgGs could be restored by adding back the adsorbed anti-PX antibody. As seen in Fig. 5 (F and G), the pups injected with the pass-through PV IgGs supplemented with anti-PX IgG eluted from the affinity column produced the PV phenotype that was indistinguishable from the epidermal acantholysis and gross skin blisters produced by non-adsorbed PV IgG (not shown). These results clearly indicated that, in addition to anti-PX antibody, the pool of disease-causing PV IgG contains autoantibodies to other keratinocyte self-antigens and suggested that a cumulative effect of anti-keratinocyte antibodies of different specificities is required to break up the integrity of live epidermis and induce skin blistering.

DISCUSSION

In this study we selected the PV IgG fraction that can both stain the epithelial substrates in the pemphigus-like pattern and induce acantholysis in keratinocyte monolayers to probe λ gt11 keratinocyte cDNA library for novel targets of disease-causing PV antibodies. The PV antibody immunoaffinity-purified on a 75-kDa keratinocyte protein band identified a novel human annexin-like molecule, which we termed PX. Recombinant PX was produced and shown to bind specifically ACh and its nicotinic and muscarinic congeners. The obtained results indicate that PX may serve as a cell surface cholinergic receptor mediating a novel ACh signaling pathway involved in the physiological control of cell-to-cell adhesion and that autoimmunity to PX may lead to acantholysis.

Pemphigus is an autoimmune disease with a complex pathophysiology. Both humoral (38) and cellular (39) effectors of autoimmune aggression against KC are involved in the pathogenesis of this disease, and it has been demonstrated that local activation of trypsin-like serine proteases, such as plasminogen activator (40), complement (41), eicosanoids (42), and proinflammatory cytokines (29, 43), all can contribute to acantholysis. The precise mechanism leading to acantholysis in PV, however, is yet to be determined. It is currently held that an autoantibody to the 130-kDa adhesion molecule Dsg 3 causes pemphigus by disrupting directly the keratinocyte cell-to-cell bridges or desmosomes (44, 45). The intuitive notion that the disease of skin adhesion is caused by an antibody to the adhesion molecule, however, awaits its direct experimental confirmation. Meanwhile, Kitajima *et al.* (46) demonstrated that desmosome formation induced by switching the incubation medium from a low to a high Ca^{2+} content is not inhibited by the binding of PV IgG to the cell membrane of cultured KC. In agreement with this report, we could not detect any morphological changes in the keratinocyte monolayers treated with the anti-130-kDa PV IgG for 16 h, whereas the acantholysis in cell monolayers usually develops within 12 h after addition of the whole PV IgG fraction (20, 29, 30). Fan *et al.* (47) attempted to create an animal model of PV by immunizing four different strains of mice, Balb/c, DBA/1, SJL/J, and HRS/J, with full-length Dsg 3 protein, recombinant extracellular portion of Dsg 3, and the synthetic peptides spanning the entire Dsg 3. However, they found no signs of pemphigus, oral or cutaneous, in any of the animals, despite relatively high, up to 1/2560, titer of circulating anti-Dsg 3 antibodies produced by immunized animals. Furthermore, even after the immune sera were concentrated 10-fold and inoculated into neonatal mice, the mice of only one strain, Balb/c, developed the lesion. These results demonstrated that, at the serum titers that are equivalent or exceeding those found in PV patients, the anti-Dsg 3 antibody is not sufficient to cause pemphigus symptoms. The suprapharmacological doses of this antibody, however, can physically interfere with cell-to-cell adhesion, as illustrated by the occurrence of microscopic changes in the oral mucosa of immuno-

deficient Rag-2 knockout mice grafted with a spleen producing anti-Dsg 3 antibodies (48). Unfortunately, the interpretation of findings in mice with adoptively transferred anti-Dsg 3 antibodies in the study of Amagai *et al.* (48) is complicated by its rather controversial nature, which includes direct conflict with the existing data. For instance, according to Amagai *et al.* (48), lack of skin changes in Balb/c mice immunized with Dsg 3 is attributed to inability of this strain of mice to produce anti-Dsg 3 antibody, whereas Fan *et al.* (47) achieved high anti-Dsg 3 antibody titers in these animals, albeit without any mucocutaneous signs of PV. Furthermore, Amagai *et al.* (48) opine that, by analogy with the interpretation of the *Dsg3^{null}* phenotype (18), a transient hair loss accompanied by transient microscopic alterations of keratinocyte adhesion in the oral cavity, which is all that can be observed in the recipient Rag-2^{-/-} mice, should be interpreted as the PV phenotype. However, the following facts argue against this interpretation: 1) hair loss is not a sign of PV (1); 2) true PV is a disease severe enough to kill approximately 90% of patients, if left untreated (reviewed in Ref. 2); and 3) neither recipient Rag-2^{-/-} mice nor *Dsg3^{null}* mice develop spontaneous skin blisters (5, 15, 18). Nevertheless, the notion about the pathophysiological significance of Dsg 3 antibody in PV has been supported by the results of *in vivo* experiments in which pemphigus antibodies affinity-purified on the rDsg3-Ig chimera induced gross skin blisters in neonatal mice (13, 14). Unfortunately, the profile of PV IgGs adsorbed by the rDsg3-Ig-His baculoprotein has never been shown, leaving unresolved the purity and specificity of the antibodies used in the passive transfer experiments. Therefore, we had to characterize the antigenic reactivity of PV IgG adsorbed with rDsg3-Ig-His in our laboratory (19). We established that the antibodies adsorbed on rDsg3-Ig-His are directed toward several keratinocyte proteins, including an unknown 130-kDa self-antigen recognized in the Western blot of keratinocyte proteins of *Dsg3^{null}* mice.

To select the PV IgG fraction that most likely contains disease-causing antibody, we screened PV IgG fractions eluted from different areas of the immunoblotting membrane for their ability to both: 1) stain epidermis in a fishnet-like, pemphigus pattern; and 2) produce acantholysis in keratinocyte monolayers. The anti-75-kDa band PV IgG met both criteria. Failure of the antibody eluted from the 130-kDa area of the immunoblotting membrane to fulfill both criteria was not surprising, because in the past this antibody was selected for the cDNA screening experiments that identified Dsg 3 based on the first criteria only (9). In our study, anti-75-kDa band PV antibody caused acantholysis, which could be observed at 0.09 mM Ca²⁺ in KGM. Although expression of Dsg 3 in KC requires preincubation of the cells at high, from 1.8 to 2.55 mM, extracellular Ca²⁺ (9, 49, 50), we and other workers have previously demonstrated that binding of disease-causing PV IgGs to KC and acantholysis in cell monolayers both occur at as low as 0.1 mM Ca²⁺ (20, 29). This fact suggests that, in addition to blocking the "adhesive sites" of desmosomal cadherins with anti-Dsg PV IgG, binding of pemphigus antibodies to KC initiates an intracellular signaling cascade that can lead to disassembly of other types of intercellular junctions comprised of classical cadherins, such as tight junctions, adherence junctions, and gap junctions, all of which can mediate keratinocyte cell-to-cell adhesion at low Ca²⁺ (51–53).

Screening of the λ gt11 keratinocyte cDNA expression library with the acantholytic anti-75-kDa band PV antibody identified PX, a novel human annexin-like molecule. It appeared that two of 3×10^6 plaques labeled with PV IgGs carried cDNA encoding for the same previously unknown annexin-like molecule with the predicted molecular mass of the translated product of 38.3

kDa. Sequence alignment with known annexins showed that PX shares the same amino acids in most of the conserved regions and is ~40% similar to annexin-2. Annexin-2 may exist as a monomer, dimer, heterodimer, or heterotetramer in which two annexin-2 molecules combine with two smaller subunits, p11, that resemble the S-100 protein of the calmodulin family (54). Because the PV IgG immunoaffinity-purified on rPX-His labeled keratinocyte proteins with apparent molecular masses of 40 and 80 kDa, it can be postulated that PX forms homodimers.

Annexins comprise a unique family of Ca²⁺- and phospholipid-binding proteins encoded by some 20 different genes, which are ubiquitous among eukaryotic organisms, single-celled organisms, and plants and animals (reviewed in Refs. 55, 56). Individual annexins have been described under the names anchorin, calcimedlin, calelectrin, calpactin, calphobindin, chromobindin, endonexin, lipocortin, and synexin. Different annexins have been shown to: 1) participate in ligand-mediated cell signaling both directly, by forming Ca²⁺-sensitive, voltage-gated Ca²⁺ channels, and indirectly, by generating membrane-derived second messengers; 2) mediate anti-inflammatory action of glucocorticosteroids via inhibition of phospholipase A₂; 3) regulate and directly mediate cell-to-cell adhesion; 4) mediate endo- and exocytosis; 5) inhibit blood coagulation; 6) regulate Ca²⁺-dependent Cl⁻ conductance; and 7) participate in the processes of cell proliferation, apoptosis, and virus infection (reviewed in Refs. 37, 57–60).

PX turned out to be a sixth protein of the annexin protein gene family identified in normal human skin to date. Annexins-1, -2, -5, -6, and -7 have been demonstrated previously (61, 62). Expression of annexins in epidermis is differentiation-dependent (63). Annexin-1 immunoreactivity is found almost entirely around the perimeter of KC, especially tonofilament/desmosome-rich prickle KC (61). It has been noted that raising intracellular Ca²⁺ results in peripheral relocations of annexins-2, -4, -5, and -6 from the perinuclear areas (64). Annexin-2 has been shown to be directly involved in regulation of cell adhesion and migration (65). The presence in PX of the conserved sites providing for Ca²⁺ binding and for bundling of actin filaments suggests that PX, just like annexin-2, regulates assembly and maintenance of the cytoskeletal units. This actin polymerization is now believed to play a crucial role in epithelial cell-to-cell adhesion, because disruption of this process in an animal model causes skin lesions indistinguishable from PV lesions (66).

Although annexins lack a leader sequence (and do not pass the Golgi apparatus), they are found on the keratinocyte cell surface, where they can function as receptors. Extracellular annexins have been demonstrated to bind collagen, tenascin, and plasminogen activator (65, 67–70). Binding of tenascin-C to annexin-2 provokes three cellular responses: loss of adhesion, lateral migration, and enhanced cell division (71). Tenascin expression is induced in pemphigus skin as well as in the skin of other blistering dermatoses (72).

To characterize PX, we produced full-length recombinant protein using pQE-30 vector, which contained IPTG-inducible promoter transformed into the *E. coli* M-15 competent cells. Plasmid purified from this clone was analyzed by restriction enzyme analysis and sequencing. Both confirmed that the PX DNA insert was 100% correct. The rPX-His was affinity-purified and used in standard receptor-ligand binding assays with the cholinergic radioligand [³H]ACh. The analysis of the saturable binding of [³H]ACh showed that PX can function as a low affinity cholinergic receptor on the cell membrane of KC. These results were expected, because choline, which itself serves as a pharmacological agonist of cholinergic receptors (73, 74), has

been shown to specifically bind to annexin-1, -2, and -3 (35). Likewise, rPX-His could be specifically tagged with a covalent cholinergic radioligand [^3H]PrBCM, which was previously used by us to label keratinocyte membrane proteins immunoprecipitated by 85% of pemphigus patients (5).

The results of pharmacological experiments demonstrated that rPX-His exhibited conformational structure, thus allowing specific binding of cholinergic ligands. Post-translational modification is not required for ligand binding to single-unit ACh receptors, such as the muscarinic receptor (75, 76). However, the affinity of ACh binding by the wild-type PX, which can form dimers, may be different from that shown by rPX-His *in vitro*, because the bacterial system in which it was expressed was not capable of post-translational modification, such as glycosylation, which is known to play an important role in ligand binding by multi-subunit ACh receptors such as the nicotinic receptor (77). Thus, PX can act as a novel keratinocyte cell surface receptor for the cytotransmitter ACh, synthesized and secreted by human KC in autocrine and paracrine fashions, and mediate known effects of ACh and cholinergic drugs on keratinocyte adhesion (reviewed in Refs. 21, 22). PX can also represent, at least in part, the putative keratinocyte cholinergic receptors targeted by PV IgG (5, 20).

The drugs that act at keratinocyte cholinergic receptors have been shown to alter cell motility and adhesion. Exposure of suspended KC to ACh results in attachment and spreading of the cells on the dish surface and development of intercellular contacts within 20–30 min, whereas non-stimulated cells accomplish this process within 90–120 min. On the other hand, exposure of a confluent keratinocyte monolayer to pharmacological antagonists of ACh leads to a characteristic acantholytic response. The cells retract their cytoplasmic projections, lose cell-to-cell attachments, detach from each other, and become round in shape and non-motile—characteristics that remarkably resemble pemphigus acantholysis *in vitro* (20). We have previously reported that ACh and its muscarinic and nicotinic congeners can prevent and reverse acantholysis produced in keratinocyte cultures by PV IgG (20). A receptor/ligand type of interaction of disease-causing PV IgG, with its target being a keratinocyte cell membrane protein, was first proposed by Patel *et al.* (78) based on the results of time-course study of the fate of the PV antibody/antigen complex. A direct evidence of activation of second messenger systems in response to PV IgG binding to KC have been obtained in the studies showing changes with phospholipase C, inositol 1,4,5-trisphosphate, transmembrane flux and intracellular levels of Ca^{2+} , intracellular cAMP/cGMP ratios, and activity and intracellular location of protein kinase C (reviewed in Refs. 5, 79). Therefore, binding of anti-PX antibody to KC may lead to acantholysis by competing with the natural agonist ACh, thus interrupting physiological regulation of keratinocyte adhesion. In keeping with the notion that autoantibody-mediated ligation of PX on the cell membrane of KC can alter the cell adhesive function are the results showing that an antibody to annexin-2 inhibits cell-to-cell attachment (80).

To determine the role of anti-PX antibody in pemphigus pathophysiology, we preabsorbed PV sera with rPX-His and tested acantholytic activities of both the PV IgGs depleted of anti-PX antibody and the PV IgG eluted from rPX-His. Neither IgG fraction could induce micro- or macroscopic mucocutaneous lesions in neonatal Balb/c mice. Addition of the adsorbed anti-PX PV IgG to the preabsorbed IgG fraction restored its acantholytic activity. These findings suggested that anti-PX antibody is one of the major contributors to skin blistering in PV patients. The fact that anti-PX PV antibody alone was sufficient to cause acantholysis *in vitro* (Fig. 1) but could not do

so *in vivo* was not surprising. Obviously, the cell-to-cell adhesion of KC cultured at low Ca^{2+} is less sophisticated than that taking place in live epidermis, with regard to a variety of adhesion molecules and control mechanisms, which include local anti-acantholytic factors such as interleukin-10 (30). Needless to say, the integrity of the epidermal barrier in higher species relies on more than a single molecule. For example, inactivation of an adhesion molecule such as Dsg 3 does not lead to skin blisters and is well compatible with the normal life span of *Dsg3^{null}* mice (5, 18), whereas a loss of immunological tolerance to keratinocyte self-antigens in PV is potentially lethal in 90% of patients (reviewed in Ref. 2). Therefore, to explain clinical and immunological correlations in PV, we propose a “multi-hit” hypothesis, which postulates that acantholysis in PV results from simultaneous and cumulative effects of autoantibodies directed toward different keratinocyte self-antigens, including the “structural” antigens, such as desmosomal cadherins, and “functional” antigens, such as cell surface receptors regulating function of the adhesion and cytoskeletal units.

The rationale behind our emphasis on the importance of “functional” targets of PV autoimmunity stems from recent discoveries of the genetic defects that underlie certain skin diseases. For instance, patients with genetic defects of the adhesion molecules Dsg1 and desmoplakin develop neither macroscopic nor light- or electron-microscopic alterations of keratinocyte cell-to-cell adhesion but produce instead a palmoplantar keratoderma, represented by linear and focal hyperkeratosis on palms and soles (81–83). In marked contrast, intra-epidermal split and PV-like skin lesions in patients with keratosis follicularis, or Darier-White disease, and patients with benign familial pemphigus, or Hailey-Hailey disease, result from a mutation in the genes coding for Ca^{2+} pumps, the ATP2A2 and ATP2C1, respectively (84, 85). Calcium metabolism in the epidermis of PV patients may also be altered. We have recently found that PV patients develop autoantibodies to the novel human $\alpha 9$ ACh receptor subunit that comprises ACh-gated Ca^{2+} channels on the cell membrane of human KC (19).

In summary, in this study we identified PX, a novel annexin-like molecule, which can function as a keratinocyte cholinergic receptor mediating biological effects of ACh on KC, including regulation of cell-to-cell adhesion. PX is targeted by PV autoimmunity and may represent one of the major targets for acantholytic autoantibodies. Further studies should be directed to elucidate the biochemical mechanisms by which the anti-PX antibody alters keratinocyte adhesion *in vitro* and the biological effect(s) caused by cholinergic ligand binding to PX. Furthermore, because annexins are well known mediators of anti-inflammatory effects of glucocorticosteroids in the skin (86), and because glucocorticosteroids can directly protect KC from the acantholytic effect of PV IgG *in vitro* (87), it will be important to elucidate possible relationships between the effects of glucocorticosteroids on PX and keratinocyte adhesion. Such an association may lead toward development of non-hormonal treatment of PV, because cholinergic drugs that, just like glucocorticosteroids, exhibit direct anti-acantholytic activity (20) may do so by competing with PV IgG for binding to PX on the cell membrane of KC.

Acknowledgments—We thank Dr. Henry Tesluk, Department of Pathology, and Drs. Thomas R. Stevenson and Thomas P. Whetzel, Department of Surgery, University of California Davis Medical Center for facilitating obtainments of large quantities of keratinocyte membrane protein for immunoblotting.

REFERENCES

1. Cohen, L. M., Skopicki, D. K., Harriest, T. J., and Clark, W. H., Jr. (1997) in *Lever's Histopathology of the Skin* (Elder, D., Elenitas, R., Jaworsky, C., and

- Johnson, B. J., eds) 8th Ed., pp. 209–252, Lippincott-Raven, Philadelphia
2. Robinson, J. C., Lozada-Nur, F., and Frieden, I. (1997) *Oral Surg. Oral Med. Oral Pathol. Oral Radiol. Endod.* 84, 349–355
3. Rosenberg, F. R., Sanders, S., and Nelson, C. T. (1976) *Arch. Dermatol.* 112, 962–970
4. Ahmed, A. R., and Moy, R. (1982) *J. Am. Acad. Dermatol.* 7, 221–228
5. Nguyen, V. T., Lee, T. X., Ndoye, A., Shultz, L. D., Pittelkow, M. R., Dahl, M. V., Lynch, P. J., and Grando, S. A. (1998) *Arch. Dermatol.* 134, 971–980
6. Stanley, J. R., Yaar, M., Hawley-Nelson, P., and Katz, S. I. (1982) *J. Clin. Invest.* 70, 281–288
7. Stanley, J. R., Koulu, L., and Thivolet, C. (1984) *J. Clin. Invest.* 74, 313–320
8. Anhalt, G. J., Labib, R. S., Voorhees, J. J., Beals, T. F., and Diaz, L. A. (1982) *N. Engl. J. Med.* 306, 1189–1196
9. Amagai, M., Klaus-Kovtun, V., and Stanley, J. R. (1991) *Cell* 67, 869–877
10. Amagai, M., Karpati, S., Prussick, R., Klaus-Kovtun, V., and Stanley, J. R. (1992) *J. Clin. Invest.* 90, 919–926
11. Memar, O. M., Rajaraman, S., Thotakura, R., Tying, S. K., Fan, J. L., Seetharamaiah, G. S., Lopez, A., Jordon, R. E., and Prabhakar, B. S. (1996) *J. Invest. Dermatol.* 106, 261–268
12. Memar, O. M. (1995) *Characterization of the Pemphigus Vulgaris Antigen (Desmoglein 3) Expressed in Insect Cells: Induction of Blister-Causing Antibodies*, University of Texas Medical Branch Editorial Offices, Galveston, TX
13. Amagai, M., Hashimoto, T., Shimizu, N., and Nishikawa, T. (1994) *J. Clin. Invest.* 94, 59–67
14. Amagai, M., Nishikawa, T., Nousari, H. C., Anhalt, G. J., and Hashimoto, T. (1998) *J. Clin. Invest.* 102, 775–782
15. Mahoney, M. G., Wang, Z., Rothenberger, K., Koch, P. J., Amagai, M., and Stanley, J. R. (1999) *J. Clin. Invest.* 103, 461–468
16. Udey, M. C., and Stanley, J. R. (1999) *J. Am. Med. Assoc.* 282, 572–576
17. Ding, X., Diaz, L. A., Fairley, J. A., Guidice, G. J., and Liu, Z. (1999) *J. Invest. Dermatol.* 112, 739–743
18. Koch, P. J., Mahoney, M. G., Ishikawa, H., Pulkkinen, L., Uitto, J., Shultz, L., Murphy, G. F., Whitaker-Menezes, D., and Stanley, J. R. (1997) *J. Cell Biol.* 137, 1091–1102
19. Nguyen, V. T., Ndoye, A., and Grando, S. A. (2000) *Am. J. Pathol.*, in press
20. Grando, S. A., and Dahl, M. V. (1993) *J. Eur. Acad. Dermatol. Venereol.* 2, 72–86
21. Grando, S. A., and Horton, R. M. (1997) *Curr. Opin. Dermatol.* 4, 262–268
22. Grando, S. A. (1997) *J. Invest. Dermatol. Symp. Proc.* 2, 41–48
23. Beutner, E. H., Chorzelski, T. P., and Jablonska, S. (1985) *Int. J. Dermatol.* 24, 405–421
24. Ohata, Y., Hashimoto, T., and Nishikawa, T. (1995) *Clin. Exp. Dermatol.* 20, 454–458
25. Nguyen, V., Kadunce, D. P., Hendrix, J. D., Gammon, W. R., and Zone, J. J. (1993) *J. Invest. Dermatol.* 100, 349–355
26. Grando, S. A., Cabrera, R., Hostager, B. S., Bigliardi, P. L., Blake, J. S., Herron, M. J., Dahl, M. V., and Nelson, R. D. (1993) *Skin Pharmacol.* 6, 135–147
27. Huynh, T. V., Young, R. A., and Davis, R. W. (1985) in *DNA Cloning: A Practical Approach* (Glover, D. M., ed) Vol. 1, pp. 49–78, IRL Press, Oxford
28. Taylor, I. K., Cuthbert, A. W., and Young, M. (1975) *Eur. J. Pharmacol.* 31, 319–326
29. Feliciani, C., Toto, P., Amerio, P., Mohammad, S., Coscione, P. S., Amerio, P., Shivji, G., Wang, B., and Sauder, S. N. (2000) *J. Invest. Dermatol.* 114, 71–77
30. Toto, P., Feliciani, C., Amerio, P., Suzuki, H., Wang, B., Shivji, G. M., Woodley, D., and Sauder, S. N. (2000) *J. Immunol.* 164, 522–529
31. Kozak, M. (1987) *Nucleic Acids Res.* 15, 8125–8148
32. Jost, M., Weber, K., and Gerke, V. (1994) *Biochem. J.* 298, 553–559
33. Jost, M., Thiel, C., Weber, K., and Gerke, V. (1997) *Eur. J. Biochem.* 207, 923–930
34. Jones, P. G., Moore, G. J., and Waisman, D. M. (1992) *J. Biol. Chem.* 267, 13993–13997
35. Zimmerman, U. J., Hennigan, B. B., Liu, L., Campbell, C. H., and Fisher, A. B. (1995) *Biochem. Mol. Biol. Int.* 35, 307–315
36. Curtis, C. A., Wheatley, M., Bansal, S., Birdsall, N. J., Eveleigh, P., Pedder, E. K., Poyner, D., and Hulme, E. C. (1989) *J. Biol. Chem.* 264, 489–495
37. Siever, D. A., and Erickson, H. P. (1997) *Int. J. Biochem. Cell Biol.* 29, 1219–1223
38. Lin, M. S., Mascaro, J. M., Jr., Liu, Z., Espana, A., and Diaz, L. A. (1997) *Clin. Exp. Immunol.* 107, Suppl. 1, 9–15
39. Grando, S. A., Glukhenky, B. T., Drannik, G. N., Kostromin, A. P., Boiko, Y., and Senyuk, O. F. (1989) *Autoimmunity* 3, 247–260
40. Hashimoto, K., Wun, T. C., Baird, J., Lazarus, G. S., and Jensen, P. J. (1989) *J. Invest. Dermatol.* 92, 310–314
41. Kawana, S., Geoghegan, W. D., Jordon, R. E., and Nishiyama, S. (1989) *J. Invest. Dermatol.* 92, 588–592
42. Grando, S. A., Glukhenky, B. T., Drannik, G. N., Epshtein, E. V., Kostromin, A. P., and Korostash, T. A. (1989) *Arch. Dermatol.* 125, 925–930
43. Grando, S. A., Glukhenky, B. T., Drannik, G. N., Kostromin, A. P., Chernyavsky, A. I., and Barabash, T. M. (1990) *J. Clin. Lab. Immunol.* 32, 137–141
44. Amagai, M. (1999) *J. Dermatol. Sci.* 20, 92–102
45. Stanley, J. R. (1995) *Ciba Found. Symp.* 189, 107–120
46. Kitajima, Y., Inoue, S., and Yaoita, H. (1987) *J. Invest. Dermatol.* 89, 167–171
47. Fan, J. L., Memar, O., McCormick, D. J., and Prabhakar, B. S. (1999) *J. Immunol.* 163, 6228–6235
48. Amagai, M., Tsunoda, K., Suzuki, H., Nishifuji, K., Koyasu, S., and Nishikawa, T. (2000) *J. Clin. Invest.* 105, 625–631
49. Iwatsuki, K., Harada, H., Yokote, R., and Kaneko, F. (1995) *Br. J. Dermatol.* 133, 209–216
50. Karpati, S., Amagai, M., Prussick, R., Cehrs, K., and Stanley, J. R. (1993) *J. Cell Biol.* 122, 409–415
51. Rajasekaran, A. K., Hojo, M., Huima, T., and Rodriguez-Boulant, E. (1996) *J. Cell Biol.* 132, 451–463
52. Witcher, L. B., Collins, R., Puttagunta, S., Mechanic, S. E., Munson, M., Gumbiner, B., and Cowin, P. (1996) *J. Biol. Chem.* 271, 10904–10909
53. Fujimoto, K., Nagafuchi, A., Tsukita, S., Kuraoka, A., Ohokuma, A., and Shibata, Y. (1997) *J. Cell Sci.* 110, 311–322
54. Creutz, C. E. (1992) *Science* 258, 924–931
55. Smith, P. D., and Moss, S. E. (1994) *Trends Genet.* 10, 241–245
56. Morgan, R. O., and Fernandez, M. P. (1997) *Cell. Mol. Life Sci.* 53, 508–515
57. Demange, P., Voges, D., Benz, J., Liemann, S., Goettig, P., Berendes, R., Burger, A., and Huber, R. (1994) *Trends Biochem. Sci.* 19, 272–276
58. Moss, S. E. (1997) *Trends Cell Biol.* 7, 87–89
59. Donnelly, S. R., and Moss, S. E. (1997) *Cell. Mol. Life Sci.* 53, 533–538
60. Reutelingersperger, C. P. M., and Van Heerde, W. L. (1997) *Cell. Mol. Life Sci.* 53, 527–532
61. Fava, R. A., Nanney, L. B., Wilson, D., and King, L. E., Jr. (1993) *J. Invest. Dermatol.* 101, 732–737
62. Culard, J. F., Basset-Seguin, N., Calas, B., Guilhou, J. J., and Martin, F. (1992) *J. Invest. Dermatol.* 98, 436–441
63. Ma, A. S., and Ozers, L. J. (1996) *Arch. Dermatol. Res.* 288, 596–603
64. Barwise, J. L., and Walker, J. H. (1996) *J. Cell Sci.* 109, 247–255
65. Chung, C. Y., and Erickson, H. P. (1994) *J. Cell Biol.* 126, 539–548
66. Vasioukhin, V., Bauer, C., Yin, M., and Fuchs, E. (2000) *Cell* 100, 209–219
67. Nakao, H., Watanabe, M., and Maki, M. (1994) *Eur. J. Biochem.* 223, 901–908
68. Falcone, D. J., Borth, W., Mathew, J., Guevara, C., and Hajjar, K. A. (1995) *FASEB J.* 9, 412 (abstr.)
69. Hajjar, K. A., and Menell, J. S. (1997) *Ann. N. Y. Acad. Sci.* 811, 337–349
70. Von Der Mark, K., and Mollenhauer, J. (1997) *Cell. Mol. Life Sci.* 53, 539–545
71. Chung, C. Y., Murphy-Ullrich, J. E., and Erickson, H. P. (1996) *Mol. Biol. Cell* 7, 883–892
72. Schenk, S., Bruckner-Tuderman, L., and Chiquet-Ehrismann, R. (1995) *Br. J. Dermatol.* 133, 13–22
73. Ulus, I. H., Millington, W. R., Buyukyuysal, R. L., and Kiran, B. K. (1988) *Biochem. Pharmacol.* 37, 2747–2755
74. Sterz, R., Peper, K., Simon, J., Ebert, J. P., Edge, M., Pagala, M., and Bradley, R. J. (1986) *Brain Res.* 385, 99–114
75. van Koppen, C. J., and Nathanson, N. M. (1990) *J. Biol. Chem.* 265, 20887–20892
76. Matus-Leibovitch, N., Mengod, G., and Oron, Y. (1992) *Biochem. J.* 285, 753–758
77. Shtrom, S. S., and Hall, Z. W. (1996) *J. Biol. Chem.* 271, 25506–25514
78. Patel, H. P., Diaz, L. A., Anhalt, G. J., Labib, R. S., and Takahashi, Y. (1984) *J. Invest. Dermatol.* 83, 409–415
79. Kitajima, Y., Aoyama, Y., and Seishima, M. (1999) *J. Invest. Dermatol. Symp. Proc.* 4, 137–144
80. Tressler, R. J., Updyke, T. V., Yeatman, T., and Nicolson, G. L. (1993) *J. Cell. Biochem.* 53, 265–276
81. Rickman, L., Simrak, D., Stevens, H. P., Hunt, D. M., King, I. A., Bryant, S. P., Eady, R. A., Leigh, I. M., Arnemann, J., Magee, A. I., Kelsell, D. P., and Buxton, R. S. (1999) *Hum. Mol. Genet.* 8, 971–976
82. Whitlock, N. V., Ashton, G. H., Dopping-Hepenstal, P. J., Gratian, M. J., Keane, F. M., Eady, R. A., and McGrath, J. A. (1999) *J. Invest. Dermatol.* 113, 940–946
83. Armstrong, D. K., McKenna, K. E., Purkis, P. E., Green, K. J., Eady, R. A., Leigh, I. M., and Hughes, A. E. (1999) *Hum. Mol. Genet.* 8, 143–148
84. Hu, Z., Bonifas, J. M., Beech, J., Bench, G., Shighara, T., Ogawa, H., Ikeda, S., Mauro, T., and Epstein, E. H., Jr. (2000) *Nat. Genet.* 24, 61–65
85. Sakuntabhai, A., Ruiz-Perez, V., Carter, S., Jacobsen, N., Burge, S., Monk, S., Smith, M., Munro, C. S., O'Donovan, M., Craddock, N., Kucherlapati, R., Rees, J. L., Owen, M., Lathrop, G. M., Monaco, A. P., Strachan, T., and Hovnanian, A. (1999) *Nat. Genet.* 21, 271–277
86. Bastian, B. C., Sellert, C., Seekamp, A., Roemisch, J., Paques, E. P., and Broecker, E. B. (1993) *J. Invest. Dermatol.* 101, 359–363
87. Swanson, D. L., and Dahl, M. V. (1983) *J. Invest. Dermatol.* 81, 258–260

Annexin I Is Phosphorylated in the Multivesicular Body During the Processing of the Epidermal Growth Factor Receptor

Clare E. Futter, Stephen Felder,* Joseph Schlessinger,* Axel Ullrich,† and Colin R. Hopkins

MRC Laboratory for Molecular Cell Biology, University College, London; and *Department of Pharmacology, New York University Medical Center, New York; †Max Planck Institute, D-8033 Martinsried, Germany

Abstract. We have previously shown that an active epidermal growth factor receptor (EGF-R) kinase is necessary for efficient sorting of the EGF-R to the lysosome, and we have shown that this occurs in the multivesicular body (MVB), where EGF-R are sorted away from recycling receptors by being removed to the internal vesicles of the MVB. The aim of the present study was to identify substrates of the EGF-R kinase associated with MVBs which might play a role in this sorting process. We used a density shift technique to isolate MVBs and show that the major substrates phosphorylated in vitro within MVBs which contain an active EGF-R kinase are the EGF-R itself and annexin I. Annexin I is associated with both plasma membrane

and MVBs in a calcium-independent manner but can be phosphorylated in vitro only in MVBs. Phosphorylation of calcium-independent annexin I in isolated MVBs converts it to a form that requires calcium for membrane association. In cells with an active EGF-R kinase the amount of calcium-independent annexin I in MVBs is reduced, suggesting that a phosphorylation-induced conversion of the calcium independent to the calcium-dependent form also occurs in vivo. Our observations, together with the known properties of annexin I in mediating membrane fusion, suggest that inward vesiculation in MVBs is induced by the EGF-R and is mediated by phosphorylated annexin I.

WHEN EGF binds to its receptor the intrinsic tyrosine kinase of the receptor is activated, resulting in phosphorylation of the receptor itself and various other proteins (Ushiro and Cohen, 1980). During this time the EGF-EGF-receptor (EGF-R)¹ complex is rapidly internalized and processed within the endocytic pathway where it becomes degraded (Carpenter and Cohen, 1976). A mutant EGF-R lacking an active kinase is internalized in response to EGF at the same rate as the wild type EGF-R but the kinase-negative EGF-R is not efficiently degraded and a significant proportion of the mutant EGF-R recycle to the cell surface (Honegger et al., 1987; Felder et al., 1990). By EM we have shown that saturating concentrations of EGF stimulate internalization of both wild type and kinase negative EGF-R to multivesicular bodies but within this compartment they have distinctly different distributions (Felder et al., 1990). Since only wild type EGF-R are efficiently transferred to the internal vesicles of the multivesicular body (MVB) we have proposed that removal of EGF-R from the perimeter membrane of the endocytic pathway allows them to be degraded.

While it is possible that the activated EGF-R kinase initiates a series of events in the plasma membrane which results in sorting at the level of the MVB it is also possible that the

EGF-R kinase is active in the endosome where it triggers the events that lead to its degradation. The aim of the present study was to determine whether there are substrates of the EGF-R kinase specifically associated with MVBs. We have adapted a previously described density shift protocol (Futter and Hopkins, 1989) to isolate highly purified MVBs containing EGF-R and show that the major substrates of the EGF-R kinase in MVBs are the EGF-R itself and annexin I. Since annexin I is a protein which interacts with membranes and actin-containing cytoskeletal elements (Glenney et al., 1987) and can promote phospholipid vesicle fusion in vitro (Ernst et al., 1990), it could regulate the production of internal vesicles within MVBs.

Materials and Methods

Cell Lines

NIH 3T3 cells, strain 2.2, transfected with plasmid bearing either the full-length cDNA for the human EGF-R (HER14 cells), or the cDNA encoding the human EGF-R with lysine 721 replaced with alanine (K721A cells), and each expressing roughly 400,000 receptors per cell, were used (Honegger et al., 1987). Cells were maintained in DME supplemented with 10% FCS at 37°C in a 5% CO₂ atmosphere.

Colloidal Gold Complexes

Gold particles (10 nm) were prepared using the tannic acid method of Slot and Geuze, (1985), and were stabilized with the mAb 108, according to

1. Abbreviations used in this paper: EGF-R, epidermal growth factor receptor; MVB, multivesicular body.

standard procedures (DeMey, 1986). The complexes were stored in 0.02% azide at 4°C, and were washed by centrifugation in an airfuge (Beckman Instruments, Palo Alto, CA) at 150,000 g for 5 min immediately before use.

Iodination

EGF (mouse EGF; Sigma Chemical Co., Poole, UK) was iodinated according to the method of Hunter and Greenwood (1962) and protein A was iodinated using iodobeads (Pierce, Chester, UK).

Incubation Procedures

All incubations were performed in DME containing 20 mM Hepes, pH 7.4, 2 mg/ml BSA. EGF was used at a concentration of 20 nM. 108-gold was used at a concentration that gave OD₅₈₀ of 0.3–0.4. Incubations were performed at 37°C unless otherwise indicated and for the times indicated in Results. Where the proportion of cell-associated ¹²⁵I-EGF that was plasma membrane bound was to be determined, cells were incubated in acetic acid-saline, pH 2.5, for 5 min at 4°C to remove plasma membrane-bound EGF, before digestion of the cells in 5 M NaOH.

Subcellular Fractionation Procedure

Cells were washed three times at 4°C with lysis buffer (10 mM triethanolamine, pH 7.4, 0.25 M sucrose, 1 mM EDTA, 200 μM orthovanadate, 1 mM PMSF). Cells were scraped off the dish in the minimum volume of lysis buffer and lysed by eight strokes through a 21 g needle. Unbroken cells and nuclei were removed by centrifugation at 800 g for 5 min at 4°C. The resulting postnuclear supernatant was layered onto a 12 ml 26–52% sucrose gradient, containing triethanolamine, EDTA, orthovanadate, and PMSF at the same concentrations and pH as the lysis buffer. Gradients were then centrifuged in a Beckman SW40 rotor at 200,000 g for 15 h at 4°C in a Beckman L70 ultracentrifuge. Gradients were fractionated from the bottom into 15 × 0.9-ml fractions.

EM

Cells and fractions were fixed in dilute Karnovsky fixative, postfixed in osmium tetroxide, and embedded and sectioned so that the full thickness of the pellet could be examined. Sections were stained in aqueous uranyl acetate and lead citrate and examined in a CM12 Philips electron microscope.

SDS-PAGE and Western Blotting

SDS-PAGE was performed under reducing conditions. Proteins on SDS-polyacrylamide gels were electrophoretically transferred to nitrocellulose for 16 h in a transfer apparatus (Bio-Rad Laboratories, Cambridge, MA) at a constant current of 100 mA. After incubation with either rabbit anti-EGF-R antiserum, RK2 (Kris et al., 1985), rabbit anti-phosphotyrosine antiserum, or rabbit anti-annexin I antiserum (a gift from S. Moss, University College, London), blots were washed and incubated in ¹²⁵I-protein A. Blots were analyzed by autoradiography and, where quantitation was performed, radioactive bands were excised, and counted.

In Vitro Phosphorylation Studies

Cell fractions were resuspended in 20 mM Hepes, pH 7.4, 150 mM NaCl. Fractions were incubated for 15 min at 4°C in the presence of 5 mM MnCl₂, 20 μM orthovanadate, and [γ -³²P]ATP (5 μM). Reactions were stopped by the addition of 10% TCA, and TCA precipitates were examined by SDS-PAGE.

To examine the effects of phosphorylation on calcium dependence of membrane association of MVB proteins, phosphorylation reactions were performed as above. MVBs were then washed twice with 20 mM Hepes, pH 7.4, 150 mM NaCl, 200 μM orthovanadate, containing either 1.5 mM EDTA or 1.5 mM CaCl₂, by centrifugation in a Beckman TL100.4 rotor at 200,000 g for 1 h at 4°C in a Beckman TLX ultracentrifuge, and the pellets were examined by SDS-PAGE.

Annexin I Immunoprecipitation

To identify annexin I, in vitro phosphorylation assays were carried out as above, but were stopped by the addition of NDET (10 mM Tris, pH 7.4, 1% NP-40, 0.4% deoxycholate, 66 mM EDTA), containing 1 mM PMSF, 200 μM orthovanadate and 0.2% SDS. Samples were clarified by centrifugation (14,000 g for 5 min), and were then incubated with a rabbit polyclonal

antibody against annexin I. Antibody-bound proteins were immunoprecipitated using *Staphylococcus aureus*, and the washed immunoprecipitate was analyzed by SDS-PAGE.

Results

Isolation of Highly Purified Endosomes by Density-shift Using EGF-R Antibody-Gold Complexes

We have previously shown in H.Ep.2 cells that antibody to the transferrin receptor complexed to colloidal gold can be used to modify the density of endocytic compartments involved in the processing of the EGF-receptor complex, so that they can be purified by sucrose density centrifugation (Futter and Hopkins, 1989). In the present study we extended this technique to NIH-3T3 cells transfected with either the wild type human EGF receptor or a human EGF receptor with a point mutation in the putative ATP binding site, rendering the receptor kinase negative (Honegger et al., 1987). To isolate endocytic compartments containing EGF-R by density shift we employed a mAb (108) to EGF-R complexed to colloidal gold. The 108 antibody binds to the external domain of the EGF-R and has been shown, when saturating EGF concentrations are used, not to stimulate internalization or kinase activity of the EGF-R, or to interfere with EGF binding (Bellot et al., 1990). To induce a sufficient increase in density of endocytic compartments containing 108-gold, it was necessary to stimulate cells with saturating concentrations of EGF. Under these conditions both the kinase positive and negative EGF-R are internalized at similar rates (Felder et al., 1990). Our previous studies using gold complexes to density shift endocytic compartments showed that gold-loaded endosomes will pellet through 52% sucrose whereas gold-loaded plasma membranes will not (Futter and Hopkins, 1989). To begin we established the rate of EGF-R internalization by following ¹²⁵I-EGF uptake, and showed that >70% was internalized within 20 min of EGF stimulation (Fig. 1 a).

Fig. 1 b shows the recovery of EGF and EGF-R in the pellet after sucrose density gradient fractionation of cells after similar stimulation with EGF. Recovery of EGF-R was assessed by Western blotting with anti-EGF-R antibody. The increase in recovery of EGF and EGF-R in the pellet with increasing lengths of incubation after EGF stimulation showed similar kinetics to that of EGF-stimulated internalization, showing that endocytic compartments rather than plasma membrane pellet under the fractionation conditions used.

Examination of the endosome pellet isolated by fractionation of 108-gold-loaded cells expressing the wild type EGF-R 20 min after EGF stimulation showed that all membranous elements labeled with gold were endosomal, many of which were clearly identifiable as MVBs (Fig. 2 a). Quantitation of the number of vesicles which contained gold by counting random sections showed that 34% of vesicle profiles found in the pellet contained gold. Vesicle profiles which lacked gold presumably contained gold particles in another section plane. Electron microscopic examination of the pellet from cells expressing the kinase negative EGF-R showed that 14% of the vesicle profiles contained gold. This lower figure compared to the wild type fraction is consistent

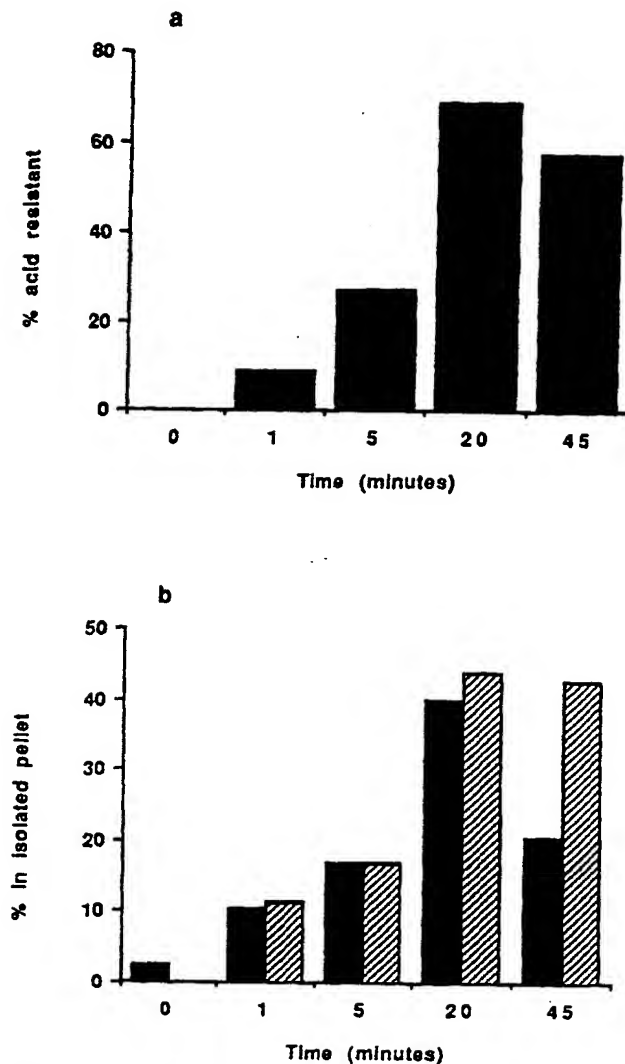


Figure 1. (a) Cells expressing wild type EGF-R were stimulated with ^{125}I -EGF for the indicated times. The percent of total cell-associated EGF that had been internalized was determined by acid stripping. (b) Cells expressing wild type EGF-R were incubated with 108-gold for 30 min and were then stimulated with ^{125}I -EGF for the indicated times. Cells were lysed and fractionated. The percent of postnuclear supernatant ^{125}I -EGF (○) and EGF-R (●) that was recovered in the pellet after sucrose density gradient fractionation was determined. Quantitation of the EGF-R was performed by blotting gradient fractions with anti-EGF-R antibody. Iodinated protein A and autoradiography were used to visualize bands, which were excised and counted.

with observations on intact cells (Felder et al., 1990) which have shown that there is significantly less EGF-R in the MVB compartment of kinase negative cells. It should be noted nevertheless that the majority of gold-loaded elements in the pellets from the kinase negative cells are MVBs (Fig. 2 b). Presumably the other gold-containing elements of the endocytic pathway were too buoyant to pellet. Previous studies have shown, through measurement of marker enzyme activities and by EM, that in a number of different cell lines nonendosomal organelles do not pellet under the fractionation conditions used (Beardmore et al., 1988; Futter et al., 1989; Beaumelle and Hopkins, 1990). However amorphous mate-

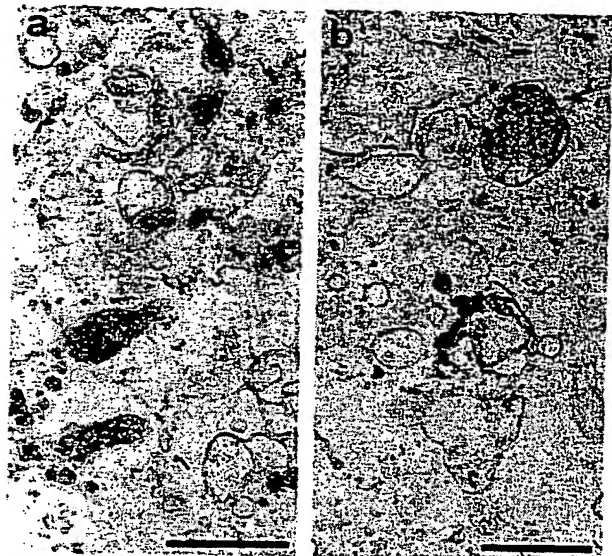


Figure 2. Cells expressing either wild type (a) or kinase negative (b) EGF-R were incubated with 108-gold for 30 min, and were then stimulated with EGF for 20 min. Cells were then lysed and fractionated, and the pellet after sucrose gradient fractionation was processed for microscopy. All membranous elements that contain gold are endosomal, many of which are MVBs. Amorphous material, presumably of cytoskeletal nature, consistently pellets with endosome fractions. Bar, 0.5 μm .

rial, presumably a component of the cytoskeleton, consistently pellets with endosome fractions.

The Fate of the Plasma Membrane during Density Shift Separation of Gold-loaded Endosomes

When cells were stimulated with EGF for 1 min after preincubation with 108-gold (when the majority of EGF-R are plasma membrane associated), the density of the plasma membrane fraction was increased. Thus, in the absence of 108-gold binding, plasma membrane was found in a peak in fractions 8-12 (Fig. 3 a) while binding of 108-gold to the plasma membrane caused a shift to fraction 6 (Fig. 3 b). After stimulation of cells with EGF for one minute EGF-R was still found in fraction 6 (Fig. 3 c). EM of this fraction showed that it was composed of large vesicle profiles bearing EGF-R-gold particles on their outer surfaces (results not shown), in contrast to MVBs where the gold particles were found only on the inner surfaces of the perimeter membrane.

Substrates Phosphorylated in Endosomes and Plasma Membrane Isolated from Cells Expressing Wild type EGF-R Kinase

To determine whether proteins are phosphorylated in MVBs as a result of activation of the EGF-R kinase, phosphorylation was examined in endosomes isolated from NIH 3T3 cells expressing either the wild type or the kinase negative EGF-R. Endosomes were isolated 20 min after EGF stimulation when the majority of both kinase negative and wild type EGF-R are in MVBs (Felder et al., 1990) and the density shifted fractions are composed primarily of MVBs (Fig. 2). When MVBs isolated from NIH 3T3 cells expressing the wild type EGF-R were incubated with $[\gamma\text{-}^{32}\text{P}]\text{ATP}$ in vitro

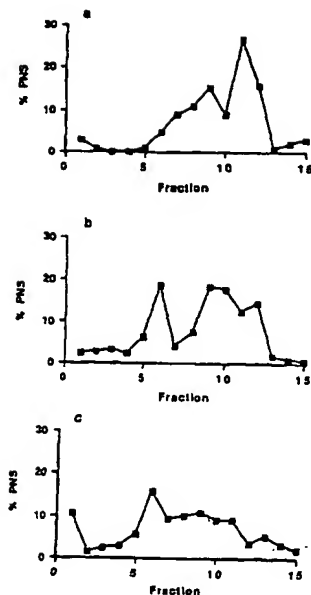


Figure 3. Cells expressing wild type EGF-R were incubated with no gold (a), 108-gold for 30 min (b), or 108-gold for 30 min, followed by stimulation with EGF for 1 min (c). Cells were lysed and fractionated and gradient fractions were analyzed by Western blotting with anti-EGF-R antibody. Iodinated protein A and autoradiography were used to visualize bands, which were excised and counted.

two major phosphorylated substrates were detected, the EGF-R itself and a protein of approximately 35 kD (Fig. 4 a). The 35-kD protein could be immunoprecipitated with anti-annexin I antibody (Fig. 4 b).

To determine whether annexin I is phosphorylated in plasma membrane fractions in addition to MVBs, plasma membrane fractions were isolated from cells stimulated with EGF for one minute. When these fractions were incubated with [γ - 32 P]ATP in vitro several substrates were phosphorylated including the EGF-R (Fig. 4 a), but immunoprecipitation with annexin I antibody showed they did not include annexin I (Fig. 4 b).

MVB and plasma membrane fractions from cells expressing the kinase negative EGF-R, used as a control, showed that neither the EGF-R nor the 35-kD protein were phosphorylated (Fig. 4, a and b).

To confirm that the phosphorylation of annexin I in the MVB was due to the presence of an active EGF-R kinase we carried out a parallel study using H.Ep.2 cells in which we have shown previously that EGF-R containing MVBs can be isolated by density shift when loaded with anti-transferrin receptor-gold complexes and stimulated with EGF (Futter and Hopkins, 1989). Western blotting the isolated MVBs showed that EGF stimulation of transferrin receptor-gold-loaded cells resulted in a fivefold increase in the amount of EGF-R that co-localized with transferrin receptor in MVBs (results not shown). In vitro phosphorylation assays showed that a number of proteins became phosphorylated in MVBs isolated from H.Ep.2 cells, but only in MVBs that contained an active EGF-R kinase did the EGF-R and a 35-kD protein become phosphorylated (Fig. 5 a). Immunoprecipitation confirmed this protein was annexin I (Fig. 5 b).

We conclude that annexin I is present in isolated MVBs and that it can be phosphorylated in vitro in the presence of an active EGF-R kinase.

Phosphorylation and the Calcium Dependence of Annexin I Binding to MVBs and Plasma Membrane

Annexin I has been isolated as an EDTA eluate of mem-

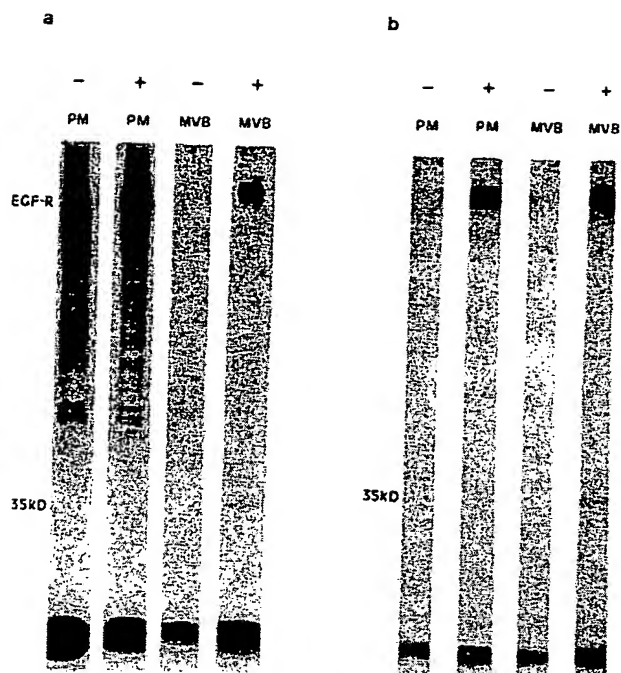


Figure 4. NIH 3T3 cells expressing either the wild type (+) or the kinase negative (-) EGF-R were incubated with 108-gold for 30 min. Cells were then stimulated with EGF for 1 min to isolate a plasma membrane fraction (PM) or for 20 min to isolate an MVB fraction (MVB). Cells were then lysed and fractionated. The PM fraction was taken from fraction 6 and the MVB fraction was taken from the pellet after sucrose gradient fractionation. In vitro phosphorylation reactions were performed on the isolated fractions as described in Materials and Methods. Either the whole fraction (a) or an anti-annexin I immunoprecipitation of the fraction (b) were analyzed by SDS-PAGE on a 10% gel. The EGF-R is present in anti-annexin I immunoprecipitations because the fractions contain anti-EGF-R gold, but in control immunoprecipitations that do not include anti-annexin I antibody, annexin I is not immunoprecipitated. Gel loadings with respect to the EGF-R are 1:2:1:1.4 for -PM: +PM: -MVB: +MVB.

branes and shown to associate with phospholipids in a calcium dependent manner (Glenney et al., 1987). Haigler et al., (1987) have shown that in addition to the calcium-dependent form there is a form of annexin I in human placenta which associates with membranes independently of calcium and can be phosphorylated by the EGF-R kinase. Phosphorylation of this form of annexin I converts the protein into a form that associates with membranes only in the presence of calcium. The MVBs used in the present study are isolated in the presence of EDTA and so the annexin I that is phosphorylated in vitro must remain associated with membranes in the absence of calcium. In order to determine the effect of phosphorylation on the calcium dependence of annexin I in MVBs, isolated fractions were incubated with [γ - 32 P]ATP and then washed two times in lysis buffer containing either 1.5 mM EDTA or 1.5 mM Ca^{2+} . The membrane pellet was examined by SDS-PAGE. After washing in EDTA phosphorylated annexin I was no longer associated with the MVB pellet. However in the presence of calcium the protein remained associated with MVBs (Fig. 6).

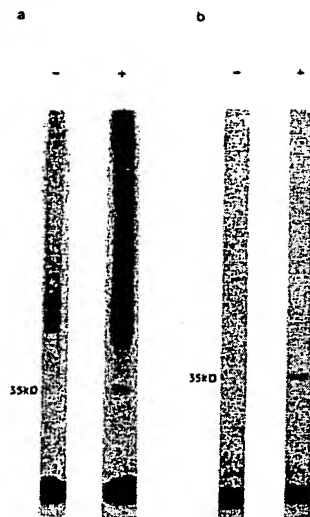


Figure 5. H.Ep.2 cells were incubated with B3/25 (anti-transferrin receptor)-gold for 60 min and were then incubated in the presence (+) or absence (-) of EGF for 20 min (in the continued presence of B3/25-gold). Cells were then lysed and fractionated. In vitro phosphorylation reactions were performed on the MVB fractions as described in Materials and Methods. Either the whole fraction (a) or an anti-annexin I immunoprecipitation of the fraction (b) were analyzed by SDS-PAGE on a 10% gel.

The Influence of EGF-R Kinase on the Amount of Annexin I Associated with Plasma Membrane and MVBs

To determine whether an active EGF-R kinase is necessary for association of annexin I with MVBs isolated MVBs were Western blotted with anti-annexin I antibody and the amount of annexin I relative to EGF-R was quantitated. Annexin I was present in MVB fractions from cells expressing the wild type EGF-R and also those expressing the kinase negative EGF-R. However MVBs from NIH 3T3 cells containing wild type EGF-R had three- to fourfold less annexin I (relative to EGF-R) than kinase negative MVBs (Fig. 7). Similarly annexin I was present in MVBs from H.Ep.2 cells iso-

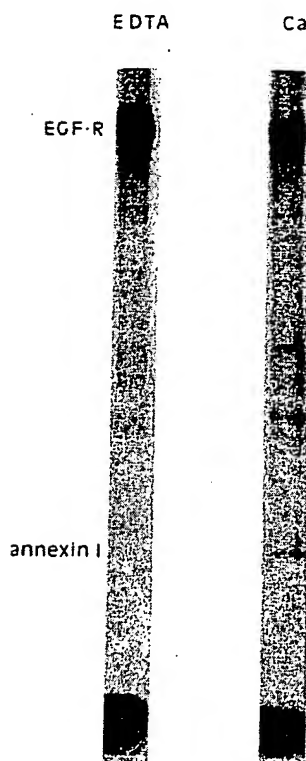


Figure 6. NIH 3T3 cells expressing wild type EGF-R were incubated with 108-gold for 30 min and were then stimulated with EGF for 20 min. Cells were then lysed and fractionated. In vitro phosphorylation reactions were performed on the MVB fractions as described in Materials and Methods. MVBs were then washed in the presence of EDTA (EDTA) or calcium (Ca). Washed pellets were analyzed by SDS-PAGE on a 10% gel.

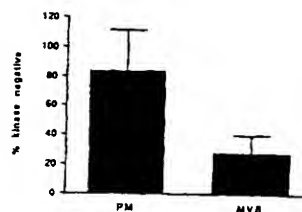


Figure 7. (a) NIH 3T3 cells expressing wild type (+) or kinase negative (-) EGF-R were incubated with 108 gold for 30 min. Cells were then stimulated with EGF for 1 min and a plasma membrane fraction isolated (PM) or for 20 min and an MVB fraction iso-

lated (MVB). Fractions were Western blotted with anti-EGF-R antibody and anti-annexin-I antibody. Iodinated protein A and autoradiography were used to visualize bands, which were excised and counted. The amount of annexin I (relative to the EGF-R) in fractions from wild type cells is expressed as a % of that in the corresponding fractions from kinase negative cells. Results are mean \pm SEM of four observations.

lated using transferrin receptor gold with or without prior EGF stimulation, but MVBs containing an active EGF-R kinase contained approximately twofold less annexin I (relative to transferrin receptor) than MVBs lacking an active EGF-R kinase (results not shown). We conclude therefore that an active EGF-R kinase is not necessary for association of annexin I with MVBs. In addition, the reduction in the amount of calcium-independent annexin I in MVBs containing an active EGF-R kinase is consistent with the phosphorylation of annexin I in vivo, as we have shown phosphorylation of annexin I in vitro to cause its release from MVBs in the presence of calcium chelator. To confirm, as our in vitro results would suggest, that the loss of calcium-independent annexin I through phosphorylation occurs in MVBs rather than on the plasma membrane, the amount of annexin I associated with plasma membrane fractions containing wild type and those containing kinase negative EGF-R was compared. Plasma membrane fractions containing wild type EGF-R and those containing kinase negative EGF-R contained similar levels of annexin I relative to EGF-R (Fig. 7), suggesting that the release of calcium independent annexin I through phosphorylation does not occur on the plasma membrane.

Discussion

We have shown in previous studies that an active EGF-R kinase is necessary for lysosomal sorting (Honegger et al., 1987; Felder et al., 1990). Other investigators have also shown a reduction in EGF-stimulated degradation of EGF in cells expressing a kinase negative EGF-R but they have concluded that this is due to a reduced internalization rate, rather than to defective lysosomal sorting (Glenney et al., 1988; Chen et al., 1989; Wiley et al., 1991). Most recently Felder et al. (1992) obtained data to suggest that the role of the EGF-R kinase in internalization concerns primarily high affinity EGF-R. At the saturating concentrations of EGF used in the present study our previous biochemical and morphological studies (Felder et al., 1990) clearly show that there is a similar rate of internalization of both the wild type and the kinase negative EGF-R and it is in the MVB that the pathways of the wild type and kinase negative EGF-R diverge. A recent study of another growth factor receptor kinase, the receptor for colony stimulating factor 1, has shown that an active kinase is not necessary for internalization but is a requirement for lysosomal sorting (Carlberg et al., 1991).

The requirement for an active EGF-R kinase for efficient degradation indicates that either the EGF-R must be autophosphorylated to be efficiently targeted to lysosomes, or the kinase phosphorylates a substrate necessary for lysosomal targeting. When kinase positive and kinase negative EGF-R are expressed in the same cell, heterodimers form in response to EGF and the kinase negative EGF-R becomes tyrosine phosphorylated (Honegger et al., 1990). However, in this system kinase negative EGF-R are still predominantly recycled. It is therefore likely that phosphorylation of a substrate accessible only in the MVB is necessary for degradation. This would require the EGF-R kinase to be active in the MVB. There is considerable evidence that the EGF-R kinase is active in the endosome. Autophosphorylation activity of the EGF-R kinase has been demonstrated *in vitro* in endosome fractions from A431 cells (Cohen and Fava, 1985) and rat liver (Kay et al., 1986; Lai et al., 1989). We and others (Carpentier et al., 1987; Nesterov et al., 1990) have shown that EGF stimulation results in prolonged autophosphorylation of the EGF-R, suggesting that the EGF-R kinase is still active after internalization *in vivo*. Wada et al. (1992) have shown that the EGF-R kinase is more highly phosphorylated in the endosome than on the plasma membrane. Moreover the internalized EGF-R kinase can phosphorylate a synthetic substrate introduced into permeabilized cells (Nesterov et al., 1990).

In this study we searched for substrates of the EGF-R kinase associated with MVBs. Western blotting isolated MVBs with anti-phosphotyrosine antibody failed to reveal any major substrates of the EGF-R kinase apart from the EGF-R itself. However, when highly purified MVBs containing the wild type EGF-R are incubated with [γ - 32 P]ATP the major proteins phosphorylated are the EGF-R itself and annexin I. Neither proteins are phosphorylated in MVBs containing the kinase negative EGF-R. Similarly when MVBs from H.Ep.2 cells are isolated using transferrin receptor gold in the presence or absence of EGF, only in endosomes isolated from cells that have been stimulated with EGF does annexin I become phosphorylated. In contrast, annexin I is not phosphorylated in plasma membrane fractions whether or not an active EGF-R kinase is present. We have demonstrated therefore that in the presence of an active EGF-R kinase annexin I can be phosphorylated in MVBs, but not plasma membrane, *in vitro*. It is likely that annexin I is phosphorylated directly by the EGF-R kinase, rather than through activation of an intermediate kinase, as annexin I is efficiently phosphorylated by purified EGF-R kinase (De et al., 1986; Huang et al., 1986) and there is no evidence of an intermediate substrate in the MVB preparations.

Our *in vitro* results are consistent with the kinetics of phosphorylation of annexin I *in vivo*. Sawyer and Cohen (1985) showed that annexin I is not phosphorylated until the majority of EGF-R have been internalized and suggested that annexin is phosphorylated by the endosomal EGF-R kinase. Cohen and Fava (1985) showed that purified annexin I added to a partially purified intracellular vesicle fraction could be phosphorylated by the EGF-R kinase, and that this reaction was dependent upon the presence of calcium. In the present study we show an association of endogenous annexin I with endosomes that is independent of calcium but this form of annexin I can be phosphorylated by the EGF-R kinase and upon phosphorylation requires calcium for membrane as-

sociation. This is in agreement with the studies of Haigler et al. (1987) who showed that phosphorylation of the calcium-independent form of annexin I in human placental membranes converts it into a form that requires calcium for membrane association. The nature of the calcium-independent interaction of annexin I with membranes is unknown but we have shown here that the association is independent of the density of EGF-R within the membrane. The interaction therefore presumably does not involve a direct interaction with the EGF-R such as has been described for the EGF-R kinase substrates, Phospholipase C γ (Miesenhelder et al., 1989), GAP (Bouton et al., 1991), Raf-1 (App et al., 1991), and Vav (Bustelo et al., 1992; Margolis et al., 1992) which interact with EGF-R via SH2 domains. Quantitation of the total amount of annexin I in plasma membrane and MVB fractions has shown that the presence or absence of an active EGF-R kinase has little effect on the amount of annexin I in plasma membrane fractions but the presence of an active EGF-R kinase causes a reduction in the amount of annexin I in MVB fractions. These results are consistent with annexin I being phosphorylated in MVBs and thus converted to a form that is eluted during fractionation in the presence of calcium chelator.

Wada et al. (1992) in a study of phosphoproteins associated with endosomes of rat liver did not report annexin I associated with endosomes. Wada et al. (1992) did however detect a 55-kD phosphoprotein associated with endosomes. We were not able to detect this substrate in either NIH 3T3 or H.Ep.2 cells, either after *in vitro* phosphorylation or by Western blotting isolated fractions with anti-phosphotyrosine antibody (results not shown). These differences may arise because different stages of processing of the EGF-R were examined. Wada et al. (1992) studied endosomes isolated a maximum of 15 min after EGF stimulation. At this time point the authors were unable to demonstrate sequestration of EGF-R within intra-luminal vesicles in the liver. That sequestration of EGF-R in intra-luminal vesicles does occur in the liver has been shown by Renfrew and Hubbard (1992). In agreement with our proposal the latter authors suggest that movement of EGF-R from the limiting membrane of endosomes to the lumen of lysosomes permits degradation of the EGF-R. Wada et al. (1992) may thus have been examining early events in the processing of the EGF-R, before removal of EGF-R from the limiting membrane.

Thus we have shown that annexin I is associated with plasma membrane and MVBs in a calcium-independent manner and can be phosphorylated *in vitro* in the presence of an active EGF-R kinase in MVBs, but not in plasma membrane. Phosphorylation of the calcium-independent form of annexin I converts it into a form that requires calcium for membrane association. MVBs, but not plasma membrane, containing an active EGF-R kinase contain less calcium-independent annexin I than those that do not contain an active EGF-R kinase. We believe therefore that calcium-independent annexin I is phosphorylated *in vivo* in MVBs whereupon it is released during fractionation in the presence of calcium chelator.

The requirement for the EGF-R kinase to be active for transfer to the inner vesicles of MVBs (Felder et al., 1990), together with the demonstration here that annexin I is a major phosphorylated substrate in MVBs, suggest that annexin I may play a role in mediating inward vesiculation. Mem-

brane invagination to form free vesicles is a well-established process at other membrane boundaries but it is important to note that in these situations the evaginating face of the membrane is cytoplasmic. In contrast, during inward vesiculation in MVBs the evaginating face of the membrane is luminal. Annexin I has been shown to mediate vesicle aggregation and a model has been proposed whereby annexin molecules bind to phospholipid vesicles and fusion between neighboring membranes is mediated by interaction of annexin molecules (Blackwood and Ernst, 1990; Ernst et al., 1991). In the MVB interaction of neighbouring molecules of annexin I on the perimeter membrane may have a role in driving inward vesiculation. Release of annexin I through phosphorylation may then be required for the inward release of vesicles from the perimeter membrane. Subfractionation of the MVB to analyse the protein composition of the perimeter membrane and inner vesicles and the development of *in vitro* systems to study inward vesiculation may allow the molecular dissection of the events leading to the formation of internal vesicles in the MVB.

The authors would like to thank Adele Gibson and Mark Shipman for expert technical assistance.

C. R. Hopkins was supported by an MRC programme grant.

Received for publication 17 July 1992 and in revised form 14 September 1992.

References

- Ando, Y., S. Imamura, Y.-M. Hong, M. K. Owada, T. Kakunaga, and R. Kanag. 1989. Enhancement of calcium sensitivity of lipocortin I in phospholipid binding induced by limited proteolysis and phosphorylation at the amino terminus as analysed by phospholipid affinity column chromatography. *J. Biol. Chem.* 264:6948-6955.
- App, H., R. Hazan, A. Zilberstein, A. Ullrich, J. Schlessinger, and U. Rapp. 1991. Epidermal growth factor stimulates association and kinase activity of Raf-1 with the epidermal growth factor receptor. *Mol. Cell Biol.* 11:913-919.
- Beardmore, J., K. E. Howell, K. Miller, and C. R. Hopkins. 1987. Isolation of an endocytic compartment from A431 cells using a density modification procedure employing a receptor-specific monoclonal antibody complexed with colloidal gold. *J. Cell Sci.* 87:495-506.
- Beaumelle, B. D., A. Gibson, and C. R. Hopkins. 1990. Isolation and preliminary characterization of the major membrane boundaries of the endocytic pathway in lymphocytes. *J. Cell Biol.* 111:1811-1823.
- Bellot, F. B., W. Moolenaar, R. Kris, B. Mirakhor, A. Ullrich, J. Schlessinger, and S. Felder. 1990. High-affinity epidermal growth factor binding is specifically reduced by a monoclonal antibody and appears necessary for early responses. *J. Cell Biol.* 110:491-502.
- Blackwood, R. A., and J. D. Ernst. 1990. Characterisation of Ca^{2+} -dependent phospholipid binding, vesicle aggregation and membrane fusion by annexins. *Biochem. J.* 226:195-200.
- Bouton, A. H., S. B. Klausner, R. R. Vines, H.-C. R. Wang, J. B. Gibbs, and J. T. Parsons. 1991. Transformation by pp60^{src} or stimulation of cells with epidermal growth factor induces the stable association of tyrosine phosphorylated cellular proteins with GTPase-activating protein. *Mol. Cell Biol.* 11:945-953.
- Bustelo, X. R., J. A. Ledbetter, and M. Barbacid. 1992. Product of the *vav* proto-oncogene defines a new class of protein tyrosine kinase substrates. *Nature (Lond.)* 356:68-70.
- Carlberg, K., P. Tapkey, C. Haystead, and L. Rohrschneider. 1991. The role of kinase activity and the kinase insert region in ligand-induced internalisation and degradation of the c-fms protein. *EMBO (Eur. Mol. Biol. Organ.) J.* 10:877-883.
- Carpenter, G., and S. Cohen. 1976. ¹²⁵I-labeled human epidermal growth factor binding, internalization and degradation in human fibroblasts. *J. Cell Biol.* 71:159-171.
- Carpentier, J. L., M. F. White, L. Orci, and C. R. Kahn. 1987. Direct visualization of the epidermal growth factor receptor during its internalization in A431 cells. *J. Cell Biol.* 105:2751-2762.
- Chen, W. S., C. S. Lazar, K. A. Lund, J. B. Welsh, C. P. Chang, G. M. Walton, C. J. Der, T. S. Wiley, G. N. Gill, and M. G. Rosenfeld. 1989. Functional independence of the epidermal growth factor receptor from a domain required for ligand-induced internalization and calcium regulation. *Cell* 59:33-43.
- Cohen, S., and R. A. Fava. 1985. Internalization of functional epidermal growth factor: receptor/kinase complexes in A-431 cells. *J. Biol. Chem.* 260:12351-12358.
- De, B. K., K. S. Misono, T. J. Lukas, B. Mroczkowski, and S. Cohen. 1986. A calcium-dependent 35-kd substrate for epidermal growth factor receptor/kinase isolated from normal tissue. *J. Biol. Chem.* 261:13784-13792.
- DeMey, J. 1986. The preparation and use of gold probes. In *Practical Applications in Pathology and Biology*. Polak, J. M., and Van Noorden, S., editors. 115-145. Wright, Bristol.
- Ernst, J. D., E. Hoyer, R. A. Blackwood, and T. L. Mok. 1991. Identification of a domain that mediates vesicle aggregation reveals functional diversity of annexin repeats. *J. Biol. Chem.* 266:6670-6673.
- Felder, S., K. Miller, G. Mochren, A. Ullrich, J. Schlessinger, and C. R. Hopkins. 1990. Kinase activity controls the sorting of the epidermal growth factor receptor within the multivesicular body. *Cell* 61:623-624.
- Felder, S., J. LaVin, A. Ullrich, and J. Schlessinger. 1992. Kinetics of binding, endocytosis, and recycling of EGF receptor mutants. *J. Cell Biol.* 117:203-212.
- Futter, C. E., and C. R. Hopkins. 1989. Subfractionation of the endocytic pathway: isolation of compartments involved in the processing of internalised epidermal growth factor receptor complexes. *J. Cell Sci.* 94:685-694.
- Glenney, J. R., B. Tack, and M. A. Powell. 1987. Calpactins: Two distinct Ca^{2+} -regulated phospholipid- and actin-binding proteins isolated from lung and placenta. *J. Cell Biol.* 104:503-511.
- Glenney, J. R., W. S. Chen, C. S. Lazar, G. M. Walton, L. M. Zokas, M. G. Rosenfeld, and G. N. Gill. 1988. Ligand-induced endocytosis of the epidermal growth factor receptor is blocked by mutational inactivation and by micro-injection of anti-phosphotyrosine antibodies. *Cell* 52:685-695.
- Haigler, H. T., D. D. Schlaepfer, and W. H. Burgess. 1987. Characterisation of lipocortin I and an immunologically unrelated 33-kDa protein as epidermal growth factor receptor/kinase substrates and phospholipase A₂ inhibitors. *J. Biol. Chem.* 262:6921-6930.
- Honegger, A. M., T. J. Dull, F. Bellot, E. Van Obberghen, D. Szapary, A. Schmidt, A. Ullrich, and J. Schlessinger. 1987. Point mutation at the ATP binding site of EGF-receptor abolishes protein tyrosine kinase activity and alters cellular routing. *Cell* 51:199-209.
- Honegger, A. M., A. Schmidt, A. Ullrich, and J. Schlessinger. 1990. Separate endocytic pathways of kinase-defective and -active epidermal growth factor receptor mutants expressed in the same cells. *J. Cell Biol.* 110:1541-1554.
- Huang, K. S., B. P. Wallner, R. J. Mattaliano, R. Tizard, C. Burne, A. Frey, C. Hession, P. McGray, L. K. Sinclair, E. Pingchang Chow, J. L. Browning, K. L. Ramachandran, J. Tang, J. E. Smart, and R. B. Pepinsky. 1986. Two human 35 kd inhibitors of phospholipase A₂ are related to substrates of pp60^{src} and of the epidermal growth factor receptor/kinase. *Cell* 46:191-199.
- Hunter, W. M., and F. C. Greenwood. 1962. Preparation of iodine-131 labeled human growth hormone of high specific activity. *Nature (Lond.)* 194:490-495.
- Kay, D. J., W. H. Lai, M. Uchihashi, M. M. Khan, B. I. Posner, and J. J. M. Bergeron. 1986. Epidermal growth factor receptor kinase translocation and activation *in vivo*. *J. Biol. Chem.* 261:8473-8480.
- Kris, R. M., I. Lax, W. Gullick, M. D. Waterfield, A. Ullrich, M. Fridkin, and J. Schlessinger. 1985. Antibodies against a synthetic peptide as a probe for the kinase activity of the avian EGF receptor and v-erbB protein. *Cell* 40:619-625.
- Lai, W. H., P. H. Cameron, J. J. Doherty, B. I. Posner, and J. J. M. Bergeron. 1989. Ligand-mediated autophosphorylation activity of the epidermal growth factor receptor during internalization. *J. Cell Biol.* 109:2751-2760.
- Margolis, B., P. Hu, S. Katrav, W. Li, J. M. Oliver, A. Ullrich, A. Weiss, and J. Schlessinger. 1992. Tyrosine phosphorylation of *vav* proto-oncogene product containing SH2 domain and transcription factor motifs. *Nature (Lond.)* 356:71-73.
- Nesterov, A., G. Reshetnikova, N. Vinogradova, and N. Nikolsky. 1990. Functional state of the epidermal growth factor-receptor complexes during their internalisation in A431 cells. *Mol. Cell Biol.* 10:5011-5014.
- Renfrew, C. A., and A. L. Hubbard. 1991. Degradation of epidermal growth factor receptor in rat liver. *J. Biol. Chem.* 266:21265-21273.
- Sawyer, S. T., and S. Cohen. 1985. Epidermal growth factor stimulates the phosphorylation of the calcium-dependent 35000-Dalton substrate in intact A-431 cells. *J. Biol. Chem.* 260:8233-8236.
- Slot, J. W., and H. I. Geuze. 1985. A new method of preparing gold probes for multiple labeling cytochemistry. *Eur. J. Cell Biol.* 38:87-93.
- Ushiro, H., and S. Cohen. 1980. Identification of phosphotyrosine as a product of epidermal growth factor-activated protein kinase in A-431 cell membranes. *J. Biol. Chem.* 255:8363-8365.
- Wada, I., W. H. Lai, B. I. Posner, and J. J. Bergeron. 1992. Association of the tyrosine phosphorylated epidermal growth factor receptor with a 55-kD tyrosine phosphorylated protein at the cell surface and in endosomes. *J. Cell Biol.* 116:321-330.
- Wiley, H. S., J. J. Herbst, B. J. Walsh, D. A. Lauffenburger, M. G. Rosenfeld, and G. N. Gill. 1991. The role of tyrosine kinase activity in endocytosis, compartmentation, and down-regulation of the epidermal growth factor receptor. *J. Biol. Chem.* 266:11083-11094.

Identification and characterization of a novel type of annexin-membrane interaction: Ca^{2+} is not required for the association of annexin II with early endosomes

Matthias Jost^{1,*}, Dagmar Zeuschner¹, Joachim Seemann², Klaus Weber² and Volker Gerke^{1,†}

¹Institute for Medical Biochemistry, ZMBE, University of Münster, von-Esmarch-Str. 56, D-48149 Münster, Germany

²Department of Biochemistry, Max Planck Institute for Biophysical Chemistry, Am Fassberg 11, D-37077 Göttingen, Germany

*Present address: Department of Cell Biology, The Scripps Research Institute, La Jolla, CA 92037, USA

†Author for correspondence

SUMMARY

Annexin II, a member of a family of Ca^{2+} and membrane binding proteins, has been implicated in regulating membrane organization and membrane transport during endocytosis and Ca^{2+} regulated secretion. To characterize the mechanistic aspects of the annexin II action we studied parameters which determine the endosomal association of annexin II. Immunoblot analysis of subcellular membrane fractions prepared from BHK cells in the presence of a Ca^{2+} chelating agent reveals that annexin II remains associated with endosomal membranes under such conditions. This annexin II behaviour is atypical for the Ca^{2+} regulated annexins and is corroborated by the finding that ectopically expressed annexin II mutants with inactivated Ca^{2+} binding sites continue to co-fractionate with endosomal membranes. The Ca^{2+} -independent membrane association

of annexin II is also not affected by introducing mutations interfering with the complex formation of annexin II with its intracellular protein ligand p11. However, a deletion of the unique N-terminal domain of annexin II, in particular the sequence spanning residues 15 to 24, abolishes the Ca^{2+} -independent association of the protein with endosomes. These results describe a novel, Ca^{2+} -independent type of annexin-membrane interaction and provide a first explanation for the observed preference of different annexins for different cellular membranes. In the case of annexin II this specificity could be mediated through specific membrane receptors interacting with a unique sequence in the annexin II molecule.

Key words: Ca^{2+} /phospholipid binding protein, Endocytosis, Membrane-cytoskeleton interaction

INTRODUCTION

The Ca^{2+} -dependent regulation of membrane-cytoskeleton and membrane-membrane interactions plays an important role in a number of biological processes ranging from the control of cell and organelle shape to that of certain membrane traffic events. Among the components thought to be involved in such Ca^{2+} -mediated processes are the annexins, members of a multigene family of Ca^{2+} /phospholipid-binding proteins widely distributed among species. Typically, all annexins share as a characteristic biochemical property the ability to bind to negatively charged phospholipids and cellular membranes in a Ca^{2+} -dependent manner, and some members of the family also interact Ca^{2+} -dependently with certain cytoskeletal elements (for reviews see Creutz, 1992; Raynal and Pollard, 1994). These annexin properties are displayed by a well conserved protein core domain which is resistant to limited proteolysis and comprises a four- or eightfold repetition of a segment of 70-80 amino acid residues, the annexin repeat. Each annexin repeat harbours one or two novel types of Ca^{2+} binding sites. These differ in architecture from the EF hand motif (Moews and Kretsinger, 1975) and involve in addition to other elements

a highly conserved acidic amino acid whose carboxyl oxygens are crucially important for Ca^{2+} coordination (Huber et al., 1990; Weng et al., 1993; Jost et al., 1992, 1994). Unique within the individual members of the annexin family is the N-terminal domain which precedes the protein core and varies in length and sequence. It is thought to be of regulatory importance as it harbours in several annexins phosphorylation sites for different signal transducing kinases (for review see Raynal and Pollard, 1994).

Annexin II is implicated in several membrane transport steps. These include the Ca^{2+} -regulated secretion since annexin II, which is a prominent component in chromaffin granule preparations, is able to aggregate these vesicles at Ca^{2+} levels which are close to those observed in stimulated chromaffin cells, and partially restores the secretory responsiveness in permeabilized chromaffin cells (Ali et al., 1989; Sarafian et al., 1991; for review see Creutz, 1992). Such Ca^{2+} -regulated function of annexin II in the exocytotic pathway seems to depend on a complex formation of the protein with its intracellular ligand, the S100 protein p11. Complex formation, which leads to an annexin IIp11 heterotetramer, is mediated through the N-terminal domain of annexin II (for review see

Weber, 1992) and is a prerequisite for anchoring annexin II in the cortical region of cultured cells (Thiel et al., 1992; Jost et al., 1994). Based on these findings it had been suggested that the annexin II-p11 complex may participate in Ca^{2+} -regulated exocytosis by linking exocytotic vesicles to the cortical cytoskeleton and/or the plasma membrane and thereby positioning the vesicle at the correct place in the cell (for reviews see Creutz, 1992; Gerke, 1996).

Several lines of evidence indicate that annexin II is also involved in endocytotic processes. The protein is found on isolated early endosomal membranes and is one of the few proteins transferred from a donor to an acceptor endosomal membrane in an in vitro fusion assay (Emans et al., 1993). Moreover, ectopic expression of a *trans*-dominant mutant for the annexin II-p11 complex, which leads to the intracellular aggregation of annexin II and p11, specifically affects early endosomes which are translocated to the site of the aggregates (Harder and Gerke, 1993). Finally, in a cell-free system purified annexin II reconstitutes in conjunction with arachidonic acid a Ca^{2+} -dependent fusion among endosomes which previously had been washed with the Ca^{2+} chelating EDTA (Mayorga et al., 1994).

The mechanism by which annexin II affects fusion properties and/or the organization and intracellular location of endosomal membranes is not known. To shed light on this mechanism and to elucidate the structural requirements for an annexin II-endosome interaction we analyzed the subcellular fractionation of ectopically expressed mutant derivatives of annexin II. We show that the co-fractionation of annexin II with endosomal membranes is not regulated by Ca^{2+} - and p11-binding. This Ca^{2+} -independent membrane association does, however, depend on the presence of amino acids 15 to 24 of the unique N-terminal domain of annexin II.

MATERIALS AND METHODS

Expression constructs

The cDNA encoding human annexin II (Huang et al., 1986) served as a template for oligonucleotide-directed mutagenesis (Kunkel, 1985) which was employed to generate mutant cDNAs encoding defective Ca^{2+} (CM) and/or p11 (PM) binding sites (Jost et al., 1994). The mutants containing a deletion of the region encoding the N-terminal 14 or 24 amino acid residues were constructed by PCR using the wild-type (WT) cDNA as a template and the oligonucleotides $\Delta 1$ (5' CTGTGCAAGCTCGAATTCGAGATGTCTCACTCTACACC 3') or $\Delta 2$ (5' CTACACCCCGAATTCATATATGTCTGTCAAAGCC 3') as sense and the oligonucleotide $\Delta 3$ (5' GACCTGTTATCTAGAAGCATGGTG 3') as antisense primers, respectively. All annexin II cDNAs also contained a single nucleotide exchange resulting in a glutamic acid for alanine replacement at amino acid position 65. This substitution installed the epitope for the monoclonal antibody H28 and thus enabled us to use this antibody to specifically detect the recombinantly expressed annexin II derivatives (Thiel et al., 1991). For expression in BHK cells the individual annexin II cDNAs were cloned into the pCMV5 vector to yield the constructs pCMV-WT, pCMV-PM, pCMV-CM, pCMV-PMCM, pCMV- $\Delta 1$ -14, and pCMV- $\Delta 1$ -24. The presence of the individual mutations was verified by dideoxy sequencing (Sanger et al., 1977).

Cell culture and transfection

Hamster BHK cells were grown in Dulbecco's modified Eagle's medium (Gibco-BRL) supplemented with 10% fetal calf serum (Boehringer,

Mannheim). Transient transfection employed a modified calcium phosphate precipitation method (Chen and Okayama, 1987) using 20 μg of the respective plasmid DNA per 100 mm dish of cells grown to 50% confluency. After addition of the DNA, cells were incubated for 12 to 16 hours at 35°C in 3% CO_2 , then washed with PBS and cultivated in fresh medium using normal culture conditions. Between 30 and 40% of the total cell population was expressing the exogenous protein 40 hours following transfection, as revealed by routine immunofluorescence analysis with the monoclonal antibody H28.

Fractionation of endosomal membranes

Labeling and fractionation of endosomes was carried out essentially as described by Gorvel et al. (1991) and Aniento et al. (1996). Briefly, four 100 mm dishes of untreated BHK cells or six dishes of transfected cells were incubated at 37°C with 2 mg/ml horseradish peroxidase (HRP) in IM (internalization medium: Dulbecco's modified Eagle's medium supplemented with 10 mM Hepes, pH 7.4). To label early endosomes the HRP incubation was carried out for five minutes. Late endosomal labeling was achieved by treating the cells for five minutes with HRP in IM followed by a 45 minute chase in IM supplemented with 2 mg/ml bovine serum albumin. Subsequently, the cells were lysed in HB buffer (0.25 M sucrose, 3 mM imidazole-HCl, pH 7.4) followed by a low speed centrifugation to yield a post-nuclear supernatant (PNS). The PNS was brought to 40.6% sucrose, 3 mM imidazole-HCl, pH 7.4, and placed at the bottom of a SW 60 centrifugation tube (Beckman). This load was overlaid with 1.5 ml of 35% sucrose, 3 mM imidazole-HCl, pH 7.4, then with 1 ml 25% sucrose, 3 mM imidazole-HCl, pH 7.4, and finally with 0.5 ml HB buffer. In some experiments, the sucrose solutions were supplemented with 1 mM EDTA to reduce the free Ca^{2+} concentration. The step gradient was centrifuged at 35,000 rpm for 60 minutes at 4°C. Fractions containing late and multivesicular endosomes were collected at the 25% sucrose-HB interface and early endosomes were enriched at the 25%-35% sucrose interface. Fractions containing heavy membranes (HM) were collected at the 35%-40.6% sucrose interface. The activity of endocytosed HRP present in the different fractions was analyzed as described (Gorvel et al., 1991) and latency was measured according to Bomsel et al. (1990). Proteins present in the different fractions were concentrated by chloroform/methanol precipitation (Wessel and Flügge, 1984) and 10 μg of each fraction (as determined according to Bradford, 1976) were separated by SDS-polyacrylamide gel electrophoresis (PAGE) (Laemmli, 1970) and analyzed by immunoblotting (Towbin et al., 1987).

Immunofluorescence analysis of annexin II and transferrin receptor distribution

BHK cells grown on glass coverslips were co-transfected with an expression construct encoding the human transferrin receptor (hTfR) cDNA (pCMV-hTfR; Harder and Gerke, 1993) and with one of the expression constructs encoding wild-type (WT) or mutant annexin II derivatives (pCMV-WT, pCMV-PMCM, pCMV- $\Delta 1$ -24). At 40 hours post transfection the cells were incubated for 1 hour in serum-free medium and then for 30 minutes in serum-free medium containing 20 $\mu\text{g}/\text{ml}$ human transferrin (Boehringer) to obtain an efficient hTfR internalization into early and recycling endosomes. Subsequently, the coverslips were washed briefly in cold PBS and placed, cells facing down, for 10 minutes at 4°C onto a 50 μl drop of a solution containing activated streptolysin O (SLO; obtained from Dr S. Bhakdi, University of Mainz, FRG; Bhakdi et al., 1993). SLO was employed at 5 $\mu\text{g}/\text{ml}$ in intracellular transport buffer (ICT; 78 mM KCl, 4 mM MgCl_2 , 8.37 mM CaCl_2 , 10 mM EGTA and 1 mM DTT; Burke and Gerace, 1986). EGTA in the ICT buffer was omitted in experiments analyzing the Ca^{2+} -dependent association of $\Delta 1$ -24 annexin II with endosomes. Following incubation at 4°C the excess SLO that did not bind to the plasma membrane was removed by two washes with cold ICT. For permeabilization the coverslips were placed on pre-warmed drops of ICT for 10 minutes at 37°C. The effectiveness of permeabilization could be

measured by LDH release. The cells were then washed for an additional 10 minutes with cold ICT to obtain an efficient depletion of the cytosol. For double immunofluorescence staining of the transfected hTfR and annexin II, the cells were fixed for 2 minutes in -20°C cold methanol, washed with PBS and incubated with the first antibodies in a humid chamber for 45 minutes at room temperature. Mouse anti-human CD71 (IgG2A; Pharmingen) was employed to label the hTfR and the mouse monoclonal H28 (IgG1; Osborn et al., 1988) was used to specifically detect the ectopically expressed annexin II derivatives. The coverslips were then washed 3×10 minutes with PBS and incubated for 45 minutes with the corresponding fluorescently labeled secondary antibodies (isotype-specific antibodies directed against mouse IgG1 and IgG2A, respectively). After three final PBS washes the coverslips were mounted in Moviol 4-88 (Hoechst). Cells were examined with a Zeiss axiophot photomicroscope and photography employed Kodak P3200 film.

Antibodies

The polyclonal rabbit antibodies directed against annexins II and IV as well as the mouse monoclonal anti-annexin II antibody H28 have been described (Gerke and Weber, 1984; Osborn et al., 1988). Antibodies against the early endosome-associated protein EEA1 (Mu et al., 1995) were kindly provided by Dr Ban-Hock Toh (Monash Medical School, Melbourne, Australia). Peroxidase coupled antibodies (Dako) were used as secondary antibodies and immunoreactive bands were visualised using the ECL chemoluminescence system (Amersham-Buchler). For double immunofluorescence analysis of transfected cells ectopically expressing hTfR and annexin II, FITC-coupled goat anti-mouse IgG2A and Texas red-coupled goat anti-mouse IgG1 (Southern Biotechnology Associated Inc.) were employed as secondary antibodies.

RESULTS

The association of annexin II with endosomal membranes in the presence and absence of Ca²⁺

To analyze whether and how Ca²⁺ ions affect the association of annexin II with endosomal membranes we probed subcellular fractions of BHK cells prepared in the absence or presence of the Ca²⁺ chelating EDTA with an annexin II antibody. In these experiments an enrichment of annexin II in a given subcellular fraction was assessed by comparing the respective immunoblot signal to that obtained when an equal amount of total protein from the starting material for gradient fractionation, the post nuclear supernatant (PNS), was analyzed. Fig. 1 reveals that annexin II is enriched in fractions containing early endosomal membranes and to a lesser extent in those containing late endosomes when cell lysis and subsequent gradient fractionation are carried out in the absence of EDTA (as already shown by Emans et al., 1993). Unexpectedly the cofractionation with early endosomes is not affected by including EDTA in all buffers used in the subcellular fractionation indicating that the annexin II binding to early endosomes still occurs at submicromolar Ca²⁺ concentrations (Fig. 1). A Ca²⁺-independent association of annexin II with endosomes is also corroborated by ultrastructural analyses of mechanically perforated MDCK cells. When these cells are incubated in a physiological buffer in the absence of Ca²⁺ prior to fixation they retain the majority of their endosome associated annexin II although the soluble protein and a substantial fraction of the plasma membrane associated annexin II is lost (Harder et al., 1997).

Further immunoblot analysis reveals that annexin IV is another annexin present in BHK cell fractions containing endosomal membranes (Fig. 1). However, in contrast to

annexin II, annexin IV is enriched to an equal extent in fractions containing early and in those containing late endosomes and its co-fractionation with the respective membrane fractions is sensitive to Ca²⁺ chelation (Fig. 1). Thus, annexin IV exhibits a behaviour typical for an annexin, i.e. a Ca²⁺-regulated interaction with membranes, whereas annexin II appears to associate with the endosomal membranes in a manner atypical for an annexin. To verify the enrichment of early endosomes in the different experiments, the gradient fractions obtained were also subjected to immunoblot analysis with an antibody against EEA1, a protein of 180 kDa specifically associated with early endosomes (Mu et al., 1995; a representative example revealing the specific enrichment of EEA1 in fractions containing early endosomes is shown in Fig. 1). Moreover, in all endosome fractionation experiments the enrichment and integrity of the different endosomal membranes was routinely monitored by following the fate of HRP internalized from the fluid phase (see Materials and Methods for details).

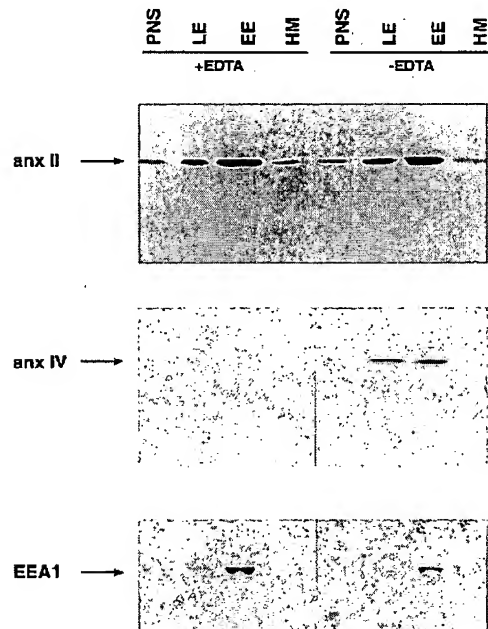
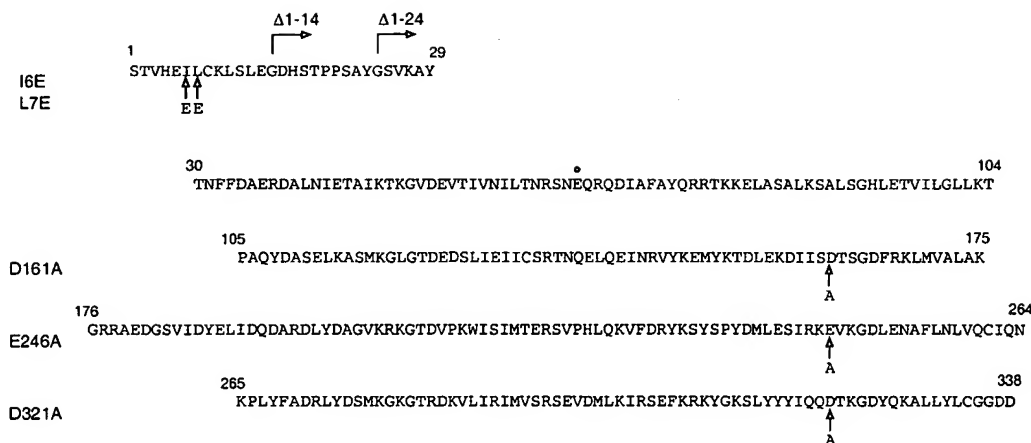


Fig. 1. Association of annexin II and annexin IV with different membrane fractions from BHK cells. A post-nuclear supernatant (PNS) was prepared from BHK cells and subjected to flotation gradient fractionation in the presence (+) or absence (-) of 1 mM EDTA. Fractions enriched in late (LE) and early endosomes (EE) as well as those containing heavy membranes (HM) were collected. Equal amounts of protein from these fractions (as determined according to Bradford, 1976) were subjected to SDS-PAGE and subsequent immunoblotting using polyclonal antibodies directed against annexins II (upper panel) and IV (middle panel). A control immunoblot using antibodies against the early endosome-associated protein EEA1 is shown in the bottom panel. Note that annexin II is enriched in fractions containing endosomal, in particular early endosomal, membranes and that this enrichment is not affected by the inclusion of the Ca²⁺ chelating EDTA. In contrast, annexin IV is equally enriched in fractions containing early and late endosomal membranes and this association is sensitive to Ca²⁺ chelation.

Fig. 2. Amino acid sequence of human annexin II and of annexin II mutants used in this study. The sequence (Huang et al., 1986) is given in the one letter code. The dot indicates a Glu for Ala replacement which is shared by all annexin II derivatives described here and which reconstitutes the epitope for the monoclonal antibody H28 (Osborn et al., 1988; Thiel et al., 1991). Vertical arrows mark the amino acid

substitutions introduced to inactivate the type II Ca^{2+} binding sites (D161A, E246A, D321A, generating CM annexin II) and the p11 binding site (I6E, L7E, generating PM annexin II). The positions of the novel N-termini of the truncation mutants, $\Delta 1-14$ and $\Delta 1-24$ annexin II, are indicated by horizontal arrows.



Intact Ca^{2+} and p11 binding sites are not required for an endosomal association of annexin II

As the subcellular fractionation data suggested a novel type of annexin-membrane interaction for the annexin II-endosome association (one not sensitive to Ca^{2+}) we analyzed the structural requirements for this association in more detail. Therefore we employed a transfection approach to express ectopically in BHK cells certain annexin II mutant proteins. The subcellular distribution of these derivatives was determined by flotation gradient fractionation of a PNS prepared from the transfected cells and subsequent immunoblot analysis of the different fractions using a monoclonal antibody specifically recognizing the ectopically expressed but not the endogenous annexin II (Thiel et al., 1991).

In a first approach we analyzed the behaviour of an annexin II mutant with inactivated type II Ca^{2+} binding sites. These sites are located in repeats 2, 3 and 4 of annexin II and they were rendered inactive by introducing alanine in place of the crucial acidic amino acids serving as so-called cap residues in this type of Ca^{2+} binding site (D161A, E246A, D321A; CM annexin II; Fig. 2). The impairment of the Ca^{2+} -sites had been verified previously by our biochemical analyses (Thiel et al., 1992; Jost et al., 1992). An expression construct encoding wild-type (WT) annexin II was used in control experiments. Fractionation of BHK cells transiently expressing the WT annexin II reveals that this ectopically expressed protein shows the co-fractionation with endosomal membranes already observed for the endogenous annexin II (Fig. 3). Moreover, this co-fractionation is observed both in the absence and in the presence of a Ca^{2+} chelating agent (not shown).

A very similar result is obtained when the subcellular distribution of the mutant protein with inactivated Ca^{2+} -sites is revealed by gradient fractionation, i.e. CM annexin II also co-fractionates with early endosomal membranes (not shown). To exclude the possibility that CM annexin II associates with endosomes through a p11-mediated binding to endogenous (intact) annexin II, we decided to analyze the subcellular distribution of a CM derivative with an inactivated p11 binding site.

p11 binding is mediated through the N-terminal 14 amino acids of annexin II with the hydrophobic side chains at positions 6 and 7 (Ile and Leu, respectively) representing major contact sites (Johnsson et al., 1988; Becker et al., 1990). Therefore, we introduced glutamic acid residues in place of Ile-6 and Leu-7 (I6E, L7E; Fig. 2) to inactivate the p11 binding site. This PM (p11-minus) mutation was combined with the CM replacements generating PMCM annexin II. As revealed by ligand blotting and Ca^{2+} -dependent liposome pelleting this mutant protein was impaired in both p11 and Ca^{2+} binding (not shown). Gradient analysis of BHK cells expressing PMCM annexin II shows that this mutant continues to co-fractionate with early endosomal membranes (Fig. 3). Since PMCM annexin II remains monomeric these results show unambiguously that Ca^{2+} binding to annexin II is not required for its cofractionation with early endosomal membranes. Interestingly, the somewhat lesser but reproducibly observed enrichment of endogenous (Fig. 1) and transfected WT annexin II (Fig. 3) in fractions containing late endosomes is not seen in the case of the PMCM derivative (Fig. 3). Likewise, the CM annexin II mutant shows an enrichment only in early endosomal but not in late endosomal fractions (not shown). This indicates that the cofractionation of annexin II with late endosomal membranes requires intact Ca^{2+} binding sites in the protein and thus differs mechanistically from the Ca^{2+} -independent association of annexin II with early endosomes.

The signal for localizing annexin II Ca^{2+} -independently to endosomal membranes resides in the N-terminal domain

To identify the region in the annexin II molecule mediating the Ca^{2+} -independent association with endosomes we generated two N-terminally truncated derivatives which were again expressed in BHK cells and subjected to the fractionation protocol described above. We chose the N-terminal domain for a more detailed analysis since this region is highly variable within the individual annexins and thus likely to be involved in mediating specific properties. In a first truncation mutant we deleted the entire p11 binding site, i.e. amino acids 1-14 (Johnsson et al.,

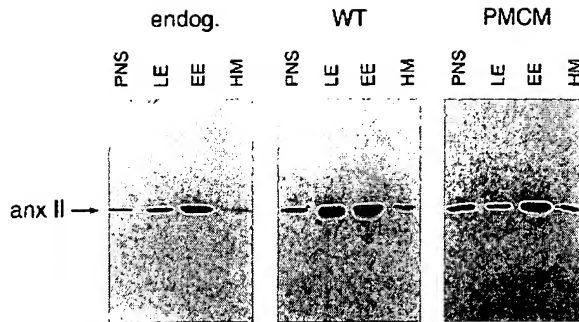


Fig. 3. Flotation gradient analysis of membranes from BHK cells ectopically expressing annexin II derivatives. BHK cells were transfected with expression constructs encoding wild-type (WT) annexin II or a mutant derivative containing inactivated Ca²⁺ binding sites as well as an inactivated p11 binding site (PMCM). Membranes present in a PNS from such cells were subjected to sucrose gradient fractionation and fractions enriched in late endosomes (LE), early endosomes (EE), and heavy membranes (HM) were analyzed by immunoblotting using a monoclonal antibody (H28) specifically recognizing the ectopically expressed annexin II. The distribution of endogenous annexin II (endog.) among the membrane fractions from non-transfected BHK cells was determined by immunoblotting with a polyclonal annexin II antibody and is given for comparison. Preparation of the PNS and gradient fractionation were carried out in the absence of EDTA to specifically analyze the consequences of the Ca²⁺-site mutations. Note that PMCM annexin II which is incapable of forming the heterotetrameric annexin II-p11 complex and which does not bind Ca²⁺ continues to co-fractionate with endosomal membranes.

1988), and introduced a novel start by replacing the amino acids at positions 14 and 15 (Gly and Asp) by methionine and serine (Fig. 2). As expected from the properties displayed by PMCM annexin II, i.e. a protein mutant incapable of binding p11, the Δ 1-14 annexin II derivative continues to co-fractionate with endosomal membranes in the presence of 1 mM EDTA (Fig. 4A). This shows again that p11 binding is not required and further reveals that the entire p11 binding site is dispensable for a Ca²⁺-independent association with endosomes.

An additional 10 amino acid residues were deleted in the second truncation mutant, Δ 1-24 annexin II, in which Gly-24 was replaced by the novel start-methionine (Fig. 2). The rationale for choosing this mutation was twofold. First, we wanted to delete or render inactive two phosphorylation sites of potential regulatory importance (Tyr-23 phosphorylated by pp60^{src} and Ser-25 phosphorylated by protein kinase C; for review see Gerke, 1992). Second, since Lys-27 is part of the discontinuous epitope of the monoclonal annexin II antibody H28 we decided to leave this residue unaffected (Thiel et al., 1991). This enabled us to detect the Δ 1-24 derivative by immunoblotting with the H28 antibody. Subcellular fractionation of BHK cells ectopically expressing Δ 1-24 annexin II reveals that this derivative fails to co-fractionate with endosomal membranes in the presence of a Ca²⁺ chelating agent (Fig. 4B). An enrichment of Δ 1-24 annexin II in membrane fractions containing endosomes is, however, observed when the preparation of the PNS and the subsequent gradient analysis are carried out in the absence of EDTA (Fig. 4B). Thus, the annexin II core starting at residue 25 displays the Ca²⁺-sensitive interaction with BHK membranes typical for an annexin, showing a preference for early and to a lesser extent late endosomes.

However, the Ca²⁺-independent association with these structures requires the sequence spanning residues 15 to 24. Fig. 4 also shows an immunoblot analysis employing EEA1 antibodies on gradient fractions prepared from BHK cells expressing the Δ 1-24 annexin II mutant. This control reveals that the fractionation properties of early endosomes are not affected by the ectopic expression of the annexin II mutant. Thus, the loss of Ca²⁺-independent membrane binding in the case of the Δ 1-24 mutant protein is solely due to the deletion of an important sequence in the protein and not caused by any putative secondary effects on the endosomal membranes in the transfected cells.

To corroborate the results obtained by subcellular fractionation we also collected morphological data on the subcellular localization of different annexin II mutants. Therefore, BHK cells were co-transfected with expression plasmids encoding the annexin II derivatives and the human transferrin receptor (hTfR) which was included as a marker for early endosomes in the transfected cells. At 40 hours following transfection the cells were permeabilized with streptolysin O (SLO) and then incubated in an intracellular transport buffer (ICT) to release

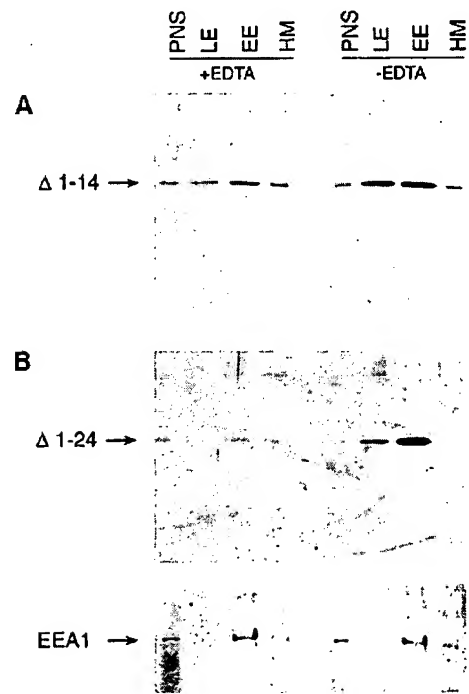
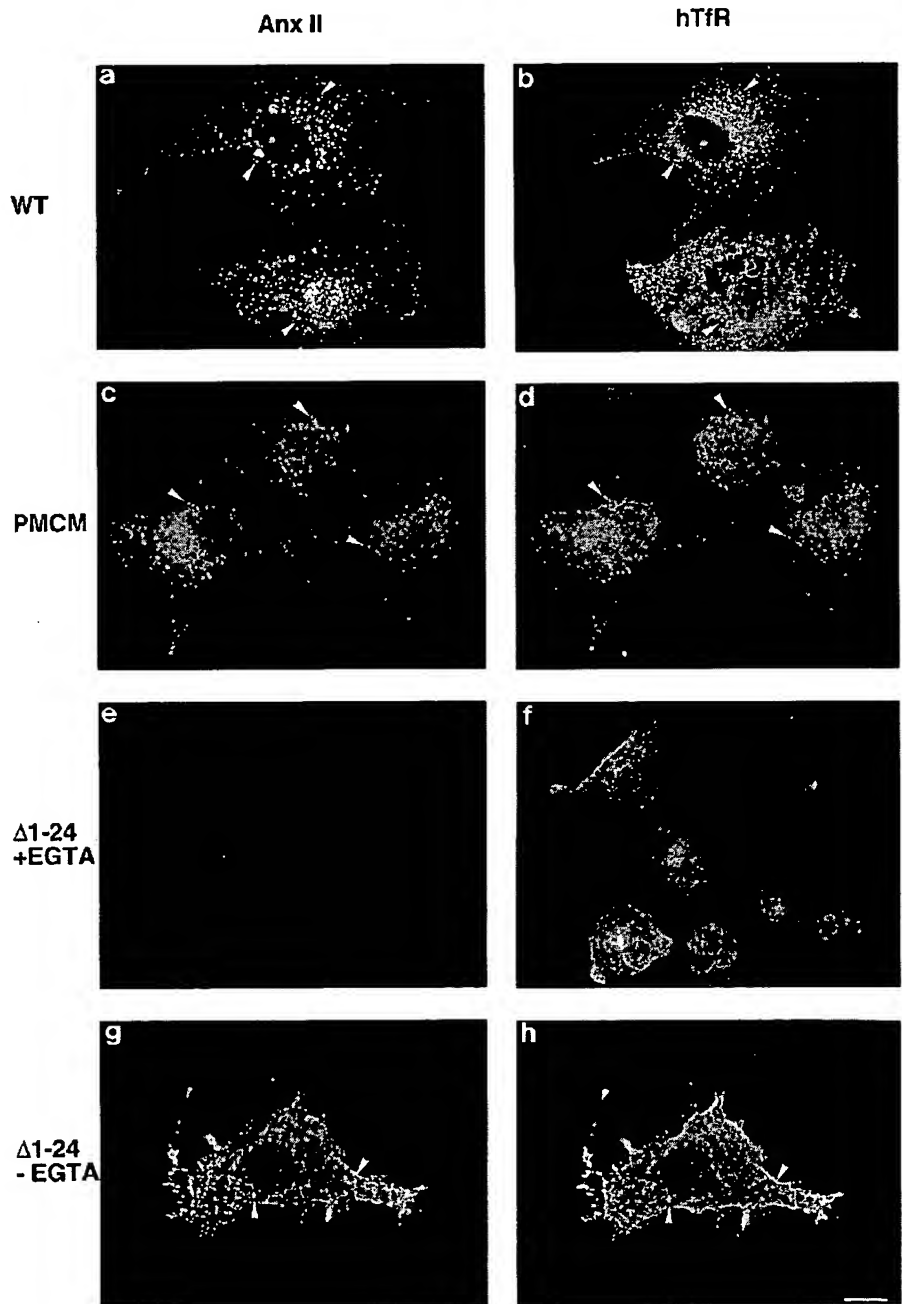


Fig. 4. Effect of N-terminal deletions on the Ca²⁺-independent co-fractionation of annexin II with endosomal membranes. Cellular membranes (LE, EE, HM) obtained by gradient fractionation of a PNS prepared from BHK cells ectopically expressing Δ 1-14 (A) or Δ 1-24 (B) annexin II were subjected to immunoblotting using the H28 monoclonal antibody specifically recognizing the mutant proteins. Subcellular fractionation was carried out in the presence (+) or absence (-) of 1 mM EDTA. Note that the deletion of amino acids 1-24 but not that of residues 1-14 renders the molecule incapable of co-fractionating with endosomal membranes in the presence of EDTA. A control immunoblot with the EEA1 antibody of the fractions obtained from Δ 1-24 annexin II-transfected cells is shown in the bottom part of B and reveals that the gradient fractionation of early endosomes is not affected in these cells.

the cytosolic fraction of annexin II (see Materials and Methods) before subjecting them to double immunofluorescence using antibodies specifically recognizing the ectopically expressed hTfR and annexin II derivatives, respectively. Fig. 5 reveals that WT annexin II and the PMCM mutant protein co-localize to a large extent with hTfR positive structures thus showing the early endosomal localization already established for endogenous annexin II at the light and electron microscope level (Emans et al., 1993; Harder and Gerke, 1993). In line with our biochemical analyses this annexin II distribution is observed after incubating the permeabilized cells prior to fixation in ICT

buffer containing the Ca^{2+} chelating EGTA (Fig. 5). In contrast, the $\Delta 1-24$ mutant protein fails to show any endosomal or other intracellular membrane association under such conditions (Fig. 5). However, when Ca^{2+} is not chelated during the incubation of the permeabilized cells in ICT buffer the $\Delta 1-24$ derivative remains associated with intracellular structures which to a large extent are hTfR positive (Fig. 5). These data are in line with the subcellular fractionation (Fig. 4) and thus support the conclusion that the unique N-terminal domain of annexin II is required for its Ca^{2+} -independent association with endosomal membranes. When this domain is truncated the resulting $\Delta 1-$

Fig. 5. Localization of ectopically expressed annexin II derivatives and human transferrin receptor in SLO-permeabilized BHK cells. BHK cells were co-transfected with expression constructs encoding the human transferrin receptor (hTfR) and one of the annexin II derivatives (WT, PMCM, or $\Delta 1-24$ annexin II, respectively). At 40 hours following transfection efficient hTfR uptake was induced by exogenously supplemented transferrin. Subsequently the cells were permeabilized with SLO and depleted of cytosol by incubation in an intracellular transport buffer (ICT) containing EGTA (see Materials and Methods). This treatment releases the cytosolic annexin II pool which to some extent masks the membrane-bound fraction in immunofluorescence analyses of directly fixed cells (Osborn et al., 1988; Harder and Gerke, 1993). In the case of cells expressing the $\Delta 1-24$ annexin II the cytosol was released either in the presence (e,f) or absence (g,h) of 10 mM EGTA to analyze the effect of Ca^{2+} on the intracellular distribution of this mutant. The cells were then fixed and processed for double immunofluorescence using antibodies directed against annexin II (a,c,e,g) and hTfR (b,d,f,h), which only recognized the ectopically expressed and not the endogenous proteins. Note that WT and PMCM annexin II co-localize to a large extent with hTfR positive endosomal structures in a manner not affected by the EGTA which is included in the ICT buffer (arrowheads in a,b and c,d, respectively). In contrast, $\Delta 1-24$ annexin II fails to show any membrane association under such conditions (e and f). A co-localization of $\Delta 1-24$ annexin II with hTfR positive endosomes is, however, observed when EGTA is omitted during cytosol depletion, i.e. in the presence of Ca^{2+} (g and h).



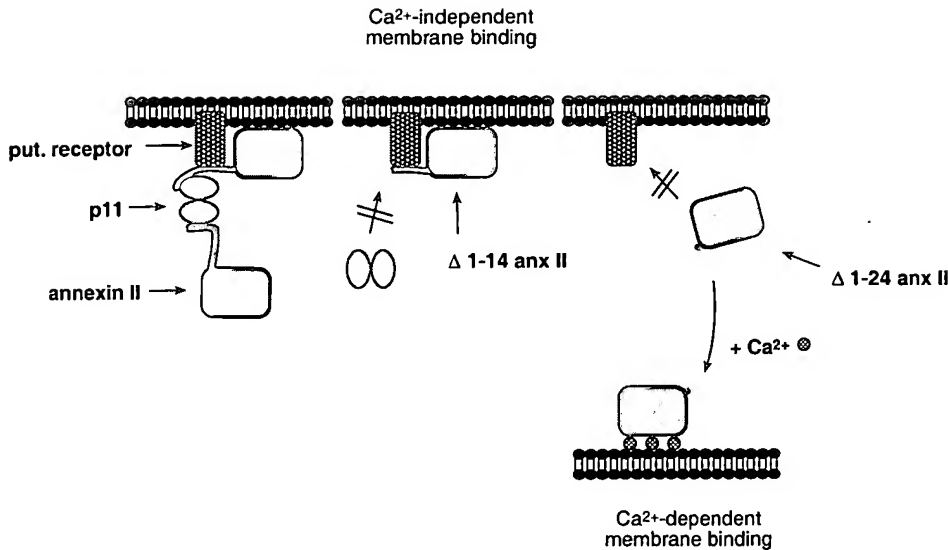


Fig. 6. Model depicting different modes of an annexin II-membrane interaction. The Ca²⁺-independent association with a target membrane described here is mediated through the sequence spanning residues 15 to 24 which could bind to a receptor specific for this membrane. This interaction would leave the very N-terminal 14 residues of annexin II accessible for p11 binding. Removal of the entire N-terminal region encompassing residues 1 to 24 generates a mutant derivative (Δ1-24 annexin II) whose membrane association strictly depends on the presence of Ca²⁺.

24 mutant protein requires Ca²⁺ for an interaction with endosomal membranes. Interestingly and as also seen in the gradient analysis the Ca²⁺-dependent membrane association of the Δ1-24 mutant protein remains to be specific for early and to a lesser extent late endosomal membranes, most likely because the phospholipid composition of these membranes is best suited for interacting with the annexin II core.

DISCUSSION

Members of the annexin family of Ca²⁺-regulated membrane binding proteins are present on most and possibly all intracellular membranes including the plasma membrane (Gruenberg and Emans, 1993). Specificity with respect to the target membrane of the individual annexins is thought to be conferred through the N-terminal domains which vary between the different members of the family. The Ca²⁺ sensitivity for a reversible and peripheral membrane binding, on the other hand, is most likely carried through the protein core comprising four or eight annexin repeats. These repeats harbour the type II and type III Ca²⁺ binding sites (for reviews see Huber et al., 1992; Swairjo and Seaton, 1994) and isolated core domains bind Ca²⁺-dependently to phospholipid vesicles and chromaffin granules (Glenney, 1986; Johnsson et al., 1986; Drust and Creutz, 1988). Most likely, the EDTA-sensitive, i.e. Ca²⁺ regulated, co-fraction of Δ1-24 annexin II with endosomes (Figs 4, 5) is the consequence of such a Ca²⁺-dependent interaction of the annexin II core domain with endosomal membranes. In this case specificity is probably carried through a certain phospholipid composition of the endosomal membranes which is better suited for binding the annexin II core than that of other cellular membranes.

A different mechanism must be responsible for mediating the Ca²⁺-independent association of annexin II with early endosomes described here. The association depends on the presence of the unique N-terminal domain of the annexin II molecule with the sequence encompassing amino acids 15-24 being of critical importance. In contrast, p11 binding and the resulting annexin II-

p11 complex formation are not required. This type of Ca²⁺-independent binding to certain cellular membranes has not been observed for an annexin before. It could be mediated through a specific receptor for annexin II on early endosomal membranes. This putative receptor would bind to the N-terminal annexin II domain, most likely to the sequence spanning residues 15 to 24, in a manner not regulated by Ca²⁺ (Fig. 6). Such an interaction could be accompanied in the presence of Ca²⁺ by a binding of the annexin II core to endosomal membrane phospholipids. Moreover, it would leave the very N-terminal region (residues 1 to 14) accessible for p11 binding thus enabling the annexin II-p11 complex formation to occur on endosomal membranes. Alternatively, the second part of the N-terminal domain, i.e. amino acids 15-24, could be involved in establishing or stabilizing a conformation of the core domain which allows for a Ca²⁺-independent interaction of this core domain with endosomal membranes. Future experiments, e.g. the identification of the putative annexin II receptor (protein or a certain lipid structure) on endosomes, have to resolve this question.

Within cells annexin II is not restricted to endosomes but is also found on the plasma membrane and/or in the cortical cytoskeleton colocalizing with molecules of the spectrin family (for review see Gerke, 1992). Interestingly, Ca²⁺ as well as p11 binding are required for establishing the tight association with the cortical cytoskeleton (Thiel et al., 1992; Jost et al., 1994) indicating that different structural requirements underlie the association of annexin II with endosomes and the cortical cytoskeleton, respectively. This could reflect the existence of functionally distinct annexin II pools and/or different modes of regulation. Cortical annexin II could be involved in stabilizing a peripheral localization of endosomes, possibly by providing a physical link between the endosomal membrane and the cortical cytoskeleton (Harder and Gerke, 1993). It may also serve an alternative or additional role in structuring or organizing endosomal membranes (or domains of the plasma membrane).

At least in certain cell types, e.g. adrenal chromaffin cells, annexin II has also been implicated in exocytotic processes, in particular in Ca²⁺ regulated secretion (Ali et al., 1989; Sarafian

et al., 1991). While the exact mechanism by which annexin II acts in exocytotic membrane transport is not known it has been suggested that a heterotetrameric annexin II-p11 complex could provide physical linkage between different chromaffin granule membranes and/or between the granule and the plasma membrane (Nakata et al., 1990; for review see Creutz, 1992). Conceptually, annexin II could therefore be involved in different membrane transport steps by serving a structural role in organizing membranes and/or membrane-cytoskeleton interactions. Specificity could then be guaranteed by certain phospholipid compositions allowing for a Ca^{2+} -dependent binding through the annexin II core domain or specific receptors (e.g. on endosomes) interacting Ca^{2+} -independently with a region in the N-terminal domain.

We thank Thomas Harder, Rob Parton and Jean Gruenberg for fruitful discussions and for communicating results prior to publication. Thanks also to Ban-Hock Toh for kindly providing antibodies against the EEA1 protein. This work was supported in part by grants from the Deutsche Forschungsgemeinschaft (Ge 514/2-2 and Ge 514/2-3) and the Human Frontier Science Program Organization (HFSPO) to V.G.

REFERENCES

- Ali, S. M., Geisow, M. J. and Burgoyne, R. D. (1989). A role for calpactin in calcium dependent exocytosis in adrenal chromaffin cells. *Nature* **340**, 313-315.
- Aniento, F., Gu, F., Parton, R. G. and Gruenberg, J. (1996). An endosomal β COP is involved in the pH-dependent formation of transport vesicles destined for late endosomes. *J. Cell Biol.* **133**, 29-41.
- Bhakdi, S., Weller, U., Walev, I., Martin, E., Jonas, D. and Palmer, M. (1993). A guide to the use of pore-forming toxins for controlled permeabilization of cell membranes. *Med. Microbiol. Immunol.* **182**, 167-175.
- Becker, T., Weber, K. and Johnsson, N. (1990). Protein-protein recognition via short amphiphilic helices; a mutational analysis of the binding site of annexin II for p11. *EMBO J.* **9**, 4207-4213.
- Bomsel, M., Parton, R., Kurznetsov, S. A., Schroer, T. A. and Gruenberg, J. (1990). Microtubule- and motor-dependent fusion in vitro between apical and basolateral endocytic vesicles from MDCK cells. *Cell* **62**, 719-731.
- Bradford, M. M. (1976). A rapid and sensitive method for quantitation of microgram quantities of protein utilizing the principle of protein dye-binding. *Anal. Biochem.* **72**, 248-254.
- Burke, B. and Gerace, L. (1986). A cell free system to study reassembly of the nuclear envelope at the end of mitosis. *Cell* **44**, 639-652.
- Chen, C. and Okayama, H. (1987). High-efficiency transformation of mammalian cells by plasmid DNA. *Mol. Cell Biol.* **7**, 2745-2752.
- Creutz, C. E. (1992). The annexins and exocytosis. *Science* **258**, 924-931.
- Drust, D. S. and Creutz, C. E. (1988). Aggregation of chromaffin granules by calpactin at micromolar levels of calcium. *Nature* **331**, 88-91.
- Emans, N., Gorvel, J. P., Walter, C., Gerke, V., Kellner, R., Griffiths, G. and Gruenberg, J. (1993). Annexin II is a major component of fusogenic endosomal vesicles. *J. Cell Biol.* **120**, 1357-1369.
- Gerke, V. and Weber, K. (1984). Identity of p36K phosphorylated upon Rous sarcoma virus transformation with a protein from brush borders; calcium-dependent binding to nonerythroid spectrin and F-actin. *EMBO J.* **3**, 227-233.
- Gerke, V. (1992). Evolutionary conservation and three-dimensional folding of the tyrosine kinase substrate annexin II. In *The Annexins* (ed. S. E. Moss), pp. 47-59. Portland Press, London.
- Gerke, V. (1996). Annexins and membrane traffic. In *Annexins: Molecular Structure to Cell Function* (ed. B. A. Seaton). Landes Science Publishers, Georgetown, TX (in press).
- Glenney, J. R. Jr (1986). Phospholipid-dependent Ca^{2+} -binding by the 36-kDa tyrosine kinase substrate (calpactin) and its 33-kDa core. *J. Biol. Chem.* **261**, 7247-7252.
- Gorvel, J. P., Chavrier, P., Zerial, M. and Gruenberg, J. (1991). rab5 controls early endosome fusion in vitro. *Cell* **64**, 915-925.
- Gruenberg, J. and Emans, N. (1993). Annexins in membrane transport. *Trends Cell Biol.* **3**, 224-227.
- Harder, T. and Gerke, V. (1993). The subcellular distribution of early endosomes is affected by the annexin IIp11₂ complex. *J. Cell Biol.* **123**, 1119-1132.
- Harder, T., Kellner, R., Parton, R. G. and Gruenberg, J. (1997). Specific release of membrane bound annexin II and cortical cytoskeletal elements by sequestration of membrane cholesterol. *Mol. Biol. Cell* (in press).
- Huang, K. S., Wallner, B. P., Mattaliano, R. J., Tizard, R., Burne, C., Frey, A., Hession, C., McGray, P., Sinclair, L. K., Chow, E. P., Browning, J. L., Ramachandran, K. L. J. T., Smart, J. E. and Pepinsky, R. B. (1986). Two human 35 kd inhibitors of phospholipase A₂ are related to substrates of p60^{src} and the epidermal growth factor receptor/kinase. *Cell* **46**, 191-199.
- Huber, R., Römisch, J. and Paques, E. P. (1990). The crystal and molecular structure of human annexin V, an anticoagulant calcium, membrane binding protein. *EMBO J.* **9**, 3867-3874.
- Huber, R., Berendes, R., Burger, A., Luecke, H. and Karshikov, A. (1992). Annexin V: crystal structure and its implications on function. In *The Annexins* (ed. S. E. Moss), pp. 105-124. Portland Press, London.
- Johnsson, N., Vanderkerckhove, J., van Damme, J. and Weber, K. (1986). Binding sites for calcium, lipid and p11 on p36, the substrate of retroviral tyrosine-specific protein kinases. *FEBS Lett.* **198**, 361-364.
- Johnsson, N., Marriott, G. and Weber, K. (1988). p36, the major cytoplasmic substrate of src tyrosine protein kinase, binds to its p11 subunit via a short amino-terminal amphipathic helix. *EMBO J.* **7**, 2435-2442.
- Jost, M., Thiel, C., Weber, K. and Gerke, V. (1992). Mapping of three unique Ca^{2+} -binding sites in human annexin II. *Eur. J. Biochem.* **207**, 923-930.
- Jost, M., Weber, K. and Gerke, V. (1994). Annexin II contains two types of Ca^{2+} -binding sites. *Biochem. J.* **3**, 553-559.
- Kunkel, T. A. (1985). Rapid and efficient site-specific mutagenesis without phenotypic selection. *Proc. Nat. Acad. Sci. USA* **82**, 488-492.
- Laemmli, U. K. (1970). Cleavage of structural proteins during the assembly of the head of bacteriophage T4. *Nature* **227**, 680-685.
- Mayorga, L. S., Beron, W., Sarrouf, M. N., Colombo, M. I., Creutz, C. and Stahl, P. D. (1994). Calcium-dependent fusion among endosomes. *J. Biol. Chem.* **269**, 30927-30934.
- Moews, P. C. and Kretsinger, R. H. (1975). Refinement of the structure of carp muscle calcium-binding parvalbumin by model building and difference Fourier analysis. *J. Mol. Biol.* **91**, 6645-6653.
- Mu, F.-T., Callaghan, J. M., Steele-Mortimer, O., Stenmark, H., Parton, R. G., Campbell, P. L., McCluskey, J., Yeo, J.-P., Tock, E. P. C. and Toh, B.-H. (1995). EEA1, an early endosome-associated protein. *J. Biol. Chem.* **270**, 13503-13511.
- Nakata, T., Sobue, K. and Hirokawa, N. (1990). Conformational change and localization of calpactin I complex involved in exocytosis as revealed by quick-freeze, deep-etch electron microscopy and immunocytochemistry. *J. Cell Biol.* **110**, 13-25.
- Osborn, M., Johnsson, N., Wehland, J. and Weber, K. (1988). The submembraneous location of p11 and its interaction with the p36 substrate of pp60 src kinase in situ. *Exp. Cell Res.* **175**, 81-96.
- Raynal, P. and Pollard, H. B. (1994). Annexins: the problem of assessing the biological role for a gene family of multifunctional calcium- and phospholipid-binding proteins. *Biochim. Biophys. Acta* **1197**, 63-93.
- Sanger, F., Nicklen, S. and Coulson, A. R. (1977). DNA-sequencing with chain-terminating inhibitors. *Proc. Nat. Acad. Sci. USA* **74**, 5463-5467.
- Sarafian, T., Pradel, L. A., Henry, J. P., Aunis, D. and Bader, M. F. (1991). The participation of annexin II (calpactin I) in calcium-evoked exocytosis requires protein kinase C. *J. Cell Biol.* **114**, 1135-1147.
- Swairjo, M. A. and Seaton, B. A. (1994). Annexin structure and membrane interactions: a molecular perspective. *Annu. Rev. Biophys. Biomol. Struct.* **23**, 193-213.
- Thiel, C., Weber, K. and Gerke, V. (1991). Characterization of a discontinuous epitope on annexin II by site-directed mutagenesis. *FEBS Lett.* **285**, 59-62.
- Thiel, C., Osborn, M. and Gerke, V. (1992). The tight association of the tyrosine kinase substrate annexin II with the submembraneous cytoskeleton depends on intact p11- and Ca^{2+} -binding sites. *J. Cell Sci.* **103**, 733-742.
- Towbin, H., Staehelin, T. and Gordon, J. (1979). Electrophoretic transfer of proteins from polyacrylamide gels to nitrocellulose sheets: procedure and some applications. *Proc. Nat. Acad. Sci. USA* **76**, 4350-4354.
- Weber, K. (1992). Annexin II: interaction with p11. In *The Annexins* (ed. S. E. Moss), pp. 61-68. Portland Press, London.
- Weng, X., Luecke, H., Song, I. S., Kang, D. S., Kim, S. H. and Huber, R. (1993). Crystal structure of human annexin I at 2.5 Å resolution. *Protein Sci.* **2**, 448-458.
- Wessel, D. and Flügge, U. J. (1984). A method for the quantitative recovery of proteins in dilute solution in the presence of detergents and lipids. *Anal. Biochem.* **138**, 141-143.

Structural and functional characterization of recombinant mouse annexin A11: influence of calcium binding

Emilio LECONA*, Javier TURNAY*, Nieves OLMO*, Ana GUZMÁN-ARÁNGUEZ*, Reginald O. MORGAN†, Maria-Pilar FERNÁNDEZ† and M^a Antonia LIZARBE*¹

*Departamento de Bioquímica y Biología Molecular, Facultad de Ciencias Químicas, Universidad Complutense, 28040 Madrid, Spain, and †Departamento de Bioquímica y Biología Molecular, Facultad de Medicina, Universidad de Oviedo, 33006 Oviedo, Spain

Annexin A11 is one of the 12 vertebrate subfamilies in the annexin superfamily of calcium/phospholipid-binding proteins, distinguishable by long, non-homologous N-termini rich in proline, glycine and tyrosine residues. As there is negligible structural information concerning this annexin subfamily apart from primary sequence data, we have cloned, expressed and purified recombinant mouse annexin A11 to investigate its structural and functional properties. CD spectroscopy reveals two main secondary-structure contributions, α -helix and random coil (approx. 30 % each), corresponding mainly to the annexin C-terminal tetrad and the N-terminus respectively. On calcium binding, an increase in α -helix and a decrease in random coil are detected. Fluorescence spectroscopy reveals that its only tryptophan residue, located at the N-terminus, is completely exposed to the solvent; calcium binding promotes a change in tertiary structure, which does not affect this tryptophan residue but involves the movement of approximately four tyrosine residues to a more hydrophobic environment. These calcium-

induced structural changes produce a significant thermal stabilization, with an increase of approx. 14 °C in the melting temperature. Annexin A11 binds to acidic phospholipids and to phosphatidylethanolamine in the presence of calcium; weaker calcium-independent binding to phosphatidylserine, phosphatidic acid and phosphatidylethanolamine was also observed. The calcium-dependent binding to phosphatidylserine is accompanied by an increase in α -helix and a decrease in random-coil contents, with translocation of the tryptophan residue towards a more hydrophobic environment. This protein induces vesicle aggregation but requires non-physiological calcium concentrations *in vitro*. A three-dimensional model, consistent with these data, was generated to conceptualize annexin A11 structure–function relationships.

Key words: calcium binding, CD spectroscopy, fluorescence spectroscopy, phospholipid binding, thermal stability.

INTRODUCTION

The annexin gene family comprises calcium-binding proteins with a unique ancestry, a tetrad structure of homologous internal repeats, and the common property of reversible binding to acidic phospholipid-rich membranes in the presence of this cation (see [1–3] for reviews), although some protein members lack the requisite consensus for high-affinity type II calcium-binding sites [4]. The annexin core structure is composed of four (eight in annexin A6) homologous domains of approx. 68 amino acids, universally conserved throughout annexin evolution [5,6]. In contrast, the N-terminal region shows greater variability in length and amino acid sequence [1,3]. Since the solution of the annexin A5 crystal structure [7], several other annexins have been crystallized; all of them display a protein core resembling a slightly curved disc in which the four repeated domains arrange around a central hydrophilic pore. Each domain comprises a folded leaf α -helix bundle (helices A, B, D and E) organized as anti-parallel cylinders capped by a fifth α -helix (helix C). The interaction with membranes takes place on the convex side of the molecule where the principal calcium-binding sites are located. Calcium binding is established with carbonyl oxygen atoms in the loop connecting helices A and B, and with a bidentate carbonyl group from glutamic or aspartic residues located in the loop connecting helices D and E, approx. 38 residues downstream

in each repeat. The N-terminal region connects domains I and IV in annexins with a short N-terminus, such as annexin A5, and is located in the concave region of the molecule, opposite to the calcium-binding sites [7]. Rosengarth et al. [8] have solved the X-ray structure of full-length annexin A1 in the absence of calcium, showing that the N-terminus interacts with domain III through an amphipathic α -helix present in the N-terminal domain replacing helix 3D.

The structural characteristics of annexins, especially A1, A2 and A5, have been extensively analysed [7–12]. However, knowledge is more limited for other members of this family, and is unavailable for annexin A11 which has an unusual N-terminus. The core domain of annexin A11 shows the highest similarity to all other human annexins [13,14] and its evolutionary origin lies near the root of this family tree [6,15], beginning with the sequential duplication of annexin A13 to annexins A7 and A11 around the emergence of chordates [16,17]. All these observations support the view of annexin A11 as a structural prototype, founding member and key functional model of chordate annexins.

Several functions have been described for annexins *in vitro*, including anti-coagulatory and anti-inflammatory activities and involvement in signal transduction, membrane fusion, endo- and exocytosis as well as calcium-channel regulation. However, little is known about their physiological role *in vivo* [1,3]. Despite their gross structural similarity, annexins have diverged

Abbreviations used: CCA, convex constraint algorithm; DTT, dithiothreitol; IPTG, isopropyl β -D-thiogalactoside; Ni-NTA, Ni²⁺-nitrilotriacetate; PA, phosphatidic acid; PC, phosphatidylcholine; PE, phosphatidylethanolamine; PG, phosphatidylglycerol; PS, phosphatidylserine; rTEV, recombinant tobacco etch virus.

¹ To whom correspondence should be addressed (e-mail lizarbe@bbm1.ucm.es).

significantly in terms of their gene regulation, tissue-specific expression patterns, subcellular localization of different isoforms and features peculiar to individual subfamilies [16,18–20]. Moreover, self-association, heterologous annexin interactions and the interaction with other proteins have been described to act as regulatory mechanisms for the function of some of these proteins [1–3].

The main structural differences among metazoan annexins appear in the non-homologous N-terminal extension, so the structural analysis of annexin A11 could reveal some features relevant to its functional specificity. This annexin possesses an extensive N-terminal region, rich in proline, glycine and tyrosine residues [21,22]. Although several studies have pointed out various functional properties of annexin A11, including its possible role in insulin secretion [23], structural data are limited to the primary structure. The N-terminal region of annexin A11 has been proposed to be responsible for its autoantigenicity [24], nuclear localization [25] and tyrosine phosphorylation [26]. Moreover, the interaction with calyculin (S100A6) is established through amino acids 45–62 [27], analogous to that described for annexins A1 and A2 with other S100 proteins, namely S100A11 and S100A10, or for p53 with S100B [28–30]. Annexin A11 also binds, through the N-terminus, to the penta-EF-hand family proteins *ALG-2* (apoptosis-linked gene-2) [31] and *sorcin* [32].

According to all these observations, annexin A11 is probably involved in several biological processes and its N-terminal region participates prominently in most of them. The aim of the present study is to perform a structural characterization of recombinant annexin A11 to allow a better understanding of the biological role of this protein. We have analysed some of the changes that take place on calcium binding as this is a key aspect of its functionality. We also studied the binding of annexin A11 to different phospholipid vesicles, as well as the consequent structural changes, to gain insight into the interaction of this protein with biological membranes, as this process may differ from other annexins due to its distinctive N-terminus.

EXPERIMENTAL

Construction of expression vectors

The mouse annexin cDNA was cloned previously (U65986) [14]. The 2.4 kb clone containing the full-length cDNA sequence was used as a template to isolate the coding portion of mouse annexin A11 by PCR. Oligonucleotide primers, 23 bp long, were synthesized according to the published sequence for both ends of the coding cDNA. The oligonucleotide sequences created *NcoI* and *EcoRI* restriction sites to facilitate the insertion of coding cDNA into either expression plasmid pPROEX-HTb (Life Technologies, Prat de Llobregat, Spain) or pTrc99A (AP Biotech, Cerdanyola, Spain). The identities of the final constructs pHisA11M and pTrcA11M were verified by restriction digestion and DNA sequencing.

Protein expression and purification

JA221 *Escherichia coli* cells were transformed with the annexin A11 expression constructs pTrcA11M or pHisA11M. Cells were grown at 37 °C in Luria–Bertani medium containing 100 µg/ml ampicillin until the cultures reached A_{600} 0.5. Recombinant protein expression was induced by the addition of 1 mM isopropyl β -D-thiogalactoside (IPTG) for different incubation times (1–16 h) and at temperatures over the range 25–37 °C. The protein expression of total cell homogenates was analysed by SDS/PAGE and then by

Coomassie Blue staining or Western blotting. Optimal conditions for the induction of the expression of recombinant annexin A11 in both cases were 4 h in the presence of 1 mM IPTG at 25 °C.

Spectroscopic characterization was performed using recombinant annexin A11 produced in bacteria transformed with the construction pHisA11M under the optimal expression conditions described above. Cells were collected after induction with IPTG by centrifugation at 6000 g for 15 min and resuspended in 50 mM Tris (pH 8.0), containing 0.1 M NaCl, 2.5 mM EGTA, 2 mM PMSF and 1 mM dithiothreitol (DTT), and ruptured by sonication cycles at 4 °C. After stirring for 90 min at 4 °C, the homogenate was centrifuged at 27000 g for 90 min at 4 °C. The supernatant was loaded on to a Ni²⁺-nitrilotriacetate (Ni-NTA)–agarose column, washed with buffer A [50 mM Tris (pH 8.0)/0.1 M NaCl/1.5 mM 2-mercaptoethanol] containing 20 mM imidazole. The recombinant protein was eluted with a linear gradient of buffer A containing 20–250 mM imidazole, and dialysed against 50 mM Tris (pH 8.0), containing 0.1 M NaCl and 1 mM EGTA. After the addition of 1 mM DTT, the protein was digested with 10 units/ml recombinant tobacco etch virus (rTEV) protease (Life Technologies) at 4 °C for 20–22 h and dialysed against buffer B [50 mM Tris (pH 8.0)/0.1 M NaCl]. Digested annexin was separated from the undigested form and from the rTEV protease by an additional Ni-NTA–agarose affinity chromatography, taking advantage of the presence of a poly(His) tag in the latter molecules. Finally, annexin A11 was dialysed against buffer B containing 1 mM EGTA, to remove traces of Ni²⁺ that induce alterations in the UV–visible spectra, and then against buffer B without EGTA.

The identity of both digested and non-digested proteins was confirmed by amino acid analysis (Beckman 6300 amino acid analyser) as described previously [33], which also allowed the determination of protein concentration. The molar absorption coefficient at 280 nm was obtained from the UV–visible spectra, after subtraction of apparent absorption due to light scattering and determination of the protein concentration by amino acid analyses from aliquots taken directly from the cuvette.

CD measurements

CD spectra were recorded at 20 °C in a Jasco J-715 spectropolarimeter equipped with a Neslab RTE-111 thermostat. The far-UV CD spectra were monitored between 200 and 250 nm using thermostatically controlled cuvettes of 0.1 cm pathlength. Melting curves were determined by monitoring the ellipticity changes at 208 or 220 nm between 20 and 80 °C at 60 °C/h. All the samples were first dialysed against 20 mM Hepes (pH 8.0) and 0.1 M NaCl, to minimize pH changes during heating. To analyse the influence of calcium concentration on the far-UV spectrum and on the melting temperature (T_m), different protein samples from the same stock were prepared with increasing CaCl₂ concentrations up to 75 mM. Samples with equivalent maximal ionic strength, obtained by the addition of NaCl instead of CaCl₂, were used as the control. Far-UV spectra and melting temperatures were also registered for annexin A11 in the presence of 50 nm phosphatidylserine (PS) small unilamellar vesicles (molar ratio of PS/annexin A11 is 800:1), in the absence (1 mM EGTA) or presence of 200 µM CaCl₂.

All spectra were averaged over six scans (ten for annexin A11 in the presence of vesicles) and were corrected by subtracting buffer contribution (with or without PS vesicles) from parallel spectra in the absence of protein; units are always expressed as molar ellipticity/residue ($[\theta]_{MRW}$). Prediction of the secondary structure from the far-UV spectra was performed using the convex constraint algorithm (CCA) as described by Perczel et al. [34].

Fluorescence spectroscopy

Fluorescence emission spectra were recorded at 20 °C on an SLM Aminco 8000C spectrofluorimeter with excitation wavelengths of 275 nm (global emission) and 295 nm (tryptophan emission), and 4 nm excitation and emission bandwidths. The spectra were monitored between 295 and 400 nm for global emission or 305 and 400 nm for tryptophan emission, using a 0.4 cm excitation pathlength and 1.0 cm emission pathlength cuvette. Scattering was minimized by crossed Glan–Thompson polarizers. Titration of calcium influence at both excitation wavelengths was performed by sequential addition of CaCl_2 in the absence or presence of 50 nm PS vesicles (molar ratio of PS/annexin A11 is 800:1) and correcting the spectra for dilution. Acrylamide quenching of tryptophan fluorescence was measured using emission spectra exciting at 295 nm at increasing acrylamide concentration, taking into account the effects of dilution as described previously [9]. Care was taken to avoid the inner filter effect and the solutions presented always UV absorption at the excitation wavelength below 0.04. The Stern–Volmer quenching constant (K_{SV}) was calculated from the plot of F_0/F at 340 nm against acrylamide concentration, according to the equation $F_0/F = 1 + K_{SV}[Q]$, where F_0 is the fluorescence intensity at zero quencher concentration and F the intensity at a given quencher concentration ($[Q]$).

Tyrosine titration

Titration was performed by the addition of aliquots of 1 M NaOH to the protein sample in the absence or presence of 50 mM CaCl_2 , using a 1 cm pathlength cuvette. After each addition, the pH was measured in the cuvette with a microelectrode and the UV–visible absorption spectrum was recorded. Absorption at 295 nm due to tyrosinate was determined after subtraction of the apparent absorption due to light scattering and taking into account the dilution of the sample. The number of tyrosine residues titrated at each pH was calculated from the molar ratio [tyrosinate]/[annexin A11], and the plot of this value against pH renders the titration curve.

Binding to phospholipids and vesicle aggregation assays

Unilamellar vesicles of PS (Avanti Polar Lipids), phosphatidylcholine (PC), phosphatidylglycerol (PG), phosphatidic acid (PA) and phosphatidylethanolamine (PE) (all purchased from Sigma) were obtained by hydration of a thin film of dried phospholipids in 50 mM Tris (pH 8.0) containing 0.1 M NaCl, followed by sonication and extrusion through polycarbonate filters of either 100 or 400 nm (Lipex Biomembranes). PE vesicles were stabilized by the addition of PC (PE/PC in the ratio 4:1) to avoid artifacts due to the formation of hexagonal-phase structures in pure PE liposomes. Small unilamellar vesicles (50 nm) were prepared from freshly obtained 400 nm vesicles by further extrusion through 50 nm polycarbonate filters.

Purified annexin A11 and 400 nm vesicles were mixed in a lipid/protein constant molar ratio of 800:1 with variable calcium concentrations in 50 mM Tris (pH 8.0) and 0.1 M NaCl and kept at room temperature (20 °C) for 15 min. The final mixture (300 μl) was ultracentrifuged at 134000 g at 4 °C for 1 h (Airfuge Beckman); the pellet and the supernatant were separated and analysed by SDS/PAGE followed by silver nitrate staining or Western blotting. Under these experimental conditions, almost no sedimentation of free protein was detected in a phospholipid-free

control. Gels or films were scanned and densitometric analysis was performed, obtaining volumograms on a photodocumentation system obtained from UVItec (Cambridge, U.K.) and using the UVIBand V.97 software.

Vesicle aggregation was studied using 100 nm vesicles (obtained by extrusion through 100 nm polycarbonate filters; 0.1 mg/ml PS) in the presence of increasing annexin A11 concentrations at 25 °C and triggering the reaction by adding the corresponding volume from a concentrated CaCl_2 stock solution. Absorption at 360 nm was measured immediately after the addition of calcium in a thermostatically controlled cuvette for at least 10 min.

Other procedures

The isolation of chicken annexin A5 was performed as described previously [9,35]. SDS/PAGE was performed by the method of Laemmli [36]. Western blotting was performed as described previously [37] using either polyclonal anti-bovine annexin A11 antibodies (dilution 1:8000; kindly provided by Dr Hiroyoshi Hidaka, D. Western Therapeutics Institute, Nagoya, Japan) and a secondary antibody conjugated with horseradish peroxidase (Bio-Rad, Madrid, Spain), or using directly a monoclonal peroxidase-conjugated anti-poly(His) (Sigma). Polyclonal antibodies against recombinant mouse annexin A11 were raised in rabbit following standard methods. Annexin A11 concentration in pure preparations was determined from the UV–visible spectra, except for CD spectroscopy, where quantitative amino acid analysis was used. Regression fitting of the experimental data to different equations was performed using SigmaPlot software v.8.02 obtained from SPSS (Chicago, IL, U.S.A.).

RESULTS

Purification of recombinant mouse annexin A11

The expression of recombinant annexin A11 cloned in the vector pTrc99A is low in all the experimental conditions assayed; the protein is extensively degraded even at 25 °C and short induction times, and is mainly expressed in an insoluble form. On the other hand, the cloning of the protein in the vector pPROEX-HTb, which introduces a His tag in the N-terminus, allows a significantly greater expression and minimizes degradation. According to the Western blots, using antibodies against the wild-type protein or against the poly(His) tag (Figure 1A), the degradation of the protein takes place from the N-terminus. Moreover, the His tag enables easy purification of annexin A11 expressed in *E. coli* at 25 °C for 4 h.

Figures 1(B) and 1(C) show the electrophoretic and Western-blot analyses of samples from the main steps of the purification process. Bacteria were collected by centrifugation and homogenized in the presence of 2.5 mM EGTA to obviate interactions of the recombinant annexin with bacterial membrane phospholipids and 1 mM DTT to prevent incorrect disulphide bond formation. Centrifugation of the cell homogenate allows the separation of the soluble and insoluble fractions (Figures 1B and 1C, lanes j–l). Approx. 50% of the recombinant annexin A11 remains insoluble either in inclusion bodies or associated with the membrane fraction. After removing EGTA by dialysis, the soluble fraction was purified by affinity chromatography in Ni-NTA–agarose. Whereas bacterial proteins do not bind to Ni-NTA–agarose (Figures 1B and 1C, lane m), annexin A11 with the His tag elutes only in the presence of imidazole (Figures 1B and 1C, lane n). Removal of imidazole by dialysis in the absence

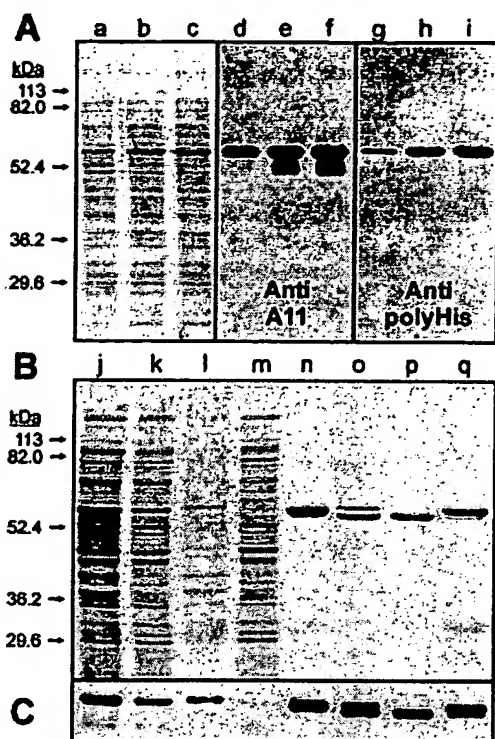


Figure 1 SDS/PAGE analysis of recombinant annexin A11 expression and purification

(A) Expression of annexin A11 was induced in exponentially growing JA221 cells by the addition of 1 mM IPTG and incubation at 25 °C for 4 h (lanes a, d and g), 6 h (lanes b, e and h) and 8 h (lanes c, f and i), and the expression was analysed by SDS/PAGE followed by Coomassie Blue staining (lanes a–c) and Western blotting using antibodies raised against either bovine annexin A11 (lanes d–f) or the poly(His) tag (lanes g–i). Purification of recombinant annexin A11 from bacterial cultures induced for 4 h with 1 mM IPTG at 25 °C was performed, followed by SDS/PAGE analysis and Coomassie Blue staining (B) and Western-blot analysis with anti-(annexin A11) antibodies (C). (B, C) Lane j, bacterial homogenate after protein expression induction; lanes k and l, supernatant and sediment respectively after centrifugation of the homogenized material in the presence of 2.5 mM EGTA; lane m, flow-through of the Ni-NTA chromatography; lane n, pool of fractions containing annexin A11; lane o, digestion of poly(His) tag containing annexin A11 with rTEV protease; lane p, purified digested annexin A11 without the poly(His) tag; lane q, material retained in the Ni-NTA-agarose chromatography after digestion with rTEV protease.

of bivalent-cation chelating agents induces the autoaggregation and precipitation of the protein containing the His tag; a similar process takes place if calcium is added to solutions of this protein. As this tag is likely to be involved in the autoaggregation of the protein, this extension was removed to perform the spectroscopic characterization of the protein. Digestion of the protein for 20 h at 4 °C in the presence of 10 units/ml rTEV protease yielded over 70% of digested protein (Figures 1B and 1C, lane o). Separation of the digested annexin A11 from the undigested protein and from the enzyme was achieved by a further chromatographic step in Ni-NTA-agarose; the protease and the undigested annexin A11 are bound to the resin, whereas the digested protein elutes in the flow-through (Figures 1B and 1C, lanes p and q).

Identity of the purified proteins was confirmed through amino acid analyses and antibodies against the recombinant protein recognized wild-type annexin A11 from cell extracts in the Western blot. The molar absorption coefficient ($51761 \text{ M}^{-1} \text{ cm}^{-1}$) was determined from the absorption spectrum in the UV-visible region after correction for apparent absorption and determination of protein concentration by amino acid analysis.

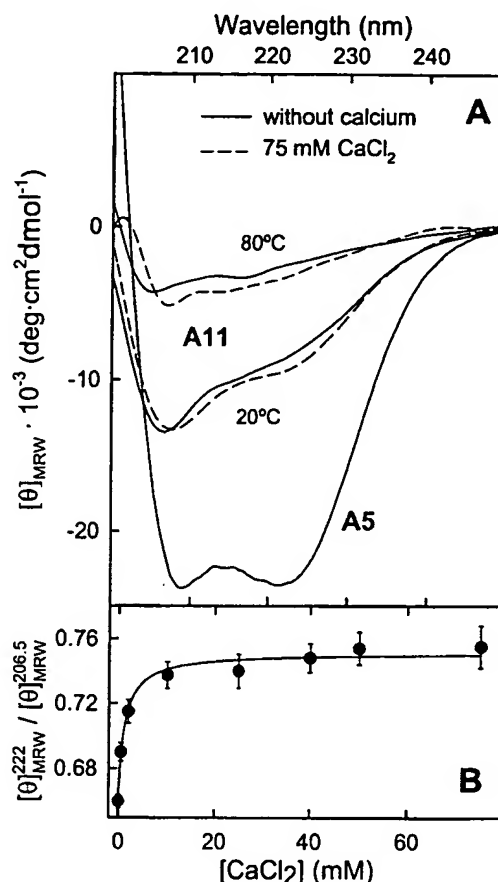


Figure 2 Far-UV CD spectra of annexin A11

(A) Representative far-UV CD spectra of annexin A11 without calcium (—) and in the presence of 75 mM CaCl_2 (---) at 20 and 80 °C are shown in comparison with that of chicken annexin A5 at 20 °C in the absence of calcium, and were registered in 50 mM Hepes (pH 8.0) and 0.1 M NaCl. (B) Variation in the ratio between molar ellipticities/residue at 222 and 206.5 nm with calcium concentration. Results are expressed as means \pm S.D. for at least three different spectra (each of them averaged over six scans).

CD analysis

The CD spectrum of annexin A11 in the far-UV region is shown in Figure 2(A) in comparison with the spectrum of chicken annexin A5 as reference. Annexin A11 in the absence of calcium presents a minimum at 206.5 nm with a molar ellipticity/residue of $-13440 \text{ degrees} \cdot \text{cm}^2 \cdot \text{dmol}^{-1}$. This spectrum differs significantly from that of annexin A5, which has a relatively short N-terminal extension of approx. 15 residues and whose spectrum in the absence of calcium presents two minima at 208 and 222 nm showing much higher negative molar ellipticities. The contribution of the different secondary-structure elements, calculated according to the CCA method, reveals that whereas annexin A5 possesses over 70% of α -helix, the main contributions to annexin A11 structure are α -helix (29%), random coil (31%) and β -turns (26%).

Calcium concentrations required for reproducing the annexin conformational rearrangements induced in the absence of phospholipids are almost three orders of magnitude higher than those required in their presence [1,2,10]. Hence, calcium concentrations in the millimolar range were used throughout these experiments. Addition of calcium to annexin A11 induces small but significant changes in the far-UV CD spectrum. Figure 2(A) also shows the spectrum of annexin A11 saturated

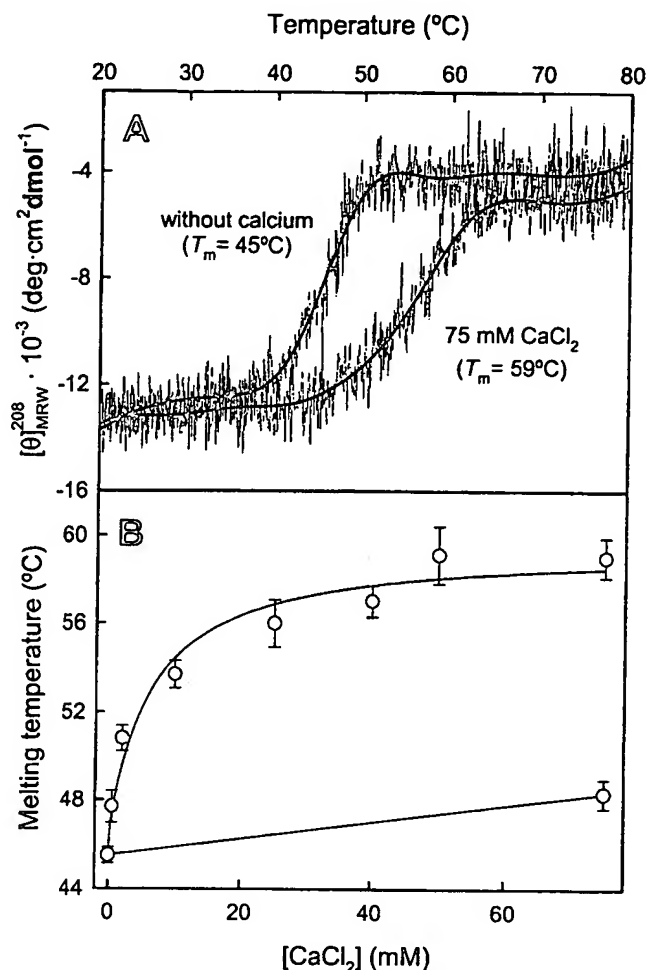


Figure 3 Influence of calcium binding on the thermal stability of annexin A11

(A) Melting curves of annexin A11 in the absence or in the presence of 75 mM CaCl_2 in 20 mM Hepes (pH 8.0) and 0.1 M NaCl. The original unsmoothed data are presented as thin lines together with the results from noise reduction using the Standard Analysis software obtained from Jasco. (B) Dependence of the melting temperature on CaCl_2 concentration (O) was analysed by determining T_m values at different calcium concentrations. Results represent the means \pm S.D. for at least two independent determinations at each CaCl_2 concentration. O \cdot , effect of an increase in ionic strength using an NaCl concentration equal to the highest CaCl_2 concentration.

with calcium (75 mM CaCl_2 ; molar ratio of calcium/protein is approx. 80000:1). These changes are not induced by the increase in the ionic strength of the solvent, since no changes in the spectrum are observed when NaCl concentration is increased up to 325 mM, equivalent to the presence of 75 mM CaCl_2 in a buffer containing 100 mM NaCl. Comparison of the spectra in the absence and presence of 75 mM CaCl_2 shows a shift in the minimum from 206.5 to 208 nm; this shift is already observed at 2 mM CaCl_2 and is maintained at higher calcium concentrations. Moreover, a gradual increase in the ratio between molar ellipticities at 222 and 206.5 nm is observed, showing a hyperbolic dependence with the calcium concentration (Figure 2B). These changes suggest a slight increase in α -helix content induced by calcium binding. In fact, CCA analysis of the spectrum at 75 mM calcium yields a 5% increase in the secondary structure (approx. 34%), with a parallel decrease in random coil (approx. 24%).

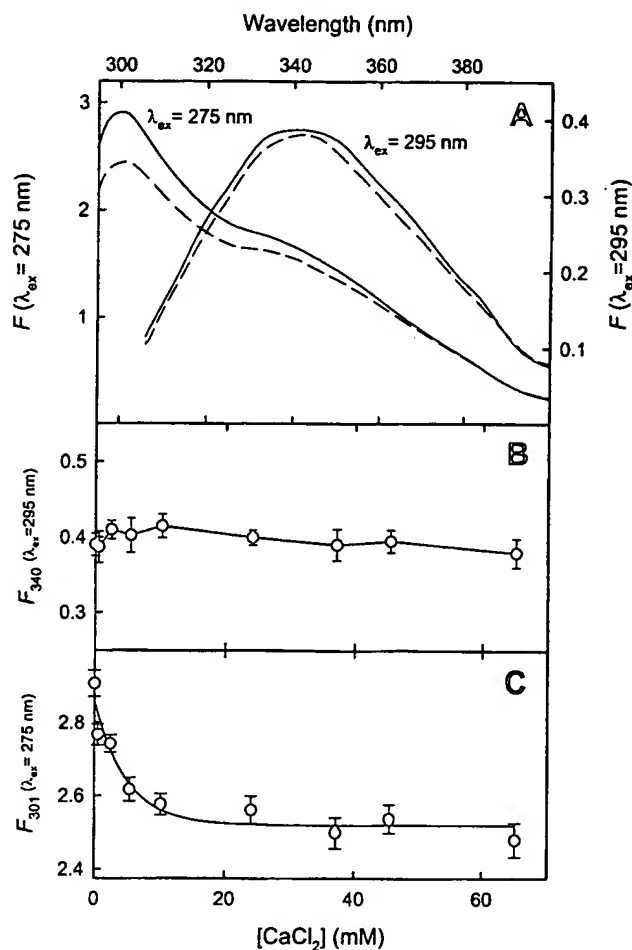


Figure 4 Fluorescence emission spectra of annexin A11 after calcium binding

(A) Emission spectra at excitation wavelengths of 275 and 295 nm in the absence of calcium (—) or presence of 75 mM CaCl_2 (---) were registered at 25 $^{\circ}\text{C}$ at 295–410 nm ($\lambda_{ex} = 275$ nm) or 305–410 nm ($\lambda_{ex} = 295$ nm). Fluorescence is expressed in arbitrary units; the scale for fluorescence emission at an excitation wavelength of 295 nm has been expanded (right axis). Variations in the fluorescence intensity in the emission maxima of tryptophan (340 nm, $\lambda_{ex} = 295$ nm) and tyrosine (301 nm, $\lambda_{ex} = 275$ nm) with calcium concentration have been plotted in (B) and (C) respectively.

Thermal stability

The stability of annexin A11 was analysed by monitoring the molar ellipticity at 208 nm as a function of temperature. In the absence of calcium, the melting curve shows a co-operative unfolding of the protein with a T_m of approx. 45 $^{\circ}\text{C}$ (Figure 3A). The binding of calcium by annexin A11 induces a highly significant increase in the thermal stability of the protein; in the presence of 75 mM CaCl_2 , there is an increase of approx. 14 $^{\circ}\text{C}$ in the T_m , with a slight loss of co-operativity (Figure 3A). The variation in the T_m with calcium concentration can be adjusted to a rectangular hyperbola, showing a midpoint effect at 6.3 mM (Figure 3B). Thermal stabilization induced by calcium is specific and is not due to alterations in the polarity of the solvent, as an increase in ionic strength with NaCl up to 325 mM induces only a slight increase in the T_m of approx. 2.8 $^{\circ}\text{C}$.

Fluorescence emission analysis

Figure 4(A) shows the fluorescence emission spectra of annexin A11 at excitation wavelengths of 275 and 295 nm in the absence

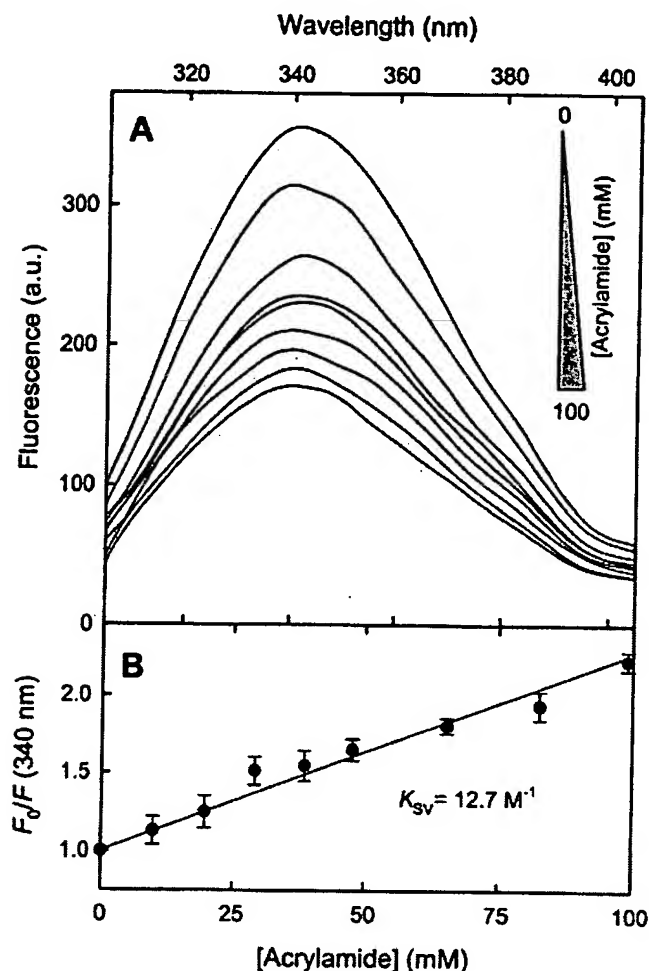


Figure 5 Acrylamide quenching of tryptophan emission

Fluorescence emission ($\lambda_{ex} = 295$ nm) at 20 °C of the unique tryptophan residue in annexin A11 was quenched by sequential addition of a concentrated acrylamide stock solution up to 100 mM. A representative experiment is shown in (A). Fluorescence intensities at 340 nm were plotted against acrylamide concentration and fitted to the Stern–Volmer equation (B). Results are expressed as means \pm S.D. for three independent experiments.

of calcium or in the presence of 75 mM CaCl_2 . The maximum in the fluorescence emission spectrum of the unique tryptophan residue of annexin A11 (Trp^{23}) appears at 340 nm and its position was not altered when calcium was added to the solvent, and no significant changes were observed in the quantum yield of this residue up to 75 mM CaCl_2 (Figure 4B). A maximum in the fluorescence emission spectrum at 301 nm is obtained using an excitation wavelength of 275 nm. This maximum is almost exclusively due to tyrosine residues and its position is not altered in the presence of calcium. However, as shown in Figure 4(C), a hyperbolic decrease of approx. 15% in the quantum yield of these residues is observed in a calcium concentration-dependent manner, showing a midpoint at 3.4 mM CaCl_2 , and this effect is almost saturated at concentrations higher than 20 mM.

Acrylamide quenching of tryptophan emission

To analyse the degree of exposure to the solvent of Trp^{23} , we have studied the effect of acrylamide on the fluorescence emission spectrum obtained at an excitation wavelength of 295 nm. Figure 5(A) shows the emission spectra of the tryptophan residue at increasing acrylamide concentrations up to 100 mM, which

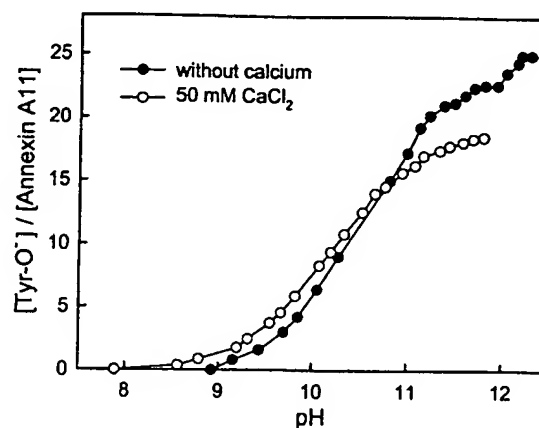


Figure 6 Tyrosine titration of annexin A11

Annexin A11 tyrosine titration was performed by sequential addition of aliquots of 1 M NaOH to a protein sample in 50 mM Tris (pH 8.0) and 0.1 M NaCl and by registration of UV–visible absorption spectra. The number of titrated tyrosine residues was calculated from the variation in absorbance at 295 nm (due to tyrosinate (Tyr-O^-)) relative to protein concentration, either in the absence of calcium (\bullet) or with 50 mM CaCl_2 (\circ).

does not induce artifacts due to the internal filter effect. A gradual decrease in the emission intensity is induced by the quencher without modification in the position of the maximum. Consequently, the tryptophan residue is accessible to acrylamide and must be at least partially exposed. The Stern–Volmer analysis of the variation in the emission intensity at 340 nm as a function of acrylamide concentration is shown in Figure 5(B); the quenching constant calculated from this plot is 12.7 M^{-1} .

Tyrosine titration

Tyrosine titration was achieved by registration of the UV–visible spectra of the recombinant annexin A11, in the absence or presence of 50 mM CaCl_2 , at increasing pH by the addition of NaOH. At this calcium concentration, binding in the absence of phospholipids should be saturated. Appearance of tyrosinate (Tyr-O^-) residues was followed at 295 nm.

Titration in the absence of calcium distinguishes two main populations of tyrosine residues: buried tyrosine residues with a pK_a of approx. 12 and tyrosine residues, which are at least partially exposed, with a pK_a of approx. 10.5; an additional subpopulation of partially exposed tyrosine residues can also be suggested with a pK_a of 11.6 (Figure 6). Under these conditions, 23 of the 25 tyrosine residues are at least partially exposed. After the addition of 50 mM CaCl_2 , only 19 of the total 25 tyrosine residues of the protein remain exposed. It was not possible to titrate the buried tyrosine residues because protein aggregates at pH higher than 11.9 in the presence of calcium.

Phospholipid binding and vesicle aggregation

We have analysed the interaction of recombinant annexin A11 with phospholipid vesicles (400 nm) by ultracentrifugation and electrophoretic analysis of the supernatants and pellets either in the absence (1 mM EGTA) or presence of 500 μM CaCl_2 . Figure 7 shows the result of the analysis using liposomes composed of acidic (PA, PS or PG) and neutral (PC or PE/PC in the ratio 4 : 1) phospholipids. Our results suggest that recombinant annexin A11 is not capable of interacting with PC vesicles in the presence or absence of calcium. However, it is capable of

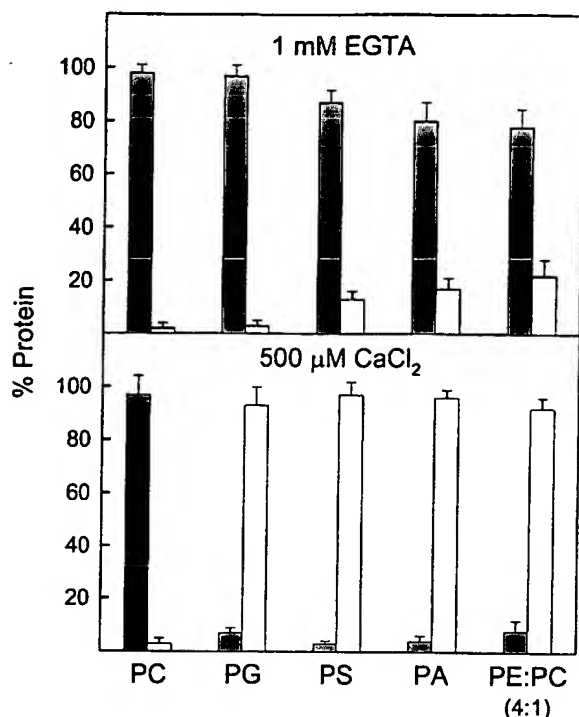


Figure 7 Binding of annexin A11 to phospholipid vesicles

The binding of annexin A11 to 400 nm vesicles with different phospholipid compositions [PC, PG, PS, PA or PE/PC in the ratio 4:1] was performed by ultracentrifugation in the absence of calcium (1 mM EGTA) or in the presence of 500 μM CaCl₂ and using a lipid/protein molar ratio of 800:1. The percentage of annexin A11 in the pellets (white bars) and in the supernatants (black bars) was analysed by SDS/PAGE followed by Western-blot analysis using anti-(annexin A11) antibodies and densitometry of the films.

interacting with the neutral phospholipid PE, and with PA, PS and PG, in the presence of 500 μM CaCl₂. Furthermore, we have found that annexin A11 interacts in a calcium-independent manner, although to a lower extent, with PE (approx. 22%) and that there is a certain degree of calcium-independent interaction with PA (approx. 17%) and PS (approx. 15%).

A more detailed analysis of the calcium dependence in the interaction of annexin A11 with PS vesicles is shown in Figure 8(A). Approx. 15% of annexin A11 binds to the vesicles in the absence of calcium, and the bound protein percentage follows a hyperbolic dependence on calcium concentration. At 28 μM CaCl₂, 50% of the total binding to PS vesicles was achieved. Additionally, annexin A11 induces aggregation of PA vesicles at 500 μM CaCl₂, but does not induce PS vesicle aggregation at calcium concentrations lower than 1 mM, even at high protein concentrations. Figure 8(B) shows that no aggregation is found at 500 μM CaCl₂ using a relatively high annexin A11 concentration (110 nM). At 1 mM CaCl₂, slow vesicle aggregation is observed in the absence of annexin, but addition of the protein speeds up this process in a concentration-dependent manner, from 5.5 to 110 nM (Figure 8B).

Spectroscopic analysis of annexin A11 in the presence of phospholipid vesicles

We have analysed the possible conformational changes in annexin A11 after its binding to PS vesicles using CD spectroscopy in the far-UV region (Figure 9A). The addition of PS vesicles (50 nm) in the presence of 1 mM EGTA induces a slight modification of

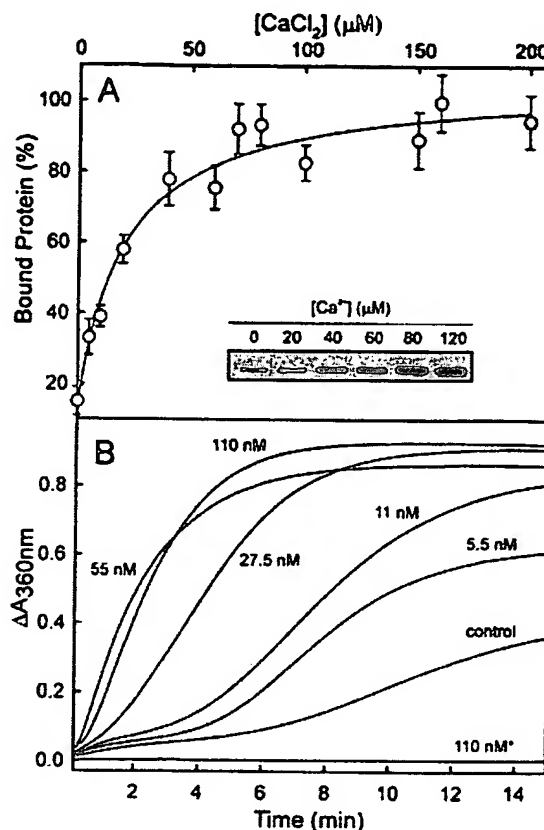


Figure 8 Calcium-dependent aggregation and binding of annexin A11 to PS vesicles

(A) Annexin A11 was mixed with PS vesicles (400 nm) at a lipid/protein molar ratio of 800:1 in the presence of increasing calcium concentrations. Quantification of the percentage of bound protein was done by ultracentrifugation and SDS/PAGE analysis of the pellets and supernatants, followed either by silver nitrate staining or by immunodetection of annexin A11. The inset shows a representative experiment analysed by Western blot. (B) Annexin A11-induced aggregation of PS vesicles (100 nm; 0.1 mg/ml) was followed by monitoring the changes in absorbance at 360 nm at 25 °C after the addition of 1 mM CaCl₂. The different protein concentrations are indicated (5.5–110 nM). The self-aggregation of PS vesicles in the presence of 1 mM CaCl₂ (control) is also shown. No vesicle aggregation was observed in the presence of 500 μM CaCl₂ even at 110 nM protein concentration indicated by an asterisk.

the spectrum, which mainly affects the region between 200 and 210 nm probably due to light-scattering effects. When 200 μM CaCl₂ is added to the mixture, a concentration high enough to induce an almost total binding of annexin A11 to PS vesicles, a more significant change is observed in the spectrum with a less negative minimum at 208 nm and an increase in the negative ellipticity at 222 nm. These changes are consistent with an increase in the α -helical content (approx. 9% according to CCA analysis) and a parallel decrease in the random-coil structure. The CD spectrum of annexin A11 with PC vesicles does not change after the addition of calcium and is almost identical with that obtained with PS in the absence of calcium (results not shown).

The influence of phospholipid vesicles, in the absence or presence of calcium, on the thermal stability of annexin A11 has been analysed by monitoring the changes in molar ellipticity at 220 nm to avoid light-scattering artifacts (Figure 9B). In the absence of vesicles, the T_m of annexin A11 is 45 °C as described above at 208 nm (Figures 3A and 9B). The addition of PS in the absence of calcium does not change this value but involves a loss of co-operativity and a modification in the final state at 80 °C. On the other hand, addition of calcium to a final concentration

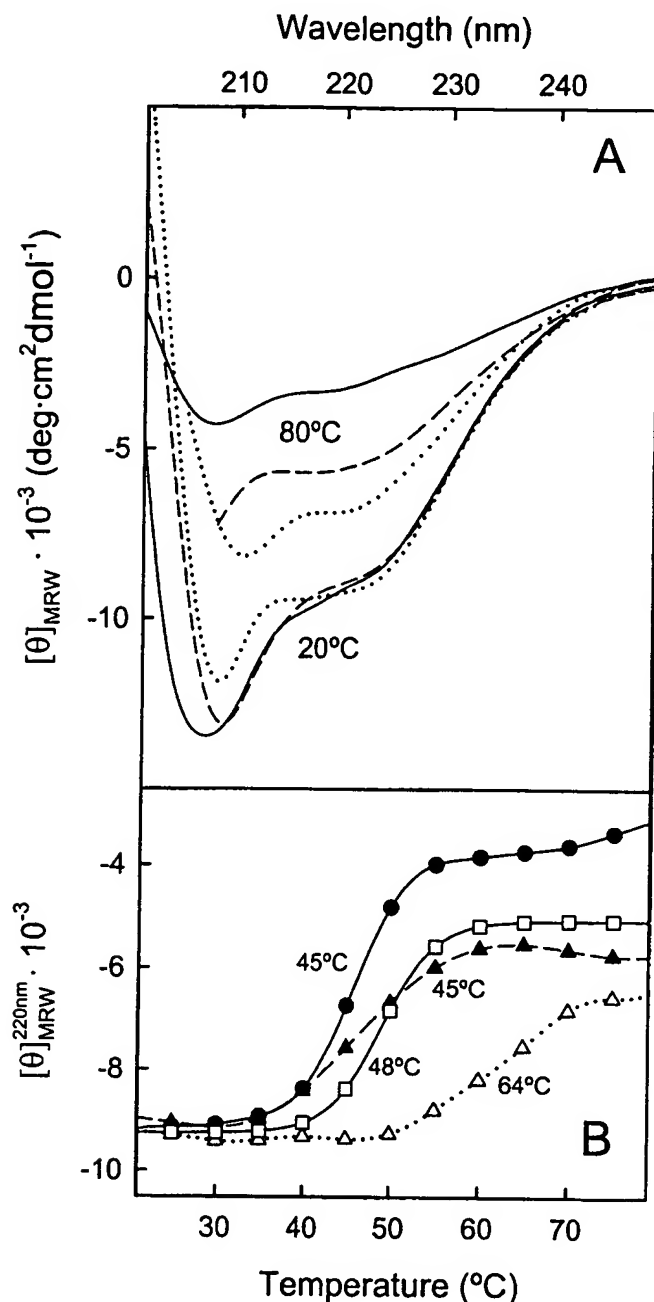


Figure 9 CD analysis of the interaction of PS vesicles with annexin A11

(A) Representative far-UV CD spectra of annexin A11 (0.12 mg/ml) in the absence (—) or presence of PS vesicles (molar ratio of lipid/protein is 800:1) either without (1 mM EGTA; ---) or with 200 μM CaCl_2 (· · · · ·) at 20 and 80 °C. Spectra of annexin A11 with PC vesicles either in the absence or presence of calcium are not shown, as they are almost identical with those with PS vesicles in the presence of 1 mM EGTA. (B) Annexin A11 melting curves in the absence (1 mM EGTA; ●) or presence of PS vesicles without (▲) or with 200 μM CaCl_2 (△) as well as in the presence of PC vesicles and 200 μM CaCl_2 (□). Molar ellipticity/residue was registered at 220 nm; noise reduction was performed using the Standard Analysis software. Melting temperatures determined from the maximum of the first derivative of each curve are also shown.

of 200 μM increases the T_m up to 64 °C; this process is less co-operative and the final denatured state is different. When this analysis is performed under the same experimental conditions but using PC vesicles in the presence of 200 μM CaCl_2 , only a slight increase in the T_m (approx. 3 °C) is observed.

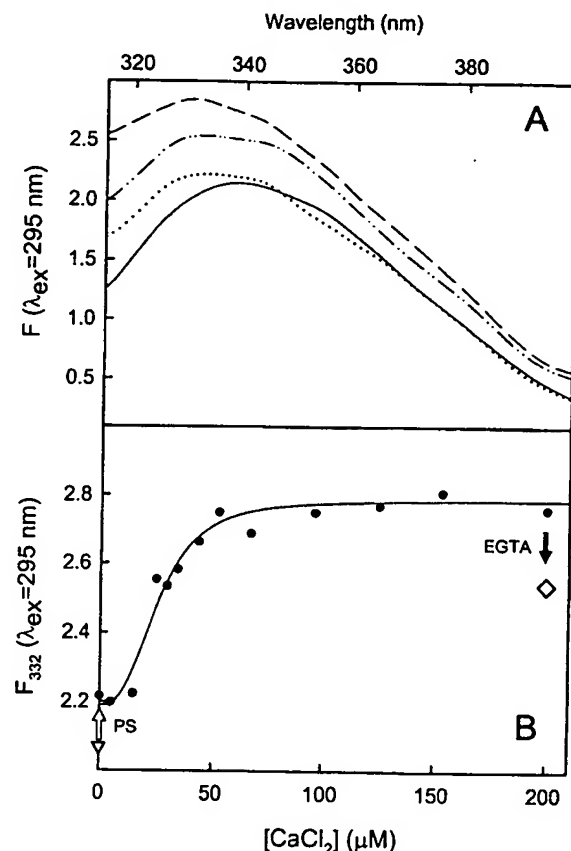


Figure 10 Analysis of the tryptophan fluorescence emission spectra after the binding of annexin A11 to PS vesicles

(A) Emission spectra at the excitation wavelength of 295 nm in the absence (—) or presence of PS vesicles without (1 mM EGTA) (· · · · ·) and with 200 μM CaCl_2 (---); - - - - shows the spectra after the addition of EGTA (1 mM final concentration) to the sample with 200 μM CaCl_2 . All spectra were recorded at 20 °C from 305 to 400 nm. (B) Effect of increasing calcium concentration on annexin A11 tryptophan fluorescence intensity at 332 nm in the presence of PS vesicles (●). The fluorescence intensities at 332 nm in the absence of PS vesicles and calcium (▽) and after the addition of PS vesicles (white arrow) and 200 μM CaCl_2 , followed by addition of EGTA at 1 mM final concentration (black arrow, ◇) are shown.

When annexin A11 is thermally denatured in the absence of phospholipid vesicles, macroscopic aggregation of the protein is observed. However, this process is prevented in the presence of vesicles with or without calcium. Thus the spectra of the denatured protein significantly differ and some secondary structure remains mainly in the presence of calcium and PS, as shown in Figure 9(A).

Fluorescence emission spectra of annexin A11 at an excitation wavelength of 295 nm are shown in Figure 10(A) in the absence or presence of PS vesicles and without (1 mM EGTA) or with 200 μM CaCl_2 . Addition of vesicles to annexin A11 induces a shift in the position of the emission maximum from approx. 340 to 332 nm. Addition of calcium does not modify this wavelength but increases the tryptophan quantum yield. The variation in fluorescence intensity at 332 nm with calcium concentration shows a midpoint effect at 25 μM CaCl_2 (Figure 10B). In Figure 10(B), the inverted triangle indicates the emission intensity in the absence of phospholipids (lower due to the maximum position shift), and the diamond indicates the decrease in intensity achieved by the addition of EGTA (1 mM final concentration) to the sample with PS vesicles and 200 μM CaCl_2 . The changes

in the fluorescence emission spectrum are not fully reversible after removal of calcium, as the tryptophan maximum remains at 332 nm and only a slight decrease in the quantum yield is observed.

Structural model

The sequence and deduced secondary structure of annexin A11 were expanded into a multiple-sequence alignment to facilitate comparative and evolutionary studies, and a virtual three-dimensional model was created by sequence-threading through the crystallography coordinates of known annexin structures. Annexin A11 homologues, identified in 20 vertebrate species, are represented by the mammal, bird, amphibian and fish proteins aligned in Figure 11(A). The greater sequence variability, alignment gaps and unique amino acid composition of the N-termini are evident, with an increased percentage of proline (28%), glycine (20%) and tyrosine (9%) and a tryptophan residue (Trp²³), which contrast with conserved type II calcium-binding sites and congruent structures of the tetrad core, in spite of the evolutionary distances between these species. Secondary-structure predictions (<http://www.expasy.org>) determined that the N-terminus would be expected to adopt a random-coil conformation except for one short α -helical segment ('h' strings in Figure 11A), whereas each tetrad core repeat contains the five α -helices common to other annexins. The observation that the 12 paralogous human annexins exhibit only 45–55% amino acid identity suggested that subfamily differences might be accounted for by variable sites non-critical for function as well as by synaptomorphic sites under functional constraint acting as determinants of subfamily specificity. Although annexin A11 was an ancestral progenitor of other paralogous annexins and thus shares many features in common [16], we sought to identify sites uniquely conserved among annexin A11 members. The DIVERGE v1.04 program from Gu [38] (available at <http://www.phyba.iastate.edu/>) computed 'evolutionary impact' values for each residue in a global sequence alignment and identified Cys²²⁴ and Cys⁴⁰⁹ as structurally relevant differences from other annexins with high divergence impact that implied functional specificity for annexin A11. Together with four other cysteine residues common to other annexins, these may contribute additional structural stability and redox susceptibility to annexin A11 members.

A three-dimensional model of annexin A11 was generated using the DeepView/Swiss-PdbViewer v3.7 computer program [39] and the Swiss-Model server (<http://www.expasy.org/>). These utilized public X-ray crystallography data [40] for full-length pig annexin A1 and human and rat annexin A5 (Protein Data Bank entries 1MCX, 1ANX and 1A8A) in the 'high-calcium' form to thread the mouse annexin A11 amino acid sequence into a three-dimensional model for the homologous tetrad core region (Figure 11B). This representation serves to illustrate the spatial proximity between residues and domains that might otherwise appear distant in sequence alignment format. Thus the residues involved in the type II calcium binding to phospholipids (mkGxGT-38aa-D/E) appear co-ordinated on the external convex surface of the molecule near Cys⁴⁰⁹, whereas the N-terminus (where Trp²³ is located) is orientated towards the opposite, concave (cytosolic) side of the molecule. DeepView program identified four tyrosine residues classified as not exposed to the solvent and within potentially buried α -helical coils: Tyr³¹² and Tyr⁴⁷¹ (<1% exposure); Tyr⁴⁹¹ (<2%); and Tyr³⁹⁶ (<4%) (Figure 11A). Thus it is highly probable that these residues are among those showing a higher pK_a value in the tyrosine titration in the presence of calcium. The other five core tyrosine residues were

predicted to be exposed (24–28% exposure). When the three-dimensional model of annexin A11 was obtained by comparison with the only known annexin X-ray structure in the absence of calcium (full-length pig annexin A1; PDB entry 1HM6), only Tyr³¹² and Tyr⁴⁷¹ were predicted to be completely buried (<1% exposure); Tyr⁴⁹¹ and Tyr³⁹⁶ present approx. 10 and 15% exposure respectively. The interchangeability of Tyr and Phe at certain positions between fish and higher vertebrates suggests the functional importance of bulky and/or hydrophobic residues at these positions relative to the interloop calcium-binding ligands. This model is consistent with our experimental findings and testifies to the structural relevance of uncharged cysteine and tyrosine residues to annexin function.

DISCUSSION

The eukaryotic annexin superfamily has been widely studied since the identification of its first members 25 years ago. The resolution of the crystal structure of some of these proteins with a short or truncated N-terminal extension [7,41–43] has provided a detailed structural knowledge of the core domain and the effects of calcium binding on this structure. However, the structural diversity of N-termini and the disparate functions assigned to these proteins emphasize the significant contribution of this distinctive extension to the functional divergence of animal annexins. The N-terminus is therefore considered to be a specific regulatory domain of annexins [1–3], although its structure and relationship with the core domain still remain poorly understood. Whereas the 314-amino-acid tetrad core region of annexin A11 is highly conserved, its extensive N-terminal region varies in length among vertebrate members (171–221 residues) and presents a high content of proline, glycine and tyrosine residues [21,22]. These unusual features aroused our interest in performing a structural study of annexin A11.

Annexin A11 has been isolated previously from bovine and rabbit lung [22,44] or as a fusion protein with glutathione S-transferase or with the mannose-binding protein [27,31]. However, to perform a spectroscopic characterization, the protein should be similar to the wild-type form and relatively large amounts of purified protein were required. We achieved a high yield in the expression of soluble annexin A11 in *E. coli* by the addition of a His tag, even though approx. 50% of the protein remains insoluble in the cell homogenate. This insertion also minimizes the extent of degradation and simplifies the purification process via affinity chromatography, which further removes N-terminally degraded forms. The requirement for chelating agents to prevent precipitation when imidazole is removed after the chromatography points out that the His tag is capable of inducing autoaggregation of annexin A11, acting as a bridge between different molecules in the presence of cations such as Ni²⁺ or Ca²⁺. Although the addition of calcium induces aggregation of the protein containing the His tag, this does not occur when the tag is removed. The use of reducing agents throughout the purification procedure prevents the oxidation of the redox-sensitive free cysteine residues that seem to be important for annexin A11 function, as mentioned above. Recombinant annexin A11 was obtained with only small modifications from the wild-type, a change in position 2 from Ser to Gly and the addition of Gly-Ala at the N-terminus, which are not likely to have any effect on the structure or functional properties of annexin A11.

The main secondary-structure element present in the highly conserved annexin core is the α -helix [7–10]. Accordingly, the CCA analysis of the CD spectrum of annexin A5, which possesses a very short N-terminus of 15 amino acid residues and whose

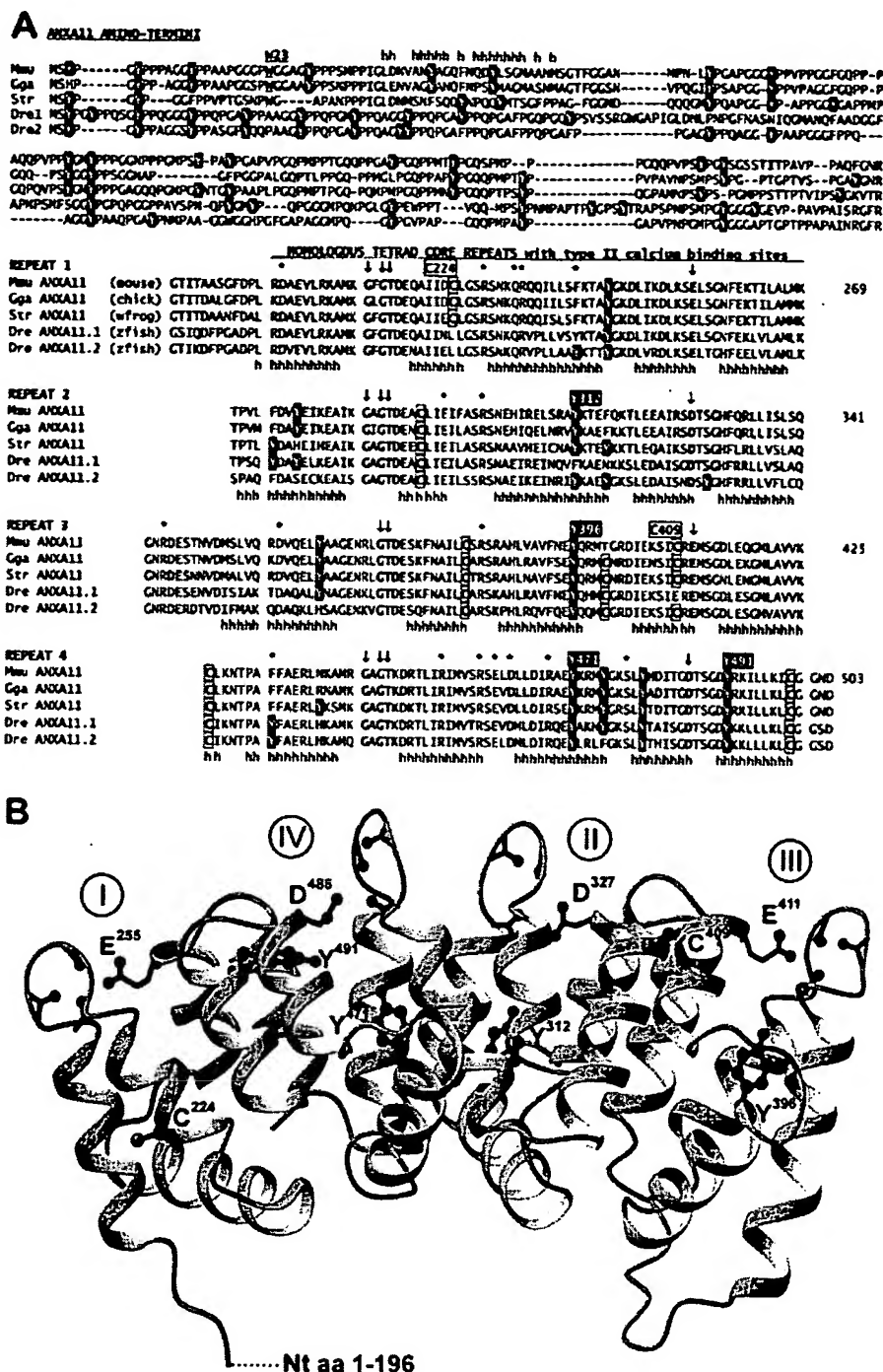


Figure 11 Annexin A11 sequence alignment and three-dimensional model

(A) Amino acid sequence alignment of annexin A11 from species representing mammal (Mmu, mouse, *Mus musculus*), bird (Gga, chicken, *Gallus gallus*), amphibian (Str, western clawed frog, *Silurana tropicalis*) and fish duplicate genes (Dre, zebrafish, *Danio rerio*). The N-termini (top panels) contain Trp²³ and increased proline, glycine and tyrosine content, whereas the four homologous repeats of the tetrad core region below identify conserved cysteine residues (boxed), tyrosine residues (reverse-shaded), type II calcium-binding motifs 'mkGxG-38aa-D/E' (beneath arrows) and residues highly preserved in all annexins (indicated by asterisks). The 'h' clusters in each repeat correspond to the five α -helical loops A, B, C, D and E. (B) A three-dimensional protein model of the homologous tetrad core of mouse annexin A11 was derived by sequence threading through X-ray crystallography coordinates of pig annexin A1 and human and rat annexin A5 by DeepView/SwissPDB v3.7 [39] and SwissModel (available at <http://www.expasy.org/>). The predominant α -helical backbone structure portrays the four major calcium co-ordination sites on the upper convex surface, together with strategically located cysteine and tyrosine residues. The carbonyl groups and acid residues proposed to be involved in calcium co-ordination are shown. The attachment origin 187 for the non-homologous N-terminus (not shown in full) extends from the lower concave side. The Figure was prepared using the MOLMOL program [54].

crystal structure is well known, shows over 70% of α -helix [9,10,35]. This is not the case for annexin A11, as can be easily observed from the comparison of the spectrum with that of annexin A5. CCA analysis reveals three main contributions:

α -helix (29%), random coil (31%) and β -turns (26%). The remaining 14% is assigned to extended β -strands; however, this percentage must arise from artifacts derived from the application of the CCA, since secondary-structure predictions based on the

amino acid sequence indicate a very low theoretical percentage of these structures. There are no structural studies concerning this annexin, but the structural features of the core domain and the relatively high degree of similarity to other annexins of known three-dimensional structure suggest that the α -helical contribution probably arises from the protein core. From the studies performed with the N-terminus, the existence of an α -helix involved in S100A6 binding has been suggested [27,45], in a way similar to those described for p53 with S100B, and annexins A1 and A2 with S100A11 and S100A10 respectively [28–30].

According to the secondary-structure predictions based on the amino acid sequence of the N-terminal extension, this region would be mainly in random coil except for the theoretical amphipathic α -helix. However, the particular amino acid sequence of the N-terminus (rich in glycine, proline, tyrosine and glutamine) suggests the formation of poly(Pro) β -turn helices that would be responsible for the high β -turn percentage detected. These atypical secondary structures have been detected in the N-terminus of annexin A7 [46], whose sequence, although shorter, is quite similar to that of annexin A11. Accordingly, the N-terminus would account for both random-coil and β -turn contributions predicted from the CD spectra.

In general, the annexin core domain is known to be quite stable, with a higher T_m for those annexins with a short N-terminus [10]. The presence of a long N-terminal extension could induce a destabilization of the core domain. In fact, the T_m for annexin A11 is approx. 6 °C lower than that of human annexin A5, which has one of the lowest T_m among mammalian annexins. The change in the negative molar ellipticity at 208 nm with increase in temperature is mainly a reflection of α -helices unfolding to unordered structure. As the melting curve shows only one co-operative transition, the unfolding of the protein core and any hypothetical α -helix from the N-terminus must take place simultaneously.

Calcium binding does not greatly affect the CD spectrum of annexin A11. For other members of the family, the secondary-structure changes described after calcium binding are also small, implying mainly three-dimensional modifications of the calcium-phospholipid-binding sites with an increase in the percentage of α -helix and a rearrangement of the protein core [9,10,47]. The analysis of the CD spectra of annexin A11 reveals a hyperbolic increase in the ratio between molar ellipticities at 222 and 206.5 nm with calcium concentration. On calcium binding, this ratio increases towards that of pure α -helix, pointing to a higher contribution of this structure with a concomitant decrease in random coil. This hypothesis is also supported by the CCA analyses of the spectra, which suggest a 5–6% increase in α -helix with an equivalent decrease in random coil. Even though it has been described that saturation with calcium of annexins with short N-termini induces a similar increase in the percentage of α -helix [9,10], the total number of residues involved should be considered. Thus, whereas only 16–19 residues change in annexin A5 core, 25–30 residues may become α -helical in annexin A11. Owing to the structural similarity among the protein cores in different annexins, the increase in the α -helical content in annexin A11 cannot be completely explained by the conformational rearrangements of the protein core, and probably involves changes in its N-terminus as well.

In contrast with the relatively small conformational changes observed, calcium induces a great thermal stabilization, increasing the T_m by approx. 14 °C. This increase is larger than that observed for other mammalian annexins such as human annexin A5 (approx. 10 °C) [10]. Moreover, the calcium-bound states of annexin A5 and annexin A11 have a similar thermal stability,

whereas calcium-free annexin A11 shows a lower stability. Taking into account the degree of homology of the annexin core, differences, quite probably in the N-terminal region, are responsible for the changes in protein stability. Therefore we propose that the long N-terminus in annexin A11 has a destabilizing effect in the calcium-free state; structural changes after calcium binding contribute to stabilization of the protein and the T_m of annexin A11 approaches that of annexin A5. It remains to be explained how this interaction could take place, but it is tempting to speculate with a mechanism resembling that described for annexin A1 [8]. This annexin binds to S100A11 through an amphipathic α -helix, which, in a calcium-free state, inserts into domain III, displacing helix 3D. The full-length crystal structure of annexin A1 has been obtained recently, showing that calcium binding induces the refolding of helix 3D pushing the N-terminus outside the annexin core [48], thus enabling the interaction with S100A11. In addition to the stabilizing effects, this mechanism also involves an increase in α -helix due to the refolding of helix 3D.

Tertiary structure analysis through fluorescence studies reveals that Trp²³ is completely exposed to the polar solvent either in the presence or absence of calcium, as the maximum of emission remains at 340 nm under both conditions and there is no decrease in intensity due to calcium binding. Acrylamide quenching also supports this observation, as the obtained Stern–Volmer constant is 12.7 M⁻¹, characteristic of an almost totally exposed tryptophan residue. Whereas free tryptophan residues or *N*-acetyl-tryptophan-amide show a K_{SV} of approx. 16 · M⁻¹, exposed tryptophan residues in proteins present values between 10 and 14 M⁻¹ [49]. On the other hand, tyrosine emission decreases with increase in calcium concentration. This decrease is probably due to a change in the microenvironment of some tyrosine residues to a more hydrophobic one, where interactions that stabilize the polar group of this residue result in the quenching of emission. To confirm this observation, tyrosine titration was performed in the calcium-free and calcium-bound state. According to the titration, in the absence of calcium two tyrosine residues are buried, whereas the calcium-bound state presents six buried tyrosine residues. Therefore the addition of calcium induces a conformational change in annexin A11 that implies the translocation of some tyrosine residues from a polar to a hydrophobic environment, whereas Trp²³ remains unaltered. Taking into account the similarity between the putative amphipathic α -helix in the N-terminus of annexin A11 and that described in the N-terminus of annexin A1, one could speculate that the N-terminus would be even more exposed to the solvent in the presence of calcium. Thus at least some of the tyrosine residues internalized in the presence of calcium are probably located in the protein core. This hypothesis is strongly supported by the surface analysis of the proposed structural model, where the highly conserved residues 312, 396, 471 and 491 are predicted to be buried in the protein core. Among these residues, Tyr³¹² and Tyr³⁹⁶ could be the ones buried in the calcium-free state, as they are the only ones predicted as buried in the calcium-free model. It is not possible to locate the remaining two tyrosine residues titrated as internal in the presence of calcium, as the three-dimensional models cannot predict the structure and position of the N-terminus.

Functionally, annexin A11 interacts with acidic phospholipid and PE vesicles in a calcium-dependent fashion, whereas no binding is observed with PC, as shown previously with wild-type annexin A11 [22]. Partial binding in the absence of calcium was observed to PE, PA and PS vesicles as described for other annexins [50–52]. Phospholipid specificity is generally conserved in calcium-independent binding, and

this is likely to be the case for annexin A11. There must be two contributions to the interaction with phospholipids under these conditions: a specific polar recognition and a hydrophobic interaction. The N-terminus of annexin A11 may be able to insert into the bilayer and establish hydrophobic contacts with the phospholipids, but this would imply a reorientation of the N-terminus from the concave/cytosolic side towards the cell membrane.

Binding of annexin A11 to PS vesicles shows a hyperbolic dependence on calcium concentration. The interaction requires calcium concentrations in the micromolar range, with 50% binding achieved at 28 μ M. Consequently, there is a great increase in calcium affinity in the presence of phospholipids as has been observed for other annexins [1,2,47]. Calcium requirement for PS binding of annexin A11 is higher than that of annexin A2 and lower than that for annexin A5 [1]. These differences could account for the development of divergent functions throughout vertebrate evolution. Annexin A11 induces PS vesicle aggregation only at non-physiological calcium concentrations (> 1 mM) at which this cation itself acts as a bridge for vesicle aggregation. However, annexin A11 is able to accelerate the aggregation process in a protein concentration-dependent manner. These results formulate a role for annexin A11 in aggregation processes *in vivo*, where the presence of other proteins such as S100A6 could modify calcium requirements, as described for other annexins. For example, calcium requirement of annexin A2 for the induction of vesicle aggregation is significantly reduced in the presence of S100A10 [53].

Spectroscopic analyses of the interaction of annexin A11 with PS vesicles give further support to the above observations. Addition of PS vesicles in the absence of calcium induces only a small change in the CD spectrum, which does not affect the thermal stability of the protein, although a loss of co-operativity in the melting curve is observed. Taking into account that annexin A11 is capable of interacting weakly with PS in a calcium-independent manner, this interaction could be responsible for the observed conformational change. However, CD spectroscopy shows that annexin A11 suffers a conformational rearrangement after vesicle binding in the presence of calcium. Calcium-dependent binding to PS vesicles induces an increase in α -helical content similar to the addition of calcium in the absence of phospholipids, but to a higher extent (approx. 9% versus 5–6%). The observed change is again too large to be exclusively due to changes in the protein core; therefore the N-terminus is likely to be involved in this process.

Calcium-dependent binding to PS vesicles is also accompanied by a large increase (approx. 20 °C) in thermal stability, higher than that described for calcium binding alone, and the loss of co-operativity is also remarkable. All these changes must be the consequence of a strong specific interaction, as they are not observed when using PC vesicles. In this case, the small increase in T_m could be due only to binding of calcium to the protein without interaction with the vesicles, and thus no loss of co-operativity is displayed.

In addition to these results, fluorescence studies support a role of the N-terminus in both calcium-independent and calcium-dependent interactions with PS vesicles. The environment of the N-terminal Trp²³ was modified when vesicles were added to the protein preparation in the absence of calcium, with a significant blue-shift in the emission maximum corresponding to a change from an almost total exposure to the solvent to a more hydrophobic environment. However, taking into account that the quantum yield was not modified significantly, this residue probably remained partially in contact with the solvent. Once again, this observation supports the notion of a weak calcium-

independent interaction, probably through the N-terminus of annexin A11 establishing hydrophobic contacts with the bilayer.

Addition of calcium to the annexin/vesicle mixture is characterized by an increase in the tryptophan quantum yield, which presents a midpoint effect almost coincident to that observed in the ultracentrifugation studies. This increase is probably due to the insertion of Trp²³ into the lipid bilayer, which would protect this residue from solvent quenching. Furthermore, the addition of excess EGTA is not able to reverse the interaction, so there must be a hydrophobic component in the binding that accounts for this effect.

This original structural characterization of annexin A11 reveals that the N-terminus, the longest of all known mammalian annexins and containing unusual composition and repeat patterns, contributes significantly to the overall annexin structure. The analysis of the structural conservation of annexin A11 using a combination of primary- and secondary-structure analyses, three-dimensional models and the evolutionary divergence offers a novel insight into its key functional determinants. This annexin has one of the lowest melting temperatures *in vitro* (45 °C) and calcium binding promotes subtle rearrangements in the secondary and tertiary structures of the protein to induce significant thermal stabilization. The recombinant protein binds to acidic phospholipids in a calcium-dependent manner as described for other annexins; it also shows calcium-independent binding, but to a lower extent. These results suggest that the binding of annexin A11 to PS vesicles presents both hydrophobic and polar contributions due to the N-terminus and the annexin core respectively. According to the spectroscopic data, a two-step mechanism can be proposed. First, a weak interaction is established through surface hydrophobic contacts with some degree of polar specificity; secondly, after the addition of calcium, a tight binding to the lipid bilayer takes place, enabling in this way the partial insertion of the N-terminus, which reinforces the interaction. It remains however to be determined whether calyculin, sorcin or ALG-2 interaction with annexin A11 will influence its binding to lipid bilayers.

We are grateful to Dr Hiroyoshi Hidaka for kindly providing a polyclonal antibody raised against bovine annexin A11. This work was supported by grant nos. PM98-0083, PB98-1529 and BMC2002-01407 from the Dirección General de Investigación (Spain).

REFERENCES

- 1 Raynal, P. and Pollard, H. B. (1994) Annexins: the problem of assessing the biological role for a gene family of multifunctional calcium- and phospholipid-binding proteins. *Biochim. Biophys. Acta* **1197**, 63–93.
- 2 Swairjo, M. A. and Seaton, B. A. (1994) Annexin structure and membrane interactions: a molecular perspective. *Annu. Rev. Biophys. Struct.* **23**, 193–213.
- 3 Gerke, V. and Moss, S. E. (2002) Annexins: from structure to function. *Physiol. Rev.* **82**, 331–371.
- 4 Morgan, R. O. and Fernandez, M. P. (1998) Expression profile and structural divergence of novel human annexin 31. *FEBS Lett.* **434**, 300–304.
- 5 Liemann, S. and Huber, R. (1997) Three-dimensional structure of annexins. *Cell. Mol. Life Sci.* **53**, 516–521.
- 6 Morgan, R. O., Jenkins, N. A., Gilbert, D. J., Copeland, N. G., Balsara, B. R., Testa, J. R. and Fernandez, M. P. (1999) Novel human and mouse annexin A10 are linked to the genome duplications during early chordate evolution. *Genomics* **60**, 40–49.
- 7 Huber, R., Römisch, J. and Pâques, E. P. (1990) The crystal and molecular structure of human annexin V, an anticoagulant protein that binds to calcium and membranes. *EMBO J.* **9**, 3867–3873.
- 8 Rosengarth, A., Gerke, V. and Luecke, H. (2001) X-ray structure of full-length annexin 1 and implications for membrane aggregation. *J. Mol. Biol.* **306**, 489–498.
- 9 Arboledas, D., Olmo, N., Lizarbe, M. A. and Turnay, J. (1997) Role of the N-terminus in the structure and stability of chicken annexin V. *FEBS Lett.* **416**, 217–220.
- 10 Turnay, J., Olmo, N., Gasset, M., Iloro, I., Arrondo, J. L. R. and Lizarbe, M. A. (2002) Calcium-dependent conformational rearrangements and protein stability in chicken annexin A5. *Biochem. J.* **363**, 2280–2291.

- 11 Burger, A., Berendes, R., Liemann, S., Benz, J., Hofman, A., Göttig, P., Huber, R., Gerke, V., Carsten, T., Römisch, J. et al. (1996) The crystal structure and ion channel activity of human annexin II, a peripheral membrane protein. *J. Mol. Biol.* **257**, 839–847
- 12 Rosengarth, A., Rösger, J., Hinz, H. J. and Gerke, V. (1999) A comparison of the energetics of annexin I and annexin V. *J. Mol. Biol.* **288**, 1013–1025
- 13 Morgan, R. O. and Fernandez, M. P. (1995) Molecular phylogeny of annexins and identification of a primitive homologue in *Giardia lamblia*. *Mol. Biol. Evol.* **12**, 967–979
- 14 Fernandez, M. P., Jenkins, N. A., Gilbert, D. J., Copeland, N. G. and Morgan, R. O. (1996) Sequence and chromosomal localization of mouse annexin XI. *Genomics* **37**, 366–374
- 15 Morgan, R. O., Bell, D. W., Testa, J. R. and Fernandez, M. P. (1998) Genomic locations of ANX11 and ANX13 and the evolutionary genetics of human annexins. *Genomics* **48**, 100–110
- 16 Bances, P., Fernández, M. R., Rodríguez-García, M. I., Morgan, R. O. and Fernandez, M. P. (2000) Annexin A11 (ANXA11) gene structure as the progenitor of paralogous annexins and source of orthologous cDNA isoforms. *Genomics* **69**, 95–103
- 17 Iglesias, J. M., Morgan, R. O., Jenkins, N. A., Copeland, N. G., Gilbert, D. J. and Fernandez, M. P. (2002) Comparative genetics and evolution of annexin A13 as the founder gene of vertebrate annexins. *Mol. Biol. Evol.* **19**, 608–618
- 18 Towle, C., Weissbach, L. and Treadwell, B. V. (1992) Alternatively spliced annexin XI transcripts encode proteins that differ near the amino-terminus. *Biochim. Biophys. Acta* **1131**, 223–226
- 19 Fiedler, K., Lafont, F., Parton, R. G. and Simons, K. (1995) Annexin XIIIb: a novel epithelial specific annexin is implicated in vesicular traffic to the apical plasma membrane. *J. Cell Biol.* **128**, 1043–1053
- 20 Sable, C. L. and Riches, D. W. H. (1999) Cloning and functional activity of a novel truncated form of annexin IV in mouse macrophages. *Biochem. Biophys. Res. Commun.* **258**, 162–167
- 21 Towle, C. A. and Treadwell, B. V. (1992) Identification of a novel mammalian annexin. cDNA cloning, sequence analysis, and ubiquitous expression of the annexin XI gene. *J. Biol. Chem.* **267**, 5416–5423
- 22 Tokumitsu, H., Mizutani, A., Minami, H., Kobayashi, R. and Hidaka, H. (1992) A calyculin-associated protein is a newly identified member of the Ca^{2+} /phospholipid-binding proteins, annexin family. *J. Biol. Chem.* **267**, 8919–8924
- 23 Iino, S., Sudo, T., Niwa, T., Fukasawa, T., Hidaka, H. and Niki, I. (2000) Annexin XI may be involved in Ca^{2+} - or GTP- γ S-induced insulin secretion in the pancreatic β -cell. *FEBS Lett.* **479**, 46–50
- 24 Misaki, Y., Puij, G. J. M., van der Kemp, A. W. C. M. and van Venrooij, W. J. (1994) The 56K autoantigen is identical to human annexin XI. *J. Biol. Chem.* **269**, 4240–4246
- 25 Mizutani, A., Watanabe, N., Kitao, T., Tokumitsu, H. and Hidaka, H. (1995) The long amino-terminal tail domain of annexin XI is necessary for its nuclear localization. *Arch. Biochem. Biophys.* **318**, 157–165
- 26 Furge, L. L., Chen, K. and Cohen, S. (1999) Annexin VII and annexin XI are tyrosine phosphorylated in peroxovanadate-treated dogs and in platelet-derived growth factor-treated rat vascular smooth muscle cells. *J. Biol. Chem.* **274**, 33504–33509
- 27 Sudo, T. and Hidaka, H. (1999) Characterization of the calyculin (S100A6) binding site of annexin XI-A by site-directed mutagenesis. *FEBS Lett.* **444**, 11–14
- 28 Mäler, L., Sastry, M. and Chazin, W. J. (2002) A structural basis for S100 protein specificity derived from comparative analysis of apo and Ca^{2+} -calyculin. *J. Mol. Biol.* **317**, 279–290
- 29 Réty, S., Sopkova, J., Renouard, M., Osterloh, D., Gerke, V., Tabaries, S., Russo-Marie, F. and Lewit-Bentley, A. (1999) The crystal structure of a complex of p11 with the annexin II N-terminal peptide. *Nat. Struct. Biol.* **6**, 89–95
- 30 Réty, S., Osterloh, D., Arié, J. P., Tabaries, S., Seemann, J., Russo-Marie, F., Gerke, V. and Lewit-Bentley, A. (2000) Structural basis of the Ca^{2+} -dependent association between S100C (S100A11) and its target, the N-terminal part of annexin I. *Structure Fold. Res.* **8**, 175–184
- 31 Satoh, H., Shibata, H., Nakano, Y., Kitaura, Y. and Maki, M. (2002) ALG-2 interacts with the amino-terminal domain of annexin XI in a Ca^{2+} -dependent manner. *Biochem. Biophys. Res. Commun.* **291**, 1166–1172
- 32 Brownawell, A. M. and Creutz, C. E. (1997) Calcium-dependent binding of sorcin to the N-terminal domain of synexin (annexin VII). *J. Biol. Chem.* **272**, 22182–22190
- 33 Gómez-Guillén, M. C., Turnay, J., Fernández-Díaz, M. D., Olmo, N., Lizarbe, M. A. and Montero, P. (2002) Structural and physical properties of gelatine extracted from different marine species: a comparative study. *Food Hydrocolloids* **16**, 25–34
- 34 Perczel, A., Park, K. and Fasman, G. D. (1992) Analysis of the circular dichroism spectrum of proteins using the convex constraint algorithm: a practical guide. *Anal. Biochem.* **203**, 83–93
- 35 Turnay, J., Plannmüller, E., Lizarbe, M. A., Bertling, W. and von der Mark, K. (1995) Collagen binding activity of recombinant and N-terminally modified annexin V (anchoring CII). *J. Cell. Biochem.* **58**, 208–220
- 36 Laemmli, U. K. (1970) Cleavage of structural proteins during the assembly of the head of bacteriophage T4. *Nature (London)* **227**, 680–685
- 37 Turnay, J., Olmo, N., Lizarbe, M. A. and von der Mark, K. (2002) Changes in the expression of annexin A5 gene during *in vitro* chondrocyte differentiation: influence of cell attachment. *J. Cell. Biochem.* **84**, 132–142
- 38 Gu, X. (1999) Statistical methods for testing functional divergence after gene duplication. *Mol. Biol. Evol.* **16**, 1664–1674
- 39 Guex, N., Diemand, A. and Peitsch, M. C. (1999) Protein modelling for all. *Trends Biol. Sci.* **24**, 364–367
- 40 Berman, H. M., Westbrook, J., Feng, Z., Gilliland, G., Bhat, T. N., Weissig, H., Shindyalov, I. N. and Bourne, P. E. (2000) The protein data bank. *Nucleic Acids Res.* **28**, 235–242
- 41 Weng, X., Luecke, H., Song, I. S., Kang, D. S., Kim, S. H. and Huber, R. (1993) Crystal structure of human annexin I at 2.5 Å resolution. *Protein Sci.* **2**, 448–458
- 42 Bewley, M. C., Boustead, C. M., Walker, J. H. and Huber, R. (1993) Structure of chicken annexin V at 2.25-Å resolution. *Biochemistry* **32**, 3923–3928
- 43 Luecke, H., Chang, B. T., Maillard, W. S., Schlaepfer, D. D. and Haigler, H. T. (1995) Crystal structure of the annexin XII hexamer and implications for bilayer insertion. *Nature (London)* **378**, 512–515
- 44 Mizutani, A., Usuda, N., Tokumitsu, H., Minami, H., Yasui, K., Kobayashi, R. and Hidaka, H. (1992) CAP-50, a newly identified annexin, localizes in nuclei of cultured fibroblast 3Y1 cells. *J. Biol. Chem.* **267**, 13498–13504
- 45 Tokumitsu, H., Mizutani, A. and Hidaka, H. (1993) Calyculin-binding site located on the NH_2 -terminal domain of rabbit CAP-50 (annexin XI): functional expression of CAP-50 in *Escherichia coli*. *Arch. Biochem. Biophys.* **303**, 302–306
- 46 Matsushima, N., Creutz, C. E. and Kretzinger, R. H. (1990) Polyproline, β -turn helices. Novel secondary structures proposed for the tandem repeats within rhodopsin, synaptophysin, synexin, gliadin, RNA polymerase II, hordein, and gluten. *Proteins* **7**, 125–155
- 47 Sopkova, J., Vincent, M., Takahashi, M., Lewit-Bentley, A. and Gally, J. (1999) Conformational flexibility of domain III of annexin V at membrane/water interfaces. *Biochemistry* **38**, 5447–5458
- 48 Rosengarth, A. and Luecke, H. (2003) A calcium-driven conformational switch of the N-terminal and core domains of annexin A1. *J. Mol. Biol.* **326**, 1317–1325
- 49 Lakowicz, J. R. (1999) Quenching of fluorescence. In *Principles of Fluorescence Spectroscopy*, 2nd edn (Lakowicz, J. R., ed.), pp. 237–265. Kluwer Academic/Plenum, New York
- 50 Jost, M., Zeuschner, D., Seemann, J., Weber, K. and Gerke, V. (1997) Identification and characterization of a novel type of annexin-membrane interaction: Ca^{2+} is not required for the association of annexin II with endosomal membranes. *Biochim. Biophys. Acta* **110**, 221–228
- 51 König, J. and Gerke, V. (2000) Modes of annexin-membrane interactions analyzed by employing chimeric annexin proteins. *Biochim. Biophys. Acta* **1498**, 174–180
- 52 Tzima, E. and Walker, J. H. (2000) Platelet annexin V: the ins and outs. *Platelets* **11**, 245–251
- 53 Lambert, O., Gerke, V., Bader, M. F., Porte, F. and Brisson, A. (1997) Structural analysis of junctions formed between lipid membranes and several annexins by cryo-electron microscopy. *J. Mol. Biol.* **272**, 42–55
- 54 Koradi, R., Billeter, M. and Wüthrich, K. (1996) MOLMOL: a program for display and analysis of macromolecular structures. *J. Mol. Graph.* **14**, 51–55

Received 4 November 2002/10 March 2003; accepted 11 April 2003

Published as BJ Immediate Publication 11 April 2003, DOI 10.1042/BJ20021721

Differential properties of two isoforms of annexin XIII in MDCK cells

Sandra Lecat^{1,2,*}, Paul Verkade^{1,2}, Christoph Thiele³, Klaus Fiedler⁴, Kai Simons^{1,2} and Frank Lafont^{1,2,†}

¹Cell Biology and Biophysics Programme, European Molecular Biology Laboratory, Meyerhofstrasse 1, D-69117 Heidelberg, Germany

²Max Planck Institute for Molecular Biology and Genetics, Pflotenhauerstrasse 110, D-01307 Dresden, Germany

³Department of Neurobiology, University of Heidelberg, Im Neuenheimer Feld 364, D-69120, Heidelberg, Germany

⁴Cell Biology Department Biozentrum, University of Basel, Klingelbergstrasse, 70, CH 4056 Basel, Switzerland

*Present address: Département des Récepteurs et Protéines Membranaires, Ecole Supérieure de Biotechnologie de Strasbourg, Strasbourg, France

†Author for correspondence at present address: Département de Biochimie, Sciences II, 30 quai Ernest-Ansermet, CH-1211 Genève 4, Switzerland (e-mail: Frank.Lafont@biochem.unige.ch)

The online version of this article contains additional data and is available at <http://www.unige.ch/sciences/biochimie/Lafont/JCSLecatY2K.html>

Accepted 9 May; published on WWW 22 June 2000

SUMMARY

Annexins form a family of proteins that are widely expressed and known to bind membranes in the presence of calcium. Two isoforms of the annexin XIII subfamily are expressed in epithelia. We previously reported that annexin XIIIb is apically localized in MDCK cells and that it is involved in raft-mediated delivery of apical proteins. We have now analyzed the properties of annexin XIIIa, which differs from annexin XIIIb by a deletion of 41 amino acids in the amino-terminal domain, and is distributed both apically and basolaterally. Annexin XIIIa binding to membranes is independent of calcium but requires its myristoyl amino-terminal modification, as observed with annexin XIIIb. Our biochemical and functional data show

that annexin XIIIa behaves differently in the apical and in the basolateral compartments. Whereas annexin XIIIa apically can associate with rafts independently of calcium, the basolateral pool requires calcium for this. Annexin XIIIa, like annexin XIIIb, stimulates apical transport of influenza virus hemagglutinin but, in contrast, only annexin XIIIa inhibits basolateral transport of vesicular stomatitis virus G protein. Our results suggest that annexin XIIIa and XIIIb have specific roles in epithelial cells, and because of their structural similarities, these isoforms offer interesting tools for unravelling the functions of annexins.

Key words: Membrane traffic, MDCK cell, Protein sorting, Annexin

INTRODUCTION

13 annexins have so far been identified in mammals, but members of the family are spread out all over the eukaryotic kingdom (Morgan and Fernandez, 1997). Each annexin has a distinct N terminus and annexins are homologous in the C-terminal core, a domain of 30 kDa that harbors calcium binding sites (Liemann and Huber, 1997). In vitro binding experiments between purified annexins and liposomes have suggested that calcium ions bridge the protein to the negatively charged head group of phospholipids. Annexins are described as calcium-dependent phospholipid-binding proteins that translocate from the cytosol to the membrane in response to an elevation of the intracellular calcium concentration. This property of the core domain was demonstrated in artificial systems but seems to operate in living cells as well (Campos et al., 1990; Ernst, 1991; Trotter et al., 1994, 1995; Selbert et al., 1995, 1996; Barwise and Walker, 1996; Chasserot et al., 1996).

How annexins perform their functions after membrane binding remains unclear (Liemann and Lewit-Bentley, 1995; Lecat and Lafont, 1999). Based on the finding that annexins can aggregate or even fuse membranes in a calcium-dependent manner in vitro, annexins have been proposed to regulate membrane fusion events (Ernst et al., 1991; Creutz, 1992;

Emans et al., 1993; Bitto and Cho, 1998). Studies in the cellular context confirmed that several annexins play a role in membrane trafficking but there is little support for their proposed function in membrane fusion (Harder and Gerke, 1993; Burgoyne and Clague, 1994; Donnelly and Moss, 1997; Carroll et al., 1998; Kamal et al., 1998; König et al., 1998). Annexins were also shown to have calcium-channel activities upon association with liposomes (Chen et al., 1993; Demange et al., 1994; Arispe et al., 1996; Liemann et al., 1996; Hofmann et al., 1997). In vitro studies have suggested that annexins I and XII can be inserted into the bilayer (Luecke et al., 1995; Langen et al., 1998; Rosengarth et al., 1998); however, studies in cells have not substantiated a role for annexins to form calcium channels. Instead, annexins have been shown to regulate the activity of several ion channels (Kaetzel et al., 1994; Nilius et al., 1996).

We previously cloned the cDNA encoding canine annexins XIIIa and XIIIb from an epithelial Madin-Darby Canine Kidney II cell (MDCKII) cDNA library (Fiedler et al., 1995). Annexin XIIIb has an insertion of 41 amino acids after the first four amino acids of the sequence that are common to both isoforms. We demonstrated that annexin XIIIb is involved in apical exocytosis of polarized MDCKII and is associated with specific lipid microdomains (Fiedler et al., 1995; Lafont et al., 1998b).

Apical exocytosis, contrary to basolateral exocytosis, is dependent on the integrity of these microdomains, called 'rafts' (Keller and Simons, 1998). Rafts consist of assemblies of sphingolipids and cholesterol (Simons and Ikonen, 1997), which form liquid-ordered phases segregated in a dynamic fashion from the other lipids (Ahmed et al., 1997; Brown and London, 1997; Brown, 1998; Rietveld and Simons, 1998). They function by forming platforms for proteins that specifically partition into these lipid assemblies (Simons and Ikonen, 1997; Brown and London, 1998). Annexin XIIIa was identified by northern blot analysis as an intestinal-specific annexin and shown by immunofluorescence studies on tissues to localize mainly at the apical plasma membrane of enterocytes with a faint staining on their basolateral plasma membrane (Wice and Gordon, 1992). The localization of annexin XIIIa could not be inferred from these studies, however, because the antibody used recognized two proteins: a 36 kDa protein corresponding to annexin XIIIa and a 40 kDa protein that we later identified as annexin XIIIb. In this paper, we have compared the subcellular distribution and functional properties of annexin XIIIa with those of annexin XIIIb in MDCKII cells.

MATERIALS AND METHODS

Reagents

Detergents were the following: SDS (BioRad Laboratories, Hercules, CA, USA), Triton X-100 (Serva, Heidelberg, Germany), NP-40 (FlukaAG, Buchs, Switzerland). IPTG, methyl- β -cyclodextrin, sodium butyrate (NaBu) and proteinase inhibitors were from Sigma Chemical Co. (Deisenhofen, Germany). Restriction endonucleases were from New England Biolabs (Schwabach/Taunus, Germany) and cloned *pfu* polymerase from Stratagene (La Jolla, CA, USA). pOPRSV1-CAT vector was from Stratagene.

Cell culture

Media and reagents for cell culture were purchased from Gibco BRL (Eggenstein, Germany). Madin-Darby Canine Kidney (MDCK) type II cells were cultured as described (Pimplikar et al., 1994) on TranswellTM polycarbonate filters (0.4 μ m pore size) from Costar (Cambridge, MA, USA) or on plastic dishes. MDCKII Lac switchable cells were given by Dr E. E. Schneeberger and cultivated the same way as wild-type MDCKII except when transfected (McCarthy et al., 1996). After transfection, the selection was maintained with 0.6 mg/ml G418 geneticin (Gibco BRL). 293 cells were grown in MEM medium supplemented with 10% fetal calf serum (FCS) and 1% non-essential amino acids in addition to the general components such as penicillin/streptomycin and glutamine.

Preparation of antibodies and Immunoblotting

The affinity-purified anti-annexin XIII-II antibody preparation was according to Fiedler et al. (1995). 12% SDS-PAGE gels were run using the BioRad mini-gel system unless otherwise mentioned. Polyclonal rabbit anti-VIP21/cav1 amino-terminal N20 was purchased from Santa Cruz Biotechnology, Inc. (Santa Cruz, CA, USA). Monoclonal mouse anti-GP114 was from our laboratory (Balcarova-Ständer et al., 1984). Goat anti-rabbit and goat anti-mouse horseradish peroxidase-conjugated antibodies were from BioRad (München, Germany). The immunoblots were revealed with ECL (Amersham International).

Construction of recombinant adenovirus expressing annexin XIIIb

Recombinant adenoviruses expressing annexin XIIIa, annexin XIIIb and non-myristoylated annexin XIIIa were produced as described

previously (He et al., 1998). Briefly, the annexin XIIIb sequences were amplified by PCR to obtain a *KpnI-XbaI* fragment using TCG GGT ACC AAA AAC GAA ATG GGC as 5' primer for the myristoylated annexins and, in order to create a non-myristoylated mutant, the codon for the amino-terminal glycine GGC was replaced by one for alanine GCC in the 5' primer. The 3' primer was ATA TCT AGA TCA GTG CAA GAG GGC C in all the constructs. The fragments were cloned in the pShuttle-CMV vector and recombinant adenoviral plasmids were generated by homologous recombination with the pAdEasy-1 vector (He et al., 1998). Transfection of 293 cells was performed by lipofection. Amplified adenoviruses were purified by CsCl gradient centrifugation and stored at -20°C in storage buffer (5 mM Tris-HCl, pH 8.0, 50 mM NaCl, 0.1% BSA, 25% glycerol).

Cloning of annexin XIIIb for stable expression in MDCKII Lac switchable cells

The annexin XIIIb sequences were amplified by PCR to obtain a *XbaI-KpnI* fragment containing a suitable Kozack sequence before the ATG and a c-myc tag at the carboxy terminus. For the amplification of the annexin XIIIb sequence, the 5' primer was TCG TCT AGA GCC ACC ATG GGC AAT CGT CAT AGC C, these last four nucleotides being replaced by GCC A for amplifying the annexin XIIIa sequence. As 5' primer for the non-myristoylated mutants, the codon for the amino-terminal glycine GGC was replaced by one for alanine GCC. For all constructs, the 3' primer was ATA GGT ACC TCA GTT CAA GTC TTC TTC GCT TAT GAG TTT TTG CTC GTG CAA GAG GGC CAC, where the bold characters correspond to the c-myc tag, EQKLISEEDLN. The fragments were inserted in pOPRSV1-1 vector, a derivative of the pOPRSV1-CAT vector containing a polylinker instead of the CAT gene (Daniele Zacchetti, EMBL; Cheong et al., 1999).

Infection and transfection of MDCKII cells

For transient overexpression of annexin XIIIb by adenovirus infection, MDCKII cells grown on 1.2 cm filters for 3 days were infected on the apical side at 37°C for 1 hour in 500 μ l of culture medium with 1 μ l of virus stock. The expression was carried on for 16 hours before further analysis. For stable overexpression of annexin XIIIb, the MDCKII Lac switchable cells were transfected by electroporation and the clones were selected for their resistance to G418. 24 clones of each transfection were screened by immunofluorescence with anti-annexin XIII-II antibody for the expression of the exogenous proteins, after having induced their synthesis with 5 mM IPTG and 1 mM NaBu for 16 hours at 37°C.

Immunoelectron microscopy and immunofluorescence analysis

The locations of the transiently overexpressed annexin XIIIa, annexin XIIIb or non-myristoylated annexin XIIIa in polarized cells were determined at the electron-microscope level using anti-annexin XIII-II antibody at 1/200 dilution, according to Lafont et al. (1998b). For immunofluorescence studies, cells grown on filters were washed twice in PBS⁺ buffer (PBS containing 0.9 mM CaCl₂ and 0.5 mM MgCl₂), fixed with methanol at -20°C for 6 minutes and then processed for immunolabeling. The myc-tag was not accessible either to the polyclonal or the monoclonal myc antibodies. The anti-annexin XIII-II antibody was used instead at a dilution of 1/300 on transient expressing cells and 1/100 on stable clones in PBS, supplemented with 0.2% gelatin for 1 hour at 37°C. The secondary antibody was a goat anti-rabbit FITC-conjugated antibody (Dianova, Hamburg, Germany). The filters were placed in mounting medium and analyzed using a Leica NTS confocal microscope as described previously (Lafont et al., 1998b).

Membrane association analysis

The two-step sucrose gradient was prepared as previously described (Fiedler et al., 1993). Briefly, the MDCKII or MDCKII Lac switchable

cells grown to confluence in 150 cm dishes were homogenized at 4°C in 500 µl of 10 mM Hepes, pH 7.4, 5 mM EGTA, 250 mM sucrose, 1 mM DTT, 25 mg/ml CLAP protease inhibitors. Then, a postnuclear supernatant (PNS) was obtained by 10 minutes centrifugation at 3000 rpm in a microfuge. The PNS was made 1.5 M sucrose, placed in a SW60 centrifuge tubes (Beckman, Munchen, Germany) and overlaid by a 1.2 M and a 0.8 M sucrose layer in Hepes-EGTA. The flotation was carried out at 4°C for 18 hours at 35000 rpm. The membranes float at each sucrose interface. 500 µl fractions were collected starting at the top of the gradient and 30 µl of each fraction was analyzed by SDS-PAGE followed by western blotting.

To prepare the total membrane fraction, MDCKII cells grown to confluence in 15 cm dishes were homogenized in 200 µl of 10 mM Tris-HCl, pH 7.5, 150 mM NaCl, 5 mM EGTA, 1 mM DTT and CLAP. The membranes from 30 µl of the subsequent PNS were collected on a 1 M sucrose cushion by a centrifugation at 100,000 g in a TLA100 rotor (Beckman). The membranes were thereafter treated for 15 minutes with agitation at room temperature (RT) in 30 µl of 10 mM Tris-HCl, pH 7.5, 150 mM NaCl, 5 mM EGTA as a control, or the same buffer supplemented with either 1 M KCl or 0.2% Nonidet P-40 (NP-40), or were treated at 4°C in 30 µl of 0.1 M NaHCO₃, pH 11. For extraction of the cholesterol, the membranes were treated with 10 mM cyclodextrin in 30 µl of buffer for 30 minutes at 37°C. The peripheral-membrane proteins released from the membranes were recovered in the supernatant following a second 100,000 g centrifugation. The samples were directly mixed with 2× loading buffer and analyzed by SDS-PAGE followed by blotting.

Cr sslinking of membrane proteins by phospholipids

The synthesis of a C18-stearic acid derivative containing a diazirin ring on the C10 carbon (10-azistearic acid) is described elsewhere (Thiele et al., 2000). MDCKII cells grown on 2.4 cm size polycarbonate filters for 2.5 days were incubated for 3 hours in medium with 5% FCS. Then cells were incubated in medium supplemented with 1% FCS and 100 µM C18-stearic acid mixed 1:1 with BSA for overnight labeling at 37°C. The fatty acid was then chased for 2 hours with 10% FCS in MEM medium. Cells were washed in PBS⁺, frozen in liquid nitrogen for 5 seconds and subjected, on dry ice, to UV irradiation by a black light lamp equipped with 100-W mercury bulb and a filter cutting wavelengths below 310 nm (Spectroline model B100/F, Spectronics Corporation, Westbury, NY, USA). The cells were 12 cm from the source for 15 minutes of irradiation. Subsequently, cells were scraped from the filters and homogenized. The membranes and the cytosol fractions were separated by a 100,000 g centrifugation, as described above, and the proteins were separated on large SDS-PAGE gels containing 8% polyacrylamide for annexin XIIIb and 13.5% for VIP21/cav1 analysis.

Raft association analysis

MDCKII or the stable MDCKII Lac switchable cells overexpressing annexin XIIIa (MDCK(lac)/55) were grown to confluence in 3 cm dishes and scraped directly after ice-cold PBS washes in 400 µl of 10 mM Tris-HCl, pH 7.5, 150 mM NaCl, 5 mM EGTA or increasing amounts of CaCl₂, 1% Triton X-100 (TX-100), 1 mM DTT, CLAP at 4°C. The cells were incubated for 30 minutes at 4°C to allow the solubilisation of the membranes to occur. Then, the material was adjusted to 40% OptiPrepTM (Nycomed-Pharma, Oslo, Norway) in a final volume of 1 ml and was overlaid with 1.2 ml of 30% OptiPrepTM, 1.2 ml 25% OptiPrepTM and 0.8 ml of 5% OptiPrepTM (all in 10 mM Tris-HCl, pH 7.5, 150 mM NaCl, 1% TX-100 plus CaCl₂ as mentioned in the text). The flotation was performed in SW60 tubes at 100,000 g for 4

hours at 4°C. 500 µl fractions were collected starting from the top of the gradient and TCA precipitated. The pellets were washed 3 times with -20°C acetone and all the material was subjected to SDS-PAGE and blot analysis.

Expression and purification of recombinant annexin XIIIa and transport assay

Myristoylated annexin XIIIa was expressed in the *Drosophila* Schneider cells and purified exactly as previously reported for annexin XIIIb (Lafont et al., 1998b). A functional assay reconstituting the transport of exocytic carriers from the TGN to either the apical or the basolateral surface has already been described in detail (Lafont et al., 1998a).

RESULTS

Annexins XIIIa and XIIIb are identical except that annexin XIIIb has a 41-amino-acid insertion in its N-terminal tail. Because of this similarity we were not able to raise an antibody specific for annexin XIIIa, so its expression was analyzed by making use of an antibody directed against a peptide sequence in the N-terminal tail common to both isoforms (Fiedler et al., 1995; Fig. 1A). This affinity-purified antibody recognizes three bands by immunoblotting of an MDCKII lysate (Fig. 1B). By

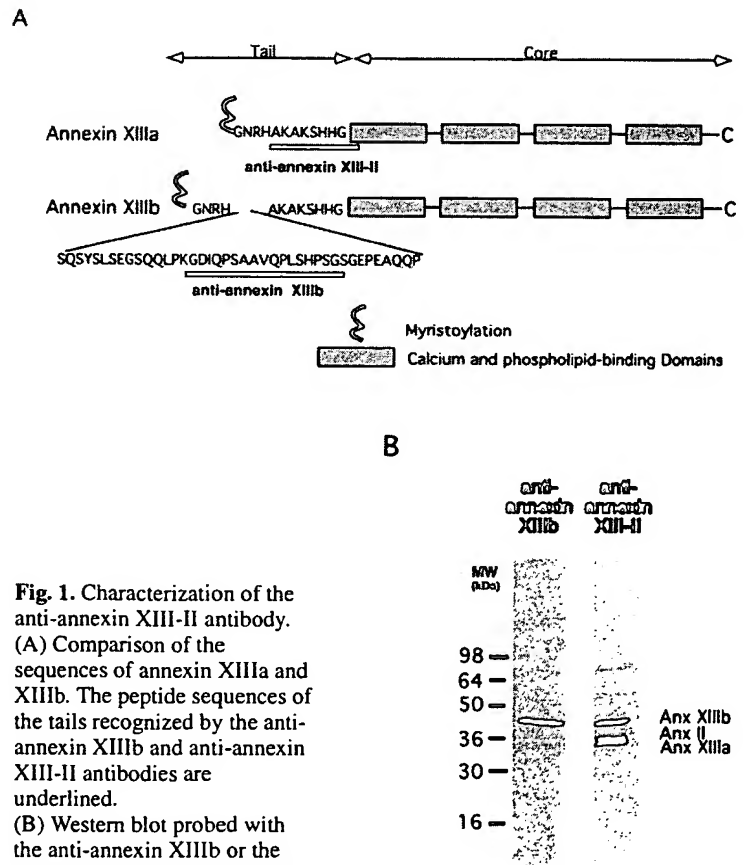


Fig. 1. Characterization of the anti-annexin XIII-II antibody. (A) Comparison of the sequences of annexin XIIIa and XIIIb. The peptide sequences of the tails recognized by the anti-annexin XIIIb and anti-annexin XIII-II antibodies are underlined. (B) Western blot probed with the anti-annexin XIIIb or the anti-annexin XIII-II antibody on MDCKII cells lysate. The positions of molecular mass markers and annexin XIIIb (40 kDa) and XIIIa (36 kDa) are indicated.

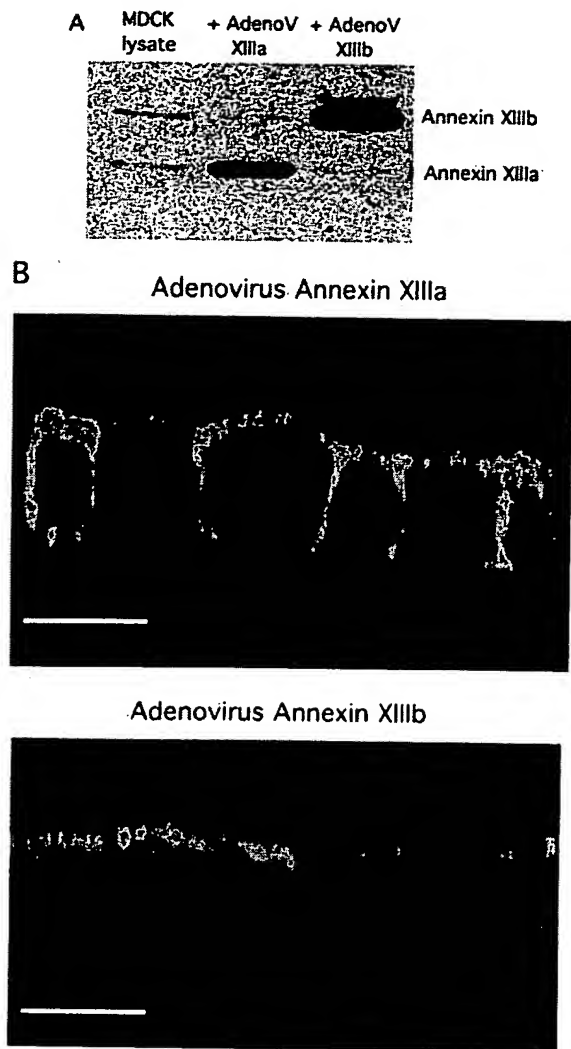


Fig. 2. Immunostaining of annexin XIIIa as compared with that of annexin XIIIb in MDCKII cells. After infection with recombinant adenoviruses overexpressing wild-type annexin XIIIa or XIIIb, MDCKII cells were analyzed by immunoblotting (A) and by immunofluorescence confocal microscopy (B) with the anti-annexin XIII-II antibody. Bar, 10 μ m.

2D-gel analysis and comparison with either overexpressed or purified annexin XIIIa and by microsequencing, we could determine that the upper band corresponds to annexin XIIIb and the lower band corresponds to annexin XIIIa. By microsequencing analysis, the intermediate band was described as being a variant of annexin II (Fiedler et al., 1997), although the amino acid sequence selected to raise the antibody does not show homology to that of annexin II. In this study, this antibody is referred as the anti-annexin XIII-II antibody.

Differential localization of annexin XIIIa versus annexin XIIIb in polarized MDCKII cells

To determine where annexin XIIIa is targeted in MDCKII cells, recombinant annexin XIII adenoviruses were generated and used to infect these cells. We used the anti-annexin XIII-II

antibody at a dilution such that the endogenous annexin XIIIa were not stained, thus allowing detection of adenovirus-expressed annexins by western blotting (Fig. 2A), immunofluorescence (Fig. 2B) and immunoelectron microscopy (Fig. 3). The overexpressed annexin XIIIb was apically localized using both anti-annexin XIIIb and anti-annexin XIII-II antibodies (Figs 2B, 3A). At the same expression level, the overexpressed annexin XIIIa was visible both at the basolateral and at the apical plasma membranes (Figs 2B, 3B). Quantitation by immunoelectron microscopy confirmed that annexin XIIIa was equally distributed between the two plasma membrane domains of MDCKII cells (3.63 ± 0.85 gold particles/ μ m membrane length on apical versus 3.15 ± 0.58 on basolateral membrane).

Calcium-independent binding of the annexin XIIIs to cellular membranes

We reported previously that half of the cellular pool of annexin XIIIb is bound to membranes when calcium ions have been chelated (Lafont et al., 1998b). To characterize the membrane binding features of annexin XIIIa, two membrane pools of high and low buoyant densities were isolated by flotation in a two-step sucrose gradient from an MDCKII cell homogenate. The protein content of the fractions was analyzed by western blotting. Caveolin-1 (VIP21/cav1) was used to follow the presence of membranes in the different peaks (Fig. 4A, fractions 4 and 8). After chelation of calcium ions with EGTA, annexin XIIIa and XIIIb were localized in the top fractions of the gradient containing the light density membranes and also in the soluble pool at the bottom of the gradient.

The myristoyl moiety is necessary for the calcium-independent interaction of annexin XIIIs with membranes

Annexin XIIIa are the only members of this protein family shown to be myristoylated on their N-terminal glycine (Wice and Gordon, 1992). In order to test how this fatty acid modification contributes to membrane linkage, MDCKII cells engineered to express exogenous genes in a regulated manner (MDCKII Lac switchable cells) were stably transfected with a pOPRSV1-1 vector encoding the myristoylated annexin XIIIa or their non-myristoylated mutants. In these cells, the synthesis of the exogenous annexin XIIIa or XIIIb is repressed due to the stable expression of the lac repressor but can be induced by adding IPTG to the cell medium, thereby inhibiting the lac repressor. Two clones of wild-type and non-myristoylated mutants of annexin XIIIa and XIIIb were selected by immunofluorescence microscopy. When membrane association of these exogenous proteins was compared using flotation in the two-step sucrose gradient the non-myristoylated annexin XIIIa were exclusively recovered in the cytosolic fractions (Fig. 4B).

To test whether the myristoyl group was anchoring the annexin XIIIa to the lipid bilayer we performed crosslinking experiments. Polarized MDCKII cells were fed with a modified saturated C18 fatty acid containing a UV-activable diazirine crosslinker. It has been previously shown that such a fatty acid is more than 80% incorporated into phospholipids with a chain length of 18 carbons (Mahoney et al., 1977; Doi et al., 1978). The crosslinker makes covalent amide bonds with the surrounding C-H from lipids or proteins upon UV irradiation.

The proteins crosslinked to additional lipids can subsequently be detected by a mobility shift in SDS-PAGE.

After crosslinking, the membranes were separated from the cytosol by centrifugation at 100,000 g and the samples were analysed by immunoblotting. In a typical experiment, the electrophoretic migration of the integral membrane protein VIP21/cav1 was shifted, while in control experiments in which the cells were either fed with fatty acids without crosslinker or were not submitted to UV irradiation, VIP21/cav1 migrated normally (see Fig. Crosslink available at <http://www.unige.ch/sciences/biochimie/Lafont/JCSLecatY2K.html>). The migration of annexin XIIIb was not shifted; however, a shadow trailing the migrating band became visible in the membrane fraction but not in the cytosolic one (see Fig. Crosslink

available at <http://www.unige.ch/sciences/biochimie/Lafont/JCSLecatY2K.html>). The shadow is probably due to the anchoring of the myristoyl group into the bilayer, arising from crosslinking to phospholipids. Because of the presence of the annexin II band overlapping the annexin XIIIa staining, we could not determine unambiguously whether a shadow was associated with annexin XIIIa using the anti-annexin XIII-II antibody. We therefore decided to analyze the membrane association of annexin XIIIa and XIIIb by different approaches.

Hydrophobic interactions are contributing to the membrane binding of annexin XIIIs

A homogenate of MDCKII cells was prepared in the absence of calcium, and membranes were collected on a sucrose

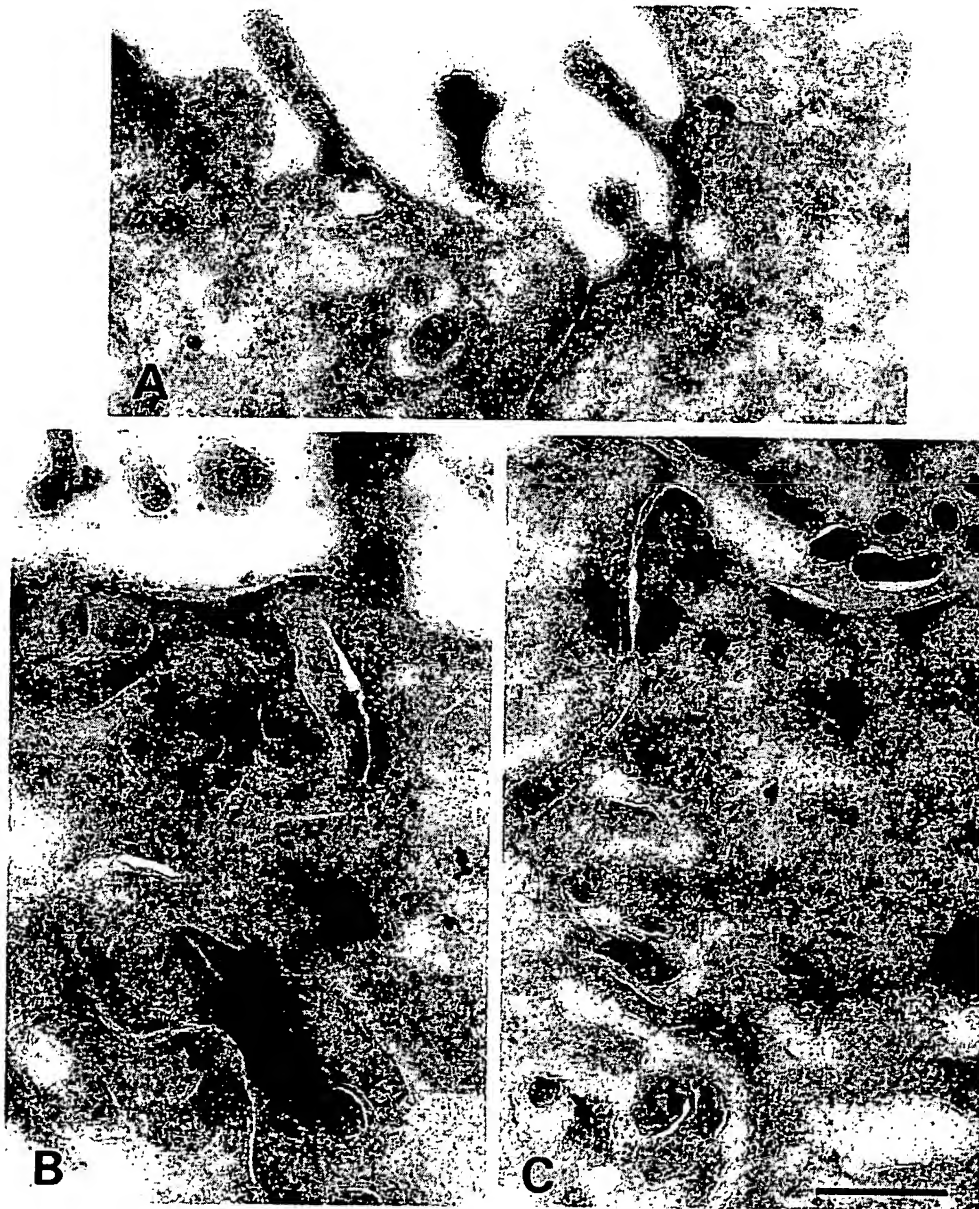


Fig. 3. Immunogold labeling of annexin XIIIa, non-myristoylated annexin XIIIa and annexin XIIIb in MDCKII cells. MDCKII cells infected with recombinant adenoviruses overexpressing annexin XIIIb (A), annexin XIIIa (B) or the non-myristoylated annexin XIIIa (C) were processed for immunoelectron microscopy with the anti-annexin XIII-II antibody (10 nm gold particles). Bar, 500 nm.

cushion by ultracentrifugation at 100,000 *g*. These pelleted membranes were washed with high salt or basic pH buffers and samples were subsequently centrifuged at 100000 *g*. The proteins released from the membrane pool were detected on western blots. The integrity of the membranes was assessed using VIP21/cav1 (Fig. 5A). For both isoforms of annexin XIII, binding to membranes was not abolished by high salt washes (Fig. 5B). Similarly, high pH stripping of the membranes released little protein (Fig. 5B). There are reports that myristoylated or palmitoylated proteins are resistant to pH 11 extraction (Song and Dohlman, 1996; Topinka and Bredt, 1998). The resistance of the annexin XIIIs to pH11 treatment shows that hydrophobic interactions are contributing to their membrane association and supports the conclusion of the crosslinking experiment described above.

Since annexin XIIIb has been shown to bind to cholesterol-sphingolipid rafts (Lafont et al., 1998b), we next analyzed whether cholesterol depletion using cyclodextrin was affecting the membrane binding of both annexin XIIIa and XIIIb.

Indeed, this was the only treatment which could significantly, although not entirely, release the annexin XIIIs into the supernatant (Fig. 5C).

A pool of annexin XIIIa is associated with rafts in absence of calcium

To demonstrate raft association of annexin XIIIb, we previously showed the presence of annexin XIIIb in lipid-protein complexes resistant to solubilisation by Triton X-100 at 4°C (Lafont et al., 1998b). These insoluble complexes are separated from solubilised proteins and from cytoskeletal elements by flotation in a density gradient. Insoluble complexes float to low density, unlike cytoskeletally bound elements and soluble proteins, which stay at the bottom of the flotation gradient. When MDCKII cells were lysed with TX-100 at 4°C in a buffer lacking calcium and the material was subsequently subjected to OptiPrep™ gradient centrifugation, part of annexin XIIIa was recovered in the low density fraction (Fig. 6A). This fraction was typically enriched in the

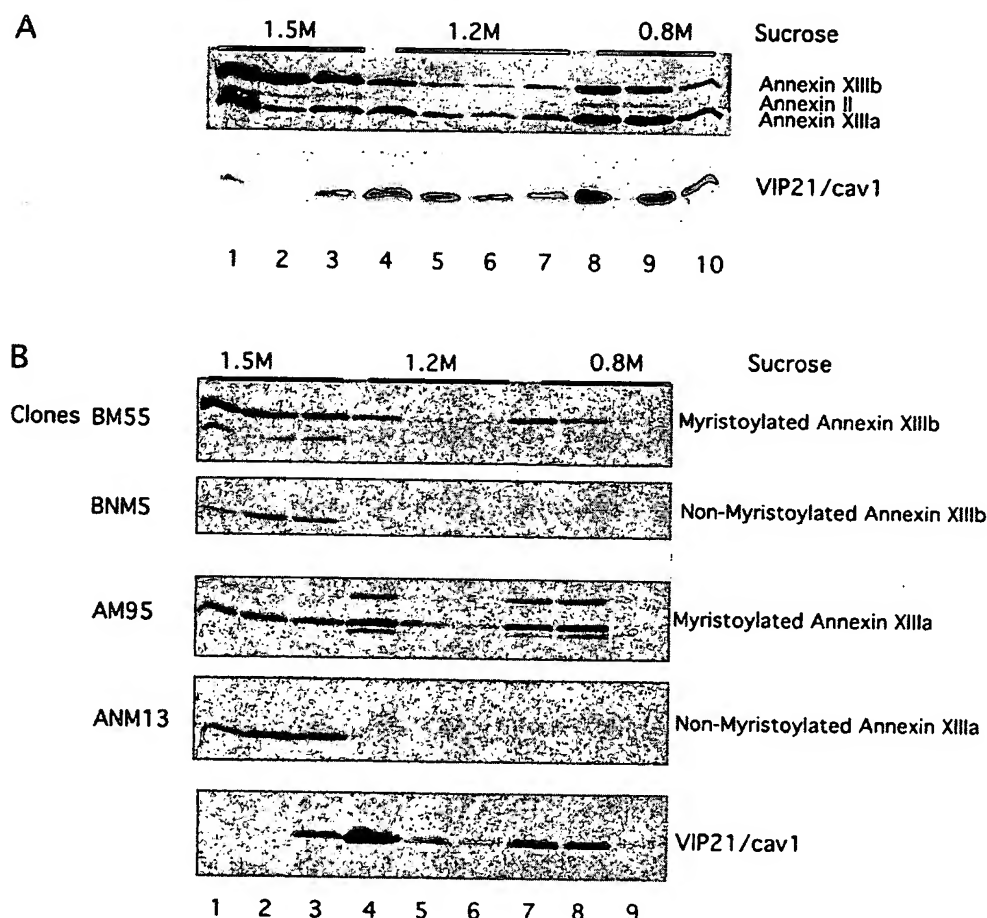


Fig. 4. Calcium-independent binding of annexin XIII to membranes. (A) MDCKII homogenate was prepared with EGTA. The membrane fractions were separated from the cytosolic proteins by a two-step sucrose gradient centrifugation. The partitioning of annexin XIIIb and VIP21/cav1 between the membranes (heavy membranes: fractions 4-5, light membranes: fractions 8-9) and the cytosolic pools (fractions 1-3) was analyzed by western blot using, respectively, anti-annexin XIII-II and anti-VIP21/cav1 antibodies. (B) Stable clones of MDCKII Lac switchable cells overexpressing either the wild-type or the non-myristoylated mutants of the annexin XIIIa were submitted to the two-step sucrose gradient centrifugation and the presence of annexin XIIIa and VIP21/cav1 in each fraction was followed by immunoblotting. Note that a band corresponding to the endogenous annexin II is visible in the immunoblot of the BM55 clone and that two bands corresponding to the endogenous annexin XIIIa (lower) and XIIIb (upper) are visible in the immunoblot of the AM95 clone.

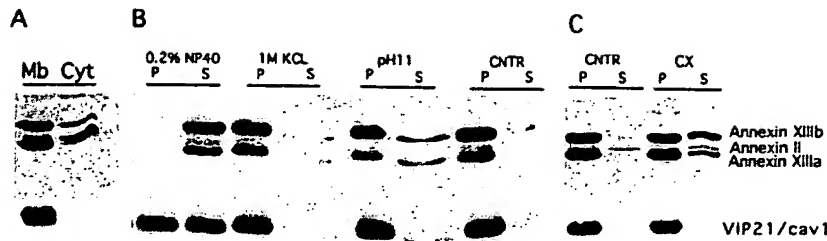


Fig. 5. Cyclodextrin treatment can partially release annexin XIIIa from membranes. (A) The total membrane (Mb) and cytosolic (Cyt) fractions of MDCKII cells were segregated by a 100,000 g spin of the PNS in the absence of calcium. (B) Membranes were subsequently subjected to no treatment (CNTR) or extracted for 15 minutes at 4°C with 0.1 M NaHCO₃, pH 11, 1 M KCl or 0.2% NP-40 at RT and then spun at 100,000 g and recovered in the pellet (P) while the released proteins were in the supernatant (S). (C) In order to extract cholesterol, membranes were treated with 10 mM cyclodextrin for 30 minutes at 37°C (CX) or left untreated as control (CNTR). The partitioning of annexin XIIIa and VIP21/cav1 between the fractions was analyzed by western blot using the respective antibodies.

cholesterol-binding protein VIP21/cav1. Neither annexin XIIIa nor XIIIb floated anymore after depletion of cholesterol by cyclodextrin (Fig. 6B). A pool of annexin XIIIa thus associates with lipid-rafts independently of calcium. However, we noticed that a fraction of annexin XIIIa was reproducibly associated with the low density fraction. We wondered whether this could reflect a differential behavior of apical versus basolateral annexin XIIIa.

To find out whether the apical and the basolateral pools of

annexin XIIIa differed in their raft-binding properties, we made use of the properties of MDCKII Lac switchable cells. This subclone differs from MDCKII cells by several criteria. For example, MDCKII Lac switchable cells express endogenous annexin XIIIa to a lower extent than MDCKII cells (data not shown) and have a lower capacity for apical delivery (Cheong et al., 1999). Another difference compared to MDCKII cells was that the overexpressed annexin XIIIa exclusively localised to the basolateral plasma membrane of MDCKII Lac switchable cells whereas the overexpressed annexin XIIIb was mostly apical (Fig. 7). This could be observed independently of the expression level by immunofluorescence after expression of annexin XIIIa either stably with pOPRSV1 vector (Fig. 7) or transiently with recombinant adenoviruses

(S. Lecat, unpublished results).

Because of the exclusive basolateral localization of annexin XIIIa in the MDCKII Lac switchable clone, we could analyze biochemically the raft association of the basolateral annexin XIIIa. We prepared detergent-insoluble material with calcium-chelating agents from stable clones expressing annexin XIIIa or XIIIb and performed step density gradient flotation. We found that annexin XIIIa was not floating while VIP21/cav1 (unpublished result) and annexin XIIIb (Fig. 8A) were floating to the same extent as in normal MDCKII cells.

Several annexins have been shown to float after Triton extraction in the presence of calcium (Parkin et al., 1996). This is particularly the case for the basolateral pool of annexin II, which has recently been observed in rafts together with CD44 (Oliferenko et al., 1999). We wanted therefore to compare the effect of calcium on the raft association of annexin XIIIa expressed in MDCKII Lac switchable cells versus that of annexin II. Increasing the calcium concentration to 200 μ M had no effect on VIP21/cav1 (unpublished result) or annexin XIIIb flotation (Fig. 8B). On the other hand, calcium triggered a drastic flotation of annexin II, as previously reported (Fig. 8B; Oliferenko et al., 1999) and a significant and reproducible flotation of a fraction of annexin XIIIa. To verify the specificity of the calcium-dependent raft association of annexin XIIIa, we made use of its non-myristoylated mutant. At a concentration of 1 mM calcium, annexin XIIIa lacking its fatty acid modification was entirely associated with the total membrane fraction recovered from a 100,000 g pellet (Fig. 8C). However, despite

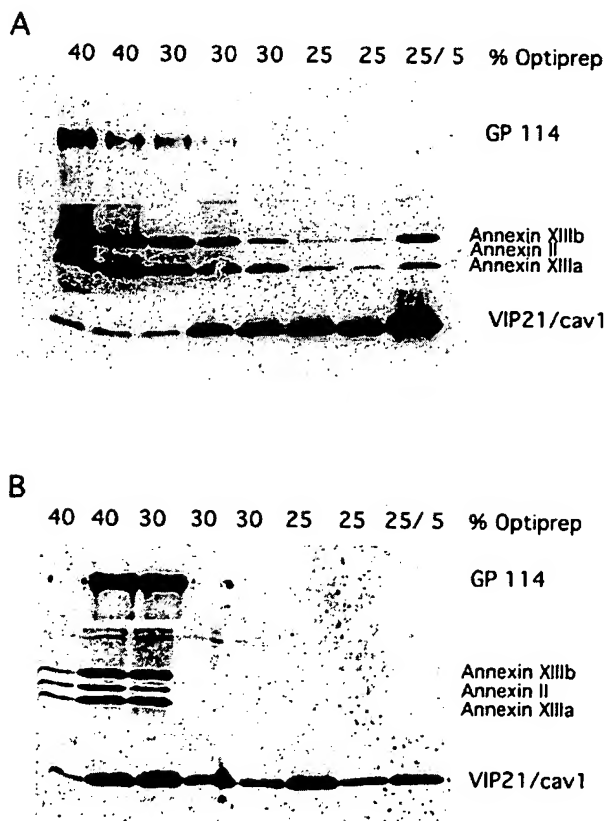


Fig. 6. A fraction of annexin XIIIa binds to detergent-insoluble glycosphingolipid enriched material (DIGs) independently of calcium. MDCKII cells were lysed in 1% TX-100 at 4°C in the absence of calcium and the DIGs were separated from the solubilised fraction by a centrifugation in an OptiPrep™ gradient. (A) The presence of GP114 (negative control), annexin XIIIa and VIP21/cav1 (positive control) in the different TCA-precipitated fractions of the gradient was analyzed by western blotting with anti-GP114, anti-annexin XIII-II and anti-VIP21/cav1 antibodies, respectively. (B) Upon extraction of cholesterol from the cell using cyclodextrin, the detergent-insoluble material is drastically reduced.

being bound to membranes, the non-myristoylated annexin XIIIa was not observed in the floating fractions.

Annexin XIIIa is differently implicated in the exocytic pathways of MDCKII cells

We previously reported that, in polarized MDCKII cells, a recombinant myristoylated annexin XIIIb could stimulate the apical delivery of exocytic carriers while the basolateral route was not affected (Lafont et al., 1998b). Here, we followed the transport of viral proteins targeted to either plasma membrane in the same functional assay as was used previously. This assay reconstitutes the trans-Golgi network (TGN)-to-apical or -to-basolateral surface transport steps in Streptolysin-O permeabilized MDCKII cells (Lafont et al., 1995). We found that the purified recombinant myristoylated annexin XIIIa (Fig. 9A), when introduced to permeabilized cells, was localized in both compartments (Fig. 9B) and could stimulate the apical delivery of transport carriers (Fig. 10C). On the contrary, basolateral transport was inhibited (Fig. 9C).

DISCUSSION

In this study, we show that both annexin XIII isoforms bind to membranes independently of calcium. Based on the cytosolic localization of the non-myristoylated mutants, we propose that the N-terminal myristoyl modification present in both isoforms

is necessary for the interaction with the lipid bilayer in the absence of calcium. Calcium-independent membrane binding has also been reported for other annexins. Annexin I interacts with the plasma membrane and with multivesicular bodies of NIH3T3 cells (Futter et al., 1993), annexins VI and II with clathrin coated pits (Turpin et al., 1998), annexin II with the plasma membrane of A549 cells (Liu et al., 1997) and with early endosomes in BHK cells (Jost et al., 1997). In the latter case, the domain important for calcium-independent binding to membrane has been mapped to amino acids 14-25 of the N-terminal tail of annexin II (Jost et al., 1997). A comparison of the known structures of annexins indicates that the N-terminal tail of annexin XIIIa should protrude out of the core domain on the face opposite to the calcium binding sites (Liemann and Lewit-Bentley, 1995). Our experiments suggest that the myristoyl group at the N terminus is inserted in the lipid bilayer. Thus, due to the shortness of the tail of annexin XIIIa (12 amino acids), the calcium binding sites of the annexin XIIIa core domain might be prevented from facing the membrane, and instead, be exposed towards the cytosol. This opens new perspectives for the function of the annexin core, which could interact in a calcium-dependent manner with proteins in addition to its lipid binding potential. Such a possibility is strengthened by the structural data obtained for the hexameric annexin XII, in which the calcium-binding sites were mediating face-to-face binding of one trimer to another (Luecke et al., 1995). A similar dual binding capacity has been

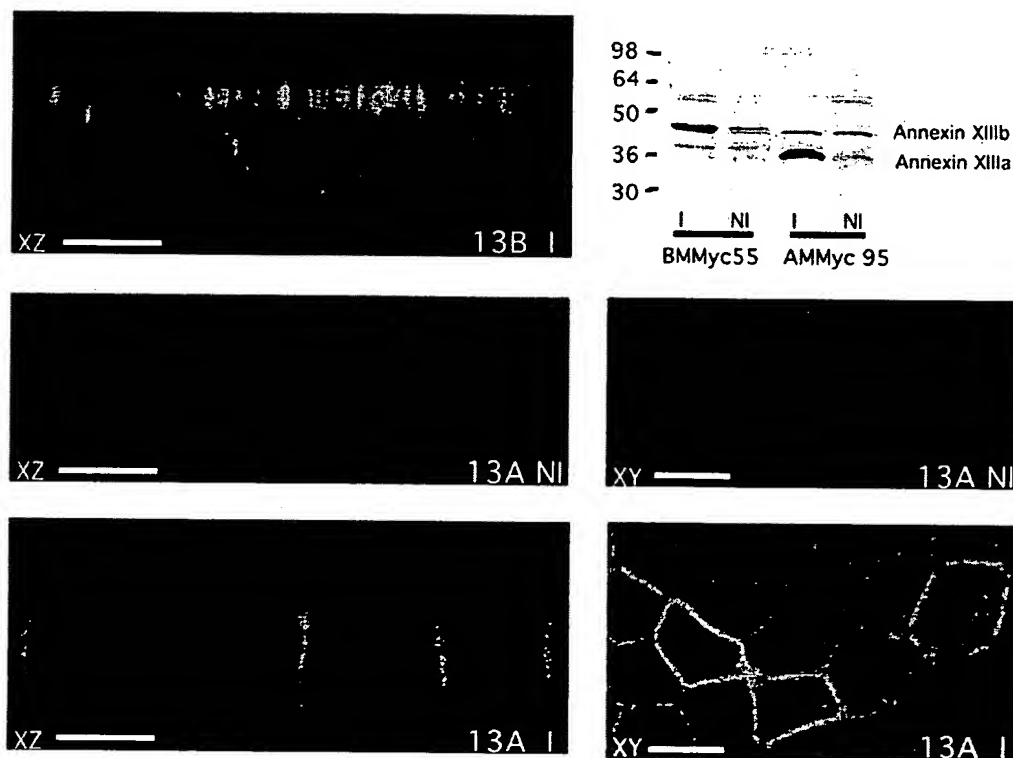


Fig. 7. Basolateral localization of annexin XIIIa in MDCKII Lac switchable cells. Stable clones of MDCKII Lac switchable cells overexpressing either annexin XIIIb (13B) or XIIIa (13A) in an inducible manner were analyzed by immunoblotting and by immunofluorescence confocal microscopy with anti-annexin XIII-II antibody. Confocal xz and xy sections are shown. I, Induced, NI, non-induced. Bar, 10 µm. Note in the immunoblots (upper right panel) that the overexpressed annexin XIIIs are running slower than the endogenous proteins due to their fusion to the myc-tag. In addition, a band corresponding to the endogenous annexin II is slightly visible in the immunoblot of the BM55 clone and a band corresponding to the endogenous annexin XIIIb is visible in the immunoblot of the AM95 clone.

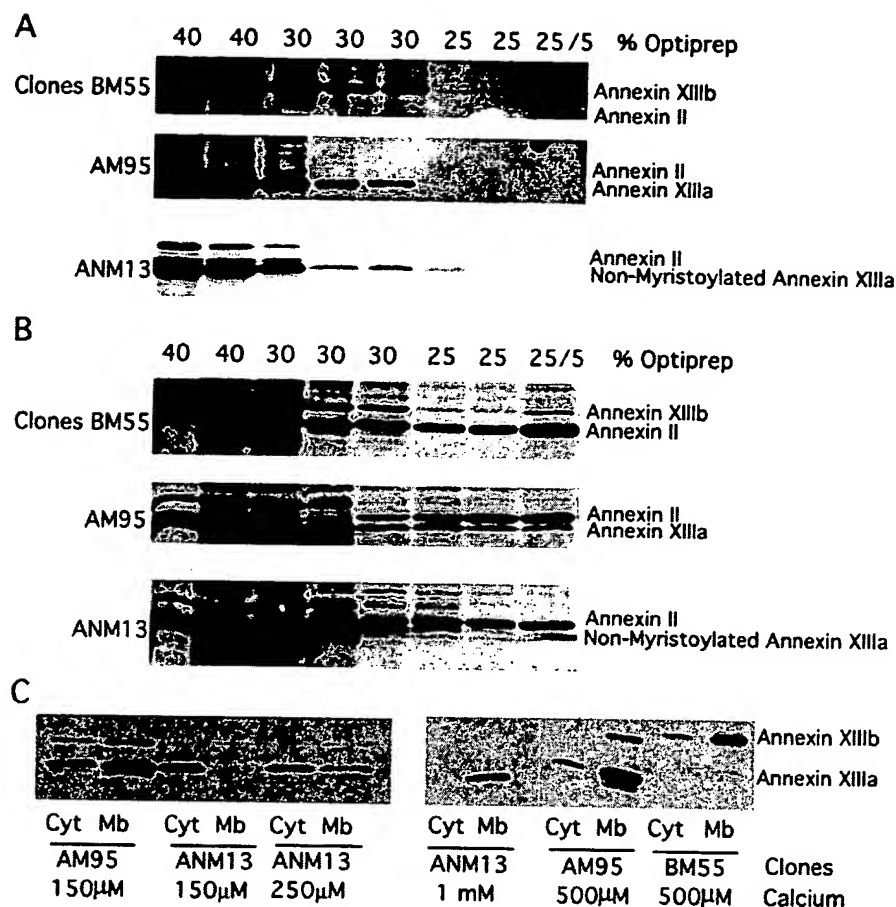


Fig. 8. Raft association of basolateral annexin XIIIa is dependent on calcium and the myristoyl group. Detergent-resistant membranes were prepared from the stable clones of MDCKII Lac switchable cells overexpressing either annexin XIIIb, annexin XIIIa or the non-myristoylated annexin XIIIa in the absence (A) or presence of 1 mM calcium (B). The different TCA-precipitated fractions collected after the OptiPrep™ gradient centrifugation were tested for their content of annexin XIIIa by western blot with the anti-annexin XIII-II antibody. Note that the endogenous annexins are visible in addition to the exogenous annexin XIIIa; in particular, the annexin II staining becomes extremely strong once the sample is prepared in presence of calcium. The membrane (Mb) and cytosolic (Cyt) pools were segregated by a 100,000 *g* spin and analyzed for their content of annexin XIIIa, myristoylated or not, by western blotting with anti-annexin XIII-II antibody. The non-myristoylated annexin XIIIa is entirely recovered in the membrane fraction at 1 mM calcium, while at 150 μM calcium it is still mostly cytosolic. The myristoylated annexin XIIIa are almost completely bound to the membrane fraction at 500 μM calcium. Note that the endogenous annexin XIIIa (lower band in clone AM95) and XIIIb (upper band in all the clones) are visible in the immunoblot.

demonstrated for the C2 domain (also called CaLB), another calcium-dependent phospholipid binding domain (Davis et al., 1998). For example, the C2A domain of synaptotagmin interacts in a calcium-dependent manner with phospholipids but can also bind to syntaxin or dimerize with itself (Popoli et al., 1997). Interestingly, the C2 domain of p120ras GAP interacts with annexin VI in a calcium-dependent manner (Davis et al., 1996).

With the exception of annexin II and annexin XIIIb, the association of annexins with lipid rafts has not been studied. Here we show by flotation after Triton X-100 solubilization that the apical annexin XIIIa is raft-associated in the absence of calcium while the basolateral annexin XIIIa only associates with rafts in the presence of calcium. Lipid rafts are present both apically and basolaterally but are enriched apically (Simons and van Meer, 1988; Benting et al., 1999). Annexin II and the integral membrane protein CD44 were shown to

partition into rafts at the basolateral plasma membrane of mammary gland epithelial (Oliferenko et al., 1999). This interaction of annexin II with the basolateral rafts was shown to require calcium. How annexin II binds to lipid rafts is not known. In the case of annexin XIIIa, this binding involves the myristoylated N-terminal tail, since in presence of calcium, the non-myristoylated annexin XIIIa was able to bind membranes but not to lipid rafts as assayed by detergent insolubility. The composition of the inner leaflet of rafts is not yet defined. The differential localization of different annexins is difficult to explain without assuming the existence of protein partners for annexin XIIIa. Identifying these putative linkers would help to understand their functions.

We have previously demonstrated that annexin XIIIb is involved functionally in apical transport from the TGN (Lafont et al., 1998b). The data suggested that annexin XIIIb could play a role both during formation of the apical transport containers

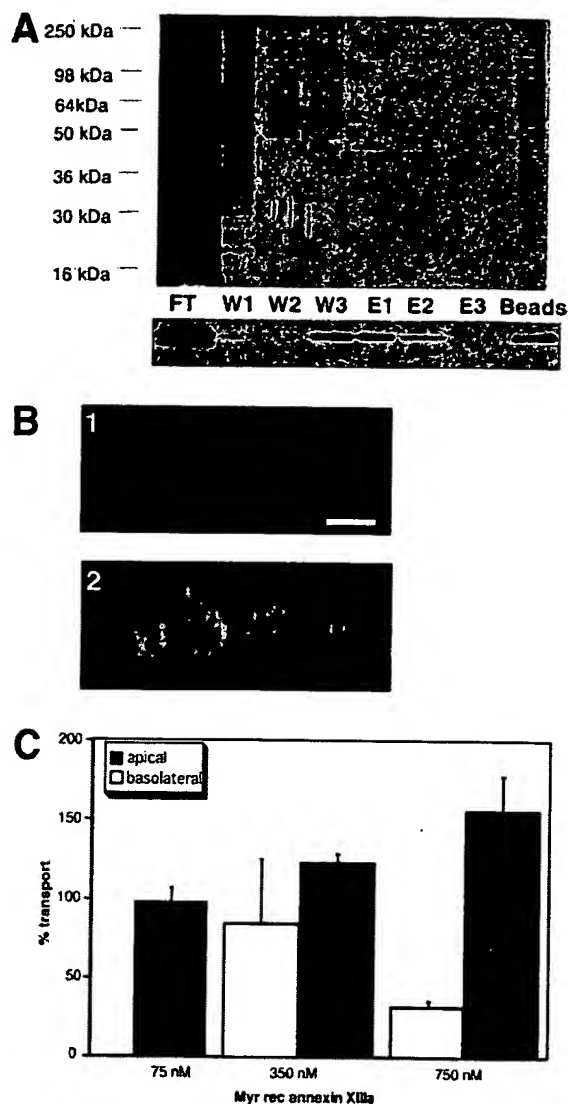


Fig. 9. Annexin XIIIa is differently involved in the exocytic routes in MDCK cells. (A) Upper panel, silver staining of the purified recombinant myristoylated annexin XIIIa expressed in Schneider cells. Lower panel, western blotting using the anti-annexin XIII-II antibody. Samples analyzed are Ni-column flowthrough (FT); imidazole washes 10 mM (W1), 20 mM (W2); 40 mM (W3); elutions 120 mM imidazole (E1-3); Ni beads (B). (B) Immunostaining of recombinant annexin XIIIa (green) in Streptolysin-O permeabilized MDCK cells. Affinity-purified anti-annexin XIII-II was used at 1:200 dilution and nuclei were visualized after DNA staining with propidium iodide. A confocal xz section is shown; bar, 15 µm. Note that the protein is present in both compartments. (C) Transport assay performed in permeabilized MDCKII cells with the hemagglutinin of influenza virus as an apical reporter and the glycoprotein of vesicular stomatitis virus as a basolateral reporter. Values of duplicate samples from three independent experiments are shown as % transport (mean \pm s.e.m.).

in the TGN and at the docking and the fusion stage of delivery. These results conform with the localization of annexin XIIIb, which has been visualized along the apical pathway from the TGN to the apical membrane. Annexin XIIIa, on the other

hand, was only localized basolaterally in the MDCKII Lac switchable cells, and both apically and basolaterally in the MDCKII cells. Thus the unique 41-amino-acid insertion in the N-terminal tail of annexin XIIIb is likely to contain an apical localization determinant. We attempted to analyze the function of annexin XIIIa using the SLO-permeabilized cell system to investigate its role in apical or in basolateral transport from the TGN. Recombinant myristoylated annexin XIIIa, when added to the permeabilized MDCK cells, was able to enhance apical delivery of influenza virus hemagglutinin as efficiently as annexin XIIIb did. However, contrary to annexin XIIIb, the recombinant annexin XIIIa had an inhibitory affect on the basolateral delivery of VSV-G; recombinant annexin XIIIb had no effect. Thus annexins XIIIb and XIIIa behave identically in the apical compartment. This is perhaps not surprising because apical annexins XIIIb and XIIIa are so similar in their properties. The exact function of annexin XIII in the apical compartment is not yet defined. The protein could help to cluster lipid rafts and associated proteins into apical transport containers, or alternatively could be involved in organizing the docking and fusion stage of the apical delivery. It cannot, however, be excluded that the protein plays its main role in regulating raft-mediated processes at the apical surface. The role of basolateral annexin XIIIa is even more difficult to pinpoint. Does the finding that annexin XIIIa is only basolaterally localized in the MDCK II Lac switchable cell strain suggest that its function is mainly there and that the apical localization in MDCKII cells is due to overexpression? Or do MDCKII Lac switchable cells lack a protein that localizes annexin XIIIa to the apical compartment? In this respect, the random redistribution of the myristoylated apical type II cGMP-dependent protein kinase occurring in the Microvillus Inclusion Disease, presumably because of a sorting deficiency, is of particular interest (Ameen and Salas, 2000). The inhibitory effect on basolateral transport in the SLO-permeabilized MDCKII cells may reflect binding to lipid rafts being transported basolaterally (Benting et al., 1999), and due to steric hindrance this binding inhibits the assembly of the basolateral transport containers. The enigma of the functional roles of the annexins remains. The fact that two very similar isoforms of annexin XIII are so different in their properties is an interesting topic for further research.

Kim Ekroos and Sigrun Brendel are acknowledged for their expert technical assistance. We are extremely thankful to Jeremy Garwood and Ulla Lahtinen for their comments and advice on the manuscript. The TCS-NT confocal laser scan microscope was provided by Leica Lasertechnik (Heidelberg, Germany) as an active participant in the Advanced Light Microscopy Facility at EMBL. This work was supported by the Commission of European Communities and the grant SFB 352 (to K.S.).

REFERENCES

- Ahmed, S. N., Brown, D. A. and London, E. (1997). On the origin of sphingolipid/cholesterol-rich detergent-insoluble cell membranes: Physiological concentrations of cholesterol and sphingolipid induce formation of a detergent-insoluble, liquid-ordered lipid phase in model. *Biochemistry* 36, 10944-10953.
- Ameen, N. A. and Salas, P. J. I. (2000). Microvillus inclusion disease: A genetic defect affecting apical membrane protein traffic in intestinal epithelium. *Traffic* 1, 76-83.

- Arispe, N., Rojas, E., Genge, B. R., Wu, L. N. and Wuthier, R. E. (1996). Similarity in calcium channel activity of annexin V and matrix vesicles in planar lipid bilayers. *Biophys. J.* 71, 1764-1775.
- Balcarova-Ständer, J., Pfeiffer, S.E., Fuller, S.D. and Simons, K. (1984). Development of cell surface polarity in the epithelial Madin-Darby canine kidney (MDCK) cell line. *EMBO J.* 3, 2687-2694.
- Barwise, J. L. and Walker, J. H. (1996). Annexins II, IV, V and VI relocate in response to rises in intracellular calcium in human foreskin fibroblasts. *J. Cell Sci.* 109, 247-255.
- Benting, J. H., Rietveld, A. G. and Simons, K. (1999). N-glycans mediate the apical sorting of a GPI-anchored raft-associated protein in Madin-Darby canine kidney cells. *J. Cell Biol.* 146, 313-320.
- Bitto, E. and Cho, W. (1998). Roles of individual domains of annexin I in its vesicle binding and vesicle aggregation: a comprehensive mutagenesis study. *Biochemistry* 37, 10231-10237.
- Brown, D. A. and London, E. (1997). Structure of detergent-resistant membrane domains: does phase separation occur in biological membranes? *Biochem. Biophys. Res. Commun.* 240, 1-7.
- Brown, D. A. and London, E. (1998). Functions of lipid rafts in biological membranes. *Annu. Rev. Cell. Dev. Biol.* 14, 111-136.
- Brown, R. E. (1998). Sphingolipid organization in biomembranes: what physical studies of model membranes reveal. *J. Cell Sci.* 111, 1-9.
- Burgoyne, R. D. and Clague, M. J. (1994). Annexins in the endocytic pathway. *Trends Biochem. Sci.* 19, 231-232.
- Campos, G. R., Kanemitsu, M. and Boynton, A. L. (1990). Epidermal growth factor induces the accumulation of calpactin II on the cell surface during membrane ruffling. *Cell Motil. Cytoskel.* 15, 34-40.
- Carroll, A. D., Moyon, C., Kesteren, P. V., Tooke, F., Battley, N. H. and Brownlee, C. (1998). Calcium, Annexins, and GTP modulate exocytosis from maize root cap protoplasts. *Plant Cell* 10, 1267-1276.
- Chasserot, G. S., Vitale, N., Sagot, I., Delouche, B., Dirrig, S., Pradel, L. A., Henry, J. P., Aunis, D. and Bader, M. F. (1996). Annexin II in exocytosis: catecholamine secretion requires the translocation of p36 to the subplasmalemmal region in chromaffin cells. *J. Cell Biol.* 133, 1217-1236.
- Chen, J. M., Sheldon, A. and Pincus, M. R. (1993). Structure-function correlations of calcium binding and calcium channel activities based on 3-dimensional models of human annexins I, II, III, V and VII. *J. Biomol. Struct. Dyn.* 10, 1067-1089.
- Cheong, K. H., Zacchetti, D., Schneeberger, E. E. and Simons, K. (1999). VIP17/MAL, a lipid raft-associated protein, is involved in apical transport in MDCK cells. *Proc. Natl. Acad. Sci. USA* 96, 6241-6248.
- Creutz, C. E. (1992). The annexins and exocytosis. *Science* 258, 924-931.
- Davis, A. J., Butt, J. T., Walker, J. H., Moss, S. E. and Gawler, D. J. (1996). The calcium-dependent lipid binding domain of P120GAP mediates protein-protein interaction with calcium-dependent membrane binding proteins. Evidence for a direct interaction between annexin VI and P120GAP. *J. Biol. Chem.* 271, 24333-24336.
- Davis, A. J., Chow, A. H. and Gawler, D. J. (1998). Protein-protein and protein-lipid interactions of the CaLB domain. *Biochem. Soc. Trans.* 26, S119.
- Demange, P., Voges, D., Benz, J., Liemann, S., Gottig, P., Berendes, R., Burger, A. and Huber, R. (1994). Annexin V: the key to understanding ion selectivity and voltage regulation? *Trends Biochem. Sci.* 19, 272-276.
- Doi, O., Doi, F., Schroeder, F., Alberts, A. W. and Vagelos, P. R. (1978). Manipulation of fatty acid composition of membrane phospholipid and its effects on cell growth in mouse LM cells. *Biochim. Biophys. Acta.* 509, 239-250.
- Donnelly, S. R. and Moss, S. E. (1997). Annexins in the secretory pathway. *Cell. Mol. Life Sci.* 53, 533-538.
- Emans, N., Gorvel, J. P., Walter, C., Gerke, V., Kellner, R., Griffiths, G. and Gruenberg, J. (1993). Annexin II is a major component of fusogenic endosomal vesicles. *J. Cell Biol.* 120, 1357-1369.
- Ernst, J. D. (1991). Annexin III translocates to the periphasosomal region when neutrophils ingest opsonized yeast. *J. Immunol.* 146, 3110-3114.
- Ernst, J. D., Hoyer, H., Blackwood, R. A. and Mock, T. L. (1991). Identification of a domain that mediates vesicle aggregation reveals functional diversity of annexin repeats. *J. Biol. Chem.* 266, 6670-6673.
- Fiedler, K., Kellner, R. and Simons, K. (1997). Mapping the protein composition of trans-Golgi network (TGN)-derived carrier vesicles from polarized MDCK cells. *Electrophoresis* 18, 2613-2619.
- Fiedler, K., Kobayashi, T., Kurzhalia, T. V. and Simons, K. (1993). Glycosphingolipid-enriched, detergent-insoluble complexes in protein sorting in epithelial cells. *Biochemistry* 32, 6365-6373.
- Fiedler, K., Lafont, F., Parton, R. G. and Simons, K. (1995). Annexin XIIIb: a novel epithelial specific annexin is implicated in vesicular traffic to the apical plasma membrane. *J. Cell Biol.* 128, 1043-1053.
- Futter, C. E., Felder, S., Schlessinger, J., Ullrich, A. and Hopkins, C. R. (1993). Annexin I is phosphorylated in the multivesicular body during the processing of the epidermal growth factor receptor. *J. Cell Biol.* 120, 77-83.
- Harder, T. and Gerke, V. (1993). The subcellular distribution of early endosomes is affected by the annexin IIp11(2) complex. *J. Cell Biol.* 123, 1119-1132.
- He, T. C., Zhou, S., da Costa, L. T., Yu, J., Kinzler, K. W. and Vogelstein, B. (1998). A simplified system for generating recombinant adenoviruses. *Proc. Natl. Acad. Sci.* 95, 3978-3983.
- Hofmann, A., Benz, J., Liemann, S. and Huber, R. (1997). Voltage dependent binding of annexin V, annexin VI and annexin VII-core to acidic phospholipid membranes. *Biochim. Biophys. Acta* 1330, 254-264.
- Jost, M., Zeuschner, D., Seeman, J., Weber, K. and Gerke, V. (1997). Identification and characterization of a novel type of annexin-membrane interaction: Ca²⁺ is not required for the association of annexin II with early endosomes. *J. Cell Sci.* 110, 221-228.
- Kaetzel, M. A., Chan, H. C., Dubinsky, W. P., Dedman, J. R. and Nelson, D. J. (1994). A role for annexin IV in epithelial cell function. Inhibition of calcium-activated chloride conductance. *J. Biol. Chem.* 269, 5297-5302.
- Kamal, A., Ying, Y. and Anderson, R. G. (1998). Annexin VI-mediated loss of spectrin during coated pit budding is coupled to delivery of LDL to lysosomes. *J. Cell Biol.* 142, 937-947.
- Keller, P. and Simons, K. (1998). Cholesterol is required for surface transport of influenza virus hemagglutinin. *J. Cell Biol.* 140, 1357-1367.
- König, J., Prenen, J., Nilius, B. and Gerke, V. (1998). The annexin II-p11 complex is involved in regulated exocytosis in bovine pulmonary artery endothelial cells. *J. Biol. Chem.* 273, 19679-19684.
- Lafont, F., Ikonen, E. and Simons, K. (1998a). Permeabilized epithelial cells to study exocytic membrane transport. In *Cell Biology: A laboratory handbook*, vol. 2 (ed. J. E. Celis) pp. 227-236. San Diego, California: Academic Press.
- Lafont, F., Lecat, S., Verkade, P. and Simons, K. (1998b). Annexin XIIIb associates with lipid microdomain to function in apical delivery. *J. Cell Biol.* 142, 1413-1427.
- Lafont, F., Simons, K. and Ikonen, E. (1995). Dissecting the molecular mechanisms of polarized membrane traffic: reconstitution of three transport steps in epithelial cells using Streptolysin-O permeabilization. *Cold Spring Harbor Symp. Quant. Biol.* LX, 753-762.
- Langen, R., Isas, J. M., Luecke, H., Haigler, H. T. and Hubbell, W. L. (1998). A transmembrane form of annexin XII detected by site-directed spin labeling. *Proc. Natl. Acad. Sci. USA* 95, 14060-14065.
- Lecat, S. and Lafont, F. (1999). Annexins and their interacting proteins in membrane traffic. *Protoplasma* 207, 133-140.
- Liemann, S., Benz, J., Burger, A., Voges, D., Hofmann, A., Huber, R. and Gottig, P. (1996). Structural and functional characterisation of the voltage sensor in the ion channel human annexin V. *J. Mol. Biol.* 258, 555-561.
- Liemann, S. and Huber, R. (1997). Three-dimensional structure of annexins. *Cell. Mol. Life Sci.* 53, 516-521.
- Liemann, S. and Lewit-Bentley, A. (1995). Annexins: a novel family of calcium- and membrane-binding proteins in search of a function. *Structure* 3, 233-237.
- Liu, L., Tao, J. Q. and Zimmerman, U. J. (1997). Annexin II binds to the membrane of A549 cells in a calcium-dependent and calcium-independent manner. *Cell Signal.* 9, 299-304.
- Luecke, H., Chang, B. T., Mailliard, W. S., Schlaepfer, D. D. and Haigler, H. T. (1995). Crystal structure of the annexin XII hexamer and implications for bilayer insertion. *Nature* 378, 512-515.
- Mahoney, E. M., Hamill, A. L., Scott, W. A. and Cohn, Z. A. (1977). Response of endocytosis to altered fatty acyl composition of macrophage phospholipids. *Proc. Natl. Acad. Sci. USA* 74, 4895-4899.
- McCarthy, K. M., Skare, I. B., Stankewich, M. C., Furuse, M., Tsukita, S., Rogers, R. A., Lynch, R. D. and Schneeberger, E. E. (1996). Occludin is a functional component of the tight junction. *J. Cell Sci.* 109, 2287-2298.
- Morgan, R. O. and Fernandez, M. P. (1997). Annexin gene structures and molecular evolutionary genetics. *Cell. Mol. Life Sci.* 53, 508-515.
- Nilius, B., Gerke, V., Prenen, J., Szucs, G., Heinke, S., Weber, K. and Droogmans, G. (1996). Annexin II modulates volume-activated chloride currents in vascular endothelial cells. *J. Biol. Chem.* 271, 30631-30636.
- Oliferenko, S., Paiha, K., Harder, T., Gerke, V., Schwarzler, C., Schwarz, H., Beug, H., Gunthert, U. and Huber, L. A. (1999). Analysis of CD44-

- containing lipid rafts: Recruitment of annexin II and stabilization by the actin cytoskeleton. *J. Cell Biol.* 146, 843-854.
- Parkin, E. T., Turner, A. J. and Hooper, N. M. (1996). Isolation and characterization of two distinct low-density, triton-insoluble, complexes from porcine lung membranes. *Biochem. J.* 319, 887-896.
- Pimplikar, S. W., Ikonen, E. and Simons, K. (1994). Basolateral protein transport in streptolysin O-permeabilized MDCK cells. *J. Cell. Biol.* 125, 1025-1035.
- Popoli, M., Venegoni, A., Buffa, L. and Racagni, G. (1997). Calcium/phospholipid-binding and syntaxin-binding of native synaptotagmin I. *Life Sci.* 61, 711-721.
- Rietveld, A. and Simons, K. (1998). The differential miscibility of lipids as the basis for the formation of functional membrane rafts. *Biochim. Biophys. Acta* 1376, 467-479.
- Rosengarth, A., Wintergalen, A., Galla, H. J., Hinz, H. J. and Gerke, V. (1998). Calcium-independent interaction of annexin I with phospholipids monolayers. *FEBS Lett.* 438, 279-284.
- Selbert, S., Fischer, P., Menke, A., Jockusch, H., Pongratz, D. and Noegel, A. A. (1996). Annexin VII relocalization as a result of dystrophin deficiency. *Exp. Cell Res.* 222, 199-208.
- Selbert, S., Fischer, P., Pongratz, D., Stewart, M. and Noegel, A. A. (1995). Expression and localization of annexin VII (synexin) in muscle cells. *J. Cell Sci.* 108, 85-95.
- Simons, K. and Ikonen, E. (1997). Functional rafts in cell membranes. *Nature* 387, 569-572.
- Simons, K. and van Meer, G. (1988). Lipid sorting in epithelial cells. *Biochemistry* 27, 6197-6202.
- Song, J. and Dohlman, H. G. (1996). Partial constitutive activation of pheromone responses by a palmitoylation-site mutant of a G protein alpha subunit in yeast. *Biochemistry* 35, 14806-14817.
- Thiele, C., Hanna, M. J., Fahrenholz, F. and Huttner, W. B. (2000). Cholesterol binds to synaptophysin and is required for biogenesis of synaptic vesicles. *Nature Cell Biol.* 2, 42-49.
- Topinka, J. R. and Brecht, D. S. (1998). N-terminal palmitoylation of PSD-95 regulates association with cell membranes and interaction with K⁺ channel Kv1.4. *Neuron* 20, 125-134.
- Trotter, P. J., Orchard, M. A. and Walker, J. H. (1994). Thrombin stimulates the intracellular relocation of annexin V in human platelets. *Biochim. Biophys. Acta* 1222, 135-140.
- Trotter, P. J., Orchard, M. A. and Walker, J. H. (1995). EGTA-resistant binding of annexin V to platelet membranes can be induced by physiological calcium concentrations. *Biochem. Soc. Trans.* 23, 375.
- Turpin, E., Russo-Marie, F., Dubois, T., de Paillerets, C., Alfsen, A. and Bomsel, M. (1998). In adrenocortical tissue, annexins II and VI are attached to clathrin coated vesicles in a calcium-independent manner. *Biochim. Biophys. Acta* 1402, 115-130.
- Wice, B. M. and Gordon, J. I. (1992). A strategy for isolation of cDNAs encoding proteins affecting human intestinal epithelial cell growth and differentiation: Characterization of a novel gut-specific N-myristoylated annexin. *J. Cell Biol.* 116, 405-422.

In vivo detection and imaging of phosphatidylserine expression during programmed cell death

FRANCIS G. BLANKENBERG^{*†}, PETER D. KATSIKIS[‡], JONATHAN F. TAIT[§], R. ERIC DAVIS[¶], LOUIS NAUMOVSKI^{||}, KATSUICHI OHTSUKI[†], SUSAN KOPIWODA[†], MICHAEL J. ABRAMS^{**}, MARILYN DARKES^{**}, ROBERT C. ROBBINS^{††}, HOLDEN T. MAECKER^{‡‡}, AND H.W. STRAUSS[†]

[†]Department of Radiology, [‡]Department of Genetics, [§]Department of Pathology, ^{||}Department of Pediatrics (Hematology/Oncology), ^{††}Department of Cardiothoracic Surgery, ^{‡‡}Department of Medicine/Oncology, Stanford University School of Medicine, 300 Pasteur Drive, Stanford, CA 94305-5105; [¶]Department of Laboratory Medicine, University of Washington, Health Sciences, Room NW-120, Box 357110, Seattle, WA 98195-7110; and ^{**}Anor MED Incorporated, 20353 64th Avenue, Suite #100, Langley, British Columbia, Canada 3A7R3

Communicated by Victor A. McKusick, Johns Hopkins University, Baltimore, MD, March 6, 1998 (Received for review January 27, 1998)

ABSTRACT One of the earliest events in programmed cell death is the externalization of phosphatidylserine, a membrane phospholipid normally restricted to the inner leaflet of the lipid bilayer. Annexin V, an endogenous human protein with a high affinity for membrane bound phosphatidylserine, can be used *in vitro* to detect apoptosis before other well described morphologic or nuclear changes associated with programmed cell death. We tested the ability of exogenously administered radiolabeled annexin V to concentrate at sites of apoptotic cell death *in vivo*. After derivatization with hydrazinonicotinamide, annexin V was radiolabeled with technetium 99m. *In vivo* localization of technetium 99m hydrazinonicotinamide-annexin V was tested in three models: fulminant hepatic apoptosis induced by anti-Fas antibody injection in BALB/c mice; acute rejection in ACI rats with transplanted heterotopic PVG cardiac allografts; and cyclophosphamide treatment of transplanted 38C13 murine B cell lymphomas. External radionuclide imaging showed a two- to sixfold increase in the uptake of radiolabeled annexin V at sites of apoptosis in all three models. Immunohistochemical staining of cardiac allografts for exogenously administered annexin V revealed intense staining of numerous myocytes at the periphery of mononuclear infiltrates of which only a few demonstrated positive apoptotic nuclei by the terminal deoxynucleotidyltransferase-mediated UTP end labeling method. These results suggest that radiolabeled annexin V can be used *in vivo* as a noninvasive means to detect and serially image tissues and organs undergoing programmed cell death.

Programmed cell death (apoptosis) plays a crucial role in the pathogenesis of a number of disorders including AIDS and other viral illnesses, cerebral and myocardial ischemia, autoimmune and neurodegenerative diseases, organ and bone marrow transplant rejection, and tumor response to chemotherapy and radiation (1-3). Since the original description of apoptosis by Wyllie in 1972, its assessment *in vivo* has required direct examination of biopsied or aspirated material (4). An imaging technique capable of localizing and quantifying apoptosis *in vivo* would permit assessment of disease progression or regression and similarly define the efficacy of therapy designed to inhibit or induce cell death (5-6).

Cells undergoing apoptosis redistribute phosphatidylserine (PS) from the inner leaflet of the plasma membrane lipid bilayer to the outer leaflet (7, 8). The externalization of PS is a general feature of apoptosis occurring before membrane bleb formation and DNA degradation (7, 8). Annexin V, a human

protein with a molecular weight of 36,000 has a high affinity for cell or platelet membranes with exposed PS *in vitro* and *in vivo* (9-13). This observation has led to testing radiolabeled annexin V in animal models of acute thrombosis and imaging of atrial thrombi in patients with atrial fibrillation (14, 15). In the current study, annexin V was derivatized with hydrazinonicotinamide (HYNIC) and coupled to technetium 99m (^{99m}Tc) (16) before i.v. administration in animal models of apoptosis. HYNIC, a nicotinic acid analog, is a bifunctional molecule capable of bonding to lysine residues of proteins on one moiety and conjugates of ^{99m}Tc on the other. The agent forms stable complexes with proteins (16) without affecting bioactivity. We performed scintigraphic imaging studies with derivatized annexin V to determine its ability *in vivo* to detect sites of apoptotic cell death occurring in Fas-mediated hepatocyte apoptosis, acute cardiac allograft rejection, and cyclophosphamide treatment of B cell lymphoma. Such *in vivo* imaging may prove useful in the clinical setting for noninvasive diagnosis, monitoring of disease progression or regression, and determining efficacy of treatment.

MATERIALS AND METHODS

Preparation of ^{99m}Tc HYNIC-Annexin V. Human annexin V was produced by expression in *Escherichia coli* as described (13, 17, 18); this material retains PS-binding activity equivalent to that of native annexin V (18). Concentrations were determined using $E_{280} = 0.6 \text{ ml/mg}^{-1} \text{ cm}^{-1}$ and molecular weight was taken as 35, 806. HYNIC-derivatized annexin V was produced by the gentle mixing of 5.6 mg/ml of annexin V in 20 mM Hepes, pH 7.4, and 100 mM NaCl for 3 hr shielded from light with succinimidyl 6-HYNIC (Anor Med, Langley, British Columbia) [222 μg in 18.5 μl (42 mM solution) of *N,N*-dimethyl formamide] at room temperature. The reaction was quenched with 500 μl of 500 mM glycine in PBS, pH 7.4, and then dialyzed at 4°C against 20 mM sodium citrate, pH 5.2, and 100 mM NaCl overnight. Precipitate was then removed by centrifugation at $15,000 \times g$ for 10 min. Then, 100 μl (100 μg) aliquots of HYNIC-annexin V were stored at -70°C. Incorporation of HYNIC into annexin V was found to be 0.9 mol/mol of annexin V by using the methods of King *et al.* (19). Membrane-binding activity of HYNIC-annexin V and decayed ^{99m}Tc HYNIC-annexin V was determined by a modified competition assay in which 5 nmol/liter fluorescein isothiocyanate (FITC)-annexin V was substituted for ¹²⁵I-annexin V (12, 17). After incubation for 15 min at room temperature, cells

The publication costs of this article were defrayed in part by page charge payment. This article must therefore be hereby marked "advertisement" in accordance with 18 U.S.C. §1734 solely to indicate this fact.

© 1998 by The National Academy of Sciences 0027-8424/98/956349-6\$2.00/0 PNAS is available online at <http://www.pnas.org>.

Abbreviations: TUNEL, terminal deoxynucleotidyltransferase-mediated UTP end labeling; PS, phosphatidylserine; HYNIC, hydrazinonicotinamide; ^{99m}Tc, technetium 99m; FITC, fluorescein isothiocyanate; HSA, human serum albumin; ROI, region of interest.

*To whom reprint requests should be addressed. e-mail: MA.FRB@Forsythe.Stanford.Edu.

were centrifuged, the FITC-annexin V bound to the pelleted cells was released with EDTA, and the released FITC-annexin V was measured by fluorometry. In this assay system, unmodified annexin V, HYNIC-annexin V, and decayed ^{99m}Tc HYNIC-annexin V inhibited 50% of the binding of FITC-annexin V at concentrations of 8 nmol/liter, 10.5 nmol/liter, and 12.3 nmol/liter, respectively.

To bind ^{99m}Tc to the HYNIC-annexin conjugate 80 μl of stannous chloride (50 mg/ml in 0.1 M HCl purged for 2 hr with N_2 gas) was first added to 50 ml of a 20 mM tricine solution (pH 7.1, purged for 1 hr with N_2 gas; tricine = *N*-[tris(hydroxymethyl)methyl]glycine). Two hundred microliters of the Sn-tricine solution was then added to 100 μl of ^{99m}Tc O_4 (4–20 mCi (1 Ci = 37 GBq) activity in 0.9% NaCl) previously mixed with a 100 μl (100 μg) aliquot of HYNIC-annexin V according to the methods described by Abrams *et al.* (20). Specific activity was 10–200 $\mu\text{Ci}/\mu\text{g}$ protein (depending on desired activity) with a radiopurity of 92–97% determined with instant thin layer chromatography using 0.9% saline solution as a solvent.

Scintillation Well Counting. Samples were counted in a Packard Cobra II gamma counter (Packard). The energy window was set at a lower level of 120 keV and an upper level of 170 keV for ^{99m}Tc . When ^{125}I was counted, samples were allowed to decay for at least 24 hr. The samples were then recounted using both the technetium window and an ^{125}I setting with a lower level of 20 keV and an upper level of 50 keV. Samples were corrected for any residual cross talk.

Radionuclide Imaging. A Technicare 420 mobile camera (Technicare, Solon, OH) equipped with a low energy high resolution parallel hole collimator was used to record the radionuclide distribution in mice and rats sedated with a mixture of 80 mg/kg ketamine and 4 mg/kg acepromazine injected i.m. Data were recorded by using a 20% window centered on the 140 keV photpeak of technetium into a 128×128 matrix of a dedicated computer system for digital display and analysis (ICON, Siemens, Hoffman Estates, IL). All images were recorded for a preset time of 10–15 min.

Murine Model of Fas-Mediated Apoptosis. Massive hepatic apoptosis can be induced within 1–2 hr in mice following i.v. injection of anti-Fas antibody (21). We used this well described model of *in vivo* programmed cell death to test the specific localization of ^{99m}Tc HYNIC-annexin to an organ undergoing apoptosis *in vivo*. Four- to five-wk-old BALB/c mice were injected i.v. with purified hamster anti-Fas mAb (Jo2, 10 $\mu\text{g}/\text{animal}$, PharMingen, San Diego, CA) using the model proposed by Ogasawara *et al.* (21). Mice were then injected i.v. with 25–50 $\mu\text{g}/\text{kg}$ of ^{99m}Tc HYNIC-annexin V (10–25 $\mu\text{Ci}/\text{animal}$ for biodistribution study and 100–150 $\mu\text{Ci}/\text{animal}$ for imaging studies) 1 or 2 hr after antibody treatment. Animals were killed 1 hr after administration of radiopharmaceutical followed by organ removal for scintillation counting of radioactivity and for histologic and immunohistochemical analyses.

Control studies with ^{99m}Tc labeled human serum albumin (HSA) also were performed in untreated and anti-Fas treated mice. Although other proteins were considered as controls, albumin was selected because distinguishing the potential vascular disruption and protein leakage associated with acute apoptosis was a major goal of this control experiment. The animals were injected with 100–150 μCi of ^{99m}Tc labeled HSA (25 mg/animal) and imaged at 1 and 2 hr, in similar fashion to the mice receiving ^{99m}Tc HYNIC-annexin.

Rodent Model of Cardiac Transplantation. Adult male ACI rats (250–350 g) received heterotopic cardiac allografts from PVG donors (obtained from Harlan-Sprague-Dawley) anastomosed to the hosts' abdominal aorta and inferior vena cava according to a modification of the technique of Ono and Lindsey (22). Syngeneic cardiac isografts from ACI donors also were transplanted to the abdomens of host ACI rats. PVG cardiac allografts in ACI recipients using the model above begin to undergo rejection between 4 and 5 days post-

transplantation as assessed by decreased pulsation to palpation. Five days after transplantation all of the animals received 700–900 μCi of ^{99m}Tc HYNIC-annexin V (10–20 μg protein/kg) via tail vein and were imaged 1 hr later. Animals were then killed, and native and transplanted hearts underwent scintillation counting and histopathologic studies.

Murine Model of Lymphoma. 38C13 murine B cell lymphomas (23) were grown in C3H/HeN mice (Harlan Breeders, Indianapolis) following s.c. injection of 400 tumor cells suspended in 200 μl of RPMI medium 1640 (without serum) into the left flank. Fourteen days after implantation mice underwent treatment with 100 mg/kg of cyclophosphamide injected i.p. Mice were injected i.v. with 25–50 $\mu\text{g}/\text{kg}$ of ^{99m}Tc HYNIC-annexin V (100–150 $\mu\text{Ci}/\text{animal}$) 20 hr after cyclophosphamide administration. Animals were then imaged and killed 1 hr after injection of radiopharmaceutical after tumor removal for scintillation counting and histopathologic studies.

Immunostaining for Bound Human Annexin V and Apoptotic Nuclei. Formalin-fixed paraffin-embedded tissues were sectioned at 5 μm for staining with hematoxylin/eosin or other techniques. Immunostaining for bound human annexin V was performed with a rabbit anti-serum raised against human placental annexin V and affinity purified with recombinant annexin V coupled to Affi-Gel (Bio-Rad). Immunohistochemical detection then was completed by sequential incubations with biotin-labeled goat anti-rabbit antibody and avidin-horseradish peroxidase complex (Jackson Immuno Research), followed by reaction with 3,3'-diaminobenzidine as described by Bindl and Warnke (24).

For the detection of apoptotic nuclei, sections were stained using a modification of the terminal deoxynucleotidyltransferase-mediated UTP end labeling (TUNEL) method described by Gavrieli *et al.* (25). After inhibition of endogenous peroxidase, deparaffinized sections were digested with proteinase K (20 $\mu\text{g}/\text{ml}$) for 15 min at room temperature. Sections were then incubated with λ exonuclease (Life Technologies, Gaithersburg, MD) at 5 unit/ml for 30 min at 37°C followed by equilibration with terminal deoxynucleotidyltransferase reaction buffer (0.2 M potassium cacodylate, 25 mM Tris-HCl, 0.25 mg/ml BSA, 1.5 mM CaCl_2 , 20 mg/ml polyvinylpyrrolidone, and 20 mg/ml Ficoll) and 5 μM dATP. The end-labeling reaction then was performed in terminal deoxynucleotidyltransferase reaction buffer also containing a final concentration of 75 unit/ml of terminal deoxynucleotidyltransferase and 100 μM of 1,N-6-ethanol-dATP (Sigma). After a 60-min incubation at 37°C, the reaction was quenched via rinsing with $1 \times \text{SSC}$ (standard saline citrate). Sections were then incubated with murine 1G4 mAb (gift from Regina Santella, Columbia University), which recognizes the ethenoadenine moiety (26). Subsequent immuno-histochemical detection was as described above, using a biotin-labeled goat anti-mouse antibody.

RESULTS

Biodistribution of Radiolabeled Annexin V in Fulminant Hepatic Apoptosis. There was a 134% and 304% increase in the hepatic uptake of ^{99m}Tc HYNIC-annexin V above controls at 1 and 2 hr after anti-Fas antibody injection, respectively, as determined by biodistribution studies (Table 1). Hepatic uptake was inversely proportional to renal uptake in treated mice with a 75% decrease in renal activity 2 hr after treatment. Of note, there was <5% excretion of administered radiopharmaceutical into the urine in control or treated animals. Splenic uptake was 108% and 54% above control values in the 1- and 2-hr treatment groups, respectively.

Subgroups of mice were co-injected with ^{125}I -HSA to control for nonspecific uptake of inert protein from the circulation caused by hepatic endothelial cell breakdown (27). Hepatic uptake was 120% above control values at 1 hr after anti-Fas antibody injection and remained unchanged in contrast to the

Table 1. Biodistribution study of radiolabeled annexin V after anti-Fas antibody treatment

A)	^{99m} Tc	Controls	1-hr anti-Fas	2-hr anti-Fas
	% ID	(n = 9)	(n = 15)	(n = 12)
	Liver	12.2 ± 1.4	28.6 ± 9.4**	49.3 ± 12.7***
	Kidneys	55.9 ± 8.9	35.2 ± 14.4*	14.0 ± 10.0***
	Spleen	1.6 ± 0.25	3.34 ± 1.42*	2.46 ± 1.22(ns)
B)	¹²⁵ I	Controls	1-hr anti-Fas	2-hr anti-Fas
	% ID	(n = 4)	(n = 6)	(n = 5)
	Liver	3.98 ± 1.09	8.77 ± 3.53*	8.4 ± 1.92*
	Kidneys	1.37 ± 0.35	1.88 ± 0.37(ns)	1.82 ± 0.38(ns)
	Spleen	0.39 ± 0.09	0.47 ± 0.15(ns)	0.37 ± 0.041(ns)
C)	Weight	Controls	1-hr anti-Fas	2-hr anti-Fas
	(grams)	(n = 9)	(n = 15)	(n = 12)
	Liver	1.06 ± 0.097	1.29 ± 0.32(ns)	1.37 ± 0.22*
	Kidneys	0.31 ± 0.061	0.32 ± 0.079(ns)	0.37 ± 0.072(ns)
	Spleen	0.12 ± 0.022	0.12 ± 0.02(ns)	0.11 ± 0.014(ns)

% injected dose (ID) per organ corrected for background, decay, and tail infiltration are listed for mice injected with 100–150 μ Ci (radiopurity >95%, specific activity 150–200 μ Ci/ μ g protein) of ^{99m}Tc HYNIC-annexin co-injected with 0.6 μ Ci (25 mg) of ¹²⁵I radiolabeled HSA. A) Biodistribution of ^{99m}Tc HYNIC-annexin V, B) ¹²⁵I-HSA, and C) Organ weight. Data are expressed as mean \pm standard error of the mean. P-values are shown in parenthesis () for Dunnett's test for multiple comparison of means of the 1- or 2-hr post-treatment groups compared with control. ns, not significant (i.e., P-value > 0.05); *, P < 0.05; **, P < 0.001; ***, P < 0.0001.

progressive rise in annexin V uptake. There was a 29% increase in liver weight at 2 hr. Renal and splenic weight and uptake of ¹²⁵I-HSA did not change significantly after treatment.

Sections of livers from mice treated with anti-Fas antibody showed a spectrum of nuclear changes characteristic of apoptosis (margination of chromatin, pyknosis, and karyorrhexis) as early as 1 hr after injection; changes were more pronounced and focally associated with hemorrhage (peliosis) 2 hr after treatment (Fig. 1A). Immunostaining for ^{99m}Tc HYNIC-annexin V was observed at the cytoplasmic border of apoptotic hepatocytes; although this result was focal, the localization pattern is consistent with PS externalization, and staining never was observed in normal hepatocytes (Fig. 1B) or in anti-Fas antibody-treated mice not injected with ^{99m}Tc HYNIC-annexin V (data not shown).

In Vivo Imaging of Fas-Mediated Fulminant Hepatic Apoptosis. A high concentration of radiolabeled annexin V activity was observed by scintillation camera imaging in the kidneys of control animals with minimal concentration in other organs (Fig. 2). Hepatic uptake in control mice [12% of injected dose (% ID)] did not permit clear delineation of the liver. In mice treated with anti-Fas antibody, there was a diffuse increase in the intensity of hepatic uptake of ^{99m}Tc HYNIC-annexin V observed at 1 hr, which continued to rise at 2 hr after treatment. The transient increase in splenic uptake and the fall in renal activity found in the biodistribution studies both were visualized readily with external imaging following anti-Fas treatment. A total of 19 mice (six control, seven 1-hr, and six 2-hr anti-Fas-treated animals) underwent biodistribution study after imaging with ^{99m}Tc HYNIC-annexin V. The percentage of whole body activity per organ determined by region of interest (ROI) image analysis correlated well with the percentage of injected dose per organ determined by biodistribution (linear correlation coefficients for the liver, kidney, and spleen of $r^2 = 0.853, 0.860,$ and 0.979 , respectively.)

There was no perceptible difference in liver, renal, or splenic uptake on the ^{99m}Tc-HSA images between the treated mice and controls (images not shown). There also was a direct correlation of observed uptake of ^{99m}Tc-HSA as seen by ROI image analysis and the biodistribution of ^{99m}Tc-HSA (data not shown), which mirrored the biodistribution of ¹²⁵I-HSA.

In Vivo Imaging of Cardiac Allograft Rejection. All of the PVG cardiac allografts (n = 4) were visualized easily with ^{99m}Tc HYNIC-annexin V 5 days after transplantation (Fig. 3).

ACI syngeneic cardiac isografts (n = 3) had no visible activity after injection of ^{99m}Tc HYNIC-annexin with uptakes of

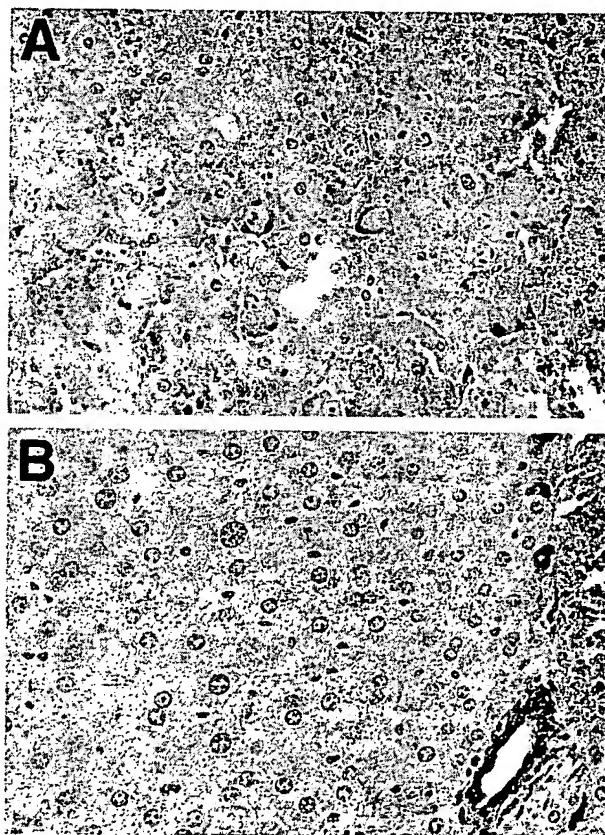


FIG. 1. Histologic sections of murine liver immunostained for exogenously administered human annexin V. (A) Two hours after anti-Fas antibody treatment there is extensive apoptotic nuclear change, slight cytoplasmic retraction, and interstitial hemorrhage. Annexin V staining (brown immunostaining product) is focally present at the cytoplasmic border of apoptotic hepatocytes. (B) No hepatocyte staining was observed in untreated mice. Staining of bile duct epithelium was caused by antibody cross-reactivity because it also was seen in the absence of exogenously administered human annexin V (data not shown). (Diaminobenzidine immunostain with hematoxylin counterstain, $\times 40$ objective magnification.)

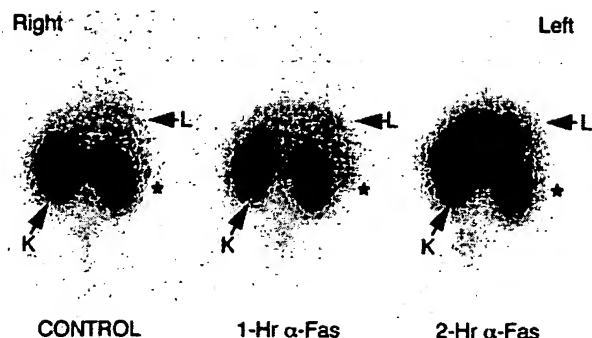


FIG. 2. Imaging Fas-mediated fulminant hepatic apoptosis with radiolabeled annexin V. One hour after injection of 150 μ Ci of radiopharmaceutical (50 μ g/kg of protein) mice were imaged in the prone anterior projection. There was a progressive increase in 99m Tc annexin V uptake of the liver of mice at 1 and 2 hr after anti-Fas antibody injection. Liver activity (L) was 111% and 239% above control values in the 1- and 2-hr mice, respectively, as shown by region of interest image analysis. Kidney activity (K) was 70% and 64% below control values in the 1- and 2-hr mice, respectively. Splenic activity (*) was 168% and 45% above control values in the 1- and 2-hr mice, respectively.

radiopharmaceutical identical to native cardiac activity as confirmed by scintillation well counting (data not shown). The percentage of whole body activity of PVG allografts was 213% above ACI isograft activity ($P < 0.005$; using a two-tailed student's t test) determined by ROI image analysis. Scintillation well-counting assay revealed a >11 -fold increase in 99m Tc HYNIC-annexin V uptake in PVG allografts as compared with native heart activity.

Sections of PVG cardiac allografts 5 days after transplantation showed a marked mononuclear inflammatory cell infiltrate in all animals; no infiltrate was observed in syngeneic or native hearts. The infiltrate surrounded areas of myocardial injury and was associated with thrombosis of myocardial vessels. In the center of these areas, there was frank necrosis, with no staining by hematoxylin, but at the periphery, there were nuclei with changes of apoptosis as confirmed by TUNEL

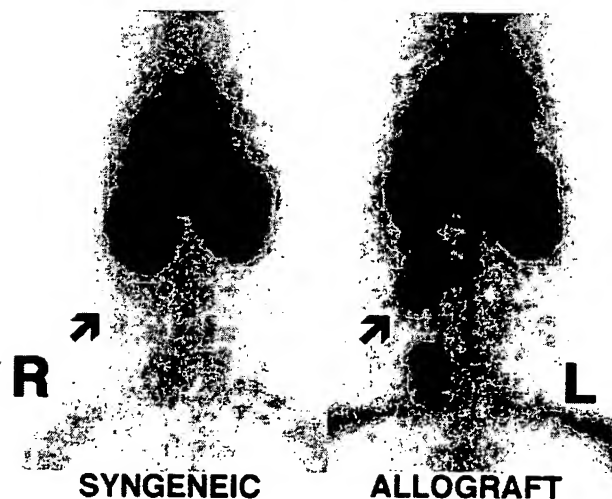


FIG. 3. Imaging cardiac allograft rejection with radiolabeled annexin V. Representative images of abdominal cardiac syngeneic ACI isograft and PVG allograft in ACI host rats 5 days after transplantation. Rats were imaged in the prone anterior projection 1 hr after injection with 900 μ Ci of 99m Tc-annexin V. Location of transplanted hearts are marked by arrows. Intense uptake of 99m Tc HYNIC-annexin V was observed in the cardiac allograft animal (Right) as compared with the lack of visualization of the syngeneic cardiac isograft (Left).

staining (Figs. 4A and B). Immunostaining for 99m Tc HYNIC-annexin V was observed in a granular pattern in cardiac myocytes at the junction of inflamed and necrotic areas; the nuclei of these cells were stained still by hematoxylin, further suggesting that they were apoptotic rather than necrotic (Fig. 5A). Anti-annexin V staining was far more extensive in terms of the number of positive myocytes and intensity compared with TUNEL. Anti-annexin staining was heavy and clumped in frankly necrotic areas as expected (Fig. 5A) but was specific; no staining was observed in syngeneic or native hearts or in staining of allografted hearts in which the primary antibody was omitted (Fig. 5B).

In Vivo Imaging of Treated Murine Lymphoma. Untreated flank tumor implants ($n = 8$) were seen easily by scintillation camera imaging (Fig. 6) and had an annexin V uptake 365% above normal soft tissue activity as shown by ROI image analysis. Treated flank tumors ($n = 6$) showed readily visualizable increases in 99m Tc HYNIC annexin V activity of 78% above control values expressed as whole body activity per gram of tumor ($P < 0.05$ using a two-tailed student's t test for significance). This result was confirmed by scintillation well counting in which treated tumors demonstrated a 132% increase in annexin V uptake expressed as percentage of injected dose per gram of tumor ($P < 0.05$) with a 58% fall in weight ($P < 0.05$) compared with the control. The whole body activity per gram of tumor as seen by ROI image analysis linearly correlated to percentage of injected dose per gram of tumor determined on biodistribution study ($r^2 = 0.831$). Histologic

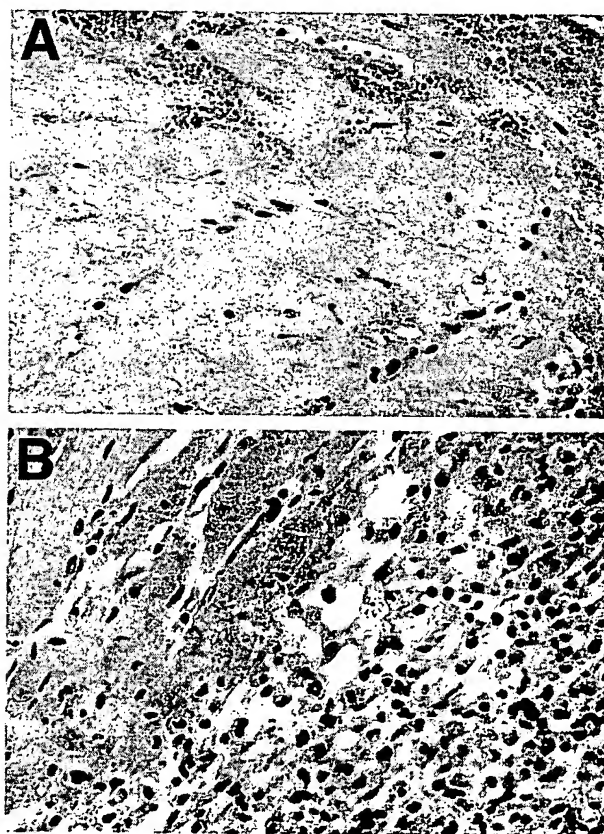


FIG. 4. Staining for apoptotic nuclei in allografted rodent heart 5 days after transplantation. (A) TUNEL staining showing apoptotic nuclei and fragments in some myocytes bordering areas of necrosis (myocytes without visible nuclei in upper half of field). (B) TUNEL positive nuclei and fragments within inflammatory infiltrate (right half of field) and in some myocytes bordering regions of inflammation. (Diaminobenzidine immunostain with hematoxylin counterstain, $\times 40$ objective magnification.)

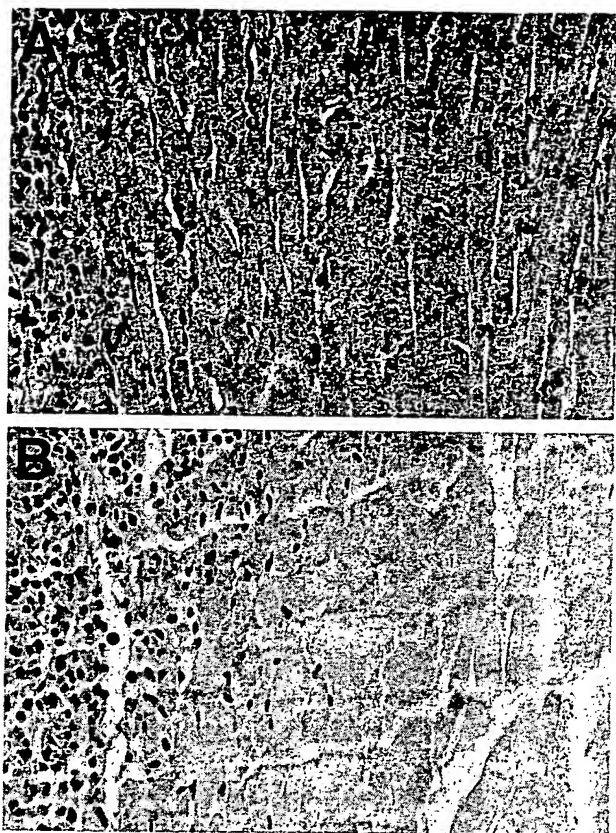


FIG. 5. Immunostaining for exogenously administered human annexin V in allografted rodent heart 5 days after transplantation. (A) Immunostaining with an antibody to human annexin V shows dense, granular staining of apoptotic myocytes at the periphery of the inflammatory infiltrate. Staining of necrotic myocytes (myocytes without visible nuclei) was clumped heavily and central. (B) Immunostaining of area similar to that shown in A omitting the primary antibody, shows no reaction product. (Diaminobenzidine immunostain with hematoxylin counterstain, $\times 40$ objective magnification.)

analysis demonstrated virtually complete ($>95\%$) apoptosis of all lymphoblasts in treated tumors with $<5\%$ apoptotic cells in controls (data not shown).

DISCUSSION

These experiments indicate that exposure of PS on the surface of cells undergoing apoptosis can be detected *in vivo* with radiolabeled annexin V in animal models including Fas-mediated fulminant hepatitis, cardiac allograft rejection, and tumor response to treatment. ^{99m}Tc HYNIC-labeled annexin V radionuclide imaging demonstrated clear and specific localization to regions of apoptotic cell death. As has been shown for annexin V reagents *in vitro*, annexin V radionuclide imaging can provide a tool which can directly assess for early stages of programmed cell death, before membrane vesicle formation and DNA degradation particularly as measured by the TUNEL method (7, 8). Imaging of tissues undergoing apoptosis could be helpful in monitoring the efficacy of therapy of diseases associated with abnormal induction or inhibition of programmed cell death. Apoptosis appears to play an important role in autoimmune and neurodegenerative diseases, cardiomyopathy, myocarditis, cerebral and myocardial ischemia, infectious diseases, cancer, viral induced hepatitis, and organ and bone marrow transplant rejection (1).

The numerous anti-annexin V positive-staining myocytes found in rejecting rodent heart transplants with nuclei which



FIG. 6. Imaging treated murine lymphoma with radiolabeled annexin V. CH3.HeN mice 14 days after implantation of 38C13 murine B cell lymphoma s.c. into the left flank were treated with 100 mg/kg of cyclophosphamide injected i.p. Twenty hours after treatment mice were injected with 150 μCi of ^{99m}Tc HYNIC annexin V (50 $\mu\text{g/kg}$ of protein). One hour after administration of ^{99m}Tc HYNIC annexin V mice were imaged in the prone anterior projection. Treated tumor demonstrated uptakes of 363% and 454% above control seen by region of interest analysis and biodistribution assay, respectively. Control tumor weight = 1.29 grams, treated tumor weight = 0.82 grams. L, left; R, right.

were only occasionally TUNEL positive implies that radiolabeled annexin V imaging may be superior to standard histopathologic assessments of apoptosis. These data suggests a far greater role for programmed cell death in cardiac allograft rejection than previously reported (28–32). Anti-annexin V staining of apoptotic myocytes (with or without TUNEL stained nuclei) was diffusely granular in appearance in contrast to the peripheral pattern of apoptotic hepatocytes. This pattern of exogenous annexin V localization may relate to the unique cellular morphology of myocardial tissue; the extensive sarcoplasmic reticulum, which communicates with the extracellular space, also may be capable of externalizing PS during apoptosis.

The ability of annexin V to bind to necrotic cells *in vivo* and bind to PS located in the inner leaflet of the plasma membrane is confirmed by finding heavy and clumped anti-annexin V staining in frankly necrotic areas in cardiac allografts. As a result, annexin V localization *in vivo* does not appear to be entirely specific for apoptosis. In the clinical setting, however, the ability of radiolabeled annexin V to noninvasively image both apoptosis and necrosis may prove useful in reducing the need for routine surveillance through endomyocardial biopsy after cardiac transplantation, which currently is the only reliable clinical means to diagnose acute transplant rejection (33, 34). Furthermore, radiolabeled annexin V imaging of the entire myocardium may provide diagnostic information superior to endomyocardial biopsy, which necessarily can only sample a limited region within the right ventricle.

These studies also demonstrate that radiolabeled annexin V imaging can detect an increase in PS exposure associated with apoptosis of implanted murine flank lymphomas after cyclophosphamide treatment. Estimates of the degree of cell death

during the first week of induction therapy using bone marrow aspirates has been shown to provide prognostic information in childhood leukemia (35, 36). Other investigators have shown a direct relationship between the degree of apoptotic cell death and subsequent tumor growth delay in murine models of lymphoma (37, 38). To date, the only noninvasive imaging method shown to detect apoptosis *in vivo* has been lipid proton NMR spectroscopy (5, 6). Lipid proton NMR spectroscopy, however, has inherent problems with magnetic susceptibility outside the central nervous system and has relatively low sensitivity.

Kidneys in control animals have marked uptake of ^{99m}Tc HYNIC annexin V. The high renal concentration did not preclude the imaging of other major organs undergoing apoptosis. The cellular site of binding is uncertain, but preliminary autoradiographs suggest the renal distribution of annexin V is cortical. The specific mechanism of renal cortical binding is uncertain but may relate to the intrinsic lipid profile of the kidney, in which there is a significantly higher concentration of PS in the cortex as compared with the papillary regions (39).

The initial increase of ^{125}I -HSA hepatic uptake after anti-Fas treatment is most likely caused by an expanded extracellular fluid volume from the early breakdown of hepatic endothelial cells as described by Lacronique *et al.* (27) and is confirmed by an increased hepatic weight of these treated animals. The initial increase of ^{125}I -HSA hepatic uptake, which subsequently remained unchanged, is in marked contrast to the progressive rise of radiolabeled annexin V hepatic uptake, which was specific for increasing numbers of apoptotic hepatocytes.

In summary, this study demonstrates the utility of ^{99m}Tc -radiolabeled annexin V for *in vivo* imaging of PS expression associated with apoptosis. Serial noninvasive assessments of PS externalization with radiolabeled annexin V may provide a more sensitive and rapid means of monitoring disease progression, determining treatment efficacy, and diagnosing a number of human disorders than is currently possible in the clinical setting.

This work was supported in part by the Child Health Research Fund, Lucile Salter Packard Children's Hospital at Stanford, and by the National Institutes of Health Grant HL-47151. The authors also gratefully acknowledge Dr. Regina Santella for the gift of 1G4 antibody.

- Thompson, B. C. (1995) *Science* **267**, 1456–1462.
- Steller, H. (1995) *Science* **267**, 1445–1449.
- Darzynkiewicz, Z. (1995) *J. Cell. Biochem.* **58**, 151–159.
- Kerr, J. F., Wyllie, A. H. & Currie, A. R. (1972) *Brit. J. Cancer* **26**, 239–257.
- Blankenberg, F. G., Storrs, R. W., Naumovski, L., Goralski, T. & Spielman, D. (1996) *Blood* **87**, 1951–1956.
- Blankenberg, F. G., Katsikis, P. D., Storrs, R. W., Bealieu, C., Spielman, D., Chen, J. Y., Naumovski, L. & Tait, J. F. (1997) *Blood* **89**, 3778–3786.
- Martin, S. J., Reutelingsperger, C. P. M., McGahon, A. J., Rader, J. A., van Schie, R. C. A., La Face, D. M. & Green, D. R. (1995) *J. Exp. Med.* **182**, 1545–1556.
- Zwaal, R. F. A. & Schroit, A. (1997) *Blood* **89**, 1121–1132.
- Koopman, G., Reutelingsperger, C. P. M., Kuijten, G. A. M., Keehnen, R. M. J., Pals, S. T. & van Oers, M. H. J. (1994) *Blood* **84**, 1415–1420.
- Verhoven, B., Schlegel, R. A. & Williamson, P. (1995) *J. Exp. Med.* **182**, 1597–1601.
- van Heerde, W. L., de Groot, P. G. & Reutelingsperger, C. P. M. (1995) *Thromb. Haemostasis* **73**, 172–179.
- Tait, J. F. & Gibson, D. (1994) *J. Lab. Clin. Med.* **123**, 741–748.
- Wood, B. L., Gibson, D. F. & Tait, J. F. (1996) *Blood* **88**, 1873–1880.
- Tait, J. F., Cerqueira, M. D., Dewhurst, T. A., Fujikawa, K., Ritchie, J. L. & Stratton, J. R. (1994) *Thromb. Res.* **75**, 491–501.
- Stratton, J. R., Dewhurst, T. A., Kasina, S., Reno, J. M., Cerqueira, M. D., Baskin, D. G. & Tait, J. F. (1995) *Circulation* **92**, 3113–3121.
- Abrams, M. J., Juweid, M., tenKate, C. I., Schwartz, D. A., Hauser, M. M., Gaul, F. E., Fuccello, A. J., Rubin, R. H., Strauss, H. W. & Fischman, A. J. (1990) *J. Nucl. Med.* **31**, 2022–2028.
- Tait, J. F., Engelhardt, S., Smith, C. & Fujikawa, K. (1995) *J. Biol. Chem.* **270**, 21594–21599.
- Tait, J. F. & Smith, C. (1991) *Arch. Biochem. Biophys.* **288**, 141–144.
- King, T. P., Zhao, S. W. & Lam, T. (1986) *Biochemistry* **25**, 5774–5779.
- Larsen, S. K., Solomon, H. F., Caldwell, G. & Abrams, M. J. (1995) *Bioconjugate Chem.* **6**, 635–638.
- Ogasawara, J., Watanabe-Fukunaga, R., Adachi, M., Matsuzawa, A., Kasugai, T., Kitamura, Y., Itoh, N., Suda, T. & Nagata, S. (1993) *Nature (London)* **364**, 806–809.
- Woodley, S. L., Gurley, K. E., Hoffman, S. L., Nicolls, M. R., Hagberg, R., Clayberger, C., Holm, B., Wang, X., Hall, B. M. & Strober, S. (1993) *Transplantation* **56**, 1443–1447.
- Maloney, D. G., Kaminski, M. S., Burowski, D., Haimovich, J. & Levy, R. (1985) *Hybridoma* **4**, 191–209.
- Bindl, J. M. & Warnke, R. A. (1986) *Am. J. Clin. Pathol.* **85**, 490–493.
- Gavrieli, Y., Sherman, Y. & Ben-Sasson, S. (1992) *J. Cell Biol.* **119**, 493–501.
- Young, T. L. & Santella, R. M. (1988) *Carcinogenesis* **9**, 589–592.
- Lacronique, V., Mignon, A., Fabre, M., Viollet, B., Rouquet, N., Molina, T., Porteu, A., Henrion, A., Bouscary, D., Varlet, P., *et al.* (1996) *Nat. Med.* **2**, 80–86.
- Seino, K., Nobuhiko, K., Bashuda, H., Okumura, K. & Yagita, H. (1996) *Int. Immunol.* **8**, 1347–1354.
- Laguens, R. P., Cabeza Meckert, P. M., San Martino, J., Perrone, S. & Favaloro, R. (1996) *J. Heart Lung Transplant.* **15**, 911–918.
- Bergese, S. D., Klenotic, S. M., Wakely, M. E., Sedmak, D. D. & Orosz, C. G. (1997) *Transplantation* **63**, 320–325.
- Jollow, K. C., Sundstrom, J. B., Gravanis, M. B., Kanter, K., Herskowitz, A. & Ansari, A. A. (1997) *Transplantation* **63**, 1482–1489.
- Matiba, B., Mariana, S. M. & Krammer, P. H. (1997) *Immunology* **9**, 59–68.
- Mannaerts, H. F., Simoons, M. L., Balk, A. H., Tijssen, J., van der Borden, S. G., Zondervan P. E., Mochtar, B., Weimer, W. & Roelandt, J. R. (1993) *J. Heart Lung Transplant.* **12**, 411–421.
- Angermann, C. E., Nassau, K., Stempfle, H.-U., Krüger, T. M., Drewello, R., Phys, D., Junge, R., Ing, D., Überfuhr, P., Weib, M., *et al.* (1997) *Circulation* **95**, 140–150.
- Asselin, B. L., Ryan, D., Frantz, C. N., Bernal, S. D., Leavitt, P., Sallan, S. E. & Cohen, H. J. (1989) *Cancer Res.* **49**, 4363–4368.
- Niemeyer, C. M., Gelber, R. D., Tarbell, N. J., Donnelly, M., Clavell, L. A., Blattner, S. R., Donahue, K., Cohen, H. J. & Sallan, S. E. (1991) *Blood* **78**, 2514–2519.
- Stephens, L. C., Hunter, N. R., Ang, K. K., Milas, L. & Meyn, R. E. (1993) *Radiat. Res.* **135**, 75–80.
- Mirkovic, N., Meyn, R. E., Hunter, N. R. & Milas, L. (1994) *Radiation Oncol.* **33**, 11–16.
- Sterin-Speziale, N., Kahane, V. L., Setton, C. P., del Carmen Fernandez, M. & Speciale, E. H. (1992) *Lipids* **27**, 10–14.

Apoptotic cell death: its implications for imaging in the next millennium

Francis G. Blankenberg¹, Jonathan F. Tait², H. William Strauss^{1,3}

¹ Department of Radiology/Division of Pediatric Radiology, Stanford University School of Medicine, Stanford, Calif., USA

² Department of Laboratory Medicine, University of Washington, Health Sciences, Seattle, Wash., USA

³ Department of Radiology/Division of Nuclear Medicine, Stanford University School of Medicine, Room H0101, 300 Pasteur Drive, Stanford, CA 94305, USA

Abstract. Apoptosis, also known as programmed cell death, is an indispensable component of normal human growth and development, immunoregulation and homeostasis. Apoptosis is nature's primary opponent of cell proliferation and growth. Strict coordination of these two phenomena is essential not only in normal physiology and regulation but in the prevention of disease. Programmed cell death causes susceptible cells to undergo a series of stereotypical enzymatic and morphologic changes governed by ubiquitous endogenous biologic machinery encoded by the human genome. Many of these changes can be readily exploited to create macroscopic images using existing technologies such as lipid proton magnetic resonance (MR) spectroscopy, diffusion-weighted MR imaging and radionuclide receptor imaging with radiolabeled annexin V. In this review the cellular phenomenon of apoptotic cell death and the imaging methods which can detect the process *in vitro* and *in vivo* are first discussed. Thereafter an outline is provided of the role of apoptosis in the pathophysiology of clinical disorders including stroke, neurodegenerative diseases, pulmonary inflammatory diseases, myocardial ischemia and inflammation, myelodysplastic disorders, organ transplantation, and oncology, in which imaging may play a critical role in diagnosis and patient management. Objective imaging markers of apoptosis may soon become measures of therapeutic success or failure in both current and future treatment paradigms. Since apoptosis is a major factor in many diseases, quantification and monitoring the process could become important in clinical decision making.

Key words: Apoptosis – Programmed cell death – Imaging methods

Eur J Nucl Med (2000) 27:359–367

Introduction

What is apoptosis?

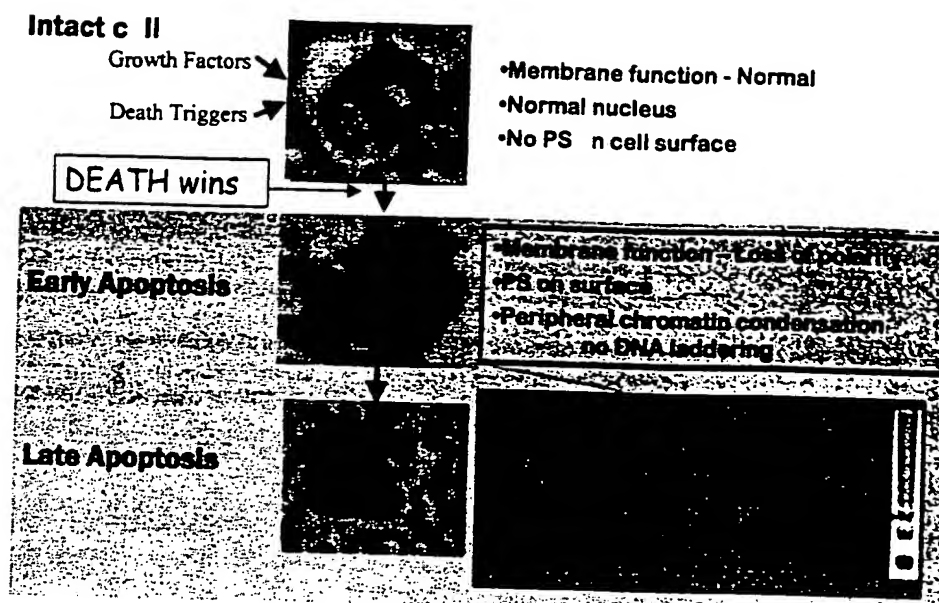
In the yin and yang of existence, it is no surprise that nature has arranged for the orderly demise of cells that have completed their useful function. The programmed disappearance of cells, apoptosis, occurs under both physiologic and pathologic circumstances. Two examples of physiologic programmed cell death are the disappearance of cells when growth factor stimuli are withdrawn (an integral component of the menstrual cycle) and the deletion of activated immune cells when cells have completed their assigned task.

When apoptosis is dysregulated, i.e., there is too little or too much programmed cell death, disease often ensues [1–6]. Diseases associated with excessive apoptosis include AIDS, neurodegenerative disorders (Alzheimer's disease), myelodysplastic syndromes (aplastic anemia, thalassemia), ischemia/reperfusion injury, progression of heart failure in cardiomyopathies, viral infections (chronic hepatitis), toxin-induced liver disease, organ transplant rejection, graft versus host disease, and adult respiratory distress syndrome (particularly when associated with toxic shock). Diseases associated with too little apoptosis include cancer and autoimmune disorders. Successful treatment of neoplasms with drugs or radiation induces apoptosis in the lesion.

Apoptosis is defined as "the dropping of a petal or leaf from a flower or tree." Kerr et al. [7] originally coined this term to define the series of morphologic changes in adrenal tissue when ACTH is withdrawn. The withdrawal of ACTH causes adrenal cells to fragment into small, variably sized vesicles (apoptotic bodies). Neighboring cells or phagocytes then ingest the apoptotic bodies, resulting in the disappearance of the cell without an inflammatory response. The outcome of this process is the controlled removal of senescent, unwanted, or deleterious cells without inciting an inflammatory reaction that might damage adjacent healthy cells and extracellular matrix (Fig. 1). The process of orderly cell auto-

Correspondence to: H.W. Strauss, Department of Radiology/Division of Nuclear Medicine, Stanford University School of Medicine, Room H0101, 300 Pasteur Drive, Stanford, CA 94305, USA

Fig. 1. Sequence of morphologic changes in apoptosis. Initially (*upper panel*) the cell is normal. Following the initiation of apoptosis, chromatin clumping and cytoplasmic condensation occur (*middle panel*). In the late phase of apoptosis (*bottom panel*) the cell begins to form apoptotic bodies and DNA is fragmented with formation for DNA laddering (as indicated on gel electrophoresis)



fragmentation is governed by a cascade of enzymatic activity. Although the original observation suggested that apoptosis is caused by a withdrawal of growth factors, it is now known that a wide array of exogenous or endogenous stimuli [8–12] can trigger the process.

Mechanism of apoptosis

Apoptosis is initiated when there is a disturbance in the local environment of the cell. Cells are constantly bathed in a sea of life-reinforcing stimuli, such as growth factors, and death signals such as tumor necrosis factor. A shift in the balance of these factors with either a decrease in survival factors or a marked increase in death signals can initiate apoptosis. Withdrawal of growth factors, severe mitochondrial damage, attempting mitosis in the presence of irreparable DNA damage, activation of cellular Fas receptors by Fas ligand expressed on activated lymphocytes, hypoxia, heat, cold, chemical injury (chemotherapy), or significant doses of ionizing radiation (causing DNA injury) can result in apoptosis.

Once apoptosis has been triggered, one of several enzymatic cascades is initiated to achieve the orderly destruction of DNA and the dissolution of other cellular elements. A major pathway involves a group of cysteine proteases, the “caspases”. Caspase activation precedes morphologic changes. At the time of caspase activation, cells destined for apoptosis appear to signal their neighbors by expressing phosphatidylserine (PS) on the cell surface [13]. PS, along with phosphatidylethanolamine, sphingomyelin, and phosphatidylcholine, is a normal constituent of the cell membrane. In contrast to the other cell membrane constituents, PS is restricted to the inner leaflet of the cell membrane. This constraint on PS distribution is the result of two enzymes, translocase and

floppase, which actively pump PS to the inner leaflet and the other lipids out. Activation of caspase is associated with inactivation of these membrane pumps, and activation of an enzyme, scramblase, which equilibrates the membrane lipids on the inner and outer leaflet of the cell membrane – resulting in the rapid appearance of PS on the outer leaflet of the membrane [14, 15]. Once the caspases are activated and PS is expressed, the execution phase of apoptosis occurs. Cellular cytoplasm condenses, nuclear DNA is degraded into 180-kDa pieces and the cell fragments into membrane-covered pieces (each expressing PS on the surface) for phagocytosis [16] (Fig. 1, “Late Apoptosis”, bottom panel).

Methods to image apoptosis in vivo

Annexin V

Annexin V [17, 18] is an endogenous human protein which binds to membrane-bound PS with an affinity of about 10^{-9} M. Annexin V, labeled with fluorescein dye, has been used to detect PS expression in studies of apoptosis in hematopoietic cell lines, neurons, fibroblasts, endothelial cells, smooth muscle cells, carcinomas, lymphomas, and all embryonic cell types, as well as non-mammalian plant and insect cells [19]. Annexin V has also been radiolabeled by iodination and coupling to linker molecules such as a diamide dimercaptide (N_2S_2) [20] or hydrazino nicotinamide [20]. The universality of annexin V binding to various cell lines is due to the composition of the phosphoserine head group of PS (the site of annexin V binding), which is identical in all multicellular organisms. In vitro cell binding studies demonstrate a 20-fold increase in annexin concentration in cells undergoing apoptosis compared with control cells.

Table 1. The biodistribution of annexin V in rats

	10 min (n=6)	30 min (n=7)	1 h (n=7)	3 h (n=6)
<i>A) % I.D./organ^a</i>				
Brain	0.0681±0.0202	0.0197±0.0035	0.0149±0.003	0.0093±0.0009
Lungs	2.611±0.367	1.558±0.191	1.000±0.30	0.821±0.085
Heart	0.372±0.0726	0.150±0.048	0.135±0.033	0.134±0.0165
Liver	20.8±1.179	15.8±2.67	21.6±4.12	17.97±1.36
Spleen	4.64±0.459	4.08±1.089	4.75±1.22	4.12±0.571
Kidneys	29.2±6.05	33.5±8.02	45.6±5.48	47.4±2.90
Stomach	0.25±0.056	0.376±0.038	0.51±0.165	0.38±0.138
<i>B) % I.D./gram^b</i>				
Small intestine	0.144±0.066	0.114±0.048	0.128±0.059	0.129±0.011
Colon	0.082±0.066	0.054±0.013	0.052±0.014	0.082±0.039
Skeletal musc.	0.035±0.009	0.024±0.007	0.026±0.008	0.022±0.002
Bone marrow	2.13±0.52	1.55±0.72	2.083±0.57	1.98±0.374
Blood	1.38±0.34	0.306±0.098	0.215±0.090	0.107±0.013

Mean values±standard error for tissue and organ samples from control Sprague-Dawley rats 10 min, 30 min, 1 h and 3 h after injection of 25 µg/kg of ^{99m}Tc-HYNIC-annexin V (500–600 µCi/animal) labeled using a ^{99m}Tc-tricine conjugate method injected via tail vein. Samples were weighed and placed in 3-ml tubes and counted

^a Mean percentage of injected dose (%I.D.) per organ (% I.D./organ)

^b Mean percentage of injected dose per gram of tissue (%I.D./g)

Tait and colleagues utilized radiolabeled annexin V to detect increased PS expression which occurs when platelets are activated in acute thrombosis [21]. Blankenberg and colleagues utilized radiolabeled annexin to detect apoptosis in vivo in animal models of transplant rejection, hypoxic cerebral injury, tumor therapy and Fas induced apoptosis [22, 23].

Following intravenous administration of radiolabeled annexin V, the agent is cleared from the blood with a half-time of less than 5 min. and is concentrated primarily in the kidneys and to a lesser degree in the liver. A summary of annexin biodistribution in rodents is presented in Table 1. Apoptosis induced by stimulation of the Fas/Fas ligand system, transplant rejection, or chemotherapy in tumor-bearing animals has been visualized with technetium-99m labeled annexin imaging.

The minimal cell mass required for successful detection of apoptosis by in vivo imaging is not known. However, in studies of heart transplant rejection by Vriens et al., histologic evidence of apoptosis was present in <10% of cells at the time when annexin imaging demonstrated remarkable focal localization in the transplant (see later discussion of heart transplant rejection). It is likely that single-photon imaging will require significant apoptosis (in at least 10% of cells) to detect the process in a small mass of tissue (~2–3 g). If the extent of the lesion involves a larger mass of tissue, such as the major portion of an organ, less extensive apoptosis will be detectable. It is likely that the contrast of annexin images will be enhanced if the protein is labeled with fluorine-18 and data recorded with positron tomography.

In addition to radionuclide imaging with radiolabeled annexin, other imaging modalities, such as magnetic res-

onance (MR), have been utilized to detect apoptosis in vivo.

MR lipid spectroscopy and diffusion-weighted MR imaging

Since 1982 numerous in vitro and in vivo MR studies have documented the presence of a narrow and intense resonance in the 1.3-ppm region of the lipid proton spectra from cultured tumor, embryonic, and stimulated lymphocyte cell lines and solid, experimental and human tumors [24, 25]. Of note, this resonance has been found to increase in solid tumors following treatment and the induction of apoptotic cell death. A rise in the 1.3-ppm resonance has also been observed acutely after hypoxic-ischemic injury of the cerebrum [26] and cerebral diffuse axonal injury due to child abuse [27] and has been found to be of prognostic significance. This resonance has now been recognized as representing the methylene proton (-CH₂-) of mobile neutral lipid fatty acid chains within the plasma membrane bilayer in vitro [23, 24] and cytoplasmic vesicles in vivo [28, 29].

Coincident with the lipid rearrangements that permit both radiolabeled annexin V and proton lipid MR spectroscopic imaging of apoptotic cells and tissues is the shrinkage of a cell's cytoplasmic volume. There is concurrent increased cytoplasmic microviscosity and restriction of water motion [30]. This apoptotic phenomenon can be imaged by MR using diffusion weighted imaging (DWI), which tags and follows the motion (diffusion or ADC = the average diffusion coefficient) of individual water molecules [31]. The use of DWI to detect and

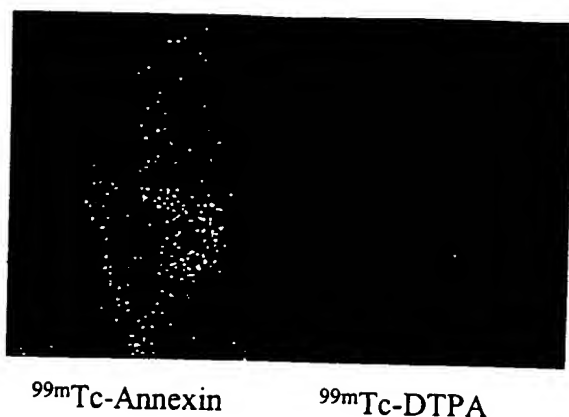


Fig. 2. Hypoxic brain injury due to transient occlusion of the right middle cerebral artery. Seven hours following occlusion/reperfusion, pinhole vertex view images of the head in intact adult rats were obtained after injection of annexin (*left panel*) to identify apoptosis and DTPA (*right panel*) to identify areas of blood-brain barrier breakdown. There is no loss of blood-brain barrier integrity, but annexin uptake is seen in the right hemisphere (*arrow*). The nose is oriented cephalad on images

track apoptotic cell death *in vivo* is only beginning to be studied and its ultimate clinical applicability, particularly outside the nervous system, remains to be defined.

The following sections describe some specific diseases where apoptosis is known to play a significant role, and where imaging the process may be helpful in clinical decision making.

Central nervous system

Stroke

Hypoxic-ischemic injury (HII) in adults (stroke, multi-infarct dementia) with delayed loss of gray and white matter is due to apoptosis [32]. Blankenberg et al. [33] have shown that moderate to severe injury, without evidence of blood-brain barrier breakdown, is associated with remarkable focal radiolabeled annexin uptake in an adult rat model of ischemic/reperfusion hemispheric injury (Fig. 2). Because the actual cell loss in these patients is gradual (delayed with respect to the insult) there may be a therapeutic window to inhibit (or reverse) early apoptosis with pharmacologic blockade. Imaging with radiolabeled annexin V may be helpful in addressing this clinical problem since annexin V has virtually no background uptake in the brain.

Ischemia/reperfusion injury in preterm/term infants

HII in preterm infants is a major cause of cerebral palsy. Because of the immaturity of the centrifugal cerebrovas-

cular circulation, full-term and preterm neonates manifest HII in a different fashion than adults [34, 35]. Preterm infants tend to suffer watershed ischemic injury in a periventricular distribution (periventricular leukomalacia or PVL) while term infants develop disease of their subcortical white matter. The delayed cell loss of these injuries is mediated by apoptosis [36]. In experimental animals ^{99m}Tc -annexin imaging has clearly delineated these lesions in the absence of blood-brain barrier breakdown.

Traditional imaging techniques do not provide the specificity needed to identify neonates at risk for development of cerebral palsy (which is usually diagnosed at 2–3 years of age) who might benefit from these novel treatments in the first several days (or hours) of life. Reversible abnormalities seen by DWI MR associated with mild transient hemispheric HII resulted in multifocal regions of abnormal annexin V cerebral and cerebellar uptake in a neonatal rabbit model of global hypoxia [37]. Histology of these neonatal rabbit brains demonstrated a correlation between radiolabeled annexin V uptake and subtle scattered ischemic changes in the hippocampus periventricular/subcortical white matter. In the future, neonates who are the products of a difficult labor or delivery could be assessed for suspected HII damage with annexin V imaging to identify patients who might benefit from therapy.

AIDS dementia/Alzheimer's disease

Neuronal and glial cell apoptosis also occurs in acquired immune deficiency syndrome, in encephalitis with or without AIDS-related dementia and in neurodegenerative disorders, such as Alzheimer's and Parkinson's disease [38]. The gradual loss of white and gray matter in Alzheimer's disease is primarily due to apoptosis. Imaging with radiolabeled annexin V could be helpful in the diagnosis and therapeutic management of this diverse group of patients.

Lung disease

High-resolution computed tomography (HRCT) of the chest has enhanced the detection and characterization of disease processes affecting the interstitium of the lung [39]. Diseases such as idiopathic pulmonary fibrosis, desquamative interstitial pneumonitis, *Pneumocystis carinii* pneumonia, lymphocytic interstitial pneumonia, fibrosis in collagen vascular diseases, sarcoidosis, drug or allergic reactions, bronchiolitis obliterans, and bronchiolitis obliterans with organizing pneumonia [40] can be readily identified. These entities, however, all involve cell-mediated inflammation and activation of T lymphocytes, at least in the acute/subacute settings. Although HRCT provides characteristic images, often obviating the need for confirmatory lung biopsy, HRCT cannot

quantify the degree of inflammation. The degree of inflammation is important to define the best management of the process. Without specific information about inflammation, clinicians manage these patients with pulmonary function tests, bronchoalveolar lavage, and serial chest radiography.

Radiolabeled annexin V imaging of the chest may be of value to quantify cell-mediated inflammation and apoptosis in the lungs. In a rat model of cell-mediated lung apoptosis, acute lung transplant rejection, radiolabeled annexin V localization was more sensitive than CT scanning in detecting the process. Other circumstances where apoptosis imaging may play a role include: adult respiratory distress syndrome, which is in part induced by the release of tumor necrosis factor, a potent inducer of apoptotic alveolar cell death; bronchopulmonary dysplasia; neonates with pulmonary oxygen toxicity; cystic fibrosis; and asthma. In each case, the extent of apoptosis will indicate the effectiveness of therapy – if apoptosis is extensive, therapy is not controlling the process.

Heart

Myocardial infarction and reperfusion injury

Like the brain, cardiomyocytes undergo apoptosis in response to hypoxic-ischemic insults that are insufficient to induce frank necrosis [41] [e.g., the peripheral (penumbral) regions of an infarct or following reperfusion of an infarct]. Interestingly, the heart also displays cytoplasmic lipid droplets, the presence of which confers a poorer prognosis in animal models of myocardial ischemia [42]. It is clear that agents which selectively inhibit activation of the apoptotic enzymatic cascade decrease the degree of "infarction" in both the heart and brain in response to an ischemic insult [43, 44]. Preliminary studies of myocardial annexin localization in rats with acute myocardial infarction suggest that apoptosis plays a major role in cell death following acute coronary occlusion (S. Hasegawa and T. Nishimura, personal communication).

Coronary disease and atherosclerosis

Recent biochemical evidence strongly suggests that activated monocytes/macrophages attracted by local vascular endothelial damage and complement activation infiltrate the arterial vascular wall [45]. With continued inflammation there is deposition of lipid at the site of injury, formation of foam cells (lipid-laden macrophages), and formation of an atheroma. Within the plaque there is significant apoptosis involving the monocytes and macrophages infiltrating the lesion, smooth muscle cells at the base of the lesion, and, in unstable plaque, the endothelial cells forming the cap of the plaque. This last

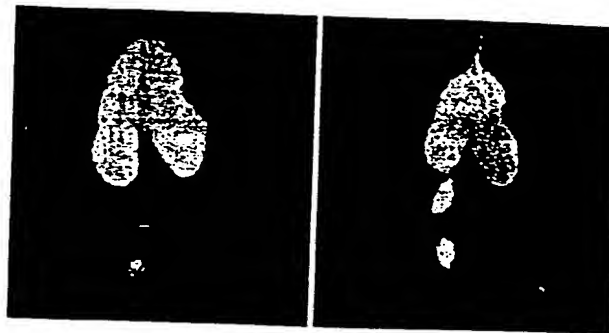


Fig. 3. Two rats with heterotopic hearts transplanted into the abdomen, below the kidneys. One hour following injection of ^{99m}Tc -annexin, anesthetized animals were placed prone on a high-resolution parallel-hole collimator. Images of the syngeneic (left) and allogeneic (right) transplants were recorded on the fourth day after transplant. The bright area in the mid abdomen is the transplant undergoing rejection/apoptosis in the allogeneic animal. Some annexin is seen in the bladder of both animals

event is particularly dangerous as the apoptotic endothelial cells expressing PS on their surface serve as thrombogenic foci.

It is unclear whether external imaging with ^{99m}Tc -annexin V will have sufficient resolution to define these lesions; however, if an intravascular probe were available such lesions might be readily identified. An alternative strategy may involve the use of radiolabeled MCP-1 (monocyte chemotactic peptide), which has a molecular weight of approximately 13,000 [46]. MCP-1 selectively binds to "activated" macrophages and has shown promise in detecting mononuclear infiltration in the subendothelial layers of mechanically traumatized arterial vessels. As activated monocytes/macrophages are intimately involved in chronic inflammation, MCP-1 may be useful as a marker of infectious or noninfectious granulomatous inflammation throughout the body [47].

Myocarditis/cardiomyopathies

Apoptotic cell death plays a major role in viral and autoimmune myocarditis and nonischemic cardiomyopathies [7]. Acute transplant rejection is primarily an immune event mediated by alloreactive T lymphocytes. In a rat model of acute cardiac transplant rejection, serial imaging with ^{99m}Tc -annexin V successfully detected rejection [48] with an accuracy exceeding that of TUNEL staining of biopsy specimens (Fig. 3). Furthermore, when immunosuppressive therapy with cyclosporine was initiated, the decrease in rejection was mirrored by a marked decrease in ^{99m}Tc -annexin localization (Fig. 4). In light of this experience with transplant rejection, annexin V imaging may also be helpful in the detection of apoptosis due to virally induced cardiomyopathies or other autoimmune diseases that affect the heart such as systemic lupus erythematosus, rheumatic fever, and Kawasaki's disease.

Fig. 4. Annexin imaging in acute cardiac transplant rejection before and after cyclosporine therapy. The four panels depict whole body images on days 1, 4, 10, and 18 after transplantation (each image was recorded 1 h after ^{99m}Tc -annexin injection). On day 1 there is no annexin imaging evidence of apoptosis. The image on day 4 demonstrates ^{99m}Tc -annexin localization in the transplanted heart. Treatment with cyclosporin commenced on day 5, and by day 10 the annexin localization has diminished. By day 18, annexin localization has declined further

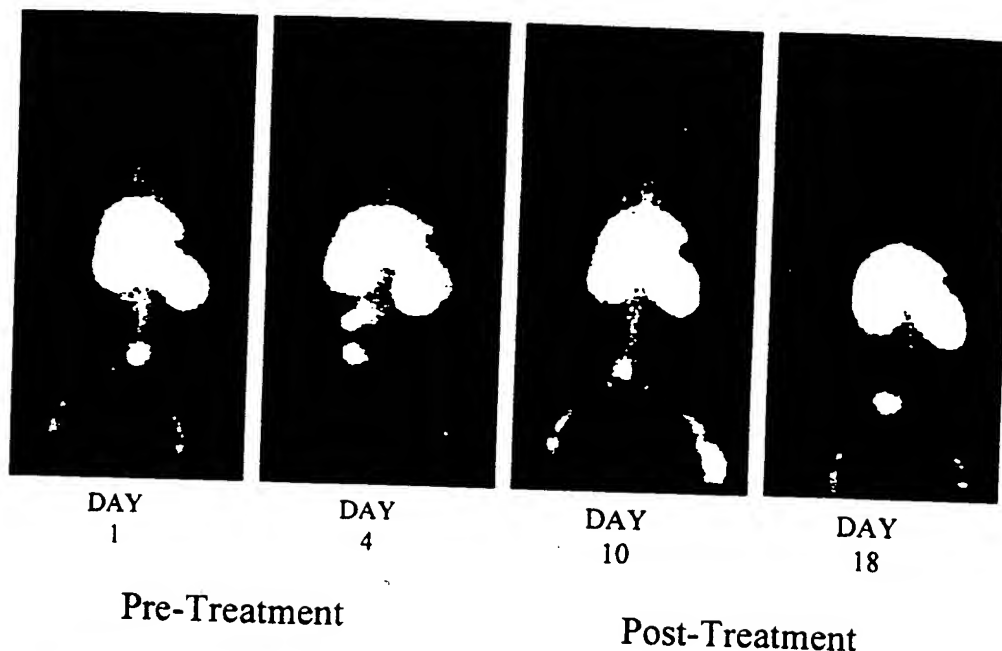
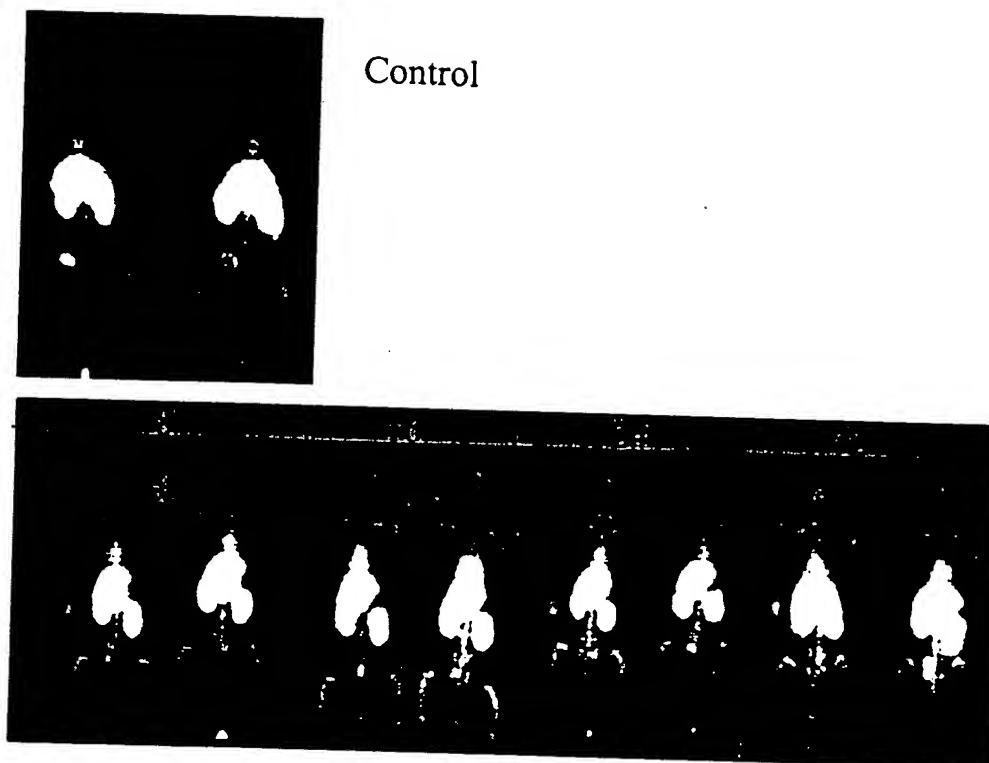


Fig. 5. Whole body posterior images in rats 1 h following tail vein injection of 1 mCi of radiolabeled annexin V before and after treatment with 100 mg/kg of cyclophosphamide administered intraperitoneally to ablate the bone marrow. One day later the animals were imaged. Control animals are shown in the *top panels* and rats that had received cyclophosphamide 8–72 h before annexin imaging are shown in the *bottom panels*. The vertebral and peripheral marrow show increased localization (350%) following cyclophosphamide-induced apoptosis



Bon marrow diseases

β -thalassemia, sickle-cell disease, aplastic anemia (myelofibrosis), parvoviral infection (and many other viral infections), autoimmune diseases, toxins, radiation, and chemotherapy cause significant apoptosis in the bone marrow [7]. Bone marrow aspiration is required to determine the degree of disease involvement of the bone marrow [49]. We have shown that cyclophosphamide (a po-

tent bone marrow suppressive and antitumor agent) treatment of otherwise normal adult rats induces a marked increase in bone marrow uptake of annexin V as compared with controls (Fig. 5). Based on this experimental observation, it is likely that ongoing apoptotic bone marrow disease processes such as aplastic anemia may be detected with annexin imaging.

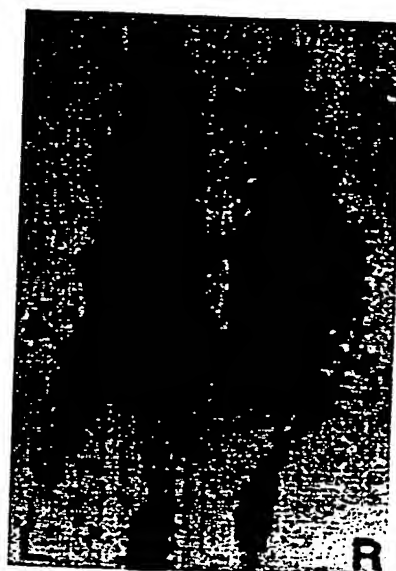
Autoimmune, crystal depositional, and idiopathic arthropathies all appear to be intimately linked to apoptotic cell death of the synovial tissues [7]. Other than symptomatic improvement there are few objective measures with which to guide anti-inflammatory therapy. Efforts are underway to characterize and quantify the quality of hyaline cartilage using a number of MR techniques [50]. Annexin V (and probably MCP-1) imaging may in fact provide an objective measure of disease severity and anti-inflammatory treatment response. Additionally, the gradual loosening and failure of joint prostheses appears to be directly linked to the apoptotic cell death of macrophages which are activated in response to foreign debris [51]. Annexin V imaging may be useful in the management of these patients as well.

Organ transplantation

Annexin V can identify acute heart, lung, and liver transplant rejection in vivo [52]. The majority of transplant recipients, however, do not have acute graft rejection, but instead suffer multiple clinically manifest and subclinical episodes of rejection. A combination of smoldering inflammation and a low level of apoptosis are some of the key findings in chronic rejection. The inflammation and apoptosis are primarily manifest as accelerated vascular disease (atherosclerosis) in the graft. Graft vasculopathy is a process that occurs over years, characterized by perivascular mononuclear cell infiltration and apoptotic cell death. The chronicity of the process may be associated with such a low level of apoptosis that the process cannot be detected by annexin V imaging.

Oncol gy

The degree of cytoreduction in response to antitumor treatment(s) directly correlates with overall disease response, disease-free interval, and ultimate survival in a number of malignancies [53]. Depending on the type of malignancy the only measures of cytoreduction are gross shrinkage or disappearance of tumor as seen by anatomical imaging with ultrasound, CT or MR imaging. Recently, there has been a renewed interest in using proton lipid MR spectroscopy and DWI MR to assess the early treatment response of tumors [26–28]. Unfortunately, these techniques cannot give information except for regional areas of tumor involvement, particularly during induction therapy, when patients can be quite ill. In addition DWI MR detection of tumoral apoptosis relies on the observable shrinkage of the cell cytoplasm during tumor cell death. However, many tumors respond to chemotherapeutic agents which specifically attack DNA, such as doxorubicin (adriamycin), by cell swelling, not



Treated
tumor in
left thigh

Fig. 6. Annexin V detection of necrotic versus apoptotic tumor cell death in flank tumors of mice following chemotherapy. The animal on the *left* demonstrated a greater than 363% increase in left flank 38C13 murine B cell lymphoma annexin V uptake 20 h after treatment with 100 mg/kg of cyclophosphamide (i.p.) compared with untreated flank lymphoma (animal on right)

cell shrinkage. Therefore, DWI MR may give misleading results in vivo. This cell swelling is due to a metabolic cell death initiated by massive activation of a normally quiescent nuclear enzyme called poly-ADP-ribose polymerase (PARP or PARS) [54]. PARP is generally activated in the later stages of apoptosis and helps induce fragmentation of a cell's DNA. Direct DNA damage by ionizing radiation, or radical ion formation by agents such as doxorubicin or HII [55] in some circumstances can induce massive direct activation of PARP. Activated PARP utilizes NAD to form poly-ADP ribose polymers. To replace lost NAD stores a cell utilizes ATP and if PARP activation is of sufficient intensity, virtually all ATP stores of a cell will be rapidly depleted. A cell depleted of ATP will simply swell and lose membrane integrity (necrosis). In an experimental model of lymphoma treated with cyclophosphamide, therapy-induced apoptosis is readily visible with ^{99m}Tc -annexin V imaging (Fig. 6). Despite these different mechanisms of cell death, annexin V imaging will demonstrate the process because annexin V binds to cells expressing PS on the outer cell surface (apoptosis) or, alternatively, annexin can gain access to inner plasma membrane leaflet PS after the onset of irreversible membrane failure (PARP-mediated cell death).

19. O'Brien IEW, Reutingsperger CPM, Holdaway KM. Annexin-V and TUNEL use in monitoring the progression of apoptosis in plants. *Cytometry* 1997; 29: 28–33.
20. Abrams MJ, Juweid M, tenKate CI, et al. Technetium-99m-human polyclonal IgG radiolabeled via the hydrazino nicotinamide derivative for imaging focal sites of infection in rats. *J Nucl Med* 1990; 31: 2022–2028.
21. Stratton JR, Dewhurst TA, Kasina S, et al. Selective uptake of radiolabeled annexin V on acute porcine left atrial thrombi. *Circulation* 1995; 92: 3113–3121.
22. Blankenberg FG, Katsikis PD, Tait JF, et al. In vivo detection and imaging of phosphatidylserine expression during programmed cell death. *Proc Natl Acad Sci USA* 1998; 95: 6349–6354.
23. Blankenberg FG, Katsikis PD, Tait JF, et al. Imaging of apoptosis (programmed cell death) with ^{99m}Tc annexin V. *J Nucl Med* 1999; 40: 184–191.
24. Blankenberg FG, Storrs RW, Naumovski L, et al. Detection of apoptotic cell death by proton nuclear magnetic resonance spectroscopy. *Blood* 1996; 87: 1951–1956.
25. Blankenberg FG, Katsikis PD, Storrs RW, et al. Quantitative analysis of apoptotic cell death using proton nuclear magnetic resonance spectroscopy. *Blood* 1997; 89: 3778–3786.
26. Hakumäki JM, Grohn OH, Pirttilä TR, et al. Increased macromolecular resonances in the rat cerebral cortex during severe energy failure as detected by ^1H nuclear magnetic resonance spectroscopy. *Neurosci Lett* 1996; 212: 151–154.
27. Ross BD, Ernst T, Kreis R, et al. ^1H MRS in acute traumatic brain injury. *J Magn Reson Imaging* 1998; 8: 829–840.
28. Remy C, Fouillhe N, Barba I, et al. Evidence that mobile lipids detected in rat brain glioma by ^1H nuclear magnetic resonance correspond to lipid droplets. *Cancer Res* 1997; 57: 407–414.
29. Veale MF, Roberts NJ, King GF, et al. The generation of ^1H -NMR-detectable mobile lipid in stimulated lymphocytes: relationship to cellular activation, the cell cycle, and phosphatidylcholine-specific phospholipase C. *Biochem Biophys Res* 1997; 239: 868–874.
30. Hakumäki JM, Poptani H, Puumalainen AM, et al. Quantitative ^1H NMR diffusion spectroscopy of BT4 C rat glioma during thymidine kinase-mediated gene therapy in vivo: identification of apoptotic response. *Cancer Res* 1998; 58: 3791–3799.
31. D'Arceuil HE, de Crespigny AJ, Rother J, et al. Diffusion and perfusion magnetic resonance imaging of the evolution of hypoxic ischemic encephalopathy in the neonatal rabbit. *J Magn Reson Imaging* 1998; 8: 820–888.
32. Du C, Hu R, Csemansky CA, et al. Very delayed infarction after mild focal cerebral ischemia: a role for apoptosis? *J Cereb Blood Flow Metab* 1996; 16: 195–201.
33. Blankenberg FG, Busch E, Yenari MA, et al. In vivo imaging of apoptotic cell death associated with cerebral hemispheric ischemia using ^{99m}Tc radiolabeled annexin V. *Stroke* 1998; 29: 330.
34. Rutherford MA, Pennock JM, Counsell SJ, et al. Abnormal magnetic resonance signal in the internal capsule predicts poor neurodevelopmental outcome in infants with hypoxic-ischemic encephalopathy. *Pediatrics* 1998; 102: 323–328.
35. Oka A, Belliveau MJ, Rosenberg PA, et al. Vulnerability of oligodendroglia to glutamate: pharmacology, mechanisms, and prevention. *J Neurosci* 1993; 13: 1441–1453.
36. Pulera MR, Adams LM, Liu H, et al. Apoptosis in a neonatal rat model of cerebral hypoxia-ischemia. *Stroke* 1998; 29: 2622–2630.
37. D'Arceuil HE, Blankenberg FG, Tait JF, et al. Radionuclide scanning combined with MR diffusion imaging investigation of apoptosis in neonatal rabbit HIE [abstract]. *Pediatr Res* 1998; 43: 317A.
38. Cotman CW, Anderson AJ. A potential role for apoptosis in neurodegeneration and Alzheimer's disease. *Mol Neurobiol* 1995; 10: 19–45.
39. Lau DM, Siegel MJ, Hildebolt CF, et al. Bronchiolitis blitans syndrome: thin-section CT diagnosis of obstructive changes in infants and young children after lung transplantation. *Radiology* 1998; 208: 783–788.
40. McAdams HP, Rosado-de-Christenson ML, Wehunt WD, et al. The alphabet soup revisited: the chronic interstitial pneumonias in the 1990s. *Radiographics* 1996; 16: 1009–1033.
41. Narula J, Haider N, Virmani R, et al. Apoptosis in myocytes in end-stage heart failure. *N Engl J Med* 1996; 335: 1182–1195.
42. Greve G, Rotevatn S, Svendby K, et al. Early morphologic changes in cat heart muscle cells after acute coronary artery occlusion. *Am J Pathol* 1990; 136: 273–283.
43. Yaoita H, Ogawa K, Maehara K, et al. Attenuation of ischemia/reperfusion injury in rats by a caspase inhibitor [see comments]. *Circulation* 1998; 97: 276–281.
44. Hara H, Friedlander RM, Gagliardini V, et al. Inhibition of interleukin 1beta converting enzyme family proteases reduces ischemic and excitotoxic neuronal damage. *Proc Natl Acad Sci USA* 1997; 94: 2007–2012.
45. Geng Y-J, Holm J, Hygren S, et al. Expression of the macrophage scavenger receptor in atherosclerosis. *Arterioscler Thromb Vasc Biol* 1995; 15: 1995–2002.
46. Torzewski J, Oldroyd R, Lachmann P, et al. Complement-induced release of monocyte chemoattractant protein-1 from human smooth muscle cells. A possible initiating event in atherosclerotic lesion formation. *Arterioscler Thromb Vasc Biol* 1996; 16: 673–677.
47. Grandaliano G, Gesualdo L, Ranieri E, et al. Monocyte chemoattractant peptide-1 expression and monocyte infiltration in acute renal transplant rejection. *Transplantation* 1997; 63: 414–420.
48. Vriens PW, Blankenberg FG, Stoot JH, et al. The use of ^{99m}Tc annexin V for in vivo imaging of apoptosis during cardiac allograft rejection. *J Thorac Cardiovasc Surg* 1998; 116: 844–853.
49. Niemeyer CM, Gelber RD, Tarbell NJ, et al. Low-dose versus high-dose methotrexate during remission induction in childhood acute lymphoblastic leukemia (protocol 81-01 update). *Blood* 1991; 78: 2514–2519.
50. Uhl M, Allmann KH, Ihling C, et al. Cartilage destruction in small joints by rheumatoid arthritis: assessment of fat-suppressed three-dimensional gradient-echo MR pulse sequences in vitro. *Skeletal Radiol* 1998; 27: 677–682.
51. Nakashima Y, Sun DH, Trainor MC, et al. Induction of macrophage C-C chemokine expression by titanium alloy and bone cement particles. *J Bone Joint Surg [Br]* 1999; 81: 155–162.
52. Blankenberg FG, Strauss HW. Non-invasive diagnosis of acute heart- or lung-transplant rejection using radiolabeled annexin V. *Pediatr Radiol* 1999; 29: 299–305.
53. Lamb JR, Friend SH. Which questimate is the best questimate? Predicting chemotherapeutic outcomes. *Nature Med* 1997; 9: 962–963.
54. Martin DS, Schwartz GK. Chemotherapeutically induced DNA damage, ATP depletion, and the apoptotic biochemical cascade. *Oncol Res* 1997; 9: 1–5.
55. Zhang J, Dawson VL, Dawson TM, et al. Nitric oxide activation of poly(ADP-ribose) synthetase in neurotoxicity. *Science* 1994; 263: 687–689.



ClustalW Results

EXHIBIT A
Docket No.: PF-0733 USN
USSN: 10/018,170

Sequences

Help

Retrieval

BLAST2

FASTA

ClustalW

GCC Assembly

Phrap

Translation

Confidential -- Property of Incyte Corporation SeqServer Version 4.6 Jan 2002

☐ g10436074☐ 2615168CD1

CLUSTAL W (1.7) Multiple Sequence Alignments

Sequence format is Pearson

Sequence 1: g10436074 345 aa

Sequence 2: 2615168CD1 345 aa

Start of Pairwise alignments

Aligning...

Sequences (1:2) Aligned. Score: 99

Start of Multiple Alignment

There are 1 groups

Aligning...

Group 1: Sequences: 2 Score: 4527

Alignment Score 2042

CLUSTAL-Alignment file created [baa4aaqV1.aln]

CLUSTAL W (1.7) multiple sequence alignment

```
g10436074      MSVTGGKMAPSLTQEILSHLGLASKTAAWGTLGTLRTFLNFSVDKDAQRLRLRAITGQGV
2615168CD1     MSVTGGKMAPSLTQEILSHLGLASKTAAWGTLGTLRTFLNFSVDKDAQRLRLRAITGQGV
*****
```

```
g10436074      RSAIVDVLTNRSREQRQLISRNQERTQQDLMKSLQAALSGNLERIVMALLQPTAQFDAQ
2615168CD1     RSAIVDVLTNRSREQRQLISRNQERTQQDLMKSLQAALSGNLERIVMALLQPTAQFDAQ
*****
```

```
g10436074      ELRTALKASDSAVDVAIEILATRTPPQLQECLAVYKHNQVEAVDGITSETSGILQDLLL
2615168CD1     ELRTALKASDSAVDVAIEILATRTPPQLQECLAVYKHNQVEAVDDITSETSGILQDLLL
*****
```

```
g10436074      ALAKGGRDSYSGIIDYNLAEQDVQALQRAEGPSREETWVPVFTQRNPEHLIRVFDQYQRS
2615168CD1     ALAKGGRDSYSGIIDYNLAEQDVQALQRAEGPSREETWVPVFTQRNPEHLIRVFDQYQRS
*****
```

```
g10436074      TGQELEEAVQNRFHGDAQVALLGLASVIKNTPLYFADKLHQALQETEPNYQVLIRILISR
2615168CD1     TGQELEEAVQNRFHGDAQVALLGLASVIKNTPLYFADKLHQALQETEPNYQVLIRILISR
*****
```

```
g10436074      CETDLLSIRAEFRKKFGKSLYSSLQDAVKGDCQSALLALCRAEDM
2615168CD1     CETDLLSIRAEFRKKFGKSLYSSLQDAVKGDCQSALLALCRAEDM
```

Submit sequences to:

